Géodynamique andine
Andean Geodynamics
Geodinámica Andina

Résumés étendus
Extended abstracts
Resúmenes expandidos

Organisateurs **Organizers** **Organizadores**

Institut de recherche pour le développement
Paris

Université Paul Sabatier
Toulouse
France

2002

IRD
Institut de recherche pour le développement

UNIVERSITE PAUL SABATIER
TOULOUSE III

GÉODYNAMIQUE ANDINE
ANDEAN GEODYNAMICS
GEODINAMICA ANDINA

5th International Symposium on Andean Geodynamics

Université Paul Sabatier, Toulouse, France,
16-18 Septembre 2002

Résumés étendus
Extended abstracts
Resúmenes ampliados

Organisateurs / Organizers / Organizadores
Institut de recherche pour le développement
Université Paul Sabatier

IRD
INSTITUT DE RECHERCHE POUR LE DÉVELOPPEMENT
Paris, 2002

COMITÉ D'ORGANISATION
COMITE ORGANIZADOR
ORGANIZING COMITTEE

P. Baby (IRD-Toulouse), J. Darrozes (Univ. Paul Sabatier-Toulouse), J. Deramond (Univ. Paul Sabatier-Toulouse), B. Dupré (CNRS-Toulouse), J.-L. Guyot (IRD-Toulouse), G. Hérail (IRD-Toulouse), E. Jaillard (IRD-Quito), A. Lavenu (IRD-Toulouse), H. Miller (Univ. München), T. Monfret (IRD-Géoscience Azur), G. Wörner (Univ. Göttingen)

Comité scientifique et représentants nationaux
Comité Científico y Representantes Nacionales
Scientific Advisory Board and National Representatives

R. Armijo (IPG, Paris), J.-P. Avouac (CEA, Paris), R. Charrier (Univ. Chile, Santiago), J.-Y. Collot (IRD, Géoscience Azur), L. Dorbath (IRD, Strasbourg), S. Flint (Univ. Liverpool), B. France-Lanord (CNRS, Nancy), L. Fontboté (Univ. Genève), Y. Gaudemer (Univ. Paris VII), R. Gaupp (Univ. Jena), F. Hervé (Univ. Chile, Santiago), T.E. Jordan (INSTOC, Cornell), J. Mojica (Univ. Bogotá), O. Oncken (Univ. Potsdam), L. Ortlieb (IRD, Bondy), R.J. Pankhurst (Brit. Antartic Surv.), V. Ramos (Univ. Buenos Aires), P. Ribstein (IRD, Paris), C. Robin (Univ. Clermont-Ferrand), S. Rosas (Univ. Lima), F. Sàbat (Univ. Barcelona), M. Schmitz (FUNVISIS, Caracas), R. Suárez Soruco (YPBF, La Paz), M. Rivadeneira (Petroproducción), W. Winkler (ETH, Zürich).

APPUIS FINANCIERS
FUNDINGS
APPOYO FINANCIERO

L'organisation de l'ISAG 2002 et les bourses accordées à un certain nombre de collègues latino-américains ont été possibles grâce au soutien financier de l'IRD (notamment de la Délégation à l'Information et à la Communication), de la région Midi-Pyrénées, de l'Université Paul Sabatier et de l'Andean Comittee de l'ILP.

SOMMAIRE / SUMMARY / SUMARIO

THIN-SKINNED TECTONICS IN THE CORDILLERA ORIENTAL, CHOROMORO BASIN, NW TUCUMAN, ARGENTINA

Liliana del Valle ABASCAL(1)

(1) Universidad Nacional de Salta. Sede regional Tartagal.Warnes 890. Tartagal. Salta. Argentina (abascal1@netscape.net)

KEY WORDS: Cordillera Oriental, Argentina, thin-skinned tectonics, structural geology

INTRODUCTION

The Choromoro Basin in northwestern Tucuman province, Argentina, is a tectonic depression that lodges about 6000 meters of Cretaceous and Tertiary sedimentary strata resting unconformably on a low-grade, Proterozoic, metamorphic basement exposed in anticlinal structures (Fig. 1). The sedimentary column comprises, at the base, strata of the Salta Group (Upper Cretaceous-lower Tertiary), deposited in the Salta Cretaceous Rift, overlain across a very low angle unconformity by beds of the Choromoro Group (Miocene-Pliocene) which comprises two major formations, the Salí Formation, consisting of red siltstones with intercalated layers of gypsum and oolithic limestones, and the India Muerta Formation, composed of thick-bedded reddish conglomeratic sandstones. Unconformably above the Choromoro Group rest conglomeratic beds of the Ticucho Formation, deposited in extensive early Pleistocene alluvial fans.

The Choromoro Basin forms part of the Cordillera Oriental geologic province (Bossi, 1969; Baldis et al., 1976; Fernández Garrasino, 1992), characterized by a thick-skinned tectonic style. In this province the low-grade Proterozoic basement is intensely involved in the Andean folding and forms the nuclei of the anticlines developed along the western and eastern borders of the basin. The western boundary of the basin is constituted by a large anticline topographically represented by the Cumbres Calchaquíes ranges, and a smaller anticline that stems from the northeastern end of the former and underlies the Altos de la Totora ranges. Both anticlines are related to high angle reverse faults with eastward vergence and offsets greater than 3 km. The eastern border is given by the Medina Ranges, which underlie an asymmetric anticline with a steep, faulted eastern limb. The faults responsible for the uplift of the blocks of metaporphic basement along the western and eastern borders of the Choromoro Basin are related to a detachment at a depth of about 20 km (Mon, 1999).

Within the Choromoro Basin a series of narrow and symmetric anticlines and synclines have been mapped. The fold axes generally plunge northwards and strike NS to NNE-SSW. The folds commonly show eastward vergence, with low dipping western limbs and eastern limbs intersected by eastward vergent reverse

faults. An analysis of the geometry of the structures indicates that they mostly originated as fault bend folds and have offsets smaller than the thickness of the Choromoro Group (approximately 2 km) as nowhere do beds of the Salta Group crop out in the hanging walls.

A second, shallower detachment level is postulated for these faults (Fig. 2). This detachment would be located in shaly, ductile beds of the Lumbrera Formation (uppermost Salta Group) at a depth of about 2 to 2.5 km. A YPF, east-west seismic line across the central Choromoro Basin shows evidence of this detachment.

In the Choromoro Basin the thick-skinned tectonic style is manifest in the structures underlying the Cumbres Calchaquies and Medina ranges, along the western and eastern borders of the basin, respectively. In contrast, within the Choromoro Basin the structural style is thin-skinned.

CONCLUSIONS

Mapping in the Choromoro Basin revealed a series of eastward vergent structures related to a detachment level located in shales of the Lumbrera Formation (Salta Group), at a depth of 2 to 2.5 km. This shallow detachment allowed the deformation of the Choromoro Group strata separately from that of the metamorphic basement. Thus, during Andean compression, a thin-skinned tectonic style developed locally in the Cordillera Oriental that is regionally characterized by a thick-skinned tectonic style.

REFERENCES

Baldis, B., Gorroño, R., Ploszkiewicz, J. and Sarudiansky, R. 1976 Geotectónica de la Cordillera Oriental, Sierras Subandinas y comarcas adyacentes. Actas 6° Congreso Geológico Argentino, 1: 3-22, Buenos Aires.

Bossi, G.E. 1969 Geología y estratigrafía del sector sur del valle de Choromoro. Acta Geologica Lilloana, v. 10, p. 19-61.

Fernández Garrasino, C. 1992 Aspectos geológicos de algunas serranías del Noroeste argentino, llanuras orientales tucumanas y valle de Trancas-Choromorro, temas exploratorios, (Provincias de Tucumán, Catamarca y La Rioja, Argentina). Boletín de Informaciones Petroleras (tercera época), Buenos Aires.

Mon, R. 1999 Cordillera Oriental. Relatorio XIV Congreso Geológico Argentino, v. 1, p. 426-431.

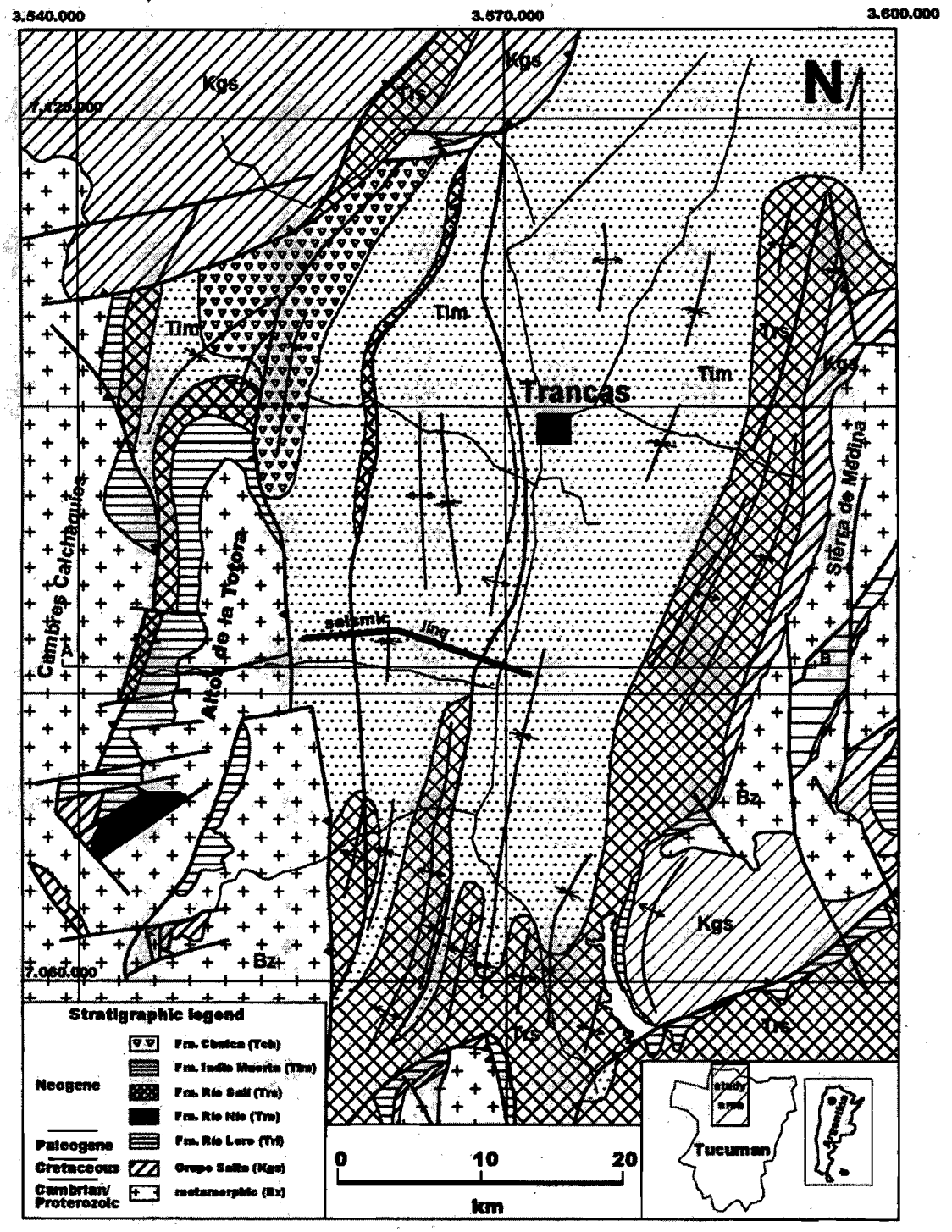

Figure 1. Geologic and structural map of the Choromoro Basin in northwestern Tucuman. Shown is the trace of a YPF seismic line mentioned in the text.

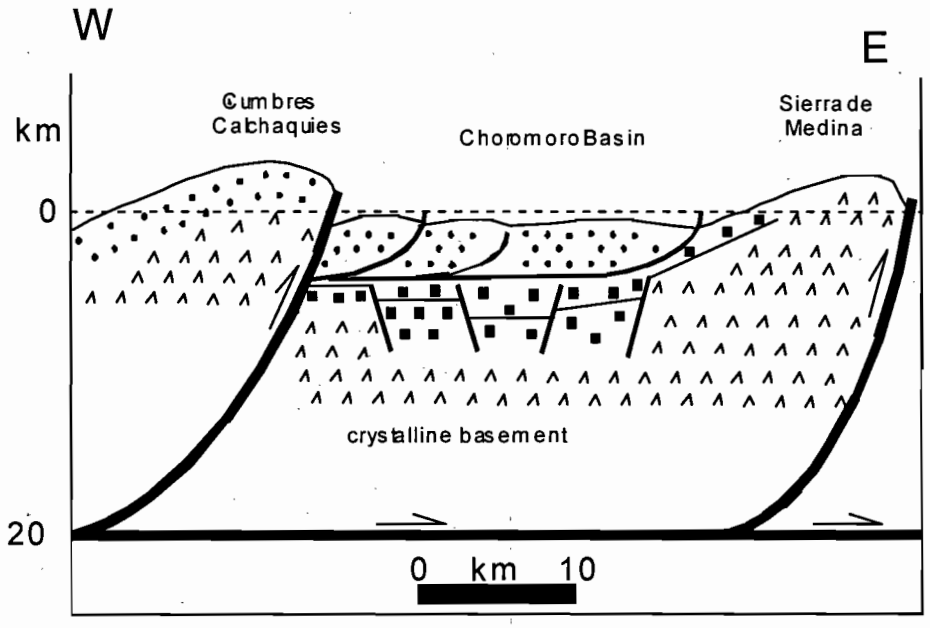

Figure 2. Schematic cross-section for the Choromoro Basin. The section shows the two detachment levels. For cross-section location see line AB in Figure 1.

LOW TEMPERATURE THERMOCHRONOLOGY AND TECTONICS IN THE CHILOE REGION, SOUTHERN CHILEAN ANDES (41°-43°S; 72°-74°W)

Alberto ADRIASOLA M.(1), Bernhard STÖCKHERT(1), Francisco HERVÉ(2)

1) Institut für Geologie, Ruhr-Universität Bochum, Universitätstr. 150, D-44780 Bochum, Germany. (alberto.adriasola@ruhr-uni-bochum.de) (bernhard.stoeckhert@ruhr-uni-bochum.de)
2) Departamento de Geología, Universidad de Chile, Casilla 13518, Correo 21, Santiago, Chile. (fherve@cec.uchile.cl)

KEYWORDS: Liquiñe-Ofqui Fault, Fission Track Analysis, Microfabrics, Erosion Rates

INTRODUCTION

One of the main important structural features controlling the late development the South-central Andes is the Liquiñe Ofqui Fault (LOFZ). In the Chiloe Region, its activiy has been well documented (Herve, 1994; Lavenu et al. 1994; Cembrano et al, 2000), but the question of uplift/erosion remains unknown. Fission track (FT) dating of zircon and apatite combined with microfabric analyses on deformed rocks are applied in this study to determine the low temperature history and uplift/erosion rates from the South-central Andes in relation to the latest movements of the LOFZ.

GEOLOGY OF THE STUDY AREA

The most prominent geological unit in the Chiloe region is the Meso-Cenozoic North Patagonian batholith. This batholith intrudes a Late Paleozoic metamorphic basement, interpreted as the remnant of an accretionary complex, the provenance of which is still poorly understood. These units are overlain by a few Meso-Cenozoic volcanosedimentary sequences, distributed as basin deposits or as roof pendants of the batholith. The Liquiñe Ofqui Fault Zone (LOFZ) extends N-S for ca. 1000 km, and has displaced dextrally all of the mentioned units since the Cretaceous (Herve, 1994; Cembrano et al., 2000). It defines a regional weakness zone which controls the location of the main volcanic arc related to present day subduction of the Nazca Plate under the South Central Andes. Additionally climate has played an important role in the development of the Andean landscape within the region. Big differences in rainfall across the Andean range have resulted in a complex interplay between the topography and uplift/erosion rates.

FIRST RESULTS AND INTERPRETATION

37 new apatite FT ages and length measurements are compared to available Rb-Sr, K-Ar and Ar-Ar ages on tectonically juxtaposed Miocene and Cretaceous plutons from the Reloncavi Sector (figure 2). Along the Fault zone itself ages vary between 5.6 +/- 2.0 and 3.3 +/- 1.2 Ma, although older ages with large errors were obtained from samples with low Uranium concentration. Apatite FT length distribution patterns from 34 samples imply increasing cooling rates from west to east on the western side of the LOFZ, whereas along the fault zone itself very rapid cooling rates are implied. Microstructural studies on deformed tonalites from Llancahue Island-Cholgo sector show quartz grains with undulose extinction, development of low angle grain boundaries, and in rare cases recrystallisation. Feldspar and micas show abundant microfractures and development of mechanical induced twinning. These microstructures imply that strain hardening processes occurred mostly under low temperature conditions (300°C, low-temperature plasticity regime for quartz). Together with the time-temperature profiles, this evidence indicates high rates of late Cenozoic cooling and hence uplift/erosion due to activity of the LOFZ. Further results concerning zircon FT ages and microstructures will be presented at the Symposium in September.

ACKNOWLEDGEMENTS

This project was partly funded by the DFG grants Sto196/11-1 and 196/11-2. A.Adriasola is funded by the DAAD exchange program. Field trips were in part sponsored by the Depto. de Geol., U. de Chile and by the SERNAGEOMIN office from Puerto Varas.

REFERENCES

Cembrano J, Schermer E, Lavenu A, Sanhueza A. (2000): Contrasting nature of deformation along an intra-arc shearzone, The Liquiñe Ofqui Fault Zone, Southern Chilean Andes. Tectonophysics, 319: 129-149.

Gallager K., Brown R; Johnson C. (1998): Fission Track Analysis and its applications to geologic problems. Annu. Rev. Earth Planet. Sci., 26: 519-72.

Hervé, F. (1994): The Southern Andes between 39° and 44°S latitude: the geological signature of a transpressive tectonic regime related to a magmatic arc. Tectonics of the Central Andes, p. 243-248.

Lavenu A; Cembrano J.(1999): Compressional- and transpressional-stress for Pliocene and Quarternary brittle deformation in fore arc and intra-arc zones (Andes of Central and Southern Chile). J.Struct. Geol., 2: 1669-1691.

Munizaga, F., Hervé, F., Drake, R., Pankhurst, R.J., Brook, M., Snelling, N.(1988): Geochronology of the Lake Region of south-central Chile (39°-42°S): Preliminary Results. South Am. Earth Sci., 1: 309-316.

SERNAGEOMIN (1994): Carta Metalogenica de la X Region.

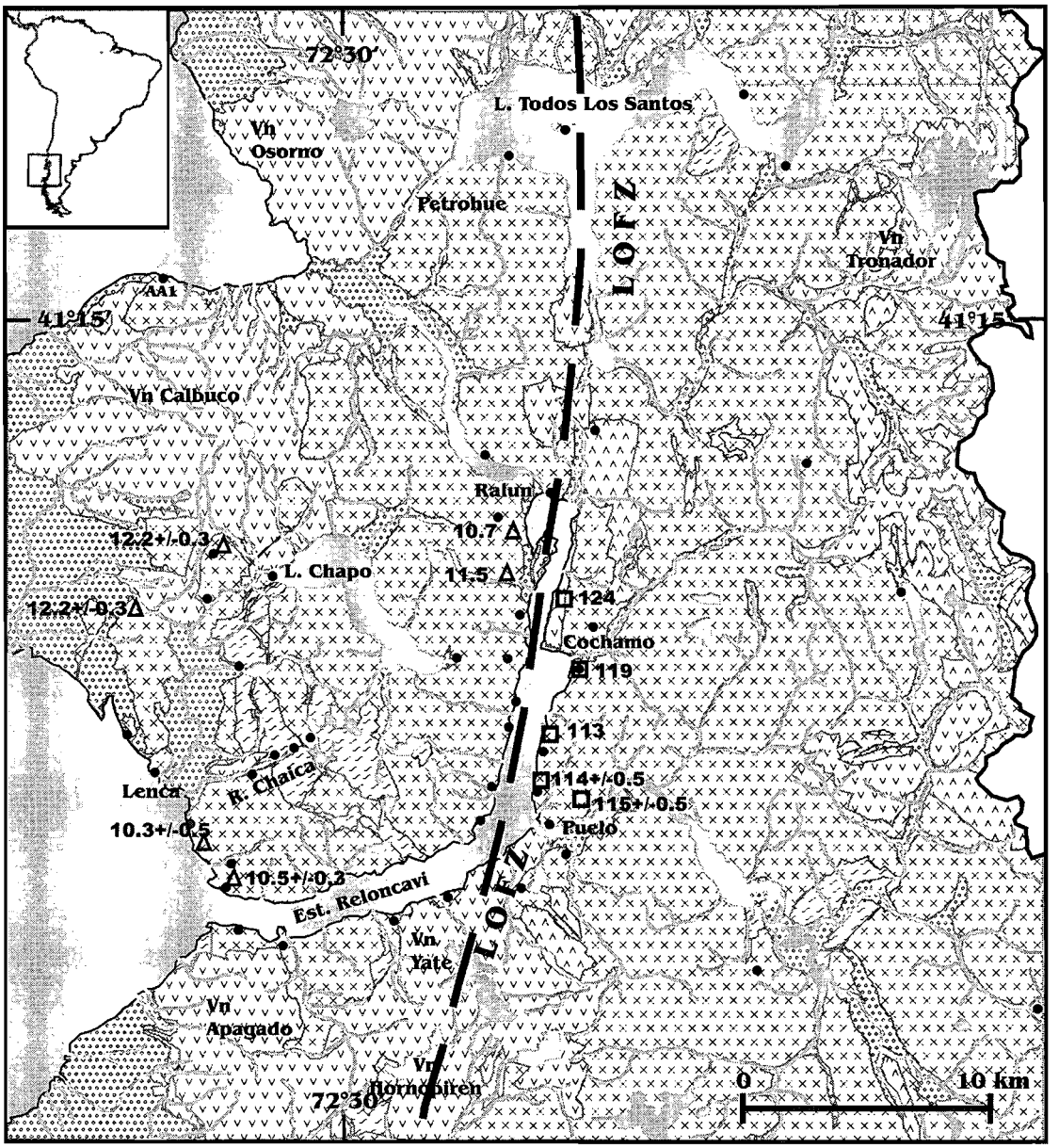

Figure 1
Geology of the Reloncavi sector of the Liquiñe-Ofqui Fault (simplified after SERNAGEOMIN, 1994). Available radiometric ages compiled after Cembrano, et al. (2000) and Munizaga et al. (1982).

- Quaternary sediments
- Quaternary volcanic rocks
- North Patagonian Batholith
- Meso-Cenozoic volcanic rocks
- Upper Paleozoic metamorphic basement
- Liquiñe Ofqui Fault Zone (LOFZ)
- Total Fusion ages on biotite
- K-Ar ages on biotite
- Samples for FT Dating

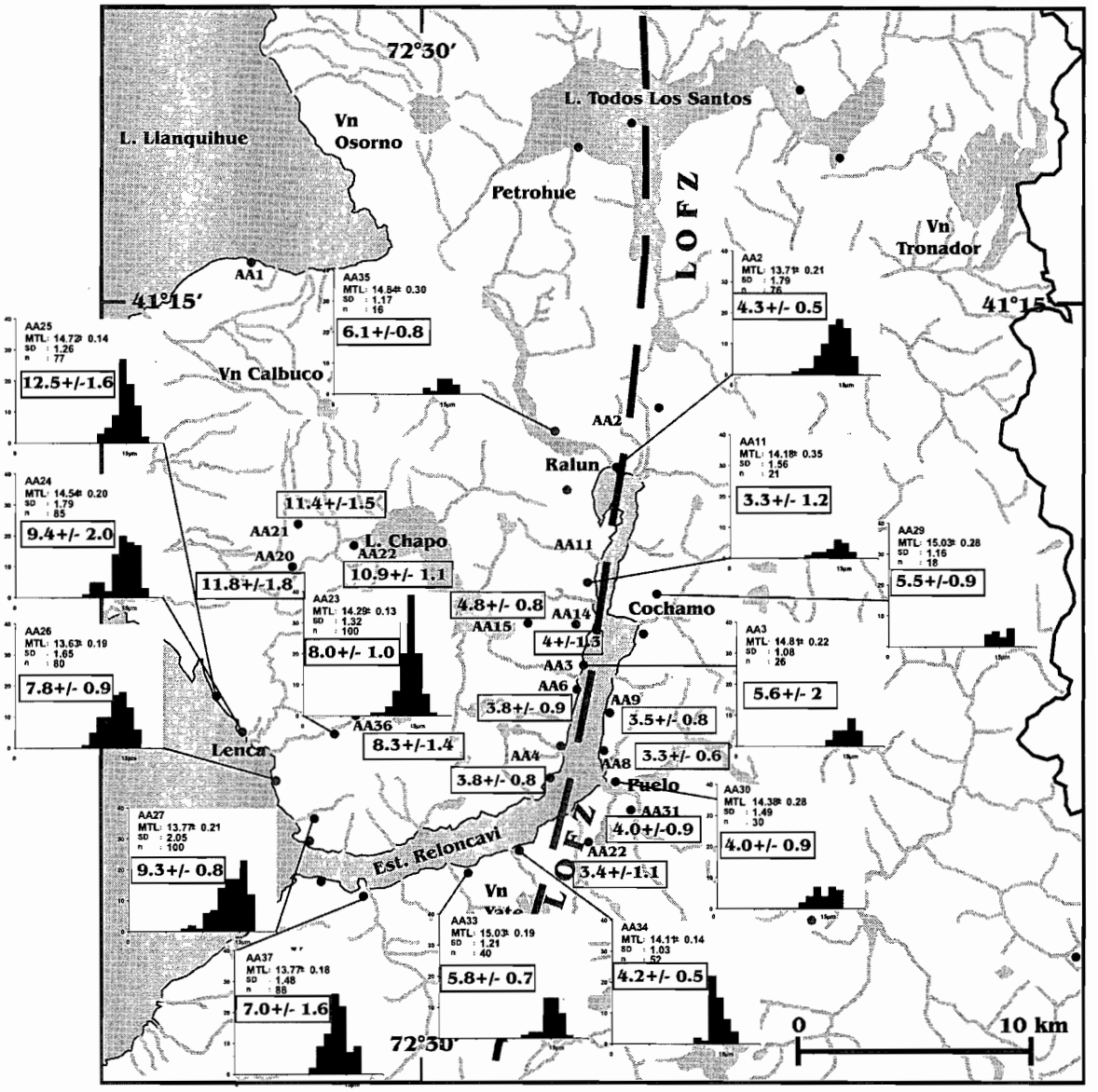

Figure2:
Apatite FT ages and length distributions in the Reloncavi Sector of the LOFZ.

- **Location of Samples for FT Dating**

6.2+/- 0.7 **Apatite ages in Ma.**

COMPOSITIONAL FEATURES AND GEODYNAMIC EVOLUTION OF VOLCANIC AND PLUTONIC COMPONENTS IN THE LOWER CRETACEOUS MAGMATIC PROVINCE (COASTAL RANGE OF CENTRAL CHILE)

Luis AGUIRRE[(1)], Miguel Angel PARADA[(1)], Diego MORATA[(1)], Gilbert FÉRAUD [(2)], Francisco FUENTES[(1)]

(1) Departamento de Geología, Universidad de Chile. Chile, luaguirr@cec.uchile.cl
(2) Unversité de Nice-Sophia Antipolis 06108, Nice, cedez 02, France, Gilbert.Feraud@unice.fr

KEY WORDS: Chile, Coastal Range, Lower Cretaceous, magmatism, ages.

INTRODUCTION

A Lower Cretaceous belt, *c.* 1200 km long and mainly composed of magmatic rocks, is exposed along the Chilean Coastal Range between latitudes 25°and 36°S. At the La Serena area, c. 29-30°S (Fig.1A), the Lower Cretaceous volcanism is represented by the Arqueros Formation which consists of basaltic andesites and marine limestone. Between 32° and 33°30'S (Fig.1B) the main units of this belt are the basic volcanic Veta Negra Formation and the Las Chilcas Formation, both largely accumulated in a subsiding basin thicker than 10 km. A pervasive and non-deformative very-low grade regional metamorphism (prehnite-pumpellyite facies) affects the volcanic products of both formations (Aguirre *et al* 1989).

Plutons belonging to this Lower Cretaceous magmatic belt are numerous. The Caleu pluton, located in the Coastal Range of central Chile *c.* 40 km northwest from Santiago, is an excellent example (Parada et al., 2002). It has good exposures covering an area of about 340 km^2 and consists in three N-S elongated zones, which define an across-pluton compositional variation characterized by a westward increasing in SiO_2 content. These three zones are: Gabbro-Diorite Zone Tonalite Zone and Granodiorite Zone.

COMPOSITIONAL FEATURES OF VOLCANIC AND PLUTONIC COMPONENTS

The magmatic development of this province is marked by two contrasting events: an older volcanic episode represented by the Veta Negra and Arqueros formations and a younger plutonic event characterized by granitoid magmatism. From latitudes 33°30' to 29°, the basic lavas are chemically homogeneous contents classifying as high-K to shoshonitic basaltic andesites and andesites (Levi *et al.*, 1988, Vergara *et al.*, 1995, Morata *et al.*, 2000). N-MORB normalized trace element patterns both for volcanic and plutonic rocks are characterized by LILE enrichment, systematic HFSE decrease and a marked Nb-Ta depletion, typical of subduction related magmatism. In spite of some chemical similarities between the volcanic and plutonic products (*e.g.* high Al_2O_3 and K_2O and low MgO), conspicuous differences between them can be recognized (Table 1).

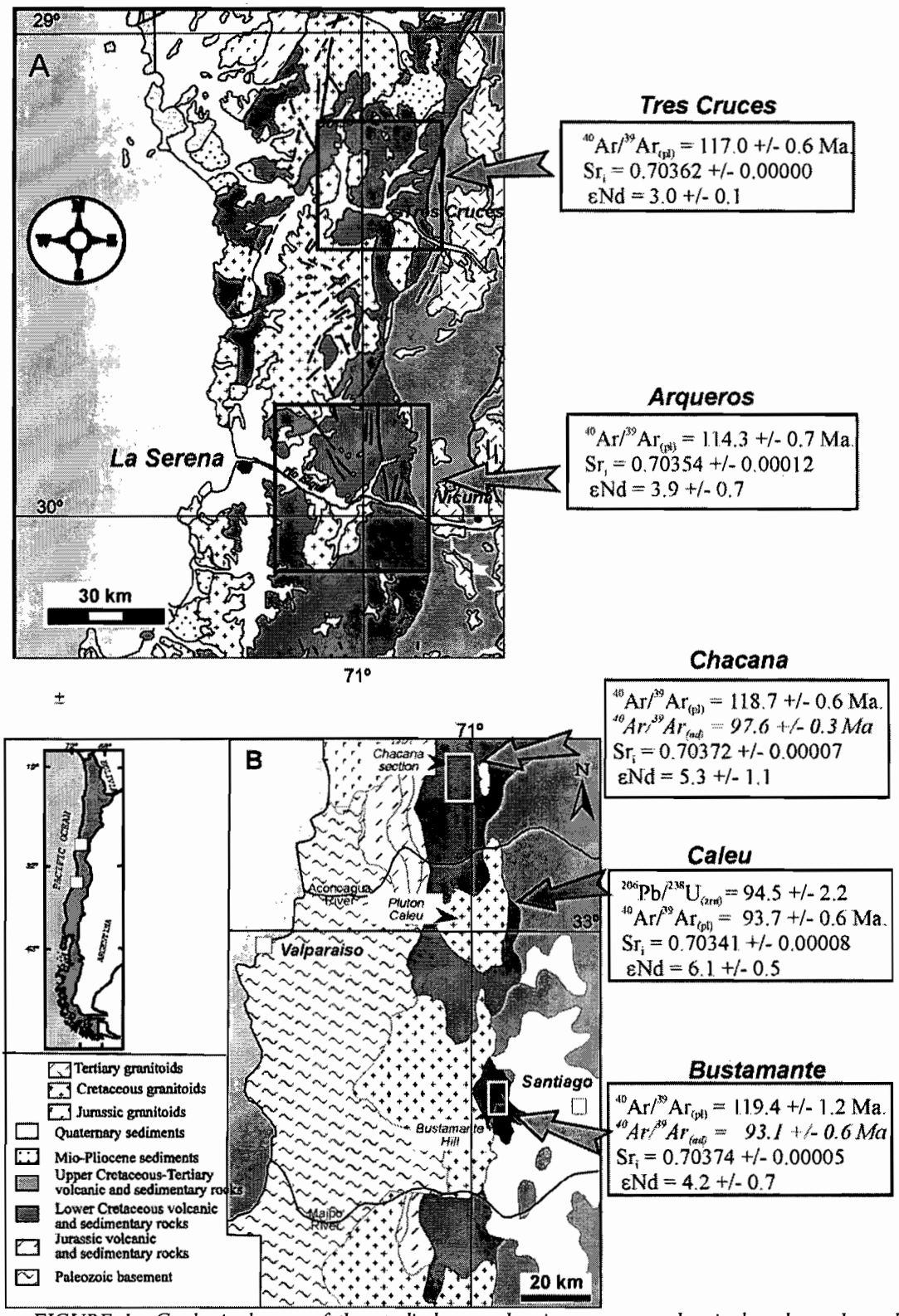

FIGURE 1.- Geological map of the studied area showing some geochemical and geochronological data.

It is of particular interest to compare the Veta Negra volcanic products with the spatially related Caleu pluton that put in evidence the fact that the Veta Negra flows are more basic and less isotopically depleted than the Caleu granitoids.

Table 1.- Summary of geochemical features and ages of the tectonic processes of the Lower Cretaceous magmatic rocks. Average and standard deviation with number of samples in parenthesis.

	Tres Cruces[1]	Arqueros[1]	Chacana[1]	Bustamante[1]	Caleu[2]
Latitude S	29°20'	29°50'	32°30'	33°25'	33°
Formation/pluton	*Arqueros*	*Arqueros*	*Veta Negra*	*Veta Negra*	*Caleu*
$\%SiO_2$	54.09±1.87(6)	53.73±1.87(8)	58.45±1.95(5)	52.39± 0.80(2)	60.33±5.72(43)
$\%Na_2O$	3.05±0.41(6)	3.96±0.80(8)	3.49±0.17(5)	3.22±0.64(2)	3.90±0.47(43)
$\%K_2O$	4.10±1.00(6)	2.61±0.87(8)	4.24±0.97(5)	2.33±0.05(2)	2.59±1.13(43)
%MgO	3.78±0.70(6)	3.05±1.29(8)	2.50±0.48(5)	3.67±0.31(2)	2.59±1.16(43)
$\%Al_2O_3$	17.64±1.12(6)	18.16±0.87(8)	16.04±1.39(5)	18.98±1.25(2)	16.90±1.43(43)
Sr_i	0.70362± 0.00000(2)	0.70354± 0.00012(4)	0.70372± 0.00007(2)	0.70374± 0.00005(2)	0.70341± 0.00008(13)
εNd^t_{CHUR}	3.0±0.1(2)	3.9±0.7(4)	5.3±1.1(2)	4.2±0.7(2)	6.1±0.5(13)
Age (Ma)	117.0±0.6	117-115	118.7±0.6	119.4±1.2	94.5±2.2
Rate of subsidence			≥0.25 mm/year	0.18 mm/year	
Age of metamorphism (Ma)			97.6±0.3	93.1±0.6	
Age of exhumation (Ma)					94-90

[1] Data from Morata *et al.* 2001

[2] Data from Parada *et al.* 2001, 2002.

GEODYNAMIC CONSIDERATIONS

The geochronological record shows the existence of a magmatic gap between 115 and 94.5 Ma, which could be explained by a decrease in intensity of the decompression melting mechanism at the origin of the Veta Negra volcanism as a consequence of progressive infilling and subsidence of its basin. Subsidence was interrumpted by fast exhumation at 94-90 Ma (Table 1) which would have been triggered by a mechanism of crustal density inversion between upper crustal basic and denser rocks, and lower crustal, felsic and lighter basement such as advocated by Martínez *et al.* (2001), to explain the presence of metamorphic core complexes in the Papua New Guinea region.

A coincidence in age between plutonism and low-grade metamorphism of the volcanic rocks (see Table 1) suggests that this last was not solely produced by burial but was related to a regional increase in thermal gradient associated with the magmatic event at the origin of the Caleu pluton. The compositional differences between the Caleu granitoids and the Veta Negra flows, already mentioned, are attributed to a lower melting

degree of deeper asthenospheric protoliths in the genesis of the former. This process would result from renewal of decompression melting associated with crustal root attenuation during the period of fast exhumation.

ACKNOWLEDGEMENTS

This work was funded by the FONDECYT Projects 1961108 and 1990980, the DID Project I001-99/2 and the CNRS-CONICYT Projets 1999, 2000 AND 2001, all of them are duly acknowledged.

REFERENCES

Aguirre, L.; Levi, B. and Nyström, J.O. 1989. The link between metamorphism, volcanism and geotectonic setting during the evolution of the Andes. In: J.S. Daly, R.A.Cliff and B.W.D.Yardley (Editors), Evolution of metamorphic belts. Geological Society of London Special Publ.ication 43, pp. 223-232.

Levi, B., Nyström, J.O., Thiele, R. and Åberg, G., 1988. Geochemical trends in Mesozoic-Tertiary volcanic rocks from the Andes in central Chile and tectonic implications. Journal of South American Earth Sciences, 1: 63-74.

Martinez, F.; Goodliffe, A.M. and Taylor, B. 2001. Metamorphic core complex formation by density inversion and lower-crust extrusion. Nature, 411, 930-934.

Morata, D.; de la Rosa, J. and Aguirre, L. 2000. A preliminary LAM-ICP-MS study on plagioclase phenocrysts from Lower Cretaceous volcanic rocks from La Serena region (Chile). IX Congreso Geológico Chileno, Actas vol. 1, 649-653.

Morata, D.; Aguirre, L.; Féraud, G.; Fuentes, F.; Parada, M.A. and Vergara, M. 2001. The Lower Cretaceous volcanism in the Coastal Range of central Chile: geochronology and isotopic geochemistry. III South American Symposium on Isotope Geology, Extended Abstracts (CD), 321-324.

Parada, M.A.; Féraud, G.; Aguirre, L.; Fuentes, F.; Morata, D.; Vergara, M. and Palacios, C. 2001. U-Pb, ^{40}Ar-^{39}Ar and fission-track geochronology of the Early Cretaceous Caleu pluton and its volcanic envelope, Coastal Range of central Chile: tectonic and metamorphic implications. III South American Symposium on Isotope Geology, Extended Abstracts (CD), 612-615.

Parada, M.A.; Larrondo, P.; Guirresse, C. and Roperch, P. 2002. Magmatic gradients in the Cretaceous Caleu Pluton (Central Chile): injections of pulses from a stratified magma reservoir. Gondwana Research, 5, 307-324.

Vergara, M., Levi, B., Nyström, J. and Cancino, A., 1995. Jurassic and Early Cretaceous island arc volcanism, extension, and subsidence in the Coast Range of central Chile. Geological Society of America Bulletin, 107: 1427-144.

A CARBONIFEROUS VOLCANIC ARC ALONG THE COASTAL CORDILLERA?

Antenor M. ALEMÁN(1) and Walther LEÓN(2)

(1) 2807 Stoney Wood, Houston TX, antenor@swbell.net
(2) INGEMET wleonlecaros@hotmail.com

KEY WORDS: Western Gondwana, arc magmatism, petrofacies

INTRODUCTION

Late Paleozoic Magmatism along the Gondwana's Pacific margin has been documented from Antarctic to northern Chile (Mukasa and Dalziel, 2000, Ramos and Aleman, 200, Bell, 1987), to southern Peru as documented by the late Silurian to early Devonian San Nicolas Batholith. However, there is an apparent absence of radiometric ages to infer the persistence of this arc-trench system throughout the Carboniferous.

The Lower Carboniferous in southern Peru is represented by the Ambo Group (Newell et al, 1953), which consists of interbedded sandstones and shales with abundant coal seams. The only direct evidence of Carboniferous igneous activity is in the Shira Mountains where Megard (1978) and Dalmayrac and others, (1980) reported interbedded andesitic to rhyolitic lavas and tuffs; however, there is little comprehension about the nature and tectonic setting of this volcanic activity in eastern Peru. Recently, indirect evidence of volcanic activity has been reported from petrofacies studies in the northern Bolivian Altiplano (Diaz Martinez, 1995). He documented significant percentage of volcanic rock fragments in the uppermost unit of the Ambo Group.

Four sections of the Ambo Group in southern Peru have been studied using Dickinson's (1983) discrimination triangles. The Paracas peninsula section plots on the undissected to transitional arc ($Qt_{15}F_9L_{76}$ and Qm13F9Lt78), however, southward, the Chala section plots in a more mature transitional to dissected arc ($Qt_{31}F_{26}L_{43}$ and $Qm_{24}F_{26}Lt_{50}$). In this section the Ambo group contains thinly bedded tuffs are interpreted to suggest the presence of a contemporaneous volcanic arc rather than the erosion of an older arc massif. Although the arc-derived debris is more abundant along the coast, near the Carboniferous forearc and interarc basins, the influence of the magmatic arc also reached the retroarc basins such as documented in the Pongo de Mainique ($Q_{50}F_{13}L_{37}$ and $Qm_{48}F_{13}Lt_{39}$) and Coñec ($Q_{64}F_9L_{27}$ and $Qm_{61}F_9L_{30}$) in the Ucayali and Madre de Dios basins respectively.

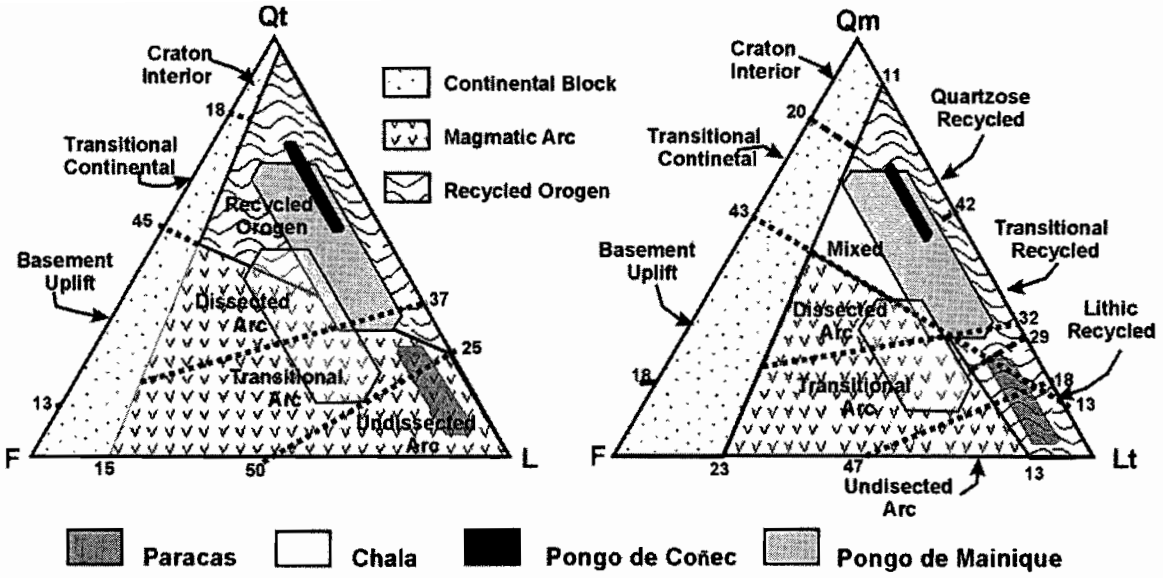

Along the coastal sections, the abundance of coal seams and low Q/F ratio (1.2 to 1.7) is interpreted to represent a warm and humid climate supporting the interpretation from the fossil flora. This climate may account for the relatively poorly preserved volcanic rock fragments and partially altered feldspars to chlorite and sericite. Variable, but relatively high feldspar content and high Lv/Lt supports a magmatic arc provenance with significant arc dissection, and episodic unroofing of batholith roots. Eastward, the Q/F ratio significantly increases in the Pongo de Mainique (3.8) and Pongo de Coñec (7.4) and is interpreted to reflect the source from recycled transitional orogen and quartz rich lithologies. The vertical modal analysis at the Pongo de Mainique section indicates random variation controlled by the source area.

This petrologic evidence provides new lines of evidence to suggest the presence of an Upper Paleozoic arc-trench system in the western margin of Gondwanaland, which may have persisted since the late Silurian to early Devonian emplacement of the San Nicolas Batholith (Mukasa and Henry, 1990). This high K calc-alkaline magmatic arc developed during closing of the Lower Paleozoic extensional basin.

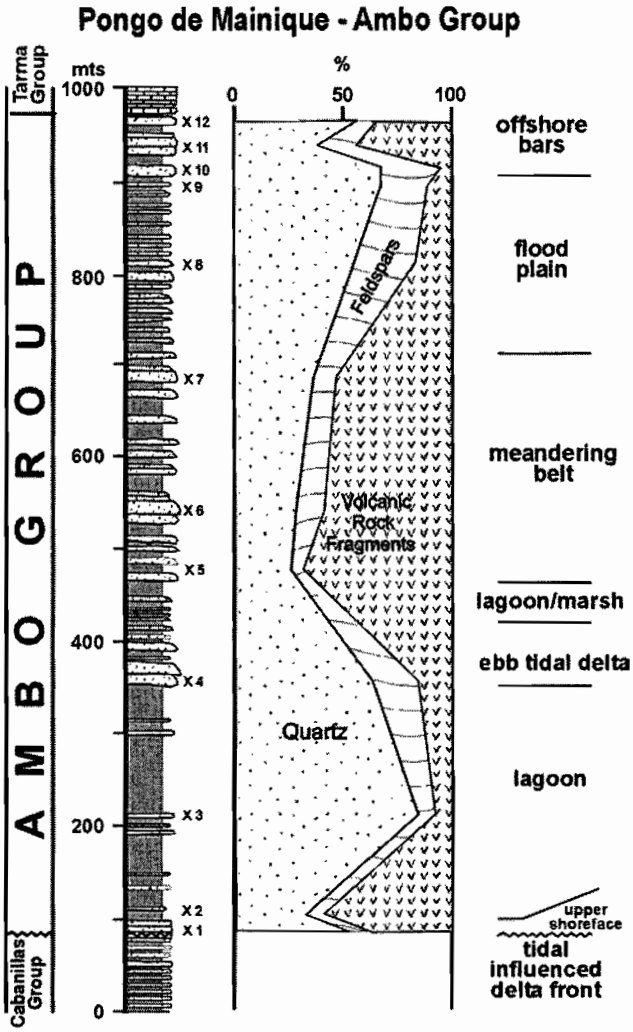

The already accreted Grenvillian Arequipa terrane was extended during the early Paleozoic ensialic and formed deep troughs where thick marine sequences interbedded with basic lava flows and sills were deposited. This facies are well documented in Bolivia and northern Argentina. Closing of this lower Paleozoic basin took place by collision and re-welding of the extended Arequipa terrane and was earlier in the south (Ocloyic Orogeny) than in the north (late Silurian to early Devonian Atico event of Shackleton and others, 1979). This event was coeval with the emplacement of the San Nicolas Batholith (Mukasa and Henry, 1990). An arc-trench system continued throughout the Carboniferous with different kinematics and subduction angle. Low angle subduction may account for a volcanic lull during the Carboniferous; however, the late Permian has been ascribed to insipient back-arc extension (Megard, 1978).

CONCLUSIONS

From Antarctica to southern Peru, the Gondwana's Pacific margin underwent a prolonged subduction-related magmatism at least since the early Devonian, which persisted through Carboniferous. The San Nicolas Batholith, formed during the closing of the early Paleozoic extensional basins, supports late Silurian to early Devonian magmatism. Petrofacies and the occurrence of thinly bedded tuffs in the Ambo Group suggest the presence of an arc-trench system along southern Peru during the Carboniferous. The lack of direct evidence for an arc may be related to a low angle subduction similar to the present day Peruvian margin. Regional analysis seems to support the presence of an arc-trench system in southern Peru at least since early Devonian.

REFERENCES

Bell, C. M., 1987, The Late Paleozoic evolution of the Gondwanaland continental margin in northern Chile. AGU Geophysical Monograph, 40, p. 29-48.

Dalmayrac, B., G. Laubacher, R. Marocco, 1980, Caractères généraux de l'evolution geologique des Andes péruviennes. Trabaux et Documents de l'ORSTOM, 122, 501 p.

Diaz Martinez, E., 1995 Evidencia de actividad volcanica en el registro sedimentario del Carbonífero inferior (Viseano Superior) del Altiplano norte de Bolivia (16^0S) y su relacion con el arco magmático de los Andes centrals, Revista Tecnica de YPFB 16, 1-2, p. 37-49.

Dickinson, W. R., Beard, L. S., Brakenridge, G. R., Erjavec, J. L., Ferguson, R. C., Inman, K. F., Knepp, R. A., Lindberg, F. A., and Ryberg, P. T., 1983, Provenance of North American Phanerozoic sandstones in relation to tectonic setting: Geol. Soc. Amer. Bull., 94, 222-235.

Dickinson, W. R., 1985, Interpreting provenance relations from detrital modes of sandstones, in Zuffa, G. G. (ed) "Provenance of Arenites", 333-361.

Mégard, F., 1978, Etude géologique des Andes du Pérou central: Memoir ORSTROM, no.86, Paris, 310 p.

Mukasa, S., and D. J. Henry, 1990, The San Nicolas batholith of coastal peru: early Paleozoic arc or continental rift magmatism?, Jour. Geol. Soc. London, 147, p.27-39

Mukasa, S. and Dalziel, I. W. D., 2000, Marie Byrd Land, West Antarctica: Evolution of Gondwana's Pacific margin constrained by zircon U-Pb geochronology and feldspar common-Pb isotopic composition, G. S. A Bull, 112, p. 611-627.

Newell. N. D., J. Chronic, and T. Roberts, 1953, Upper Paleozoic of peru, Geological Society of America memoir 58, 276p.

Ramos, V., and Aleman, A., 2000, Tectonic Evolution of the Andes, in Cordani, U. G., Milani, E. J., Thomaz Filho, A., and Campos, D. A., (eds) "Tectonic Evolution of South America", p. 635-685. Rio de Janeiro 2000.

Shackleton, R. M., Ries, A. C., Coward, M. P., and Cobbold, P. R., 1979m Structure, metamorphism and geochronology of the Arequipa Massif of coastal Peru: Geological Society of London, v. 136, 195-214.

TECTOSEDIMENTARY EVOLUTION OF TRIASSIC JURASSIC EXTENSIONAL BASINS IN THE HIGH ANDES OF ARGENTINA AND CHILE (32°-34° SL)

P. Pamela ALVAREZ (1),(2), Laura B. GIAMBIAGIi (1),(3) ,Estanislao GODOY (4) and Victor A. RAMOS (1)

(1) Laboratorio de Tectónica Andina, Universidad de Buenos Aires, Ciudad Universitaria s/n, Pabellón II, 1428 Capital Federal, Argentina. andes@gl.fcen.uba.ar
(2) Actually, Sipetrol, Vitacura 2236 piso 8, Santiago de Chile palvarez@sipetrol.cl
(3) Centro Regional de Investigaciones Científicas y Tecnológicas, Parque San Martín s/n, 5500 Mendoza, Argentina. lgiambiagi@lab.cricyt .edu.ar
(4) Servicio Nacional de Geología y Minería. Casilla 10465, Santiago, Chile. egodoy@sernageomin.cl

KEY WORDS: High Andes, Argentina, Chile, Triassic – Jurassic, Rift Systems, tectonostratigraphy

INTRODUCTION

The Triassic oil basins of central Argentina present a north-west trend, oblique to the main structures of the Andes. Most of the present knowledge from these basins was derived from eastern foothills, where the Cuyo and Neuquén basins are one of the main producers of the Mendoza area.

A series of rift systems along the western margin of Gondwana were formed during Late Triassic – Early Jurassic times. Their inception was controlled by mayor crustal boundaries, usually the Early Paleozoic terrane sutures (Ramos and Kay, 1991). Examples of these systems are the Mercedario Rift System in La Ramada Basins and La Valenciana – Río Atuel, Alvarado, Nieves Negras and Yeguas Muertas depocenters in the Mendoza – Aconcagua Basin, along the High Andes (Figure 1).

Basin infill of the different rifts share a common history, mainly controlled by eustatic sea level changes and tectonics events.

LA RAMADA BASIN

La Ramada is a composite basin that begun in the Late Triassic to Early Jurassic as a rift depocenter isolated from the main Andes of Argentina and Chile and continued during early Cretaceous time as a retroarc basin. An important topographic high, present from the Triassic to mid Jurassic, separated the La Ramada basin from the Mendoza – Neuquén basin to the south (Alvarez and Ramos, 1997).

The initial infill is exposed in a series of half –grabens, controlled by west-dipping normal faults. The highly variable thickness of the Rancho de Lata Formation (Late Triassic) is interpreted as indicative of synrift

facies. Above this break-up unconformity, a sequence of shales and sandstones of Los Patillos Formation (Early to Middle Jurassic), with tabular development, overstep the different grabens, without being affected by the normal faulting. The La Manga Formation limestones cover this sequence.

Two cycles have been identified within the thermal sag phase. The lower one corresponds to early sag, where the marine sequences of Los Patillos Formation developed within the initial generalized subsidence. The relationship between both sag sequences is characterized by a coastal onlap. The jurassic sequence ends with gypsum deposits of the Auquilco Formation (Late Oxfordian – Kimmeridgian). A new extensional cycle began with the continental red beds of Tordillo Fomation. These continental deposits are related to a synrift stage and the thermal subsidence is linked to development of a Tithonian – Early Neocomian carbonate platform.

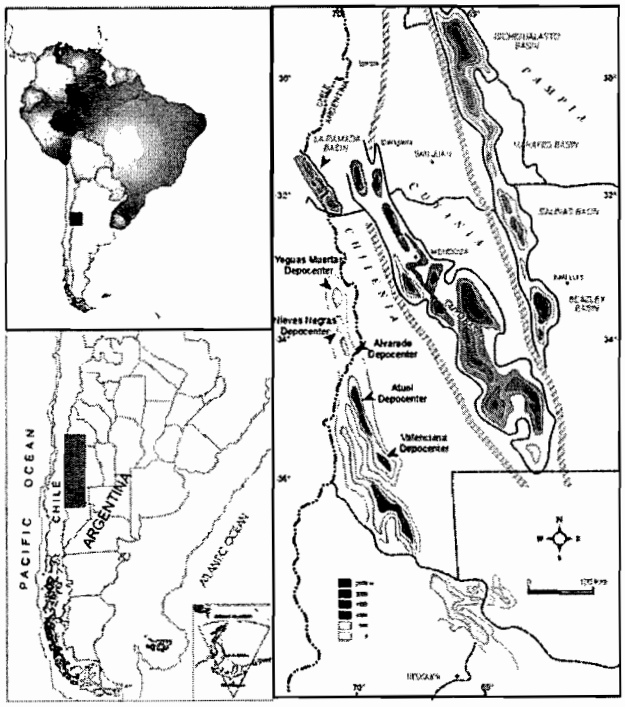

Figure 1: Location of the episutural Ramada and northern Neuquén Triassic depocenters, treated in this paper.

ACONCAGUA BASIN

In the Nieves Negras, Alvarado and Yeguas Muertas depocentres, located in the northern Neuquén basin, rifting may also have begun in the Late Triassic, though field evidence is lacking (Giambiagi et al., 2002). Their sag phase is reflected by the deposition of thick Middle Jurassic black shales outcropping in the three depocenters, the Nieves Negras Formation (Alvarez et al., 2000). This unit is characterized by 450 meters of black shales first interbedded with fine and medium sandstones and then with both thin and nodular mudstones. During the Middle and Late Callovian the basin was completely desiccated due to a rapid relative sea level fall and some tens of metres of evaporites, referred to as the Tábanos Formation, were deposited.

A new extension phase was developed between 32°30′ and 34° S.L. towards the Middle Jurassic. It is recorded south of Mount Aconcagua by normal faults that enclose the synrift Lotena Formation deposits. Thickness of its coarse conglomerates, sandstones and siltstones is highly variable (10 to 400 meters).

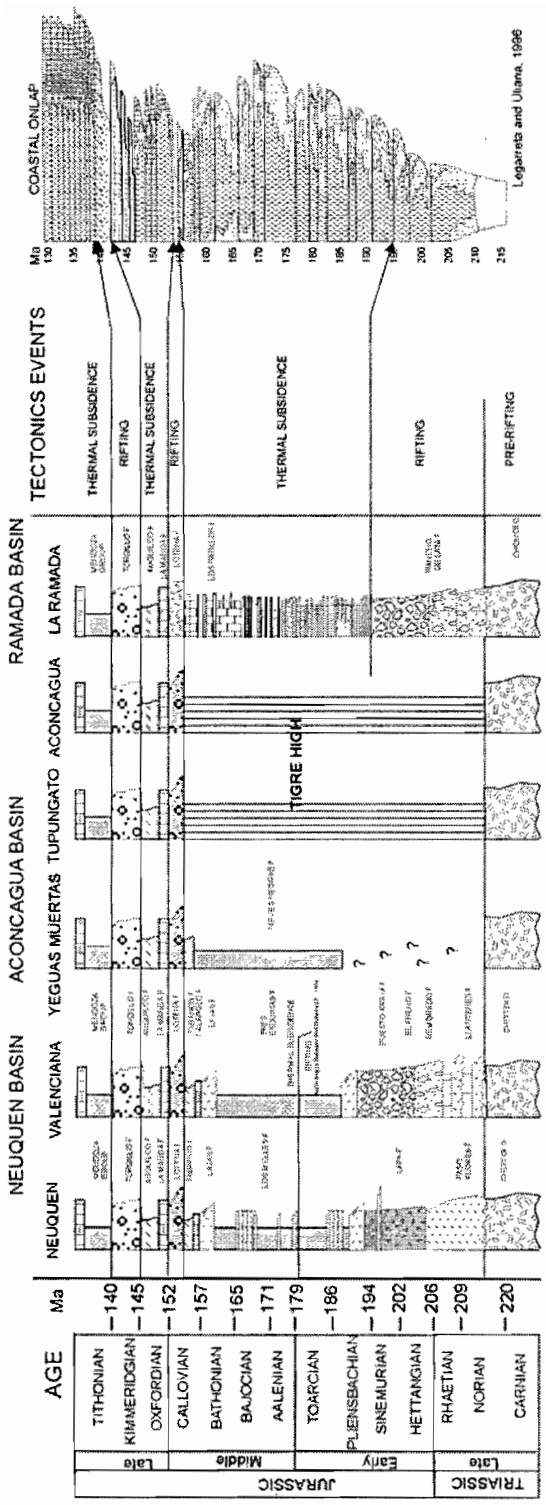

Figure 2. Correlation between different depocenters and Neuquén basin onlap curve

The La Manga Formation carbonate platform paraconcordantly overlies these deposits in such a way that the Alto del Tigre (Fig. 29) is covered and all the Late Jurassic depocenters were connected. During the Late Oxfordian to Early Kimmeridgian a new important sea level fall event is represented by the evaporites of Auquilco Formation.

A similar development as in the La Ramada basin is observed in this area: thick sequences of red conglomerates, sandstones and shales of the Tordillo Formation were deposited in half-grabens. Thickness of these continental sequences is highly variable, between 100 to more than 1000 metres. This synrift characteristic has, however, been related to sea level fall in the Neuquén Basin.

After deposition of the Tordillo Formation, the Mendoza Group represents flooding of the basin related to a new thermal subsidence during the Early Tithonian – Neocomian. It consists of three lithostratigraphic units: fetid black shales bearing levels of calcareous nodules with abundant nektonic fauna, the Vaca Muerta Formation, corresponding to offshore - basinal environment. This unit is followed by bioturbated packstones of big oysters, first interbedded with wackestones: the Chachao and Agrio Formations. These sequences represent a shallow platform environment.(Aguirre-Urreta and Alvarez, 1998).

CONCLUSIONS

Stratigraphic boundaries that have been interpreted as eustatic sea level changes in the central argentinian-chilean Triassic to Jurassic basins seems to be generated by other processes. Coastal onlap may be caused by downwarp of extensional continental margins, while relative sea level falls could be caused by thermal doming of accompanying rifting (Figure2).

The Triassic Jurassic basins of the High Andes of Argentina and Chile were affected by an extensional tectonic regime during de Mesozoic and many of the sequences-boundary events and stratigraphic architectures are now interpreted in terms of local or regional episodes of extensional faulting and thermal subsidence. These episodes are:

- 210 Ma Rifting and halfgraben formation associated with the breakup of Pangea
- 210 to 195 Ma Renewed extension and synrift deposits
- 195 to 155 Ma Thermal subsidence associated with eustatic changes that controlled the sedimentary infill
- 155 to 153 Ma New extensional event and synrift deposits
- 153 to 141 Ma Generalized thermal subsidence, all depocenters were connected
- 141 to 139 Ma Extension and synrift deposits
- 139 to 129 Ma Thermal subsidence and sag facies

ACKNOWLEGDEMENT: Partial founding was provided by PICT 07-06729.

REFERENCES

Aguirre – Urreta M.B. and Alvarez P. P., 1998. Late Jurassic stratigraphy of the High Andes of Argentina and Chile (34 S). 5th International Symposium on the Jurassic System, Abstracts:2, Vancouver.Alvarez, P. P. and Ramos V. A., 1999. The Mercedario rift system in the Principal Cordillera of Argentina and Chile (32° SL). J. South Am. Ear. Sc., 12: 17-31.

Giambiagi L., Alvarez P., Godoy E., and Ramos V.,2002. The control of pre-existing extensional structures in the development of the southern sector of the Aconcagua fold and thrust belt, Chile and Argentina. Tectonophysics (in press).

Ramos, V. A. and Kay S. M., 1991. Triassic rifting and associated basalts in the Cuyo basin, central Argentina. En R. S. Harmon y C. W. Rapela (Eds.): Andean magmatism and its tectonic setting. Geol. Soc. Am., Spec. Pap., 265: 79-91.

STRUCTURE OF THE PRECORDILLERA ALONG THE 30° LATITUDE CROSS-SECTION (JACHAL RIVER, NW ARGENTINA)

Joaquina ALVAREZ-MARRON(1), Roberto RODRIGUEZ-FERNANDEZ(2), Nemesio HEREDIA(2), Pere BUSQUETS(3) and Ferran COLOMBO(3)

1. Instituto de Ciencias de la Tierra, CSIC, Barcelona.
2. Instituo Geológico Minero de España, Madrid.
3. Universidad de Barcelona.

KEY WORDS: Paleozoic thrust systems, Cenozoic overprint, Andean Precordillera

INTRODUCTION

The Argentine Precordillera that corresponds to the foothills of the 29°-33° S segment of the Andes, forms a N-S mountain chain, bounded in the west and east by active large Cenozoic basins. The western basin covers the structural boundary between the Precordillera and the Cordillera Frontal. In the east, the foreland basin includes large Proterozoic basement uplifts of Sierras Pampeanas (Ramos, 1988). At 30° latitude, the Precordillera includes an E-verging set of mostly emergent thrust faults that carry Paleozoic and younger cover rocks (Almendinger et al., 1990). Synorogenic Tertiary deposits indicate that major E-verging thrusts moved between about 20 Ma ago and present (Jordan et al. 1993). In addition, the Precordillera registers a Paleozoic compressional deformation event that resulted in faulting and folding of Early Paleozoic sedimentary strata [Gossen, 1994].

Along a 50 km wide band centered at 30° S latitude the morphology of the Precordillera is dominated by rhomb-shaped domains that form ridges and depressions. The ridges show outcrops of Paleozoic age strata and the depressions form intermontane basins of different dimensions that are filled by Cenozoic age strata. Along most of the ridge slopes and depressions there appear large active Quaternary alluvial fans that continue to efficiently fill the lower topographic areas. The deeply incised valley of the Jachal River that runs perpendicular to the strike of the Andean foothills, offers a complete section of the Precordillera (30° latitude) that is very well exposed in an almost continuous 50 km long section. A field-based study has been carried out aided by 1:50.000 scale aerial photographs, TM satellite images and available 1:250,000 scale geological maps of the Argentinean Geological Survey (SEGEMAR) [Cardo, in press; Gonzalez, in press]. The main objective was to produce a complete geological cross-section across the Precordillera that depicts the structural style of Paleozoic deformation and to distinguish this from later Cenozoic structures.

CONCLUSIONS

Along a W-E cross-section of the Precordillera at 30° S latitude two major sets of structures reveal the different deformation styles that were superposed through time during the Paleozoic to present tectonic evolution of this sector of the Andes.

1) A Paleozoic age E-verging thrust stack consisting of three main thrust units that exhibit important variation in structural style and stratigraphy, that may be due to large horizontal displacements. The thrust wedge includes, a) the Western Allothton at the rear that consists mostly of clastic Ordovician age rocks folded by large-scale asymmetric, E-verging folds with a well-developed axial planar cleavage and very low-grade metamorphism, b) the Central Imbricate deforms mostly Siluro-Devonian rocks in a system of imbricate E-verging thrusts that merge into a detachment near the base of Ordovician carbonates and include associated fault propagation folds, c) the Paleozoic deformation in the Frontal Unit possibly consisted in a protothrust structure at the core of an open anticline.

2) A Cenozoic set of steep thrust faults with a probabilly component of left lateral along strike displacement is responsible for the characteristic morphology of rhomb-shaped domains. The steep faults have uplifted and breached through the previous thrust wedge and have associated intramontane basins. The intramontane basins on top of the Western Allochton and Central Imbricate appear along N-S trending valleys and include Tertiary to Quaternary sediments that unconformably onlap onto the Paleozoic rocks of the highest topographic borders. In some cases, reactivation of Paleozoic thrust faults resulted in overthrusting of the younger sediments and in other cases progressive unconformities are developed due to continuous uplift at the unconformable contact. Cenozoic faults have also caused passive block rotations of Paleozoic structures.

REFERENCES

Allmendinger, R. W., Figueroa, D., Snyder, D., Beer, J., Mpodozis, C., and Isacks, B. L., 1990, Foreland shortening and crustal balancing in the Andesat 30 degrees S latitude: Tectonics, v. 9, no. 4, p. 789-809.

Cardo R., in press. Carta Geológica 3169-I Rodeo, escala 1:250.000. Instituto de Geología y Recursos Minerales, Subsecretaría de Mineria, SEGEMAR. Republica Argentina

Gonzalez P., in press. Carta Geológica 3169-II San José de Jachal, escala 1:250.000. Instituto de Geología y Recursos Minerales, Subsecretaría de Mineria, SEGEMAR. República Argentina

Gosen W. von, 1997. Early Paleozoic and Andean structural evolution in the Rio Jachal section of the Argentine Precordillera. J. South Am. Earth Sci., 10 (5-6), 361-388.

Jordan, T. E., Allmendinger, R. W., Damanti, J. F., and Drake, R. E., 1993, Chronology of motion in a complete thrust belt; the Precordillera, 30-31 degrees S, Andes Mountains: Journal of Geology, v. 101, no. 2, p. 135-156.

Ramos, V. A., 1988. The tectonics of the Central Andes; 30° to 33° S latitude. In: Processes in Continental Litospheric Deformation, S. Clark and D. Burchfiel (Eds.). Geol. Soc. Amer., Spec. Paper, 218, 31-5

MID-CRETACEOUS CRUSTAL SHORTENING, UPLIFT AND EXHUMATION: EVIDENCE FROM A REGIONAL-SCALE DUCTILE SHEAR ZONE IN THE COASTAL RANGE OF CENTRAL CHILE (32°S)

Gloria ARANCIBIA (1)

(1) Departamento de Geología . Universidad de Chile. Casilla 13518, Correo 21, Santiago, Chile. (gloarancibia@123.cl)

KEYWORDS: Mid-Cretaceous crustal shortening, shear zone, Coastal Range, central Chile

INTRODUCTION

Previous studies indicate a complex tectonic evolution of the Coastal Range of Central Chile during the Cretaceous. The following regional tectono-magmatic events have been documented between the 27° and 33°S: 1) Widespread volcanism associated with extensional volcanosedimetary intra-arc or back-arc basins developed during the Lower Cretaceous (*e.g.* Vergara *et al.*, 1995); 2) an extensive very low-grade metamorphism, coeval with basins closure (*ca.* 93-94 Ma), which affected the Upper Jurassic and Lower Cretaceous stratified rocks (*e.g.* Aguirre *et al.*, 1999); and 3) the first stages of the Coastal Range formation and uplift during mid-Cretaceous, associated with a marked increase in the exhumation/erosion rate (*e.g.* Vergara *et al.*, 1995; Parada and Larrondo, 1999; Gana and Zentilli, 2000). These three events indicate a major change from a mainly extensional tectonic regime, associated with Lower Cretaceous volcanism, to contractional regime associated with the closure of the Lower Cretaceous basins, uplift, and increase of the exhumation/erosion rate in the Coastal Range during mid Cretaceous time. However, no Cretaceous contractional shear zones compatible with crustal shortening have been documented to date. In this study, we first document a regional-scale, reverse ductile shear zone (the Silla del Gobernador Shear Zone, SGSZ), whose geometry, kinematics and timing are consistent with mid-Cretaceous crustal shortening.

THE SILLA DEL GOBERNADOR SHEAR ZONE (SGSZ)

The SGSZ is a NNE-striking shear zone located in the western border of the present-day Coastal Range in central Chile (Fig. 1). This shear zone consists of: (a) NS-striking micaceous mylonite belts with moderately-

dipping foliation to east, subvertical mineral/stretching lineation and reverse-slip kinematic indicators; and (b) NE-striking cataclastic belts with subvertical foliation and oblique lineations (striae) with dextral-reverse and reverse-dextral kinematic indicators. Mylonitic and cataclastic fabrics are consistent with a regional transpressive regime (predominantly reverse) resulting from EW to NWW shortening; with a small dextral shear component. Thermodynamic and microstructural data indicate deformation temperatures between 300° and 400°C. Mesoscopic fabric and microstructure are strongly controlled by the protolith rheology. The best estimate for the absolute age of mylonitic deformation, obtained through *in situ* ^{40}Ar-^{39}Ar laser ablation on neophormed micas from high strain mylonites zones, is 108 ± 12 Ma (Arancibia, 2002) (Fig. 1).

DISCUSSION AND CONCLUSIONS

The increase in the erosion rate during mid-Cretaceous times is based on the presence of Upper Cretaceous coarse grain deposits, interpreted as a consequence of fast erosion rates of the Jurassic to Cretacic volcanosedimetary units (*e.g.* Las Chilcas Formation, Vergara *et al.,* 1995). This event is coeval with a fast exhumation (fission track ages) of the Paleozoic, Jurassic and Lower Cretaceous plutons forming the bedrock of the Coastal Range between the 27° to 34°S. These data suggest that the plutonic rocks crossed the 80°-125°C zone at 110-90 Ma ago (Parada and Larrondo, 1999; Gana and Zentilli, 2000). Pre-Cretaceous plutonic rocks, in turn, were probably located at a shallow crustal level as far back as the Middle Jurassic.

The increase in the erosion/exhumation rates documented for the mid-Cretaceous can be interpreted as coeval with the onset of uplift of the Coastal Range (*e.g.* Gana and Zentilli, 2000). This also is compatible with a major change from a predominantly extensional regime in which the Lower Cretaceous basins opened (Fig. 2a), to another more compressional regime coeval with the closure of these basins and the peak of the very low-grade metamorphism which affected the Lower Cretaceous rocks (Fig. 2b). The ^{40}Ar-^{39}Ar age of 108 ± 12 Ma, the calculated 300 - 400°C deformation temperature and the geometry and kinematics of the ZFSG, suggest that the increase in the erosion/exhumation rates is coeval with crustal shortening and uplift during this time and is a clear evidence of a switch on the regional tectonic regime (Fig. 2b).

ACKNOWLEDGMENTS

This work is part of the author Ph.D. Thesis and was funded by a FONDECYT PROJECT 2000011 and a CONICYT Scholarship. Reynaldo Charrier (University of Chile) is thanked for field work and discussions.

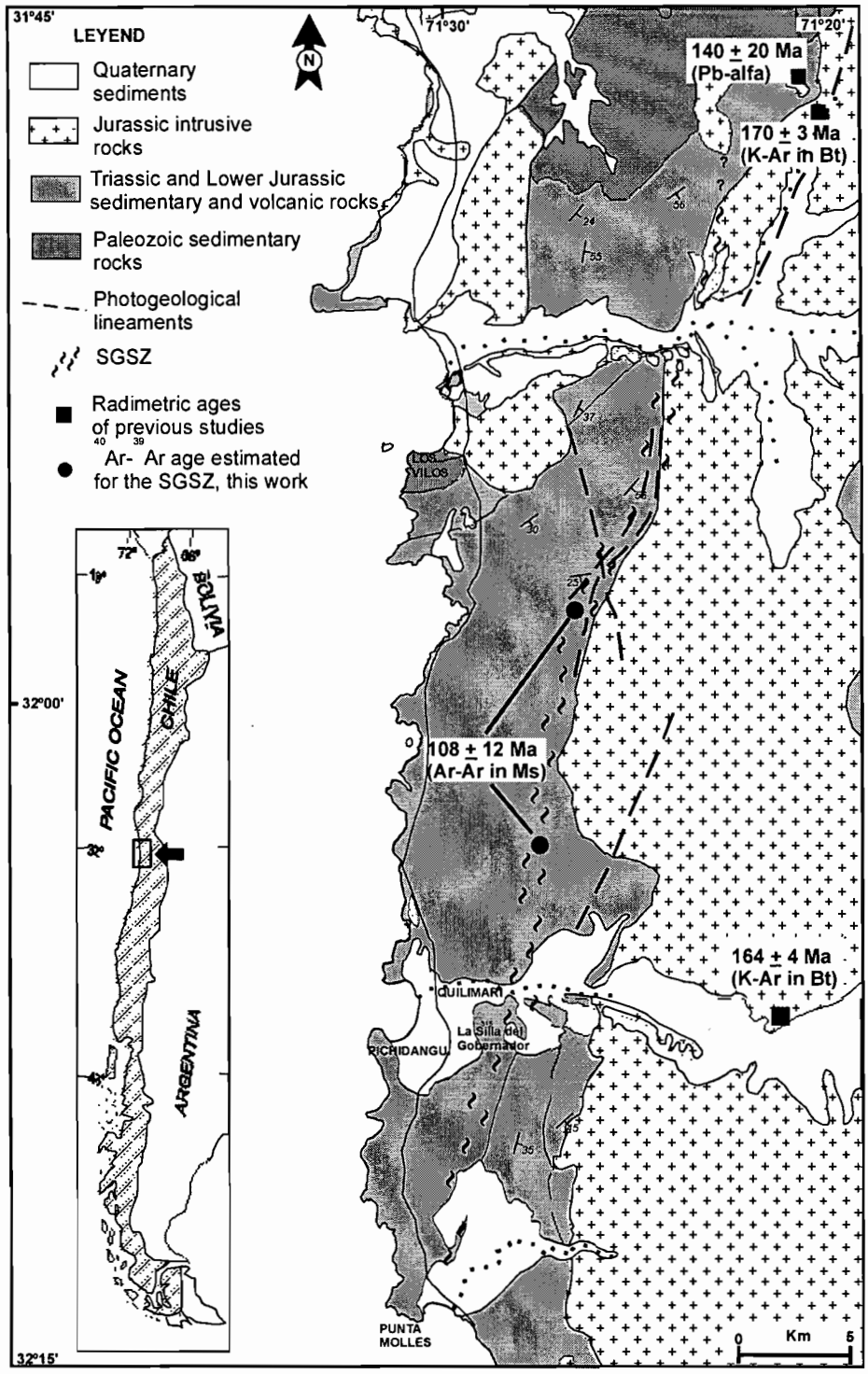

Figure 1. Simplified geological map of the Silla del Gobernador Shear Zone (SGSZ) (modified from Rivano *et al.*, 1993) and location of study area (lower-left).

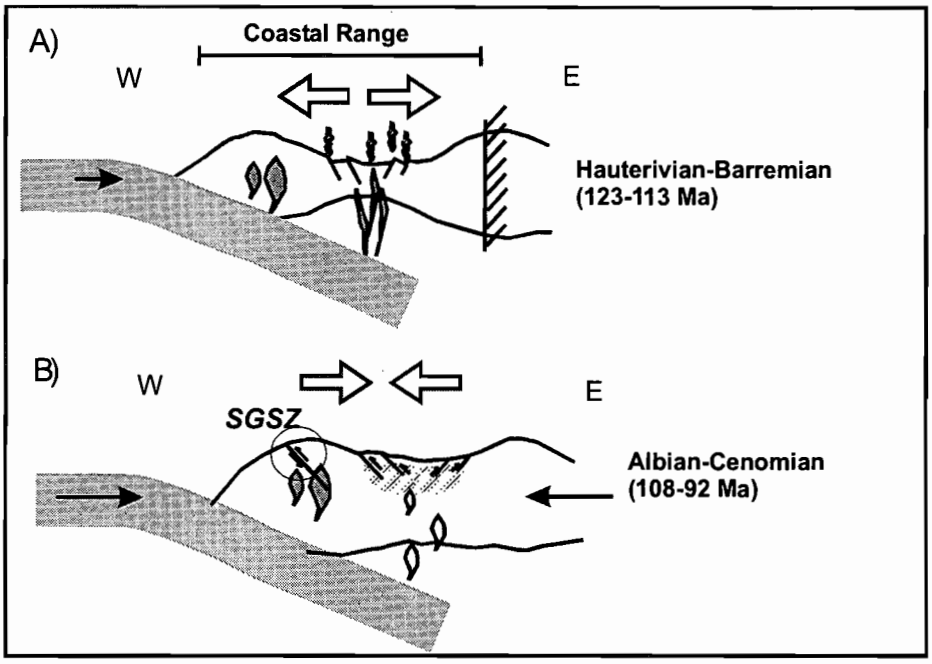

Figure 2. Schematic tectonic W-E section in the Coastal Range at 32°S. A) Predominantly extensional in which the Lower Cretaceous basins were opened (123-113 Ma). B) More compressional regime with the closure of these basins and the peak of the very low grade metamorphism (108-92 Ma) SGSZ suggest that the increase in the erosion/exhumation rates is coeval with crustal shortening uplift during middle Cretaceous and is a clear evidence of a switch on the regional tectonic.

REFERENCES

Aguirre, L., Fëraud, G., Morata, D., Vergara, M., Robinson, D. 1999. Time interval between volcanism and burial metamorphism and rate of basin subsidence in a Cretaceous Andean extensional setting. Tectonophysics, 313: 433-447.

Arancibia, G. 2002. Geometría, cinemática, condiciones y edad de la deformación milonítica en rocas volcánicas. El caso de la Zona de Falla Silla del Gobernador, Chile central (32°S). Unpublished Ph.D. Thesis, Departamento de Geología, Universidad de Chile.

Gana, P., and Zentilli, M. 2000. Historia termal y exhumación de intrusivos de la Cordillera de la Costa de Chile central. In: IX Congreso Geológico Chileno, 2: 664-668.

Parada, M., and Larrondo, P. 1999. Thermochronology of the Lower Cretaceous Caleu Pluton in the coast range of central Chile: Tectonostratigraphic implications. In: 4th ISAG, Göttingen, Germany, 563-566.

Rivano, S., sepúlveda, P., Boric, R., Espiñeira, D. 1993. Hojas Quillota y Portillo, Servicio Nacional de Geología y Minería, escala 1:250.000.

Vergara, M., Levi, B., Nyström, J., Cancino, A. 1995. Jurassic and Early Cretaceous island arc volcanism, extension, and subsidence in the Coast Range of central Chile. Geological Society of America Bulletin, 107 (12): 1427-1440.

TABULAR PLUTONS FROM THE COASTAL CORDILLERA OF COPIAPÓ-VALLENAR (27°00´-28°30 S) AND AN APPROACH TO THEIR EMPLACEMENT MECHANISMS, ATACAMA REGION, CHILE

Carlos AREVALO (1), John GROCOTT (2), Justiniano VALENZUELA, (1) and Daniela WELKNER (1)

(1) SERNAGEOMIN. Av. Santa María 0104. Santiago. Chile (carevalo@sernageomin.cl)
(2) KINGSTON UNIVERSITY. Kingston-upon-Thames. Surrey KT1 2EE. UK (j.grocott@kingston.ac.uk)

KEY WORDS: Coastal Cordillera of Atacama, tabular plutons, roof-uplift, floor-depression, feeding dykes

INTRODUCTION

Traditional methods like mapping and geochronology have been applied to the Andean Orogen over the last two decades allowing the recognition that in much of the chain an eastward migration of the magmatic focus took place (Zentilli 1974, Brook *et al.* 1986, Dallmayer 1996). In the case of the Mesozoic of Northern Chile, volcanic arcs were abandoned and uplifted allowing erosion to act and expose the plutonic roots. Whereas the study of the volcanic products of the Cenozoic modern chain permits indirect inferences about the lithospheric processes, the eroded roots of the Mesozoic arcs offer a unique opportunity to study, in the field, the processes of arc building, emplacement of magmas and their interaction with deformation and the associated processes of mineralisation. Progress made recently in the Coastal Cordillera of Taltal-Chañaral have focused the attention into the plutons themselves and their relationships with contemporary structural systems (Grocott & Wilson 1997, Wilson 1998, Wilson & Grocott 1999, Grocott & Taylor in press). These works have interpreted the plutons as tabular bodies and inferred for them roof-uplift and floor-depression emplacement mechanisms. The present contribution present some of the most relevant results of our current research, within a 130 km N-S segment of the Coastal Cordillera immediately south of Chañaral between Copiapó and Vallenar (Fig. 1), which are consistent which are consistent with findings made in the north. Current works will incorporate gravimetry and AMS studies to reach a general model for the construction of the Coastal Batholith.

REGIONAL SETTING

In the Atacama Region, the magmatic ascent during the Mesozoic was mainly focused in the current coastal range building up a multiplutonic complex that intruded a Devonian-Carboniferous basement and its related volcanic products. This complex constitutes a morphotectonic unit which is denominated Coastal Cordillera by analogy with the southern (south of 33° S) and northern counterpart (north of 27° S) where a well defined Central Valley separates it from the western ranges of the main Cordillera (Jordan *et al.* 1983, Mpodozis & Ramos 1990). The mainly sedimentary Mesozoic back-arc elements extend to the east of the Coastal Cordillera as single basins or as systems of interconnected basins, resting on a Carboniferous to Triassic basement as far as the current Chilean-Argentinean border.

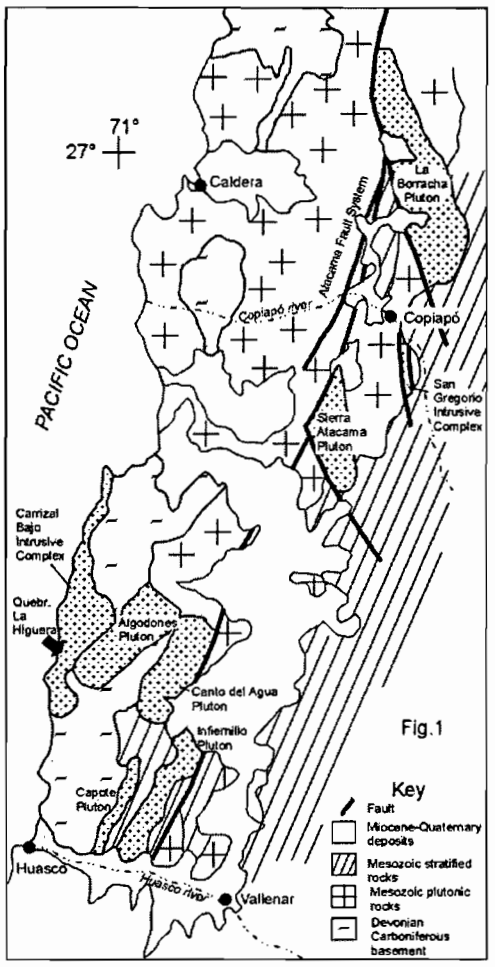

PLUTONS FROM THE COPIAPO-VALLENAR AREA

(1) Three types of plutons have been recognised so far in the Coastal Cordillera of the Copiapó-Vallenar region: Multilayered mylonite bounded plutons

These plutons have parallelogram-shaped outcrops determined by the existence of syn-emplacement planar structural features. Straight borders are generally defined by one NNE-trending, sub-vertical and syn-plutonic mylonitic margin, often coinciding with a branch of the Atacama Fault System (Brown *et al.* 1993), and by other NW straight border interpreted as syn-plutonic fault (Grocott & Taylor in press). Outside non-structural borders, where layered wall rocks are well exposed, outward-dipping homoclines are often visible. Outliers of volcanic and volcaniclastic rocks in the roofs show that they are flat to gently-dipping and generally concordant. The existence of locally transgressive contacts suggest us the presence, although still unproven, of low-angle, country-rock faulting. The floors are generally unexposed. However unique outcrops at the base of the Carrizal Bajo Plutonic Complex (Welkner & Arévalo 2002) imply shallow bottom surfaces. The plutons are composite bodies internally formed by two o more distinctive, flat-lyingintrusive layers. Contacts between them are sharp, planar and generally parallel to each other and to the roof where it is exposed. Examples of these intrusives (Fig. 1) are the Infiernillo pluton (130 Ma; Gipson in prep., Valenzuela 2002), San Gregorio Intrusive Complex (111 Ma; Arévalo 1999), the La Borracha pluton (107-104 Ma, Dallmayer 1996) and the Carrizal Bajo Intrusive Complex (243-208 Ma, Welkner & Arévalo 2002).

(2) Single-layered, mylonite bounded plutons

The plutons have subvertical rounded walls. They have elliptical to semi-elliptical outcrops with NE to NNE long axes. Often, specially where the walls juxtapose the plutonic rocks with sedimentary or volcanic panels, mylonitised shear zones are developed. No clear outliers of countryrock at the top of the plutons are exposed indicating erosion of most of the intrusive roofs. The Canto del Agua dioritic pluton exposes at its eastern border panels of older shallowly dipping, hornfelsified-andesitic rocks as remains of flat-lying roof. The plutons are internally homogeneous suggesting that they are probably formed by only one single layer although the possibility of erosion of other facies cannot be ruled out. Examples of these intrusives are the Algodones pluton (197-192 Ma, Arévalo & Welkner in prep.), the Sierra Atacama pluton (111-104 Ma, Arévalo in prep.) and the Canto del Agua pluton (155-150 Ma; Arévalo & Welkner in prep.).

(3) Single-layered plutons unrelated to mylonites

These correspond to minor scale, single layer intrusives with well defined floors and roofs, steep sides and no mylonitic envelopes. Generally they are emplaced within flat lying surfaces like basement-cover interfaces (Capote pluton, 189 Ma; Valenzuela 2002) or internal sedimentary contacts (Los Puntudos diorite; Arévalo & Welkner in prep.).

3-D GEOMETRY AND AN APPROACH TO EMPLACEMENT MECHANISMS

No research has been done so far to determine the geometry in depth of these plutons. However. characteristics such as shallow-dipping roofs, steep sides, flat lying internal interfaces between plutonic layers and shallow plutonic floors are all consistent with flat-lying tabular pluton geometry (Vigneresse 1995, Cruden 1998). In the case of the multilayered plutons the pluton-down sense of shear indicators within synplutonic mylonitic rocks in the walls and down-warping of primary structures in the host rocks toward the mylonitic envelop and the pluton are consistent and imply a floor depression emplacement mechanism. The presence of outward dipping homoclines in well layered country rock around these plutons is somehow inconsistent with the latter mechanism. Although it is a matter of current research two explanations are possible: (1) vertical bending of the upper plutonic layers as a result of an upward doming of the pluton roof due to a drop in the space-creation rate producing a subsequent rising in the magma pressure or (2) syn/late stage tectonic folding. Cruden (1998) evaluated the mechanisms by which Cordilleran plutons depressed their floors utilising two possible end models: the cantilever and the piston model which differ in the existence of vertical shear within one single wall (cantilever) or all around the pluton border (piston). In the light of the evidence given the multilayered plutons were emplaced mostly through the operation of the Cantilever mode of floor depression. In the case of single layered intrusives, the pluton-up sense of shear within mylonitised walls and the existence of open synclines outside and parallel to plutonic margins imply emplacement via roof-uplift for most of them. Explanations for the absence of layering exhibited by the pluton types 2 and 3 are matters for further research. One possibility could invoque the tendency of magma to favour lateral propagation to create single sheets rather than layered complexes in a scenario of increasing overburden thickness (Roman-Berdiel *et al.* 1995). On the other hand, removal of putative upper layers by erosion should not be discarded. This latter case seems to be the situation of the San Gregorio Intrusive Complex where complete panels of a shallow layers have been removed by erosion during inflation of a deeper layer via dip-slip of bounding faults

DYKE ASCENT OF MAGMAS

Dykes are well known as the most efficient way to feed upper crustal plutons (Petford 1996). In the Copiapó-Vallenar zone dykes of basic to intermediate composition cross cut the intrusives and their hosting rocks throughout the region. However places where demonstrable spatial linkages between tabular bodies and vertical dykes are scarce. One exceptional place is Quebrada La Higuera (Fig. 1) where deep incision of the valley allows to see a complete section of the Carrizal Bajo Intrusive Complex. Along this valley a stack of four compositionally distinct plutonic sheets are exposed. Interfaces between each layer are defined by sharp contacts or by horizon of intrusion breccias (Welkner & Arévalo 2002). The lower most sheet is a homogeneous diorite exposed throughout on a marine terrace. La Higuera valley has deeply eroded this terrace exposing at the base of the dioritic layer windows of strongly deformed biotite schists from a Permo-Triassic basement cross cut by a

pervasive andesitic to dacitic dyke swarm. The absence of these minor intrusives in the upper plate implies that the dykes expanded upward to feed the horizontal body. Additionally the existence of vertical shear surfaces parallel to the dykes and ductile shear bands as dyke walls indicate that some of these bodies also acted as structurally active channels to feed and to eventually create space for the upper layers.

CONCLUSIONS

In the Copiapó-Vallenar region three type of plutons have been identified: multilayered mylonite bounded plutons, single layered mylonite bounded plutons and single-layered plutons unrelated to mylonites,

(1) Characteristics such as shallow dipping roofs, flat lying internal interface between layers and shallow plutonic floors are consistent with flat-lying tabular geometry,
(2) The tabular character and the existence of marginal, synplutonic, dip-slip ductile shear zones, implies that the intrusions were emplaced by roof-uplift or floor-depression,
(3) Clear evidence of dyke ascent of magma is exposed at the Quebrada La Higuera.

REFERENCES

Arévalo, C. & Welkner, D. in prep. Mapa Geológico del sector Carrizal Bajo-Chacritas, Región de Atacama: Servicio Nacional de Geología y Minería (Chile). Mapas Geológicos. Escala 1:100.000.

Arévalo, C. 1999. *The Coastal Cordillera/ Precordillera boundary in the Tierra Amarilla Area (27°20'-27°40'S/70°05'-70°20'W), Northern Chile, and the structural setting of the Candelaria Cu-Au ore deposit.* PhD Thesis, Kingston University, Kingston-upon -Thames, U.K.

Arévalo, C. in prep. Mapa Geológico de la Hoja Copiapó: Región de Atacama. Servicio Nacional de Geología y Minería.

Brook, M., Pankhurst, R.J., Shephard, T.J. & Spiro, B. 1986. ANDCHRON; Andean geochronology and metallogenesis. *Overseas Development Agency Open-file Report*, 1-83.

Brown, M., Díaz, F. & Grocott, J. 1993. Displacement History of the Atacama Fault System, 25°00'S 27°00'S, Northern Chile. *Geological Society of America Bulletin*, **105**, 1165-1174.

Cruden, A.R. 1998. On the emplacement of tabular granites. *Journal of the Geological Society,* **154**, 853-862.

Dallmeyer, D., Brown, M., Grocott, J., Taylor, G.K. & Treloar, P. 1996. Mesozoic Magmatic and Tectonic Events Within the Andean Plate Boundary Zone, 26°-27°30', North Chile: Constraints from $^{40}Ar/^{39}Ar$ Mineral Ages. *Journal of Geology*, **104**, 19-40.

Gipson, M. in prep. PhD Thesis, University of Plymouth, Plymouth, U.K.

Grocott, J. & Taylor, G. in press. Deformation partitioning, magmatic arc fault systems and emplacement of granitic complex in the Coastal Cordillera, north Chilean Andes (25°30´S to 27°00´S). *Journal of the Geological Society.*

Grocott, J. & Wilson, J. 1997. Ascent and emplacement of granitic plutonic complexes in subduction-related extensional environments. *In:* HOLNESS, M.B. (ed) *Deformation-enhanced fluid transport in the Earth's crust and mantle.* Chapman & Hall, London, 173-195.

Jordan, T.E., Isack, B., Allmendinger, R., Brewer, J., Ramos, V. & Ando, C. 1983. Andean tectonics related to geometry of subducted Nazca plates. Geological Society of America Bulletin, **94**, 341-461.

Mpodozis, C. & Ramos, V. 1989. The Andes of Chile and Argentina. *In:* ERICKSEN, G.E., CAÑAS-PINOCHET, M.T. & REINEMUND, J.A. (eds) *Geology of the Andes and its relationship to hydrocarbon and mineral resources.* Circum-Pacific Council for Energy and Mineral Resources Earth Science Series, **11**, Houston, 59-90.

Petford, N. 1996. Dykes or diapers ? Transactions of the royal Society of Edimburgh, **87**, 105-114.

Roman-Berdiel, T., Gapais, D. & Brun, J.P. 1995. Analogue models of laccolith formation. *Journal of Structural Geology*, 16, 447-466.

Valenzuela, J. 2002. Caracterización, geocronología y mecanismos de emplazamiento del Batolito de la Costa a la latitud de Vallenar (28°22´-28°41´ Lat.S y 70°45´-71°7´ Long. W), III Región, Chile. Memoria de Título, Universidad de Concepción.

Vigneresse, J.L. 1995. Control of granite emplacement by regional deformation. *Tectonophysics*, **249**, 173-186.

Welkner D. & Arévalo C. 2002. The Carrizal Bajo Breccias: indications of contemporaneity between two end member magmas in a Late Triassic Extensional setting, Costal Cordillera, northern Chile (27°45/28°20 S).

Wilson J. & Grocott, 1999. The emplacement of the Las Tazas complex, northern Chile: the relationship between local and regional strain. *Journal of Structural Geology*, **21**, 1513-1523.

Wilson, J. 1998. Magnetic suscetibility patterns in a Cordilleran granitoid: The Las Tazas complex, northern Chile. *Journal of Geophisical Research*, **103**, 5257-5267.

Zentilli, M. 1974. Geological evolution and metallogenic relationships in the Andes of Northern Chile between 26° and 29°. PhD Thesis Queen's University, Kingston, Canada.

CRETACEOUS TO PALEOGENE COMPRESSIONAL TECTONICS DURING DEPOSITION OF THE PURILACTIS GROUP, SALAR DE ATACAMA

César ARRIAGADA (1), Peter COBBOLD (2), Constantino MPODOZIS (3) and Pierrick ROPERCH (4).

(1) Departamento de Geología, IRD, Universidad de Chile, Santiago, Chile.(cearriag@cec.uchile.cl)
(2) Géosciences-Rennes (UMR6118 du CNRS), 35042 Rennes, France.(cobbold@univ-rennes1.fr)
(3) SIPETROL, Santiago, Chile.(constantino.mpodozis@sipetrol.cl)
(4) Departamento de Geología, IRD, Universidad de Chile, Santiago, Chile.(properch@dgf.uchile.cl)

KEY WORDS: Purilactis Group, Salar de Atacama, compressional tectonics, growth strata.

INTRODUCTION

On the western edge of the Salar de Atacama, continental deposits of the Purilactis Group, mid Cretaceous to Eocene-Oligocene in age, are up to 5 km thick (Mpodozis et al., 1999) (Fig. 1). Deposition is generally assumed to have occurred during extensional tectonics, in an arc or back-arc setting, even if syn-sedimentary extensional faults have not been described (Hartley et al., 1992; Flint et al., 1993; Charrier and Reutter, 1994). Similarly, uncomformably overlying Oligo-Miocene sequences have been attributed to a stage of relaxation, following Late Eocene compressional tectonics (Götze et al., in press). Here we discuss new evidence for deposition of the Purilactis Group in a context of compressional tectonics, during uplift and eastward overthrusting of Cordillera Domeyko.

EVIDENCE FOR A COMPRESSIONAL CONTEXT

In the northern part of the area, on the western limb of the large cylindrical Barros Arana syncline (Fig. 1), a westward-verging back-thrust has detached the Purilactis Formation (in the hanging wall) from evaporites of the Tonel Formation (in the footwall). The back-thrust can be traced all along the El Bordo escarpment (Fig. 1). In the central part of the area (Cerro Quimal, Fig. 1), the syncline becomes tighter, adopting a chevron style, and its axial plane dips westward. In the footwall of the detachment between Purilactis and Tonel formations is an anticline, overturned to the E (Fig. 2a). About 1 km to the SE, a syncline and adjacent anticline mark the lower part of the Tonel Formation (Fig. 2b), whereas no folds are visible in the upper part. Another 5 km to the S, the basal section of the Tonel Formation shows growth strata. These were deposited over pre-growth strata, which form kink folds (Fig.2c).

Further S, on the eastern side of Cerro Quimal, Late Paleozoic (and early Triassic?) volcanic rocks overthrust the Tonel Formation (Fig. 2e) above an eastward-verging footwall syncline (Fig. 2d).

DISCUSSION

Along the northern part of El Bordo escarpment, the overturned anticline appears to be a fault-propagation fold, above a thrust front that roots into the eastern edge of Cordillera Domeyko (Figs. 2a & 2e). From structural styles and growth strata, we infer that at least the lower section of the Tonel Formation accumulated in a compressional context. Fission track ages for the Cerro Quimal intrusion indicate fast uplift at about 63 Ma (Andriessen and Reutter, 1994). They thus account for Paleocene alluvial facies of the Naranja unit, which unconformably overlies Maastrichtian volcanic rocks (Fig. 1, Mpodozis et al., 1999). However, the main tectonic event in the area was probably the Eocene Incaic phase, which accounted for deposition of more than 1000 m of proximal alluvial facies (Loma Amarilla strata), large clockwise tectonic rotations, uplift and eastward overthrusting of Cordillera Domeyko (Arriagada et al., 2000). Evidence for Oligocene or post-Oligocene compressional tectonics can be found to the S of Cerro Quimal, where the Tonel Formation overthrusts Eocene (and perhaps Oligocene) deposits of the Loma Amarilla strata (Fig. 1). In conclusion, the western edge of the Salar de Atacama appears to have developed in a compressional foreland setting, from mid-Cretaceous to Paleogene times.

REFERENCES

Andriessen, P., Reutter, K-J. 1994. K-Ar and fission-track mineral age determination of igneous rocks related to multiple magmatic arc system along the 23°S latitude of Chile and NW Argentine. In: Tectonics of the Southern Central Andes (edited by Reutter, K.-J., Scheuber, E., Wigger, P.), Springer-Verlag, Berlin, p. 141-153.

Arriagada, C., Roperch, P., Mpodozis, C. 2000. Clockwise block rotations along the eastern border of the Cordillera de Domeyko, Northern Chile (22°45'-23°30'S). Tectonophysics, 326, 153-171.

Charrier, R., Reutter, K.-J. 1994. The Purilactis Group of Northern Chile: Boundary Between Arc and Backarc from Late Cretaceous to Eocene. In: Tectonics of the Southern Central Andes (edited by Reutter, K.-J., Scheuber, E., Wigger, P.), Springer-Verlag, Berlin, pp. 189-201.

Flint, S., Turner, P., Jolley, E., Hartley, A. 1993. Extensional tectonics in convergent margin basins; an example from the Salar de Atacama, Chilean Andes. Geological Society of America Bulletin, 105, 603-617.

Götze, H.-J., Krause, S. The Central Andean gravity high, a relic of an old subduction complex? Journal of South American Earth Sciences (in press).

Hartley, A., Flint, S., Turner, P., Jolley, E. 1992. Tectonic controls on the development of a semi-arid, alluvial basin as reflected in the stratigraphy of the Purilactis Group (Upper Cretaceous-Eocene), northern Chile. Journal of South American Earth Sciences, 5, 275-296.

Mpodozis, C., Arriagada, C., Roperch, P., 1999. Cretaceous to Paleogene geology of the Salar de Atacama Basin, Northern Chile: A reappraisal of the Purilactis Group stratigraphy. 4th International Symposium on Andean Geodynamics, Göttingen, Germany, Editions IRD, pp. 523–526.

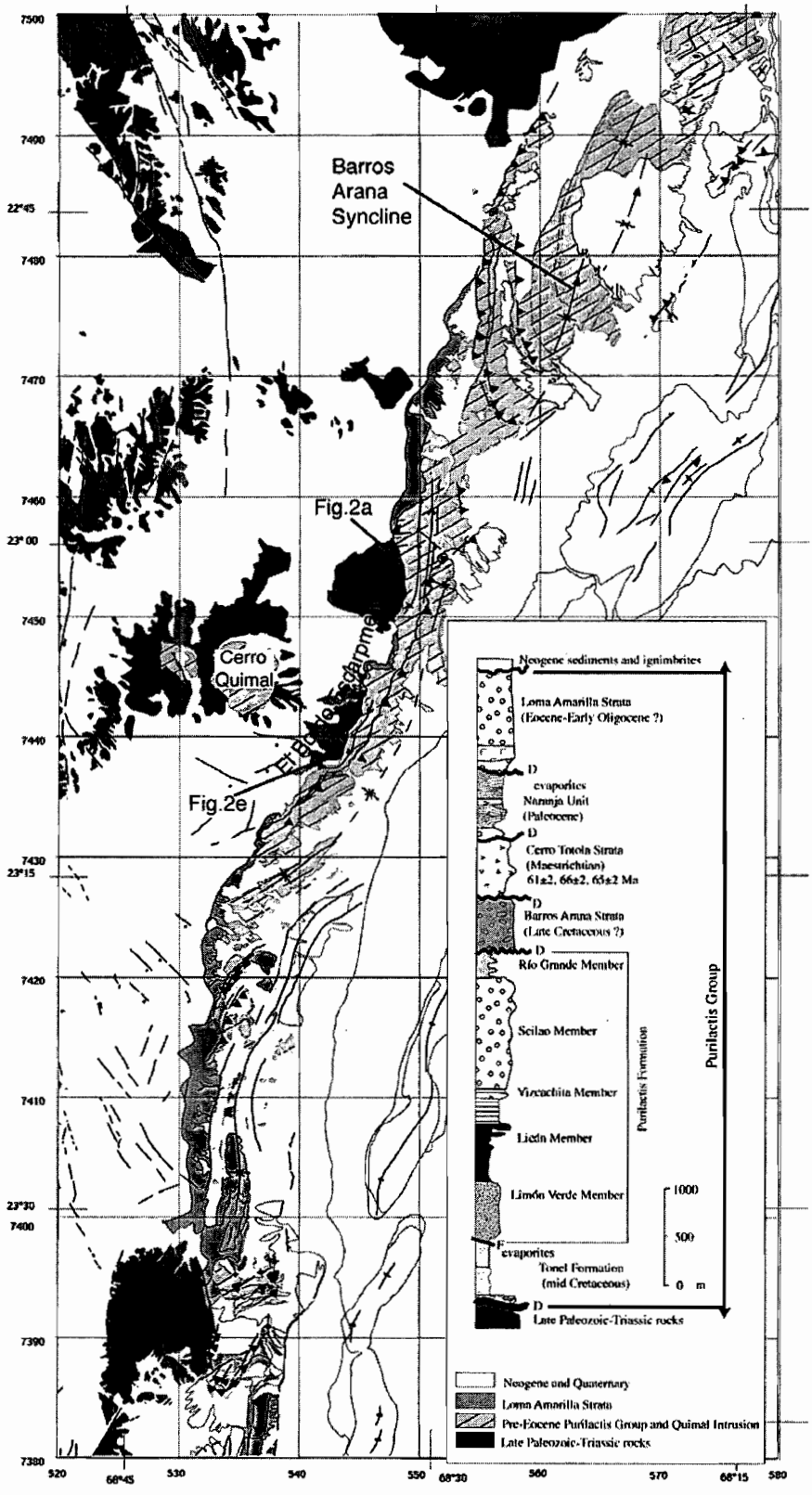

Figure 1: Simplified geological map and stratigraphy for the western edge of the Salar de Atacama basin

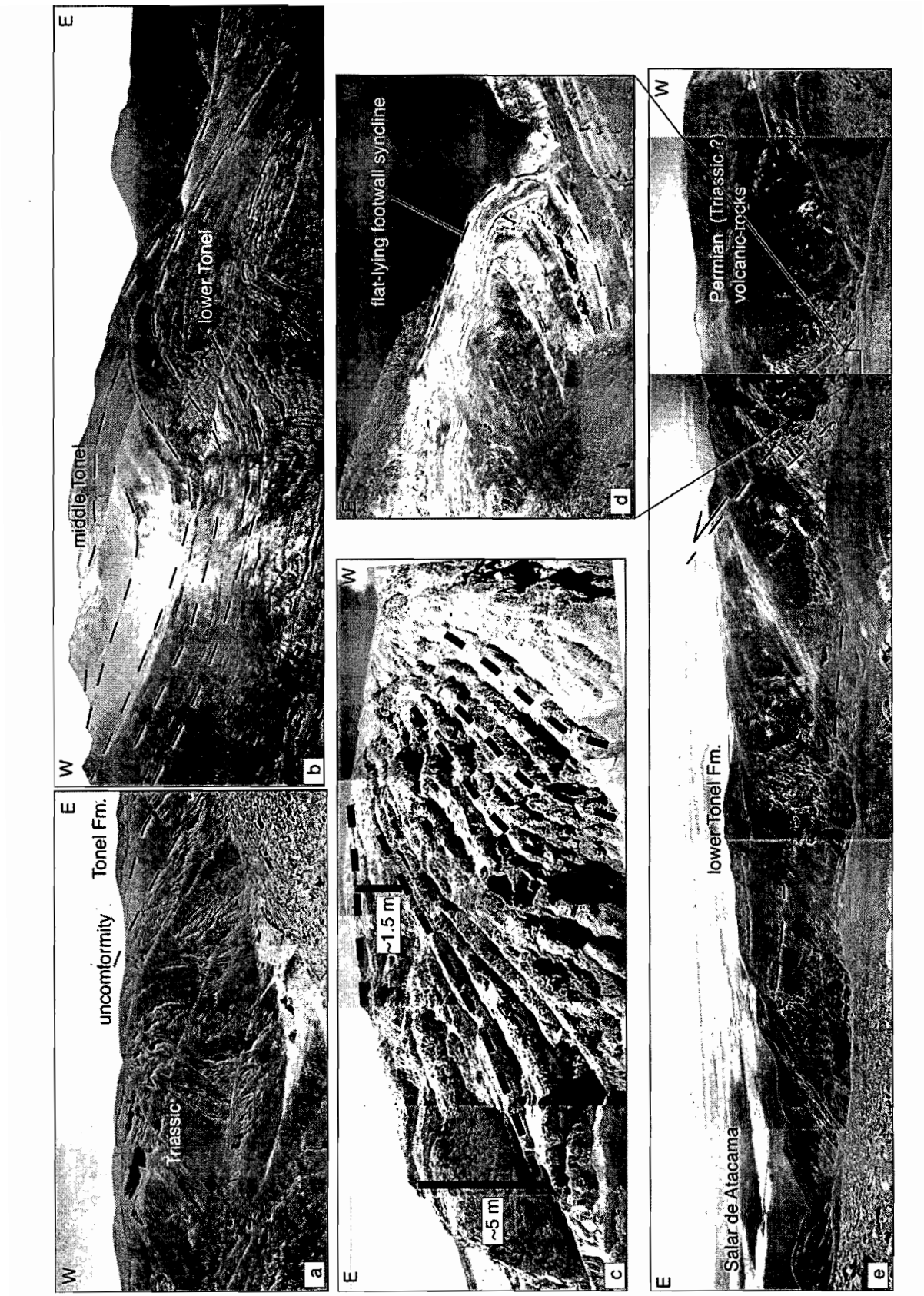

Figure 2: Structures at selected localities (see Fig. 1). a. Anticline overturned to E in Triassic and lower Tonel strata. b. Growth syncline in lower Tonel Fm. c. Growth strata in lower Tonel Fm. d. Footwall syncline in lower Tonel Fm (located in e). e. Thrust front at eastern edge of Cordillera de Domeyko.

LATE CRETACEOUS TO TERTIARY EVENTS IN THE WESTERN CORDILLERA OF ECUADOR

John A ASPDEN (1) and William J McCOURT (1)

(1) British Geological Survey, Keyworth, Nottingham, NG12 5GG (jaa@bgs.ac.uk)

KEY WORDS: Accretion, Continental Margin Magmatism-Sedimentation.

INTRODUCTION

Between 1995-2000 the British Geological Survey (BGS) in partnership with the Dirección Nacional de Geología (DINAGE, ex-CODIGEM) carried out systematic geological mapping and geochemical surveys of the Cordillera Occidental between 1^0N - 4^0S, some 36,000 km^2. As a result of the survey it is possible to recognise a series of regional events that provide a temporal and spatial geotectonic framework for the Late Cretaceous-Miocene evolution of this part of the Northern Andean margin.

CONCLUSIONS

Three separate oceanic terranes were identified during the 5 year mapping programme, from oldest to youngest they are the Pallantaga, Naranjal and Macuchi Terranes. Regional stratigraphic combined with detailed geochemical evidence suggests they are distinct both from each other and the coastal Piñon Terrane (cf. Kerr et al. 2002). The construction of the modern Cordillera Occidental began in the Late Cretaceous (c.65-85Ma) following the incorporation of the oceanic Pallatanga Terrane (**PT**) on to the Andean margin. **PT** comprises the Pallatanga Unit (McCourt et al. 1997) which is dominated by oceanic plateau basalts, together with its associated sedimentary cover sequences (Boland et al., 2000; Dunkley and Gaibor, 1997; Hughes and Bermudez 1997; McCourt et al., 1997;). The eastern limit of the **PT** is defined by the Calacali-Pallatanga Fault Zone (**CPFZ**) (Aspden et al., 1987) and its, poorly exposed, western margin is defined by the Toachi Fault, locally corresponding to the Mulaute Shear Zone (**MSZ**) of Hughes and Bermudez, (1997), which continues south as the buried Chimbo Lineament. The age of the Pallatanga Unit is not well established, although Reynaud et al. (1999) quote an Sm/Nd isochron age of 123 ±13 Ma from the west of Quito. The precise timing of the **PT** accretion is unknown but various observations (Aspden et al., 1992; Noble et al., 1997; Jaillard et al. 1999) suggest that it approached obliquely from the south/south west and first came into contact with the then continental edge prior to the Late Campanian. Subsequent marginal parallel transport of the **PT** probably continued throughout much of the Paleocene.

In the 0°-1^0N sector of the cordillera immediately to the west of the Toachi Fault (**MSZ**) is the Naranjal Terrane (**NT**) comprising lavas of the Naranjal Unit together with its associated volcanosedimentary sequences.

Radiolarian remains indicate consistent Campanian-Maastrichtian ages. The Naranjal Unit consists mainly of volcanic arc andesites and basalts but some analyses have geochemical signatures more compatible with an oceanic plateau setting (Kerr et al., 2002; Boland et al., 2000). Based on sedimentary and geochronological evidence the timing of the **NT** accretion is well constrained as Early Eocene.

Following the **NT** accretion, there was a widespread marine transgression which led to the deposition of the Middle to Late Eocene Zapallo and Tortugo units in the 0-1° N sector. Further east, the Silante Unit was also deposited and although previously poorly dated the discovery of foraminiferal remains of probable Middle- Late Eocene-Early Oligocene age (Boland et al., 2000) confirms its age. Although the exact nature and timing of the **NT** accretion most likely varied from place to place, nevertheless from about the Middle Eocene significant changes in the sedimentological record are apparent over large areas of the Northern Andes. For example, in the coastal regions of western Ecuador (with the exception of the Progresso Basin) Paleocene and Cretaceous sequences are unconformably overlain by late Early Eocene to Late Eocene shallowing upwards successions (Benitez, 1995; Jalliard et al., 1995; Reynaud et al., 1999). Similarly in southern Colombia, Middle Eocene-Oligocene marine sediments of the Calcareous Detrital Formation occur along the cordilleran foothills and Pacific Coastal Plain overlying Cretaceous-Tertiary basement sequences (McCourt et al., 1991).

Southwards of the Naranjal outcrop is the Macuchi Terrane (**MT**) which is dominated by the Macuchi Unit a volcanic-rich clastic sequence which also includes pillow lavas/breccias, minor limestones and diabase bodies. Geochemical evidence indicates that the unit varies in composition from basaltic to andesitic and represents the remnants of an oceanic island arc (Hughes and Pilatasig, 2002). Kerr et al. (2002) while noting the geochemical similarities between these rocks and those of the Naranjal Unit also suggested that some of the more 'primitive' (MgO rich) lavas of the Macuchi Unit may have formed in a back-arc basin. Poorly constrained palaeontological and radiometric evidence (Eguez, 1986) suggests that part of the Macuchi is of Early Eocene age. Although the along strike physical continuity between the **NT** and **MT** is interrupted by extensive alluvial fan deposits, both occupy analogous structural positions within the cordillera juxtaposed against the western margin of the **PT** along the line of the Toachi Fault-**MSZ**-Chimbo Lineament. Detailed structural analysis of the **MSZ** is still required but the presence of gently dipping to subhorizontal stretching lineations and dextral kinematic indicators within the zone and its southern continuation are consistent with a model of oblique emplacement from the southwest (Boland et al., 2000). It is tempting to suggest a similar (Early Eocene) accretionary age for both terranes. Evidence from the southern part of the cordillera, however, suggests that the final accretion of the Macuchi Terrane possibly did not occur until the latest Eocene-earliest Oligocene (Dunkley and Gaibor, 1997).

To the south of the Equator the Angamarca Group, which is everywhere separated from the Macuchi Unit to the west by the Chimbo Lineament, was deposited. It comprises a turbiditic, quartzo-feldspathic, often sericitic, sandstone/siltstone/mudstone sequence that includes conglomerate and breccia horizons and minor limestone. Abundant palaeontological evidence (Santos and Ramirez, 1986; Eguez, 1986) indicates Middle to Late Eocene ages for parts of the group but it is possible that sedimentation continued into the Oligocene since the upper, eastern, portion of the section has not been dated. Samples from the western Angamarca outcrop, towards its contact with the Macuchi Unit, yielded sparse but diagnostic planktonic foraminifera of Early to Middle Paleocene age and McCourt et al. (1997) proposed that the Angamarca Group ranges from Paleocene to Eocene in age. In view of the regional evidence mentioned above, however, this interpretation seems open to question

and our preferred working hypothesis would be to suggest that, in common with other areas in the Northern Andes, sedimentation in the Angamarca basin probably commenced in the Middle Eocene.

In addition to the changes in sedimentation, changes in subduction zone dynamics during the Eocene lead to the development of widespread volcano-plutonic arc activity along the continental margin. In the north west of the cordillera the 44-35Ma Santiago plutons represent the intrusive base of this arc which helped source the post-accretion, andesitic, sedimentary units such as the Silante. Further north intrusive ages of 44-39Ma recorded from dioritic plutons which intrude the Timbuqui volcanic arc (McCourt et al., 1991) suggest that correlatives of both the Naranjal Unit and the Santiago plutons are present in Colombia. Elsewhere in Ecuador, however, the peak of batholithic emplacement seems to be much later with ages of 26-15Ma.

Between 2^0S-4^0 S extensive continental margin volcanic activity gave rise to the Saraguro Group a calc-alkaline sequence of intermediate to acidic composition consisting mainly of lavas, welded ash-flow tuffs and reworked volcaniclastic rocks (Dunkley and Gaibor, 1997). Based on radiometric evidence the group ranges from Middle Eocene to Early Miocene in age c.40-20Ma (Dunkley and Gaibor,1997; Pratt et al., 1997; Steinmann, 1997; Hungerbuhler, 1997). In the southern/central portion of the cordillera the deformation and erosion of older dacitic-rhyolitic volcanic units and the change to less evolved, andesitic material within the Saraguro Group led Dunkley and Gaibor (1997) to propose an 'end Eocene-basal Oligocene' age for the **MT** accretion. Although the regional significance of the 'intra-Saraguro deformation' remains to be established, the radiometric age data clearly indicates that 'Saraguro Arc' activity continued until the Early Miocene.

From about Middle Miocene time, possibly influenced by the arrival of the aseismic Carnegie Ridge at the Ecuador Trench, there was a change in Andean geodynamics which saw the development of a series of extensional basins (Steimann, 1997; Hungerbuhler, 1997; Spikings et al., 2001). In the cordillera a period of erosion and regional deformation preceded the deposition of a series of post-Early Miocene volcanic and volcanoclastic dominated units and the development of a new magmatic arc which continues until the present-day. These include the Tarqui, Quimsacocha, Turupamba, Turi, Uchucay, Santa Isabel Fms/Units and the Ayancay Group (Pratt et al., 1997) ranging in age from c. 20-8Ma. At this time the Chaucha Batholith (12-8Ma) was also emplaced. Further north is the Cisaran Formation (16.8-8.0Ma) which in part rests unconformably on folded Saraguro Group strata (Dunkley and Gaibor, 1997) and the Zumbagua Group (12.5-6.0Ma) which also has discordant contact with the underlying Angamarca Group sediments (Hughes and Bermudez, 1997).

REFERENCES

Aspden J. A., Litherland M. L., Duque P., Salazar E., Bermudez R., Viteri. 1987. Un nuevo cinturon ofiolitico en la Cordillera Real, su posible signicaion regional. Politecnica, Monografia de Geologia, XII, 2, 81-94, Quito.

Aspden, J. A., Harrison, S. H., Rundle, C C. 1992. New geochronological control for the tectono-magmatic evolution of the metemorphic basement, Cordillera Real and El Oro Province of Ecuador. Jour. S American Earth Sciences, 6, 77-96.

Benitez, S. 1985. Evolution géodynamique de la province côtière sud-équatorienne au Crétacé supérieur-Tertiaire. Geol. Alpine 71, 3-163.

Boland, M. L., Pilatasig, L. F., Ibadango, C. E., McCourt, W. J., Aspden , J. A., Hughes, R. A.,Beatte, B. 2000. Geology of the Cordillera Occidental of Ecuador between 0^0 – 1^0 N. Proyecto PRODEMINCA, Programa de Informacion Cartografica y Geologia. Informe 10, CODIGEM-BGS, Quito.

Dunkley, P.N. and Gaibor A. 1997 Geology of the Cordillera Occidental of Ecuador between 2^0 – 3^0 N. Proyecto PRODEMINCA, Programa de Informacion Cartografica y Geologia. Informe 2, CODIGEM-BGS, Quito.

Eguez,E. 1986.Evolution Cenozoique de la Cordillere Occidentale Septentrionale d' Equateur: Les mineralisation associees. Unpublished PhD thesis, Universite Pierre et Marie Curie, Paris.

Hughes, R. A and. Bermudez, R. 1997. Geology of the Cordillera Occidental of Ecuador between 0^0 – 1^0 S. PRODEMINCA, Programa de Informacion Cartografica y Geologia. Informe 4, CODIGEM-BGS, Quito.

Hughes, R. L. Pilatasig L. F. 2002. Cretaceous and Tertiary terrane accretion in the Cordillera Occidental of the Andes of Ecuador. Tectonophysics, 35 (1-4), 29-48

Hungerbuhler, D. 1997. Neogene basins in the Andes of southern Ecuador:evolution, deformation and regional tectonic implications. PhD thesis, Swiss Federal Institute of Technology Zurich. (Diss ETHZ No. 12371).

Jaillard, E., Ordonez, M., Benitez, S., Berrones, G., Jimenez, N., Montenegro, G., Zambrano, I. 1995. Basin development in an accretionary, ocean-floored forearc setting: southern coastal Ecuador during late Cretaceous to late Eocene times. American Association of Petroleum Geologists, Memeoir 62, 615-631.

Jaillard, E., Laubacher, G., Bengtson, P., Dhondt, A. V., Bulot, L. G. 1999. Stratigraphy and evolution of the Cretaceous foearc Celica-Lancones basin of southwestern Ecuador. Jour S American Earth Sciences, 12, 51-68.

Kerr, A. C., Aspden, J. A., Tarney, J., Pilatasig, L. (2002). The nature and provenance of accreted ocanic terranes in western Ecuador: geochemical and tectonic constraints. Journal of the Geological Society, London,

McCourt, W. J., Duque, P., Pilatasig. 1997. Geology of the Cordillera Occidental of Ecuador between 1^0 S– 2^0 S. PRODEMINCA, Programa de Informacion Cartografica y Geologia. Informe 3, CODIGEM-BGS, Quito.

McCourt, W.J, Muñoz, C. A., Villegas, H. 1991. Regional geology and gold potential of the Guapi-Napi Upper Timbiqui drainage basin Department Cauca SW Colombia, MPP-11. BGS Technical Report WC/90/34

Noble, S. R., Aspden, J. A., Jemielita, R. 1997. Northern Andean crustal evolution: new U-Pb geochronological constraints from Ecuador. Bulletin of the Geological Society of America, 109, 789-798.

Reynaud, C., Jaillard, E., Lapierre, H., Mamberti, M., Mascle, G. 1999. Oceanic plateau and island arcs of south-western Ecuador: their place in the geodynamic evolution of north-west South America. Tectonophysics, 307, 234-254.

Santos, M., Ramirez, F. 1986. La Formacion Apagua, una nueva unidad eocenica en la cordillera occidental ecuatoriana. Memorias del Cuarto Congreso Ecuatoriano de Geologia, Minas y Petroleo, Tomo 1, 179-189.

Spikings, R.A., Winkler, W., Seward, D., Handler, R. 2001. Along-strike variations in the thermal and tectonic response of the continental Ecuadorian Andes to collision with heterogeneous oceanic crust. Earth Planetary Science Letters, 186, 57-73.

Steinmann, M. 1997. The Cuenca basin of southern Ecuador: tectono-sedimentary history and the Tertiary Andean evolution. PhD thesis, Swiss Federal Institute of Technology Zurich. (Diss ETHZ No. 12297).

Pratt, W. T., Figueroa, J., Flores, B. 1997. Geology of the Cordillera Occidental of Ecuador between 3^0 S– 4^0 S. PRODEMINCA, Programa de Informacion Cartografica y Geologia. Informe 1, CODIGEM-BGS, Quito.

Van Thournout, F., 1991. Stratigraphy, magmatism and tectonism in the Ecuadorian Northwestern Cordillera: metallogenic and geodynamic implications. PhD thesis Katholieke Universiteit, Leuven.

STABILITY OF QUATERNARY MORAINIC COMPLEXES CUT BY THE BOCONÓ FAULT, MÉRIDA ANDES, WESTERN VENEZUELA

Franck AUDEMARD[1], Christian BECK[2], Victor CANO[1], Eduardo CARRILLO[3], Raymi CASTILLA[1], Michel COUSIN[2], François JOUANNE[2], Luis MELO[1] and Thierry VILLEMIN[2]

[1] Funvisis, Earth Sciences Dept., Apdo. Postal 76.880, Caracas 1070-A, Venezuela. e-mail: **dptoct@internet.ve**
[2] Univ. de Savoie, Lab. de Géodynamique des Chaînes Alpines, 73376 Le Bourget du Lac Cedex, France.
[3] Univ. Central de Venezuela, Fac. de Ciencias, Inst. de Ciencias de la Tierra, Caracas, Venezuela.

KEY WORDS: Paleoseismic limnology; Liquefaction; Deep-seated sliding; Boconó fault, Venezuelan Andes.

INTRODUCTION

The Mérida Andes (MA) is a prominent geomorphic feature in the landscape of western Venezuela. It extends in SW-NE direction for some 350 km from the colombian-venezuelan border to the city of Barquisimeto (**Fig. 1a**). Its highest peaks reach 5000 m in elevation in the central portion, near Mérida. This chain appears to be in the northeastward topographic prolongation of the Eastern Cordillera (EC) of the Colombian Andes. However, the MA and EC do not keep any direct genetic relationship between them. While the SA Andes uplift results from convergence across a conventional type-B subduction, The present MA chain build-up results from Pliocene-Quaternary transpression due to oblique convergence between two continental blocks: SA and Maracaibo Triangular Block. This present geodynamic setting is responsible for ongoing strain partitioning along the MA where the foothills and the chain are shortened transversely in a NW-SE direction whereas the axially-located Boconó fault (BF) accommodates right-lateral strike-slip (RLSS; Audemard & Audemard, 2002).

Audemard (in press) indicates that the MA exhibits four distinct types of active deformations, but all linked to strain (stress) partitioning: (1)- sub-axial RLSS along the BF and related transtensional basins at releasing geometries or deep erosional valleys sitting on heavily-fractured bedrock; (2)- vertical uplift supported by: either erosional or depositional staircased alluvial terraces, disruption of pull-apart basins and deep transverse-to-chain incision; (3)- shortening across the chain, mostly attested in both foothills and not in the chain core due to lack of young deposits and (4)- seismically-induced mass wasting (slides, avalanches/flows, etc.), deep-seated slope instabilities (i.e.: gravitational spreading) and earthquake-triggered soft-sediment deformation. This contribution intends to bring supporting evidence to the last type of ongoing active deformation, triggered by the Quaternary activity of the BF in the lake Mucubají (LM) region, some 60 km northeast of Mérida.

BOCONÓ FAULT

The BF is a spectacular NE-SW trending RLSS fault that extends for about 500 km, partly along the backbone of the MA. It runs slightly oblique to the MA chain axis and bounds the Caribbean Coast range of northern Venezuela on the west, thus extending between the Tachira depression, at the border between Colombia and Venezuela, and Morón -on the Caribbean coast of Venezuela-. This fault has been identified, mapped and characterized rather easily since the pioneering work of Rod (1956) by the large number of along-strike geomorphic features, among which: continuous series of aligned 1-5 km wide valleys and linear depressions, passes, saddles, trenches, sag ponds, scarps and sharp ridges. Among those, the alignment of

valleys along the fault is the most conspicuous feature as it makes the fault easily recognizable in radar (SLAR) images (**Fig. 1a**).

The study area partly lies in the northeastern end of the Apartaderos basin that corresponds to a releasing bend of the BF (Soulas, 1985; Audemard et al., 1999). In fact, this part of the BF has a slightly more easterly strike with respect to the overall NE-SW trend. Here, the BF is well preserved along a 3,500-m-high drainage divide that separates the southeasterly flowing streams (Orinoco basin) from the northwesterly flowing streams (Maracaibo basin). This divide is nestled in the area of lake Mucubají (LM), belonging to the Sierra Nevada National Park. The BF here comprises two conspicuous sub-parallel active strands located at about 1-1.5 km apart, both exhibiting magnificent geomorphologic expression preserved in latest Pleistocene and Holocene deposits (**Fig. 1d and e**). Even though the vertical component of slip appears to be significant at some localities (*e.g.*: near El Cerrito, in the village of Apartaderos, Los Zerpa and near Las Tapias), most of the fault geomorphology is typical of a RLSS fault (**Fig. 1**). At present time, this high-altitude basin is being deeply dissected by both the Chama and Santo Domingo (SD) river headwaters, whose drainage divide is exactly at the LM, even though this depression seems to have accumulated a rather thick sequence of Pleistocene glacial deposits as those preserved at Mesas del Caballo and Julián. This sedimentary evolution seems to be strongly dependent on marked hydric changes between glacial and interglacial periods, there is no doubt though that the deactivation of sedimentation in this perched basin is due to generalized chainwide uplift that induces parallel-to-chain axis deep incision along the heavily-fractured bedrock or brecciated material generated by the present activity of the axial BF (**Fig. 1e**; notice perfect match between bottom valley and fault trace under Pleistocene moraine fill). The BF exhibits is highest slip rate at this basin, where the southern and northern strands respectively carry about 75% and 25% of the 7-to-10 mm/a net slip rate measured in this sector (Audemard et al., 1999). From the LM area, the BF slip rate decreases towards both ends.

BOCONO FAULT AND QUATERNARY MORAINIC SYSTEMS INTERPLAYS

Besides the direct permanent ground deformation (surface fault rupturing) and its cumulative expression in landscape by repeat of earthquakes (geomorphic evidence of active faulting), moderate-to-large earthquakes induce other phenomena gathered under the name of indirect permanent ground deformations that includes soil liquefaction (soft-sediment deformation) and mass wasting of very diverse types (deep-seated and shallow slides, falls, flows and lateral and gravitational spreadings). Some of these permanent features are also been utilized to determine the seismic history of a fault or region, beyond the simple trenching of active surface faulting. This is the case for the LM sector of the BF where both deep-seated slides and soft-sediment deformation (including soil liquefaction and lateral spreading) in late Pleistocene morainic systems are being induced by coseismic fault slip and direct disruption of the morainic systems by the BF (Audemard et al., 2001). Two particular cases will be dealt with in this contribution: LM and Los Zerpa moraines. In both sites, both sesimically-induced effects are preserved in late Pleistocene lake and alluvial sediments.

Lake Mucubají morainic complex

This late Pleistocene morainic complex sits on the high-altitude water divide of the Chama and SD rivers. The Mucuñuque river –running along the moraine bottom- used to pour its waters into the Chama basin on the southwest before shifting to the SD basin on the northeast, as attested by the abandoned spillway of LM preserved on the southwestern side of the outermost frontal moraine (**Fig. 1c**). This glacial system is cut across by the southern and main strand of the Boconó fault composing the Apartaderos pull-apart basin, along the

southeast edge of the present LM (**Fig. 1c**). This morainic complex shows the particularity of preserving an active lake (LM) leaning against the outermost frontal moraine (**Fig. 1c**) instead of being in a more rangeward position, as expected in a retreating moraine system, likewise in the La Victoria moraine. Besides, the present Mucuñuque river leans against the NE lateral moraine. We believe that these three issues are related to down-slope motion of the entire morainic complex that has also been slightly tilted to the north, inducing the spillway shift to the northeast as well as the present water ponding against the frontal moraine farthest to the northwest. This gravitational motion of the morainic complex is attested by a 5-6-m-high northwest-facing scarp that cuts across the Mucubají morainic complex near the moraine complex/underlying bedrock contact (**Fig. 1c**). We believe that destabilization of the Quaternary moraine complex is induced when the BF progressively disrupted and displaced coseismically the end section of the moraine complex to the northeast, thus reducing the confining horizontal forces that used to keep the moraine as one single resistant horse-shoe-shaped piece. The above-mentioned scarp exposes the penultimate lake sedimentary sequence, which exhibits soft-sediment deformation at the sequence top and slumping. Nowadays, it is being eroded by a set of rather small Holocene staircased alluvial terraces.

Los Zerpa morainic system and its paleo-lake

In the upstream section of the SD valley, several late Pleistocene morainic complexes are preserved, among which are La Victoria, Los Zerpa and Las Tapias, from SW to NE. All three are crosscut by the BF, and particularly by its main strand along the southern edge of the Apartaderos basin.

Los Zerpa moraines do not contain any lake at present but it used to be ponded behind the end moraine, next to the BF trace that just disconnects the frontal moraine from its lateral counterparts. The late Pleistocene paleolake sequence is also disturbed (rotational sliding, small-scale faulting, seismically-induced tight folding and liquefaction; Audemard et al., 2001), as in the penultimate paleo-lake at Mucubají, and the staircased late Pleistocene-Holocene(?) alluvial terraces are also down-faulted. But here, all these sedimentary disturbances are directly related to the formation of a narrow pull-apart basin along a very short segment of the main strand of the BF that strikes slightly more east than the fault trend, all exhibiting a releasing bend geometry. However, the upper section of the lateral moraines, as well as the post-glacial alluvial terraces, are also tractioned by the void effect introduced by the pull-apart sinking (**Fig. 1b**), that induces down-slope motion driven by gravity. The creation of this pull-apart basin is responsible for deactivation of the original Los-Zerpa-paleolake spillway.

REFERENCES

Audemard, F. A., under review. Geomorphic and geologic evidence of ongoing uplift and deformation in the Mérida Andes, Venezuela. Quaternary International (pre-print).

Audemard, F. A. and Bellier, O., 1997. Trenching site selection for paleoseismic assessment on the Bocono fault, southern Venezuelan Andes. In web page: http://io.ingrm.it/sfit/Bocono_1996.html.

Audemard, F. A., Beck, C., Carrillo, E., Cousin, M. & Paterne, M., 2001. Sedimentary record of late Pleistocene seismic activity along the Boconó fault (Mérida Andes, Venezuela): the Los Zerpa moraine-dammed paleo-lake. Congrès 2001 de l'Association des Sédimentologues Français, Orléans (abstract).

Audemard, F. A., Pantosti, D., Machette, M., Costa, C., Okumura, K., Cowan, H., Diederix, H. and Sawop Participants, 1999. Trench investigation along the Merida sectión of the Boconó fault (central Venezuelan Andes). Tectonophysics, 308: 1-21.

Audemard, F. E. and Audemard, F. A., 2002. Structure of the Mérida Andes, Venezuela: relations with the South America-Caribbean geodynamic interaction. Tectonophysics, 345(1-4): 299-327.

Rod, E., 1956. Strike-slip faults of northern Venezuela. AAPG Bulletin 40, 457-476.

Soulas, J-P., 1985. Neotectónica del flanco occidental de los Andes de Venezuela entre 70°30' y 71°00'W (Fallas de Boconó, Valera, Piñango y del Piedemonte). VI Congreso Geológico Venezolano, Caracas, 4, 2690-2711.

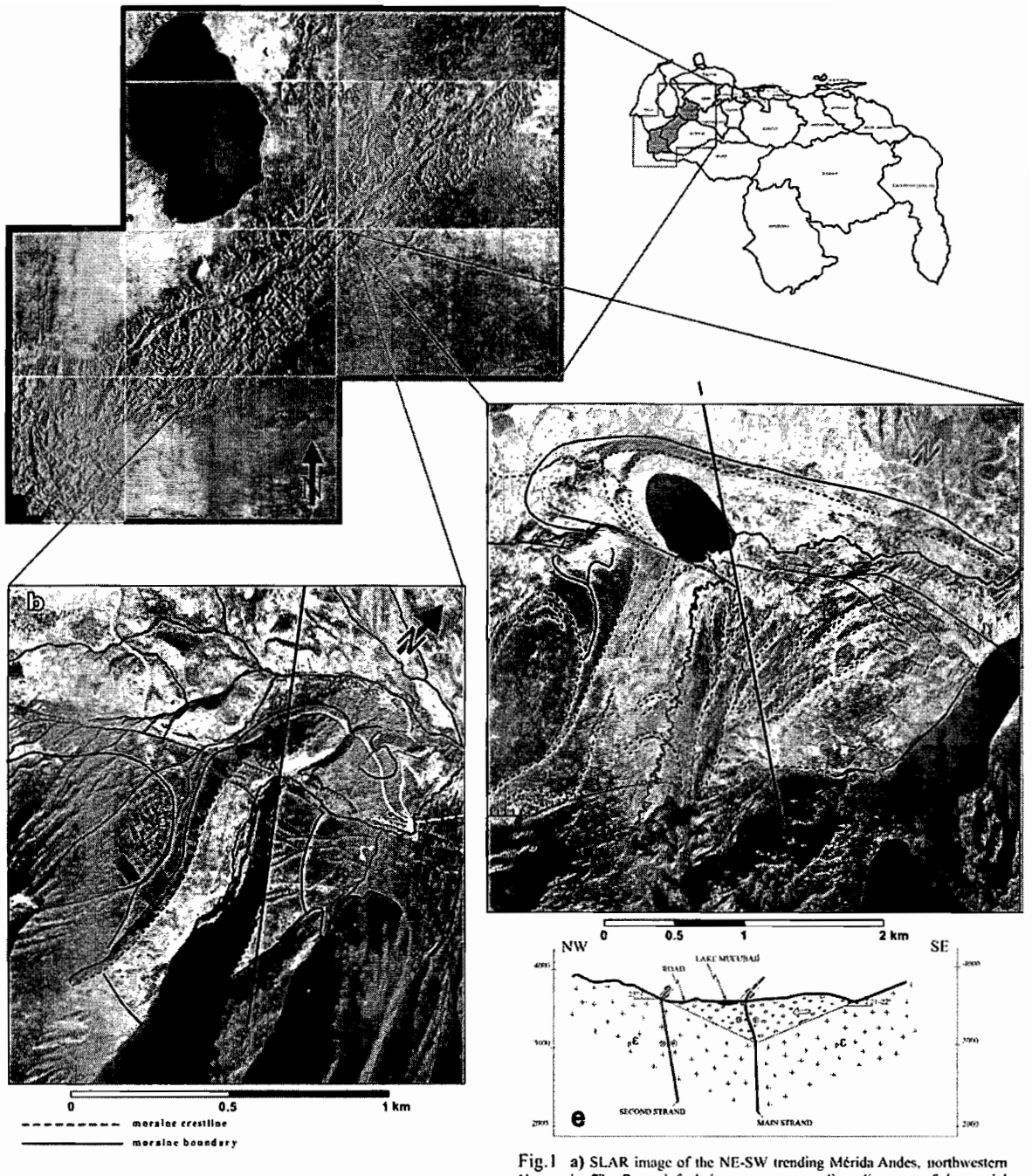

Fig. 1 **a)** SLAR image of the NE-SW trending Mérida Andes, northwestern Venezuela. The Boconó fault images an outstanding alignment of deep axial valleys. **b)** Los Zerpa moraine system cut by main strand of the Boconó fault that offsets the end section of the moraine and generates a small pull-apart basin into the last glacial deposits where fault shows a slightly more east trend. **c)** Main Boconó fault strand across the Mucubaji moraine complex exhibiting and en echelon R shear pattern that indicates that fault is cutting across a thick poorly-consolidated moraine deposit, as shown in **e**. In lower part of the image, scarp of deep-seated slide runs along bedrock-moraine contact, that pushes off fault trace to the northwest. **d)** Cross-section along Los Zerpa lateral moraine (along heavy line) imaging the sedimentary and tectonic environment. **e)** Cross-section across the Mucubaji morainic complex, showing its significant thickness (≈ 500 m)

NEOTECTONICS ON THE WESTERN FLANK OF THE DOMEYKO CORDILLIER AND CENTRAL DEPRESSION (NORTHERN CHILE)

Laurence AUDIN (1), Gérard HERAIL (1), Rodrigo RIQUELME (2,1)
José DARROZES (3), Joseph. MARTINOD (1, 3), Manuel MOREIRA (4)

(1) IRD (audin@lmtg.ups-tlse.fr, gherail@siege.paris.ird.fr)
(2) Université de Santiago du Chili (riki29rodi@yahoo.es, jmartino@cec.uchile.cl)
(3) LMTG, Université P. Sabatier (darrozes@lmtg.ups-tlse.fr)
(4) Géochimie, Insitut de Physique du Globe de Paris (moreira@ipgp.jussieu.fr)

KEY WORDS: Neotectonics, Geomorphology, Erosion, Intracontinental basin, Cosmogenic Dating

INTRODUCTION

In northern Chile, Neogene debris flows and alluvial fans are trapped in the Central depression, also known as the Longitudinal Valley, part of the Atacama arid area. This depression presents an NS trend and an average EW width of 70 km (Figure 1). On its western flank, the Central depression is bounded by the Coastal Cordillera and the Atacama Fault system. On its eastern flank runs the Domeyko fault zone, a NS trending fault system that controls much of the structure of the Chilean Precordillera. (Mortimer, 1973). The Cenozoic was characterized by an important magmatic activity along volcanic arcs, migrating step by step towards the East up to its present-day location, along the Western cordillera. Although the timing and kinematics of the Domeyko fault system is poorly constrained, studies suggest that the Domeyko fault system was active during the life-span of Eocene-Lower Oligocene magmatic arc, showing both important strike-slip and shortening composants (Reutter et al., 1991; Tomlinson et al., 1993).Based on the relationships between tectonics and morphology, this paper aims to demonstrate the presence of active faulting and folding, lying along the piemont of the Precordillera and the Central Depression, and cutting trough the Recent alluvial deposits (Figure 1). It also discusses relative chronology between the intermittent rivers and the tectonic normal scarps.

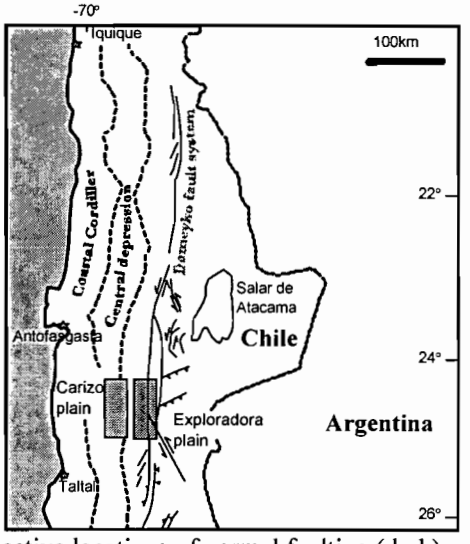

Figure 1: Respective locations of normal faulting (dark) and folding along the western flank of the Precordillera.

BASIN INFILLING MORPHOLOGY

The Central Depression is bounded on the west by the Coastal Cordillera, which separates the Depression from the Pacific Ocean since the Neogene. Throughout the Neogene, the Depression acted as a significant drainage basin for water input from the east that flowed into the area without reaching the sea. In the Exploradora and Carizo plains, between 25°S and 26°S, alluvial fan systems reach dimensions of kilometer wide and tens of metres in thickness. The topography responsible for this drainage arrangement was partly generated during the Upper Palaeogene, as a result of the Incaic orogenic phase (lower alluvial complex; Sáez et al., 1999). From this time to the Pliocene (Mortimer, 1973; Riquelme et al., submitted), the Central Depression was an endorheic area, and the Coastal Range acted as a barrier to drainage to the sea. North or south of this area, the development of large-scale salars and evaporitic deposits took place during the Neogene, mostly from Upper Miocene to Recent (Hartley and Chong, 2002). The basin fill in Pampa Exploradora and Carizo comprises a sequence of Neogene to Quaternary continental deposits, more than 300 meters thick. The neogene sequence correspond fluviatil conglomerats (Atacama gravels). The upper surface covers an erosional paleotopography that developed in the previously deformed sediments. Some volcanic layers, mostly ignimbritic flows are interstratified in the sedimentary sequence. A 10.2±0.9Ma old ignimbrite (Tomlinson *et al.*, 1993) can provide the oldest age for the Atacama gravels formation. Previous studies (Alpers and Brimhall, 1988, 1989) suggest that desertification in the Atacama region began at 14 Ma during global climate desiccation. Sedimentologic data from middle Miocene to upper Pliocene formations in the modern Atacama desert indicate that a semi-arid climate persisted from 8 to 3 Ma, punctuated by a phase of increased aridity at ca. 6 Ma (Hartley and Chong, 2002). In those plains, large coalescing and dissected alluvial fans, deposited by streams coming directly from the Precordillera, cover the valley floor. These alluvial deposits cover between 60% and 70% of the Central depression. Oldest abandoned surfaces are dissected and partly covered by inter-bedded debris flows and fluvial gravels, which are incised by intermittent rivers. The Quaternary recent alluvial fans interact with the preexisting drainage. A short, narrow and steep drainage network develop as range perpendicular watersheds came from the higher Precordillera. Well-developed desert pavements and big darkly varnished pebbles (50-100cm large) cover the oldest preserved surfaces of the fans, indicating that some surfaces are stable over long time periods..

MORPHOTECTONICS

1/ Normal Faulting and EW extension in the Pampa Exploradora (Figure 2)

The Exploradora fault (Figure 2) zone forms a network of more or less NS striking, parallel normal faults. The fault scarps are almost continuously distributed along the Precordillera. They are usually developed in the Atacama gravel deposits cutting through the intermittent river beds. The tectonic escarpements intersect the pre-existing drainage and cause the river deflection or interruption (Figure 2).

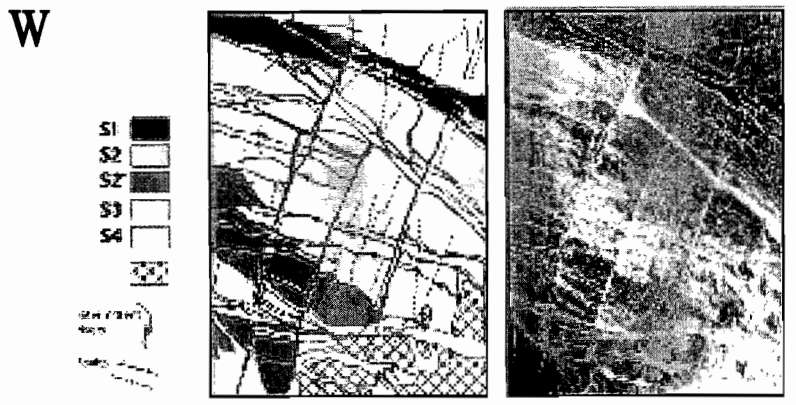

Figure 2: Aerial photography and interpretation of the normal faulting area, in the Pampa Exploradora around 3500 m of altitude.

Figure 2, based on the analysis of aerial photographs and sattelite images shows that the fault segments offset at least four alluvial fan generation (4 nested surfaces, Figure 2) that deposited at the piemont of the Domeyko cordillera in the Exploradora plain. These segments form small vertical and sometimes composite scarps about 2 meters high, The dip direction of which, (toward the East), never change along strike Mapped from an air photo enlargement and field work , Figure 2 focuses on some of the normal faults. The successive surface deposits are cut by three main normal fault scarps, parallel, East dipping, nearly perpendicular to the dry river runoff that dissects the fans surfaces. The vertical throws become smaller as the offsett surface gets younger. The faults also affects the most recent sediments deposited inside the intermittent valleys. This attests of the ongoing activity of the faults during the fan emplacement and dissection phases. No lateral offset can be systematically identified along these fault traces.

2/ Folding and NW-SE compression in the Pampa Carrizo (Figure 3)

To the west, and topographically lower (2000m), the Carrizo plain shows the same surface deposits: the Atacama gravels. Some evapotitic deposits can also be recognized of the top of the alluvial deposits (Figure 3).

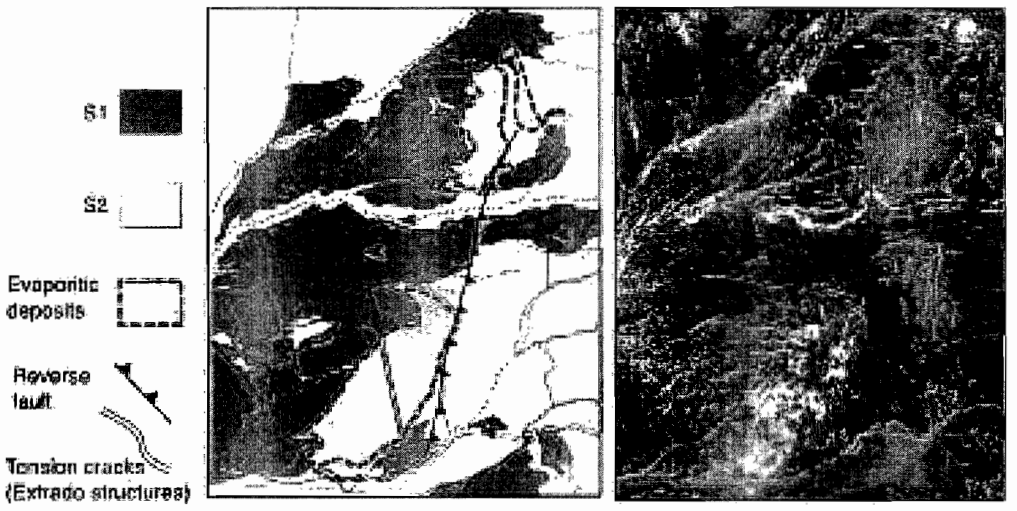

Figure 3: Aerial photography and interpretation of the folding area, in the Pampa Carrizo around 2000 m of altitude.

These two most recent surfaces are affected by an undescribed NE-SW fold system, outcropping under the Atacama gravels, that has been recently activated (Figure 3). A recent field trip has evidenced a number of

normal faults and tension cracks that cross a network of intermittent channels. This secondary fault set can be recognized, with a more NS trend than the fold direction. The Carrizo normal fault zone comprises short, parallel and antithetic fault scarps, very different from what is observed in the Exploradora first area, and we interpret them as extrado structures.

CONCLUSIONS

Clear-cut signs of neotectonics were not previously described in this region, and the known seismic activity is low. But two constrasting tectonic regimes can be distinguished in the study area, as already observed in the north of Chile (Victor, 2000). We propose here a new hypothesis in favor of neotectonic activity in the region of the Central depression. A NW-SE compressional regime in the lower part of the Central depression (Pampa Carizo) seem to predate or at least to coexist with a NW-SE extensionnal regime (Pampa Exploradora), present-day active, in the upper part of the Central depression (Figure 4). This could be reconciliated in one single model, either the normal faulting and folding could be the result of a regional tilting to the West of the whole Andean chain.

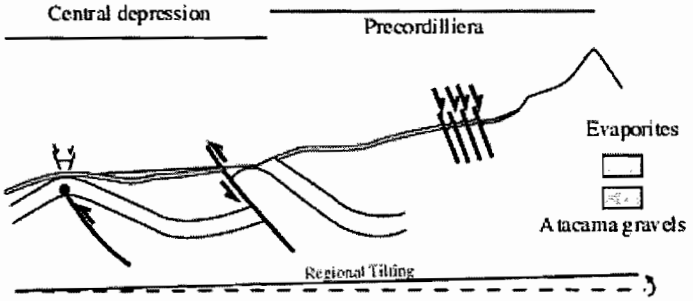

Figure 4: Proposed interpretation to explain both extension and compression evidences of deformation in the Andean Precordillera.

REFERENCES

Alpers, C. and Brimhall, G. H, 1988, Middle Miocene climatic change in the Atacama Desert, northern Chile: Evidence from supergene mineralization at La Escondida: Geol. Soc. Amer., v. 100, p. 1640-1656.

Alpers, C. and Brimhall, G. H, 1989, Paleohydrologic evolution and geochemical dynamics of cumulative supergene metal enrichment at La Escondida, Atacama Desert, northern Chile: Econ. Geol., v. 84, p. 229-255.

Hartley and Chong, 2002, Late Pliocen age for the Atacama Desert: Implications for the desertification of western south America

Mortimer C., 1973, The Cenozoic history of southern Atacama Desert, Chile. J. G. Soc. Of Lond, 129, 505-526.

Reutter K.J. et al., 1991, Structural evidence of orogen-parallel strike slip displacements in the Precordillera of Northern Chile. Geol. Rndsch., 80, 135-153.

Riquelme et al., Neogne tectonics of the Central Depression and Precordillera (Andes of northern Chile) from the analysis of a drainage basin evolution, submitted.

Sáez etal., 1999 Late Neogene lacustrine record and palaeogeography in the Quillagua Llamara basin, Central Andean fore-arc (northern Chile), Palaeogeo., Palaeoclimat., Palaeoeco.,151, 1-3, 5-37

Tomlinson, A.J.; Cornejo P., Mpodozis,C; Ramirez,C, 1993, Structural geology of the Sierra Castillo-Agua Armaga fault system, Precordillera of Chile, El Salvador Potrerillos. 2nd International symposium on Andean Geodynamics, pp 259-262. Editions de l'Orstom, Colloques et Séminaires Paris.

Victor P. Die Entwicklung der Altiplano Westflanke und ihre Bedeutung fur die Plateaubildung und Krustenverdickung in N-Chile (20-21°S). PhD thesis, FU Berlin, Berlin, Germany, 2000.

CATHODOLUMINESCENCE OF QUARTZ AS PROVENANCE INDICATOR FOR LATE PALAEOZOIC METASEDIMENTS OF SOUTHERN ANDEAN PATAGONIA

Carita AUGUSTSSON (1) and Heinrich BAHLBURG(1)

(1) Geologisch-Paläontologisches Institut, Westfälische Wilhelm-Universität, Corrensstraße 24, 481 49 Münster, Germany (E-mail: *augustss@uni-muenster.de*, *bahlbur@uni-muenster.de*)

KEY WORDS: cathodoluminescence, provenance, Patagonia

INTRODUCTION

Mature sediments dominated by quartz grains usually have been modified considerably from source area to depositional basin. With a lack of provenance indicative rock fragments, the general petrography of quartz rich sandstones is not always reliable as provenance indicator.

Along with other techniques, the cathodoluminescence (CL) characteristics of quartz can be used as provenance indicator. The CL characteristics of quartz differ, depending on the thermal events that have affected the quartz crystals and its host rocks. Thus, the CL signal of single quartz grains of sedimentary rocks can be used to reveal characteristics of the source rocks. This assumes that the CL signal of the quartz grains has remained unchanged from the original source. Brown luminescing quartz is assumed to be of regional metamorphic origin, red, violet and bright blue of volcanic origin and dark blue of plutonic origin (Zinkernagel, 1978). The CL colours of quartz are very weak and the brightness of the luminescence depends on excitation conditions. Further the perception of colours is subjective.

METHOD

To get an objective tool for the identification of CL colours of quartz, measured CL spectra of individual quartz grains have been compared. The CL spectra are usually dominated by one peak in the blue wavelength interval at 460-490 nm and one in the red range at 610-640 nm. For bright blue luminescing quartz, the blue peak is higherst, and for red luminescing quartz the red peak is dominating. A general wavelength

increase in peak positions, as well as a decrease in relative peak heights, appears with decreasing temperature reached by the thermal events.

We have compared the spectra of 392 quartz grains in seven greywacke and arenite samples of Late Devonian to Early Carboniferous age from the Andean Patagonia of southern Chile and Argentina (47°-49°S, 72-73°W). The spectra of individual quartz grains have been sorted into groups for spectral types typical of different CL colours, as they were identified by Zinkernagel (1978). This gave a lower percentage of dark luminescing quartz grains compared to optical identification. The population of brown luminescing quartz grains was for example reduced from 49 % by the optical identification to 35 % with the spectra classification, and bright blue luminescing quartz grains increased from < 1 % to 8 %.

The wavelength positions of the two main peaks were compared with the position of the trough between the peaks. This resulted in a good separation of quartz with different spectral types. Almost no overlap between quartz grains with spectra typical of blue and brown luminescing quartz occurs. The CL spectra typical of red and violet luminescing quartz could not be well separated with the used quartz grain population. The comparison of the relative heights of the two main peaks with the depth of the trough resulted in good separation for all spectral types. The large height difference between the two main peaks, especially between bright blue and red luminescing quartz, made it possible to separate red and violet luminescing quartz from quartz with blue and brown CL colours. Due to the small overlaps observed, interpretations based on the peak and trough positions and their relative heights give similar results as the more time consuming classification into different spectral types.

PROVENANCE

The first indications of easterly directed subduction under southern Patagonia at the Pacific margin of Gondwana (present coordinates) are of Late Carboniferous age. In Early to Middle Devonian times a stable platform fauna existed, thus bracketing the onset of subduction between the Middle Devonian and the Late Carboniferous for this region.

The studied sediments are metaturbidites of Late Devonian to Early Carboniferous age, belonging to the Eastern Andean Metamorphic Complex in Chile and the Bahía de la Lancha Formation in Argentina. The quartz grain populations in the analyses rocks samples are dominated by grains with a probable metamorphic and plutonic origin (brown and dark blue luminescing quartz grains). This can be expected both for active tectonic margins without volcanism, and for passive margins. Thus, in this case it is necessary to combine CL analysis with other techniques for further qualification.

The metasediments from the Eastern Andean Metamorphic Complex have a felsic geochemical composition with active margin affinity, negative $\varepsilon_{Nd}(T)$ values (-7 to -2) indicative of older continental sources, and Nd model ages of 1170-1490 Ma (Augustsson & Bahlburg, in review). Evidence of syn-depositional intrusive activity is absent. This was taken to indicate that the sediments were deposited at a passive margin, but that they were fed by material produced at ancient active margins (Augustsson & Bahlburg, in review). The CL results, with its dominance of quartz grains crystallized during metamorphic and plutonic conditions, give further support to this interpretation.

REFERENCES

Augustsson C. & Bahlburg H. in review. Active or passive margin ? Geochemical and Nd isotope constraints of metasediments in the backstop of a pre-Andean accretionary wedge in southernmost Chile (46°30'-48°30'S). In: Tracing tectonic deformation using the sedimentary record (Ed. by T. McCann), Geological Society of London Special Publication.

Zinkernagel U. 1978. Cathodoluminescence of quartz and its application to sandstone petrology. Contributions to Sedimentology, 8, 1-69.

FACTORS CONTROLLING PARTITION OF DEFORMATION DURING PLATEAU FORMATION

Andrey BABEYKO (1) and Stephan V. SOBOLEV (1)

(1) GeoForschungsZentrum-Potsdam, Telegrafenberg, 14473 Potsdam, Germany, (babeyko@gfz-potsdam.de, stephan@gfz-potsdam.de)

KEY WORDS : numerical modelling, collision, plateau formation, strain localization

INTRODUCTION

Altiplano-Puna plateau of the Central Andes is believed to be formed during the last 10-30 Myrs mainly due to crustal thickening produced by tectonic shortening [*Allmendinger et al., 1997*]. Various studies report strong spatial and temporal variations of the deformation pattern during this shortening [*e.g., Isacks, 1988; Kley et al., 1997; Allmendinger et al., 1997; Elger and Oncken, this volume*]. Of particular interest are lack of tectonic activity in the Central Altiplano during ca. 28-15 Ma when deformation was active in the Eastern and Western Cordilleras, and migration of the deformation from the Altiplano to the east into the Subandean Range at ca. 10 Ma.

In this study we employ 2-D numerical thermomechanical modelling to test three possible factors, which could strongly effect partition of deformation during tectonic shortening. Our modelling technique (explicit, finite element algorithm) allows simulation of strongly non-linear rheologies such as temperature dependent power-law visco-elasticity and Mohr-Coloumb elasto-plasticity. The technique is able to model strong strain localization (faults) in the brittle crust by allowing strain softening (decrease of cohesion or friction in Mohr-Coloumb model) as well as large ductile deformation in the lower crust including thermal convection.

First, we explore the role of initial local thermal softening of the lithosphere (Fig. 1). In the case of the Altiplano-Puna plateau, the initial thermal heterogeneity could be attributed to the pre-Andean rift system in the Eastern Cordillera [*Sempere, 1994*].

Secondly we study effect of rheological softening of the crust as a result of advective crustal heating (Fig. 2). In the Central Altiplano there was a low tectonic activity until ca. 15 Ma. Followed increase of shortening rate coincides in time with the onset of extensive ignimbrite magmatism. *Babeyko et al. [2002]* showed that available geological and geophysical observations in the Altiplano-Puna Volcanic Complex are well explained by ongoing intracrustal bulk convection as a respond to increased mantle heat flux at ca. 25 Ma.

And finally, we present a preliminary result for the shortening model incorporating highly east-west contrasting rheologies resembling hot and weak Altiplano and cold and strong Brasilian shield (Fig. 3).

RESULTS

Shortening of the lithosphere with the domain where temperature is slightly increased (+100°C at Moho relative to the surrounding lithosphere) first results in strain localization within the domain (Fig. 1). At some 5 My a W-dipping crustal subduction structure within the heated domain is formed. After 8-10 My deformation is migrated to the west of the heated domain and at about 15 My an E-dipping crustal subduction structure is formed there.

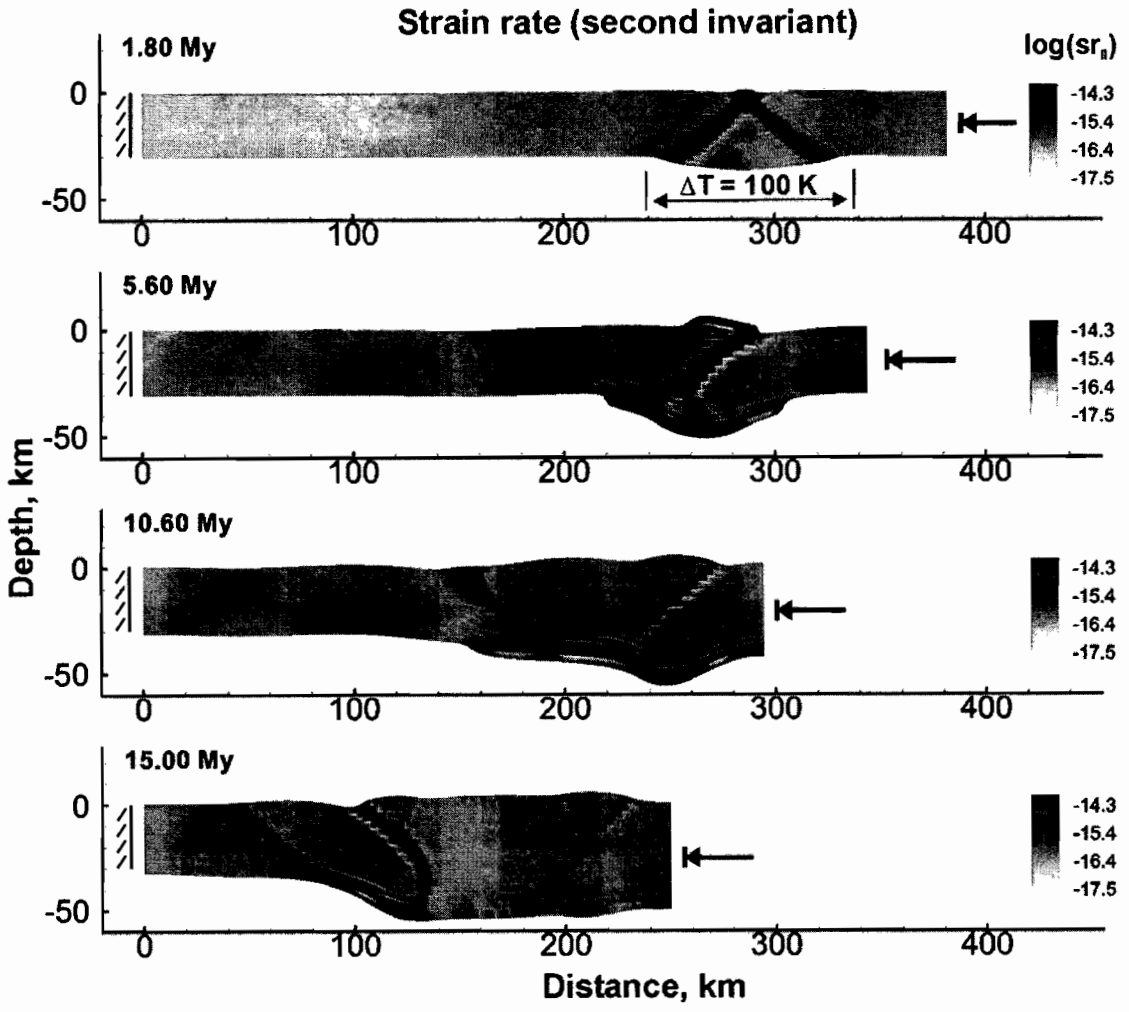

Figure 1. Evolution of deformation during shortening of the lithosphere containing domain with slightly higher temperature.

Asthenospheric upwelling (e.g. due to mantle lithosphere delamination) strongly increases basal heat flow to the crust. When combined with ongoing tectonic shortening and weak (quartz dominated) crustal rheology, high basal heat flow may result in partial melting and bulk convection in the lower and midlle crust (Babeyko et al., 2002) (Fig.2). This, in turn, leads to rapid weakening of the crust and changes in style of deformation in the upper crust.

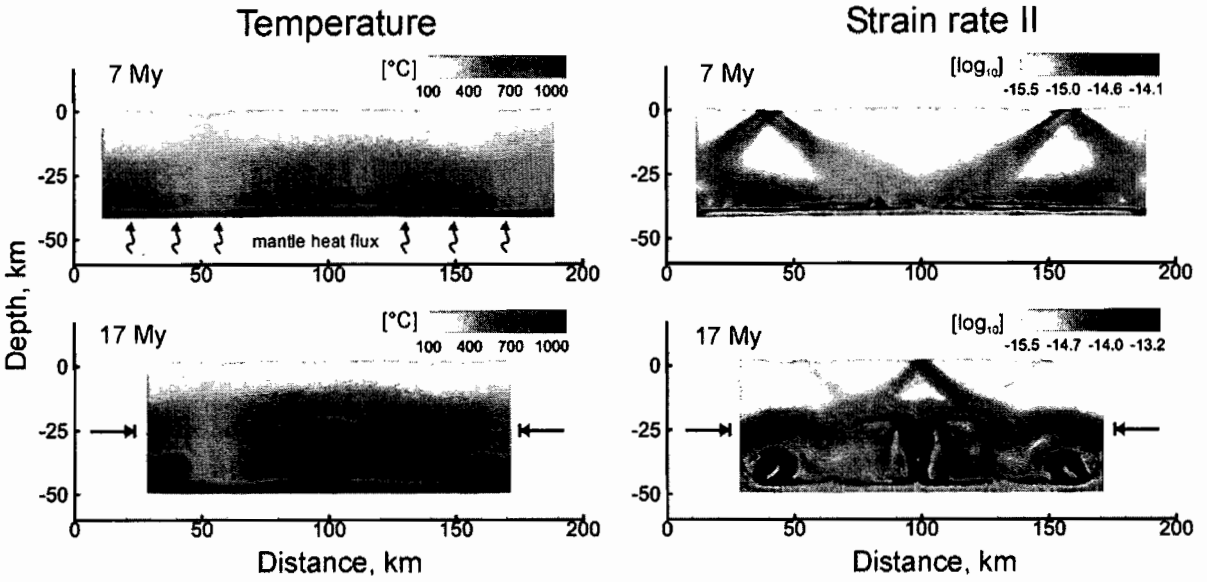

Figure 2. Crust with weak (quartz-dominated) rheology is shortened and heated from below by heat flux = 60 mW/m^2.

Fig.3 presents shortening of two contrasting lithospheric blocks: hot and weak block with convective-type temperature distribution in the middle/lower crust (Altiplano-Puna) in contact with cold and strong block (Brazilian shield). The cold block contains weak uppermost crust (10 km thick layer of sediments possibly with high pressure fluids) with the Mohr-Coloumb friction coefficient of 0.1, which is 6 times lower than in the rest of the crust. In the beginning of shortening deformation is concentrated in the lower crust of the heated block and shortening of the upper crust is accommodated by faults in its center and at eastern margin. After few million years the upper crustal deformation migrates eastwards, to the weak upper crustal body. However, cold lower crust and mantle undernearth deforming upper crust remain undeformed, i.e., at deeper levels deformation remains to be confined to the heated block. The gross deformation pattern looks like simple shear despite of the pure shear boundary conditions. This type of evolution is consistent with the last 10 My years deformation evolution in the Central Andes.

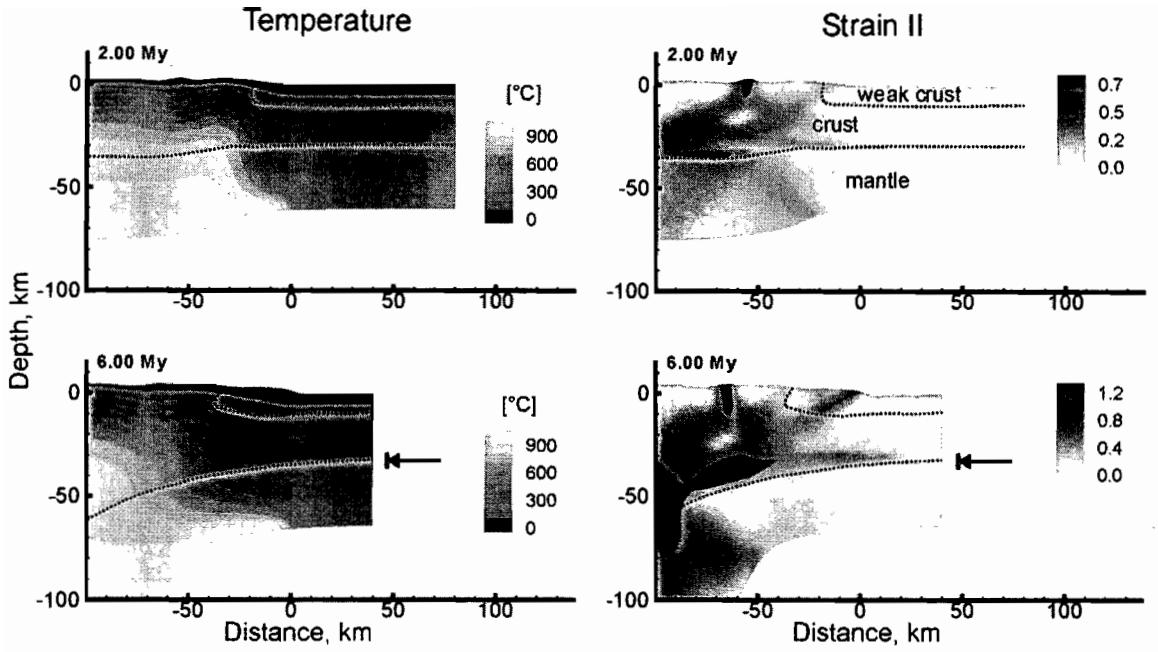

Figure 3. Shortening of the lithosphere containg two blocks with strongly contrasting rheology. The western block is strongly heated (Altiplano–Puna). The eastern block is cold and strong (Brazilian shield) but contains weak upper crust (young sediments + fluds).

REFERENCES

Allmendinger, R.W., T.E. Jordan, S.M. Kay and B.L. Isacks (1997). The evolution of the Altiplano-Puna plateau of the central Andes, *Annu. Rev. Earth Planet. Sci.*, 25, 139-174.

Babeyko, A.Yu., S.V. Sobolev, R.B. Trumbull, O. Oncken, and L.L. Lavier (2002). Numerical models of crustal scale convection and partial melting beneath the Altiplano-Puna plateau, *Earth Planet. Sci. Lett.*, in press.

Elger, K. and Oncken, O. (2002). The pattern of deformation related to growth of the Southern Altiplano plateau (Bolivia), *this volume.*

Isacks, B.L., (1988). Uplift of the Central Andean Plateau and bending of the Bolivian Orocline, *J. Geophys. Res.*, 93, 3211-3231.

Kley, J., J. Müller, S. Tawackoli, V. Jacobshagen, and E. Manutsoglu (1997). Pre-Andean and Andean-age deformation in the Eastern Cordillera of Southern Bolivia, *J. South Amer. Earth Sci.*, 10, 1-19.

Sempere, T. (1994). Kimmeridgian? to Paleocene tectonic evolution of Bolivia, In: *Cretaceous Tectonics of the Andes,* J.A. Salfity (ed.), p. 168-212, Vieweg, Braunschweig, Germany.

THE 1999-2000 SEISMIC EXPERIMENT OF THE SWARM OF MACAS (ECUADOR) IN RELATION WITH A SUBANDEAN UNEXPECTED WRENCH FAULT SYSTEM

Patrice BABY (1), Denis LEGRAND (2), Séverine BES DE BERC (1)(2), Francis BONDOUX, Marco RIVADENEIRA (3)

(1) IRD (UR104), Université Paul Sabatier, Toulouse, France (baby@cict.fr)
(2) IFEA : Institut Français d'Etudes Andines, Whymper 442 y Coruña, Quito, Ecuador (legrandenis@yahoo.com)
(3) Petroproducción, Av. 6 de Diciembre 4226 y Gaspar Cañero, Apartado 17-01-1006, Quito, Ecuador, (asicad3@petroecuador.com.ec)

KEY WORDS: Seismic swarm, Macas, Ecuador, seismotectonic, subandean

INTRODUCTION

A seismological experiment of 10 portatile short-period stations has been carried out in 1999-2000 around a swarm close to the city of Macas, Ecuador. The corresponding event locations have been correlated with respect to structural geology. Two main trends have been found. One corresponds to the already well established NNE-SSW trend of the big aftershocks of the M_w=7.0 1995 Macas earthquake, in agreement with its focal mechanism and the orientation of one of the complex subandean faults systems. The other one in an unexpected NNW-SSE trend where most of the registred events occurred. In fact, this trend is also in agreement with Subandean structures and can be explained in a more general tectonic pattern.

The purpose of this study is to present and correlate our seismological results and structural analysis in order to characterize the active Subandean deformation, and to explain the origin of the Macas swarm. Tectonic implications at the Andean scale are discussed.

REGIONAL SEISMIC SETTINGS

Ecuador is situated near the change of orientation of the SSE-NNW Central Andes and the SSW-NNE Northern Andes. Hence, this particular elbow-like position (Huancabamba Deflection) is submitted to high stress changing and, as a consequence, may be responsible of the high volcanic and seismic activity of Ecuador respect to Peru and Colombia. In order to have a rough idea of stress tensors, we calculate them from CMT Harvard focal

mechanisms for shallow (depth < 50 km) events of magnitude M_w bigger than 5.0. The whole region has been split into 10 regions for which a unique stress tensor could be calculated (Figure 1). The general tectonic behavior can be deduced from the shape factor R (Rivera and Cisternas, 1990) of the stress tensor ($R<0$ for a pure compression, $R>1$ for a pure extension and $0<R<1$ for an intermediate state). All the stress tensors are compressional (with a vertical σ_3, figure 1 *i.e.* with $R<0$) except for two regions: the Southern part of Colombia Coast (crosses in figure 1), which is a small extensional region ($R>1$). The second region is the Macas swarm (diamonds in figure 1), which has an intermediate shear stress tensor ($0<R<1$). Hence, this Macas region is a transition zone between two compressional regions (Peru and Northern Ecuador), characterizing a transpressive deformation, in an elbow-like position between the change of Peru and Ecuador mountain orientation mentioned before. These results are close to the one of Ego et al. (1996), except for the region of Bogota (stars in figure 1) and for the Macas region (diamonds in figure 1). This difference may be attributed to the fact that those authors have not taken into account the 1995 M_w =7.0 Macas earthquake and its aftershocks and the 1995 M_w =6.5 earthquake and its aftershocks in the Bogota region (these events occurred after their study). This particular situation of Macas region will be discussed latter on in a geological pattern.

MACAS SEISMIC SETTINGS

In 03/10/1995 an M_w=7.0 shallow (25 km depth) earthquake occurred at 2.55°S, 77.53°W (event 10 in Figure 2) near Macas city. The main trend of the biggest USGS events (mainly aftershocks of the 1995 Macas earthquake) is NNE-SSW, in agreement with the focal mechanism of the main shock (Figure 2) and the orientation of some subandean reverse faults. Nevertheless, many small aftershocks (of local magnitude $M_L<4.0$) have been recorded in a NNW-SSE orientation few days after the main shock (Yepes et al., 1996, Alvarado et al., 1996) and more than 5 years after (this study).

LOCATION OF THE 1999-2000 EVENTS

In a first step, events have been pre-located using hypoellipse code (Lahr, 1995). In a second step, relative localisations using the Master Event technique (Spence, 1980) have been done (with the *a priori* information of the hypocenters given by hypoellipse code) and are shown in Figure 3. The model of propagation has been deduced from seismic sections done by Petroproduccion (Rivadeneira and Baby, 1999). Most events are between 0 and 25 km depth, and few events are deeper, until 181 km depth, corresponding to the subduction of the Nazca plate. The two NNE-SSW and NNW-SSE seismic trends still appear, but the NNW-SSE orientation is most dominant.

CONCLUSIONS

The seismic risk in the region of Macas is high, as proved by the M_w=7.0 1995 Macas event. Many people feel earthquakes each year even at present times (2001) in that region. The stress tensor of the Macas swarm corresponds to a local transpressive deformation along a local blind NNE-SSW reverse fault, associated to a NW-SE vrench faults system which explains the principal trend of the swarm. It expresses the active

deformation of the transition zone of the Huancabamba Deflection between the central and northern Andes. In the Ecuadorian Andes, the NNW-SSE structural orientation, in addition to the classical NNE-SSW one, is probably a major trend of deformation which can be correlated with others Ecuadorian swarms.

ACKNOWLEDGEMENTS : Research supported by INSU grant 99PNSE59 and IRD (Tectonique, érosion et sédimentation dans le bassin de l'Amazone : du Mio-Pliocène à l'Actuel).

REFERENCES

Alvarado A., Segovia M., Yepes H., Guillier B., Chatelain JL., Egred J., Villagómez D., Ruiz M., Samaniego P., Santacruz R., 1996: The Mw=6.8 Macas earthquake in the subandean zone of Ecuador, October 3, 1995. Third ISAG, St Malo (France), 17-19/09/1996, 129-132.

Ego F., Sébrier M., Lavenu A., Yepes H., Egues A., 1996: Quaternary state of stress in the Northern Andes and the restraining bend model for the Ecuadorian Andes. Tectonophysics, 259, 101-116.

Lahr, J., 1995. HYPOELLIPSE/Version 3.0: A computer program for determining hypocenter, magnitude and first motion pattern of local earthquake. U. S. Geol. Surv., Open-file rep., 95: 90 pp.

Rivadeneira V., M., Baby P., 1999: La Cuenca Oriente: estilo tectónico, etapas de deformación y caracteristicas geológicas de los principales campos de Petroproducción. PETROECUADOR-IRD edition, Quito, Ecuador, 88 pp.

Rivera, L. and Cisternas, A., 1990: Stress tensor and fault plane solutions for a population of earthquakes. Bull. Seism. Soc. Am., 80: 600-614.

Spence W., 1980: Relative epicenter determination using P-wave arrival-time differences. Bull. Seism. Soc. Am., 70: 171-183.

Yepes H., Chatelain JL., Guillier B., Alvarado A., Egred J., Ruiz M., Segovia M., 1996: The Mw 6.8 Macas earthquake in the Sub-Andean zone of Ecuador, October 3, 1995. Seis. Res. Let., 67, 27-32.

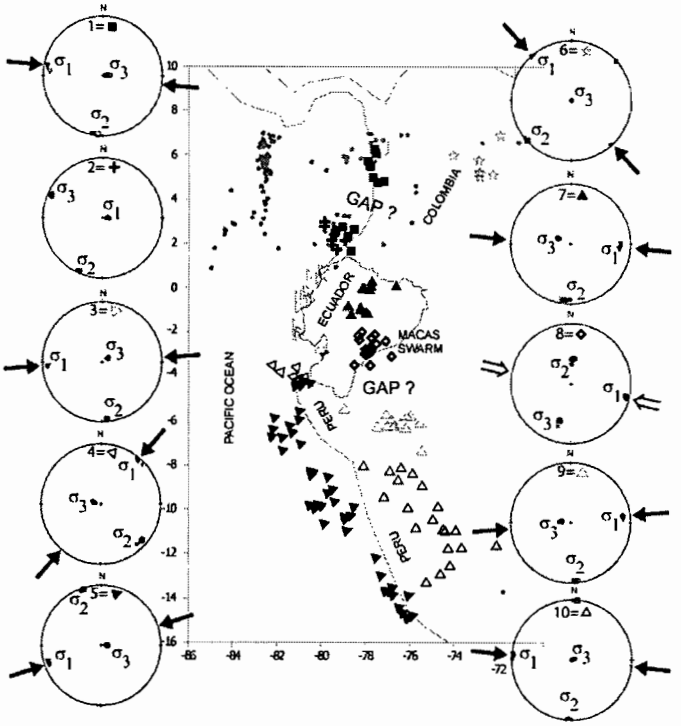

Fig. 1: Shallow (depth < 50 km) earthquakes (of M_w > 5.0) of the Harvard catalog (1973-2000) that have focal mechanism for 10 different regions and the corresponding stress tensors. Circles correspond to earthquakes that have not been used for stress tensor determinations. For the swarm of Macas, 3 additional events have been included (10/05/1963, 03/11/1963, 21/06/1967, see figure 2)

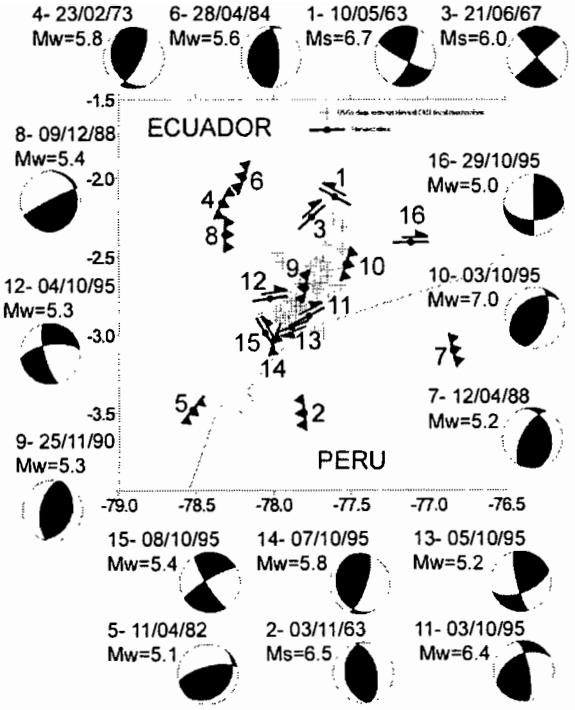

Fig. 2: Focal mechanisms of shallow (depth < 50 km) earthquakes (of M_w > 5.0) of the Harvard catalog (1973-2000) in the Macas region (region 8 of figure 1). 3 additional events have been included (10/05/1963, 03/11/1963, 21/06/1967). The fault planes selected during the stress tensor determination are shown. Cross correspond to the USGS data that have no Harvard focal mechanism (between –77.5/-78.6 and –2.1/-3.1).

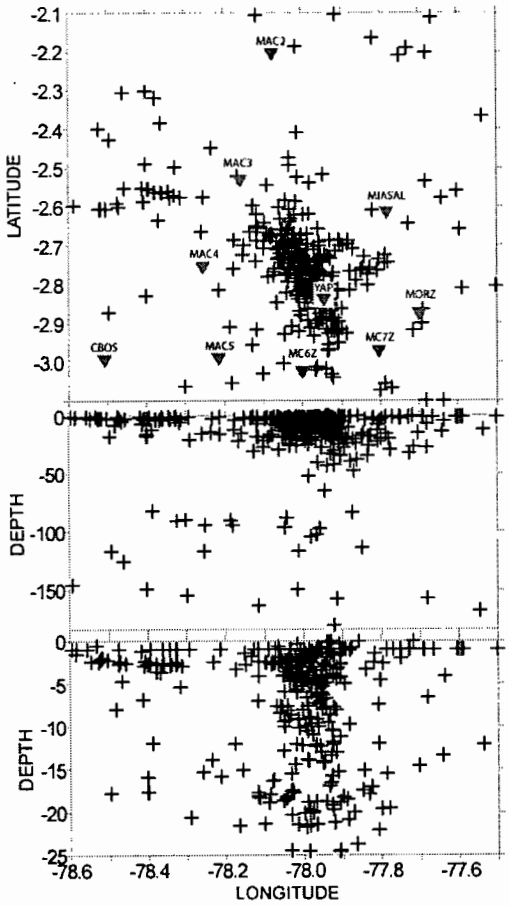

Fig. 3: Locations of the seismic portatile stations of the 1999-2000 experiment, and the seismicity recorded during this experiment.

OLLANTAYTAMBO FORMATION: A PROBABLY ARC-DERIVED VOLCANICLASTIC SUCCESSION OF CAMBRIAN TO ORDOVICIAN AGE IN THE CORDILLERA ORIENTAL OF SOUTHERN PERU

Heinrich BAHLBURG (1), Victor CARLOTTO (2), José CÁRDENAS (2), and Eva WESTERVOSS (1)

(1) Geologisch-Paläontologisches Institut, Westfälische Wilhelms-Universität, Corrensstrasse 24, 48149 Münster, Germany (bahlbur@uni-muenster.de)

(2) Departamento Académico de Geología, Universidad San Antonio Abad del Cusco, Cusco, Peru

KEY WORDS : Peru, Ordovician, volcaniclastic successions

INTRODUCTION

The Ollantaytambo Formation is exposed extensively in the vicinity of the Inca archeological site of Ollantaytambo located in the Cordillera Oriental of southern Peru. This lithostratigraphic unit was first mentioned by Marocco (1978) who described the 'Serie de Ollantaytambo' as a Cambrian to possibly Early Ordovician succession of quartzites, ignimbrites, tuffaceous, partly dark shales, and sandstones of at least 1000 m thickness. Until now no fossils have been found in the rocks. To our knowledge the volcanic rocks included in the Ollantaytambo Formation represent the only evidence of syndepositional volcanic activity in the Early Paleozoic of the Cordillera Oriental of southern Peru and northern Bolivia. It is therefore of key significance for the interpretation of the plate tectonic evolution of the Early Paleozoic Gondwana margin in the northern Central Andes.

STRATIGRAPHIC RELATIONSHIPS

The base of the Ollantaytambo Formation is not exposed. At the top it is overlain concordantly by Ordovician conglomerates and sandstones of the Veronica Formation, which, in turn, is separated from overlying finer grained sandstones and shales of biostratigraphically dated Arenig-Llanvirn age (San José Formation) by an unconformity (Carlotto and others, 1996). Furthermore, Carlotto and others (1996) indicate the presence of an unconformity in some localities between the Ollantaytambo and San José Formations where the Veronica Formation is missing. However, this contact we now interpret as a duplex structure within the Ollantaytambo Formation related to the Tertiary Andean deformation in an otherwise conformable stratigraphic succession of the Ollantaytambo and Veronica Formations. However, there may be some syndepositional scouring at the base

of the Veronica Formation which appears to represent an up to 500 m thick and c. 10 km wide complex of stacked channels. In the continued absence of biostratigraphically indicative fossils the Ollantaytambo Formation has to be considered as Cambrian—Early Ordovician or Early Ordovician in age.

LITHOLOGY AND GEOCHEMISTRY

The most notable unit within the Ollantaytambo Formation is a ca. 100 m thick hydroclastic breccia which constitutes the foundation on which the Ollantaytambo archeological site has been built. The breccias occur above an at least 100 m thick succession of relatively quartz-rich sandstones and interbedded thinner shales and is associated with green shales which probably represent redeposited tuff. The breccias consist of a recrystallized former glassy groundmass with angular mafic clasts of variable size, but not larger than c. 6 cm. Most of the clasts show chilled rims indicative of the extrusion of hot magma into ambient water. The breccia is overlain by green colored fine grained volcaniclastic sandstones, siltstones and shales which pass into quartz-rich sandstones and shales, some of which show normal grading indicative of deposition from turbidity currents.

The petrographical and geochemical study of the different lithologies of the Ollantaytambo Formation is presently under way First results of the geochemical analysis of the breccias, of individual larger hydroclasts contained in the breccias, as well as of the associated tuffs, shows that these rocks are the product of calc-alkaline basaltic to andesitic volcanism which at least in parts took place subaqueously. Chondrite-normalized element patterns show a moderate enrichment of the LREE with La_N/Yb_N ratios of 7-14, and a weak Eu anomaly. Pronounced negative Nb and Ta anomalies are considered indicative of a magma evolution in an arc environment.

In contrast to this, the overlying sandstones and shales are compositionally relatively mature and have geochemical features reflecting upper crustal sources.

CONCLUSIONS

The Cambrian—Ordovician basin in the Cordillera Oriental of southern Peru and northern Bolivia has been variably interpreted as an aulacogen, a back-arc rift or a passive margin (Sempéré, 1995; Gohrbrandt, 1992; Keppie and Ramos, 1999). These interpretations were mainly based on regional considerations, as well as the compositional maturity, large areal extent and considerable thickness of the Early Paleozoic sedimentary rocks in the Cordillera Oriental. Our new and still preliminary data indicate the presence of an active Cambro—Ordovician volcanic arc in this region. In view of the limited exposure and stratigraphical range of the volcanic rocks of the Ollantaytambo Formation this arc may have been of only limited spatial and temporal extent. However, it may alternatively represent a northern extension of the Famatinian arc system in the southern Central Andes and thus form part of a large scale plate tectonic feature.

REFERENCES

Carlotto V., Gil W., Cárdenas J., and Chavez R. 1996. Geología de los cuadrangulos de Urubamba y Calca, hojas 27-r y 27-s 1:100,000. Instituto Geológico Minero y Metalurgico Boletin 65, Serie A: Carta Geológica Nacional, 245.

Gohrbrandt K.H.A. 1992. Paleozoic paleogeographic and depositional developments on the proto-Pacific margin of Gondwana: their importance to hydrocarbon accumulation. Journal of South American Earth Sciences 6, 267-287.

Keppie J.D. and Ramos V.A. 1999. Odyssey of terranes in the Iapetus and Rheic oceans during the Paleozoic. In: Ramos V.A. & Keppie J.D., eds., Laurentia-Gondwana connections before Pangea. Geological Society of America Special Paper 336, 267-276.

Marocco R. 1978. Un segment E-W de la chaîne des Andes peruviennes: la déflexion d'Abancay. Etude géologique de la Cordillère orientale et des hauts plateaux entre Cuzco et San Miguel, sud de Pérou (12°30'S à 14°00 S). Géologie des Andes péruviennes, Travaux et documents de L'O.R.S.T.O.M. 94, 195 pp.

Sempéré T. 1995. Phanerozoic evolution of Bolivia. In: Tankard A.J., Suarez-Soruco S., and Welsink H.J., eds., Petroleum basins of South America. American Association of Petroleum Geologists Memoir 62, 207-230

VOLCANOGENIC EVIDENCES OF THE NORTH ANDEAN TECTONIC SEGMETATION: VOLCANOES SUMACO AND EL REVENTADOR, ECUADORIAN SUBANDEAN ZONE

Roberto BARRAGAN (1) and Patrice BABY(2)

(1) Amerada Hess Corporation, P.O.Box 20316, Libreville, Gabon, Africa
(2) IRD (ex-ORSTOM), Unité de Recherche 104, Université Paul Sabatier, Toulouse III, 38 rue des Trente-Six Ponts, 31400 Toulouse, France.

KEY WORDS: *shoshonites, adakites, partial melting, incompatible elements, HFS, LILE*

INTRODUCTION

The Ecuadorian Andes, characterized by two parallel chains called the Occidental Cordillera (west) and the Cordillera Real (east), present a third volcanic zone consisting of back-arc volcanoes along the northern subandean zone (Napo uplift) (Fig 1). In spite of being developed along the same basement, corresponding to the Phanerozoic sedimentary section of the Amazonian Oriente Basin, these subandean volcanoes show a strong compositional variation :

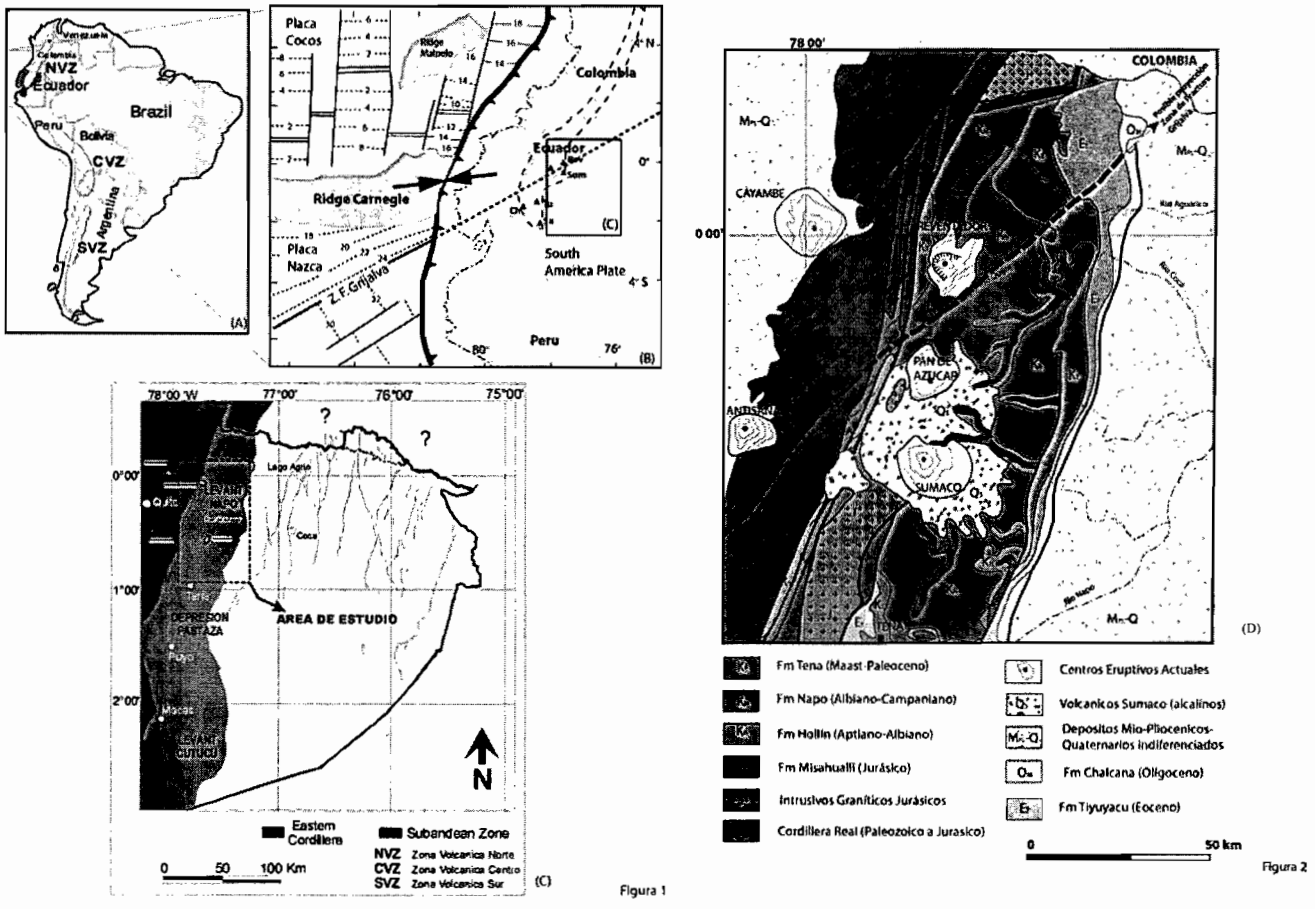

Figura 1

Figura 2

Figure 1: Location map: (A) active volcanic zones along de Andean Cordillera. (B) present-day subduction system along the Ecuadorian margin (modified from Monzier et al., 1999). (C) Northern Ecuadorian Subandean Zone and (D) synthetic geologic map of the study area (Napo uplift).

The Sumaco volcano, located towards the South of the Napo uplift, is characterized by distinct alkaline lavas strongly subsaturated in silica (Fig. 2). They are feldespathoid-bearing phonolites, basanites and tephrites (Barragan, 1998). The alkaline mineral assemblage is reflected in the major elements compositions of the lavas, which shows their shoshonitic affinity. Sumaco's lavas are enriched in all of the incompatible and light-REE elements compared with the rest of volcanoes of the northern Andean zone.

The Reventador volcano, located in the northern part of the subandean Zone and separated just 50 km from Sumaco volcano (Fig. 1), is characterized by a succession of basaltic andesites, andesites and dacites lavas that belong to the medium-high-K calc-alkaline clan (Fig. 2). The lavas of El Reventador are distinguished by high contents in Al_2O_3 (> 18%) and Sr (> 800 ppm), by low values of Y (13-17ppm) and Yb (< 1,57 ppm), in addition to Sr/Y ratios > 47, which suggest a typical adakitic affinity (Defant and Drummond, 1990; 1993).

The $^{87}Sr/^{86}Sr$ and $^{143}Nd/^{144}Nd$ ratios of lavas from volcano Sumaco and El Reventador range from 0,704195-0,704538 and 0,512895-0,512715, within the global range of island arc lavas and similar to the values observed in the Southern Volcanic Zone (Hawkesworth et al., 1993; Davidson et al., 1990) (Fig. 3), suggesting small extents of crustal assimilation.

Trace element abundances in the studied volcanoes and from other Holocene volcanic centers of the present Ecuadorian magmatic arc are plotted normalized to MORB values (Fig. 4). Absolute concentrations of most of the incompatible and REE elements increase strongly towards Sumaco volcano enriched in a 5 to 1 relation with respect to the rest of Ecuadorian Andean volcanoes (Table 1). All of the compared volcanoes are characterized by anomalously low concentration of HFS relative to LIL elements which is a nearly ubiquitous feature of subduction-related lavas and is considered to be inherent from fluids derived from the subducted lithosphere (Hickey et al., 1986). Although the Sumaco's lavas are most strongly enriched in all incompatible elements, they have the lowest LIL/HFS ratios, similar to the observed range in basalts of oceanic islands, suggesting less slab contribution (Barragan et al., 1998) (Fig. 5).

The concentrations of incompatible elements increase towards Sumaco volcano as does the La/Yb ratios, suggesting that magmas of this volcano are the result of progressively lower degrees of partial melting of the mantle wedge associated to normal subduction processes (Hickey et al., 1986). The anomalous adakitic signature observed in El Reventador lavas suggests that a lithospheric tear is present allowing melting of oceanic subducted lithosphere and limiting the distal portions of the aseismic zone that marks the Carnegie Ridge flat slab segment (Gutscher et al., 1999). Although, it has been suggested an affinity of the Sumaco shoshonitic lavas to basalts of high Nb (Bourdon et al., 2001). Nevertheless, this observation is opposite by the high values in the Ba/La (> 20), and La/Nb (> 2) ratios, ruling out any type of relation nor with high Niobium basalts (Reagan and Gill, 1989), nor with respect to the adakitic signature observed in El Reventador lavas.

CONCLUSIONS

The subandean volcanoes, El Reventador and Sumaco, show a strong compositional variation in spite of being developed along the same basement. The systematic variation in the composition is demonstrated to be controlled by the depth of the Benioff zone suggesting that independent subduction zones control the generation of these magmas.Then, it is proposed a volcanogenic limit oriented NE-SW that separates two different volcanic

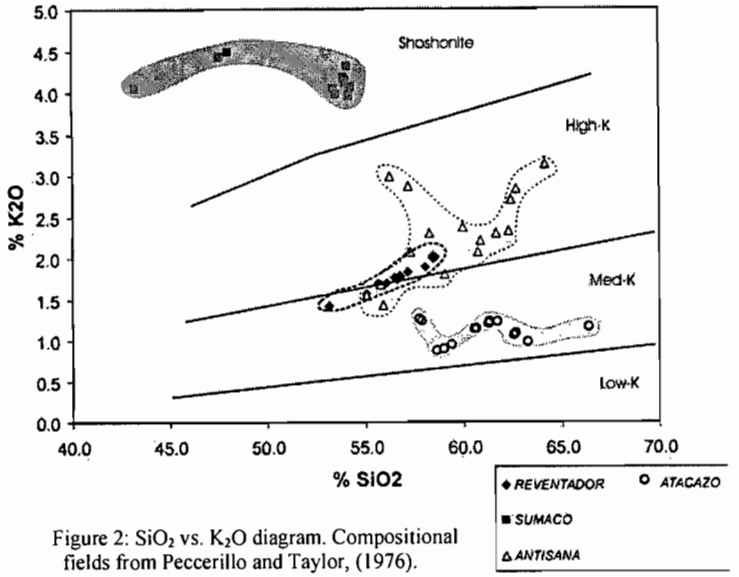

Figure 2: SiO_2 vs. K_2O diagram. Compositional fields from Peccerillo and Taylor, (1976).

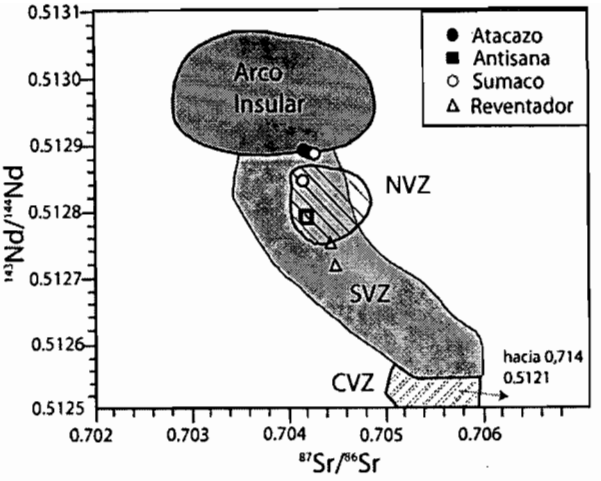

Figure 3 Sr and Nd isotopic ratios for the Sumaco and Reventador volcanoes. Additional compositional fields correspond to the different Andean volcanic zones (modified from Barragan et al., 1998)

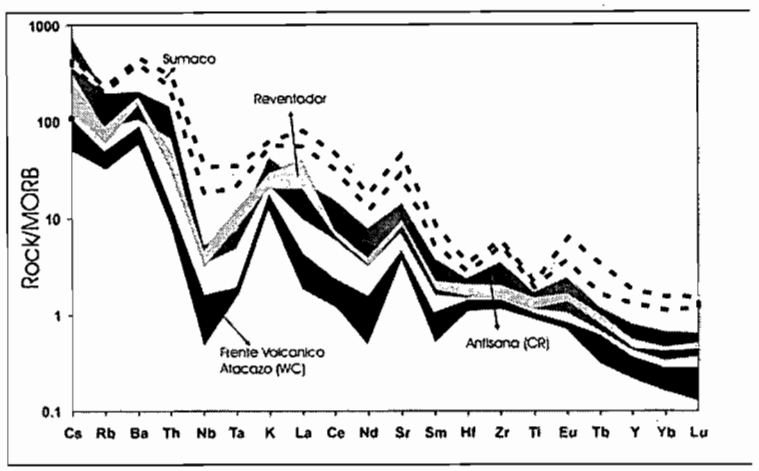

Figure 4: MORB-normalized spider diagram

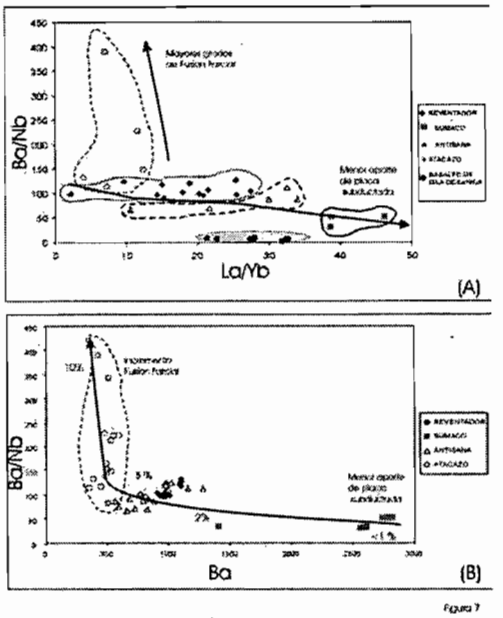

Figure 5: a) LIL/HFS vs. LIL (i.e., Ba/Nb vs. Ba) and (b) Ba/Nb vs. La/Yb. 1 to 10% values are hypothetical

zones or subduction systems. To the north, El Reventador volcano, characterized the distal part of the aseismic zone corresponding to the adakitic trend of the northern Ecuadorian Andes that mark the flat slab subduction of the Carnegie Ridge (Gutschter et al., 1999). To the south, the Sumaco volcano is associated to normal subduction event of the older Oligocene Farallon oceanic crust in the Ecuadorian Andean back-arc. The shoshonitic signature results from low degrees of partial melting and a smaller contribution of the subducted slab. Thus, the volcanogenic limit corresponds to a Tear Zone along the Grijalva fracture zone projected towards the continent previously defined by Hall and Wood (1985) and Gutschter et al. (1999).

ACKNOWLEDGEMENTS : Research supported by INSU grant 99PNSE59 and IRD (Tectonique, érosion et sédimentation dans le bassin de l'Amazone : du Mio-Pliocène à l'Actuel).

REFERENCES

Barragán R., Geist, D., Hall, M., Larson, P., and Kurz, M., 1998. Subduction controls on the compositions of lavas from the Ecuadorian Andes, Earth Planet. Sci. Lett. **154**, 153-166.

Bourdon, E., Eissen, E., Gutscher M., Monzier, M., Robin, C., Samaniego, P., Hall, M., Maury, R., Martin, H., Bassoullet, C., Cotteen, J., 2001. Respuesta magmática a la subducción de una cordillera asísmica: el caso de la margen Ecuatoriana. Cuartas Jornadas en Ciencias de la Tierra, Memorías-Anexos.

Davidson, J., McMillan, N., Moorbath, S., Worner, G., Harmon, R., Lopez-Escobar, L., 1990. The Nevados de Payachata volcanic region (18°S/69°W, N. Chile), II. Evidence fro widespread crustal involvement in Andean Magmatism, Contrib. Mineral. Petrol. **105**, 412-432.

Defant, M., and Drummond, M., 1990. Derivation of some modern arc magmas by melting of young subducted lithosphere. Nature, **347**, 662-665.

Gutscher, M., Malavieille, S., Lallemand, S., and Collot, J., 1999a. Tectonic segmentation of the North Andean margin: impact of the Carnegie Ridge collision, Earth Planet Sci. Lett. **168**, 255-270.

Hall, M., and Wood, C., 1985. Volcano-tectonic segmentation of the northern Andes, Geology, 13, 203-207.

Hawkesworth, C., Gallagher, K., Hergt, J., McDermott, F., 1993. Mantle and Slab contributions in arc magmas. Annu. Rev. Earth. Planet. Sci., **21**, 175-204.

Hickey, R., Frey, F., Gerlach, D., Lopez Escobar , L., 1986. Multiple sources for basaltic ans rocks from the southern volcanic zone of the Andes (34°-41°S): trace element and isotopic evidence for contributions from subducted oceanic crust, mantle and continental crust. Journal of Geophys. Reser., **91**, 5963-5982.

Monzier. M., Robin, C., Hall, M., Cotton, J., Mothes, P., Eissen, J., and Samaniego, P., 1997. Les adakites d'Equateur: modele preliminaie, C. R. Acad. Sci. Paris, **324**, 545-552

Reagan, M., and Gill, J., 1989. Coexisting Calcalkaline and High Niobium Basalts from Turrialba Volcano, Costa Rica. Jour. Geophys. Res., **94**, B4, 4619-4633.

	Volcan Reventador		Volcan Sumaco	
	REV-2	*REV-11*	*3D2*	*GS-8*
SiO2	58.46	55.062	47.56	54.33
TiO2	0.779	0.934	1.29	0.77
FeO*	5.78	7.298	8.99	6.36
MgO	3.41	4.646	2.49	1.68
K2O	2.02	1.575	4.43	4.06
Na2O	4.28	3.888	6.77	6.35
P2O5	0.367	0.366	0.64	0.46
Zr	137	124	441	406
Ni	17	28	4	10
Ba	1107	834	2563	2822
Rb	49	36	125	104
Sr	846	802	4059	2605
Y	13	17	49	35
Nb	8.7	9.2	82	53
$^{87}Sr/^{86}Sr$	0.704538	0.704429	0.704243	0.704195
$^{143}Nd/^{144}Nd$	0.512715	0.512756	0.512893	0.512894
La	32	24	173	138
Ce	52.55	50.57	302	240
Nd	24.64	24.36	121	88.7
Sm	4.98	5.22	18.5	14.4
Eu	1.47	1.64	5.03	3.79
Tb	0.55	0.65	1.59	1.12
Yb	1.26	1.57	4.67	3.67
Lu	0.20	0.25	0.63	0.52
Th	5.13	4.58	27.8	29.8
U	1.60	1.36	7.26	10.1

Table1. Representative Geochemical analyses from Sumaco and Reventador volcanoes

CONCORDANT TITANITE U-Pb AGES OF CAMBRIAN TO SILURIAN HIGH T METAMORPHISM AT THE WESTERN EDGE OF GONDWANA (SOUTHERN PUNA AND WESTERN SIERRAS PAMPEANAS, ARGENTINA, 26 - 29°S)

Raul BECCHIO(1)(2) and Friedrich LUCASSEN(3)(4)

(1) Universidad Nacional de Salta, Buenos Aires 177, 4400 Salta, Argentina, (tato@unsa.edu.ar)
(2) Servicio Geológico y Minero Argentino. Av. Bolivia 4650 4400 Salta, Argentina
(3) GeoForschungsZentrum Potsdam, Telegrafenberg, 14473 Potsdam, Germany (Lucassen@gfz-potsdam.de)
(4) Freie Universität Berlin, FB Geowissenschaften, Malteserstr. 74-100, 12249 Berlin, Germany

KEY WORDS: Puna, Sierras Pampeanas, metamorphic rocks, isotopic dating

INTRODUCTION

The western margin of Proterozoic Gondwana has been substantially reworked by metamorphism and magmatism in an Early Palaeozoic mobile belt (ca 18° - 32°S) active between Cambrian and Silurian times (recent summaries ca 30° - 32°S, Pankhurst and Rapela (eds), 1998; ca 18 - 27°S, Lucassen et al., 2000). The metamorphism with widespread anatexis and extended crust-derived magmatism indicates high temperatures at a midcrustal level. High pressure rocks typical of collisional tectonic regimes are unknown. The mobile belt north of ca 28°S and east of the Argentine Precordillera south of ca 28°S formed part of Gondwana throughout its thermo-tectonic evolution, whereas the Argentine Precordillera is considered as an exotic terrane (Fig. 1) with a possible Early Ordovician age of docking (e.g. Casquet et al., 2001). Published ages of metamorphism indicate thermal events at ca 510 Ma in the Puna and at ca 470 - 460 Ma with a possible continuation of the high T into Silurian in the northern Sierras Pampeanas (Lucassen et al., 2000; Büttner et al., in revison) and at ca. 530-520 Ma and ca 460 Ma in the Southern Sierras Pampeanas south of ca 30°S (in: Pankhurst and Rapela (eds), 1998). The age of the metamorphism is unknown in many areas of the mobile belt and the evolution of the high T regime either in discrete peaks, i.e. at ca. 510 and 460 Ma, or as continuum is not well constraint. Timing of the high grade metamorphism is the base for any interpretation of the geodynamic setting, e.g. the docking of a terrane as an example for a discrete event or the long-standing activity of a continental magmatic arc. This study presents 16 new U-Pb ages of titanite mainly from calcsilicate rocks, two from migmatites and one amphibolite, all from upper amphibolite - granulite facies metamorphic rocks extending from the southern Puna into the western Sierras Pampeanas to ca. 30°S, east of the Precordillera exotic terrane (Fig. 1). Our results indicate that there is more than one 'event' and possibly a continuos evolution of the high T metamorphism at least from Mid-Ordovician to Silurian time.

PETROLOGY OF THE HIGH-GRADE METAMORPHIC ROCKS

In our working area, the Early Paleozoic metamorphic belt comprises the southern Puna which is part of the Cenozoic Andean High-Plateau and the Sierras Pampeanas which extend east and south of the Andean Plateau and east of the Andean Mountain chain (Fig. 1). In the southern Puna and in the Sierras Pampeanas the bulk of

the high-grade metamorphic rocks have silici-clastic protoliths and form monotonous gneiss - migmatite areas with little variation in the lithology. The mineral paragenesis of the gneiss-migmatite is quartz - plagioclase - biotite - minor garnet with potassic feldspar, alumo-silicate and cordierite in the more pelitic compositions. Marbles, calcsilicate rocks and amphibolites occur locally within this unit. Their thickness varies between dm and tens to hundred of meters. The typical mineral paragenesis of the calcsilicate rocks is calcite - quartz - plagioclase - clinopyroxene - garnet and accessory titanite with epidote, scapolite and amphibole in some samples. The temperature of metamorphism at all locations was above the wet granite solidus as indicated by

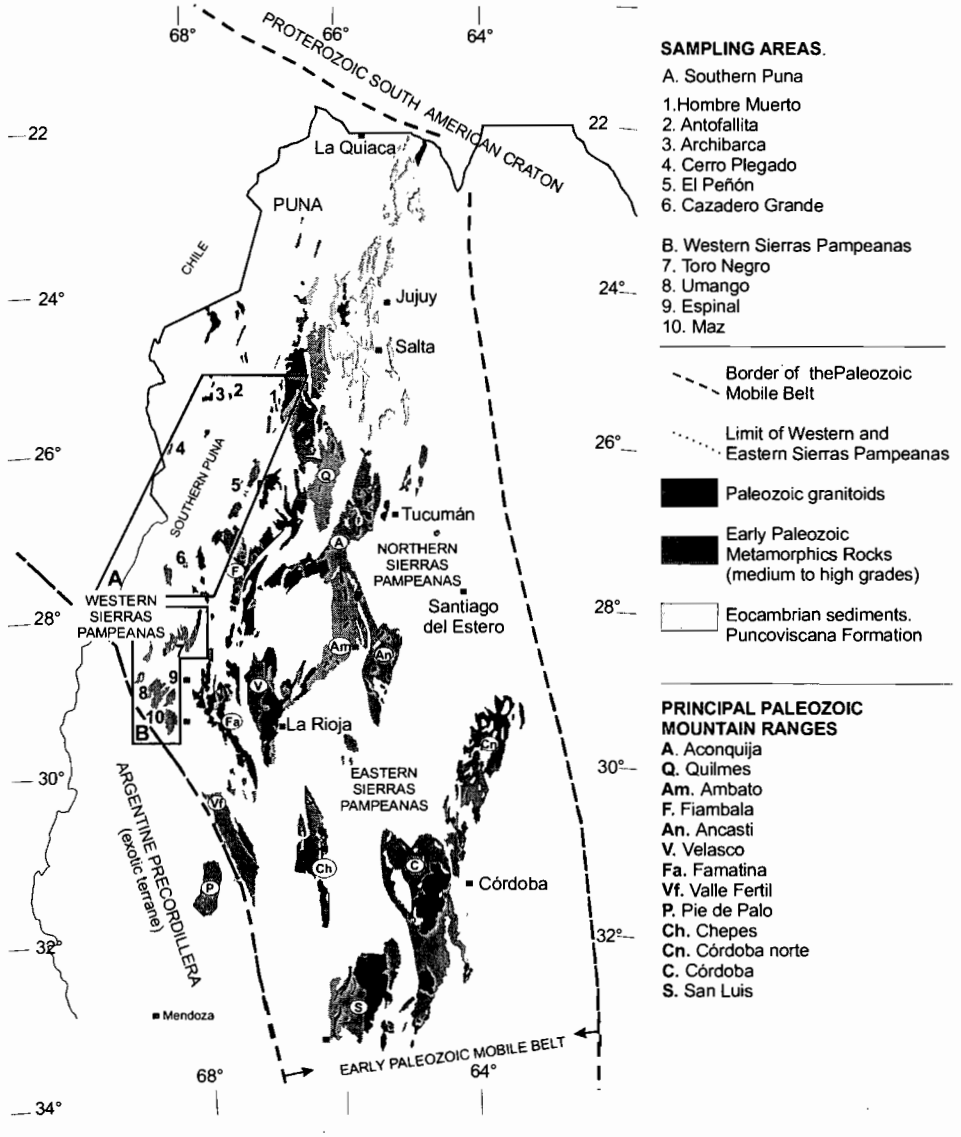

Figure 1 Geological map showing the distribution of Paleozoic magmatic and metamorphic rocks, our sample locations and the principal Paleozoic Mountain Ranges. Weighted means of the $^{206}Pb/^{238}U$ and $^{207}Pb/^{235}U$ *ages in Ma* and errors at the 95% confidence level for our sample sites are: (1) Hombre Muerto #4-164 *515±2, 514±2* (2,3) Antofalla-Archibarca #AN-25 *455±5, 452±4*; AN3-39 *464±10, 464±10* (5) El Peñon #01-22 *528±3, 525±3*; #01-24 *520±8, 523±7*; #7-100 *517±6, 515±6* (6) Cazadero Grande #01-35 *451±4, 449±5;* #01-43 *444±3, 446±3* (7)Toro Negro #01-54 *454±3, 451±2;* #01-60 *432±2, 433±5* (8) Umango #01-80 *425±4, 424±5;* #01-89 *422±5, 421±5* (9) Espinal #01-69 *465±1, 465±1;* #01-70 *466±1, 465±1* (10) Maz #01-108 *393±23, 381±25;* #01-111 *443±3, 443±3;* #01-116 *535±4, 539±4;* #01-125 *606±30, 657±30 (strongly discordant);* #01-128 *428±6, 431±3.* Ages of metamorphism (ca 530 Ma, U-Pb, Rb-Sr) are reported from Sierras de Cordoba (in Pankhurst and Rapela (eds), 1998) and ca 470 Ma (U-Pb ages Monazite and titanite) from Sierra de Quilmes (Büttner et al., in revision).

widespread anatexis of pelitic compositions. The peak metamorphic parageneses are preserved without thorough retrogression. Deformation occurs at T close to peak-metamorphic conditions in all sample areas with subsequent recovering of the microfabric still at high T. Subsequent deformation is located in shear zones (cm - km scale) and overprints the annealed fabrics still at high T and without change of the mineral paragenesis.

U-Pb DATING

Titanite characteristics. Titanite has long been recognised as suitable for U-Pb dating and its closure T is reasonable high (> 650°C) to record age of metamorphism of upper amphibolite facies grade. Euhedral titanite forms part of the stable mineral paragenesis in the calcsilicate. Optical and compositional zoning is absent in titanite. Major element patterns from microprobe analysis indicate no systematic overgrowth, inherited cores, or gradual compositional core-rim zoning by diffusion. We conclude from the textural position of the titanite and from its compositional pattern that it formed close to upper amphibolite facies conditions and has not been altered during retrogression. Thorough deformation at high temperature in shear zones is observed in the field and in the development of microfabrics. Dynamic recrystallization of the metamorphic mineral assemblage during deformation at high T would leave the stable mineral assemblage unchanged but may reset the U-Pb isotope system in the titanite.

U-Pb ages. The average values of $^{206}Pb/^{238}U$ and $^{207}Pb/^{235}U$ ages of five to six different titanite fractions from each sample are listed in Figure 1. The titanite shows a high content of radiogenic ^{206}Pb ($^{206}Pb/^{204}Pb$ > ca. 200 - 700) in most calcsilicate rocks, and, therefore, the uncertainties in the correction of the common lead content are minor. Most samples and fractions plot on or very close to the U-Pb concordia and only one sample is clearly discordant. Different size fractions of euhedral titanite from one sample yield identical ages and no influence of the cooling history or possible reheating is seen in their U-Pb systematics. In addition, the chemical homogeneity of the titanites and their appearance in the metamorphic fabric without reaction textures largely exclude a multistage development of titanite within a single sample. The following discussion is based on the assumption that the U-Pb ages present the age of formation of the titanite.

DISCUSSION

Reliable age data of high grade metamorphic rocks from Sierras Pampeanas and the Puna Plateau are scarce and only recently few U-Pb and Sm-Nd ages using metamorphic minerals became available (northern Sierras de Pampeanas; Büttner et al., in revision; 21-27°S; Lucassen et al., 2000; ca 30-32°S; southern Sierras Pampeans and Argentine Precordillera: in Pankhurst and Rapela (eds.), 1998). The Neoproterozoic - Cambrian Pampean orogeny and the Ordovician - Silurian Famatinian orogeny have been previously constrained by the ages of two distinct magmatic - sedimentary cycles (def. by Aceñolaza and Toselli, 1976; see also in Pankhurst and Rapela (eds.) 1998). Pampean (530 - 510) and Famatinian ages (470- 400) are now well established in the high temperature metamorphic rocks in the southern Puna and western Sierras Pampeanas (Fig. 1). Famatinian ages have been also found in high grade metamorphic rocks of the Chilean Precordillera at ca 21°S (ca 470 - 420 Ma, U-Pb ages on titanite; own unpublished data,F. Lucassen). Proterozoic ages of metamorphism seem to be absent in the whole area. The age gap of ca 40 Ma between Pampean and Famatinian metamorphism might be an artefact of the scarce data. The ages of Famatinian crust-derived magmatism of Sierras Pampeanas and south-eastern Puna (ca 495 - 460 Ma; e.g. Pankhurst et al. 2000) suggest a continuation of the Cambrian high T conditions in the crust during the Early Ordovician. Ages of metamorphic rocks from Sierras de Maz, Umango

and Espinal (Fig. 1), at the eastern edge of the Argentine Precordillera, show the complexity of age relations: concordant U-Pb ages of ca. 530, 460, 440, 430, 420, 400 Ma and one strongly discordant titanite sample (#01-125, Fig.1) document a polymetamorphic (or polydeformational) development. A meaningful interpretation of these ages of high grade metamorphism (deformation) in terms of tectonic events is not possible at the present state of knowledge. Provided the proposed eastern boundary of the Precordillera terrane is correct, the Sierras de Maz , Umango and Espinal formed part of the western leading edge of Gondwana. Sierra de Maz was metamorphosed at ca 530 Ma before docking of the Precordillera terrane, contemporaneous and at similar high T and moderate P as the Pampean orogen in the southern Sierras Pampeanas, Southern Puna, and N Chile. Given the docking age of the Precordillera was lower Ordovician (>460 Ma; Casquet et al., 2001) high T metamorphism and deformation occurred after the possible collision of the Precordillera at ca 460, 440, 430, 420 and 400 Ma, contemporaneous with the widespread magmatism and metamorphism of the Famatinian orogeny in the Sierras Pampeanas, the southern Puna and N Chile. Pampean and Famatinian metamorphism formed a regional important belt with more than 1000 km N-S extension of metamorphic rocks at the western edge of Gondwana. Age data of metamorphic and magmatic rocks indicate high T conditions in this crust over a time span of at least 70 Ma, possibly 130 Ma. However, variations in the metamorphic grade are small and mineral parageneses are similar at the different sample-sites. At least for the Ordovician history heating - deformation- cooling - reheating - deformation etc. seems unlikely and we propose reset of the U-Pb isotope system by repeated deformation and dynamic recrystallization in shear zones which all formed at similar P-T conditions. High grade shear zones are observed e.g. in Sierra Umango and described in detail from Sierra de Quilmes (northern Sierras de Pampeanas; Büttner et al., in revision). To unravel details of the timing and regional importance of deformation in the high-grade metamorphic rocks detailed fieldwork on their structural features is necessary.

REFERENCES

Aceñolaza F.G. and Toselli, A.J. 1976. Consideraciones estratigráficas y tectónicas sobre el Palozoico inferior del Noroeste Argentino. Mem. II Congreso Latinoamaricano de Geologia 1976, 2, 755-764, Caracas

Büttner et al. (in revision) Static heating and retrograde Ordovician extension in the Sierra de Quilmes, Sierras Pampeanas (NW Argentina): A non-collisional evolution. Journal of Metamorphic Geology

Casquet et al. 2001. Involvement of the Argentine Precordillera terrane in the Famatinian mobile belt: U-Pb SHRIMP and metamorphic evidence from the Sierra de Pie de Palo. Geology 29, 703-706.

Lucassen et al., 2000. Proterozoic-Paleozoic development of the basement of the Central Andes (18-26°S)- a mobile belt of the South American craton. Journal of South American Earth Sciences 13, 697-715.

Pankhurst R.J. and Rapela C.W. (eds) 1998. The Proto-Andean Margin of Gondwana. Geological Society of London Special Publication 142, London.

Pankhurst et al., 2000. Age and origin of coeval TTG, I- and S-type granites in the Famatinian belt of NW Argentina. Trans Royal Soc Edinburgh Earth Sciences 91, 151-168.

NATURE AND ORIGIN OF HYDROTHERMAL FLUIDS DURING THE LOW-GRADE METAMORPHISM OF JURASSIC-TERTIARY VOLCANIC SUCCESSIONS IN THE CHILEAN ANDES (35° S) - PRELIMINARY RESULTS

Mauricio BELMAR(1), Susanne Th. SCHMIDT (2), Joseph MULLIS(3)

(1) Departamento de Geología, Universidad de Chile, Casilla 13518, c 21, Santiago.(mbelmar@ing.uchile.cl)

(2) Département de Minéralogie, Rue des Maraîchers 13, CH-1211 Genève, Switzerland

(3) Mineralogisch-Petrographisches Institut, Bernoullistr. 30, CH-4056 Basel, Switzerland

KEY WORDS: Fluid inclusion study, stable istope analysis, low-grade metamorphism, zeolite facies, prehnite-pumpellyite facies

GEOLOGICAL SETTING

A ca. 6000 m thick section of mainly volcanic and volcanoclastic as well as some marine and alluvial sedimentary rocks is exposed in the upper Río Tinguiririca and Río Damas valleys. It comprises the Río Damas Formation, characterized by a ca. 3700 m thick sequence of red continental detrital and volcanic rocks. The lower part contains abundant volcanic breccias of various sizes, whereas in the upper part andesitic basaltic lava flows are intercalated. A Kimmeridgian age is assumed based on the fossiliferous age of younger and older rock units. The Baños del Flaco Formation lying on top of the Río Damas Formation has an approximate thickness of 390 m and is a marine fossiliferous unit. Calcarenites and calclutites represent a platform facies whereas the shale horizons indicate a facies evolution to a deep shelf environment (Arcos, 1987). Based on several ammonite species, a Tithonian age was determined (Covacevich et al., 1976; Biro-Bagoczky, 1984). The Baños del Flaco Formation is conformably overlain by the ca. 200 - 250 m thick Brownish-red Clastic Unit. It represents a continental unit with mainly volcanic breccias in the lower part and conglomerates and conglomeratic sandstones in the stratigraphically thicker upper member. The Brownish-red-Clastic unit is unconformably overlain by the Coya-Machalí Formation (Zapatta, 1995). The ca. 1600 m thick sequence is of a volcanic character with alternating basaltic lavas and pyroclastic and detrital sediments. Various plutons, hypabyssal or subvolcanic bodies, dikes, and sills of mostly unknown age are exposed in the study area. The biggest pluton of the study area occurs at the Río Damas Pass. It is not explicitly dated but geochemical similarities suggest that it probably belongs to a group of intrusive bodies known as the Nacimiento Río Cortadera pluton, described only a few kilometers to the North. Age determinations on biotite cluster at 8.4±0.3 Ma. Intrusive bodies to the west give

age determinations of 14.1±0.4 Ma (in Spichiger 1991) and correspond to the belt of lower Miocene Intrusions of Santa Rosa de Rengo and La Obra.

LOW-GRADE METAMORPHISM

The metamorphic pattern in the study area will be documented by the distribution of several index minerals from a large data base of ca. 4000 microprobe analysis of volcanic rocks as well as by X-ray diffraction of individual minerals such as zeolites and phyllosilicates. The illite and chlorite crystallinity method was applied to marine and fine-grained sediments, effusive volcanic and hypabyssal rocks. The vitrinite reflectance was also measured in all shales of the sequences (Belmar, 2000; Belmar et al., submitted).

Two metamorphic zones are observed. A zeolite zone with laumontite as the main index mineral in the Tertiary Coya-Machalí Formation, as well as in the upper Cretaceous Brownish-Red-Clastic Unit and the Upper Jurassic Baños del Flaco Formation. The lower Upper Jurassic Río Damas Formation lying below the Baños del Flaco Formation has experienced prehnite-pumpellyite facies in the lower part of the unit, whereas the upper part displays a non-diagnostic celadonite-K-mica-chlorite assemblage. No discontinuity in metamorphic grade is observed along the major unconformities, as between the Tertiary Coya-Machalí Formation and the Cretaceous Brownish-Red-Clastic Unit or the Cretaceous Brownish-Red-Clastic Unit and the Upper Cretaceous Baños del Flaco Formation. In the Coya-Machalí Formation, higher metamorphic prehnite-pumpellyite assemblages are observed within sills and dikes.

In addition, illite crystallinity, chlorite crystallinity and coal rank were determined and confirm the metamorphic facies pattern. The Coya-Machalí formation, belonging to the zeolite facies, yielded values of 221-276 °C with the "chlorite geothermometer. The Baños del Flaco Formation, belonging to the late diagenetic zone according to illite and chlorite crystallinity data, yielded peak temperatures derived from vitrinite reflectance data of 150-168 °C for a burial heating model and 175-204 °C for a hydrothermal metamorphism model. The Río Damas Formation, recording the transition from zeolite to prehnite-pumpellyite facies, yielded values of 223-272 °C with the "chlorite geothermometer.. In contrast to other low-grade metamorphic terranes where the smectite to chlorite transition is characteristic for the transition from the zeolite to the prehnite-pumpellyite facies, a K-mica/celadonite transition occurs which seems to be characteristic for the transition from the upper zeolite to the prehnite-pumpellyite facies in the K-rich rocks of the study area.

PRELIMINARY RESULTS

As described in the introduction, volcanic and volcanogenic rocks dominate in the study area. It is generally difficult to differentiate between effusive and hypabyssal intrusive rocks in the field, and the occurrence of amygdules or fluidal texture cannot be used as criteria for the determination of the effusive character of a rock. In addition, in the immediate proximity of intrusive rocks the regional metamorphic pattern is overprinted by contact metamorphism producing hornfels assemblages. The first results on the fluid inclusions indicate that in the Termas del Flaco area various types of hydrothermal/meteoric/basinal fluids can be observed. An amygdule with pumpellyite followed by quartz and calcite towards the center of the amygdule (TF10-12) is

considered to be the result of the regional metamorphic prehnite-pumpellyite facies. Four different fluid inclusion populations are observed in quartz. Fibrous quartz overgrowths pumpellyite and contains a metastable aqueous fluid. A second generation of quartz occurs at the top of the quartz fibers as a prismatic overgrowth. The homogenisation temperature of the fluid inclusions of this second quartz generation was determined at 92 °C and the salinity corresponds to 15 NaCl %equiv. The continous overgrowth of quartz shows in the third fluid inclusion generation an increase of the salinity to ca. 30% NaCl %equiv and a T_{hom} of 85 °C. A fourth fluid inclusion populationis similar to the second generation with T_{hom}=93°C and a salinity of 14 NaCl %equiv. A specimen close to an intrusion shows a population with a low salinity, a high CO2 content.and a T_{hom}=290 °C. Another specimen was taken from a vein within the marly shists of the Baños del Flaco Formation (TF1-10): It shows 2 fluid inclusion populations. The first generation contains higher hydrocarbons and a T_{hom}=222°C, and the second generation contains a nearly pure propan-dominated population. The preliminary results indicate that various types of fluids circulated within the various rock types ranging from meteoric to high saline and organic rich compositions. A stable isotope analysis on quartz and and calcite is currently being carried out to help to constrain the conditions and the nature of the altering fluids in the Termas del Flaco area .

ACKNOWLEDGEMENTS

This researchs are financially supported by "Fundación Andes Grant" and from the Universidad de Chile and Ministerio de Educacion through the "MECESUP Grant". We would like to thank the Servicio Nacional de Geología y Minería (SERNAGEOMIN) for logistic support in the field. The Swiss National Science Foundation Grants Nr. 20-43122.95, 20-50625.97 and 20-56842.99 supported the previous metamorphic study in the region.

REFERENCES

Arcos, R. (1987). Geología del Cuadrangulo Termas del Flaco, Provincia de Colchagua. VI región, Chile. Memoria de título, *Departamento de Geología, Universidad de Chile.*

Belmar, M. (2000) Low-grade metamorphism in Central Chile at 35ª S. Ph D. Thesis, Basel, Switzerland. University of Basel, 189p.

Belmar, M., Schmidt, S. Th.. Frey, M. Ferreiro-Mählmann, R., Mullis, J., Stern, W.B. (under review) Diagenesis, low-grade and contact metamorphism in the Triassic-Jurassic of the Vichuquén-Tilicura and Hualañe-Gualleco Basins, Coastal Range of Chile. *Submitted to the Swiss Bulletin of Mineralogy and Petrology.*

Biro-Bagoczky, L. (1984). Nuevos antecedentes paleontológicos y estratigráficos de algunos afloramientos Titono-Neocomianos en la Cordillera Chilena, entre los 33°45' y 35° lat. Sur. *International Geological Programme, Project 171; Circum-Pacific Jurassic*, Repot 2, Special Paper 3.

Charrier, R.,Wyss, A., Flynn, J. 1996. New evidence for late Mesozoic-Early Cenozoic evolution of the Chilean Andes in the Upper Tinguiririca Valley (35ª), Central Chile. Journal of South American Earth Sciences 9,393.

Covacevich, V., Varela, J. & Vergara, M. (1976). Estratigrafía y sedimentación de la Formacion Baños del Flaco al sur del Río Tinguiririca, Cordillera de los Andes, Provincia de Curicó, Chile,. *1*, A191-A211. Primer Congreso Geológico Chileno, Santiago, Chile.

Spichiger, S. (1993). Geología y estilo estructural de un perfil de los Andes chilenos a 35° de lat. Sur, con énfasis en la Cordillera de la Costa, VII Región. Memoria de titulo, 112p, *Departamento de Geologia, Universidad de Chile*

Zapatta, F. (1995). Nuevos antecedentes estratigráficos y estructurales del área de Termas del Flaco, valle del Río Tinguiririca, VI Región, Chile. Memoria, 122p, *departamento de Geologia, Universidad de Chile.*

UPLIFT AND ACTIVE DEFORMATION OF THE PASTAZA ALLUVIAL FAN (SUBANDEAN ZONE OF ECUADOR)

Séverine BÈS DE BERC (1),(2), Patrice BABY. (2), Jean-Claude SOULA (2), SOURIS M. (3) and Jaime ROSERO (4)

(1) IFEA (Institut Français d'Etudes Andines), Whymper 442 y Coruña, AP 17 12 857 - Quito, Ecuador (sevebdb@interactive.net.ec)

(2) IRD/ LMTG – UPS, 38, rue des 36 Ponts – 31400 Toulouse (baby@cict.fr ; jcsoula@cict.fr)

(3) IRD, Quality House Convent, 38 Convent Rd, Silom, Bangrak, Bangkok 10500 (souris@ird.fr)

(4) PerezCompanc – Suiza 209 y Eloy Alfaro – Quito, Ecuador (jrosero@pecom.com.ec)

KEYWORDS : Ecuador, Subandean zone, Fluvial Terrace, Volcanic Terrace, Quaternary, Aluvial Fan, Lahar

INTRODUCTION

The Pastaza megafan constitutes the largest humid tropical fan in the world (Räsanen et al., 1992). The apex of this megafan is situated between the Ecuadorian Subandean domes of Cutucú and Napo at the outlet of the Rio Pastaza (Fig.1), whose catchment is situated in the Interandean depression. Actually, the Rio Pastaza runs across the Cordillera Oriental before debouching into the megafan. It drains the flanks of the Ecuadorian stratovolcanoes Cotopaxi, Sangay, Tungurahua, Altar, Chimborazo and Carihuairazo, and continues to receive massive amounts of volcanoclastic debris (Hall, 1977).

The Pastaza megafan is made up of Miocene to Pleistocene deposits (Chambira Fm.), including the late Pleistocene Mera Formation (Tschopp, 1953) mainly composed of catastrophic volcanoclastic (andesitic) debris flows from the Tungurahua volcano, interfering with pure fluvial sedimentation.

The Eastern Cordillera constitutes a relatively narrow thrust and fold belt, which overrides the Subandean Zone (Baby et al., 1999) along the Abitagua batholite thrust (Fig. 2 and 3), still active to day as revealed by the Baeza seismic event (Ms = 6.9, 1987). Both the Eastern Cordillera and Pastaza megafan are incised by the Pastaza River and principal tributaries, which indicates general uplift in the orogen. The present paper is aimed at comparing incision and incision rates in the megafan and the Eastern Cordillera in order to distinguish overall and local incision and analyze their causes by means of a study of the construction of the fluvial terraces.

THE UPPER PASTAZA VALLEY

In most of the Upper Pastaza valley (Fig.3), large-volume catastrophic deposits and lava flows interferes with the normal pure fluvial deposits. These deposits form a series of aggradations terraces and lava (flows) deeply incised by the present-day Pastaza River, which have been used as geomorphic and age markers for incision rate measurements.

The most spectacular example is provided by an andesitic lava-flow, the "Juive Chico Pre-historic" flow produced by the Tungurahua volcano, which filled the Pastaza valley over at least 30 km. It sealed a fluvial pebbles level and provides actually an excellent geomorphic surface. Dating of the basis and top of this lava flow has given ages of 1470 +/- 85 y.BP and 2215 +/- 90 y.BP (Hall *et al.*, 1999). Differential GPS measurements show that the height of the lava above the present-day stream bed varies between 65 m along the 30 km elongate lava flow. Incision rate thus appear as ranging here from **4.74 to 7.14 cm/year**.

The importance of incision is also spectacularly shown in the small Santa Ines – Rio Negro piggy-back basin formed on the rear of the Abitagua thrust sheet, where are preserved rather thick and wide terraces (Fig.3). There, charcoal from the best-preserved fluvial terrace, 54m above present-day river level, gives a ^{14}C age of 1 ky BP, which indicates an incision rate of **5.4 cm/year**.

THE PASTAZA MEGAFAN

Morphoscopic studies show that the upper surface of the Pastaza fan constitutes, at least in the whole upper part of the fan, a well characterized geomorphic marker which can be used as a reference surface because of the scarcity of post-depositional tectonic structures. This surface is incised by the antecedent Pastaza River and main tributaries, which now shifted toward the southeast.

On the apex of the alluvial fan (near Mera), where the Pastaza River emerges onto the lowlands (Oriente basin), a thick unit of andesitic breccias with chaotic internal structure typical of debris avalanche deposits (lahar) forms a broad terrace (Mera Fm.; Tschopp, 1953). It constitutes the remnant mounds of a massive avalanche related to a sector collapse that followed the Tungurahua I constructional period (Hall *et al.*, 1999).

At the top of this Mera lahar terrace (Figs. 1 and 3), an organic soil recognized under braided-stream deposits, gives a ^{14}C age of 17 920 +/- 70 y.BP. These fluvial sediments are now located 80 m above the present-day Pastaza stream, which indicates an incision rate of at least **0.44 cm/years.**

DISCUSSION AND CONCLUSIONS

The incision measurements in the Pastaza megafan indicate values ten times lower than in the Upper Pastaza. Since no tectonic event has deformed significantly the fan surface from late Pleistocene to present-day

and no base level comparable with the measured incision was recorded during this period, the incision measured in the fan is likely to represent the overall orogen uplift.

The much higher incision rated measured in the Upper Pastaza valley indicates the occurrence of local events. The high incision rate, measured in the Santa Ines – Rio Negro back limb basin, can be attributed to the uplift due to the Abitagua thrust, which limits the Cordillera Oriental from the Subandean zone (Figs. 2 and 3). The modern activity of this fault is attested by the strong seismicity of the Subandean region (see Baby et al., this issue). This strong incision indicates that active headward erosion was associated with thrusting. Although somewhat higher, the values of incision rates measured in the Upper Pastaza valley are actually comparable with those obtained in the outer Himalayan thrust and folds (Avouac, 1991; Van Der Woerd et al., 2001). These high incision rates are thus likely to have a result of local tectonics accompanying overall orogenic uplift.

ACKNOWLEDGEMENTS : Research supported by INSU grant 99PNSE59, IRD and IFEA (Tectonique, érosion et sédimentation dans le bassin de l'Amazone : du Mio-Pliocène à l'Actuel).

REFERENCES

Avouac J.P. 1991 - Application des méthodes de morphologie quantitative à la néotectonique. Modèle cinématique des déformations actives en Asie centrale - *Thèse de Doctorat Paris VII.*

Baby P., Rivadeneira M., Christophoul F., Barragan R. 1999 - Style and timing of deformation in the Oriente Basin of Ecuador, *4nd International Symposium on Andean Geodynamics (ISAG'99)*, Univ. Göttingen (Germany), Extended Abstracts Volume, 68-72.

Hall M.L. 1977. El Volcanismo en El Ecuador. – *Instituto Panamericano Geográfico Historico*, Quito, 120 p.

Hall M.L., Robin C., Beate B., Mothes P., Monzier M. 1999. Tungurahua Volcano, Ecuador : structure, eruptive history and hazards – J. Volcanol. Geotherm. Res. 91, 1-21.

Baby P., Legrand D, Bes de Berc S., Bondoux F., Rivadeneira M.2002. The 1999-2000 seismic experiment of the swarm of Macas (Ecuador) in relation with a SUBANDEAN unexpected wrench fault system - Isag 2002, this issue.

Räsänen M., Neller R., Salo J. and Jungner H. 1992. Recent and ancient fluvial deposition systems in the Amazonian foreland basin, Peru. – Geol. Mag. 129 (3), pp. 293-306

Tschopp H. 1953. Oil Explorations in the Oriente of Ecuador. – A.A.P.G. Bulletin, v. 37, pp. 2303-2347.

Van Der Woerd J., Xiwei Xu, Haibing Li, Tapponnier P., Meyer B., Ryerson F. J., Meriaux A.-S, Zhiqin Xu. 2001. Rapid active thrusting along the northwestern range front of the Tanghe Nan Shan (western Gansu, China) – J. Geophys. Res., 106, 30,475-30,504.

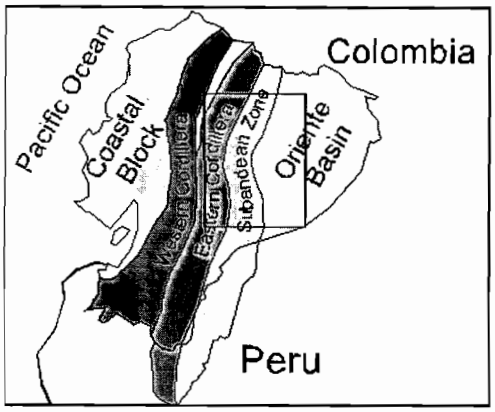

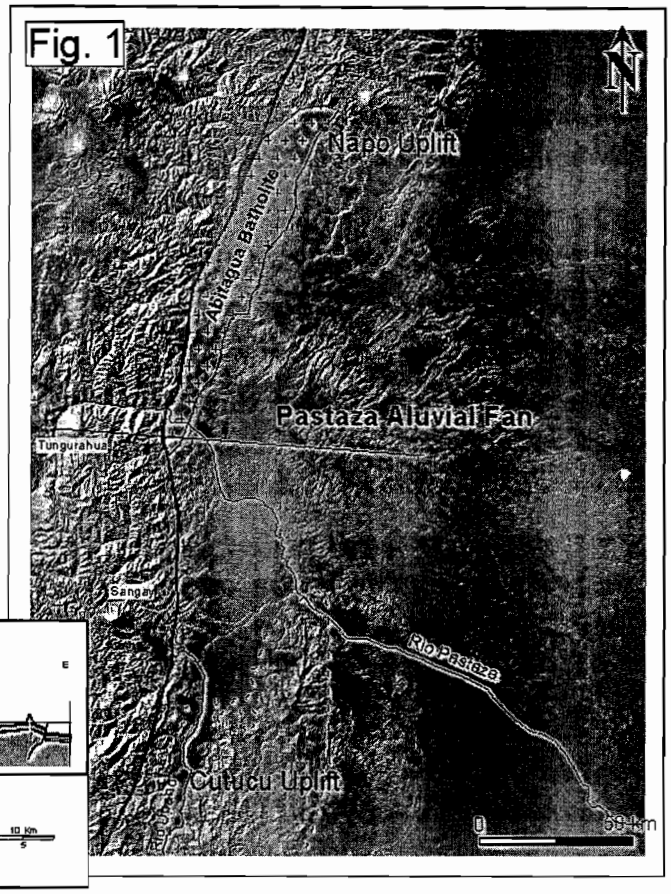

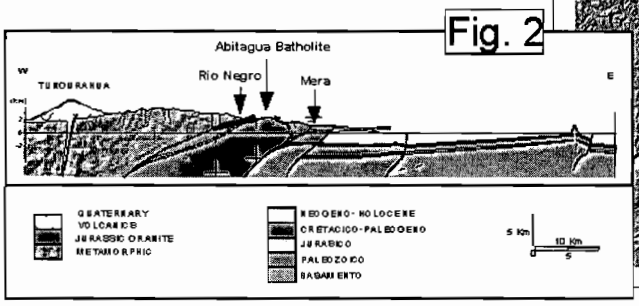

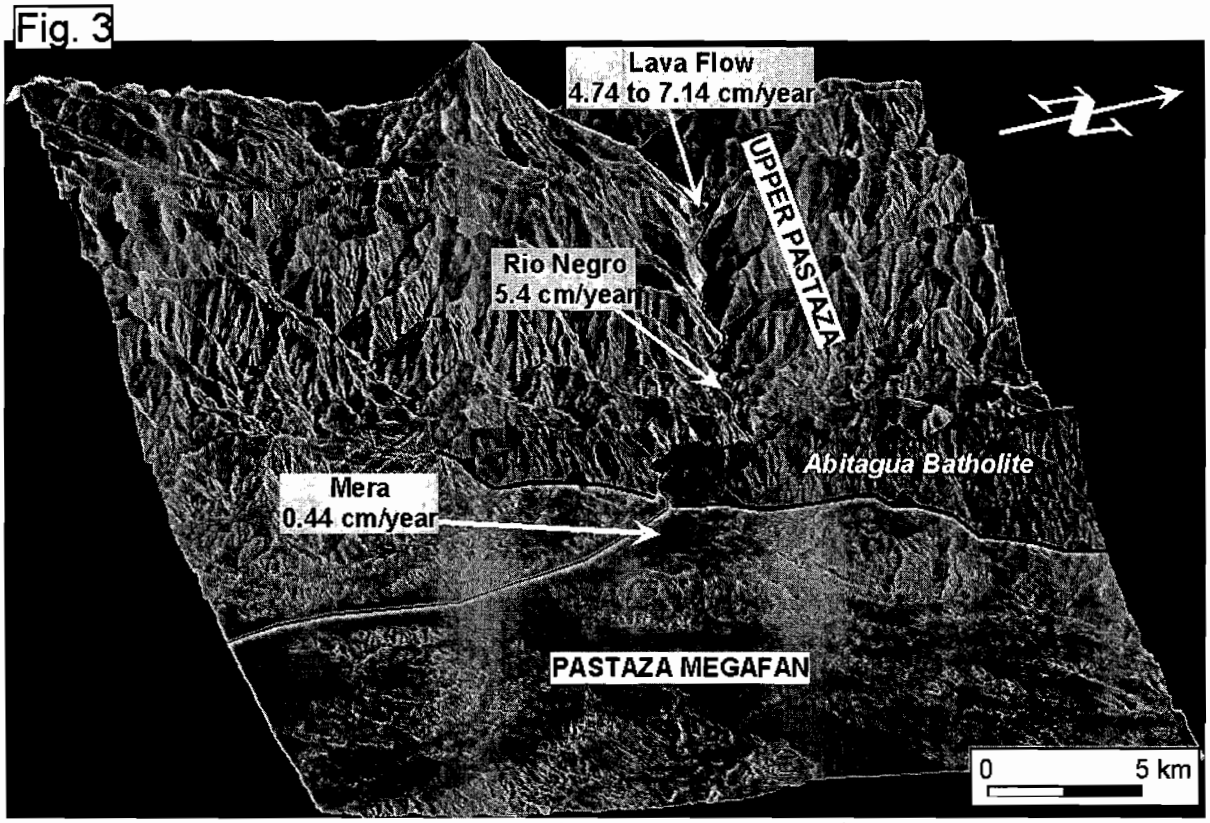

Fig. 1: Detailed topography (from *Savane* processing of 1: 50000 topographic maps) of the Pastaza alluvial megafan and its relationships with the Ecuadorian Eastern Cordillera and Subandean zone. Fig. 2: Structural cross-section across the Eastern Cordillera and the Pastaza megafan (location on fig. 1). Fig. 3: 3D detailed topography (from *Savane* processing of 1 : 50000 topographic maps) of the Upper Pastaza and Pastaza megafan.

ASSESSMENT OF GIS ANDES: PREDICTIVE MAPPING OF NEOGENE GOLD-BEARING MAGMATIC-HYDROTHERMAL SYSTEMS IN THE CENTRAL ANDES

Mario BILLA, Daniel CASSARD, Laurent GUILLOU-FROTTIER, Andor LIPS, Bruno TOURLIERE

BRGM, Mineral Resources Division, BP 6009, 45060 ORLEANS cedex 2, France
m.billa@brgm.fr, d.cassard@brgm.fr, l.guillou-frottier@brgm.fr, a.lips@brgm.fr, b.tourliere@brgm.fr
http://www.brgm.fr/sigand/

KEY WORDS: Central Andes, GIS, gold deposits, epithermal, porphyry, favorability maps

INTRODUCTION

GIS Andes is designed by BRGM to be a homogeneous information system of the entire Andes Cordillera based on original compilations. It covers an area of 3.83 million km² and extends for some 8500 km from the Guajira Peninsula (Colombia) to Cape Horn (Tierra del Fuego). It has been conceived as a tool aimed primarily at the mining and academic sectors. For the former it will be an invaluable aid to mineral exploration and mine development. For the latter it will stimulate in the developing of new metallogenic models (Cassard, 1999). This contribution aims to quantitatively integrate the different regional datasets that exist in the GIS to provide the link between the tectonic development of the Andean margin and the spatial and temporal distribution of ore deposits. The integration of the data is achieved by the production of favorability maps, highlighting the regional metal potential. Due to the complex evolution of the Andean margin, to avoid ambiguities in the less constrained older history, and to incorporate data on the present morphology of the convergent margin, this study considers only one element, gold, in the youngest timeframe, the Neogene to Recent, in the best studied part of the belt, between 5° and 33°.

GIS ANDES DATASETS

GIS Andes contains numerous datalayers which can be subdivided into five main categories:

- Geographic datasets: a DCW® geographic base; three digital elevation models with a structural analysis of the detailed topography; and SPOT 4 VEGETATION® satellite imagery.

- Geological datasets; a geological synthesis at 1:2,000,000 scale; a present state of the geological coverage (presenting the distribution of more than 1100 georeferenced maps); and the distribution of the Holocene volcanism.
- Geophysical datasets; more than 50,000 seismic records; a 3-D model of the subduction plane; gravimetric layers (Bouguer anomaly, including isostatic correction and residual anomalies, vertical gradient calculation and structural analysis, and a gravity model of the Nazca plate); and heat flow information (251 oceanic and 239 continental datapoints).
- Geochemistry; a database with 3935 whole-rock analyses (which allows e.g. to identify zones of adakitic magmatic activity – a recent gold metallotect).
- Metallogeny; an ore deposit database under Access® with more than 3300 records and using new metallogenic lexicons; data on, mineralogy, fluid inclusions and isotopic data on the 350 main ore deposits; and a datalayer showing locations, main features and mining potential of the main mining districts and provinces.

FAVORABILITY MAPPING

Consideration of metallogeny at a continental scale requires knowledge of the parameters that may control, at this scale, the spatial and temporal distribution of the ore deposits. A "data association model" results from the search for pertinent relational criteria within existing databases through statistical analysis. Multicriteria processing (using SynArc®) of GIS Andes data has been employed to create maps presenting the favorability score for different parameters to magmatic-hydrothermal ore formation. The individual digital maps have been combined to result in a synthesized favorability map, also known as predictive map.

The interest of this study relates to "the metallogenic crisis" of gold in the Neogene (Sillitoe, 1991; Noble and McKee, 1999; Petersen, 1999; Oyarzun, 2000) characterized along the Central Andes by the occurrence of giant epithermal and porphyry gold deposits, e.g. the Yanacocha district (Peru) and El Indio belt (Chile), and the Maricunga belt (Chile) and Bajo de la Alumbrera district (Argentina), respectively. The studied corpus consists of 113 Neogene epithermal or porphyry gold deposits. In total the corpus contains 30% of all different ore deposits in this zone, representing 75% of the total stock metal. The applied method is an empiric approach which aims to search the GIS for relational properties between the ore deposit occurrences and other data from different layers in order to quantify their individual favorabilities for gold deposition (e.g. Knox-Robinson et al., 1997; Groves et al., 2000).

Five regional criteria have been extracted from the GIS and are applied based on their apparent association with the studied deposits. They are (see table 1);

- The lithology of the host rock,
- The contact between two different lithologies,
- The structural discontinuities (faults and lineaments),
- The modeled depth of the Wadati-Benioff zone,
- The modeled slope of the Wadati-Benioff zone (e.g. Fig. 1).

The criteria are assessed by a favorability score for every individual criterion (non, or poorly, favorable 0, favorable 1, highly favorable 2), based on their metal content per surface unit or per length unit, as summarized in the following table.

Criterion	Highly favorable Score: 2	Favorable Score: 1	Poorly favorable Score: 0
Lithology	Mainly Tertiary plutonic and volcanic rocks Paleozoic plutonic and volcano sedimentary rocks		Sedimentary rocks Mesozoic sequences
Lithologic contacts	Boundaries of Tertiary igneous rocks Paleozoic plutonic and volcano sedimentary rocks		Contacts between sedimentary rocks
Structural discontinuities	Transversal faults: N080° to N100°E N110° to N120°E	N050° to N060°E N070° to N080°E N160° to N170°E	Longitudinal faults: N000° to N050°E N060° to N070°E N100° to N110°E N120° to N160°E N170° to N180°E
Depth of Wadati-Benioff zone	75 to 150 km	150 to 250 km 225 to 250 km	Areas over 250 km
Slope of Wadati-Benioff zone	Flat areas: Slopes from 8° to 22°		Steep areas

Table 1. Favorability values assigned to regional criteria which may contribute to the spatial distribution of magmatic-hydrothermal gold deposits.

PREDICTIVITY MAP

A final synthesized "favorability map" or "predictivity map" presents the cumulative favorability scores of the individual criteria (Fig. 2). As the resulting map has not been directly derived from the distributions of known ore deposits, the existing deposits allow us to verify the favorability scores.

The zones of high gold potential (favorability > 4) correspond to 65% of the known magmatic-hydrothermal gold deposits and to 95% of the total metal content (50% of the deposits and 71% of the metal content fall within a favorability >5, and 24% of the deposits and 51% of the metal content are located in the favorability regions > 6).

The gold districts of Portovelo (Ecuador), Yanacocha (Peru), Orcopampa (Peru), and the Maricunga belt (Chile) are particularly expressed in the highly favorable zones. Other important districts like El Indio (Chile) and Bajo de la Alumbrera and Agua Rica (Argentina) are less defined, but are still hosted by the highly favorable zones. The Bolivian districts of Kori Kollo and Tasna-Chocaya are clearly outside the favorability criteria and fall in the regions of average to low favorabilities.

Parallel to the verification of the predictivity map by the distribution of the known gold deposits, the map also indicates new favorable zones (e.g. east of Pierina (Peru), west of Bajo de la Alumbrera (Argentina), a favorable zone in southwest Bolivia). As for the areas with known deposits, these new areas are put forward by the assumptions and calculations as being sensitive in hosting undiscovered magmatic-hydrothermal gold deposits.

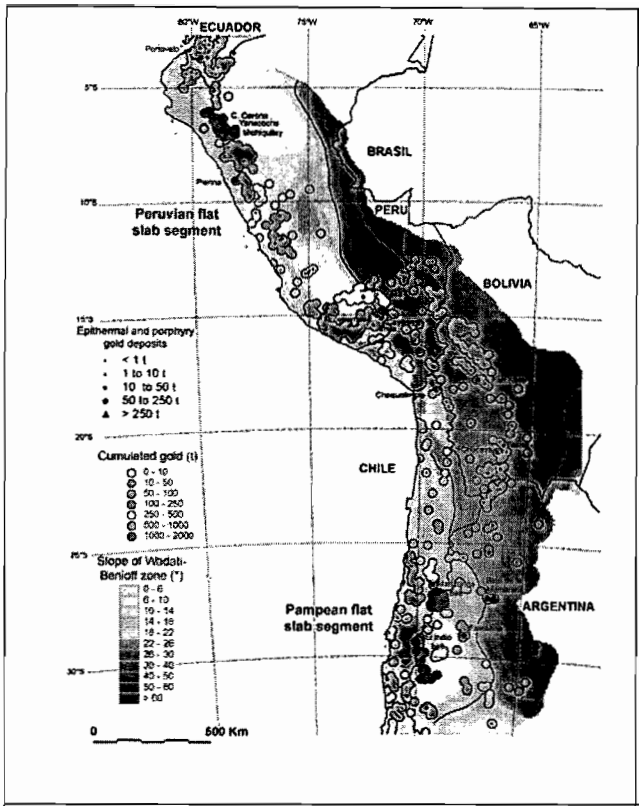

Figure 1. Location of gold districts with respect to the slope of Wadati-Benioff zone (in degrees)

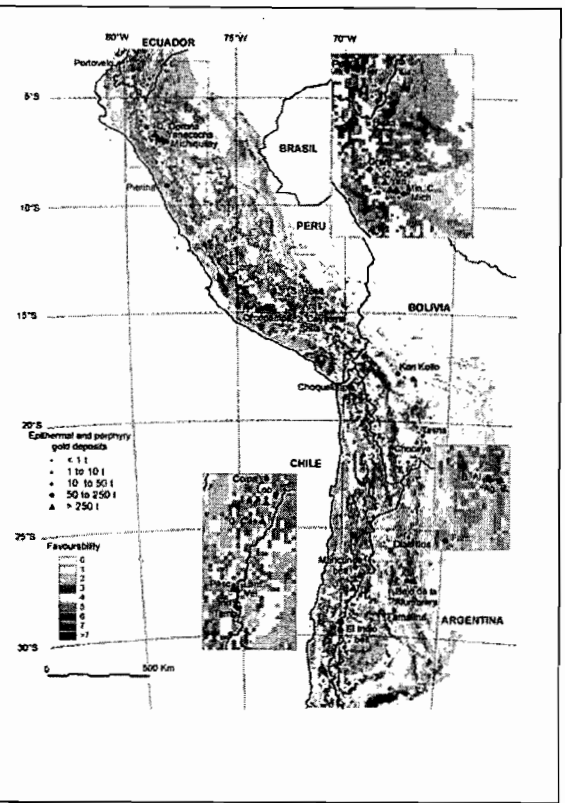

Figure 2. Predictivity map for epithermal and porphyry gold deposits

REFERENCES

Cassard D. 1999. GIS Andes: A metallogenic GIS of the Andes Cordillera. Proceedings of the Fourth ISAG, Goettingen (Germany), 147-150.

Groves D.I., Goldfarb R.J., Knox-Robinson C.M., Ojala J., Gardoll S., Yun G.Y. and Holyland P. 2000. Late-kinematic timing of orogenic gold deposits and significance for computer-based exploration techniques with emphasis on the Yilgarn Block, Western Australia. Ore Geology Reviews, 17, 1-38.

Knox-Robinson C.M. and Groves D.I. 1997. Gold prospectivity mapping using a Geographic Information System (GIS) with examples from the Yilgarn block of Western Australia. Chron. Rech. Min. N°529.

Noble D.C. and McKee E.H. 1999. The Miocene Metallogenic Belt of Central and Northern Peru. In: Skinner, BJ. (Ed.), Geology and ore deposits of the Central Andes: Society of Economic Geologists Special Publication, 7, 155-193.

Oyarzun, J. 2000. Andean Metallogenesis. A synoptical review and interpretation. Tectonic evolution of South America, proceedings of the IUGS conference. Rio Janeiro, 725-753.

Petersen U. 1999. Magmatic and Metallogenic Evolution of the Central Andes. In: Skinner, BJ. (Ed.), Geology and ore deposits of the Central Andes: Society of Economic Geologists Special Publication 7, 109-153.

Sillitoe R.H. 1991. Gold metallogeny of Chile-an introduction. Economic Geology, 86, 1187-1205.

THE SOUTHERN ANDES BETWEEN 36° AND 40°S LATITUDE: A 3-D IMAGE OF THE LITOSPHERIC STRUCTURE INFERRED FROM LOCAL EARTHQUAKE DATA

Mirjam BOHM (1), Günter ASCH (1), Klaus BATAILLE (2), Carsten BRUHN (3), Andreas RIETBROCK (3), ISSA working group

(1)GeoForschungsZentrum Potsdam, Telegrafenberg, 14473 Potsdam, Germany (mirjam@gfz-potsdam.de, asch@gfz-potsdam.de)

(2)Departamento Ciencias de la Tierra, Universidad de Concepción, Concepción, Chile (bataille@udec.cl)

(3)Institut für Geowissenschaften, Universität Potsdam, 14476 Golm, Germany (cbruhn@geo.uni-potsdam.de, andreas@geo.uni-potsdam.de)

KEY WORDS : Andes, crustal structure, seismic velocities, subduction, tomography

INTRODUCTION

A temporary seismological network was installed as part of the project ISSA 2000 (Integrated Seismological experiment in the Southern Andes) between 36° and 40°S above the active continental margin in the Southern Andes reaching from the Chilean Pacific coast to 68°W in Argentina. This project took place within the framework of the Special Research Programm SFB 267 « Deformation Processes in the Andes » and in cooperation with partners from Germany (FU Berlin, Universität Potsdam, GFZ Potsdam, GEOMAR Kiel) and Chile (Universidad de Concepción, Universidad de Antofagasta, SEGMI Santiago). Aimes of the project are to investigate the local seismicity and to determine the 3-D velocity structure of the crust and upper mantle of the region by local earthquake tomography.

The network consisted of 62 three-component seismographs recording continuously from November 1999 to April 2000. The mean station spacing was about 50 km. We recorded on average 2 to 3 local earthquakes per day, mainly concentrated in the northwestern part of the network. The resulting data set comprises 264 seismic events with more than 8 P and S wave observation per event and a RMS error less than 0.6 s.

The data used for an arrival time inversion should be of high quality and provide a good spatial distribution of ray paths. Only earthquakes with an azimuthal gap less than 180° were selected resulting in a final data set of 120 events that provided 1945 P and 1119 S wave observations. An initial Vp/Vs ratio of 1.75 was estimated from linear regression on a set of Wadati diagrams.

The arrival times were inverted simultaneously for 1-D velocity structure, hypocentral coordinates and station corrections. The minimum 1-D velocity model serves as initial reference model for local earthquake tomography (*Kissling*, 1988; *Kissling et al.*, 1994). The same local earthquake data set has been used to determine the 3-D velocity structure of the region by a simultaneous inversion for hypocentres and 3-D Vp and Vp/Vs ratios (*Thurber*, 1983, 1993; *Eberhart-Phillips*, 1993). We performed series of inversions of increasing complexity starting with 2-D inversions followed by 3-D inversions. This procedure ensures a smooth regional model in places of low resolution (*Reyners et al.*, 1999).

The dimension of the inversion grid and the spacing of the grid point coordinates are chosen according to station and hypocentre distribution, and ray density in between. The orientation of the grid is parallel to the strike of the subducted plate (N11°E). The 2-D model has constant velocities in NS direction.

As the damping parameter will vary with the model grid and the data set, it was determined for each inversion by evaluating trade-off curves of data variance and solution variance (*Eberhart-Phillips*, 1986).

CONCLUSIONS

The ISSA 2000 seismological network provides a local earthquakes data catalogue with precise earthquakes locations for the Southern Andes (36°-40°S and 68°-75°W).

Crustal seismicity concentrates in the forearc region along fault zones. Benioff seismicity is observed down to 150 km depth resulting in the first accurate image of the Wadati-Benioff zone in this region. Two maxima are at 20 to 30 km and at 60 km depth, the first of which can be attributed to the coupling between the upper and the lower plate. The second might be due to intermediate depth seismicity caused by dehydration embrittlement. This occurs at relatively shallow depth compered to the Central Andes where the centre of intermediate depth seismicity is at roughly 100 km depth.

Average P wave velocities in the continental crust are 6.3 km/s for the upper crust and 6.9 to 7.4 km/s for the lower crust indicating felsic to mafic composition. Mantle velocities near 8.0 km/s are found below 55 km depth, rising to 8.34 km/s at 90 km depth. The down-going slab is defined by the location of the earthquakes and characterized by fast velocities (8.2 km/s). Low Vp values in the crust beneath the Coastal Cordillera are due to basal accretion of sediments (*Lohrmann et al.*, 2001). Increased Vp values beneath the Longitudinal Valley correlate with negative values of the station corrections belonging to the 1-D velocity model and with the relatively fast velocities obtained by the refraction seismic survey (*Lüth et al.*, 2000).

REFERENCES

Eberhart-Phillips D. 1986. Three-Dimensional Velocity Structure in Northern California Coast Ranges From Inversion of Local Earthquake Arrival Times. BSSA, 76(4), 1025-1052.

Eberhart-Phillips D.1993. Local Earthquake Tomography: Earthquake Source Regions. in *Seismic Tomography:*

Theory and Practice. edited by H. Iyer and K. Hirahara, pp. 613-643, Chapman & Hall, London.

Kissling E. 1988. Geotomography with Local Earthquake Data. Rev. Geophys., 26(4), 659-698.

Kissling E. Ellsworth W.L. Eberhart-Phillips D. Kradolfer U. 1994. Initial Reference Models in Seismic Tomography. J. Geophys. Res., 99(B10), 19635-19646.

Lohrmann J. Kukowski N. Adam J. Oncken O. 2001. The Role of Parameters Controlling Tectonically Erosive and Accretive Forearcs - Results of 2-D Sandbox Experiments. Eos. Trans. AGU, 82(47), Fall. Meet. Suppl.

Lüth S. Wigger P. Asch G. Bohm M. Bruhn C. Rietbrock A. 2000. The Crustal Structure of the Southern Andes Based on 3-Component Refraction and Wide-Angle Seismic Data. Eos. Trans. AGU, 81(48), Fall. Meet. Suppl.

Reyners M. Eberhart-Phillips D. Stuart G. 1999. A Three-Dimensional Image of Shallow Subduction: Crustal Structure of the Raukumara Peninsula, New Zealand. Geophys. J. Int., 137, 973-890

Thurber C. 1983. Earthquake Locations and Three-Dimensional Crustal Structure in the Coyote Lake Area, Central California. J. Geophys. Res., 88, 8226-8236.

Thurber C. 1993. Local Earthquake Tomography: Velocities and Vp/Vs-Theory. in *Seismic Tomography: Theory and Practice*. edited by H. Iyer and K. Hirahara, pp. 563-583, Chapman & Hall, London

ASSESSEMENT OF GROUND DEFORMATION MEASUREMENTS ON ANDEAN VOLCANOES USING RADAR INTERFEROMETRY AND GPS DATA

Sylvain. BONVALOT (1), Dominique. REMY (1*), Germinal. GABALDA(1*),*
Andres. PAVEZ (1,2), Michel DIAMENT (2), Patricia. MOTHES(3)

(1) IRD (Institut de Recherche pour le Développement), UR104, France. * presently at Universitad de Chile, Dept. de geofisica, Santiago, Chile (bonvalot@dgf.uchile.cl, remy@dgf.uchile.cl, gabalda@dgf.uchile.cl)
(2) Institut de Physique du Globe de Paris, Laboratoire de gravimétrie et géodynamique, France (pavez@ipgp.jussieu.fr, diament@ipgp.jussieu.fr)
(3) Escuela Politecnica Nacional, Intituto Geofisico, Quito, Ecuador

KEY WORDS : Radar interferometry, GPS, Guagua Pichincha, Cotopaxi, Lascar, volcano monitoring

INTRODUCTION

Recent studies have demonstrated the potentialities and the limitations of satellite SAR (Synthetic Aperture Radar) interferometry for measuring ground deformations related with volcanic activity (see for instance Zebker et al., 2000). Basaltic shield volcanoes or large calderas appeared as good targets for radar interferometry and studies conducted on these volcanoes have significantly improved the understanding of magmatic fluid migrations at various depths. On the other hand, explosive andesitic volcanoes appeared to be less suited for interferometry studies due to specific geometry or environmental conditions (sleep slopes, vegetation, ice cover, etc.) which may contribute to reduce the quality of the acquired radar data. As a matter of fact, very few studies have been conducted on stratovolcanoes even though significant topographic changes are likely to occur at various scales (lava dome collapse, flank destabilization, etc.). Moreover, the rough field conditions (elevation, access conditions) such as observed on Andean volcanoes, do not allow to properly perform ground monitoring tasks. For such volcanoes, precise geodetic observations are often rare or inadequate to improve our knowledge of ground deformation processes and contribute to hazard mitigation.

In the present study, we have combined SAR interferometry and GPS techniques on some Andean volcanoes with the following objectives :

- to attempt a better quantification and understanding of possible ground deformations associated with lava dome extrusion and collapse,
- to evaluate the potentialities of using satellite interferometric data for ground deformation studies in remote or dangerous areas where geodetic networks cannot be easily maintained,

- to set up precise GPS repetition networks and to determine baseline measurements for a better monitoring of future activities.

We present here the results obtained on Guagua Pichincha and Cotopaxi (Ecuador) and Lascar (Chile) volcanoes and discuss their significance in relation with the current activity and with the potentialities for future monitoring. ERS and JERS datasets have been selected in order to compute interferograms from various time periods (from several years to one day) for coherence analysis between 1992 to 2000. The differential interferograms have been generated with Diapason software (CNES). On these volcanoes, we set up GPS networks and acquired observations using dual frequencies Z-code receivers with full wavelength data. Static or kinematic survey procedures have been used according to the field conditions and the required accuracy. The precise coordinate solutions have been computed according to classical protocols for precise GPS processing.

CASE STUDIES

(1) Guagua Pichincha and Cotopaxi volcanoes (Ecuador)

Guagua Pichincha (4785 m) and Cotopaxi (5911 m) are located in the vicinity of the capital Quito (1,5 Million Inhab.). Both of them have been very active in the historical times, but only the Guagua-Pichincha has undergone eruptive activity within the last decades (repetitive dome growth and destruction). The last reactivation, started during summer 1998 was characterized by a series of phreatic explosions which took place within the 2-km-wide summit caldera hosting a dacitic lava dome. It culminates with a paroxysmal explosion occurred in October 1999 that produced partial destruction of the lava dome and ash fall over Quito. This recent volcanic crisis offered a good opportunity to study ground deformations related with growing lava dome and to evaluate the SAR interferometry method for monitoring such dangerous areas. Moreover, both Pichincha and Cotopaxi volcanoes are representative of South American strato-volcanoes that constitute extreme cases for SAR interferometry applications (steep slopes, variable vegetation, possible ice cap).

Data acquisition (ERS, GPS) : We carried out a first GPS survey on Pichincha volcano in October 1998, consecutively to the reactivation of the Guagua Pichincha. A total number of 34 GPS stations have been determined (21 in the summit area on the eastern side of the active crater) from static or kinematic measurements (figure 1a). The western part of the volcano has not been investigated due to the bad field conditions (absence of access path, dense vegetation) that would require high difficulties for network installation and reiteration. For same reasons, other geophysical monitoring networks are also mainly deployed on the eastern part of the volcano. The GPS network has been partially reoccupied in March 2000 after the major explosion of October 1999. On Cotopaxi volcano, the first GPS observations have been realized by USGS in 1993 (network of 4 stations). In November 1996, we reoccupied the USGS sites and installed 14 new sites distributed from the base of the volcano up to the base of the ice cap (figure 1b). A control survey based on kinematics observations has been realized in March 2000.

Results : The SAR dataset includes ERS images acquired between October 1992 and January 2000. We first attempted to determine from coherence analysis of ERS radar images, the areas where SAR interferometry might be successfully used for ground deformation studies (see results on table below). Despite of the low coherence level of the interferograms, the dataset revealed that no large scale deformation affected the Pichincha volcano before and during the recent volcanic crisis. This result is consistent with our precise GPS measurements realized

during 1998-2000 on the eastern part of the volcano up to the caldera rim. By stacking temporal series of amplitude radar images we attempted to obtain a higher resolution of SAR imaging of the summit active zone. This process allowed to evidence morphologic change of the lava dome consecutively to the Oct. 1999 event (figure 2). This study confirms that ground deformations were confined within the caldera and that no important magmatic fluid migration or gaz pressure occurred at shallow levels to produce large scale surface deformation.

	Guagua Pichincha	**Cotopaxi**
SAR interferometry	**(10/1992–01/2000)**	**(05/1992–05/1997)**
ERS availability	poor (1992-2000)	poor (1992-1997)
Spatial coherence	limited (eastern flank, summit)	quite good (below ice cap, lahars)
Temporal coherence	6 months	up to few years (lahars deposits)
Observed changes	within the caldera	none (05/1992-05/1997)
Potentialities	short term deformations	short to mid terms deformations
GPS data	**(11/1998–03/2000)**	**(11/1996–03/2000)**
Network / Baseline	26 stations (since 1998)	18 stations (since 1996)
Network accuracy	Static (1 to 3 cm) - Kinematics (2 to 5 cm)	Static (1 to 3 cm) - Kinematics (2 to 5 cm)
Observed changes	Below network accuracy (< 2 cm horiz.)	Below network accuracy (< 2 cm horiz.)

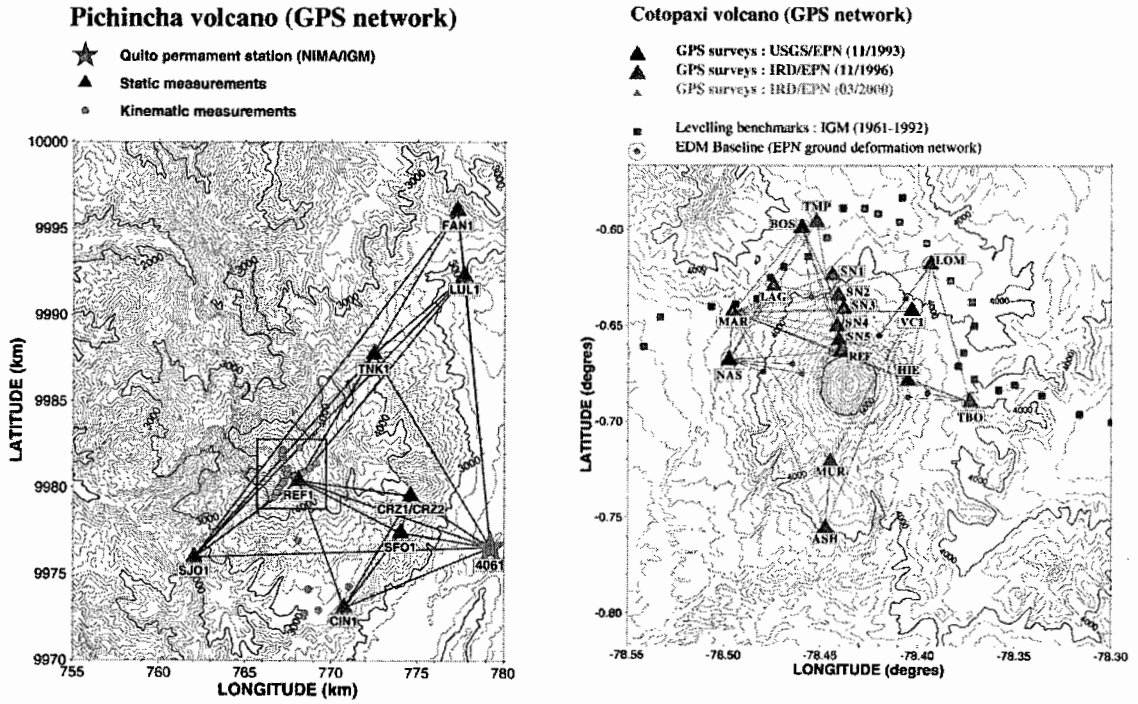

Figure 1 : Topography and GPS networks of Guagua Pichincha (a) and Cotopaxi (b) volcanoes (Ecuador)

Figure 2 : Example of amplitude radar image on Pichincha volcano and Quito capital (a). Detailed views of the active caldera obtained from stacking of images acquired before (a) and after (b) October 1999 show morphologic changes of the lava dome.

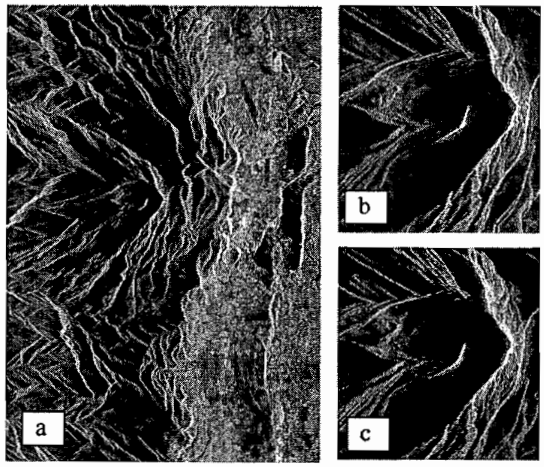

(2) Lascar volcano (North Chile)

Lascar (5592 m) is one of the most active volcanoes of the northern Chilean Andes. Its recent activity is characterized by repetitive dome growth and subsidence (4 cycles between 1984 to 1993) accompanied by vigorous degassing and explosive eruptions of various magnitude Matthew et al. (1997). In April 1993 the largest historical eruption of Lascar produced ash column up to 25 km altitude. Remote sensing and ground based geodetic data are combined here for the first time to enhance if ground deformations are associated with episodes of dome extrusion and collapse and attempt to better constrain the internal dynamics (localization of pressure source for instance). Moreover, due to the absence of vegetation and to arid climatic conditions, this volcano presents the most favorable conditions of for radar interferometry and can be considered as a test site.

Data acquisition (ERS and JERS) : We analysed a series of radar images taken between July 1993 and October 2000. In addition, the use of ERS and JERS data provided a comparative information of the potentialities of different satellite radar data according with the sensor specifications. The longer wavelength of JERS signal (23,5 cm) compared to ERS signal (5,66 cm) is less sensitive to the ground cover and thus presents a better response to the underlying geology. Moreover, as shown on figure 3, the larger JERS incidence angle (35°) reduces the foreshortening and layover effects as observed for ERS satellite (23°). Unlike to ERS for which precise orbits data are available, the low accuracy of the JERS orbits decreases the quality of the interferograms.

Figure 3 : Comparison of layover and foreshortening effects on Lascar volcano from ERS and JERS data. The black pixels correspond to interferometric decorrelated areas.

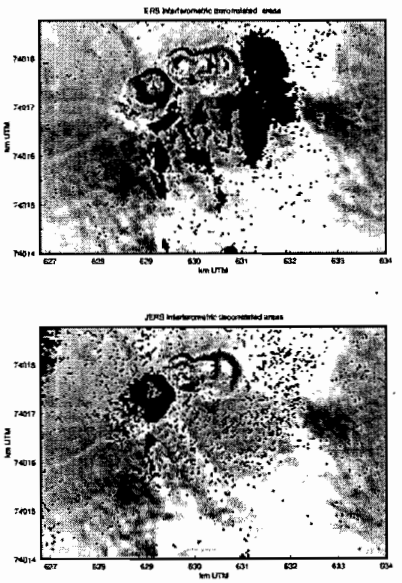

Results : The analysis of ERS and JERS data on Lascar confirmed the high quality of ground response to radar imaging. First results also revealed that more precise Digital Elevation Model would be required to better remove local effects of the topography in the summit area and to enhance small scale ground deformation. With this aim, a more precise DEM generated from aerial photogrammetry and constrained by GPS data acquired in early 2002 is in progress.

REFERENCES

Zebker H.A., Amelung F., Jonsson S, 2000. Remote sensing of volcano surface and internal processes using Radar interferometry. Remote sensing of Active volcanism. AGU Geophysical monograph 116. pp179-205.

Matthews S.J., Gardeweg M.C., Sparks, R.S.J., 1997. Bull. Volcanology, vol 59, pp72-92.

This study has been supported by INSU (PNRN) and IRD.

THRUST KINEMATICS AND FORELAND BASIN DYNAMICS OF THE SOUTHERN SUBANDEAN ZONE OF BOLIVIA: NEW INSIGHT FROM APATITE FISSION TRACK ANALYSIS

Stéphane BRUSSET (1), Philippe ROCHAT (2), Patrice BABY (1,3), Joan FLINCH (4)

(1) LMTG, Geodynamics, UMR 5563, 38, rue des 36 ponts, 31400 TOULOUSE, FRANCE, stephane.brusset@cict.fr
(2) TOTALFINAELF CSTJF avenue Larribau, 64000 Pau, France philippe.rochat@totalfinaelf.com
(3) IRD UR104, LMTG, Geodynamics, UMR 5563, 38, rue des 36 ponts, 31400 TOULOUSE, FRANCE, patrice.baby@cict.fr
(4) TOTALFINAELF CSTJF avenue Larribau, 64000 Pau, France joan.flinch@totalfinaelf.com

KEY WORDS :: Foreland basin system, AFTA, stratigraphic implications.

INTRODUCTION

It is now well-known that the subandean zone of Bolivia (fig.1) is structured by thrust-related folds (Baby et al., 1992). Such structures are controlled by two main décollement levels located in the Silurian Shales and in the Devonian Los Monos Fm. Several balanced-cross sections have been proposed for the studied area. The aim of this paper is to discuss the geodynamics evolution of the thrust-wedge using Apatite Fission Track Analysis on samples collected on each structure and to combine this analysis with a sedimentary facies study of Neogene deposits. The evolution of the thrust-wedge controls the foreland basin system configuration, so a step-by-step reconstruction will give good information about the propagation of the Neogene Subandean retroforeland basin system.

METHODOLOGY

The information obtained from AFTA allows deducing a maximum burial history for each anticline-syncline pair. The combination of this information with source rock maturity analysis defines precisely these burials. The kinetic parameters used to constrain the deformation sequences are: i/the dating of the cooling of the apatites (rising); ii/two new ages obtained in tufaceous strata; and iii/ages of youngest grain population of apatites located in the basal part of Neogene series and resulting from recent volcanic explosion. The sedimentologic and morphologic analyses allow relating the facies associations and the relevant surfaces recognized in the Neogene series to depozones of a modern foreland basin system.

The interpretation of new seismic sections allows a better geometric definition of the deep structures. This new information is used for the construction of balanced cross-sections.

RESULTS

Between 20.9±2.7 and 9.9 ±1.3 Ma, the distribution from west to east of the ages obtained in the base of the Neogene series shows the diachrony in the foreland basin system structure development. The burial computation using temperature constraints on apatite samples allows constructing the pre-thrusting configuration of the foreland basin system. Thickness variations can be interpreted as the result of a bending of the foreland lithosphere determining distal foreland system depozones. These depositional areas are distributed from west to east as follow: the foredeep depozone in the present day Domo Oso and west-Iñiguazu anticlines; the forebulge depozone from west-San Alberto to west-Aguarague and the backbulge depozone from Aguarague to the Chaco plain. During this period, the southern Subandean zone was submitted to large wavelength tectonic tied to the flexion of the Brazilian shield owing to the load of an orogenic prism located westward in the Camargo area.

The facies records that the studied area was in the part distal of such a system (foredeep - forebulge - backbulge depozones).

From 9.6 ± 0.8 Ma, thrust-related folds propagated eastward with two décollements one at the very base of the wedge (Silurian - Kirusillas Fm) and other within the wedge itself (Upper Devonian –Los Monos Fm). Link thrust developed between the décollements and involved Kirusillas, Icla and Huanapama Fms in a hinterland dipping duplex associated with large structures. From the second décollement (Los Monos Fm) merged thrusts with associated box folds (antiformal stack).

The décollement at the base of Los Monos Fm authorizes a decoupling between the most top structures and the lowest structures. Therefore the shortening of Aguarague's structure gets accommodated partly in the antiformal stack of the San Alberto anticline. On the other hand, in the more internal structures (Domo Oso, Iniguazu), the shortening of the lowest duplex gets accommodated directly in surface by the development of a transported syncline. The deformation sequence corresponds globally to forward thrust propagation. This type of spread is obvious well in the lowest duplex, and registered by the sedimentary sequences near the structures Aguarague and La Vertiente. On the other hand, the geometry of the most top units seems to show a more anarchic organization. The existence of several décollement levels and the shortening are characterized by the synchronous development of the thrusts (Boyer, 1993). This synchronism is proved by the ages of cooling of the apatites.

CONCLUSIONS

Several conclusions can be pointed out (fig. 2)

1- the classical stratigraphy of Neogene rocks based on facies recognition is inconsistent with stratigraphic implication of apatite fission track analysis. For example the basal part of Neogene strata is eastward younger and younger. This trend agrees with the progressive onset of flexural subsidence controlling the first stages of foreland system occurrence;

2- two radiometric ages (K/Ar) have provided by tuffaceous layers interbedded in Neogene formations. One gives 3.3 ± 0.1 Ma at the very base of the wedge-top depozone I sequence in the eastern part of the Chaco plain the other is dated at 5.3 ± 0.2 Ma in the eastern syncline of San Alberto in the basal part of the wedge-top depozone II sequence.

3- to interpret this new stratigraphic constraints, the propagation of a typical foreland basin system is required. The first stage corresponds to the occurrence of distal depozones (distal foredeep, forebulge and backbulge) with an axis of the forebulge located in the present day San Alberto area.

4- as demonstrated by the cooling ages of apatites, thrust reached the Iñiguazu area between 9.6±0.8 Ma and 6.7±0.6 Ma and developed throughout the study area until around 6 Ma, the latest cooling of one sample occurred around 3 Ma at the western rear of the wedge suggesting out-of-sequence thrust reactivation;

5- geomorphologic observations (terrace tilting; growth onlaps) evidence the ongoing of thrust-related deformation.

REFERENCES

Baby P., Herail G.; Salinas R.; Sempere-Th. 1992. Geometry and kinematic evolution of passive roof duplexes deduced from cross section balancing; example from the foreland thrust system of the southern Bolivian subandean zone. Tectonics; 11; 3, 523-536.

Boyer S.E. (1992). Geometric evidence for synchronous thrusting in the southern Alberta and northwest Montana thrust belts. In Thrust Tectonics, (eds) K.R. Mc Clay, 377-390.

DeCelles P.G. and Giles K.A.1996) Foreland basin systems. Basin Research, 8, 105-123.

Horton, B.K, and DeCelles, P.G., 1997, The modern foreland basin system adjacent to the central Andes: Geology, ²25, 895-898.

Horton, B.K., and DeCelles, P.G., 2001. Modern and ancient fluvial megafans in the foreland basin system of the central Andes, southern Bolivia: Implications for drainage network evolution in fold-thrust belts: Basin Research, 13, 1, 43-65

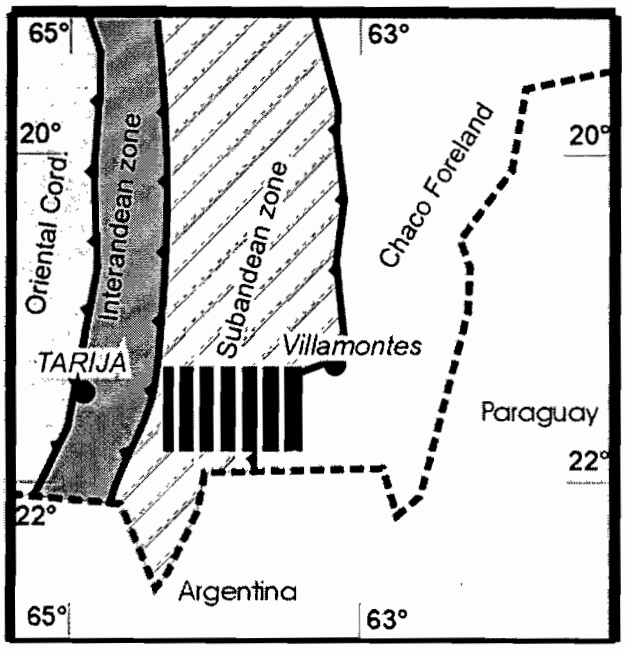

Figure 1: Schematic map of Bolivia. Strip area corresponds to the studied zone

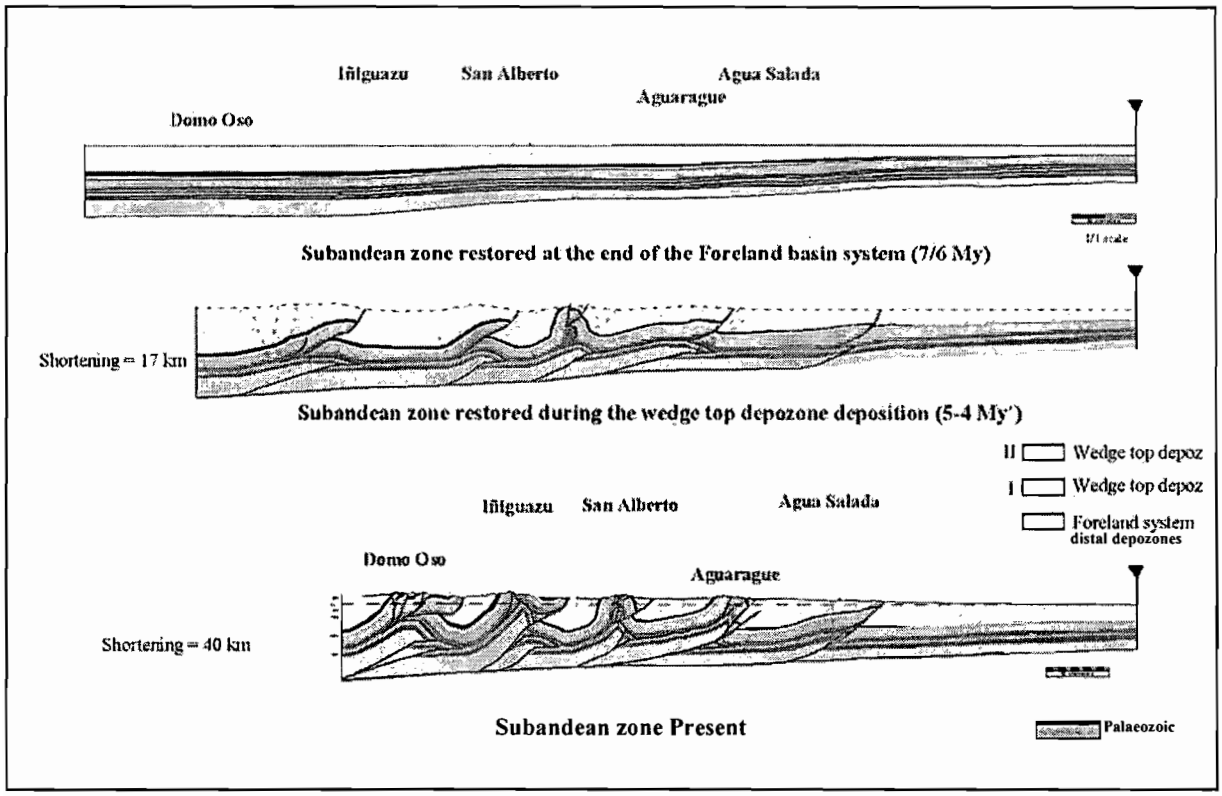

Figure 2: Sequential restoration of the studied cross-section displaying the eastward progression of the thrust wedge in the southern Subandean zone.

THE UPPER CARBONIFEROUS IN FRONTAL CORDILLERA (SAN JUAN PROVINCE – ARGENTINA): REGIONAL IMPLICATIONS

Pedro BUSQUETS(1), Ferran COLOMBO(1), Nuria SOLE de PORTA(1), Nemesio HEREDIA(2), L. Roberto RODRÍGUEZ-FERNÁNDEZ(3) and Joaquina ÁLVAREZ-MARRÓN (4)

(1) Dep. Estratigrafia, Paleontologia y Geociencias Marinas. C/Martí i Franqués s/n. Universidad de Barcelona. Pedralbes. E-08071 Barcelona, Spain. pere@natura.geo.ub.es; colombo@natura.geo.ub.es

(2) Instituto Geológico y Minero de España. Av. República Argentina 30, 1° B, E-24004 León. nheredia@jet.es

(3) Instituto Geológico y Minero de España. C/Ríos Rosas 23. E-28003 Madrid. roberto.geo@jet.es

(4) Instituto de Ciencias de la Tierra, Jaime Almera. CSIC. C/Lluis Solé i Sabarís, s/n. E-08028, Barcelona. jalvarez@ija.csic.es

KEY WORDS: lithofacies, palynology, chronostratigraphy, Andean ranges.

INTRODUCTION

The age of the stratigraphic successions that outcrop in the Castaño Viejo area (NW of San Juan Province, Argentina) of the Andean Frontal Cordillera (Groeber, 1938) is not well known. These have important implications in the understanding of the Paleozoic tectonic evolution of this sector of the Andes. The Famatinian and Gondwanic deformation cycles are responsible for the Paleozoic structures that appear in this area overprinted by the Permo-Triassic and Tertiary structures associated to volcanic and volcanoclastic rocks together with Mesozoic and Tertiary granitoids. The main structures associated with the Gondwana Orogenic cycle are thrust systems and related folds that caused 60 to 70% shortening (Heredia et al. 2002).

In the Castaño Viejo area, a sedimentary sequence that can be correlated with the Agua Negra (Polanski, 1970) and La Puerta Formations (Caballé, 1986) of Upper Carboniferous-Lower Permian age (Aparicio, 1969, González, 1977) appears along Quebrada de las Animas and Quebrada de las Ñipas. This sequence unconformably overlies Devonian sediments deformed during the Famatinian Orogenic Cycle, and is organised in two sedimentary cycles interpreted as pre- and syn-orogenic with Gondwanic orogenic Cycle. However, in Quebrada de las Animas, the limestone that appear at the upper part of the syn-orogenic cycle had been dated as Silurian-Devonian by Pöthe de Baldis et al (1987). In an attempt to solve this age contradiction, a detailed study of the main lithofacies together with exhaustive sampling for analysis of palinomorphs has been

carried out along the two Quebradas. Special emphasis has been given to the study of microfacies in the upper limestones.

The sediments corresponding to the syn-orogenic cycle have an estimated total thickness of around 400 m., and occupy a stratigraphic position between the Agua Negra Formation and the Choiyoi Group. The upper limestones consist of microbioliths (in the sense of Burne and Moore, 1987) which form large interconnected stromatolithic domes. Thrombolithic structures overlaid by stromatolithic structures are organised in sequences of metric thickness (from 1 to 6 meters) with paleosoils at the top, suggesting shallowing upwards sequences. Silt size quartz grains found in the limestones are aeolian in origin, and clays with possible Devonian palynomorphs probably reached the basin in the same way. The best palynological results have been obtained from the fine sediments between the limestones.

In the lower part of the Quebrada de las Ánimas, three samples provided the following palynomorphs: *Ancistrospora verrucosa* Menéndez & Azcuy 1972, *Apiculiretusispora tuberculata* Azcuy 1975, *Cristatisporites* sp., *Lundbladispora* cf. *braziliensis* (Pant & Srivastava) Marques-Toigo & Pons 1974, *Raistrickia paganciana* Azcuy 1975, *Raistrickia* cf. *rotunda* Azcuy 1976, cf. *Reticulatisporites pseudopalliatus* Staplin 1960, *Colpisaccites granulosus* Archangelsky & Gomerro 1979, *Limitisporites* sp., *Platysaccus papilionis* Potonie & Klaus 1954, *Bisaccate* spp. The upper part of the section contains *Raistrickia paganciana* Azcuy 1975 and some undetermined bialate remains. Samples from Quebrada de las Ñipas contain *Ancitrospora* sp. *A* Azcuy 1975, *Convolutispora muriornata* Menéndez 1965 and *Platysaccus* sp.

Although, there are scarce palynological studies in this sector of the Carboniferous Calingasta-Uspallata basin, some palynomorphs such as *Granulatisporites*, *Apiculiretusispora* y *Cristalisporites,* which are characteristic of the Lower Permian-Upper Carboniferous times have been found in Cerro de Agua Negra Fm (Gutiérrez, 1992). In addition, Ottone & Rosello (1996) found palynomorphs such as: *Limitisporites*, *Lueckisporites*, *Lunatisporites* y *Vittatina*, which are considered to be characteristic of the Permian in the La Puerta Fm. In all of the samples from Castaño Viejo, the trilete spores are accompanied by some bialate forms, and only one striated form (*Lunatisporites*) was found. The lack of striated forms that are characteristic of the Permian is noticeable. The samples that contain the better-preserved association of palynomorphs include spores and bialates that correspond to an Upper Carboniferous environment. The presence of remains of some highly metamorphosed large, black spores with coarse processes or tubercles difficult to identify and chitinozoa indicative of a Devonian age are considered reworked or redeposit in the basin in Upper Carboniferous times.

The associations of palynomorphs found in all samples correspond to the *Ancistrospora* palynological zone identified by Azcuy (1986) in the Paganzo Basin. The characteristic forms in this zone such as *Ancistrospora verrucosa* and *Convolutispora muriornata*, both indicative of an Upper Carboniferous age are found in the samples from Castaño Viejo analysed in this study.

CONCLUSIONS

The association of palynomorphs found in the samples from Castaño correspond to the Raistrickia densa – Convolutispora muriornata Biozone (César & Gutierrez, 2000) corresponding to an Upper Carboniferous age. Reworked palynomorphs and chitinozoa of an earlier age, possibly Devonian are also found, which are

interpreted to have reached the basin by aeolian transport. These recycled palynomorphs originated from exposed Devonian rocks of surrounding topographic relieves.

The abundance of spores such as Lycopsida, Philicopsida and Sphenopsida types of Pteridophyta, are indicative of a flat swampy humid area (Azcuy 1978), and in which microbioliths grow. These spores are associated with bisaccate forms, some of which may belong to the Coniferae, possibly transported from higher land partially covered by vegetation from more arid climatic conditions.

During the Gondwana Cycle this region of the Frontal Cordillera passed from being a retroarc basin (Ramos 1988), in which the sediments come from eroding relieves of the Precordillera and the Sierras Pampeanas, to a position in which the growing relieves of the volcanic arc that provided sediments also caused the partial cannibalisation of previously accumulated sediments. Previous interpretations of the Frontal Cordillera (Chilenia Terrane) being placed in a paleolatitude away from Gondwana were based in the presence of Silurian-Devonian hot water stromatolithic limestones. Our results suggest that previous geodynamic interpretations should be reviewed.

ACKNOWLEDGMENTS

We thank I. Zamarreño for her suggestions in the limestone study. This paper uses the results obtained for the Castaño Viejo and Castaño Nuevo sheets (1:100,000) of the Argentine Geological Map, funded by SEGEMAR (Argentine Geological Survey), AECI (ICI) (Spanish Cooperation Agency) and IGME (Spanish Geological Survey). It has also been funded by DGESIC PB 98-1189 (Spanish Science and Tecnology Agency) and by Comissionat per Universitats i Recerca, Generalitat de Catalunya, Grup de Qualitat GRQ97-0073.

REFERENCES

Aparicio, E.P., 1969. Contribución al conocimiento de la edad de los sedimentos del arroyo de Agua Negra, Departamento de Iglesia, San Juan, República Argentina. Revista Asociación Geológica Argentina, 31 (3), 190-193.

Azcuy, C.L., 1978. Posible significado paleoecológico de microfloras Gondwanicas del Paleozoico Superior, especialmente Argentinas. Ameghiniana, 15(1-2), 85-95.

Azcuy, C.L., 1986, Algunas precisiones sobre palinozonas Carbónico – Pérmicas de la Cuenca Paganzo. Ameghiniana 23 (1-2), 97-100.

Burne,R.V. and Moore, L.S., 1987, Microbiolithes:organosedimentary deposits of the benthic microbial communities. Palaios,2, 241-254.

Caballé, M.F., 1986. Estudio geológico del sector oriental de la Cordillera Frontal entre los ríos Manrique y Calingasta (Provincia de San Juan). Tesis Doctoral, Universidad Nacional de La Plata (unpublished).

Césari, S.N. and Gutiérrez P.R., 2000, Palynostratigraphy of Upper paleozoic sequences in Central-Western Argentina. Palynology, 24, 113-146.

González, C.R., 1977. Oriocrassatella y Stutchburia (Bivalvia) en la ingresión marina del Pérmico inferior de la quebrada del Agua Negra, provincia de San Juan (Argentina). Ameghiniana 13 (2), 127-140.

Groeber, P., 1938. Mineralogía y Geología. Espasa-Calpe Argentina. 492 pp.

Gutiérrez, P.R., 1992, Microflora de la Formación Cerro Agua Negra (Carbonífero Superior-Pérmico Inferior) de la quebrada Las Leñas, provincia de San Juan, Argentina. 8° Simposio Argentino de Paleobotánica y Palinologia, Corrientes. Asociación Paleontológica Argentina. Publicación Especial, 2, 63-66.

Heredia, N., Rodríguez Fernández L.R., Gallastegui, G., Busquets, P. and Colombo, F., 2002. Geological setting of the Argentine Frontal Cordillera in the flat-slab segment (30°00' to 31° 30' S latitude). In: Ramos, V., and McNulty, B., (Eds.), Flat Subduction in the Andes. Jour. South Am. Earth Sci., Special Issue, 15(1), 000-000.

Ottone, E.G. and Rosello, E.A., 1996, Palinomorfos Pérmicos de la Formación La Puerta, Cordillera Frontal, Argentina. Ameghiniana, 33(4), 453-455.

Pöthe de Baldis, E.D., Cardó, R. and Pelichotti, R., 1987. Silúrico-Devónico en Castaño Viejo, Cordillera Frontal, Provincia de San Juan. Revista de la Asociación Geológica Argentina, XLII (3-4), 469-471

Polanski, J., 1970. Carbónico y Pérmico en la Argentina. Eudeba, Buenos Aires, 216 pp

Ramos, V. A., 1988. The tectonic of the Central Andes: 30° to 33° S latitude. In: Clark, S., Burchfiel, D. (Eds.), Processes in Continental Lithospheric Deformation. Geological Society of America, Special Paper 218, 31-54.

CHRONOSTRATIGRAPHY OF THE SAN JUAN DE ORO BASIN AND ITS TECTONIC IMPLICATIONS FOR THE NORTHERN PUNA DURING THE MIOCENE

Pablo J. CAFFE(1) and Beatriz L. COIRA(2)

Instituto de Geología y Minería - UNJu. C.C. 258. S. S. de Jujuy (4600). Jujuy. Argentina. (1) email: pabcaf@idgym.unju.edu.ar (2) email: bcoira@idgym.unju.edu.ar

KEY WORDS: chronostratigraphy; compressive deformation; Miocene; northern Puna.

INTRODUCTION

The detailed stratigraphic study of Cenozoic basins in the Central Andes has been one of the keys to understanding the evolution of compressive deformation in the high Puna-Altiplano plateau. While Cenozoic sedimentary basins in the Bolivian Altiplano (16°-22°S) were indeed the object of intense field and geochronologic regional work in the last decade (e.g. Kennan et al, 1995; Sempere et al., 1997), data on the stratigraphy of northern Puna basins (22°S-24.5°S) –obtained by the Argentine Geological Survey during 1960 to 1980 (e.g. Turner, 1978; Coira, 1979)– were rather general so far.

In this work we expose part of the K-Ar geochronologic (Table 1) and stratigraphic results attained by our group in the last years, as a consequence of the surveying of the Mina Pirquitas geologic chart (Coira et al., in press). With this information, we will intend to appraise the tectostratigraphic history of the northern Puna during the tectonic phases previous to the Upper Miocene, when compressive deformation ended in this sector of the Andean plateau (i.e. 10-8 Ma; Cladouhos et al., 1994).

SAN JUAN DE ORO BASIN

The record of most northern Puna basins mainly shows a Neogene history of sedimentation, although the first Cenozoic deposits seem to have been as old as Eocene-Oligocene, just post-dating the rifting event occurred in the Cretaceous (Jordan and Alonso, 1987). Among the older Cenozoic units, the Peña Colorada Fm. (Paleocene to Lower Miocene?; Bellmann and Chomnales, 1960) –a thick fluviatile red bed sequence (up to 1200 m)- is the most conspicuous infill of the large San Juan de Oro basin (Fig. 1). The Peña Colorada Fm. overlays pre-Cenozoic (Palaeozoic or Cretaceous) basement rocks, and represents the first deposits sedimented in the SJOB. The sequence is conglomeratic in its basal portion (~150 m), but rapidly becomes finer (sandy to silty) upwards. The lack of coarse deposits on the top of the Peña Colorada Fm., even for outcrops near the Sierra de Rinconada mountain range (Fig. 1), as well as the presence of small relics of red beds inside this elevated structure (Bellmann and Chomnales, 1960; Turner, 1978) indicate that the latter was considerably lower than today. At the same time this assumption suggests either broader extensions for the SJOB east of its current western boundary (Western Sierra de Rinconada Thrust, WSRT, Fig. 1), or alternatively a partial connection with the Laguna de Pozuelos basin (Fig. 1) by that time.

According to Jordan and Alonso (1987), the fragmentation of Puna foreland basins was synchronous to the first Andean volcanic phases. This early volcanism (late Oligocene to early Miocene) is concentrated in some intramontane piggy back basins, mainly located to the east of SJOB (i.e. Abra Moreta, 20±2 Ma; Tupiza, 22.7 Ma; Coira et al., 1993; Soler y Jiménez, 1993). Inside the SJOB, volcanism did not occur until the late Early Miocene, when the upper member of Cabrería Fm. was deposited. The Cabrería Fm. is an extremely thick sequence of conglomeratic beds (up to 1000 m) deposited along the western margin of the Sierra de Rinconada, which cover an erosional unconformity carved over the Peña Colorada Fm. The upper levels of Cabrería Fm. are entirely formed by prymary –mostly ignimbrites– and reworked -laharic and alluvial- volcaniclastic deposits dated in 17.4 ± 0.8 Ma (Table 1), but its base must be relatively much older. The coarse grain size and lack of roundness of clasts form the Cabrería Fm. suggest that the latter would have been originated from alluvial fans going downslope to the west from the rising Sierra de Rinconada.

The Cabrería Fm. as well as the underlaying Peña Colorada Fm. are folded in their contact with the western margin of the Sierra de Rinconada; this folding is caused by the dragging of an important structure –the Western Sierra de Rinconada Thrust (WSRT; Fig. 1)- which overthrusted Palaeozoic basement rocks onto SJOB sedimentary sequence. Though younger, the Cabrería Fm. conglomerates correlate with the San Vicente Fm. (~20 Ma; Fornari et al., 1989), which outcrops to the north of the studied area, flanking the Altiplano- Eastern Cordillera structural boundary (the San Vicente Thrust, northernward extension of WSRT).

The Cabrería Fm. is covered by a 200 m-thick succession of sandstones, psefites and mudstones, commonly intercalated with ignimbrites and tuffs (the Tiomayo Fm. of Seggiaro and Aniel, 1989). The basal member of Tiomayo Fm. consists of coarse (sandy to conglomeratic), red-to-gray-coloured beds which have rather an uniform age across the western boundary of SJOB: to the north (Casa Colorada, 22°15'S; Fig. 1), an intercalated dacitic ignimbrite is dated in 15.7 ± 0.6 Ma (Table 1); to the southern SJOB edge (Mina Pirquitas, 22°40'S; Fig. 1) another ignimbrite with a similar position in the sequence brought an age of 14.9 ± 0.5 Ma (Table 1). Meanwhile to the west, in the SJOB axis (Tiomayo: 22°20'S; Fig. 1), the Cabrería Fm. dissapears, and the Tiomayo Fm. discomformably overlays the Peña Colorada Fm. (pre-18 Ma). The Tiomayo Fm. is a thinning- and fining-upward succession, which changes from red fluvial conglomerates and sandstones at the base to mostly yellow and greenish lacustrine mudstones at the top, predominating the latter aspect in direction to the depocentre (Tiomayo; Fig. 1). Interbedding with tuffs and pyroclastic flow deposits is also common in that direction. An outstanding characteristic of the upper levels of the Tiomayo Fm is that they horizontally onlapped the southern border of the Sierra de Rinconada (Mina Pirquitas, Fig. 1). The same as the base of the sequence, the younger beds of the Tiomayo Fm. also show a fairly similar age across the SJOB: in the western part, underlying the Cerro Panizos volcanic rocks (Fig. 1), a tuff on top of the Tiomayo Fm. was dated in 12.43 ± 0.08 Ma (^{40}Ar-^{39}Ar; Ort, 1991); at the east (Orosmayo, 22°35'S) another air-fall tuff gives a K-Ar age of 12.1 ± 0.7 Ma (Coira et al. in press). The deposition of this sequence finished before the eruption of the basal ignimbrite in the Orosmayo Volcanic Complex (Coira et al., 1996) which was dated in 10.3±0.5 Ma (Table 1).

The Tiomayo Fm. beds are practically horizontal, covering at least one third of the WSRT length (the southernmost one) being neither affected by that structure nor defformed in any way by other thrusts or compressive faults. Although the Tiomayo Fm. does not exhibit continuity to the north of Panizos, it would correlate with the Upper Quehua Fm. in the Altiplano (Fornari et al., 1989).

TECTONIC IMPLICATIONS

From the chronostratigraphic framework outlined above, it is possible to infer that the first segmentation events of the Andean foreland between 22° and 23° S would have postdated the Upper Oligocene (the Pehuenche tectonic event). The time of breaking of Puna foreland basins is represented by the deposition of the Cabrería Fm., whose characteristics are suggestive of a strong uplift in the eastward Sierra de Rinconada during the late Lower Miocene, a fact that seems to be little important prior to that moment. A similar event was proposed by Hèrail et al. (1994) for the Altiplano-Eastern Cordillera structural boundary –the northern extension of the WSRT-, but those workers considered the San Vicente Thrust to have started its motion well before the Lower Miocene. Then, the progression of segmentation would have been diachronous from north to south. Similarly, the last compressive events in the western border of the Bolivian Eastern Cordillera occurred between 20 and 18 Ma (Kley et al., 1996), but thrusting of the Palaeozoic basement to the south continued until later, as is inferred from the deformation of the ~18 Ma Cabrería Fm. Thus, the WSRT would have stopped its motion between the Cabrería Fm. folding event (post-18 Ma) and the deposition of the undeformed Tiomayo Fm. (pre-15 Ma). During the Middle Miocene the compressive deformation moved out from the SJOB to the east. Such an assumption is evident from the stratigraphic record in the Laguna de Pozuelos basin, where sedimentary sequences equivalent in age to the Tiomayo Fm. (14-12 Ma) show intense deformation (Cladouhos et al., 1994; Gangui, 1998).

REFERENCES

Bellmann, R. and Chomnales, R. 1960. Estudio hidrogeológico del Valle Puesto Viejo y sus posibilidades económicas. *Acta Lilloana* III : 59-84.

Coira, B. 1979. Descripción Geológica de la Hoja 3c, Abra Pampa, Pcia. de Jujuy. *Boletín del Servicio Geológico Argentino* **170**, 1-90.

Coira, B., Caffe, P.J., Kay, S.M., Díaz, A. and Ramirez, A. 1996. Complejo volcánico Vilama - Sistema caldérico del Cenozoico superior en Puna, Jujuy. *XIII Congreso Argentino de Geología, Buenos Aires*, 603-620.

Coira, B., Caffe, P.J., Ramírez, A., Chayle, W., Díaz, A., Rosas, S.A., Pérez, A., Pérez, E.M.B., Orosco, O. & Martínez, M. Hoja Geológica 2366-I Mina Pirquitas (1:250.000). *SEGEMAR,* (in press).

Cladouhos, T.T., Allmendinger, R.W., Coira, B. and Farrar, E. 1994. Late Cenozoic deformation in the Central Andes: Fault kinematics from the Northern Puna, Northwestern Argentina and Southwestern Bolivia. *Journal of South America Earth Science* **7**, 209-228.

Fornari, M., Hèrail, G., Pozzo, L. and Vizcarra, G. 1989. Los yacimientos de oro de Los Lipez (Bolivia). T I, Informe N 19. ORSTOM en Bolivia. Mission de La Paz. 26 pp.

Gangui, A. 1998. Seismic stratigraphy of the Pozuelos basin: Northern Puna, Argentina. *X Congreso Latinoamericano de Geología, Buenos Aires, Actas* **1**, 12-17.

Hèrail, G., Baby, P. and Soler, P. 1994. El contacto Cordillera Oriental-Altiplano en Bolivia: Evolución tectónica, sedimentaria y geomorfológica durante el Mioceno. *VII Congreso Geológico Chileno, Concepción, Actas* **1**, 62-66.

Jordan, T.E. and Alonso, R. 1987. Cenozoic stratigraphy and basin tectonic of the Andes Mountains. 20°-28°, South latitude. *American Association of Petroleum Geologists Bulletin* **71**, 49-56.

Kennan, L., Lamb, S. and Rundle, C. 1995. K-Ar dates from the Altiplano and Cordillera Oriental of Bolivia: implications for Cenozoic stratigraphy and tectonics. *Journal of South American Earth Science* **8**: 163-186.

Kley, J., Muller, J., Tawackoli, S., Jacobshagen, V. and Manutsoglu, E. 1996. Pre-Andean and Andean-age deformation in the Eastern Cordillera of Southern Bolivia. *Journal of South American Earth Sciences* **10**, 1-19.

Ort, M.H., 1991. Eruptive dynamics and magmatic processes of Cerro Panizos, Andes. PhD thesis, Univ. California, Sta. Barbara. 474 pp.

Seggiaro, R. and Aniel, B. 1989. Los Ciclos Volcánicos Cenozoicos del Area Coranzulí-Tiomayo, Jujuy, Argentina. *Revista de la Asociación Geológica Argentina* 44 (1-4): 394-401.

Sempere, T., Butler, R.F., Richards, D.R., Marshall, L.G., Sharp, W. and Swisher, C.C. 1997. Stratigraphy and chronology of Upper Cretaceous-lower Paleogene strata in Bolivia and northwest Argentina. *GSA Bulletin*, 109: 709-727.

Turner, J.C. 1978. Descripción Geológica de las Hojas 1a y b, Santa Catalina y 2a, San Juan de Oro. Provincia de Jujuy. *Boletín del Servicio Geológico Nacional,* **156-7**: 1-56.

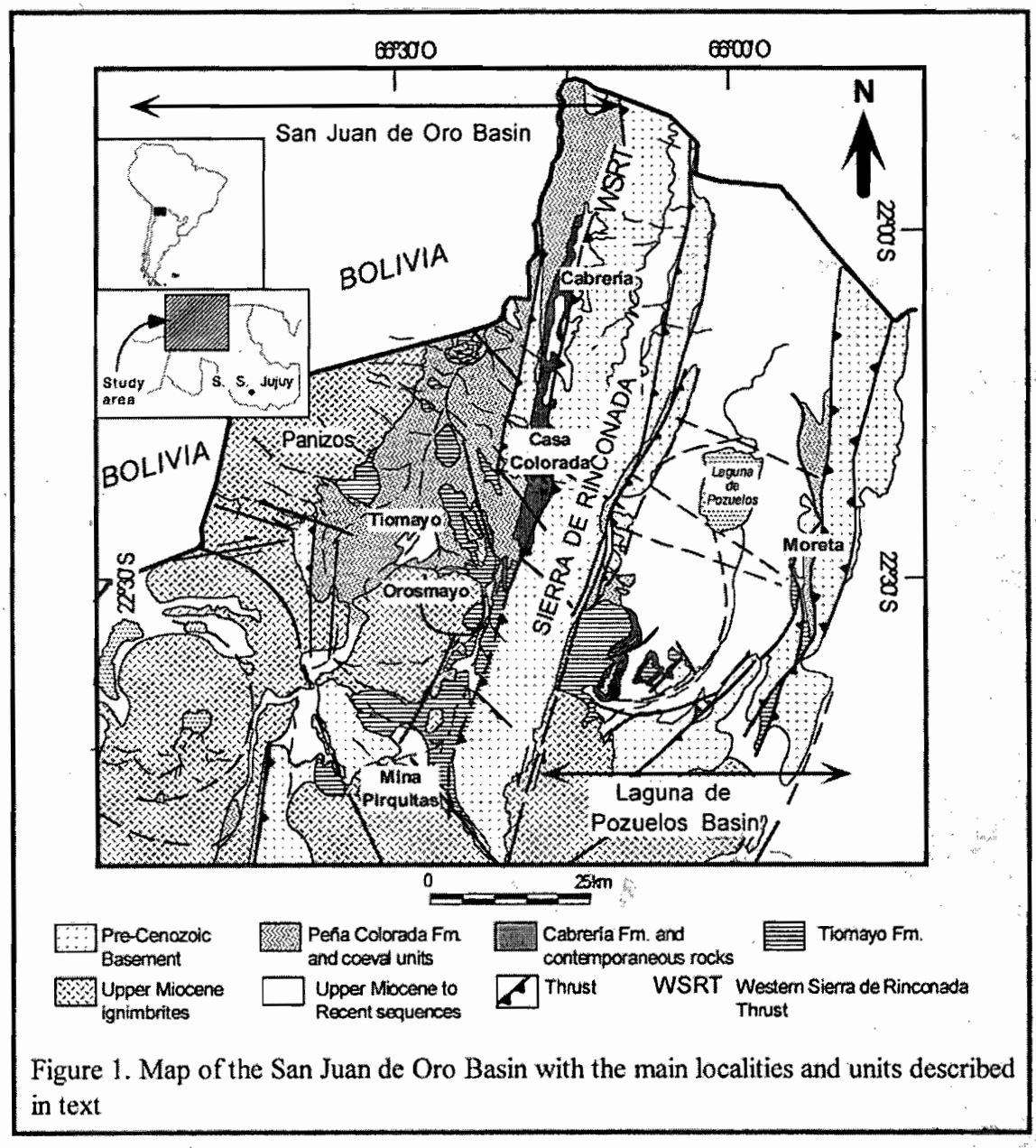

Figure 1. Map of the San Juan de Oro Basin with the main localities and units described in text

Sample	Unit	Location	Material	% K (wt.%)	^{40}Ar rad (nl/g)	% atm ^{40}Ar	Age Ma	Error (2 sig.)
CCl-dat 1	Cabrería Fm. ignimbrite	22°14'S 66°20'W	Biotite	7.365	5.000	57	**17.4**	**0.8**
CCl-dat 3	Ign. in Lower Tiomayo Fm.	22°19'S 66°25'W	Biotite	7.315	4.490	36	**15.7**	**0.6**
Clau-1	Ign. in Lower Tiomayo Fm.	22°40'S 66°30'W	Biotite	7.037	4.095	43	**14.9**	**0.5**
StaAna-6	Orosmayo Ignimbrite	22°35'S 66°29'W	Biotite	7.563	3.149	42	**10.3**	**0.5**

Tabla 1: K-Ar analytical data and calculated ages by Geochronology Lab – SERNAGEOMIN.

BIOTITES $^{40}AR/^{39}AR$ AND ZIRCON FISSION TRACK DATING IN THE ZALDÍVAR PORPHYRY COPPER, NORTHERN CHILE

Eduardo A. CAMPOS S. (1), Jan R. WIJBRANS (2), Paul A. M. ANDRIESSEN (3)

(1) Universidad de Concepción, Casilla 3-C Concepción, Chile (came@geo.vu.nl, ecampos@udec.cl)

(2) De Boelelaan 1085, 1081 HV, Amsterdam, The Netherlands (wijj@geo.vu.nl)

(3) De Boelelaan 1085, 1081 HV, Amsterdam, The Netherlands (andp@geo.vu.nl)

KEY WORDS : Porphyry copper deposit, $^{40}Ar/^{39}Ar$ geochronology, zircon fission tracks, hydrothermal system.

INTRODUCTION

The dating of mineral having isotopic systems with different closure temperature provides an excellent opportunity to study the cooling history of ore deposits that are genetically related to intense hydrothermal activity such as the porphyry copper deposits (PCDs), regarding the selection of appropriated minerals whose isotopic system have not been modified by alteration or thermal events.

The Zaldívar deposit is located 175 km SE of the city of Antofagasta, in the western margin of the Atacama plateau of Northern Chile. The main pit, at the intersection of a NW and a NE trending fault system, is mainly dug in the Llamo porphyry (Fig. 1), a subvolcanic, NNE elongated granodioritic to rhyolitic intrusion emplaced within the Late Eocene-Early Oligocene West Fissure Structural Belt, which includes several of the world's largest PCDs. The Llamo porphyry is responsible for the primary mineralization event, its intrudes the Zaldívar porphyry, a sub-volcanic rhyolite of 290 ± 4 Ma age, as well as the fine-grained to porphyritic andesites from the Augusta Victoria Formation (between 66.6 ± 2.2 and 41.2 ± 2.2 Ma) (Fig. 1).

A previous geochronology study by Richards et al., 1999, in one sample collected at the Llamo porphyry reported a crystallization age (U/Pb in zircon) of 38.7±1.3 Ma and a weighted mean $^{40}Ar/^{39}Ar$ plateau of 37.40 +/- 0.18 Ma. Although this result is in agreement with data from other PCDs in the neighboring area (Escodida and Chimborazo), it can only be considered preliminary, as the exact location of the sample within the deposit is unknown. The present research is a more focused study aiming to further constrain the thermal history of the Zaldívar deposit during the period that follows the hydrothermal magma-related mineralizing event.

METHODS AND ANALYTICAL RESULTS

The sample preparation and all experimental and analytical work were carried out in the Department of Isotopic Geology at the Vrije Universiteit Amsterdam.

The ceasing time of the main magma-related hydrothermal system would be defined by applying the $^{39}Ar/^{40}Ar$ isotope dating method (closure temperature of about 350°C) (Harrison et al, 1985), on relatively unaltered igneous biotites phenocrysts from the Llamo porphyry. Complementarily, the application of zircon fission-track (ZFT) dating method may shed light on the time of cooling of the whole thermal event as fission tracks produced in zircons are only retained at temperature below ca. 250°C (Tagami et al., 1996); this temperature is lower than those usually defined for hydrothermal events in porphyry copper systems (mostly above 300°C),

$^{40}Ar/^{39}Ar$ systematics in biotites where carried out by the laser step heating technique in an argon laser probe. Incremental-heating experiments yield ages that vary from 37.68 ± 0.4 (sample S-05, Fig. 1) to 35.55 ± 0.7 Ma (sample S-03, Fig. 1). No major compositional or textural difference can be found between the older and younger biotites, except for biotites from sample S-03. These biotites show physical, optical and compositionally properties markedly different from those found in all other studied samples, and they are most likely of hydrothermal origin. Despite the different origin of biotites, the yielded age is undistinguishable between the igneous and hydrothermal biotites; therefore not separation will be made on further interpretations.

To minimize the effect of outliers and to identify modes in the data that will lead to a better age determination, the ages were analyzed on a cumulative probability plot (Fig. 2). The plot for all the measured samples indicates that the most probable date for this set of samples is 36.5 Ma, similar to the weighted mean age of all samples 36.57 ± 02.

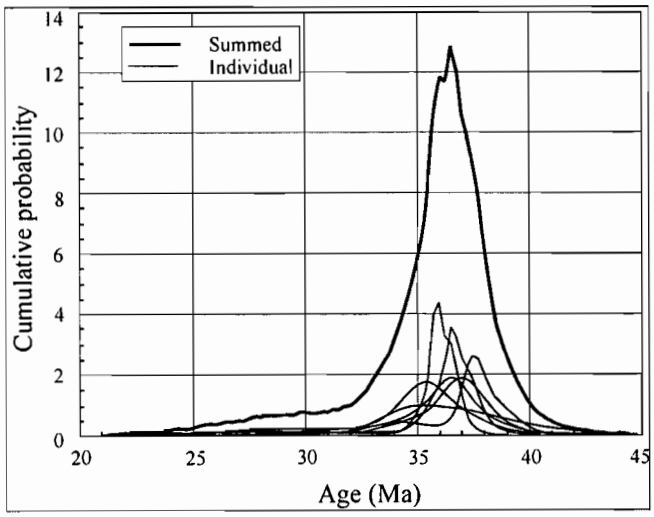

Figure. 2. Cumulative probability plot of step-heating $^{39}Ar/^{40}Ar$ ages in biotites from the Llamo porphyry. The enveloping curve is generated by summing the probability curves for each individual sample.

Because hydrothermal alteration events may disturb to varying degrees the $^{40}Ar/^{39}Ar$ systematics and in consequence affect the final outcome of the ages, it is necessary to evaluate this potential perturbing effect in the lights of the hydrothermal alteration observed in the analyzed samples. All studied samples are within the potassic alteration zone, which is stable between 350° to 700° C (Titley, 1982), and are not affected by lower temperature hydrothermal alteration such as phyllic or propylitic. The potassic alteration is overprinted by the supergene alteration that characterized by the kaolinitization of biotites and feldspars.

Because the closure temperature for the $^{40}Ar/^{39}Ar$ system in biotite is below the lower temperature range defined for potassic alteration, and the supergene kaolinite is not stable at temperatures higher that 300°C (Hemley et al., 1971, *in* Moore and Nash, 1974). The system $^{40}Ar/^{39}Ar$ should not be thermally disturb by the hydrothermal alteration, and the only perturbation that may be expected would be chemical and will be related to the supergene alteration.

All studied samples yield comparable ZFT ages of about 29 Ma, independently of the provenance of the sample or the host rock of the zircon grains (Andesites, Llamo porphyry or Zaldívar porphyry) (Fig. 1). In fact, sample S-03 taken east of the Portezuelo fault, the major structure in the site, and sample S-11 taken west of this fault, show comparable ZFT ages, although they yield contrasting $^{39}Ar/^{40}Ar$ ages (Fig 1). The weighted mean age of all ZFT ages is 29.08 ± 1.2 Ma.

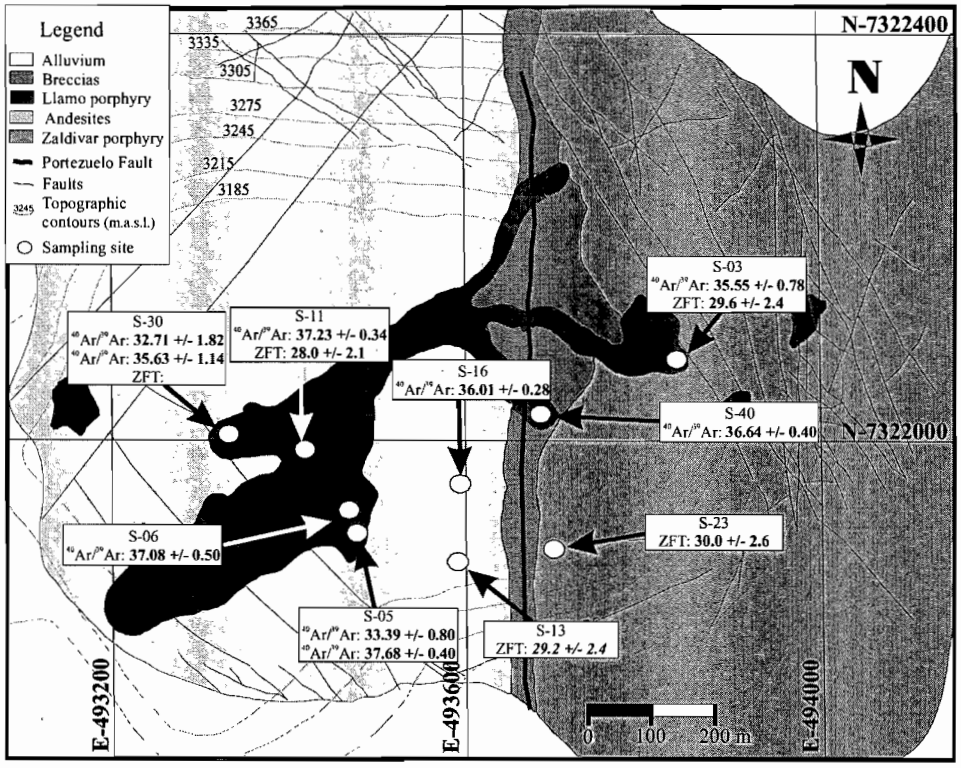

Figure 1. Geochronology data from $^{40}Ar/^{39}Ar$ in biotites and zircon fission track (ZFT).

DISCUSSION AND CONCLUSIONS

The weighted mean age for the $^{40}Ar/^{39}Ar$ ages in biotites from Llamo porphyry yield 36.57 ± 0.2 Ma and is in satisfactory agreement with, but more comprehensive than, the 37.4 ± 1.8 Ma also measured in igneous biotites reported by Richards et al., 1999. Because the closure temperature for the $^{40}Ar/^{39}Ar$ system in biotites is about 345°C, the biotite $^{40}Ar/^{39}Ar$ age will constrain the time at which the samples were cooled below this temperature, furthermore the homogeneous plateau ages imply that reheating has never occurred. As the closure temperature for the $^{40}Ar/^{39}Ar$ system in biotite is closely similar to the lower temperature defined in the magma-related hydrothermal fluids (~350°C) (Campos et al., 2001), the yielded $^{40}Ar/^{39}Ar$ ages will represent the ceasing of the main mineralizing hydrothermal system.

The crystallization age for the Llamo porphyry defined by U/Pb in zircon is 38.7 ± 1.3 Ma (Richards et al., 1999), in combination with $^{40}Ar/^{39}Ar$ ages (ca. 36.5 Ma) and fluid inclusions microthermometry data (Campos et al., 2002), defines a time span between the crystallization of the intrusives and the ceasing of the main mineralization-alteration event at the Zaldívar deposit of about 2 Ma, in agreement with the intrusive-mineralization-alteration timing defined for other PCDs of northern Chile (e.g. Reynolds, 1997; Clark et al., 1998).

In the Escondida mine (5 km south of Zaldívar), a PCD that is coeval with Zaldívar deposit (Richards et al., 1999), the magmatic activity continues long after the main mineralization event and is represented by a suite of dacitic dikes that yield ages as young as 31 Ma (K-Ar whole-rock) (Alpers and Brimhall, 1988). This value is comparable with the ZFT age defined in the Zaldívar mine (29, 1 ± 1.2 Ma). Although no direct evidences of post mineralization magmatic activity similar to the one observed in the Escondida area has been found in the Zaldívar deposit, the ZFT age most probably is dating the end of the magmatic activity in the Zaldívar-Escondida area, specifically signaling the time when the whole site cooled through the temperature of ca. 250°C.

REFERENCES

Alpers, H. C., Brimhall, G. H., 1988, Middle Miocene climatic change in the Atacama Desert, northern Chile: Evidences from supergene mineralization at La Escondida: *Geological Society of America Bulletin*, v 100, p. 1640-1656.

Clark, A. H., Archibald, D. A., Lee, A. W., Farrar, E., and Hodgson, C. J., 1998, Laser probe $^{40}Ar/^{39}Ar$ ages of early- and late-stage alteration assemblage, Rosario porphyry copper-molybdenum deposit, Collahuasi District, I Region, Chile: *Economic Geology*, v. 93, p. 326-337.

Harrison, T. M., Duncan, I., and McDougall, I., 1985, Diffusion of ^{40}Ar in biotite: Temperature, pressure and compositional effects: *Geochimica et Cosmochimica Acta*, v. 49, p. 2461-2468.

Moore, W. J., and Nash, J. T., 1974, Alteration and fluid inclusion studies of the Porphyry Copper ore body at Bingham, Utah: *Economic Geology*, v. 69, p. 631-645.

Richards, J. P., Noble, S. R., Pringle, M., 1999, A revised late Eocene age for porphyry copper magmatism in the Escondida Area, Northern Chile: *Economic Geology*, v. 94, p. 1231-1248.

Reynolds, P., Ravenhurst, C., Zentilli, M., and Linsay, D., 1997, High precision $^{40}Ar/^{39}Ar$ dating of two consecutive hydrothermal events in the Chuquicamata porphyry copper system, Chile: *Geological Association of Canada-Mineralogical Association of Canada*, Program with abstracts, v. 22, p. A-125.

Tagami, T., Carter, A., and Hurford, A. J., 1996, Natural long-term annealing of zircon fission-track system in the Vienna Basin deep borehole samples: constrains upon partial annealing zone and closure temperature: *Chemical Geology*, v. 130, p. 147-157.

Titley S., 1982, The style and Progress of Mineralization and Alteration in Porphyry Copper Systems, America Southwest: *in* Tetley, S. R., ed., Advances in Geology of the Porphyry Copper Deposits, Southwestern North America. 93-116.

PALEOGEOGRAPHIC CONTROL ON THE EVOLUTION OF TERTIARY BASINS IN THE WESTERN CORDILLERA AND ALTIPLANO OF SOUTHERN PERU (CONDOROMA-CUSCO-AYAVIRI)

Victor CARLOTTO(1), Gabriel CARLIER(2), Etienne JAILLARD(2), Georges MASCLE (3) José CARDENAS(1), Michel FORNARI(2), Luis CERPA(1)

(1) Universidad Nacional San Antonio Abad del Cusco. Peru, carlotto@chaski.unsaac.edu.pe
(2) IRD France: gabi@cimrs1.mnhn.fr, ejaillar@ecnet.ec, Michel.Fornari@unice.fr
(3) LGCA-Grenoble-France, Georges.Mascle@ujf-grenoble.fr

KEY WORDS: Paleogeography, strike-slip basin, Tertiary, Southern Peru, Western Cordillera, Altiplano.

INTRODUCTION

The lithosphere of the southern Peruvian Central Andes results from a long history of orogen superposition. The structures inherited during this process originate a high mechanical heterogeneity which controlled the deformation of the lithosphere each time it is subject to a new stress field. The evolution of the Andes of southern Peru offers a good example of the influence of lithospheric heterogeneity within a context of type-A subduction. Mesozoic paleogeography shows, from W to E, a Western Basin (Western Cordillera), a structural high called Cusco-Puno Swell (CPS, western Altiplano), and the Putina and Eastern Basin (eastern Altiplano and Eastern Cordillera) (Jaillard, 1994). This swell was limited from the western marine basin by the Cusco-Lagunillas-Mañazo (CML) fault system, and from the eastern marine and continental basin by the Urcos-Sicuani-Ayaviri (USA) fault system (Fig. 1) (Carlotto, 1998). These two systems formed during the Mesozoic. They are structures inherited from the Paleozoic or even older, and they separate two Proterozoic basements. During the Mesozoic, the CPS was covered by an average of 1 km thickness of sediments, mostly continental and occasionally restricted marine. However, during the Tertiary, it received continental sediments which may locally exceed 10 km thicknesses. Tertiary evolution was controlled by this paleogeographic feature, affecting not only the evolution of the basins, but also the deformation, the tectonic style, and the vergence of thrusting.

EVOLUTION OF TERTIARY BASINS

Andean deformation events began in southern Peru during the Late Cretaceous affecting the Western Cordillera, and continued during the Paleocene, migrating towards the NE. Thickening and loading of the crust

beneath the Western Cordillera resulted in the development of a Paleocene foreland basin with continental deposits at the boundary zone between the Western Cordillera and the Altiplano (Quilque and Chilca Formations) (Fig. 2).

Early Eocene (approx. 50 to 42 Ma) sedimentary record is absent from the Western Cordillera and adjacent Altiplano, where younger deposits overlie Cretaceous and locally Paleocene units with strong unconformity, suggesting the erosion of the Western Cordillera during this period. We interpret this as a result of important uplift due to thickening of the crust, which became unstable and underwent delamination. At the same time, basic calc-alkaline magma (gabbro, cumulates and diorites) developed in the Western Cordillera, as exposed along its northern margin at the Andahuaylas-Yauri batholith. This magmatism probably resulted from fusion of the asthenosphere, which rose and was emplaced in the space left over by the lithosphere after sinking during delamination. Uplift and magmatism along the Western Cordillera resulted in its erosion, as well as feeding and filling of the San Jerónimo Red Beds Basin to the north, i.e., over the former structural high of the Cusco-Puno Swell (Western Altiplano). A thick alluvial and fluvial thickening-coarsening sedimentary pile exceeding 4 km (Kayra Formation) (Fig. 2) developed between approx. 50 and 42 Ma. The basin was bounded by the CLM and USA fault systems (Fig. 1), with right-lateral strike slip, and apparently corresponding to former faults separating the swell from the western and eastern basins. These faults did not lead to a classical pull-apart basin because the swell has an apparently thick substrate which behaves as a rigid massif which prevents thinning. Uplifted areas, located mainly to the south, are due both to delamination and right-lateral strike slip in relation with regional stress and plate kinematics taking place during that time.

Compressive deformation along the NE margin of the Western Cordillera and in the Altiplano took place around 44-40 Ma, initiating alluvial and fluvial coarse-grained deposits of the Pichu basin in the Western Cordillera, and in the Anta basin along its NE margin, with thicknesses exceeding 3 km. This coarsening sequence coincided with calc-alkaline andesitic and dacitic volcanism dated between 37 and 38 Ma towards the base, and alkaline towards the top, where it is dated in 29.9 Ma (Carlotto,1998). Meanwhile, sedimentation and deformation continued in the Altiplano, with the development of progressive unconformities within the San Jerónimo basin (Soncco Formation, 3 km thick, and dated at the top in 29.9 Ma) of the former CPS. This compressive event affected the delaminated zone, i.e., the Western Cordillera, which had a thin crust but still allowed the development of smaller calc-alkaline subvolcanic intrusive bodies (36-32 Ma). Compression also developed thrusting along the faults limiting the basin and the swell, particularly the northern margin of the Western Cordillera over the Altiplano. Within this context, the Pichu and Anta basins are interpreted as piggy-back basins located behind the CML fault system, with the San Jerónimo basin (Soncco Formation) in a foreland position (Fig. 1).

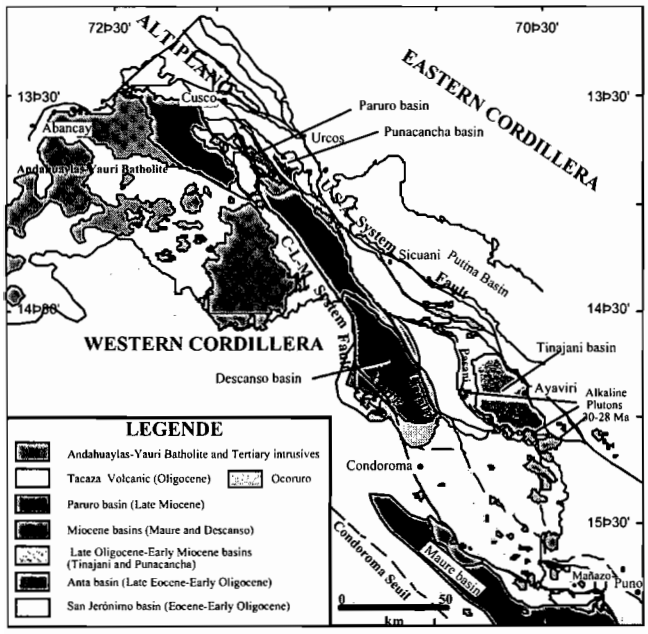

Fig. 1 Structural sketch-map of the Cusco-Ayaviri-Condoroma region showing the Tertiary basins, intrusives and volcanics rocks

The first potassic and shoshonitic alkaline magmatic events appear in the area between 30 and 28 Ma (Carlier et al., 1996). Potassic and ultrapotassic magmatism originated from fusion of rocks resulting from thermal re-equilibrium between a thick lithosphere (Altiplano) and a thinner lithosphere after delamination (Western Cordillera). The shoshonitic rock is originated from mixing of ultrapotassic and calc-alkaline magmas. This magmatism was also controlled by the CML and USA fault systems.

Around 30-28 Ma, and up to 20 Ma (late Oligocene-basal Miocene), an important volcanic activity took place in the Western Cordillera, and particularly along its NE margin (Tacaza volcanism). At the same time, the northern margin of the Western Cordillera locally received the Ocoruro conglomerates, indicating that the fault systems limiting the Western Cordillera and Altiplano were still active and served as conduits for the vulcanism (Figs. 1 and 2). Intermontane basins began to form in the Altiplano, in relation with the strike-slip faults of the CLM and USA fault systems (Fig. 1). Deposition in the Tinajani basin began around 28 Ma with a 600m, fluvial-lacustrine fining-upwards sequence controlled by the Pasani fault to the south, and Ayaviri fault to the north (Flores & Rodriguez, 1999). In Cusco, the Punacancha basin also developed during this period, with a 400m fluvial fining-upwards sequences controlled to the south by the Anyarate fault. The structures controlling these basins are part of the CML and USA fault systems, and had left-lateral strike-slip displacements, in agreement with the regional E-W tensors active at the time (Figs. 1 and 2).

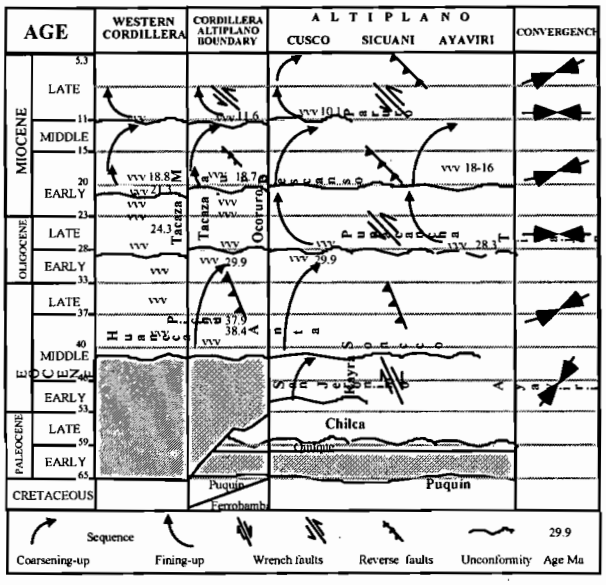

Fig. 2. Correlation chart of the main Tertiary stratigraphic formation of the Western Cordillera and Altiplano of Southern Peru

Between 22 and 12 Ma (Early-Middle Miocene) the Maure basin developed within the Western Cordillera (Fig. 1 and 2) and was filled with a 500 m coarsening sequence of lacustrine and fluvial deposits contemporaneous with explosive volcanism (21.39 and 18.82 Ma, Ar-Ar: Fornari, unpublished). This basin is located to the north of the Condoroma high, which apparently is a paleostructural high within the Western Cordillera, south of the CLM fault system, and continues into Bolivia (Fig. 1). At the boundary between the Western Cordillera and the Altiplano, the Descanso basin also developed during the same period as the Maure basin (Early-Middle Miocene), with a similar evolution of 800 m fluvial-lacustrine coarsening sequence and volcanism (Cerpa & Meza, 2001). The Langui and Yauri faults controling this basin are part of the CLM system (Fig. 1). In the Altiplano, continental sedimentation continued in the Tinajani (600m) and Punacancha (>1200m) basins during the Early-Middle Miocene, with a thickening-coarsening fluvial-alluvial sequence resulting from NE-SW compressive stress along the boundary thrust faults controling the basin.

Between 12 and 7 Ma (Middle-Late Miocene), sedimentation continued in the Maure basin of the Western Cordillera (Fig. 1 and 2), with a 500 m fining sequence unconformably overlain by volcanics dated in 4.92 Ma Ar-Ar (Fornari, unpublished). At the boundary between the Western Cordillera and the Altiplano, sedimentation also continued in the Descanso basin (Fig. 1 and 2) with a 200 m thinning-fining sequence mainly controled by the Langui fault (Cerpa & Meza, 2001). In the Altiplano, a new smaller basin began to

develop, the Paruro basin, with a 500 m thinning-fining alluvial-fluvial-lacustrine sequence related with the Yaurisque fault located to the south (Jaimes & Romero, 1996; Carlotto, 1998). During this period, all the basins were subject to an almost E-W regional stress, with boundary faults undergoing left-lateral strike-slip (Fig. 2).

Between 7 and 5 Ma (Late Miocene) important deformation and volcanism took place in the Western Cordillera. The deposits of the Maure basin are unconformably overlain by volcanics dated in 4.92 Ma. However, at the Western Cordillera-Altiplano boundary the tectonic compression seems to be buffered, particularly south of the Descanso basin, where the lacustrine deposits at the top of the Descanso basin sequence grade into volcanic deposits dated between 7 and 5 Ma. Meanwhile, in the Altiplano of Cusco, the Paruro basin underwent important compressive tectonic activity, with deposition of alluvial-fan coarsening sequences (600m) prograding to the north, and displaying progressive unconformities controlled to the south by the Yaurisque fault, which now behaves as a thrust. The regional stress was compressive and NE-SW oriented, in accord with plate kinematics.

CONCLUSIONS

The mechanical heterogeneity of the Andes of southern Peru greatly conditioned the Mesozoic paleogeographic scheme, which in turn controlled the evolution of Andean deformation and Cenozoic basins. The Mesozoic normal and strike-slip fault systems of Cusco-Lagunillas-Mañazo (CLM) and Urcos-Sicuani-Ayaviri (USA) defined a structural high (Cusco-Puno Swell). During the Tertiary these faults acted mostly as strike-slip and reverse faults, and currently display an en echelon pattern. The CLM fault system controlled the uplift of the northern margin of the Western Cordillera, in relation with both Early Eocene delamination and right-lateral strike-slip leading to development of the San Jerónimo Red Beds (Kayra). Beginning at this time (42 Ma), the regional stress field changed first to NE-SW compression, and later to alternating E-W compression. This resulted in left-lateral strike-slip movements and NE-SW compression, with reverse displacements along the CLM and USA fault systems controlling the evolution of the basins. These faults also controlled the highly-potassic alkaline magmatism present from the Oligocene (30 Ma) and with a deep magmatic source.

REFERENCES

Carlier, G., Lorand, J.-P., Bonhomme, M. & Carlotto, V. 1996. A reappraisal of the Cenozoic Inner Arc magmatism in the Southern Peru. 3rdISAG, St Malo, ORSTOM ed., 551-554.

Carlotto, V, 1998. Evolution andine au niveau de Cusco (Pérou). Ph.D., Université de Grenoble, France, 159 p.

Cerpa, L., Meza, P. 2001. La cuenca Descanso-Yauri (Mioceno). Tesis Universidad de Cusco, Perú, 121 p.

Flores, T., Rodriguez, R. 1999. La cuenca Tinajani: (Ayavir-Puno). Tesis Universidad de Cusco, Perú, 68 p.

Jaillard, E. 1994. Kimmeridgian to Paleocene tectonic and geodynamic evolution of the Peruvian (and Ecuadorian) margin. In: Cretaceous tectonics in the Andes, Salfity, Ed., 101-167, Earth Evolution Sciences.

Jaimes,F., Romero, D. 1996. La cuenca Paruro (Mioceno superior). Tésis Universidad de Cusco, 71 p.

GEOCHEMICAL ASPECTS OF HOST-ROCKS OF POLYMETALLIC VEINS PARAMILLOS DE USPALLATA, MENDOZA, ARGENTINA

Silvia Irene CARRASQUERO

Facultad de Ciencias Naturales y Museo (Universidad Nacional de La Plata), Paseo del Bosque, s/nº, (1900) La Plata, Argentina (scarras@museo.fcnym.unlp.edu.ar).

KEYWORDS: polymetallic veins, volcanism, geochemistry, Andes, Argentina

INTRODUCTION

The Paramillos de Uspallata mining district is located in the south argentine Precordillera: 32° 30'LS and 69° 05 LW and at 3500 m of altitude.

The "Paramillos de Uspallata" mineralised veins extend over some 16 km^2. They are located centre-west of the porphyry deposit sector, hosted by the Uspallata Group diabase and sediments, together with andesitic porphyrys. In this region there are various ore deposits (Carrasquero, 1999): porphyry-type "Paramillos Norte" and "Paramillos Sur", epithermal ore deposit, "Oros del Norte" and "Oros del Sur".

This research was undertaken as part of doctoral studies by the author (University of La Plata, Argentina)

REGIONAL GEOLOGIC SETTING

The Paramillos de Uspallata mining district is located in tectonically complex Precordillera. The stratigraphy is composed by (Fig. 1):

Villavicencio Group (Devonian): The oldest rocks in the district are metamorphized sediments, slates, green schists, phyllites, limestone and banded schists (Harrington, 1971). These rocks form the basement in the region. Pircas Conglomerate (Upper Devonian?): Overlain unconformably under Villavicencio Group: they are sedimentary rocks with slates and schist clasts (not shown in Fig. 1). The Pircas Conglomerate is a slope deposit in the Lower Paleozoic surface with thickness of 35 meters. Choiyoi Group (not shown in Fig. 1) is composed by andesites, rhyolitic ignimbrites, quartz porphyry and breccias. Their thickness is 60 to 1000 m. These rocks were dated upper Permian to lower Triassic. It is composed by pyroclastic levels with rhyolitic sequences and alkaline volcanism.

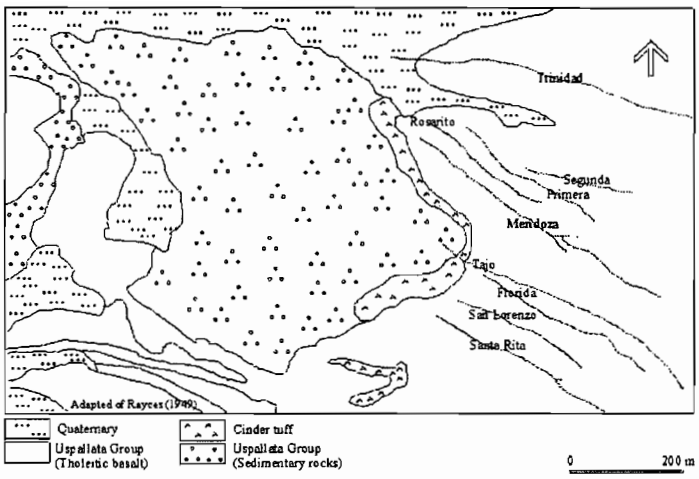

Geological map of polymetallic ore deposit
Paramillos de Uspallata, Mendoza, Argentina

Figure 1 Geological simplified map

Uspallata Group: Clastic sediments (Middle-Late Triassic): red conglomerates, yellow dark sandstones, slates and bituminous schists. The group presents the intercalations of sills and volcanic rocks, with characteristics of rifting stage (middle Triassic). The intraplaque volcanism is formed by tholeitic alkaline basalt and andesite basalt. Miocene volcanism: The distribution and character of Miocene volcanism in this region suggest that the subducted zone has shallowed over the last 18 Ma. After this processus, the magmatic arc is located in Precordillera. The volcanism include stocks, sills, dykes, andelacitic porphyrys and monzodiorite rocks Cortés et al.(1997).

In this region there are several deformation events; after Paleozoic phases, in the Triassic age developped extensional hemi-grabens. This deformation is continuated in the Tertiary by a contraction tectonic, accordingly produced the inversion of basins. The main structural trend in the region is NW and NE. The faulting NW is the most important structure because it controlled sulfide mineral distribution, along with parallel faults. The hydrothermal system vein is controlled by the intersection of two systems of faults trending E-W and NW-SE, with mineralization extending along strike 300-1500 m with a maximum thickness of 3 m.

GEOCHEMISTRY AND PETROGRAPHY OF HOST-ROCKS OF POLYMETALLIC ORE DEPOSITS

This volcanism is basic (Table 1), with 48 % SiO2; moderaly to high TiO_2 (0.42-2.51 %), the Al_2O_3 is > 13.99 %. The Fe_2O_3 contents are variable (4.26-10.75 %) and the MgO-rich < 2.80 %.

Ba contents is variable 117-1241 ppm, Ba/La is 3.7 (one sample > 22), normal relation for within plate volcanism), Zr (208-346 ppm), Y high, (16-34 ppm), the comportment of Zr and Y is characteristic of inmobile REE (Fig. 2); high Cr (48-221 ppm) shows their primitive nature (Fig. 3).

This volcanism is associated with the early opening of the South Atlantic Ocean; the volcanic rocks (sills and lava flows, Fig. 4) are composed of tholeiitic to slightly alkaline within-plate olivine basalts. The chemical analyses show the basic to alkaline signature; the mineralogy is formed with phenocryst plagioclase, olivine and opaque minerals. Where as the texture is porphyritic (Carrasquero, 2001).

Sample	SiO_2	Ti_2O	Al_2O_3	Fe_2O_3	MnO	MgO	CaO	Na_2O	K_2O	P_2O_5	LOI
Gn 3	48.96	2.22	18.25	10.75	0.20	2.30	2.13	6.43	0.41	0.42	4.36
Gn 8	48.28	2.51	16.62	8.32	0.17	2.79	4.84	5.24	2.15	0.64	4.18

Sample	Ba	Rb	Sr	Nb	La	Nd	Y	Zr	Cr	Hf	Ni
Gn 3	133	11	442	5	36	31	16	208	221	2	110
Gn 8	1084	40	701	10	46	43	28	346	29	4	3

Table 1: Analyses of Volcanic rocks of Paramillos de Uspallata Group.

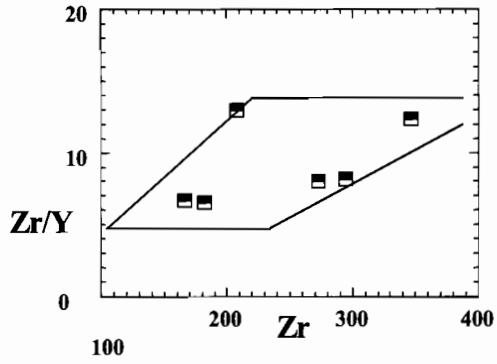

Figure 2. Plots of Zr/Y-Zr, the within-plate lavas are inside of polygon figure.

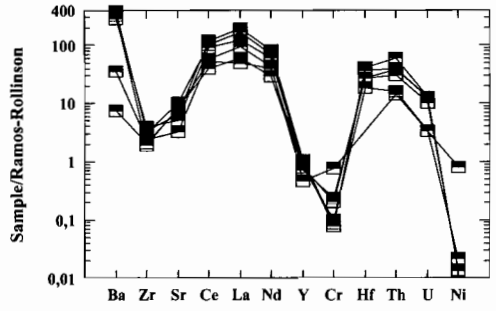

Figure 3. Spider diagram after Bevins et al. 1984 (in Rollinson, 1995) and Ramos and Kay, (1991).

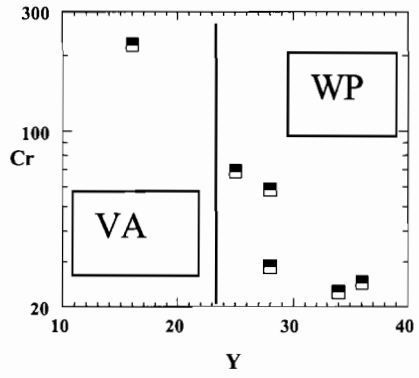

Figure 3. Plots of Cr-Y. Field arc volcanic (VA) and within-plate (WP).

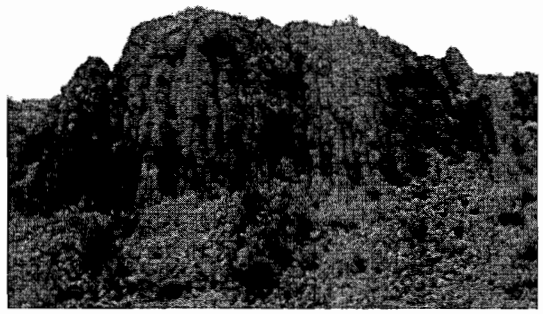

Figure 4. Picture of basaltic rocks (columnar jointing).

POLIMETALLIC ORE DEPOSITS

This ore deposit comprises forty principal and secondary veins: "Santa Rita", "San Lorenzo", "Tajo", "Vallejos", "Belén", etc. The veins show breccias structures with fine grained groundmass between host rock and mineralization: an example of this is shown in the "Vallejos" vein. In the "San Miguel" and "Rosario" veins, banded siderite, and sphalerite with a central infilling composed of fine grained siderite with quartz veinlets is developed. The mineralogy veins is composed of one primary zone, with pyrite, silver galena, tetrahedrite,

sphalerite, proustite-pyrargirite. The oxidation zone is formed by limonite, manganese oxides, crisocole, malachite and azurite. Where as the cementation zone have argentite, red silver. The gangue presents calcite, chalcedony and barite.

Fluid inclusions studies on the Paramillos de Uspallata mineralized veins (Tajo vein) have been done according to Garrido et al. (2001); the studies on quartz and sphalerite indicate homogenisation temperatures (Th) between 170-260° C and salinities between 4-19 %wt eq. NaCl. The $\delta^{18}O$ values of quartz vary between 11.5 and 13.8, the $\delta^{18}O$ values of siderite range from 15.5 to 19.1. Generally, the $\delta^{34}S$ values vary between 0.9 ± 5 to 8.0 ± 5 from galena and 2.8 ± 5 to 4.2 ± 5 from sphalerite. These data are consistent with a hydrothermal system invoking mixing of magmatic fluids with meteoric water.

CONCLUSIONS

The host-rocks of polymetallic veins Paramillos de Uspallata (Pb-Zn-Ag) are volcanic rocks; this volcanism (middle Triassic) is associated with the early opening of the South Atlantic. The volcanic rocks are composed of tholeiitic within-plate olivine basalts and they are intercalated with a Triassic sedimentary section and are formed sills and basalt lavas. The chemical analyses show the basic to alkaline signature whereas the mineralogy is formed with phenocryst plagioclase, olivine and opaque minerals and the porphyritic texture.

The mineralization shows 40 veins with silver minerals: Ag-galena and tetrahedrite principally; lead minerals and zinc mineral's, for example sphalerite. The data of isotopic studies and fluid inclusions suggests the mixing of hydrothermal system with meteoric water.

REFERENCES

Carrasquero, S. I. 1999. Porphyry-type and epithermal ore deposits in the Paramillos de Uspallata district, Mendoza, Argentina. Proceedings of the fifth biennal SGA meeting and the tenth Quadrennial IAGOD symposium, London. In: *Mineral deposits: processes to processing.* Edited by Stanley et al. I: 487-490. Balkema, Rotterdam.

Carrasquero, S. I. 2001. Nuevos aportes a la geoquímica del volcanismo de intraplaca en la región de Paramillos de Uspallata, Mendoza, Argentina. XI Congreso Latinoamericano de Geología y III Congreso Uruguayo. (Actas edición electrónica).

Cortés J. M.; González Bonorino, M. G.; Koukharsky, M. M. L.; Pereyra, F. X. and Brodkorb, A. 1997. Memoria de la hoja 3369-09, Uspallata, provincia de Mendoza, escala 1:100.000. Servicio Geológico Minero Argentino (Inédito). Buenos Aires, 1-164.

Garrido, M.; Domínguez, E. and Schalamuk, I. 2001. Veta Tajo, Paramillos de Uspallata, Mendoza. Características del sistema hidrotermal. Revista de la Asociación Geológica Argentina. 56 (1): 99-110.

Harrington, H. 1971. Hoja geológica "22c Ramblón" Boletín 114. Dirección de Minería de la Nación. Buenos Aires, 1-89.

Ramos, V. and Kay, S. M. 1991. Triassic rifting and associated basalts in the Cuyo basin, central Argentina. In Harmon, R. S. and Rapela, C. W. (Eds.) "Andean magmatism and its tectonic setting": boulder, Colorado, Geological Society of America Special Paper, 265: 79-91 pp.

Rollinson, H. R. 1995. Using geochemical data: evaluation, presentation, interpretation.

SEDIMENTARY DISTURBANCES IN LATE QUATERNARY FLUVIO-LACUSTRINE DEPOSITS OF THE LOS ZERPA MORAINE INDUCED BY THE BOCONÓ FAULT, MÉRIDA ANDES, VENEZUELA

Eduardo CARRILLO (1), Franck AUDEMARD (2), Christian BECK (3) and Michel COUSIN (3)

(1) Univ. Central de Venezuela, Fac. de Ciencias, Inst. Ciencias de la Tierra. (ecarrill@gea.ciens.ucv.ve)

(2) Fundación Venezolana de Investigaciones Sismológicas, Apartado Postal 76.880, Caracas 1070-A.

(3) Lab. de Geodynamique des Chaînes Alpines UMR, cnrs 5025, Univ. de Savoie, Bourget du Lac, France.

KEY WORDS: Paleoseismology, Sedimentation, Liquefaction, Boconó fault, Los Zerpa, Venezuela

INTRODUCTION

During the late Pleistocene glaciation in the Venezuelan Andes, known as the Mérida Glaciation, an important advance of moraines took place in the northern (shaded) slope of the Sierra de Santo Domingo (Schubert and Vivas, 1993). These moraines, among which are Mucubají, La Victoria, Los Zerpa and Las Tapias, were prominent landforms in that area at that time (**Fig. 1**). Not only climate has played a role in their sediment preservation and distribution, since they have also been subject to general Neogene-Quaternary chain uplift and to the tectonic activity of the right-lateral strike-slip Boconó fault. Therefore, climate and tectonic signatures are both simultaneously recorded in the late Quaternary high-altitude sediments of the Mérida Andes, in the lake Mucubají surrounds.

The sedimentary record in the fluvio-lacustrine deposits preserved inside Los Zerpa moraine is an outstanding example of sedimentation and active tectonics interplays (Audemard et al., 2001). The terminal part of this moraine is cut and right laterally offset by the main strand of the Boconó Fault, where a rather narrow and small pull-apart basin is being created, which in turn induces down-slope motion of the entire upstream section of the moraine (Audemard et al., in this volume). Therefore, these fluvio-lacustrines sediments deposited after the last glaciation (< 15 ka) are controlled by both climatic variability and local tectonics; the latter being chiefly due to the active Boconó Fault (BF).

SEDIMENT DISTRIBUTION AND TERRACING

A thick package of coarse conglomerates is the first fluvial sediments to fill the moraine bottom, after retreat of the Los Zerpa glacier. This aggradational terrace is about 25 m thick. Subsequently, this terrace was eroded due to runoff increase, leaving a slightly lower terrace with no pair on the right bank. Then, a second episode of valley fill is

attested by an aggradational terrace. This terrace is presently hanging about 10 m high over the river bed, but it was subsequently cut by two other lower sets of terrace flights (**Fig. 2**). We presume that age of these terraces could give clues about the largest earthquakes on the BF. The second aggradational terrace used to end up into a small lake as an underwater delta. These alternating aggradation/erosion terraces, besides denoting a few-thousand-year-long climatic cyclity, have also recorded local tectonic instability because of exhibiting anomalous (sideward and back-) tilts, as well as quick river down-cutting. Tilting is attested by paleocurrent changes in some Los Zerpa lake-shore sediments (**Fig. 3**). The Mucubají, La Victoria and Las Tapias moraines and infills also show anomalous tilting.

LAKE SEDIMENTS AND SOFT-SEDIMENT DEFORMATION

Because lake deposits are specially prone to earthquake–induced deformation (Sims, 1973), they are excellent earthquake recorders. The pore-pressure build-up in unconsolidated well-saturated sands by a strong earthquake induces soil liquefaction which is typically recognized by structures such as: convoluted bedding, ball and pillows, sand dikes, sand boils and flame structures (Audemard and De Santis, 1991; Obermeier, 1996).

In the Los Zerpa paleolake sediments, locally cross-cut by the BF main strand, the most distal facies are almost totally clay-laminated. Occasionally, their are intercalated with some few-centimeter-thick sand beds that display flames and ball and pillow structures attesting earthquake-induced liquefaction (**Fig. 4**). Besides, small-scale slumps are also present in some clayey intervals. In the proximal lake facies, near the southeastern edge and closer to the submarine delta front, sand content and number of sand beds increase. Three clay beds intercalated within such sand units display slumping. Slumping is so intense that folds are almost isoclinal. Orientation of fold axial surfaces indicates that shortening is transverse to river flow and subparallel to the BF trend. Besides, many other few-centimeter-thick sand beds also underwent liquefaction. Chronology of the paleo-earthquakes recorded in these sediments is still under evaluation, but we believe that several (~5) earthquakes happened in the region in a shorter time span than the recorded by the flight of alluvial terraces.

FLUVIO-DELTAIC SEDIMENTS AND DEFORMATION

The distal facies of the alluvial deposits essentially corresponds to an underwater front delta that used to pour into the previously-described lake. This delta exhibits a well-developed foreset, made of sands, micro-conglomerates and conglomerates. In the foreset sequence, seven stratigraphic packages bounded by unconformities ("tectono-sequence") were recognized (**Fig. 5**). These unconformities show progressive tilting to the NW although the two youngest unconformities lie almost subhorizontal. Both packages and unconformities are affected by SE-dipping normal listric faults, that seem to have also been progressively tilted. South of here, the delta sequence is crosscut by normal faulting conjugate to the previous one. We interpret that all these deformations correspond to a knee (?) fold propagating above a blind normal throw (slide-related) that simultaneously induces extension in the outer fold hinge (normal bending-moment faults). Each unconformity would correspond to a seismic event on the close BF and sedimentation would be definitely controlled by local tectonics/instabilities.

CONCLUSION

We presume that deformed clay beds, earthquake-induced liquefaction of sands and progressive fluvio-deltaic unconformities are all related to at least 4 to 7 large paleoearthquakes. This new paleoseismic record could complement the seismic history of the BF derived by Audemard et al. (1999) for the northern strand at the Apartaderos pull-apart basin. It is very likely that the number of recognized events shall increase with more detail and thorough sedimentological and paleoseismic analyses that are now in progress.

REFERENCES

Audemard F. and De Santis, F., 1991. Survey of liquefaction structures induced by recent moderate earthquakes. Bulletin of the International Association of Engineering Geology 44, 1-16.

Audemard, F., Pantosti, D.; Machette, M.; Costa, C.; Okumura, K.; Cowan, H.; Diederix, H., Ferrer C. and SAWOP participants, 1999. Trench investigation along the Mérida section of the Boconó fault (Central Venezuelan Andes), Tectonophysics 308, 1-21.

Audemard, F.; Beck, C.; Cano, V.; Carrillo, E.; Castilla, R.; Cousin, M.; Jouanne, F.; Melo, L. and Villemin T., in this volume. Stability of morainic complexes cut by the Boconó fault and their sedimentary signature, Mérida Andes, Venezuela. V International Symposium on Andean Geodynamics, Toulouse, France, september -2002.

Audemard, F.; Beck, C.; Carrillo, E.; Cousin, M. and Paterne, M., 2001. Sedimentary record of late Pleistocene seismic activity along the Boconó Fault (Mérida Andes): preliminary observations on the Los Zerpas Moraine-dammed paleo-Lake. 8ème Congrès Français de Sédimentologie, Novembre 2001-Orlèans, France- (Abstract).

Obermeier, S., 1996. Use of liquefaction-induced features for paleoseismic analysis –An overview of how seismic liquefaction features can be distinguished from other features and how their regional distribution and properties of source sediment can be used to infer the location and strength of Holocene paleo-earthquakes. Engineering Geology 44, 1-76

Sims, J., 1973. Earthquake-induced structures in sediments of Van Normal Lake, San Fernando California, Science, v. 182, 161-163.

Schubert, C. and Vivas, L., 1993. El Cuaternario de la Cordillera de Mérida. Universidad de los Andes-Fundación Polar, 345 pp.

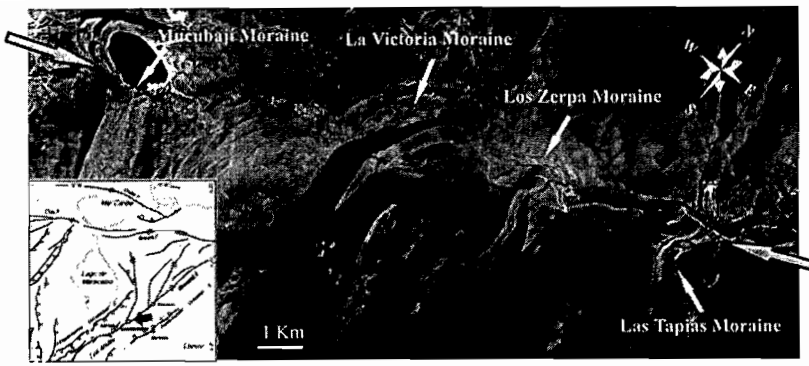

Figure 1. Los Zerpa, La Victoria, Mucubají and Las Tapias moraine locations at the Mérida Andes, Northern South America. The Yellow arrows point out the main Boconó fault trace. Notice how moraines are dextrally offset by fault.

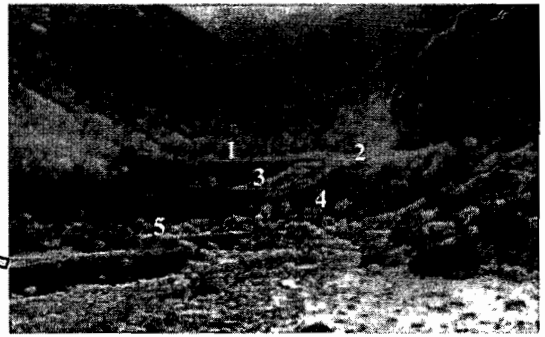

Figure 2. Flight of terraces in Los Zerpa Creek. Terraces 1 and 3 are post glacial fill periods and terraces 2, 4 and 5 correspond to erosional episodes. Paleoclimatic variability and Boconó fault activity control these sedimentary/erosion cycles.

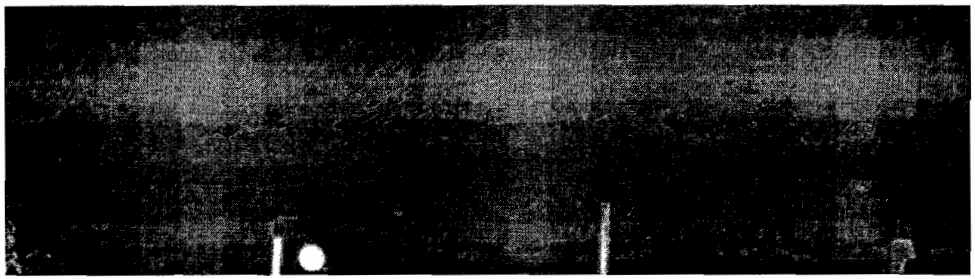

Figure 2. Earthquake-Induced liquefaction in Los Zerpa paleolake clayey sediments. The flame structure has been highlighted.

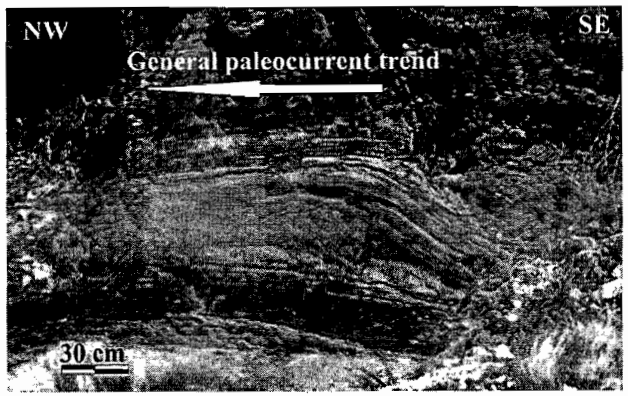

Figure 3. Small SE-prograding conglomeratic package against NW general fluvio-lacustrine paleocurrent direction in Los Zerpa Creek. Earthquake-induced back tilt in the paleolake basin momentarily changed the paleocurrents and facies distribution.

Figure 4. Los Zerpa paleolake underwater-delta sediments: these progressive unconformities bounded sequences show tectonics control in sediment distribution. The five oldest tilted sequences are truncated by subhorizontal sediments. It implies that sequences are folded during ongoing extension. The two youngest sequences represent a post-earthquake fill in the 10-m- high terrace. These unconfomity-bounded sequences are clear evidence of tectonic control on sedimentation.

BRITTLE DEFORMATION AND FLUID TRANSPORT IN MAGMATIC ARCS: A CASE STUDY FROM THE ATACAMA FAULT ZONE

José CEMBRANO(1), Gabriel GONZÁLEZ (2), Ivo AHUMADA (3) and Gloria ARANCIBIA (4)

(1) Depto. Ciencias Geológicas, U. Católica del Norte, Angamos 0610, Antofagasta, Chile. jcembrano@ucn.cl
(2) Depto. Ciencias Geológicas, U. Católica del Norte, Angamos 0610, Antofagasta, Chile. ggonzale@ucn.cl
(3) Depto. Ciencias Geológicas, U. Católica del Norte, Angamos 0610, Antofagasta, Chile. iac001@ficg.ucn.cl
(4) Depto.de Geología, Universidad de Chile,Casilla 13518, Correo 21, Santiago, Chile. garancib@cec.uchile.cl

KEYWORDS: Tectonics, Atacama fault system, fluids, faults, duplex

INTRODUCTION

Several workers (e.g. Etheridge, 1983; Sibson, 1996; 2000) have set theoretical constraints on the dynamic interaction between fluid transport and faulting, especially for mesothermal ore deposits associated with reverse faulting (e.g. Sibson, 1988; Cox, 1999) and epithermal veins associated with strike-slip faulting (Sibson, 1987). However, to date there is little published field evidence that accounts for the operation of those processes in real examples (e.g. Bonson et al. 1997; Foxford et al. 2000). Furthermore, although the theoretical constraints on the dynamic interaction between fluid transport and deformation seem clear, few studies concentrate on the consequences of active deformation on the time-space physical and chemical evolution of hydrothermal fluids transported and emplaced in fracture networks (e.g. Coombs et al. 1993).

Fracture meshes, hydrothermal fluid circulation and mineral deposition in strike-slip environments

Sibson (1987, 1990, 1996) emphasizes the close relationship between the earthquake cycle and hydrothermal fluid migration and subsequent mineral precipitation in strike-slip settings. During a slip event on one master strike-slip fault, pre-existing and/or newly created vertical fractures that face the instantaneous extension direction will be sites of a sudden, significant decrease in fluid pressure. This local depressurization drives fluids into the extension fractures; a geologically instantaneous process lasting until internal fluid pressures re-establish equilibrium with the environmental hydrostatic pressures typical of upper crustal levels (< 4 km) (Figure 1a). This sort of dynamic interaction between brittle deformation and fluid flow is known as the suction pump mechanism. Under certain conditions, this mechanism can result in the precipitation of hydrothermal minerals triggered by boiling, mixing with cold meteoric waters and/or hydration reactions (e.g. Drummond and Ohmoto, 1985; Sibson, 1987, 1990; Coombs, 1993). According to Sibson (1990, 1996), the theoretical geometry of interconnected fault-veins networks at dilational jogs in strike-slip settings consists of vertical strike-slip barren master faults and subvertical extensional fault-vein networks with different geometries (Figure 1b). In particular, our experience shows that other subsidiary fractures, similar to those reported in Riedel type models, also host mineralized veins.

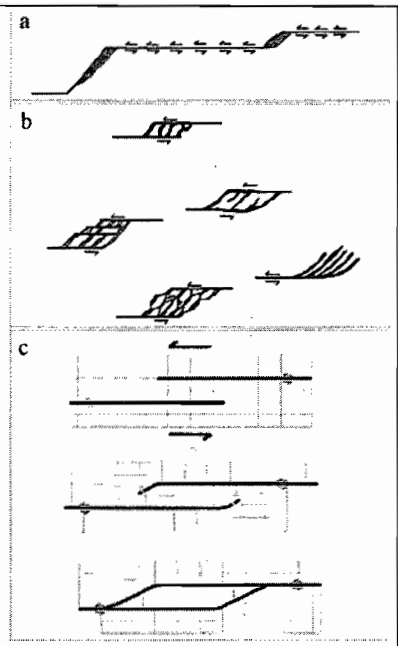

Figure 1. (a) Dilational jog linking two overstepping sinistral strike-slip fault zones. Rupture propagation is from right to left. Sudden drop in fluid pressure inside the jog during rapid slip transfer between master faults induces fluid flow towards the jog. This process may trigger mineral precipitation in response to boiling and/or by mixing with meteoric waters (e.g. Sibson, 1987). Internal geometry and kinematics of fault-vein networks forming at dilational jogs (b) is very similar to that resulting from the structural development of extensional strike-slip duplexes (c)
(Modified from Sibson, 1990; Woodcock and Fisher, 1986).

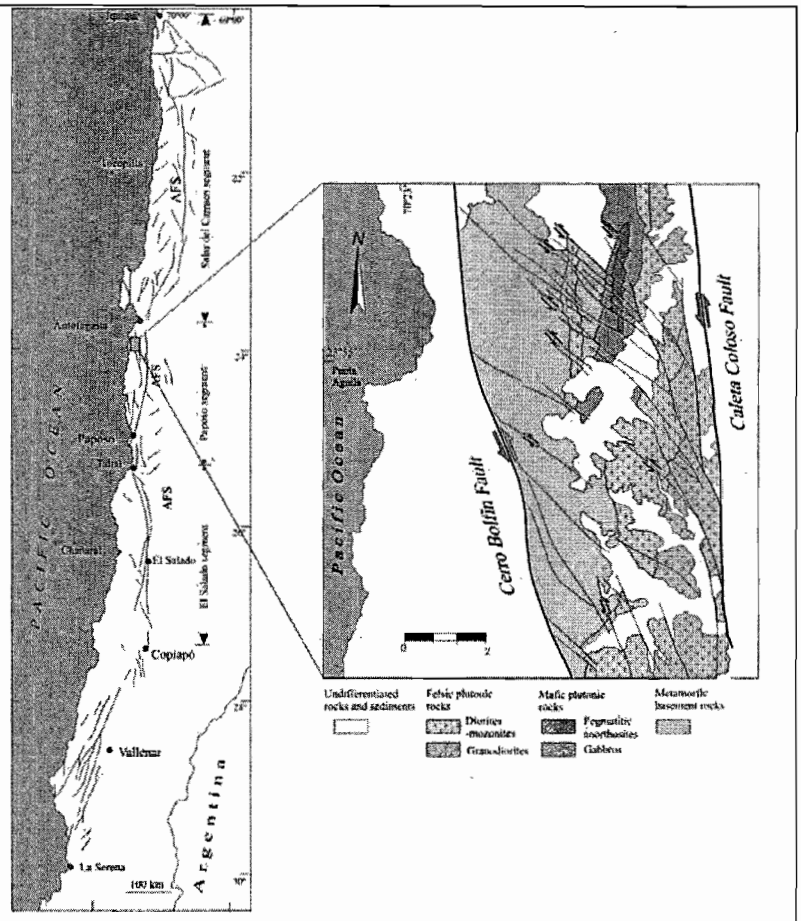

Figure 2. Regional scale geometry of the Atacama Fault System (AFS) in the Coastal Cordillera of northern Chile. Inset shows the Caleta Coloso Duplex formed by NW striking faults linking the ~NS-striking Bolfin and Caleta Coloso faults (modified of Brown et al. 1993; Scheuber and González, 1999).

If one compares the geometry and kinematics of extensional strike-slip duplexes described by Woodcock and Fisher (1986) and the structural mesh concept suggested by Sibson (1996) for fluid flow in strike-slip settings, there are remarkable similarities that demand further attention (Figure 1a,b, c). For instance, a requirement for the suction pump mechanism to operate in strike-slip settings is that slip occurs in one of two flanking strike-slip overstepping master fault (Figure 1a). Potential slip transfer from one master fault to the other is accomplished via propagation of extensional and/or hybrid fractures from one master fault to the other at a dilational jog. This propagation may result in a physical linkage between the two overstepping master faults in an analogous way to that proposed by Woodcock and Fisher (1987); to form strike-slip duplexes (Figure 1b,c). According to these authors, extensional duplexes may form from progressive propagation of Riedel-type shears from the tip of both overstepping master faults (Figure 1c). Consequently, we propose that extensional strike-slip duplexes play a twofold role of accommodating strike-slip displacement and serve as channelways for the migration of hydrothermal fluids in the upper crust.

In this contribution we focus on the processes related to the formation of a mid-Cretaceous strike-slip duplex belonging to the intra-arc Atacama Fault System in northern Chile. This structure, the Caleta Coloso Duplex, meets many of the requirements needed to address the problem of deformation and fluid migration. Master and subsidiary faults that form the duplex are filled with hydrothermal mineral associations constituting fault-veins, oblique extension veins and extension veins. Fault and veins show spectacularly well-preserved

internal structures such as mineral fibers, striated planes, banding, etc, that allow to reconstruct the deformation-mineralization history at both the local and regional scale.

THE CALETA COLOSO DUPLEX

The Caleta Coloso Duplex is part of the Atacama fault system (AFS) in the Central Andes (Figure 2). It is flanked by the Caleta Coloso Fault and the Bolfin Fault, two important regional-scale brittle structures of the AFS. The geometry, kinematics and timing of deformation of the AFS are very well known at the regional-scale (e.g. Brown et al. 1993; Grocott et al. 1994; Taylor et al. 1998; Scheuber and Gonzalez, 1999). Although the kinematics and timing of deformation vary along-strike, most authors agree that intra-arc transtensional to transpressional sinistral displacement was active during arc construction at least from 190 to 110 Ma along most of the present-day Coastal Cordillera from Antofagasta to Vallenar. Absolute age determinations of ductile deformation document coeval sinistral and dip-slip normal displacement at around 145 Ma and sinistral displacement around 125 Ma in the Paposo segment where the duplex is located (Scheuber et al. 1995; Scheuber and Gonzalez, 1999). Published data and our own field observations indicate that the Caleta Coloso strike-slip duplex formed during the last stages of activity of the AFS, shortly after 125 Ma, the age of mylonites near Cerro Paranal, 100 km farther to the south (Scheuber and Andriessen, 1990). Fission tracks in apatite from rocks crosscut by the duplex document that the rocks passed through the ~100° C geotherm at ca. 118 Ma (Scheuber and Andriessen, 1990), constraining the age of the duplex formation between 125 and 118 Ma . This time span is widely accepted to be the age of cooling and waning stages of arc magmatism in the Coastal Cordillera.

The Caleta Coloso duplex constitutes a structural arrangement that is representative of the AFS along the Coastal Cordillera between Paposo and Antofagasta. The first duplex-like structure of the area was described by Herve (1987), who identified some northwest striking faults with sinistral separation linking major north-south striking faults. All faults affect volcanic and plutonic rocks of the Coastal Cordillera magmatic arc. Preliminary structural investigations carried out in the faults of the Caleta Coloso Duplex show that bulk deformation was accommodated in a complex way. The subvertical Caleta Coloso fault strikes NNW and is marked by an hectometric-wide zone of striated faults, fault gouge, foliated cataclasites and foliated breccia that locally overprint and early mylonitic fabric. The matrix of the cataclastic rocks is filled with chlorite an epidote. Kinematic indicators document sinistral and sinistral-oblique normal displacement. The Cerro Bolfin fault strikes NNW, has a curved shape, and consists of a meter-wide zone of fault gouge. Last movement on the fault seems to be normal dip slip. Multiple sets of subsidiary northwest striking faults splay off the Caleta Coloso fault joining it with the Bolfin fault as a duplex structure. The northwest structures dip steeply to the southwest and consist of sinistral meter-wide fault-fracture zones and epidote-chlorite veins whose overall branched geometry and synthetic kinematics resembles consecutive sets of Riedel shears as seen in analog experiments (e.g. Naylor et al. 1986). Individual veins, up to 10 cm thick, are commonly banded and show isolated inclusions of altered wallrock fragments. The dioritic wallrock shows alteration haloes of albite and sericite. Under the microscope, the bands consist of coarse-grained and fine-grained isotropic aggregates of euhedral and anhedral epidote respectively. Preliminary SEM analysis of veins indicates that narrow zones of ultracataclasite cut the epidote bands, which are made of least two types of epidote according to its iron content.

CONCLUSION

We propose that the fault-fracture network forming the Caleta Coloso duplex in the Atacama fault system is one remarkable example of a regional scale geological structure resulting from the dynamic interaction between brittle deformation and hydrothermal fluid migration and mineral precipitation in the upper crust Northwest striking chlorite-epidote-bearing veins and fault veins likely formed in response to sudden pressure drops at dilational sites during multiple slip events along the flanking Caleta Coloso and Bolfin faults. Our observation that the master and subsidiary faults contain a range of rocks from mylonites to cataclasites and fault gouge strongly suggests the extensional strike-slip duplex developed during progressive cooling in a magmatic arc dominated by margin-parallel sinistral deformation. As the arc cooled down, deformation became brittle, allowing the suction pump mechanism, well known for epithermal systems, to operate during major slip events of the master faults. In this tectonic setting, veins are expected to occur at the oblique-slip/extensional sites represented by linking faults of the duplex, as is observed in the present study. Regional-scale cooling of arc rocks may have resulted from regional exhumation accompanying a mid-Cretaceous sinistral transpressional event and/or from the well-documented migration of the magmatic foci towards the east during mid-Cretaceous time.

ACKNOWLEDGEMENTS

Fondecyt Project 1020436 (JC) is currently funding this research. We thank Dr. Mauricio Belmar, University of Chile, for his help with SEM analysis.

REFERENCES

Bonson, C., Grocott, J., Rankin, A. 1997. A structural model for the development of Fe-Cu mineralisation coastal cordillera, Northern Chile (25°15'S-27°15'S). *In*: 8° Congreso Geológico Chileno, Universidad de Antofagasta (eds., v. III, p. 1608-1612, Antofagasta, Chile.

Brown, M., Díaz, F. and Grocott, J. 1993. Displacement history of the Atacama fault system, 25°00'S-27°00'S, northern Chile. Geological Society of America Bulletin, 105: 1165-1174.

Coombs, D.S. 1993. Dehydration veins in diagenetic and very-low-grade metamorphic rocks: features of the crustal seismogenic zone and their significance to mineral facies. J. Metamorphic Geology, Vol. 11.

Cox, S.F. 1999. Deformational controls on the dynamics of fluid flow in mesothermal gold systems. In MacCaffrey, K., Lonergan, L., and Wilkinson, eds. Fractures, flow and mineralization. Geological Society of London Special publication v. 155, 123-140.

Drummond, S.E., and Ohmoto, H. 1985. Chemical evoltuion and mineral deposition in boiling hydrothermal systems. Economic Geology. 80, 126-147

Etheridge, M.A. 1986. Differential stress magnitudes during regional deformation and metamorphism: upper bound imposed by tensile fracturing. Geology 11, 231-234.

Foxford, K.A., Nicholson, R., Poyla, D.A. and Hebblethwaite, R.P.B., 2000. Extensional failure and hydraulic valving at Minas da Panasqueira, Portugal-evidence of vein spatial distribution, displacements and geometries. Journal of Structural Geology 22, 1065-1086.

Grocott, J., Taylor, G., Treloar, P., Wilson, J. 1994. Magmatic arc fault systems and the emplacement of mesozoic plutonic complexes in northern Chile. *In*: 7° Congreso Geológico Chileno, Universidad de Concepción (eds.), v. II, p. 1360-1364, Concepción, Chile.

Naylor, M.A., Mandl, G. and Sijpesteijn, C.H. 1986. Fault geometries in basement-induced wrench faulting under different initial stress states. *Journal of Structural Geology* v. 8, p. 737-752.

Scheuber E. and Gonzalez, G. 1999. Tectonics of the Jurassic-Early Cretaceous magmatic arc of the north Chilean Coastal Cordillera (22°-26°S). Tectonics 18, p. 895-910.

Scheuber, E & Andriessen, P. A. M. 1990. The kinematic significance of the Atacana fault zone, northern Chile. Journal Of Structural Geology, Vol. 12, p. 243-257.

Scheuber, E.; Hammerschmidt, K.; & Friedrichsen H. 1985. Ar and Rb-Sr analyses from ductile shear zones from the Atacama Fault Zone, northern Chile: the age of deformation. Tectonophysics, Vol. 250, 61-87

Sibson, R. H., Robert, F. & Poulsen, K. H. 1988. High-angle.reverse faults, fluids pressure cycling and mesothermal gold-quartz deposits. Geology. 16, 551-555.

Sibson, R.H. 1987. Earthquake rupturing as a hydrothermal mineralizing agent. Geology 15, 701-704.

Sibson, R.H. 1990. Faulting and fluid flow. Mineralogical Association of Canada short course on fluids in tectonically active regimes of the continental crust. B.E. Nesbit eds. Chapter four: p.93-132.

Sibson, R.H. 1996. Structural permeability of fluid driven fault-fracture meshes. Journ. of Struct. Geol. 18, 1031-1042.

Sibson, R.H. 1996. Structural permeability of fluid driven fault-fracture meshes. Journ. of Struct. Geol. 18, 1031-1042.

Sibson, R.H. 2000. A brittle failure mode plot defining conditions for high-flux flow. Economic Geology 95, 41-48.

Taylor et al. 1998. Mesozoic fault systems, deformation and block rotation in the Andean forearc: a crustal-scale strike-slip duplex in the Coastal Cordillera of Northern Chile. Tectonophysics 299, 93-110.

Woodcock and Fisher, 1986. Strike-slip duplexes. Journal of Structural Geology 8, 725-735.

GEODYNAMIC EVOLUTION OF THE MIOCENE DESCANSO-YAURI BASIN, CUSCO REGION, PERU

Luis CERPA (1), Victor Carlotto (2), Thierry SEMPERE (3) & Paola MEZA (1).

(1) Convenio UNSAAC-IRD. Av la cultura s/n. e-mail: geoloco_x@hotmail.com
(2) Departamento academico de Geologia. UNSAAC. e-mail: carlotto@chaski.unsaac.edu.pe
(3) IRD. e-mail: sempere@terra.com.pe

KEY WORDS : Miocene, Sinorogenic basins, Cusco, Peru.

ABSTRACT

The Descanso-Yauri Basin is located south of Cusco (Peru), at the boundary between the Altiplano and the Western Cordillera. The basin has a NW-SE-oriented rhombohedric shape, and a continental sedimentary fill of Miocene age grouped in 3 members, all resulting from fault displacements along the boundaries of the basin. Folding along the northern margin dies out towards the basin's center. The stress tensors controlling the evolution of the basin are related with the regional stress field.

INTRODUCTION

The Neogene evolution of the Central Andes led to the development of small intermontane basins with their sedimentary and tectonic evolution tightly related to a continuous tectonic deformation. The Descanso-Yauri Basin belongs to a group of basins located along the transition zone between the Altiplano and Western Cordillera of southern Peru, immediately to the south of Sicuani (Cusco Dept.). It is NW-SE oriented, and covers an approximate surface of 2000 km2. The substrate of the basin presents rocks belonging to either the Altiplano or the Western Cordillera paleogeographic domains (Cárdenas et al, 1997; Carlotto, 1998). The boundary between these two domains is characterized by thepresence of regional faults controlling its evolution and mostly cropping out along the northern margin. The most conspicuous are the Langui, Descanso, and Yauri-Ocoruro faults . The basin has an elongated rhombohedric shape, limited to the northby the Descanso fault system, and to the SW by paleoreliefs of Mesozoic and Cenozoic rocks. The sedimentary infill is known as El Descanso Formation, consisting of conglomerates mostly crpping out towards the north, as well as sandstones, mudstones, and some limestone beds towards the south. To the E it unconformably overlies Eocene to earliest Miocene conglomerates and volcanic rocks, also sealing the NW-SE-oriented Yauri-Ocoruro fault. El Descanso Formation includes two volcanic tuff beds, onetowards thebase with an approximate age of 19 Ma, and another towards the top, with an average age of

11.5 Ma, which allow to consider this unit as Miocene. The NE margin of the basin presents tight folds which die out towards the center of the basin and are absent along the southern margin.

TECTONIC AND SEDIMENTARY EVOLUTION

The sedimentary evolution of the basin may be subdivided into 3 stages, corresponding to the 3 members of the El Descanso Formation. Member A (20-100 m) corresponds to the beginning of sedimentary infill of the Descanso-Yauri Basin. About 20 Ma ago, alluvial fan development began along the NW margin, due the activity along the Descanso and Langui faults. The SW margin remained apparently stable, and lacustrine deposition tookplace in the central part. The reliefs formed along the NW margin were active until about 19 Ma (Cerpa & Meza, 2001), as indicated by the lateral and foreward progradation of the alluvial fan deposits towards lacustrine deposits. The upper part of this member includes the Atunhuasi Tuff, which is used as the limit with the overlying member. This pyroclastic bed is dated in the region as being deposited at about 19 Ma (Boudesseul et al, 2000; Cerpa & Meza, 2001), and consists of a regional explosive event resulting in rhyolitic tuffs. The tuffs are subalkaline acid rocks, oversaturated in silica, peraluminous and potassic, transitional between the calcalkaline and shoshonite series.

Member B (50-700 m) corresponds to most of the sedimentary infill of the basin, and is unconformable with Member A. Deposition of Member B began at about 18 Ma with a SSE-sourced fluvial system probably due to reactivation of the Yauri-Ocoruro Fault. The slope of the system was rather low, thus leading to the developmentof small lakes in the central and NW areas. However, tectonic and sedimentary activity along the NE margin of the basin must have been continuous since 20 Ma, because the main drainages in Member B were along synclinal axes. Synclines formed between 18 and 19 Ma, and affect conglomerates of Member A. This rather continuous deformation originated progressive unconformities within the alluvial and fluvial deposits along the northern border of the basin. Sedimentation of Member B seems to have lasted until 13-12 Ma.

Deposition of Member C (50-200) began around 12 Ma with the development of deep braided which evolved towards a fine meandering fluvial system. The fluvial system comes from the SE and SW, due to the activation of the southern margin, i.e., the Yauri-Ocoruro fault, where alluvial fans and progressive unconformities developed. The NW margin continued active and developed alluvial fans nearby. Deposition of the base of the member is contemporaneous with explosive volcanic activity,which was dated (Ar/Ar ages on sanidine) as 12.82 ± 1.08 Ma (Cerpa et al. 2000), 11.74 ± 0.09 Ma and 11.66 ± 0.13 Ma (M. Fornari, *in* Cerpa & Meza, 2001). Later, deposition becomes lacustrine and *overfilled*, sealing progressive unconformities along the southern margin. However, this lacustrine system was subject to tectonic and climatic changes, leading to alternating depositional styles between *overfilled* and *balanced fill*. Lacustrine deposition progressively increased, until the basin filled in and greatlyextended its limits towards the south and west. Periferal areas developed small shallow lakes with carbonate deposition including algae. These beds have diatoms (De la Cruz, 1995), which provide a middle to late Miocene

age (Servant *in* Cerpa & Meza, 2001). Lacustrine sedimentation of Member C sealed progressive unconformities as well as the Yauri-Ocoruro fault, and lasted until about 10-9 Ma.

The Yauri tuff, interbedded towards the base of Member C of the El Descanso Formation, was deposited at about 11.5Ma. This rhyolitic tuff is transitional between the alkaline and subalkaline series. It is an acid, peraluminous and potassic rock, supersaturated in silica.

CONCLUSIONS

Deposition of the El Descanso Formation took place in a strike-slip basin beginningat about 20 Ma. Relief developed in relation to the Langui and Descanso faults, due to E-W oriented stress. The evolution of the sedimentary environments and of the synsedimentary tectonic structures show that the sedimentary fill of the Descanso-Yauri basin took place under a rather constant tectonic regime. The thickenning-coarsening sequence of Member B is related with NE-SW compression. As for Member C, the Yauri-Ocoruro fault acted as a sinistral strike-slip fault under E-W stress. The Descanso Faultwas active throughout the evolution of the basin, and was responsible for progressive unconformities along the northern margin. Folds along the northern margin die out towards the center (SW) of the basin, indicating a migration of strain in that direction. The Langui and Descanso faults are old structures which also controlled magmatism in the area. Stress tensors controlling the evolution of the Descanso-Yauri basin agree with the regional stress field for southern Peru (Carlotto, 1998).

References

Boudesseul, N.; Fornari, M.; Sempere, T.; Carlier, G.; Mamani, M.; Ibarra, I.; Meza, P. & Cerpa, L. (2000). Un importante evento volcánico de edad Mioceno inferior en la zona de Descanso-Ayaviri-Condoroma-Santa Lucía (Dptos. de Cusco, Puno y Arequipa). X Congreso Peruano de Geología, Resúmenes, p. 8.

Carlotto, V. (1998). Evolution andine et raccourcissement au niveau de Cusco (13-16°s), Pérou. Ph.D. Graduate Thesis, Université Joseph Fourier, Grenoble, 158 p.

Cárdenas, J.; Carlotto, V.; Flores, T.; Mamani, M.; Rodríguez, R.; Latorre, O.; Cano, V. & Jaimes, F. (1997). Estratigrafía de la región de Sicuani y sus correlaciones con las regiones de Cusco y Puno. IX Congreso Peruano de Geología, Resúmenes extendidos, p. 255-259.

Cerpa, L. & Meza, P. (2002). Las cuencas neógenas del Sur del Perú. La Cuenca Descanso - Yauri (Mioceno): Evolución sedimentológica y tectónica. Tesis de Ingeniero. Universidad Nacional San Antonio Abad del Cusco, 102 p.

Cerpa, L.; Meza, M.; Sempere, T.; Fornari, M.; Boudesseul, N.; Carlotto, V. & Carlier, G. (2000). Análisis sedimentológico y estratigráfico de una cuenca intramontañosa mio-pliocena: la cuenca Descanso-Yauri (Cusco). X Congreso Peruano de Geología, Resúmenes, p. 14.

De la Cruz, N. (1995). Geología de los cuadrángulos de Velille, Yauri, Ayaviri y Azángaro. INGEMMET, Bol. 58, serie A, 144 p.

RAPID TECTONIC AND PALEOGEOGRAPHIC EVOLUTION: THE CHUCAL ANTICLINE, ALTIPLANO OF ARICA, NORTHERN CHILE

Reynaldo CHARRIER(1), Andres CHAVEZ (2), Sara ELGUETA (3), Gérard HERAIL (4), John J. FLYNN(5), Darin CROFT (6,5), Andres WYSS (7) and Marcelo GARCIA (8)

1. Dpto. de Geología, Univ. de Chile, Casilla 13518, Correo 21, Santiago, Chile. rcharrie@cec.uchile.cl
2. SIPETROL S.A., Vitacura 2736, 8° Piso, Providencia, Las Condes, Santiago. achavez@esfera.cl
3. Carlos Silva Vildósola 1110, Depto. 303, Providencia, Santiago. elkine@entelchile.net
4. IRD, LMTG, 38 rue des 36 Ponts, 31400 Toulouse, France. gherail@paris.ird.fr
5. Dpt. of Geology, Field Museum of Nat. Hist., 1400 S. Lake Shore Dr., Chicago, USA. jflynn@fieldmuseum.org
6. Dpt. of Organ. Biol. & Anat., Univ. of Chicago, 1025E. 57 St., Chicago, USA. dacroft@midway.uchicago.edu
7. Dpt. of Geological Sc., Univ. of California, Santa Barbara, California 93106, USA. wyss@magic.geol.ucsb.edu
8. Servicio Nacional de Geología y Minería, Avda. Santa María 0104, Santiago. mgarcia@sernageomin.cl

KEY WORDS: Neogene, Paleoenvironment, Tectonics, Andes, Altiplano, Chucal.

INTRODUCTION

An east-vergent structural system composed of the Jaropilla Fault, and the Chucal Anticline (Riquelme, 1998; Riquelme and Hérail, 1997), is located on the S-E side of the fault-controlled Chapiquiña-Belén Ridge (Charrier et al., 2000), Altiplano of Arica (Fig. 1). This system deformed lower to upper Miocene rocks and caused the development of several progressive unconformities, located on the E-flank of the anticline (Riquelme, 1998; Riquelme and Hérail, 1997). The deformed stratigraphic series formed by the Lupica, Chucal, and Quebrada Macusa Fms. (Muñoz, 1991; Riquelme, 1998) ranges in age between 21.7±0.8 Ma and 10.4±0.7 Ma. The latter age corresponds to a less deformed lava covering the Quebrada Macusa Fm. (Riquelme, 1998).

New stratigraphic and structural studies, radioisotopic datings of tuff layers and discoveries of mammal fossils enable us to (1) better constrain the chronology of the tectonic evolution of the Chucal Anticline, and the development of the progressive intraformational unconformities, and (2) understand the effects of deformation on the stratigraphic sequence, sedimentation, and paleogeographic development of the Chucal-Lauca Basin.

STRATIGRAPHY AND CHRONOLOGY OF DEFORMATION

The core of the Chucal Anticline exposes the upper part of the Lupica Fm. formed by a >50 m thick, 21.7±0.8 Ma old, massive, white tuff (Riquelme, 1998) covered by a thin stratified series of white tuffaceous, lenticular, fluvial sandstones layers. On the W-flank it is 66 m thick and on the E-flank, 50 m thick. It is conformably covered with minor erosional discontinuities by the Chucal Fm. (Muñoz, 1991).

On the **western flank** of the anticline (Fig. 1), the Chucal Fm. (600 m thick) is a 35 to 40° west-dipping series, covered further west by the Quebrada Macusa Fm. It is composed by:

-Member W1 (60 m) begins with a lenticular, orange colored, channelizing paraconglomerate and is formed by three upwards-fining, fine grained sequences, ending with a 4-6 m thick calcareous series.

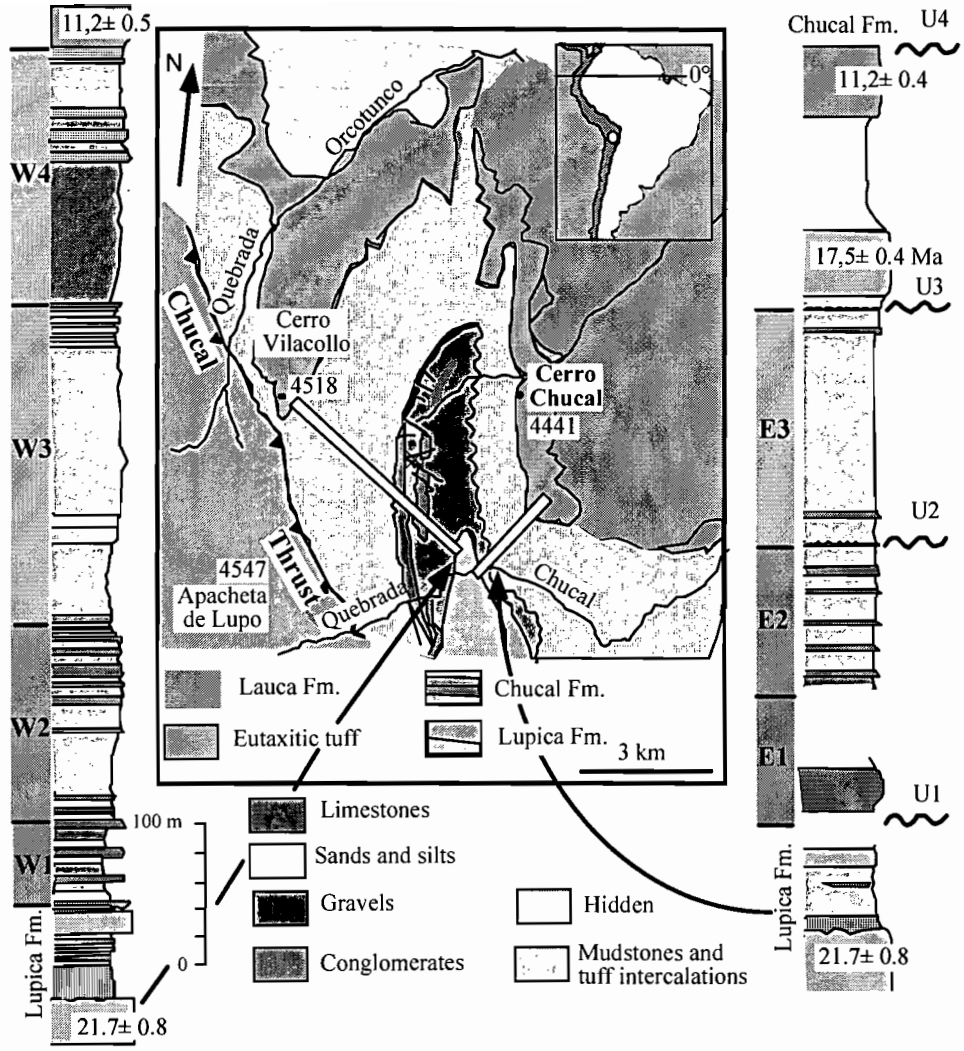

Fig. 1 - The Chucal Anticline: tectonic and stratigraphic columns.

-Member W2 (144 m) is white colored series composed of fine grained sandstones with intercalations of tuffaceous material, mudstones, and limestones. Limestones correspond to laminated marls (with plants remains), chert nodules, massive marls, fine calcareous sandstones, and micrites.

-Member W3 (225 m) corresponds to an alternation of green sandstones, mudstones, and a few, thin, external red in color, limestone intercalations. Plant remains are frequent in this member.

-Member W4 (172 m): This is the upper member of the Chucal Fm. and is characteristically comprised of brownish-grey mudstones. The upper part contains some conglomerate and tuff intercalations.

The W-flank series represents evolution from fluvial (Lupica Fm.) to lacustrine conditions (Member W2), lake filling and flood-plain development (Member W3), and new subsidence (Member W4). Mammal fossils were mainly found in the flood-plain facies, and some lacustrine-influenced strata.

On the **eastern flank**, the Chucal Fm. (<365 m) is a steeply E-dipping series, unconformably covered by the 17.5±0.4 Ma old lower tuff (Bond and García, 2002) of the Quebrada Macusa Fm. It is composed by:

-Member E1 (~100 m) is a white calcareous series deposited above the Lupica Fm.. Its exposed thickness is ~30 m. The gap between the Lupica Fm. and Member E2 is 100 m (its maximum possible thickness). Member E1 corresponds to the thicker Member W2 on the W-flank.

-Member E2 (100 m) is green in color, and corresponds to the thicker Member W3 on the W-flank. It contains limestone intercalations with an external red color. Its contact with Member E1 is not exposed.

-Member E3 (165 m) is a grey, massive, mammal-fossils bearing, fluvial sandstone series with hard, calcareous intercalations. The contact with the underlying member is slightly unconformable; it is less steeply dipping than Member E2. It has no equivalent on the W-flank. Considering its position between Member E2 and the Quebrada Macusa Fm., it can be chronologically correlated to all or to part of Member W3 on the W-flank.

The E-flank strata represent a series, interrupted by unconformities, of evolving paleoenvironmental conditions, from fluvial (Lupica Fm.), to lacustrine (Member E1), to lake filling and flood-plain systems with lacustrine influence (Member E2), and finally abruptly changing back to fluvial and flood-plain conditions, also with some lacustrine influences indicating continuing proximity to and persistence of a lake within the system.

Member W1 is not developed on the E-flank. The calcareous Member W2 is considerably thicker than its correlative Member E1, and the green sandstone Member W3 is thicker than its correlative Member E2. Member W4 has no equivalent on the E-flank. Considering its position between Member W3 and the lower white tuff of Quebrada Macusa Fm. it can be considered as a chronologic equivalent of Member E3 on the E-flank. Member E3 represents a major increase of transport energy not represented on the W-flank.

The W-flank column is relatively continuous. Interruptions in the sedimentation process in the E-flank have been interpreted as progressive unconformities (Riquelme, 1998; Riquelme and Hérail, 1997).

A major change in depositional regime occurred at the base of the Chucal Fm., with the deposition of the basal, orange colored conglomerates of Member W1, which is formed by upwards finning cycles, each one ending with lacustrine limestones. Deformation began after deposition of the orange colored member, and caused on the E-flank side: 1. Erosion of the orange colored member (U1), 2. reduction in thickness of Member E1 (U2), 3. reduction in thickness of Member E2 (U3), and 4. the progressive unconformity U4 on the E-flank.

FOSSIL MAMMALS

Abundant mammalian remains have been recovered from numerous horizons within the Chucal Fm. In the anticline's W-flank fossils generally occur in flood-plain facies and lacustrine-influenced intervals (i.e., in the lower parts of Members W3 and W4), whereas on the E-flank they predominantly occur in fluvial facies (i.e., Members E3 and E1), reflecting the distinctly different depositional systems on either side of the anticlinal.

The fauna (Flynn et al., 2002) appears to represent a single, short temporal interval, most likely Santacrucian or Friasian in age (e.g., between 14 and 17.5 Ma). The new date, from basal Quebrada Macusa Fm. strata overlying the mammal fossils, emphasizes that deposition and deformation of most of the Chucal Fm. was very rapid. It also suggests that this fauna more likely correlates to Santacrucian than any younger SALMA; additional work on the fauna and geochronology will clarify this point. At least eight fossil mammal taxa are currently identified from the Chucal Fm. (Flynn et al., 2002), including five notoungulates (*Nesodon imbricatus*, a toxodontid; three mesotheriid species; hegetotheriine), the litoptern *Theosodon*, a glyptodontoid, and the oldest known chinchilline rodent. Abundant new material and additional localities discovered in 2001 suggest that at least 6-7 additional species occur in this formation. Preliminary identifications include a notohippid notoungulate (supporting a Santacrucian age), a second (diminutive chinchilline, an armadillo, and several other interesting but as yet unstudied very small-bodied taxa. The large chinchilline, *Nesodon*, mesotheres, and hegetotheres are

known from multiple levels and on both flanks of the anticline. Bond and García (2002) report the existence of *Palyeidodon* in the upper levels of the Chucal Fm. on the E-flank.

CONCLUSIONS

Sedimentation of the 600 m thick Chucal Fm., pulses of development of the Chucal Anticline, development of progressive unconformities (U1 to U4), associated erosion, and development of at least partially isolated paleogeographies with abundant associated fauna (likely Santacrucian SALMA=17.5-16.3 Ma; Flynn and Swisher, 1995) and flora on both sides of the anticline occurred between about 21.7±0.8 Ma and 17.5±0.4 Ma. This rapid episode of deformation occurred within less than a 4 my interval. Further deformation affecting the Quebrada Macusa Fm. (U5) occurred after 11.2±0.5 Ma and before 10.4±0.7 Ma. The total time represented by this series, between the Basal Tuff (Lupica Fm.), and the upper tuff in the Quebrada Macusa Fm. is ~11 my.

ACKNOWLEDGEMENTS. We thank the National Geographic Society (U.S.A.) for Grant 5371-94, U.S. NSF Grant DEB-9317943, Chile FONDECYT Grant 1224-91, Field Museum Department of Geology, John S. Guggenheim Foundation, and the IRD for field-work and other support, and for supporting A. Chávez thesis. We thank G. Carrasco, A. Charrier, C. Hérail, the Flynn family, and S. Villagrán for collaboration in the field, and the Field Museum preparator staff for their excellent preparation of the mammal fossils.

REFERENCES

Bond, M. and García, M., 2002. Nuevos restos de un Toxodonte (Mammalia; Notoungulata) en el Mioceno (Formación Chucal) de la Cordillera Occidental de Arica, Norte de Chile. Rev. Geol. de Chile, in press.

Charrier, R., Hérail, G., Flynn, J.J., Riquelme, R., García, M., Croft, D. and Wyss, A.R., 2000. El Cordón Chapiquiña-Belén en el borde occidental del Altiplano chileno: Significado paleogeográfico y contexto tectónico regional. Proc. 9th Congr. Geol. Chileno, Vol. 1, p. 763-767.

Flynn, J.J., Croft, D.A., Charrier, R., Hérail, G. and Wyss, A.R., 2002. The first Cenozoic mammal fauna from the Chilean Altiplano. Journal of Vertebrate Paleontology, Vol. 22, N° 1, p. 200-206.

Flynn, J.J. and Swisher, C.C., 1995. Cenozoic South American Land Mammal Ages: Correlation to global geochronologies; *In:* Geochronology, Times Scales and Global Stratigraphic Correlation, SEPM Sp. Publ. 54, p. 317-333.

Muñoz, N., 1991. Marco geológico y estratigráfico de un sistema fluvio-lacustre Paléogeno, Altiplano de Arica, Norte de Chile. Proc. 6th Congr. Geol. Chileno, p. 201-204.

Riquelme, R. and G. Hérail, 1997. Discordancias progresivas en el Cenozoico Superior del borde occidental del Altiplano de Arica: Implicancias en la interpretación tectónica de la Cordillera Occidental. Proc. 8th Congr. Geol. Chileno, Vol. 1, p. 231-235.

Riquelme, R., 1998. Evolución tectosedimentaria post-oligocénica del borde occidental del Altiplano, entre Tignámar y Salar de Surire, I Región, Chile. Thesis, Depto. de Geología, Univ. de Chile, Santiago, 123 p.

STRUCTURE OF THE SUBDUCTION CHANNEL AT THE ECUADOR CONVERGENT MARGIN FROM WIDE-ANGLE SEISMIC MODELING AND INVERSION

Philippe CHARVIS, Audrey GAILLER, Valenti SALLARES, Jean-Yves COLLOT, David GRAINDORGE, Alcinoë CALAHORRANO, Ruth VILLAMAR

Géosciences Azur, IRD, BP 48, 06235, Villefranche-sur-mer, France (philippe.charvis@obs-vlfr.fr)

KEY WORDS: Ecuador, convergent margin, seismogenic zone, subduction channel, seismic tomography

INTRODUCTION

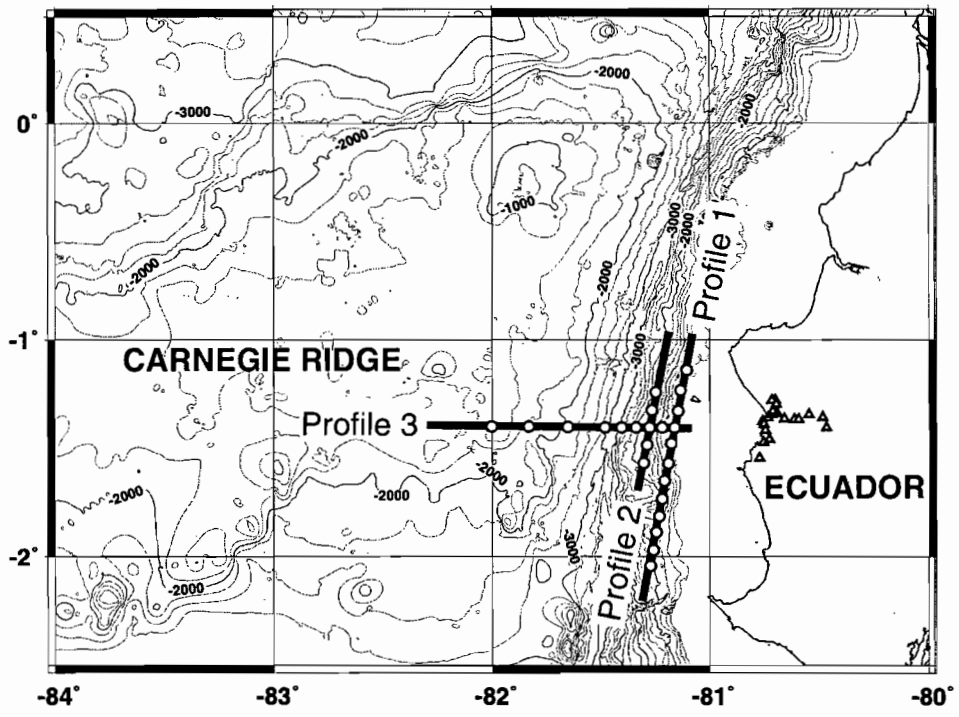

***Figure 1**: bathymetric map of the study area. Locations of the wide-angle seismic lines shot during the Sisteur experiment are shown: black lines stands for the shooting line; open circles for OBSs and open triangles for land seismometers.*

The North Andean convergent margin located at the boundary between the Nazca and South American plates has remained poorly studied, although since 1901, six great subduction earthquakes have ruptured the plate boundary between 3°S and 3°N. Several factors have been proposed as controlling inter-plate coupling and tectonic regime of the margin including reactivation of seafloor relief when subducted, and the subduction or accretion of sediment [*Cloos and Shreve*, 1996].

A major east-west trending bathymetric feature, the Carnegie Ridge (Figure 1), characterizes the Nazca plate. This ~200-km wide volcanic ridge, related to the interaction between the Galápagos hotspot and the

Galápagos spreading center to the west, is subducting beneath the Ecuador convergent margin. The frontal subduction of the Carnegie Ridge, has produced a segmentation of the upper plate expressed in lateral variations of uplift, seismicity, deformation, arc magmatism as well as sediment distribution along the margin [*Collot et al.*, 2002; *Gutscher et al.*, 1999].

Seismic investigations at convergent margins are critical to understanding the mechanics of the interplate seismogenic zone. During the SISTEUR experiment (Sept.-Oct. 2000) conducted by our group on board the French research vessel *Nadir* (IFREMER) and the Ecuadorian research vessel *Orion* (INOCAR), we collected deep multichannel seismic reflection and wide-angle seismic data recorded by ocean bottom seismometers (OBSs) and land seismometers on the Nazca-north Andean plate boundary. The objectives of this cruise were to study the crustal structure and its possible correlation with the occurrence of great subduction earthquakes in the area of the Ecuador and southern Colombia margin. We focus in this paper on imaging the geometry and the properties of the subduction channel in front of the subduction of the Carnegie Ridge (Figure 1).

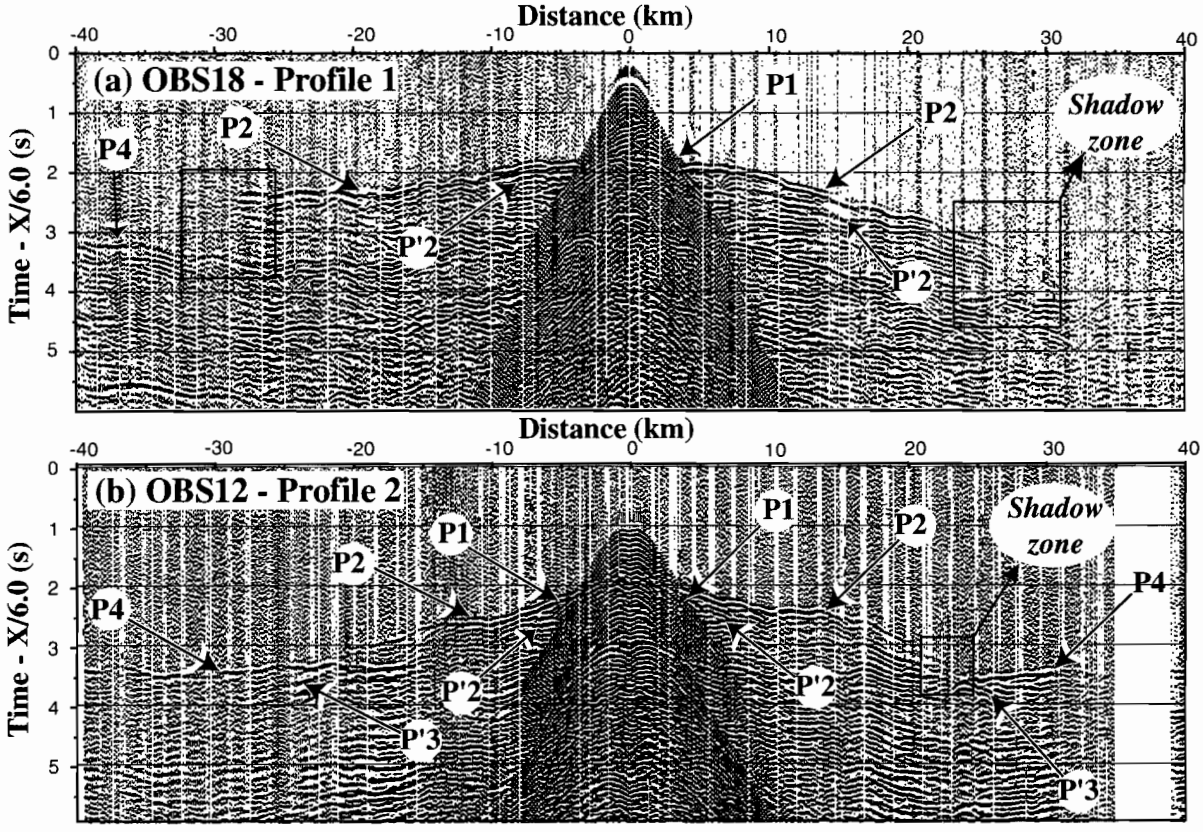

***Figure 2**: Wide-angle seismic record sections from OBS 18 (Profile 1) and OBS 12 (Profile 2). The reducing velocity is 6.0 km/s. Data were bandpass filtered between 3 and 18 Hz and amplitude scaled proportional to offset. Main arrivals used for modeling and inversion: P1 refraction in the sedimentary cover; P2 refraction in second layer (upper plate); P4 refraction in fourth layer (subducting plate); P'2 reflection from the base of layer 2, P'3 reflection from the base of layer 3. On both sections a clear shadow zone is interpreted as related to a low-velocity layer 3. It reaches ~1 s delay along profile 1 and only ~0.3 s along profile 2.*

DATA ACQUISITION AND MODELING

Three seismic lines were shot on the Ecuador margin over a network of 24 OBSs and 10 land stations (Figure 1). 350-km of in-line shots were recorded providing a unique set of high quality data (Figure 2). Profiles

1 and 2 were shot parallel to the trench respectively on the top of the continental platform and in the middle of the slope. One of the striking characteristics of the wide-angle record sections is the presence of a clear shadow zone between arrival P2, refracted in the upper plate and phase; P3, refracted in the top of the plunging plate.

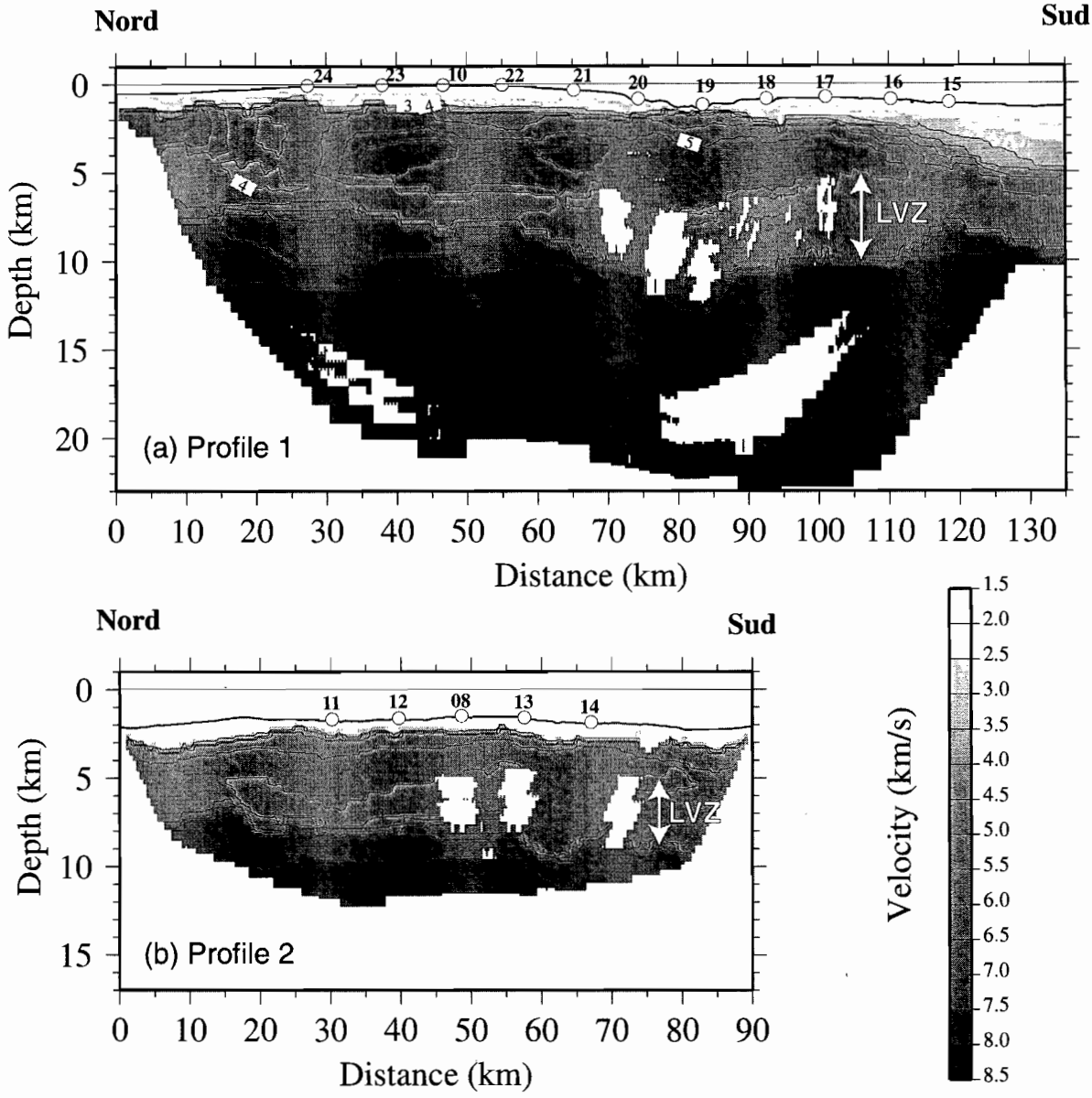

***Figure 3**: Velocity models obtained from the inversion of the travel time of the first arrival [Korenaga and et al., 2000]. The starting model was based on forward modeling of wide-angle and coincident multichannel reflection data [Zelt and Smith, 1992]. (a) Model along profile 1. (b) Model along profile 2. The low velocity channel is indicated on both models. It reaches 3 km along profile 2 and 5 km along profile 1.*

CONCLUSIONS

Along profile 2 the top and the base of low velocity layer are underlined by reflections visible at wide-angle and at vertical incidence as well. The average velocity in this layer, constrained by the wide-angle reflec-

tion at its base, is 4.0 to 4.5 km/s, only slightly lower than in the basement of the upper plate (5.0 km/s). The thickness of this layer varies from zero to the north of the profile to approximately 3 km to the south.

Along profile 1 the low velocity channel is thicker (3 to 5 km) and there is clear reflection at its base. Seismic velocities, as high as 6.0 km/s, determined in the overriding plate are possibly related to the Piñon formation composed of mafic rocks [e.g., *Reynaud et al.*, 1999]. Beneath this profile, the uppermost part of the down-going plate could be part of the low velocity layer and the actual subduction channel is not clearly defined.

On the contrary, the low velocity layer is clearly related to the subduction channel beneath profile 2 as the top of the down-going plate is clearly defined. The sedimentary cover of the Carnegie Ridge consists of a ~1 km thick layer of material with an average seismic velocity of ~2.5 km/s. This preclude that the subduction channel consists only of sediments of the down-going plate dragged along in the subduction. Several hypotheses could explain the velocity models: material possibly comes from both the down-going and the overriding plates, material of the subduction channel should be compacted as it is buried beneath ~ 2 km of rocks and because of the deformation, material should be accreted between the 2 plates to explain the thickness of the subduction channel.

Amplitude modeling and waveform inversion will provide additional constrains on the geometry and characteristics of the subduction channel.

REFERENCES

Cloos, M., and R.L. Shreve, Shear-zone thickness and seismicity of Chilean- and Marianas-type subduction zones, *Geology*, *24* (2), 107-110, 1996.

Collot, J.-Y., P. Charvis, M.-A. Gutscher, S. Operto, and the SISTEUR scientific Party, Exploring the Ecuador-Colombia active margin and inter-plate seismogenic zone, *EOS, Transaction, American Geophysical Union, in press*, 2002.

Gutscher, M.A., J. Malavieille, S. Lallemand, and J.Y. Collot, Tectonic segmentation of the North Andean margin: impact of the Carnegie Ridge collision, *Earth and Planetary Science Letters*, *168*, 255-270, 1999.

Korenaga, J., and et al., Crustal structure of the southeast Greenland margin from joint refraction and reflection seismic tomography, *Journal of Geophysical Research*, *105*, 21591-21614, 2000.

Reynaud, C., E. Jaillard, H. Lapierre, M. Mamberti, and G.H. Mascle, Oceanic plateau and island arcs of southwestern Ecuador: their place in the geodynamic evolution of northwestern South America, *Tectonophysics*, *307*, 235-254, 1999.

Zelt, C.A., and R.B. Smith, Seismic traveltime inversion for 2-D crustal velocity structure, *Geophysical Journal International*, *108*, 16-34, 1992.

LEAD ISOTOPE EVIDENCE FOR LATITUDINAL MANTLE HETEROGENEITY BENEATH THE ANDES

Massimo CHIARADIA and Lluís FONTBOTE

Section des Sciences de la Terre, Département de Minéralogie, Université de Genève, Rue des Maraîchers 13, CH-1211 Genève 4, Switzerland; e-mail: massimo.chiaradia@terre.unige.ch

INTRODUCTION

Geochemical data suggest that Andean arc melts are generated in the mantle wedge whence they migrate into and become variably contaminated by continental crust. This model is supported also by lead isotopes, which, among the radiogenic systems, represent the most extensive database of the Andes, including analyses on both magmatic rocks and associated ore minerals.

Many studies have shown that the Pb isotope variability of arc magmas in segments of the Central Andes is mainly due to crustal contamination. In this paper we discuss 234 new lead isotope data on Late Cretaceous-Tertiary magmatic arc rocks and associated ores of the Northern Andes of Ecuador (N=165) and mining districts of Peru (N=69) together with literature data on magmatic arc rocks and associated ore deposits of the Central Andes. The new data allow us to compare lead isotope reservoirs for arc magmatism of the Northern and Central Andes (10°N-40°S). We present, for the first time, evidence that the sub-Andean mantle is characterised by a systematic decrease in the $^{206}Pb/^{204}Pb$ ratio from north to south, and propose a possible explanation for this heterogeneity.

THE DATABASE

This study is based on about 500 lead isotope data, 234 of which are from analyses performed at our laboratories while the remainder is from previous investigations. They include magmatic arc rocks and related mineralization (VHMS, porphyry, epithermal, skarn) with Late Cretaceous to Late Tertiary ages. The time span chosen is determined by the homogeneous distribution of magmatism and associated mineralization along the whole Andean chain in the Late Cretaceous-Tertiary, and by the availability of a much larger database than for older periods, thus permitting a reasonable comparison of different segments of the Cordillera. Ores of province III of Macfarlane et al. (1990) have been excluded because they do not have magmatic signatures, deriving most of the lead from hydrothermal leaching of crustal basements. The Tertiary-Quaternary volcanics of the Arequipa massif and Belén segment in Chile, which have low radiogenic lead isotope signatures due to contamination by lower crust-type basements, have also been excluded.

The Pb isotope data have been subdivided into four latitudinal areas: 8°N-5°S (Ecuador and Colombia); 5°S-15°S (Northern Peru); 15°S-20°S (Southern Peru); 20°S-40°S (Chile). These subdivisions coincide with major geomorphologic features (Huancabamba deflection at 5°S; Arica elbow at 20°S) and/or with lead isotope

provinces of Macfarlane et al. (1990) (e.g. the 15°S limit between subprovinces Ib, II to the north and subprovince Ic to the south).

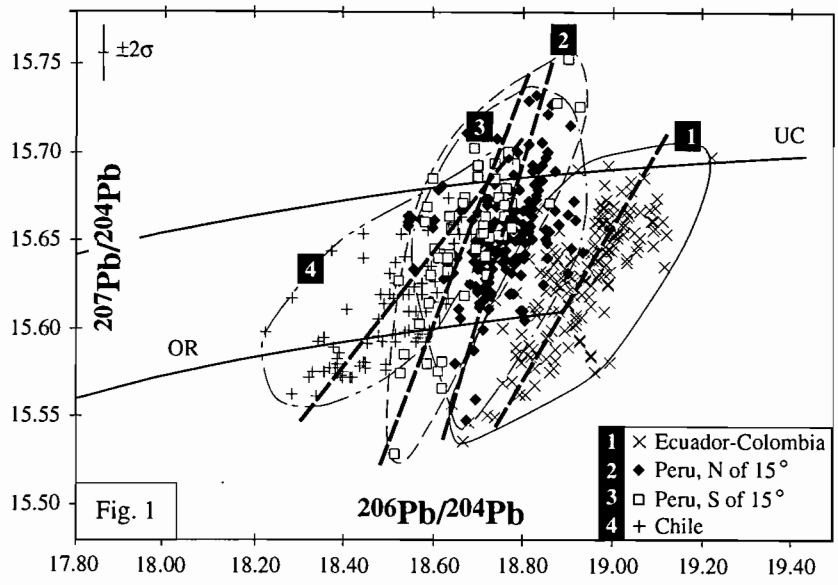

Fig. 1: $^{208}Pb/^{204}Pb$ and $^{207}Pb/^{204}Pb$ vs. $^{206}Pb/^{204}Pb$ plots of Late Cretaceous-Tertiary magmatic rocks and associated ores of the Andean Cordillera, subdivided according to the geographic provinces of this work.

RESULTS AND DISCUSSION

Late Cretaceous-Tertiary ores and magmatic arc rocks of each of the four Andean provinces define distinct steep elliptical arrays in conventional plots (Fig. 1), indicating that the majority of lead within each province derives from mixing of two main end-members characterised respectively by low and high $^{207}Pb/^{204}Pb$ and $^{208}Pb/^{204}Pb$ ratios. The prolateness of the ellipses indicates that the 2-end-member mixing is disturbed by secondary sources, by short time-evolved reservoirs, and, probably, by $^{206}Pb/^{204}Pb$ variability of the main sources. Like previous studies (e.g. Macfarlane, 1995) we interpret these arrays as mixing lines between the mantle, possibly enriched by pelagic sediments, at the low $^{207}Pb/^{204}Pb$ (and $^{208}Pb/^{204}Pb$) end, and upper crustal rocks at the high $^{207}Pb/^{204}Pb$ (and $^{208}Pb/^{204}Pb$) end. Comparison of the arrays, especially in the uranogenic plot that allows the best discrimination between mantle and upper crust reservoirs, shows two remarkable features (Fig. 1): (1) Arrays are systematically shifted towards lower $^{206}Pb/^{204}Pb$ values from Ecuador-Colombia to Chile. (2) The low radiogenic (mantle) end-members of each array contain progressively ^{206}Pb-poorer lead from north to south.

Lead isotope systematics of the Late Cretaceous-Tertiary Andean mantle end-members

The compositional differences of the four mantle end-members cannot be attributed to a single time-evolved reservoir because of the similar Late Cretaceous-Tertiary ages of the investigated magmatic rocks and associated ores in all provinces. We also exclude the possibility that the different mantle end-members are an artefact of crustal contamination. Indeed, arrays of the four provinces being sub-parallel (Fig. 1), the low radiogenic end-members cannot derive from mixing between a homogeneous low $^{207}Pb/^{204}Pb$ and $^{208}Pb/^{204}Pb$ mantle and heterogeneous (variable $^{206}Pb/^{204}Pb$) high $^{207}Pb/^{204}Pb$ and $^{208}Pb/^{204}Pb$ reservoirs like upper crustal rocks and pelagic sediments. The $^{206}Pb/^{204}Pb$ spread of the mantle end-members cannot derive either from

assimilation of low radiogenic lower crust by mantle-derived melts during melting-assimilation-storage-homogenisation (MASH) processes. This would imply enrichment in thorogenic lead concomitant with the southward decrease of $^{206}Pb/^{204}Pb$ values of the low radiogenic end-members, which is not observed (not shown). In contrast, the isotopic differences of the mantle end-members can be related to mixing between MORB components characterised by different $^{206}Pb/^{204}Pb$ and consistently low $^{207}Pb/^{204}Pb$ ($^{208}Pb/^{204}Pb$) ratios (Fig. 2). Mixing of DMM and enriched mantle components is considered responsible for MORB isotope variability (Zindler and Hart, 1986). Mixing between a low radiogenic MORB mantle, possibly carrying a DMM or EM I component, and a more radiogenic MORB mantle, possibly carrying an HIMU component, best explains the $^{206}Pb/^{204}Pb$ range of the Andean mantle end-members (Fig. 2). Note that the mantle end-member of the Ecuador-Colombia trend is ^{206}Pb-richer than E-Pacific MORB (Fig. 2).

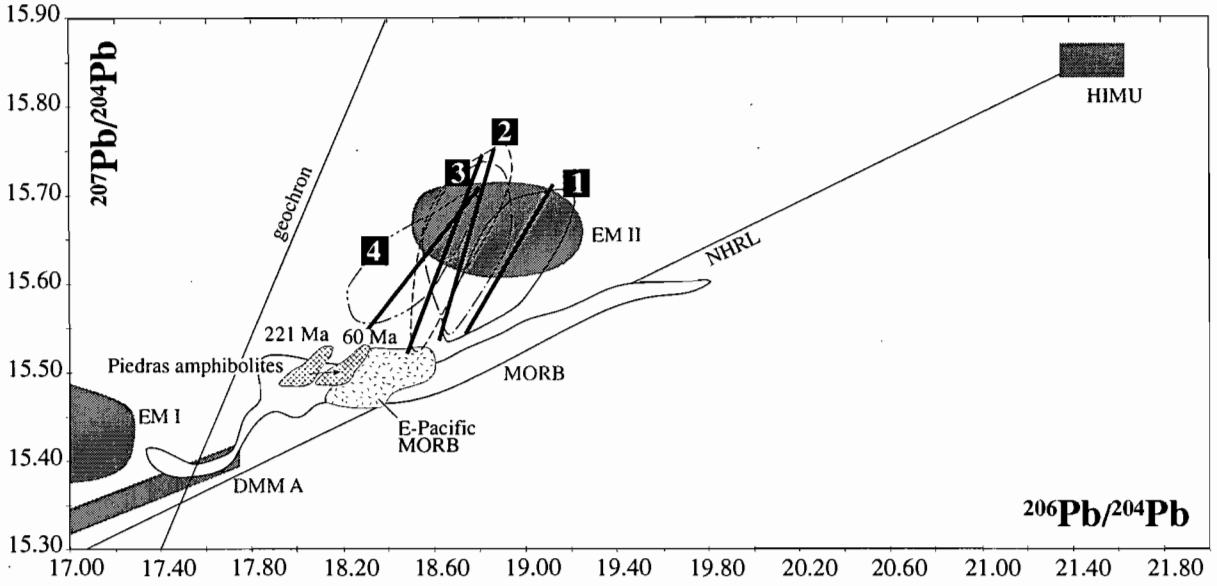

Fig. 2: $^{207}Pb/^{204}Pb$ vs. $^{206}Pb/^{204}Pb$ plot of the four trends of Fig. 1 together with the compositional fields of the main mantle reservoirs of Zindler and Hart (1986).

Although the presence of a true HIMU component in the northern sub-Andean mantle remains elusive, mixing of a low radiogenic and a high radiogenic mantle is further revealed in the Northern Andes by Triassic amphibolites (U-Pb zircon age of 221±17 Ma, Aspden et al., 1995) of the Piedras Group, which is part of a metamorphic complex cropping out in southwestern Ecuador. The Piedras amphibolites have MORB-type geochemical features with no signs of crustal contamination (Aspden et al., 1995) and Pb isotope compositions less radiogenic than the E-Pacific MORB field (Fig. 2). Lacking crustal contamination, they allow us to explore Pb isotope geochemistry of the Triassic mantle beneath northern South America. If this mantle had the isotopic composition of the Piedras amphibolites, with a μ ($^{238}U/^{204}Pb$)=9 and an ω ($^{232}Th/^{204}Pb$)=32, by Late Cretaceous-Tertiary times it would be far less radiogenic not only than the mantle end-member of the Ecuador-Colombia trend, but also of the Northern and Southern Peru trends (Fig. 2). Therefore, it could not be the source of the Late Cretaceous-Tertiary arc magmatism of the Northern Andes. In contrast, spiking of the time-evolved Triassic mantle by radiogenic MORB material (possibly carrying an HIMU component) between Triassic and Late Cretaceous times can explain the enriched mantle end-member in the Northern Andes (Fig. 2).

What could cause the lead isotope heterogeneity of the Andean mantle?

At the present stage it is very difficult to identify the cause of the sub-Andean mantle Pb isotope heterogeneity pointed out by our data. As working hypotheses, we propose two tentative scenarios of post-Triassic mixing between a radiogenic mantle, possibly carrying an HIMU-type component, and a low radiogenic mantle to explain the sub-Andean mantle heterogeneity. Oceanic plateaus generated by the mid-Cretaceous superplume event have been subducted during the Mesozoic beneath Central America and Northern South America but not beneath Central South America (Larson, 1991). These oceanic plateaus, characterised by ^{206}Pb-rich compositions, could have enriched the sub-Andean mantle of the Northern Andes or, if underplated under the continental crust, could have contaminated mantle-derived magmas on their way to the surface. Another speculative scenario is that Mesozoic plume events occurred at the northern edge of South America, e.g. the 90 Ma old Galapagos hotspot and the 106-82 Ma old hotspot in the Ecuadorian Oriente basin (Barragan and Baby, 1999), could have dispersed ^{206}Pb-rich material into the surrounding upper mantle creating the isotopic gradient observed along a distance of several hundreds of kilometres.

The main implication of our results is that, although crustal contamination is responsible for most of the Pb isotope variability in segments of the Central Andes (e.g. Davidson and de Silva, 1992; Wörner et al., 1992), mantle heterogeneity is an additional factor responsible for Pb isotope variability of the Andean provinces at the continental scale. Our data would also document the first example of a possible HIMU-type component in the source of continental arc magmas thus complementing similar conclusions drawn by Hickey-Vargas (1992) on the source of island arc magmatism.

REFERENCES

Aspden, J.A., Bonilla, W. and Duque, P., 1995. The El Oro metamorphic complex, Ecuador: geology and economic mineral deposit. BGS Overseas Geology and Mineral Resources, Keyworth, U.K., N. 67, 63 pp.

Barragan, R. and Baby, P., 1999. A Cretaceous hot spot in the Ecuadorian Oriente Basin: geochemical, geochronological, and tectonic indicators. In: Proc. 4th Int. Symp. Andean Geodynamics, October 4-6 1999, Göttingen, Germany, pp. 77-80.

Chiaradia, M. and Fontboté, L. (2002) Lead isotope systematics of Late Cretaceous-Tertiary Andean arc magmas and associated ores between 8°N and 40°S: evidence for latitudinal mantle heterogeneity beneath the Andes. Terra Nova, in press.

Davidson, J.P. and de Silva, S.L., 1992. Volcanic rocks from the Bolivian Altiplano: insights into crustal structure, contamination, and magma genesis in the Central Andes. Geology, 20, 1127-1130.

Hickey-Vargas, R., 1992. A refractory HIMU component in the sources of island-arc magma. Nature, 360, 57-59.

Larson, R.L., 1991. Latest pulse of Earth: evidence for a mid-Cretaceous superplume. Geology, 19, 547-550.

Macfarlane, A.W., Marcet, P., LeHuray, A.P. and Petersen, U., 1990. Lead isotope Provinces of the Central Andes inferred from ores and crustal rocks. Economic Geology, 85, 1857-1880.

Wörner, G., Moorbath, S. and Harmon, R.S., 1992. Andean Cenozoic volcanic centres reflect basement isotopic domains. Geology, 20, 1103-1106.

Zindler, A. and Hart, S., 1986. Chemical geodynamics. Annual Reviews of Earth and Planetary Sciences, 14, 493-571.

THE LOADING AND RELAXATION PROCESSES IN THE NORTHERN CHILE SUBDUCTION ZONE USING SAR INTERFEROMETRY AND GPS MEASUREMENTS

M. CHLIEH[1], J.B. de CHABALIER[1], J.C. RUEGG [1], R. ARMIJO[1]
K. FEIGL[2] and J. CAMPOS[3]

[1]Institut de Physique du Globe de Paris, France. chlieh@ipgp.jussieu.fr
[2] OMP, Toulouse, France. [3]DGF, Santiago, Chile.

KEY WORDS : earthquake cycle, coupling, subduction, Insar, gps

INTRODUCTION

The North Chile region, located between 18°S and 23°S is one of the most important seismic gaps in the world (Nishenko, 1985) with no rupture having occurred since 1877 in this area. The two extremities of this gap have experienced major earthquakes in recent years (the Mw=8.1 Antofagasta earthquake in 1995; the Mw=8.4 South Peru earthquake in 2001). Sar interferometry and GPS measurements are powerfull tools to constrain the loading (inter-seismic) and the relaxation (co- and post-seismic) processes that take place on the subducting interface.

1995 ANTOFAGASTA EARTHQUAKE

Combined with GPS and seismic modelling (Ruegg & al, 1996; Ihmlé & al, 1997), SAR interferometry (figure 1) has proved to be essential to constrain the surface deformation and to characterize the source mechanism of 1995 Antofagasta earthquake. The slip direction is parallel to Nazca-South America relative plate convergence indicating no slip partitionning; the variation of slip distribution on the fault plane indicates non homogeneous strain release reaching a maximum of 5.5m; blocked in the north by the presence of the geometrical asperity of Mejillones penninsula, the rupture propagates toward to the south and do not reach the 1877 northern Chile gap (Delouis, 1997).

INTERSEISMIC AND POSTSEISMIC PROCESSES

We have mapped the crustal deformation by processing interferograms of ERS satellites during the three years immediately after the 1995 earthquake (figure 2) and by determining the GPS vectors of 40 points measured between 1996 and 2000, on an area of more than 700 km long by 100 km wide including the 1877 Chile gap and Antofagasta rupture zone. The GPS signal observed in the central part of the gap is dominated by an elongated interseismic velocity gradient parallel to the arc with 20-30 mm/yr eastward displacement with respect to stable South America (Ruegg & al, in preparation; Kendrick & al, 2001). This is consistent with the 15-20 mm/yr range

decrease determined by SAR interferometry. South of this gap, the interferometric map exhibits a different pattern and the GPS vectors are significantly different in direction and amplitude. This change is located in the area where the M=8.1 Antofagasta earthquake occured in 1995 and is interpreted to be post-seismic relaxation.

We model the interseismic with points source embeded in an elastic half-space by 100% coupling of the thrust interface of the subduction to a depth of 35km with a 50km wide transition zone beneath. The slip in this zone increases linearly from zero to the plate convergence rate (79mm/yr from NUVEL-1).

We model the postseismic relaxation following Antofagasta earthquake as after-slip located in the transition zone (35-55km depth). The maximum post-seismic slip reach 75cm, in the prolongation in depth where the maximum of energy have been release during the 1995 earthquake (5.5m of slip).

Between the 1877 gap and the 1995 rupture, the structures associated with the Mejillones Peninsula seem to have an important role. The 1995 event nucleated in this region appears to have acted as a barrier to northward propagation. During the 4 years following the earthquake some slip within lower part of seismogenic depth zone (20-45 km) is also required in this area to explain the observations. We propose a simple slip model for the seismic cycle where the transition zone has alternating behaviour with both plastic shear (inter-seismic) and seismic slip (co-seismic). The sum of co-seismic and inter-seismic slip do not explain the whole cycle. The post-seismic slip occurring in the transition of the thrust interface fills the remaining gaps with both seismic and aseismic slip.

Acknoledgments: The ERS data were provided by the European Space Agency, in the frame of the Announcement of Opportunity AOT F310 and AO-3 302.

References :

Delouis B., Monfret T., Dorbath L., Pardo M., Rivera L., Comte D., Haessler H., Caminade J.P., Ponce L., Kausel E., Cisternas A., The Mw=8.0 Antofagasta (Northern Chile) earthquake of 30 July 1995, a precursor to the end of the large 1877 gap, Bull. Seismo. Soc. Am., Vol.87, N°2, 427-445, 1997.

DeMets C., Gordon R.G., Argus D.F. and Stein S., Current plate motions, Geophys. J. Int., 101, 425-478, 1990.

Ihmlé P.F.and J.C. Ruegg, Source tomography by simulated annealing using broad-band surface waves and geodetic data: application to the Mw=8.1 Chile 1995 event, *Geophys. J. Int.,* 131, 146, 158, 1997.

Kendrick E., Bevis M., Smalley R. Jr., Brooks B., An intergrated crustal velocity field for the Central Andes, Geochem. Geophys. Geosyst, 2,10.1029/2001GC000, 191, 2001.

Nishenko S.P., Seismic potential for large and great interplate earthquakes along the Chilean and Southern Peruvian margins of South America: a quantitative reappraisal, *J. Geophys. Res.,* Vol.90, N°B5, 3589-3615, 1985.

Ruegg J.C., Campos J., Armijo R., Barrientos S., Briole P., Thiele R., Arancibia M., Cañuta J., Duquesnoy T., Chang M., Lazo D., Lyon-Caen H., Ortlieb L., Rossignol J.C., Serrurier L., The Mw=8.1 Antofagasta (North Chile) earthquake of July 30, 1995: First results from teleseismic and geodetic data, *Geophys. Res. Lett.* Vol.23, N°9, 917-920, 1996.

Figure 1 - 1995 Antofagasta earthquake displacement field in North Chile.

The map corresponds to a mosaic of 7 ERS interferograms surperimposed on shaded topography. Positive displacements (in cm) correspond to range increase (increase of ground satellite distance). In the Antofagasta region where the 1995 Mw=8.1 subduction earthquake occured, range is increased and corresponds to a combination of subsidence and westward displacement as shown by GPS measurements (red arrows) during the same period. This is interpreted as coseismic elastic rebound. Plate convergence from De Mets & al. (1990). Focal mechanism from Ruegg & al. (1996). White star is location of the 1995 epicenter.

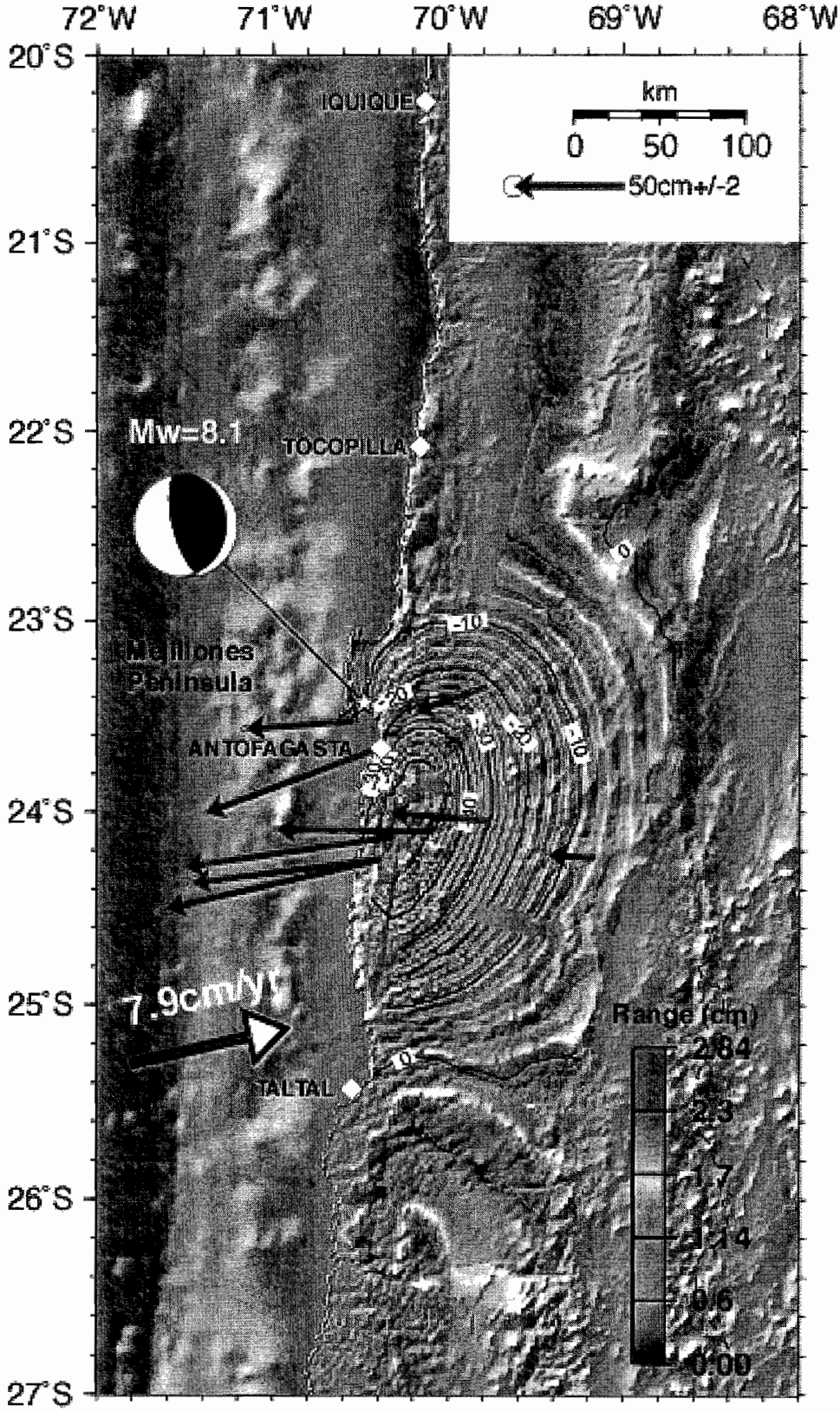

Figure 2 - 1995-1999 displacement field in North Chile.

Each Interferogram Pair (1 and 2) covers 3.6 years (a) and 3.3 years (b) after the Antofagasta earthquake (c). Pair 1 starts 6 hours after the earthquake. The GPS vectors (black arrows) recover same time period and are represented relatively to stable South America.

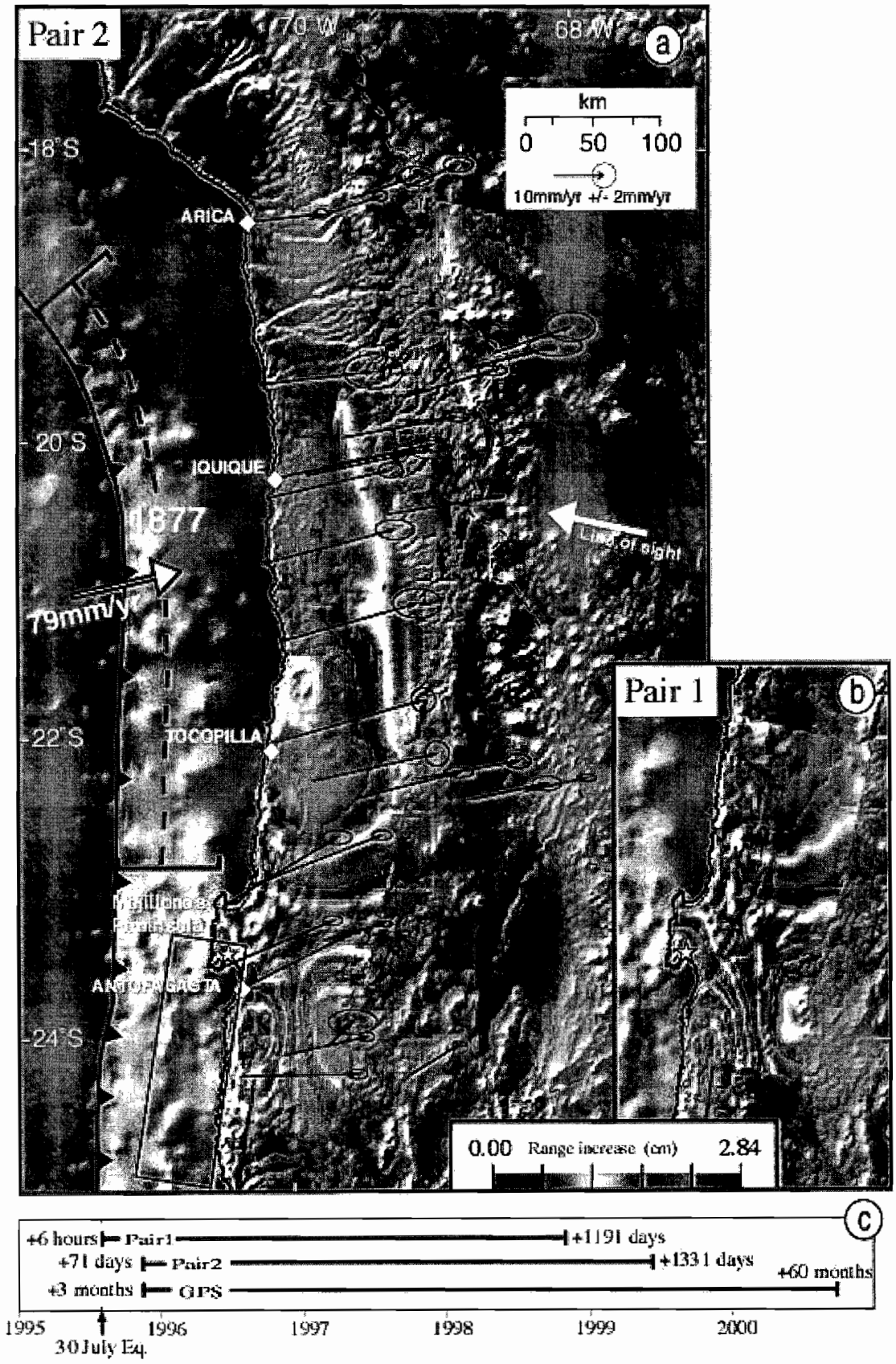

PHASES OF ANDEAN DEFORMATION, FOOTHILLS OF THE NEUQUEN BASIN, ARGENTINA

Peter R. COBBOLD (1), Eduardo A. ROSSELLO (2)

(1) Géosciences-Rennes (UMR6118 du CNRS), Université de Rennes I, 35042 RENNES Cedex, France (peter.cobbold@univ-rennes1.fr)
(2) CONICET y Departamento de Ciencias Geológicas, Universidad de Buenos Aires, 1428 BUENOS AIRES, Argentina (rossello@gl.fcen.uba.ar)

KEY WORDS: Deformation, Andean phases, Neuquén, basin, foothills.

INTRODUCTION

The Neuquén Basin lies on the eastern side of the Andes. It formed as a rift basin in the early Mesozoic. Regional extension resulted from slow subduction of oceanic crust beneath the Pacific margin of South America. The Triassic to Early Cretaceous basin fill, some 5000 m thick, includes marine strata of Pacific affinity (Urien and Zambrano, 1994; Legarreta and Uliana, 1999; Vergani et al., 1995).

From 100 Ma to the present, the Neuquén Basin developed in a foreland setting. Late Aptian evaporites heralded the end of marine (Pacific) influence. Above a Cenomanian unconformity, up to 1300 m of fluvial and alluvial conglomerates (Neuquén Group) filled a Late Cretaceous foreland basin. Towards the end of the Cretaceous, an incursion of Atlantic waters resulted in shallow-marine carbonates, followed by early Eocene fresh-water diatomites. A late Eocene unconformity marked a return to continental conditions but no regional foreland basin. Cenozoic volcanic rocks and shallow intrusions spread over the foothills. Although early workers (for example, Groeber, 1929) recognized Peruvian (Late Cretaceous), Incaic (Eocene) and Quechua (Neogene) phases of Andean deformation, there are no modern syntheses of their history or style.

MAJOR STRUCTURES

Gentle folds mark the foreland: the Chihuidos anticline in Late Cretaceous strata and the Huantraico syncline in Neogene lavas and sediment (Fig. 1). In the foothills, the Tromen and neighbouring volcanoes line the hanging wall of the east-verging Tromen thrust, which involves Pre-Mesozoic basement. To the south, narrow tight anticlines and wide flat synclines trend N-S or NW-SE. Associated reverse faults involve basement and have formed by reactivation of Mesozoic extensional faults (Zapata et al., 1999).

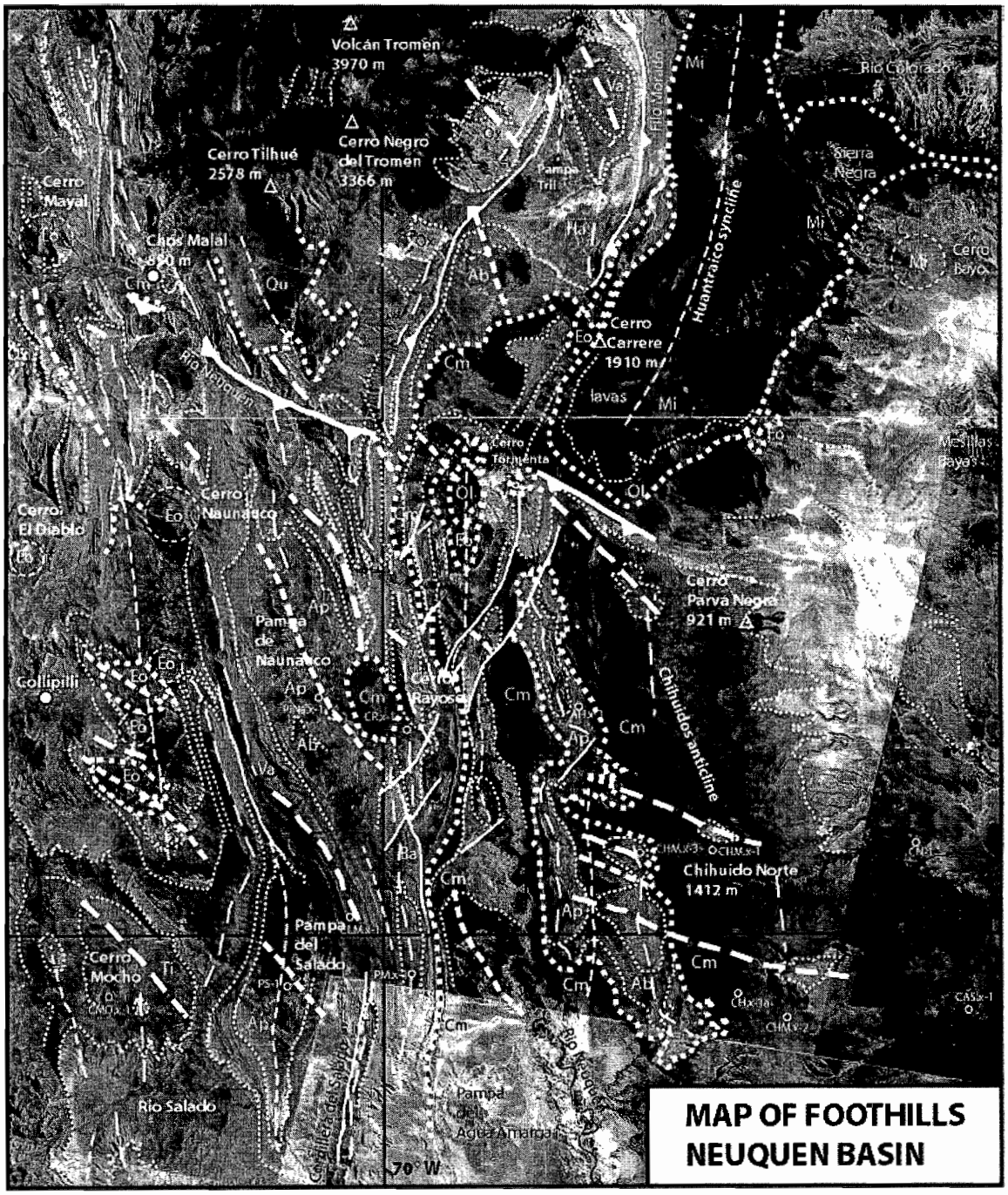

KEY

Chos Malal 850 m	Town or village		Eocene anticline	Ox	Oxfordian
Cerro Carrere 1910 m	Peak		Eocene syncline	Tl	Tithonian
CHM.x-2	Oil well		Neogene anticline	Ba	Barremian
	Bedding trace		Neogene syncline	Va	Valanginian
	Unconformity		Eocene fault	Ha	Hauterivian
			Neogene fault	Ap	Aptian
				Ab	Albian
				Cm	Cenomanian
				Eo	Eocene
				Ol	Oligocene
				Mi	Miocene
				Qu	Quaternary

P.R. Cobbold, E.A. Rossello, 2002

Figure 1

INCAIC AND QUECHUA PHASES

1. Incaic phase. Near Collipilli (Fig. 1), volcano-clastic rocks and andesitic lavas have been dated as late Eocene (Llambías and Rapela, 1989). They fill synclines trending NW-SE. 2. At Cerro Caycayén, andesitic dykes and sills have been dated as middle Eocene (Llambías and Rapela, 1989). They pierce pre-existing folds. 3. At Cerro Mayal (Fig. 1), we have dated a sill at 39.7 ± 0.2 Ma (late Eocene) by Ar-Ar on whole rock. That sill also pierces pre-existing folds. 4. West of the Cordillera del Viento, andesitic lavas have been dated as late Eocene (Jordan et al., 2001). They overstep a folded sequence (Triassic to Cretaceous). 5. At Puesto de las Liebres, volcano-clastic deposits overlie Eocene diatomites and underlie basal lavas of the Palaoco Formation, which have been dated as Oligocene (Ramos and Barbieri, 1989). We have found volcano-clastic growth strata in the footwall of a major fault trending WNW-ESE (Fig. 2). 6. At Chos Malal, the same fault system puts Cretaceous marine strata over conglomerates of the Neuquén Group (Fig. 1). In general, Eocene folds and thrust faults trend NW-SE (Fig. 1), whereas right-lateral faults trend N-S. Associated bitumen dykes trend NE-SW (Cobbold et al., 1999). We infer transpressional deformation and attribute it to oblique convergence at the Pacific margin of South America. This is compatible with plate-tectonic reconstructions (Pardo-Casas and Molnar, 1987).

2. Quechua phase. This produced less than 10% of E-W shortening in the Huantraico syncline (Fig. 1). In the foothills, it tightened pre-existing structures and re-oriented them in a N-S direction. The Tromen thrust and Filo Morado triangle zone may have been active at this time, but evidence is lacking.

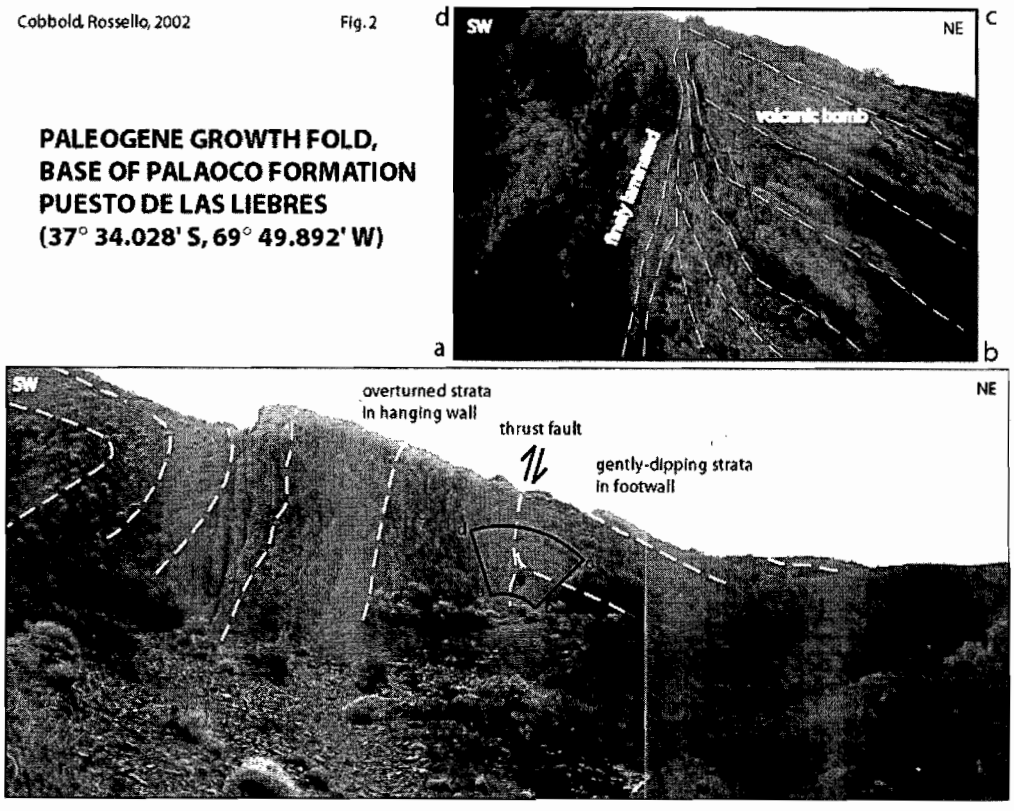

CONCLUSIONS

1. In the foothills of the Neuquén basin, the Peruvian, Incaic and Quechua phases of Andean deformation have all left their marks.
2. The Peruvian phase resulted in major unconformities and a foreland basin.
3. The Incaic phase resulted in strong transpressional deformation. Evidence for this includes a major unconformity, volcano-clastic growth strata and shallow magmatic intrusions, all dated to the Eocene. We attribute Incaic deformation to oblique convergence at the Pacific margin.
4. The Neogene Quechua phase resulted in E-W shortening, but this may not have been intense.

REFERENCES

Cobbold, P.R., Diraison, M., Rossello, E.A. 1999. Bitumen veins and Eocene transpression, Neuquén Basin, Argentina. Tectonophysics, 314, 423-442.

Groeber, P. 1929. Líneas findamentales de la geología del Neuquén, sur de Mendoza y regiones adyacentes. Dirección General de Minería Geología e Hidrología, Buenos Aires, Publicación 58, 1 -110.

Jordan, T.E., Burns, W.M., Veiga, R., Pángaro, F., Copeland, P., Kelley, S., Mpodozis, C. 2001. Extension and basin formation in the southern Andes caused by increased convergence rate: A mid-Cenozoic trigger for the Andes. Tectonics, 20, 308-324.

Legarreta, L., Uliana, M.A. 1999. El Jurásico y Cretácico de la Cordillera Principal y la Cuenca Neuquina. I. Facies Sedimentarias. In: Geología Argentina (edited by Caminos R.), Instituto de Geología y Recursos Minerales, SEGEMAR (Buenos Aires, Argentina), Anales 29, Capítulo 16, 399-416.

Llambías, E.J., Rapela, C.W. 1989. Las volcanitas de Collipilli, Neuquén (37°S) y su relación con otras unidades paleógenas de la cordillera. Asociación Geológica Argentina Revista, 44, 224-236.

Pardo-Casas, F. and Molnar, P. 1987. Relative motion of the Nazca (Farallon) and South American plates since Late Cretaceous time. Tectonics, 6, 233-248.

Ramos, V.A., Barbieri, M. 1989. El volcanismo Cenozoico de Huantraico: edad y relaciones isotópicas iniciales, provincia del Neuquén. Asociación Geológica Argentina Revista, 43, 210-223.

Urien, C.M., Zambrano, J.J. 1994. Petroleum systems in the Neuquén Basin, Argentina. In: The petroleum system - from source to trap (edited by Magoon, L.B., Dow, W.G.), American Association of Petroleum Geologists Memoir, 60, 513-534.

Vergani, G.D., Tankard, A.J., Belotti, H.J., Welsink, H.J. 1995. Tectonic evolution and paleogeography of the Neuquén basin, Argentina. In: Petroleum basins of South America (edited by Tankard, A.J., Suárez S., R., Welsink, H.J.), American Association of Petroleum Geologists Memoir, 62, 383-402.

Zapata, T., Brissón, I., Dzelalija, F. 1999. La estructura de la faja plegada y corrida andina en relación con el control del basamento de la Cuenca Neuquina. Boletín de Informaciones Petroleras, 60, 112-121.

CORRELATIONS BETWEEN CRUSTAL STRUCTURES OF THE NORTHERN-ECUADOR SOUTHERN COLOMBIA MARGIN FROM MCS DATA, AND RUPTURE ZONE OF 1942, 1958 AND 1979 GREAT SUBDUCTION EARTHQUAKES

J-Y COLLOT(1), B. MARCAILLOU(1), M-A GUTSCHER(2), P. CHARVIS(1), W. AGUDELO(1) and F. MICHAUD(1).

(1) UMR Géosciences Azur, BP 48, 06230 Villefranche sur Mer, collot@obs-vlfr.fr,
(2) UMR Domaines Océaniques, Place Nicolas Copernic, 29280, Plouzané, gutscher@univ-brest.fr

KEY WORDS : Subduction, margin segmentation, great subduction earthquake, multichannel seismic reflection

INTRODUCTION

Along the north Andean margin, the Nazca plate subducts eastwards beneath the Ecuador and Colombia at ~ 6 cm/yr. (Trenkamp et al., 2002). The margin consists of oceanic terranes accreted against the continent from Late Jurassic to Eocene (Gansser, 1973, Reynaud et al., 1999). During the XXth century, six great earthquakes have ruptured the subduction plate-interface. The largest, in 1906 (Mw 8.8), had an estimated rupture zone of ~ 500 km in length (Kelleher, 1972), which was partially reactivated by three subsequent thrust events, from Baya de Caraques to Tumaco, in 1942 (Mw=7.9), 1958 (Mw=7.8) and 1979 (Mw=8.2) (Beck and Ruff, 1984; Swenson and Beck, 1996). The cause of the segmentation between adjacent rupture zones (as defined by the aftershocks distribution), as well as the nature of seismological asperities (as defined by regions of maximum co-seismic displacement on the fault plane), have remained unclear. Deep multichannel seismic reflection (MCS) data collected across the Ecuador-Colombia margin during the SISTEUR cruise (Collot et al., 2002) in September-October 2000, together with conventional bathymetry are used to establish correlations between the margin segmentation, limits of earthquake rupture zones and seismological asperities. MCS data were recorded across the Ecuador-Colombia margin using a 45-L airgun seismic source and a 360-channel streamer. Shots were fired every 50-m, providing a 45-fold coverage. Single beam bathymetry was collected with MCS data.

CONCLUSIONS

The northern segment of the margin extends offshore Esmeraldas and Tumaco between 1°-2°30'N (Fig. 1). It is ~100-120 km wide, with a large, 800-1000 m deep reentrant containing a 3 km-thick sedimentary fore-arc basin, and a discontinuous outer ridge as shallow as 60 m below sea level. The Colombia trench that contains up to 3 km of sediment bounds the margin seaward, whereas a subsiding coast dominated by marshes and mangroves flanks the margin landward. This margin segment contrasts with the southern segment (South of 1°N) adjacent to the Carnegie Ridge, which shows a short (40-70km) trench-coast distance, thin (<100 m) trench fill, a

shallow (100m) continental shelf and an uplifted coastline. The boundary between the two margin segments is sharp and outlined by the steep, NW-trending southern flank of the reentrant that is deeply incised by the active Esmeraldas canyon. This boundary coincides with the offshore extension of the major NW-trending, inherited, crustal fault ES, and matches the limit between the 1942 and 1958 rupture zones (Fig. 1).

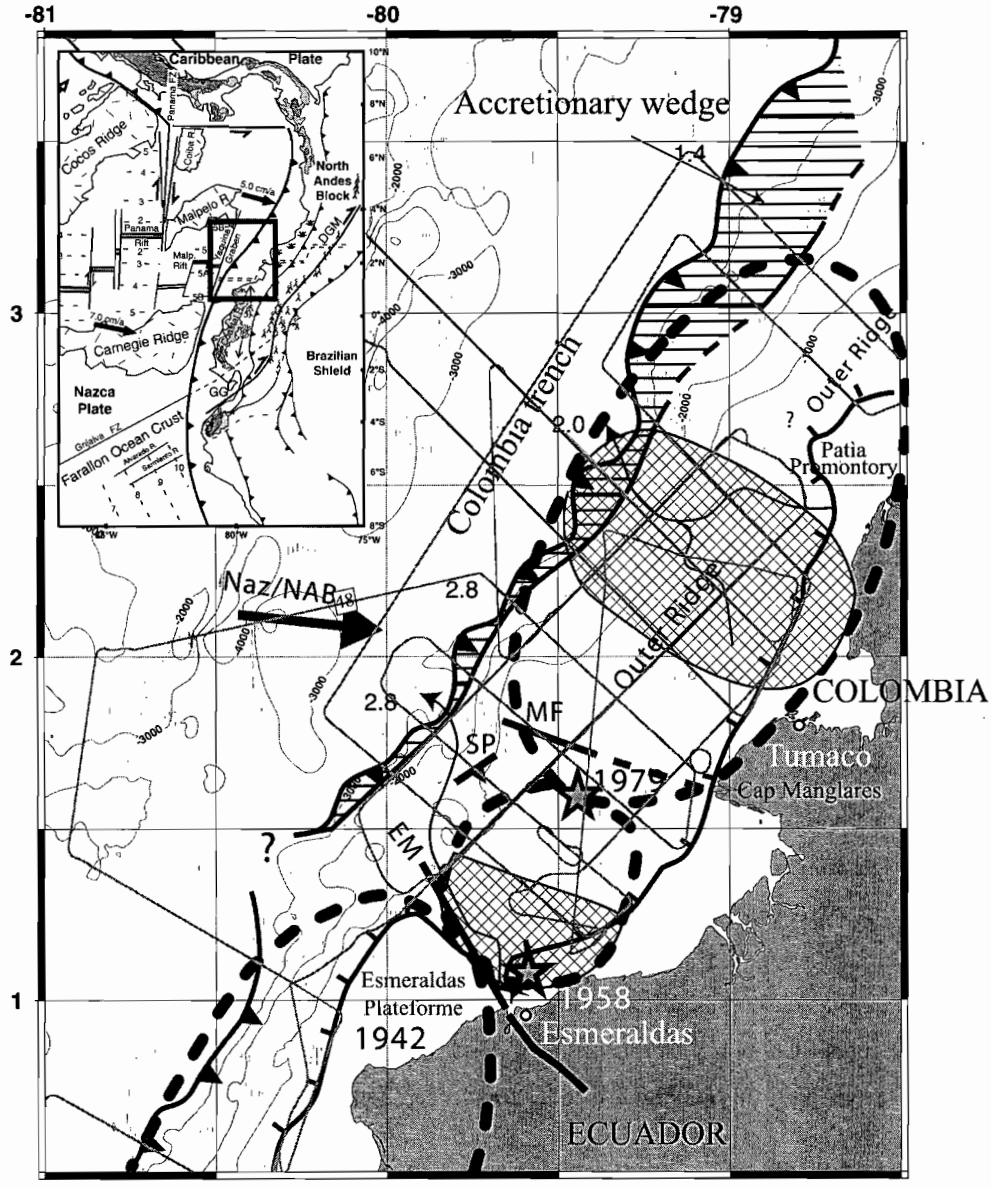

Fig. 1 Bathymetric and structural map of the northern Ecuador-southern Colombia margin with 1942, 1958 and 1979 subduction earthquake rupture zones. Bathymetric contour = 100 m

earthquake rupture zones and seismological asperity

earthquake epicenter

2.8 trench fill thickness (stwt)

thrust front

Nazca Plate-North Andean block convergence

canyons

EM = Esmeraldas Fault; **SP** = Splay Fault; **MF** = Manglares Fault

Sisteur MCS-lines

MCS data across the northern segment of the margin show evidence of a second major NW-trending crustal fault named the Manglares Fault (MF in Fig. 1). Fault MF projects seaward from Cap Manglares, a N-105°E rectilinear coast segment, and divides the margin into two areas of different deformation style. The fault

coincides approximately with the limit between the rupture zones of the 1958 and 1979 earthquakes. Immediately south of fault MF, most of the active deformation occurs specifically between the margin front and a major landward-dipping crustal splay fault SP (Fig. 1), which soles out at a 12-13 km depth on the plate interface. From MCS data, the plate interface dips landward and returns strong reflections as deep as 22-24 km near the coast line. The 1979 and 1958 earthquake hypocenters project onto the seismically-imaged plate interface at depths of about 18 and 20 km respectively. Interestingly, between fault MF and Esmeraldas, the fore-arc basin is 55 km-wide and shows no evidence for recent shortening. North of fault MF, active deformation, which is dominantly compressive, is distributed over a much larger area than south of the fault. The deformation zone includes an incipient accretionary wedge, an imbricated margin front, a shallow outer basement ridge and the seaward flank of a narrow fore-arc basin. Although both faults ES and MF may no longer be active, they bound margin segments of different structural history, and seem to act as lateral barriers to the propagation of the inter-plate rupture during earthquakes of Mw 7.8 to 8.2.

The seismological asperities associated with the1958 and 1979 earthquakes correlate with drastically different seafloor and structural expressions, which may reflect different stress or friction conditions. The 1958 asperity projects onto the fore-arc basin seafloor as a smooth, long wavelength, 150-200 m-high bulge that is incised by the Esmeraldas canyon. The absence of active thrusting across the bulge together with the restriction of the 1958 earthquake rupture zone to the fore-arc basin area, suggests that the major crustal splay fault and corresponding plate interface segment accommodate most co-seismic motion and probably the long-term thrust motion. Aseismic motion may occur on secondary faults near the margin front. Sediments in the fore-arc basin appear to have recorded earthquake shaking. Continuous, sub-horizontal stratification changes locally into incoherent reflections or sequences disrupted by 100-200 m long disturbances, indicating debris flows, slumps and small-scale failures, possibly triggered by earthquakes.

The 1979 asperity is associated with part of the highly shortened margin segment, north of fault MF. The distribution of folds and active thrust faults from the deformation front to the outer basement ridge and fore-arc basin suggests a weak margin and a relatively high inter-plate friction. This wide distribution of active deformation, associated with the fact that the asperity and rupture zone areas match the margin width, indicate that the co-seismic motion and possibly the long term deformation are not accommodated by a single splay fault, but by a set of landward-dipping crustal faults in addition to the plate interface.

In the region of the 1958 and 1979 rupture zones, variations of trenchfill thickness, as well as the location of the decollement within the trenchfill, reveal along-strike changes in the accretionary process, which may reflect margin structural complexities associated with the seismological asperities. In the northernmost part of the study area, the décollement lies within the trenchfill, allowing accretion of the upper 1/2 to 2/3 trenchfill, and sediment subduction of the corresponding lower trenchfill. Further south, the décollement lies dominantly at the roof of the subducting trenchfill, thus forming a 2-3 km thick subduction channel. Consequently, despite the thick trenchfill, a narrow or no accretionary wedge has developed seaward of the 1958 and 1979 rupture zones indicating an unstable, transient-state tectonic regime (Fig. 1).

Possible explanations for these along strike variations include: 1) Rapid accumulation of trench fill may not have allowed tectonic accretion to develop fully in the south. 2) Along strike variations in physical properties within the incoming trench sediment could cause the basal friction to vary along the decollement and affect the accretionary style. 3) An underthrusting structural high beneath the margin may have locally deflected the

decollement upward so that a shadow zone develops in the wake of the high, allowing the entire trench fill to be dragged into the subduction (Dominguez et al., 2000). 4) The margin may be locally exhibiting cyclical accretion, alternating between underthrusting of the entire sedimentary sequence and periods of frontal accretion with rapid local growth of an accretionary wedge. Sandbox models with a high basal friction have demonstrated this accretionary style for sedimentary input at the trench (Gutscher et al., 1998). The unusual location of the decollement at the top of the trenchfill, and the very localized deformation zone in the outer ridge supports a high-friction inter-plate surface beneath the ridge. This high friction together with the seismological asperity identified in the 1979 earthquake source function (Beck and Ruff, 1984) may correlate with an oceanic asperity buried beneath the margin.

REFERENCES

Beck, S.L., and L.J. Ruff, 1984. The rupture process of the great 1979 Colombia earthquake: evidence for the asperity model, Journal of Geophysical Research, 89, 9281-9291.

Collot, J.-Y., P. Charvis, M.A. Gutscher, S. Operto, and SISTEUR Scientific Party, 2002. Exploring the Ecuador-Colombia active margin and inter-plate seismogenic zone, EOS Transactions, American Geophysical Union, in press.

Dominguez, S., J. Malavieille, and S. Lallemand, 2000. Deformation of margins in response to seamount subduction insights from sandbox experiments, Tectonics, 19 (1), 182-196.

Gansser, 1973. Facts and theories on the Andes, Jounal Geological Society London, 129, 93-131.

Gutscher, M.-A., Kukowski, N., Malavieille, J. and Lallemand, S., 1998. Episodic imbricate thrusting and underthrusting: Analog experiments and mechanical analysis applied to the Alaskan accretionary wedge. Journal of Geophysical Research, v. 103, p. 10161-10176

Kelleher, J., 1972. Rupture zones of large South American earthquakes and some predictions, Journal of Geophysical Research, 77, 2087-2103.

Reynaud, C., E. Jaillard, H. Lapierre, M. Mamberti, and G.H. Mascle, 1999. Oceanic plateau and island arcs of southwestern Ecuador: their place in the geodynamic evolution of northwestern South America, Tectonophysics, 307, 235-254.

Swenson, J.L., and S.L. Beck, 1996. Historical 1942 Ecuador and 1942 Peru subduction earthquakes, and earthquake cycles along Colombia-Ecuador and Peru subduction segments, Pageoph., 146 (1), 67-101.

Trenkamp, R., J.N. Kellogg, J.T. Freymueller, and P. Mora, H, , 2002. Wide plate margin deformation, southern Central America and northwestern South America, CASA GPS observations, Journal of South American Earth Sciences, in press.

STUDY OF INTRAPLAQUE SEISMICITY TRIGGERED IN NORTHERN CHILE BY THE JUNE 23, 2002 PERUVIAN SUBDUCTION EARTQUAKE

Diana COMTE (1), Catherine DORBATH (2, 3), Jaime CAMPOS (1), Louis DORBATH (2,3) and Henri HAESSLER (3)

(1) U. de Chile, Santiago
(2) IRD, UR 104
(3) IPGS, UMR 7516

KEY WORDS: Intraplaque seismicity, triggering, northern Chile

ABSTRACT

An earthquake of magnitude Mw = 8. 4 occurred in the southern Peru subduction zone on June 23, 2002. This event was immediately followed by a significant increase of the crustal seismicity of the forearc in the southern Peru and northern Chile regions. This activity culminated with the July 24, 2002 Mw=6.3 Aroma crustal earthquake. We modelized the broad band teleseismic records and studied the aftershocks sequence using the local network complemented by temporary stations. This event occurred on an even known fault zone not yet recognized as active, the Ausipar Thrust. The focal mechanism shows right lateral movement on a north-south east dipping plane, corresponding to a jog of the main fault. The aftershocks zone extends about 25 km suggesting some segmentation. In depth, the seismic activity extends below the aftersocks zone down to the subducted slab. This earthquake and its aftershocks sequence are located on a major P-wave velocity jump evidenced down to the Moho by a previous tomographic study. On january 14, 2002, a magnitude Mw=5.7 earthquake occurred there, with about the same epicentral area but at a depth of about 70 km. This depth is well controlled by nearby stations, and therefore this event is not crustal neither in the subducted slab. The obtained depth agrees well with the CMT solution determined by global agencies, showing a similar focal mechanism of the Mw=6.3 crustal event It is was followed by other events in the same range depth. We present some possible interpretation of this unusual spatial and temporal seismic sequence and its mechanical pattern.

ASSIMILATION OF MAFIC-ULTRAMAFIC CUMULATES BY ARC BASALTS MAY BE AN IMPORTANT PROCESS IN MODIFYING MAJOR AND TRACE ELEMENT SIGNATURES: EVIDENCE FROM THE TATARA-SAN PEDRO COMPLEX (TSPC), 36E S, CHILEAN ANDES

Laurie CORTESI[1], Michael DUNGAN[1], Jon DAVIDSON[2], Fred FREY[3], Fidel COSTA[4], Andrea MARZOLI[1]

(1) Sciences de la Terre, Université de GenΠve, 13 rue des Maraîchers, 1211 GenΠve 4, Switzerland
(2) Department of Geological Sciences, University of Durham, Durham DH1 3LE, United Kingdom
(3) Department of Earth, Atmospheric & Space Sciences, MIT, Cambridge MA 02139, USA
(4) Institut des Sciences de la Terre d'Orleans-CNRS, 1A Rue de la Ferollerie, 45071 Orleans, Cedex 2, France

KEY WORDS: Open-system magmatic processes, assimilation, SVZ, Tatara-San Pedro volcanic complex

ASSIMILATION OF MAGMATIC CUMULATES BY BASALTS: GENERAL CONSIDERATIONS

Arc magmas are notorious for the presence of disequilibrium mineral assemblages. Magma mixing and crustal assimilation are both recognized as contributors to the mineralogical complexities of continental arc magmas, as well as to their chemical diversity: closed-system fractional crystallization is rarely the sole differentiation mechanism recorded in evolved magmas. In this contribution we suggest that assimilative recycling of gabbroic to ultramafic plutonic lithologies (not phenocryst accumulation), both as partially solidified crystal mush from conduit systems (*e.g.,* Cole *et al.,* 2000) and as previously solid material, is a common and potentially important open-system process that may substantially impact the major and trace element compositions of contaminated basaltic magmas. Gabbroic rocks are by far the most common and abundant xenolith type throughout the history of the long-lived Tatara-San Pedro complex (TSPC, 36E S, Chilean Andes; 930 ka - Holocene), and many lavas contain 5-15 vol. % of such lithologies dispersed as xenocrysts and angular micro-xenoliths (1-10 mm) in which solid-solid grain boundaries are preserved.

In long-lived continental arc magmatic systems, plutonic roots comparable in volume to that of erupted magma are left behind during differentiation. Heliker (1995) has shown that even highly refractory anhydrous gabbroic rocks may be partially melted and dispersed in silicic host magma during short residence times (<3 years). Cumulate rocks containing amphibole and mica would be more susceptible to grain boundary melting, disaggregation, and dispersion of refractory solids if incorporated by hot basaltic magma. Among the xenolith suites at the TSPC are diverse (chemically, mineralogically, modally) groups of hybridized gabbros and gabbronorites containing up to 50 vol. % amphibole + phlogopite, wherein hydrous phases are the products of reaction between partially to completely solidified cumulate assemblages (oliv+Cr-spinel+augi+plag) and percolating hydrous dacitic melts that apparently originated outside the gabbroic plutons (Costa *et al.,* 2002).

As the hydrous phases in such rocks are enriched in alkalies and incompatible trace elements relative to a refractory cumulate pile, assimilation of hybrid cumulates would impose a chemical imprint on contaminated magmas in which both highly compatible elements (Mg, Cr, Ni, Sc, Sr) and incompatible elements are added in ratios that deviate markedly from what would be typical for two-component magma mixing, bulk assimilation of

evolved upper crustal lithologies, or AFC, particularly where the contaminated magma is basalt with low initial abundances of incompatible elements. Adding such a chemically 'bi-polar' component to basalt may greatly modify its initial incompatible element signature and maintain or increase compatible element abundances.

AN EXTREME CASE OF CUMULATE ASSIMILATION AT THE TSPC: THE UPSPS LAVAS

Among the suites of lavas at the TSPC in which assimilative recycling of gabbroic-ultramafic rocks appears to have been important, are the Upper Placeta San Pedro sequence basalts (UPSPS, 235 ka), which previously have been discussed in these terms by Dungan *et al.* (2001). The UPSPS lavas are an unusual suite for the TSPC in that they are entirely basaltic (~49.9-52.3 wt. % SiO_2; ~5.4 to ~9 wt. % MgO), and on the basis of paleomagnetic constraints (unpublished data, L. Brown and J. Pickens) were emplaced during a short time interval. We have analyzed 66 samples of ~30 flows (top eroded) from six stratigraphic sections. Some flows are compositionally heterogeneous and chemical variations with respect to eruptive order define a complex temporal evolution. Fractional crystallization is definitively eliminated as the dominant differentiation mechanism responsible for variations among UPSPS lavas, although even the inferred parental compositions are substantially evolved (Ol Fo_{83-80} + Pl An_{95-50}). Two consecutive flows in the lower third of the pile: **(1)** have low incompatible element abundances (~6 wt. % MgO; 8 ppm Rb, 0.9 ppm Th, 0.6 wt.% K_2O, 50-60 ppm Cr), **(2)** are free of the xenocrystic olivine-rich and augite-rich crystal clots which are present in all other flows, **(3)** are apparently the least contaminated magmas preserved in the UPSPS (K/Rb = 600), and **(4)** are inferred to be approximations of the prevalent parental magma composition (Dungan *et al.*, 2001; p. 591-595).

UPSPS flows with the higher Mg, Fe, and Cr (lowest Al_2O_3) than the parent magmas contain the highest modal abundances of coarse-grained olivine (single crystals as well as multi-grain clots, commonly embayed and cut by healed fractures), and they are characterized by higher K, Th, and Rb (*e.g.*, 20 ppm Rb, but up to 180 ppm Cr) and large departures in elemental ratios (high Rb/SiO_2, Rb/Y, La/Yb, Th/Yb, and low K/Rb, Sr/Rb, Ba/Rb, Ba/Th: poorly correlated with SiO_2) relative to the inferred parental magmas. Dungan *et al.* (2001; p. 591-595) showed that neither mixing with a wide range of TSPC magmas, nor simple olivine accumulation can account for the compositional arrays defined by this subset of UPSPS lavas. Doubling the number and increasing the diversity of mixing end-members has not led to a satisfactory model, which in any case would require many highly diverse end-members to account for the total array. Other UPSPS lavas contain less olivine, but larger quantities of augite-rich micro-xenoliths, and they display positive correlations between increasing SiO_2 and increasing incompatible element abundances (up to 27 ppm Rb). These lavas are characterized by the same low Cr and MgO as the parental magmas. Some mixing models approximate the general compositional characteristics of some magmas for some elements and ratios, but almost all such models fail in detail when applied to reproducing the compositions of individual lavas.

Numerous arguments mitigate against inheritance of these compositional variations from compositionally variable parental magmas: **(1)** plots of incompatible elements and ratios define fan-shaped arrays radiating from the xenocryst-free and incompatible element-poor inferred parental magmas, **(2)** $^{87}Sr/^{86}Sr$ *decreases* from the uncontaminated magmas (0.70409) to those with the highest incompatible element abundances (0.703905), **(3)** variations in trace elements and elemental ratios are not consistent with variable degrees of partial melting from a homogeneous mantle source or with a heterogeneous source due to varying amounts of slab-derived fluid

components. Evidence supporting the assimilation of hybrid cumulates comes from the mineralogy and mineral chemistry of coarse-grained multi-phase aggregates that fill embayments and channels in olivine and augite xenocrysts. These embayed olivines closely resemble those in the amphibole- and phlogopite-bearing cumulates studied by Costa *et al.* (2002). We are currently investigating all aspects of the compositional variations and zoning profiles of mineral phases and rare glass in these lavas, but in this contribution we present preliminary results from minerals filling large embayments and channels in xenocrystic olivine and augite.

We have analyzed feldspar-rich assemblages that occur as large pockets (100-200 μm) in olivines from Mg-rich flows, and a feldspar-rich vein that cuts an augite. The pockets in olivine contain plagioclase zoned from normal ($An_{45-40}Ab_{50-52}Or_{3-4}$) to ternary compositions ($An_{12-20}Or_{12-21}Ab_{60-70}$), minor Afsp ($Or_{30-50}$), orthopyroxene, phlogopite, amphibole, and coarse magnetite. Blades of phlogopite are common in felsic pockets within such olivines. Glass in these segregations it is rarely preserved in thin section, perhaps due to fragility related to vesiculation. The vein that cuts the augite xenocryst preserves feldspar (sub-equal amounts of plag and Afsp Or_{30-70}), magnetite, and orthopyroxene and compositions of the two feldspars are similar to those in the pockets within olivines. Both contaminated and uncontaminated UPSPS basalts contain plagioclase phenocrysts with similar high-An cores (An_{92-40}), but zoning trends in plagioclase from contaminated lavas trend toward higher Or ($An_{50}Or_{2-3}$) than those in uncontaminated lavas ($An_{50}Or_{1.8}$). The unusual assemblage amphibole + high-Mg phlogopite + Afsp + orthopyroxene (En_{75-80}) must have an origin extraneous to the host magmas, as it is not compatible with crystallization of primitive or evolved low-K arc basalts, regardless of water content.

We conclude that these unusual mineral assemblages are not the crystallization products of magmas: they

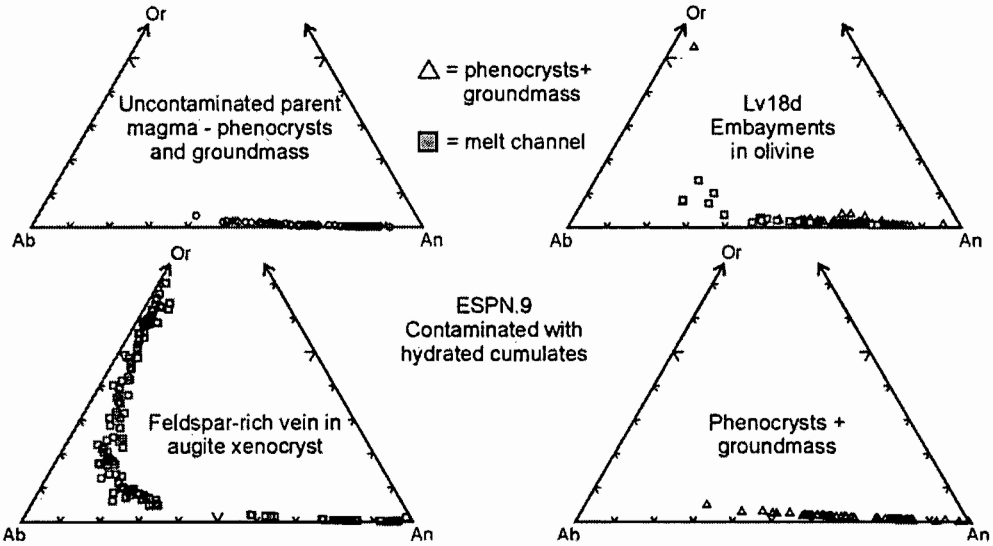

reflect syn-eruptive crystallization within confined melt pockets (embayments in assimilated olivine and augite) that formerly consisted of hydrous minerals plus orthopyroxene and magnetite that were formed at an earlier stage by replacement of olivine and augite (Costa et al., 2002). Syn-eruptive crystallization of minor quantities of phlogopite in association with alkali feldspar apparently after partial degassing of secondary alkali-rich melts, leading to an assemblage dominated by sodic + potassic feldspar. The alkali-rich character of these pockets was preserved by their physical inclusion within refractory mineral phases, whereas the overall enrichments of alkalies and incompatible trace elements in the lavas reflects efficient melting of hydrous phases that initially surrounded olivine and augite, followed by blending of these melts and xenocrysts with host basalt. The departure of UPSPS basalt compositions from a simple variation pattern involving a few components is

explained by: (**1**) primary heterogeneities in the assimilated cumulate lithologies (phase proportions and compositions), (**2**) differences in the fraction of incorporated mafic xenoliths, (**3**) different histories of partial melting, disaggregation, dispersion, and reaction of the refractory and non-refractory mineral phases of these xenoliths depending on the temperatures of the host magma and cumulates and residence time after xenolith ingestion, and (**4**) post-assimilation settling-out of dense, refractory solids from magmas, leaving the resulting hybrid incongruently enriched in components contributed by wet, low-density melts of hydrous minerals.

IMPLICATIONS

Whereas quantitative modeling of magmatic evolution of UPSPS lavas, and the physical processes invoked above, falls outside current thinking and methodology and will be difficult, it would be an error to dismiss such compositional variations as inconsequential noise, or to contend that the UPSPS lavas are a unique aberration: similar compositional variations on a smaller scale linked to similar textural-mineralogical clues are observed in basalts from several sequences of the TSPC. As all long-lived arc volcanoes must be underlain by volumetrically important plutonic roots that originated during differentiation from primitive to evolved magmas, it must be assumed that other volcanic centers are associated with comparable reservoirs of gabbroic to ultramafic lithologies at depth, and that many of these will contain hydrous minerals. The TSPC is built on a deformed pile of mainly Tertiary arc volcanic and volcaniclastic rocks that is several kilometers thick, and which is presumably complimentary to a large volume of gabbroic-ultramafic cumulates at depth.

A long-standing problem in understanding magmatic evolution in the Andean SVZ is the small range in Sr isotopic compositions, even where magmas have evolved by open-system processes in which crustal assimilation is implicated by incompatible trace element enrichments. This observation is conventionally explained by the assumption of low crust-magma isotopic contrast, even though Rb-enriched crustal lithologies would evolve to $^{87}Sr/^{86}Sr$ ratios much higher than those of most SVZ basalts (0.7038-0.7040) in a geologically short interval. Are some open-system trace element signatures in plausibly contaminated continental arc basalts the products of assimilation of broadly coeval (*i.e.,* isotopically unevolved) mafic-ultramafic cumulates that contained abundant non-refractory, incompatible element-enriched hydrous minerals? The observations of Heliker (1995) demonstrate that this mechanism is not as thermally and mechanically possible.

REFERENCES CITED

Cole, J.W., Thordarson, T. & Burt, R.M. (2000) Magma origin and evolution of White Island (Whakaari) Volcano, Bay of Plenty, New Zealand. *Journal of Petrology,* **41,** 867-895.

Costa, F., Dungan, M. & Singer, B. (2002) Hornblende and phlogopite-bearing gabbroic xenoliths from Volcán San Pedro (36E S), Chilean Andes: Evidence for melt and fluid migration and reactions in subduction-related plutons. *Journal of Petrology*, **43,** 219-241.

Dungan, M.A., Wulff, A. & Thompson, R. (2001) Eruptive stratigraphy of the Tatara-San Pedro complex, 36E S, Southern Volcanic Zone, Chilean Andes: Reconstruction method and implications for magma evolution at long-lived arc volcanic centers. *Journal of Petrology* **42,** 555-626.

Heliker, C., 1995. Inclusions in Mount. St. Helens dacite erupted from 1980 through 1983. *J. Volcanol. Geotherm. Res.*, **66,** 115-135.

PETROLOGY OF THE HUALPÉN STOCK: EVIDENCES OF LATE TRIASSIC CRUSTAL EPIZONAL PLUTONISM AT THE WESTERN MARGIN OF GONDWANA (36°45' S – 73°10' W).

Christian CREIXELL(1), Friedrich LUCASSEN(2), Gerhard FRANZ(3), Paulina VÁSQUEZ(1) & Oscar FIGUEROA(1).

(1) Universidad de Concepción, Chile, Depto. Ciencias de la Tierra, casilla 160-C, Concepción, (ccreixell@yahoo.com).
(2) GeoForschungsZentrum Potsdam, Telegrafenberg, 14473 Potsdam, Germany (lucassen@gfz-potsdam.de).
(3) TU-Berlín, Petrologie-EB15, Strasse des 17 Juni 135, 10623 Berlín, Germany (gerhard.franz@tu-berlin.de).

KEY WORDS: Hualpén Stock, epizonal, Late Triassic magmatism, isotopic composition, Rb-Sr isochron.

INTRODUCTION

The Coastal Range of south – central Chile (between 32°30' and 38°00' S) is mainly built of Late Paleozoic sedimentary, metamorphic and intrusive rocks (Hervé, 1988). During the Late Triassic – Lower Jurassic, rift – type basins developed on this basement at the south western margin of Gondwana due to continental extension. The NW-SE striking basins follow the main tectonic lineaments in the Palaeozoic basement. Continental and minor marine sedimentation occured contemporaneously with volcanic activity (lavas and pyroclasts, Charrier, 1979; Franzese and Spalletti, 2001) and plutonism, both with locally bimodal composition (Parada *et al.*, 1991; Morata *et al.*, 2000).

Isolated Late Triassic intrusions occur at the westernmost edge of the Coastal Range in Central Chile. They are small granitic stocks that intrude the Western Series (Aguirre *et al.*, 1972) of the Palaeozoic Basement. The principal occurrences of Late Triassic intrusions are near the towns of Pichilemu (34°30' S, Hervé *et al.*, 1984), Constitución (35°10' S, Gana and Hervé, 1983) and Concepción (Hualpén Stock, Hervé *et al.*, 1988 and this study). This study presents new geological, geochemical and age data of the Hualpén Stock.

GEOLOGY AND PETROGRAPHY

The Hualpén Stock is located on the Hualpén Peninsula, approximately 15 km NW of the city of Concepción (ca. 36°45' S and 73°10' W; fig. 1). It intrudes into weakly metamorphic rocks of the Western Series, generating a narrow contact aureole with biotite and minor andalusite. The contacts to the wall rocks are sharp and no xenoliths are observed. Some tonalitic dykes with abundant plagioclase phenocrysts and other felsic dykes cut the basement rocks. The Hualpén Stock is a medium grained leucocratic monzogranite with quartz, perthitic ortoclase, plagioclase (An_{20}), biotite (phlg 17-23) and minor white mica, turmaline and cordierite, the latter forming intergrowths with quartz. Monazite occurs as an accessory mineral in biotite. In the

northern part of the peninsula, the stock locally shows sub-circular (5 to 30 cm diameter) miarolitic cavities with cores of turmaline + quartz and rims with alkali feldspar, suggesting a shallow emplacement of the stock.

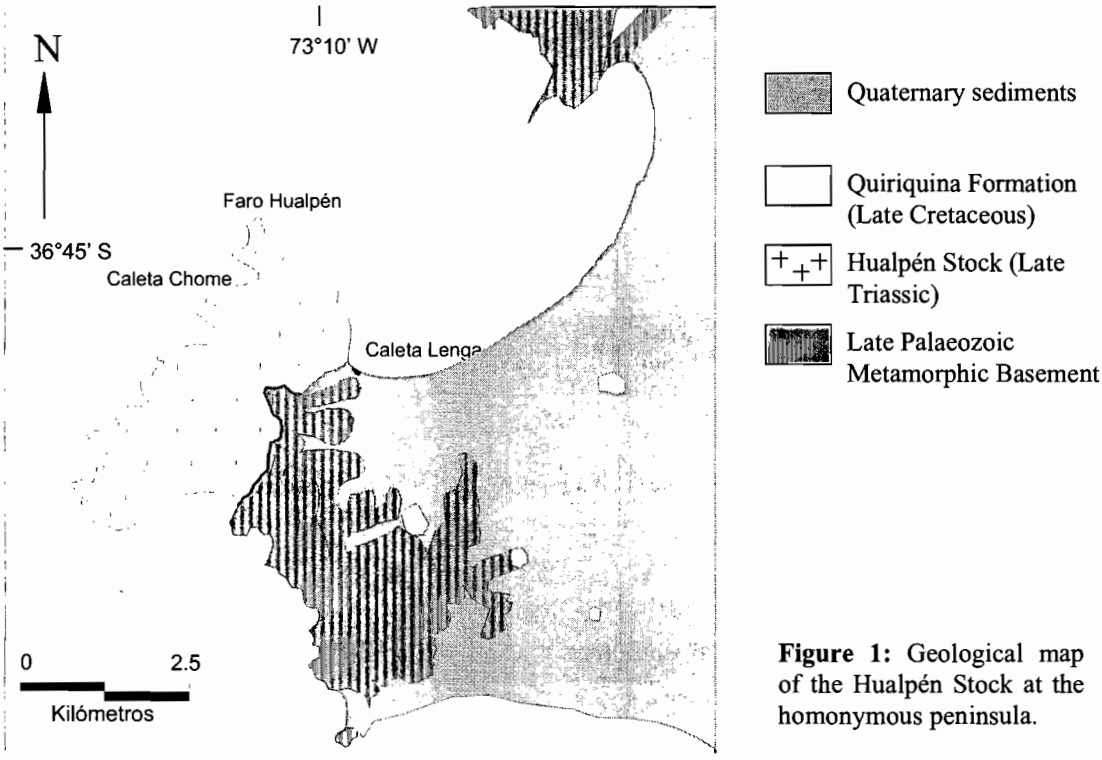

Figure 1: Geological map of the Hualpén Stock at the homonymous peninsula.

GEOCHEMISTRY, ISOTOPIC COMPOSITION AND AGE

The Hualpén Stock shows little variation in its composition with SiO_2 (ca.75 wt%), K_2O (ca. 4.5%), Na_2O (ca. 3.5%), Al_2O_3 (13.2 to 14%), CaO (0.3 to 0.69%), Fe_2O_3 (ca. 1.2%), MgO (0.16 to 0.27%), and TiO_2 (ca. 0.10%). Ca, Fe and Mg contents are low in all samples. The rocks are peraluminous (A/CNK = 1.1 – 1.26) and cordierite is a stable mineral phase in these rocks. The trace element abundance diagram, normalized to chondrite (fig. 2), shows an enrichment of incompatible elements, especially U and Th, and a relative depletion of Ba, P, Sr and Ti. The rare earth elements patterns are relatively flat (La_N/Yb_N= 3 – 3.9) and show a large negative Eu anomaly. Initial isotope ratios of $^{87}Sr/^{86}Sr$ (0.7080-0.7120), $^{143}Nd/^{144}Nd$ (0.51224-0.51226), $^{207}Pb/^{204}Pb$ (15.65), $^{206}Pb/^{204}Pb$ (18.40-18.50) and $^{208}Pb/^{204}Pb$ (38.47-38.51) show little variation. Two samples have been dated by the Rb-Sr method. The mineral whole rock isochrons yield ages of ca. 215 Ma (figure 3). This is consistent with a K-Ar age on biotite of 215 Ma from this intrusion (Hervé *et al.*, 1988).

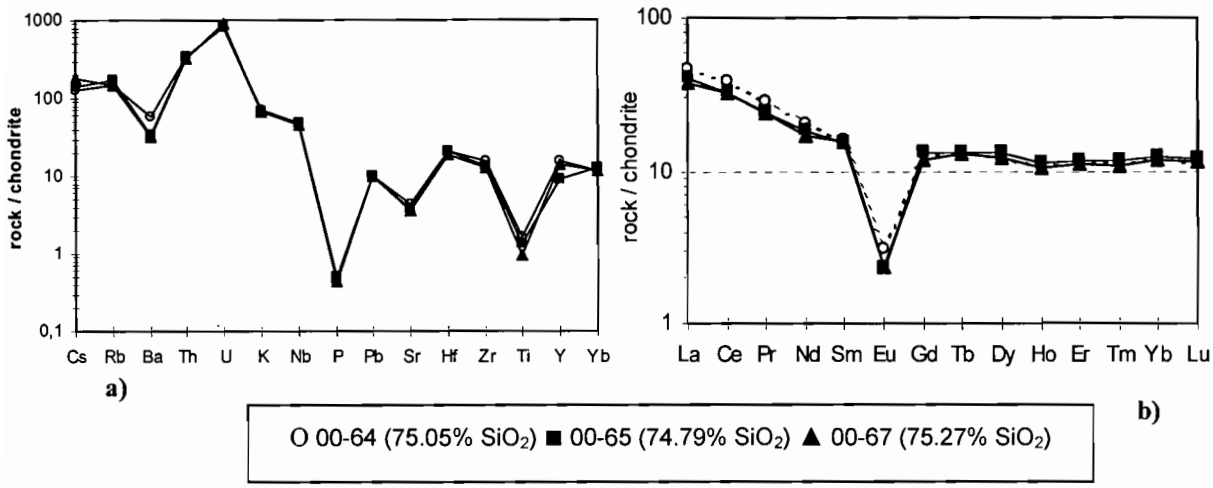

Figure 2: a) Trace element diagram for granitic Hualpén Stock, normalized to C1 chondrite (Sun and McDonough, 1989).b) Chondrite-normalized REE patterns.

DISCUSSION

The occurrence of cordierite + quartz intergrowths in presence of biotite, suggest that cordierite formed from the Fe-rich biotite by two simultaneous reactions, indicating a crystallisation pressure near 2 kbar (Barbey *et al.*, 1999) and, therefore, a shallow level of intrusion of the Hualpén Stock. The REE pattern and the low Ca and Sr contents may have been caused by prominent fractionation of plagioclase. The crustal magma is highly evolved also by fractionation of Fe-Mg minerals (low Fe, Mg and Ti) and possibly apatite (the P content is below chondritic value). Isotope ratios of Hualpén Stock indicate that his parental magma received a major contribution of rocks with isotopic signatures similar to those of the local Late Palaeozoic basement (Lucassen *et al.*, 2001). The intrusion age (ca. 215 Ma) is similar to the sedimentation age of the Santa Juana Formation, whose locus locality is situated 25 km SE of Hualpén Peninsula. This sediments has been deposited in an extensional (rift-related?) basin (Charrier, 1979; Ferraris, 1981). The spacial – temporal relation between these two units suggest an emplacement of the Hualpén Stock in an extensional tectonic setting.

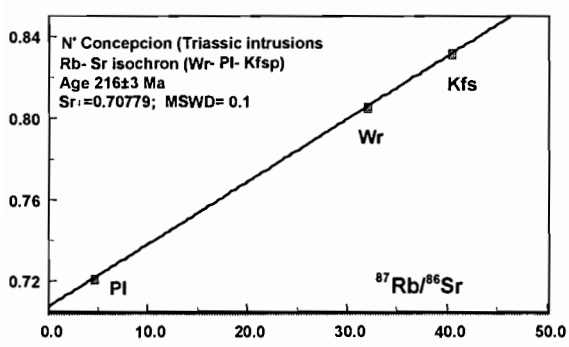

Figure 3: Rb-Sr mineral – whole rock isochron indicate a Late Triassic age of the Hualpén Stock

Acknowledgments: this study is a contribution within the SFB 267 "Deformations prozesse in den Andes" and proyecto DIUC N° 200.025.018-1 of the Dirección de Investigación of Universidad de Concepción.

REFERENCES

Aguirre, L.; Hervé, F. y Godoy, E. 1972. Distribution of metamorphic facies in Chile-An outline. *Kristalinikum* 9, 7-19.

Barbey, P.; Marignac, C.; Montel, J.; Macaudiere, J.; Gasquet, D. y Jabbori, J. 1999. Cordierite growth textures and the conditions of genesis and emplacement of crustal granitic magmas: the Velay Granite Complex (Massif Central, France). *Journal of Petrology*, 40, 1425 – 1441.

Ferraris, F., 1981: Hoja Los Angeles-Angol, *Mapas geológicos preliminares de Chile*, escala 1:250.000, Instituto de Investigaciones Geológicas. Santiago.

Franzese, J. R. and Spalletti, L.A., 2001. Late Triassic – early Jurassic continental extension in southwestern Gondwana: tectonic segmentation and pre-break-up rifting. Journal of South American Earth Sciences 14, N°3, 257 – 270.

Gana, P.; Hervé, F., 1983. Geología del basamento cristalino en la Cordillera de La Costa entre los ríos Mataquito y Maule, VII Región. *Revista Geológica de Chile*, 19-20, 37-56.

Hervé, F. 1988. Late Paleozoic subduction and acretion in Southern Chile. *Episodes* 11, N°3, 183-188.

Hervé, F.; Kawashita, K.; Munizaga, F.; Bassei, M. 1984. Rb-Sr isotopic ages from Late Palaeozoic metamorphic rocks of Central Chile. *Journal of geol. Society London*, 141, 877-884.

Hervé, F.; Munizaga, F.; Parada, M.A.; Brook, M.; Pankhurst, R.; Snelling, N.J.; Drake, R. 1988. Granitoids of the Coast Range of central Chile: geochronology and geologic setting. *Journal of South American Earth Sciences*, 1, N°2, 185-194.

Lucassen, F.; Franz, G.; Trumbull, R.; Romer, R.; Vásquez, P.; Creixell, C. 2001. Sr, Nd, Pb – isotopic composition of metasedimentary and magmatic rocks of the Late Paleozoic and Mesozoic basement in Chile and W Argentina (36°30'-40° S; 70°30'-73° W)-implications for the source regions of the pre-cenozoic basement. III Symposium on Isotopic Geology, Abstracts, Session 6, Pucón, Chile.

Morata, D.; Aguirre, L.; Oyarzún, M.; Vergara, M. 2000. Crustal contribution in the genesis of the bimodal Triassic volcanism from the Coastal Range, central Chile. *Revista Geológica de Chile*, 27, N°1, 83-98.

Parada, M. A.; Levi, B. and Nystrom, J. O. 1991. Geochemistry of the Triassic to Jurassic plutonism of central Chile (30 to 33° S); petrogenetic implications and a tectonic discussion. Andean Magmatism and its tectonic setting (Harmon, R. S., and Rapela, C. eds.). Geological Society of America Special Paper 256, 99-111.

Sun, S.S.; McDonough, W.F. 1989. Chemical and isotopic systematics of oceanic basalts: implications for mantle composition and processes. In *Magmatism of ocean basins*. Geological Society, Special Publication 42, 313-345.

INTRACONTINENTAL SEISMICITY AND NEOGENE DEFORMATION OF THE ANDEAN FOREARC IN THE REGION OF ARICA (18.5°S-19.5°S)

Claire DAVID (1), Joseph MARTINOD (1, 2), Diana COMTE (1), Gérard HÉRAIL (2), Henri HAESSLER (3),

(1) Universidad de Chile, Casilla 2777, Santiago, Chile (dcomte@dgf.uchile.cl, d.claire@dgf.uchile.cl)
(2) IRD, LMTG, 38 rue des 36 Ponts, 31400 Toulouse, France (jmartino@cec.uchile.cl, gherail@paris.ird.fr).
(3) IPGS, 5 rue Rene Descartes, 67084 Strasbourg Cedex France, (henri@sismo.u-strasbg.fr)

KEY WORDS : Forearc, Shortening, Tilting, Intraplate Seismicity, Altiplano.

INTRODUCTION

The superficial crustal seismic activity in Chile is remarkably moderate. Almost all the Chilean earthquakes are located on the subduction plane, and most of the intracontinental seismicity that results from the growth of the Cordillera occurs on the Eastern side of the Andes, in Bolivia and Argentina. Geological data, indeed, in agreement with the seismological measurements, show that the Chilean forearc suffered very moderate deformations in the Neogene [e.g. Lamb et al., 1997; García et al., 1997], in spite most of the surrection of the Altiplano probably occurred at that time [e.g. Gregory-Wodzicki, 2000]. The only region in Chile where significant crustal seismicity has been reported in the forearc is the northernmost part of the country, near Arica, where a permanent seismic network evidences an intracontinental forearc seismicity that vanishes south of 19.7°S. In this work, we describe the main characteristics of this seismicity, the associated tectonics of the area, and its possible relations with the growth of the Altiplano.

GEOLOGICAL DATA

The forearc and volcanic arc of the Andes near Arica can be divided in four main longitudinal morphological units, which are from west to east: (1) The Coastal Cordillera composed by Jurassic and Cretaceous volcanic rocks, (2) the Central Depression filled by Cenozoic sediments, (3) the Precordillera mainly composed by Miocene ignimbrites and detritic series overlying Mesozoic rocks, and (4) the Western Andean Cordillera behind which the present-day volcanic arc is developed. The Precordillera corresponds to a regular slope that joins the Central Depression whose mean elevation is 1000 m, with the 4000 m high Western Cordillera.

Active folds, thrusts and faults are scarce in the forearc of the Arica zone [e.g. Muñoz and Charrier, 1996; Lamb et al., 1997]. The Quaternary activity of the East-vergent thrust-faults and related growth anticlines that separate the Western Cordillera from the Altiplano (Lauca Basin) [Riquelme, 1998] is not well documented, although near Guallatire, the Quaternary sediment of the Lauca river is deformed. The so called "west vergent Thrust System" [Muñoz and Charrier, 1996] that emerges in the Putre-Belen area West of the Western

Cordillera may also be active, as suggested by the vertical displacement of the Upper Pliocene ignimbrites. The Precordillera is bounded to the West by the Ausipar fault, that has essentially been active during the Miocene. Anyway, the Neogene shortening accommodated by all these thrust-faults has been smaller than 10 km, which represents only a marginal part of the shortening accommodated in the Central Andes, and cannot explain much of the thickening of the continental crust below the Western Cordillera at that time [e.g. Rochat et al., 1999; Rochat, 2000; García, 2001].

SEISMOLOGICAL DATA

The data used in this work can be divided into two sets, 12000 events registered by the Arica permanent network, and 3000 events registered during temporary field works. The Arica permanent network (Fig. 1) is composed of 13 telemetric short period stations and is operating since December 1994. The two additional temporary field works (Fig. 1) deployed dense local short period seismic networks, providing reliable data that permit to better constrain the shallow seismicity recorded by the permanent network. Hypocenters were determined using a modified version of the HYPOINVERSE program [Klein, 1978]. We located about 60 intracontinental earthquakes West of the Altiplano at depths between 10 km and 60 km, and obtained 30 well-constrained focal mechanisms with good azimuth coverage.

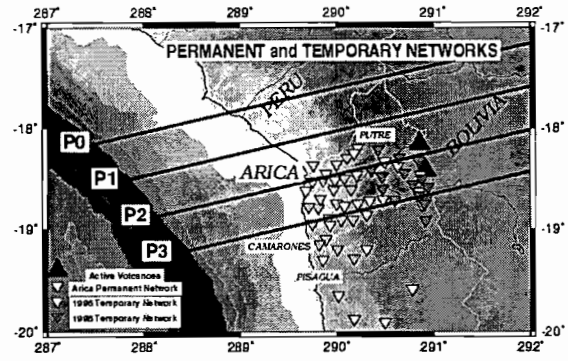

Figure 1 : Spatial distribution of the permanent and temporary networks in the Arica region.

INTRACONTINENTAL SEISMICITY OF THE ARICA REGION

The two cross sections presented in Fig. 2 show that most of the earthquakes occur on the east-dipping Wadati-Benioff zone, where a double-layered seismic zone appears at intermediate depths [Comte et al, 1999]. Many earthquakes, however, are located above the subduction zone, and evidence seismic deformations within the South America continental plate. In the Altiplano, seismicity is very shallow (0-10 km). Although some earthquakes could be correlated with the activity of volcanoes (e.g. Guallatire), most of them should result from the activation of crustal faults. In the forearc below the Precordillera and the Central Depression, crustal events are defining a seismic zone that dips about 45° toward the trench, and that is almost perpendicular to the dip of the subducting slab at that depth (David et al., 2001).

The 31 reliable focal mechanisms of intracontinental events show a wide variability of focal mechanisms between nearby events (Fig. 2), which is the usual expression of microseismic events. We performed formal inversions of the best fitting stress-tensor, following the technique developed by Rivera and Cisternas [1990],

first for the profile P2 forearc events, then for those of profile P3, and finally for all the forearc seismicity. The three calculated stress tensors show the same compressive regime, with a maximum stress axis σ_1 oriented N75E° and dipping 30° to the West. This result suggests that the intracontinental west-dipping seismic corresponds to an east-vergent reverse fault (Fig. 3).

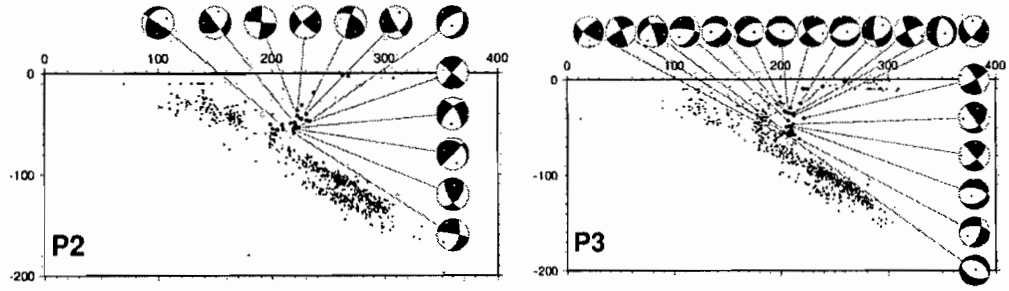

Figure 2 : Cross-sections showing the seismic events localized on profiles P2 and P3 (see Fig. 1 for the location of the cross sections). Focal mechanism solutions are projected on the northern hemisphere.

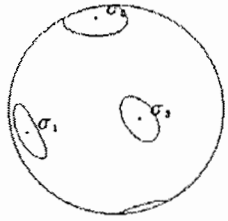

Figure3 : Stress Tensor obtained from the intraplate forearc seismic events.

DISCUSSION AND CONCLUSIONS

Forearc earthquakes are located between 2 km and 59 km depth with a large concentration of earthquakes at the largest depths, between 50 km and 59 km. The intracontinental seismicity belongs therefore both to the upper lithospheric mantle and to the crust of the South America plate, the depth of the Moho varying from 40 km under the coastal Cordillera to 60 km under the volcanic arc. The contrast between the seismic behavior of the forearc on the one hand, and that of the Western Cordillera and Altiplano on the other hand, is remarkable. The western Altiplano does not show any seismicity at depths larger than 10 km, while in the forearc earthquakes are observed from the surface up to 60 km depths. This different behavior probably results from the difference between the rheological profile of the forearc, that remains cold, rigid and brittle at large depths, and that of the Altiplano and Western Cordillera, that is characterized by a ductile low viscosity middle and lower crust. The west-dipping forearc seismic plan may correspond to the thermal and rheological boundary between the rigid forearc block and the soft crust of the magmatic arc (David, 2002).

This seismic plan emerges in the Western Cordillera (Fig. 4). Its position suggests that the superficial thrust-faults that have been reported on both sides of the Western Cordillera may be associated with this deep east-vergent reverse fault. The geometry of the superficial Western Cordillera tectonic structures does not constrain the vergence of the deep related thrust-fault. The Neogene thrust-faults of the Western Cordillera are minor accidents that do not accommodate much shortening, and they cannot have accommodated much of the surrection of the Altiplano. This surrection has essentially been accommodated west of the volcanic arc, by the weak tilting of the entire chilean forearc, and in the Altiplano by the flow of weak ductile crust coming from the

East and resulting from the underthrusting of the Brazilian Craton [Lamb et al., 1997]. Then, we propose that the deep thrust-fault that results in the shortening of the Western Cordillera in the Arica region dips to the West below the forearc. This fault may be expected to result from the westward flow of lower crust below the Altiplano. The surrection of the Altiplano resulting from this deep flow, in turn, may have been accommodated by the tilting of the forearc above this deep east-vergent thrust fault (Fig. 4).

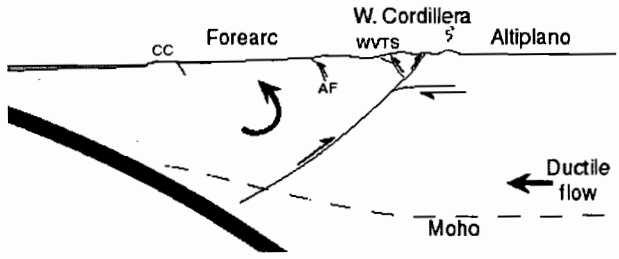

Figure 4 : Diagram illustrating the Neogene to recent kinematics of the western Margin of the Central Andes.

ACKNOWLEDGEMENTS This work was partially founded by FONDECYT 1020104.

REFERENCES

Comte, D., Dorbath L., Pardo M., Monfret T., Haessler H., L. Rivera, Michel Frogneux, B. Glass and C. Meneses, *Geophys. Res. Lett.*, 26, 1965-1968, 1999.

Comte, D., H. Haessler, L. Dorbath, C. David, B. Glass, E. Correa, C. Meneses, J. Vergara, J. Tapia, I. Balmaceda and G. Hérail., *IX Congr. Geol. Chileno, Jornadas de Geofísica*, Puerto Varas, pp 409-412, 2000.

David, C.; Comte, D.; Dorbath, L.; Haessler, H.; Frogneux, M.; Glass, B.; Balmaceda, I.; Correa, E.; Meneses, C.; Cruz, A.; Ruz, L., *European Geophysical Society, XXVI General Assembly*, Nice, France, 2001.

David, C., Tesis de Magíster en Ciencias, Mención Geofísica, Universidad de Chile, 46 p., 2002.

García, M., Hérail G., and Charrier R., *Actas VIII congreso geológico chileno*, 60-64, 1997.

García, M., PhD thesis, Université de Grenoble, 2001.

Gregory-Wodzicki, K., *Geol. Soc. Am. Bull.*, 112, 1091-1105, 2000.

Haessler, H., Comte, D., L. Dorbath, C. David, B. Glass, E. Correa, C. Meneses, I. Balmaceda, A. Tapia, J. Vergara and G. Herail. *American Geophysical Union Fall Meeting*, San Francisco, Ca.-USA., EOS, 2000.;

Klein F., Hypocentral location program HYPOINVERSE, *U. S. Geol. Survey Open File Rep.*, 78-694, 1978.

Lamb, S., Hoke L., Kennan L. and Dewey J., *Geol. Soc. Spec. Pub.* , 121, 237-264, 1997.

Muñoz, N., and Charrier R., *J. South Am. Earth Sci.*, 9, 171-181, 1996.

Riquelme, R., Tesis de Magíster en Ciencias, Mención Geología, Universidad de Chile, 124 p., 1998.

Rivera, L., and Cisternas A., *Bull. Seism. Soc. Am.*, 80, 600-614, 1990.

Rochat, P., Hérail G., Baby P., and Mascle G., *C. R. Acad. Sci.*, 328, 189-195, 1999

Rochat, P., PhD thesis, Université de Grenoble, 2000.

QUATERNARY MINOR VOLCANIC CENTRES IN SOUTHERN PERU: VOLCANOLOGY, PETROLOGY, AND GEOCHEMISTRY

Adélie DELACOUR(1), Perrine PAQUEREAU(2), Marie-Christine GERBE(1), Jean-Claude THOURET(2), and Gerhard WÖRNER(3)

(1) Département de Géologie-Pétrologie-Géochimie, Université Jean Monnet et UMR CNRS 6524 Magmas et Volcans, 23 rue du Dr. Paul Michelon, 42 023 Saint Etienne cedex, France
(2) Laboratoire Magmas et Volcans, Université Blaise Pascal et CNRS, OPGC, 5 rue Kessler, 63038 Clermont-Ferrand cedex, France
(3) Göttinger Zentrum Geowissenschaften, CZG, Abt. Geochemie, Universitat Göttingen, Germany

KEY WORDS: Peru, monogenic volcanoes, basalts, contamination, graben.

INTRODUCTION

Several fields of small monogenetic scoria cones and associated lava flows are found throughout the Central Andean Volcanic Zone (CVZ). Some are located in southern Peru on the western Cordillera west of the Colca valley. The Andahua valley located 30 km NE of Nevado Coropuna and currently known as the "Valley of the volcanoes" is certainly the most spectacular (Venturelli, 1978). This field extends north to south over a distance of about 40 km from Orcopampa to Ayo, the youngest centres being concentrated near Andahua. Another field is found near Huambo, 20 km south of Andahua, on the left side of the Rio Colca valley. Their morphologies and a few ^{14}C datations point to of quaternary ages, from late Pleistocene to historic ages. These volcanic fields are located close to the huge quaternary stratovolcanoes (Nevados Coropuna and Sabancaya), and are related to N160 rift structures oblique to the NW-SE-trending Western Cordillera. They mainly consist of basaltic andesite to andesite lavas.

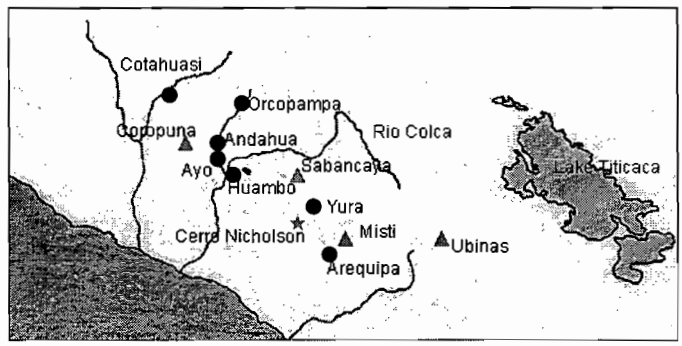

Figure 1: Location map of area of study in Southern Peru.

This study presents volcanological, mineralogical and geochemical data for a set of samples collected from various volcanic cones and lava flows of Pleistocene and Holocene ages. We test the postulate that they represent magmas rather preserved from interactions with crustal materials and consequently that they may reflect more accurately the petrological characters of the source magmas.

VOLCANIC AND STRUCTURAL SETTINGS

The CVZ lies 220-250 km from the Peru-Chile Trench and about 100-130 km above the Benioff zone (Barazangi and Isacks, 1976). The Nazca plate moves towards N80° (Sébrier and Soler, 1991) and the subduction plate is dipping 25-30° beneath the thick continental lithosphere of South America. The minor

centres of Andahua – Orcopampa and Huambo are located at the northern edge of the CVZ, where the dip of the Benioff zone is decreasing to 5-15°.

In the Western Cordillera, tensional faulting has prevailed since Cenozoic time and has been associated with an intense brittle tectonic and voluminous calc-alkaline volcanism. On a regional scale, the current tectonic regime is controlled by a N-S stretching related to the collapse of the Andean Cordillera and N80°-trending compression which are thought to be weak since the late Pleistocene (Sébrier and Soler, 1991, Mering and al., 1996). Three groups of active or recently active faults are identified within the studied area on the basis of the analysis of air photographs and satellite scenes (fig. 2). Firstly, the inactive N150-160-trending faults, characterized by dip-slip motions with small sinistral strike-slip component, limit the north and the south zones of the Rio Andahua valley, near Orcopampa and Ayo respectively. They form the overall shape of the rift structures. Secondly, the normal N120-135-trending fractures, characterized by a sinistral strike-slip component best recognized near Andahua, offset the first group of N160 faults. Thirdly, the Huambo area and the south side of the Rio Colca Valley show inactive N130-striking inverse faults, which have been re-activated by the recent extensional regime, and N70-80-striking normal faults, whose southwards dip-slip motion offsets late Pleistocene lava flows.

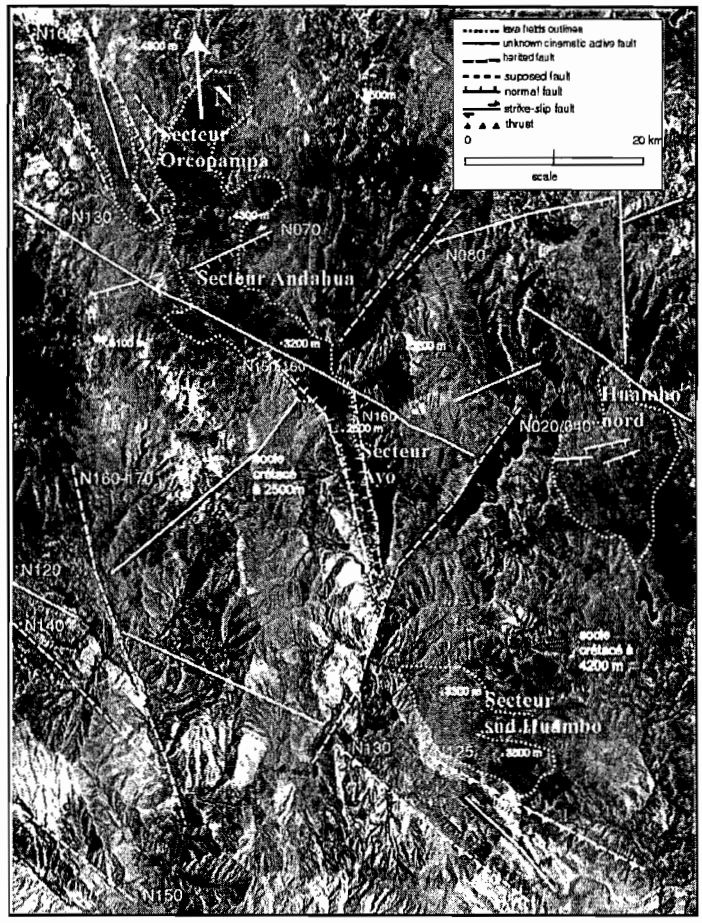

Figure 2: Structural map of Andahua-Orcopampa and Huambo areas.

Within the volcanic fields, four main phases of growth may be distinguished on the basis of few ^{14}C datations and the systematic analysis of the stratigraphic relationships of the cinder cones and lava flows (direct field observations, interpretation of aerial and satellite photos and morphometry): late Pleistocene age, early to mid-Holocene age (the ash fall of Cerro Tichso cone is dated at 4060 ± 50 yr B.P., near by the town of Andahua), upper Holocene age (2650 ± 50 B.P. for the Cerro Keyocc near Huambo, and 2860 ± 50 B.P. for a exposed ash fall layer 10 km north of Orcopampa), and historical age (the ash fall of Chilcayoc Grande is dated at 360 ± 50 yr B.P.).

PETROLOGY AND MINERALOGY

A total of 80 samples were collected in the Andahua-Orcopampa and Huambo volcanic fields. Two samples of the small isolated Cerro Nicholson cinder cone, located about 40 kilometres west of Arequipa, were added to the

sampling. The lavas consist mainly of basaltic andesites (about 20%), and andesites (about 78%) with few dacites (< 2%).

Basalts and basaltic andesites

The most basic rocks are found in Huambo (52% SiO_2, 6-7 % MgO) and Cerro Nicholsson and are quite scarce. Two groups of basaltic andesite lavas can be distinguished.

The first group consists of lavas, which are similar to basalt in composition and mineralogy. The phenocryst assemblage is normally zoned plagioclase (An_{63-72}), olivine (Fo_{80-86}) and clinopyroxene (Wo_{31-39} En_{32-47} Fe_{3-14}). Olivines are rich in Ni, Cr, and contain small crystals of chrome spinel, suggesting cristallization from a relatively primitive magma. The groundmass consists of laths of plagioclase (An_{53-67}) and Fe-Ti oxides (titano-magnetite). The second group is similar to andesite in composition. These porphyric lavas show phenocrysts of normally zoned plagioclase (An_{53-71}), olivine (Fo_{74-83}), clinopyroxene (Wo_{31-43} En_{37-51} Fe_{4-15}) and Fe-Ti oxides. The groundmass consists of laths of plagioclase (An_{44-64}) and Fe-Ti oxides (titano-magnetite).

Andesites

The andesites are porphyric in the lavas of Andahua and Huambo and microporphyric in the lavas of Orcopampa. The paragenesis consists of plagioclase, rare olivine, pyroxene ± amphibole and Fe-Ti oxides in Andahua and Huambo, whereas the mineral phases in Orcopampa are represented only by plagioclase, clinopyroxene and Fe-Ti oxides. The plagioclase crystals (An_{34-60}) show normal compositional zoning. However reverse compositional zoning are also found ($An_{60-76-56}$), suggesting variations in the conditions of plagioclase crystallization. This disequilibrium is further indicated by the fact that the olivines (Fo_{71-79}) show coronae of clinopyroxene or orthopyroxene. The clinopyroxene crystals are Wo_{31-43} En_{39-48} Fe_{5-15} and the orthopyroxenes are En_{67-75} Fe_{22-30}. The amphibole (magnesio-hastingsite) crystals are sometimes present, often destabilized, and are rimmed by Fe-Ti oxides. The Fe-Ti oxides are represented by titano-magnetites and ilmenites. The groundmass contains mainly plagioclase microlites and microcrystals of the other phases within glass. The glass is dacitic (66 % SiO_2) in composition.

GEOCHEMICAL DATA AND MAGMATIC PROCESSES

The lavas of the Andahua-Orcopampa and the Huambo fields show a more basic SiO_2 range (51,8-64,6 wt%SiO_2), in contrast to the lavas of the Nevado Sabancaya-Ampato stratovolcano massif (57-67 wt%SiO_2) which is located about 50 km of Andahua on the Altiplano (fig. 3A). The geochemical data have suggested the role of two magmatic processes for the evolution of the Andahua-Orcopampa and Huambo lava series.

Firstly, the fractional crystallization process is dominant and is indicated by the evolution of major elements. Most of the element contents decrease with increasing SiO_2 content and may be related to the fractionation of plagioclase, olivine, pyroxene, amphibole and Fe-Ti oxides. Several stages of fractionation are evidenced by the behaviour of some elements such as Na_2O and Al_2O_3. They show a positive correlation with SiO_2 content during a first step (< 58% SiO_2), which may be consistent with a predominant role of mafic minerals (olivine, pyroxene), and a slight decrease for higher SiO_2 content (>58% SiO_2) suggesting the main role of plagioclase during the end of the fractionation process. The influence of the fractional crystallization process is reinforced by a similar evolution of trace elements. The Ni, Cr, Sr, and V contents decreasing with increasing SiO_2 content are

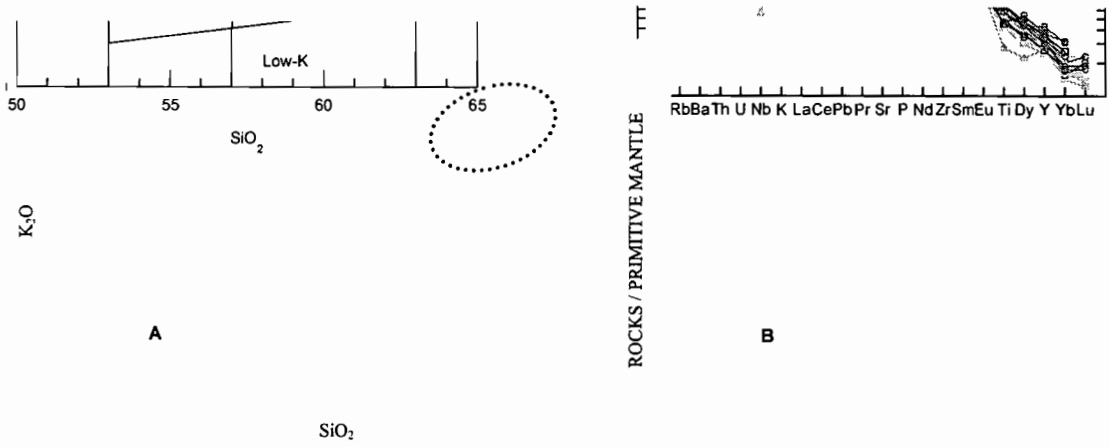

Figure 3: A: K_2O vs SiO_2 (Gill, 1981); B: REE patterns normalized to chondrites (Sun and Mc Donough, 1989). Square: Huambo; circle: Orcopampa; triangle: Andahua; cross: Cerro Nicholsson. The big circle represents the field of Nevado Sabancaya compositions

probably related to crystal fractionation, as well as the parallel patterns of REE normalized to chondrites. The role of crustal contamination in magma evolution is inferred by the scattered trends of elements such as Ba, Zr, Nb and by the relative enrichment of LILE (as Rb and Th). Further the O, Sr, Nd isotopic data ($^{87}Sr/^{86}Sr$= 0,7063-0,7067, $^{143}Nd/^{144}Nd$= 0,5123-0,5124, and $\delta^{18}O$=7,07-8,45 ‰ SMOW) exclude a direct mantle source origin and suggest also a crustal component. Secondly, concerning the source of these magmas, the REE patterns normalized to primitive mantle show positive anomalies of Sr, Ba, Th and negative anomalies in HFSE (Rb, Nb), which are typical features of continental arc magmas (fig. 3B). The "peaks" of Sr, Ba and Th reflect the participation of enriched fluids in subduction zone and (or) a crustal component. The relative depletion of HREE in Spider diagrams suggests a residual phase in source material (as amphibole or garnet), which concentrates the HREE.

CONCLUSIONS

The Andahua-Orcopampa and Huambo lavas were formed by fractional crystallization from a primitive magma, which is possibly enriched by fluids from dehydration of the subducted lithosphere. The crustal contamination also plays a role in the magma evolution. Variable rates of contamination affect the lavas whether they are stored within the crust or rapidly erupted from their deep reservoir. The less evolved lavas are found in the Huambo area and may be related to deeper faults, which have promoted the basic magma ascent. In that respect, the Huambo "basalts" may represent the best witness of source magmas within this part of the Central Volcanic Zone.

REFERENCES

BARAZANGI M. and ISACKS B. (1976). Spatial distributions of earthquakes of the Nazca plate beneath South America, v 4, pp. 686-692

MERING C. and *al.* (1996). New data on the geodynamics of southern Peru from computerized analysis of SPOT and SAR ERS-1 images, Tectonophysics, n°259, pp.153-169

SEBRIER M. and SOLER P. (1991). Tectonics and magmatism in the Peruvian Andes from late Oligocene time to Present, Geological Society of America, Special Paper 265

VENTURELLI and *al.* (1978). Trace element distribution in the Cainozoic lavas of Nevado Coropuna and Andagua Valley, Central Andes of Southern Peru, Bulletin Volcanologique, vol 41-3

VENEZUELAN ANDEAN TECTONICS REVEALED BY SAR JERS IMAGERY

Damien DHONT (1), Guillaume BACKE (1), Yves HERVOUËT (1), Leonardo GONZALES M. (1, 2), José T. CASTRILLO (2)

(1)UMR 5831 Imagerie Géophysique, Géologie Structurale et Télédétection, IPRA CURS, BP 1155, 64013 PAU, France, E-Mail : damien.dhont@univ-pau.fr
(2)Escuela de Ingeniera Geologica, Universidad de los Andes, Mérida, Venezuela

KEYWORDS : radar imagery, neotectonics, fault mechanism, pull-apart, extrusion, gravity collapse, Andes

Observations on satellite imagery with 3D (Dimensional) GIS (Geographic Information System) permit to implement the mapping of the large neotectonic structures of the Venezuelan Andes. Radar images are particularly useful for the detection of fault scarps, which can be related either to active faults or to lithologic contrasts because they express sensitive changes in the morphology (Chorowicz et al., 1995; Dhont et al., 2002). A mosaic of Synthetic Aperture Radar (SAR) scenes of the Japanese Earth Resources Satellite-1 (JERS-1) was used for geomorphic analysis at regional scale.

The NE-SW Venezuelan or Mérida Andes (Figure 1) extend from the Colombian border in the SW to Barquisimeto in the NE, and constitute a 100 km wide belt with peaks reaching up to 5000 m. This chain began to uplift in the Miocene, probably as a consequence of the collision of the Panama arc against the South American plate (Audemard, 1993). Uplift of the Mérida Andes accelerated during the Plio-Quaternary due to transpression related to oblique convergence between two independent blocks belonging to the South America plate, the Maracaibo block to the north and the Guyana shield to the south.

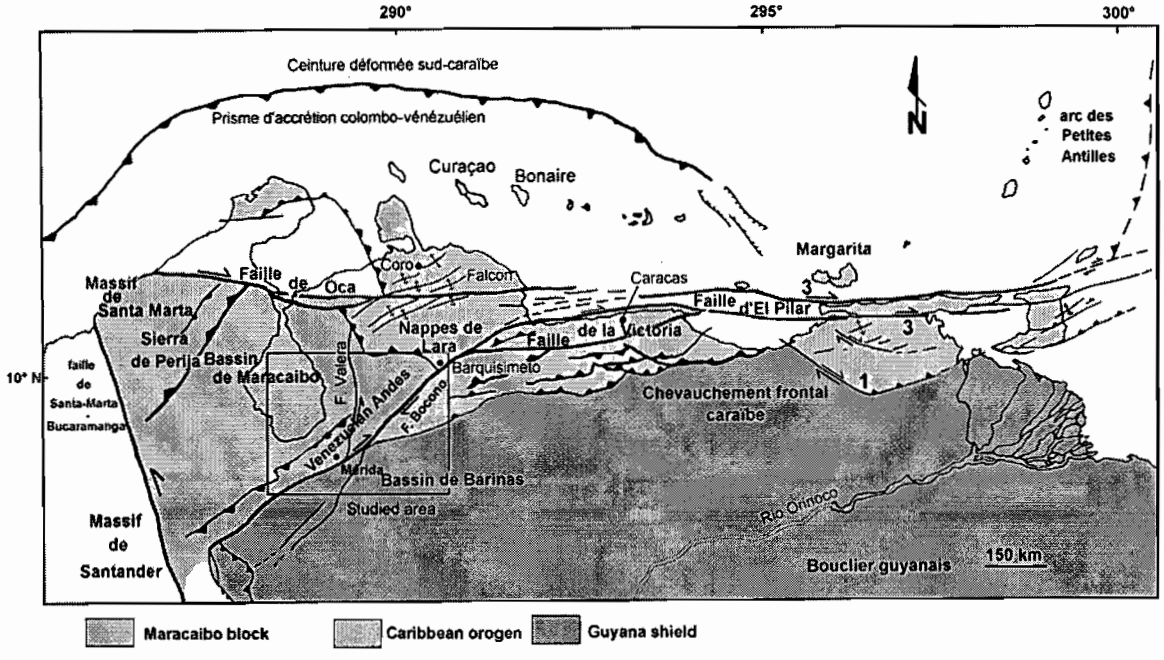

Figure 1. Structural map of the northwestern part of South America and location of the studied area.

Important strike-slip faults are associated to these oblique movements. The right-lateral strike-slip Bocono fault divides the Venezuelan Andean belt in two parts along its NE-trending direction. The N-S left-lateral strike-slip Valera fault is another main accident, which branches to the Bocono fault in a triple-junction geometry. These two faults individualise the Trujillo triangular block (Hervouët et al., 2001), extruded to the NNE as a consequence of the relative convergence between the Maracaibo block and the Guyana shield.

From fault plane solutions of large earthquakes affecting the area (Figure 2), we have plotted the horizontal projections of the slip vectors in these earthquakes, in which the direction of motion is shown of the south side relative to the north (Figure 3). On the southern and northern flank of the Mérida Andes, slip vectors are perpendicular to the belt. Focal mechanisms indicate that gravity collapse occurs within the belt. Slip vectors along the Bocono and Valera faults clearly indicate that they are respectively purely dextral and sinistral. The N-trending El Empedrado fault does not seem active. Within the Trujillo block, slip vectors are directed north to northeast, consistent with NNE lateral escape of the block.

Figure 2. Lower hemisphere fault plane solutions of earthquakes (Harvard cmt, Choy et al., 2000, Audemard and Audemard, 2002) plotted on a Digital elevation Model (pixel size = 5000 m) of the northernmost part of the Andes.

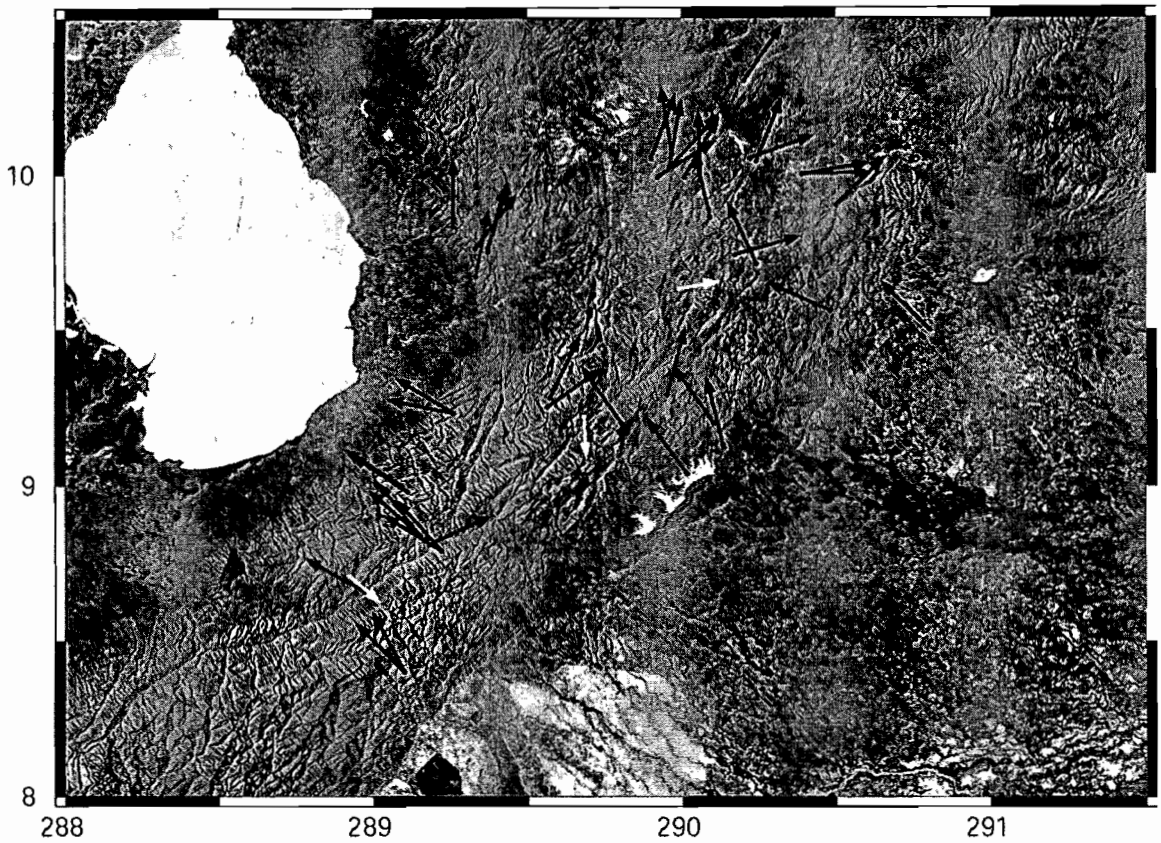

Figure 3. Mosaic of SAR JERS-1 image (negative print, looking west) of the sudied area, and horizontal projections of slip vectors from the earthquakes of Figure 2. White arrows indicate gravity collapse of blocks.

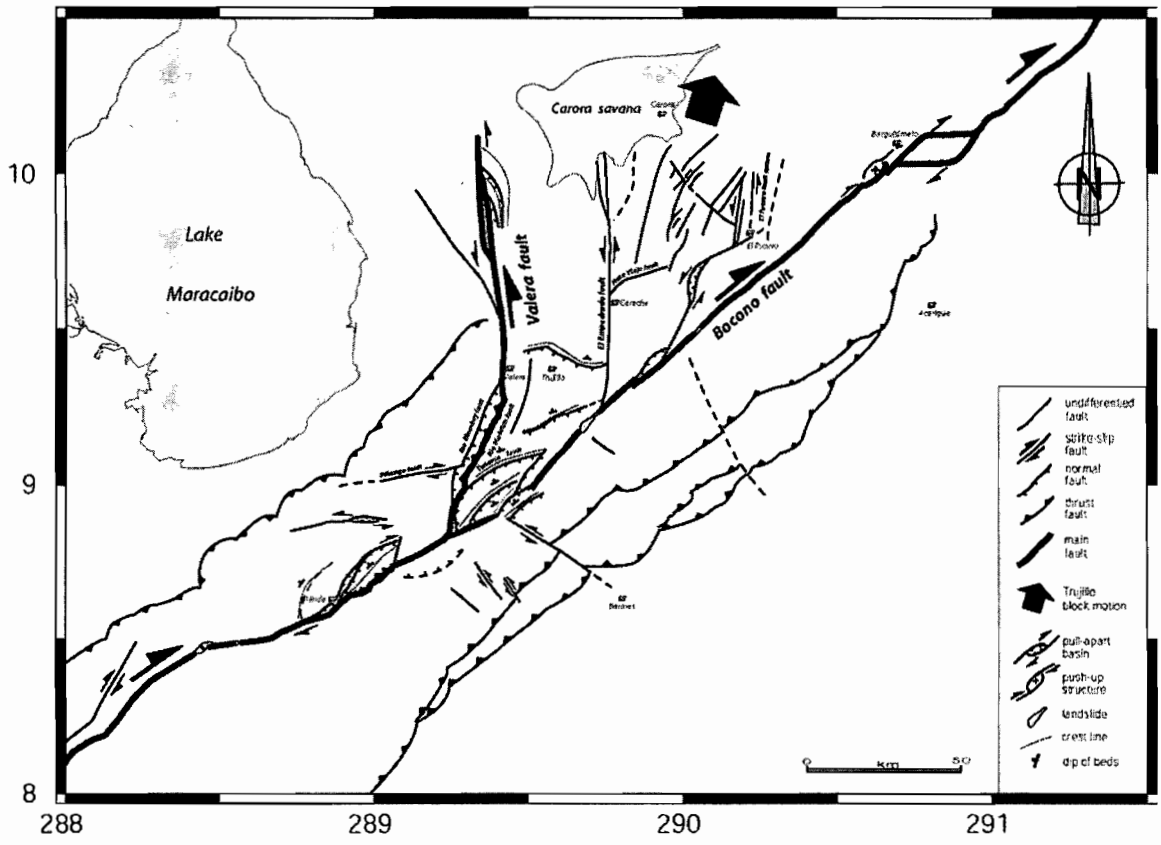

Figure 4. Structural interpretation of the mosaic of radar images of Figure 3.

Radar imagery permit to map precisely the Bocono and Valera faults (Figure 4). The Bocono fault is a continuous but broken line bordered by pull-apart and push-up structures. Pull-apart basins constitute troughs where gravity collapse can occur. We have been able to map collapse structures with dimensions reaching several tens of kilometres along the Bocono and Valera faults. These structures initiate by means of listric faults having a curved trace in plan view. The Tuñame and Rio Momboy faults are interpreted as normal faults bounding such collapse structures. Others can be observed north of Mérida along the Rio Mucujun and at the northern end of the Valera fault. Radar imagery shows that Trujillo block is intensively deformed within the Barbacoas area, consistent with active seismicity of this area.

REFERENCES

Audemard, F.A., 1993. Néotectonique, sismotectonique et aléa sismique du nord-ouest du Venezuela (Système de failles d'Oca-Ancon). Ph.D Thesis, Université Montpellier II, France, 369 pp + appendix.

Audemard, F.E., and Audemard, F.A., 2002. Structure of the Mérida Andes, Venezuela: relations with the South America-Caribbean geodynamic interaction. Tectonophysics, in press.

Chorowicz, J., Koffi, B., Chalah, C., Chotin, P., Collet, B., Poli, J.-T., Rudant, J.-P., Sykioti, O. and Vargas, G., 1995, Possibilités et limites de l'interprétation géologique des images SAR ERS-1. Bulletin de la Société Française de Photogrammétrie et Télédétection, 138, 82-95.

Choy, J., Palme, C. and Morandi, M., 2000. Observaciones acerca del estado de esfuerzos tectonicos en el norte de los Andes Merideños.

Dhont, D., Chorowicz, J, and Cadet, J.-P., 2002. Detection of compression structures from SAR ERS imagery : example of the Central Japan seismic area. Int. J. Remote Sensing, in press.

Hervouët, Y., Castrillo, J.T., and Odreman, O., 2001. - Interaction entre un chevauchement imbriqué et une zone transcurrente: le flanc nord-ouest des Andes vénézuéliennes. *Bull. Soc. Géol. France,* t 172, n° 2, 159 - 175.

AKNOWLEDGEMENTS

This study has been made possible by means of the agreement ULA-UPPA, ULA-PDVSA, the ECOSNORD project (V00U02) and the SPOT ISIS program

PALEOZOIC EVOLUTION OF THE CENTRAL ANDES: A NON-ACCRETIONARY MODEL FOR GONDWANA'S ACTIVE MARGIN

Enrique DÍAZ-MARTÍNEZ

Centro de Astrobiología (CSIC-INTA), Carretera a Ajalvir km 4, 28850 Torrejón de Ardoz, Madrid, Spain (diazme@inta.es)

KEY WORDS: Paleozoic, Central Andes, Gondwana, active margin.

INTRODUCTION

The Paleozoic geologic evolution of South America's western margin is frequently considered to include the complex accretion of exotic terranes. This concept has been widely promoted after the wealth of information recently provided to prove the collision of the Precordillera terrane with southwestern Gondwana (Astini et al., 1995; Rapela et al., 1998, and references therein). However, a review of other evidence present in the Central Andean region indicates that this may not be the norm. In fact, a large part of the Central Andes, in particular that between 5°S and 27°S, allows for an alternative overall interpretation. The area here considered covers central and southern Peru, most of Bolivia, northern Chile, and northwestern Argentina, and therefore excludes the Amotapes of northwestern Peru and southern Ecuador, as well as the Precordillera of western Argentina. This abstract attempts to synthesize the paleogeographic and geodynamic evolution of this part of the Central Andes during the Paleozoic, as recently proposed by Díaz-Martínez et al. (2000) and Jaillard et al. (2000). Apart from submitting this conceptual model to the scientific community working on Andean geodynamics for discussion and constructive criticism, the main objective of this abstract is to draw attention to one of the its main implications: that a large part of the Central Andean margin of Gondwana never underwent continental accretion of allochthonous terranes during the Phanerozoic, as opposed to what may be inferred from immediately adjacent regions north of 5°S (Colombia, Ecuador and NW Peru) and south of 27°S (Chile and Argentina). Those interested in the details of the model are encouraged to read the original and references therein.

PALEOZOIC GEODYNAMIC EVOLUTION OF THE CENTRAL ANDES

A review of the information published during the last two decades allowed us to establish a conceptual model with a coherent sequence of events for the Paleozoic of the Central Andes (Figure 1; Díaz-Martínez et al., 2000; Jaillard et al., 2000). The model proposed is schematic and considers the lack of evidence for the accretion of allochthonous terranes during the Phanerozoic. In brief, Paleozoic rocks of the Central Andes record the breakup of the Late Proterozoic Protopangea (Rodinia) in the latest Proterozoic-Early Cambrian to form a passive margin along western Gondwana, and its later evolution as an active margin during most of the Paleozoic and until present times (Sempere, 1995). The continuous superposition of magmatic, tectonic and sedimentary events has led to complex lateral variations, both transverse to the orogen and along strike.

The crustal basement in most of the Central Andes formed part of the Grenville orogen, as a result of the collision between Laurentia and Amazonia in the Middle Proterozoic (Wasteneys et al., 1995; Sadowsky and Bettencourt, 1996). The reconstruction of the remains of the Grenville orogen in South America (Sadowski and Bettencourt, 1996) indicates that the Central Andes corresponds to an area intermediate between the magmatic arc (represented by the Sunsas igneous province, in eastern Bolivia and western Brazil) and the thrust belt (SE Canada) of the Grenville orogen (Figures 1a and 1b). This interpretation explains the similar trends identified between the Proterozoic outcrops along the Andes, and those of the Brazilian shield (Litherland et al., 1985, 1989). The geochronology of basement rocks indicates that Paleoproterozoic ages represent the pre-Grenville Laurentian-Amazonian protolith, whereas Mesoproterozoic ages represent the main collisional events of the Grenville orogen (Wasteneys et al., 1995; Sadowski and Bettencourt, 1996). Rifting during break-up of Protopangea (Rodinia) in the Neoproterozoic-Early Cambrian led to separation of Laurentia from Amazonia (Figure 1c), leaving behind the parautochthonous Arequipa-Antofalla craton attached to Amazonia (Central Brazil shield). The boundary zone between the two crustal blocks, located beneath the Altiplano and Eastern Cordillera, constitutes a paleosuture inherited from the Mesoproterozoic evolution of the Grenville orogen (Figure 1b). This crustal weakness zone remained active during the Paleozoic, and ever since, with variable behavior depending on the regional state of stresses (Ramos, 1988; Forsythe et al., 1993).

After the breakup of Rodinia, and opening of the Southern Iapetus Ocean between eastern Laurentia and western Gondwana passive margins, subduction began in the Late Cambrian with the development of an active continental margin lasting most of the Phanerozoic until present times (Figures 1d, 1e, and 1f). Marginal magmatic arcs developed as a result of eastward subduction, with different rates of activity and sense of migration of the arc depending on regional plate stresses and inhomogeneities. Basin development also changed according to these plate interactions. An extensional regime during the early Paleozoic (Late Cambrian-Middle Ordovician) resulted in the development of a backarc basin over a strongly subsiding thinned crust (Figure 1d), with partial rifting and synsedimentary basic volcanism reaching from SE Peru through Bolivia and into N Argentina, and limiting the Arequipa-Antofalla craton to the west (Ramos et al., 1986) and the Amazon craton to the east (Teixeira et al., 1989). The progressive increase of rigidity of the crust, in conjunction with a shift to a compressional regime, resulted in the development of a large retroarc foreland basin during the mid Paleozoic (Middle Ordovician-Early Carboniferous), with progressive onlap of units over the distal cratonic margin of the basin, and episodic development of transpressional uplifts (Figure 1e). The San Nicolás batholith of Peru is interpreted as the roots of the magmatic arc resulting from east-ward subduction of oceanic crust along the active margin of Gondwana during the Ordovician-Devonian (Mukasa and Henry, 1990). An extensional regime during the late Paleozoic (Late Carboniferous-Early Triassic) resulted in the development of forearc, intra-arc and backarc basins, with local transpression and transtension (Figure 1f). A change from an overall accretionary to an overall erosive plate margin took place during the Late Paleozoic, and resulted in the progressive tectonic erosion of the margin during the Mesozoic and Cenozoic. As deduced from the aforementioned sequence of events, this part of western Gondwana (i.e., the Central Andes between 5° and 27°S) does not show any evidence for allochthonous terrane accretion during the Phanerozoic, and only the Arequipa-Antofalla craton may be considered as para-authochthonous.

ACKNOWLEDGMENTS

Research funded by the Spanish Government, and supported by IRD, SERGEOMIN, and YPFB. G. Laubacher helped with the compilation of data. E. Jaillard and T. Sempere crytically read earlier versions of the manuscript.

REFERENCES CITED

Astini, R.A., Benedetto, J.L., Vaccari, N.E., 1995. The early Paleozoic evolution of the Argentina Precordillera as a Laurentian rifted, drifted, and collided terrane: a geodynamic model. GSA Bulletin, v. 107, p. 253-273.

Díaz-Martínez, E., Sempere, T., Isaacson, P.E., Grader, G., 2000. Paleozoic of western Gondwana active margin (Bolivian Andes). Pre-Congress Fieldtrip Bft 27, 31st International Geological Congress, Brazil, 31 pp.

Forsythe, R.D., Davidson, J., Mpodozis, C., Jesinkey, C., 1993. Lower Paleozoic relative motion of the Arequipa block and Gondwana: paleomagnetic evidence from Sierra de Almeida of northern Chile: Tectonics, v. 12, p. 219-236.

Jaillard, E., Hérail, G., Monfret, T., Díaz-Martínez, E., Baby, P., Lavenu, A., Dumont, J.F., 2000. Tectonic evolution of the Andes of Ecuador, Peru, Bolivia and northernmost Chile. In: Cordani, U.G., Milani, E.J., Thomaz Filho, A., Campos, D.A. (eds.), "Tectonic Evolution of South America", Rio de Janeiro, p. 481-559.

Litherland, M., Klinck, B.A., O'Connor, E.A., and Pitfield, P.E.J., 1985. Andean-trending mobile belts in the Brazilian shield. Nature, v. 314, p. 345-348.

Litherland, M. and 10 more authors, 1989. The Proterozoic of Eastern Bolivia and its relationship with the Andean Mobile Belt. Precambrian Research, v. 43, p. 157-174.

Mukasa, S.B., Henry, D.J., 1990. The San Nicolás batholith of coastal Peru: early Palaeozoic continental arc or continental rift magmatism? Journal of the Geological Society of London, v. 147, p. 27-39.

Ramos, V.A., 1988. Late Proterozoic-Early Paleozoic of South America - a collisional history. Episodes, v. 11, no. 3, p. 168-174.

Ramos, V.A., Jordan, T.E., Allmendinger, R.W., Mpodozis, C., Kay, S.M., Cortés, J.M., Palma, M., 1986. Paleozoic terranes of the central Argentine-Chilean Andes. Tectonics, v. 5, n. 6, p. 855-880.

Rapela, C.W., Pankhurst, R.J., Casquet, C., Baldo, E., Saavedra, J., Galindo, C., 1998. Early evolution of the Proto-Andean margin of Gondwana. Geology, v. 26, p. 707-710.

Sadowsky, G.R., Bettencourt, J.S., 1996. Mesoproterozoic tectonic correlations between eastern Laurentia and the western border of the Amazonan Craton. Precambrian Research, v. 76, p. 213-227.

Sempere, T., 1995. Phanerozoic evolution of Bolivia and adjacent regions. AAPG Memoir 62, p. 207-230.

Teixeira, W., Gaeta Tassinari, C.C., Cordani, U.G., Kawashita, K., 1989. A review of the geochronology of the Amazonian craton: tectonic implications. Precambrian Research, v. 42, p. 213-227.

Wasteneys, H.A., Clark, A.H., Farrar, E., Langridge, R.J., 1995. Grenvillian granulite-facies metamorphism in the Arequipa Massif, Peru: a Laurentia-Gondwana link. Earth and Planetary Science Letters, v. 132, p. 63-73.

Figure 1: Simplified conceptual model for the pre-Andean geodynamic evolution of the Central Andes (5-27°S) as proposed in the text. Overall regional stress field: 1, transcurrent; 2, tensional; 3, compressional.

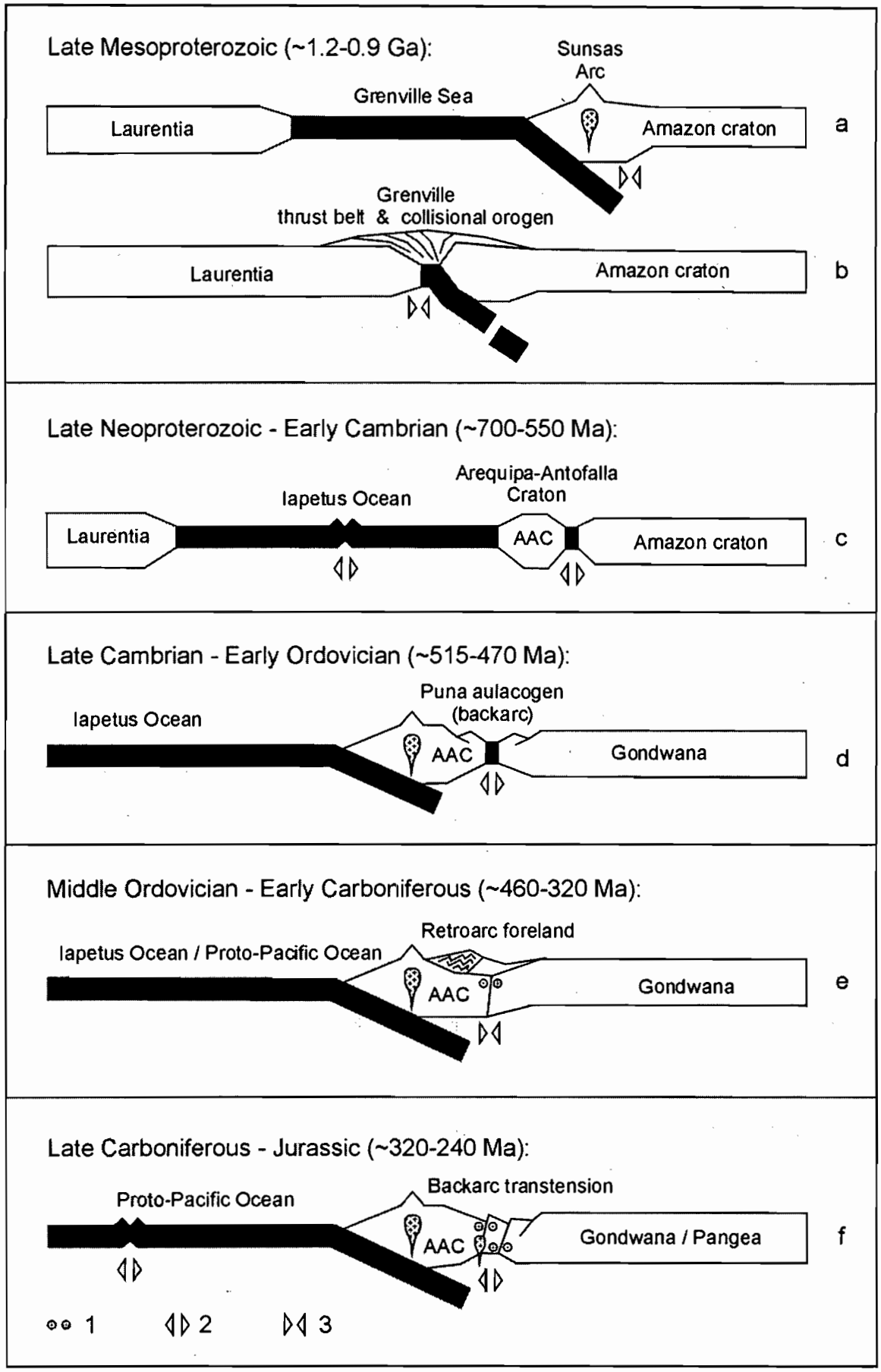

SEISMOTECTONICS ON THE CENTRAL REGION OF THE COLOMBIAN EASTERN CORDILLERA

Cristina DIMATE (1),(2), Alfredo TABOADA (3), Luis RIVERA (2), Armando CISTERNAS (2), Domenico GIARDINI (4)

(1) INGEOMINAS, Diag. 53 No 34-53, Bogotá, Colombia. (cristina@eost.u-strasbg.fr)
(2) Inst. de Physique du Globe, ULP, 5 rue René Descartes, F67084 Strasbourg Cedex, France. (luis@eost.u-strasbg.fr - armando@eost.u-strasbg.fr)
(3) UMR 5573, Laboratoire de Géophysique, Tectonique et Sédimentologie, CNRS, Université Montpellier II, Montpellier, France (Alfredo.Taboada@dstu.univ-montp2.fr)
(4) ETH, Inst. of Geophysics, ETH, Hoenggerberg. CH-8093, Zurich, Switzerland (giardini@seismo.ifg.ethz.ch)

KEYWORDS: Seismotectonics, Colombian Andes, Eastern Cordillera, inversion tectonics

INTRODUCTION

In this work, existing geologic, geophysical and neotectonic data, jointly with historic and recent instrumental seismicity, are re-examined to investigate on a regional scale the active tectonics of the Central Region of the Colombian Eastern Cordillera.

The Colombian Andes is an extended zone of continental deformation which constitutes the link between three tectonic domains: (1) the South American craton in the east, (2) The Caribbean Complex in the north, and (3) the Cocos and Nazca Plates in the west. The relative convergence between these plates is mainly absorbed by subduction along the Colombian-Ecuatorian Trough, the Northern Colombia Caribbean Trench and by deformation along major active fault zones parallel to the foothills of the Western, Central and Eastern cordilleras. On the regional scale the Eastern Cordillera exhibits different structural styles which can be identified from north to south. The *northern domain* between Tunja and Bucaramanga characterized by folds and thrusts of N-NE azimuth, consistent with shortening in E-SE direction. The *central domain* between Tunja and the Paramo de Sumapaz characterized by tigth folds and thrusts in NS and NNE direction in the western flank, and by NE *en echelon* thrusts in the eastern flank; these thrusts constitute the borders of the wide plateau ot the Sabana de Bogota. The *southern domain*, to the south of the Paramo de Sumapaz, corresponds to a zone of narrowing of the cordillera, and is characterized on the eastern flank by major high dipping faults oriented in NE direction with transpressive motion, and on the western flank by thrusts with western vergency and wide and elongated folds.

Distinct seismic and neotectonic activity characterize these domains. In the *northern sector* morphotectonic evidences of activity are scarce and feeble, in general. However; important seismic activity is observed.

Microseismicity may be associated, in the western flank to reverse faults with NW vergency buried under the Magdalena Valley sediments and to the piedmont faults of the Salinas System, in the axial zone to the SE vergency faults of Suarez and Soapaga-Boyaca System, and in the eastern flank to the SE vergency faults of the Frontal Fault System (Pajarito F., Guaicaramo F. and Yopal F.) and to the E vergency Sacama Fault limiting the Sierra Nevada del Cocuy. Four historic events of moderated magnitude (1646, 1724, 1755 and 1928) have been associated to activity in the axial zone and none historical earthquake is known on the western flank.

In the *central sector* seismic activity is essentially confined to the flanks of the cordillera. On the western flank a narrow corridor of epicenters along the southern Honda and Alto del Trigo faults, suggests that present activity in this sector is constrained to the most external segments of the southern Salinas System. The 1805 earthquake (M~6.7) which ruined the city of Honda is probably associated to one of those segments. Strong morphologic indicatives of activity have been observed at the Cambao Fault. On the eastern flank instrumental seismicity is important and it is associated to the most external traces of the NW verging faults of the Piedemonte Llanero Fault System (Yopal, Guaicaramo, Tesalia and Guayuriba-Restrepo faults), where sound morphotectonic evidences of activity have been observed also. On this flank of the cordillera, three significant earthquakes are known to have occurred: 1743, M~6.7; 1923, M~6.7, and 1995, M_w=6.5.

In the *southern sector* seismicity is abundant and it is confined to the eastern flank of the cordillera and to the axial zone at the south of Bogota. Seismicity is well correlated with the large transpressive faults of the Algeciras-Altamira system which limits the Precambrian and Paleozoic structures of the Garzón and Quetame massifs, respectively. It is along those structures where the largest crustal historic earthquakes in Colombia have had origin. The most recent in 1967 (M_w=7.0) had an strike slip mechanism with right lateral movement on the SW-NE plane. This mechanism agrees with the copious geomorphologic evidences of activity observed at the southern segments of the Algeciras System. The large 1827 earthquake (M_w~7.7) ruptured the southern segment of the Algeciras System. In the axial zone to the south of Bogota some microseismic activiy has been registered and at least one large historic earthquake, in 1917 (Ms=7.1), is located in this sector.

An important event occurred in 1785 which largely affected Bogota (intensity VIII) and originated intensity VII in towns as far as Neiva, and intensity VI in Pasto and Popayan (more than 350 km away from Bogota). The location of this earthquake remains uncertain; an intermediate focus related to the known seismicity under the Eastern Cordillera could explain the so wide isoseismals but the data are not enough to firmly constrain the location.

CONCLUSION

The central region of the Colombian Eastern Cordillera is a complex tectonic region, subjected to compressive stresses associated to fast eastward convergence of the Nazca Oceanic Plate and slow, E-SE convergence the Caribbean Plate referred to South America. The lack of large earthquakes in some regions, the weakness of morphological evidences on others, and the scarcity of microseismic records where evidences of activity were

known demonstrate the necessity of a multidisciplinary approach. Following this approach we identified and characterized the major active faults in the region. The Algeciras-Altamira Fault System stands as the most active system in the region with abundant evidences of all types. In the central sector of the cordillera, both, the eastern and western piedmont fault systems are identified as active, the eastern system showing the most contundent evidences. Activity on the axial faults of the cordillera has been identified, moderate on the SE vergency thrusts at the north of Tunja and higher on the west vergency thrust to the south of Bogota.

In analyzing the configuration of the structures exhibiting neotectonic activity, the role of the geometry of the ancient normal faults and major structures affecting the basement of the cordillera has been recognized. Activity rates and tectonic styles along the cordillera can be explained in terms of the variation in the tectonic stress field associated to convergence of the major plates.

REFERENCES

Taboada A., Rivera L., Fuenzalida A., Cisternas A., Philip H., Bijwaard H., Olaya J. and Rivera C., 2000. Geodynamics of the northern Andes: Subduction and intracontinental deformation (Colombia). *Tectonics*, **19**, 787-813.

Colleta B., Hebard F., Letouzey J., Werner P. and Rudkiwercz L., 1990. Tectonic style and crustal structure of the Eastern Cordillera (Colombia) from a balanced cross section. En J. Letousey ed. *Petroleum and Tectonics in mobile belts*, Paris, Editions Technip, p.81-100.

Kellogg J. and. Vega V., Tectonic development of Panama, Costa Rica, and the Colombian Andes: Constraints from Global Positioning System geodetic studies and gravity, *Spec. Pap. Geol. Soc. Am.*, ***295***, 75-90, 1995.

Vergara, H., A. Taboada, J. Romero, G. Paris, and Castro E., 1996. Principales fuentes sismogénicas de la región central de Colombia. paper presented at *VII Congreso Colombiano de Geologia,* INGEOMINAS,Bogota.

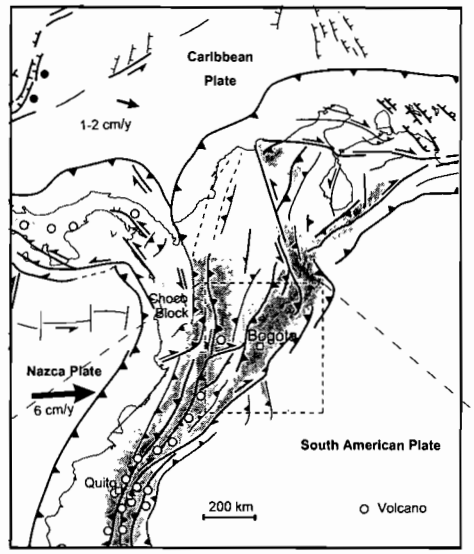

After Taboada et al. 2000

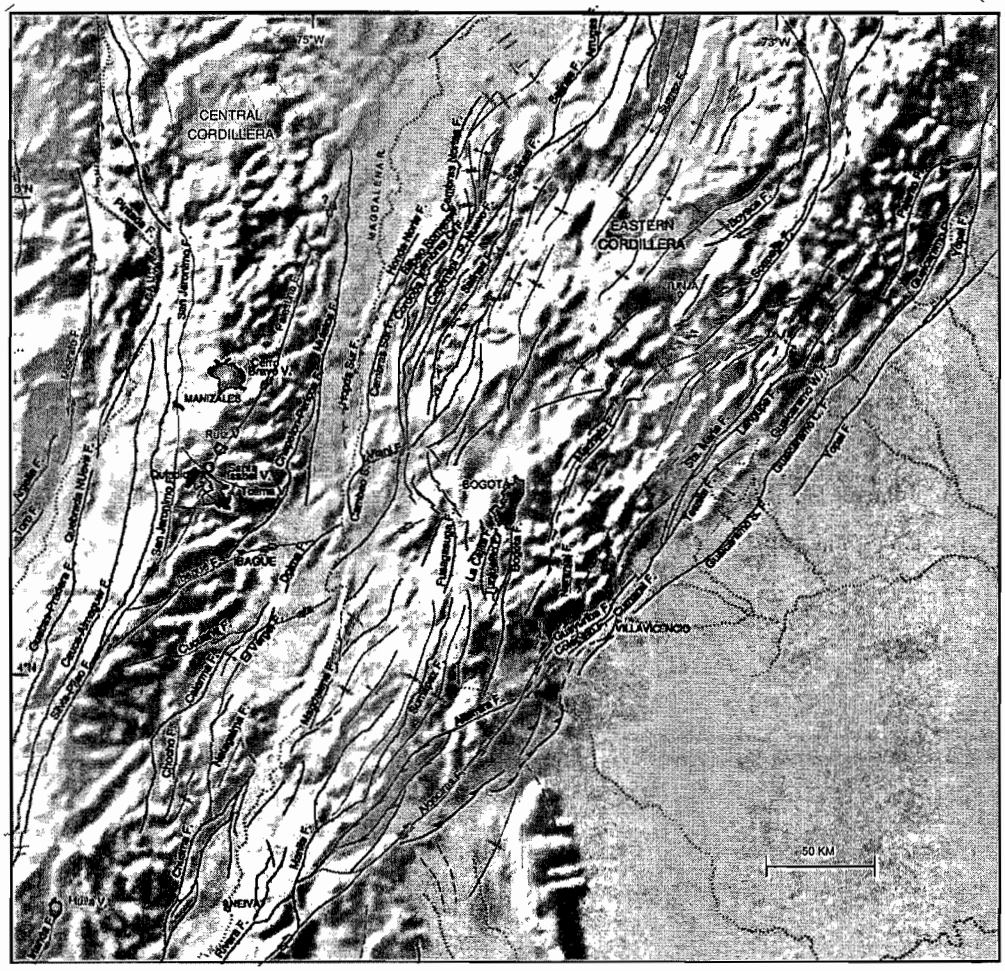

THE NEOTECTONIC EVOLUTION OF THE GULF OF GUAYAQUIL: A TAIL STRUCTURE BETWEEN CONVERGING PLATES

J.F. DUMONT [A,*], *E. SANTANA* [B], *W. VILLEMA* [C], *M. ORDOÑEZ* [C], *N. JIMENEZ* [C], *I. ZAMBRANO* [C], *and K. PEDOJA* [D]

[a] IRD, URM Geosciences Azur, AP 0903 30096, Guayaquil, Ecuador
[b] INOCAR Base Maritima Sur, Av. 24 de Julio, Guayaquil Ecuador
[c] Petroproducción, CIG-G, Km 6,5 via a Salinas, Guayaquil, Ecuador
[d] UPMC, UMR Geosciences Azur, La Darse, 06235 Villefranche s/Mer, France

KEY WORDS: Gulf of Guayaquil, Quaternary tectonics, active margin

INTRODUCTION

The Gulf of Guayaquil opens during the Neogene at the south tip of the North Andean Block (Fig. 1A) (Kellogg and Bonini, 1982; Pennington, 1981). This block is the northwestern broken corner of the South American continent, in the position of a triple junction between the Nazca, Caribbean and South American plates (Ego et al., 1996). It moves northward along a NE trending wrench fault zone joining Santa Clara and Puná Islands to Pallatanga (Fig. 1A). The Gulf of Guayaquil opens along the southwest segment of this fault zone, at the junction with the Ecuadorian subduction zone (Fig. 1B).

The recent evolution of the Gulf is characterized by transtension deformation involving flower structures and diapirism, with very important accumulation of Pliocene sediments (Benitez, 1995; Deniaud et al., 1999; Lions, 1995).
The present study is based on field works in the Santa Clara and Puná Islands.

DATA

Three major neotectonic events are observed in Pliocene to early Pleistocene shallow marine sediments:

- 1) a NW-SE shortening evidenced by right and left hand faults is observed in the Zambapala Cordillera. This shortening is coherent with 300 m uplift of the Zambapala Cordillera during the early Pleistocene, in relation to a positive flower structure.

- 2) a E-W shortening is observed in several places. It is principally represented by right hand movement along the NE-SW trending Zambapala-Lechuza wrench zone. Drainage offset of up to 300 m are observed, and a cumulated 3 km offset is registered by the Lechuza pull apart.

- 3) The more recent event are all extension trending NNW-SSE to NNE-SSW. In Santa Clara this event post date, transtension deformation along the northward extension of the Amistad structure. This event emphasizes faults and structures trending parallel to the Santa Elena and Progresso Basin. This is the main style of deformation in the north of Puná Island, as well as probably all the Guayas area located north of the Zambapala-Pallatanga wrench zone.

CONCLUSIONS

The strong shortening rising the Zambapala Cordillera and the following and probably related W-E shortening are interpreted in relation to a compressive event originated in the subduction system. The introduction of the Grijalva Scarp in the subduction may be responsible for this shortening event which predate and postdate transtension or extension events. The Grijalva scarp is a South looking scarp separating an old and morphologically lower oceanic crust to the south from a younger crust post dating the break of the Farallon platform to the north. It constitutes not only an asperity but also a major break in the subducting plate.

The recent and roughly N-S extension initiates a new morphostructural pattern, resulting in partitioning of the deformation between the Zambapala-Pallatanga wrench zone and the subsiding Guayas Basin. The opening of the Del Moro Channel since the last interglacial period, as well as the cluster of shallow seismicity located below Guayaquil is results of this partitioning.

REFERENCES

Benitez, S., 1995. Evolution géodynamique de la province cotière sud équatorienne au Crétaca supérieur Tertiaire. Géologie Alpine, 71: 208p.

Deniaud, Y. et al., 1999. Ouverture et évolution tectono-sédimentaire du golfe de Guayaquil: basin d'avant-arc néogene et quaternaire du Sud des Andes équatoriennes, Tectonique, pp. 181-187.

Ego, F., Sebrier, M., Lavenu, A., Yepes, H. and Egues, A., 1996. Quaternary state of stress in the Northern Andes and the restraining bend model for the Ecuadorian Andes. Tectonophysics, 259: 101-116.

Kellogg, J.N. and Bonini, W.E., 1982. Subduction of the Caribbean Plate and basement uplifts in the overriding South America Plate. Tectonics, 1(3): 251-276.

Lions, R., 1995. Evolution geodynamique d'un bassin d'avant-arc néogène en contexte decrochant: l'ouverture du Golfe de Guayaquil. DEA Thesis, Université Joseph Fourier, Institut Dolomieu, Grenoble, 83 pp.

Pennington, W.D., 1981. Subduction of the Eastern Panama Basin and seismotectonics of northwestern south America. Journal of Geophysical Research, 86(B11): 10753-10770.

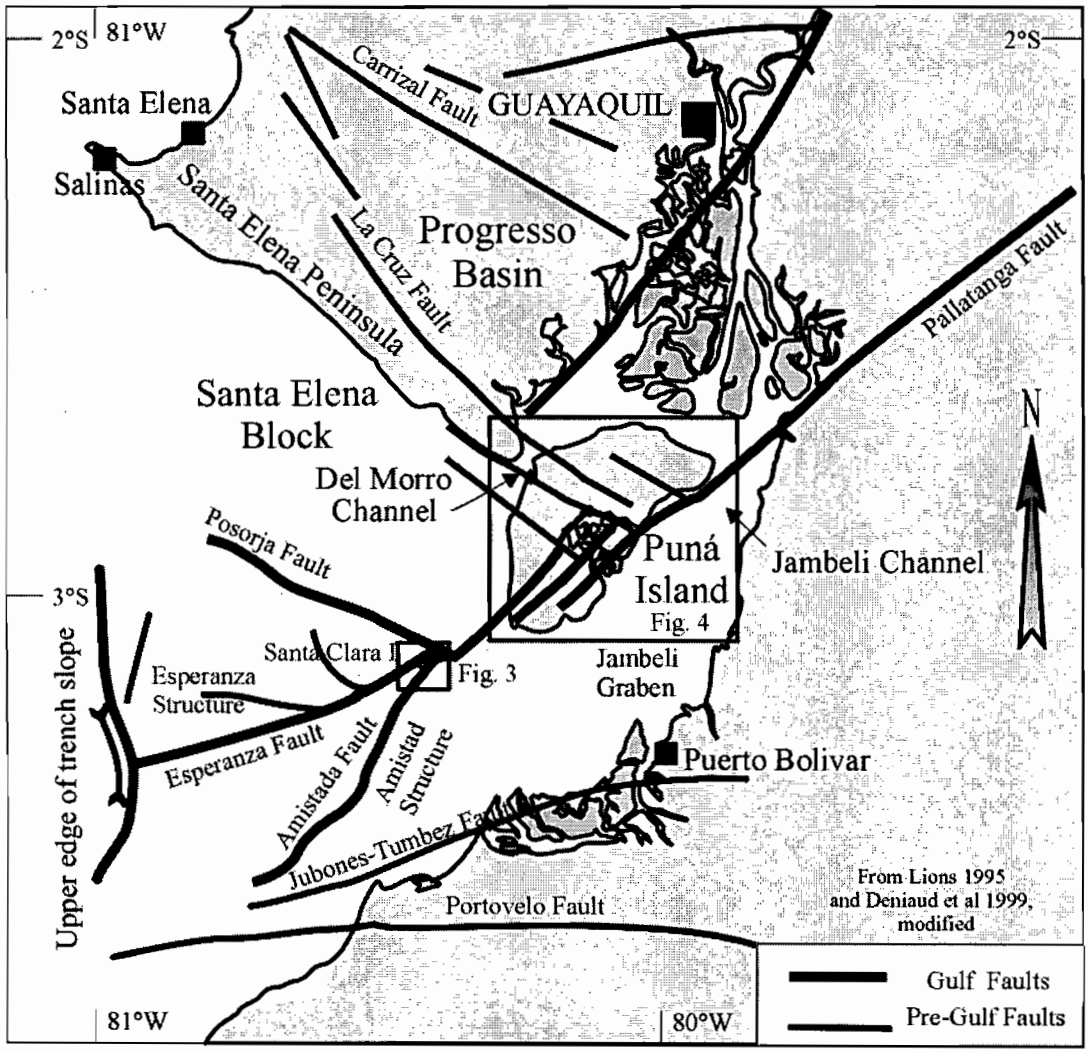

Fig. 1. Structural scheme of the Gulf of Guayaquil. From Lions (1995), Deniaud et al., (1999), simplified.

OBSERVATIONS AND SPECULATIONS PERTAINING TO REGIONAL MAGMATIC PATTERNS IN THE ANDEAN SOUTHERN VOLCANIC ZONE

Michael DUNGAN (1), Wes HILDRETH (2), Fred FREY (3), Jon DAVIDSON (4), Leonardo LÓPEZ-ESCOBAR (5), Daniel SELLÉS (1) and Carolina RODRIGUEZ (1)

(1) Section des Sciences de la Terre, Université de GenΠve, 13 rue des Maraîchers, 1211GenΠve 4, Switzerland (Michael.Dungan@terre.unge.ch)
(2) U.S. Geological Survey, 345 Middlefield Rd, Menlo Park, CA 94025, USA (hildreth@usgs.gov)
(3) Dept. Earth, Atmospheric & Space Sciences, MIT, Cambridge MA 02139 USA (FAFrey@mit.edu)
(4) Dept. of Geological Sciences, University of Durham, Durham DH1 3LE UK (J.P.Davidson@durham.ac.uk)
(5) Geologico Ecomómica Aplicada, Univ. de Concepción, Casilla 160-C, Concepción, Chile (llopez@udec.cl)

KEY WORDS: SVZ, Tatara-San Pedro complex, magma evolution,

ARC SEGMENTATION AND THE ROLE OF THE CRUST IN MAGMA DIFFERENTIATION

The accessible portion of the Southern Volcanic Zone (SVZ 33-42E S), is divided into three structural segments characterized by eastward-stepping en echelon offsets (SΨN) from the topographic front to the crest of the Andes (Hildreth & Moorbath, 1988; Dungan *et al.*, 2001). Segment boundaries occur at 36E and 34.5E S (Fig. 1), and the volcanoes of each segment are internally relatively similar in comparison to jumps in the character of magmatic evolution trends across segment boundaries. In particular, many compositional indices in Quaternary magmas change dramatically across the boundary at 36E S, where there is also an inflection in the trend of SΨN increasing regional elevation of the Cordillera that is inferred to reflect increasing SΨN crustal thickness (Hildreth & Moorbath, 1988). The NE projection of the Mocha Fracture Zone, which separates relatively young and old oceanic lithosphere (older to the north), intersects the SVZ near 36.5-37ES. Distinguishing contributions from subducting oceanic lithosphere and sediment to sub-arc mantle sources from components added to magmas during ascent through the continental lithosphere is a fundamental problem in arc volcanism, and it is a controversial topic with respect to regional variations of magma chemistry in the SVZ (*e.g.*, Hickey *et al.*, 1986; Hildreth & Moorbath, 1988; Davidson *et al.*, 1987; Stern, 1991; Tormey *et al.*, 1991). As a contribution this debate, we present a synthesis of >1600 new and previously published major and trace element

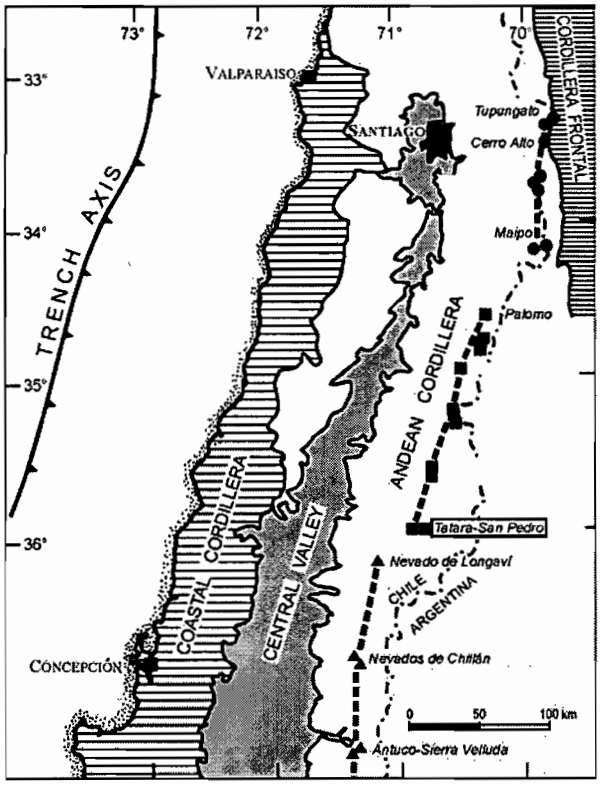

analyses from the SVZ, as well as reconnaissance results from Cenozoic plutons between 35E and 37.5E S. Although regional variations as a function of latitude (particularly data regressions) are not sufficient to resolve the relative contributions of multiple mantle and crustal components, they are a useful framework for interpreting results from detailed investigations of individual centers (*e.g.,* Davidson *et al.,* 1987; Ferguson *et al,* 1992; Feeley & Dungan, 1996; Dungan *et al.,* 2001).

RHYOLITIC VOLCANISM

One marked difference between Quaternary volcanic centers north and south of 36E S is the abundance of high-SiO_2 rhyolite (SiO_2>74 %), Plio-Quaternary silicic ash-flow tuff calderas, and large Tertiary porphyry copper deposits, to the north and their absence along the axis of the arc to the south (to our knowledge). Quaternary high-SiO_2 rhyolites north of 36E have vastly different trace element signatures from rhyolites in the south (*e.g.,* Puyehue-Cordón Caulle; Gerlach *et al.,* 1988), where such magmas have been derived by extreme fractional crystallization of mafic parental magmas. We favor the interpretation that northern high-SiO_2 rhyolites are partial melts of the crust (perhaps hybridized crust), but the conditions of magma generation and source lithologies remain unconstrained.

MAGMA DIFFERENTIATION

In keeping with evidence for production of southern rhyolitic magmas by fractionation-dominated evolution, contrasts between evolved mafic to intermediate magmas north and south of 36E are: **(1)** trace element signatures verify minimal upper crustal contributions in the south, whereas even some northern basalts are substantially modified by crustal interaction, and **(2)** southern SVZ evolved magmas are dominantly the products of low-pressure fractional crystallization, whereas northern evolved magmas have probably differentiated at various pressures and by a combination of differentiation mechanisms. Typical southern andesites and dacites rarely contain hydrous minerals (see below), and differentiation trends characterized by limited increases in Th/Yb and Rb/Y (high HREE & Y) plus low and decreasing Sr and Sr/Sc indicate derivation by shallow closed-system fractionation (plagioclase-rich assemblages), without important contributions from upper crustal lithologies. In contrast, the diversity of evolved magma compositions characterized by trends to higher, and highly variable K, Rb, Sr, Th, Rb/Y, Th/Yb (lower Y & HREE), and Sr/Sc leads to the inference that open-system differentiation paths (substantial crust-magma interaction) dominate at the Tatara-San Pedro complex (TSPC, 36E; Dungan *et al.,* 2001). Recent studies at the TSPC have led to the conclusion that assimilation of gabbroic lithologies containing hydrous minerals may also substantially modify incompatible element signatures in contaminated magmas (Cortesi *et al.,* 2002). The TSPC lies in a completely different petrologic realm from those located to the south across the 36E segment boundary, despite the fact that there is no correspondingly large jump in regional elevation or expression in basement geology.

LOW-K HYDROUS MINERAL-BEARING ANDESITES & DACITES

Well characterized SVZ frontal arc centers from Nevados de Chillan (36.8E S) to Volcán Osorno (41.1E S) are mainly basaltic andesite-mafic andesite cones with minor proportions of basalt and silicic magmas. This

coherent chain is bracketed by two dominantly andesitic cones, Nevado de Longaví (36.25E S; Sellés *et al.*, 2002) and Calbuco (41.2E S; López-Escobar *et al,* 1995) that are distinct in most respects from the intervening centers. Some Longaví low-K andesites (<1.3 % K_2O; 61-64 % SiO_2) contain hbl±biot, but such assemblages are only sporadically present in dacite (>2.5 % K_2O; 66-69 % SiO_2) of the adjacent Tatara-San Pedro complex and hydrous phases are essentially absent at Chillan (and southward to Osorno until Calbuco). The trace element signatures and trends of Longaví andesites (up to 64 % SiO_2) resemble high-Sr/Y magmas of Mt. Burney (54.4E S), but they are not associated with subduction of hot, young oceanic crust. We suggest that the dominantly andesitic mode and anomalous compositions of volcanoes such as Longaví and Calbuco are not derived directly by differentiation of more mafic parent magmas or as partial melts of a young, hot slab. Is the origin of Longaví andesites linked to their occurrence at a segment boundary, to anomalous local crustal compositions, to the impact of the subducted Mocha Fracture Zone on basaltic compositions, or some heretofore unrecognized factor?

SPECULATION

The degree to which mantle-derived magmas incorporate crust plays a large role in determining the major and trace element character of evolved magmas in the SVZ, and the influence of the crust is far greater in the northern SVZ (36-33E S; Dungan, 1999). However, many first-order observations are not consistent with a framework wherein the degree to which crust-magma interactions have modified evolved magma compositions is a linear function of increasing crustal thickness northward. We speculatively suggest that an important factor may be a step-function decrease in the fertility of deep sub-arc crust south of 36E. A more 'oceanic', less fertile deep crust in the southern SVZ is favored by fragmentary, circumstantial evidence such as the extremely depleted gabbroic xenoliths at Calbuco (Hickey *et al.,* 1995), but more work needs to be done to evaluate this hypothesis.

Distinctions between granitoids at 37.3E and 36E S are consistent with the regional differences in Quaternary silicic magmas originating in the crust. Although uncontaminated basaltic rocks throughout the SVZ have low Rb/Y (~0.4-0.7) all volcanic centers north of 36E display variable but significant increases in Rb/Y (~2-13) and Th/Yb with increasing SiO_2 that require open-system addition of crustally-derived components with high Rb/Y and Th/Yb, in contrast to centers from Nevados de Chillan southward that generally exhibit limited increases in Rb/Y consistent with nearly closed-system fractionation (Rb/Y generally < 2-3 in rhyolite). Granitoids at 36E have higher Rb/Y (~3-22) than the Quaternary volcanic rocks at a given SiO_2, whereas the granitoids at 37.3E (basement beneath Antuco-Sierra Velluda) have comparably low Rb/Y (<3.5, except for one aplite dike). An origin for volumetrically minor silicic magmas south of 36E by low-pressure closed-system fractionation of basaltic parent magmas is explicable if the crust below the southern SVZ is infertile, dense, and thin. Quantifying the roles of crustal inputs versus variable mineral assemblages and/or differentiation mechanisms is far more difficult where magmas have evolved through polybaric, multi-component open-system differentiation during passage through fertile crust (*i.e.,* north of 36E S).

REFERENCE CITED

Cortesi, L., Dungan, M., Davidson, J, Fred Frey F., Costa, F. & Marzoli, A. 2002. Assimilation of mafic-ultramafic cumulates may be an important process in modifying major and trace element signatures: Evidence from the Tatara-San Pedro complex (TSPC), 36E S, Chilean Andes (this volume)

Davidson, J.P., Dungan, M.A., Ferguson, K.M. & Colucci, M.T. 1987. Crust-magma interactions and the evolution of arc magmas. The San Pedro-Pellado volcanic complex, southern Chilean Andes. *Geology* 15, 443-446.

Dungan, M.A., Wulff, A. & Thompson, R. 2001. Eruptive stratigraphy of the Tatara-San Pedro complex, 36ES, Southern Volcanic Zone, Chilean Andes: Reconstruction method and implications for magma evolution at long-lived arc volcanic centers. *Journal of Petrology* 42, 555-626.

Feeley, T.C. & Dungan, M.A. 1996. Compositional and dynamic controls on mafic-silicic magma interactions at continental arc volcanoes: evidence from Cordón El Guadal, Tatara-San Pedro Complex, Chile. *Journal of Petrology* 37, 1547-1577.

Ferguson, K.M., Dungan, M.A., Davidson, J.P. & Colucci, M.T. 1992. The Tatara-San Pedro volcano, 36° S Chile: a chemically variable, dominantly mafic magmatic system. *Journal of Petrology* 33, 1-43.

Gerlach, D.C., Frey, F.A., Moreno-Roa, H. & López-Escobar, L. 1988. Recent volcanism in the Puyehue-Cordon Caulle region, Southern Andes, Chile (40.5ES): Petrogenesis of evolved lavas. *Journal of Petrology* **29,** 333-382.

Hildreth, W. & Moorbath, S. 1988. Crustal contributions to arc magmatism in the Andes of central Chile. *Contributions to Mineralogy and Petrology* 98, 455-489.

Hickey, R.L., Frey, F.A., Gerlach, D.C. & López-Escobar, L. 1986. Multiple sources for basaltic arc rocks from the Southern Volcanic Zone of the Andes (34E-41ES): trace element and isotopic evidence for contributions from subducted oceanic crust, mantle, and continental crust. *Journal of Geophysical Research* 91, 5963-5983.

Hickey-Vargas, R., Abdollahi, M.J., Parada, M.A., López-Escobar, L. & Frey, F.A. 1995. Crustal xenoliths from Calbuco Volcano, Andean Southern Volcanic Zone: implications for crustal composition and magma-crust interaction. *Contributions to Mineralogy and Petrology* 119, 331-344.

Lara, L., Moreno, H. & Lavenu, A. 1999. Volcanism and tectonics in the Pleistocene-Holocene volcanic arc, Southern Andes (40.5-41.5E S), Fourth ISAG, Goettingen, Abs. p. 417-421

López-Escobar, L., Parada, M.A., Hickey-Vargas, R., Frey, F.A., Kempton, P.D. & Moreno, H. 1995. Calbuco Volcano and minor eruptive centers distributed along the LiquiZe-Ofqui Fault Zone, Chile (41E-42E S): contrasting origin of andesitic and basaltic magma in the Southern Volcanic Zone of the Andes. *Contributions to Mineralogy and Petrology* 119, 345-361.

Sellés, D., Rodriguez, C. & Dungan, M.A. 2002. Nevado de Longaví: Anomalous incompatible element-poor compositions in the SVZ of the Andes (36.25E S). (This volume)

Stern, C.R. 1991. Role of subduction erosion in the generation of Andean magmas. *Geology* 19, 78-81.

Tormey, D.R., Hickey-Vargas, R., Frey, F.A. & López-Escober, L. 1991. Recent lavas from the Andean volcanic front (33 to 42° S); interpretations of along-arc compositional variations. In: Harmon, R.S., and Rapela, C.W. eds., Andean Magmatism and its Tectonic Setting. Boulder Colorado. *Geol. Society of America. Special Paper* 265, 57-77.

SECOND PARTIAL MELTING STAGE OF A SLAB-MELT METASOMATIZED MANTLE AT SUMACO VOLCANO (NORTHERN VOLCANIC ZONE, ECUADOR)

Jean-Philippe EISSEN(1,2), Erwan BOURDON(1,3), Bernardo BEATE(4), Silvana HIDALGO(2) & Joseph COTTEN(5)

(1) IRD, UR Processus et aléas volcaniques, Whymper 442 y Coruña, Ap. 17-12-857, Quito, Ecuador (eissen@ird.fr)
(2) Departamento de Geofísica, Escuela Politécnica Nacional, Ap. 17-01-2759; Quito, Ecuador
(3) IRD, UR Processus et aléas volcaniques, Royal Holloway University of London, Egham, Surrey TW20 0EX, UK
(4) Dept. Geología, Petroleo y Minas, Escuela Politécnica Nacional; Ap. 17-01-2759, Quito, Ecuador.
(5) UMR 6538, Université de Bretagne Occidentale, BP 809, 29285 Brest Cedex, France

KEY WORDS: Andes, Northern Volcanic Zone, Ecuador, mantle metasomatism, high-Nb basalts, absarokites.

INTRODUCTION

Sumaco is one of the less known volcanoes of Ecuador, partially because of its remoteness as it is the only recent volcano located in the amazonian forest of the NVZ. However, it has been known for a while that most of its products are understaturated alkaline lavas, with frequently more then 15% of normative nepheline and normative apatite (Colony & Sinclair, 1928). The aim of this contribution is to present the first results obtained on this isolated and peculiar volcano after a recent survey (january 2001) in order better to constrain the petrogenetic process active in the geodynamic setting of Ecuador.

LOCATION AND MORPHOLOGY OF SUMACO VOLCANO

Located some 90 km ESE of Quito, Sumaco volcano rises above the rain forest of the Amazonian province of Ecuador on the eastern foothills of the andean chain. It is the volcano situated the farest from the trench of all the NVZ, in rear-arc position (Fig. 1). It is at the latitude of Sumaco the the width of the NVZ arc reachs its maximum, with more then 100 km. Sumaco exibits a regular cone well preserved morphology, suggesting that it may have experienced recent volcanic activity. At least one major avalanche event disected its northeast flank and its semi-circular scar is still visible in the topography. The summit cone build inside the avalanche scar, is mainly constituted by scorias intercalated with massive lava flows.

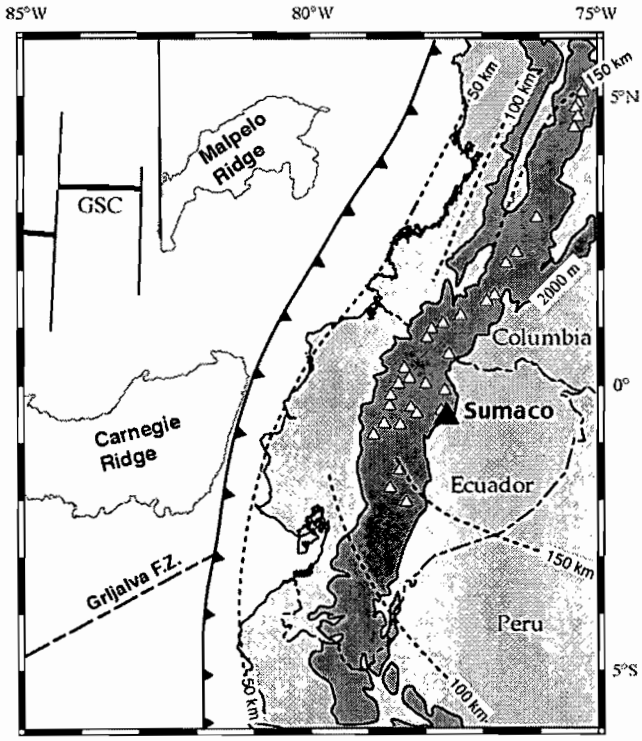

Figure 1 :
Map of the northwestern part of South America including main oceanic features, as well as the inferred position of the subducted slab beneath Colombia and Ecuador.
Depth contours to the Wadati-Benioff zone indicated as dotted lines (from Gutscher et al., 1999).
Andes Cordillera defined by 2000 m contour.
Trench is defined by toothed line.
Active volcanoes are designed by open triangles.
GSC: Galápagos Spreading Center.

PETROLOGY AND GEOCHEMISTRY OF SUMACO LAVAS

The mineralogical composition of the rocks of Sumaco volcano includes clinopyroxene, abundant hauyne and apatite, Fe-Ti oxides, ± amphibole, ± plagioclase, ± olivine in accordance with a first studies (Colony & Sinclair, 1928; Barragan *et al.*, 1998; Bourdon, 1999). Some lavas exibit a high countain of felsdpathoid in absence of plagioclase, corresponding to the initial definition of absarokite (Iddings, 1895).

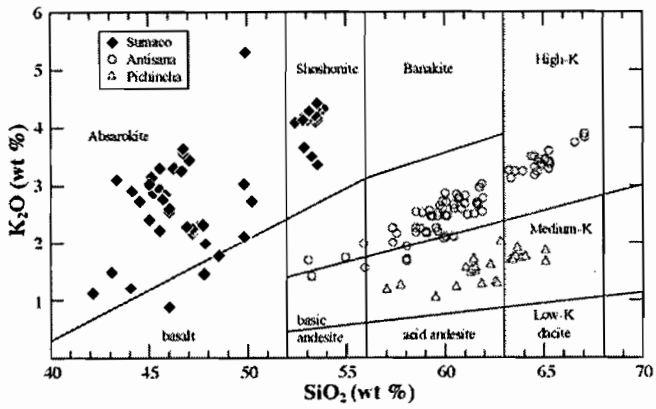

Figure 2 : K_2O versus SiO_2 classification diagram for orogenic magmas, modified from Peccerillo & Taylor (1976) showing Pichincha (triangles), Antisana (circles) and Sumaco (diamonds) lavas.

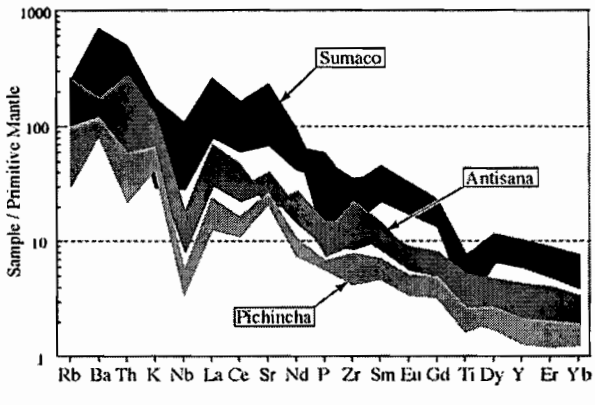

Figure 3 : Extended trace elements patterns of rocks from Pichincha, Antisana and Sumaco volcanoes. Normalization to the primitive mantle (normalization values from Sun & McDonough, 1989).

Geochemically, they are constituted by K-rich ($0.9 < K_2O\% < 5.3$) undersaturated lavas ranging in composition from basic absarokite to shoshonite ($44 < SiO_2\% < 5$ 4; Fig. 2) with high concentrations in all incompatible elements (Fig. 3). They also present a strong enrichment of LREE over HREE (La/Yb = 28-50), unless these later are significantly enriched (*e.g.* Yb = 2.02-3.9 ppm) compared to other rocks from the NVZ in Ecuador. On primitive mantle-normalized trace element patterns, a significant positive anomaly in Sr is observed (Fig. 3). But the most remarkable feature of these lavas is their strong enrichment in Nb (21-79 ppm): therefore, these lavas can be designated as high-niobium basalts (HNB ; Defand *et al.*, 1992). Isotopicaly, these lavas show unradiogenic characteristics with Sr ($^{87}Sr/^{86}Sr \approx 0.7042$), Nd ($^{143}Nd/^{144}Nd > 0.512880$) and Pb isotope data that are virtually the same than those from the adakites from the Western Cordillera (Bourdon, 1999; Bourdon *et al.*, 2002).

DISCUSSION : GEODYNAMIC IMPLICATIONS

The geochemical characteristics of Sumaco absarokites are close to those of HNB found in others arc settings in association with adakites (Saunders *et al.*, 1987; Defand *et al.*, 1992). The close association HNB-adakites has suggested to many authors that HNB could be the partial melting product of a mantle metasomatised by slab melts (Defand *et al.*, 1992). Indeed, slab melts are likely to transport Nb in the mantle, unlike hydrous fluids (Kesson & Ringwood, 1989).

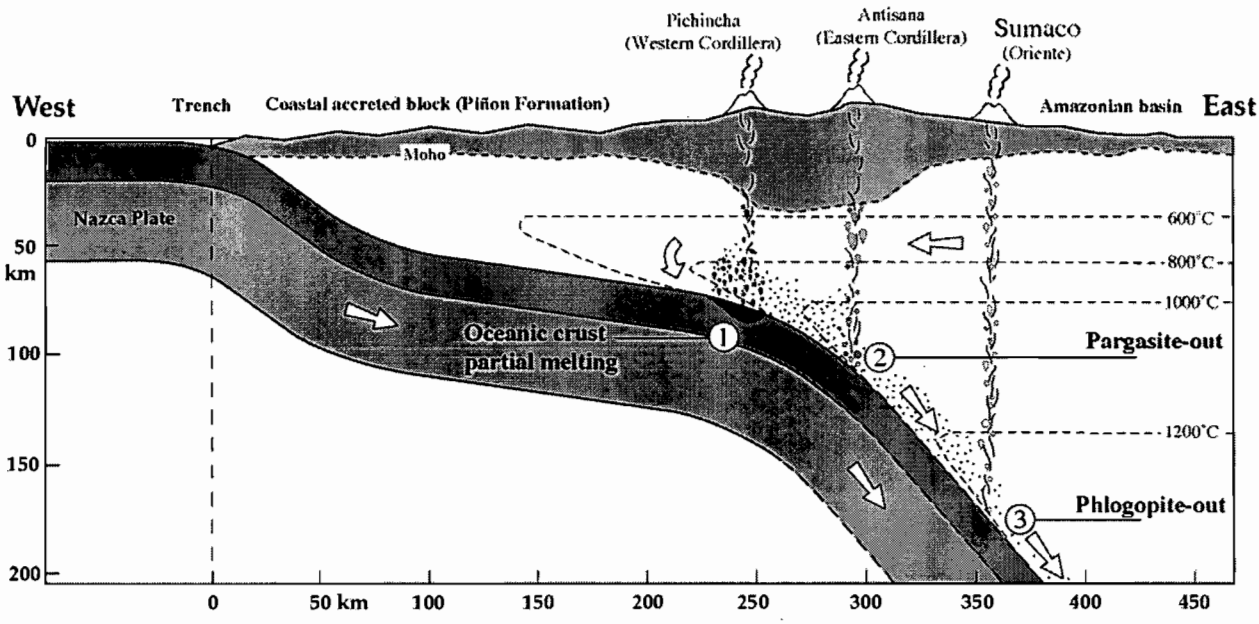

Figure 4: Schematic petrogenetic model in three steps for the NVZ in Ecuador, see the last paragraph (from Bourdon *et al.*, 2002).

Furthermore, Tatsumi & Koyaguchi (1989) experimentally showed that an absarokite with geochemical characteristics close to the most basic basalts of Sumaco was in equilibrium with a phlogopite-rich peridotitic mantle, suggesting that the source of this type of magma is likely to be a metasomatised mantle with significant amounts of phlogopite. Other studies on HNB related to adakites have shown that their low HREE concentrations could be related to a genesis in a garnet-rich mantle, resulting of a metasomatism by slab melts (Defand *et al.*, 1992). But

unlike most HNB, Sumaco basalts display no strong HREE depletions, suggesting that garnet is no longer present in the source. They could, however, be produced by the destabilization of phlogopite (Tatsumi & Koyaguchi, 1989).

But could Sumaco lavas be related to an intracontinental hotspot or an old enriched mantle and not to subduction processes ? In the absence of extensional structures in the eastern Andean foothills, the lavas from the Sumaco cannot be related to the partial melting of an adiabatically uplifted mantle. Moreover, the Nb anomalies of the Sumaco lavas are a clear imprint of a "subduction component". Lastly, the exact "match" between the isotopic signature of magma types from the arc front and the Sumaco is an irrefutable proof that their genesis are closely related to one another and thus to the subduction processes (Bourdon *et al.*, 2002).

In our schematic petrogenetic model in three steps (Fig. 4), the magmas of the fore-arc ([1] *e.g.* Pichicnha volcano) are mainly alimented today by adakitic magmas resulting from the direct partial fudion of the oceanic slab, but the adakitic melts are also metasomatising the mantle wedge. Therefore, below the Eastern Cordillera ([2] *e.g.* Antisana volcano), the melts are mainly pseudo-adakites producted by the partial fusion of these metasomatised peridotites. And finally in rear-arc positon, ([3] *e.g.* Sumaco volcano), the melts result a deeper, second partial fusion stage at a much lower fusion rate.

REFERENCES

Barragan R., Geist D., Hall M.L., Larson P. & Kurz M., 1998 - Subduction controls on the composition of lavas from the Ecuadorian Andes. *Earth Planet. Sci. Lett.* 154:153-166.

Bourdon B., Eissen J.-P., Gutscher M.-A., Monzier M., Hall M.L. & Cotten J., 2002 - Magmatic response to early aseismic ridge subduction: the Ecuadorian margin case (South America). *Earth Planet. Sci. Lett.*, (in press).

Bourdon E. 1999. Conséquences pétrogénétiques de la subduction d'une ride asismique: l'exemple du volcanisme de la marge équatorienne. Université de Bretagne Occidentale, Brest. *PhD Thesis*, 190 p.

Colony R.J. and Sinclair J.H., 1928 - The lavas of the Sumaco, eastern Ecuador, *American J. Sci.*, 216:299-312.

Defant M.J., Jackson T.E., Drummond M.S., De Boer J.Z., Bellon H., Feigenson M.D., *et al.*, 1992 - The geochemistry of young volcanism throughout western Panama and southeastern Costa Rica: an overview. *J. Geol. Soc. London*, 149:569-579.

Gutscher M.-A., Malavieille J., Lallemand S. & Collot J.-Y. 1999 - Tectonic segmentation of the North Andean margin: impact of the Carnegie Ridge collision: *Earth Planet. Sci. Letters*, 168:255-270.

Iddings J.P., 1895 - Abarokite-shoshonite-banakite series, *J. Geology*, 3:935-959.

Kesson S.E. & Ringwood A.E., 1989 - Slab-mantle interactions 1. Sheared and refertilized garnet peridotite xenoliths - samples of Wadati-Benioff zones ? *Chem. Geol.*, 78:83-96.

Peccerillo P. & Taylor S.R., 1976 - Geochemistry of Eocene calc-alkaline volcanic rocks from the Kastamonu area, Northern Turkey, *Contrib. Mineral. Petrol.* 58:63-81.

Saunders A.D., Rogers G., Marriner G.F., Terrell D.J. *et al.*, 1987 - Geochemistry of cenozoic volcanic rocks, Baja California, Mexico: Implications for the petrogenesis of post-subduction magmas. *J. Volcan. Geotherm. Res.*, 32:223-245.

Sun S.-S. & McDonough W.F., 1989 - Chemical and isotopic systematics of oceanic basalts : implications for mantle composition and processes. *in* Magmatism in the Ocean Basins, A.D. Saunders & M.J. Norry, eds., *Geol. Soc. Spec. Pub., London,* 42: 313-345.

Tatsumi Y. & Koyaguchi T., 1989 - An absarokite from a phlogopite lherzolite source. *Contrib. Mineral. Petrol.* 102(1):33-40.

THE PATTERN OF DEFORMATION RELATED TO GROWTH OF THE SOUTHERN ALTIPLANO PLATEAU (BOLIVIA)

Kirsten ELGER. (1), Onno ONCKEN (1)

(1) Geoforschungszentrum Potsdam, PB 3.1, Telegrafenberg, 14473 Potsdam, Germany.
kelger@gfz-potsdam.de, oncken@gfz-potsdam.de

KEY WORDS: Southern Altiplano, balanced cross sections, deformation partitioning, plateau uplift, tectonics and magmatism

ABSTRACT:

Structural studies on the Southern Altiplano in Bolivia based on reflection seismic data yield more shortening than previously estimated (56-72 km). Deformation was accumulated during several deformation increments since the Eocene. The spatially and temporally strongly variable fault activation is a characteristic feature during plateau formation. Field data and geophysical observations indicate that the style, timing, and location of deformation in the plateau can be interpreted as a consequence of magmatically controlled thermal weakening of the middle crust.

INTRODUCTION

The Altiplano-Puna Plateau is the most prominent feature of the Central Andes. It covers large parts of southern Peru, Bolivia and NW Argentina and has an average elevation of 4000 m. The Bolivian Altiplano is bordered by the bivergent thrust system of the Eastern Cordillera to the east and the active magmatic arc of the Western Cordillera to the west. The latter is also part of the plateau. The high topographic elevation is compensated by an up to 70 km thick crust that reaches its maximum underneath the Eastern Cordillera (Wigger et al., 1994; Yuan et al., 2000).

Crustal thickening and plateau uplift in the arc-backarc domain of the South American convergent margin took place during the Cenozoic (e.g. Allmendinger et al., 1997; Gregory-Wodzicki, 2000; Isacks, 1988; Lamb and Hoke, 1997). Tectonic shortening is believed to be the prime mechanism for crustal thickening and so far many workers directed their interest at the plateau's eastern margin (e.g. Baby et al., 1997; Kley and Monaldi, 1998; Kley et al., 1997; Lamb and Hoke, 1997; Sheffels, 1990). Tectonic shortening in the bivergent thrust system of the Eastern Cordillera and the foreland fold-and-thrust belt of the Interandean and Subandean ranges sums up to ~180-210 km of contraction. This value explains some 60-70% of the required crustal thickness of the Andes (Kley and Monaldi, 1998). Deformation at the western flank of the plateau is characterised by a thick-skinned basement ramp with only very minor horizontal shortening (Victor, 2000).

The structural style associated with plateau formation and uplift is poorly constrained in the central plateau area due, mostly, to widespread coverage with syn- and posttectonic sediments. This study is aimed at constraining style, magnitude and age of tectonic shortening on the southern Altiplano in Bolivia through

incrementally balanced cross sections (at ~21°S) based on reflection seismic profiles, 3D-strain analysis, gravity data, age dating, and field observations (see fig. 1 for location).

CONCLUSIONS

The southern Altiplano is segmented in two structural domains. The Eastern Altiplano domain (EAP) is interpreted as westernmost part of the N-S-trending west-verging thin-skinned thrust belt of the Eastern Cordillera. The buried deformation front lies ~12 km west of the Vilque well in the EAP (fig. 1). The shallow to medium dipping thrusts merge into a slightly eastward dipping detachment that lies at a depth of ~6-9 km in the Eastern Altiplano within Lower Paleozoic sediments and continues in the Eastern Cordillera.

The Central Altiplano domain (CAP), west of the NNW-SSE trending Khenayani Uyuni fault zone (KUFZ), is characterised by a bivergent thrust system with steep to shallow basement-involving thrusts in the East and fault controlled folds in the west.

The buried thin-skinned deformation front of the Eastern Cordillera has accumulated a minimum shortening of ~6 km (thrusting and folding). Tectonic shortening of the Central Altiplano sums to ~39 km. First results of the 3D-strain analysis show that a significant amount of strain at the grain scale has also been accumulated on the Altiplano (6-15%, i.e. 11-27 km). Including this, total shortening in the plateau increases to 56-72 km (29-35%), about twice the value reported from earlier studies.

Despite the differences in structural style and magnitude of shortening, it is noteworthy that deformation occurred rather synchronous in both, the Eastern and the Central Altiplano domain, but at different relative magnitudes. The oldest structures that recorded contraction are of Lower Oligocene age (>28 Ma). This deformation increment was responsible for ~4,5 km horizontal shortening in the EAP, and for 15-21 km shortening in the CAP, resulting in the uplift of Paleozoic basement ridges that provided a sediment source for the intervening intermontane basins.

Most shortening in the CAP took place during the Middle Miocene (15-8Ma, 18-24 km), resulting in formation of several small thrust top basins filled with equivalent continental sediments. Seismic sequence analysis, map interpretation, and field observations revealed the relative order of fault activation. The absolute ages of the younger deformation increment are based on isotopic ages of angular unconformities and interbedded tuffaceous horizons in the syntectonic thrust-top basins. Horizontal contraction on the Altiplano ended between 11-8 Ma as indicated by the age of overlying undeformed volcanic rocks. Prior to contractional deformation, the CAP experienced a Paleocene/ Eocene extensional increment resulting in significant thickness variations of the Eocene/ Oligocene sediments in a major halfgraben with maximal thickness near the western part of the Khenayani-Uyuni fault zone (>3 km) and reduced thickness (<1 km) on the graben shoulder in the eastern part of the KUFZ. The latter thus is, in part, an inverted normal fault system.

Seismic stratigraphy and interpretation reveals a complex deformation history characterised by spatially and temporally varying fault activity that does not show a systematic pattern. Observing the Eastern Altiplano domain jointly with the adjacent parts of the Eastern Cordillera, tectonic activity is almost continuous from Lower Oligocene to Middle Miocene times. During this period, however, faults were repeatedly reactivated in a complex pattern as evidenced from the infill architecture of thrust top basins. In contrast, deformation in the

CAP is restricted to the main increments given above. Last not least, the Western flank of the plateau developed in two increments, a Late Eocene with high strain rate ("incaic", 14 km)(Günther, 2001), and a low strain rate stage between 29 and ~10 Ma (~5 km shortening)(Victor, 2000). The younger increment shows continuous deformation in the same time span as the Eastern Cordillera and EAP (see above).

In the CAP, as in the EAP, the activation of faults does not reflect a prograding deformation front in either direction. The spatially and temporally strongly variable fault activation is a characteristic feature during the entire plateau formation and requires a probably self-organized steady state between driving forces, mechanical properties of the faults and underlying basement, and mass redistribution at the surface. Moreover, the syntectonic stratigraphic units of the Central and Eastern Altiplano domain overlie shallow marine Upper Cretaceous sediments that still form a subhorizontal regional near sea level. Surface uplift in this part of the plateau is nearly entirely controlled by sedimentary infilling (3-5 km) of structurally controlled basins with internal drainage.

At the western flank of the plateau, active shortening is coeval with magmatism that resulted from crustal melting (Victor, 2000). In the plateau area we observe a positive correlation between the spatial and temporal distribution of Miocene volcanic centres and the activity of the Altiplano imbricate system. Moreover, the bivergent thrust system of the Central Altiplano is spatially related to a variety of geophysical anomalies. The interpretation of partial melts in the middle crust is based on the presence of a seismic low velocity zone whose upper limit correlates with a bright seismic reflector from the ANCORP'96 section and also with the upper limit of an extremely high conductivity anomaly (Brasse et al., in press; Yuan et al., 2000). Accordingly we favour a model explaining style, timing, and location of deformation in the plateau as a consequence of magmatically controlled thermal weakening of the middle crust.

REFERENCES

Allmendinger, R.W., Jordan, T.E., Kay, S.M. and Isacks, B.L., 1997. The evolution of the Altiplano-Puna Plateau of the Central Andes. Annual Reviews Earth Planet Sciences, 25: 139-174.

Baby, P., Rochat, P., Mascle, G. and Herail, G., 1997. Neogene shortening contribution to crustal thickening in the back arc of the Central Andes. Geology, 25(10): 883-886.

Brasse, H., Lezaeta, P., Rath, V., Schwalenberg, K., Soyer, W. and Haak, V., in press. The Bolivian Altiplano conductivity anomaly. Journal of geophysical research.

Gregory-Wodzicki, K.M., 2000. Uplift history of the Central and Northern Andes: a review. GSA Bulletin, 112(7): 1091-1105.

Günther, A., 2001. Strukturgeometrie, Kinematik und Deformationsgeschichte des oberkretazisch-alttertiären magmatischen Bogens (nord-chilenische Präkordillere, 21,7-23°S). Ph. D. Thesis, Freie Universität Berlin, Berlin.

Isacks, B.L., 1988. Uplift of the Central Andean Plateau and bending of the Bolivian Orocline. Journal of Geophysical Research, 93(B4): 3211-3231.

Kley, J. and Monaldi, C.R., 1998. Tectonic shortening and crustal thickness in the Central Andes: How good is the correlation? Geology, 26(8): 723-726.

Kley, J., Müller, J., Tawackoli, S., Jakobshagen, V. and Manutsoglu, E., 1997. Pre-Andean and Andean-Age Deformation in The Eastern Cordillera of southern Bolivia. Journal of South American Earth Sciences, 10(1): 1-19.

Lamb, S. and Hoke, L., 1997. Origin of the high plateau in the Central Andes, Bolivia, South America. Tectonics, 16(4): 623-649.

Sheffels, B.M., 1990. Lower bound on the amount of crustal shortening in the central Bolivian Andes. Geology, 18: 812-815.

Victor, P., 2000. Die Entwicklung der Altiplano Westflanke und ihre Bedeutung für die Plateaubildung und Krustenverdickung in N-Chile (20-21°S). Scientific Technical Report, STR00/13: 1-89.

Wigger, P., Schmitz, M., Araneda, M., Asch, G., Baldzuhn, S., Giese, P., Heinsohn, W.-D., Martinez, E., Ricaldi, E., Röwer, P. and Viramonte, J., 1994. Variations of the crustal structure of the Southern Central Andes deduced from seismic refraction investigations. In: Reutter K.-J. et al. (Editor), Tectonics of the Southern Central Andes, New York, pp. 23-48.

Yuan, X. et al., 2000. Subduction and collision processes in the Central Andes constrained by converted seismic phases. Nature, 408: 958-961.

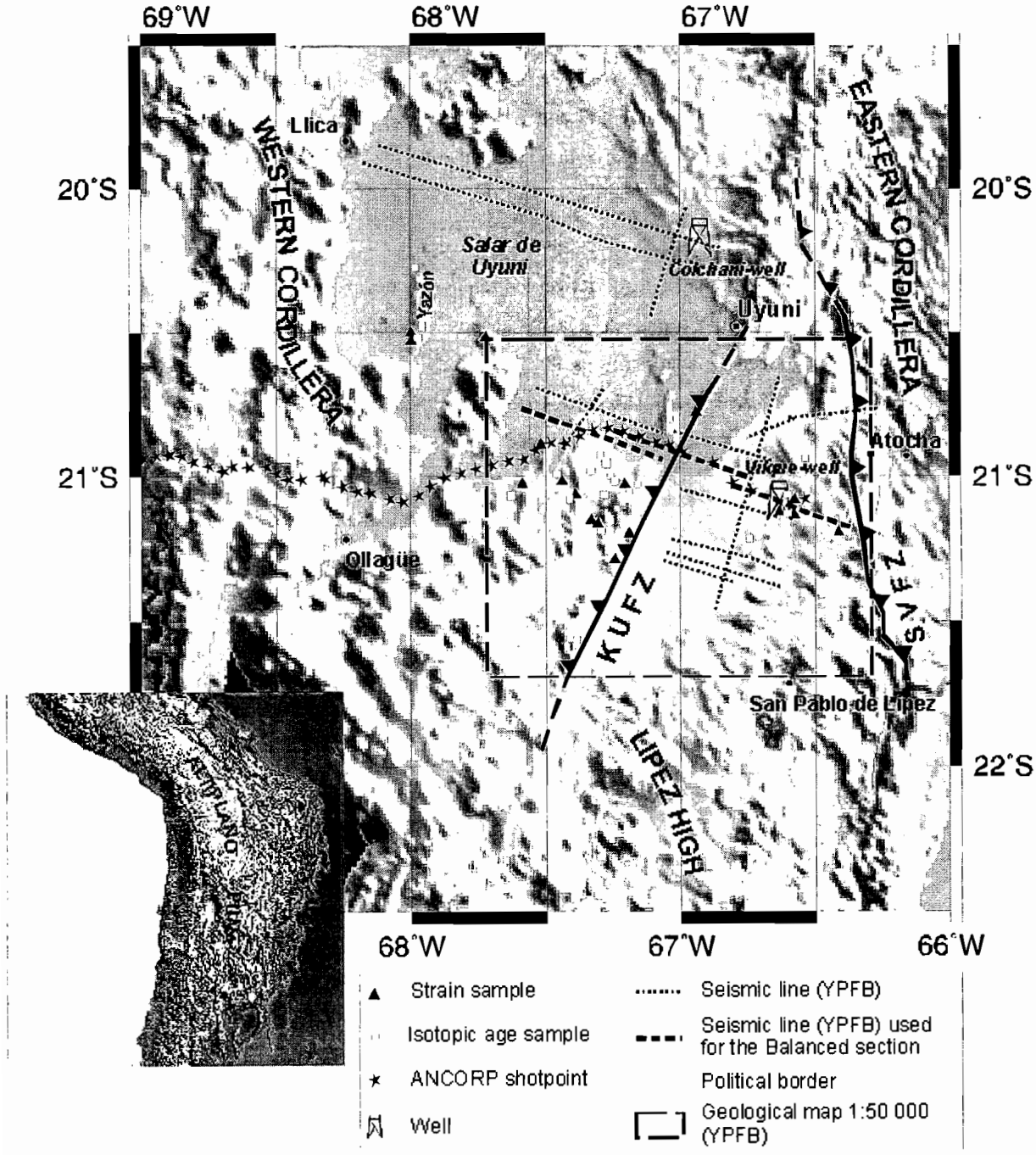

Fig. 1: Schematic map of the Southern Altiplano in Bolivia showing the geological and seismic database including sample and well locations and the outline of the geological map from YPFB (Bolivia). The Khenayani-Uyuni fault zone (KUFZ) divides the Southern Altiplano in the Eastern and Central Altiplano structural domain. The San Vicente fault zone (SVFZ) marks the boundary between the Altiplano and the Eastern Cordillera. The Lipez high marks the transition to the Argentine Puna.

NAVIDAD FORMATION: DELTAYC SEDIMENTATION THAT REFLECTS THE TECTONIC CHANGE DURING THE LOWER MIOCENE IN SOUTH AMERICA

Alfonso ENCINAS (1)

(1) aencinas@cec.uchile.cl

KEY WORDS: Bouma sequences, pumice, breccias, tectonic change

INTRODUCTION

The Navidad Formation was described by Darwin in 1846 (Darwin, 1900). Is a fosiliferous marine sequence 500 m thick of mudstones, siltstones, sandstones and conglomerates. Overlies granitoids of Paleozoic and Triasic-Jurasic age and underlies eolian and aluvial deposits and quaternary soils.

From a Sedimentological point of view at the base of the sequence there is a conglomerate formed by clasts of granitoids and mafic rocks. Some of this clasts have metric sizes. In the rest of the sequence the most important facies are those of masive sandstones and high energy paralel lamination sandstones. These are interbeded with mudstones and siltstones of centimetric and metric width. There are also facies of sandstones whit planar cross bedding and current ripples. This facies usually form Bouma sequences. Pumice clasts, mudstones rip up clasts, burnt wood clasts and more rarely, granitoids and mafic rock clasts in a sandstones or siltstone matrix are abundant. Concreccions esferic or ovoidal are abundant too. These have a carbonatic cement and inside them there are an abundant fosiliferous content. Sandstones have in many ocassions water-scape marks. There are also levels made of sedimentary breccias, slumpas and sinsedimentary faults.

The fosiliferous content is very abundat and consist of tree trunks and branches, leeves, bivalves, braquiopods, gastropods, solitary corals, shark theet and whales bones.

As regards the age of the formation there is some disagreetment; it has been described as late Oligocene to early Miocene based on macrofossils (Tavera, 1979), late middle to late Miocene based on ostracods (Osorio, 1976), and 19-10 Ma based on planktonic foraminifera (Martínez-Pardo, 1990)

CONCLUSIONS

The presence of numerous leaves and tree trunks fosils, masive sandstones, high energy paralel lamination, planar cross bedding, current ripples, water-scape marks, slumps and sedimentary breccias indicates that the Navidad Formation was deposited in the distal part of a delta complex with dominant turbiditic and gravity proceses. The base conglomerate whit oversized clasts and the presence of sinsedimentary breccias and faults indicate that there was an intense tectonic activity at the moment of the deposition. This tectonic activity was produced because of the transformation of Farellones plate, 25 Ma ago, into the Cocos and Nazca plates. This change was produced as a consequence of the Thetys sea clousure. This changed the organization of the earthe plates. The Farellones plate had a convergence direction NNE-SSW whit the Southamerican plate that

changed to an ortogonal convergence with the new Nazca plate. This gave rise to a much bigger compression changing from a distensive regime that dominated during the Oligocene, to a compresive one during the Miocene. This increase of the compression and an eustatic sea level rise between 25 and 10 Ma. was the cause of the sedimentation of the Navidad Formation.

The presence of many pumice rounded clasts, volcanic ash reworked by the sea and burnt wood clasts in the Navidad Formation indicate that an explosive volcanic activity was present during the deposition of this formation during lower Miocene. As the volcanic arc in this period, represented by Farellones Formation, was 80 km east is quite unlikely that this pumice clasts could travel that distance by the air nor that they could be transported by rivers due to the low resistance of pumice to transport. Nevertheless there is a small outcrop of volcanic lava known as Lavas las Patagua (Wall, R., 2001) about 20 km east of the coastal Navidad outcrops and with a K-Ar age of 18 Ma which is similar to that of the base of Navidad Formation. It is posible that this lavas are the reminder of a volcanic complex producer of the explosive volcanism responsible of the sedimentation of pumice within the Navidad Formation and the burning of woods. This burnt wood would be transported and sedimentated as burnt wood clasts. As this lava outcrop is situated in the intersection of two big faults is quite probable that the volcanism was controled by this faults.

Paleoclima of the Navidad Formation. Studies realized on plantonic foraminifera (Martínez-Pardo, 1990) suggest sea surface temperatures of 25°c. In terms of terrestrial climate the studies of fosil floras (troncoso, 1991; Hinojosa 2000) suggest temperatures between 15 and 21°c. and precipitation between 800 and 1200 mm. The present temperature and precipitation at this site is aproximately 13.5°c and 750 mm. respectively which are quite lower that the Miocene ones.

These dates of temperature and precipitation puzzles climatologists because the opening of the Drake Passage, based in magnetic and isotopic studies, was produced in the upper Oligocene (30-25 Ma). At this moment the Humboldt and Circumpolar Antactic current should have beggin and so should the termal isolation of Antarctica. The presence of a warm to tropical fauna during lower to middle Miocene (19 to 10 Ma) and a flora of a climate much warmer and rainy than the actual in the Navidad Formation indicate that the opening of the Drake passage was produced step by step during most of Miocene and lower Pliocene (magnetic anomalies 6 to 3) with subsidence processes by stages as a consequence of the sea floor spreading. The most important of this stages took place 10 Ma ago and in that moment the deep of the oceanic floor reached 2000 m. With this depth the water circulation was effective and so was the Humboldt current.

The age of 10 Ma coincide with the first register of the modern Psychrophera.

REFERENCES

-Darwin, C. 1900. Geological Observations on the Volcanic Islands and Parts of South America Visited During the Voyage of the H.M.S. Beagle: London, Ward, Lock and Col

- Hinojosa, L. F. 2000. Análisis fisonómico-foliar de las paleofloras del Mioceno de Chile Central: Magnitud del cambio climático Neógeno-Paleógeno, In XI Simposio Argentino de Paleobotánica y Palinología, Tucuman, Argentina, p. 48.

- Martínez- Pardo R., and Martínez-Guzmán R. 1997. Neogene Southeast Pacific Paleoceanography, the opening of the Drake Passage and the Humboldt Current history: The Chilean micropaleontological perspective. VIII Congreso Geológico Chileno, Antofagasta, p. 525-527

- Martìnez-Pardo, R. 1990. Major Neogene events of the Sutheaster Pacific: the Chilean and Peruvian record: Paleo-3, v. 77, p. 263-278.

- Osorio, R. 1976. Edad de la base de la Formación Navidad S.S. (Etchart, 1973) en Punta Perros, in Primer Congreso Geológico Chileno, p. C59-C66.

- Tavera, J. 1979. Estratigrafía y paleontología de la Formación Navidad, Provincia de Colchagua, Chile: Boletín del Museo Nacional de Historia Natural, vol. 36, 176 pag.

- Troncoso, A. 1991. Paleomegaflora de la Formación Navidad, Miembro Navidad (Mioceno) en el área de Matanzas, Chile Central Occidental. Boletín del Museo Nacional de Historia Natural, Chile, V. 43, p. 155-178

- Wall, R., Lara, L. 2001. Lavas Las Pataguas: volcanismo alcalino en el antearco andino del Mioceno Inferior, Chile Central. Revista Geológica de Chile, Vol. 28, N° 2, pag. 243-258.

ACTUAL EROSION BY RIVERS IN THE BOLIVIAN ANDES

Naziano FILIZOLA, Pascal FRAIZY, Jean Loup GUYOT, Frédérique SEYLER
Patrice BABY & Gérard HERAIL

IRD – LMTG, 38 rue des 36 ponts, F-31400 Toulouse

KEY WORDS : Erosion, Hydrology, Andes, Bolivia.

INTRODUCTION

In Bolivia, the Andean Mountain belt is very large and deformed by thin-skinned tectonics (Baby et al., 1997). The back arc orogenic wedge is formed by the Cordillera Oriental – which limits the Altiplano enigmatic high plateau (Rochat et al., 1999) - and the Subandean zone, and characterized by an elbow shape of the mountain range (Bolivian orocline) and high relief (several summits over 6000 m). It over thrusts and supplies its adjacent foreland sedimentary basin with sediments since upper Oligocene times. The present axis of the Bolivian orocline separates the High Amazonian drainage basin in the north from the Pilcomayo drainage basin in the south. Little data is available to measure the actual erosion of the Andes cordillera. However, the measurement of sedimentary yields at the hydrological stations makes it possible to estimate these actual rates of erosion and their geographical variability.

DATA AND METHODS

In the Andes of Bolivia, the data obtained at the hydrological networks of various national services (ENDE, SENAMHI, SEARPI) made it possible to select 42 gauge stations (Figure 1) including 23 on the Amazon River basin, 13 on the basin of the Paraguay River and 5 on the endoreic Altiplano basin. In spite of different observation times and durations, the great quantity of samples collected on the Andean rivers (28 167) allows a realistic estimate of sedimentary flows. With extreme altitudes of 170 m (station of piedmont) to 6400 m (tops of the Real Cordillera), the studied basins show very contrasted characteristics, with mean basin altitude varying from 1175 to 4925 m (Guyot et al., 1990, 1996). The selected hydrological stations drain nested basins, of variable area (from 160 to 81 300 km^2) and slope (from 7 to 37%). Basin area extraction followed the methodology described in Seyler et al. (in press). The GTOPO30 DEM, river network extracted from JERS 1 mosaic (TRFIC project) , digitalized maps, and D8 algorithm were used. The flow accumulation threshold has been chosen as the minimum area necessary to delineate the streams gauged. For each delineated basin, the slope has been calculated, and used in the statistical exploration. Processing involved Arc-View, Erdas Imagine, and avenue scripts developed by the University of Texas at Austin (Maidment et al., 1997).

These basins, distributed on the whole of the Andean domain of Bolivia, are subjected to very contrasted climates: of 350 mm/yr in the arid regions of the altiplano, with more 3800 mm/yr in the Andean piedmonts of the Amazonian basin, and present runoff coefficients from 10 to 72% (Roche et al., 1992). The lithological index was calculated by using the Probst indices. The lithology of each basin was extracted from the geological map of Bolivia by using a SIG. The forest cover index (from to 0 to 100% depending of the sub-basin) was also extracted with the SIG from the Bolivian chart of vegetation.

RESULTS

The results obtained show a very strong heterogeneity, with suspended sediment concentrations varying from 46 to 19600 $mg.l^{-1}$ during the hydrological cycle, and a rate of current erosion varying from 21 to 18200 $t.km^{-2}.yr^{-1}$ according to the basins (Guyot et al., 1990, 1996). Using a forward stepwise multiple regression analysis with the whole dataset, the significant control variables are only drainage area and slope, with a multiple regression coefficient r=0.53. The same trend was observed with a smallest dataset not including the Altiplano Rivers (Aalto et al., in press).

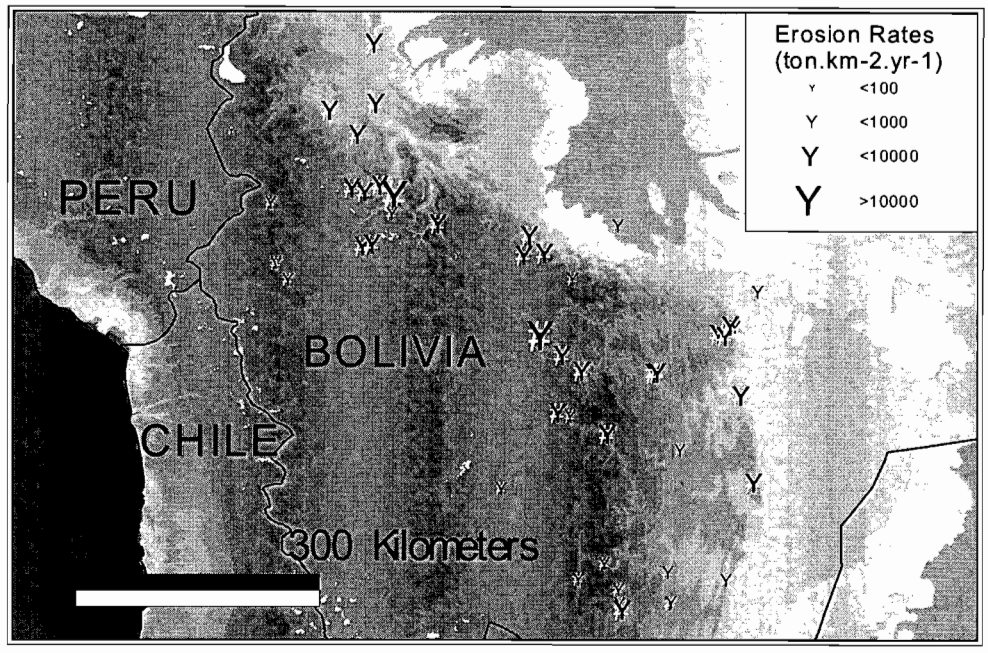

Figure 1 : Gauge stations location in the Bolivian Andes, with Erosion Rates values.

Table 1 : Drainage basin characteristics and Erosion rates

	Code	River	Gauging Station	Area (km2)	Slope (%)	Rainfall (mm.yr-1)	Runoff (%)	Lithologic Index	Forest Cover (%)	Erosion Rate (t.km-2.yr-1)
Altiplano	ESC	Suchez	Escoma	3 100	10	498	16	24	0	21
	TIW	Tiwanaku	Tiwanaku	320	7	669	22	36	0	107
	MAU	Mauri	Calacoto	9 420	20	450	16	16	0	640
	CAL	Desaguadero	Calacoto	9 770	11	580	29	36	0	59
	ULL	Desaguadero	Ulloma	22 800	20	510	20	28	0	289
Amazonas	MAP	Mapiri	A.Quercano	9 400	22	1 284	42	7	44	3 920
	COR	Coroico	Santa Rita	4 700	26	1 886	57	6	78	1 620
	VBA	Tamampaya	V.Barrientos	1 900	31	1 283	46	6	9	4 120
	CAJ	La Paz	Cajetillas	6 500	32	808	43	10	1	18 200
	COT	Cotacajes	Cotacajes	5 600	34	1 129	41	7	0	7 250
	AIN	Alto Beni	A.Inicua	29 900	37	1 366	47	11	38	3 850
	AB	Beni	A.Bala	68 000	37	1 615	50	12	57	3 220
	LOC	S.Isabel	Locotal	200	19	2 610	69	8	84	3 340
	ICO	J.Corani	Icona	2 300	17	3 450	67	7	70	4 940
	PAL	E.Santos	Palmar P.	160	21	3 470	72	7	97	6 660
	SEH	Ivirizu	Sehuencas	420	22	1 400	59	6	16	227
	PV	Ichilo	P.Villarro	7 580	21	3 800	65	20	99	712
	ANG	Pirai	Angostura	1 420	12	1 000	24	6	100	2 080
	TAR	Pirai	Taruma	1 590	12	1 050	15	8	100	840
	BEL	Pirai	Belgica	2 880	12	1 300	10	17	86	792
	AMO	Caine	A.Molinero	9 200	21	654	20	13	0	13 700
	HUA	Chayanta	Huayrapata	11 200	27	664	35	9	0	1 260
	PAR	Grande	P.Arce	23 700	28	659	28	10	0	6 500
	PNA	Grande	P.Nava	31 200	28	650	34	10	0	6 620
	MIZ	Mizque	P.Nava	10 800	21	653	20	7	3	1 310
	PAZ	Azero	P.Azero	4 360	21	780	19	8	10	520
	AP	Grande	Abapo	58 900	28	750	18	10	18	2 110
	SAN	Parapeti	S.Antonio	7 500	17	800	19	24	83	2 590
Paraguay	ATA	Pilcomayo	A.Talula	6 340	23	480	23	8	0	1 910
	NUC	Cachimayu	Nucchu	1 600	19	720	23	14	0	661
	VQU	Pilcomayo	V.Quemada	13 200	24	490	20	10	0	1 670
	SLE	Yura	S.Leon	4 200	17	370	13	9	0	106
	ELP	SJ.Oro	El Puente	20 100	20	345	18	15	0	120
	CHI	Pilaya	Chillcara	42 900	23	360	11	12	0	323
	SJO	Pilaya	S.Josecito	47 500	32	390	14	11	5	645
	VIL	Pilcomayo	Villamontes	81 300	32	478	14	12	15	890
	ERI	S.Ana	Entre Rios	290	11	912	27	14	43	223
	PAJ	Pajonal	Entre Rios	220	13	917	30	16	66	499
	CAN	Chamata	Canasmoro	230	12	834	37	11	6	197
	OBR	Guadalquivir	Obrajes	920	19	810	30	14	2	439
	SJA	Tolomosa	S.Jacinto	460	21	1 020	45	18	0	3 340

Using the same forward stepwise multiple regression analysis, but separating in different geographical groups, the multiple regression coefficients present better values, and it becomes possible to calculate a rate of erosion for each sub basins (Figure 2). For the Altiplano basin rivers (r=1.00), the control factors are drainage area, slope and rainfall. For the Pilcomayo basin rivers (r=0.98), the control factors are also drainage area, runoff and lithologic index. In the Amazon basin, erosion rates in the Beni (r=0.96) and Chapare (r=0.99) basins are controlled by rainfall and runoff, whereas in the Grande (r=0.97) basins, these erosion rates depend of lithologic index and forest cover.

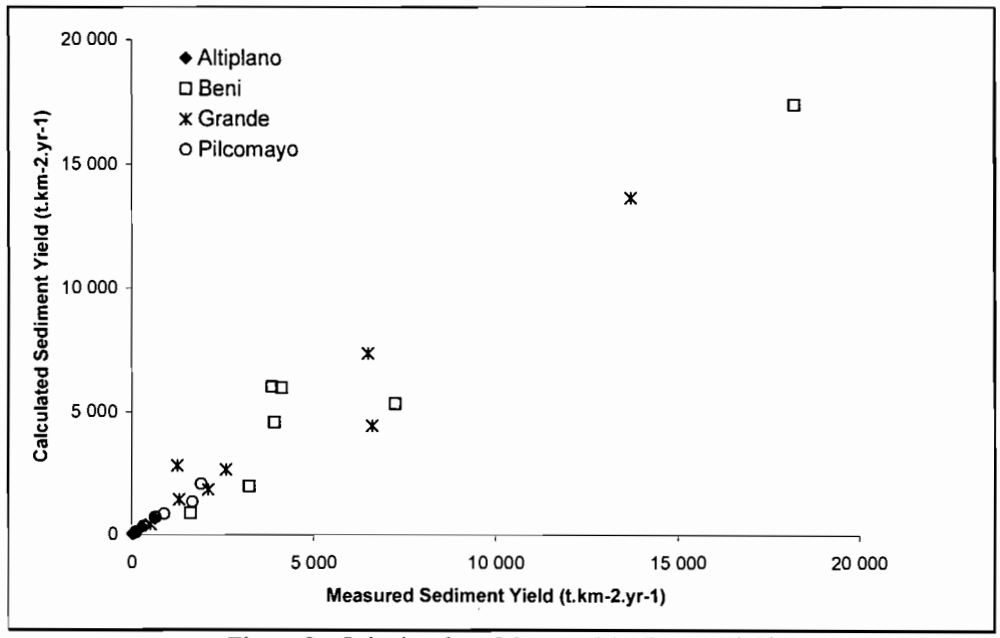

Figure 2 : Calculated vs. Measured Sediment Yield

For each geographical group, the largest basin corresponds either to the Andean piedmont (Angosto del Bala for the Beni river, Abapo for the Grande river, Villamontes for the Pilcomayo river), or to the station of Ulloma on Altiplano. The compared hypsometry of these four basins show different stages of evolution (Fig. 3). The Altiplano basin presents a more advanced stable profile, with erosion stopped by the regional endoreism. The Beni, Grande and Pilcomayo basins correspond to different levels of erosion, with a positive gradient from South towards North: profile of Beni River being more advanced than that of Pilcomayo.

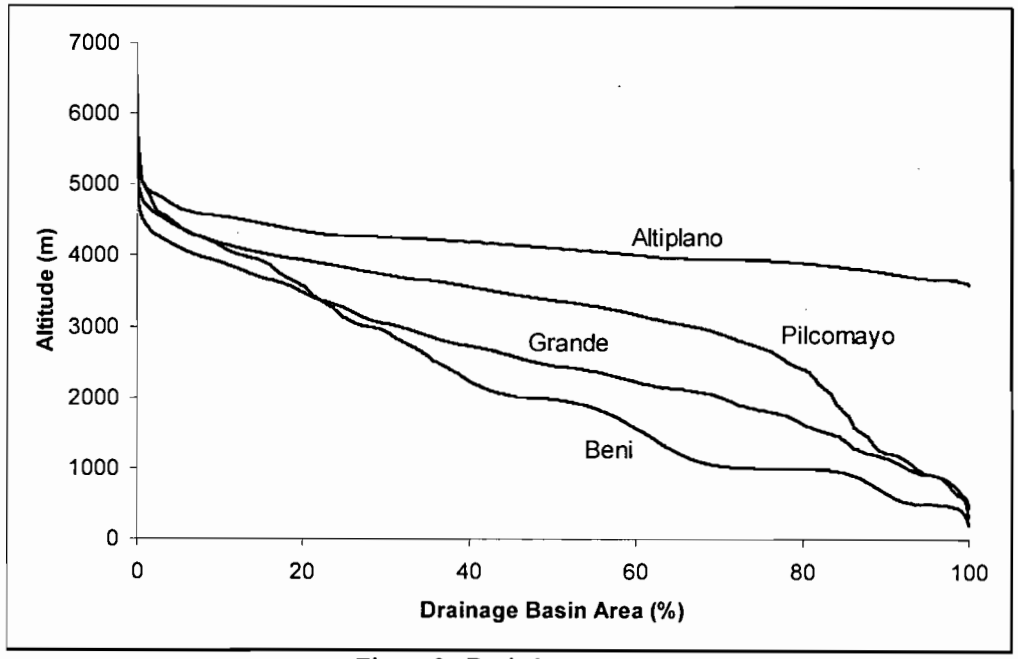

Figure 3 : Basin hypsometry

It is interesting to compare the degree of evolution of the basin with the current rate of erosion measured at the hydrological gauging stations. For that, we calculated the volume of the basin comprised between the today curve and a theoretical initial profile. Considering the current rates of erosion, the time that had been necessary to obtain the observed profiles varies from 1.4 to 2.4 MY. The results (fig. 4) show a good adjustment between current measurements (few years observation) and evolution of topography related to long scales of time.

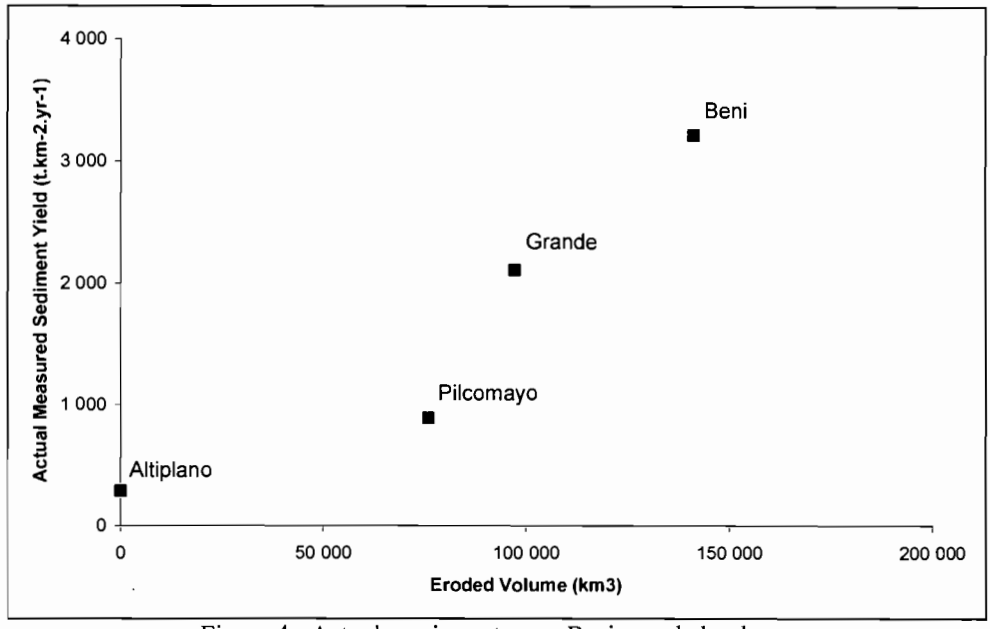

Figure 4 : Actual erosion rates vs. Basin eroded volume

REFERENCES (alphabetical order)

Aalto R., Dunne T., Guyot J.L. in press. Geomorphic controls on Andean denudation rates. Journal of Geology.

Baby P., Rochat P., Mascle G., Hérail G. 1997. Neogene shortening contribution to crustal thickening in the back arc of the Central Andes. Geology 25: 883-886.

Guyot J.L., Calle H., Cortes J., Pereira M. 1990. Transport de matières dissoutes et particulaires des Andes vers le Rio de La Plata par les tributaires boliviens (rios Pilcomayo et Bermejo) du Rio Paraguay. Hydrological Sciences Journal, 35(6), 653-665.

Guyot J.L., Filizola N., Quintanilla J., Cortez J. 1996. Dissolved solids and suspended sediment yields in the Rio Madeira basin, from the Bolivian Andes to the Amazon. Erosion and Sediment yield : Global and Regional Perspectives, IAHS Publ. 236, 55-63.

Guyot J.L., Roche M.A., Noriega L., Calle H., Quintanilla J. 1990. Salinities and Sediment Transport in the Bolivian Highlands. Journal of Hydrology, 113, 147-162.

Maidment D.R., Reed S.M., Akmansov S., McKinney D.C., Olivera F., Ye Z. 1997. Digital atlas of the world water balance. Center for Research in water Resources, University of Texas at Austin.

Rochat, P., Hérail G., Baby P, Mascle G. 1999. Bilan crustal et contrôle de la dynamique érosive et sédimentaire sur les mécanismes de formation de l'Altiplano. *C. R. Acad. Sci. Paris, Sciences de la terre et des planètes/ Earth and Planetary Sciences,* **328**: 189-195.

Roche M.A., Fernandez C., Aliaga A., Peña J., Salas E., Montaño J.L. 1992. Balance hídrico de Bolivia. Publ. UNESCO-PHICAB, 16 p.

Seyler F., Muller F., Cochonneau G., Guimarães V., Guyot J.L. (in press). Watershed delineation of the Amazon sub-basins system using GTOPO30 DEM and a drainage network obtained from JERS SAR images. Hydrological processes.

CENOZOIC ANDEAN PALEOENVIRONMENTS AND TECTONIC HISTORY: EVIDENCE FROM FOSSIL MAMMALS

John J. FLYNN (1)

Dept. Geology, The Field Museum, 1400 S. Lake Shore Dr., Chicago, IL 60605 USA;
(jflynn@fieldmuseum.org)

KEYWORDS: fossil mammals, paleontology, tectonics, Andes, Cenozoic, paleoenvironment

INTRODUCTION

Fossil mammals have long been one of the most useful tools for establishing the age of Cenozoic terrestrial sequences, particularly in those that cannot be dated radioisotopically. Mammals also are key sources of data for understanding evolution, documenting faunal change through time, and assessing environmental transformations. In contrast, tectonic studies typically have relied on geophysical, structural, and geochemical data to constrain deformation and uplift histories. For almost 200 years, knowledge of South American fossil mammals has been derived almost exclusively from the remarkable, but gap-riddled record from Patagonia and other Argentine lowland, high-latitude sites. But broader availability of data from the tropics and tectonically-active regions are required to understand continent-wide or Andean patterns and their possible causal processes. Similarly, a precise and reliable terrestrial geochronology, integrating magnetostratigraphic and radioisotopic calibration with the biochronology of South American Land Mammal "Ages" (SALMAs), had not been available until very recently[1]—this is an essential prerequisite to accurately determining timing and duration of events *throughout* the continent (e.g. refs. 1-4), and employing data from fossil mammals in more extensive tectonic, paleoecologic or evolutionary analyses. As Andean fossil mammal discoveries continue increasing, integrating paleontological data with those typically used in tectonic analyses can yield new or deeper insights into both.

South America has long been considered a model system for studying "evolution in isolation," as the continent was basically an island from its final split from Africa during Gondwana fragmentation by 80 Ma, until its reconnection to North America ~3.5 Ma. By the mid-1900s, G.G. Simpson had developed a "3-stratum" concept of South American Cenozoic mammal evolution and environmental change during isolation, and it remains a reasonable basic summary today. There is growing evidence, however, of much greater complexity in the geological connections and the biotic interchanges than had been believed, and that Cenozoic faunas record and responded in more complicated ways than had been envisioned to both global and regional biogeographic, climatic, tectonic, sea level, ecological, and environmental changes (e.g., refs. 1, 4-6).

CONCLUSIONS

This paper focuses on review of paleoenvironmental and tectonic inferences derived from recent analyses of Andean mammal faunas, emphasizing those from Chile. In broad terms, South American environments were largely forested across the entire continent in the early Cenozoic, with two subsequent phases of widespread habitat change during the middle (Eo-Olig.; earliest global appearance of widespread open, grassland/woodland habitats) and late (Plio-Pleist.; glacial-interglacial oscillations, increased aridity, pulsed shifts of grassland-forest biomes, and major faunal reorganization and extinctions as part of the Great American Biotic Interchange ["GABI"] following the final formation of the Isthmus of Panama connecting North and South America) Cenozoic. These phases appear to have marked relatively rapid transformations, likely in response to more global rather than regional causes, although the key driving-forces, duration, and "tempo" or rate of change are still being clarified. The large-scale faunal provinciality observed today, in which there is marked "endemism" (species restricted to certain regions) and differentiation (tropical biotas share very few species or genera with high-latitude faunas, and montane assemblages differ markedly from lowland faunas) due to climatic and elevational gradients and barriers, existed by the middle to late Miocene[3]. New data from Andean and foreland sequences suggests that regional or continent-wide provinciality may have been present earlier, by the Eocene and perhaps even within the earliest parts of the Cenozoic[2,4-6]. Our current knowledge, greatly enhanced by discovery of the first South American assemblages of transitional Eo-Oligocene age (Andean [1-2,4,7-18]) also suggests that the evolutionary events of "stratum 2" (dispersal of rodents and primates to South America, "modernization" of mammal groups and entire mammalian communities, and appearance of first extensive grassland habitats [in South America only]) occurred rapidly, by the earliest Oligocene. These changes almost certainly were caused by dramatic geological, climatic, and environmental changes that occurred across the Eocene/Oligocene boundary (~34 Ma) interval.

Periodically, smaller-scale changes were superimposed on the large-scale transformations, including several mid-Cenozoic episodes of poleward expansion of forested habitats as late as the middle Miocene (indicated by presence of obligate humid forest-dwelling primates as far south as 50° in southern Patagonia) and expansion and contraction of major epicontinental seaways along the Andean foreland during the Eocene and Miocene. Of particular note is that Andean data are crucial to resolving the age and extent of some of these smaller-scale fluctuations, as well as testing models for the effects of larger-scale changes.

Exceptionally diverse or important Tertiary mammal faunas from the Andean highlands are now known from Chile, Bolivia, Colombia, Ecuador and elsewhere. These range in age across the early Paleocene (Tiupampa, Bolivia[19-21]), Eocene-Oligocene boundary interval (Tinguiririca, Chile; part of a series of sites in the Abanico Formation of central Chile spanning the Eocene-middle Miocene[1-2,4,7-18, 22-25]), early Oligocene (Salla, Bolivia[13,26-29]; with other important Miocene-Pliocene sites elsewhere in the Bolivian Altiplano), early Miocene (Pampa Castillo, Patagonian Chile[30]; Chucal, Altiplano, Chile[31-34]), and middle Miocene (LaVenta, Colombia[3,35-36]). In contrast to most lowland temperate sequences, some of these are precisely dated because of their Andean setting and associated abundance of volcaniclastics. A few others, especially in Bolivia[14,27,37-38] and Colombia[3,35], include paleobotanical, sedimentological and stable isotope evidence complementing mammal-based paleoenvironmental inferences.

Discussion will present exemplar "case-studies" of published and in-progress work on key regions and conclusions. Perhaps the best-sampled temporal interval in the Andes is now the early-middle Miocene (~20-11 Ma), with important Andean assemblages complementing the classical record from foreland and coastal

Argentina now known from southern Chile (47°S) to north-central Colombia (3°N), a range of some 50° of latitude. At the southern extreme, the diverse, late early Miocene (Santacrucian SALMA, ~16-17.5 Ma) Pampa Castillo fauna[30] of Chile is the westernmost high latitude mammal fauna known from South America, and its similarity to coastal Santacrucian faunas suggest similar habitats[39] (increasing aridity, extensive grasslands) across all of Patagonia. The mammal fauna transitionally overlies fossiliferous marine strata, documenting the NW-most extent and last significant incursion of Patagonian early Miocene Atlantic epicontinental seaways, and constrains initiation of uplift in this region by 16 Ma in response to tectonic events associated with the nearby Chile Margin Triple Junction.

At the northernmost extreme, the tropical LaVenta fauna[3,35-36] (13.5-11.8 Ma) documents marked provinciality (similar to modern systems in sharp "icehouse" latitudinal climatic gradients) by the middle Miocene, presence of extensive and varied forest biotopes throughout (rather than the expansive savanna grasslands inferred in previous studies), and environmental regimes of high rainfall (>1,500-2,000 mm/yr) and low seasonal aridity. The fauna and associated geochronologic studies also provide new insights into Andean tectonics, including dramatic basin subsidence shortly before 13.5 Ma, a short and rapid phase of uplift and volcanism in the Central Cordillera at about 12.9 Ma coincident with initiation of uplift in the Eastern Cordillera at 12.9 Ma (completed by 11.9 Ma) and major depositional changes in the intervening Magdalena basin, and some of the fastest sediment accumulation rates observed in any tectonic setting. Significant global and regional plate tectonic and sea level changes may be coincident with, and related to, the major changes in the terrestrial system beginning at 12.9-11.8 Ma.

Intervening Andean Miocene sequences occur throughout southern-central Chile (Abanico Formation of Ríos Maipo, Las Leñas, Teno, and Upeo[22,24]; and equivalents at Lonquimay[40] and Laguna del Laja [newly discovered by the author and colleagues]), the first mammal assemblage from the Chilean Altiplano (Chucal, Santacrucian? SALMA[31-34]), and others from the Bolivian Altiplano[37] and Ecuador[3]. The 4,500 m high Chucal site better constrains the age of the strata, timing of deformation, and initiation of major uplift in the Chilean Altiplano. Preliminary study suggests that this region probably was already an intermontane basin, but not yet extremely high, with a mixed habitat of grasslands and significant riparian regions flanked by forests and woodlands. An unusual hoofed herbivore group (mesotheres) are abundant and diverse here and in the Bolivian Altiplano, but rare elsewhere (Patagonia, LaVenta), while chinchilline rodents (a montane group today) appear to originate within this Andean region, 10-15 million years before they appear elsewhere. Miocene Altiplano faunas (Chile and Bolivia) are similar compositionally, but differ from contemporaneous faunas in both the low-latitude tropics (Colombia) and the high-latitudes (Patagonia)—these patterns may be due to marked regional provinciality in the Miocene, which in turn may be the result of significant global climate changes, Andean tectonics, and associated paleoenvironmental changes[3-4].

Some of the most interesting Andean data are derived from a growing array of sites in unusual (relative to standard mammal-preserving environments) volcaniclastic deposits of central Chile. The first assemblage discovered in this sequence, the Tinguiririca Fauna[1-2,4,7-18, 22-25], documents a new earliest Oligocene biochronologic interval, suggests some faunal provinciality by the Oligocene or earlier, dramatically alters understanding of the age and tectonic history of a large Andean lithosome (Abanico Formation; part of Darwin's "Porfiritica"), includes the oldest South American rodent (indicating origin from African ancestry and Eocene transoceanic dispersal), and yields key insights into environmental change in South America around the E/O

boundary. Paleoenvironmental analyses reveal some non-analog aspects of middle Cenozoic South American localities, that a relatively dry habitat was present at Tinguiririca, and that the most dramatic shift in Cenozoic South American paleoecology and paleoenvironment occurred by the earliest Oligocene. The data provide compelling indications that open habitat, grassland/woodland environments flourished 15-20 million years earlier in South America than on other continents, likely related to the E/O boundary and earliest Oligocene climatic "deterioration", and associated paleoenvironmental events. The younger fauna from Salla, Bolivia[14,26-29] complements this record of change, and documents some intracontinental provinciality by the early Oligocene.

The series of other mid-Cenozoic localities in central Chile represent at least 6 temporal intervals, and are just beginning to be studied in similar detail to Tinguiririca. For example, the Las Leñas fauna[22] documents monkeys in the Colhuehuapian (20 Ma) of the Andes, in addition to Colhuehuapian and Santacrucian primates previously reported from higher latitudes, supporting one or more early-middle Miocene climatic ameliorations and poleward spread of major forested habitats (New World monkeys are limited to tropical, forested environments). Further analysis of the Las Leñas/Cachapoal area has yielded a new regional model of early Cenozoic extensional tectonics followed by later compression, inversion and uplift[25]. Radioisotopic and biochronologic data suggest that deposition began by the earliest Oligocene, more likely within the Eocene, and that compression and uplift postdated the middle Miocene[23,25]. Similar thrusting has been documented in the Abanico Formation along the Río Tinguiririca valley well to the south, although it is of uncertain timing relative to that farther northward[2,9,11-12,41-43].

REFERENCES

[1]Flynn & Swisher 1995. In Berggren et al. (eds.) *SEPM Spec. Pub.* 54:317-333. [2]Wyss et al. 1994. *Amer. Mus. Novitates* 3098:1-31. [3]Kay, Madden, Cifelli, Flynn (eds.) 1997. *Vertebrate Paleontology in the Neotropics.* Smithsonian Inst. Press., 592 pp. [4]Flynn & Wyss 1998. *Trends Ecol. Evol.* 13:449-454. [5]Pascual & Ortiz J. 1990. *J. Human Evol.* 19:23-60. [6]Pascual et al. 1996. *Münchner Geowiss. Abh. (A)* 30:265-319. [7]Wyss et al. 1990. *J. Vert. Paleo.* 10:518-522. [8]Wyss et al. 1993. *Nature* 365:434-437. [9]Wyss et al. 1996. *PaleoBios* 17:13-27. [10]Charrier et al. 1990. *2º Symp. Terciario Chile,* Actas:73-84. [11]Charrier et al. 1994. *7º Cong. Geol. Chileno,* Actas II:1316-1319. [12]Charrier et al. 1996. *J. S. Amer. Earth Sci.* 9:393-422. [13]Hitz 1997. *Ph.D. thesis.* U. California-Santa Barbara.
[14]Hitz et al. 2000. *Fieldiana* 42:1-26. [15]Flynn & Wyss 1999. *J. Vert. Paleo.* 19:533-549. [16]Croft 2000. *Ph.D. thesis.* U. Chicago. [17]Croft 2001. *Diversity and Distributions* 7:271-287. [18]Reguero et al. in press. *Fieldiana.* [19]De Muizon et al. 1997. *Nature* 389:486-489. [20]De Muizon 1991. In Suarez-Soruco (ed.), *Rev. Téc. Y.P.F.Boliv.*:575-624. [21]Gayet et al. 1991. In Suarez-Soruco (ed.), *Rev. Téc. Y.P.F.Boliv.*:303-433. [22]Flynn et al. 1995. *Nature* 373:603-607. [23]Flynn & Wyss in press. *Amer. Mus. Bulletin.* [24]Charrier et al. 1997. *8º Cong. Geol. Chileno,* Actas:465-469. [25]Charrier et al. 2002. *J. S. Amer. Earth Sci.* [26]MacFadden et al. 1985. *J. Geol.* 93:223-250. [27]MacFadden et al. 1996. *Palaios* 11:319-327. [28]Kay et al. 1998. *J. Vert. Paleo.* 17:189-199. [29]Kay et al. 1999. *Proc. Nat. Acad. Sci. US* 96:13235-13240. [30]Flynn et al. 2002. *J. S. Amer. Earth Sci.* 15(3). [31]Flynn et al. 2002. *J. Vert. Paleo.* 22:200-206. [32]Charrier et al. 1994. *7º Cong. Geol. Chileno,* Actas I:430-433. [33]Charrier et al. 1999. *Fourth ISAG*:155-158. [34]Charrier et al. 2000. *IX Cong. Geol. Chileno,* Actas I:763-767. [35]Hoorn et al. 1995. *Geology* 23:237-240. [36]Kay & Madden 1997. *J. Human Evol.* 32:161-199. [37]MacFadden et al. 1994. *Palaeogeog., Palaeoclimat., Palaeoecol.* 107:257-268. [38]Gregory-Wodzicki et al. 1998. *J. S. Amer. Earth Sci.* 11:533-560. [39]Tauber 1997. *Ameghiniana* 34:517-529. [40]Croft et al. submitted. *Revista Geol. Chile.* [41]Godoy & Lara 1994. *7º Cong. Geol. Chileno,* Actas II:1344-1348. [42]Godoy et al. 1999. *Tectonophys.* 306:217-236. [43]Sempere et al. 1994. *Tectonophys.* 229:251-264.

INSTABILITY OF SOUTHERN ANDEAN STRAIN DURING THE LAST 25 Ma

[1]Andrés FOLGUERA, [1]Victor A. RAMOS, [2]Daniel MELNICK

[1]Laboratorio de Tectónica Andina, Universidad de Buenos Aires, Ciudad Universitaria, Pabellón II, (1428) Buenos Aires, Argentina. [2]Universidad de Concepción, Departamento de Geología.
(email: folguera@gl.fcen.uba.ar, andes@gl.fcen.uba .ar, Dmelnick@udec.cl)

KEY WORDS: Southern Central Andes, Patagonian Andes, Strain Partitioning, Oblique Subduction.

STRAIN PARTITIONING ALONG THE SOUTHERN ANDES TODAY

Strain partitioning defines the geometry of orogenic belts and this geometry reveals the orogen-scale dynamics of the deformation. The Andes at 38°S represent a transitional zone between a high, wide area of deformation to the North identified as the Austral Central Andes (Ramos et al., in press) and a low, narrow belt to the South, the Northern Patagonian Andes (Fig. 1). The latter are characterized by a strong strike and dip-slip deformation along the arc (Lavenu y Cembrano, 1999) and no retroarc seismicity (Figs. 1 and 2–A). The Austral-Central Andes are known for their important intraplate seismicity along the orogenic front (Fig. 1). The strike-slip axial system of the Northern Patagonian Andes is known as the Liquiñe-Ofqui fault zone and presents dextral offset in a transpressive setting along most of its length (Fig. 2–A). The Eastern Central Valley of Chile and the Barreal-Calingasta Valley concentrate the main locus of movements parallel to the trench, in the Austral Central Andes (Figs. 1 and 2–C). Both areas are developed in the inner domains of the Andean orogen. Construction of high and wide mountains in an oblique convergent subduction setting only seems to be possible when partitioning becomes large.Otherwise deformation stays at the arc line and the orogenic front does not penetrate towards the retroarc.

The extension developed in the Northern Patagonian Andes (37°-40°S) 5 million years ago after a period of orogenic deformation during the Upper Miocene (Ramos y Folguera, 1998; Folguera et al., 2001), is associated with the steepening of the Nazca plate while the volcanic arc shifts to the trench (Stern, 1989; Ramos, 1998). However, the fact that this process is restricted to a latitudinal band between the Central Andes and the Patagonian Andes seems to indicate that there exists some kind of local process controlling this tectonic setting (Fig. 2).

Extension would be a necessary transitional step between highly imbricated systems in the retroarc, linked to highly partitioned segments of the cordillera and systems without active shortening in the retroarc in a lowly partitioned setting (Fig. 2) (Folguera et al., 2001).

STRAIN PARTITIONING THROUGH TIME, RELATED TO OCEAN FLOTABILITY

The Northern Patagonian Andes, between 37° and 46°S, present a striking feature : A wide area of Upper Paleogene deformation in the foreland of the Andean region, not associated to upper crustal intraplate

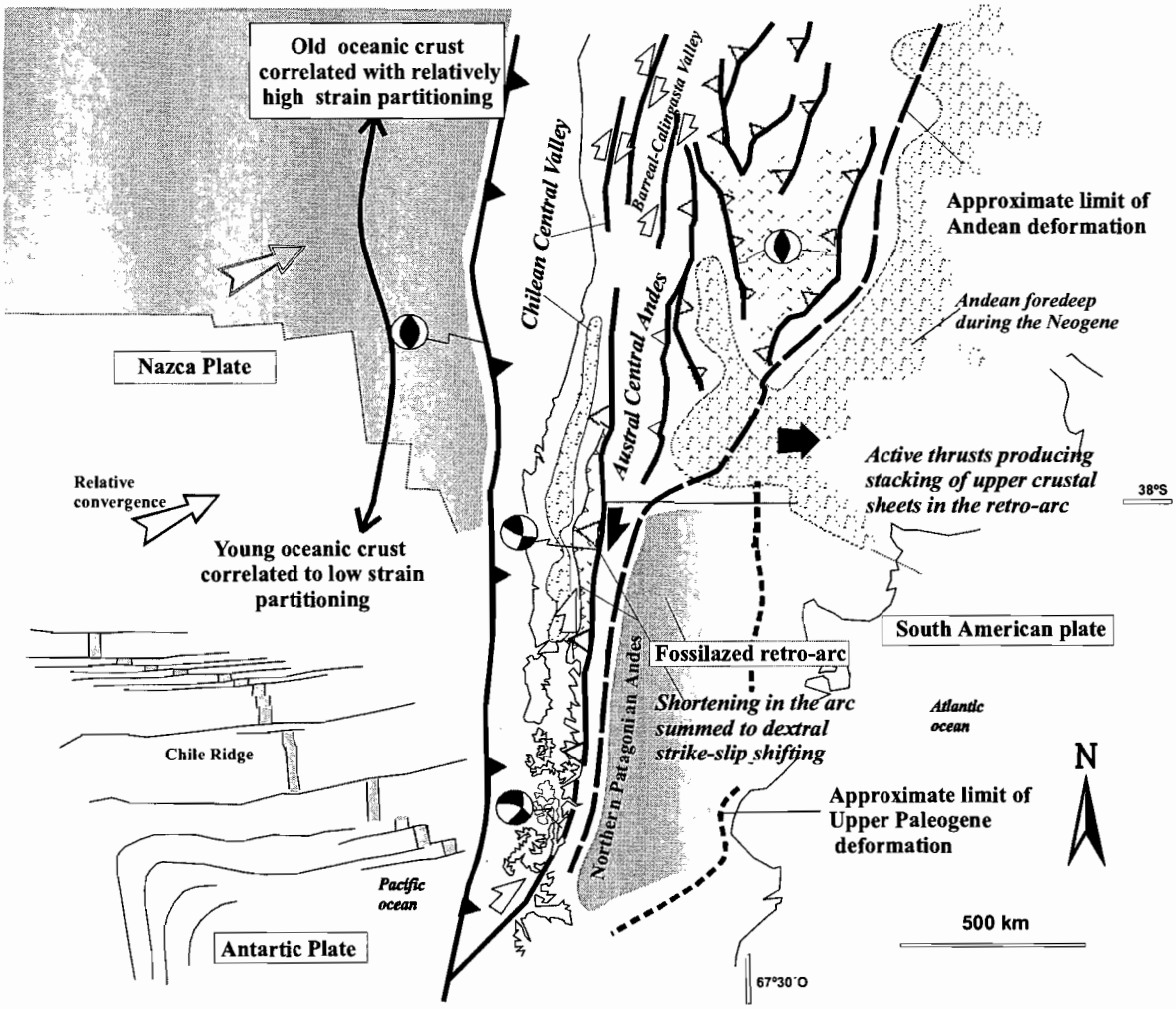

Figure 1: Strain partitioning distribution along the Southern Andes, as a function of oceanic age.

seismicity (Fig. 1). Such a fossil-imbricated system is not easy to fit with the present geodynamic setting of Western Patagonia. The present Central Andes, north of 38°S, could be an analogue of the retroarc Patagonian dynamics that existed approximately 15 million years ago. This analogy could be explained with the current picture: Strain partitioning along different segments plays an important role in defining areas of stacking of upper crustal sheets (Lavenu and Cembrano, 1999), and partitioning is also strongly correlated with the age of the subducting ocean floor.

As the ocean floor configuration along the Chilean trench changed with time, following the collision of the Chile ridge to the North (Fig. 1), the partitioning scheme significantly varied. The ancient areas of upper crustal shortenning became not active in a low strain partitioned setting.

STRAIN PARTITIONING THROUGH TIME, RELATED TO BENIOFF'S ZONE GEOMETRY

The Andes between 36° and 39°S were built by a broad range of processes during the last 25 Ma. These processes can be classified in two alternating types: periods of parallel to trench–strained homogeneous shear zones, encompassing areas hundreds of kilometers wide (Fig. 2–A, 2–B1), and periods of discrete strike-slip

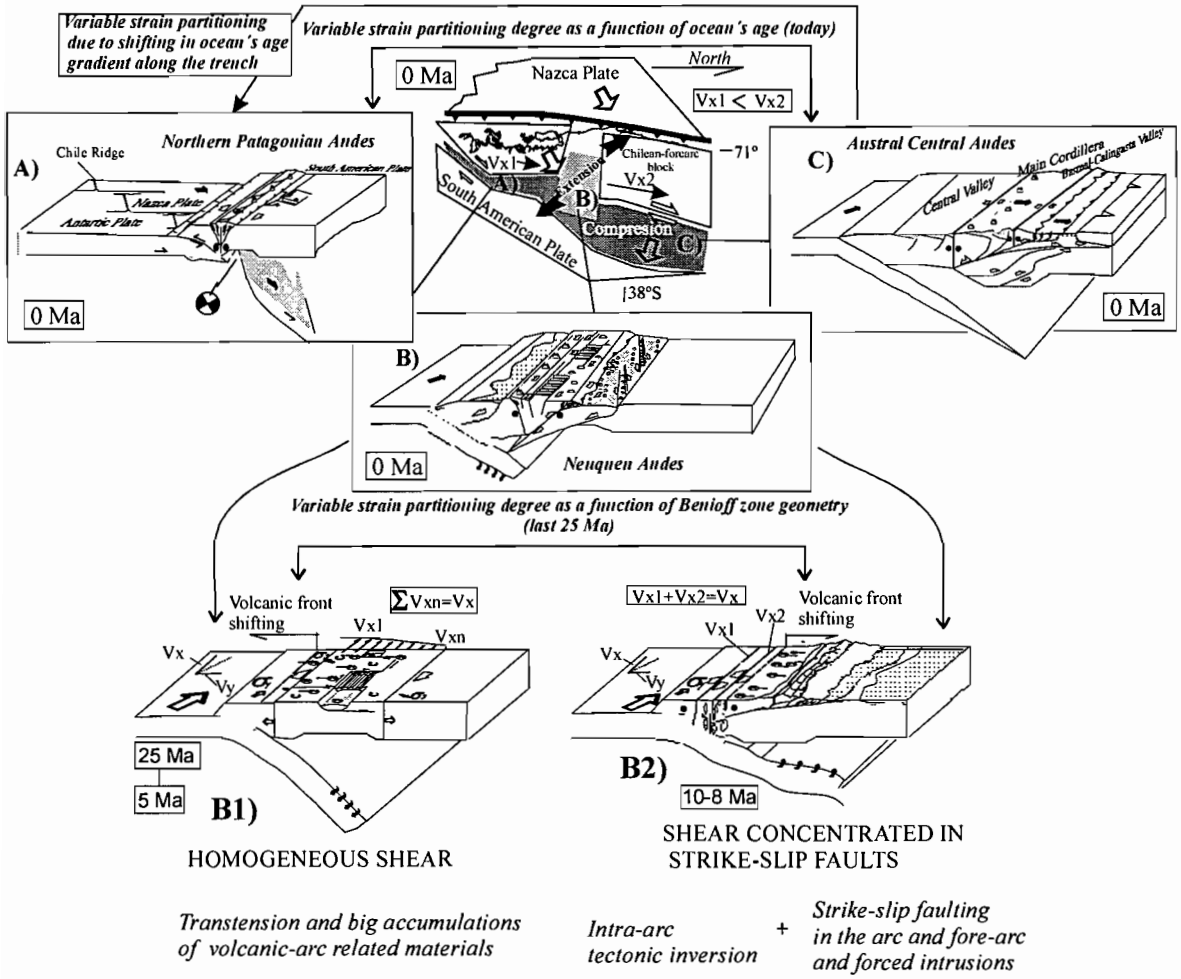

Figure 2: Variability of strain partitioning degree and spectrum of mechanical responses present and pastimes

fault displacements in the orogenic inner domains associated with uplift of retro-arc mountains constructed by stacking of upper crustal sheets (Fig. 2–C, 2–B2).

Transtension dominated the upper crust at 36°–39°S, between 25 and 15 Ma and the arc was the locus of small volcanogenic basins in a belt over 100 kilometers wide perpendicularly to the trench (Jordan et al., 2001) (Fig. 2–B1). Later, at 12-10 Ma, the arc concentrated the intrusions of large volumes of magma along strike-slip lithospheric systems (Hervé et al.,1993), and basin formation was inhibited, while the retro-arc was deformed in a pure shear setting, which triggered basin inversion (Fig. 2–B2) . Finally, after 5 Ma conditions became more alike to those at 25-15 Ma, in which homogeneous transtension affected broad areas over 50 kilometers wide (Fig. 2–B1).

Strain partitioning controls the distribution of the shear component, which is linked to the parallel component of convergence, either in discrete or broad areas of deformation, therefore defining the availability of basin formation processes along the arc.

Steepening and flattening of the Wadati-Benioff zones locally controlled the strain partitioning behavior of the upper crust in the Andes between 36° and 39°S, defining discrete periods of accumulation of large volumes of volcanic materials in the inner domains of the orogen, alternating with periods of arc-related intrusions along discrete strike-slip fault systems (Fig. 2–B1, 2–B2).

ACKNOWLEDGEMENTS

This research project was developed with funding from PIP 4162 (Conicet) and PICT 059 for the "Study of the segment of normal subduction -33° to 38°S-".

REFERENCES

Folguera, A., Yagupsky, D., Zlotnik, S., Iaffa, D., Melnick, D. 2001. Transtensión como mecanismo de transición entre estados de baja y alta partición de la deformación entre 37° y 40°S en el Plioceno y Cuaternario. 11° Congreso Latinoamericano de Geología, Simposio sobre evolución tectónica de los Andes, 3. Electronic files. Montevideo.

Hervé, F., Pankhurst, R., Drake, R., Beck, M., Mpodozis, C. 1993. Granite generation and rapid unroofing related to strike-slip faulting, Aysén, Chile. Earth and Planetary Science Letters, 120, 375-386.

Jordan, T., Burns, W., Veiga, R., Pángaro, F., Copeland, P., Kelley, S., Mpodozis, C. 2001. Extension and basin formation in the Southern Andes caused by increased convergence rate: A Mid-Cenozoic trigger for the Andes. Tectonics, 20 (3), 308-324.

Lavenu, A.y Cembrano, J. 1999. Compressional and tranpressional stress pattern for Pliocene and Quaternary brittle deformation in fore arc and intra arc zones (Andes of Central and Southern Chile). Journal of Structural Geology , 21, 1669-1691.

Ramos, V.A. y Folguera, A. 1998. The Andes of Neuquen (36°-38°S): Evidence of Cenozoic transtension along the arc. IV Andean Geodynamic Symposium, Extended Abstracts, 606–609. Göttingen.

Ramos, V.A. 1998. Estructura del sector occidental de la faja plegada y corrida del Agrio, Cuenca Neuquina Argentina. X Congreso Latinoamericano de Geología, 2, 105-110.

Ramos, V., Zapata, T., Cristallini, E., Introcaso, A. In Press. The Andean thrust system: Latitudinal variations in structural styles and orogenic shortening. En: *Thrust Tectonics* (K. McClay, Ed.). AAPG. Memoir.

Stern, C. 1989. Pliocene to present migration of the volcanic front, Andean Southern Volcanic Front. Revista Geológica de Chile, 16 (2), 145-16

AR-AR DATING OF LATE OLIGOCENE-EARLY MIOCENE VOLCANISM IN THE ALTIPLANO

Michel FORNARI(1), Eddy BALDELLON(2), Felix ESPINOZA(2), Ivanoff IBARRA(3), Nestor JIMENEZ (4), Miriam MAMANI(3)

(1) IRD, UMR Géosciences Azur, Parc Valrose, 06108 Nice Cedex 02 (fornari@unice.fr)
(2) SERGEOMIN, La Paz, Bolivia.
(3) Departamento de Geología,Universidad Nacional San Antonio Abad del Cusco, Peru
(4) Facultad de Ciencias Geologicas, Universidad Mayor de San Andres, La Paz, Bolivia

KEY WORDS: Peru, Bolivia, Altiplano, magmatism, Ar-Ar dating

INTRODUCTION

In the Altiplano, the volcanic activity appears to have been very reduced during Eocene and Lower Oligocene when several kms of mainly detrital sediments accumulated. Volcanic activity increased during late Oligocene - early Miocene, forming a succession of outcrops in a SW-NE belt of more than 800 km long located in the Altiplano and oblique to the subduction related magmatism. The aim of this contribution is to present new Ar-Ar data that constrain the time of initiation and the duration of this volcanic activity.

GEOCHRONOLOGICAL RESULTS

^{40}Ar-^{39}Ar laser step-heating age determinations were made on single grains of biotite and sanidine from the crushed rock samples; whole rock fragments were used for basaltic samples lacking of K-rich phenocrysts as separation of suitable minerals was not possible. The laser step-heating experiments were performed following the method described in Féraud (1982) and Ruffet et al. (1991). The criteria used to define a plateau age are: (1) the plateau should include at least 70 % of released ^{39}Ar; (2) there should be at least three successive steps in the plateau; and (3) the integrated age of the plateau should agree with each apparent age of the plateau segment within 2σ error confidence level.

The first occurrences of this volcanic activity are represented by pyroclastic products and also by basic lava flows. In the area of Chivay (Box A in fig. 1), a slightly chloritised biotite from a pyroclastic tuff included in a thick conglomeratic succession, shows a plateau age of 29.66 ± 0.88 Ma (sample 990513-3). In the area of Ayaviri (Box B in fig. 1), pyroclastic levels included in a thick red-beds sequence, were sampled en 2 sites (Sipi Sipi and Co Incanan) located near the limit with of the Eastern Cordillera. They furnish plateau ages on biotite of 28.03 ± 0.15 (sample 990521-4) and 28.03 ± 0.24 Ma (sample 990524-4).

- In the northern part of Laguna Lagunillas (Box C in fig. 1), basalt-andesite lava flows overly unconformably conglomerates of the Puno Formation. A whole-rock sample (sample 981011-3, Pinaya area) yielded a nice plateau age of 29.8 ± 0.06 Ma, accounting 86% of the total ^{39}Ar.

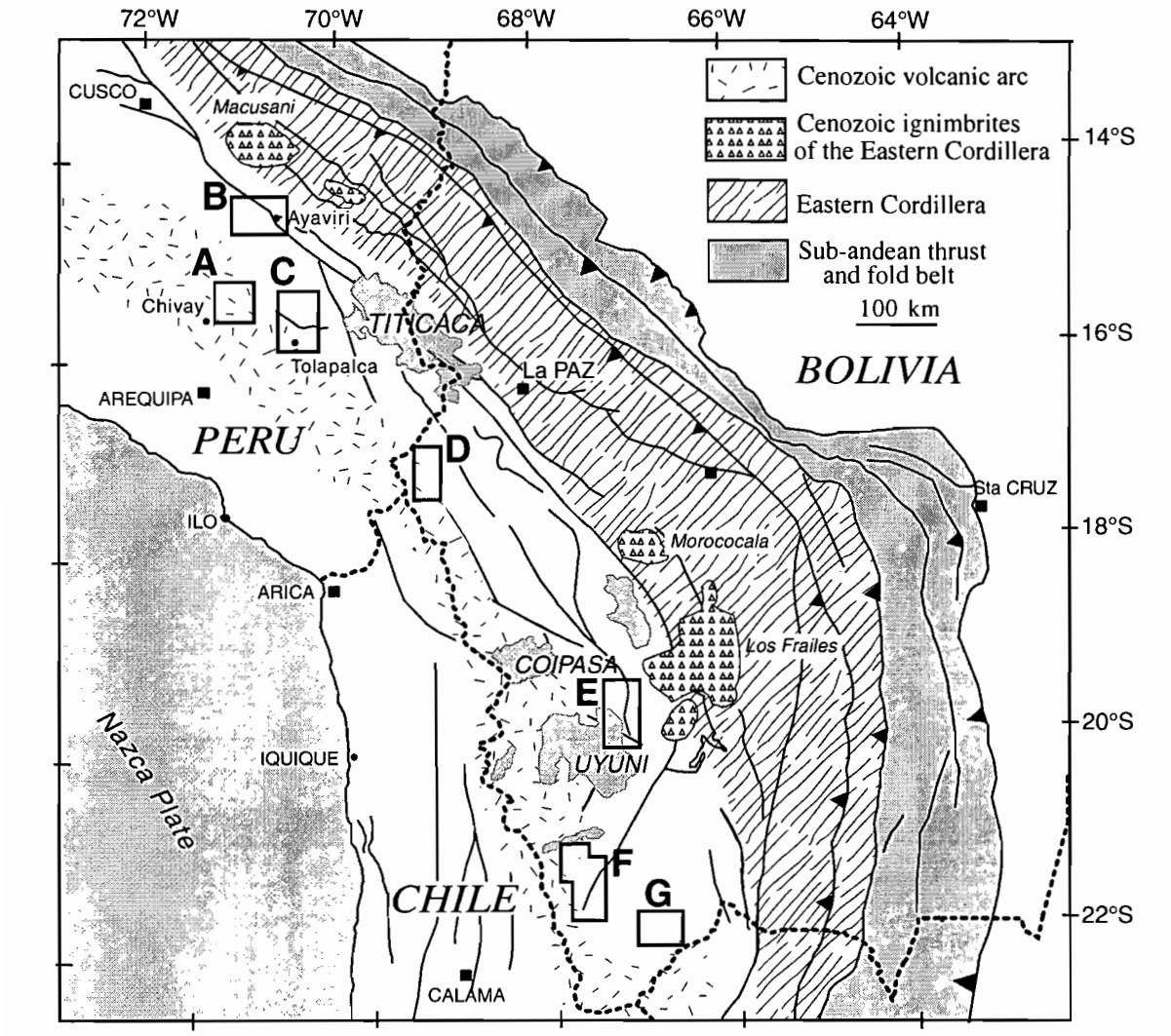

Fig 1: sketch map of the Central Andes showing the location of the sampled area (labeled boxes).

In the same area, basaltic lava flows, sills, dykes and volcanic brecchias form outcrops of several hundred of meters-thick; but they have been strongly altered by hydrothermal circulation and meteorization thus they could not be dated. So we include the sample (970815-1) of a microgabbroic lava from Tolapalca, located at 40 km south of Pinaya. In spite of a disturbed age spectrum due to alteration and ^{39}Ar recoil during irradiation, evidenced by decreasing apparent ages with temperature. Nevertheless, the "mini-plateau" age of 26.50 ± 0.09 Ma, (accounting only for 42% of the total ^{39}Ar released), is probably not far from the true age of the rock. Moreover, biotites from two pyroclastic flows located about 150 m above the basic lava display plateau ages of 24.48 ± 0.11 and 24.09 ± 0.81 Ma (samples 981005-2 and 9981005-1).

These ages are in the same range than the age of 25.23 ± 2.34 Ma (sample 970823-1) from a cluster of plagioclase from a nephelinic lava flow near Ayaviri. The data present a high error because of the low K content of the plagioclase but agree with the 28-25 Ma K/Ar ages of Bonhomme (1985).

In Bolivia similar lavas are identified with different local names from North to South e.g., Abaroa Formation, Tambillo Fm, Julaca Fm., Rondal Fm., but because of the lack of stratigraphic data, the age of the magmatic episode was poorly constrained. These lavas crop out mainly as flows, sills, dykes and small intrusives stocks; ash falls deposits are present in some locations (e.g., Tambillo Fm). A characteristic feature of this volcanism is

the presence of thick and extended deposits of flow breccias that indicates the presence of several volcanic centers.

- In the area near the border between Chile, Bolivia and Peru (box D in fig. 1), determinations were made on basic whole-rocks of the Abaroa Fm. The sample ABM1 yielded a plateau age of 27.84 ± 0.05 Ma, accounting for 95% of the total ^{39}Ar released. Three determinations display disturbed spectra with decreasing apparent ages versus temperature. These shapes are due to ^{39}Ar recoil; in that case, we consider that intermediate to high temperature ages may represent geological valid ages; the ages are 27.97 ± 0.13 for sample ABA9 with 47% of the total ^{39}Ar released, 27.34 ± 0.08 for sample ABM2, with 35 % of the total ^{39}Ar released and 27.5 ± 0.2 for sample ABA12 with 30 % of the total ^{39}Ar released.

These dates are much older than the K/Ar determinations (18-13 Ma) of Lavenu et al. (1989) for the Abaroa Fm and also older than the age of 25.2 ± 1.0 Ma for a basalt flow they attributed to the Mauri Formation.

- Near the eastern border of the Salar de Uyuni, outcrops of the Serrania de Urachata (box E in fig 1) contain several hundred meters thick of basic volcanism and some tuffs within detrital sediments (Espinosa, 1995). Several samples of basic lava were analyzed and yielded dates about 23-24 Ma. The basaltic sill from Cerro Chiar Kullu shows a ^{39}Ar-^{40}Ar plateau-age of 24.2 ± 0.4 (sample 95BL18) which is the oldest age from the basic magmatism in this area; the date is in concordance with the K/Ar age of 25.2 ± 0.9 Ma of Hoke et al., (1993) and Khennan et al., (1995). The Chiar Kullu sill is overlain by about 500 m of sandstones and a >100 m-thick basaltic sill with plagioclase phenocrysts up to 3 cm. This sill which forms the Kapora-Tambo Tambillo syncline, shows a whole rock plateau-age of 23.8 ± 0.1 (sample 941112-1). It was probably sampled very close to the sample Rod-91, which yielded a K/Ar date of 23.1 ± 1.2 Ma (Khennan et al., 1995).

The Cerro Picacho (southern part of boxE) shows a section of about 1000 m thick, with more than 15 basaltic levels included in detrital sediments; a lava flow in the basal part of Cerro Picacho section yields a plateau age of 23.45 ± 0.08 Ma (sample FD7S1). An other sample in the top of the same section shows a disturbed age spectrum (^{39}Ar recoil) but contains a "mini-plateau", accounting for 51% of the total ^{39}Ar released with an age of 23.6 ± 0.1 Ma. Morerever a biotite crystal from a basic dyke which cuts several flows and sills provides a plateau-age of 23.5 ± 0.1 Ma (sample 930402-2). Thus it appears that most of the basic lava emplaced very quickly. Above the sequence of basic lava, several hundred meters of conglomeratic levels were deposited (member 2 of the Tambillo formation. They contain thin levels of tuff. The upper part of the Chiar Punta section, which crops out in the border of the Salar of Uyuni contains more than 1000 m of coarse conglomerates. In the lower part of the conglomeratic sequence, a sanidine from a ash-fall horizon above the basaltic sill and lava flows yielded a plateau age of 22.26 ± 0.06 (sample F4).

In the Kapora -Tambo Tambillo syncline, sample 95BL21 was collected from a cineritic level at the base of the Tambillo Formation. The cinerite is located ca. 20 m above the thick porphyric basaltic sill and shows a biotite single grain plateau-age of 25.2 ± 0.3 Ma. Another cineritic level ca. 150 m above 95BL21 displays a plateau-age of 23.6 ± 0.3 Ma (sample 95BL20). Both samples are located in the fine-grained part of the Tambillo formation, which rapidly coarsens upwards. In the eastern flank of the syncline, the conglomeratic upper part of the sequence contains a welded tuff located ca 2500 m above the basaltic horizon. It presents a biotite single grain plateau-age of 16.0 ± 0.2 Ma (sample 95BL22). Presumably the same tuff gave a K/Ar age of 15.8 ± 0.5 Ma, (Hoke et al., 1993, Khennan et al., 1995).

These data permit to calculate low sedimentation rates of about 60 m by million of years for the base of the Tambillo Formation and of about 250 m by million of years for the upper conglomeratic sequence indicating that the area was not affected by an intense tectonic activity at this time although the Member 2 of the Tambillo Formation consists of an up-coarsening sedimentary sequence.

- In the southern part of the Bolivian Altiplano (box F in fig. 1), basic lava flows, sills and dykes occur within detrital sediments in the Serranias de las Minas. Two samples display concordant whole rock plateau-ages of

21.9 ± 0.2 (Khonas, sample 95BL9) and 21.8 ± 0.2 Ma (Suri Puquio, sample EG69). Two age spectra show decreasing apparent ages versus temperature (^{39}Ar recoil) but intermediate to high temperature steps (from 35 to 66% of total ^{39}Ar released) may represent geological valid ages of 21.9 ± 0.2 Ma (sample EG31) and 21.9 ± 0.3 (sample 941115-3). All these dates are in the same range whereas a significantly lower plateau-age of 19.9 ± 0.3 Ma is displayed by the sample 95BL16 (laguna Chuan). Despite the existence of a plateau-age, the age spectrum apparently shows a slight ^{39}Ar recoil effect at low temperature.

A basalt-andesitic dyke near Guadalupe (box E in fig. 1) gave a whole rock plateau-age of 22.18 ± 0.26 (sample S5, Rondal Fm). This age is slightly older than the plateau-age of 21.4 ± 0.1 Ma given by a biotite single crystal from a andesitic sill (sample 910914-1, Rondal lava) and than the plateau-age of 21.1 ± 0.3 from a basic lava flow (sample 3010-4).

Theses lava flows are apparently the first ones that occur in the detrital sedimentary sequence (Baldellon, 1995), and so, the volcanism onset seems to be younger here than in the northern part of the Altiplano.

CONCLUSION

Ar-Ar data evidence magmatic activity in the range of 29-21 Ma; a more subtle difference may exist between the North and the South of the Altiplano (ages between 29 and 25 Ma in Peru, 24.5 and 22.5 Ma in Tambillo area and around 22-21Ma in the Serrania de las Minas - Guadalupe area). The High-K, alkaline affinity of this volcanism indicates a deep origin and may be related to the transtensive tectonic conditions and the reactivation of main fracturation.

The late Oligocene-Early Miocene episode of magmatic activity appears to coincide with an extended period of structural deformation and crustal shortening; it appears also that the onset of volcanism and tectonism followed a period of major plate reorganization in the southeast Pacific following the Farallon plate brake up, with fast plate convergence (Pilger, 1984; Pardo-Casas & Molnar, 1987).

REFERENCES

Baldellon P. E. 1995. Geologia y etapas de deformacion de la zona de Serrania de las Minas (Dpto de Potosi). Thesis de grado, Universidad Mayor de San Andrés, La Paz, Bolivia, 158 p. Inedito.

Bonhomme M. G., Audebaud E, Vivier G. 1985. K-Ar ages of Hercynian and Neogene rocks along an East West cross section in Southern Peru. Comunicaciones, 35, 27-30.

Espinoza R. F, 1995 Geologia al nor este del Salar de Uyuni. Petrologia de las rocas igneas de la formation Tambillo. Thesis de grado,Universidad Mayor de San Andrés, La Paz, Bolivia, 148 p. Inedito.

Hoke L., Lamb S., Entenmann J. 1993. Volcanic rocks from the Bolivian Altiplano: Insights into crustal structure, contamination and magma genesis: Comment and Reply. Geology, 1147-1149.

Kennan L., Lamb S., Rundle C. 1995. K-Ar dates from the Altiplano and Cordillera Oriental of Bolivia: implications for the Cenozoic stratigraphy and tectonics. Journal of South American Earth Sciences, 8, 163-186

Lavenu A, Bonhomme M. G, Vatin-Perignon N, De Pachtere P. 1989. Neogene magmatism in the Bolivian Andes between 16°S and18°S: stratigraphy and K/Ar geochronology. J. of South American Earth Sciences, 2, 35-47.

Pilger R.H. 1984. Cenozoic plate kinematics, subduction and magmatism: South American Andes. Journal of the Geological Society of London, 141,793-802.

Pardo-Casas F., Molnar P. 1987. Relative motion of the Nazca (Farallon) and South American plates since late Cretaceous time. Tectonics, 6, 233-248

THE HIGH PRESSURE ULTRAMAFIC SEQUENCE OF THE EL TORO FORMATION (EL ORO METAMORPHIC COMPLEX, SW ECUADOR): CHARACTERISATION AND METAMORPHIC EVOLUTION

Piercarlo GABRIELE (1), Giovanni B. PICCARDO (2), Giorgio MARTINOTTI (3) and Jean HERNANDEZ (4)

(1) Institut de Minéralogie et Géochimie, Université de Lausanne, BFSH-2, CH-1015 Lausanne, Suisse (Piercarlo.Gabriele@img.unil.ch)
(2) Dipartimento per lo Studio del Territorio e delle sue Risorse (DIPTERIS), Università di Genova, Corso Europa 26, 16132 GENOVA, Italy (piccardo@dipteris.unige.it)
(3) Dipartimento di Scienze della Terra, Università di Torino, Via Valperga Caluso 35, 10125 Torino, Italy (martinotti@dst.unito.it)
(4) Institut de Minéralogie et Géochimie, Université de Lausanne, BFSH-2, CH-1015 Lausanne, Suisse (Jean.Hernandez@img.unil.ch)

KEY WORDS: Ecuador; Ultramafic rocks, Eclogite-facies metamorphism, Exhumation.

GEOLOGICAL SETTING

In the south-western part of Ecuador (between 3°S and 4°S of latitude; 79°30'W and 80°50'W of longitude), in the "El Oro" province, various metamorphic terranes (Feininger, 1982) were grouped under the name of "El Oro Metamorphic Complex" (Aspden et al., 1995). These terranes have been interpreted as independent allochtonous or parautochtonous bodies (Feininger, 1987); as large displaced blocks (Mourier et al., 1988), or as a late Jurassic - early Cretaceous tectonic mélange representing part of an accretionary prism (Aspden et al., 1995). The El Oro Metamorphic Complex is characterised by different lithologies ranging in age from Palaeozoic to Cretaceous (Aspden et al., 1995). This area is crosscut by several E-W-trending faults that subdivide the El Oro Metamorphic Complex into smaller units.

One of these units, the El Toro formation (as defined by Feininger, in Bristow and Hoffstetter, 1977) is bounded to the North by the "La Palma - El Guayabo" fault, and to the South by a major tectonic contact. The El Toro formation consists mainly of variably-serpentinised massive metaperidotites with subordinated amphibole-diopside-chlorite-rich bands. Small dykes of primary mafic rocks (now metabasites) crosscut the ultramafic sequence. The El Toro ultramafites are particularly well exposed in the quarries located immediately to the east of the Tahuin dam, in the "Cerro El Toro" area.

PETROGRAPHY

The metaperidotites with diopside-amphibole-chlorite bands are characterised by a variably pervasive schistosity defined by aligned crystals of antigorite. Olivine, clinopyroxene and orthopyroxene porphyroclasts together with variable amount of brown spinel define the relict primary mantle assemblage in the metaperidotite. The mineral assemblage related to the metamorphic peak is represented by neoblastic olivine, diopside, antigorite and variably amount of clinohumite, which are in textural equilibrium.

The bands in metaperidotites are composed by chlorite and amphibole porphiroblasts; the peak assemblage in these bands is represented by diopside and antigorite.

The mafic dikes consist of amphibole-rich rocks with massive to poorly schistose fabric. They are mainly composed of green to blue-green inequigranular amphibole. Zoisite porphyroblasts are concentrated in domains and they are in textural equilibrium with amphibole. Relicts of clinopyroxene and garnet are present: they are clearly replaced by the amphibole and the zoisite. Titanite and rutile are common accessory phases.

MINERAL CHEMISTRY

Relict clinopyroxene porphyroclasts (cpx-1) in metaperidotites are chromian diopside (Cr = 0.083 a.p.f.u.). The neoblastic clinopyroxene (cpx-2) is diopside both in metaperidotites and diopside-amphibole-chlorite bands, showing only minor variations in the Mg and Ca contents, ranging respectively from 0.86 to 0.96 p.f.u. and from 0.87 to 0.98 a.p.f.u. Orthopyroxene is present only in metaperidotites: it shows enstatite composition with an average Mg# 90. The two generations of olivine, olivine-1 porphyroclasts and olivine-2 neoblasts, evidenced on a textural basis, show significantly different composition. Primary mantle olivine (Ol-1) has an higher XMg (in the range 0.90-0.91), and lower Mn (average MnO = ~0.16 wt%). The neoblastic olivine (Ol-2) has a slightly lower XMg (averaging around 0.87), while MnO is up to 0.28 wt%. The serpentine minerals show a wide compositional range: chrysotile is characterised by high Mg values (2.8-2.9 a.p.f.u.) and by very low Al (a.p.f.u. 0.0-0.02). Antigorite has lower Mg (2.6-2.7 atoms a.p.f.u). and higher Al (up to 0.12 atoms p.f.u.). Chlorite is magnesium-rich (XMg varying from 0.94 to 0.96). The analysed clinohumites are fluorine free titanian-clinohumites having significant amounts of Ti (in the range 0.42-0.45 a.p.f.u.). Two generations of amphiboles are present in the metaperidotites and in the diopside-amphibole-chlorite bands: older porphyroblasts (amphibole-1) and small fibrous crystals or neoblastic grains (amphibole-2). The former are calcic amphiboles (pargasite), the latter are sodic-calcic amphiboles (magnesiokatophorite or richterite, according to the Si content).

In the mafic dykes the analysed pyroxenes are omphacites, which are characterised by an average jadeite content of 34 mol%. Garnets are characterised by an high grossular content (around 76 mol%), and by an average XFe of 0.91. Zoisites are characterised by a Fe3+/(Al+Fe3+) ratio averaging around 0.10. Amphibole is present as i) unzoned pargasites or as ii) grains having a sodic-calcic core (magnesiotaramite) grading to a calcic (pargasite) rim.

WHOLE ROCK CHEMISTRY

The metaperidotites are characterized by relatively low SiO_2 and high MgO (37.03-38.84wt%) contents, typical of olivine-rich mantle peridotites, and CaO (~2.05wt%) and Al_2O_3 (1.48-2.88wt%), closely similar or slightly lower than estimated concentrations in fertile mantle peridotites (Hofmann, 1988; Jagoutz et al., 1979). The amphibole-diopside-chlorite band in metaperidotites has lower MgO (24.89wt%) and significantly higher CaO (10.04wt%) and Al_2O_3 (8.73wt%), which indicate for a mafic composition of the protolith.

The amphibolite-rich mafic dykes have MgO (11.78-17.40), CaO (10.67-15.02wt%) and Al_2O_3 (10.54-13.53wt%) similar to or slightly higher than those of common basaltic compositions.

Concerning the trace elements composition, the metaperidotite sample displays an almost flat C1-normalized Rare Earth Element (REE) pattern, from HREE to MREE, at about 1xC1, significantly depleted for the LREE (Ce_N/Sm_N = 0.26): the trace element spiderdiagram evidences a strong Sr enrichment. The diopside-amphibole-rich bands in metaperidotite show a REE pattern, from HREE to MREE, slightly lower than 10xC1, with a significant LREE negative fractionation (Ce_N/Sm_N = 0.30): the trace element spiderdiagram evidences a slight Sr enrichment.

The amphibole-rich samples can be divided in two groups. The first group has almost flat REE patterns, form HREE to MREE, at about 6-7xC1,with a slight LREE fractionation (Ce_N/Sm_N = 0.34-0.54) and an evident Eu_N positive anomaly; these samples show, moreover, strong Sr enrichment. The second group shows almost flat REE patterns, at about 20xC1, with a slight LREE fractionation (Ce_N/Sm_N = 0.48-0.67).

PRIMARY AND METAMORPHIC EVOLUTION

The geochemical characteristics of the metaperidotite are typical of moderately depleted mantle peridotites. One of the analysed diopside-amphibole-rich band has a REE pattern, and overall trace element contents, closely similar to that of LREE-depleted pyroxenite bands in orogenic and ophiolitic peridotites.

The trace element compositions suggest that amphibole-rich rocks, which crop out as dykes crosscutting the ultramafic body, can be divided in two groups: the first one, showing an evident Eu_N positive anomaly, is similar to gabbroic rocks, characterized by cumulus of plagioclase: their protoliths could have been plagioclase-bearing intrusive mafic rocks. The second group most probably derives from rocks of basaltic compositions. These amphibole-rich rocks are commonly characterized by variable LREE negative fractionation, which is strongly indicative of a MORB affinity of the parental melts of their magmatic protoliths.

Available petrographic and compositional data suggest that pristine mantle peridotites, with pyroxenite layers, were characterized by spinel-facies assemblages, indicative of equilibrium recrystallization at moderate pressure conditions (P ranging 10-20 Kb). The development of amphiboles (pargasite and tremolite) and/or chlorite, stable with olivine (amphibole and/or chlorite peridotite facies assemblages), indicates transition to lower pressure and temperature conditions. The intrusion of MORB-type gabbros and basalts suggests progressive decompressional evolution in an oceanic setting: oceanic metamorphic overprint is evidenced by the development of crysotile, chlorite, and tremolite at the expense of mantle minerals and by the Sr enrichment of the whole rocks.

The subsequent metamorphic evolution is related to the subduction of the ultramafic body, which reached eclogite facies conditions. The olivine+diopside+antigorite+Ti-clinohumite assemblage, representing the metamorphic peak in metaperidotites, indicates temperature not higher than 500-550°C (Engi and Lindsley, 1980; Trommsdorff and Evans, 1980), whereas the garnet+omphacite+rutile association in amphibolite-rich mafic dykes indicates the high-pressure conditions. A retrograde evolution is evidenced by the amphibole and zoisite growth in the amphibole-rich rocks.

The El Toro ultramafic rocks can be thus defined as depleted mantle peridotites with pyroxenites bands that recorded a metamorphic HP event. The occurrence of HP metamorphic rocks in SW Ecuador is well documented by the Raspas Complex mafic and pelitic eclogites (Feininger, 1980, Gabriele et al., 1999, Gabriele

et al., 2001). The identification of the El Toro ultramafic body as a new high pressure metamorphic unit provides new insights into the subduction-exhumation processes in active margin setting.

REFERENCES

Aspden, J. A., Bonilla, W., and Duque, P. 1995. The El Oro metamorphic complex, Ecuador: geology and economic mineral deposits. Overseas Geology and Mineral Resources, No. 67.

Bristow, C. R., and Hoffstetter, R., 1977. Lexique stratigraphique international, Amérique Latine, Equateur. Paris, Centre National de la Recherche Scientifique, 5, 139-140.

Engi, M. and Lindsley, D. H. 1980. Stability of titanian-clinohumite: experiments and thermodynamic analysis. Contributions to Mineralogy and Petrology, 72, 414-424.

Feininger, T. 1980. Eclogite and related high-pressure regional metamorphic rocks from the Andes of Ecuador. Journal of Petrology, 21, 1, 107-140.

Feininger, T., 1982. The metamorphic "basement" of Ecuador. Geological Society of America Bulletin, 93, 87-92.

Feininger, T., 1987. Allochtonous terranes in the Andes of Ecuador and northwestern Peru. Canadian Journal of Earth Sciences, 24, 266-278.

Gabriele, P., Ballèvre, M., Jaillard, E., Hernandez, J., 1999. Decompression at decreasing temperatures in eclogite-facies metapelites (El Oro metamorphic complex, SW-Ecuador): a record of fast exhumation rates. 4th Internat. Symp. Andean Geodyn.-ISAG, Göttingen 1999, 245-248, IRD publ., Paris.

Gabriele, P., Ballèvre, M., Martinotti, G., Jaillard, E., Hernandez, J., 2001. P-T paths of the Mesozoic Raspas eclogites, Andean belt (Ecuador): possible constraints on exhumation. EUG XI, European Union of Geosciences, Strasbourg, France. Journal of Conference Abstracts, 6, 350.

Hofmann A. W. 1988. Chemical differentiation of the Earth.: the relationships between mantle, continental crust and oceanic crust. Earth Planet. Sci. Lett., 90, 297-314.

Jagoutz E., Palme H., Baddenhausen H., Blum K., Cendales M., Dreibus G., Spettel B., Lorenz V., Wanke H 1979. The abundance of major, minor and trace elements in the Earth's mantle derived from ultramafic nodules. Proc. Lunar Planet. Sci. Conf. 10th , 2031-2050.

Mourier, T., Laj, C., Megard, F., Roperch, P., Mitouard, P., and Farfan-Medrano, A. 1988. An accreted continental terrane in northwestern Peru. Earth and Planetary Science Letters, 88, 182-192.

Trommsdorff, V. & Evans, B. W. 1980. Titanian hydroxyl clinohumite: formation and breakdown in antigorite rocks (Malenco, Italy). Contributions to Mineralogy and Petrology, 72, 229-242.

SPATIAL AND TEMPORAL VARIATIONS OF THE QUALITY FACTOR (Q) BEFORE AND DURING THE 1999 GUAGUA PICHINCHA ERUPTIONS

Alexander GARCÍA-ARISTIZÁBAL (1), Álvaro Pablo ACEVEDO (2), Mario C. RUIZ (1)

(1) Departamento de Geofísica – Escuela Politécnica Nacional. P.O. Box 17-01-2759, Quito – Ecuador. (Email: algari@terra.com.co)

(2) Ingeominas. Observatorio Vulcanológico y Sismológico de Manizales. Av. 12 de Octubre No. 15-47. Manizales – Colombia. (Email: apa@latinmail.com)

KEY WORDS: Seismic wave attenuation, Quality factor (Q), volcanic unrest.

INTRODUCTION

Guagua Pichincha volcano (GGPV) is part of the quaternary volcanic chain of the Ecuadorian "Cordillera Occidental". It is located at 0°10' S – 78° 36' W and 4739 m in altitude. Located at its western margin, it is the youngest emission center of the Pichincha volcanic complex. Quito city, the political and administrative capital of Ecuador (with a population of about 1'800.000) is located about 12 km to the East (fig. 1).

During 1998 important earthquake activity (actually called Distant-volcano tectonic events, or DVT (R. White, pers. comm.)) began 15 km NE of the caldera. On august 4 a 7.1 Ms earthquake occurred at the Ecuadorian subduction zone 220 km West of the volcano, and on august 7 recurrent phreatic activity suddenly began at Guagua Pichincha. This activity was characterized in the initial weeks by explosions followed by various hours/days of tremor and hybrid earthquake swarms.

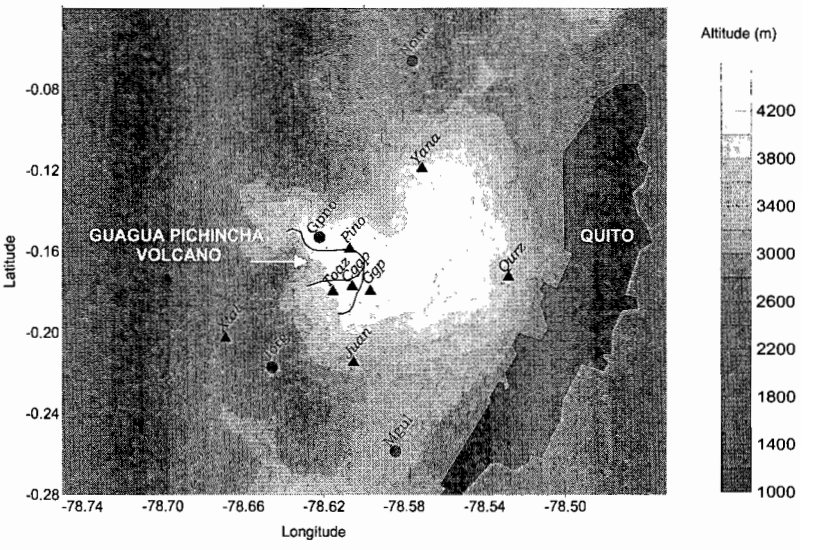

Figure 1. Guagua Pichincha volcano. Geographic location and the seismic network. Data from stations denoted by triangle were used in this study.

In September 1999 activity changed from phreatic to a magmatic character. Strong swarms of Long Period (Lp) events began a process in which 8 lava domes were extruded into the caldera center subsequently destroyed by explosions, generating at least 3 light ash fall (<3mm) over Quito and the surrounding area, and 4 pyroclastic flows down the Western flank (Cristal river).

Using the data from the seismological network operated by the Departamento de Geofísica – EPN (before Instituto Geofísico) since 1981 for Guagua Pichincha monitoring (fig. 1) and taking the events from the NE Quito swarm (Calahorrano, 2001), a methodology for the Q calculation at different frequencies (between 2 and 12 Hz) was developed. Starting in October 1998 through December 1999, both the spatial and temporal variations as a frequency-dependant process were studied, and correlations were made with other geologic and geophysical parameters observed at the volcano.

THEORETICAL BASIS

In an idealized, purely elastic Earth, geometric spreading and the reflection and transmission of energy at boundaries control the amplitude of a seismic pulse. Once excited, these waves would persist indefinitely. The real earth is not perfectly elastic, and propagating wave *attenuate* with time due to various energy-loss mechanisms. We usually describe these processes collectively as "internal friction" and it is generally modeled with phenomenological descriptions because the microscopic process are complex (Lay and Wallace, 1995). The simplest description of attenuation can be imagined by an oscillating mass on a spring over any surface. The relationship which describes its movement in time shows an harmonic oscillation with an exponential loss of amplitude.

RESULTS

Frequency dependence

The derived Q values show a clear dependence with frequency, and thus arriving at the next relationship which could be called "The Q law" for both P and S waves.

General expression...	Q law for P waves	Q Law for S waves:
$Q_{(f)} = Q_0 f^{\gamma}$	$Q^{P}_{(f)} = 1.23 f^{0.96}$	$Q^{S}_{(f)} = 0.711 f^{0.92}$
	Standard deviation: Qo= 0.28 γ= 0.21	Standard deviation: Qo= 0.28 γ= 0.21

For Guagua Pichincha, it's observed that the Q value increases directly with frequency. The value is increasing more or less constantly for frequencies lower than 6 hz. However, at higher frequencies (6-12 Hz) the Q value tends to have a steeper slope as seen in figure 2.

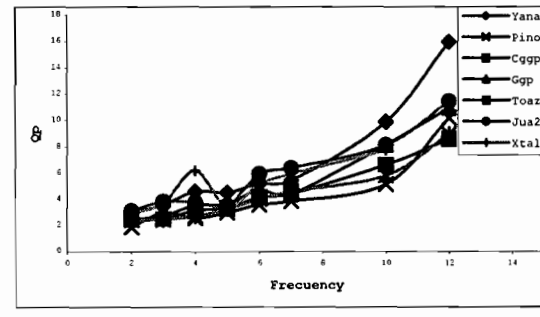

Figure 2. Q variations (for P waves) Vs. frequency

This variation was observed in both P and S waves, and in all the stations in which the measurement was done.

Temporal Changes

During the period of time when Q was calculated (October 1998 – December 1999) the greatest variations in the Q value were observed, mainly in those stations located directly over the volcanic edifice. Distal stations YANA and QUR, showed lesser changes with time. However the stations of PINO, CGGP, GGP1 and TOAZ, located around the caldera, and JUA2, located on the southern flank, showed a very important decrease in Q during the period January-May 1999. Figure 3 shows the Q variation during the whole period of study at GGP1 station, and it is possible to determine at least tree periods of time with significant changes in the Q behavior: The first period, at the beginning, between October and December 1998, with the highest values, the second one: between January and May 1999, where an important decrease in the Q value is seen, and finally, the third period: between June and December 1999, when the Q is more or less stable with respect to the preceding months.

Spatial Changes

Using the different stations and the Q values calculated in each one, we interpolated the values (using the Kriging method) looking for any spatial distribution of the factor. In the same way, trying to infer a general idea about the internal volcanic structure, an inversion methodology was applied (which can be reviewed in García, 2001).

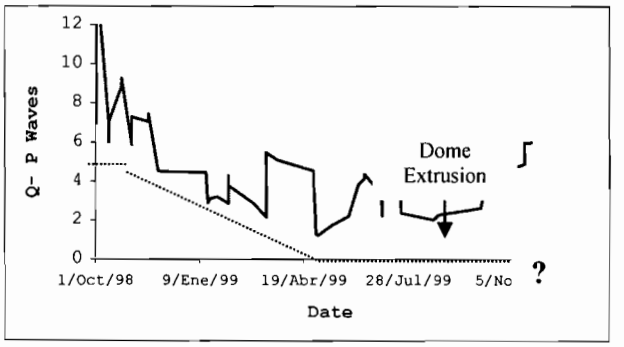

Figure 3. Q value: Temporal variation Oct/98 – Nov/99. GGP1 Station

Figure 4 shows the Q-spatial distribution found for P waves at 7 Hz. The map is showing the surface projection of the anomalies. Note that the lower Q values found are around the Guagua Pichincha caldera.

On the other hand, figure 5 shows a cross section along a NNE-SSW profile. It is possible to see the higher attenuation zone located about 3 to 5 km depth. Additionally, it has been overlapped with the most important volcano seismicity associated with the dome extrusion between September and December 1999.

Discussion

As is described by Jin & Aki (1989), Q value determinations are geophysical measurements that shows one of the best correlations with the current tectonic activity. The Andean volcanism is directly related with the tectonic activity around the Pacific trench, so in general terms, it's expected to have low Q values. Around Guagua Pichincha volcano we have found a strong frequency-dependence of Q, and relatively low values (between 3 and 9 in the lower frequencies measured (2-4 Hz) and between 5 and 40 for the higher frequencies (6-12 Hz)). However, it was possible to find both spatial and temporal changes in the factor. In time, an important Q decrease was observed between January and may 1999.

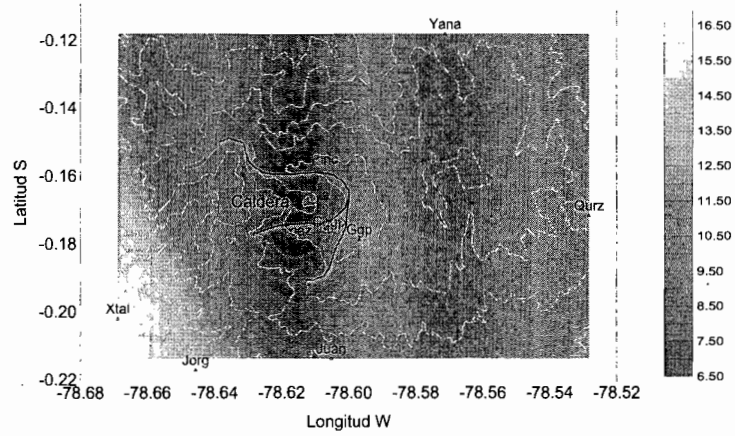

Figure 4.
Spatial variation of Q values at 7 Hz. Surface projection of the anomalies. Note, that the lower Q values are located under the GGPV caldera.

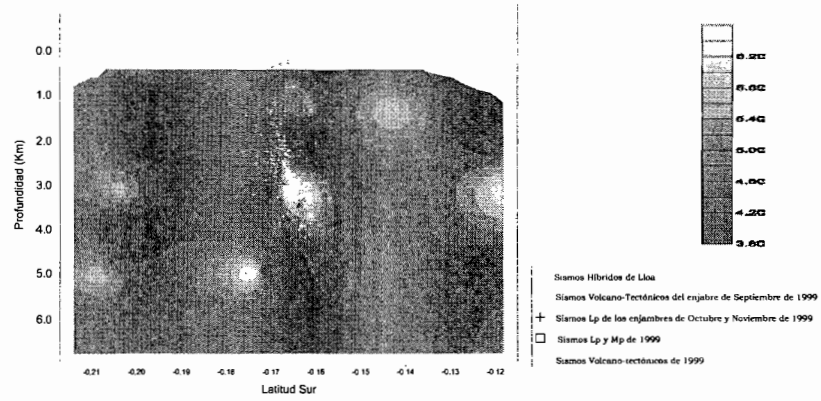

Figure 5.
Q distribution in depth. The darkest shade equal the lower Q. Volcano seismicity associated with dome extrusion is overlapped.

This change preceded by about tree months the beginning of the magmatic activity, when lava domes were extruded. The decrease in the Q values is correlated with an increment in the b value (from the Gutenberg-Richter law) observed by Villagomez (2000) calculated from Volcano-tectonic events. Spatially, there is a low Q area around the Guagua Pichincha Caldera, located approximately between 3 and 5 km depth beneath the caldera floor. It is presumed that at this depth there is the geologic contact between the basement rock and the volcanic building (Hall, pers. Comm). So, due to the low Q calculated, and its temporal decrease, (and taking in account that the seismicity correlated with the dome grouth is located directly over this low Q area, see fig. 5), we have interpreted this zone as a trap formed in this discontinuity. This Q anomaly is best outlined with frequencies between 5 and 7 Hz. Both, P and S waves show more or less the same Q anomaly, so this anomaly should be associated not only with intrinsic media properties, but with a high density of fractures and probably thermal anomalies (conditions which probably exist beneath the caldera).

References

Calahorrano, A. 2001. Origen del enjambre sísmico de la zona norte de Quito. Trabajo de Grado. Escuela Politécnica Nacional, Facultad de Ingeniería en Geología, minas y Petróleos. Quito - Ecuador

García, A. 2001. Atenuación de ondas sísmicas en un volcán dacítico: El Guagua Pichincha. Trabajo de Grado. Universidad de Caldas, Facultad de Geología y minas. Manizales – Colombia.

Jin, A. and Aki, K. 1989. Spatial and temporal correlation between Coda Q and seismicity and its physical mechanism. Journal of Geophysical Research, vol. 94, No. B10, p. 14,041 – 14,059.

Lay, T. and Wallace, T. 1995. Modern global seismology. San Diego, California. Academic press. 521pp.

Villagómez, D. 2000. Sismicidad del volcán Guagua Pichincha 1998-1999. Trabajo de Grado. Escuela Politécnica Nacional, Facultad de Ingeniería en Geología, minas y Petróleos. Quito – Ecuador

OLIGOCENE-NEOGENE TECTONIC EVOLUTION OF THE ALTIPLANO OF NORTHERN CHILE (18-19°S)

Marcelo GARCIA (1), Gérard HERAIL (2), Reynaldo CHARRIER (3), Georges MASCLE (4), Michel FORNARI (5) and Carlos PEREZ de ARCE (1)

(1) SERNAGEOMIN. Av. Santa María 0104, Providencia, Santiago, Chile (mgarcia@sernageomin.cl)
(2) IRD, LMTG. Université P. Sabatier, 39 Allées Jules Guesde, 31000 Toulouse, France (gherail@paris.ird.fr)
(3) Universidad de Chile. Casilla 13518, Correo 21, Santiago, Chile (rcharrie@cec.uchile.cl)
(4) LGCA, UMR. BP 53, 38041 Grenoble, France (Georges.Mascle@ujf-grenoble.fr)
(5) IRD, UMR. Géosciences Azur, Université Nice-Sophia Antipolis, 06108 Nice, France (fornari@unice.fr)

KEY WORDS: Altiplano, Oligocene-Neogene, tectonic, compression, Chile.

INTRODUCTION

The Oligocene-Neogene tectonic evolution of the eastern Altiplano (Bolivia) is characterised by important compression (Sempere et al., 1990; Lamb et al., 1997) with an horizontal shortening from 190 to 240 km (Roeder, 1988; Baby et al., 1997). By contrast, in the western Altiplano (northern Chile), studies are few and, in part, contradictory (Muñoz and Charrier, 1996; García et al., 1996; Lamb et al., 1997; Wörner et al., 2000a). Here, we describe the evolution of the western Altiplano at the latitude of Arica, based on new balanced cross-sections and chrono-stratigraphic data. In this region four physiographic units are recognised (Fig. 1). The Coastal Cordillera (up to 1200 m in altitude) is a smooth relief. In the Central Depression the altitude increases from 500 to 2300 m. The Precordillera (1900-3600 m high) is an elongated plateau. The Western Cordillera is mainly volcanic, with an irregular topography (altitude of 3800-4500 m and maximum of 6350 m).

DEFORMED SEQUENCES: COMPOSITION AND AGE

The extensive Oligocene-Neogene sequence (more than 90% of the area; Fig. 1) is formed by volcanic and continental sedimentary rocks, which overlie unconformably a Precambrian-Paleocene substratum.

Pre-Oligocene substratum. In the Western Cordillera, in Belén, this corresponds to blocks of Precambrian-Paleozoic metamorphic rocks (Basei et al., 1996; Wörner et al., 2000b). To the west the substratum is of Mesozoic-Paleocene intrusive and sedimentary rocks (Salas et al., 1966; Muñoz et al., 1988).

Oligocene-Neogene sequences. To the east they are thick (<5000 m), essentially volcanic, and locally strongly deformed. To the west they are horizontal, essentially sedimentary, and their thickness decreases to 0-200 m. The Azapa Fm. (Salas et al., 1966; Parraguez, 1998), in the Central Depression, consists of up to 500 m of Oligocene fluvial conglomerates and sandstones, proceeding from the NE and E. It is covered by the Oxaya Fm. (Salas et al., 1966; García, 1996), which is constituted by large ignimbrites and minor sediments; its thickness decreases from 1000 m (Precordillera) to 50 m (Central Depression). Several K-Ar and Ar-Ar determinations give a 26-19 Ma age (Naranjo and Paskoff, 1985; Parraguez, 1998; Wörner et al., 2000a; this work). In the Central Depression, the Oxaya Fm. is covered by the El Diablo Fm. (Tobar et al., 1968; Parraguez, 1998), less than 400 m in thickness. The lower part of the El Diablo Fm. is composed of distal-fluvial and lacustrine deposits. The upper part is formed by fluvial gravels coming from the Western Cordillera; two fresh andesitic

clasts were dated (K-Ar whole rock) in 14.7±0.8 and 11.9±0.6 Ma. To the south these gravels are covered by a 8.4±0.6 Ma lava flow (Naranjo and Paskoff, 1985; Muñoz and Charrier, 1996), indicating end of the deposition between 12 and 9 Ma. In the Coastal Cordillera, small Oligo-Miocene basins are filled by alluvial sediments and minor tuffs,similar in composition and age to the Oxaya tuffs. In the eastern Precordillera, the upper Oxaya Fm. is interstratified with the 20-18 Ma Quevilque andesites (Wörner et al., 2000a), and is covered by the Sucuna (15-12 Ma) and Marquez (11-9 Ma) volcanoes and the16-12 Ma andesites of the Zapahuira Fm.. The east-dipping Oxaya and Zapahuira Fms. are onlapped, in low-angle progressive unconformity, by the fluvial Huaylas Fm. (Salas et al., 1966; García et al., 1996). In the upper gravels an ignimbrite has been dated (Ar-Ar biotite) in three sites, giving a mean age of 10.7±0.3 Ma. Uppermost gravels (9-7 Ma) cover partly the Lupica Fm. (to the E). The east-derived Huaylas gravels are coeval to the uplift of the Western Cordillera.

In the Western Cordillera, the Belén Metamorphic Complex is directly overlain by the Lupica Fm. (Salas et al., 1966), constituted by 1500-2500 m of andesitic to rhyolithic flows and alluvial-lacustrine sediments. Ar-Ar, U-Pb and K-Ar ages give Late Oligocene-Early Miocene (18.6±0.6 to 25.5±0.6 Ma) (García, 1996; Riquelme, 1998; this work). The Lupica and Oxaya tuffs are identical in composition and age. In Chucal, the Lupica Fm. is overlain by sediments (Chucal Fm.) with Lower-Middle Miocene vertebrates (Flynn et al., 2002), which are overlain by the 17-10 Ma old Macusa Fm.. In the eastern Western Cordillera, the Lupica Fm. is unconformably covered by Late Miocene-Quaternary volcanoes (Wörner et al., 1988) and Plio-Pleistocene (5-1 Ma) sediments and tuffs of the Lauca Fm. (Kött et al., 1995). The <150 m thick Lauca Ignimbrite, extending over most of the region, yield reliable ages close to 2.7 Ma (Kött et al., 1995; Wörner et al., 2000; this work).

GEOMETRY OF DEFORMATION

The Oligocene-Neogene sequences of Arica are affected by essentially west-vergent compressive structures striking N-S to NNW-SSE (Muñoz and Charrier, 1996; García et al., 1996, 1999; Riquelme, 1998).

Western Cordillera. Structures form a complex fold-and-thrust belt affecting the Lupica Fm. and partially covered by Neogene sediments and volcanics. In the eastern part, gentle deformation is represented by the east-vergent growth Churiguaya Anticline, with flanks dipping less than 35°; Neogene shortening is about 1 km. To the west, a high-deformed domain is developed, with a west-vergent system in the north (Putre-Belén) and an east-vergent system in the south (Chucal-Macusa). The Putre-Belén System produces a great change of altitude (from 3000 to 5300 m). In Socoroma area, a west-vergent syncline is thrust (30° east-dipping) over the subhorizontal Oxaya Fm. and Quevilque Volcano. In Belén-Tignámar area, the system is characterised by a large involving-basement anticline (wavelength of 35 km) associated, in the front, to folds and thrusts that include sheets of syntectonic conglomerates and volcanics, dipping 20-60° east. East Belén, the basement is in contact with the lower Lupica Fm. by a local high-angle east-dipping fault, which is covered by the middle Lupica Fm. For the Putre-Belén System, the minimum Neogene shortening is estimated from 8.3 to 6.4 km. In Chucal, an east-vergent growth anticline (flanks dipping from 10 to 80°), 5 km in wavelength, interprets as a fault-propagation fold. To the west, this anticline is cut by an important thrust (40-50°W) that places the lower Lupica Fm. over Chucal Fm.. More to the west, the Macusa folds are short, tight and west-vergent. For the Chucal-Macusa System the shortening is of 6.6 km. Thus, the Western Cordillera is characterised by west-vergent basement-involved deformation whose Neogene shortening is estimated of 8 km.; this deformation is geometrically compatible with that observed in the eastern Altiplano, but of lesser magnitude.

Precordillera. It is a domain of gentle deformation, affecting essentially the Oxaya Fm. To the north the large Huaylillas Flexure is exposed. To the south (Sucuna Monocline), the west-dipping (2-4°) surface is very gently folded. In the central part the Oxaya Anticline is a well-developed west-vergent fold (flanks of up to 10°W and 4°E). Its shortening is very negligible (<100 m) respect to the vertical displacement (<850 m). The straight western border of the fold is a very open half-syncline. It corresponds to the surface projection of an east-dipping subvertical blind reverse fault (Ausipar Fault), whose upward propagation formed the anticline.

Central Depression and Coastal Cordillera. The deformation is gentle, represented by large flexures and minor faults affecting the El Diablo Fm. The Humayani Flexure is west-vergent, producing vertical displacement up to 500 m and minor shortening (<50 m). It formed by movement of a blind subvertical reverse fault (Taltape Fault) in the western border. Other flexures produce up to 100 m of displacement. In the Coastal Cordillera, locally curved subvertical faults are reverse, normal and strike-slip, and strongly controlled by pre-Oligocene tectonics. These faults show displacements less than 50 m in the Oligo-Miocene deposits; some laterally separate intermittent valleys. The western part of the Arica region is strongly incised (up to 1000 m) by exorreic rivers (Lluta, Azapa, Vitor and Camarones) after the deposition of the El Diablo Fm.

TIMING OF DEFORMATION

It has been constrained from radiometric ages of the syntectonic volcanic and sedimentary horizons.

Oligocene. Deformation of this age is registered in the Taltape and Ausipar faults; these show also Miocene reactivation. The Taltape Fault, below the unfolded Upper Oligocene-Miocene (upper Azapa, Oxaya and El Diablo Fms.), places in direct contact the Mesozoic substratum with the lower Azapa Fm. (and probably older), implying an uplift of the eastern block during the Early Oligocene (and probably prior). The Ausipar Fault, below the unfolded Upper Oligocene-Miocene (Oxaya Fm.), places the Mesozoic substratum against the upper Azapa Fm., indicating an Oligocene age (prior to ~25 Ma) for faulting.

Miocene. Miocene deformation has been previously recognised (Muñoz and Charrier, 1996; García et al., 1996, 1999; Riquelme, 1998). In the eastern Western Cordillera, the Churiguaya Anticline involves the overall Lupica Fm. (26-18 Ma), and is covered unconformably by the 7-6 Ma Choquelimpie Volcano, giving a 22-7 Ma age by the folding. In the Chucal area, the Oligo-Miocene sequence is thrust and folded, and the Upper Miocene (17-10 Ma) seals partially the deformation; it is gently folded but covered by 5-1 Ma horizontal Lauca Fm. To the west, Macusa folds involve 17-10 Ma volcanic rocks and are covered unconformably by the 7 Ma Familiani Volcano. Thus, for the Chucal-Macusa System the deformation developed between 21-18 and 5 Ma. In the Putre-Belén System, to the north, folds and thrusts affecting the Lupica Fm. are covered unconformably by Middle Miocene lavas (13 Ma), indicating compression between 18 and 13 Ma. To the south, on the eastern flank of the Belén Anticline, a 20 Ma ignimbrite is unconformity covered by a 16 Ma dacite; this latter is unconformity overlain by the Lauca Fm.. This implies continuous folding between <20 and >5 Ma. The thrusts of Belén cut the 18-15 Ma syntectonic conglomerates (Joracane Beds) and 16-12 Ma Zapahuira Fm., and some are locally sealed by the uppermost Huaylas Fm. (9-7 Ma). The frontal thrust cuts the lowermost Huaylas Fm. (11-10 Ma) and gently displaces the Pliocene. So, the thrusts of the Putre-Belén System were developed in-sequence (to the west) and their major activity is between 18 and 6 Ma. In the Precordillera, the eastern limb of the Oxaya Anticline is covered, in progressive unconformity, by the Huaylas Fm.: the lowermost sandstones being tilted while the

upper gravels are horizontal. This implies that the folding occurred between 11.7±0.7 Ma and 10.7±0.3 Ma. Faults and flexures of the Central Depression and Coastal Cordillera postdate Late Miocene sediments.

Pliocene-Quaternary. Tectonic activity of this age is lesser compared to that Miocene. This is registered in the frontal thrust of Belén, which displace the 2.7 Ma Lauca Ignimbrite vertically about 100 m. Neotectonic activity in the Western Cordillera is confirmed by shallow seismicity, down to 20 km in depth (Comte et al., 1999). In the Coastal Cordillera strike-slip faults separate valleys suggesting a relatively recent activity.

Figure 1. Simplified structural map of the Andes of Arica

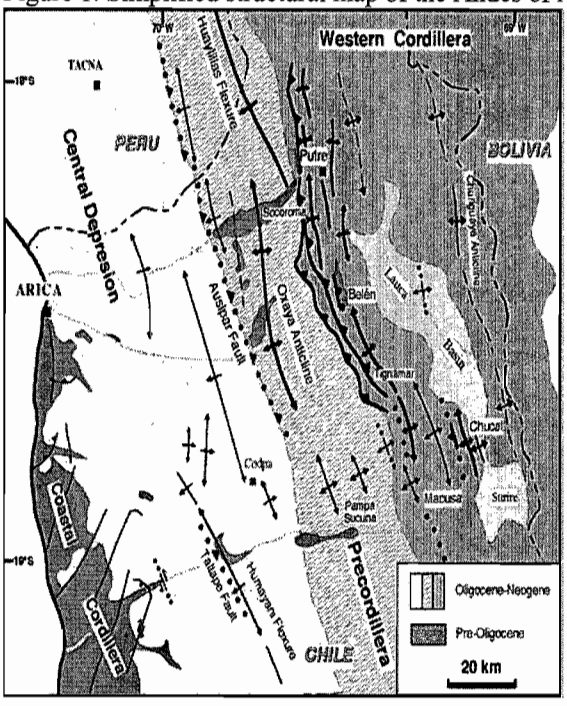

REFERENCES

Basei, M., A.; Charrier, R.; Hervé, F.; 1996. New ages (U-Pb, Rb-Sr, K-Ar) from supposed Pre-cambrian units in northern Chile: Some geotectonic implications. Third I.S.A.G., Saint Malo, France, p. 763-766.

Comte, D.; and 8 authors; 1999. A double-layered seismic zone in Arica, Northern Chile. Geophys. Res. Letters, V. 26 (13), p. 1965-1968.

García, M.; Hérail, G.; Charrier, R.; 1996. The cenozoic forearc evolution in northern Chile: The western border Altiplano of Belén (Chile). Third I.S.A.G., Saint Malo (France), p. 359-362.

García, M.; Hérail, G.; Charrier, R.; 1999. Age and structure of the Oxaya Anticline, a major feature of the Miocene compressive structures of northernmost Chile. Fourth I.S.A.G., Göttingen (Germany), p. 249-252.

Flynn, J.; Croft, D.; Charrier, R.; Hérail, G.; Wyss, A.; 2002. The first Cenozoic mammal fauna from the Chilean Altiplano. Journal of Vertebrate Paleotology, 22(1), p. 200–206.

Kött, A.; Gaupp, R.; Wörner, G.; 1995. Miocene to Recent history of the Western Altiplano in Northern Chile revealed by lacustrien sediments of the Lauca Basin (18°15'-18°40'S / 69°30'-69°05'W). Geol. Rundsch., V. 84, p. 770-780.

Lamb, S.; Hoke, L.; Kennan, L.; Dewey, J.; 1997. Cenozoic evolution of the Central Andes in Bolivia and northern Chile. In J. P. Burg et M. Ford (eds.), "Orogeny Through Time". Geol. Soc. Special Publication N° 121, p. 237-264.

Muñoz, N.; Charrier, R.; 1996. Uplift of the western border of the Altiplano on a west-vergent thrust system, Northern Chile. J. South Amer. Earth Sci., V. 9, p. 171-181.

Muñoz, N.; Elgueta, S.; Harambour, S.; 1988. El Sistema Jurásico (Formación Livilcar) en el curso superior de la quebrada Azapa, I Región: Implicancias paleogeográficas. Actas V Congreso Geológico Chileno, Santiago, Tomo 1, p. A403-A415.

Naranjo, J.A.; Paskoff, R.; 1985. Evolución Cenozoica del piedemonte andino en la Pampa del Tamarugal, norte de Chile (18°-21° S). Actas IV Congreso Geológico Chileno, Antofagasta, V. 5, p. 149-164.

Parraguez, G.; 1998. Sedimentología y geomorfología producto de la tectónica cenozoica, en la Depresión Central, I Región de Tarapacá, Chile. Memoria de Título. Depto. de Geología, U. de Chile, 108 p.

Riquelme, R.; 1998. Evolución tectono-sedimentaria post-oligocénica del borde occidental del Altiplano, I Región, Chile. Tesis de Magister y Memoria de Título. Depto. de Geología, U. de Chile, 123 p.

Roeder, D.; 1988. Andean-age structure of Eastern Cordillera (Province de La Paz, Bolivia). Tectonics, V. 7, N° 1, p. 23-39.

Salas, R.; Kast, R.; Montecinos, F.; Salas, I.; 1966. Geología y recursos minerales del Departamento de Arica, Provincia de Tarapacá. Instituto de Investigaciones Geológicas, Boletín 21, 130 p.

Sempéré, T.; Hérail, G.; Oller, J.; Bonhomme, M.; 1990. Late Oligocene-early Miocene major crisis and related basins in Bolivia. Geology, V. 18, p. 946-949.

Tobar, A.; Salas, I.; Kast, R.; 1968. Cuadrángulos Camaraca y Azapa. Provincia de Tarapacá. Inst. de Invest. Geol., Carta Geol. de Chile N° 19 y 20, 13 p.

Wörner, G.; and 8 authors; 1988. The Nevados de Payachata volcanic region (18°S/ 69°W, N. Chile). I. Geological, geochemical, and isotopic observations. Bull. of Volcanology, V. 50, N° 5, p. 287-303.

Wörner, G.; Hammerschmidt, K.; Henjes-Kunst, F.; Lezaum, J.; Wilke, H.; 2000a. Geochronology (Ar-Ar, K-Ar and He-exposure ages) of Cenozoic magmatic rocks from northern Chile (18-22°S): Implications for magmatism and tectonic evolution of the central Andes. Revista Geológica de Chile, V. 27, p. 205-240.

Wörner, G.; Lezaun, J.; Beck, A.; Heber, V.; Lucassen, F.; Zinngrebe, E.; Rössling, R.; Wilke, H.G.; 2000b. Precambrian and Early Paleozoic evolution of the Andean basement at Belén (northern Chile) and Cerro Uyarani (western Bolivia Altiplano). Journal of South American Earth Sciences. V. 13, N° 8, p. 717-737

U-Pb DATING WITH SUB-MILLION YEAR PRECISION OF EARLY ANDEAN PLUTONIC ROCKS IN THE COASTAL CORDILLERA OF CHAÑARAL, NORTHERN CHILE

Sergio H. GELCICH (1), Donald W. DAVIS (2), Edward T.C. SPOONER (3)

(1) SERNAGEOMIN (Chile) - University of Toronto, Ontario, Canada, gelcich@geology.utoronto.ca
(2) Earth Science's Department, Royal Ontario Museum, Toronto, Ontario, Canada
(3) Department of Geology, University of Toronto, Ontario, Canada

KEY WORDS: U-Pb, Zircon, Coastal Cordillera, Magmatism, Geochronology

INTRODUCTION

The central Andes represents a continental boundary complex characterised by subduction of oceanic crust beneath the western margin of the South American continent. Subduction has been active and continuous since the Jurassic, i.e. since the Pangea-Godwana breakup (Mpodozis and Ramos, 1990). The associated deformation, magmatism and metamorphism define what is called the Andean orogeny (Mpodozis and Ramos, 1990) or Andean Cycle (Coira et al., 1982). The tectonic conditions along the margin during the Jurassic and early Cretaceous (early stages of the Andean Cycle) were characterised by an extensional regime with the consequent development of an arc–back arc pair (Mpodozis and Ramos, 1990). The Jurassic-Cretaceous magmatic complexes in northern Chile developed above a basement that consists of a penetratively deformed, Palaeozoic, low-grade metasedimentary sequence associated with a fore arc basin and plutonic (S and I type) and volcanic units of Permo-Triassic age (Berg and Baumann, 1985; Dallmeyer et al., 1996). The Jurassic-Cretaceous plutonic complexes range from calc-alkaline hornblende-biotite gabbros, through diorites, tonalites and granodiorites with subsidiary granites that were emplaced in the upper crust (Dallmeyer et al., 1996).

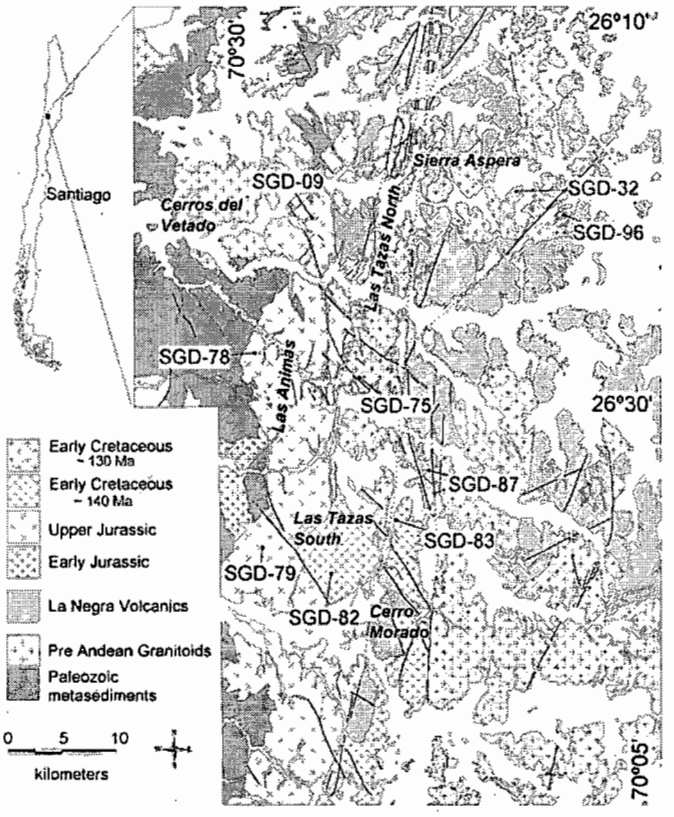

Fig.1 Geological Map of the Coastal Cordillera in the Chañaral area; based on Godoy and Lara (1998) and Lara and Godoy(1998). The main plutons and U-Pb sample locations are shown.

The present research presents preliminary results of U-Pb zircon geochronology on nine Jurassic and Cretaceous plutonic rocks in the Coastal Range of

Chañaral (Fig. 1). The new data are compared with published data allowing a discussion of magmatic evolution in the early Andean stages.

GEOLOGICAL CONTEXT

Detailed regional geological maps (scale 1:100.000) have recently been published by the Geological Survey of Chile covering the area of interest (Godoy and Lara, 1998; Lara and Godoy, 1998). The geology of the area has also been examined by Berg and Baumann (1985); Brown et al (1993) and Dallmeyer et al., (1996). The oldest rocks are grouped into the Paleozoic Chañaral metamorphic complex and consist of marine sequences with turbiditic facies of quartzites and slates. The metamorphosed sequences are intruded by S-type Permo-Triassic plutons (e.g Cerros del Vetado pluton).

The first record of "Andean" magmatic activity in the area is represented by the basal levels of the La Negra volcanic formation, which is composed of andesites and basaltic andesites with a few intercalations of conglomerate and calcareous sandstone (Godoy and Lara, 1998). In the Antofagsta region andesitic lavas have given a Rb-Sr age of 186 ± 14 Ma (Rogers and Hawkesworth, 1989), which we interpret as a minimum age.

Plutons or plutonic complexes in the area usually present elongate shapes, sometimes bordered by mylonite zones such as the trench parallel Atacama Fault system (Brown et al., 1993). Previous geochronologic data show that plutonic activity has four main peaks in the study area (Early Jurassic, ~190-180 Ma; Late Jurassic ~160 Ma; ~140 Ma and ~130 Ma). Each distinct episode of magmatism was located successively eastward, inboard from the subduction zone.

METHODS

U-Pb analyses were carried out at the Royal Ontario Museum using methods described in Krogh (1973, 1982) except that dissolution capsules and columns were scaled down to reduce blank. All errors are given at 2 sigma levels. Current Pb blank levels of less than 1 picogram permit precise analyses of fractions consisting of one or several grains. Only grains that showed no evidence of cores, cracks or alteration were selected for laboratory abrasion and analysis. Precise ages on Mesozoic zircon must rely on the $^{206}Pb/^{238}U$ decay system. Corrections for ^{230}Th disequilibrium are no more than 0.1 Ma but these ages can be biased by secondary Pb loss as well as inheritance from Phanerozoic sources while still preserving concordancy. Reproducibility of concordant data is the best argument that sources of bias have been avoided.

RESULTS AND DISCUSSION

Most of the data are concordant and $^{206}Pb/^{238}U$ ages from individual samples agree within analytical error for six of the nine samples (Fig 2). Only one sample, SGD-83, contained evidence for much older inheritance in the form of an imprecise discordant datum (off scale on Fig 2), which gives an upper concordia intercept of about 1100 Ma when regressed with the concordant data.

Zircons from disturbed samples show a large range in U concentrations, which seem to be correlated with age. The youngest datum from SGD-09 (155.2 ± 0.6 Ma) shows a U concentration of 200 ppm versus 20-40 ppm for the two older data, which agree in age at 156.4 ± 0.3 Ma. Th/U ratios are uniform and unusually high for

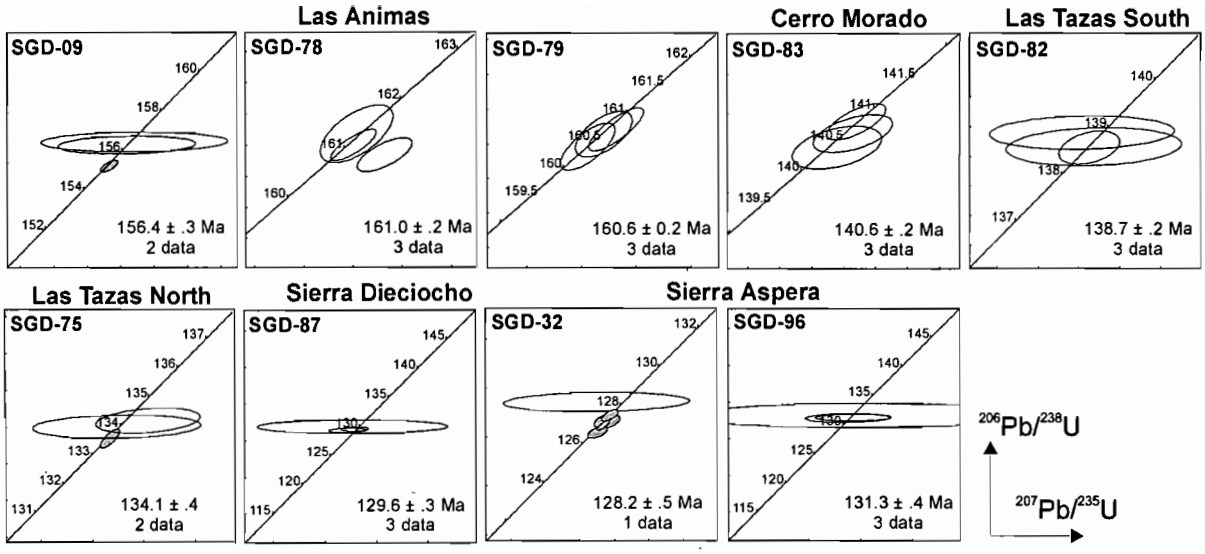

Fig. 2 Concordia diagrams for the 9 new U-Pb zircon dates; samples locations given in Fig. 1. Ages are calculated using $^{206}Pb/^{238}U$ on the unfilled error ellipses (see text for discussion).

zircon, which suggests that none the grains are inherited. The fact that the higher uranium fraction shows a younger age suggests that it may have suffered minor secondary Pb loss (<1%) and that the age of the two low U fractions is closer to the time of crystallization. Similarly with SGD-32, an exceptionally low U fraction (14 ppm vs 100-300 ppm) gives the oldest $^{206}Pb/^{238}U$ age of 128.2 ± 0.5 Ma, which is most likely to represent primary crystallization. Data from the other fractions range in age down to 126.6 ± 0.3 Ma. The two oldest data from SGD-75, which agree at 134.1± 0.3 Ma, are more likely to give the primary age than a slightly younger, higher U datum (16 ppm versus 140 ppm). Further work will be required to confirm the accuracy of these ages.

The new ages can be assigned to three of the main plutonic peaks: Upper Jurassic, Jurassic-Cretaceous and Early Cretaceous. Late Jurassic samples are from the Las Animas complex, quartz diorites to granodiorites that intrude Palaeozoic metamorphic rocks and the lavas of the La Negra formation. Its eastern border is sharp and defines one of the main lineaments of the Atacama Fault Zone. Three ages range from 156.4 ± 0.3 to 161.0 ± 0.2 (SGD-09, SGD-78 and SGD-79; Figs. 1 and 2) with the youngest pluton appearing in the north.

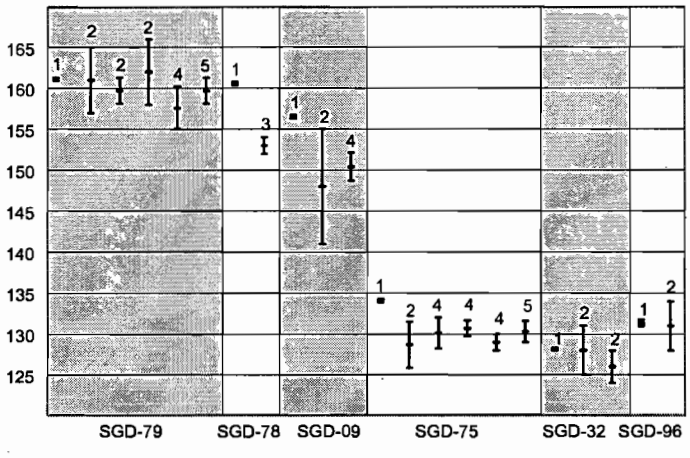

Fig. 3 Comparison of new U-Pb zircon ages with pre-existing geochronology, including errors. Numbers identify radiometric methods; 1: U-Pb zircon age, this work; 2: K-Ar; 3: Ar-Ar; 4: Rb-Sr; 5: previous U-Pb. References in Godoy and Lara (1998) and Lara and Godoy (1998).

A monzodiorite from the Cerro Morado pluton (SGD-83) has been dated at 140.6 ± 0.2, indicating a slightly older age for the pluton than the one suggest by Lara and Godoy (1998). A granodiorite (SGD-82) from the southern pluton of the Las Tazas complex is 138.7 ± 0.2 Ma old.

The Early Cretaceous northern Las Tazas complex appears to be distinctly younger than the southern segment, according to the 134.1 ± 0.3 Ma age obtained from a quartz diorite (SGD-75). A quartz monzodiorite of the Sierra Dieciocho pluton, partially mineralised with iron oxide

stockwork in the area of the Manto Verde iron mine, gives an age of 129.6 ± 0.3 (SGD-87). A preliminary age of 128.2 ± 0.5 Ma was obtained from the interior of the Sierra Aspera pluton (SGD-32) while a sample from the pluton margin (SGD-96) proved to be 3 m.y. older (131.3 ± 0.4 Ma). Both results are comparable to previous less precise ages (Fig. 3) but are clearly resolved, indicating that the compositional zonation in Sierra Aspera (interior granodiorite grading to exterior quartz diorite) was established over at least several million years and is unlikely to have resulted from crystallization of a single magma.

Geobarometry studies in some of the plutons indicate an epizonal emplacement (Dallmeyer et al., 1996) suggestive of later rapid cooling processes. This is corroborated in some areas by the similarity in ages obtained using isotopic systems and minerals with different closure temperatures (Fig. 3; SGD-79, SGD-32 and SGD-96). Despite this general agreement differences are evident when comparing some previous ages with the new U-Pb data for closely located samples of the same plutonic units (Fig. 3; SGD-78, SGD-09 and SGD-75). Berg and Baumann (1985) noted such discrepancies and inferred that major thermal events perturbed the Rb-Sr system. In these cases, less robust systems in terms of closure temperature have probably suffered some degree of resetting due to post-crystallization thermal effects related to emplacement of adjacent plutons, shearing and /or widespread dyke intrusions.

REFERENCES

Berg, K., Baumann, A. 1985. Plutonic and metasedimentary rocks from the coastal range of northern Chile: Rb-Sr and U-Pb systematics. Earth and Planetary Science Letters, 75, 101-115.

Brown, M., Diaz, F., Grocott, J. 1993. Displacement history of the Atacama fault system, 26°00'S-27°00'S, northern Chile. Geological Society America Bulletin, 105, 1165-1174.

Coira, B., Davidson, J., Mpodozis, C., Ramos, V. 1982. Tectonic and magmatic evolution of the Andes of northern Argentina and Chile. Earth Science Reviews, 18, 303-332.

Dallmeyer, R.D., Brown, M., Grocott, J., Graeme, K.T., Treolar, P. 1996. Mesozoic magmatic and tectonic events within the Andean plate boundary zone, 26°-27°30'S, north Chile: constraints from 40Ar/39Ar Mineral Ages. The Journal of Geology, 104, 19-40.

Godoy, E., Lara, L. 1998. Hojas Chañaral y Diego de Almagro, region de Atacama. Servicio Nacional de Geologia y Mineria. Mapas Geologicos No 4. 1 map scale 1:100.000, Santiago.

Krogh T. E. 1973. A low-contamination method for hydrothermal decomposition of zircon and extraction of U and Pb for isotope age determinations. Geochim. Cosmochim, 37, 485–494.

Krogh T. E. 1982. Improved accuracy of U-Pb zircon ages using an air abrasion technique. Geochim. Cosmochim, 46, 637–649.

Lara, L., Godoy, E. 1998. Hoja Quebrada Salitrosa, Region de Atacama. Servicio Nacional de Ggeologia y Mineria. Mapas Geologicos No 3. 1 map scale 1:100.000, Santiago.

Mpodozis, C., Ramos, V.A. 1990. The Andes of Chile and Argentina: Circum-Pacific Council for Energy and Mineral resources, Earth Science Series, 11, 59-90.

Rogers, G., Hawkesworth, C., 1989. A geochemical traverse across the North Chilean Andes; evidence for crust generation from the mantle wedge. Earth and Planetary Science letters, 91, 271-285.

NUMERICAL MODELLING OF DEFORMATION PROCESSES IN THE ANDES

Muriel GERBAULT (1), Gérard HERAIL (1), Joseph. MARTINOD (2)

(1) IRD UR 104, 38 rue des 36 Ponts, 31400 Toulouse, FRANCE (gerbault@lmtg.ups-tlse.fr)
(2) LMTG Université Paul Sabatier, 38 rue des 36 Ponts, 31400 Toulouse, FRANCE

KEY WORDS: faulting, lithospheric deformation, rheology, plate boundary, numerical modelling

INTRODUCTION

Numerical models taking into account the pressure and temperature dependent rheology of the lithosphere are developed in order to bring insights on the distribution of deformation across the Andean orogeny. A general question concerns the extent of the plate boundary, which is the understanding of deformation that is either directly linked to the subducting plate beneath the South American continent, or deformation that is typical of intra-continental domain. Constraints provided by data such as geological reconstructions, geochronology, geomorphology, or seismicity, allow to propose models or mechanisms of deformation, and numerical models help to validate some of these propositions. At this stage we develop a parametric study, exploring the spatial distribution of strength and thermal heterogeneities within the continental lithosphere, and how the rheological properties are modified by the advancing subducting plate. Proposed subjects of study concern 1) deformation of the fore-arc portion of the continental lithosphere in the Central Andes, 2) the role of inherited structural heterogeneities on the differences in height, crustal thickness and mode of deformation in between the Altiplano and the Puna.

1. NUMERICAL METHOD

We use a finite differences two-dimensional code modified from Parovoz (Poliakov & Podladchikov, 1992). It is based on the Fast Lagrangian Analysis Continuum method (FLAC, Cundall & Board, 1988), which incorporates an explicit time-marching scheme, and allows the use of a wide range of constitutive laws such as brittle-elastic-ductile rheology derived by rock experimentalists (Ranalli, 1995). It handles initiation and propagation of non-predefined faults (shear bands).

As a general approach, the lithosphere and part of the asthenosphere are modelled as a medium of about 100 to 500 km thick and about 10 times longer in width. Each element is 1 to 5 km^2, depending on the specific question that the model addresses. Both lateral borders are free to slip vertically, and a horizontal velocity V_x is applied from the sides. The lithosphere+asthenosphere medium floats on a 'perfect-fluid' asthenosphere within the gravity field; hydrostatic boundary conditions are applied at the bottom of the model.

The equation of motion is resolved for each element and at each time-step, constrained by the boundary conditions. At the stress-free surface, erosion and sedimentation processes are modelled using a diffusion equation. The heat equation is resolved with time, while the initial temperature field is calculated according to an age dependent procedure (e.g. Burov & Diament, 1992), linked to the inherited thermal history.

The modelled lithospheric plate is composed of crustal layers and a lithospheric mantle, which have different densities and rheological properties. Elastic-viscous-brittle behaviour is modelled with pressure-dependent, non-associative, Coulomb criterion for brittle failure and temperature-dependent creep power-law for

ductile behaviour. The brittle-ductile transition is self-consistently defined in the modelling, and is empirically referred to as the depth at which the deviatoric shear stress becomes lower than 20 MPa (for a discussion see Ranalli, 1995).

2. LITHOSPHERIC FAULTING IN THE CENTRAL ANDES FOREARC

Numerical models of ongoing subduction incorporate a subducting oceanic lithosphere in contact with the continental lithosphere, and a part of the asthenosphere. Preliminary modelling consists of testing the effects of relative strength contrasts between the different oceanic and continental layers that are in contact: the brittle yield stress and the power-law parameters defined by a dominant composition, together with the geotherm, all contribute to control the localisation of deformation (and the geometry of faults), at the scale of several millions of years convergence.

These models investigate not only the effect of the advancing oceanic lithosphere on surrounding crustal and mantle continental material, but also the far field reaction of the intra-plate domain. A preliminary model (figure 1) containing a relatively high friction between the oceanic plate and the continental plate, displays two main features: 1) shear zones (fault zones) that initiate from the subducting plate, 2) shear zones that develop far into the continental domain, where an initially warmer area has been inserted.

The first set of shear zones result from the compression exerted by the bended slab on the continental lithosphere, and do not require any specific strength contrast within the continental lithosphere. The 'western most' shear zone initiates at the base of the ductile continental crust, while the second one to the east initiates above the base of the 'strong' continental lithosphere; they both propagate to the surface. At the surface, these shear zones emerge as two bulges, bounding a crustal wedge and a lithospheric wedge. They form the western boundary of a domain subjected to crustal scale folding (oscillations of the topography seen in fig. 1).

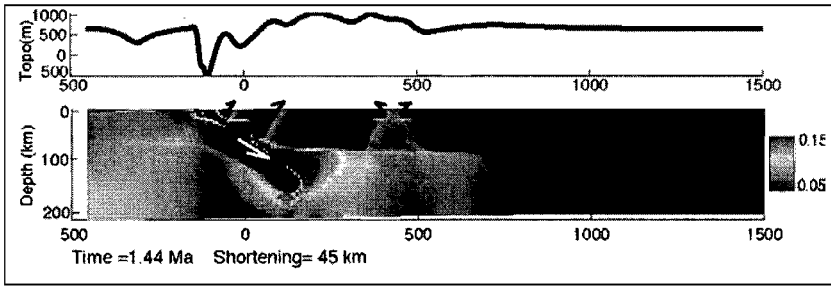

Figure 1 : Preliminary model of continental deformation above a subduction zone : development of shear bands (or fault zones) 1) at the base of the crust and of the lithosphere, 2) strain localisation in an area far away from the subduction zone, where an initial weak rheology has been inserted.

In order to link modelled shear zones with observational data, these models require further investigations such as their sensitivity to rheological variations within the lithospheric plates but also at their contact. However the first set of shear zones initiating from the subducting plane finds some support in seismic and geological records. David et al. (ISAG, 2002) studied the crustal seismicity recorded in the northern most part of the Chilean forearc from about 18°S to 19°S. Below the Precordillera and the Central Depression, seismic events define a zone under compression dipping about 45° towards the trench, connecting nearly perpendicular to the subducting plane. Focal mechanisms and stress tensors show a consistent compressive stress regime for earthquakes occurring down to 59 km depth. David et al (ISAG, 2002) suggest that this quasi-planar zone of seismicity probably results from the difference in rheology of the forearc and of the Altiplano and Western Cordillera. However, our preliminary models indicate that such a rheological boundary is not necessary to the formation of such a shear zone.

3. LATERAL FLOW FROM THE PUNA TOWARDS THE ALTIPLANO?

The subduction styles are quite similar in the Central Andes in the Puna and in the Altiplano (no significant internal deformation or rotations in Neogene times neither in the fore-arc nor in the Brazilian Craton), but geological and geophysical studies indicate different features:

1) On a general east-west direction, the amount of crustal shortening across the Altiplano is twice as large as that across the Puna (about 100 km difference). Crustal shortening in the Altiplano would contribute for 20% less than the present day crustal volume (Kley et Monaldi, 1998; Rochat et al. 1999).
2) Paleomagnetism measurements show clockwise rotation of crustal blocks in the southern part of the Altiplano (Roperch et al. 2000).
3) Seismic velocities attenuation at depths ~50 to ~150 km is stronger under the Altiplano than under the Puna. Amongst several different interpretations, Whitman et al. (1992) suggested this could be due to the absence of continental mantle lithosphere below the Puna (the crust is directly in contact with the asthenosphere).
4) Best fitting models of interseismic crustal velocities in the central Andes (Bevis et al. 2001) are inclined about 30° to much towards the west with respect to measured GPS velocities.

Although aware that other data may contradict these features, we propose to explain them by an active lateral flow of the lower crust, from the Puna towards the Altiplano. Preliminary 2D numerical models show that for a higher average elevation of the Puna, upper crustal material flows towards the Altiplano, which is however compensated by a strong counter flow at the base of the crust. However, if in addition the continental mantle lithosphere under the Puna is lighter or thinner than under the Altiplano, crustal-scale flow from the Puna towards the Altiplano develops on a large time-scale, at a rate of about 2 mm/yr (Fig. 2). This velocity cannot be precisely constrained, since its value is highly dependent on the poorly known lower crust viscosity. The value obtained in this example shows, however, that this phenomenon may occur at non-negligible geological rates.

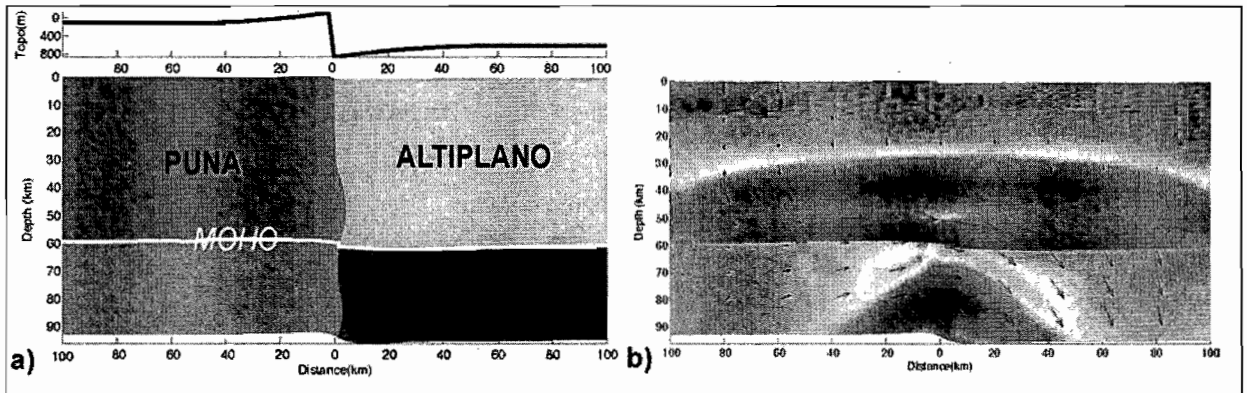

Figure 2: 2D north-south model in which the Puna crust to the left is initially higher and thinner than the Altiplano crust to the right. **a)** Surface topography after 2 Ma, with the Puna and Altiplano crusts respectively in blue and green, and the Puna and Altiplano mantle, respectively in orange and brown. **b)** Shear strain rate and velocity vectors, showing lower crustal flow in red, at rate of about 2mm/yr. The Puna crust is initially higher by 1 km than the Altiplano crust. When a density difference exists between the mantle lithospheres of the Puna and Altiplano, then a sustained flow from the Puna towards the Altiplano develops.

This mechanism of lateral flow is one amongst other ways to explain, by initial mechanical heterogeneities, the origin of observed different styles of deformation between the Puna and the Altiplano. This study is still in very preliminary stage and requires a deeper investigation of geological and geophysical information.

CONCLUSIONS

Preliminary modeling can reproduce the development of crustal and lithospheric scale shear zones as a result of the advancing subducting plane into the continent, and without introducing pre-existing rheological heterogeneities. However, rheological or thermal heterogeneities could explain the localization of deformation in an intraplate domain, such as for example where a Proterozoic basin would exist. Crustal thickness or densities variations may also explain large-scale south-to-north crustal flow.

These preliminary results are promising but still require improvement of specific initial and boundary conditions, which can only be provided by adequate and precise geological and geophysical information. The numerical method is still under development, for its application to the large scale of the Andes, requiring to take into account phase transitions and other temperature dependent deformation processes, for the implementation of surface processes, capable of reproducing geomorphologic markers, and finally for the development of a 3D approach, necessary to reproduce fundamental features in the Andes.

REFERENCES

Bevis M., Kendrick E., Smalley R., Brooks B., Allmendinger R., Isacks B., 2001. On the strength of interplate coupling and the rate of back-arc convergence in the central Andes: an analysis of the interseismic velocity field, Geochemistry Geophys., Geosystems 2, nov.

Burov E.B., Diament M., Flexure of the continental lithosphere with multilayered rheology, *Geophys. J. int 109*, 449-468, 1992.

Comte, D., Dorbath L., Pardo M., Monfret T., Haessler H., L. Rivera, Michel Frogneux, B. Glass and C. Meneses, *Geophys. Res. Lett.*, 26, 1965-1968, 1999.

David C., Martinod J., Comte D., Hérail G., Haessler H., Intracontinental seismicity and neogene deformation of the andean forearc in the region of Arica (18.5°s-19.5°s), ISAG abstracts 2002.

Gerbault, M., E. B. Burov, A. N. B. Poliakov, and M. Daignières, Do faults trigger folding in the lithosphere?, *Geophys. Res. Lett. 26*, 271-274, 1999.

Poliakov, A., and Y. Podladchikov, Diapirism and topography, *Geophys. J. Int. 109*, 553-564, 1992.

Ranalli G. *Rheology of the Earth*, 2nd ed.,Chapman & Hall eds., 413p, 1995.

Rochat, P., Hérail G., Baby P., and Mascle G., *C. R. Acad. Sci.*, 328, 189-195, 1999.

Romanyuk T.V., Gotze H.J., Halvorson P.F., A density model of the Andean subduction zone, *The Leading edge*, 264-268, 1999.

Roperch P., Fornari M., Hérail G., Parraguez G. Tectonic rotations within the Bolivian Altiplano; implications for the geodynamic evolution of the Central Andes during the late Tertiary. *J. Geophys. Res. 105-1*, 795-820, 2000.

DEFORMATIONAL HISTORY OF THE ANDES, BETWEEN 33° AND 34° SOUTH LATITUDE, CHILE AND ARGENTINA

Laura B. GIAMBIAGI [1,2], Victor A. RAMOS [1], Estanislao GODOY [3] and P. Pamela ALVAREZ [1]

[1] Laboratorio de Tectónica Andina, Universidad de Buenos Aires, Ciudad Universitaria s/n, Pabellón II, Capital Federal, Argentina. Email: andes@tango.gl.fcen.uba.ar
[2] Centro Regional de Investigaciones Científicas y Tecnológicas, Parque San Martín s/n, Mendoza, Argentina. CONICET. Email: lgiambia@lab.cricyt.edu.ar
[3] Servicio Nacional de Geología y Minería. Casilla 10465, Santiago, Chile. Email: egodoy@sernageomin.cl

KEYWORDS: Southern Central Andes, Cenozoic deformation, Aconcagua fold and thrust belt, Cordillera Frontal.

INTRODUCTION

It is generally accepted that compression of the active margin between the Nazca and South American plates controls the development of the Andean orogenic belt. Timing of the onset of Andean deformation and the different structural phases remain, however, uncertain. The present-day structure of the chain is characterized from west to east by the Cordillera Principal and Cordillera Frontal. The Oligocene to Miocene volcanic arcs and the Neogene Aconcagua fold and thrust belt make up western and eastern Cordillera Principal respectively. The foreland, on the other hand, is marked by the inversion of Triassic extensional faults of the Cuyo basin.

The structure of the western Cordillera Principal is dominated by the inversion of an Oligocene – Early Miocene extensional basin in a bivergent sense (Charrier et al., 1997; Godoy et al., 1999). The easternmost extension of the basin corresponds to an out-of-sequence thrust, which marks the border between western and eastern sectors, assumed to ramp up from a mid-level detachment in the basement (Fig. 1). The Aconcagua fold and thrust belt has been divided in three major domains: the eastern foreland basin domain, the central thin-skinned domain and the western basement-involved domain (Giambiagi and Ramos, 2002). The eastern sector, where Neogene synorogenic units crop out, comprises thin-skinned fold-thrust sheets above a decollement developed in Upper Cretaceous siltstones. The central thin-skinned domain is characterized by a dense array of imbricate thin-skinned thrusts and exhibits flat and ramp geometries. In the western domain the basement does not crop out; its involvement is deduced on the geometry of the structure, rift stratigraphy and significant thickness variations of the deformed Mesozoic succession exposed (Alvarez et al., 2000; Giambiagi et al., 2002).

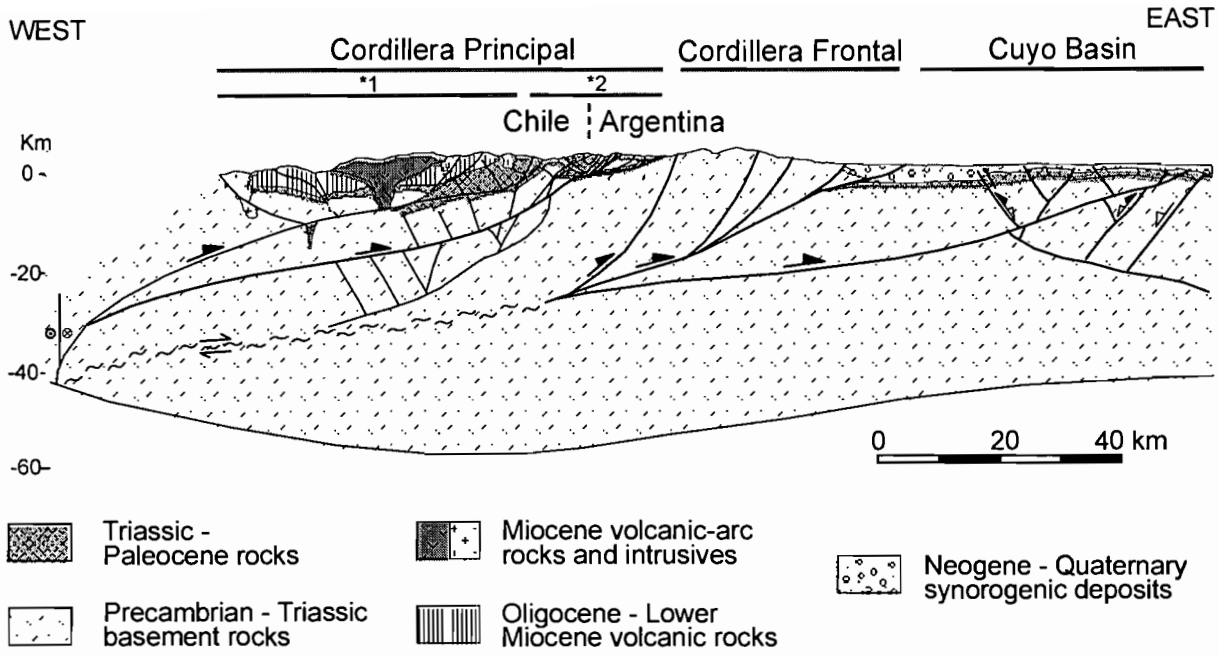

Figure 1: Cross-section through the southern Central Andes, at 33°40′S. *1 Oligocene to Miocene volcanic arcs. *2 Aconcagua fold and thrust belt.

The Cordillera Frontal consists of several basement blocks that form the backstop behind the Aconcagua fold and thrust belt (Fig. 1). During Late Cenozoic compression this morphostructural unit behaved as rigid blocks disrupted by medium to high angle faults. At the study latitudes it is composed, from north to south, by the Cordón del Plata (32°40' to 33°20′S), Cordón del Portillo (33°20′ to 33°50′S) and Cordillera de las Llaretas (33°50′ to 34°10′S) ranges. The Cordón del Plata is uplifted by the La Carrera fault system consisting of four N to NNE-trending high-angle faults. This system involves the metamorphic basement in the deformation, constituting a thick-skinned system that was generated during the Late Paleozoic compression (San Rafael orogeny) and reactivated during the Andean deformation. In the Cordón del Portillo two trends of regional structures exist: NNE-trending faults in the northern region and N to NNW-trending faults in the southern half, related to Late Paleozoic structures. The Cordillera de las Llaretas was uplifted along two NNW-trending high angle faults.

The Triassic – Neogene Cuyo basin, located in the Andean foreland, is characterized by a series of spaced elongate anticlines, locally broken by reverse faults displaying eastward or westward vergence (Dellapé and Hegedus, 1995). These structures are aligned along two NNW-striking structural trends. The basin was marginally uplifted and subjected to moderate structural inversion of Triassic half-grabens and its related relay transfer faults bounded during Late Cenozoic compression.

CONCLUSIONS

Accurate recording of surface structural and sedimentological data has been integrated with available magnetostratigraphical data (Irigoyen et al., 2000) and geochemical studies (Kurtz et al., 1995; Ramos et al., 1996) to show the progressive development of the Andes at the latitudes between 33° and 34° S during Cenozoic times.

Deformational stage D1: Early to Middle Miocene (20? – 15 Ma)

There are several lines of evidence supporting the hypothesis that compressional deformation started only around 20 to 18 Ma at the study latitudes: (1) the first indication of tectonism and uplift of the Cordillera Principal represented by deposition of the synorogenic strata in the Early-Middle Miocene (~ 18 Ma); (2) the slow uplift and cooling of intrusives during the Early Miocene (20-16 Ma) (Kurtz et al., 1995); (3) the presence of an extensional basin in western Cordillera Principal during Oligocene – Early Miocene times; and (4) the existence of the retro-arc geochemical signature of the Contreras volcanism in eastern Cordillera Principal which indicates an unthickened crust until ~ 18 Ma (Ramos et al., 1996). During the first 1 or 2 Ma the uplift was concentrated in the Oligocene extensional basin of western Cordillera Principal. At around 18 Ma, inversion of the Mesozoic extensional basin located in the eastern Cordillera Principal took place after the extrusion of retro-arc volcanic rocks.

Deformational stage D2: Middle to Late Miocene (15 – 9 Ma)

As deformation migrated progressively eastward, it involved the Mesozoic sequences and generated the Aconcagua fold and thrust belt. Basement thrusts transported the inverted structures of the western Cordillera Principal, forming a hybrid thin and thick-skinned belt. Overprinting relationships indicate that the fold and thrust belt evolved by a forward propagating thrust sequence with constant periods of out-of-sequence thrust emplacement. During this stage uplifting of the Cordillera Frontal was confined north of 33°S to the Cordillera del Tigre.

Deformational stage D3: Late Miocene (9 – 6 Ma)

During this stage, the deformation of the Cordillera Frontal progressed southward, uplifting the Cordón del Plata and then the northern part of the Cordón del Portillo. This event was responsible for the generation of a broken foreland basin and the development of a cumulative wedge represented by the proximal synorogenic deposits. During this time the emplacement of out-of-sequence thrusts took place in western Cordillera Principal.

Deformational stage D4: Late Miocene – Early Pliocene (6 – 4 Ma)

The uplift of the Cordillera Frontal generated a sticking point, preventing the propagation of the thrust belt towards the foreland. As a result, a series of out-of-sequence thrusts developed in the eastern Cordillera Principal. Deformation of the Cordillera Frontal continued during this time with the uplift of the southern sector of the Cordón del Portillo and Cordillera de las Llaretas. The Cordón del Plata continued uplifting by the emplacement of the easternmost faults of the La Carrera fault system.

Deformational stage D5: Early Pliocene - present (4 – 0 Ma)

Thrusting along the Cordillera Principal had terminated by ~4 Ma and subsequently, the deformation front migrated to the Precordillera foothills, north of 33°S, and to the Cuyo basin and Cordillera Frontal foothills,

south of 33°S. At this time the basal decollement of the Cuyo basin began to move, reactivating pre-existing normal faults as inverted faults and generating new thrust faults.

REFERENCES

Alvarez, P. P., V. A. Ramos, L. B. Giambiagi, and E. Godoy, 2000. Relationships between different depocenters of Triassic – Jurassic rift systems in the Main Andes of Argentina and Chile. XXIII Geological International Congress, Proceedings in CD, Brasil.

Charrier, R., J. J. Flynn, A. R. Wyss, F. Zapatta, and C. C. Swisher, 1997. Antecedentes bio y cronoestratigráficos de la Formación Coya Machalí – Abanico, entre los ríos Maipo y Teno (33°55′ y 35°10′S), Cordillera Principal, Chile Central. VIII Congreso Geológico Chileno, 1, 465-469, Chile.

Dellapé, D., and A. Hegedus, 1995. Structural inversion and oil occurrence in the Cuyo basin of Argentina. In: Petroleum basins of South American, A. J. Tankard, R. Suárez and H. J. Welsink (Eds.), 359-367, AAPG Memoir 62.

Giambiagi, L. B., and V. A. Ramos, 2002. Structural evolution of the Andes between 33°30′ and 33°45′ S, above the transition zone between the flat and normal subduction segment, Argentina and Chile. Journal of South American Earth Sciences 15(1) (in press).

Giambiagi, L. B., P. P. Alvarez, E. Godoy, and V. A. Ramos, 2002. The control of pre-existing extensional structures in the evolution of the southern sector of the Aconcagua fold and thrust belt. Tectonophysics (submitted manuscript).

Godoy, E., G. Yañez, and E. Vera, 1999. Inversion of an Oligocene volcano-tectonic basin and uplift of its superimposed Miocene magmatic arc, Chilean Central Andes: first seismic and gravity evidence. Tectonophysics, 306, 217-326.

Irigoyen, M. V., K. L. Buchan, and R. L. Brown, 2000. Magnetostratigraphy of Neogene Andean foreland-basin strata, lat 33°S, Mendoza Province, Argentina. Geological Society of America, Bulletin 112, 803–816.

Kurtz, A., S. Kay, A. Tittler, M. Mpodozis, and E. Godoy, 1995. Neogene magmatism in the Andean Cordillera (26°S to 34°S): evidence for spatial and temporal changes in crustal thickness. Eos, 76, S272.

Ramos, V. A., E. Godoy, V. Godoy, and F. Pángaro, 1996. Evolución tectónica de la Cordillera Principal argentino-chilena a la latitud del Paso de Piuquenes (33°30′S). XIII Congreso Geológico Argentino y III Congreso de Exploración de Hidrocarburos, 2, 337-352

TECTONIC IMPLICATIONS OF PERMIAN TO JURASSIC PALEOMAGNETIC RESULTS FROM THE PERUVIAN CORDILLERA

Stuart GILDER (1), Sonia ROUSSE (1), Daniel FARBER (2), Brendan MCNULTY (3), Victor TORRES (4), Oscar PALACIOS (4)

(1) Institut de Physique du Globe de Paris, Laboratoire de Paléomagnétisme, 4 place Jussieu, 75252 Paris Cedex 05 FRANCE (gilder@ipgp.jussieu.fr, rousse@ipgp.jussieu.fr)
(2) Lawrence Livermore National Laboratory, Livermore, CA, 94550 USA (Farber2@llnl.gov)
(3) Earth Science Dept., California State University Dominguez Hills, Carson CA 90747 USA (bmcnulty@csudh.edu)
(4) Instituto de Geológico Minero y Metalurgico, Lima, 1470 Avenida Canadá, San Borja, Lima 41, PERU, (torresbazanvictor@hotmail.com)

KEY WORDS: Jurassic, Paleomagnetism, Permian, Peru, Tectonics

We report paleomagnetic data from 28 sites of Permian and Jurassic strata. A stable magnetic component from six sites of Mitu Formation red beds from northern Peru (Bagua region) passes fold and reversal tests and likely represents a primary magnetization (Figure 1). The overall mean pole agrees well with Permian to Triassic poles from cratonal South America, suggesting this part of northern Peru has experienced neither significant rotation nor latitudinal transport since the Permo-Triassic. Thermal demagnetization isolates stable magnetic components in 18 of 22 sites collected from a region spanning 2° in latitude and 5° in longitude from Lake Titicaca to Pisac/Cusco to Ayacucho. The 18 sites are rotated significantly (25° to 125°) counterclockwise and pass a fold test based solely on magnetic inclinations. Three Permo-Triassic sites, two from the La Paz, Bolivia area (Roperch and Carlier, 1992) and another from the Huancayo region (Creer, 1970) are also rotated significantly counterclockwise. Importantly, the amount of the paleomagnetic rotations is similar for both Permian and Jurassic rocks, which would indicate that the rotations occurred after the Jurassic (Figure 2). Because Cretaceous to Neogene rocks from the Cordillera are rotated much less, it would suggest that the age of rotation lies between the Upper Jurassic and the Upper Cretaceous, consistent with an important deformation event observed at that time. Counterclockwise rotation of the Permian to Jurassic rocks implies that the tectonic regime responsible for the rotations included an important component of sinistral shear. However, the paleolatitudes of these sites show no important difference with respect to cratonal South America arguing against the hypothesis that the sites were part of an accreted terrain. The northern limit of sinistral shear lies between about 12°S and 6°S, south of the 6 sites from Bagua (Figure 2).

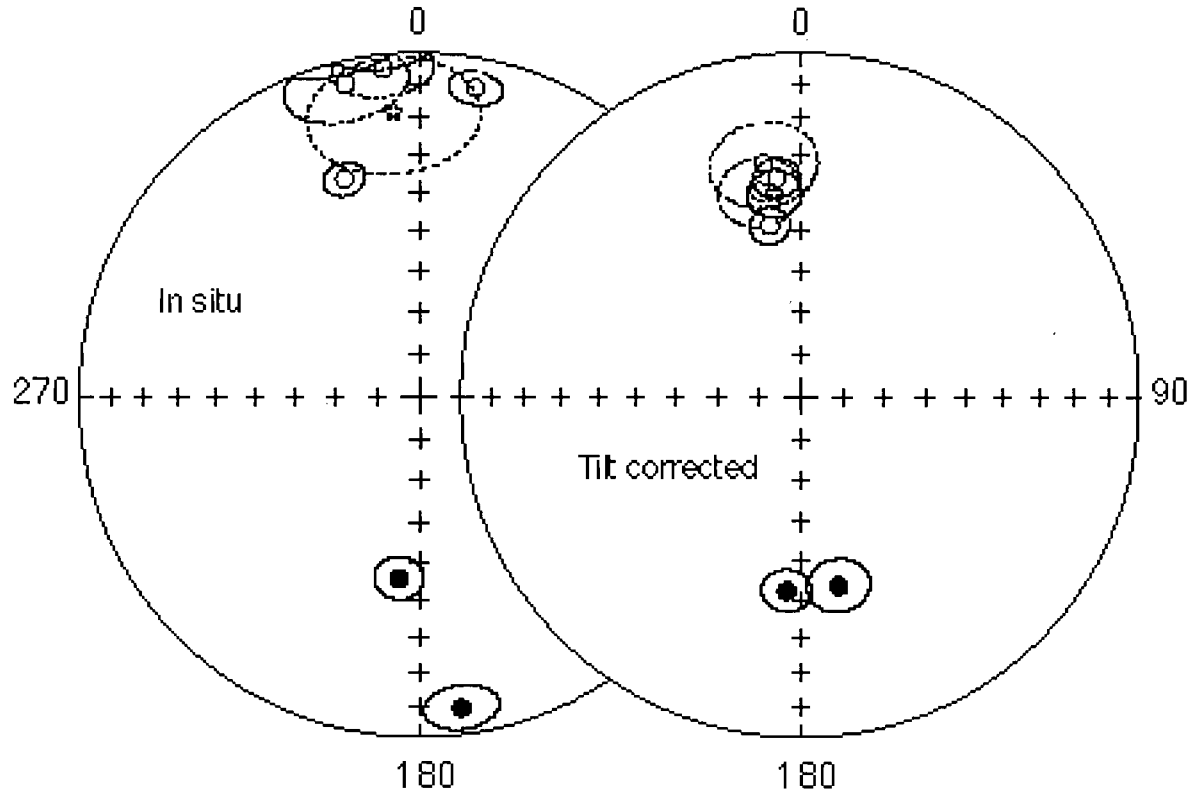

Figure 1. Site mean directions (circles) and 95% confidence envelopes of Mitu Group sites from Northern Peru (Bagua region sites PP938-943). Fold test is positive at the 95% significance level.

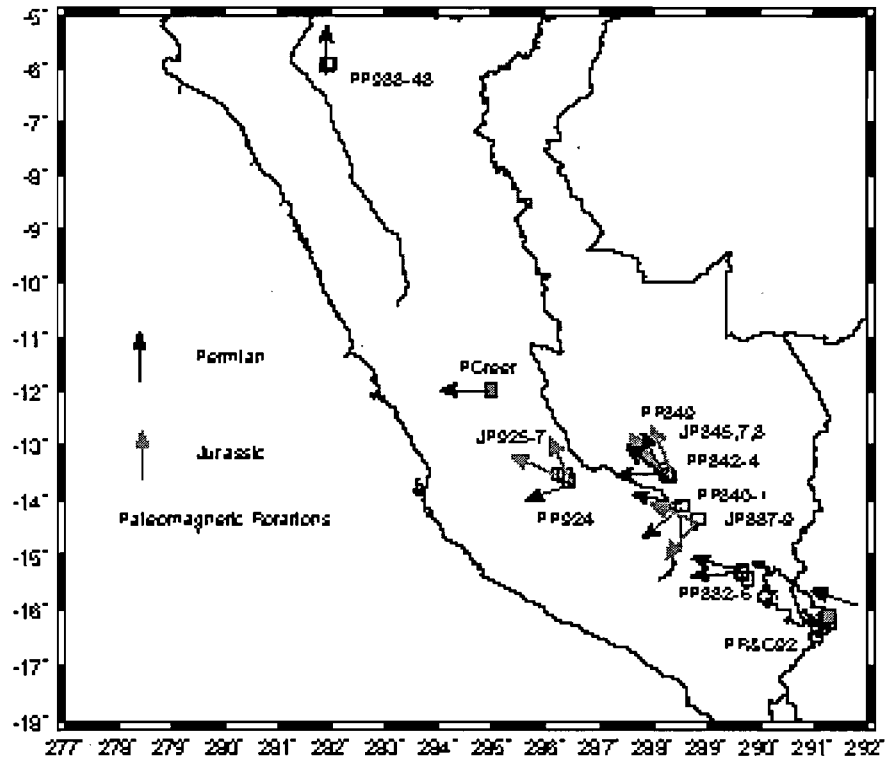

Figure 2. Paleomagnetic rotations in Peru. Sites beginning with a P are Permian; sites beginning with a J are Jurassic. Site PCreer from Creer (1970); site PR&C92 from Roperch and Carlier (1992).

REFERENCES

Creer, K.M., 1970. A palaeomagnetic survey of South American rock formations. Phil. Trans. Roy. Soc. London Ser. A, 267: 467-558.

Roperch, P. and Carlier, G., 1992. Paleomagnetism of Mesozoic Rocks from the Central Andes of Southern Peru : Importance of Rotations in the development of the Bolivian Orocline. Journal of Geophysical Research, 97(B12): 17,233-17,249.

THE MUD-DIAPIR TREND IN THE EASTERN VENEZUELAN BASIN

Carlos GIRALDO (1), Eduardo ALVAREZ (2), and Marco ODEHNAL (3)

(1) giraldoc@pdvsa.com
(2) alvareezez@pdvsa.com
(3) odehnalm@pdvsa.com

KEY WORDS: Eastern Venezuelan, Arcilokinesis, Lower Miocene Shale, Carapita Formation, Mud-Diapir.

INTRODUCTION

The Eastern Venezuelan basin is located south of the Serrania del Interior Oriental range, which represents the easternmost branch of the Andean uplift (Figure 1). The northernmost boundary of the Serrania del Interior Oriental range, is controlled by right lateral strike-slip motion. It includes the El Pilar Fault system, a major dextral fault, considered to be the main contact between Caribbean and South American plates (Fig. 2); it's dextral movement, seems to have started in the Upper Miocene; current slip rate is about 1 cm / year and total offset is around 70 km (Audemard and Giraldo, 1997). An igneous – metamorphic and sedimentary Caribbean belt, lying to the north of the El Pilar fault, was progressively thrusted over, against the South American passive margin (from west to east), during the Eocene / Miocene times (Audemard and Lugo, 1994). Towards the east, the Serrania del Interior Oriental range, ends up against a series of plio / pleistocene grabens (i.e. San Juan) , related to a NE -SW tectonic extension. More information, about seismic stratigraphy and tectonics, appears in Di Croce (1995), Hung (1997) and Ysaccis (1997). The mud diapir tract and its related structures occupies an WSW - ENE trending belt that stretches from Tonoro, to the west, to Pedernales in the Orinoco delta. These features, two hundred kilometers long and ten wide, have also been reported offshore and onshore in Trinidad with various degrees of activity that range from mud emanations to mud volcanoes, which occasionally rise above sea level. Also associated to this diapir trend a number of oil and gas seeps as well as asphalt lakes have been discovered. The age of diapirism seems to be restricted to a period from Pliocene to Recent. Seismic transects perpendicular to diapir development evidence both their geometry and growth (Fig.2).

CONCLUSIONS

The Plio-Pleistocene Mud-diapir trend has been well documented from seismic sections, south of the Serrania del Interior Oriental range. The age of remobilized shales is lower Miocene, and have been identified as part of the shaly section of the Mid. Miocene Carapita Formation, considered as a major seal in the basin. This trend runs parallel to the negative gravimetric anomaly located in the foredeep. The most intense arcilokinetic effect lies inmediatly southeast of the San Juan graben system; the observed gravimetric anomaly (Fig. 2) reaches its minimum value (200mgals); intensity of arcilokinesis decreases progressively disappearing altogether toward the west. The associated Mud ridges are very conspicous, and formed during Pliocene to Recent times, causing the onlapping geometry of youngest sediments (Figs.3 and 4). The uplift of Miocene shale is about 2.5 seconds

(TWT) and rotated onlaps are good indicators of recent uplift Probably, the shale remobilization, produces a void effect towards the north, that acomodates normal faulting at the San Juan Graben. This Mud diapir trend, has been identified by oil explorationists, since the beginning of this century (Hedberg, 1950) ,documented from seismic lines by Liliú (1990) and Duerto (2002).

REFERENCES

Audemard,F. and Giraldo C., 1997, Desplazamientos dextrales a lo largo de la frontera meridional de la placa Caribe, Venezuela septentrional, VIII Congreso Geológico Venezolano, Porlamar, I:101-108.

Audemard, F. and Lugo, J. 1994, An Updated Overview of Venezuela's Petroleum Basins, Short course #2 & 6, VII Congreso Venezolano de Geofísica, Caracas, (course Notes), 230 pp.

Di Croce, J., 1995, Eastern Venezuela Basin: Sequence Stratigraphy and evolution, PhD Thesis, Rice Univ., 225 pp.

Duerto L., (2002) Three-Dimensional Geometry and Evolution of Shale diapirs in the eastern Venezuelan Basin, AAPG, Houston (Poster Session).

Giraldo, C. 1999, Late Tertiary-Quaternary Structural styles: Serrania del Interior Oriental Foothills, Northeastern Venezuela, 6th International Congress of the Brazilian Geophysical Society, SBGf42899, 4pp.

Hedberg, H., 1950, Eastern Venezuela Basin (Anzoategui-Monagas-Sucre-Eastern Guárico), BGSA V.61,11:1173-1216.

Hung, E., 1997, Foredeep and Thrust Belt interpretation, Maturin Basin, Eastern Venezuela, MsC Thesis, Rice Univ.125 pp.

Liliú A., 1990, Geophysical Interpretation pf Maturin Foreland Northeastern Venezuela, MsC Thesis, Rice Univ.124 pp.

Pimentel, N., 1984, Mapa Geológico Estructural de Venezuela, Esc. 1:2.500.000, MEM., Caracas.Ysaccis, R. ,1997, Tertiary evolution of the Northeastern Venezuela offshore, PhD Thesis, Rice Univ., 285 pp

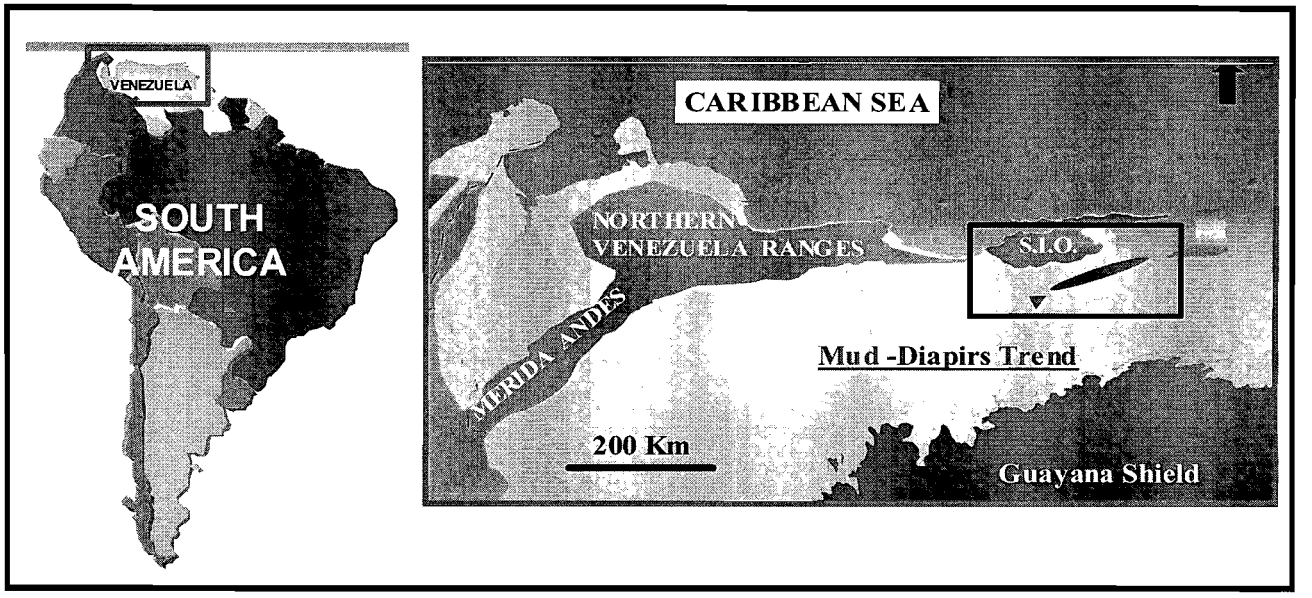

Figure 1. Location of the Mud –Diapirs Trend (S.I.O.= Serranía del Interior Oriental).

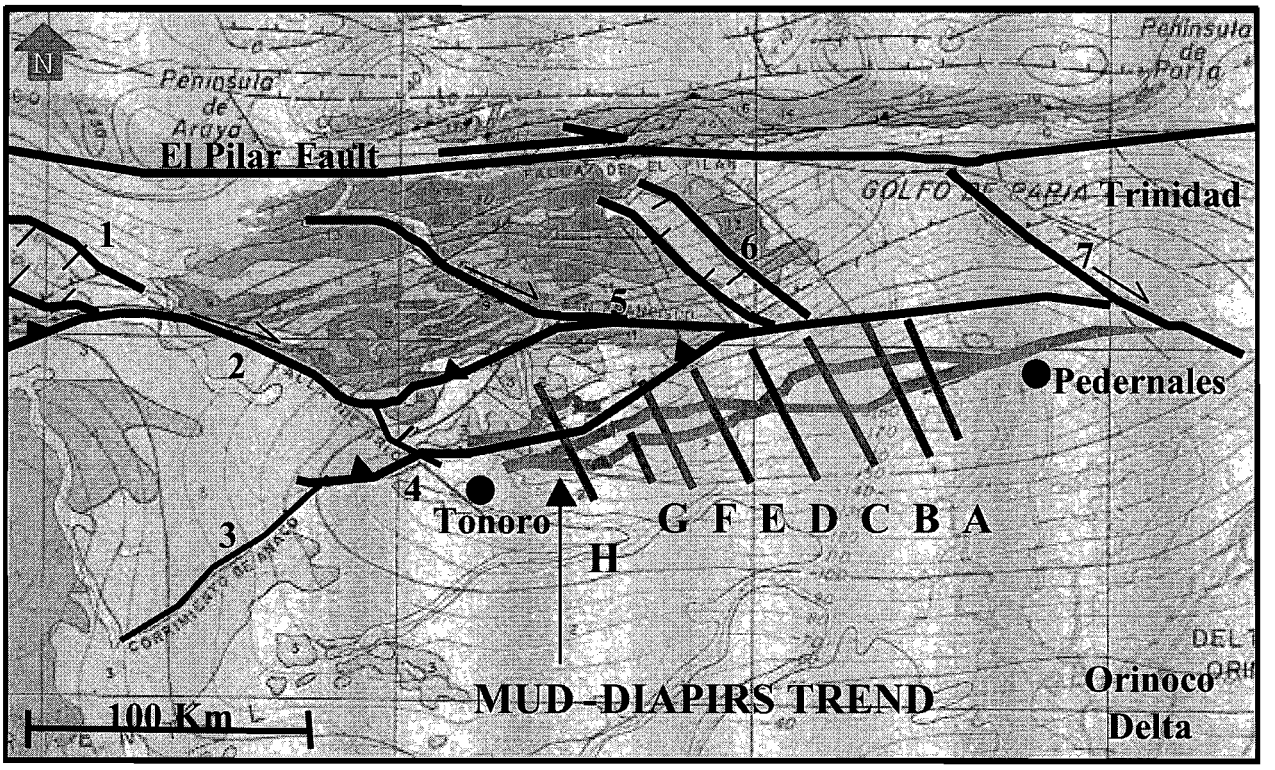

Figure 2. Tectonic setting: 1.Píritu Graben, 2. Urica Fault, 3. Anaco Thrust, Tala-Pirital Thrust, 5. San Francisco Fault, 6. San Juan Graben, 7. Los Bajos-El Soldado Fault (Mod. From PIMENTEL,1984).

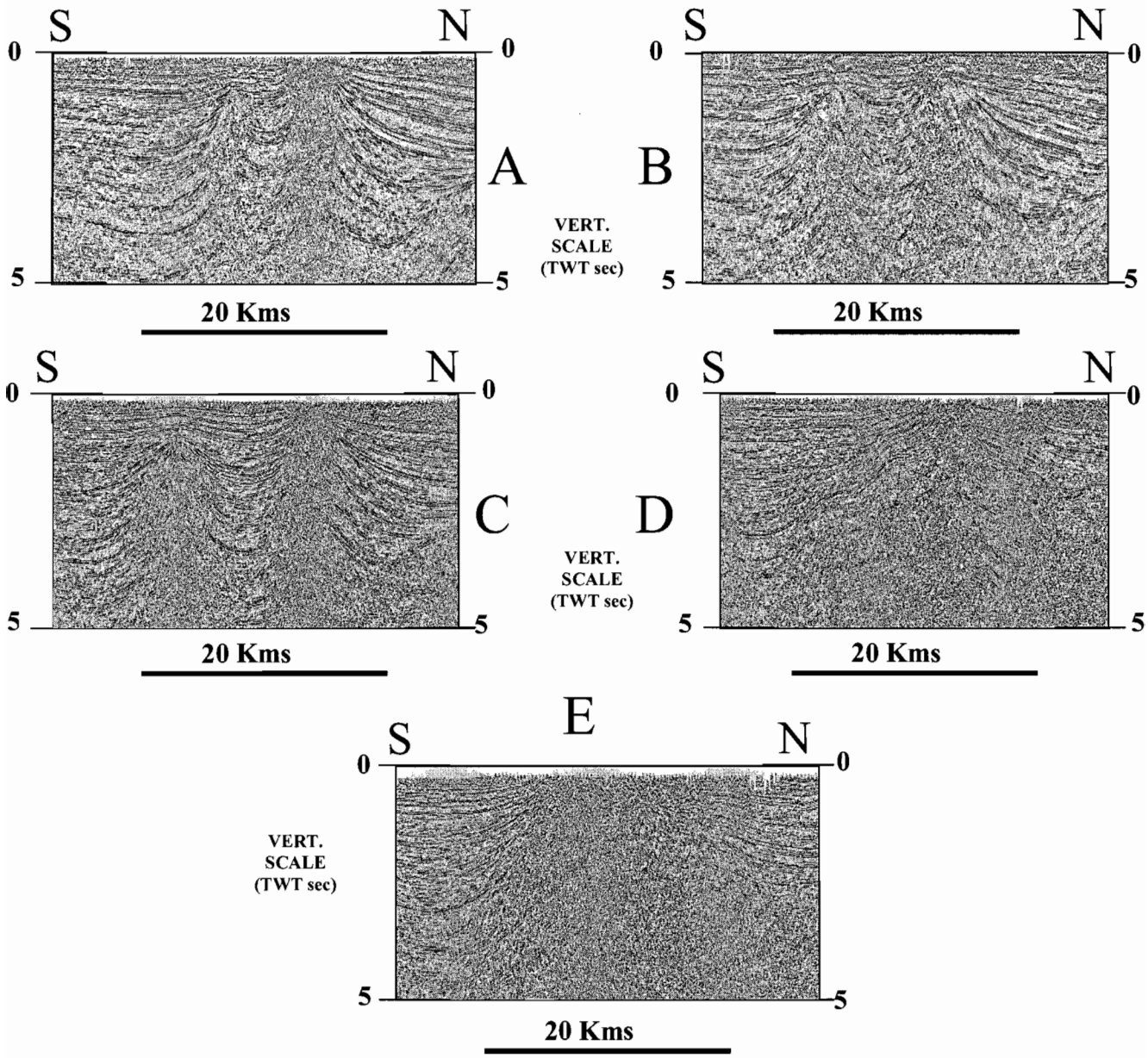

Figure 3 Seismic sections showing Mud-Diapirs (see Figure 2 for location).

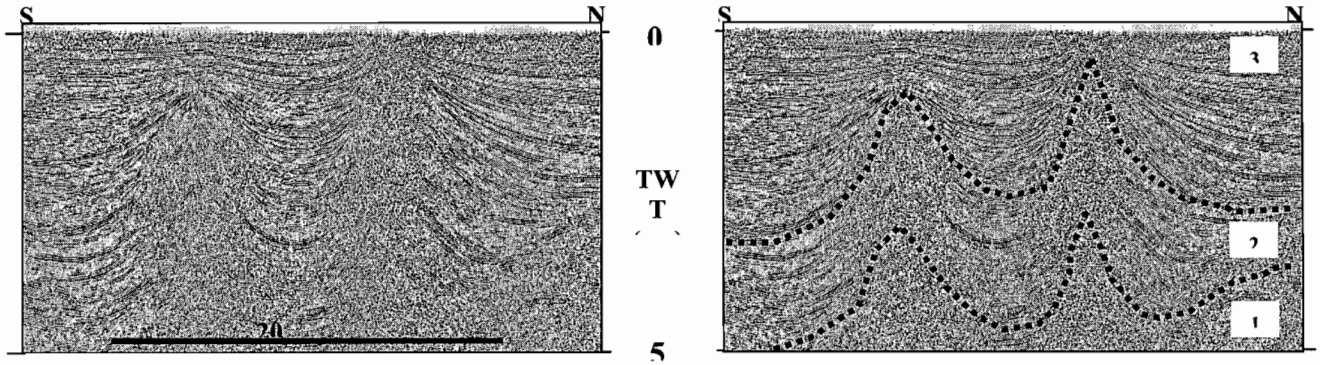

Figure 4 Interpretation of Section C; 1: L. Mioc. Shale, 2:Mid. Miocene, 3:Plio-Q., Unc=Unconformity.

GEOCHRONOLOGICAL CONSTRAINTS ON MATERIAL CYCLING VELOCITIES, STRUCTURAL EVOLUTION, AND EXHUMATION OF A PALEO-ACCRETIONARY WEDGE: THE BAHIA MANSA COMPLEX, SOUTH CENTRAL CHILE.

Johannes GLODNY [1], Jo LOHRMAN [1], Wolfgang SEIFERT [1], Kirsten GRÄEFE [1], Helmut ECHTLER [1], Oscar FIGUEROA [2]

(1): GeoForschungsZentrum Potsdam, Telegrafenberg, 14473 Potsdam, Germany. (email: glodnyj@gfz-potsdam.de)
(2): Depto. de Ciencias de la Tierra, Universidad de Concepción, Chile (email: ofiguero@mail.udec.cl)

KEY WORDS: Geochronology, sandbox simulation, deformation, exhumation, Coastal Cordillera, Chile.

INTRODUCTION

The basement of the Coastal Cordillera of South Central Chile (38°S – 42°S) is dominated by a high-P/T metamorphic complex. Metamorphism reached transitional greenschist to blueschist facies conditions, with maximum pressures around 9 kbar. This complex, known as the Bahia Mansa complex and sometimes termed "Western Series", consists of metapelites, metagreywackes and metapsammites, with intercalated mafic to ultramafic rocks, and is interpreted as a forearc accretionary complex (e.g. Hervé 1988, Martin et al. 1999). Almost all lithologies, with the exception of some metabasites, are characterized by an intense mylonitic deformation. Locally, the metamorphic complex was post-tectonically intruded by Cretaceous subvolcanic granitoids (Martin et al. 1999). Preexisting geochronological data from the metasedimentary and metabasic rocks (cf. Duhart et al. 2001) comprises U/Pb zircon data, interpreted as detritus ages, as well as numerous K-Ar and $^{40}Ar/^{39}Ar$ ages which were interpreted as cooling ages. From these data, the time frame for the exhumation of the metamorphic complex was constrained to be Permo-Triassic (Duhart et al. 2001). However, the exact timing of the metamorphic evolution remains unclear as there is considerable debate on whether the straightforward interpretation of K-Ar and $^{40}Ar/^{39}Ar$ white mica dates as cooling ages is justified. In particular, in highly strained lithologies like in the Bahia Mansa Complex, K-Ar-based dates for mica phases may represent deformation rather than cooling ages (Villa et al. 1998, DiVincenzo et al. 2001).

The present study integrates sandbox simulation of mass-transfer processes in the South Chilean accretionary complex, macro- and microstructural observations, thermobarometry, and various geochronologic approaches (U/Pb and Rb/Sr internal mineral isochrons as well as apatite and zircon fission track dating). It aims towards a comprehensive model of the dynamic P-T-t-deformation history of the Bahia Mansa complex.

EXPERIMENTAL APPROACH, RESULTS AND INTERPRETATION

Based on field observations, a series of 2D-scaled sandbox experiments was set up to simulate the dynamics and mass transfer mode of an accretionary forearc (e.g. Kukowski et al., in press) as found in South Central Chile. The experiments allow for frontal accretion as well as for underthrusting and basal accretion. Results

indicate a "circulating" mode of mass transfer in the complex: Material is eroded at the surface of the forearc complex and in the arc region. This material is then transported to the trench where it enters the subduction channel. With tectonic transport to depth, dehydration and prograde metamorphism is paralleled by imbrication of the metasediments with oceanic lithologies of the lower plate. With further increasing overburden due to continuing subduction, the material is intensely deformed and basally accreted to the upper plate. The process of basal accretion induces duplex tectonics and consequently uplift, bending and extension of the overlying, previously accreted material. Surface erosion finally leds to exposure of the high-P/T metamorphic rocks.

The described mass-transfer mode is linked to development of specific metamorphic assemblages and structural elements, some of which are suitable for radioisotopic dating. U/Pb ages of detrital zircons, found in the metasediments, date crystallization of zircons most probably derived from the magmatic arc. The youngest concordant U/Pb ages of the zircon detritus age spectra define a maximum age for sediment entrance in the subduction channel. During prograde metamorphism, the mineral assemblages comprise phases which are very resistant with respect to subsequent deformation and isotopic resetting (e.g. garnet, amphibole, sphene and epidote). U/Pb mineral isochrons are suited to date such prograde assemblages (cf. Mattinson 1986). Basal accretion of the material takes place at the plate boundary, in a setting characterized by high velocity gradients. It is therefore related to intense, penetrative mylonitic deformation. Penetrative ductile shearing is strictly confined to the inferred late prograde to early retrograde stage; later, retrograde ductile deformation can be ruled out (Willner et al. 2001). We used internal Rb/Sr mineral isochrons to date this shearing event, exclusively analyzing phases that recrystallized during deformation. This approach was shown to have the potential for precise dating of the waning stage of deformation in mylonites (e.g. Freeman et al. 1997, Hetzel and Glodny 2002). During continuous basal accretion, uplift of the metamorphic complex is accompanied by extension, increments of which can be dated by internal Rb/Sr mineral isochrons as well. Extensional deformation at semi-ductile conditions leds to formation of distinct shear zones, while mineralized tension gashes are formed in the brittle regime at higher crustal levels.

Fieldwork and sampling for geochronology was carried out along a N-S profile, near Quidico (38°15'S), Valdivia (39°50'S), Bahia Mansa (40°35'S) and at Playa Guabun, Chiloé (41°48'S). For the Valdivia region, we arrive at the following scenario: A maximum age for material entrance in the accretionary system is placed by a 278 Ma U/Pb age of a detrital zircon (data of Duhart et al. 2001). Prograde metamorphism occurred at about 250 Ma, and was closely followed by mylonitic deformation, at 250-245 Ma / 8.5 kbar. Extensional semi-ductile shear zones developed about 10 Ma later, at ~237 Ma / 7 kbar. Tension gashes formed ca. 30 Ma after the mylonitic deformation, at ~215 Ma / 3 kbar. The other regions under investigation show very similar age distribution patterns, i.e. very similar structural evolutions. However, the absolute age values differ, and clearly document a southward propagation of the accretionary system: the ages for mylonitic deformation grade from ~285 Ma (Quidico) through 245-250 Ma (Valdivia) to ~233 Ma (Bahia Mansa). The southward younging of the age values for tension gashes is proportional (~252 Ma at Quidico vs. ~200 Ma at Bahia Mansa). The southward propagation of the accretionary system is reflected in the internal structure of the metamorphic complex which exhibits a pronounced asymmetry with respect to the present day continental margin. Mineral stretching lineations and fold axes trend systematically in a NW-SE direction, thus oblique to the NNE-SSW-trending morphology of the modern oceanic trench and the Andes.

The data allow to deduce exhumation rates for different time slices since the Permian. During ongoing basal accretion (>250 Ma – 215 Ma in the Valdivia region), exhumation proceeded with rates of 0.5 – 0.7 mm/a. In the Valdivia region, basal accretion ceased at about 215 Ma, and correspondingly, time-averaged exhumation rates for the period between ~215 Ma and ~90 Ma are very low, on the order of ~0.03 mm/a. Exhumation rates between ~90 Ma and recent times are low as well: Near Valdivia, the roof zone of a subvolcanic granitoid intrusion is exposed, which was dated at 91.3 ± 4.9 Ma by Martin et al. (1999), using zircon U/Pb systematics. The crystallization depth of this intrusion is less than 3 km (Al-in-hornblende barometry), which indicates that total denudation since the Cretaceous was no more than a few km. This is corroborated by new apatite fission track data (Gräfe et al., this volume), implying that the metamorphic rocks passed the apatite fission track closure temperature (~100°C) in Early Paleogene times. We conclude that, despite of that the Bahia Mansa metamorphic complex remained in a forearc position since at least Early Permian times, its internal structural evolution was terminated in a southward-propagating process in the Triassic. Since then, the complex remained stable and almost unaffected in its present-day position. Furthermore, there was no major basal accretion in the position of the Bahia Mansa metamorphic complex since Late Triassic times, which places close constraints to geodynamic models of the Cenozoic Andean "subduction factory".

REFERENCES

DiVincenzo G., Ghiribelli B., Giorgetti G., Palmeri R. 2001. Evidence of a close link between petrology and isotope records; constraints from SEM, EMP, TEM and in situ $^{40}Ar/^{39}Ar$ Ar laser analyses on multiple generations of white micas (Lanterman Range, Antarctica). Earth and Planetary Science Letters 192(3), 389-405.

Duhart P., McDonough M., Muñoz J., Martin M., Villeneuve M. 2001. El Complejo Metamórfico Bahía Mansa en la cordillera de la Costa del centro-sur de Chile (39°30'-42°00'S); geochronología K-Ar, $^{40}Ar/^{39}Ar$ y U-Pb e implicancias en la evolución del margen sur-occidental de Gondwana. Revista Geológica de Chile 28(2), 179-208.

Freeman S.R., Inger S., Butler R.W.H., Cliff R.A. 1997. Dating deformation using Rb-Sr in white mica: Greenschist facies deformation ages from the Entrelor shear zone, Italian Alps. Tectonics 16: 57-76.

Gräfe K., Glodny J., Seifert W., Rosenau M., Echtler H. 2002. Apatite fission track thermochronology of granitoids at the South Chilean active continental margin (37°S - 42°S): implications for Denudation, tectonics and mass transfer since the Cretaceous. ISAG (this volume).

Hervé F. 1988. Late Paleozoic subduction and accretion in southern Chile. Episodes 11, 183-188.

Hetzel R., Glodny J. 2002. A crustal-scale, orogen-parallel strike-slip fault in the Middle Urals: age, magnitude of displacement, and geodynamic significance. Int. J. Earth Sciences 91, 231-245.

Kukowski N., Malavielle J., Gutscher M.-A., Lallemand S.E. 2002. Mechanical decoupling and basal duplex formation observed in sandbox experiments with application to the Western Mediterranean Ridge. Marine Geology 187(3-4), in press.

Martin M.W., Kato T.T., Rodriguez C., Godoy E., Duhart P., McDonough M, Campos A. 1999. Evolution of the late Paleozoic accretionary complex and overlying forearc-magmatic arc, south central Chile (38°-41°S): Constraints for the tectonic setting along the southwestern margin of Gondwana. Tectonics 18(4), 582-605

Mattinson J.M. 1986. Geochronology of high-pressure-low-temperature Franciscan metabasites: A new approach using the U/Pb system. In: Evans B.W., Brown E.H. (eds.): Blueschists and Eclogites. Geol. Soc. of America, Memoirs, 164, 95-105.

Villa I.M. 1998. Isotopic closure. Terra Nova 10(1), 42-47.

Willner A.P., Pawlig S., Massonne H.J., Hervé F. 2001. Metamorphic evolution of spessartine quartzites (Coticules) in the high-pressure, low-temperature complex at Bahia Mansa, Coastal Cordillera of South-Central Chile. Canadian Mineralogist 39, 1547-1569.

DOES CRUSTAL THINNING TRIGGER SUBSEQUENT BUILDING OF THE ANDES?

Estanislao GODOY

Serv. Nac.de Geología y Minería Sta.María 0104 Santiago, Chile. egodoy@sernageomin.cl

KEY WORDS: southern Andes, Oligocene extension, Miocene crustal thickening

INTRODUCTION

Crust under the Andes of central Chile and Argentina has been thickened several times. Mechanisms invoked range from microplate collisions during the Paleozoic to Mesozoic underplating and Late Cenozoic underplating combined with tectonic shortening. The last of these thickening events, an ongoing process that started during the early Miocene, has been linked by Jordan et al.(2001) to "a more stable state of the subducting plate" which allowed structural inversion of "active basins" built on crust extended during a previous high convergence rate. The model is rather extreme, in that it considers extension as "a necessary condition to subsequent building of the modern Andes Mountains". Godoy et al (1999), for example, have included inversion of a central Andean extensional basin as only a part of that thickening process Based mainly on studies by previous authors in the chilean-argentinian central and south-central Andes we comment on the validity of such triggering mechanism.

THE CHILEAN-ARGENTINIAN ANDES AT 33°-34° S.L

The **Coya-Machalí Formation** is a *ca* 2 km thick pile of continental volcaniclastics and minor lacustrine sediments, deposited in an Oligocene to earliest Miocene "active-margin" basin. that crops out along the western half of the Andean Main Range, from 33° to 35° S.L. In its northern end, Nystrom et al (1993) report a depleted ε_{Nd} and $^{87}Sr/^{86}Sr$ signature in its tholeitic volcanic rocks, which they relate to an "episode of mantle upwelling and crustal thinning". They also recognized a reverse trend, away from MORB, for the overlying Farellones Miocene calc-alkaline volcanics, a formation that in some huge relict volcanic edifices, such as the Aconcagua, may reach a thickness of over 3 km.

According to Kay et al, (2002).the low pressure pyroxene-bearing phenocryst and residual mineral assemblages of the Oligocene low- to mid-K tholeiitic magmas at 34° show a depleted isotopic signature similar to that at 33° and is also linked with crustal thinning. The high pressure garnet-bearing residual mineral assemblages and enriched isotopic signatures of the Farellones volcanics is, on the other hand, related to dramatic crustal thickening. They recognize distinctive breaks in trace elements trends and isotopic enrichment in the younger high-K calc-alkaline magmas at 18 and 6 to 5 Ma, which coincide with eastward shifts in the arc front and regional uplift. The related thickening events correlate well with early in-sequence and major out-of-sequence thrusting, the latter taking place mainly along the western margin of the Miocene volcanic arc (Fierro Thrust, Godoy et al., 1999). The geochemical breaks are explained by both increases in the depths of basal crustal MASH processes and enrichment of mantle wedge magma sources through incorporation of crustal blocks removed during forearc subduction erosion.

In the Kay et al.(2002) modeling, "changing plate convergence vectors" are held responsible for peaks in forearc subduction erosion, arc migration and ductile thickening of the subarc crust in concert with shortening in the foreland fold-thrust belt. Even though it implies an initial stage of subarc crustal softening, this is a different, more dynamic scenario in which no extensional triggering is needed.

TRIGGERING AT THE 36°-44°s.l. SEGMENT

A late Oligocene to early Miocene magmatic belt also crops out, from 36° to 44° s.l., west of the Main Range. South of the 38° it interfingers with marine sediments deposited during the initial subsidence of the Central Valley. According to Muñoz et al. (2000) its variable trace-element and isotopic composition "could reflect the interaction between melts derived from upwelling asthenospheric mantle and the subcontinental mantle lithosphere previously contaminated by slab-derived fluids". They link this transient period of invigorated asthenospheric circulation to the late Oligocene three-fold increase in trench-normal convergence rates between the Nazca and South American plates, both processes inducing a 800 km wide crustal extension by rollbacking of the former plate. Minor subsequent deformation of the belt, untriggered by the previous extension and unrelated to crustal thickening, is assigned by Muñoz et al. (2000) to decrease in subduction angle of the Nazca plate, which returned the magmatic activity to its current locus in the Main Cordillera.

Oligocene to middle Miocene volcanic rocks, interdigitated and transitional to thick piles of lacustrine sediments (formational names **Cura-Mallín** in the north and **Ñirihuau** in the south), crop out south of 36° s.l, east of the present arc. They seem to represent an extension of the Coya-Machalí setting yet, south of 40°, their abundant volcanics are not tholeiitic. The NNW trending Ñiriguau depocenters have moreover been interpreted as pull-apart basins (Dalla Salda and Franzese, 1987). These mid-Tertiary rocks overlie Paleocene to Eocene calc-alkaline rhyolitic ignimbrites and andesites of the Pilcaniyeu Formation (Rapela et al., 1988). In contrast, under the Coya-Machalí Formation,.a 30 My long Paleocene-Eocene hiatus seems unavoidable.

CONCLUSIONS AND DISCUSSION

The Andean Oligocene-Early Miocene basins between the 33° and 44°s.l. do not share a common evolution. Three different tectonic settings may be recognized in them:

In the **Coya-Machalí basins** a strong late Miocene inversion has blurred, through marginal tight folding and out-of-sequence thrusting, their original boundary normal faults, some of which may be inherited from Triassic and late Jurassic rifting. The geochemistry of its lavas is compatible with a thin crust during basin formation, while that of the overlying volcanics matches that of magmas generated under a crust thickened by incorporation of crustal blocks removed during forearc subduction erosion.

In the **Curamallín type basins**, on the other hand, east vergent folding is widespread (Niemeyer and Muñoz, 1983). However, in only one half-graben at 37° s.l.. has a border fault, gently inverted during the middle Miocene, been recognized (Jordan et al.,2001) and no Miocene crustal thickening is reported.

At the latitude of the **Ñirihuau type basins** Oligocene extension was the widest, over 800 km. According to the seismic profiles quoted in Jordan et al.(2001), the western basins, under the Chilean Central Valley, were developed on metamorphic basement and show only moderate inversion. This major extensional event, however, did not trigger crustal thickening.

According to the thermomechanical modeling of Thompson et al. (2001) softening under active rifts are precursors to thickened Orogenic belts, yet and in agreement with Muñoz et al.(2000), "continental back arcs become extended in response to the roll-back of subduction". Jordan et al. (2001), however, consider that lithosphere subducted during the Oligocene in this part of the south-eastern Pacific was not old and cold enough to comply with. the "typical" Molnar and Atwater (1978) situation. They therefore dismiss this extension mechanism in favor of abnormally complex transient invigorated circulation patterns within the asthenospheric wedge. Sharing the slab window proposition of Muñoz et al. (2000), Yañez et al. (2002) relate this invigorated circulation to "a detached segment of the subducted slab south of " 33°S whose "unbalanced slab pull force triggered...the abrupt change in the Nazca pole of rotation at 25 Ma".

Either with or without rollbacking contribution, a long-wedge of the andean crust did extend during the Oligocene-early Miocene, yet only south of 33°S and later shortening was concentrated only close to its northern end.

García et al (2002) give convincing evidence that during the oligo-miocene at 18° S deformation was wholly compresional. The small oligo-miocene normal faults used by Jordan el al, (2001) in that area as a hint that the stress state was initially extensional up to that latitude must be forgotten. Margin-parallel extension, also coincident with rapid seafloor spreading, did prevail during the early Cretaceous in much of the Andes. Only locally, however, was it followed by a compressional event. Many of its normal faults were inverted only during the late Miocene.

REFERENCES

Dalla Salda, L. y Franzese, J. 1987. Las megaestructuras del Macizo y la Cordillera Norpatagónica argentina y la génesis de las cuencas volcano-sedimentarias terciarias. Revista Geológica de Chile, 31, 3-14.

García, M., Herail, G., Charrier, R., Mascle, G. and Fornari, M. 2002. Oligo-Eocene deformation of the western altiplano, northern Chile (18-19°S). (this meeting).

Godoy, E., Yáñez, G. and Vera, E.. 1999, Inversion of an Oligocene volcano-tectonic basin and uplifting of its superimposed Miocene magmatic arc in the Central Chilean Andes: first seismic and gravity evidences: Tectonophysics, 306, 217-236.

Jordan, T., Burns, M., Veiga, R., Pángaro, F., Copeland, P., Kelley, S. and Mpodozis, C. 2001. Extension and basin formation in the southern Andes caused by increased convergence rate: A mid-Cenozoic trigger for the Andes. Tectonics, 20, 3, 308-324.

Kay, S., Godoy, E. and Kurtz, A., 2002. Role of Crustal Thickening and Forearc Subduction Erosion Processes in the Evolution of Neogene Southern Andean Volcanic Zone Magmas. Geological Society of America Bulletin (in press)

Molnar, P. and Atwater, T. Interarc spreading and cordilleran tectonics as alternates related to the age of subducted oceanic lithosphere. Earth and Planetary Science Letters, 41, 330-340.

Muñoz, J., Troncoso, R., Duhart, P., Crignola, P., Farmer, L. and Stern, C. 2000. The relation of the mid-Tertiary coastal magmatic belt in south-central Chile to the late Oligocene increase in plate convergence rate. Revista Geológica de Chile, 27, 2, 177-203.

Niemeyer, H. y Muñoz, J. 1983. Hoja Laguna de la Laja. Carta Geológica de Chile, n° 57. Servicio Nacional de Geología y Minería. 52 p.

Nystrom, J., Parada, M. and Vergara, M. 1993. Sr-Nd isotope compositions of Cretaceous to Miocene volcanic rocks in Central Chile: a trend towards a MORB signature and a reversal with time. Second ISAG, Oxford (UK), 411-414.

Rapela,C., Spalletti, L., Merodio, J. and Aragón, E. 1988. Temporal evolution and spatial variation of early Tertiary volcanism in the Patagonian Andes. Journal of South American Earth Sciences, 1, 1, 75-88.

Thompson, A., Schulmann, K., Jezek, J., Tolar, V. 2001. Thermally softened continental extensional zones (arcs and rifts) as precursors to thickened orogenic belts. Tectonophysics, 332, 115-141.

Yañez, G., Cembrano, J., Pardo, M., Ranero, C. and Sellés, D. 2002. The Challenger-Juan Fernández-Maipo major tectonic transition of the Nazca-Andean subduction system at 33-34°S: geodynamic evidence and implications. Journal of South American Earth Sciences (in press)

NEOGENE TO QUATERNARY DEFORMATION OF THE SALAR GRANDE AREA, COSTAL CORDILLERA OF NORTHERN CHILE: IMPLICATIONS FOR FOREARC TECTONICS

Gabriel GONZÁLEZ L (1)., Alejandro MACCI; Daniel CARRIZO (3) and José CEMBRANO (4)

(1) Departamento de Ciencias Geológica, Universidad Católica del Norte, Chile; ggonzale@ucn.cl
(3) dcarrizos@yahoo.com
(4)jcembrano@ucn.cl

Keywords: Central Andes, Chile, forearc, extensional tectonics and strike-slip faulting.

Introduction

The continental margin of northern Chile is an excellent place to study the interaction between near-surface forearc deformation and deep-seated tectonics related to plate convergence. Well-exposed structures formed during the Neogene to Recent deformation history of the forearc, provide important information of the long-term and short-term tectonic processes that have dominated at the margin surface. Several contributions regarding the local Neogene tectonics of Antofagasta area and the Mejillones Peninsula have been published over the last years (Armijo and Thiele 1990; Niemeyer et al., 1996; Delouis et al., 1998). In this contribution, we present new field structural data of the Salar Grande (20°45', Fig. 1) and provide a first integrated model of the Neogene to Quaternary deformation of this part of the Coastal Cordillera. This area is very important to improve the current understanding of long-term and large-scale processes operating in Andean-type margins.

Fault arrangement and timing of deformation

The fault architecture of the Salar Grande area consists of three north-west-striking strike-slip faults and several north-south to north-northeast striking normal faults. The most important northwest-striking faults are the Salar Grande Fault and the Chomache Fault; both structures splay towards the west from north-south trending faults (Fig. 1). The Chomache Fault shows dextral-slip displacement, which is evidenced by the lateral offset of alluvial fans and streams, small-scale pull-apart structures formed along releasing bends, and push-up swells occur along restraining bends. The Salar Grande Fault trends parallel to the Chomache Fault along the inner part of the Coastal Cordillera, cutting the Salar Grande Basin which is filled with 100-150 m thick pure halite (Chong et al. 1999). Along this fault, morphological kinematic indicators, such as displaced streams, evidence consistently a dextral-strike slip character for this fault. Dextral kinematics is also documented by a drag fold in the northern part of the Salar Grande Fault, which affects Late Jurassic-Early Cretaceous red beds. Both the Chomache and the Salar Grande Faults have subhorizontal striae and dextral strike-slip outcrop-scale kinematic indicators. They are consistent with the kinematics arising from morphological analysis.

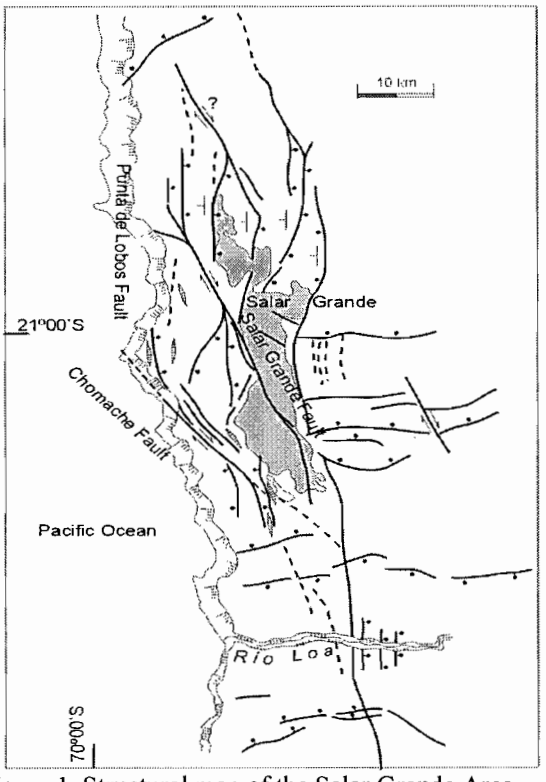

Figure 1. Structural map of the Salar Grande Area

The north-south-striking normal faults of the Salar Grande area, exert an important control on the morphology of the Coastal Cordillera at this latitude. They define asymmetric horst and graben morphology; the grabens are located on the eastern side of the faults and are limited by 50-100 m east-facing scarps. In the vast majority of cases, fault surfaces are not exposed and thus they do not provide any direct evidence of their kinematic character. Dip-slip component of motion on these faults is indirectly deduced from the displacement of both stratigraphic markers and pediplain surfaces of the top of the Coastal Cordillera. The Punta the Lobos Fault is the best exposed north-south striking fault. It dips 82° east and forms the boundary between a 1000 m in high, north-south oriented range and a fault-parallel alluvial basin, located at the west of the fault. The exposures of this fault show down-the-dip striae and have outcrop-scale kinematic indicators that evidence a normal dip-slip character of the displacement.

A complex system of open cracks that affect both sediments and country rocks are present in the Salar Grande area. The cracks are hectometric in length, 0.3-5 m in width and 1-7 m in depth. They strike mainly north-south, north-northwest and less commonly northeast and east-west. The north-south open cracks occur locally in the footwall of north-south striking normal faults, such is the case of Punta de Lobos Fault and the Geoglifo Fault. The north-northwest cracks are developed in low-land topographic zones affecting the alluvial graben-infill of north-south striking normal faults. The northeast and east-west cracks occur in clusters mainly in the highest parts around the Salar Grande. Some of these cracks are localized in the uplifted part of old east-west oriented fault scarps, whereas others are not spatially related to faults. Because open cracks affect both highlands and lowlands, an origin exclusively by topographically-controlled gravitational movement can be discarded.

Because both the Chomache Fault and the Salar Grande Fault show well-defined fault traces, displace streams and have well preserved fault scarps, it is likely that the dextral displacements along these faults occurred in the Pliocene or Quaternary. In fact, the observation that the Chomache Fault cuts the youngest alluvial fan deposits and displaces the Plio-Pleistocene Coastal Cliff (Niemeyer et al., 1996) suggests that the dextral slip along this fault has a Pleistocene or younger age. The Salar Grande Fault has a more strongly eroded morphological scarp and does not show fresh ruptures, it can then be interpreted that the dextral displacement along this fault has an older age than the Chomache Fault. The Punta de

Lobos Fault, deforms alluvial fan deposits with interbedded tuffs that in other parts of the Coastal Cordillera yielded 3-5 Ma-K-Ar ages. Thus, a Late Pliocene or younger age for this fault is likely.

Kinematic Analysis

Using the attitude of the fault plane, the orientation of the slip direction and the sense of slip, we applied the kinematic graphical reconstruction of Marrett and Allmendinger (1991) to obtain the P and T-axes, the principal incremental shortening axis (P) and the principal extensional axis respectively (T). The Salar Grande Fault, the Chomache Fault and the Punta de Lobos Fault show well-developed striae and very well exposed kinematic indicators. The T-axes obtained from the two dextral strike-slip faults have a subhorizontal, east-west orientation. The attitude of the P-axes is nearly subhorizontal and trends north-south. The linked Bingham distribution of the tensor axes for the right lateral faults yielded a N89°E-trending, subhorizontal T axis and N01W-trending, subhorizontal P axis. For the Punta de Lobos Fault, the P-T analysis shows that the T axes are subhorizontal and trend east-west. In contrast with the Salar Grande Fault, the P-axis derived from the Punta the Lobos Fault is subvertical, which is determined by the normal character of the fault. In other normal faults, we found a similar orientation of the T and P axes. Applying the same Bingham analysis to the whole normal fault population, we obtained a N78°E-trending, horizontal T axis. This attitude is similar to that yielded by the dextral faults.

Using crack orientation we tried to obtain the T axes related to their formation. We assume that for each crack the fracture-plane pole correspond with the orientation of the T axes. In the Salar Grande area the fracture orientation define a maximum pole located between N60-70E, a secondary maximum is oriented N80-90E.

The comparison between the T axes obtained from the fault slip data and those derived from crack orientation show that there is some correlation. However, a detailed analysis of the cracks-data shows that there is a group of cracks having T axes oriented N60-70E, which departs from the T axes orientation related to the faults.

Concluding remarks

The fault-slip data of Salar Grande evidence a kinematic compatibility within an overall east-west extensional regime. The northwest striking dextral strike-slip faults act as high-oblique transfer structures on the nearly east-west extensional deformation. We base this idea on the following field observations: (1) the Salar Grande Fault and the Chomache Fault do not crosscut the Salar del Carmen Fault at the southern tip of the Salar Grande and (2) the Chomache and Salar Grande Faults connect two north-south striking normal faults with opposite dip senses; and (3) the obtained T axes for the strike-slip and normal faults have similar attitude and orientation. Thus, we propose that the normal and the strike-slip faults of this area form a linked fault system related to the bulk east-west directed extension. The extensional direction is nearly parallel to the trench normal at this latitude. Trench perpendicular

extension is also documented by north-south trending tensional cracks, which are exposed along the Coastal Cordillera. However, oblique extension relative to the normal component of the trench orientation also has been recorded, this is the case the north-northwest striking open cracks of the Salar Grande area, whose T axes are oriented N60-70E.

Our field data indicate that the part of the forearc structures exposed at the Coastal Cordillera has experienced near-surface extensional deformation which is trench normal orientated. The mechanism that controls this extension is probably related to plate-convergence. Several marines terraces exposed at this Coastal Cliff of this area attest to currently active uplift of the Coastal Cordillera. By the uplift process, the forearc surface between the trench and the Coastal Cordillera forms an upward flexure. The west flank of this flexure is subjected to gravitationally-driven movement towards the trench that promotes extensional deformation. Thus, extensional deformation results from a sort of large-scale buckle folding, where normal faulting is concentrated in a thin sheet, above a neutral surface that separates it from an underlying sheet undergoing contraction. This hypothetical configuration may explain why most faults of the Coastal Cordillera and Mejillones Peninsula are listric in section. The depth at which the faults become flat may represent the neutral surface, above which the crust is detached and moved towards the trench.

According to the fracture data processing, the cracks formation mechanism is related to the same extensional deformation. This is the case of the nearly north-south trending cracks, which are closely related to the normal faults. However, considering that the extensional direction, derived from the N20-30W trending open cracks, deviates from the north-south direction, it is plausible to suppose that other mechanism are intervening in the formation of open cracks. Because this type of cracks are nearly normal to the convergence vector, we propose that they are related to coseismic extension arising from elastic rebound during great earthquakes in the subduction zones.

References

Armijo, R. & Thiele, R., 1990. Active faulting in northern Chile: ramp stacking and lateral decoupling along a subduction plate boundary. Earth Planet. Sci. Lett., **98**, 40-61.

Chong, G., Mendoza, M. García-Veigas, J., Pueyo, J. L., & Turner, P., 1999. Evolution and geochemical signatures in a Neogene forearc evaporitic basin: The Salar Grande (Central of Chile). Palaegeogra., Palaeoclimatol., Palaeoecol, 151, 39-54.

Delouis, B. Philip, H., Dorbath, L., & Cisternas, A., 1998. Recent crustal deformation in the Antofagasta region (northern Chile) and the subduction process. Geophys. J. Int, **132**, 302-338.

Niemeyer, H., González, G. & Martinez-De Los Rios, E., 1996. Evolución tectónica cenozoica del margen continental activo de Antofagasta, norte de Chile. Revista Geológica de Chile, **23**, 165-186.

POLYPHASED TECTONICS IN THE NORTHERN VENEZUELAN ANDES

Leonardo GONZALEZ M. (1,2), Yves HERVOUET (1), Damien DHONT (1), José T. CASTRILLO (1)

(1)UMR 5831 Imagerie géophysique, Géologie structurale et télédétection, IPRA-CURS. , BP 1155, 64013 PAU, France. E-mail : yves.hervouet@univ-pau.fr

(2)Escuela de Ingenieria Geologica, Universidad de Los Andes, Mérida, Venezuela. cjoset@ing.ula.ve

KEYWORDS : inversion tectonics, transpression, reactivation, Barbacoas, Andes

The northern part of the Mérida Andes (figure 1) correponds to a complex area referred as the Barbacoas platform, comprising a sedimentary sequence which age ranges from Cretaceous to Paleogene.

Our study is based on analysis of Landsat TM (06-053; 1990), Spot (KJ 652-330, 652-331, 653-331; 1998) and Radarsat satellite imagery, aerial photographs, and complemented by geological studies in the field. We describe that different tectonic styles and structures in the Northern Venezuela Andes.

Remnant of the Caribbean orogeny affects the Rancheria Formation near Puente Gomez (southwesten part of the studied area, figure 1) where N130°E-trending folds having a fault propagation fold geometry can be observed.

The Barbacoas platform (figures 1, 2) is bounded to the northwest and to the southeast by folds of several tens of kilometres (San Pedro and Humocaro anticlines) trending NE-SW. To the northwest, the San Pedro antiform affects the Jurassic-Cretaceous sedimentary layers. This structure is 10 kilometres wide and is overturned to the NW. To the southeast, the Humocaro antiform affects sedimentary sequences dated Cretaceous-Paleogene. Laterally to the northeast, the Jurassic continental layers (Fm. La Quinta) are visible. The Humocaro anticline is 9 kilometres wide and is overturned to the SE. The Paleozoic does not outcrop at the core of these two antiforms, but is affected by the folding.

At the core of the Humocaro structure, the geometry of the La Peña anticline indicates that it was built as a consequence of the positive inversion of a preexisting graben. This can be generalised for the San Pedro and Humocaro antiforms, which cores comprise Jurassic sedimentary layers (Fm. La Quinta; figure 2).

A wide strip of Cretaceous terranes outcrop in between these anticlines. It corresponds to the Barbacoas synclinorium (figure 2), that we considered as an ancient horst during the Jurassic. This structure is cut by subvertical faults containing small or no vertical offset (figure 4). The latest movement along these faults occurred lately after the graben inversion. These accidents are connected with N020°E-trending anticlines which dimensions are some hundred of metres wide. One of the best exemple is the Nunca Jamas structure (figure 3) near Barbacoas. Analysis of the geometry of this anticline shows that it was affected by different tectonic stages. The Caribbean stage is responsible for NE-trending tension fractures. Left-lateral strike-slip

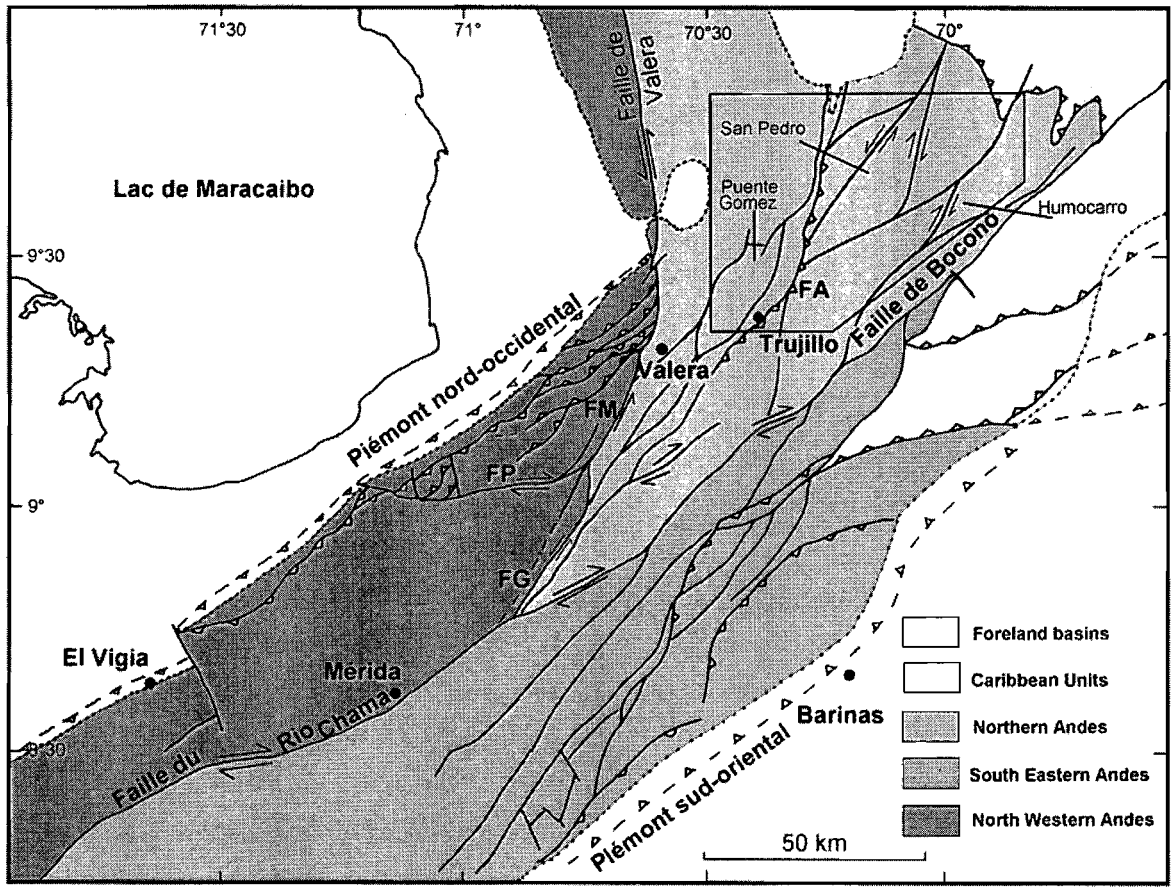

Figure 1. Location of the study area

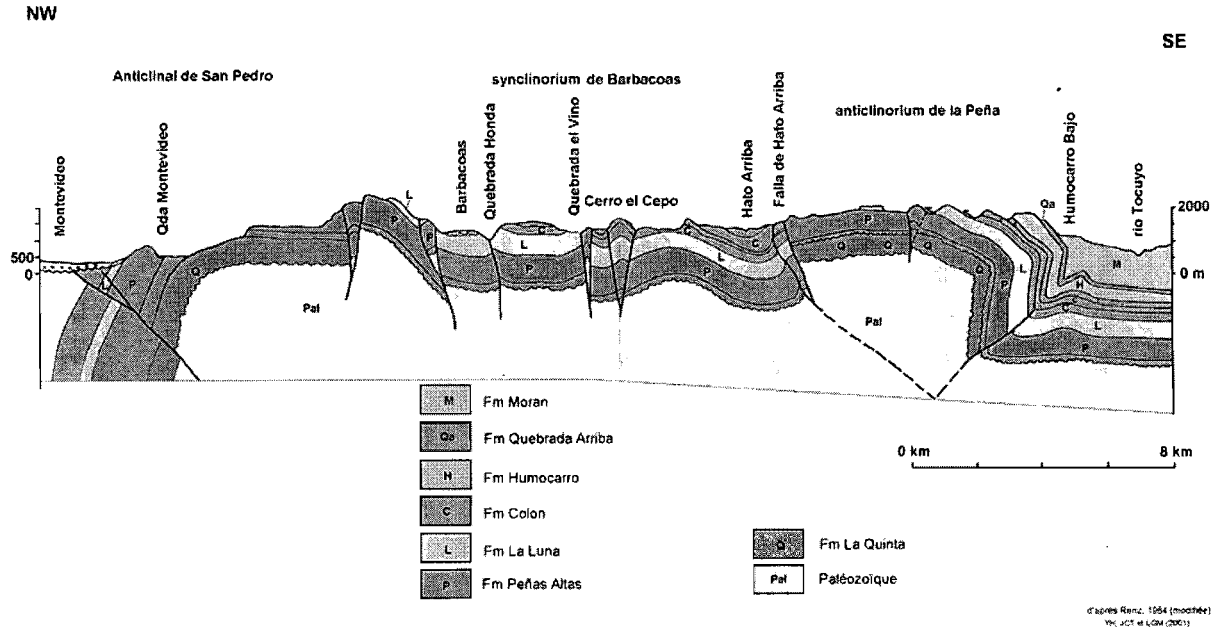

Figure 2. Synthetic cross-section of the Barbacoas platform (modified from Renz, 1964)

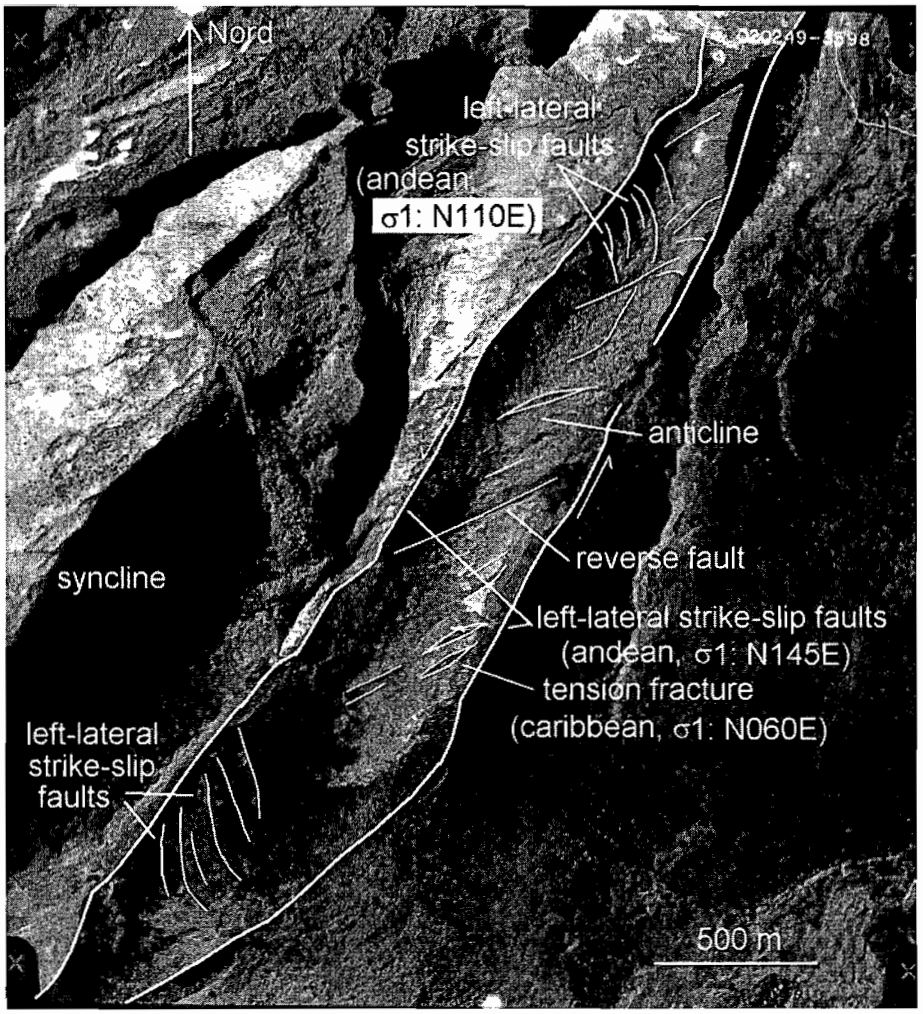

Figure 3. Structural interpretation of the Nunca Jamas anticline from aerial photograph analysis

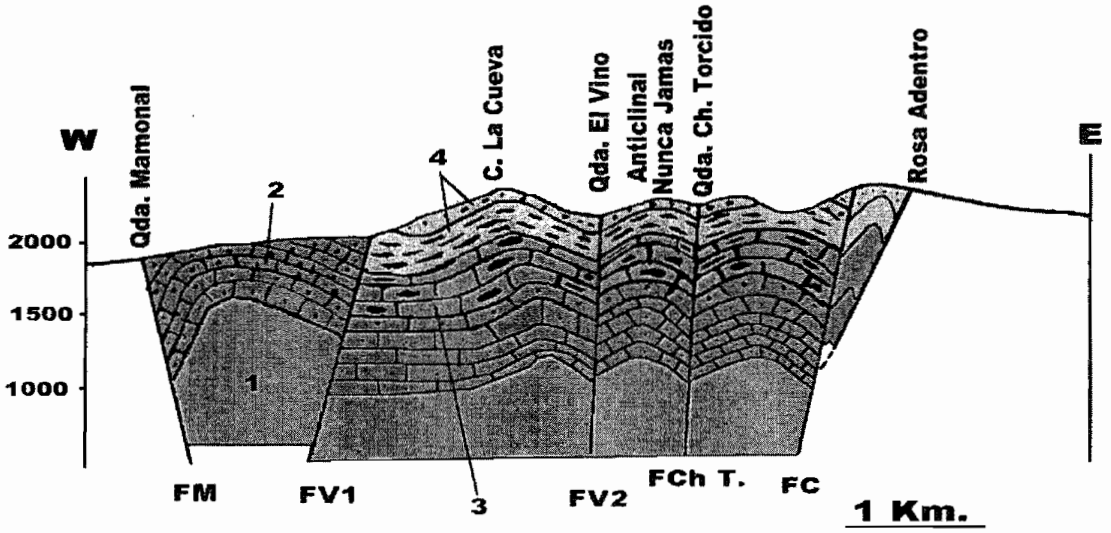

Figure 4. Geological cross-section in the core of the Barbacoas synclinorium 1: Paleozoic; 2: Fm Peñas Altas; 3: Fm La Luna; 4: Fm Colón and Cujisal member; FM: Mamonal fault; FV1 and 2: La Quebrada El Vino faults; FChT: Chorro Torcido fault; FC: El Cepo fault.

movement along the N020°E-striking faults, and N060°E-trending reverse faulting occurred later on during a second compressive Andean event. N020°E-trending the folds and NW-trending left-lateral strike slip faults occured at local scale during the last compressive Andean event. It can be explained by anticlockwise rotation.

CONCLUSIONS

The Barbacoas area is affected by polyphased tectonics. The oldest tectonic stage corresponds to the Caribbean movements, which is reponsible for thrusting and formation of tension fractures.

Andean movements can be individualised into several tectonic stages. The first one corresponds to the inversion of the Jurassic grabens, giving rise to the San Pedro and Humocaro anticlines, which dimensions are tens of kilometres wide. The second one corresponds to formation of N20°E-trending left-lateral strike-slip faults. At local scale, by anticlockwise rotation of the stress, this later stage permitted the formation of narrow anticlines (some hundred of meters wide). The Andean tectonics then globally changes from compression to transpression.

REFERENCES

Audemar F., (1997).- Los Andes Venezolanos, Vision Alterna. Mem. III, *Cong. Soc. Venezolana de Géol.*, T1, 85-92.

Hervouet Y., Castrillo J.T., & Odreman O. (2001) . - Interaction entre un chevauchement imbriqué et une zone transcurrente: le flanc nord-ouest des Andes vénézuéliennes. *Bull. Soc. Géol. France,* t 172, n° 2, 159 - 175.

Parnaud F., Gou Y., Pascual J. C., Capello M.A., Truskowski I., & Passalacqua H., (1995). - Stratigraphic synthesis of Western Venezuela. *In*: Tankard, A.J.; Suarez R. & Welsink H.J. Eds, Petroleum basins of South America, *A.A.P.G.*, memoir 62, 681-698.

Scheurs G. & Colletta B., (1998). - Analogue modelling of faulting in zones of continental transpression and transtension. *Geological Society*, London, Special publications, 135, 59 -79.

Stéphan J. F. (1977).- El contacto cadena Caribe-Andes Merideños entre Carora y El Tocuyo, Estado Lara: Observaciones sobre el estilo y la edad de las deformaciones cenozoicas en el Occidente Venezolano. Memoria, *V Cong. Geol. Venez.*, Caracas, tomo 2, 7.

AKNOWLEDGEMENTS

This study has been made possible by means of the agreement ULA-UPPA, ULA-PDVSA, the ECOSNORD project (V00U02) and the SPOT ISIS program

APATITE FISSION TRACK THERMOCHRONOLOGY OF GRANITOIDS AT THE SOUTH CHILEAN ACTIVE CONTINENTAL MARGIN (37°S - 42°S): IMPLICATIONS FOR DENUDATION, TECTONICS AND MASS TRANSFER SINCE THE CRETACEOUS

Kirsten GRÄFE, Johannes GLODNY, Wolfgang SEIFERT, Matthias ROSENAU, Helmut ECHTLER

GeoForschungsZentrum Potsdam, Telegrafenberg, 14473 Potsdam, Germany; (email: graefe@gfz-potsdam.de)

KEY WORDS: apatite fission track thermochronology, exhumation, South Central Chile, forearc, magmatic arc

INTRDUCTION

Seismicity, faulting and uplift reflect active deformational processes along the South Central Chilean continental margin and makes this area a natural laboratory for investigations of long term mass transfer patterns at convergent margins. Understanding the factors controlling the tectonic behaviour of the continental margin has some general implications for continental growth and the mass transfer processes in "subduction factories". The present study is part of an interdisciplinary project combining structural, geothermochronological, petrological and extensive geophysical investigations (e.g. SALT, South American Lithosphere Transect), and aims towards better understanding of the long-term dynamics of this active continental margin.

Main geological and tectonic features of the study region are illustrated in Fig. 1 and comprise a) Eocene to Miocene sediments in the coastal region, b) the Coastal Cordillera, which north of the Gastre Fault Zone (GFZ) consists of granitoids and high T metamorphic rocks of Carboniferous age, while south of this fault zone the Coastal Cordillera is made up by a Permo-Triassic high p/T metamorphic complex. This complex, known as "Western Series" (Aguirre et al., 1972; Willner et al., 2001), is interpreted as a forearc accretionary wedge. Its internal structural evolution was terminated in the Late Triassic. Since then the complex remained stable and almost unaffected in its present day position (Glodny et al., this volume). Major activity of the Gastre Fault Zone was inferred for Mesozoic times, with possible Cenozoic reactivation (Rapela and Pankhurst 1992; Rapela 1997). Further east, the c) Chilean Longitudinal Valley is bordered to the east by the main Cordillera with the active Andean magmatic arc. Here, one of the most

striking tectonic and morphological features is the Liquiñe-Ofqui Fault Zone (LOF), a major trench-parallel intra-arc strike-slip fault system (Cembrano et al. 1996).

In the present study we apply fission track (FT) thermochronology to rocks of the forearc and the magmatic arc between 37°S and 42° S in order to provide information on the timing and magnitude of basal accretion in the forearc accretionary complex, on the thermal history of the granitoids and on the timing of activity of the major fault systems.

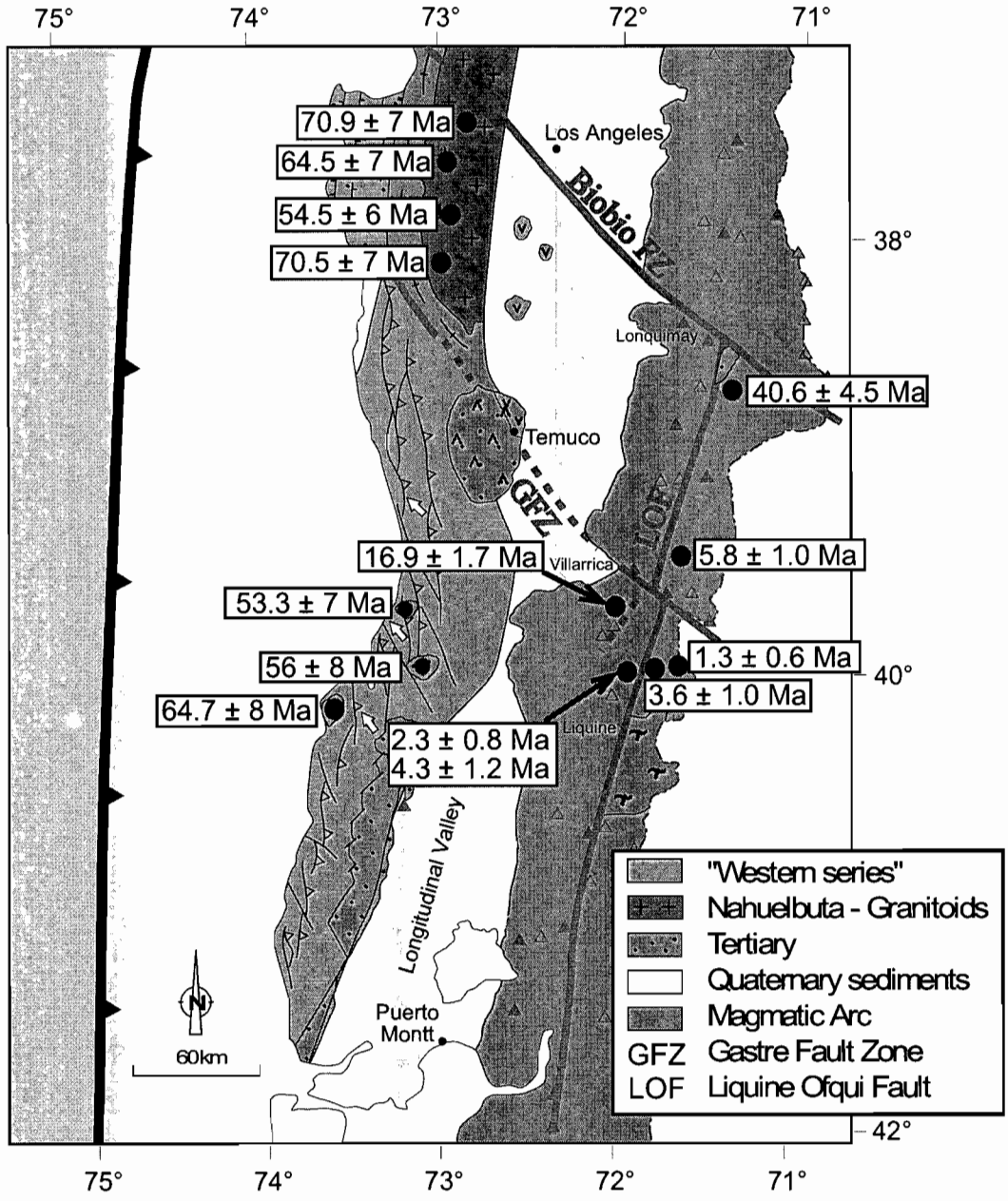

Fig. 1: Geological map of South-Central Chile between 37° and 42°, with the (●) locations of apatite fission track ages.

RESULTS AND CONCLUSIONS

Apatite FT analysis was performed on granitoid rocks from the forearc region (Coastal Cordillera) and from the Main Cordillera (Fig. 1). In the Coastal Cordillera, south of the Gastre Fault Zone, apatite FT ages range from 64.7 to 53.3 Ma, indicating that exhumation of less than 4 km occurred since the Early Tertiary. The exhumation rates were variable with time: While geomorphology and sedimentary cover on the basement rocks indicate uplift of several 100 m during Pliocene and Quaternary, sedimentary basins suggest subsidence during Miocene times. Therefore, the main exhumation must be Paleogene in age. The slow and discontinuous exhumation suggests that if basal underplating occurred, it was similarly discontinuous and not a dominant process during the Cenozoic. The Late Cretaceous to Early Tertiary apatite FT ages both north and south of the Gastre Fault Zone (Fig. 1) imply that at least vertical displacement along this fault was restricted to the Mesozoic.

In the Main Cordillera, the apatite FT ages of the area around the village of Liquiñe (40°S, Fig.1) range between 4.3 and 1.3 Ma, revealing that exhumation there is recent and rapid, with rates of nearly 1 km/Ma during the last 4 Ma. Estimates on the crystallization depths of the Miocene granitoids of the region suggest that Late Miocene denudation rates may have been comparable to the present rates. There is no detectable control of the LOF on the apatite age distribution pattern. Therefore, the LOF seems to be predominantly a strike-slip transform fault, without major vertical displacement at least since the Pliocene. We observe a clear tendency towards older apatite FT ages west and particularly north of Liquiñe: In the area of Lonquimay (38°30'S) at the northern end of the LOF, an Eocene apatite age of 40.6±4.5 Ma indicates that exhumation there was more than an order of magnitude less efficient than in the Liquiñe area. This pattern is supported by tectonic investigations (Rosenau et al., this volume) which show that in contrast to the Liquine area, the Lonquimay area is characterized by extensional deformation. Furthermore, the granitoids of the Lonquimay area are subvolcanic, shallow intrusions, which corroborates low long-term denudation rates. Although variations of the geothermal gradient and tectonics may have influenced the age distribution pattern, climate seems to be an important factor. Younger ages towards the south correlate with drastic increases of precipitation rates and intensity of Pleistocene glaciation.

REFERENCES

Aguirre, L., Hervé, F., Godoy, E. 1972. Distribution of metamorphic facies in Chile, an outline. Krystalinikum, 9, 7-19.

Cembrano J., Hervé F., Lavenu A. 1996. The Liquiñe-Ofqui fault zone: A long-lived intra-arc fault system in southern Chile. Tectonophysics, 259, 55-66.

Glodny, J., Lohrmann, J., Seifert, W., Gräfe, K., Echtler, H., Figueroa, O. 2002. Geochronological constraints on material cycling velocities, structural evolution and exhumation of a paleo-accretionary wedge: The Bahia Mansa complex, South Central Chile. ISAG (this volume).

Rapela C.W. 1997. El sistema de fallas de Gastre: e pur si muove. Rev. Asoc. Geol. Argentina, 52 (2), 219-222.

Rapela C.W., Pankhurst R.J. 1992. The granites of northern Patagonia and the Gastre fault system in relation to the break-up of Gondwana. In: Storey B.C., Alabaster T., Pankhurst R.J. (eds.): Magmatism and the causes of continental break-up. Geol. Soc. of London Special Publications, 68, 209-220.

Willner, A.P., Pawlig, S., Massonne, H.J., Hervé, F. 2001. Metamorphic evolution of spessartine quartzites (Coticules) in the high-pressure, low-temperature complex at Bahia Mansa, Coastal Cordillera of South-Central Chile. Canadian Mineralogist, 39, 1547-1569.

SHALLOW MELTING OF OCEANIC CRUST DURING SPREADING RIDGE SUBDUCTION: ORIGIN OF NEAR-TRENCH QUATERNARY VOLCANISM AT THE CHILE TRIPLE JUNCTION

Christèle GUIVEL (1), Yves LAGABRIELLE (2), René C. MAURY (2), Nicolas ARNAUD (3), Jo COTTEN (2), Jacques BOURGOIS (4), Serge FOURCADE (5) and Hervé MARTIN (3)

(1) Université de Nantes, UMR 6112 Planétologie et Géodynamique, 2 rue de la Houssinière 44322 Nantes Cedex 3 France (guivel@chimie.univ-nantes.fr)
(2) IUEM, UMR CNRS 6538, Place Nicolas Copernic, 29280 Plouzané, France (Yves.Lagabrielle@sdt.univ-brest.fr, René.Maury@sdt.univ-brest.fr, Jo.Cotten@univ-brest.fr)
(3) UMR 6524 Magmas et volcans, Université Blaise Pascal, 5 rue Kessler, 63038 Clermont-Ferrand, France (N.Arnaud@ opgc.univ-bpclermont.fr, H.Martin@opgc.univ-bpclermont.fr)
(4) Institut de Recherche et Développement (IRD) and Centre National de la Recherche Scientifique (CNRS), Université Pierre et Marie Curie, Boîte 119, 4 place Jussieu, 75252 Paris Cédex 05, France (bourgois@ccr.jussieu.fr)
(5) UMR 6118 Géosciences Rennes, Université de Rennes I, Avenue du Général Leclerc, 35042 Rennes, France (Serge.Fourcade@univ-rennes1.fr)

KEY WORDS: Chile triple junction, ridge subduction, near trench magmatism, adakites

INTRODUCTION

Pleistocene basaltic andesites and dacites carrying a subduction-related geochemical imprint were dredged along the Chilean continental margin off the Taitao Peninsula during the Chile Triple Junction (CTJ) cruise of the N/O L'Atalante in 1997 (Bourgois et al., 2000). These rocks, although similar in several respects to the Chilean arc lavas located 200 km landward, are located within the active Chile trench axis itself or in the forearc domain less than 20 km away from the trench (Figure 1). Considering their spatial and temporal distribution, the CTJ lavas were undoubtedly emplaced near the trench during a ridge subduction event. This peculiar geodynamic context is not consistent with the generally accepted model of origin of Andean arc magmatism, i.e. the deep partial melting of the metasomatized mantle wedge triggered by the release of hydrous fluids from the subducting slab.

The Chile Triple Junction volcanic rocks range in SiO_2 from 50.3 to 69.5 wt%. Basaltic to intermediate lavas, ranging in composition from 50.3 to 57.5 SiO_2 wt% coexist with felsic lavas displaying a more restricted SiO_2 range (from 65.5 to 69.5 wt%). In the N-MORB-normalized plot (Figure 2), representative basaltic to dacitic CTJ lavas display LILE and LREE enrichments and Nb and Ti depletions relative to adjacent incompatible elements. These features are characteristic of arc magmas. Their Sr and Nd isotopic signatures are rather juvenile ($^{87}Sr/^{86}Sr$= 0.703679 to 0.704555±6 +0.8, ϵNd= +2.9 to +5.3), suggesting that the magma source was not strictly MORB-type but contained in addition a continental crust or sedimentary component, a feature also consistent with their $\delta^{18}O$ values (+5.9 to +6.9 ‰). The trace element patterns (see Figure 2) which are not parallel from basalt to dacites and the isotopic variations among the CTJ lavas preclude a simple closed-system fractionation of a single primitive magma and fractional crystallization coupled with assimilation of continental crust and/or sediments from basalts to dacitic magmas.

Major and trace element data allow to distinguish two groups of dacites sampled in the same dredge site CTJ17. The distinction between low-Si and high-Si dacites is especially based on the higher Sr contents, lower Y and heavy REE (HREE) concentrations, and the lack of negative Eu anomaly in the former (Figure 2). These features are characteristic of adakitic (slab-melt) compositions (Defant and Drummond, 1990). Evolved lavas (SiO_2>63 wt%) from the Austral Volcanic Zone (AVZ) and from the Southern Volcanic Zone (SVZ), respectively, have been plotted together with the CTJ17 dacites in the Sr/Y vs. Y diagram of Figure 3. The latter are intermediate between normal calc-alkaline mantle-derived magmas (SVZ magmas in Figure 3) and adakites/slab melts (AVZ magmas in Figure 3).

We show that both groups derive from the melting of a basaltic protolith plus sediments and do exist within a same dredge site, which srongly suggests relatively close sources at depth. The high-Si dacites are likely to derive from the hydrous melting of a mixture of 75% MORB + 25% sediments at high temperatures (800-1000°C) under low pressures (<0.8 GPa) in the plagioclase stability field. Low-Si dacite melts originate in a pressure field where both garnet and plagioclase are stable that is between 0.8 and 1.5 GPa (Green, 1982) corresponding to depths ranging from 25 to 45 km. Assuming a Benioff plane dip of 20°, the top surface of the oceanic crust underthrusted below the edge of the Chile continental crust is at a maximum depth of only ca. 10 km below the dredge sites. Therefore, the occurrence of residual garnet in the source of the low-Si dacites is not consistent with the present-day structure of the investigated area. If we consider that the slab dip cannot be lower than few tens of degrees, only a combination of several tectonic processes implying a very complex history with rapid burying and uplift of slabs fragments close to the CTJ should account for the genesis of the adakitic melts. The tectonic context of the CTJ is indeed characterized by strike-slip faulting, rapid tectonic erosion and changes in sedimentary wedge configuration in relation with glaciary-driven sedimentary supply variations occurrences (Bourgois et al., 2000; Lagabrielle et al., 2000). In such an atypical subduction context, tectonic slices of oceanic crust may follow a complex pathway. For this reason we favour a model in which parts of the slab should be subducted rapidly to depths of 20-30 km right under the trench (Figure 4). The proposed model of figure 4 is based on a specific character of the Chile Triple Junction. The oceanic lithosphere entering the trench at the CTJ is indeed characterized by the occurrence of a group of transform faults. In our model, transform faults are considered as stress free boudaries that allow the partition of the slab into successive independant portions. We assume that the youngest slab portions may bend drastically in response to mantle counterflow in the mantle wedge, moving from the back-arc to the trench. Such a bending might allow portion of relatively young and still hot portions of oceanic crust to reach rapidly depths of 20-30 km. The CTJ region is unfortunatly devoid of significant seismicity and seismological data are not available in order to constrain the dip of slab under the CTJ. As a consequence, we are well aware that our model remains highly hypothetical. However, at present, it is the only hypothesis that integrates some of the fundamental parameters provided by the petrogenetical modeling constraints as summarized below.

- 1. Melting of the downgoing slab needs a great amount of water. The serpentinites that are present in very high volume in the transform zones can be regarded as good feeder for the water,
- 2. Only a configuration with an almost vertical slab may lead to the presence of two groups of dacites emplaced in the same site.

The basaltic andesites, which contain Mg-rich olivines in desequilibrium with their host rocks and which display lower MREE and HREE contents than the Chile ridge basalts, are thought to result from the mixing of MORB-type magmas from the buried spreading ridge with dacitic magmas.

CONCLUSIONS

Numerous past examples in which calc-alkaline magmas were emplaced in near-trench conditions, for instance as intrusions crosscutting the accretionary prism metasediments, have been documented and attributed to ridge subduction processes (Cole and Basu, 1995; Sisson and Pavlis, 1993; Lytwyn et al., 2000; Maeda and Kagami, 1996). The CTJ basaltic andesites and dacites provide the first Quaternary example of magmas carrying subduction-related signatures being emplaced in the forearc domain, less than 20 km away from the active Chile trench. The very unusual tectonic context of the Chile Triple Junction, which involved the successive subduction of several ridge segments below the same zone, was able to produce the quite exceptional conditions of melting required for the above models: temperatures of 800-1000°C at depths lower than ca. 20-30 km, and availability of considerable amounts of water probably arising from the shallow dehydration of downgoing sediments or from serpentinites present in the transform faults.

REFERENCES

Bourgois, J., Guivel, C., Lagabrielle, Y., Calmus, T., Boulègue, J., and Daux, V. 2000. Glacial-interglacial trench supply variation, spreading-ridge subduction, and feedback controls on the Andean margin development at the Chile triple junction area (45-48°S), J. Geophys. Res., 105, 8355-8386.

Cole, R.B., and Basu, A.R. 1995. Nd-Sr isotopic geochemistry and tectonics of ridge subduction and middle Cenozoic volcanism in western California, Geol. Soc. Am. Bull., 107, 167-179.

Defant, M.J., and Drummond, M. S. 1990. Derivation of some modern arc magmas by melting of young subducted lithosphere, Nature, 347, 662-665.

Forsythe, R.D., Drake, R., and Olsson, R. 1995. Data report: 40Ar/39Ar and additional paleontologic age constraints, Site 862, Taitao Ridge. *Proceedings of the Ocean Drilling Program, Scientific Results, 141*, 421-426.

Green, T.H., Anatexis of mafic crust and high pressure crystallization of andesite, in: Thorpe, R.S. (Ed.), Andesites. Wiley, New York, 466-487, 1982.

Guivel, C., Bourgois, J., Fourcade, S., Lagabrielle, Y., Martin, H., and Maury, R.C. 1999. New constraints for the origin of ridge-subduction-related plutonic and volcanic suites at the Chile Triple Junction (Taitao Peninsula and Site 862, Leg ODP 141 on the Taitao ridge), Tectonophysics, 311, 83-111.

Lagabrielle, Y., Guivel, C., Bourgois, J., Fourcade, S., and Martin, H. 2000. Magmatic-tectonic effects of high thermal regime at the site of active ridge subduction: the Chile Triple Junction model, Tectonophysics, 326, 255-268.

Lopez Escobar, L., Kilian, R., Kempton, P.D., and Tagiri, M. 1993. Petrography and geochemistry of Quaternary rocks from the southern volcanic zone of the Andes between 41°30' and 46°00'S, Chile, Revista Geologica de Chile, 20, 33-55.

Lytwyn, J., Lockhart, S., Casey, J., and Kusky, T. 2000. Geochemistry of near-trench intrusives associated with ridge subduction, Seldovia Quadrangle, southern Alaska, J. Geophys. Res., 105, 27 957-27 978.

Maeda, J., and Kagami, H. 1996. Interaction of a spreading ridge and an accretionary prism: implications for MORB magmatism in the Hidaka magmatic zone, Hokkaido, Japan, Geology, 24, 31-34.

Sisson, V., and Palvis, T. 1993. Geologic consequences of plate reorganization: an example from the Eocene southern Alaska fore arc, Geology, 21, 913-916.

Stern, C.R., and Kilian, R. 1996. Role of the subducted slab, mantle wedge and continental crust in the generation of adakites, from the Andean Austral Volcanic Zone, Contrib. Mineral. Petrol., 123, 263-281.

Sun, S:S., and McDonough, W.F. 1989. Chemical and isotopic systematics of oceanic basalts: implications for mantle composition and processes, In: Saunders, A.D. and Norry, M.J. (eds), Magmatism in the Ocean Basins, Geol. Soc. Spe. Publ., 42, 313-345.

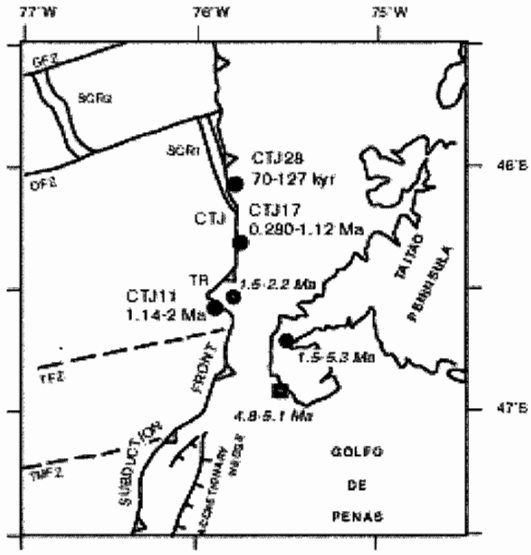

Figure 1 : Location of the Pliocene to Quaternary calk-alcaline magmatic rocks in the vicinity of the Chile Triple Junction. Note the good correlation of magmatic ages older from south to north in agreement with northward migration of the Chile Margin Triple Junction. Filled circles: new $^{40}Ar/^{39}Ar$ dates on basaltic andesites and dacites from the CTJ lava population obtained by NA; Empty circles: $^{40}Ar/^{39}Ar$ dates on rhyolitic samples from Leg ODP 141, Site 862 on the Taitao ridge (Forsythe et al., 1995) and nannoplankton assemblages ages (Bourgois et al., 2000) from volcanic-sedimentary Chile margin unit on the Taitao Peninsula; Empty square: $^{40}Ar/^{39}Ar$ dates on the Cabo Raper granodioritic pluton on the Taitao Peninsula (Guivel et al., 1999). GFZ: Guamblin fracture zone; DFZ: Darwin fracture zone; TFZ: Taitao fracture zone; TMFZ: Tres Montes fracture zone; SCR2 and SCR1 : Southern Chile Ridge segment 2 and segment 1 respectively; CTJ: Chile Triple Junction; TR: Taitao Ridge.

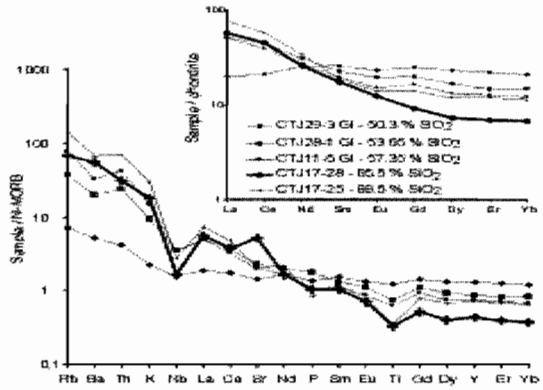

Figure 2 : Trace-element abundance patterns for representative CTJ cruise lavas, ranging from basalt to dacites, normalized to the composition of N-MORB (Sun and Mac Donough, 1989). Inset: Rare earth element patterns for the same samples normalized to chondritic values (Sun and Mac Donough, 1989). The trace element patterns are not parallel and we observe a general decrease in MREE and HREE from basalt to dacites, which is incompatible with fractional crystallization process.

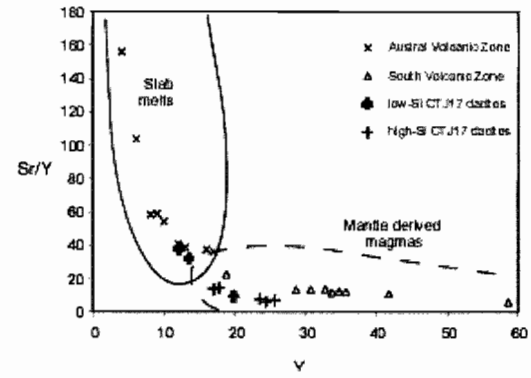

Figure 3 : Sr/Y versus Y diagram showing fields expected for slab melts (solid curve) and mantle-derived magmas (dashed curve). All CTJ17 dacites plot between the slab melt field and the mantle-derived field. The Austral Volcanic Zone (AVZ) lavas classified as adakites (Stern and Kilian, 1996) and the Southern Volcanic Zone (SVZ; Lopez-Escobar et al., 1993) lavas that include "normal" dacites from the Southern SVZ are also shown for comparison.

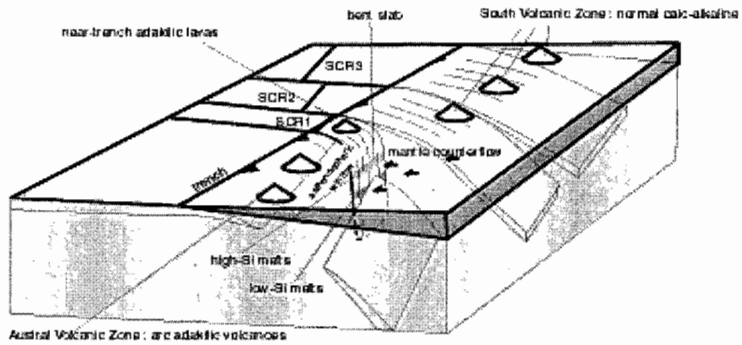

Figure 4: Near-trench dacitic magmas on the Chile triple junction derive from the melting of a basaltic protolith plus sediment at various depths. In this atypical subduction context, tectonic slices of oceanic crust may follow a complex pathway supplying P-T-H_2O conditions necessary to allow shallow (20-45 km) slab melting (see text for discussion).

TECTONIC-MAGMATIC EVOLUTION OF THE MINERAL DISTRICT AGUA DE DIONISIO (YMAD), ARGENTINA

Adolfo Antonio GUTIÉRREZ (1), Shoji Kojima (2) and Sergio ESPINOZA R.(2)

(1) Universidad Nacional de Tucumán, Facultad de Ciencias Naturales e IML. Miguel Lillo 205, (4000) San Miguel de Tucumán, Argentina: terres@csnat.unt.edu.ar

(2) Universidad Católica del Norte, Departamento de Ciencias Geológicas. Av. Angamos 0610, Antofagasta, Chile: skojima@ucn.cl – sespinoz@ucn.cl

KEY WORDS: Tectonics, volcanism, Central Andes, deposits.

INTRODUCTION

The Volcanic Complex Farallon Negro is located westward the 66°30'W meridian and northward the 27°30'S parallel. A structure scheme of YMAD district has been depicted after a visual interpretation of Landsat images at scales 1:1.000.000 and 1:2.500.000 B&N MSS 7 of 1975 (Figure 1). In Figure 3, sub-volcanic dikes mapped by Llambias (1970) are shown.

The volcanic stratus have began its activity approximately at 13Ma through 5Ma (Sasso, 1997). During its development, a series of sub-volcanic intrusive and sub-vertical dikes (dated by Caelles et al., 1971; Sasso, 1997) have settled. They present a main NW-SE orientation. In a lesser extent, other sub-volcanic bodies and dikes follow a NE-SW direction (Figure 2). Dikes and sub-volcanic intrusives have settled in the volcanic complex following a structure pattern which at the beginning of the volcanic activity had a main NE-SE direction. Afterwards, this direction shifted to a NW-SE position following the rotation of the shrinking axis from NE-SW to NNW-SSE (Gutiérrez, 2000b) (Figure 2).

The structure and the parallel dike arrangements of main NW-SE direction, and inclination between 65° and sub-verticals, follow a transpresive twisting scheme with rotation of the shrinking axis from NE-SW to NNW-SSE. This axis was developed by parallel forces of NW-SE direction originated by the dextral fault system of Amanao and Ampujaco at the end of the Tertiary (Gutiérrez, 2000a) (Figures 1 and 2).

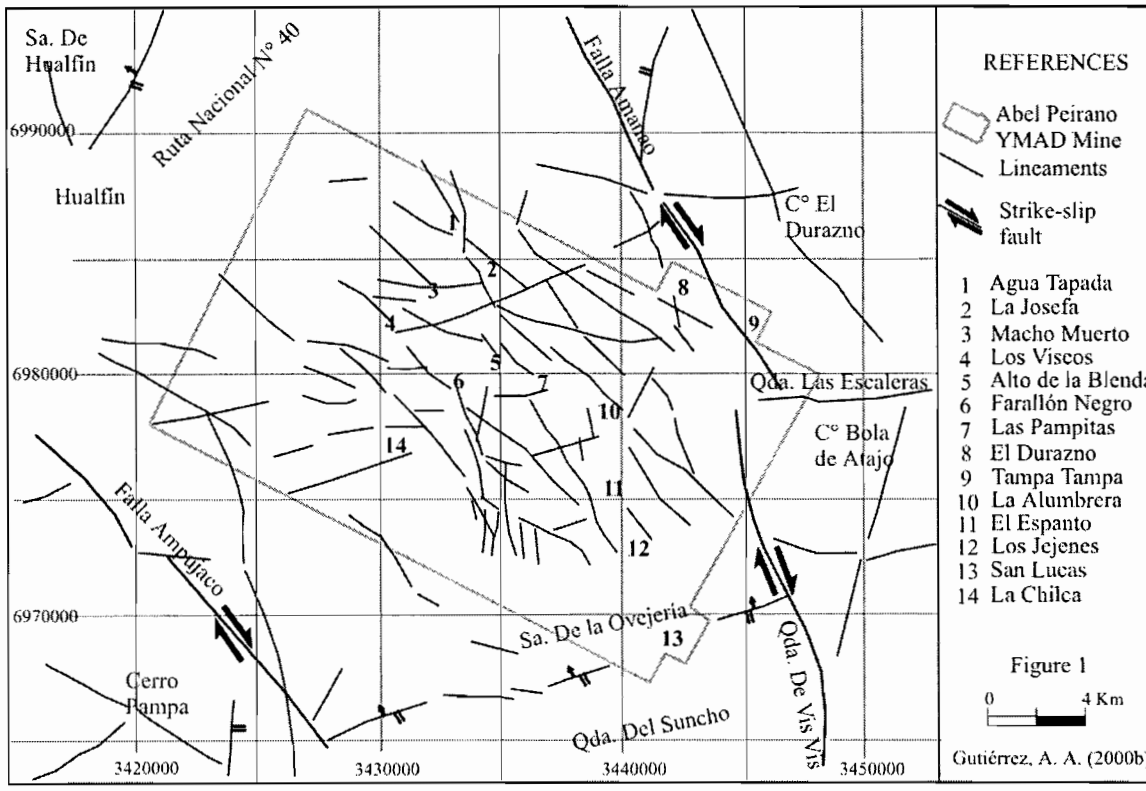

The transitional-compressive position NE-SW of the shrinking axis until 6.7Ma at YMAD district, would have given birth to the copper porfid deposits El Durazno, Agua Tapada, La Alumbrera and Las Pampitas (Figure 3). During the stress tectonic regime, the shrinking axis followed a NNW-SSE direction, giving rise to the epithermal deposits of low sulfurization Alto de la Blenda and Farallón Negro, and to the epithermals Santo Domingo, La Josefa and Morro Bola (Figure 3). The location of the epithermal deposits Agua Tapada, Santo Domingo, La Josefa, Morro Bola and the copper porfid deposits El Durazno, Agua Tapada and Las Pampitas shown in Figure 3, are relative since its ages are unknown.

CONCLUSIONS

The sequential development in space and time of the volcanic complex intrusives, evince the shrinking axis variation from a NE-SW to a NNW-SSE position, taking place approximately between 8.59Ma and 5.0Ma (Figure 2).

The epithermal deposits of low sulfurization originate in a tectonic regime of stress character, while the copper porfid deposits, in a tectonic regime of compressive regime, alike the mentioned examples (Watanabe, 1995; Watanabe et al., 1996, Kojima, 1999).

The relative movement of the Nazca Plate together with the action of the Dorsal de Juan Fernandez, would have given rise to sinestral parallel forces of NE-SW direction between 27°S and 33°S, originating structures of

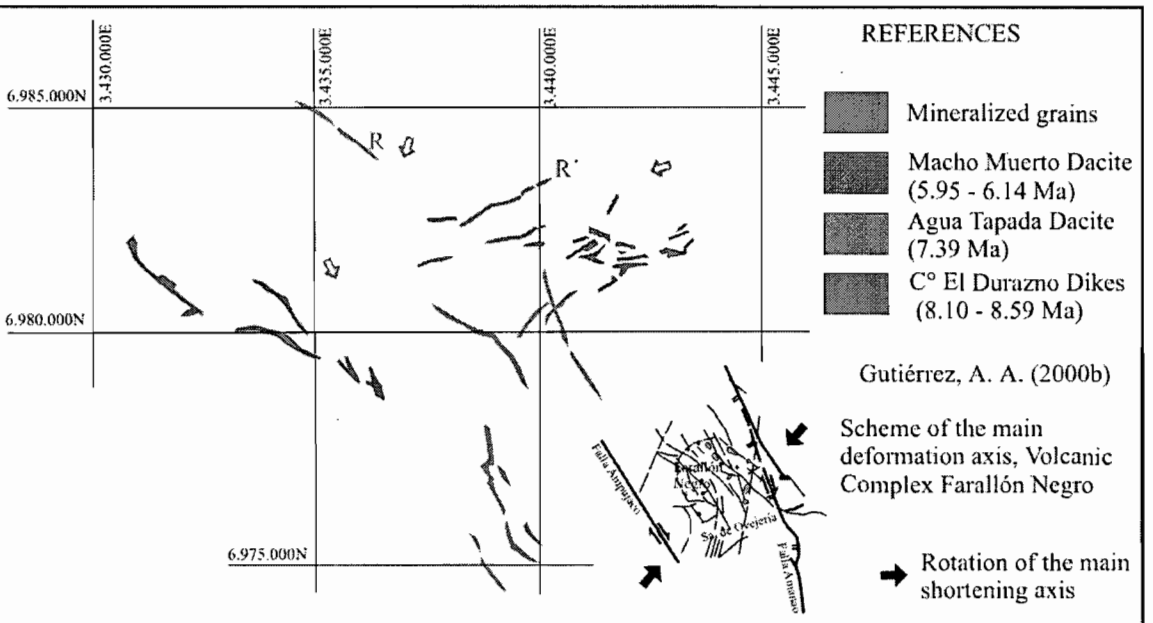

Figure 2 - Structural evolution of the YMAD district dikes

NE-SW and NW-SE direction and the formation of an incipient retroarc rift which favored the YMAD deposits formation in a tectonic environment of tranpressive twisting (Gutiérrez, 2000b).

Mineralizing age	?Ma	?Ma	6.75Ma	?Ma	6.55Ma	?Ma
Deposits	El Durazno	Agua Tapada	La Alumbrera	Las Pampitas	Alto de la Blenda / Farallón Negro	Epitermales
Tectonic regime	Compressive		Transitional		Stressing	
	NE-SW				NNW-SSE	

Epithermals: Vetiformes de Agua Tapada, Santo Domingo, La Josefa y Morro Bola

Figure 3: Ages and tectonic regimes of the YMAD district deposit

ACKNOLEDGMENTS

We thank the National University of Tucumán, Argentina and the Magister Program of the Northern Catholic University, Antofagasta, Chile. We also thank the valuable assistance of Dr. Guillermo Chong D.

REFERENCES

Caelles, J. C., A. H. Clark, E. Farrar, S. L. Mc Bride & S. Quirt, 1971. Potassium-argon ages of porphyry copper deposits and associated rocks in the Farallón Negro-Capillitas District, Catamarca, Argentina. Economic Geology, Vol. 66, 961-964.

Gutiérrez, A. A., 2000a. Morphotectonic Evidences of Sinestral Rotation of the Pampeanas Mountain Ranges, Argentina. Revista Profil, XVII Simposio Latinoamericano de Geología, Stüttgart, Germany.

Gutiérrez, A. A., 2000b. Dispersión Geoquímica Primaria y Metalogénesis de Depósitos Tipo Pórfido Cuprífero y Epitermal, Distrito Minero Agua de Dionisio, Argentina. Universidad Católica del Norte, Antofagasta, Chile. Tesis de Magíster, 131p.

Kojima, S., 1999. Some aspects Regarding the Tectonic Setting of high- and low-sulfidation epithermal gold deposits of Chile. resource Geology, Vol. 49, N° 3, 175-181.

Llambías, E. J., 1970. Geología de los Yacimientos Mineros de Agua de Dionisio: Revista de la Asociación Argentina de Mineralogía, Petrología y Sedimentología; Tomo 1, Vol. 2, 2-32.

Sasso, A. M., 1997. Geological Evolution and Metallogenetic Relationships of the Farallón Negro Volcanic Complex, NW Argentina. Queen's University, Kingston, Ontario, Canadá. Tesis Doctoral, v. 1 y 2.

Watanabe, Y., 1995. Tectonic setting for the formation of high-and low-sulfidation epithermal gold deposits. Abstracts with Programs, Annual Meetting of the Society of Resource Geology, Tokyo, Japan: O35.

Watanabe, Y., M. Aoki and N. Nakajima, 1996. Age and style of epithermal gold mineralization in the Minamikayabe area, Southwestern Hokkaido. Resource Geology, Vol. 46(6), 317-326.

THE STRUCTURE AND MECHANICAL PROPERTIES OF THE ANDEAN LITHOSPHERE FROM GRAVITY-BASED STUDIES

Ron HACKNEY (1), Hans-Jürgen GÖTZE (2), Sabine SCHMIDT (3), Zuzana TAŠÁROVÁ (4), Susann WIENECKE (5)

Institut für Geologische Wissenschaften, Freie Universität Berlin, Malteserstr. 74–100, D-12249 Berlin, Germany
(1) rhackney@geophysik.fu-berlin.de
(2) hajo@geophysik.fu-berlin.de
(3) sabine@geophysik.fu-berlin.de
(4) zuzana@geophysik.fu-berlin.de
(5) susann@geophysik.fu-berlin.de

KEYWORDS: gravity anomalies, isostasy, rigidity, Andes.

INTRODUCTION

During the course of the Collaborative Research Project SFB267, "Deformation Processes in the Andes", a large amount of gravity data have been collated at Freie Universität in Berlin. This database comprises around 140,000 gravity stations that cover two main areas in the central and southern Andes. In conjunction with data from other disciplines, the quantity and quality of the data in this database enable comprehensive studies of Andean crustal structure and mechanical properties. We present here a summary of our gravity-based studies in these areas.

THE GRAVITY DATABASE

Gravity data collated at Freie Universität are sourced from measurement campaigns conducted as part of SFB267, existing data from Geological Surveys of Chile and Argentina, the Universities of Chile and Buenos Aires and the Institute of Geodesy in Buenos Aires. Large amounts of data have also been obtained from the Bolivian and Argentinean State Oil Companies and Empresa Nacional del Petroleo. All stations in the database have been tied to the IGSN71 gravity datum and complete Bouguer anomalies have been computed by applying terrain corrections based on elevation data from the GTOPO30 global digital elevation model (USGS, 1997).

METHODS

Most computations are based on the IGMAS modelling package developed over many years at Freie Universität Berlin (e.g. Schmidt & Götze, 1998). IGMAS is an interactive program for the three-dimensional forward modelling and interpretation of potential field data. Three-dimensionality is achieved by triangulating between common interfaces in a series of two-dimensional cross-sections constructed through the region of interest.

Interpretation is further aided by the integration of a GIS-based system which allows direct visualisation of constraints provided by other disciplines. IGMAS also has the capabilty to directly compute internal crustal loads from the density structure invoked during forward modelling. From these loads, lithospheric rigidity can be derived. The results from this approach can be compared to results derived from techniques based on admittance and coherance functions.

INTERPRETATION OF THE GRAVITY FIELD

In the Central Andean region (Fig. 1a,b), where until recently most work has been focussed, onshore complete Bouguer anomalies reach a minimum of -450 mGal (Fig. 1c). This anomaly low reflects crustal thickening and the generally low densities associated with the volcanic arc. Residual isostatic anomalies (Fig. 1d), computed using a Vening-Meinesz model for regional compensation of topography (plate rigidity 10^{23} Nm), vary between about -120 and 120 mGal. These anomalies show several significant correlations with geological structure.

One of the most important residual anomaly features is the positive NW–SE trending Central Andean Gravity High (Fig. 1d). This feature extends over at least 5° in latitude from Calama (Chile) in the north to east of Catamarca (Argentina) in the south. It reflects deep (>10 km), high-density (~3000 kg/m^3) rocks that are postulated to be related to the volcanic arc of a pre-Andean subduction zone (Götze & Krause, 2002). This high-density mid-crustal body is likely to have exerted a strong influence on the location of fault-zones and the style of deformation, as well as having a role in the formation of structurally controlled porphyry copper deposits found at the margins of the feature.

Other notable features of the residual anomaly field include:

- A prominent and continuous positive residual anomaly paralleling the Chilean margin. This feature correlates with dense igneous rocks exposed in the Coastal Cordillera.

- Negative residual isostatic anomalies that correlate with the Miocene to Quaternary volcanic arc of the Western Cordillera (Fig. 1b,d).

- Extreme local anomaly minima in the southern Altiplano that is associated with young collapsed calderas (Coira et al, 1998; Chmielowski, et al, 1999).

- Positive isostatic residual anomalies associated with the Bolivian Altiplano region, suggesting the dominance of mass excess in the upper crust (Fig. 1b,d).

RIGIDITY OF THE ANDEAN LITHOSPHERE

Rigidity values for the Central Andean region vary between about 10^{20}Nm (effective elastic thickness of ~5 km)

in areas associated with young, large volcanic calderas, and about 10^{24} Nm (effective elastic thickness of 55 km) in the Coastal Cordillera. The regions of low rigidity associated with volcanic calderas are also well correlated with low electrical resistivity, and the most rigid areas of the Central Andes lie adjacent to the coast where regions of high seismic velocity also exist.

SUMMARY AND CONCLUSIONS

In the next three-year stage of the SFB267 project, we aim to improve existing three-dimensional gravity models and to construct new models in other areas (e.g. Southern Andes). These detailed models will allow us to extend the isostatic analyses beyond the Central Andes and to improve simple finite element modelling of Altiplano uplift by incorporating density structure and zones of lower rigidity inferred from the gravity modelling. Continued integration of results based on gravity data with those from other disciplines will remain a primary focus of this work. Additionally, comparisons with other orogenic systems will lead to a better understanding of the dynamic processes associated with the formation and evolution of the Andes.

REFERENCES

Chmielowski J., Zandt G. & Haberland, Ch. 1999. The Central Andean Altiplano–Puna magma body. Geophysical Research Letters, 26, 783–786.

Coira B., Caffe P., Diaz A. & Ramirez A. 1998. Sistema de calderas andinas del cenozoico superior: Vilama – Coruto, Puna (Argentine) – Altiplano (Bolivia). Memorias del XII Congreso Geologico de Bolivia, 991–1002.

Götze H.-J. & Krause S. 2002. The central Andean gravity high, a relic of an old subduction zone? Journal of South American Earth Sciences, 14, 799–811.

Schmidt S. & Götze H.-J. 1998. Interactive visualisation and modification of 3D models using GIS functions. Physics and Chemistry of the Earth, 23, 289–296.

USGS 1997. GTOPO30 Digital Elevation Model, United States Geological Survey EROS Data Centre, Sioux Falls, South Dakota. http://edcdaac.usgs.gov/gtopo30/gtopo30.html

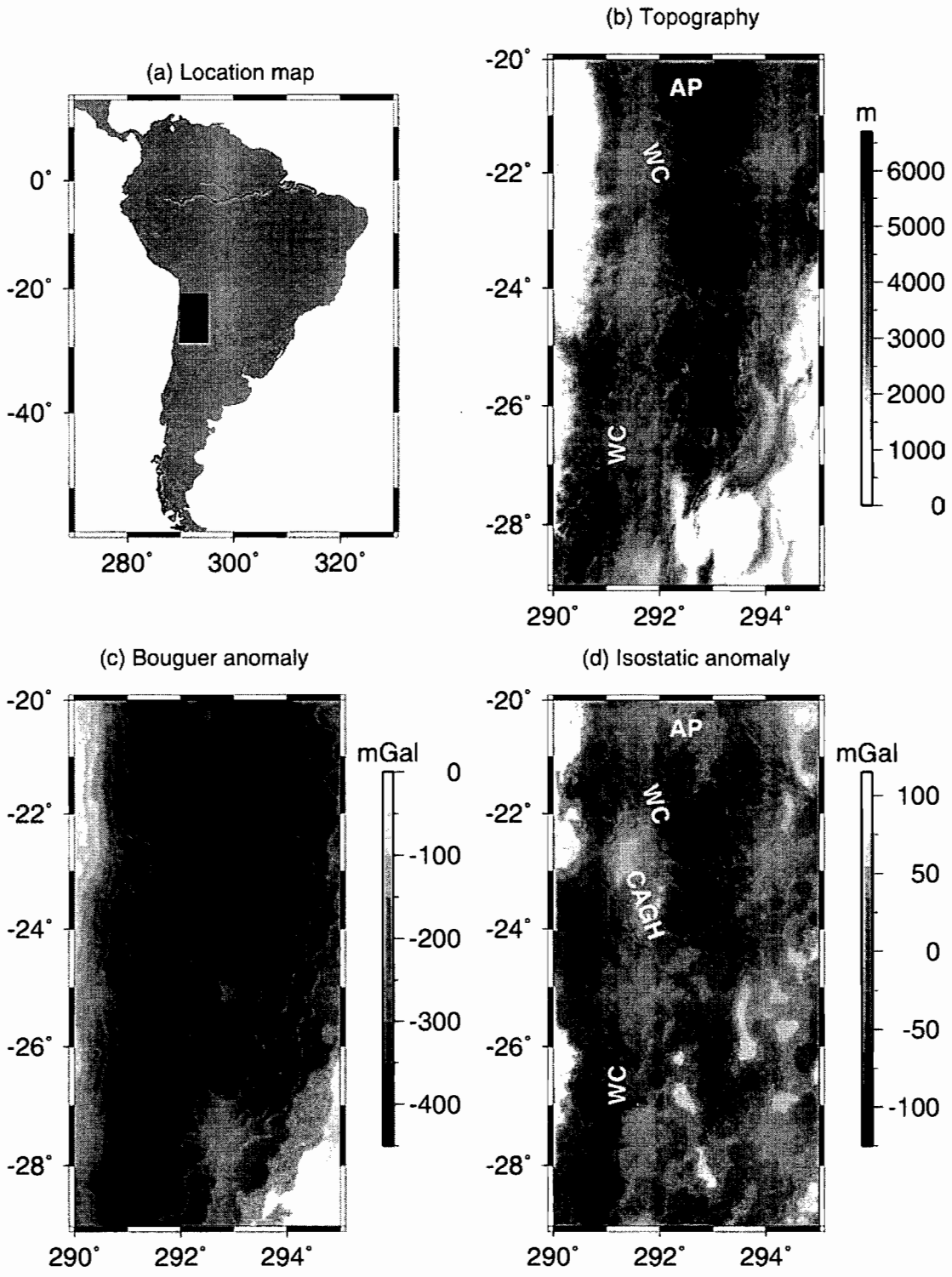

Figure 1: (a) Map of South America showing the region of the Central Andes included in b, c and d. (b) Topography in the Central Andes from the GTOPO30 digital elevation model. AP marks the Altiplano, WC marks the volcanic arc of the Western Cordillera. (c) complete Bouguer anomalies. (d) Isostatic residual anomalies. CAGH is the Central Andean Gravity High.

THE OBLIQUELY SUBDUCTING NAZCA RIDGE AT THE PERUVIAN ACTIVE MARGIN: THE PRESENT COLLISION ZONE AND A RE -EVALUATION OF ITS MIGRATION HISTORY

Andrea HAMPEL (1), Nina KUKOWSKI (1), Joerg BIALAS (2), Udo BARCKHAUSEN (3)

(1) GeoForschungsZentrum Potsdam, Telegrafenberg, D-14473 Potsdam, Germany (andrea@gfz-potsdam.de)
(2) GEOMAR Research Center of Marine Geosciences, Wischhofstr. 1-3, D-12148 Kiel, Germany
(3) BGR, Stilleweg 2, D-30361 Hannover, Germany

KEYWORDS: Peru, Nazca Ridge, collision zone, plate reconstructions, migration history, ridge subduction

ABSTRACT

At the Peruvian convergent margin, the oceanic Nazca Plate subducts obliquely beneath the South American continent at a convergence rate of ~61 mm/a. The age of the subducting plate varies from 28 Ma to 38 Ma at the trench south and north of the Mendana Fracture Zone, respectively (Fig.). A prominent feature off Peru, which plays an important role in the evolution of the margin, is the 1.5 km high and 1000 km long submarine Nazca Ridge. This ridge migrates southward along the margin due to its oblique orientation to both the convergence direction and the trench line. The present collision zone of the Nazca Ridge and the Peruvian margin between 14°S and 17°S is characterized by deformation of the upper plate and several hundred meters of uplift in the forearc which is expressed by a narrowing of the shelf, an eastward shift of the coastline and the presence of marine terraces. South Peru also suffered from strong earthquakes of magnitude M_w = 8.1 and M_w = 7.7 in 1942 and 1996, respectively, which occurred near the continuation of the crest of the ridge and south of it. On 23 June 2001, an earthquake with a magnitude of M_w = 8.4 and several aftershocks of magnitude M_w = 6.0 and larger ruptured the coastal area at the southern edge of the intersection zone of the Nazca Ridge and the margin.

The Nazca Ridge and its collision zone with the trench was imaged by bathymetric and wide-angle seismic data during the RV "Sonne" cruise SO146–GEOPECO in spring 2000 off Peru between 5°S and 15°S. The data reveal that the southeastern flank of the ridge, which marks its leading edge entering the trench, has a rather smooth topography compared to the rough relief of the surrounding Nazca Plate. The sediment cover on the ridge does not exceed a thickness of 300 m. Several volcanic structures of different size and elevation can be identified on its surface. As they seem quite intact, they may have formed after the origin of the main part of the ridge. Towards the trench, an increasing number of trenchparallel normal faults, which are caused by the bending of the ridge into the subduction zone, can be identified. The trench is characterized by a rough surface and little to no sediment fill. Where the crest of the ridge enters the trench, the water depth decreases to 5000 to 5300 m compared to a water depth of 6500 m and more south of the intersection area. This is consistent with the amount

of uplift recorded in marine terraces along the coast (Hsu, 1992; Macharé and Ortlieb, 1992). The lower continental slope is very steep and shows features typical of erosion. There is no evidence for the presence of a former or present accretionary prism. The wide-angle seismic profiles indicate a thickened crust of up to 17 km for the ridge with seismic velocities typical of oceanic crust. The depth of the Moho varies laterally, thus the ridge seems to have a slightly assymmetrical root. The incoming sediments are assumed to be completely subducted since an accretionary wedge cannot be identified in the seismic data. The angle of the lower slope is larger than north of the Nazca Ridge, therefore, the continental slope may undergo enhanced short-term erosion due to the ridge subduction which is superposed on a long-term erosional regime of the Peruvian margin. The Nazca Plate, which can be traced to a depth of about 28 km, subducts at an angle of about 9°.

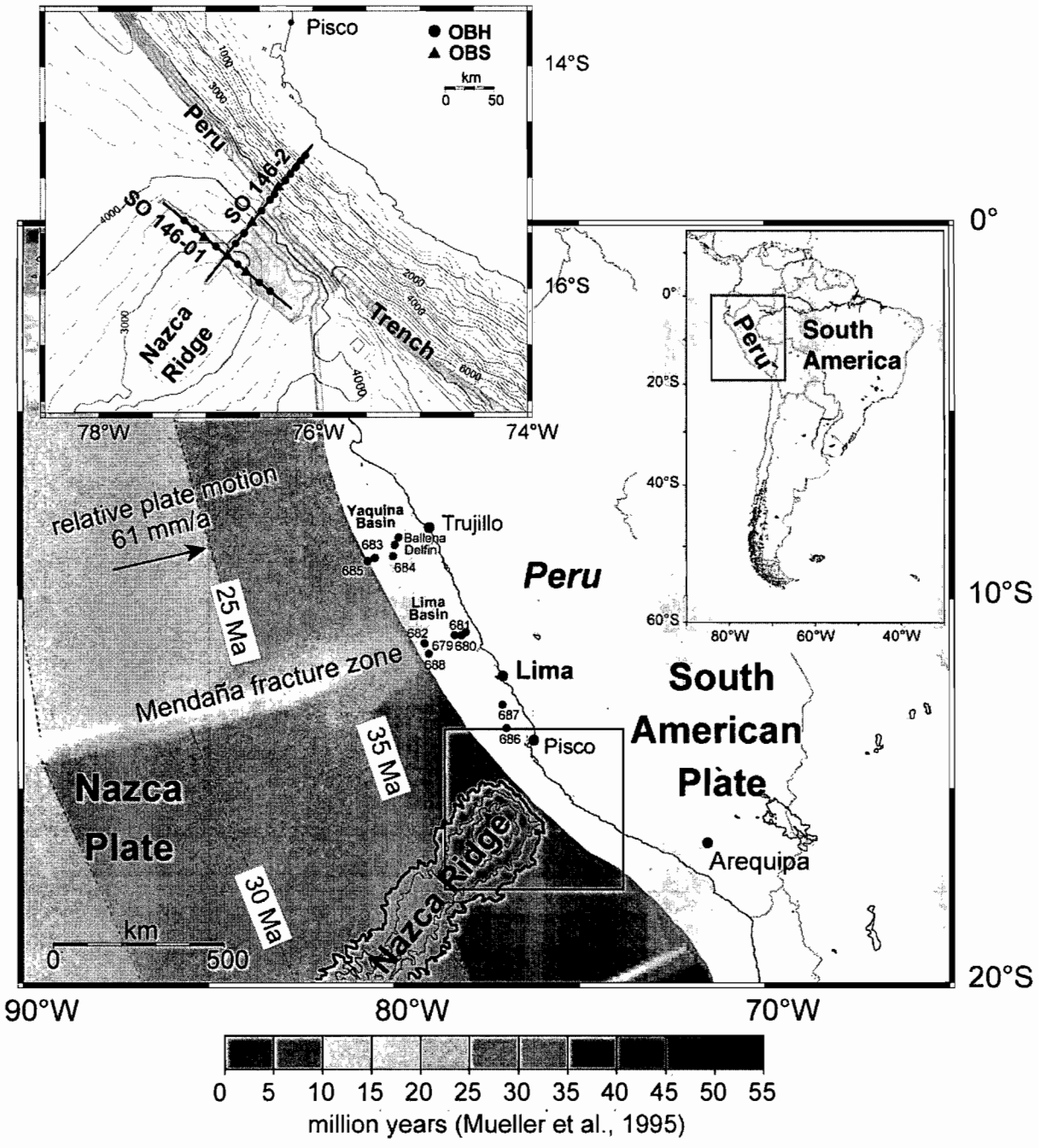

Fig.: Location map of the Peruvian margin. The working area of the SO146-GEOPECO cruise at the Nazca Ridge is marked by box (grey: area covered by multibeam bathymetry; black lines: wide-angle seismic profiles) Black circles mark drilling sites (ODP Leg 112 and two industrial wells).

For reconstructing the migration history of the Nazca Ridge, updated plate motion data (Somoza, 1998), resulting from a revision of the geomagnetic time scale (Cande and Kent, 1995), are used to construct paleo-positions of the Nazca Ridge. Due to the deceleration of the Nazca Plate motion and the variable orientation of the ridge with respect to the trench, the ridge crest moved at a significantly decreasing velocity parallel to the margin. During the 4.9-0 Ma time interval, the average lateral migration velocity of the ridge has been 4.3 cm/a. Constraining the length of the original Nazca Ridge by its conjugate feature on the Pacific Plate yields that the subduction of the ridge began ~11 Ma ago at 11°S. Therefore, the Nazca Ridge did not affect the northern sites of Ocean Drilling Program (ODP) Leg 112 located at 9°S. For the Lima Basin region at 11.5°S, the model suggests the passage of the ridge crest 9 Ma ago. The results of the model are supported by the marine and subaerial sedimentological record of the Peruvian forearc.

The results of the reconstruction of the migration history offer the possibility to compare regions that have not been affected by the ridge passage (9°S) with regions that have been (12°S) and are presently (15°S) influenced by the ridge, but otherwise have similar geodynamic boundary conditions. The data collected at different latitudes during the SO146-GEOPECO cruise enables to compare these regions of different tectonic development to better quantify the geodynamic influence of the Nazca Ridge on the Peruvian margin.

REFERENCES

Cande S.C., D.V. Kent, Revised calibration of the geomagnetic timescale for the Late Cretaceous and Cenozoic, J. Geophys. Res. 100 (1995) 6093-6095.

Hsu, J.T., Quaternary uplift of the Peruvian coast related to the subduction of the Nazca Ridge: 13.5 to 15.6 degrees south latitude, Quaternary Int. 15/16 (1992) 87-97.

Macharé, J., L. Ortlieb, Plio-Quarternary vertical motions and the subduction of the Nazca Ridge, central coast of Peru, Tectonophysics 205 (1992) 97-108.

Mueller, R.D., W.R. Roest, J.-Y. Royer, L.M. Gahagan, J.G. Sclater, Digital isochrons fo the world's ocean floor, J. Geophys. Res. 102 (1997) 3211-3214.

Somoza, R.,Updated Nazca (Farallon)- South America relative motions during the last 40 My: implications for mountain building in the central Andean region, J. South Am. Earth Sci. 11, 3 (1998) 211-215.

FORELAND BASIN SYSTEM EVOLUTION OF THE PERUVIAN ANDES: NEW INSIGHTS FROM MASS BALANCE COMPUTATION

Wilber HERMOZA(1), Patrice BABY(2), Stéphane BRUSSET(3), Frederic CHRISTOPHOUL(4), Wily GIl(5)

(1) IRD UR 104 LMTG-UMR 5563, 38 rue des 36 Ponts 31400 Toulouse-France ; hermoza@lmtg.ups-tlse.fr
(2) IRD UR 104 LMTG-UMR 5563, 38 rue des 36 Ponts 31400 Toulouse-France ; baby@cict.fr;
(3) IRD UR 104 LMTG-UMR 5563, 38 rue des 36 Ponts 31400 Toulouse-France ; brusset@cict.fr
(4) LMTG-UMR 5563, 38 rue des 36 Ponts 31400 Toulouse-France ; christop@cict.fr;
(5) LMTG-UMR 5563, 38 rue des 36 Ponts 31400 Toulouse-France ; wf_gilrodriguez@hotmail.com

KEY WORDS: Foreland Basin, Geodynamic, Mass balance, Huallaga, Marañón, Peruvian Andes.

INTRODUCTION

The Huallaga-Marañón basins are part of the NE Subandean basins of the Peruvian Andes (Fig. 1). The Huallaga basin, which is deformed by thrust-and-fold structures, represents the Subandean zone s.s. (wedge-top depozone), whereas the poorly deformed Marañón basin corresponds to the actual foredeep depozone. Wells, seismic sections and surface data of the Marañón and Huallaga basins permit to calculate the masses of sediments accumulated since the Eocene. The mass balance computations are performed using the method developed by Métivier & Gaudemer (1997), and modified by Deniaud (2000). The results of this study coupled with sedimentary and structural data allow us to reconstruct the evolution of the northern Peruvian foreland basin system from the Eocene to the Present.

GEOLOGICAL AND STRUCTURAL SETTING

The development of the eastern Andean foreland basin system started at the Late Cretaceous times in a marine environment (Barragan, 1999). The Huallaga and Marañón Subandean basins are individualized since Eocene times. They propagated eastward during the deposition of mainly continental series. In this study, we consider exclusively the Huallaga- Marañón stage of the foreland basin evolution.

In the Huallaga Basin (Fig. 2), the Eocene to Pliocene series corresponds to a prograding sequence evolving from estuarine facies to deltaic and continental facies. Reflection seismic data show that the upper part of this succession is characterized by progressive unconformities displaying the occurrence of thrust-related folding. In the Marañón basin, wells and seismic data show that the Eocene to Pliocene sedimentary fill comprises two sequences (Fig 2). The 1st sequence (Middle Eocene to Middle Miocene) developed above an erosive surface and started with the conglomerates (Lower Pozo Fm). This conglomerates have been interpreted as a consequence of orogenic unloading (Chistophoul et al., 2002; Gil, 2001). Above this conglomerates, marine argillaceous sediments have been deposited (Upper Pozo or Orteguaza Fm. of the Oriente basin) from Middle Eocene to Lower Oligocene (biostratigraphic age ROBERTSON RESEARCH, 1990). In the Oriente basin, the lateral equivalent of the Lower Pozo conglomerate have been dated (Upper Tiyuyacu Fm 46.0+0.4 My, Chistophoul et

al., 2002). The Sequence II (Upper Miocene-Pleistocene) displays a coarsening and thickening upward pattern. The basal part consists of green clays and red-grey limestones indicating a shallow marine environment, which gradually passes to continental (Fm. Pebas: Gabb, 1969; Sanchez & Romero, 2000). According to palynologic dating, the deposition occurred between the Middle Miocene and the Late Miocene (16,3-10,4 My) (Hoorn M, 1993; Sanchez & Romero, 2000).

The Huallaga and Marañón basins present different styles of deformation. The Huallaga basin or Subandean zone is deformed by thrusting, tectonic inversions and halokinesis (Baby, 1995). The Marañón basin is only affected by slight tectonic inversions of pre-Cretaceous grabens (Baby et al., 1999; Gil et al., 2000; Gil 2001).

MASS BALANCE COMPUTATION

The mass of sediments deposited since Eocene times in the Huallaga and Marañón basins is determined using isopach maps obtained from the interpretation of seismic sections, and applying the Métivier 's formula in each of its points (petroleum wells or virtual wells deduced from the seismic). The average accumulation rates are determined for Sequence I (Middle Eocene to Middle Miocene) and Sequence II (Upper Miocene to Pleistocene). In the Huallaga basin, the highest accumulation rates (30.10^7 t/My/m^2) are registered during the Middle Eocene. These rates decrease during the Upper Miocene and Pleistocene times (10.10^7 t/ My/m^2). These calculations show general decrease of the average mass accumulation rates during the Neogene (Fig. 3). In the Marañón basin, lowest accumulation rates are registered from Middle Eocene to Middle Miocene (Fig. 3), i.e. during the deposition of the Sequence I (25.10^7 t/My/m2). During the Upper Miocene and Pliocene (Sequence II), accumulation rates considerably increase and reach 110.10^7 t/My/m^2. The tectonic-sedimentary evolution of the Marañón basin is then marked by a general increase of the Neogene accumulation rates, which is the contrary to the Huallaga basin evolution.

DISCUSSION AND CONCLUSION

The Eocene-Neogene geodynamic evolution of the Peruvian Andes was recorded by two sedimentary sequences deposited in the Subandean basins. Each sequence shows an evolution of the dynamic subsidence, where the tectonic loading increases progressively.

In the Sequence I (Eocene-Middle Miocene), during the Eocene–Lower Oligocene, the Huallaga-Marañón foreland basin system experienced orogenic unloading. The marine sediments of the Lower Pozo Fm. have been deposited in a foresag depozone (*sensu* Catuneanu et al. 2000). From the Lower Oligocene to the Middle Miocene, the Marañón basin was gradually filled up by a prograding sequence. At the same period, the Huallaga basin experienced an estuarine to continental sedimentation with high accumulation rates characterizing a foredeep depozone. In the Marañón basin, the sediments accumulation rates are lower. Such small rates can be interpreted as the result of backbulge subsidence. This backbulge can be located east of the Contaya Arch.

During Upper Miocene times (base of the Sequence II), the Subandean basins are controlled by orogenic unloading, which allowed a marine transgression to reach these basins. The deposition of the Pebas Fm. occurs in near shore environments (tidal facies in the Marañón basin and deltaic facies in the Huallaga basin). After this marine incursion, the foreland basin system is again controlled by tectonic loading. As a result, the Huallaga

basin is affected by thrust-tectonics as shown by the development of growth strata overlying Miocene deposits. Sedimentation accumulation rates indicate a lower subsidence corresponding to the flexural subsidence minus the thrust related uplift. In the same period, the Marañón basin transformed in foredeep depozone with a sharp increase of the accumulation rates.

ACKNOWLEDGEMENTS : Research supported by INSU grant 99PNSE59 and IRD (Tectonique, érosion et sédimentation dans le bassin de l'Amazone : du Mio-Pliocène à l'Actuel).

REFERENCES

Baby P. 1995. Informe final convénio ORSTOM-PETROPERU, Rapport inédit, 15.

Baby P., Rivadeneira M., Christophoul F., Barragan R. 1999. Style and timing of deformation in the Oriente Basin of Ecuador, 4nd International Symposium on Andean Geodynamics (ISAG'99), Univ. Göttingen (Germany), Extended Abstracts Volume, 68-72.

Barragan R. 1999. Relations entre volcanisme, tectonique d'inversion et sédimentation dans le Bassin Crétacé équatorien Oriente. Thèse Université Paul Sabatier de Toulouse. 223 pp.

Catuneanu O. Sweet A. R. & Miall A. D. 2000. Reciprocal stratigraphy of the Campanian – Paleocene Western Interior of North America. Sedimentary Geology, 134, pp. 235-255.

Chistophoul F. Baby P. & Davila C. 2002. Stratigraphic responses to a major tectonic event in a foreland basin : the Ecuadorian Oriente Basin from Eocene to Oligocene times. Tectonophysics 345, pp. 281-298.

Deniaud Y. 2000. Enregistrements sédimentaire et structural de l'évolution géodynamique des Andes Equatoriennes au cours du Néogène: étude des bassin d'avant arc et bilans de masse. Géologie Alpine, 200, Mémoire Hors Série 32. Université Joseph Fourier, Grenoble, 157.

Gabb W. M. 1869. Descriptions of fossils from the clay deposits of the Upper Amazon. American Journal of Conchyology, 4, 197-200.

Gil W. 2001. Evolution latérale de la déformation d'un front orogénique: Exemple des bassins subandins entre 0° et 16°S. Thèse de doctorat de l'Université Paul Sabatier Toulouse III, 150.

Gil W., Baby P. & Rivadeneira M. 2000. Estilo tectónico e histórico de la deformación de las cuencas Marañón y Oriente. Ximo Congreso Peruano de Geología. Lima, 4.

Hoorn M. C. 1993. Geología del Nororiente de la Amazonia Peruana : La Formación Pebas. En : Amazonía Peruana-Vegetación humeda tropical en el llano subandino. Proyecto Amazonia Universidad de Turku (PAUT) y ONERN, Jyväskylä, 69-85.

Métivier F., Gaudemer Y. 1997. Mass transfer between eastern Tien Shan and adjacent basins : Constraints on regional tectonics and topography. Geophysical Journal International, 128, 1-18.

ROBERTSON RESEARCH 1990. Palynological zonation. Inf. inédito Petroperu Robertson Research.

Sanchez A. et Romero D. 2000. Sedimentologia y paleogeografia de la Formacion Pebas (Mioceno medio a Superior), del nororiente peruano (región Loreto). X Congreso de Geología, Lima, 11.

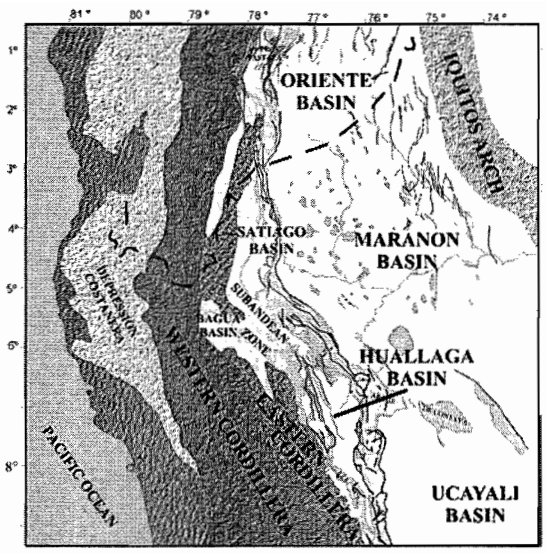

Fig. 1: Sketch map showing the Andean Foreland Basin System of Northern Peru.

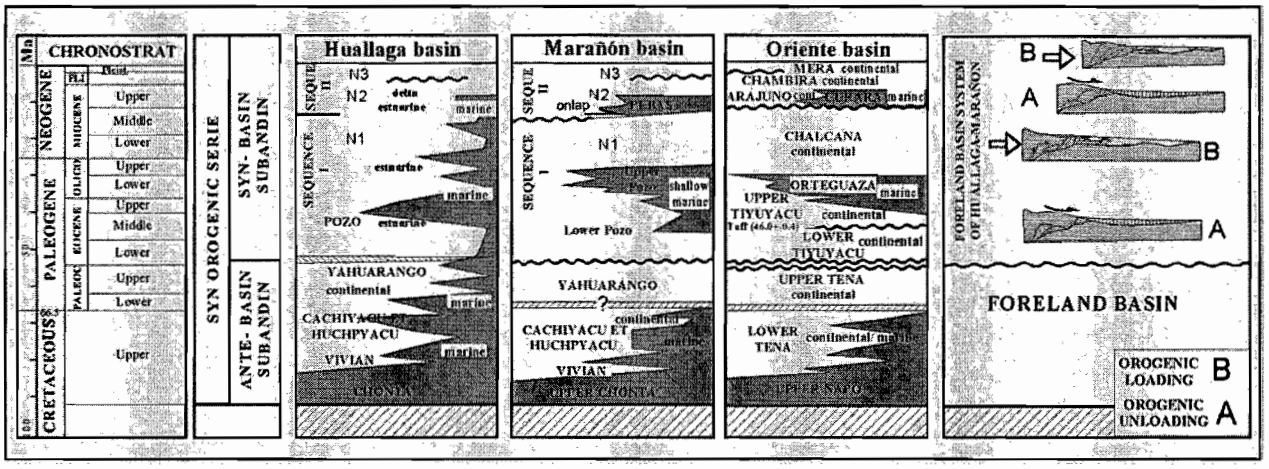

Fig. 2: Stratigraphic correlation chart between different basins in Northern Peru

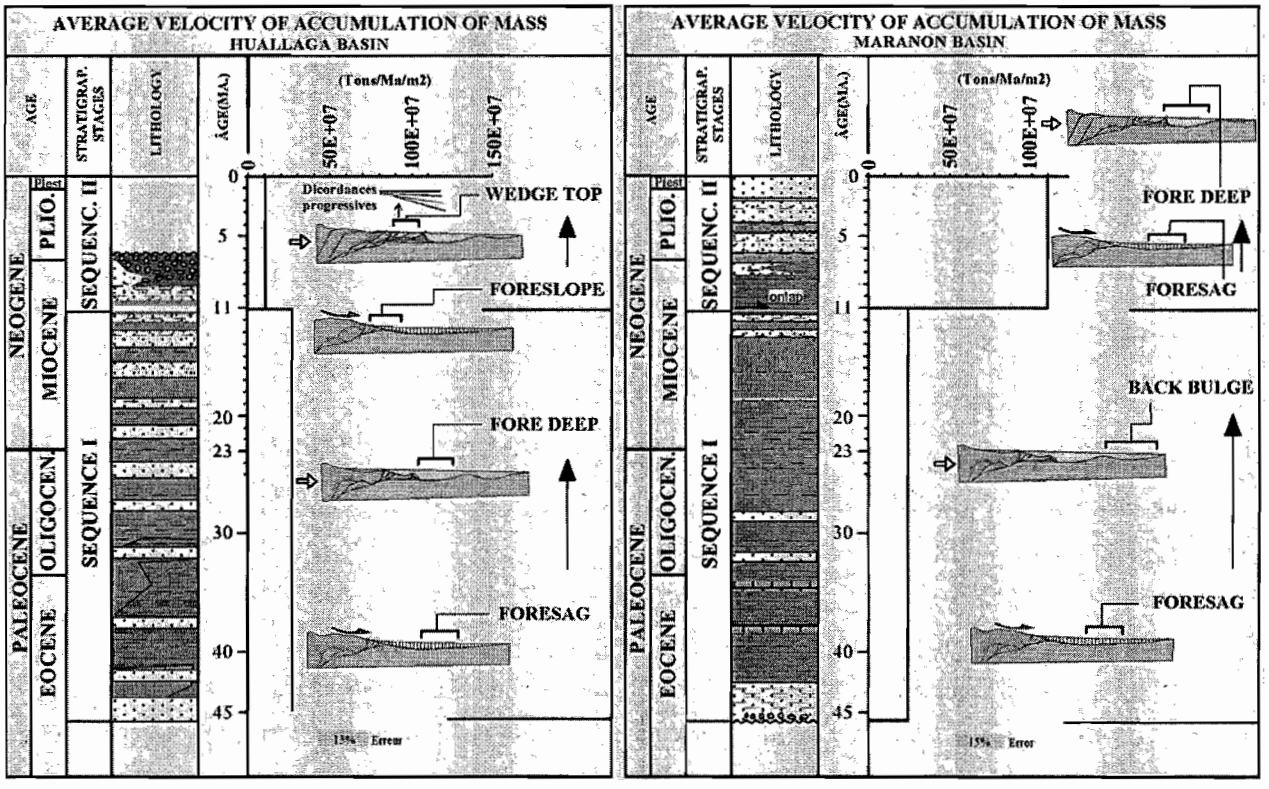

Fig. 3: Geodynamic and sedimentary accumulation rates evolution during Eocene to Pleistocene.

LOW-GRADE EARLY PERMIAN (?) METASEDIMENTARY COMPLEXES AT THE WESTERN ENTRANCE OF THE STRAIT OF MAGELLAN, SOUTHERN CHILE

Francisco HERVE (1), John BRADSHAW (2), Robert J. PANKHURST(3)

(1) Departamento de Geología, Universidad de Chile, Casilla 13418, Correo 21, Santiago, Chile .
e-mail : fherve@cec.uchile.cl
(2) Geology Department, University of Canterbury, Christchurch, New Zealand
e-mail : j.bradshaw@geol.canterbury.ac.nz
(3) British Antarctic Survey, c/o NERC Isotope Geosciences Laboratory, Keyworth, Nottingham, UK
e-mail: rjpt@bas.ac.uk

KEY WORDS: chert, psammite, pelite, accretionary complex, Late Paleozoic

INTRODUCTION

The accretionary complexes of the Pacific margin of southern Chile (Aysén and Magallanes), have different lithologies, and sedimentary and metamorphic ages. The Chonos Metamorphic Complex in Aysén has a Late Triassic age. The Tarlton Limestone and the Denaro Complex of the Madre de Dios accretionary complex have Late Carboniferous to Early Permian depositional ages. The Duque de York complex has a late Early Permian maximum depositional age. On the other hand, the age of the metamorphism appears to have been uniformly Late Triassic to Early Jurassic according to fission track dating (Thompson & Hervé, submitted). The Diego de Almagro Metamorphic Complex includes rocks of Late Jurassic age, as is apparently also the case for the Diego Ramírez islands.

We present here some field data on very remote islands where largely unknown low-grade metasedimentary complexes crop out. This is the case of Isla Desolación, which extends for 100 km to form the southern shore at the western entrance of the Strait of Magellan (SM), and islas Ramírez and Contreras, immediately north of the SM. To our knowledge, no previous account of the geological constitution of Isla Desolación has been published ever, and islas Ramírez and Contreras have been only briefly described (see below). The purpose of this presentation is to describe the rocks of these areas, and to compare them with the other units previously described in the region. The lack of age determinations, at this stage of our research, means that our conclusions are partly speculative.

Field Geology

Isla Desolación

The bedded nature of the rocks underlying the western part of Isla Desolación is very distinctive when approaching the island from the north on a sunny day, although this is possibly why it has never been described before! There are conspicuous rock bodies with red and white strata within predominant grey metasediments. A ca. 200 m vertical

section of these rocks was studied at Bahía Vio, in the northwestern part of the island, where red rocks reach the shore line.

In this section, the predominant rock types are massive sandstones in beds up to 10 m thick, with interbeds of thin fine sandstone and mudstone in which cleavage is developed. Graded bedding, ripple cross lamination and truncated convolutions are well preserved in thin ABC and BC turbidites. The red rocks (ca.30m) comprise thinly bedded chert, some with visible radiolarian fossils. At the top and botthom there are white and grey cherts interbedded with mudstone. On a large scale the red chert forms macroboudins across the north face of the mountains, the bodies of red chert being connected to each other by thinner bands of the white chert. In detail, the cherts are stratified on a 1–5 cm scale, and show abundant isoclinal folds of decimetric dimensions, which are not observed in the surrounding sandstones. The pattern of hinge closures strongly suggests sheath folds. The axial plains are roughly parallel to the main trend of the chert band, which is roughly NW to WNW with steep dip to the SW.

The studied succession is mostly in normal stratigraphic position, but is inverted immediately below the cherts. This relationship suggests the existence of an overturned asymmetric fold of regional dimensions. Bedding-parallel thrust planes probably separate the overturned limb from the adjacent upright parts of the succession. Undeformed andesitic dykes, 3 to 8 meters thick, cut across the structure.

The outcrops of the low-grade metasedimentary rocks are limited to the east by intrusions of the South Patagonian Batholith, which have been dated locally at 49 Ma (Weaver et al, 1990).

Islas Contreras and Ramírez

Cecioni (1955) was the first to describe the presence of a succession of fine-grained, thinly laminated psammites and pelites in this area. The succession observed at Seno Vargas is mainly composed of sandstones and pelites, with a low grade of metamorphism. The presence of worm ichnites and sedimentary structures, showed that some parts of the succession are overturned. The main trend of the stratification planes is NW-SE, and the structure is characterized by the presence of numerous overturned metre-scale isoclinal folds with development of axial plane cleavage. Cherts were only recognized as small bodies in the contact aureole against the western margin of the South Patagonian Batholith, which delimits outcrops to the east.

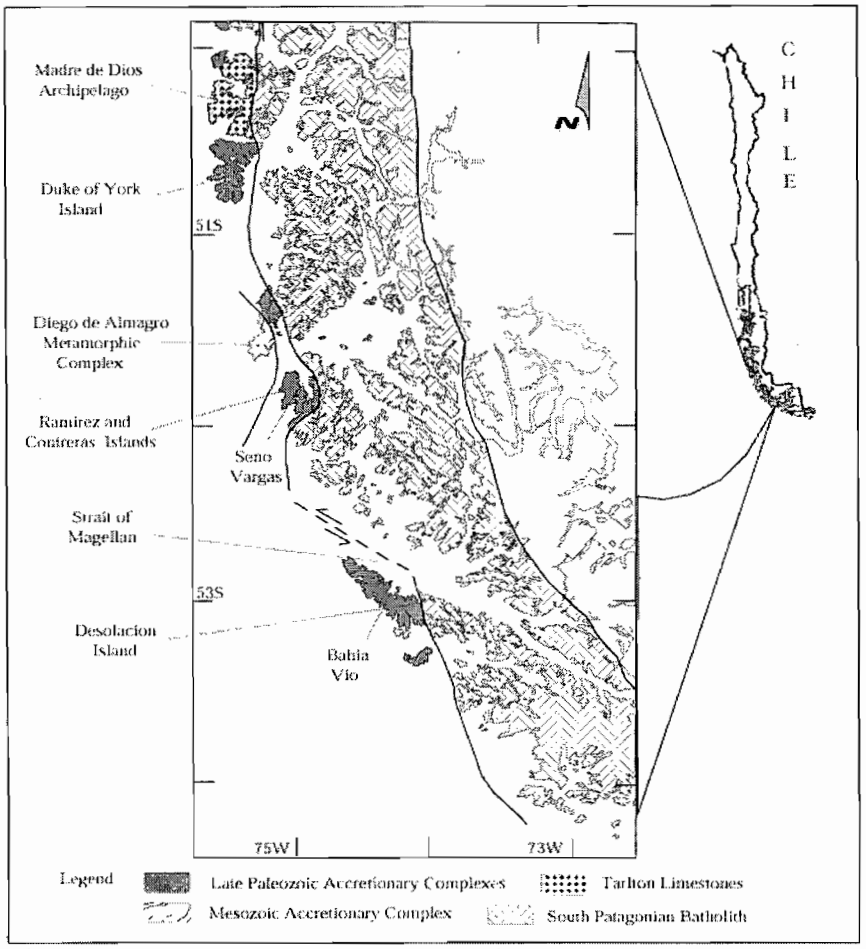

Figure 1. Sketch map showing the distribution of the accretionary complexes and the South Patagonian Batholith

Discussion and Conclusions

The rocks exposed at islas Ramírez, Contreras and Desolación exhibit similarities in lithologies, in structure, and in their low-grade metamorphism. They are very probably part of the accretionary complexes which form the westernmost exposed rocks of the archipelagos of Aysén and Magallanes between the Strait of Magellan and the Chonos archipelago. On lithological grounds, a tentative correlation can be made with the Duque de York complex (DYC), a unit made up of alternating sandstone and mudstone with subsidiary conglomerate beds, and minor greenschists, which locally is seen to be deposited over a palaeokarst surface in the latest Carboniferous – Early Permian Tarlton limestone. Forsythe & Mpodozis (1979) suggest that the DYC was deposited near the continental margin of Gondwana when the exotic Denaro and Tarlton units approached that margin.

The succession studied at Desolación Island, contains red radiolarian cherts associated with the turbidites. This feature may indicate that the rocks here were deposited farther away from the continental influences than the DYC in its type locality, 200 km to the north. South of Isla Desolación, Ling and Forsythe (1987) have described the presence of Early Permian radiolaria in red cherts at Isla Recalada, but give no information of the geological context of the sampled rocks, except that they are highly deformed, thus hampering establishment of their stratigraphical relationships. It is possible, as a preliminary conclusion, to consider the succession at Isla Desolación to be of the

same age. If these correlations are correct, they would form part of a ~300 km long semi-continuous belt of Early Permian detrital rocks, with minor intercalations of chert and basic rocks, extending from the area of Madre de Dios archipelago to Isla Recalada. This unit is flanked to the west by the Jurassic blueschist-bearing Diego de Almagro and Diego Ramírez complexes, that represent more deeply buried (and at present the westernmost) components of the subduction complex of southern Chile. The apparent left lateral displacement of ca. 40 km of the western margin of the South Patagonian Batholith along the Strait of Magellan needs to be supported by dating of the rocks and observation of the metasediment-batholith contact in Isla Desolación.

ACKNOWLEDGEMENTS

The research is funded by FONDECYT Grant 1010412. This is a contribution to IGCP Project 436 "The Ancestral Pacific Gondwana Margin" and to the BMBF-CONICYT Project "HighPressure Metamorphism in Southern Chile". Captain Conrado Alvarez and crew took us safely to these remote regions in his yacht "Penguin". M. Calderón helped with the figure, and together with V.Faundez, J. Cembrano, S. Thomson, H. Massone , C. Augustsson & H. Bahlburg participated in part of the field work.

REFERENCES

Cecioni, G. (1956). Primeras noticias sobre la existencia del Paleozoico Superior en el Archipiélago Patagónico entre los 50^0 y los 52^0 S. Universidad de Chile, Facultad de Ciencias Físicas y Matemáticas , Anales, 13, 183-202, Santiago.

Forsythe, R.D. & Mpodozis, C. (1979). El archipiélago Madre de Dios, Patagonia Occidental, Magallanes: rasgos generales de la estratigrafía y estructura del basamento pre-jurásico Superior. Revista Geológica de Chile, 7, 13-29.

Ling, H.Y. & Forsythe, R.D. (1987). Late Paleozoic pseudoalbeillellid radiolarians from Southernmost Chile and their geological significance. In: Mackenzie,G.D. (ed.), Gondwana Six: Structure, Tectonics and Geophysics, AGU Geophysical Monograph, Washington, 40, 253 – 260.

Thomson, S & Hervé, F. (submitted) Integration of detrital zircon fission-track and U-Pb SHRIMP ages to better estimate the timing of deposition, metamorphism and later reheating of metamorphic basement complexes at the ancestral Pacific Gondwana margin of southern Chile (42°S-52°S). Revista Geológica de Chile.

Weaver, S.G., Bruce, R., Nelson, E., Brueckner, H.K & LeHuray, A.P. (1990). The Patagonian batholith at 48°S latitude, Chile: Geochemical and isotopic variations. In Kay, S.M. and Rapela, C.W. (eds.), Plutonism from Antarctica to Alaska, Boulder, Colorado. Geological Society of America Special Paper, 241, 33-50.

THE TIPA SHEAR ZONE (NW-ARGENTINA): ISOTOPIC DATING AND GEOCHEMICAL PROCESSES

Martin HÖCKENREINER (1), Frank SÖLLNER (2) and Hubert MILLER (3)

(1) Department für Geo- und Umweltwissenschaften (Department of Geo- and Environmental Science)
Lehrstuhl für Allgemeine und Angewandte Geologie, Luisenstr. 37, D-80333 München, Germany
marthock@iaag.geo.uni-muenchen.de
(2) see above; frank.soellner@iaag.geo.uni-muenchen.de
(3) see above; hubert.miller@iaag.geo.uni-muenchen.de

KEY WORDS: shear zones, geochronology, geochemistry, deformation, NW-Argentina, Famatina

INTRODUCTION

Absolute age determination of a deformational event is often difficult. It needs to be verified that complete isotopic (re-) homogenisation in minerals used for dating took place during deformation and below or subsequently to passing their corresponding closure temperature. Otherwise, the obtained ages will only represent the cooling of the system. Furthermore, mixing with an older, incompletely homogenised component should be considered additionally. It is assumed that due to intracrystalline processes like grain boundary migration, diffusion in mylonites is orders of magnitudes faster (GROMET, 1991) and thus, deformation should reduce the corresponding closure temperature. A decrease of the closure temperature can also be achieved by fluid-assisted recrystallisation during ductile deformation (VILLA, 1998). Also, new mineral growth can take place in shear zones due to migration of huge quantities of fluids/melts mobilised from deeper crustal levels. This mineral growth may happen below the corresponding closure temperature.

In the present paper, we focus on the TIPA shear zone (LOPEZ & TOSELLI, 1993) in NW Argentina. The shear zone mainly crosscuts granitic rocks which were formed during the Ordovician Famatinian orogeny. In the studied area near Tinogasta (Catamarca province) the granitic protoliths do not contain any garnet whereas the granitic mylonites often contain plentiful garnet. This indicates that garnet growth is cogenetic with deformation and thus, dating of this mineral will provide the age of this process.

Furthermore, the mylonites are geochemically different from their parent rocks. As pegmatoid veins are almost exclusively bound to the shear zone, we correlate this change in geochemistry with a mechanical mixing and homogenisation of the mobilised pegmatoid melts with the precursor rocks during shearing.

GEOLOGICAL SETTING

The TIPA shear zone separates two major geotectonic units. East of the shear zone a metasedimentary sequence is developed which is thought to represent part of the Pampean System (Los Ratones formation, NEUGEBAUER & MILLER, 1993). West of the shear zone a mostly volcano-sedimentary sequence built on continental crust occurs (Famatina system). Between these two units sediments of a back-arc basin are found which was squeezed between these two units during the Famatinian orogeny (Las Termas belt, SÖLLNER et al., 2001). Due to the intrusion of large quantities of granitoids during the Famatinian orogeny, the border between these two units is smudged. Granitoids of that orogeny can be observed westward in the Famatina system as well

as in the Sa. de Mazán in the East (Pampean system; see Fig. 1). These granitoids date around 495 to 465 Ma (e.g. SÖLLNER et al., 2001, PANKHURST et al., 2001).

The TIPA shear zone mainly crosscuts these granitoids. It is the prominent one of at least four larger subparallel mylonite zones which strike NNW-SSE and are steeply dipping to the East. Kinematic indicators point to an ENE-WSW directed compression with the Pampean ranges being thrusted onto the series of the Famatina system. Temperatures during deformation are estimated to be in the order of 500 to 550 °C as inferred from the ductile behaviour of minerals like feldspar. Tectonic activity ceased in Carboniferous times as indicated by post-deformational granitoids which date around 335 Ma (U-Pb on Zircon, GRISSOM et al., 1998). Hence, data of the geological frame constrain the age of mylonitisation between 465 and 335 Ma.

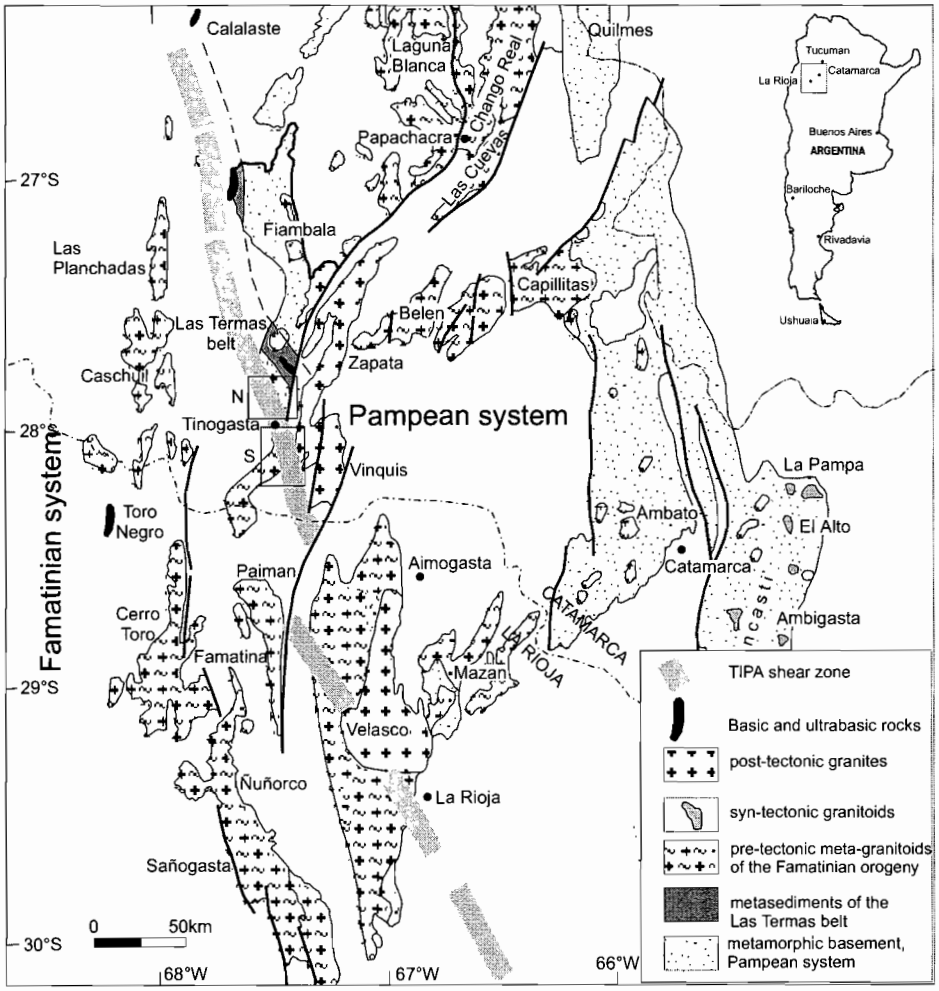

Figure 1: Geographical position of the studied areas (rectangles) and the TIPA shear zone in general. Modified after Ramos (2000).

GEOCHEMISTRY

The meta-granodiorites (HUE1 and FLO2) are homogeneous in chemical composition, furthermore, a sample from the Sa. de Paimán, 80 km to the south, yielded identical geochemical data and thus granitoids seem to be very homogeneous over a large area. The mylonites (PUN4 and KAP) are geochemically also very similar. Almost all element concentrations of a protomylonite (PUN6) figure between these two groups. REE patterns of the mylonitic samples show a rather flat pattern in comparison to that of the undeformed samples. PUN6 (protomylonite) again plots between these two groups (Fig. 2). Mylonites show enrichment in Si and K, whereas

element concentrations of Fe, Mg, Ti, V, Ca, Ga, Sr, Zr, Hf, Ba, REE and Nb are well below in the mylonitic rocks. We guess, the chemical composition of the pegmatoids (PUN1) is similar to that of the fluid/melt composition pouring through the rocks during deformation and thus, mylonites can be seen as a mixture of the granodioritic protolith and the syntectonic pegmatoids. In fact, many element concentrations (including LREE, Zr, Hf, V, Sr, Ti, Fe, K, ± Si) of the mylonites coincide with a calculated mixture of three parts PUN1-pegmatoid and one part of the protolith. A possible explanation for this observation could be that large amounts of pegmatoid melt were mobilised in deeper crustal regions and mechanically mixed with the protoliths during mylonitisation. Depletion of the REE content in the mylonitic rocks in the order of 70% is better explained by dilution than by fluid/rock interaction (PUN1 is depleted in REE and many trace elements in comparison to the protoliths HUE1 and FLO2).

In the field, C-parallel elongated bodies with nearly absence of biotite and a higher enrichment in K-feldspar may represent those older pegmatoid veins mixed up with the host rock to such an extend that their identification happens only due to their deviating mineralogy. In support of our idea the mobilised pegmatoid melts ascended almost exclusively in the mylonitic zone.

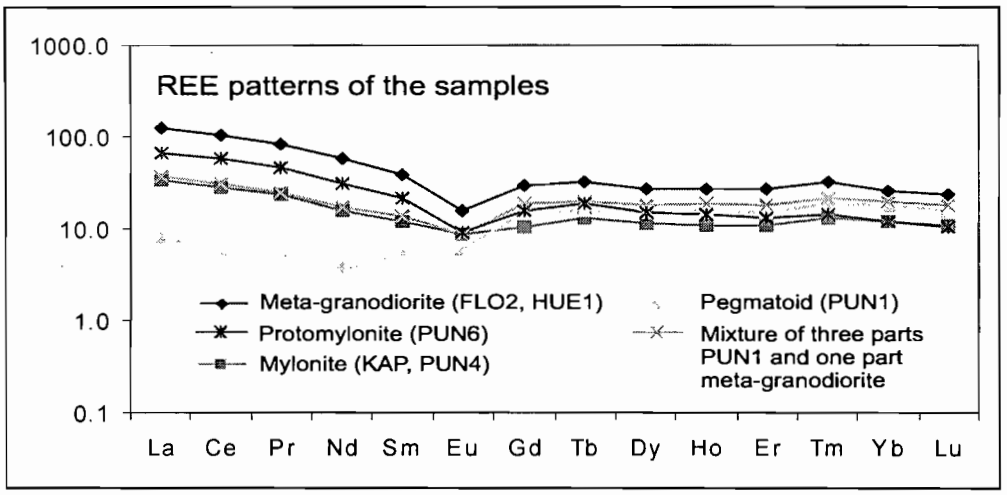

Figure 2: Chondrite-normalized REE patterns of meta-granodiorite (mean of samples FLO2 and HUE1, protoliths of the mylonites), protomylonite (PUN6), mylonite (mean of samples KAP and PUN4) and pegmatoid (PUN1). The LREE pattern of a calculated mixture of three parts pegmatoid and one part meta-granodiorite is equal to the pattern of the mylonite.

GEOCHRONOLOGY

Sample	Rock type	WR-grt age Ma	2 σ Ma	$^{143}Nd/^{144}Nd$ init.	2 σ	Nd model age Ga	ε (t)
KAP	mylonite	416.5	3.3	0.511788	0.000010	1.61	-5.8 (470 Ma)
PUN4	mylonite	435	14	0.511777	0.000019	1.60	-5.7 (470 Ma)
PUN6	proto-mylonite	412.7	5.2	0.511793	0.000012	1.60	-5.7 (470 Ma)
PUN1	pegmatoid	408.5	2.6	0.511732	0.000054	1.68	-7.4 (405 Ma)
		Garnet isochron age					
All garnets without WR		403.4	1.2	0.511849	0.000011		

Table 1: Isotopic Sm-Nd garnet and whole rock analyses

Garnets are completely absent in the heavy mineral fraction of the undeformed samples HUE1 and FLO2. Protomylonite PUN6 contains only about 120 mg of garnets on a 6 kg sample, whereas the rocks within the

shear zone (PUN4, KAP, PUN1) have plenty of garnets (up to 5 g and more) indicating a direct correlation between deformation, fluid/melt activity and garnet growth. The whole rock-garnet ages point to a single garnet-growth event. However, the ages are not identical within limits of error (Table 1). The main reason, we think may result from missing of total homogenisation of Nd-isotopes within the whole rock system. There has been no complete exchange of Nd-isotopes between new grown mineral phases and those, who recrystallised during deformation. A distinct lower Nd-initial ratio in mylonites than in new grown garnets as observed, would result in a too high inclination of the isochron and therefore, in an older apparent age.

In respect, that the garnets grew at a single event under support of a fluid/melt providing most of the elements, a better appraisal of the time of deformation should be obtained by excluding the factors of possible isotopic disequilibration (whole rock). This model also excludes later isotopic disturbance due to possible open system behaviour of other minerals.

The resulting four-point garnet isochron is well defined with a MSWD of 0.19. This clearly confirms our interpretation. Hence, all garnets are cogenetic and crystallized during mylonitisation at 403.4 ± 1.2 Ma (Early Devonian). The $^{143}Nd/^{144}Nd$-initial ratio of the garnet isochron is significantly higher than the initials of each garnet-whole rock isochron. This implies that garnet isotopic composition is additionally controlled by other factors than the isotopic composition of the parent rock.

CONCLUSIONS

Within the working area, for the first time major thrust tectonics were successfully dated. Garnets grew due to high fluid/melt activity within the shear zone. The higher Nd initial ratios in garnets in comparison with the whole rocks argue for an origin of the melts/fluids from older and deeper crustal levels. These melts were mechanically mixed and homogenised with the protoliths within the shear zone during deformation (403.4 ± 1.2 Ma) as indicated by model calculations on REE patterns and major and trace elements. The age of deformation along the TIPA shear zone agrees well with overthrust movement of the Sierras Pampeanas onto the rocks of the Famatina system due to crustal shortening in connection with continuing subduction on the western border of Gondwana. A possible terrane/continent collision during that time cannot be excluded.

REFERENCES (alphabetical order):

Grissom G., Debari S. M., Snee L., 1998. Geology of the Sierra de Fiambalá, northwestern Argentina: implications for Early Palaeozoic Andean tectonics.- in: Pankhurst, R. J., Rapela C. W. (eds.): The proto-Andean margin of Gondwana. Geological Society (London) Special Publication 142, pp 297-323.

Gromet P., 1991. Direct dating of deformational Fabrics.- in: Heamann L., Ludden J. N. (eds.): Applications of radiogenic isotope systems to problems in geology; Short Course Handbook 19, pp. 167-189.

López J. P., Toselli A. J., 1993. La faja milonítica TIPA: Faldeo oriental del Sistema de Famatina. 12° Congreso Geológico Argentino y 2° Congreso de Exploración de Hidrocarburos, Actas 3: 39-42.

Neugebauer H., Miller H., 1993. Las milonitas de la Sierra de Fiambalá: Sutura oriental del Sistema de Famatina (Pcia. De Catamarca, Argentina).- XII Congreso Geológico Argentino, II Congreso de Exploración de Hidrocarburos, Actas III: 34-38; Mendoza.

Pankhurst R. J.; Rapela C. W., Fanning C. M., 2001. Age and origin of coeval TTG, I- and S-type granites in the Famatinian Belt of NW Argentina.- Geol. Soc. America, Special Paper 350, pp. 151-168.

Ramos V. A., 2000. The Southern Central Andes. In: Cordani U. G., Milani E. J., Thomaz Filho A., Campos D. A. (Eds.), Tectonic evolution of South America, 561-604, Rio de Janeiro.

Söllner F., Höckenreiner M., Miller H., 2001. Constraints on the ages of Famatinian igneous intrusions and subsequent deformation in the Sierra de Fiambalá (Catamarca/NW-Argentina).- Comunicaciones 52, p. 167, Santiago.

Villa I. M., 1997. Isotopic closure.- Terra Nova 10/1, 42-47.

A GROUNDWATER GENESIS FOR THE GIANT QUEBRADAS OF THE ATACAMA DESERT, NORTHERN CHILE

Gregory D. HOKE (1), Teresa E. JORDAN (2), and Bryan L. ISACKS (3)

(1) Dept. of Earth and Atmospheric Sciences, Cornell University, Ithaca, NY, 14853 USA, (gdh7@cornell.edu)
(2) Dept. of Earth and Atmospheric Sciences, Cornell University, Ithaca, NY, 14853 USA, (tej1@cornell.edu)
(3) INSTOC, Cornell University, Ithaca, NY, 14853 USA, (bli1@cornell.edu)

Keywords: Geomorphology, Drainage networks, Groundwater, Spring Sapping, Neogene

INTRODUCTION

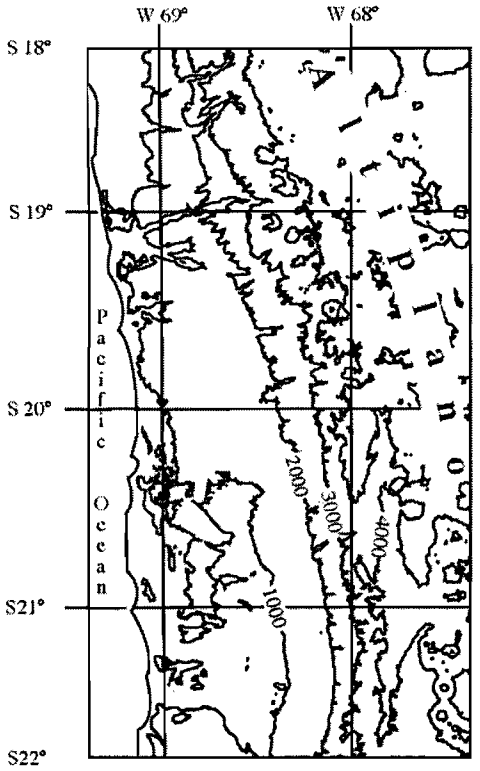

Figure 1. Map of the central Andes Illustrating the relatively uniform and simple topography of the western slope. Nicks in the 2000 and 3000 meters contours are largely from the incision of drainages. The deeply incised quebrada de Camarones is visible just south of 19°

The western slope of the central Andes between 18° and 22° S is a remarkably simple large-scale landform. The simplicity of this landform can in part be related to persistently arid conditions since the middle Miocene. Two very different drainage patterns coexist with one another on the western slope: (1) a wide valley, deeply incised network and (2) a narrow valley, shallowly incised network of parallel to sub-parallel channels. The deeply incised, wide valley drainages (Quebradas) of northernmost Chile, between 19° 30' and 18° S, are an anomalous features in the otherwise uniform landscape of the western slope (Figure 1). Explanation of these deeply incised quebradas requires water in excess of the local precipitation, while the shallowly incised, parallel channels may result from local precipitation. Comparison of this region of Chile with studies in Hawaii, USA, suggests that groundwater has been the dominant influence on the formation of these deeply incised quebradas.

METHODS

All observations presented here were made remotely using digital elevation models (DEMs) (90 m or 20 m pixel resolution), Advanced Spaceborne Thermal Emission and Reflection Radiometer (ASTER) imagery (15 m pixel resolution) and Landsat Thematic Mapper (TM) imagery (30 m pixel resolution). Drainage network data were extracted from digital topography using RSI's Rivertools software and validated with TM and ASTER imagery.

CLIMATE

The study area lies in the heart of the modern day, hyper-arid Atacama Desert. The onset of Aridity in the region is postulated to have begun at some point during the Miocene (Alpers and Brimhall, 1991) with hyper-aridity becoming stable in the Pliocene (Hartley and Chong 2002). Recent work has detected climate variations at frequencies of millions of years, tens of thousands of years and thousands of years (Rech, 2002; Latorre, 2002). However it is reasonable to assume that since the Middle Miocene, past climates never became more humid than semi-arid in this region (Alpers and Brimhall, 1991; Hartley and Chong 2002).

GEOLOGY/GEOMORPHOLOGY

The western slope of the central Andes between 22°S and 18°S is a simple, uniform surface which has been subject to relatively minor amounts of incision. The regional slope is paralleled by a thin veneer of Miocene to recent strata which lie unconformably over Mesozoic age basement (Isacks, 1988). Two styles of drainage patterns, dendritic and parallel to sub-parallel, are readily identifiable and are developed throughout the western slope. We focus on the region from 18° to 20° capped by the Oxaya ignimbrite because of its relative simplicity. The Oxaya ignimbrite is a 19 Ma, large-volume ignimbrite flow which is a convenient marker, because it formed as an initially low-relief surface of known age and uniform composition. Because both types of drainage networks extend beyond the extents of the Oxaya ignimbrite between 22°S and 18°S we assume that the influence of any pervasive jointing in the ignimbrite does not exact a strong control on drainage network development.

Shallowly incised, Parallel to sub-parallel drainage patterns dominate the western slope of the central Andes and are well developed and easily observed in the ignimbrite covered area (Wörner et al., 2002). The development of parallel drainage networks is common in young, steep landscapes (Ritter, 1995). Experimental studies on initially flat surfaces have demonstrated that parallel drainage networks are the first to form on slopes $\geq 2°$ (Schumm et al., 1987). Over time the network evolves towards a progressively more dendritic pattern. The average slope of the western slope of the central Andes is on the order of 2-3° and therefore favors parallel drainage development. Rain falling directly on the slope itself is the other essential ingredient in the formation of parallel drainage networks (Ritter, 1995), which in this area, is approximately 1-10 cm/yr in the modern probably has not exceed 30 cm/yr since the middle Miocene. The small amount of local precipitation, age of the ignimbrite surface, and the geomorphic youthfulness of the drainage pattern developed on it suggests that landscape evolution in this region is extremely slow.

Dendritic drainage patterns correspond to the deeply incised drainage networks. The most extreme examples of dendritic-patterned drainage networks are found between 19°30" and 18°S. These drainages all terminate at the Pacific Ocean, crossing the waning topographic barrier of the coastal Cordillera. The approximate age of these drainages is somewhere between 11-2.7 Ma based on constraints from Mortimer, (1980) and Wörner et al. (2000). The parallel drainage networks developed on the western slope of the central Andes indicate local precipitation is far too low to be solely responsible for the formation of such deeply incised valleys. All of the valleys are similar in morphology indicating that the processes responsible for their formation are the same. Specific morphologic characteristics include: 1) Steep-walled canyons with relief between the interfluves and valley floor exceeding 1500 meters; 2) Junction angles between drainage segments ranging from 45° and 80°; (3) Segments containing areas of lateral expansion by landsliding; 4) Drainages heading in

amphitheater heads or relict amphitheater heads which are readily visible in all datasets (relatively recent capture of smaller, morphologically distinct streams high on the Altiplano tend to obscure what were once sharp amphitheater heads); and 5) the ratio of canyon area to total drainage area is high (preliminary DEM analysis of two drainage basins). Correspondingly, drainage density is low. A dendritic drainage pattern and all of the features described above are indicative of a strong spring sapping influence on the development of drainage networks (Baker et al., 1990; Howard et al.; 1988, Dunne, 1990). Dendritic patterned drainages appear to cross-cut and interrupt, not necessarily captured, the parallel drainages.

COMPARISON WITH HAWAII

Hawaiian coastal areas studied by Baker et al., (1990) are morphologically similar to the northern Chile study site with both parallel and dendritic drainage patterns present in the same area. We suggest that Hawaii is an excellent analog for the northern Chile study area because, to a first order, the dipping layers of successive generations of lava flows serve as a reasonably good approximation to the dipping strata on the western slope of the central Andes. However, the two sites differ by up to two orders of magnitude in measured rainfall (250 cm/yr vs. ~1-10 cm/yr), and valleys are much longer in Chile (120 km) than in Hawaii (5-10 km). Nevertheless, the landscapes appear very similar (Figure 2) which suggests that similar processes are acting to shape the landscape, even in such dramatically different climates. Baker et al. (1990) attributed the development of two distinct valley morphologies in Hawaii to two distinct causes of valley formation, surface runoff and spring sapping. In both northern Chile and Hawaii, runoff and near surface groundwater flow contribute to the formation of high density, parallel valleys while deeper groundwater flow, independent of the origin of the groundwater, contributes to the formation of wide, steep-walled, low drainage density valleys. In northern Chile, the only feasible source of groundwater is from the Altiplano Plateau, but in Hawaii the groundwater is most likely derived from piping of local precipitation along fractures and dikes.

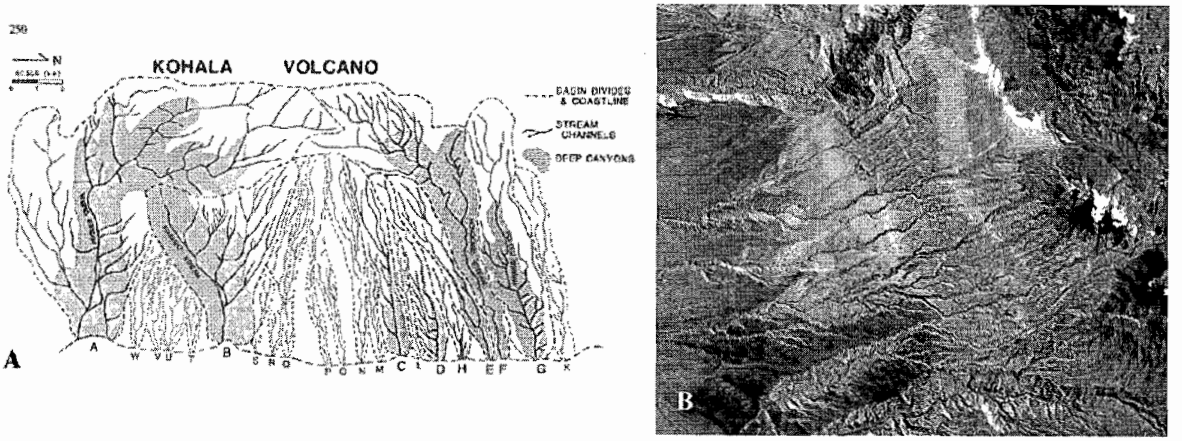

Figure 2. A) Map of the drainages coming off the flanks of the Koahala Volcano, Hawaii from Baker et al., (1990). Deep canyons (A-K) are emphasised by grey shading. B) A greyscale Landsat 5 TM (spectral bands 5,4,2) showing the drainages coming off the western slope of the central Andes. The scene is 67 km across with the upper left corner at S18° 28", W69° 59" and lower right at S18° 59", 69° 21". The drainage patterns of the two regions are comparable despite differences in scale.

CONCLUSIONS

Two morphologically distinct drainage networks have evolved independently on the western slope of the Central Andes of northern Chile: shallowly incised networks with parallel drainage pattern and deep, wide canyons with dendritic drainage pattern. Portions of the Hawaiian Islands exhibit a similar morphology for which Baker et al., (1990) demonstrated that steep-walled, low drainage density canyons result from focused groundwater sapping. We advocate the application of this model, with groundwater being supplied from the adjacent Altiplano plateau, to explain the genesis of the large quebradas in the Atacama Desert.

REFERENCES

Alpers, C.N., and Brimhall, G.H., 1988, Middle Miocene climatic change in the Atacama Desert, northern Chile: evidence from supergene mineralization at La Escondida: Geological Society American Bulletin, v. 100, p. 1640-1656.

Baker, V.R., 1990, Spring sapping and valley network development, in Higgins, C.G., and Coates, D.R., eds., Groundwater Geomorphology: the role of subsurface water in earth-surface processes and landforms: Boulder, Colorado, Geological Society of America Special Paper 252. p. 235-265.

Hartley, A.J. and Chong G., 2002, Late Pliocene age for the Atacama Desert: Implications for the desertification of western South America; Geology, v30:1 p. 43-46.

Howard A.D., and Kochel, R.C., 1988, Introduction to cuesta landforms and sapping processes on the Colorado Plateau, in Howard A.D., and Kochel, R.C. and Holt, H.E. eds, Sapping features of the Colorado Plateau, Washington D.C.: NASA, SP-491.

Isacks, B.L., 1988, Uplift of the Central Andean plateau and bending of the Bolivian orocline: Journal Geophysical Research, v. 93, p. 3211-3231.

Latorre C, Betancourt JL, Rylander K, and Quade, J, 2002, Vegitation invasions into absolute desert: A 45,000 yr rodent midden record from the Calama-Salar de Atacama basins, Norther Chile: Geological Society of America Bulletin, vol. 114:3, p349-366.

Mortimer, C., 1980, Drainage evolution in the Atacama Desert of northernmost Chile: Revista Geológica de Chile, v. 11, p. 3-28.

Ritter D.F, Kochel, R.C. and Miller J.R., 1995, Process Geomorphology: Boston, William C. Brown, 546 pp.

Rech, J.A., Quade, J., and Betancourt, J.L., 2002, Late Quaternary paleohydrology of the Central Atacama Desert, (lat 22°-24°), Chile: Geological Society of America Bulletin, vol. 114:3, p334-348.

Schumm S.A., Mosley M.P., and Weaver, W.E., 1987, Experimental Fluvial Geomorphology: New York, Wiley and Sons, 413 p.

Wörner, G, Uhlig, G., Kohler, I., and Seyfried, H., 2002, Evolution of the West Andean Escarpment at 18°S (N. Chile) during the last 25 Ma: uplift, erosion and collapse through time: Tectonophysics, vol. 345:1-4 p.183-198

Wörner, G., Hammerschmidt, K., Henjes-Kunst, F., Lezaun, J., Wilke, H 2000. Geochronology (40Ar/39Ar, K-Ar and He exposure ages) of Cenozoic magmatic rocks from northern Chile (18-22°S): implications for magmatism and tectonic evolution of the central Andes, Revista de Geologia de Chile, v27:2 p205-240

ALTIPLANO UPLIFT FROM GRAVITY DRIVEN CHANNEL FLOW

Laurent HUSSON (1) and Thierry SEMPERE (1)

(1) I.R.D.-Perú, La Mariscala 115, Lima 27 ; apartado postal 18-1209, Lima 18, Peru (laurent.husson@ens-lyon.fr, sempere@terra.com.pe)

KEY WORDS: Altiplano, uplift, channel-flow, strain, mid-lower crust, rheology

INTRODUCTION

The discrepancies between several observations and a homogeneous crustal deformation in convergence zones led numerous authors in the last decade to propose alternative models. Bird (1991) showed from an analytical approach that a temperature dependent rheology implied that a low resistance zone prevails at the base of thickened crusts. The lateral variations in crustal thickness induce stress gradients on this low viscosity zone, which in turn can easily be driven from thickened, high stress zones towards lowlands where gravity stresses are lower.

In the Central Andes, the measured shortening of the upper crust does not show much correlation with crustal thickness (e.g. Kley & Monaldi, 1998; Rochat et al., 1999). The very thick crust is however globally related to its elevated thermal regime (e.g. Springer, 1999). As a consequence, the crust matches the conditions required for a low viscosity and a mid-lower crustal flow.

In this paper, we adapt a gravity driven channel flow model to explain the uplift of the Altiplano and explain the mismatch between upper crust deformation and crustal thickness.

GEODYNAMIC EVOLUTION OF THE CENTRAL ANDES

Although the Central Andes beneficiated from numerous studies in the last decades, the Altiplano area remains widely misunderstood. The uplift history is however now fairly well constrained (Kennan, 2000; Gregory-Wodzicki, 2000) and provides useful data in the comprehension of the Andean history. The Western Cordillera initiated its surrection 60 Ma ago and was followed by the more gentle uplift of the Eastern Cordillera. This former stage lasted until 30-40 Ma BP as the Western and Eastern Cordilleras reached elevations of about 1000 m and 2000 m respectively. Eventually, the rapid uplift of both Cordilleras increased from 20 Ma BP until now, leading to very high elevations (more than 4000 m on average). The Altiplano *sensu stricto*, in between these two Cordilleras, mainly uplifted during the last 20-10 Ma.

The formation of the Eastern Cordillera and subsequent crustal thickening can be easily explained by a considerable stacking of crustal slices. We emphasize that the *in situ* crustal thickening of the Western Cordillera is often under-evaluated, as the Late-Cretaceous-Paleogene deformation was certainly more intense in the western part of the Andes than generally mentioned; magmatism and other processes (which are not dicussed herein) also contributed to crustal growth. On the other hand, the upper crustal structure of the Altiplano does not indicate any significant shortening in this area (e.g. Rochat et al., 1999). Its high crustal thickness (up to 60-70 km, Beck et al., 1996) is hence to be explained invoking other mechanisms. Fig. 1 illustrates the mismatch between upper crustal shortening and crustal thickness in the Central Andes.

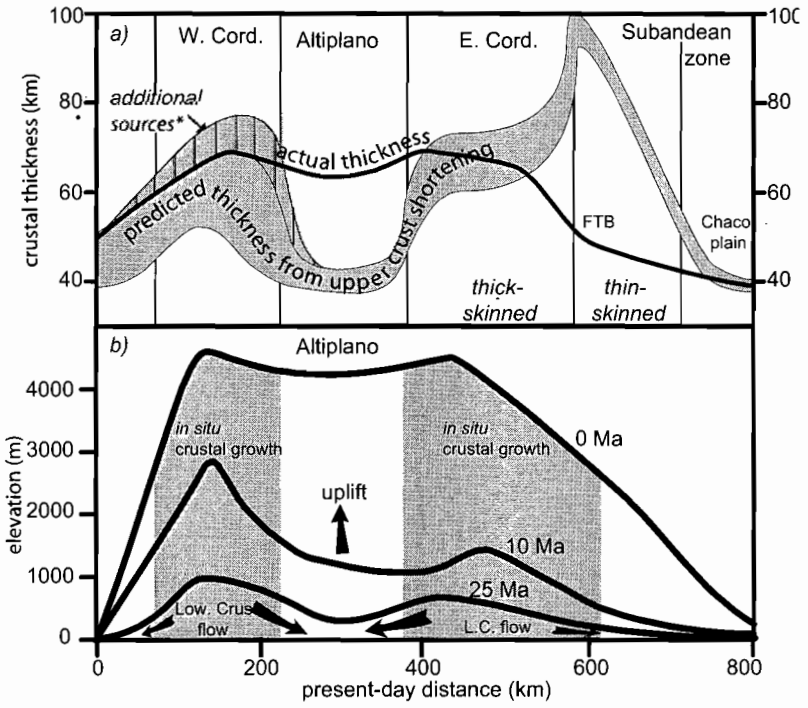

Figure : a) discrepancy between the actual crustal thickness (solid line) and predicted thickness from upper crust total shortening (shaded area) in the Central Andes (~20°S); note the volume excess in the E. Cordillera and Subandean Zone and the deficit below the Altiplano; b) crustal growth through time. Data are adapted from Rochat et al., 1999; Beck et al., 1996; Kennan, 2000.

MODELING THE ALTIPLANO UPLIFT

Homogeneous crustal thickening and lateral extrusion of the mid-lower crust constitute two end-members models which are commonly used to explain the formation of high plateaus (Medvedev & Beaumont, 2001). In the case of the Central Andes, the observations discussed above tend to suggest that the hypothesis of a lower crust channel flow can be explored. Isacks (1988) formerly suggested that the uplift of the Altiplano can be explained by a viscous lower crustal flow. Although some authors have suggested that the Altiplano could correspond to deep crustal imbrications (*e.g.* McQuarrie and DeCelles, 2001), we emphasize that evidence for a partially molten mid-lower crust (Yuan et al., 2000) more likely implies a ductile behavior at depth.

In the following model, we assume that both Cordilleras thickened *in situ* (although controversial for the W. Cordillera). As they thickened, the lateral pressure gradients drove the lower crust below the Altiplano area, inducing its uplift without shortening of the upper crust. We derive the uplift data from Kennan (2000) to calculate the crustal thickness through time assuming isostasy, only for both Cordilleras, but not for the Altiplano, where no upper crustal shortening can be invoked.

The mid-lower crustal flow is described by a Poiseuille flow in a channel of constant thickness C. The governing equations can be derived after Turcotte & Schubert (1982). After algebra, the change in elevation h through time writes (accordingly to *e.g.* Clark & Royden, 2000):

$$\frac{\partial h}{\partial t}=\frac{\rho_m-\rho c}{\rho_m}g\frac{C^3}{12}\frac{\partial}{\partial x}\left(\frac{1}{\eta}\frac{\partial h}{\partial x}\right)$$

where ρ_m and ρ_c are the mantle and crust densities, g the gravitational acceleration, η the viscosity of the channel and h the elevation. The flow will mainly depends on the viscosity, which can vary by several orders of magnitude, while the uncertainties and variations in the other parameters are negligible in comparison. Changes in crustal thickness S can now write in a simple form as $\frac{\partial S}{\partial t}=A\frac{\partial}{\partial x}\left(\frac{1}{\eta}\frac{\partial h}{\partial x}\right)$ which emphasizes the role of the viscosity η, A now being a constant.

Because viscous deformation is restricted to the lower crust, this approach somehow considers that the upper crust behaves with an elastic rheology, and this model subsequently constitutes an intermediate between pure viscous and elastic deformation theories for the crust.

Creep flow law relates the strain rate $\dot{\varepsilon}$ to rheological constants (*Ea, D, n*), shear stress σ and an exponential form of the temperature T as $\dot{\varepsilon}=D\sigma_s^n e^{-Ea/RT}$. Temperature thus appears as the main variable in the equation. Moreover, as very little is known on both rheological constants and thermal regime of growing orogens, we assume for a first order approximation that ductility in the channel is (non linearly) depth-dependent. According to the results of Bird (1991), we assume that viscosity drastically increases with crustal thickness. The large uncertainty in rheological parameters does not allow to predict its actual temperature dependence; we prefer to invert the dynamic evolution of the Altiplano to calibrate the evolution of viscosity with depth.

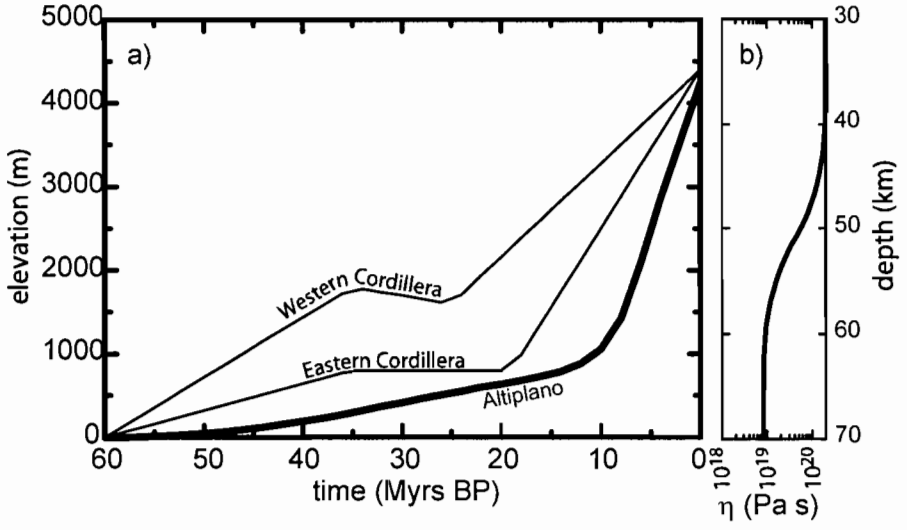

Figure 2: a) *A priori* uplift of the E. Cordillera and W. Cordillera for the model (thin lines, after Kennan, 2000), due to *in situ* crustal thickening, and predicted uplift for the Altiplano area (thick line); b) viscosity of the crustal channel as a function of crustal thickness.

In the model, the mid-lower crust flows from the surrounding growing Cordilleras towards the Altiplano. We assume that the flow from high elevation zones is instantaneously compensated.

The best fit between predicted and observed uplift histories (Fig.2) is obtained for a critical thickness of about 50 km, where the viscosity drops from 2 10^{20} Pa s to 8 10^{18} Pa s.

CONCLUSIONS

Our model confirms the possibility for a mid-lower crustal channel flow to be responsible for the Altiplano uplift. The calculated rheology is similar to the one proposed by Medvedev (2001) or Royden (1996) with the existence of a low viscosity (< 10^{19} Pa s) channel below 50 km depth.

However, the assumptions of *in situ* crustal growth for the Cordilleras raises the problem of volume balance, particularly for the Western one, where only little crustal shortening is generally mentioned. The possibility that crustal growth in the W. Cordillera might have benefited from subduction-related magmatic addition, in proportions which are difficult to assess, can also be addressed.

REFERENCES

Beck, S.L., Zandt, G., Myers, S.C., Wallace, T.C., Silver, P.G. and Drake, L., 1996. Crustal scale variations in the Central Andes, Geology, 24: 407-410.

Bird, P., 1991. Lateral extrusion of lower crust from under high topography, in the isostatic limit, J. Geoph. Res., 96, 10,275-10,286.

Clark, M.K. & Royden, L.H., 2000. Topographic ooze: building the eastern margin of Tibet by lower crustal flow, Geology, 28, 703-706.

Gregory-Wodzicki, K.M., 2000. Uplift history of the Central and Northern Andes: a review, Geol. Soc. Am. Bull., 112, 1091-1105.

Isacks, B., 1988. Uplift of the Central Andes and bending of the Bolivian orocline, J. Geoph. Res., 93, 3211-3231.

Kennan, L., 2001. Large-scale geomorphology of the Andes: interrelationships of tectonics, magmatism and climate, in Geomorphology and Global Tectonics, ed. M.A. Summerfield, Wiley.

Kley, J. & Monaldi, C.R., 1998. Tectonic shortening and crustal thickness in the Central Andes: how good is the correlation?, Geology, 26, 723-726.

McQuarrie, N. & DeCelles, P., 2001. Geometry and structural evolution of the Central Andean backthrust, Bolivia, Tectonics, 20, 669-692.

Medvedev, S. & Beaumont, C., 2001. Growth of continental plateaux: channel-flow or tectonic thickening ? (abstract), AGU Fall Meet., San Francisco.

Rochat, P., Hérail, G., Baby, P. & Mascle, G., 1999. Bilan crustal et contrôle de la dynamique érosive et sédimentaire sur les mécanismes de formation de l'Altiplano, C.R. Acad. Sci., 328, 189-195.

Royden, L., 1996. Coupling and decoupling of crust and mantle in convergent orogens: implications for strain partitioning in the crust, J. Geophys. Res., 101, 17679-17705.

Springer, M. and Forster, A., 1998. Heat Flow density across the Central Andean subduction zone, Tectonophysics, 29, 123-139.

Turcotte, D.L. & Schubert, G., 1982. Geodynamics. Applications of continuum physics to geological problems, Wiley and sons, 450 p.

Yuan, X. et al., 2000. Subduction and collision processes in the Central Andes constrained by converted seismic phases, Nature, 408, 958-961.

CRUSTAL THICKNESSES AND GENERAL ISOSTATIC BALANCE OF THE PERUVIAN ANDES FROM OBSERVED AND PREDICTIVE SHORTENING

Antonio INTROCASO (1), Iris Rosalía CABASSI (2)

(1) Facultad de Cs. Exactas, Ingeniería y Agrimensura – IFIR – U.N.R. – CONICET – Av. Pellegrini 250, 2000 Rosario - ARGENTINA (geofisic@fceia.unr.edu.ar)
(2) Facultad de Cs. Astronómicas y Geofísicas – U.N.L.P. – Paseo del bosque s/n, 1900 La Plata - ARGENTINA (rosy@fcaglp.fcaglp.unlp.edu.ar)

KEY WORDS: crustal thicknesses, shortenings, isostasy

INTRODUCTION

Peruvian Andes are bounded in the west by the Perú-Chile trench and in the east by the Brazilian shield. This part of the Andes is formed by two parallel cordilleras named Western Cordillera and Eastern Cordillera. From the middle part and to the south, a significant widen of the system takes place. An elevated plateau between the two cordilleras is present: the Altiplano, which has a mean elevation of 4 km. Morphological units are completed with the Subandean zone to the east of the Eastern Cordillera and the Cordillera de la Costa to the southwest of the Western Cordillera and coastal plain. See Benavídez-Cáceres (1999) for more information.

Andean geodynamics, in particular Peruvian Andes, involve two processes at global scale: (a) subduction of a young oceanic lithosphere (Nazca plate) below the Sudamerican coastal margin, and (b) continuous progress of the Sudamerican plate westwards.

Peruvian Andes from 5° S to 18° S latitudes involve the greatest « flat-slab » type subduction zone of the world, located between 5° S and 15 ° S latitudes. It exhibits low heat flow and has not active volcanism. It has been considered that the buoyancy is connected with the delay of the basalt-eclogite phase change (Sacks, 1983). Then, southwards, the oceanic slab gradually takes its normal dip. There, there is high heat flow and active volcanism.

The goal of this study is to find crustal thicknesses and to determine the large scale isostatic state of the Peruvian Andes to better understand the tectonic style and deformation.

CRUSTAL THICKNESSES

Crustal thicknesses have been determined on seven Peruvian Andes cross sections (Fig. 1) from inversion of the regional Bouguer anomalies using wavelengths that agree with the Andean width. Crustal thicknesses change from 64 km to 71 km (Table I) in very good agreement with those of Bolivian Andes (Miranda and Introcaso, 2000) and Argentina-Chile Andes (Introcaso et al.., 2000) until 33° S – 34° S latitude. Peruvian Andes crustal thickness is approximately 67 km ± 3 km in average.

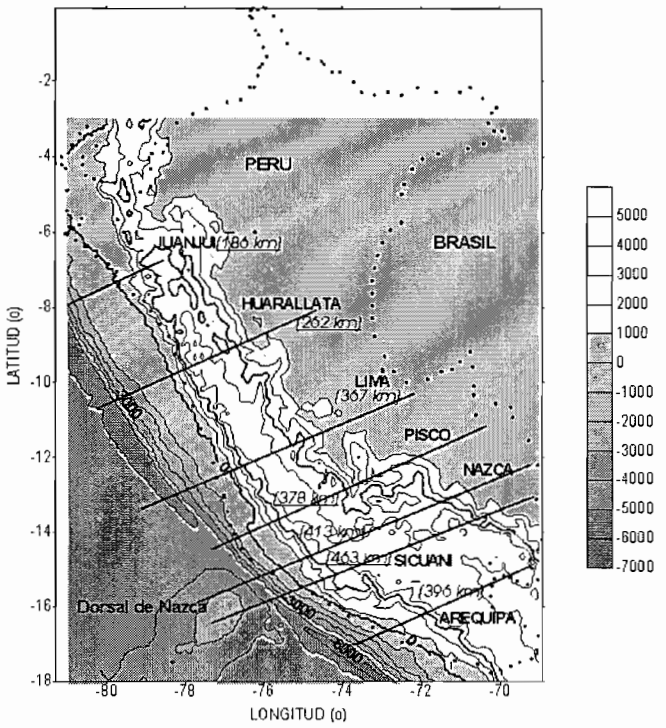

Fig. 1. Peruvian Andes. Topography and location of the studied cross sections

PREDICTIVE (S'_h) SHORTENING AND OBSERVED (S_h) SHORTENING

Shortenings and crustal thicknesses control both the tectonic style and the deformation (Ramos et al., 2002). Knowing the isostatic state (compensation or no compensation and the mechanisms present: Airy, flexural, ...) it is possible to determine crustal deformation at large scale.

By comparing both observed and predictive shortenings: $S_h - S'_h = \Delta S$ (1) we have indicators of general isostatic state ($\Delta S>0$, $\Delta S=0$, $\Delta S<0$). In fact, to calculate the predictive shortening S'_h an exact balanced theoretical model is used, in which the topographic elevation is the only input. From this value, and using - for instance - hydrostatic formulas, it is possible to obtain Andean roots. Observed shortening S_h, obtained from Andean elevation and Andean root values (from gravity inversion, seismic depths, etc.), must be compared with S'_h according to (1).

In fact, expression (1) is similar to an isostatic anomaly (AI) because it is obtained by comparing the observed gravity effect of the real crust with the gravity effect originated by a theoretical crustal model. And the latter is similar to an observed model, although it is exactly compensated.

We have calculated shortenings on crustal scale at the following Peruvian Andes cross sections: Juanjuani (J), Huarallata (H), Lima (L), Pisco (P), Nazca (N), Sicuani (S) and Arequipa (A) (Fig. 1). Before this work, Isacks (1988) and Introcaso et al. (2000) among others, have carried out similar studies. The excess of Andean masses (Andean elevations) have been calculated here in 2D and named A_t [km^2]. We have assumed a standard crustal thickness T_n = 33 km (Bullen, 1963; Woollard, 1969; Introcaso et al., 1992) and the following density values: σ_t (sea level and upwards) = 2.67 g/cm^3; σ_c (crust below sea level) = 2.90 g/cm^3; σ_m (upper mantle) = 3.30 g/cm^3. So, we have (Introcaso et al., 1992; Introcaso et al., 2000):

A_r (crustal root area) = 6,.675 A_t (topographic area) (2)

with A_r and A_t in km^2. From (2), and with T_n = 33 km, the predictive shortening S'_h [km^2] will be:

$S'_h = (A_t + A_r)/ T_n = 0,.23257\ A_t$ (3)

With the density values informed by Woollard (1969) and Isacks (1988): σ_c (density of the whole crust) = 2.93 g/cm^3, σ_m (upper mantle density) = 3.32 g/cm^3 and keeping T_n = 33 km, we have:

$S'_h = 0,.25796\ A_t$ (km^2) (4)

With density values with only one decimal digit: σ_c = 2.9 g/cm^3 and σ_m = 3.3 g/cm^3, we will have:

$S'_h = 0,.25\ A_t$ (km^2) (5)

S'_h for each section have been obtained assuming expression (3) with σ_t = 2.67 g/cm^3, or the same density of Bouguer correction that is more realistic than 2.93 g/cm^3 or 2.9 g/cm^3 of (3) or (4), and evaluating A_t (km^2) in the seven cross sections of Fig. 1, using the moving window method (Isacks, 1988; Introcaso et al., 1992).

Keeping A_t (km^2) calculated for the seven sections we have defined the observed Andean root A_r (observed in km^2 from inversion of regional Bouguer anomaly with: $\sigma_c - \sigma_m$= -0.4 g/cm^3 agreeing with (3)).

Table I involves: crustal thicknesses, A_t, $A_{r\,pred}$, $A_{r\,obs}$, S'_h, S_h and the differences in absolute value of $A_{r\,obs}/ A_t$ and 6.675 (exact compensation from (2)), and relative errors of S'_h and S_h.

Location	Maximum crustal thickness (km)	A_t (km^2)	$A_{r\,pred}$ (km^2)	S'_h (km)	$A_{r\,obs}$ (km^2)	S_h (km)	$\lvert A_{r\,obs}/A_t - 6.675 \rvert$	$(S_h - S_h')/S_h'$ (%)
J, -7° S	64	751	5,011	175	5,400	186	0.52	6.3
H, -10° S	71	999	6,666	232	7,631	262	0.96	12.9
L, -11.9°S	67	1,071	7,145	249	11,034	367	3.62	47.4
P, -13.1°S	69	1,425	9,514	331	11,058	378	1.08	14.2
N, -14.1°S	68	2,035	13,585	473	11,583	413	0.98	-12.6
S, -14.9°S	64	2,374	15,847	552	12,901	463	1.24	-1.6
A, -16.1°S	65	1,668	11,137	388	11,396	396	0.15	2.1

Table I. Predictive and observed shortenings of the seven studied sections

DISCUSSION AND CONCLUSIONS

Cabassi (doctoral thesis, 2002) has added the following methods for isostatic analysis of Peruvian Andes:

A – Linear relationships between mean Bouguer anomalies (or Free Air anomalies) and mean altitudes

B – Elastic crustal flexion

C – Airy system

D – Isostatic geoid undulation

The linear formulas obtained using (A) for Peruvian Andes were compared with similar relationships informed by Introcaso et al. (2000) for the isostatically compensated Chile-Argentina Andes (22° S – 34° S latitudes), and so Cabassi (2002) concluded that Peruvian Andes are compensated, at least in general terms.

However, this method does not point out which is the isostatic mechanism present in Peruvian Andes. From (B), (C) and (D) it was possible to analyse the general isostatic balance and the local mechanism present in each section. So, Peruvian Andes taken as a whole are compensated in Airy system as pointed out by the very low elastic thickness (5 km to 10 km necessary to justify the Bouguer anomalies) in (B), the low amplitude of the isostatic anomalies in (C), and the isostatic metric anomalies in (D) consistent with (C). The local isostatic analysis in each section with wavelengths lower than the Andean width has revealed no compensation in some areas.

Our isostatic analysis from shortening points out no isostatic compensation in Lima cross section (relative error: 47 %), only general tendency to compensation in Huarallata, Pisco and Nazca (relative errors lower than 15 %, between –12.6 % and 14.2 %), and very good isostatic compensation in Juanjuani, Sicuani and Arequipa sections (low relative errors: 6 %, -2 % and 2 % respectively).

From 15° S latitude and southwards, heating could have an effect in the Andean building.

The evaluation of isostatic balance in Peruvian Andes from shortening is a quick and general method that involves the whole Andean masses. However, we must point out the isostatic shortening indicators (ΔS) informed here have no more resolution than the corresponding to general Andean width. In spite of this, the ΔS indicators can be used on partial widths, for example only in the Eastern Cordillera or only in the Western Cordillera.

Finally, from 7° S to 34° S latitudes, the Airy compensation system is present with crustal thicknesses that, in general terms, doubles the normal crustal thickness.

REFERENCES

Benavides-Cáceres V. 1999. Orogenic evolution of the Peruvian Andes: The Andean Cycle. Economic Geology, 94, chapter 3, 61-107.

Bullen K.E. 1963. An Introduction to the Theory of Seismology. 3th. Ed., Cambridge University Press, 381 pp.

Cabassi I. R. 2002. Análisis de la evolución tectónica de los Andes Peruanos a partir del método gravimétrico. Tesis doctoral inédita (U.N.Rosario, Argentina), 243 pp.

Introcaso A., Pacino M.C. and Fraga H. 1992. Gravity, isostasy and Andean crustal shortening between latitudes 30° and 35°S. Tectonophysics, 205, 31-48.

Introcaso A., Pacino M.C. and Guspí F. 2000. The Andes of Argentina and Chile: Crustal configuration, Shortening and Tectonic features from gravity data. Temas de Geociencia 5, UNR Editora, ISSN N° 1514-4149, 31 pp.

Isacks B.L. 1988. Uplift of the central Andean plateau and bending of the Bolivian Orocline. Journal of the Geophysical Research, 93 (B4), 3211-3231.

Miranda S. and Introcaso, A. 2000. Acortamientos corticales para los Andes Centrales bolivianos a partir de datos de gravedad. Congreso Geológico Boliviano, La Paz, Bolivia, 72-76.

Ramos V.A., Zapata T., Cristallini E. and Introcaso A. 2002. The Andean thrust system: Latitudinal variation in structural styles and orogenic shortening. American Association of Petroleum Geologist. In press.

Sacks I.S. 1983. The subduction of young lithosphere. Journal Geophysical Research, 88, 3355-3366.

Woollard G.P. 1969. Regional variations in gravity. In: The Earth's crust and upper mantle, Pembroke J. Hart (ed.), Geophysical Monograph, 13, AGU, Wash. D. C., 320-341

STRUCTURAL CHARACTERISTICS OF THE INCAPUQUIO FAULT SYSTEM, SOUTHERN PERU

Javier JACAY (1), Thierry SEMPERE (2), Laurent HUSSON (2), Adán PINO (3)

(1) Escuela de Ingeniería Geológica, Universidad Nacional Mayor de San Marcos, apartado postal 3973, Lima 100, Peru (J_Jacay@yahoo.com)
(2) I.R.D.-Perú, La Mariscala 115, Lima 27; apartado postal 18-1209, Lima 18, Peru (sempere@terra.com.pe; lhusson@yahoo.com)
(3) Escuela de Ingeniería Geológica – Geotecnia, Universidad Nacional Jorge Basadre Grohmann, Av. Miraflores s/n, Tacna, Peru (adan_pino@yahoo.com; alefloro@yahoo.com; conrado@docentes.unjbg.edu.pe)

KEY WORDS: Peru, transcurrent fault system, transpression, flower-structure, mylonite

INTRODUCTION

The Pacific piedmont of the Cordillera Occidental of southern Peru is characterised by a N125E-trending senestral transcurrent system that is at least 400 km-long and locally >10 km-wide. This contribution describes this structural system in southernmost Peru, where it is known as the Incapuquio-Challaviento fault system (Tacna department, 69°50'-70°45'W; Wilson and García, 1962) or as the Incapuquio, Micalaco and Capillune faults (Moquegua department, 70°45'-71°20'W; Bellido, 1979). In order to simplify this structural nomenclature, we use here the simpler denomination "Incapuquio fault system" (SFI in Spanish).

STRUCTURE OF THE INCAPUQUIO FAULT SYSTEM

Although it presents significant variations along strike, the Incapuquio system (SFI; Fig. 1) is characterised by a number of transpressional characteristics, including positive flower-structures. Although a rhomboidal core of Precambrian and Paleozoic rocks occur in one part of its axial strip, rocks cropping out along the SFI are mainly thick Jurassic volcano-sedimentary marine strata in the SE (Yura Group; Wilson y García, 1962; Vicente, 1989), and thick Late Cretaceous-Early Paleogene igneous and subordinate sedimentary rocks in the NW (Toquepala Group and related intrusions). The SFI was the NE active boundary of the basin in which the Oligocene Moquegua Group accumulated. Sharp and usually angular unconformities separate the deformed Moquegua, Toquepala, and Yura groups, but contacts between these units are locally tectonic. Stratigraphic and structural variations occur across the SFI.

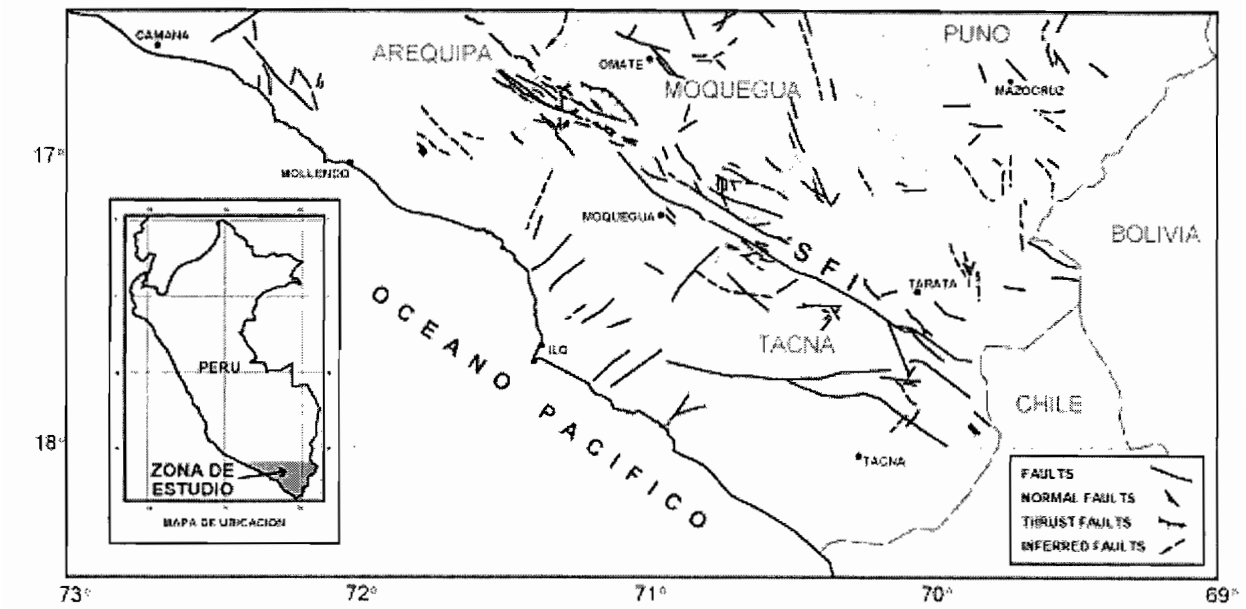

Fig. 1: The tectonic sketch map of southern Peru is dominated by the prominent Incapuquio fault system (SFI).

A variety of observations indicates or is in agreement with the fact that senestral transcurrent motions have occurred along the SFI. Its area of influence include *en échelon* faults and anticlines, subparallel sinuous and anastomosed faults and fractures, asymmetric flower-structures, as well as folds with subvertical axes. The Mal Paso flower-structure (Fig. 1) has exhumed Precambrian basement and overlying Paleozoic strata and is fringed by subvertical mylonite bands. This asymmetric structural "rhomb" presently reaches >4000 m altitude. In the eastern area of the structure, Jurassic strata are intensely faulted and complexly folded, especially near the corners of the "rhomb".

A variety of fault rock fabrics are observed. In the Moquegua area, fault rocks related to the SFI display cataclastic to mylonitic textures and subvertical dips. East of 70°10'W, gouge facies grade into subvertical mylonites that locally reach ultramylonite and possibly pseudotachylite facies farther east. Gouge-mylonite zones may be 100 m to 3 km - wide.

At least near Cuajone and Mirave, the SW fringe of the SFI includes a few SW-verging reverse faults, with dips as low as 35°, that place thick, massive lavas of the Toquepala Group onto thick conglomerates of the lower Moquegua Group. The distribution and thickness of these conglomerates show that the SFI was the active NE boundary of the Oligocene Moquegua basin.

Late Cretaceous-Early Paleogene dioritic, granodioritic, and monzonitic intrusions, locally ore-bearing, are associated with the SFI (Concha y Valle, 1999) and coeval with the thick and dominantly volcanic Toquepala Group. As magma ascension was probably favored by a contemporaneous transcurrent regime of the SFI crustal shear zone, it is likely that the latter was already active in the Late Cretaceous-Early Paleogene. Following Saint-Blanquat et al.'s (1998) model, coeval transpression along the SFI would provide a tectonic framework compatible with the abundant magmatism represented by the Toquepala Group.

CONCLUSIONS

On the whole, the structural characteristics observed along the Incapuquio fault system (SFI) indicate that it is a dominantly transcurrent system, and that it functioned principally in transpression. This transpression possibly represents a Late Cretaceous and/or Cenozoic inversion of a specific part of the Jurassic basin (which had developed by lithospheric thinning; Sempere et al., 2002a&b).

The SFI probably facilitated the Late Cretaceous-Early Paleogene abundant magmatism (Toquepala Group), and remained active during the Oligocene, forming the NE active border of the Moquegua basin. The SFI is currently still seismically active.

The SFI prolongates to the NW (Arequipa department) with some similar characteristics. At 71°45'W, it splits into two main branches that bound the large Huatiapa flower-structure (most probably a compressional jog that inverted a particularly weak area of the Jurassic basin). The SW branch, the El Castillo fault system, represents the true prolongation of the SFI because, as the latter, it shows a SW-verging reverse component. The NE branch has long been described as the Cincha-Lluta fault system (Vargas, 1970; Vicente, 1979) and shows a NE-verging component. Between these fault sytems, the Huatiapa flower-structure mostly consists of Precambrian rocks and Jurassic, Late Cretaceous, and Early Paleogene intrusions. Because it continues northwest at least as far as 72°30'W, we propose the denomination "Incapuquio-El Castillo fault system" (SFIEC in Spanish) to unify the entire system, restraining the name Incapuquio (SFI) for its southern segment.

REFERENCES

Bellido, E., 1979. Geología del cuadrángulo de Moquegua. Boletín del Instituto Geológico Minero y Metalurgico, N° 15, 78p.

Concha, O., Valle, J., 1999. Prospección, exploración y desarrollo del yacimiento de Cuajone. In: IIMP y ProEXPLO (eds.), *Primer Volumen de Monografías de Yacimientos Minerales Peruanos*, p. 117-143.

Saint-Blanquat, M. de, Tikoff, B., Teyssier, C., & Vigneresse, J.-L., 1998. Transpressional kinematics and magmatic arcs. In: R.E. Holdsworth, R.A. Strachan & J.F. Dewey (eds), *Continental transpressional and transtensional tectonics*, Geological Society, London, Special Publications, v. 135, p. 327-340.

Sempere, T., Carlier, G., Soler, P., Fornari, M., Carlotto, V., Jacay, J., Arispe, O., Néraudeau, D., Cárdenas, J., Rosas, S., Jiménez, N., 2002a. Late Permian - Middle Jurassic lithospheric thinning in Peru and Bolivia, and its bearing on Andean-age tectonics. Tectonophysics, v. 345, p. 153-181.

Sempere, T., Jacay, J., Pino, A., Fornari, M., Marocco, R., Flores, A., Acosta, J., Bedoya, C., 2002b. Adelgazamiento litosférico triásico-jurásico en el extremo sur del Perú. XI Congreso Peruano de Geología, in press.

Vargas, L., 1970. Geología del cuadrángulo de Arequipa. Boletín del Servicio Geológico Minero, n° 24, 64 p.

Vicente, J.-C., Sequeiros, F., Valdivia, M.A., Zavala, J., 1979. El sobre-escurrimiento de Cincha-Lluta: elemento del accidente mayor andino al NO de Arequipa. Boletin de la Sociedad Geológica del Perú, v. 61, p. 67-99.

Vicente, J.-C., 1989. Early Late Cretaceous overthrusting in the Western Cordillera of southern Peru. In: Ericksen, G.E., Cañas, M.T., & Reinemund, J.A. (eds.), *Geology of the Andes and its relation to hydrocarbon and mineral resources*, Houston, v. 11, p. 91-117.

Wilson, J.J., García, W., 1962. Geología de los cuadrángulos de Pachía y Palca. Comisión de la Carta Geológica Nacional, v. 2(4), 82 p.

EVOLUTION OF THE CRETACEOUS CELICA-LANCONES FOREARC BASIN (NW PERU-SW ECUADOR)

Etienne JAILLARD (1), Raynald ETHIEN (1), Henriette LAPIERRE (1), Cédric REYNAUD (1), Marc MAMBERTI (1) and Piercarlo GABRIELE (2).

(1) IRD-LGCA, Maison des Géosciences, BP 53, 38041 Grenoble Cedex, France [ejaillar@ujf-grenoble.fr]
(2) IMG, BFSH2, University of Lausanne, CH-1015 Lausanne, Switzerland [Piercarlo.Gabriele@imp.unil.ch]

Key-Words : Cretaceous, forearc pull-apart Basin, wrench movements, deformations, convergence direction.

INTRODUCTION

The Celica-Lancones Basin is located in the present-day forearc zone of Southern Ecuador and Northern Peru (Fig. 1). It is characterized by unusual turbiditic series of Cretaceous age. According to the authors, this basin has been interpretad as an extensional basin (Kennerley 1973), an aborted marginal basin (Aguirre 1992), or a transcurrent forearc Basin (Jaillard et al. 1999). New observations presented here support the latter interpretation and suggest that the evolution of this forearc zone was controlled by the convergence regime.

STRATIGRAPHY AND GEOCHEMISTRY

The Celica-Lancones Basin is bounded to the Southeast by a volcanic arc (Celica Fm, San Pedro Gp), and to the Northwest by the Amotape-Tahuin Paleozoic Massif. Two series may be distinguished (Fig. 2).

To the Southeast, the Celica-San Pedro volcanic rocks are mostly of Albian age, but their upper part yielded Early Cenomanian faunas (Reyes and Caldas 1987, Carlier pers. com.). Their geochemistry is marked by depletion in Nb, Ta and Ti, and concentrations in Th, which indicate a volcanic arc affinity (Reynaud 1996, Fig. 3). These volcanic facies laterally grade NW-ward into volcaniclastic, high-density turbidites (Lancones, Alamor Fms, Reyes & Caldas 1987, Jaillard et al. 1999). Intercalated volcanic rocks exhibit volcanic arc affinity, and include dacites marked by high LREE and high Sr/Y relation, suggesting an adakitic nature (Reynaud 1996, Fig. 3). In the northeastern part of the Basin, thin-bedded alternations of black shales and fine-grained greywackes yielded Late Cenomanian-Turonian inoceramids (Jaillard et al. 1999).

This deformed and eroded Albian-Turonian series is unconformably overlain by a transgressive marine series (marls, limestones, sandstones), the base and top of which yielded Early Campanian, and Late Campanian ammonites, respectively (Jaillard et al. 2002). It is overlain by coarse-grained fan conglomerates ascribed to the Late Campanian-Early Maastrichtian (Fig. 2). They are unconformably overlain by latest Maastrichtian to Paleocene subaerial volcanic rocks (Sacapalca Fm, Hungerbühler 1997, Fig. 2) of continental volcanic arc affinities

(anomalies in Nb, Ta and Ti, Reynaud 1996, Fig. 3).

To the Northwest, the Paleozoic Amotape-Tahuin Massif is unconformably overlain by transgressive beds, which are, from base to top : (i) undated sandstones and conglomerates, (ii) massive, fossiliferous shelf limestones, locally interbedded with volcanic tuffs and conglomerates, grading into black laminated limestones of Middle Albian age, (iii) laminated black shales and fine-grained volcanogenic turbidites of Middle to Late Albian age (Huasimal Fm), (iv) a coarsening upwards turbiditic sequence of arkosic to volcaniclastic composition (Copa Sombrero Gp, Olsson 1934), the top of which yielded an ammonite of Late Albian age (Fig. 2). Volcanic tuffs are locally known between (i) and (ii) (Puyango). Although reflecting heterogeneous sources (MORB to EMII types), scarce lava flows interbedded in the Copa Sombrero Gp exhibit volcanic arc affinity (Ethien 2000, Fig. 3). Since fossils of Early Coniacian age have been mentionned (Reyes & Caldas 1987), deposits of that age may be locally preserved beneath the overlying unconformity.

Along the Basin axis, from Chiclayo to Chaguarpamba, and West of Lancones, this series is intruded by large volumes of gabbros and minor diorites of Santonian-Campanian age (86-82 Ma, Mourier 1988, Alemán pers. com.). Geochemical and isotopic data (Pb, Sr, $\varepsilon Nd \approx 0$) indicate a depleted source contaminated by continental crust or sediments, suggesting that they result from partial melting of the forearc mantle (Ethien 2000).

The deformed and partly eroded turbidites and gabbros are unconformably overlain by a latest Cretaceous marine series which comprises, from base to top : (a) transgressive, shallow marine arkosic or calcareous beds overlain by black shales and siltstones of Middle to Late Campanian age (Jaillard et al. 2002), (b) undated, thick quartz-conglomerates of shoreline environments (Monte Grande Fm, Olsson 1934), and (c) black shales and medium-bedded quartz-turbidites of Early Maastrichtian age (Fig. 2). In the Pazul area (NW Peru), these are overlain by marine fossiliferous beds of Paleocene age (Balcones Fm), and the succession ends up with unconformable, coarse-grained quartz-conglomerates of latest Paleocene-Early Eocene age (Mogollón Fm), overlain by the Eocene marine deposits of the Talara Forearc Basin (Morales 1993).

TECTONIC EVOLUTION AND GEODYNAMIC INTERPRETATION

The Early Albian is marked by the beginning of the Celica-San Pedro volcanic arc activity. Therefore, the Cretaceous Celica-Lancones Basin can be unequivocally interpreted as a Forearc Basin (Fig. 1).

Scattered, **bimodal** volcanic manifestations of Early Albian age (Puyango) may be related to the extensional opening of the Celica-Lancones Basin. Subsidence of the Basin increased in the Middle Albian. Unpublished seismic lines (Alemán pers. com.) indicate that WNW-trending, S-ward dipping normal faults controlled the extension and turbiditic sedimentation (102-96 Ma). This evidence of a roughly trench-parallel extension, together with the rhombic shape of the Celica-Lancones Basin, strongly suggests that it is a pull-part basin, related to the NNE-ward, trench-parallel migration of the Amotape-Tahuin forearc sliver.

Remnants of Cenomanian-Turonian fine-grained deposits suggest that tectonic activity significantly decreased between 96 and 89 Ma. Around 84 Ma, basic intrusions emplaced in the center of the basin and along a suture line joining its NE and SW tips. They are regarded as resulting from the adiabatic partial melting of the forearc mantle (Ethien 2000), due to significant crustal thinning in the center of the Basin, and to the play of the Cross-Basin Fault Zone (suture) that achieves the evolution of pull-apart basins (Dooley & McClay 1997).

The Campanian unconformity (≈84-80 Ma) seals the Late Cretaceous deformations. In the northern part of

the basin, the deformation is dominated by NNW-ward thrustings, associated with ENE-trending isoclinal to cylindrical folds. In Peru, seismic data suggest that the Albian normal faults were slightly inverted, provoking the formation of mild, basin-scale, ENE-trending folds. Progressive discordances in the overlying deposits indicate that similar mild deformations continued during the Late Campanian-Maastrichtian (80-69 Ma). Moreover, the Pazul area is a WNW-trending syncline, which results from the Late Paleocene deformation phase, since it involves Paleocene beds and is sealed by unconformable conglomerates of Early Eocene age.

These observations suggest that the Late Cretaceous-Paleocene evolution of the Celica-Lancones Basin was dominated by trench parallel stress regimes, *i.e.* in Albian-Santonian times, NNE-trending extension related to wrench motions, and NNE-trending compression during Campanian-Paleocene times. Conversely, Paleocene-Eocene deposits are only deformed by NNE-trending folds, indicating that post-Paleocene deformations are dominated by an East-trending, trench-normal contractional regime, without significant wrench movements.

This change in the stress regime of the forearc zone coincides with a drastic change in the oceanic convergence in the Late Paleocene. About 58 Ma ago, the convergence of the oceanic plate abruptly changed from a North- or NNE-ward direction, to a NE-ward direction (e.g. Pardo-Casas & Molnar 1987).

REFERENCES

Aguirre L. 1992. Metamorphic pattern of the Celica Formation, SW Ecuador, and its geodynamic implications. Tectonophysics, 205, 223-237.

Dooley T., McClay K. 1997. Analog modelling of Pull-Apart Basins. AAPG Bull., 81, 1804-1826.

Ethien R. 2000. Les magmatismes d'avant-arc crétacés et néogènes de la marge andine Nord (Équateur-Pérou). Implication géodynamiques. Mémoire DEA, Univ. Aix-Marseille III, 29 p., unpubl.

Hungerbühler D. 1997. Neogene basins in the Andes of southern Ecuador: evolution, deformation and regional tectonic implications. PhD thesis, ETH Zürich, n° 12371, 182 p.

Jaillard É., Laubacher G., Bengtson P., Dhondt A., Bulot L. 1999. Stratigraphy and evolution of the Cretaceous forearc "Celica-Lancones Basin" of Southwestern Ecuador. J. South Am. Earth Sci., 12, 51-68.

Jaillard É., Bengtson P., Dhondt, A. 2002. Late Cretaceous stratigraphy of Northern Peru and Ecuador, a preliminary revision. J. South Am. Earth Sci., in press.

Kennerley J.B. 1973. Geology of the Loja Province, Southern Ecuador. London Inst. Geol. Sci., Rep. 23, 34 p.

Morales W. 1993. Reinterpretación geológica del área de Lagunitos (NW Perú) en base a sísmica reflexión. 3rd INGEPET, INGP-055, 1-19, Lima.

Mourier T. 1988. La transition entre Andes marginales et Andes cordilléraines à ophiolites. Evolution sédimentaire, magmatique et structurale du relais de Huancabamba. Dr Thesis, Univ. Paris XI, 275 p., unpubl.

Olsson A.A. 1934. The Cretaceous of the Amotape region. Bull. Amer. Paleont., 20, 104 p., New-York.

Pardo-Casas F., Molnar P. 1987. Relative motion of the Nazca (Farallón) and South America plate since late Cretaceous times. Tectonics, 6, 233-248.

Reyes L., Caldas J. 1987. Geología de los cuadrángulos de las Playas, la Tina, las Lomas, Ayabaca, San Antonio, Chulucanas, Morropón, Huancabamba, Olmos y Pomahuaca. Bol. INGEMMET, A, 39, 83, Lima.

Reynaud C., 1996. Géochimie et géodynamique des plateaux océaniques, arcs insulaires et arcs continentaux crétacé-paléocènes de l'Ouest équatorien. Mémoire DEA Univ. Grenoble I, 36 p., unpubl.

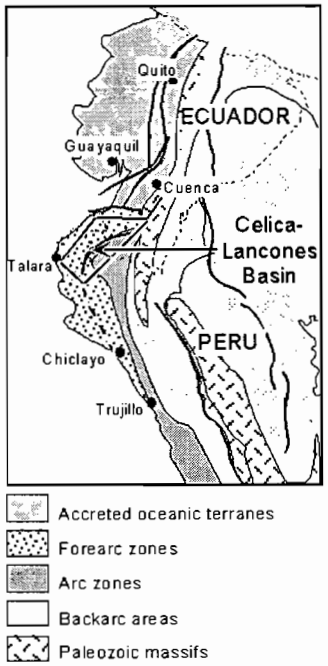

Fig. 1: Location of the Celica-Lancones Forearc basin

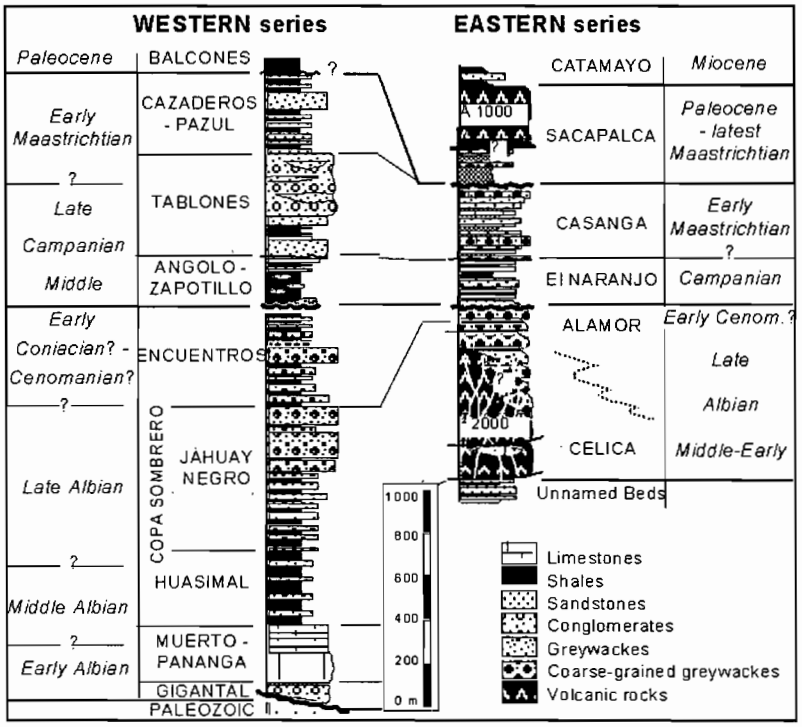

Fig. 2: Stratigraphic successions of the Celica-Lancones Basin (after Jaillard et al. 1999)

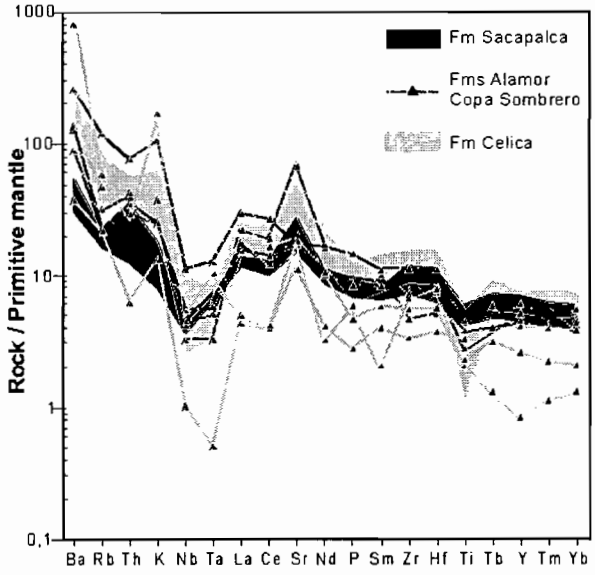

Fig. 3: Spiderdiagram of the Cretaceous-Paleocene volcanic arc rocks of the Celica-Lancones Basin (after Mamberti unpubl., Reynaud 1996, Ethien 2000)

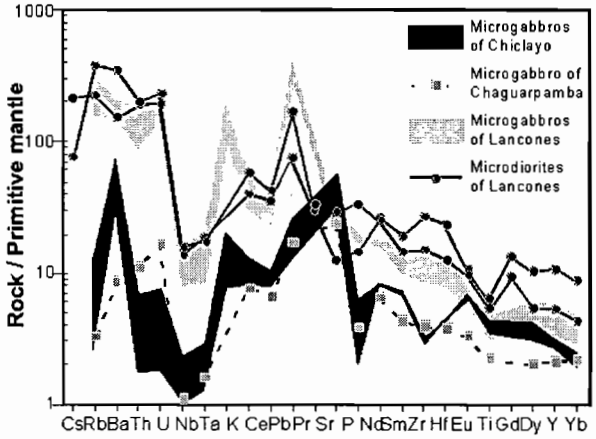

Fig. 4: Spiderdiagram of the Santonian-Early Campanian plutonic rocks of the Celica-Lancones Basin (after Ethien 2000)

GEOCHEMICAL CHARACTERISTICS OF THE CRETACEOUS BASEMENT OF WESTERN ECUADOR

Diego JAYA, Liliana TRONCOSO & Arturo EGUEZ

Instituto Geofísico, Escuela Politécnica Nacional, Ap. Pos. 2759, Quito-ECUADOR. geofisico@accessinter.net

KEY WORDS: Boninites, Plateau, "back-arc" basin.

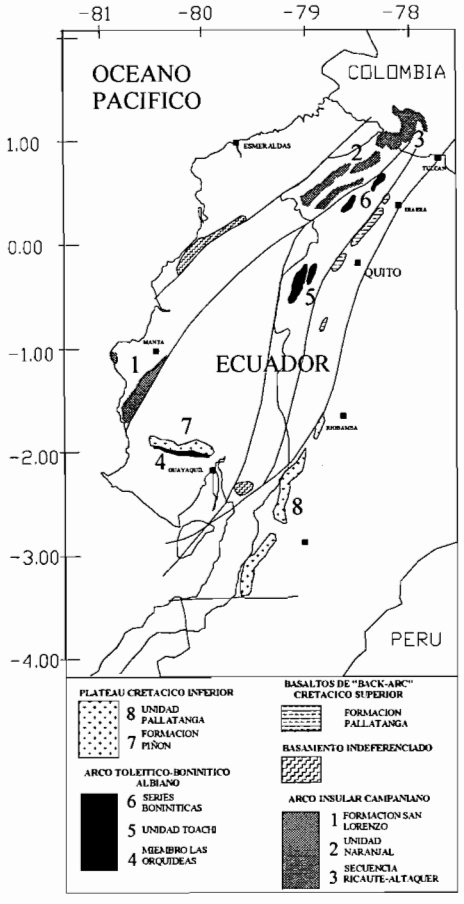

***Fig. 1** Location map of ambient in the basement of Western Ecuador*

INTRODUCTION

The basement of the Western Cordillera and the Coastal plain from the Gulf of Guayaquil toward the north are considered constituted by terrains originated in different oceanic scenarios and accreted to the continent. This work considers the studies and chemical analysis made on rocks of the Cretaceous basement, referred in different publications since 1987, and interpreted in a new geodynamic context based on the new published cartography of those regions of the Ecuador (10). We conclude with the existence of an old plateau of the Lower Cretaceous, an Albian boninitic-toleithic arc, a pre-Campanian back-arc basin and a Campanian mature insular arc (Fig. 1).

GEOLOGICAL SETTING

The simplest interpretation of the Cretaceous basement considered the Piñón Formation on the Coastal plain with its equivalent one within the Western Cordillera (8).

The present knowledge indicates that the coastal basement is constituted by the Piñón Formation (FP) of the Lower Cretaceous showing characteristics of oceanic plateau (11), by the Las Orquídeas Member (MLO) (11), corresponding to an Upper Albian to pre-Turonian Island Arc, and by the San Lorenzo Formation (FSL) dated 85-65 Ma (7) with the same affinities. The Cretaceous basement of the Western Cordillera (COE) is considered formed by the Pallatanga Unit (UP) (2) generated in a probable oceanic plateau environment and correlated with the Diabasic Group from Colombia (GDC), by the Toachi Unit attributed to an pre-Turonian insular arc (3) and by the Naranjal Unit (UN) of the Late Campanian (2). Thick volcano-sedimentary turbiditic sequences of the Campanian-Turonian age are known in the Western Cordillera and the Central Northern Coast (2). The accretion age for those oceanic terrains remains uncertain, however two events

have been accepted, a former Santonian to Later Campanian accretion of the UP, and a late Eocene to Oligocene event, involving the FP and the Macuchi Unit. Nevertheless, another important tectonic event is suggested during the Late Paleocene to Early Eocene, correlated with the FP and MLO collision (6).

The process under similar criteria of the geochemical data included in the published works, allows a new characterization and a coherent structural distribution for the recognized oceanic terrains during Cretaceous times.

OCEANIC PLATEAU PIÑÓN (FP) AND PALLATANGA SOUTH (UPS) (Lower Cretaceous)

The rocks of the UP are considered similar in age and geological environment to those of the FP (2, 7). The age of FP is Lower Cretaceous (11), while the age of the UP is not clearly defined, because toward the north a Santonian- Early Campanian age is reported (2) whereas in the southern part an age range from Middle Jurassic? to Early Cretaceous is suggested (9). Also, the geochemical data show differences between the UP outcropping in the Northern Western Cordillera in front of the southern portion of this.

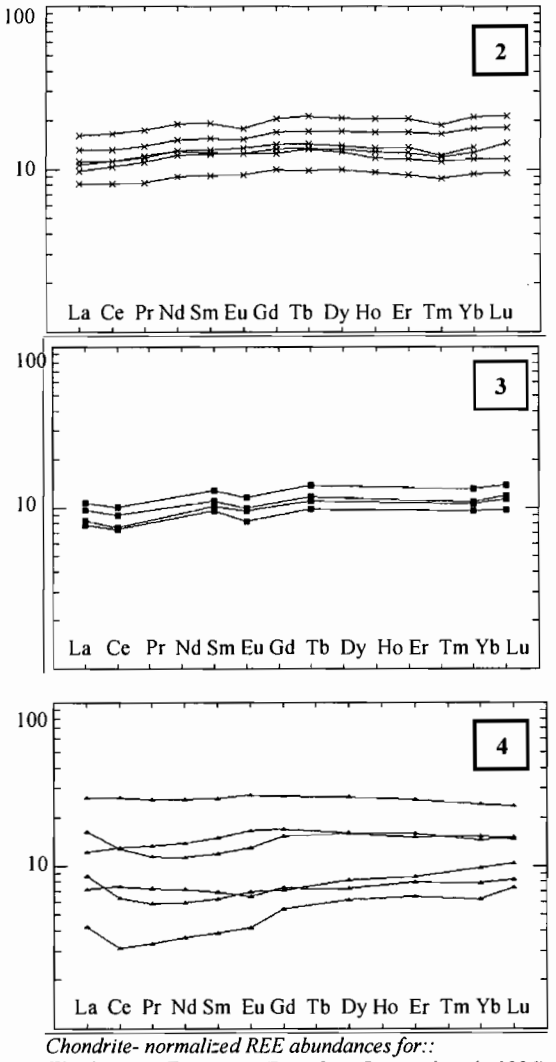

Chondrite- normalized REE abundances for::
***Fig. 2** Piñón Formation (Data from Reynaud et al., 1996)*
***Fig. 3** Pallatanga Unit, south part (Data from Lebrat, 1987)*
***Fig. 4** Pallatanga Unit, north part (Data from Boland et al., 2000)*

The rocks of the UPS, FP and GDC are similar in the following features: all samples are plotted in the field of sub-alkaline basalt using the discriminatory diagram of Zr/TiO_2 vs. Nb/Y; models of REE sub parallel ($0.8 < (La/Yb)N < 1.4$) (Figs. 2, 3); models of REE show intermediate characteristics between N-MORB and OIB; samples show abnormal Eu, reflecting plagioclase removal or accumulation; and high Nb values, comparable to those of GDC ($4 < Nb < 9$), differentiating them of rocks originated by subduction. In the diagram La-Nb, most of samples belong to the E-MORB (OIB) field, with some of them in the limit of N-MORB (Fig. 5).

Thus, it is possible that FP and UPS have been originated in a "Hot Spot" older than the plateau involving GDC within the Caribbean domain.

BACK-ARC BASIN PALLATANGA NORTH (UPN) (Pre-Campanian)

The UP of north central Ecuador shows geochemical characteristics different than the previous rocks. The samples plot in the field of basaltic andesites. The values of Nb ($1 < Nb < 8$) show a larger range than the FP, the UPS and the GDC, the values of some samples being similar to rocks of an arc. An uncommon Ce anomaly, is similar to that found in rocks of the "back-arc" of the northern Mariana Trough of the Western Pacific Ocean, where the expansion area is close to the volcanic arc (4).

The UPN also present a wide range of geochemical signatures, showing characteristic of rocks N-MORB in their majority, with two samples with characteristics of T- MORB and orogenic lavas (Figs. 4, 5). In the graphic La/Nb it is observed that the rocks of UP of the part center north form a different group, having bigger affinite with rocks N-MORB (Fig. 5).

Associated to these rocks are thick volcano-sedimentary turbiditic sequences of the Pilatón Unit (COE), the Cayo Formation (Coast) and the Natividad Unit (COE), of Turoniano-Maastrichtiano age (2) and that they could represent the filling of a " back-arc " basin.

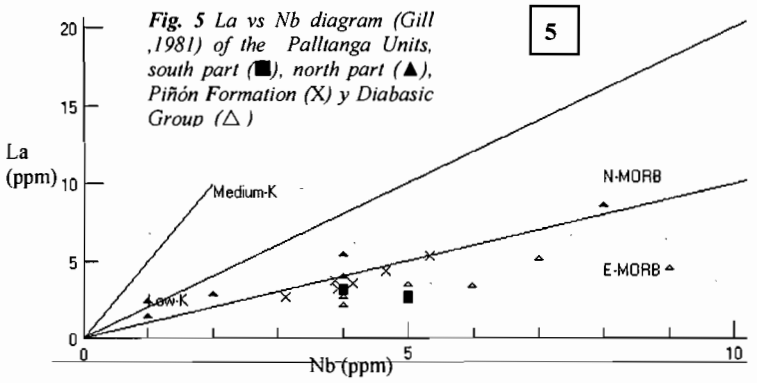

Fig. 5 La vs Nb diagram (Gill ,1981) of the Palltanga Units, south part (■), north part (▲), Piñón Formation (X) y Diabasic Group (△)

BONINITIC-TOLEITIC ARC: LAS ORQUÍDEAS (MLO)– TOACHI (UT) (Albian)

The MLO of Upper Albian-Cenomanian and the UT of pre-Coniacian (3,5) exhibit geochemical caracteristics of sub-alc-alcaline basalts, basic andesites and andesites, with an orogenic arc affinity.

The REE diagrams of MLO show low concentrations and an enrichment in LREE (Fig. 6), whereas UT rocks have a flat profile (Fig. 7). In respect to N-MORB, they present low concentration in Nb, a sign related to subduction magmatism. They present high content in MgO, Ni, Cr and low content in Al_2O_3, TiO_2, Y and Zr, abnormal to rocks of a typical arc, suggesting the presence of a source of primary magma. The $^{87}Sr/^{86}Sr$ ratio show the involment of some subducted sediments in the source or fluids recycled from the hydrothermalised subducted slab. Following these geochemical caracteristics, the MLO group could be assimilated to boninites (1), in relashioship with the generation of the primitive UT arc. Furthermore, north of the COE, in the Pilatón Unit, some rocks presenting boninitic geochemical caracteristics have been described (13) (Fig. 6), a unit that could have genetical relationships with the MLO and the UT.

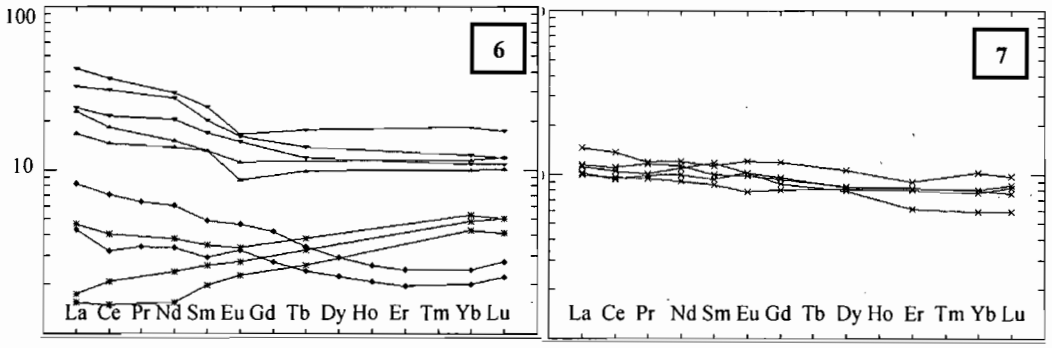

Chondrite-normalized REE abundances for:
***Fig. 6** MLO (◆) (Data from Reynaud et al., 1996), Boninite series (✳) and island-arc normal (▽) (Data from Van Thournout et al., 1991).*
***Fig. 7** Toachi Unit (cf. Macuchi Unit of Hughes and Bermúdez 1997)*

OCEANIC ISLAND ARC NARANJAL-SAN LORENZO-RICAURTE (Campanian)

The FSL of Campanian (6), the UN of Late Campanian (2) and the Ricaute-Altaquer sequence of Campanian (12) are geochemicaly basaltic andesites with affinity toleitic and/or calco-alkaline, they have REE models rich in LREE. With respect to MORB show depletion in Nb (Figs. 8, 9, 10), typical to subduction. The low values of Cr, Ni y Mg suggests that they didn't generate of primitive magmas, different than Albian arc. The values of TiO_2, Al_2O_3, Y and Zr, are normal to arc basaltic andesites, in conclution this suite have affinity with normal

UNDIFFERENT BASAMENT

In the Northwest Coast zone and next to Gulf of Guayaquil (Fig. 1), there are rocks mapped like the FP and UPS, but their age and geochemistry are not know; nevertheless, given their structural position the rocks in the north-west zone of the Coast should be related to the Caribbean-Colombian Oceanic Plateau of Late Cretaceous.

CONCLUSIONS

The following geodynamic domains can be recognized during the Cretaceous evolution of the Western Cordillera and Coastal plain of Ecuador: 1. An Early-Cretaceous oceanic plateau involving the FP and UPS; 2. An Albian to pre-Turonian toleitic-boninitic arc former to the extensive basin in the Late Cretaceous; 3. A Santonian-Campanian back-arc basin involving the UP North and a thick sedimentary sequence; and, 4. A Campanian-Maastrichtian normal island arc showing evolution from toleitic to calc-alkaline composition, overlying an oceanic floor of N-MORB. The recognized structural features define a right-lateral to transpression pattern where thrusting could be expected in spite of no field evidences.

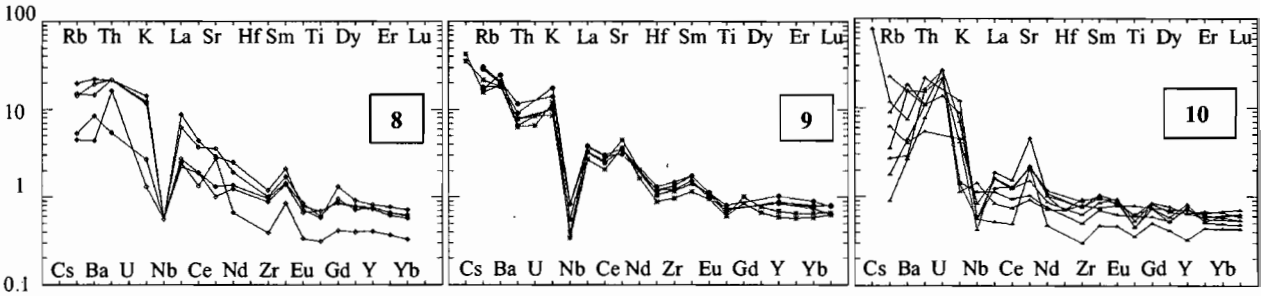

MORB-normalized trace element pattern for: ***Fig 8*** *Ricaute-Altaquer Sequence (Data from Spadea y Espinoza, 1996),* ***Fig 9*** *San Lorenzo Formation (Data from Reynaud et al,1999, Lebrat 1987),* ***Fig 10*** *Naranjal Unit (Data from Boland et al., 2000)*

REFERENCES

1) Bloomer, S. & Hawkins, J., 1987. **Contributions to Mineralogy and Petrology**, 97: 361-377
2) Boland, M., Pilatasig L., Ibadango, E., McCourt, W., Aspden, J., Hughes, R. & Beate, B., 2000. PRODEMINCA Report No. X: Geology of the Cordillera Occidental of Ecuador between 0° y 1°N. BGS, Nottingham-CODIGEM. Ecuador
3) Cosma, L., Lapierre, H., Jaillard, E., Laubacher, G., Bosch, D., Desmet, A., Mamberti, M., Gabriele, P., 1998. **Bulletin Societé Géologique de France**, 169 No.6: 739-751.
4) Gribble, R., Stern, R., Bloomer, S., Stuben, D., O'Hearn, T., & Newman, S., 1996. **Geochimica et Cosmochimica Acta**, 60, 12: 2153-2166
5) Hughes, R & Bermúdez, R. (1997). PRODEMINCA Report No. IV: Geology of the Cordillera Occidental of Ecuador between 0° y 1°S. BGS, Nottingham-CODIGEM. Ecuador
6) Jaillard, E., Soler, P., Carlier, G & Mourier, T., 1990. **Geol. Soc. London**, 147: 1009-1022.
7) Lebrat, M., Megard, F., Dupuy, C & Dostal, J.., 1987. **Bulletin of the Geological Society of America 99**: 569-578.
8) Litherland, M., Zamora, A.& Eguez, A., 1993. Nacional Geological Map of the Republic of Ecuador, scale 1:1000000, British Geological Survey, Nottingham and CODIGEM, Quito
9) McCourt, W., Duque, P., & Pilatasig, L., 1997. PRODEMINCA Report No. 3: Geology of the Cordillera Occidental of Ecuador between 1° and 2° S. BGS, Notthingham-CODIGEM, Quito
10) British Geological Survey & Corporacion de Desarrollo e Investigación Geológico-Minero y Metalurgica (BGS-CODIGEM). Mapas Geológicos de la Cordillera Occidental del Ecuador. Escala 1:200.000, Quito.
11) Reynaud, C., Jaillard, E., Lapierre, H., Mamberti, M. & Mascle, G., 1999.. **Tectonophisic** 307: 235-254.
12) Spadea, P., & Espinosa, A., 1996.; **Journal of South Earth Sciences**, 9, ½.: 79-90
13) Van Thournout, F., Hertogen, J. & Quevedo, L., 1992. **Tectonophysics** 205: 205-222

OROGENIC-SCALE GROUND WATER CIRCULATION IN THE CENTRAL ANDES: EVIDENCE AND CONSEQUENCES

T.E. JORDAN (1), L.V. GODFREY (2), N. MUNOZ (3), R. ALONSO (4), T. LOWENSTEIN (5), G. HOKE (6), P. PANNANONT (7), N. PERANGINANGIN (8), B.L. ISACKS (9), and L. CATHLES (10)

(1) Earth & Atmospheric Sciences, Cornell University, Ithaca, NY, 14853-1504, USA (tej1@cornell.edu)
(2) Earth & Environmental Sci, Lehigh University, Bethlehem, PA,. USA 18015 (lig5@Lehigh.edu)
(3) SIPETROL (UK) Ltd., St. Andrew's House, Woking Surrey, GU21 1EB, UK (nmunoz@sipetrol.co.uk)
(4) Univ. Nac. Salta, Buenos Aires 177, 4400 Salta, Argentina (rnalonso@sinectis.com.ar)
(5) Geological Science and Environmental Studies, Binghamton University, Binghamton, NY, 13902 USA (lowenst@binghamton.edu)
(6) Earth & Atmospheric Sciences, Cornell University, Ithaca, NY 14853-1504, USA (gdh7@cornell.edu)
(7) Earth & Atmospheric Sciences, Cornell University, Ithaca, NY 14853-1504, USA (pananon@geology.cornell.edu)
(8) Biological & Environmental Engineering, Cornell Univ., Ithaca, NY 14853, USA (np34@cornell.edu)
(9) Earth & Atm. Sci., Cornell University, Ithaca, NY 14853-1504, USA (bli1@cornell.edu)
(10) Earth & Atm. Sci., Cornell University, Ithaca, NY 14853-1504, USA (cathles@geology.cornell.edu)

KEY WORDS: halite, Atacama, groundwater, uplift, ignimbrites, paleolakes

INTRODUCTION

The Salar de Atacama, Chile, accumulated an estimated 3000 km³ of halite during the last roughly 5 million years. We propose that the principal water supply to the closed drainage salar during that time has been deep ground water (Fig. 1). It is the ground water that transports the Na, Cl, and associated ions to the salar, where evaporation under a hyperarid climate generates evaporite minerals. Precipitation infiltrates in the less arid Altiplano-Puna plateau, located E, N, and S of the Atacama basin, and flows as ground water toward into the Atacama basin. Ground water circulation from the Andean interior to the lowland flanks would have existed since uplift began but, we propose, the halite initiation near 5 Ma marks the time when the magnitude and form of the topography reached states similar to today's.

AGE AND VOLUME OF ATACAMA HALITE

The subsurface geology of the Salar de Atacama is constrained by hundreds of km of seismic reflection data (property of ENAP), a 5000 m deep borehole (Toconao-1) for which cuttings descriptions and wireline logs exist, and tens of cores ranging in length from 40 to 500 m (property of brine-mining company SQM). Direct age constraints come from U-series dates of halite in two SQM cores (Bobst et al., 2001; Lowenstein et al. in review) and a K-Ar date of an ignimbrite horizon in core 2106 in the SE zone of the salar (Bevacqua, 1991).

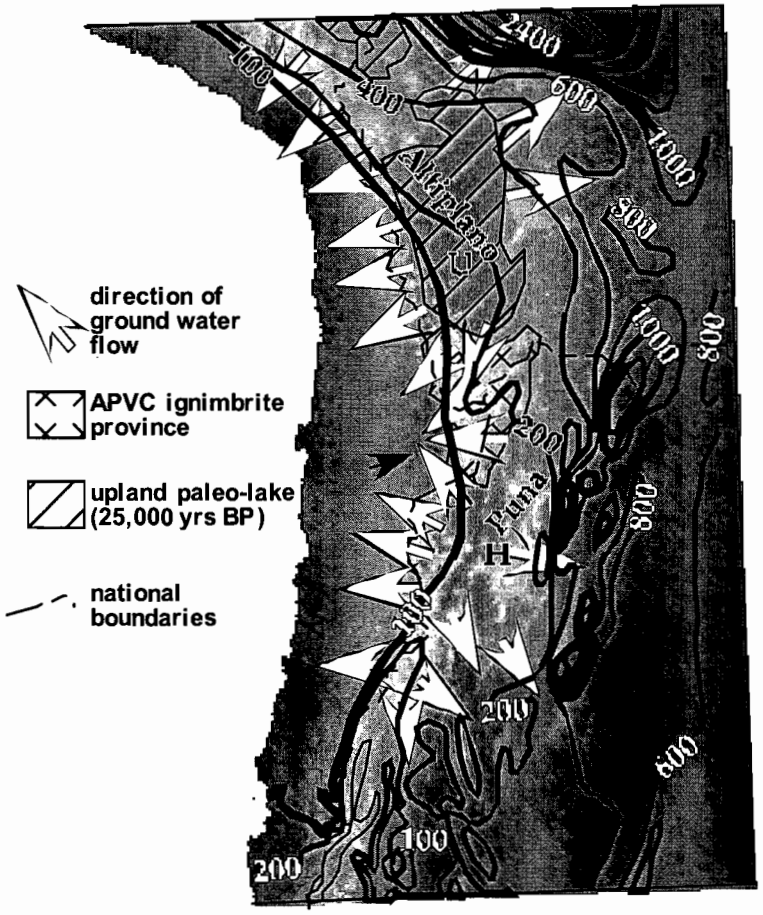

Figure 1. Grayscale topography of the Central Andes, showing location of Atacama Basin and major elements of the hydrology. White to light gray represents high elevations, mostly in the Altiplano-Puna plateau. Salars for which the history of late Pleistocene lakes is well documented are Uyuni (U), Hombre Muerto (M), and Atacama. Contours are mean annual precipitation (mm).

We mapped the base of the Halite Unit, as defined in Toconao-1, throughout the salar subsurface following reflection continuity (Jordan et al., in review). We also mapped 8 stratigraphic sub-sequences within the Halite Unit. Conversion of the seismic travel time to depth leads to the estimate that the volume of the Halite Unit is approximately 3000 km^3.

The ages of two Pliocene horizons are well constrained. First, the dated 3.1 Ma ignimbrite of core 2106 (Bevacqua, 1991) correlates with the 3.1 Ma Patao Ignimbrite and/or 3.2 Ma Tucucaro Ignimbrite, which cover broad regions immediately E and S of the salar (Ramirez and Gardeweg, 1982). We interpret a prominent negative-polarity reflection at the depth of 2106's dated ignimbrite as the seismic signal of ignimbrite. A reflection of similar character, likely also ignimbrite, occurs widely in the eastern periphery of the salar within Stratigraphic Subsequence 4. We correlate that seismically identified ignimbrite (?), which underlies the 3.1 Ma horizon and spans the length of the salar, with the 4.0 Ma Atana - Toconao Ignimbrites. Lindsay et al. (2001) showed that the Atana-Toconao Ignimbrites totaled some 2500 km^3 in volume east of the salar, and are 35 m thick in outcrop only 20 km east of the salar margin. Consequently, the thick and widespread Atana-Toconao Ignimbrite set is anticipated to persist into the salar region. At greater depths in the E and NE, similar reflection characteristics below Stratigraphic Subsequence 4 likely reveal other ignimbrites, but we lack criteria for assigning ages to specific horizons. Comparison of the base of the Halite Unit to the seismically-identified ignimbrites (?) reveals that the base of the Halite Unit is younger than the oldest ignimbrites(?). The oldest exposed ignimbrites are approximately 10 Ma N of the salar, although near the E margin of the salar the oldest exposed ignimbrites are 5.8 Ma (Gardeweg and Ramirez, 1987; DeSilva, 1989; Lindsay et al., 2001). We bracket the base of the Halite Unit as older than 4 Ma and younger than 5.8 Ma or, at greatest, 10 Ma.

GROUND WATER AND NaCl

The majority of halite in the upper 200 m near the center of the salar crystallized a few tens of centimeters beneath the solid top crust of the desiccated salar, at the water table - air interface (Lowenstein et al., in review)). Times during the late Quaternary when Salar de Atacama was a salt lake correlate well with the history of high lake stands in the southern Altiplano (Bobst et al., 2001; Lowenstein et al., in review; Baker et al., 2001) but are markedly out-of-phase with the precipitation history of the Salar de Atacama drainage basin (Betancourt et al., 2000). This is easily reconciled if Salar de Atacama is fed by ground water, rather than by surface water, and if the ground water source is the plateau. A source of the water in the Altiplano is consistent with the isotopic composition of paleo-lake waters trapped as fluid inclusions (Godfrey et al., in review).

The traditional explanation of the upper Neogene halite has been its derivation by dissolution of the Oligocene-lower Miocene San Pedro Formation halite. In contrast, we interpret that the original volume of halite in the San Pedro was much less than the 3000 km^3 in the Plio-Quaternary Halite Unit. Instead, we propose that much of the NaCl must be delivered to the Atacama basin from other sources, including dehydration of the underlying Nazca plate, residual waters distilled from arc magmas, and surface weathering and subsurface leaching of Cl from typical crustal bedrock. For the modern drainage basin we estimate that the sum of NaCl supplied by operation of all of these processes is only a fraction of the halite now in the Atacama basin. However, the volume of halite in the Atacama basin can be accounted for if the source area of the solutes greatly exceeds the surface drainage area of the basin, and if the ground water that feeds the salar circulates deeply.

Deep circulation of ground water sourced in the Altiplano-Puna plateau toward the Chilean lowlands is the average response to the high elevation of the plateau. Indentation of the western slope of the plateau by the Atacama basin focuses flow toward the Atacama basin. Consequently, the Atacama basin receives an enhanced flux of ground water and dissolved ions. Ground water flow through hundreds of km of rock, to depth on the order of 10 km, would mobilize solutes from dehydration and/or magmas, and react with average crustal rock.

We hypothesize that halite came to dominate the Salar de Atacama basin when the topography reached a state similar to today's. An increase in elevation of the western half of the Andes Mountains between 10 and 5 Ma is consistent with major shortening of the upper crust along the Subandean eastern flank of the Andes commencing near 9 Ma (Echavarría et al., in review).

The Altiplano-Puna Volcanic Complex lies between the major late Pleistocene lakes of the Altiplano and the Atacama basin, and many of the largest ignimbrite eruptions were contemporaneous with halite accumulation. Topographically driven ground water flow would pump very large amounts of Altiplano-derived water through the APVC crust, possibly contributing to the wet conditions needed for explosive eruptions (Lindsay et al., 2001).

REFERENCES

Baker, P. A., Rigsby, C. A., Seltzer, G. O., Fritz, S. C., Lowenstein, T. K., Bacher, N. P., Veliz, C., 2001, Tropical climate changes at millennial and orbital timescales on the Bolivian Altiplano: Nature, v. 409, 698-701.

Betancourt, J.L., Latorre, C., Rech, J.A., Quade, J., and Rylander, K.A., 2000, A 22,000-year record of

monsoonal precipitation from Northern Chile's Atacama desert: Science, v. 289, p. 1542-1546.

Bevacqua, P., 1991. Geomorfología del Salar de Atacama y estratigrafía de su núcleo y delta, segunda región de Antofagasta, Chile, (Geomorphology of the Salar de Atacama, and stratigraphy of the nucleus and delta; Second region of Antofagasta, Chile), Masters Thesis, Universidad Católica del Norte, Antofagasta, Chile, 284 p.

Bobst, A.L., Lowenstein, T.K., Jordan, T.E., Godfrey, L.V., Hein, M.C., Ku, T.-L., and Luo, S., 2001, A 106 ka paleoclimate record from the Salar de Atacama, northern Chile: Palaeogeography, Palaeoclimatology, Palaeoecology, v. 173, p. 21-42.

De Silva, S.L., 1989, Geochronology and stratigraphy of the ignimbrites from the 21°30'S to 23°30'S portion of the Central Andes of northern Chile: Journal Volcanology and Geothermal Research, v. 37, p. 93-131.

Echavarria L., Hernandez R., Allmendinger R., and Reynolds, J.R., in review, Subandean thrust and fold belt of northwestern Argentina: Geometry and timing of the Andean evolution: submitted to GSA Bulletin

Gardeweg, M., and Ramírez, C.F., 1987, La Pacana caldera and the Atana Ignimbrite -- a major ash-flow and resurgent caldera complex in the Andes of northern Chile: Bull. Volcanology, v. 49, p. 547-566.

Godfrey, L.V., Jordan, T.E., Lowenstein, T.K., Li, J., Bobst, A.L., Hein, M.C., Ku,T-L. , Luo, S., Stable isotope constraints on the transport of water to the Andes between 20° and 30°S during the last glacial cycle: in review for Palaeogeography, Palaeoclimatology, Palaeoecology

Jordan, T.E., Muñoz, N.,Hein, M.T.,Lowenstein, T., Godfrey, L.V., and Yu, J., in review 2001, Active faulting and folding without topographic expression in an evaporite basin, Chile: submitted to GSA Bulletin

Lindsay, J.M., Schmitt, A.K., Trumbull, R.B., De Silva, S.L., Siebel, W., and Emmermann, R., 2001, Magmatic evolution of the La Pacana caldera system, Central Andes, Chile: compositional variation of two cogenetic, large-volume felsic ignimbrites: Journal of Petrology, v. 42, p. 459-486.

Lowenstein, T.K., Hein, M.C., Bobst, A.L., Jordan, T.E., Ku, T.-L., and Luo, S., in review, Paleoclimate records from closed-basin lake sediments: Assessment of stratigraphic completeness, tectonic influences and climate controls, Salar de Atacama, Chile: Journal of Sedimentary Research (submitted August, 2001)

Ramírez, C., and Gardeweg, M., 1982, Hoja Toconao, Región de Antofagasta: Servicio Nacional de Geología y Minería, Carta Geológica de Chile, no. 54, 122 p. plus map at 1:250,000.

LATE PLEISTOCENE AND HOLOCENE TEPHROSTRATIGRAPHY AND CHRONOLOGY IN SOUTHERN PERU

Etienne JUVIGNE(1), Jean-Claude THOURET(2), , Jersy MARIñO(3), Marcela MOSCOL(4), A. LEGELEY-PADOVANI(5), Isabelle LOUTSCH(2)

(1)Laboratoire de Géomorphologie, Université de Liège, 4000 Liège, Belgique (ejuvigne@ulg.ac.be)
(2)Laboratoire Magmas et Volcans (UMR 6524 CNRS), Université Blaise Pascal, 63038 Clermont-Ferrand, France (thouret@opgc.univ-bpclermont.fr)
(3)Instituto Geofisico del Peru, Calle Clatrava 216, Urb. Camino Real, La Molina, Lima 12, Peru (jrmasa@axil.igp.gob.pe)
(4)Université Montpellier II, Institut des Sciences de l'évolution, UMR CNRS 5554, 34095 Montpellier cedex 05 (mcmakosso@care2.com)
(5)Institut de Recherche pour le Développement, Centre Ile de France, 34 rue Henri-Varagnat, 93170 Bondy cedex, France (Annick.legeley-Padovani@bondy.ird.fr)

KEY WORDS: tephra, stratigraphy, chronology, Late Pleistocene, Holocene, Peru.

INTRODUCTION

Multidisciplinary investigations of stratigraphic sections and cores extracted from peat-bogs and lakes in the Western Cordillera of the southern Peruvian Andes, have enabled us to trace more than 40 tephras over the past 50,000 ^{14}C years. At least eight pumice-fall deposits are widespread (>1,000 km^2) and voluminous (≥1 km^3), as shown in bold squares in Table 1.

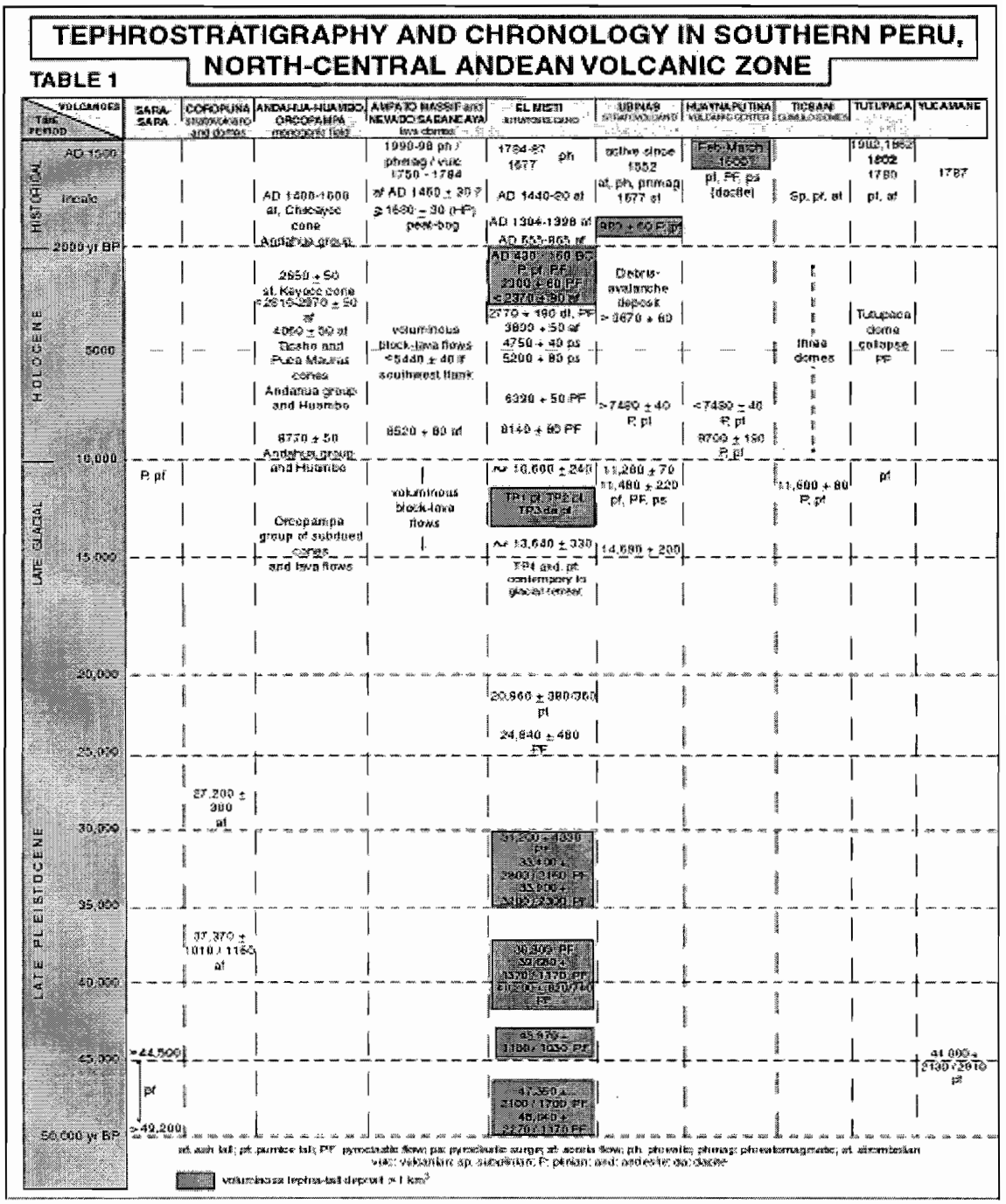

LATE PLEISTOCENE TEPHRA

Late Pleistocene tephra have been dated on the west flank of Nevado Sara Sara between ca. 49,200 and 44,500 yr BP and ca. 44,000 yr BP on the south flank of Yucamane. Nevado Coropuna has probably been active before the Late Glacial; ashfalls in a soil section outside of the Last Glacial Maximum moraines yielded ^{14}C ages of ca. 27,200-37,370 yr BP. The composite Misti edifice comprises a stratovolcano termed Misti 1, partially overlapped by two stratocones termed Misti 2 and 3 (≤112 ka), and a summit cone Misti 4 ≤11 ka. Sustained explosive eruptions have delivered at least 12 pumice falls during the past ca. 50,000 years (Thouret et al., 2001b).

LATE-GLACIAL AND HOLOCENE TEPHRAS

Two cores extracted from the *salar* of Laguna Salinas, 35 km east of Arequipa, include 7 tephra-fall deposits from Huaynaputina, Misti, and Ubinas over the past 15,000 years (Juvigné et al., 1997). Two recent tephra falls are found around the Ticsani domes: a dacitic pumice-fall deposit of 0.4 km^3 has been dated ca.11, 600 yr BP; bombs and pumice preceding the youngest dome overlie the AD 1600 Huaynaputina ash. The recent explosive behaviour of Ubinas produced several tephra falls, including two widespread plinian pumice falls. The pumice-fall deposit >7840 yr BP and the ca. 980 yr BP-old pumice-fall deposit have a volume >1 km^3 and may be linked to the formation of the summit caldera (Rivera et al., 1998). The peat sequence in the Sallalli peat-bog 10 km SE from the Nevado Sabancaya includes 4 tephra-fall layers: the AD 1600 Huaynaputina ash, an AD 1200-1400 Sabancaya/Ampato ash, a thin black ash probably from Misti ca. 2,370 yr BP, and a Sabancaya/Ampato ash of ca. 8,550 yr BP (Juvigné et al., 1998).

HISTORICAL TEPHRAS

The last subplinian explosive episode ca. 2,300-2,050 yr BP at Misti produced pumice-fall and flows ca. 1 km^3 in volume. Spanish chronicles refer to an explosive eruption ca.AD 1440 and 1470: the small volume 'Pachacútec ash' affected the Incaic towns of Cayma and Chiguata (Thouret et al., 1999a, 2001a). The AD 1600 Huaynaputina plinian eruption produced the most widespread and voluminous (12 km^3) pumice-fall deposit in the Andes in historical times (Thouret et al., 1999b). Tephra falls, pyroclastic flows, and surges disrupted life ~60 km around the volcano and ashfall was reported 250-500 km away in south Peru, west Bolivia and north Chile. Persistent eruptions of Nevado Sabancaya have dispersed a small volume of ash from May 1990 until 1998 as far as 20 km towards the east (Thouret et al., 1995, 2001b).

CONCLUSIONS

In sum, 1) heavy ashfall can recur every 500 to 1500 years on average but small ashfall can occur on a 100-years basis; 2) voluminous pumice-fall deposit can occur every 2000 to 4000 years on average; 3) three voluminous (≥1 km^3) plinian eruptions occurred over the past 2,000 years; (4) the large-scale plinian and ignimbritic eruption of Huaynaputina produced 12 km^3 of tephra and caused havoc and famine in southern Peru 400 years ago.

REFERENCES

Juvigné E., Thouret J.-C., Gilot E., Gourgaud A., Legros F., Uribe M., Graf K., 1997. Etude téphrostratigraphique et bioclimatique du Tardiglaciaire et de l'Holocène de la Laguna Salinas, Pérou méridional. Géographie physique et Quaternaire (Canada), 51, 2: 219-231.

Juvigné E., Thouret J.-C., Gilot E., Leclercq L., Gourgaud A., 1998. L'activité du volcan Nevado Sabancaya (Pérou) au cours de l'Holocène.Quaternaire, Hommes et Volcans, 9, 1, 45-51.

Rivera M., Thouret J.-C. y Gourgaud A., 1998. Ubinas, el volcan más activo del Sur del Perú desde 1550: geología y evaluación de las amenazas volcánicas. Boletin Sociedad Geológica del Perú, 88, 53-71.

Thouret J.-C., Gourgaud A., Uribe M., Rodriguez A., Guillande R., Salas G., 1995. Geomorphological and geological survey, and spot remote sensing of the current activity of Nevado Sabancaya stratovolcano (south Peru): assessment for hazard-zone mapping. Zeit. für Geomorphology, 39, 4, 515-535.

Thouret J.-C., Suni J., Eissen J.-Ph., Navarro P., 1999a. Assessment of volcanic hazards in the Arequipa area based on the eruptive history of Misti volcano, Southern Peru. Zeitschrift für Geomorphology, Suppl.-Bd.114, 89-112.

Thouret J.-C., Davila J., and Eissen J.-Ph., 1999b. Largest historic explosive eruption in the Andes at Huaynaputina volcano, south Peru. Geology, 27, 5, 435-438.

Thouret J.-C., Suni J., Finizola A., Fornari M., Legeley-Padovani, and Frechen M., 2001a. Geology of El Misti volcano near the city of Arequipa, Peru. Accepted to Geological Society of America Bulletin, June 2001.

Thouret J.-C., Juvigné E., Loutsch I. et Chávez Chávez J.A., 2001b. Activité volcanique historique et sacrifices humains chez les Incas au Pérou méridional. In: E. Juvigné & JP Raynal, eds.,Tephras : chronologie/chronology, Arqueologie/arquaeology, p. 219-226, Les dossiers de l'Arquéo-Logis n°1, CDCRAD, Goudet.

ENDOGENEOUS ARC-RELATED PROCESSES AND THEIR FINGERPRINTS IN LAKE SEDIMENTS
- LONQUIMAY BASIN, SOUTH-CENTRAL CHILE

Helga KEMNITZ

GeoForschungsZentrum Potsdam, Telegrafenberg, D-14473 Potsdam, e-mail: heke@gfz-potsdam.de

KEY WORDS: Chile, Miocene, lake sediments, stratigraphy, tectonic control, detritus

INTRODUCTION

In the study area, main control on the pre- and syn-sedimentary dynamic processes of basin formation and filling was exerted by endogeneous processes related to the subsidence and exhumation of the magmatic arc. Early Late Cretaceous exhumation of the basement, including Mid - to Late Mesozoic magmatic rocks, and a synchronous closure of marine back-arc basins was followed by a renewed period of strongly increasing convergence/subduction rate (Drake, 1976). Bound to the reorganization of the South Pacific plates in Late Oligocene, which caused extensional tectonics in the magmatic arc of the Central and Southern Andes, a chain of Oligocene - Miocene pull-apart basins opened (Somoza, 1998). The Lonquimay Basin (37°45´ and 39° S), which represents a continental intra-arc basin (Cisternas & Diaz, 1985), is one of the newly formed Cura-Mallín subbasins.

The deposits of the Lonquimay Basin are built of alternating fluvial to lacustrine siliciclastic and calcarenitic sediments, pyroclastic rocks, and debris flows of more than 2000 m thickness in an eastern and of at least 1400 m in a western sediment pile. The uppermost Miocene formation has been reduced in thickness by denudation since post-Miocene times. Its upper boundary is obscured by discordantly overlying lava flows of Pliocene age. Synsedimentary, the entire lacustrine succession images tectono-magmatic triggered variations of the lake level and periods of non-sedimentation.

Referred to short-time lowstands and other local, small-scaled events throughout the depositional record, the mountaineous humid, continental climate also had some, but minor impact. Climate and vegetation obviously steered mainly lateral and vertical facies changes. Thus, the stratigraphic division of the Lonquimay Formation into four members (LON I - IV; Cisternas & Diaz, 1985) has been modified and a tectonostratigraphic subdivision introduced. Detrital component analysis has proved to be an important tool to clarify the stratigraphic positions of problematic outcrops, especially, if lithologic markers are lacking.

DISCUSSION AND CONCLUSIONS

The Lonquimay Basin has existed morphologically at least since lowermost Miocene, filled with lava flows interfingering the fluvial - alluvial silicilastics of LON I, the lateral equivalents of which at the northern basin margin are coal beds (Cisternas & Diaz, 1985). Both lithologies indicate long-lasting subsidence. The sandstones and conglomerates already contain the complete spectrum of the Jurassic basement that was uplifted during extensional tectonics before the Lower Miocene.

Continuous basin deepening and termination of nearby volcanic activity led to deeper lake basin sequences in LON II1. This sequence can be connected to a change in the local tectonic setting of the Lonquimay Basin, with an apparent abrupt isolation from the basement source area evidenced by detrital fragments. From LON II1 (Lower Miocene) up to LON III3 (uppermost Middle Miocene), the detrital input is widely restricted to short-distance transport of volcanogenic material, with increasing portions of redeposited fragments in LON II2. This might have been due to synsedimentary seismic activity, related to movement along the reactivated Liquiñe-Ofqui Fault Zone, which has a contact with the Jurassic basement to the west of the Lonquimay Basin. Intercalated layers of dilute volcaniclastic mass flows in LON II1 emphasize the denudation dominated character of this period.

With LON II2, the lake basin becomes shallower. Damming of the lake by the surrounding volcanoes and simultaneous growth of relief eventually resulted in lake filling in LON III3. Arc related volcanism, very likely coupled with seismic activity is indicated by proximal detrital avalanches and volcaniclastic mass flows, especially from LON III1 on. The beginning of this latter sequence, controlled by volcanogenic processes, is marked by bombs and lapilli occuring in palustral sediments in the western profile, increasing both laterally and vertically with time, followed by lava breccias in LON III2. In the eastern profile only discordant volcanic breccias of somewhat younger age (?LON III2) appear, showing that the area of immediate volcanic activity is restricted to the west to northwest (cf. Wall, 1993).

A temporary increase of thicknesses of the western sediment pile compared to the eastern one seems to support the assumption of Carpinelli (2000) that during Lower to upper Middle Miocene the basin subsided more in the west. Deltaic siliciclastic of LON III3 still show the basin to be isolated as they contain exclusively detrital components from the preceding Middle Miocene volcanic rocks or those from reworked older Miocene volcanism.

LON IV1 enters into another local tectonic setting. Compared to LON I, the lithoclast contents of the fluvial - alluvial siliciclastic sequence of LON IV1 indicates new access to the basement as a source rock area from both the southeast and southwest, but still contains parts of the mineralogy typical for the Middle Miocene volcanism.

The post-sedimentary history of the Lonquimay Formation is one of compressional tectonics and uplift. The Lonquimay Formation is characterized by undulating open folds of small amplitudes (meter- to decameter-scale) and half-wavelength of a few 100 m. This is thought to be the result of compressional movements along the Liquiñe-Ofqui Fault Zone and across the arc in the Lower Pliocene (Rosenau, this volume). Furthermore,

overthrusting of marine Jurassic successions on LON IV2, exposed in the southeastern part, was probably synchronous with this compressional process.

The principal E- to ESE-dip of bedding planes is a further postsedimentary structural feature of the Lonquimay Formation. It may have resulted from block tilting, in context with uplift of the western to northwestern block adjoining the Liquiñe-Ofqui Fault Zone between 37° to 39° S, subsequent to folding. Synchronously or subsequently, isolated blocks of the Miocene succession were relatively uplifted mainly in the west, along normal faults of a general E - W strike.

REFERENCES

Carpinelli, A. A. (2000): Analisis estratigrafico, paleoambiental, estructural y modelo tectono-estratigrafico de la cuenca de Cura-Mallín. VIII y IX Región, Chile - Provincia Del Neuquén, Argentina. - unpubl. MD, Universidad de Concepción, Departamento de Ciencias de la Tierra, Chile, 158 p.

Cisternas, M. E. & Diaz, L. L. (1985): Los depósitos terciarios lacustres de Lonquimay, Chile. - Zbl. Geol. Paläont. I, Stuttgart, 1985: 9/10, 1351 - 1362

Drake, R. E. (1976): Chronology of Cenozoic igneous and tectonic events in the central Chilean Andes; latitudes 35 degrees 30' to 36 degrees S. - Journal of Volcanology and Geothermal Research, Amsterdam, 1: 3, 265-284

Rosenau, M. (this volume): The Liquiñe-Ofqui Fault Zone - stretching between the oroclines ?

Somoza, R. (1998): Updated Nazca (Farallon) - South America relative motions during the last 40 My: implications for mountain building in the central Andean region. Journal Of South American Earth Sciences 11: 3, 211-215

Wall, R. (1993): Sistema depositacional deltaico - lacustre en el cerro Rucañanco (38°38´S; 71°08´W), Mioceno de Lonquimay, Chile. - unpubl. MD, Universidad de Concepciòn, Departamento de Ciencias de la Tierra, Chile, 180 p.

TECTONICS OF THE TRES CRUCES BASIN, EASTERN CORDILLERA, NORTHERN ARGENTINA: SEISMIC AND OUTCROP EVIDENCE OF INVERTED CRETACEOUS NORMAL FAULTS

Jonas KLEY (1), Eduardo A. ROSSELLO (2), César R. MONALDI (3), Björn HABIGHORST (4)

(1) Institut für Geowissenschaften, Universität Jena, Burgweg 11, D-07749 Jena, Germany, email: kley@geo.uni-jena.de
(2) CONICET-Depto. Cs. Geológicas, Universidad de Buenos Aires, Pabellón II, Ciudad Universitaria. 1428 Buenos Aires, Argentina, email: rossello@gl.fcen.uba.ar
(3) Universidad Nacional de Salta-CONICET, Buenos Aires 177, 4400 Salta, Argentina
(4) Geologisches Institut, Universität Karlsruhe, Kaiserstr. 12, D-76131 Karlsruhe, Germany

KEY WORDS: Eastern Cordillera, Argentina, Seismic lines, Inversion tectonics, Transverse structures

INTRODUCTION

The Tres Cruces Basin is located in northern Argentina, in the westernmost part of the Eastern Cordillera where it borders the Puna plateau. This basin originated in Eocene time, very probably as part of a much more extensive basin (Jordan and Alonso, 1987) and further developed into a thrust-bounded syntectonic depression (ramp basin) that was filled by up to 5 km of locally derived clastic sediments. Deposition and deformation in the Tres Cruces Basin apparently ceased in the Middle Miocene. Its Eocene to Miocene infill disconformably overlies Paleocene strata belonging to the post-rift stage of the Cretaceous to Paleogene Salta rift and exhibits an overall upward coarsening trend. Several unconformities have been described from this succession and correlated with regional tectonic phases (Boll and Hernández, 1986) but the contacts between different units are always conformable on outcrop scale. Today, the Tres Cruces Basin is overthrust by the regional El Aguilar thrust sheet from the west. The eastern border is structurally more varied and marked by a monocline or west-verging thrust faults. Within the basin, two synclinal zones to the west and east are separated by a central anticlinal high (Cerro Colorado trend). In detail, however, the internal structures are extremely variable along strike. Sigmoidal structure contours are common. Fold axes often plunge steeply, producing abrupt, box-shaped fold terminations. None of the internal structures can be traced along the length of the basin without lateral offset or change in structural style. For example, the central high switches rapidly from a simple east verging thrust sheet to a broad, short, doubly plunging anticline. The most pronounced structural changes are aligned on two NW trending oblique zones, whose continuity suggests an influence of basement faults on the higher level structures. The Tres Cruces basin has been explored for hydrocarbons in the 80s, resulting in a dense network of seismic lines and drilling of four wildcat wells.

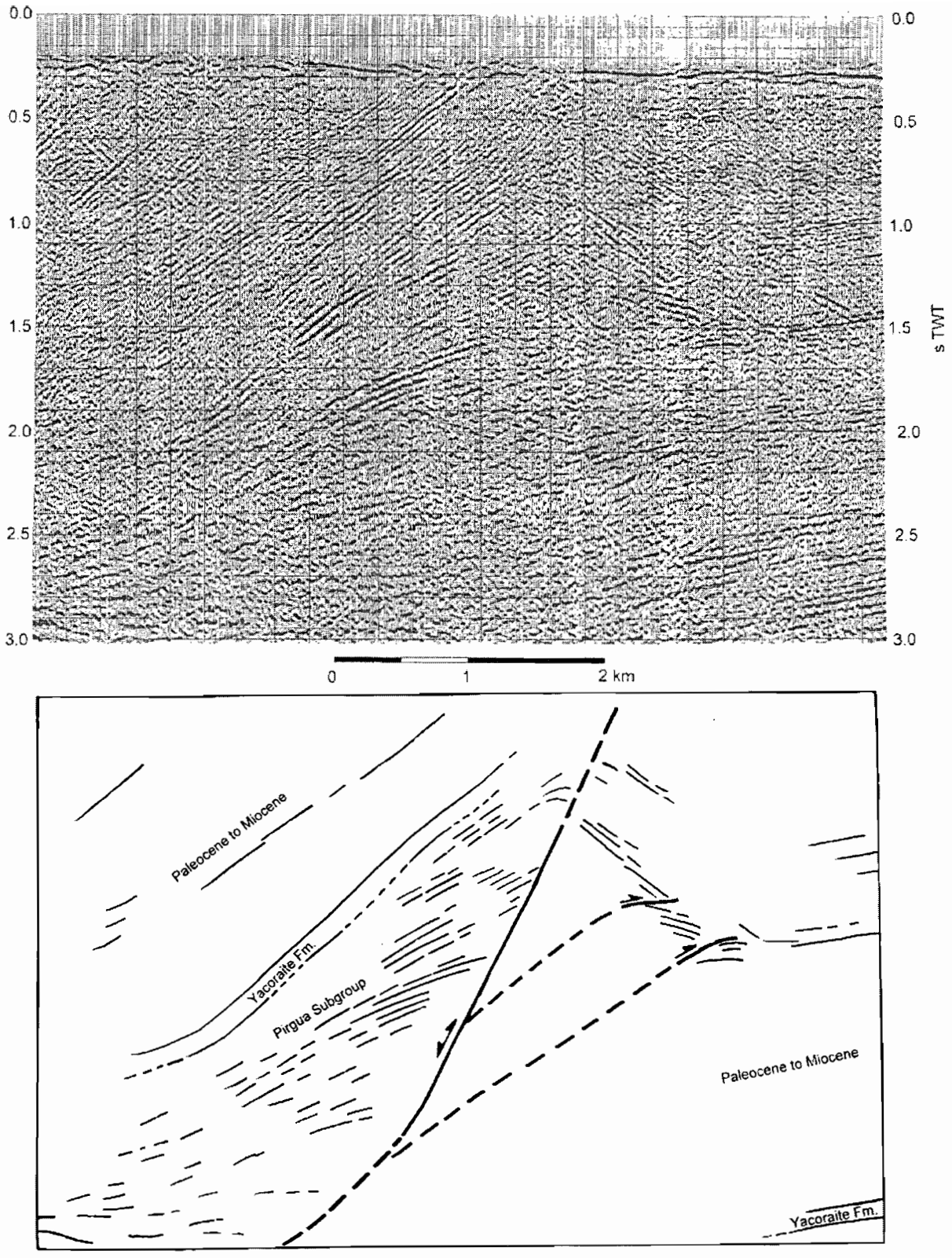

Figure 1: Detail from seismic line in the Tres Cruces basin (above) and interpreted line drawing (below). Notice the fanning reflector pattern in the syn-rift Pirgua subgroup.

Some seismic lines have been published with interpretations from different authors (Boll and Hernández, 1986; Gangui and Götze, 1996; Gangui, 1998; Coutand et al. 2001). So far, only Gangui and Götze (1996) and Gangui (1998) have interpreted inversion structures and high-angle faults at the northern termination of the Tres Cruces basin. The interpretations of lines across the center of the basin propose a simple structural style with listric thrust faults that sole into a detachment in Early Paleozoic rocks or the underlying very low grade metamorphic schists, contrasting with the complexity evident in map view.

NORMAL FAULT REACTIVATION

On most seismic lines, the stratigraphy is clearly imaged down to the prominent reflector of the Yacoraite limestone horizon near the base of the post-rift succession. Below, the interpretation becomes more ambiguous. Nevertheless, a close examination in some cases reveals fanning reflector patterns immediately beneath the Yacoraite reflector and adjacent to the major faults (Figure 1). We interpret this to indicate Pirgua synrift strata thickening into fault-bounded half grabens and hence an origin of thrust faults in the Tres Cruces Basin as Cretaceous listric normal faults. From the thickness variations of the Pirgua subgroup across them, we estimate the maximum normal offset on these faults to have been as high as 1500 m.

Observations on structures outcropping farther east along the Quebrada de Humahuaca valley suggest that also the oblique NW trending lineaments segmenting the Tres Cruces basin may have been established during Cretaceous rifting. Thickness values of the Pirgua synrift succession jump across W to WNW trending faults in Quebrada de Humahuaca. Offsets on these faults which today appear as strike slip faults due to rotation by Neogene folding and thrusting are up to 2500 m. Thin or absent Pirgua sections often correlate with incomplete Paleozoic successions, indicating erosion from uplifted hanging walls during the early stages of rifting.

CONCLUSIONS

The highly variable directions of faults that were demonstrably active during the main phase of Cretaceous rifting corresponds with the complex overall geometry of the Salta rift system (e.g. Salfity and Marquillas, 1994) and suggests a poorly defined extension direction, with S_{Hmax} practically equal to S_{hmin}. It is not yet clear if a sequence of different extension directions can be established.

Although Cretacous normal faults striking parallel to the Neogene Andean structural grain can be identified in the subsurface, most examples that have been described from outcrops are transverse or oblique structures. This probably implies that many normal faults have been strongly modified during inversion. In particular, the hanging-wall cutoff angles are likely to have decreased by shear associated with folding as the thrust sheets moved over listric fault planes. We suspect that a substantial number of former normal faults has passed unnoticed, and that the structural geometry of the rift system remains to be fully understood.

REFERENCES

Boll, A., Hernández, M. 1986. Interpretación estructural del área Tres Cruces, Boletín de Información Petrolera, Junio 1986, 2-14.

Coutand, I., Gautier, P., Cobbold, P.R., de Urreiztieta, M., Chauvin, A., Gapais, D., Rossello, E.A., Lopez Gamundi, O. 2001. Style and history of Andean deformation, Puna Plateau, northwestern Argentina. Tectonics 20(2), 210-234.

Gangui, A.H. 1998. A combined structural interpretation based on seismic data and 3-D gravity modeling in the Northern Puna / Eastern Cordillera, Argentina. Berliner Geowiss. Abh. (B) 27, 176 pp.

Gangui, A., Götze, H.-J. 1996. The deep structure of the northern Puna, Argentina – constraints from 2D seimic data and 3D gravity modeling. XIII Congr. Geol. Argent. Y III Congr. de Exploración de Hidrocarburos, Actas II, 545-565.

Jordan, T.E., Alonso, R.N. 1987. Cenozoic stratigraphy and basin tectonics of the Andes mountains, 20°-28° south latitude. AAPG Bull. 71(1), 49-64.

Salfity, J.A., Marquillas, R.A. 1994. Tectonic and sedimentary evolution of the Cretaceous-Eocene Salta Group basin, Argentina. In: J.A. Salfity (ed.) Cretaceous tectonics of the Andes, Vieweg, Braunschweig, 266-315.

DETERMINATION OF EROSION RATES IN A DECOUPLED RIVER AND PEDIPLANE SYSTEM IN THE CENTRAL ANDES, NORTHERN CHILE

F. KOBER (1), F. SCHLUNEGGER (2), R. WIELER (3), S. IVY-OCHS (4), G. SIMPSON (5)

(1) Institute of Geology, ETH Zürich, Sonneggstr. 5, 8092 Zürich, kober@erdw.ethz.ch
(2) Institute of Geology, ETH Zürich, Sonneggstr. 5, 8092 Zürich, schlunegger@erdw.ethz.ch
(3) Institute of Geochemistry and Mineral Resources, ETH Zürich, Sonneggstr. 5, 8092 Zürich, wieler@erdw.ethz.ch
(4) Institute of Particle Physics, ETH Zürich, Hönggerberg, 8093 Zürich, ivy@particle.phys.ethz.ch
(5) Institute of Geology, ETH Zürich, Sonneggstr. 5, 8092 Zürich, simpson@erdw,ethz.ch

KEY WORDS: cosmogenic nuclides, Central Andes, landscape evolution

RESUME

Nous présentons des valeurs de taux érosifs mesurés sur des surfaces dans la région d'Arica dans le nord du Chili, l'une des régions les plus arides du globe. Ces taux d'érosion ont été déterminés par la méthode des nucléides cosmogéniques stables, ainsi que des isotopes radiogéniques. Les taux d'érosion mesurés atteignant approximativement 200 mm/ma, sont environ 1000 fois inférieurs aux taux d'érosion fluviatile observés dans les vallées adjacentes. Les rivières coulant dans ces vallées prennent leur source dans les zones élevées des Andes. Il semble que les contrastes entre les taux d'érosion superficielle et les taux érosifs observés dans les vallées adjacentes soient dus au gradient climatique caractérisé par des conditions hyperarides dans la cordillière côtière et un climat semi-aride dans les zone plus élevées des Andes. Ce gradient climatique est tenu comme responsable du découplage existant entre l'érosion fluviatile et les processus superficiels induisant des taux érosifs extrêmement différents.

Introduction

The Central Andes of Northern Chile are a tectonically active mountain belt with a high topographic gradient and an orogen-parallel climatic system that is characterized by hyperarid conditions in the Coastal Cordillera, and semiarid climate in the high Andes. For the situation in Northern Chile, supergene enrichments of porphyry copper deposits have been used to infer a Middle Miocene age for establishment of the present-day dry climatic conditions (Alpers & Brimhall, 1988). It was then believed that due to the dry climate, erosion became negligible, which in turn was hold responsible for formation of stable landscapes since the early phases of the Andean growth (Mortimer 1980, Uhlig 1999). In favour of such an interpretation are the abundant

remnants of surfaces formed between the Middle Miocene and the Pliocene. Recently, however, it was argued that climate hasn't been completely hyperarid since the Miocene. Specifically, Hartley & Chong, (2002) revealed that Late Pliocene climate fluctuations led to higher erosion rates during this period, which in turn prohibited landscapes to remain stable also in hyperarid climatic zones (Zhang et al., 2001). In contrast, it has been proposed that erosions rates especially in fluvial systems are enhanced if climate shifts towards more arid conditions. This is considered to be the case because an augmentation of aridity appears to increase the frequency of large floods leading to enhance rates of fluvial erosion (Molnar, 2001).

As outlined above, the Arica area that is situated in Northern Chile displays such remnants of surfaces that document the various stages of landscape formation and, therefore, the evolutionary steps of Andean orogenesis. These surfaces are characterized by planar geometries tens to hundreds of km^2 wide that generally dip at a low angle (<1°) towards the coast. In addition, smooth ridges and U-shaped valleys found on these surfaces result in formation of a local relief of ca. 50 m. In the Arica region, these surfaces are made up of top of the Oxaya ignimbrite sheets [formation age of the upper ignimbrite sheet of 19.3My (Walfort et al., 1995) places a lower limit on the age of surface formation] and by the top of the Diablo Fm. that has a fluvio-lacustrine origin (Garcia et al, 1999). These surfaces are cut by major rivers (e.g. Lluta and Azapa rivers) that are sourced in the high Andes and that have formed >1500 m deep valleys.

In this project, we determine exposure ages and erosion rates on the gently dipping planar surfaces and in the deeply incised valleys of the Arica region. Specifically, we intent of determine how the present-day gradient of precipitation to extremely dry from the Coastal Cordillera to semiarid in the high Andes is mirrored in the pattern of erosion rates on the surfaces and in the valleys. We also aim at extracting information about the historical record of surface erosion in that area as a function of climate change. As a tool, we use the technique of cosmogenic nuclides (radionuclides and stable cosmogenics) for determination of exposure ages and erosion rates. If implemented in a digital elevation model, the results yield information about the spatial and temporal pattern of rates of landscape forming processes.

Preliminary Results

Apparent ^{21}Ne minimum ages measured on quartz minerals that are extracted from rocks exposed on the top the gently dipping surfaces range from the Pliocene to the Pleistocene, much younger than expected [>10 Ma based on regional geological information (e.g. Uhlig, 1999; Wörner et al., 2002)]. It is important to note here that the boundary conditions for age determination comprise correction for surface uplift of 0.2mm/yr (Gregory Wodzicki, 2000) and assumption of zero or negligible erosion. In addition, these young 'exposure' ages display a distinct pattern that correlates with the modern distribution of humidity and precipitation, i.e. the more rainfall the lower the ages. Specifically, ages become apparently younger as samples are taken at higher altitudes. It appears, therefore, that the assumption of zero (or at least negligible erosion) on even the flattest surface in the driest area is certainly not valid. Consequently, we estimated erosion rates by applying a combination radionuclide (^{10}Be) with a stable cosmogenic nuclide (^{21}Ne) studies that allow estimations of long-term (however, with unknown range) erosion rates (Ivy-Ochs, 1996). This is the case because radionuclides have experienced the same exposure history as the stable cosmocenic nuclides, but they record a different history of exposure (which also includes erosion rates) due to the half-life decay. Using this methodology, we determine

erosion rates in the order of 200mm/my for the supposedly several My-old surfaces. Interestingly, these rates are >1000 times higher than those in the Lluta and Azapa valleys. Indeed, for these systems, Wörner et al. (2002) estimated erosion to occur at rates of ca. 300 m/My using the difference between the elevations of the 2.7 Ma-old Lauca-Peréz Ignimbrite and the present-day base level. It appears, therefore, that the climatic gradient between the Coastal Cordillera and the high Andes has resulted in (i) decoupling between the fluvial valleys and the bordering slopes/surfaces, (ii) contrasting rates of processes operating in valleys and on surfaces, and (iii) establishment of a transient stage in landscape evolution.

References

Alpers, C.N. & Brimhall, G.H. (1988): Middle Miocene climate change in the Atacama Desert, northern Chile: evidence from supergene mineralization at La Escocndida. GSA Bull. 100, 1640-1656.

Garcia, M., Herail, G. & Charrier, R. (1999): Age and structure of the Oxaya Anticline: A major feature of the Miocene compressive structures of northernmost Chile. 4th ISAG, Goettingen. pp. 249-252.

Gaupp, R., Kött, A. & Wörner, G. (1999): Paleoclimate implication of Mio-Pliocene sedimentation in the high altitude intra-arc Lauca-Basin of northern Chile. Paleogeography, Paleoclimatology, Paleoecology 151, 79-100.

Gregory-Wodzicki, K.M. (2000): Uplift history of the Central and Northern Andes: A review. GSA Bulletin 112, 1091-1105.

Hartley, A.J. & Chong, G. (2002): Late Pliocene age of Atacama Desert: Implication for the desertification of western South America. Geology 30, 43-46.

Ivy-Ochs, S. (1996): The dating of rock surface using in situ produced ^{10}Be, ^{26}Al and ^{36}Cl, with examples from Antarctica and the Swiss Alps. PhD-thesis, Zuerich.

Molnar, P. (2001): Climate change, flooding in arid environments, and erosion rates. Geology 29,1071–1074.

Mortimer, C. (1980): Drainage evolution in the Atacama desert of northernmost Chile. Rev. Geol. Chile 11, 3-28.

Uhlig, D. (1999): Die Westabdachung der Zentralanden in den Provinzen Arica und Parinacota, Nordchile: Landschaftsentwicklung und Geologie. Profil 17, pp. 167-244.

Walfort, B., Hammerschmidt, K. & Wörner, G. (1995): New Ar/Ar ages from Tertiary volcanics in the North Chilean Andes (18°S): Implication for tectonic and magmatic evolution. EUG-meetingc Strasbourg. Terra Abstract 7, 334.

Wörner, G., Uhlig, D., Kohler, I. & Seyfried, H. (2002): Evolution of the West Andean Escarpment at 18°S (N. Chile) during the last 25 Ma: uplift, erosion and collaps through time. Tectonophysics 345, 183-198.

Zhang P., Molnar, P. & Downs, W.R. (2001): Increased sedimentation rates and grain sizes 2-4Myr ago due to the influence of climate change on erosion rates. Nature 410, 891-897.

GEOPHYSICAL INVESTIGATIONS OF THE CENTRAL CHILEAN CONTINENTAL MARGIN

Heidrun KOPP (1), Ernst R. FLUEH (1), Peter THIERER (1), Dirk KLAESCHEN (1), Frederik TILMANN (1), Christoph GAEDICKe (2)

(1) Geomar Research Center, Wischhofstr. 1-3, 24148 Kiel, Germany, hkopp@geomar.de
(2) BGR Bundesanstalt fuer Geowissenschaften und Rohstoffe, Stilleweg 2, 30655 Hannover, Germany, christoph.gaedicke@bgr.de

KEY WORDS: Chilean continental margin, seamount subduction, crustal structure, refraction seismics, tomography, bathymetry,

INTRODUCTION

The central Chilean margin was the target of RV SONNE cruise SO161, which acquired seismic wide-angle and reflection data, high-resolution bathymetry data, gravity and magnetics. A local seismogenic network was operated over a period of 2 months, accompanying investigations on land. From October 13-15, 2001 (Leg 1) an array of 23 ocean bottom hydrophones (OBH) and seismometers (OBS) were deployed and recovered in December. Here we present preliminary results of the seismic and swath surveys across the subduction zone and volcanic structures entering the trench.

The Chilean margin is defined by the compressional underthrusting of the oceanic Nazca plate of Eocene age beneath the South American continent. The subduction process is characterized by a change in dip angle of the downgoing plate along the strike of the trench, resulting in a segmentation of the margin. 'Flat' slab segments have been identified underneath central and northern Peru, as well as beneath Central Chile. North and south of these subhorizontal subduction domains, a steeply dipping slab is present (Barazangi and Isacks, 1976). The flat slab segments correlate with the absence of Quaternary volcanism and a central valley on the South American plate, whereas active volcanism occurs above the steeply dipping segments. The origin of the flat slab geometry is still enigmatic. Segment boundaries commonly coincide with bathymetric elevations, ridges, or fracture zones on the oceanic plate (Pilger, 1981). There may exist a correlation between the buoyancy of the subducted seafloor relief and the occurrence of shallow subduction. It has been proposed that these oceanic plate asperities form earthquake-nucleating features (von Huene et al., 1997). The fundamental effects of ridge subduction on the margin suggest a linkage of the subducting Juan Fernandez chain on the Nazca plate to the flat slab segment of the central Chilean margin, which poses one aspect investigated in the scope of the SPOC project presented here. Another aspect concerns the mass transfer along the margin. Sediment accretion leads to the evolution of voluminous accretionary wedges, whereas erosive margins, which dominate in the Pacific region, pose the other end-member of subduction zone types. These margins are typically composed of a backstop of continental rock against which a small accretionary wedge or non-accretionary prism has accumulated. The Chile subduction zone

is unique in that the growth and destruction of the margin may be observed in regions of subduction accretion and subduction erosion, respectively. It is a key area for investigating the interplay of processes that shape subduction zones.

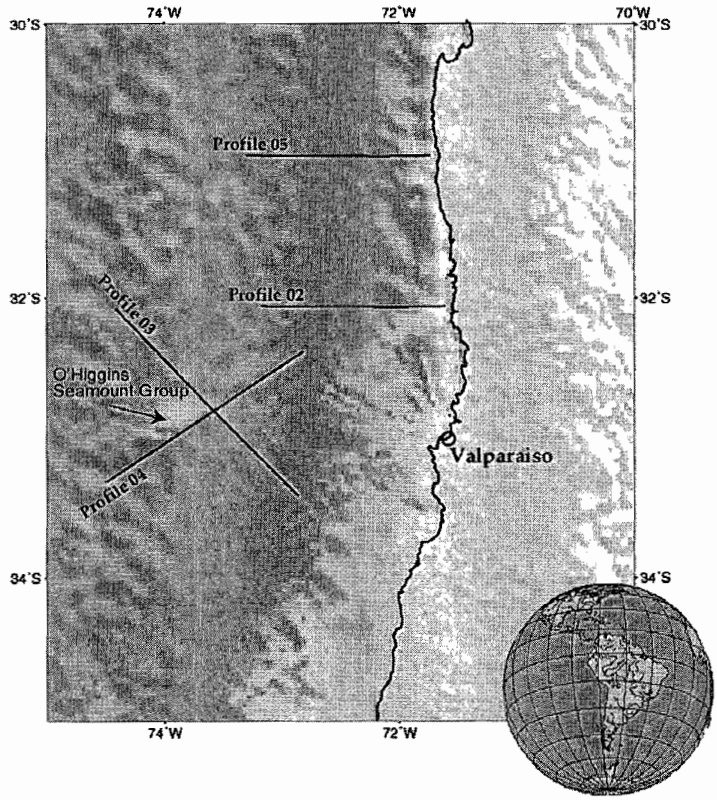

Fig. 1: Location map of refraction seismic profiles acquired during cruise SO161-4 of RV SONNE across the central Chilean subduction zone and the Juan Fernandez Ridge with the pronounced O'Higgins seamount group.

The study area covers the eastern part of the aseismic Juan Fernandez Ridge and the continental slope (31°-34°S) off Valparaiso (Flueh et al., 2002). Four wide-angle profiles were laid out: Profiles P02 and P05 are W-E oriented and located across the subduction complex at latitudes 32°S and 31°S, respectively. Profiles P03 and P04 cross the Juan Fernandez Ridge at the O'Higgins seamount and lie perpendicular to each other. Seismic arrivals over offsets of more than 120 km are present on many record sections, especially along profiles covering the oceanic crust.

Wide-angle profile P02 is approximately 190 km long with a total of 25 instruments which cover 80 km of oceanic crust seaward of the trench, as well as the continental slope. Only a thin sedimentary blanket is recognizable on the rough seafloor of the oceanic crust, which shows a thickness of about 7 km. Different velocity gradients divide the crust into an upper part (Layer 2 and 3a) and a lower portion (Layer 3b), with velocities increasing from 4.8 km/s to 7.2 km/s at the crust-mantle boundary. The oceanic Nazca plate subducts beneath the South American plate with only a small slope inclination angle. In contrast to the landward part of the profile, the Moho is clearly visible on the seaward side of the trench, at a depth of about 11.5 km. The

continental Moho cannot be resolved, which leaves the continental structures below 15 km unidentified. One important aspect deduced from this wide-angle profile concerns the lateral increase of seismic velocities at the lower part of the continental slope. A backstop probably consisting of Paleozoic basement is clearly defined by the high p-wave velocities ranging from 5.5 km/s to 5.8 km/s. Toward the trench, a wedge-shaped body of reduced velocities is observed and interpreted as accreted compressed and reworked trench material.

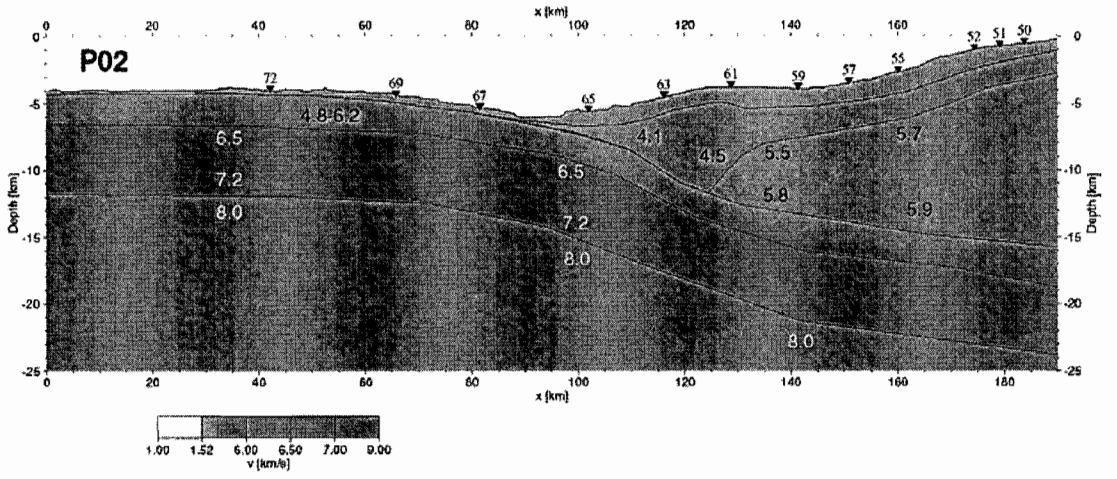

Fig. 2: Preliminary velocity-depth model of Profile 2 crossing the subduction complex at 32°S.

The O'Higgins seamount group was the target of profiles P03 and P04. An investigation of the velocity-depth distribution was aimed at determining the rate of underplating or the ratio of extrusive vs. intrusive melt generated when the plate moved over the hotspot that is currently forming Alexander Selkirk Island at the western termination of Juan Fernandez Ridge. The instrument spacing along the profiles of ca. 2.2 nm guarantees high ray coverage. The ocean floor topography results in considerable travel time variability; most pronouncedly expressed in the seismic arrivals are the volcanic edifices. Towards the trench, which shows a significant sedimentary fill in this area south of the entrance point of the Juan Fernandez Ridge into the subduction zone, numerous fractures and faults result in an increasingly rough seafloor. A combined modeling of the two perpendicular profiles reveals a Moho deflection underneath the seamounts by up to 4 km.

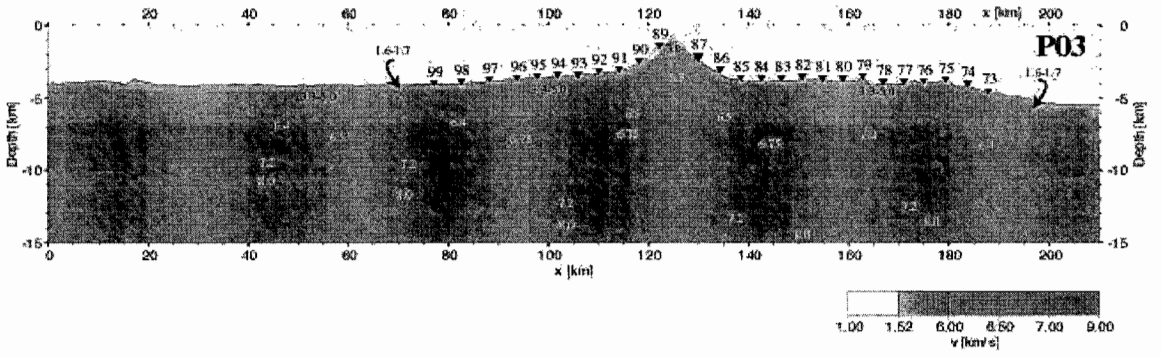

Fig. 3: Velocity-depth model of profile P03 across the O'Higgins seamount group. A clear Moho deflection is detected centered underneath the seamounts, indicative of a hotspot-related volcanic origin.

This zone of anomalously thick crust is centered underneath O'Higgins Seamount and Guyot, but extends beyond it, forming a structure typical of hotspot related seamount chains. Tomographic investigations across the ridge and seamounts include a top-to-bottom approach and a first-arrival inversion process, which has been modified to also consider later arrivals. This will be of advantage for this dataset, as clear PmP arrivals are present on all of the record sections, whereas the Pn phases are more difficult to identify at larger offsets.

REFERENCES:

Barazangi, M., Isacks, B. L. 1976. Spatial distribution of earthquakes and subduction of the Nazca plate beneath South America. Geology, 4, 686-692.

Flueh, E. R., Kopp, H., Schreckenberger, B. (edts). 2002. SPOC: Subduction processes off Chile. Cruise Report, Geomar, 383 pp.

Pilger, R. H. 1981. Plate reconstructions, aseismic ridges, and low-angle subduction beneath the Andes. Bull. Geol. Soc. Am., 92, 448-456.

Von Huene, R., Corvalan, J., Flueh, E. R., Hinz, K., Korstgard, J., Ranero, C. R., Weinrebe, W. and CONDOR Scientists. 1997. Tectonic control of the subducting Juan Fernandez Ridge along the Andean margin near Valparaiso, Chile. Tectonics, 16, 3, 474-488

SUBDUCTION PROCESSES OFF CHILE (SPOC) – COMBINED OFFSHORE-ONSHORE EXPERIMENTS IN CENTRAL CHILE

Charlotte KRAWCZYK (1), Onno ONCKEN (2), SPOC and IMTEQ Working Groups (3)

(1) GFZ Potsdam, Telegrafenberg, D-14473 Potsdam, Germany, lotte@gfz-potsdam.de
(2) GFZ Potsdam, Telegrafenberg, D-14473 Potsdam, Germany, oncken@gfz-potsdam.de
(3) See text for detail

KEY WORDS: combined onshore-offshore observations, multi-component (seismic) network, seismogenic coupling zone, Interplate MegaThrust EarthQuake Processes (IMTEQ), southern Central Chile

INTRODUCTION

Convergent continental margins are the Earth's principal locus of important earthquake hazards. Some 90% of global seismicity and nearly all interplate megathrust earthquakes with magnitudes >8 occur in the seismogenic coupling zone between the converging plates. Despite the societal, economic, and scientific importance associated with the coupling zone, the processes that shape it and its relation to surface deformation are poorly understood. Seismogenic coupling zones occupy a limited depth range of convergent plate interfaces between 5 to 10 km depth at the updip end and 30 to 60 km at the downdip end (e.g. Tichelaar & Ruff 1993). The location of rupture nucleation and the distribution of slip are probably mainly constrained by stronger asperities or a variation of the material state that control the strength of the otherwise rather weak coupling zone and subduction channel (Ruff 1999, Pacheco et al. 1993). The related extent and degree of seismic coupling plays a major role in the generation mechanism of great interplate earthquakes (e.g. Hyndman & Wang, 1993).
The vision of our integrated study is a quantitative understanding of megathrust earthquake seismicity in subduction zones and its relation to processes at depth *and* at the surface. We have started with a series of experiments in the area of the 1960 Southern Chile earthquake that are designed to image the processes operating at the seimogenic plate interface and their effect for surface deformation. These experiments – the first integrated marine experiment (SPOC: Subduction Processes Off Chile) completed in early 2002 - are planned in national and international cooperation within the scope of the SALT project (South American Lithospheric Transect) under the auspices of the ILP program. A series of field and lab studies will (1) image a complete seismogenic plate interface from the updip to below the downdip end, in order to (2) yield key petrophysical and mechanical properties. We will also (3) test the variation of properties along different segments of a plate interface which are at different stages of the seismic rupture cycle, and (4) observe and model the surface response to seismic rupture and identify the controls of hazard distribution. Here, we report first results of project SPOC (Subduction Processes Off Chile) and the scope of future plans within project IMTEQ (Interplate MegaThrust Earthquake Processes).

The southern Chilean convergent margin provides a first test site and natural laboratory for our studies (Fig. 1). Here, the largest instrumentally recorded earthquake occurred in 1960 (Mw = 9.5). It ruptured the

margin starting at 38°S at a hypocentral depth of some 30 km below the continental forearc towards the south for approximately 1000 km (Cifuentes 1989) with a coseismic slip of up to 40 m, up to 2 m vertical displacement and a tsunami up to 15 m high that affected the entire Pacific (Kanamori & Cipar 1974, Plafker & Savage 1970). Recent GPS data reveal this part of the upper plate to still be in the post-seismic relaxation stage. The unusual width of the seismogenic coupling zone in this area with a downdip end well inland allows observation of this part of the plate interface with onshore based experiments, while most of the ruptured surface is situated beneath the offshore forearc (Diaz Naveaz 1999).

CONCLUSIONS

The first component of the study, the ship-borne integrated geophysical experiment SPOC with R/V SONNE, took place in fall and winter 2001/2002 (operated by The Federal Institute for Geosciences and Natural Resources, in cooperation with GEOMAR and the Berlin-Potsdam Andes research group, SFB 267). It will yield a near 3D image of the offshore forearc including the updip parts of the seismogenic coupling zone of the great 1960 Chile-earthquake segment and the seismic gap segment to the north (Reichert & SPOC Scientific Shipboard Party, 2002). The offshore profiles reveal that the slope area in the region is overprinted by a faint lineation pattern with a dominant azimuth of some 120 degrees correlating with onshore structures. The upper plate is split into many segments with pronounced forearc basins and strikingly narrow accretionary wedges. The relatively thick trench fill of up to more than 2.000 m seems to be subducted through a thick subduction channel, thereby suggesting a non-accretionary subduction type here.

Between 36° and 39° S, a combined onshore-offshore, active-passive seismic experiment was carried out linking the marine profiles to the subduction features observed onshore. It comprised: (1) a 3D-wide angle reflection/refraction component simultaneously recording the airgun pulses from the R/V SONNE with 32 3-component stations deployed in an array and 50 stations along 3 W-E profiles; (2) recording of explosive shots fired at the ends of the three profiles; and (3) an additional pilot seismic reflection experiment covering the coastal onshore-offshore transition at the southern E-W line in order to provide a complete link between the offshore dataset and the landbased experiments with the first complete high resolution coverage of an entire seismogenic plate interface (see also Lüth et al., Stiller et al., this volume).

The first results from the near-vertical incidence reflection (NVR) seismic experiment component, (located at 37° 15`S) yields an image of the part of the subduction zone between the S-America and Nazca-Plate that is located in the offshore-onshore transition zone. The 54 km long line recorded the offshore profile shot by the R/V SONNE with the airgun array and a series of shots in the Pacific Ocean, and on land resulting in a 45 km long 2-fold CDP line, and a single-fold coverage along 72 km profile length. The preliminary data processing of single shots gives an image of different reflection bands in the upper and middle crust. On the entire profile, a 1 s TWT thick strong reflection band is observed between 3 and 4 s TWT, which shows almost no dip. On the western half of the profile, prominent reflections dip eastward from ca. 6 s TWT down to ca. 8 s TWT. Finally, in the central part of the seismic reflection profile, some relatively weaker reflections are found between 10 to 14 s TWT. All theses eastward dipping reflection bands between 6 and 14 s TWT correlate with Wadati-Benioff seismicity and can be interpreted as imaging the top of the downgoing plate with a change of the downdip image that approximately correlates with the downdip end of the seismogenic plate interface. Further inland, a velocity

anomaly coincides with a break in the reflectivity located below the axis of the coastal cordillera which might be indicative for the intersection of the oceanic plate and the continental Moho.

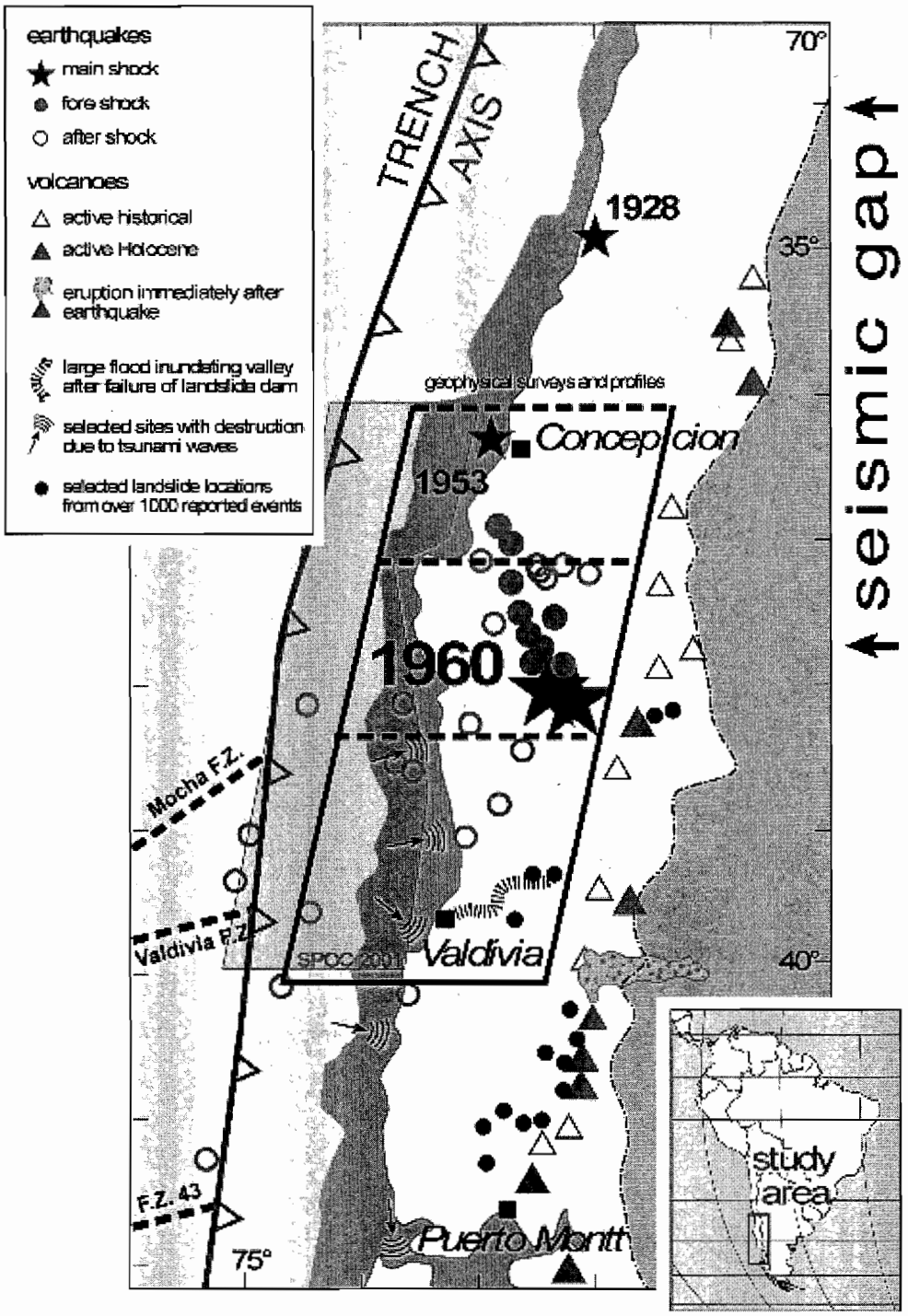

Figure 1: Schematic map of the investigation area in southern Chile with earthquake locations and hazards related to the 1960 earthquakes (F.Z.-fracture zone).

The SPOC Working Group-onshore:

M. Araneda [1], K. Bataille [2], J. Bribach [3], A. Cser [4], C.M. Krawczyk [3], S. Lüth [5], S. Martin [6], J. Mechie [3], L. Rabenstein [5], W. Schnurr [5], M. Stiller [3], P. Wigger [5]

[1] SEGMI (Santiago, Chile)

[2] Universidad de Concepcion (Concepcion, Chile)
[3] GeoForschungsZentrum Potsdam (Germany)
[4] Universidad de Concepcion (Los Angeles, Chile)
[5] Free University Berlin (Germany)
[6] Potsdam University (Germany)

REFERENCES

ANCORP-Working Group 1999. Seismic reflection image revealing offset of Andean subduction-zone earthquake locations into oceanic mantle. Nature, 397, 341-344.

Beck S., Barrientos S., Kausel E., Reyes M. 1998. Source characteristics of historic earthquakes along the Central Chile subduction zone. Journal of South American Earth Sciences, 11 (2), 115-129.

Cifuentes I.L. 1989. The 1960 Chilean Earthquakes. JGR, 94 (B1), 665-680.

Diaz Naveas J.L. 1999. Sediment subduction and accretion at the Chilean convergent margin. PhD thesis, Kiel University, pp. 130.

Hyndman R.D. Wang K. 1993. Thermal constraints on the zone of major thrust earthquake failure. JGR, 98 (B2), 2039-2060.

Kanamori H., Cipar J.J. 1974. Focal process of the great Chilean earthquake May 22, 1960. Physics of the Earth and Planetary Interiors, 9, 128-136.

Pacheco J.F., Sykes L.R., Scholz C., 1993. Nature of seismic coupling along simple plate boundaries of the subduction type. JGR, 98, 14133-14159.

Plafker G., Savage J.C. 1970. Mechanism of the Chilean earthquakes of May 21 and 22, 1960. Geol. Soc. Am. Bull., 81 (4), 1001-1030.

Reichert C. & SPOC Scientific Shipboard Party, 2002. Subduction Processes off Chile: Initial Geophysical Results of SONNE Cruise SO-161(2+3). Geophysical Research Abstracts, 4.

Ruff L. 1999. Dynamic stress drop of recent earthquakes: variations within subduction zones. Pure and Applied Geophysics, 154 (3-4), 409-431.

Tichelaar B.W., Ruff L. 1993. Depth of seismic coupling along subduction zones. JGR, 98 (B2), 2017-2037.

LONG-TERM AND SHORT TERM TECTONIC EROSION AT THE PERUVIAN ACTIVE MARGIN BETWEEN 9°S AND 15°S: EVIDENCE FROM BATHYMETRY DATA AND 3D SANDBOX ANALOGUE MODELLING

Nina KUKOWSKI (1), Andrea HAMPEL (1), Joerg BIALAS (2), Anne BROSER (2), Christian HUEBSCHER (3), Udo BARCKHAUSEN (4), Jacques BOURGOIS (5)

(1) GeoForschungsZentrum Potsdam, Telegrafenberg, D-14473 Potsdam, Germany (nina@gfz-potsdam.de)
(2) GEOMAR Research Center of Marine Geosciences, Wischhofstr. 1-3, D-12148 Kiel, Germany
(3) Institut für Geophysik, Universität Hamburg, Bundesstr. 55, 20146 Hamburg, Germany
(4) BGR, Stilleweg 2, D-30361 Hannover, Germany
(5) LGTE-UPMC-CNRS, Boite 119, 4 place Jussieu, Paris Cedex 05, F-75252, France

KEY WORDS: convergent margin, Peru, tectonic erosion, bathymetry, seismics, 3D analogue modelling

ABSTRACT

Bathymetric, wide-angle and reflection seismic data were acquired between 5°S and 15°S off Peru during RV Sonne cruise SO-146 GEOPECO in spring 2000 to image the Nazca Plate and the continental slope at different latitudes as well as the present collision zone of the Nazca Ridge and the Peruvian trench. Data sets acquired in preparation of ODP Leg 112 and during a French cruise have been added (Fig.).

At 8°S to 9°S, the oceanic crust is extraordinarly rough with a relief of up to 800 m between narrowly spaced highs. Locally, the highs and lows have slope angles steeper than 20°. As the roughness does not increase towards the trench, the structures are inherited and not caused by the bending of the plate. The sediment input along the margin varies, but never exceeds a thickness of about 300 m. The great variety of structures, which are all oblique to the strike of the trench, have different directions and do not seem to be related to each other or the current convergence direction. Surface deformation found at the very steep lower slope occurs at a very small local scale inferring mass wasting and the slope being at failure everywhere. Observed linear trends may result from the oblique convergence direction. The transition to the upper slope is marked by numerous steep gullies. At 10°S, where the Mendana Fracture Zone enters the trench, the oceanic crust is also characterized by high roughness but has a completely different pattern with parallel ridges are crossed by trenchparallel normal faults. The lower slope shows ridge-shaped features that are not related to the directional structures on the plate. At 13°S and 12°S, the Nazca Plate has a rough topography with trench-parallel normal faults. The steep lower slope shows erosional features. The roughness of oceanic plate and lower slope is of small scale, however, compared

to other margins, the latter is still extraordinarily steep and rough. A small wedge is revealed by the wide-angle seismic data. The sea floor of the adjacent mid slope terrace is cut by numerous narrow furrows and canyons which may result from mass wasting through surficial erosion. A probable slump has also been identified in the mapped. On the upper slope, the Lima Basin opens towards the lower slope and comprises a pronounced drainage system.

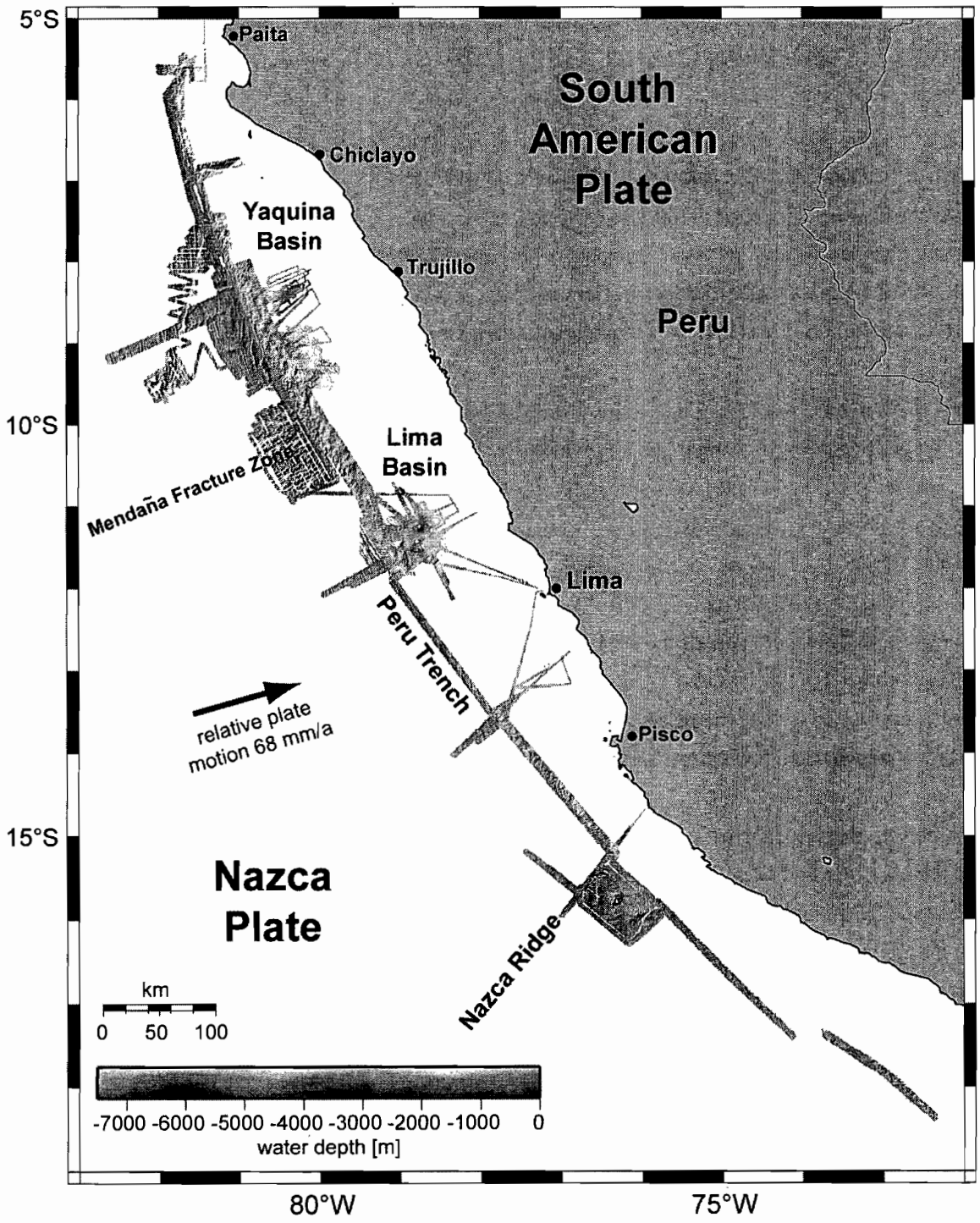

Fig.: Bathymetric data acquired during the RV Sonne cruise SO146-GEOPECO. In the Lima and Yaquina Basin area, data from the French SEAPERC cruise and data collected in preparation of ODP Leg 112 has been added.

Compared to the rough relief of the Nazca Plate, the Nazca Ridge has a rather smooth surface, as imaged at the southeastern flank of the ridge. The sediment cover on the ridge does not exceed a thickness of 300 m. Several volcanic structures of different size and elevation are located on the flank of the ridge. Towards the trench, an increasing number of trenchparallel normal faults caused by the bending of the plate into the subduction zone occur. The trench is characterized by a rugged surface and little to no sediment fill. Where the crest of the ridge enters the trench, the water depth decreases to 5000 to 5300 m compared to a water depth of 6500 m and more south of the intersection area. The lower continental slope is very steep and shows features typical of erosion.

To quantify the roughness of the sea floor, in general several factors contributing to the roughness have to be taken into account: the incremental mean surface slope, the distance coefficient, i.e. the ratio of surface length to base line length, the magnitude of the peaks and the void volume. A comparison between bathymetric profiles at different latitudes shows that they have a steep slower slope, escarpements and basins in common, but that their roughness differs significantly. The roughness of the oceanic crust increases from south to north and is significantly higher than at the Nazca Ridge. As the oceanic crust is older in the south than in the north, the roughness of the oceanic crust is not a function of the age. High values of distance coefficients indicating high rouhgness coincide with sections that have a steep slope. Towards the shelf, the slope angle variations and distance coefficients decrease, with exception of the areas around the escarpements.

The bathymetry data set is the base for characterizing the mechanics of the Peruvian margin. In terms of the taper stability field, the margin can be classified as near or at failure everywhere. To further determine the parameters which control the mechanics of the margin, 3D sandbox experiments with an accretive phase at the beginning and an erosive phase afterwards have been carried out. In an experiment with 20° obliquity, which simulates the setting off central Peru, with high basal friction and no sediment input produces an wedge that is at failure throughout. The effect of the oblique convergence direction is not very pronounced. The slope shows a morphology, e.g. escarpements, that is characteristic for a erosive regime. Small ridges of similar size as the structures at 9°S that have been attached to the subducting "plate" are not mirrored in the slope during their subduction.

The analogue experiments suggest that long term tectonical erosion is governed by the nature of the plate interface in absence of sediment supply. The conditions for tectonic erosion are a large dip of the subducting plate, a steep lower slope, no sediment input and high sea floor roughness accompanied by surficial wass masting and the development of a characteristical morphology of the slope (e.g. escarpements). All these factors are met off Central Peru. Therefore, this margin can be classified as long term tectonically erosive. Regarding the tectonic evolution of the Peruvian margin, the Nazca Ridge has caused short term erosion of the continental slope, however, this effect is superposed on a long-term tectonic erosion.

SEDIMENTARY PROVENANCE AND TECTONIC REGIME OF THE DEPOSITIONAL BASIN OF THE DUQUE DE YORK METAMORPHIC COMPLEX, MAGALLANES, CHILE

Juan Pablo LACASSIE (1) and Francisco HERVÉ (1)

(1) Departamento de Geología Universidad de Chile, Casilla 1351, Correo 21, Santiago, Chile (jlacassi@cec.uchile.cl), (fherve@cec.uchile.cl)

KEYWORDS: Gondwana; tectonic setting; geochemistry; metaturbidites; Patagonian Andes; Chile.

INTRODUCTION

The Duque de York metamorphic complex (CDY) constitutes a well exposed post-Early Permian – pre-Early Cretaceous metasedimentary succesion of greywacke, siltstone, shale and conglomerates that crops out at the Madre de Dios and Diego de Almagro archipelagos, West Patagonian Andes, Chile. It was considered by Forsythe and Mpodozis (1983) as a continent-derived detrital succesion, which was unconformably deposited over the other two units of the achipelago, the Late Carboniferous-Earliest Permian Tarlton Limestone (TL; Douglass and Nestell, 1976) and the coeval Denaro Complex (DC), as they came close to the continent as an alloctonous terrane. The three units were then tectonically interleaved into the forearc of the Gondwana margin by subduction processes. Petrographic and whole-rock major and trace elements compositions of CDY sandstones and mudstones were studied in order to establish the provenance of their clastic components and the tectonic setting of their depositional basin. The data described in this paper contribute to a broader understanding of the development of the "Pacific" margin of Gondwana, which in the time bracket in which the studied unit was deposited, was continuous with Antarctica and New Zealand (e.g.Veevers et al., 1994).

FIELD OBSERVATIONS

The rocks of the DYC study area consist of very low metamorphic grade metaturbidites, with locally preserved sedimentary structures such as bioturbated beds, flute and groove casts attesting to erosive current action, and sandstone load balls in mudstone indicating post-depositional instability. Most of the succesion is structureless but

planar, cross- and convolute-laminations were observed together with rare mesoscopic slumping and syn-sedimentary faulting. They are composed of rhythmical intercalations of light grey sandstones, black to grey mudstones and graywackes between massive outcrops of polymictic conglomerate beds, occasionally normally graded. The bed thickness ranges from millimetric to metric scale. The conglomerate clasts correspond to sandstones, acid plutonic and volcanic rocks, limestones and chert in decreasing order of frequency. Some conglomerate and mudstone beds have ovoidal shaped milimetric scale fossils presumably fusulinids. The stratigraphic relations are obliterated because there is a complex tectonic imbrication between the different units that compose the basement in this area as a result of two events of deformation (Forsythe and Mpodozis, 1983).. However, a TL paleokarstic surface, containing fossiliferous black mudstone lenses, close to the TL–DYC contact area, and a stratigraphic DC-DYC contact were recognized. At Seno Soplador area a kilometric scale sill intrudes TL (Fig 1), wich is also intruded by concordant, highly weathered, centimetric dikes and by discordant, northwest trending and mainly sub-vertical, basic metric dikes, that also intrude the DYC.

METHOD

Five DYC sandstones plus 1 sandy mudstone where selected for point count analysis following Dickinson **(1983)**. Whole-rock major and trace element concentrations of 5 DYC sandstones and other 6 DYC mudstones were determined by ICP-AES at the Geology Department, Universidad de Chile.

RESULTS AND DISCUSSION

Modal analysis of sandstones indicates derivation from a dissected magmatic arc source (Fig 2). The DYC Chemical Index of Alteration (CIA; Fig 3) indicates moderate weathering at the source area or during transportation. Assuming a common source of granodioritic composition, the DYC A-CN-K scatter could be explained by grain size fractionation coupled with different degrees of weathering and k-metasomatism. In figure 4 this source composition coincides with the proximity of rhyodacite to the DYC sandstones and mudstones projection, wich indicates a felsic igneous provenance for them. In the diagram of figure 5 the DYC scatter points to an active continental margin. The Th/Sc ratio of figure 6 suggests a petrologically mature DYC source with an intermediate to acid composition. The high Zr/Sc indicates a source rich in zircons or that the sediment endured long transportation and sorting, previous to its deposition.. DYC sandstones and mudstones are compared with metasedimentary rocks of similar age of the Torlesse terrane of New Zealand, and the LeMay Group of central Alexander Island, Antartica. There is a great coincidence between the modal composition between sandstones from the three units (Fig 2), and between DYC and Torlesse PF1-PF3 petrofacies proyections (Fig. 3, 4 and 6). These Permian-Late Triassic Torlesse petrofacies were interpreted as derived from the gradual unroofting of a continental margin volcano-plutonic arc (McKinnon, 1983; cited in Roser and Korsch, 1999). Also in terms of their modal composition Tranter (1991) interpreted the LeMay Group sandstones as derived from a magmatic arc.

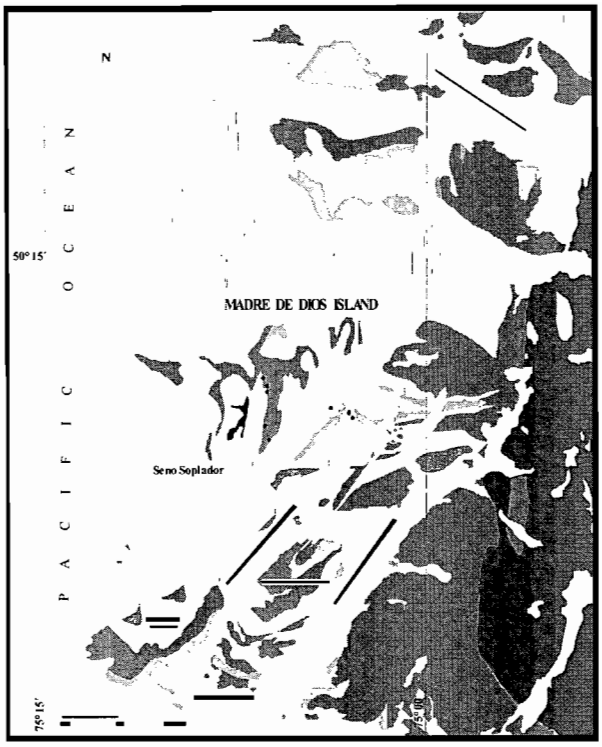

Figure 1. Geologic map of Madre de Dios Island (modified after Forsythe & Mpodozis, 1983)

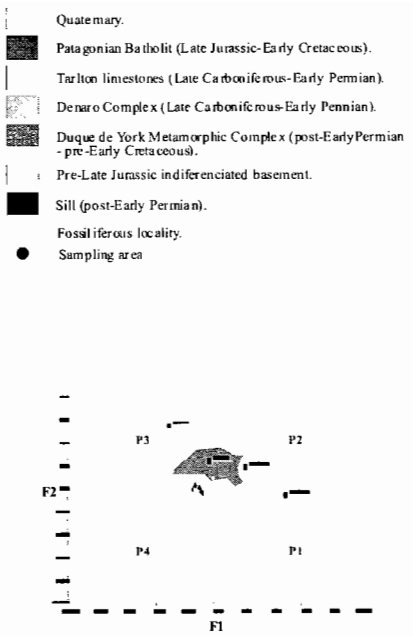

Figure 4. Sedimentary provenance diagram of Roser and Korsch (1988). Source type: P1: mafic; P2: intermediate; P3: felsic; P4: recycled. Igneous rocks averages from Roser & Korsch (1988). Shaded area: Torlesse sandstones - mudstones projection area (PF1 -PF3 petrofacies). Symbols as in Fig. 3.

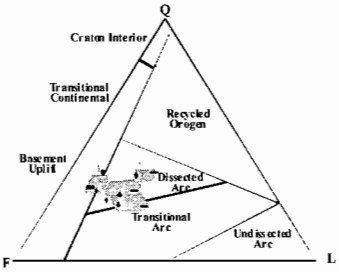

Figure 2. QFL diagram (Dickinson et al., 1983). Q: Total Quartz; F: Total Feldspars; L: Total Lithics. Dashed line: LeMay Group sandstones projection area (Tranter, 1991). Shaded areas: Torlesse petrofacies PF1- PF4 sandstones projections (MacKinnon, 1983).

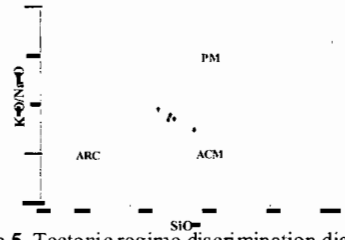

Figure 5. Tectonic regime discrimination diagram of Roser and Korsch (1986). PM: Passive margin; ACM: Active continental margin; ARC: Oceanic island arc. Symbols as in Fig. 3.

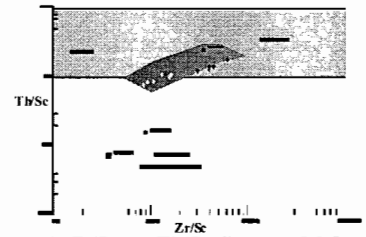

Figure 6. Zr/Sc vs. Th/Sc diagram (McLennan et al., 1993). UCC:Upper Continental Crust; HMSC:Heavy Minerals Sorting and Concentration. Shaded area: North Island PF1-PF3 Torlesse terrane sandstones - mudstones projection. Igneous averages as in Fig. 4. Symbols as in Fig. 3.

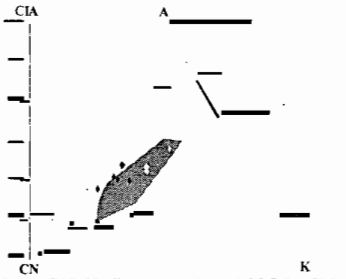

Figure 3. A-CN-K diagram A = Al2O3, CN = CaO + Na2O, K = K2O, WL: Feldspar weathering line. Typical igneous rocks values from Le Maitre (1976). Black diamons: DYC sandstones; White diamonds: DYC mudstones. Shaded area: Torlesse (PF1 - PF3) sandstones-mudstones projection area.

CONCLUSIONS

The combination of petrographical and geochemical analyses of DYC sandstones and mudstones indicates that they derive from a source averaging near granodiorite composition that was part of an active margin, probably a continental margin volcano-plutonic arc. Although this source may have been deeply dissected, this erosion was not accompanied by intense weathering. DYC geochemical and modal composition similarities with Torlesse terrane and LeMay Group, suggest the possibility of a closer relation between them.

REFERENCES

Dickinson, W.R., Beard, L.S., Brakenridge, G.R., Erjavec, J.L., Ferguson, R.C., Inman, K.F., Knepp, R.A., Lindberg, F.A., Ryberg, P.T. 1983. Provenance of North American Phanerozoic sandstones in relation to tectonic setting. Geological Society of America Bulletin 94, 222 – 235.

Douglass, R.C., Nestell, M.K. 1976. Late Paleozoic foraminifera from southern Chile. U.S. Geological Survey Special Paper 858, 49 p.

Forsythe, R.D., Mpodozis, C. 1983. Geología del Basamento pre-Jurásico Superior en el Archipiélago Madre de Dios, Magallanes, Chile. Servicio Nacional de Geología y Minería, Boletín 39, 63 p.

McLennan, S. M., Hemming, S., McDaniel, D. K., Hanson, G. N. 1993. Geochemical approaches to sedimentation, provenance and tectonics. In: Johnnson, M. J. & Basu, A. (eds.) Processes controlling the composition of clastic sediments. Geological Society of America Special Papers 285, 21 – 40.

Roser, B.P., Korsch, R.J. 1986. Determination of tectonic setting of sandstone – mudstone suites using SiO_2 content and K_2O/Na_2O ratio. J. Geol. 94. 635 – 650.

Roser, B.P., Korsch, R.J. 1988. Provenance signatures of sandstone - mudstone suites determined using discriminant functions analysis of mayor element data. Chemical Geology 67, 119 – 139.

Tranter, T. 1991. Accretion and subduction processes along the Pacific margin of Gondwana, central Alexander island, Antartica. 437 – 441.

Veevers, J.J., Powell, C., Collinson, J.W., López Gamundi, O. R. 1994. Synthesis. In Permian-Trassic Pangean Basin and Foldbelts along the Panthalassan Margin of Gonwanaland. (Veevers, J.J. and Powell, C., editors). Geological Society of America. Memoir 184. Boulder, Colorado.

MARGIN-PARALLEL V/S MARGIN-ORTHOGONAL COMPRESSION ALONG A CONVERGENT MARGIN: THE ANDES OF CENTRAL - SOUTHERN CHILE AND WESTERN ARGENTINA

Alain LAVENU (1), José CEMBRANO (2), Carlos COSTA (3)

(1) Alain Lavenu IRD-LMTG, Université Paul Sabatier, 38 rue des 36 Ponts, 31000 Toulouse France (lavenu@cict.fr)
(2) José Cembrano UCN, Antofagasta, Chile (jcembrano@socompa.ucn.cl)
(3) Carlos Costa, Univ. San Luis, Argentina (costa@unsl.edu.ar)

KEY WORDS: Andes, state of stress, oblique convergence, slip partitioning

INTRODUCTION

The central and southern Andes constitute a segment of the type-example of mountain building related to subduction of an oceanic plate beneath a continental plate margin. Oceanic plate subduction is commonly believed to drive significant margin-orthogonal shortening in the overriding plate which in turn is throught to produce mountain-building.

In particular, forearc deformation should be strongly coupled with the plate convergence vector, however, the relationship between convergence and tectonics on the overriding plate is not yet fully understood. Evolution of this zone appears to be controlled by several other processes such as margin consumption, margin accretion, subsidence, uplift and formation of sedimentary basins.

Even in those cases when the convergence vector is oblique and partitioned into trench-orthogonal shortening and trench-parallel strike-slip displacement, the instantaneous shortening direction across the orogen does not seem to depart much from that of the convergence vector. Theory and observation predict that trench-orthogonal shortening is accommodated in the forearc regions whereas strike-slip displacement is accomodated within the magmatic arc (e.g. Fitch, 1972; Beck, 1983; Jarrard, 1986; McCaffrey, 1992; Saint-Blanquat *et al.*, 1998). Therefore, in the forearc region, the direction of the maximum horizontal compression should be nearly parallel to the slip vector. While this may be true for the forearc base close to the subduction zone itself, a much more complex geometry of the stress tensor is found at the forearc surface.

In the southern part of the Central Andes of Argentina,Quaternary deformation is characterized by east-verging thrusting giving way inland to high-angle reverse faults that bound the assymetric foreland uplifts of the Sierras Pampeanas (Costa, 2002).

We here document regional-scale margin-parallel compression along a large (>1000 km long) tract of the Chilean Andes forearc that poses important questions regarding the way by which subduction zone deformation is tranferred up to surface. We show that margin-parallel compression may be more common than previously recognized because second-order forces arising from slip partitioning can overcome those directly related to trench-orthogonal displacement.

The Andean segment between 30°S and 45°S lie at the Nazca-South America plate boundary zone. Convergence has been slightly dextral-oblique during the last 20 Ma, at relatively high rates (5-8 cm/year) giving

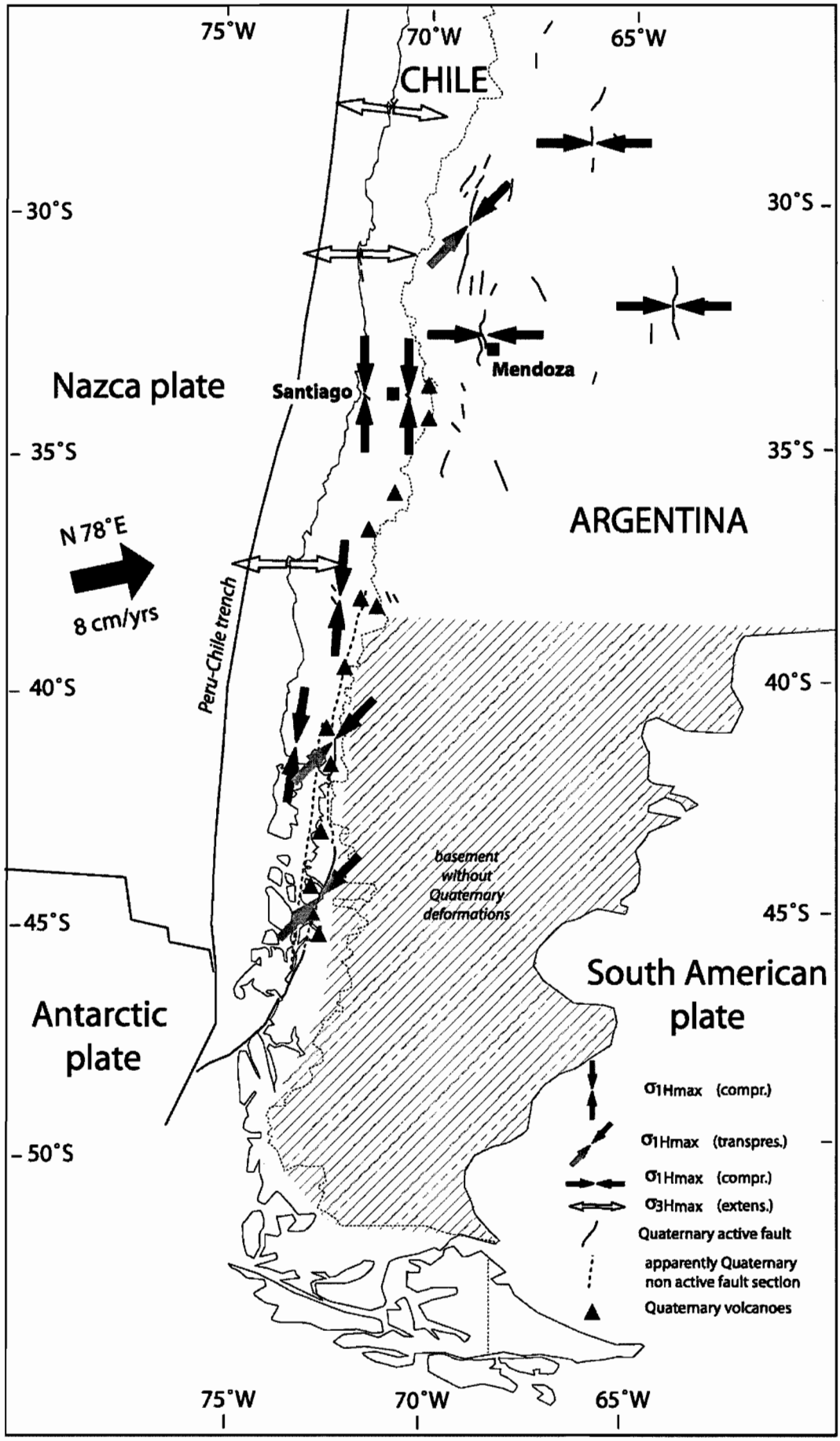
75°W
70°W
65°W
CHILE
30°S
30°S
Nazca plate
Santiago
Mendoza
35°S
35°S
ARGENTINA
N 78°E
8 cm/yrs
Peru-Chile trench
40°S
40°S
basement
without
Quaternary
deformations
45°S
45°S
South American
plate
Antarctic
plate
50°S
σ1Hmax (compr.)
σ1Hmax (transpres.)
σ1Hmax (compr.)
σ3Hmax (extens.)
Quaternary active fault
apparently Quaternary
non active fault section
Quaternary volcanoes
75°W
70°W
65°W

rise to bulk transpressional tectonics in the magmatic arc south of 39°S (Hervé, 1994; Lavenu and Cembrano, 1999)

The forearc region of central and southern Chile is marked by three major, north-south trending morphological units: the Coastal Cordillera, the Central Depression and a significant portion of the Main Range lying west of the present-day volcanic chain. The Coastal Cordillera; up to 2km high, is made up of Paleozoic to Mesozoic metamorphic, plutonic and volcanic rocks. The Central Depression is a low relief region, up to 500 m high, constituted by a thick Oligocene-Quaternary sedimentary infill. The Main Range, whose altitudes west of the volcanic change vary from 4km in central Chile to 2 km in the southern Chile, is formed by highly deformed Mesozoic to Cenozoic volcano-sedimentary rocks cut by Miocene plutons.

The foreland region is characterized by a narrow and eastward-migrating fold and thrust belt, the Sierras Pampeanas basement block uplifts, and the absence of active volcanism.

The present-day tectonic front lies ca. 100 km east of the Andean divide between latitudes 30° and 35°S (Sierras Pampeanas); from latitudes 35° to 47°S, in turn, no significant active deformation has been documented in the foreland region. The Liquine-Ofqui fault zone appears to take up much of the plate boundary crustal deformation, in the magmatic arc between 39° and 47°S.

Forearc deformation was studied by using geometric and geomorphologic analysis of satellite images and from kinematic studies of faults in the field. Major lineaments and subsidiary structures were identified and then checked in the field to search for evidence of nature and timing of motion. When, possible, fault-slip analyses for the stress tensor was carried out through the Carey-Mercier inversion algorithm (Carey and Brunier, 1974; Carey, 1979). This method assummes that the slip direction on a given fault represents the shear stress component of a force F and allows for calculating a stress tensor and the three principal components of the stress tensor, $\sigma 1$, $\sigma 2$, $\sigma 3$.

Our results show that, in contrast to widespread Pliocene E-W compression, the Quaternary stress field is not a single one for the entire range, despite the fact that the convergence vector has been essentially the same for the last 20 Ma [a N-S trending compression in the fore arc (slip vector orthogonal to the convergent motion), a NE-SW trending transpression in the intra arc (slip vector oblique to the convergent motion), and an E-W trending compression in the foreland (slip vector parallel to the convergent motion)]. However, the decrease in convergence rate, may have led to less interplate coupling. On the other hand, significant crustal blok rotations have not been documented for the Quaternary (Roperch *et al.*, 1999).

CONCLUSION

Nazca-South America convergence rate decreased since the Pliocene. The strain partitioning model, as discribed by previous authors (e.g. Fitch, 1972; Jarrard, 1986; Dewey and Lamb, 1992) cannot account for the actual regional stress patterns we have obtained from fault-slip analysis.

Several processes can contribute to this somewhat unexpected strain partitionning in the Andean Range:

- changes in the subduction regime as velocity, coupling, temperature/age of the oceanic plate (DeMets *et al.*, 1994; Somoza 1998);
- concave-convergent margin with "buttress effect" (Beck, 1991; McCaffrey, 1992);
- plate margin geometry;
- slip-vector partition.

REFERENCES

Beck M.E. 1983. On the mechanism of tectonic transport in zones of oblique subduction. Tectonophysics, 93, 1-11.

Beck M. E. 1991. Coastwise transport reconsidered : lateral displacement in oblique subduction zones, and tectonic consequences. Phys. Earth Planet. Inter., 68, 1-8.

Carey E., Brunier B. 1974. Analyse théorique d'un modèle mécanique élémentaire appliqué à l'étude d'une population de failles. C. R. Acad. Sci., Paris, 279, 891-894.

Carey E. 1979. Recherche des directions principales de contraintes associées au jeu d'une population de failles. Revue de Géographie physique et de Géologie dynamique, 21, 1, 57-66.

Costa C. 2002. Geomorphic signature of Quaternary deformation and strategies for regional neotectonic mapping in Argentina. (in press).

DeMets, C., Gordon, R.G., Argus, D.F., Stein, S., 1994, Effect of recent revisions to the geomagnetic reversal time scale on estimates of current plate motions: Geophysical Research Letters, v. 21, p. 2191-2194.

Dewey J. F., Lamb S.H. 1992. Active tectonics of the Andes. Tectonophysics, 205, 79-95.

Fitch T. J. 1972. Plate convergence, transcurrent faults, and internal deformation adjacent to southeast Asia and the western Pacific. Journal of Geophysical Research, 77, 4432-4460.

Jarrard, R.D., 1986. Relations among subduction parameters. Reviews of Geophysics, 24, 217-284.

Hervé F. 1994. The southern Andes between 39° and 44°S latitude: the geological signature of a tranpressive tectonic regime related to a magmatic arc. In K.J. Reutter, E. Scheuber and P.J. Wigger (eds.), Tectonics of the Southern Central Andes, Springer, Berlin, 243-248.

Lavenu A., Cembrano, J., 1999, Compressional- and transpressional-stress pattern for Pliocene and Quaternary brittle deformation in fore arc and intra-arc zones (Andes of central and southern Chile): Journal of Structural Geology, v. 21, p. 1669-1691.

McCaffrey R. 1992. Oblique plate convergence, slip vectors, and forearc deformation. Journal of Geophysical Research , 97, 7, 8905-8915.

Roperch P., Hérail G., Fornari M. 1999, Magnetostratigraphy of the Miocene Corque basin, Bolivia: implications for the geodynamic evolution of the Altiplano during the late Tertiary: Journal of Geophysical Research, 104, 20,415- 20,429.

Saint-Blanquat M., Tikoff B., Teyssier C, Vigneresse J.L. 1998. Transpressional kinematics and magmatic arcs. In Holdsworth R.E., Strachan R.A., Dewey J.F. (eds.), Continental transpressional and transtensional tectonics, Geological Society, London, S.P., 135, 327-340.

Somoza R., 1998, Updated Nazca (Farallon)-South America relative motions during the last 40 My: implications for mountain building in the central Andean region: Journal of South American Earth Sciences, 11, 211-215.

MAXIMUM AND MINIMUM VOLUME ESTIMATES OF AN ASH FALL LAYER FROM THE AUGUST 2001 ERUPTION OF MT TUNGURAHUA (ECUADOR)

Jean-Luc LE PENNEC (1,2), Patricia MOTHES (2), Minard L. HALL (2), Patricio RAMON (2), Gorki A. RUIZ (2)

(1) IRD, Whymper 442 y Coruña, AP 17-12-857, Quito, Ecuador (Jean-Luc.Le-Pennec@ird.fr)
(2) Departamento de Geofísica, Escuela Politécnica Nacional, casilla 17-01-2759, Quito, Ecuador

KEY WORDS: Volcanology, tephra, ash fall, volume, Tungurahua, Ecuador

INTRODUCTION

After eight decades of quiescence, Tungurahua volcano (5023 m a.s.l.) in the Cordillera Real of Ecuador (Hall et al., 1999) progressively reawakened between August and October 1999. The magmatic activity, which began after a phreatic vent-clearing phase, has been characterized by alternating episodes of gas and ash emissions, short-lived "vulcanian" explosions and strombolian eruptive styles. The intensity of the eruption fluctuated during the year 2000 and decreased drastically in October of the same year. A new eruptive phase started in May 2001 with small-scale lava fountaining, accompanied by occasional "vulcanian" explosions in June and July, and by deep LP seismic events. With no clear immediate precursory warning, a strong increase in tremor amplitude took place on August 04, 2001, marking the onset of a relatively intense strombolian phase which lasted until August 23. The eruptive event coincided with significant rainfall in the area. Wet ash falls and associated acidic rains severely affected livestock and agricultural resources to the west of the volcano, prompting the intervention of several national and international humanitarian organizations.

For various reasons, quantitative tephra volume estimates (ballistics or ash falls) were not obtained during the 1999-2000 eruptive phases. On the contrary, during the relatively intense phase of August 2001 more favorable conditions permitted obtaining reliable thickness measurements within several weeks of the emplacement of the ash fall deposit, which resulted in an isopach map. In this note we present two preliminary estimates of the bulk volume of the ash fall layer. In contrast to most recent studies on tephra fall volume calculations (e.g. Legros, 2000; Pyle, 1995; 1989; Fierstein and Nathenson, 1992), we concentrate here on two simple methods that do not require any mathematical assumption of the thickness decay rate. Estimating the volume of ballistic tephra falls or other eruptive parameters like DRE volumes, magnitude or intensity is beyond the scope of this abstract and will be presented in forthcoming notes.

DATA COLLECTION

Ninety thickness measurements were made during and after the eruptive phase. Twelve isopachs in the thickness range 0.3 – 12 cm were contoured on a map with satisfactory precision. We also attempted to assess the area of two additional isopachs based upon the following arguments. On the Pan-American highway a thickness of 0.2 cm of ash was measured 28 km downwind from the volcano. Considering an elliptical isopach 28 km long and 14 km wide we

obtain an area of 308 km^2. In addition, the icecap of Chimborazo volcano, located about 50 km west of Tungurahua, appeared coated with a dark layer of ash at the end of the eruption. By analogy with what we have observed at many other localities, we think that a minimum thickness of 0.05 cm is required to obtain such a uniform ash cover. This permitted us to relate the area of the 0.05 cm isopach to that of an ellipse 50 km-long and 20 km-wide. Data of isopach thicknesses and areas are given in Le Pennec et al. (2002), along with results of others estimates of bulk ash fall volume.

ASH FALL THICKNESS VARIATIONS AND VOLUME ESTIMATES

Pyle (1989) and Fierstein and Nathenson (1992) have shown that the data (thickness, T – isopach area, A) of many natural deposits plot as one or two straight lines on a Log$T$ – $A^{1/2}$ diagram. From these and other findings, Houghton et al. (1999) concluded that the thickness of proximal and medial tephra fallout deposits decay exponentially with distance from the source. For this reason, most models of tephra fall volume calculations are based on the exponential decay assumption (e.g. Legros, 2001; Pyle, 1995; 1989; Fierstein and Nathenson, 1992).

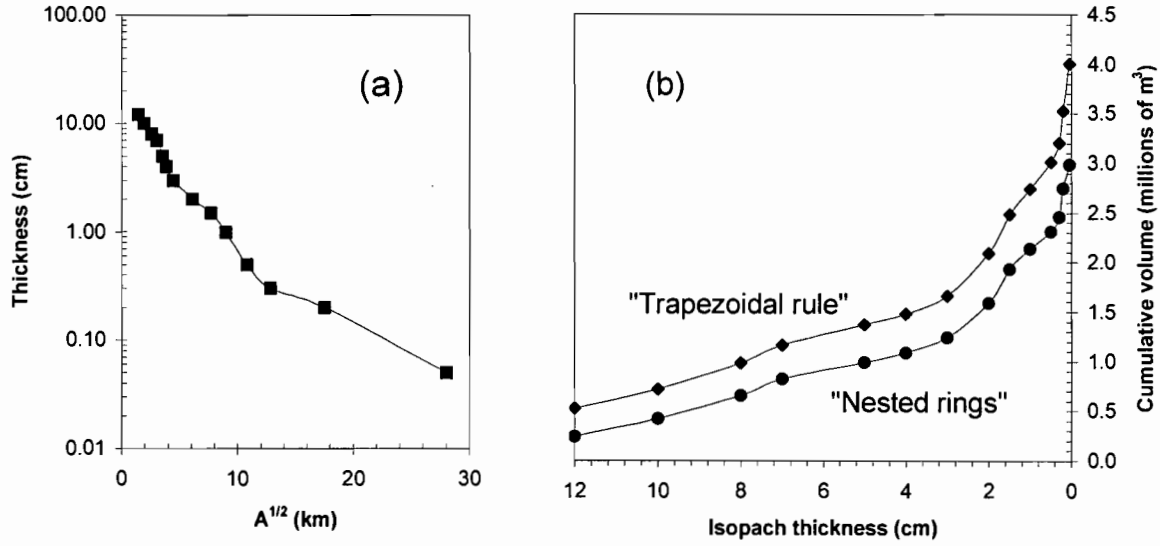

Figure 1. (a) Plot of Log$T$ versus square root of isopach area. **(b)** Cumulative volume against isopach thickness from 12 cm to 0.05 cm using the "trapezoidal rule" (upper curve) and the "nested rings" (lower curve) approximations.

However, other studies point out limits to this widely accepted model. For example, Bonadonna et al. (1998) modeled the influence of particle Reynolds numbers on final tephra fall thickness. They found that coarse ejecta with high Reynolds numbers should correspond to a deposit displaying an exponential decay rate. On the other hand, settling of fine-grained ash with low Reynolds numbers should form a deposit whose thinning rate is better described by a power law.

Various other processes may lead to additional departures from the exponential decay rate model. For instance, the effect of ash aggregation or the control of rain flushing on the final thinning rates is poorly known. These processes were at work during the August 2001 eruptive phase of Tungurahua volcano. Moreover, work in progress

suggests that the deposit contained a significant fraction of low Reynolds number particles, even close to the source. Altogether, this may partly explain the complex thinning rate observed at Tungurahua (Figure 1a). Because the thinning rate does not clearly follow the simple exponential decay rate model, we propose here to simply evaluate the bulk volume of ash using two extreme models which do not require any assumption on the mathematical formulation of the decay rate. Below we use first a method called the "trapezoidal rule" approximation that has been applied to pyroclastic deposits by various authors (e.g. Fierstein and Nathenson, 1992 and references therein) to calculate a maximum bulk ash fall volume. Secondly, a new method is presented here, called the "nested rings" approximation. It allows estimating a minimum bulk volume of the deposit.

"Trapezoidal rule" approximation. This method overestimates the true volume (see details in Fierstein and Nathenson, 1992). However, it tends to give reasonable maximum values, if closely spaced isopachs are provided and if a $T = 0$ isopach can be defined. In this method the thinning rate is a discontinuous function of the isopach area and the thickness varies linearly with area between two successive isopach data. Here we need an estimate of T_0, the ash fall thickness at the vent. According to a mountain climber who reached the crater in December 2001, the fallout thickness on the northern crater rim was about 40-60 cm (Alexander García, pers. comm., 2001). Because the dispersal axis was oriented to the west of the crater, and because the crater rim is still situated about 100 m from the major eruptive vents, we have assigned a value of 80 cm for T_0. The second problem is to estimate the area of the isopach $T = 0$. If we consider the dispersion of the ash monitored by NOAA satellites, along with witness accounts of ash fall near the Ecuadorian coast, we propose that the westernmost limit of the $T = 0$ isopach coincided with the 81° meridian, offshore of the Ecuadorian coast. We thus approximate the $T = 0$ isopach area to that of a 300 x 80 km ellipse. Finally, we obtain a bulk cumulative volume V_{tr} (subscript "tr" is for "trapezoidal rule") of 3.61 x 10^6 m^3 if the most distal isopach has a thickness $T_d = 0.3$ cm (Figure 1b); 4.41 x 10^6 m^3 if $T_d = 0.05$ cm, and 8.93 x 10^6 m^3 if $T_d = 0$. This latter value should represent a maximum estimate of the ash fall layer volume.

"Nested rings" approximation. This method is newly defined here and consists in dividing the ash fall layer in a succession of concentric structures (or eccentric structures if isopach contours are elliptical in shape), each being bounded by two isopachs of thickness T_n and T_{n+1} (with $T_n > T_{n+1}$), corresponding to areas A_n and A_{n+1} ($A_{n+1} > A_n$) respectively. Between T_n and T_{n+1} the thickness is supposed to be constant and equal to T_{n+1}. This method does not necessitate extrapolating the thinning rate neither to the vent nor to infinity but requires many closely spaced isopachs to provide an acceptable minimum volume. Application to our data collection gives a cumulative volume V_{nr} (subscript "nr" is for "nested rings") of 2.46 x 10^6 m^3 if the most distal isopach has a thickness $T_d = 0.3$ cm; 2.75 x 10^6 m^3 if $T_d = 0.2$ cm, and 2.98 x 10^6 m^3 if $T_d = 0.05$ cm. This latter value should represent a minimum estimate of the ash fall layer volume (Figure 1b).

CONCLUSION

Sustained strombolian activity took place at Tungurahua volcano in the Ecuadorian Andes in August 2001. The three weeks long eruptive phase produced a notable plume of ash whose deposits were concentrated by strong to moderate winds to the west of the edifice. With two complementary methods we have estimated a maximum and a

minimum volume for the ash fall deposit. Using thickness extrapolations to the vent and distally to zero, the "trapezoidal rule" approximation gives a maximum volume V_{tr} close to 9 x 10^6 m^3, while the "nested rings" approximation provides a minimum volume V_{nr} close to 3 x 10^6 m^3, i.e. only three times smaller than the maximum volume V_{tr}. The average of these two extreme volumes is 6 x 10^6 m^3, in close agreement with other preliminary volume estimates based on exponential or power law thinning rate assumptions (Le Pennec et al., 2002). The August 2001 ash fall layer is thus remarkably small if compared to other tephra falls deposited during the recent (<3000 yr BP) geological history of the volcano (Hall et al., 1999). In summary, the August 2001 eruptive phase of Tungurahua volcano illustrates how a small-size eruption can have a pronounced impact on human activities and properties, twenty-three months after the onset of the magmatic activity.

REFERENCES

Bonadonna, C., Ernst, G.G.J., and R.S.J. Sparks, 1998. Thickness variations and volume estimate of tephra fall deposits: the importance of particle Reynolds number. J. Volcanol. Geotherm. Res., 81: 173-187.

Fierstein, J., and M. Nathenson, 1992. Another look at the calculation of fallout tephra volumes. Bull. Volcanol., 54: 156-167.

Hall, M.L., Robin, C., Beate, B., Mothes, P., and M. Monzier, 1999. Tungurahua Volcano, Ecuador: structure, eruptive history and hazards. J. Volcanol. Geotherm. Res., 91: 1-21.

Houghton, B.F., Wilson, C.J.N., and D.M. Pyle, 1999. Pyroclastic fall deposits. In Sigurdsson et al. (coord.) "Encyclopedia of volcanoes": 555-570.

Le Pennec, J.-L., Ruiz, A.G., Mothes, P., Hall, M.L. and P. Ramón, 2002. Estimaciones del volumen global del depósito de ceniza de la erupción de Agosto 2001 del volcán Tungurahua. Boletín de Investigación en Geociencas, Instituto Geofísico – Escuela Politécnica Nacional, Quito, (in press).

Legros, F., 2000. Minimum volume of a tephra fallout deposit estimated from a single isopach. J. Volcanol. Geotherm. Res., 96: 25-32.

Pyle, D.M., 1995. Assessment of the minimum volume of tephra fall deposits. J. Volcanol. Geotherm. Res., 69: 379-382.

Pyle, D.M., 1989. The thickness, volume and grainsize of tephra fall deposits. Bull. Volcanol., 51: 1-15.

A MIOCENE SUBMARINE CANYON IN NORTH-CENTRAL CHILE: IMPLICATIONS FOR ANDEAN TECTONISM

Jacobus P. LE ROUX (1), Carolina GÓMEZ (1), Heather MIDDLETON (2), Juliane FENNER (3), Binyamin BUCHBINDER (4) and Kathryn M. GREGORY-WODZIKI (5)

(1) *Departamento de Geologìa, Facultad de Ciencias Fisicas y Matemáticas, Universidad de Chile, Casilla 13518, Correo 21, Santiago, Chile*
(2) *Time Frames Group, CSIRO Petroleum, Riverside Corporate Park, Delhi Rd., North Ryde, NSW 2113, Australia*
(3) *Bundesanstalt für Geowissenschaften und Rohstoffe, Stilleweg 2, D-30655 Hannover, Germany*
(4) *Geological Survey of Israel, 30 Malkhe Yisrael St., Jerusalem, Israel*
(5) *Lamont-Doherty Earth Observatory of Columbia University, Palisades, New York 10964-8000, U.S.A.*

KEY WORDS: Marine sedimentation, debris-flow, continental platform

Exceptionally good outcrops of a submarine canyon are exposed along the length of Quebrada Chañaral at Carizalillo, north of La Serena. The most proximal facies consists of channel fill-deposits interbedded with coarse debris-flows directly abutting the canyon wall from which they originated. The beds dip 28° against the cliff but flatten out within a few meters away from it. The normal canyon-fill deposits consist of yellow, fine to very fine-grained sandstone with broken shells dominated by oysters and pecten. Lenticular beds of coquina with larger fragments and occasionally whole shells of oysters, pecten and barnacles occur within the shelly sandstone. They generally display irregular, sharp basal contacts and also contain angular basement clasts up to 40 cm in diameter.

The fine- to very fine grained, shelly sandstones are not unlike the deposits filling modern submarine canyons. Scott and Birdsall (1978), for example, described samples collected at water depths between 14 and 400 m along the Hueneme Canyon along the Californian coast. Sediments occurring along the canyon wall in this case also consist of thinly laminated, silty sands with pelecypod and gastropod shells and few biogenic structures, contrasting with the highly bioturbated canyon floor deposits. The presence of mostly disarticulated, fragmented shells of oysters, pecten, barnacles and turitella in the Coquimbo Formation suggests that these sediments were probably derived from shallower water and were transported down the canyon by currents.

The debris-flow deposits are characterized by angular basement clasts, mixed with perfectly rounded cobbles, in a sandstone matrix similar to the normal channel-fill deposits. The rounded cobbles probably formed as basal gravel on a wave-cut platform during a lowstand period, subsequently accumulated at the canyon edge and were incorporated into the debris flow when the latter collapsed. The poor sorting, inverse grading and protruding, outsize clasts are representative of classical debris flows (e.g. Sohn, 2000), but the good clast imbrication probably indicates compressional shear straining during transport.

An intermediate facies is represented by wide, shallow channels occurring about 1 km further downslope. Flutes and giant flutes at the channel base indicate the passage of highly erosive, turbulent flows, which may also have been responsible for scouring the channels into the soft, silty substrate. A thin (1-2 cm) sandstone layer is present at the channel base, partially filling the flutes but apparently representing a subsequent event. It is interpreted as a traction-carpet developing at the base of the overlying hyperconcentrated flow. A frictional basal zone and an overlying collisional zone containing a higher concentration of shell hash can be distinguished. The hyperconcentrated flow deposited shell conglomerates with scattered, angular to rounded basement clasts. The coquinas contain disarticulated bivalves orientated with their convex side down, indicating large-scale upward fluid escape. Towards the channel centre, however, the shelly conglomerate shows stratification and cross-stratification, with most of the bi-valves orientated convex side up. Large rip-up clasts of the underlying siltstone are also present in the deeper parts of the channel, which evidently became more dilute and turbulent along its axis.

The most distal facies occurs another 6 km downchannel, where finer-grained turbidites onlap and backlap onto the stoss and lee sides of a channel obstacle formed by cohesive debris flow deposits. These deposits show a good resemblance to the inclined sandy macroforms recently described for the first time in submarine channel settings (Pickering et al., 2001). They are interbedded with bioturbated, volcanic ash beds showing cross-stratification dipping upcurrent, reflecting the influence of flood tidal currents along the deeper part of the canyon. Microfossils indicate that the canyon developed in fairly deep water, probably on the continental platform to upper continental slope.

$^{87}Sr/^{86}Sr$ dating on clamshells near the base of the succession indicates that a period of marine transgression started to inundate the basement coastal platform at around 15.5 Ma. Considering the global sea-level of about +50 m at the time (Prentice and Matthews, 1988), a relative sea-level rise of 80-150 m would have been required to submerge the area to continental shelf depths. Since 15.5 Ma, sea levels did not rise to more than about 100 m above present base level, which could imply tectonic submergence of up to 50 m. A minimum tectonic uplift of 200 m must also have taken place after 3.6 Ma (as indicated by microfossils) to expose upper continental slope deposits at an elevation of 20 m on the present coastal plain.

REFERENCES

Scott, R.M. and Birdsall, B.C. 1978. Physical and biogenic characteristics of sediments from Hueneme submarine canyon, California coast. In: Sedimentation in Submarine Canyons, Fans and Trenches (eds. D.J. Stanley and G. Kelling), Dowden, Hutchinson & Ross, Inc. Stroudsburg, Pennsylvania, p. 51-64.ñ

Pickering, K.T., Hodgson, D.M., Platzman, E., Clark, J.D. and Stephens, C. 2001. A new type of bedform produced by backfilling processes in a submarine channel, Late Miocene, Tabernas-Sorbas Basin, SE Spain. Journal of Sedimentary Research, 71, 692-704.

Prentice, M.L. and Matthews, R.K. 1988. Cenozoic ice volume history: development of a composite oxygen isotope record. Geology, 16, 963-966.

Sohn, Y.K. 2000. Depositional processes of submarine debris flows in the Miocene fan deltas, Pohang Basin, SE Korea with special reference to flow transformation.

STRESS TENSOR ANALYSIS OF THE 1998-99 TECTONIC SWARM OF NORTHERN QUITO RELATED TO THE VOLCANIC SWARM OF GUAGUA PICHINCHA VOLCANO, ECUADOR.

Denis LEGRAND (1,2), Alcinoe CALAHORRANO (2,3), Bertrand GUILLIER (2,4), Luis RIVERA (5,6) Mario RUIZ (2), Darwin VILLAGÓMEZ (2), Hugo YEPES (2)

(1) IFEA: Institut Français d'Etudes Andines, Whymper 442 y Coruña, Quito, Ecuador. (legrandenis@yahoo.com)
(2) IG-EPN: Instituto Geofísico de la Escuela Politécnica Nacional, apartado 17-01-2759, Quito, Ecuador
(3) Géosciences Azur, Laboratoire Océanologique, BP 48, 60235, Villefranche sur Mer, France.
(4) IRD: Institut de Recherche pour le Développement, 209-213 rue La Fayette, 75 480 Paris Cedex 10, France.
(5) Seismolab #252-21, Caltech, 1200 E. California Blvd., Pasadena, California 91125, USA.
(6) EOST, ULP-CNRS, 5 rue René Descartes, 67084 Strasbourg Cedex, France.

KEY WORDS : stress tensor, volcanic and tectonic swarm, Guagua Pichincha volcano, Ecuador.

INTRODUCTION

Phreatic activity and subsequent dacitic dome growth in 1998-99 at Guagua Pichincha volcano, Ecuador, was associated with two seismic swarms: One located in the northern part of Quito and another one, just below the active volcano, about 15-20 km SW from the first one. We registered more than 3.200 events (among which 2.354 events of $1.4 \leq M_L \leq 4.2$) between June 1998 and December 1999, at [-2 km; -17 km] depth. Approximately 130.000 events were registered between September 1998 and December 1999 at [+2.4 km; -3.5 km] depth. We study here the stress tensors of these two swarms deduced from the polarities of P first motions and compare them to the regional stress tensor deduced from CMT Harvard focal mechanisms. Movement of fluids (magma, gas and/or groundwater) produced by the close active Guagua Pichincha volcano seems to have influence in the acceleration of generation of seismic events.

SEISMOLOGICAL NETWORK AND DATA:

In this study, we use 35 of the 40 stations of the Ecuadorian network (Figure 1), mainly 1 Hz vertical component with a good azimuthal distribution and distance range with respect to both swarms. In the period 1998-99, about 130 000 tectonic and volcanic events have been recorded by the IG-EPN. In this study, we only select the best events and relocated them with a new velocity model (Villagómez et al., 1999; Villagómez, 2000; Calahorrano et al., 1999; Calahorrano, 2001). We show (Figure 2) the most reliably constained events of the swarm of Quito (1.662 over more than 3.200 events) corresponding to a RMS<0.5 and at least one S arrival time.

STRESS TENSOR ANALYSIS:

The joint inversion for focal mechanisms and stress tensor shape and orientation has been performed. The best stress tensors are shown in Figure 3. For Quito swarm two principal kinds of focal mechanisms exist: strike slip and reverse faults. These differences can be expected with the shape factor R = -1. Focal mechanisms of Guagua Pichincha are very different from these of the swarm of Quito. They are mainly normal and strike slip faults, compatible with respect to a 0.4 R shape factor.

A classical question is to check whether the stress tensor beneath a volcano is the same as the regional stress tensor. In order to answer this question, we compare the local Quito and Guagua Pichincha stress tensors with respect to the regional tectonic stress tensor. We consider focal mechanisms of large ($M_w \geq 5$) and shallow (depth≤50 km) earthquakes (Figure 4). The corresponding data split naturally into 2 regions called the coast and the cordillera. Hence, we calculate the stress tensor for each region. The results are shown in figure 4 and show an almost identical stress tensor for both regions. This regional tectonic stress tensor with σ_1 aligned E-W is consistent with compression caused by the convergence between the Nazca and South America plates. Additionally, the subduction collision of the Carnegie Ridge may locally increase plate coupling (Gutscher et al., 1999a and 1999b) and is similar to Quito swarm.

CONCLUSIONS

Quito swarm stress tensor (Figure 3 bottom-right) has a major compressive stress direction σ_1 almost in a horizontal direction, oriented N116.5°E, compatible with 1) the regional plate motion direction of N102°E deduced from GPS (Kellogg and Vega, 1995) 2) the results of Ego et al., 1996 and 3) the σ_1 N91.5°E direction we found using large earthquakes of the cordillera of Mw≥5 (Figure 4 up-right). The extensional direction σ_3 of the swarm of Quito (Figure 3 bottom-right) is almost vertical, in agreement with the regional stress tensor (Figure 4). Hence, the stress tensor of the swarm of Quito is similar to the regional stress tensor, small differences can be due to the effect of the close active Guagua Pichincha volcano, situated 15-20 km SW.

In contrast, the stress tensor of Guagua Pichincha volcano (Figure 3 middle-left) is very different from the regional tectonic (Figure 4) and the Quito swarm (Figure 3 bottom-right) ones. This suggests a very local stress regime directly associated to Guagua Pichincha volcano activity. The horizontal σ_3 direction beneath the volcano is compatible with what should be expected under a volcano were many up-going fluids (water, gas and/or magma) can generate such horizontal extensional direction.

We speculate that Quito swarm is directly submitted to the regional stress tensor, slightly modified by the close (15-20 km) active Guagua Pichincha volcano, whereas the stress tensor of the swarm under the volcano is a local response to this regional stress tensor.

The presence of two stress tensors relatively different within a small region (at about a distance of 15-20 km) suggests that the stress tensor may be rather heterogeneous in that region, and that the volcano may have an influence upon the regional stress tensor within a distance of at least 20 km from which Quito swarm is located.

Acknowledgements:

We thank all the staff (technicians, researchers, engineers and students) of the Instituto Geofísico of the Escuela Politécnica Nacional of Quito (IG-EPN) for the monitoring and the maintenance of the seismological stations in Ecuador. We thank the IFEA (Institut Français d'Etudes Andines), the IRD (Institut de Recherche pour le Développement) and the MAE (Ministère des Affaires Etrangères) for supporting portions of this study.

Al amigo, Diego Viracucha, quien cayó el domingo 14 Enero del 2001 en el crater del Guagua Pichincha. Un recuerdo sincero para todos tus efuerzos y devoción a la volcanología. Te dedicamos este pequeño trabajo.

REFERENCES

Calahorrano, A., 2001. Estudio del origen del enjambre sísmico de la zona norte de la ciudad de Quito, durante 1998-99. Escuela Politécnica Nacional, facultad de geología, minas y petróleos, tesis de ingeniera geóloga, Quito, Ecuador, 190 pp.

Calahorrano, A., Yepes, H., Guillier, B., Ruiz, M., Segovia, M., Villagómez, D. and Andrade, D., 1999. Seismic swarm in Quito (Ecuador): tectonic or volcanic origin? In: Fourth ISAG, Goettingen (Germany), pp. 119-122.

Ego, F., Sébrier, M., Lavenu, A., Yepes, H. and Eguez, A., 1996. Quaternary state of stress in Northern Andes and the restraining bend model for the Ecuadorian Andes. Tectonophysics, 259: 101-116.

Gutscher, MA., Malavieille, J., Lallemand, S. and Collot, JY., 1999a. Tectonic segmentation of the North Andean margin: impact of the Carnegie Ridge collision. Earth Planet. Sc. Let., 168: 255-270.

Kellogg, J. and Vega, V., 1995. Tectonic development of Panama, Costa Rica, and the Colombian Andes: constraints from Global Positioning System geodetic studies and gravit. In Mann P. (Ed.), Geologic and tectonic development of the Caribbean plate boundary in Southern Central America, Geol. Soc. Am. Spec. Pap., 75-90.

Villagómez, D., 2000. Sismicidad del volcán Guagua Pichincha, 1998-1999. Escuela Politécnica Nacional, facultad de geología, minas y petróleos, tesis de ingeniero geólogo, Quito, Ecuador, 114 pp.

Villagómez, D., Ruiz, M., Yepes, H., Hall, M., Guillier, B., Alvarado, A., Segovia, M. and Calahorrano, A., 1999. Seismic activity at Guagua Pichincha volcano, Ecuador. Fourth ISAG, Goettingen (Germany), 793-796.

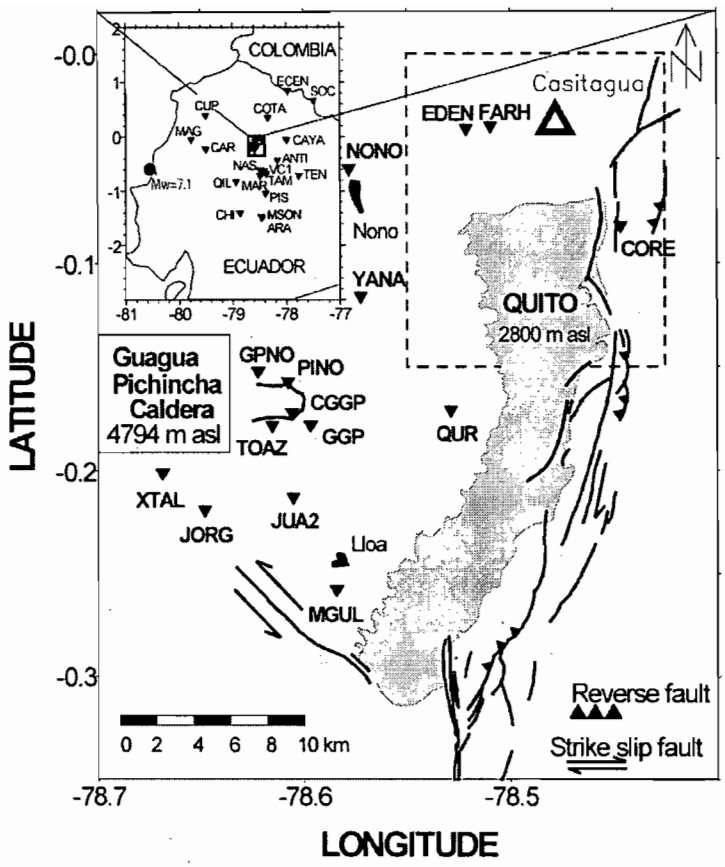

Fig 1. **Up-left rectangle**: The 35 seismic stations (inverse triangles) of IG-EPN used for this study. The rectangle corresponds to the limits of the main figure.

Main figure: Local seismic stations and main faults near Quito. The station TERV is at the same place as CGGP. The open triangle corresponds to the Casitagua (3519 m) old volcano. We represent also the 4675 m limit of the caldera of Guagua Pichincha volcano (4794 m). The rectangle corresponds to the limits of Quito swarm.

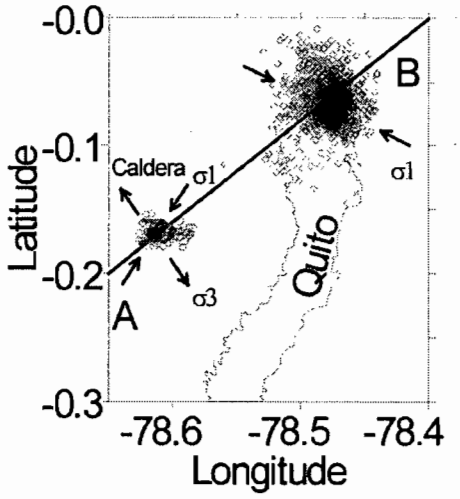

Fig 2. Location of the events of Quito swarm (diamonds) and VTs swarm under the Guagua Pichincha caldera (circles). The line AB corresponds to a vertical cut of figure 3.

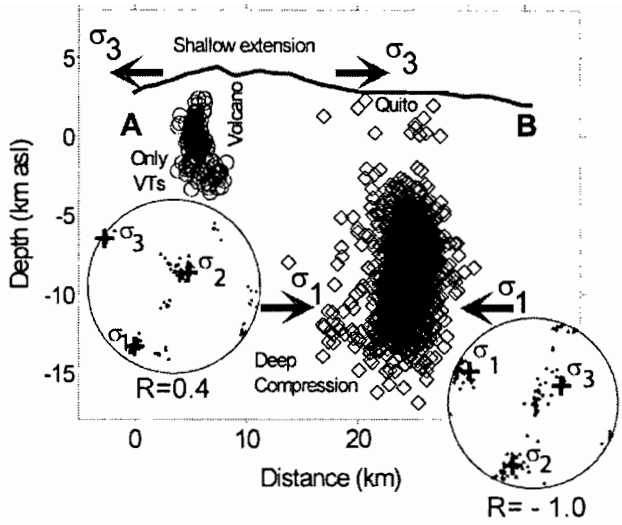

Fig 3. Vertical cut AB of figure 2. Stress tensors of the swarm of VTs swarm below Guagua Pichincha volcano (up-left) and Quito swarm (bottom-right). The direction σ_1 may affect the deep events under Quito (diamonds) and generate a deep compression (convergent arrows) and a shallow extension at the level of the volcano (divergent arrows). The stress tensors are represented in the inferior half sphere, equal-area Schmidt projection. $\sigma_1>\sigma_2>\sigma_3$ are the eigen directions of compression, intermediate and extension respectively. The 50 best solutions are plotted, the cross corresponds to the best solution.

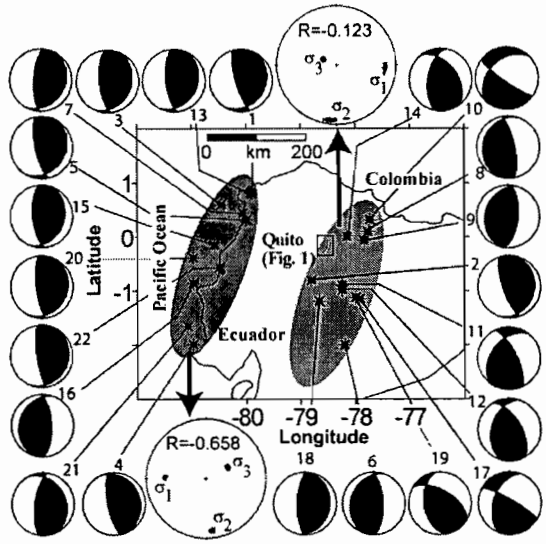

Fig 4. CMT Harvard focal mechanisms of shallow earthquakes (less than 50 km deep), and $M_w \geq 5$. $\sigma_1>\sigma_2>\sigma_3$ are the eigen directions of compression, intermediate and extension respectively. The square corresponds to limits of figure 1.

FOREARC EXTENSION: TECTONICS, SEDIMENTOLOGIC AND STRATIGRAPHY EVOLUTION OF THE EAST PISCO BASIN

Walther LEÓN (1) and Antenor M. ALEMÁN (2)

(1) INGEMET wleonlecaros@hotmail.com

(2) 2807 Stoney Wood, Houston TX, antenor@swbell.net

KEY WORDS: Forearc basin, transtension, oblique convergence

INTRODUCTION

The East Pisco forearc basin was built over a basement varying in age and lithologies from Precambrian gneisses and schist, to Devonian granitoids to Jurassic volcaniclastics. Eastward, the Cerrillos Fault limited the distribution of the Cretaceous arc massif rocks. The Coastal Batholith arc magmatism terminated in the Paleocene and migrated eastward. As a result, pervasive regional igneous underplating and regional forearc basin uplift took place until the Middle Eocene worldwide plate reorganization. Oblique convergence, strong coupling and lithosphere heterogeneities were the main factors controlling strain partitioning and strike-slip deformation in the upper plate (Molnar and Pardo Casas, 1987).

Crooked fault pattern may reflect the influence of pre-existing fabrics. However, identification of transfer zones provides important information to explain fault geometry, graben polarity changes, and along strike changes in fault throw. Rhombic fault geometry produced by zigzag faults was a tempting pattern for a transtensional interpretation of the East Pisco Basin. Regardless of the structural origin, a tectonic-sedimentary model is proposed that may explain the Cenozoic basin evolution in four distinctive stages (Fig.1):

1. Middle Eocene extension and half-graben formation.
2. Late Oligocene extension, polarity change and full graben formation.
3. Middle Miocene uplift and extension renewal.
4. Late Pliocene to Pleistocene basin inversion and uplift.

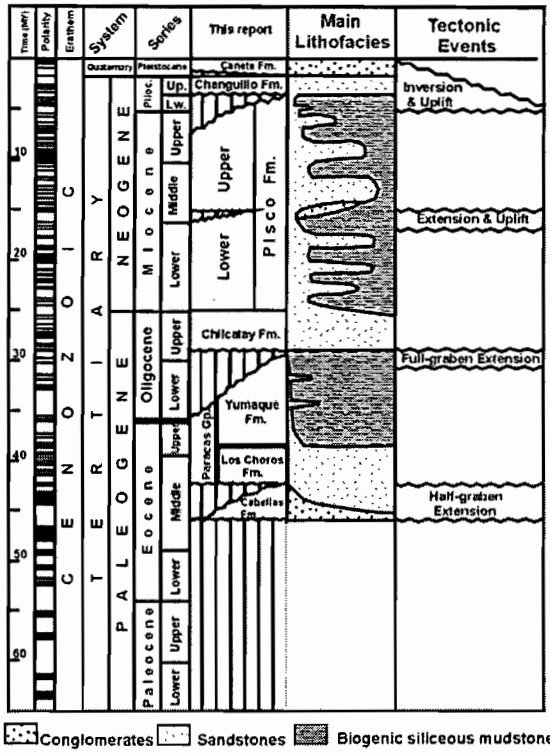

Fig.1 Lithofacies and tectonic events in the East Pisco Basin

Middle Eocene extension is inferred from the Caballas Formation alluvial fan to fluviatile siliciclastic progradation wedges made of material derived directly from fault scarp erosion. As extension continued, the first marine incursion and transgression took place as interpreted from the overlying shallow water, low to high energy Los Choros Formation. Episodic equilibrium between faulting and sediment supply caused repeated and vertical stacked progradational events. Large olistoliths, syndepositional faults, bed rotation, thick debris flows and conglomerates in this formation are interpreted to confirm active faulting. Fault-driven subsidence accounts for marine flooding and deposition of tuffaceous and diatomaceous-rich mudstones of the Yumaque Formation. In addition, large sandstones and mudstones olistoliths are thought to indicate active faulting during deposition.

A slight angular unconformity, interbedded conglomerates and debris flows associated with the shallow marine sandstones of the Chilcatay Formation are interpreted to be the result of late Oligocene extension (Fig. 1 and 2). Locally, footwall uplift caused fault scarp retreat and alluvial fan deposition was interbedded with nearshore facies. Discontinuous, repeated and vertical stacked shoreface progradational events were deposited until the equilibrium between faulting and sediment supply was broken. Glass shards in the sandstones imply important airfall volcanic contribution and rapid beach cementation. Continuous faulting caused marine flooding and deposition of thinly bedded, tuffaceous, and diatomaceous rich mudstones of the Lower Pisco Formation. Distinct thin layers of tuffs, phosphatic pellets, dolomite and diatomites are present throughout the section. Upwelling was not as important in the Pisco Formation as in the Yumaque Formation deposition (Dumbar and Baker, 1988). Isolated interbedded sandstones are interpreted to result from terrigenous input during footwall uplift that moved axially and along the grabens flanks. Structural and depositional history varies along and across the basin and was characterized by either reactivation of boundary faults, formation of new synthetic fault or generation half-grabens with different polarity. The graben polarity change caused full-graben formation exemplified by abandonment or decrease in activity of older boundary faults and development of relatively widely spaced minor faults.

Middle Miocene uplift and short-lived compressional was caused by a change in the regional stress field orientation prior to extension renewal along pre-existing faults. Extension was accompanied by footwall uplift, fault scarp retreat and slight bed rotation and triggered stream incision and rejuvenation. As a result deep scouring caused formation of incised valleys filled with fluviatile conglomerates. Continuous fault-controlled subsidence caused rapid incised valley flooding and deposition of the Upper Pisco Formation biogenic and tuffaceous mudstones below storm wave base. Similar to the Yumaque Formation, the presence of dolomite, phosphate pellets, and diatomite oozes and laminations are interpreted to indicate upwelling conditions similar to the present day Humboldt Current (Dumbar,

1988; Marty, 1989). The presence of tuffs and glass shards dispersed in the mudstones records active Miocene arc volcanism to the east. Thick interbedded sandstones are interpreted as episodic terrigenous input during continuous footwall uplift.

Late Pliocene to Pleistocene basin inversion and uplift was the result of subduction of the Nasca aseismic ridge as it migrated southward along the coast beneath the Peruvian forearc basins (Pilger, 1981; Macharé and Ortlieb, 1993). Hence, modification in the regional stress at the plate boundary resulted in regional uplift. This large orientation change in the original stress field was a predictable event since grabens tend not to develop under long-lived stable stress conditions.

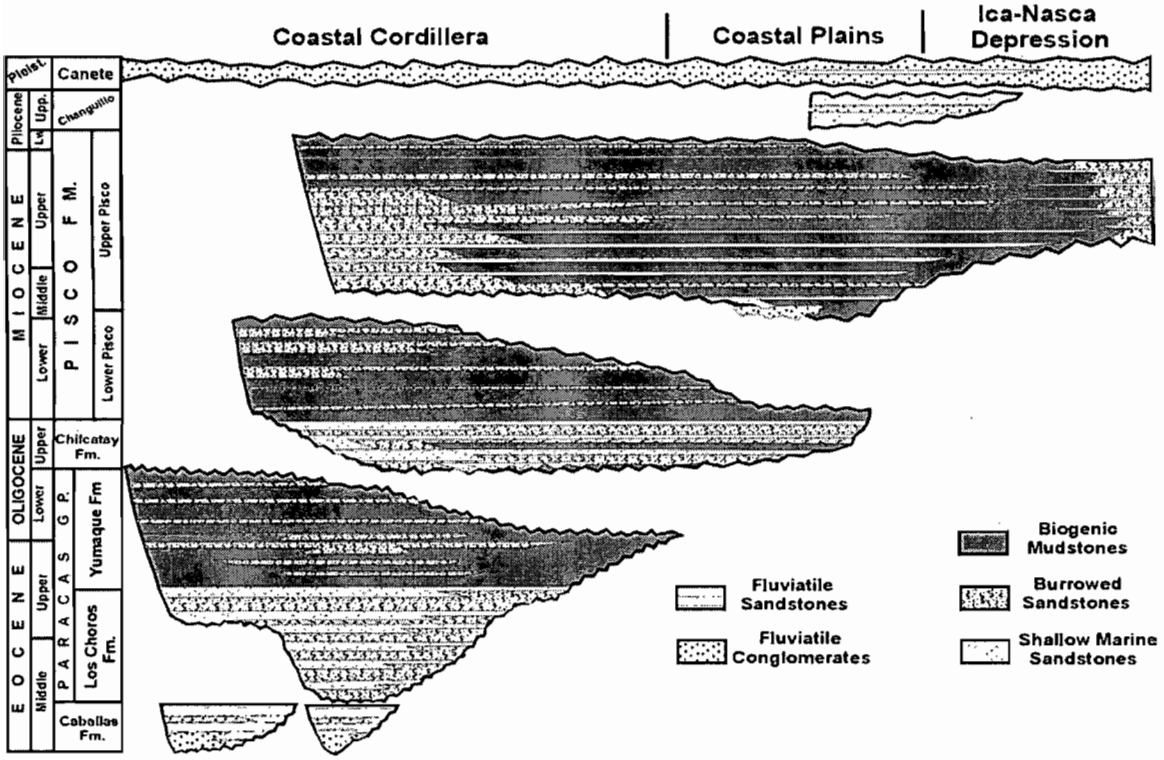

Fig. 2. Chronostratigraphic chart of the east Pisco basin

Cenozoic rocks provenance diagrams are plot mainly on older volcanic arc massif and may be interpreted as a constant source (Fig.3). However, important variations in the degree of arc dissection as well as increased quartz content are interpreted to be related to depositional process. The Caballas, Chilcatay, Pisco and Changuillo Formations have similar provenance, however the Los Choros Formation contains more quartz grains. This is interpreted to be related to longer resident time in the high-energy shoreface environment.

CONCLUSIONS

Deformation in the East Pisco forearc basin is related to oblique extension characterized by widespread development of grabens developed along a narrow corridor following the Coastal Cordillera structural grain. The

grabens were inverted during the late Neogene impinging of the Nasca Ridge. The basin has undergone four distinctive episodes of deformation characterized by different degree of extension. Modal analysis suggest that petrofacies variations is related to local source variations.

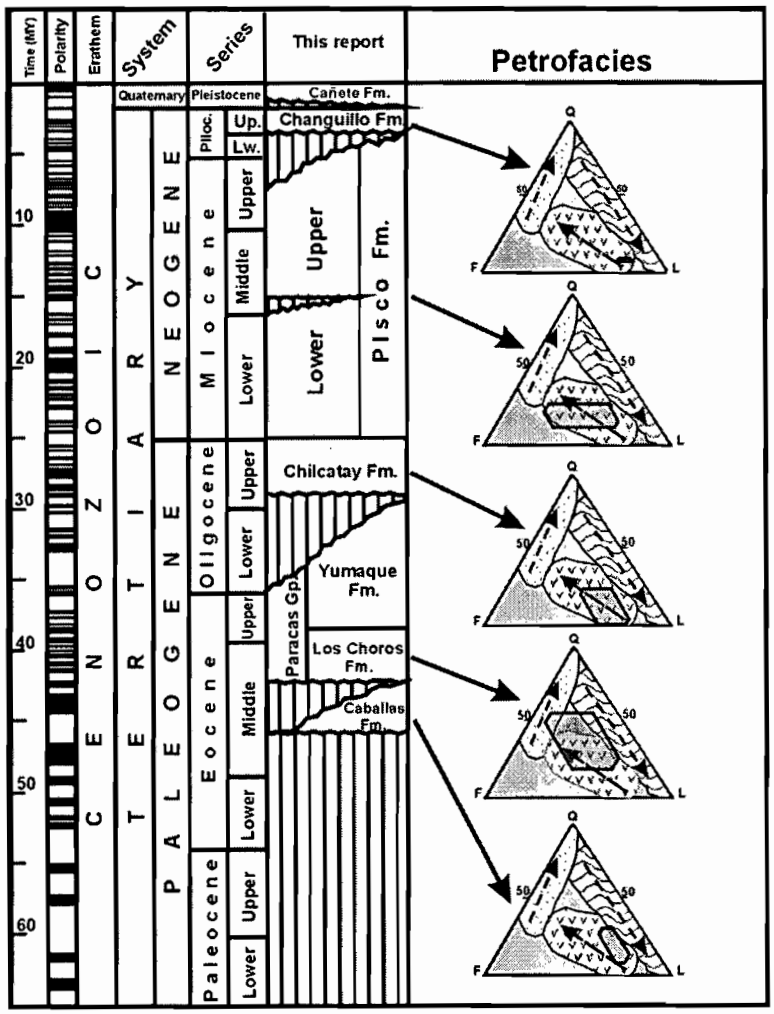

Fig. 3. Stratigraphy and Tertiary petrofacies

REFERENCES

Dumbar, R. B. Baker, P.A., 1988, Cenozoic Geology of the Pisco Basin, IGCP no. 156 Guidebook to Field Workshop, 253 pp.

Macharé, J., and Ortlieb, L., 1993, Coastal Neotectonics in Peru: Subduction regime and Quaternary vertical motions, Second Intern. Symp. of Andean Geodynamics, Oxford, 107-110.

Marty, R. C., 1989, Stratigraphy and chemical sedimentology of Cenozoic biogenic sediments from the Pisco and Sechura Basins, Peru. Thesis Rice University, Houston, Texas, 238.

Pilger, R. H., 1981, Plate reconstructions, aseismic ridges, and low-angle subduction beneath the Andes: Geolog. Soc. Amer. Bull. , v.92, 448,456.

Molnar, P., and F. Pardo Casas, 1987, relative motion of the Nasca (Farallon) and South American plates since Late Cretaceous, Tectonics, 6, p.233-248.

PRELIMINARY COMPARISON BETWEEN ANTUCO AND SIERRA VELLUDA VOLCANOES (SOUTHERN ANDES)

Silke LOHMAR (1), Leopoldo LÓPEZ-ESCOBAR (1) and Hugo MORENO (2)

(1) Magmatic Group. Instituto de Geología Económica Aplicada, Universidad de Concepción. Casilla 160-C. Concepción, Chile. (E-mail: slohmar_2000@yahoo.com_E-mail: llopez@udec.cl)

(2) Observatorio Volcanológico de los Andes del Sur (OVDAS). Servicio Nacional de Geología y Minería. Cerro Ñielol s/n. Casilla 23 D. Temuco, Chile. E-mail: ovdassis@chilesat.net

KEY WORDS: Volcanism, Quaternary, Geochemistry, Southern Andes, Central-south Chile.

INTRODUCTION

The Antuco - Sierra Velluda volcanic complex is located in the Southern Volcanic Zone (SVZ) of the Chilean Andes at 37°21' - 37°33'S (Fig. 1). Its position is related to a N50-70°E lineament (López-Escobar *et al.*, 1995) which is associated with the NNE-SSW trending Liquiñe-Ofqui Fault Zone (LOFZ; Hervé *et al.*, 1979).

Sierra Velluda is a strongly eroded stratovolcano. Activity commenced around 500 ka ago and ended ca. 300 ka ago (dikes cutting through the edifice have been dated at less than 150 ka). Antuco, by comparison, is a composite, compound stratovolcano with an almost perfect cone, whose volcanic activity commenced at 130 ka and continues to the present (K/Ar ages; Moreno et al., 1986).

This work presents geochemical data for Antuco and preliminary data for the neighbouring and older Sierra Velluda, which is a previously unstudied Southern Andean stratovolcano.

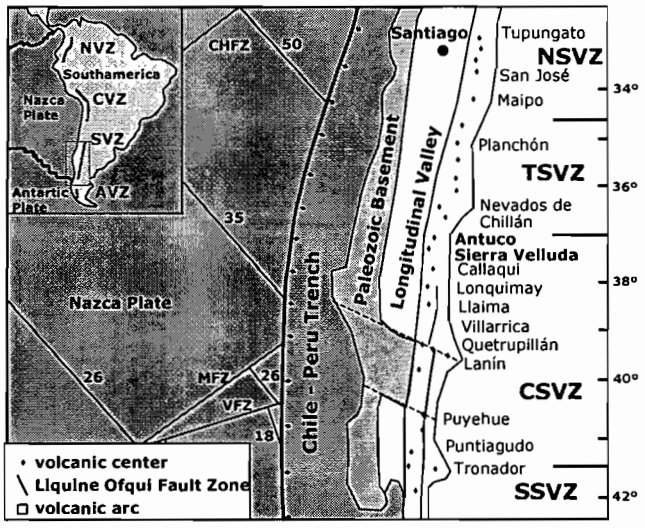

Figure 1: Location map of the Antuco-Sierra Velluda volcanic complex in the Southern Volcanic Zone (SVZ) (modified from López-Escobar *et al.*, 1993).
NSVZ: northern SVZ, TSVZ: transitional SVZ, CSVZ: central SVZ, SSVZ: southern SVZ.

GEOLOGICAL FRAMEWORK

Two main units are distinguished during the evolution of Antuco volcano: 1) a primary edifice (Antuco I), formation of which was terminated ca. 6.2 ka ago by a large scale (> 5 km^3) sector collapse to the west, with a westward opening, and 2) a younger eruptive cone (Antuco II) building at the same location. Antuco I lavas range in composition from basalt to dacite, with olivine basalts and basaltic andesites being the most abundant lithologies. In contrast, Antuco II lavas are mainly basalts and basaltic andesites (Lohmar *et al.*, 1999).

Sierra Velluda Volcano consists of lava flows and clastic deposits (laharic and pyroclastic) which radiate from the current peak. The lava flows extend over more than 10 km from the vent area and have been partially eroded by glacial activity, generating several radial valleys. Regionally, flows unconformitably overlie intrusive rocks of Miocene age and volcaniclastic rocks belonging to the Curamallin Formation (Eocene-Miocene). They underlie lava flows of Antuco volcano. Moreno *et al.* (1986) have distinguished two units at Sierra Velluda which are lithologically different and separated by a depositional unconformity: Sierra Velluda I is the oldest and is principally formed of laharic and pyroclastic deposits, while Sierra Velluda II consists mainly of lava flows.

PETROGRAPHY

- **Antuco:** Basalts and basaltic andesites (Antuco I and II) are porphyrytic, with little vesiculation, and contain phenocrysts of predominantly plagioclase, and lesser olivine and clinopyroxene. Orthopyroxene is mainly observed in Antuco I lavas. Plagioclase phenocrysts are compositionally zoned (center=An 80-76; rim=An 75-65) and occassionally contain inclusions of glass and groundmass minerals ("sieve" texture). The groundmass is composed of plagioclase, olivine, clinopyroxene (and orthopyroxene, in case of Antuco I), opaque minerals and variable amounts of glass. Texture varies from intergranular to intersertal, and occasionally pilotaxitic. Andesites and dacites (Antuco I) are also porphyrytic and contain phenocrysts of strongly zoned plagioclase, and lesser quantities of clinopyroxene, orthopyroxene and olivine. Olivine phenocrysts are mantled with a thin orthopyroxene rim. All mafic phenocrysts are rimmed by iron oxides. This evidence, together with the "sieve" textured plagioclases, indicates disequilibrium between phenocrysts and the host magma. The groundmass is composed of plagioclase, olivine, clinopyroxene, orthopyroxene, opaque minerales and glass. Texture varies from pilotaxitic and hialopilitic to intergranular and intersertal. All Antuco I dacites exhibit flow textures.
- **Sierra Velluda:** Initial studies of the lava units of Sierra Velluda show that compositions are restricted to basaltic andesites and andesites (Fig. 2). Rocks are porphyrytic and contain phenocrysts of mainly plagioclase, with lesser quantities of clinopyroxene, orthopyroxene and olivine. The groundmass is composed of plagioclase, clinopyroxene, orthopyroxene, olivine, opaque minerals and variable amounts of glass. Textures vary from intergranular to intersertal and hialopilitic.

GEOCHEMISTRY

All Antuco and Sierra Velluda lavas are typically calc-alkaline (according to Irvine and Baragar, 1971) with high Al_2O_3 contents. Antuco I lavas vary in SiO_2 content from 51 to 64 wt.%. The SiO_2 range is more restricted in the case of Antuco II lavas (50 to 57 wt.%). In general, basaltic and andesitic basaltic rocks are the most common compositions in Antuco lavas (Fig. 2).

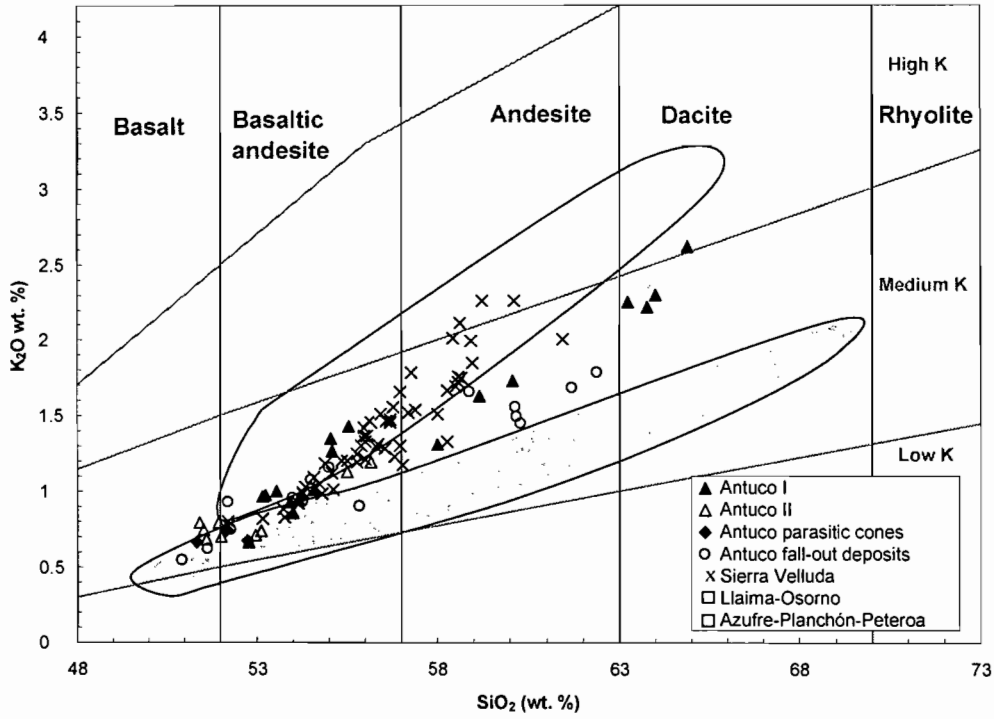

Figure 2: Classification diagram (Peccerillo and Taylor, 1976) for Antuco and Sierra Velluda samples. For comparison, fields occupied by other volcanoes of the SVZ are shown: Azufre-Planchon-Peteroa (35°S), Llaima (38,5°S) and Osorno (41°S) (López-Escobar, unpublished data).

Sierra Velluda compositions vary between 52 and 61 wt.% SiO_2 and show slightly higher K_2O contents compared with Antuco lavas of similar silica contents, above all for andesitic rocks (Fig. 2).

Variation of major and trace elements versus SiO_2 indicates an important fractionation of olivine (decrease in Mg, Co and Ni), clinopyroxene (decrease in Cr and Ca), plagioclase (decrease in Al and Sr) and magnetite (decrease in Fe and V) during the evolution of the Antuco and Sierra Velluda magmas.

Antuco basalts (regardless of their age) are relatively evolved magmas with low MgO (<7,5 wt.%), Ni and Cr, which have experienced fractionation of olivine and pyroxene prior to emplacement.

Limited variability in Rb/Y (Antuco: 0.64 - 2.39, Sierra Velluda: 0.57 - 2.84), Rb/La (Antuco: 1.45 - 3.97, Sierra Velluda: 1.41 - 4.18), Rb/Ba (Antuco: 0.05 - 0.15, Sierra Velluda: 0.05 - 0.18), K/La (Sierra Velluda: 546.54 - 1006.74, Antuco: 432.02 - 941.49) and K/Ba (Antuco: 18.78 - 36.95, Sierra Velluda: 25.29 - 39.77) in both Antuco and Sierra Velluda lavas suggest that magmas have not been significantly contaminated during their evolution, or have assimilated material with a similar geochemical signature. Regardless, Sierra Velluda lavas are slightly more enriched in Rb than Antuco lavas of similar SiO_2 content (54.5 - 59 wt.%).

Antuco volcano is one of the isotopically most primitive stratovolcanoes of the Southern Andes ($^{87}Sr/^{86}Sr$ between 0.70369 and 0.70391 in the range of basalt to andesite (Lohmar *et al.*, 1999).

CONCLUSIONS AND FURTHER STUDIES

Preliminary investigation of Sierra Velluda lavas show that they are more evolved than those of the neighbouring and younger Antuco. We intend to investigate if this is only due to a different degree of differentiation (bigger magma chamber and longer residence time in the case of Sierra Velluda, as would be apparent from higher Rb and K of Sierra Velluda lavas) or assimilation of different types of crust material. Further work will include mineral chemistry studies in Antuco rocks and isotopic analysis of dacites. The same type of investigation will be carried out on Sierra Velluda samples to generate a comparative data set, including the first isotopic analyses for this volcano.

ACKNOWLEDGEMENTS

Special thanks to Michael Dungan from University of Geneva. Funding has been provided by the Swiss FNSRS. Leopoldo López-Escobar acknowledges the support given by FONDECYT-Chile grant 800-0006.

REFERENCES

Hervé, F.; Araya, E.; Fuenzalida, J. and Solano, A. 1979. Edades radiométricas y tectónica neógena en el sector costero de Chiloé continental, X Región. II Congreso Geológico Chileno, 1, F1-F18.

Irvine, T. and Baragar, W. 1971. A guide to chemical classification of the common volcanic rocks. Canadian Journal of Earth Science, 8, 523-548.

Lohmar, S.; López-Escobar, L., Moreno, H. and Déruelle, B. 1999. Antuco Volcano: One of the isotopically most primitive stratovolcanoes of the Southern Andes (37°25'S). Fourth International Symposium on Andean Geodynamics, 437-440.

López-Escobar, L.; Cembrano, J. and Moreno, H. 1995. Geochemistry and tectonics of the Chilean Southern Andes basaltic Quaternary volcanism (37°-46°S). Revista Geológica de Chile, 22, 2, 219-234.

López-Escobar, L.; Kilian, R.; Kempton, P. and Tagiri, M. 1993. Petrography and geochemistry of Quaternary rocks from the Southern Volcanic Zone of the Andes between 41°30' and 46°00'S, Chile. Revista Geológica de Chile, 20, 1, 33-55.

Moreno, H.; Lahsen, A.; Varela, J. and Vergara, M. 1986. Edades K-Ar de rocas volcánicas cuaternarias del Grupo Volcánico Antuco-Sierra Velluda, Andes del Sur, 37°27'S. Comunicaciones, 36, 21-25.

Peccerillo, R. and Taylor, S.R. 1976. Geochemistry of Eocene calc-alcaline volcanic rocks from the Kastamonu area, northern Turkey. Contributions to Mineralogy and Petrology, 658, 63-81

PROGRESS REPORT ON A PETRO-GEOCHEMICAL AND MINERALOGICAL STUDY OF THE "EL TENIENTE BELT", CENTRAL CHILE: IMPLICATIONS OF LOWER CRUSTAL MELTING PROCESSES AND THE LINKS TO GIANT ANDEAN PORPHYRY Cu-Mo MINERALIZATION

Leopoldo LOPEZ-ESCOBAR,(1), Robert W. KING (1), Osvaldo M. RABBIA (1) and Laura B. HERNANDEZ (1)

(1) Grupo Magmático, Instituto GEA, Casilla 160-C, Universidad de Concepción, Concepción 3, Chile (llopez@udec.cl; rking@udec.cl; rabbia@udec.cl; laherna@udec.cl)

KEY WORDS: porphyry copper; high-Al TTG; boron; tourmaline; rutile; apatite

OVERVIEW

Over the past few years, our research group has been actively engaged in the study of magma genesis in subductive regimes and on the use of resistate minerals as a monitor of environment of formation. A major portion of this research has been funded by CONICYT-Chile through Fondecyt research grants. This present Fondecyt Lineas Complementarias project builds on these accomplishments and a much broader scale project has emerged to further develop the scientific understanding of deep crustal/subduction zone-related magmatism associated with active continental margins and its constraints on the formation of economic porphyry Cu-Mo systems.

INTRODUCTION

The main objective of the project is to evaluate processes that took place deep in or below the Andean crust of the El Teniente Belt of Central Chile and link them to those processes that formed some of the giant to supergiant Miocene-Pliocene porphyry copper deposits characteristic of this belt. This presentation outlines findings to date on several fronts of the project. The majority of the works focuses on the El Teniente supergiant porphyry copper deposits as data from the other two systems (Los Pelambres and Río Blanco-Los Bronces) are still being collected at the time of writing.

HIGH-Al TTG ANALOGOUS INTRUSIVE ROCKS IN THE SUPERGIANT EL TENIENTE PORPHYRY COPPER DEPOSIT.

The main igneous units at the El Teniente deposit are: the pre-ore "Andesitas de la mina" (subvolcanic mafic bodies), "Diorita Sewell" (leuco-quartz-diorite to trondhjemite stock) and the syn-ore "Pórfido Teniente" (leuco-dacite porphyry) and minor leuco-tonalitic apophyses.

The distinctive petrographic and geochemical features of the felsic intrusive units include: leucocratic character, high Na_2O (>4.5wt%) and Al_2O_3 (>15.5wt%) contents, high Sr/Y (>80), La/Sm (>5) and La/Yb (>25) ratios with low $HREE_{chn}$ (~2x), Y (<7ppm) and Sc (<10ppm) contents, sub-alkaline (calc-alkaline) affinity and metaluminous character (ASI<1). The evidence suggest that these rocks were mainly derived from a garnet(±pyroxene±amphibole)-bearing basaltic source. Additionally, the lack of a negative Eu anomaly in conjunction with high Sr (550-1050 ppm) content for a silica range of 60 to 70wt%, preclude significant plagioclase in the source residue. Furthermore, #Mg <0.55 coupled with relatively low Ni (≈10 ppm) and Cr (≈ 20 ppm) contents of these rocks, preclude any significant interaction of the silicic magmas with the mantle wedge.

From the isotopic point of view, these porphyries have less radiogenic $Sr_{(i)}$ values (≈0.7040) and higher $\varepsilon Nd_{(i)}$ values (+3.4 to +3.9) than those exhibited in Quaternary volcanics at the same latitude, but are almost identical to modern lavas erupted through the thinnest SVZ crust. The Pb isotopes, are clearly more radiogenic than Nazca Plate Basalts, but less radiogenic than those from the Juan Fernández aseismic Ridge.

Overall, petrographic, geochemical and isotopic evidence points to a general petrogenetic model based on high pressure partial melting of young mafic Andean lower crust, as the main magma source from which this high-Al TTG analogous suite associated with the El Teniente porphyry Cu-Mo deposit was derived.

BORON BEHAVIOUR IN SVZ ROCKS: IMPLICATION OF BORON, CRUSTAL/ SUBDUCTION PROCESSES AND SUPERGIANT COPPER MINERALIZATIONS

In order to understand the origin of the large amounts of B associated with the supergiant porphyry copper deposits of the Central Chile Andes, we have investigated the behaviour of B in simpler basaltic to basaltic andesite systems belonging to the central and southern provinces of the southern volcanic zone of the Andes (CSVZ, 33°-41.5°S; SSVZ 41.5°-46°S). Samples are from small eruptive centers (SEC) and large stratovolcanoes. While SEC are controlled by the 1000 km long, N10°E, Liquiñe-Ofqui Fault Zone (LOFZ), which is located behind the volcanic front, the stratovolcanoes in contrast are controlled by fractures tranverse to this fault. Volcanic front stratovolcanoes are richer in B (12.8-16.2 ppm) than SEC. With the exception of Huellemolle and Mirador (12.1 and 11.5 ppm B respectively), the studied SEC have B contents < 10 ppm. The lowest value (1.6 ppm) is found in a basalt (48.8% SiO_2) from the Puyuhuapi volcanic group, which is located well behind the volcanic front. Puntiagudo stratovolcano, also located behind the front and controlled by the LOFZ, has low B content (2.9 ppm)

similar to SECs. The affinity of B to aqueous fluids phases and its positive correlation with ^{10}Be suggests that B is firstly controlled by the amount of aqueous fluids liberated from the slab which, in turn, is related to its surface temperature and position of centers with respect to depth of the slab, and secondly to the evolution styles of magmas and eruptive behaviour of each center. This, together with the low concentrations of B in the lower crust suggest that B increases as the hydrothermal solutions increase during the rise of the magmas through the crust. Thus, it is expected higher concentrations of B in deposits emplaced in a thick crust.

MINERAL CHEMISTRY OF TOURMALINE, RUTILE AND APATITE FROM THE SUPERGIANT EL TENIENTE PORPHYRY COPPER DEPOSIT: IMPLICATIONS FOR SOURCE REGIONS, MAGMATIC AND HYDROTHERMAL PROCESSES

a. Tourmaline

A survey of tourmaline from the El Teniente porphyry copper deposit is reported with emphasis on distribution, texture, compositional varieties, minor, trace and REE abundances, together with stable isotope (O, H, B) signatures. Tourmaline occurs 1) as a trace constituent in veins and wallrocks associated with stockwork mineralization and alteration and 2) as the primary matrix material associated with tourmaline breccia pipes. Texturally, the tourmaline occurs as scattered needles, as radial groups of crystals, as massive granular aggregates and as intergrown aggregates of fine-grained fibrous needles.

The tourmaline have characteristic major and trace element compositions. SiO_2 and B_2O_3 contents generally display little variations, whereas Al_2O_3 (36.9 to 18.7 wt%), FeO (19.3 to 1.9 wt.%) and MgO (10.0 to 5.7 wt%) have significant compositional ranges. Abundances of K_2O (0.10 to 0.02 wt%), and CaO (0.95 to 0.19 wt%) are systematically low, while Na_2O varies from 2.7 to 1.9 wt. %. Contents of MnO and Cr_2O_3 are commonly below detection limits. TiO_2 varies widely between 3.89 to 0.06 wt%. On the Al-Fe-Mg ternary diagram, the tourmaline plots within the schorl-dravite solid solution series, with a tendency for Mg-rich members (dravite) to dominate. Calculation of the structural formula indicates Fe^{3+} substitution for Al^{3+} is common. Zonation in the tourmaline can be either optically and chemically distinct or non existent. Two styles of chemical zonation have been observed including a Fe-Mg zonation were the Al content remains uniform and a Fe-Al zonation with a stable Mg content.

The results are discussed in terms of the significance of tourmaline in the copper forming system, as well as its relevance as a potential pathfinder for source regions and crustal/subduction processes.

b. Rutile

At the El Teniente deposit, rutile is the main Ti mineral in the hydrothermal alteration envelopes, particularly in the potassic core. Rutile is formed under hydrothermal conditions from the breakdown of Ti-bearing

minerals. Minor anatase was also identified, yet it tends to occur in distal carbonate veins in the deposit fringe. Sampling covered the main hydrothermal alteration zones and lithologies present in the ore deposit.

EPMA (n=326) and PIXE (n=85) analyses of rutile(-anatase) show relatively high minor and trace elements contents (~3 wt%), where Fe, W and V account for almost 90% of the impurities. The remaining ~10% includes traces of Mn, Cr, Si, Al, Nb, Ta, Sn, Sc, Mo, Cu, Zn, Sb, Pb, As, Ni, Zr and U.

Results shows that in spite of the super-giant nature of this deposit and its complex history of alteration and mineralization, rutile(-anatase) composition changes systematically with position in the deposit. Most indicative elements are: Mo, Zr, Nb, Ta, U, As and Pb. Molybdenum is high (186 ppm) in rutiles from porphyries but very low (~5 ppm) in rutiles from the wallrock. In the same way total HFSE content is almost 5 time higher in rutiles from the porphyries (1307 ppm) than in those from the wallrock (269 ppm). Uranium in rutile shows a similar, but less marked, concentration contrast, with 49 ppm in the porphyries and 18 ppm in wallrock rutiles. One exception is anatase, which is enriched in U (78 ppm) and also in lead. Arsenic is enriched in rutile(-anatase) from the marginal low ore-grade propylitic zone (46 ppm), while it is very low (6 ppm) in rutile from the potassic core.

The fact that rutile produced by mineralizing fluid alteration can allocate a broad spectrum of different cations makes this Ti-oxide a potential "monitor" of the chemical evolution of hydrothermal fluids.

c. Apatite

Sulfur is an essential component in magmatic and hydrothermal fluids that produce porphyry copper deposits. Its speciation ($S^{=}$ or S^{+6}) is strongly dependent on the oxygen fugacity of the magma, being $S^{=}$ dominant at low fO_2, and S^{+6} at high fO_2. Oxydized magmas prevent early sulfide fractionation, producing S and metals concentration towards the later stage of magmatic crystallization, favoring in turn, ore deposit formation.

From the crystal chemistry point of view, S can enter in apatite structure when it is as S^{+6}. Therefore its content in apatite could be a good monitor of magma oxydation state. We have analyzed apatites from the silicic porphyries at El Teniente ("Porfido Teniente" (PT), "Diorita Sewell " (DS) and "Diorita La Huifa" (LH)).

Preliminary results based on EPMA analyses allow us to establish: 1) All analyzed grains have measurable SO_3 content. 2) It varies within a) the same grain (generally lower toward rims), b) between different grains (depending on the texture: apatite inclusions are richer than microphenocrysts and groundmass grains), and c) between different rock-units (apatites from the PT (related to Cu mineralization), have the highest values (0.69wt% compared to DS (0.55wt%) and LH (0.37wt%). 3) In LH, two apatite populations have been identified: one with a turbid appearance, and low minor element content, and another, clear in appearance, with characteristically high chlorine content (up to 2.8wt% Cl, while the highest value in PT and DS is 0.9wt%). 4) S enters into the studied apatite by the following coupled substitution mechanisms: a) $S^{+6} + Si^{+4} \_ 2P^{+5}$ and/or b) $S^{+6} + Na^{+} \_ P^{+5} + Ca^{+2}$. 5) Additionally Si and Na also participate in other coupled exchange reactions to explain the main chemical features of the studied apatites: a) $REE^{+3} + Si^{+4} \_ P^{+5} + Ca^{+2}$ and b) $REE^{+3} + Na^{+} \_ 2\ Ca^{+2}$.

ACKNOWLEDGMENTS: This is a contribution to Fondecyt Líneas Complementarias project #800-000

CRUSTAL RECYCLING AND JUVENILE ADDITIONS: THE PALEOZOIC TO RECENT TECTONIC AND COMPOSITIONAL EVOLUTION OF THE CHILEAN CONTINENTAL MARGIN (36°-40°S)

Friedrich LUCASSEN(1,2), Helmut ECHTLER(1), Robert TRUMBULL(1), Gerhard FRANZ(3), Rolf L. ROMER(1), Oscar FIGUEROA(4)

(1) GeoForschungsZentrum Potsdam, Telegrafenberg, 14473 Potsdam, Germany; lucassen@gfz-potsdam.de
(2) Freie Universität Berlin, FB Geowissenschaften, Malteserstr. 74-100, 12249 Berlin, Germany
(3) TU-Berlin, Petrologie-EB15, Strasse des 17.Juni 135, 10623 Berlin, Germany;
(4) Universidad de Concepción, Chile, Depto. Ciencias de la Tierra, Barrio Universitario s/n, casilla 150

KEYWORDS: Crustal evolution, magmatism, isotopic composition, Gondwana margin, Paleozoic orogen

GEOLOGICAL FRAMEWORK AND TECTONICS

The Southern Andes are in contrast to the Central Andes characterized by normal crustal thicknesses (~40 km), a rather low-relief and narrow mountain chain with an important erosive exogene mass transfer from the cordillera to the trench under wet climatic conditions. Though the general plate boundary conditions are identic since the Mesozoic, there the subduction-related magmatic input into the arc is not reflected by crustal thickening and isostatic uplift. The tectonic architecture of the upper plate is dominated by metamorphic and magmatic basement with scattered sedimentary basins that developed during a) Early Paleozoic and Late Paleozoic to Triassic orogenies along the Gondwana margin and b) the ongoing Andean cycle since the Jurassic. The Late Paleozoic to Triassic orogenic wedge is caracterized by the formation of an accretionary wedge with subduction related accreted hP-metasediments incorporating metabasites and mafic rocks (western series) and extended granitoid batholiths forming part of the eastern series in the Nahuelbuta Range (Hervé, 1988; Martin et al., 1999). The eastern series comprises also non-metamorphic to medium grade siliciclastic rocks and could also present part of a late Paleozoic accretionary wedge, however, mafic rocks are generally absent. Here, contact metamorphism around extensive late Paleozoic granite batholiths is abundant (ca. 300 Ma; Hervé, 1988; Martin et al., 1999). The metamorphic rocks probably formed during or have been overprinted by a regional contact metamorphism (ca. 300 Ma; Sm-Nd mineral isochron from garnet bearing migmatite, eastern series; our data; Rb-Sr mineral isochrons, Glodny et al. this volume). Late Paleozoic granitoids are also present in the Eastern Andean foothills of the Aluminé area /Argentina (ca 300 Ma Rb-Sr mineral isochron; our data). Small Triassic granites are found at the Coast north of Concepcion (ages ca 215 Ma from Rb-Sr mineral isochrons, our data). The age of possible regional metamorphism in the eastern series is bracketed by the presumably Carboniferous to Permian depositional age of the sedimentary protoliths (Bandel and Quinzio-Sinn, 1999), non-metamorphic Triassic intra-mountain basins upon the basement and undeformed intrusions of late Paleozoic granites. In the Aluminé - Piedra de Aguila (Argentine foothills) high grade metamorphic gneiss and migmatite have an age of ca 390 Ma (concordant U-Pb age on titanite and Rb-Sr mineral isochron; our data). They presumably belong to the western part of the 'cratonic' foreland of the North Patagonian Massif in the east of the Andes for which Devonian ages of metmophism have been discussed (Ostera et al., 2001).

The Andean cycle, starting in the Jurassic, shows alternating phases of uplift and exhumation and periodically crustal shortening. The Mesozoic -Tertiary history of this belt shows a mainly continental margin evolution with granitoid magmatism and basin tectonics. The main processes during this active margin evolution are :

Jurassic(?) – L. Cretaceous: emplacement of intra-arc batholiths and scattered intrusions in the fore-arc, intra-arc volcanism and back-arc basins (Neuquen).

Upper Cretaceous: cessation of the plutonism, inversion of the back-arc basins and uplift/exhumation of the intra-arc batholiths.

Eocene – M. Miocene: fore-arc basin development by uplift-induced arc-orthogonal extension and intra-arc/back-arc basins along arc-parallel transtensional faults. Emplacement of intra-arc batholiths

Late Miocene: Weakening of plutonism, basin inversion and uplift/exhumiation of parts of the Miocene intra-arc batholiths along arc-parallel transpressive zones.

Pliocene - recent: general extensional tectonics with strike-slip deformation along intra-arc shear zones and frontal and basal accretion with uplift in the fore-arc. As well as volcanism of the active continental magmatic arc.

During this evolution and actually the upper plate mechanics is largely controlled by the inherited pre-andean basement structures. The focus of the Cretaceous - Recent magmatic activity is in the area of the Andean Cordillera. The Cordillera and the eastern foothills in the Aluminé area hosts large intrusive complexes of late Mesozoic to Cenozoic age which intruded into clastic sediments. Their age in the Aluminé area is ca. 100 Ma (K-Ar data; Latorre et al., 2001). Although age relations are poorly constrained among the late Mesozoic intrusions, these rocks could correlate with the Jurassic to Tertiary North Patagonien batholith (e.g. Pankhurst et al., 1999). Both the late Mesozoic intrusions and the late Paleozoic granites intruded at shallow levels.

COMPOSITIONAL EVOLUTION – RESULTS AND DISCUSSION

Granitic to intermediate compositions predominate in Late Paleozoic to Tertiary intrusions and basic compositions are mainly found within the Mesozoic-Tertiary magmatic rocks. Chilean Paleozoic (meta) sediments follow trends typical for sedimentary rocks with variable clay mineral - quartz -feldspar proportions. The Argentine Paleozoic metasediments have quartz-rich protoliths. REE patterns of most samples from the different magmatic and metasedimentary groups are relatively flat (La/Yb ratios < 10) and the patterns of all magmatic rocks show negative Eu-anomalies, pointing to plagioclase fractionation at crustal levels. The REE-pattern of the late Mesozoic magmatic rocks are among the least evolved. Sr - Nd and Pb - Sr isotope ratios distinguish clearly between the Paleozoic (meta) sediments and granites of the Coastal Range and eastern foothills and the late Mesozoic - Tertiary intrusions and volcanic rocks. Nd and Pb isotope ratios of the late Paleozoic granites are very similar to those of the Paleozoic (meta) sedimentary rocks. Single-stage Nd depleted mantle model ages (t_{DM}) of granites and (meta) sediments are between 1.5 - 2.1 Ga. These Nd model ages are typical of the Central Andean and the Pampean Early Paleozoic basement south of 18°S (Lucassen et al., 2000; 2001 and references therein). The granites contain large proportions of this old continental crust and formed mainly by crustal recycling. The late Mesozoic to Recent magmatic rocks show little variation in their Sr, Nd and Pb isotope ratios (Figs. 1 and 2). Their isotope ratios are not correlated with indicators of differentiation and possible crustal contamination as the

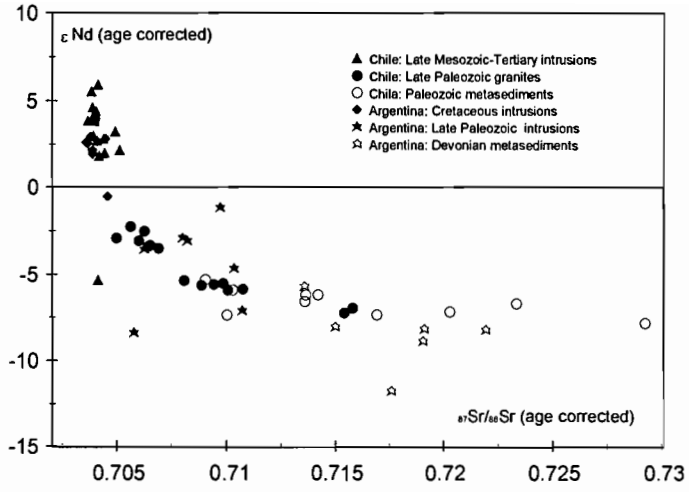

Figure 1 Nd and Sr isotope composition corrected for insitu decay. All but two late Mesozoic – Tertiary intrusions plot in the depleted mantle field.
The Paleozoic metasediments show a relativly broad spread in their Sr isotope ratios probably due to inherited inhomogeneities in their protoliths.

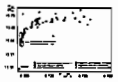

SiO_2 content (Fig. 3). Initial Sr and Nd isotope ratios plot in the compositional array of the depleted mantle (Fig. 1). Pb isotope compositions are displaced from the values of the Paleozoic rocks towards MORB ratios in the Pb-Sr isotope diagram (Fig. 2) and indicate some contamination by crustal material if a MORB composition is assumed for the mantle source (Figs. 1 and 2). Less than 10% addition of bulk Paleozoic crust or its younger sedimentary derivative (e.g. slope and trench sediments) to MORB-like composition would explain the isotope ratios observed. The minor variation of isotope compositions in these rocks of different age

Figure 2 $^{207}Pb/^{204}Pb$ and Sr isotope ratios are not corrected for in situ decay. Corrections would be minor for the $^{207}Pb/^{204}Pb$ ratio and moderate for the Sr isotope ratios (see Figure 1). The small array of Pb and Sr isotope compositions of the late Mesozoic to Tertiary intrusions from Chile and Argentina coincides with the compositional field of Cenozoic volcanic rocks of the active arc from the same section of the arc (Hildreth and Moorbath, 1988).

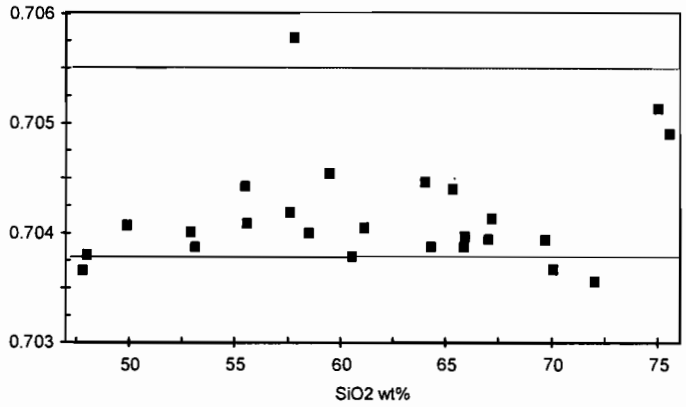

Figure 3 Sr isotope ratios and SiO_2 content of the late Mesozoic to Tertiary intrusions (solid squares) are not correlated. The compositionally more evolved rocks developed by fractionation from isotopically homogeneous parent magmas. The two lines delineate the compositional field of the Cenozoic volcanic rocks (Fig.2; Hildreth and Moorbath, 1988) which show also no correlation between Sr isotopic composition and SiO_2 content.

(ca 100 - 0Ma) at a large degree of differentiation (50-76wt% SiO_2) requires isotopically homogeneous parent magmas. The constant isotopic composition over a long time span including Cretaceous intrusions and Recent volcanic rocks makes an assimilation process within the crust unlikely. In this case one would expect a large variation especially in the Pb isotope ratios between the two endmembers, MORB and old continental crust (Fig. 2). Source contamination in the mantle wedge, e.g. by mixing of subducted sediment derived from the continent,

is the preferred process to explain the small variation of isotopic composition. The Late Mesozoic - Recent magmatic rocks present a prominent juvenile addition to an elsewhere old (ca. 1.6-2.0 Ga) continental crust. The presence of considerable volumes of differentiated, intermediate to granitic, mantle derived rocks implies the presence of a more mafic equivalent in the crust, because the magmas differentiated at relatively moderate pressures without major residual garnet.

CONCLUSION

The geochemical data on the crystalline basement of the South-Central Andes document two major geodynamic cylces of magma generation during the Phanerozoic. The Paleozoic to Triassic orogeny is characterised by crustal recycling of Proterozoic continental basement. The Andean evolution instead shows a remarkable stable and simple subduction-related magmatism with significant addition of juvenile material to the active margin upper plate. Magmatism thereon seems to reflect a rather unvariable active margin evolution in time and space concerning the subduction related magmatism during the Andean cycle in the South Central Andes.

REFERENCES

Bandel K, Quinzio-Sinn LA, 1999. Paleozoic trace fossil from the Cordillera Costal near Concepción, connected to a review of the Paleozoic history of central Chile. Neues Jahrbuch Geolgisch Paläontologische Abhandlungen, 211(1/2), 171-200

Glodny J et al. Geochronological Constraints on material cycling velocities, structural evolution and exhumation of a Paleo Accretionaryx Wedge – the Bahia Mansa Complex, South Central Chile, this volume

Hervé F, 1988. Late Paleozoic subduction and accretion in southern Chile. Episodes 11, 183-188.

Hildreth W, Moorbath S, 1988. Crustal contributions to arc magmatism in the Andes of Central Chile. Contributions to Mineralogy and Petrology 98. 455-489.

Lucassen F et al., 2000. Proterozoic-Paleozoic development of the basement of the Central Andes (18°-26°) - a mobile belt of the South American craton. Journal of South American Earth Science 13, 697-715.

Lucassen F et al., 2001. Composition and density model of the continental crust at an active continental margin-the Central Andes between 21°and 27°S. Tectonophysics 341, 195-223.

Martin, M.W. et al. 1999. Evolution of the late Paleozoic accretionary complex and overlying forearc-magmatic arc, south central Chile (38°-41°S): Constraints for the tectonic setting along the southwestern margin of Gondwana. Tectonics 18, 582-605.

Pankhurst R.J. et al., 1999. Mesozoic–Cenozoic evolution of the North Patagonian Batholith in Aysén, southern Chile. Journal of the Geological Society 156, 673-694

Latorre et al., 2001. K-Ar ages of rocks from Lago Aluminé, Rucachoroi and Quillen, North Patagonien Andes, Neuquen, Republica Argentina. III Simposio de Geologia Isotopica, Pucon, Chile, Abstract Volume on CD-ROM.

Ostera et al., 2001. A widespread Devonian metamorphic episode in Northern Patagonia, Argentina. III Simposio de Geologia Isotopica, Pucon, Chile, Abstract Volume on CD-ROM.

SUBDUCTION PROCESSES OFF CHILE (SPOC) - N-S VARIATIONS OF CRUSTAL STRUCTURE FROM OFFSHORE-ONSHORE WIDE-ANGLE SEISMIC OBSERVATIONS IN CHILE (36°-39°S)

Stefan LÜTH(1), James MECHIE(2), Peter WIGGER(1) and SPOC Working Group

(1) Freie Universität Berlin, Fachrichtung Geophysik, Malteserstr. 74-100, D-12249 Berlin (stefan@geophysik.fu-berlin.de) (wigger@geophysik.fu-berlin.de)
(2) GeoForschungsZentrum Potsdam, Telegraphenberg, D-14473 Potsdam (jimmy@gfz-potsdam.de)

KEY WORDS: Southern Andes, Seismic Wide-Angle Reflection, Seismic Refraction, Crustal Structure

INTRODUCTION

During the third leg of RV Sonne Cruise SO 161 off the Chilean Pacific coast additional onshore seismic observations were performed in order to extend the data coverage to the near coastal and onshore part of the foreac. The onshore seismic observations were located between 36° and 39° S and reached from the Pacific coast up to the Chilean-Argentinean border in the main cordillera (Fig. 1).

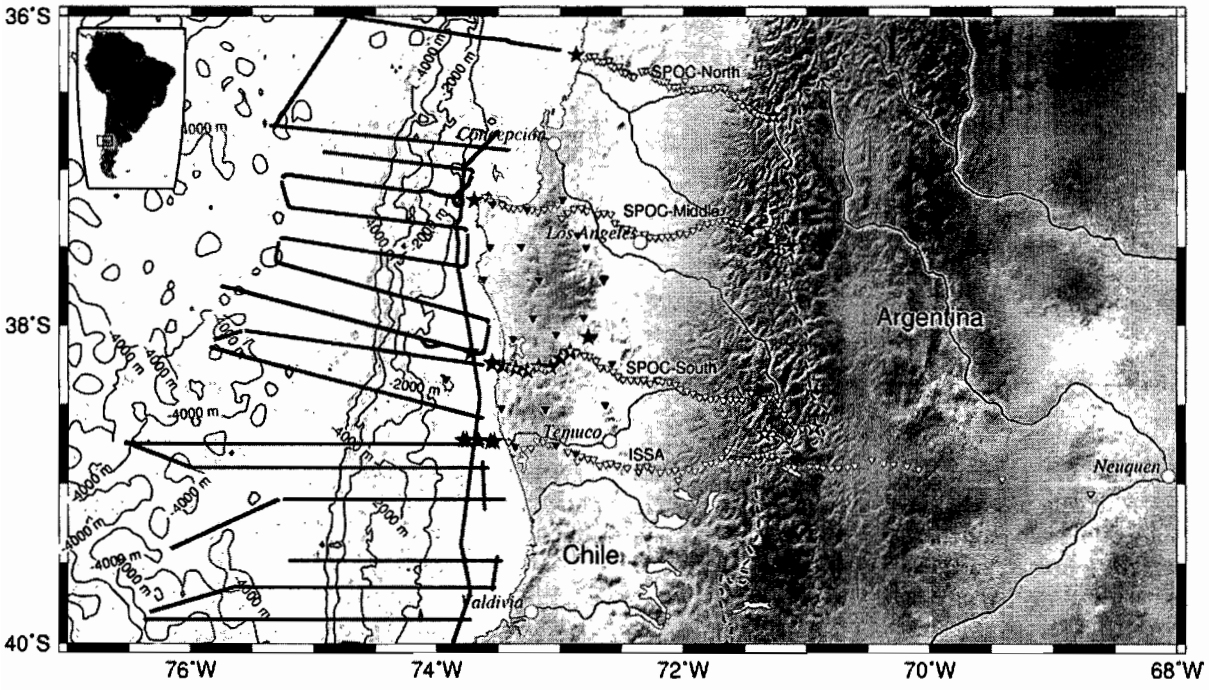

Fig. 1: Map showing the receiver and shotpoint locations of the onshore part of the SPOC experiment and of the ISSA 2000 seismic refraction profile. The SO 161/3 airgun profiles are indicated as black lines. Receivers of the seismic refraction/wide-angle reflection profiles are shown as inverted triangles with white filling. Stations of the seismic array are represented by inverted triangles with black filling. Chemical explosions in the shallow water region of the Pacific Ocean and in boreholes in the Chilean main cordillera are shown as black stars.

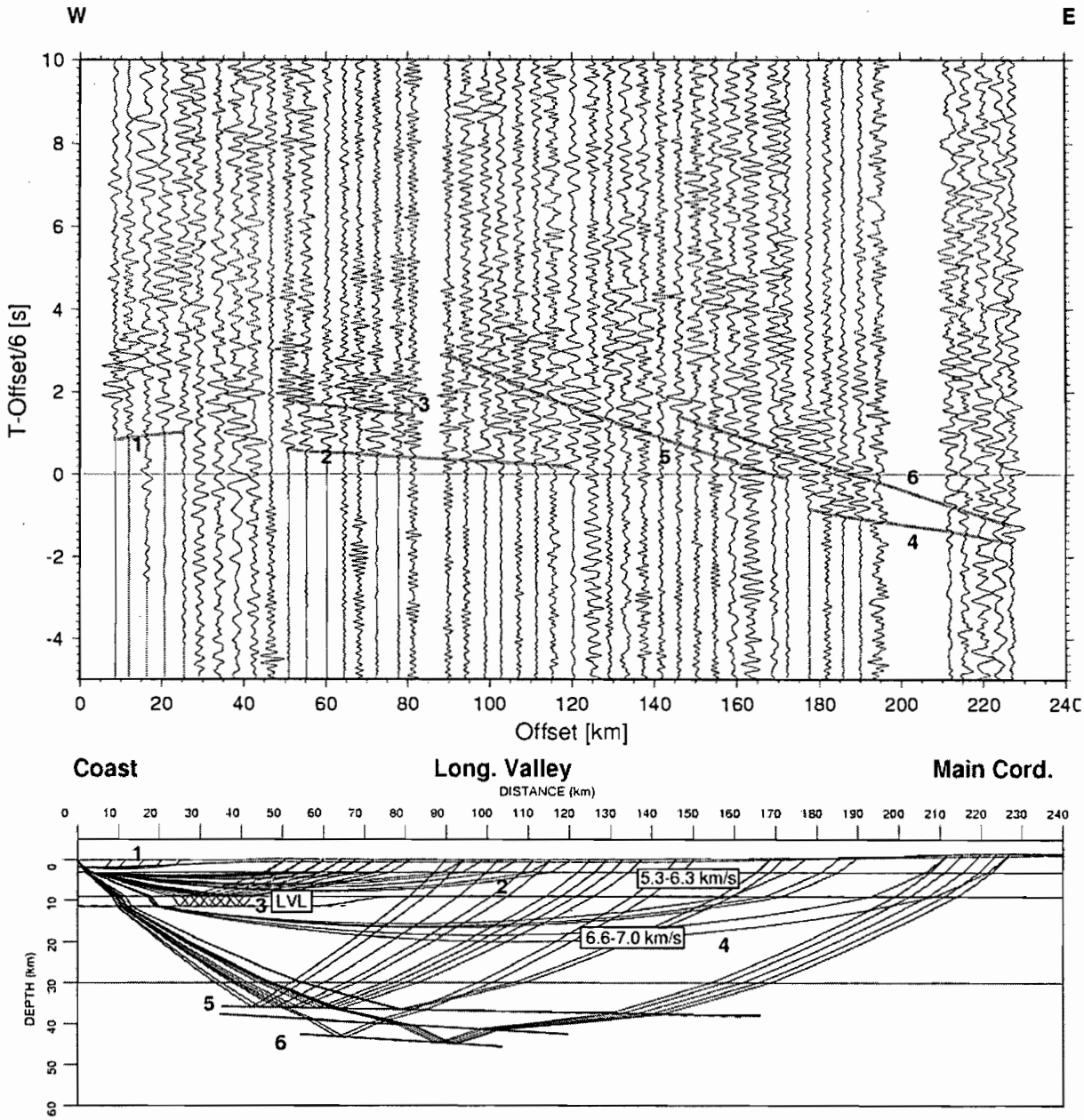

Fig. 2: Shot-gather from shot M1 on profile SPOC-Middle. Shotpoint is located at western end of the profile (0 km). Trace data has been bandpass-filtered (1-7 Hz) and traveltime-reduced using 6 km/s. Grey lines labeled 1 through 6 indicate modelled traveltimes based on ray-tracing in model shown below. 1: Refracted wave through upper crust (upper part); 2: refracted wave through upper crust (lower part); 3: reflected wave from lower boundary of low-velocity layer (LVL); 4: refracted wave through lower crust; 5 and 6: reflected waves from imbricated layering at lower boundary or below the lower continental crust. Only the velocities are shown which are well constrained by refracted phases.

Three seismic refraction profiles with 52 3-component recorders were installed and shot by chemical explosions at both ends of the profiles. Additionally, these profiles recorded the airgun pulses of the RV Sonne who was cruising on offshore profiles in the linear prolongation of the onshore seismic lines (Fig. 1).

A seismic network of 30 stations was installed in the coastal cordillera which recorded the chemical explosions as well as the Sonne airgun pulses and natural seismicity. Finally, a near-vertical seismic reflection profile was

acquired on the southernmost of the SPOC wide-angle profiles. The results of the onshore near-vertical seismic reflection measurements are presented on an accompanying poster (Stiller et al., 2002). The seismic refraction and wide-angle reflection observations in that area are completed by a profile which had been realized by the German Collaborative Research Center (SFB) 267 in the first three months of 2000 (Lüth et al., 2002).

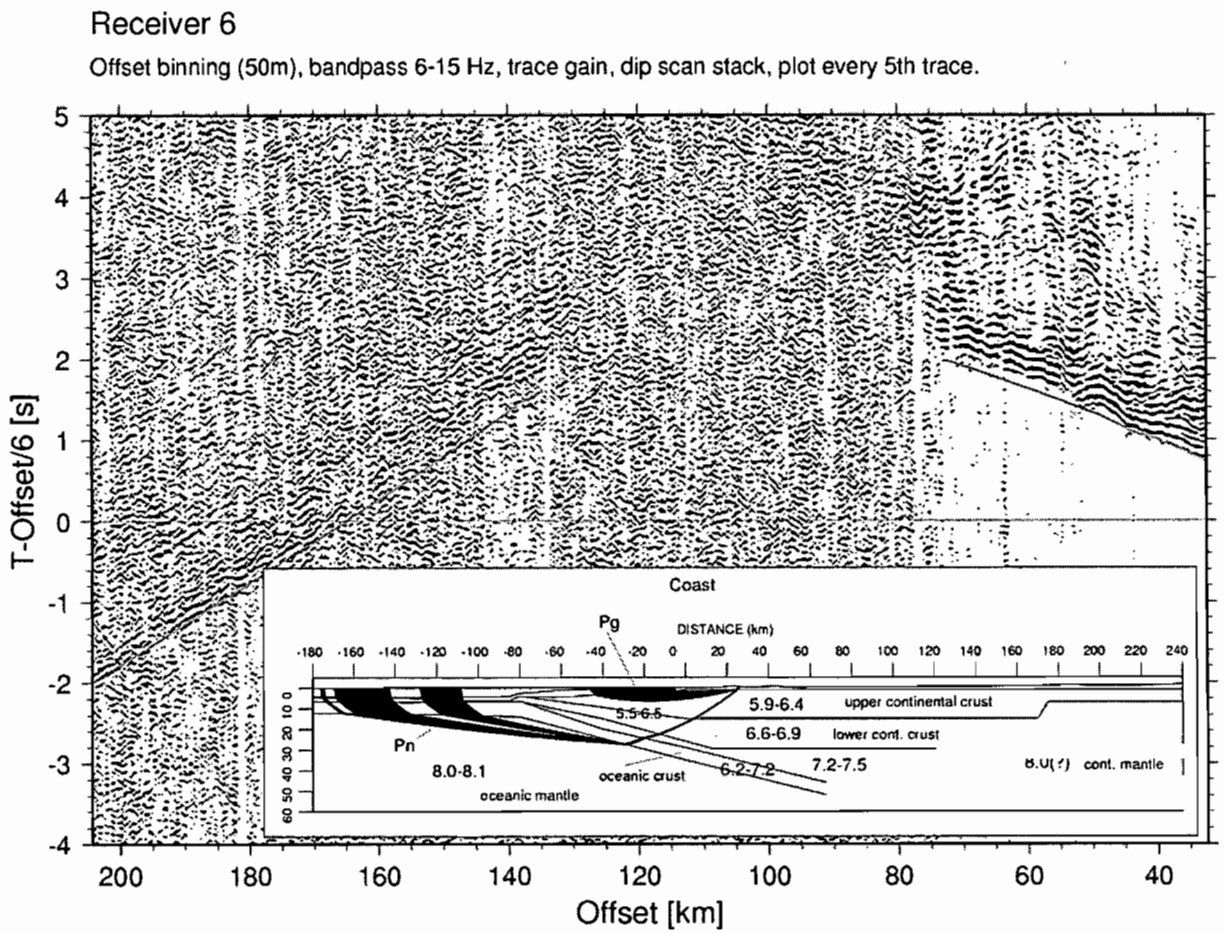

Fig. 3: Receiver-gather from station 6 on profile SPOC-South. The station has recorded the airgun pulses of RV Sonne in an offset range of 35 to 205 km. The signal/noise ratio of the refracted wave through the upper continental crust (Pg) is excellent up to 80 km offset. A refracted wave through the oceanic mantle (Pn) can be correlated between 130 and 205 km offset. In spite of coherency enhancing processing the signal/noise ratio appears extremly high. The modelled traveltimes of the phases Pg and Pn are shown as grey lines in the section.

RESULTS

The onshore seismic refraction profiles constrain the crustal structure basically of the continental crust underneath the Chilean Longitudinal Valley, but also the Moho of the subducting oceanic crust can be modelled based on registrations on the profiles SPOC-South and ISSA (not shown here). The oceanic moho is at 45 km depth below the coastal cordillera underneath the two southernmost profiles. A clear oceanic moho can not be correlated on the sections of the profiles SPOC-Middle and SPOC-North. On the section of SPOC-Middle (Fig. 2), a low-velocity layer is modelled below the coastal cordillera which is not the case on the other profiles. This may be the first indication for an anomalous crustal structure exactly underneath the Arauco peninsula with

respect to the sections north and south of it. Integration of the Airgun pulses recorded by the receivers of the profiles SPOC-Middle and SPOC-North is expected to yield further constraints on variations of crustal structure. Figure 3 gives an example of data quality of these registrations. Evaluation of these data sets has recently started. In general the quality of the airgun recordings at wide-angle distances on land declines from north to south, in that it becomes more difficult to record the Pn wave at offsets greater than about 100 km as one goes south. The example shown in Fig. 3 represents one of the clearest registrations on the southern profile and correlation is only possible after strong coherency enhancement of the data.

REFERENCES:

Lüth, S., Wigger, P. and ISSA Research Group. 2002. A Crustal Model along 39degS From a Seismic Refraction Profile - ISSA 2000. Submitted to Revista Geologica de Chile.

Stiller, M., Krawczyk, Ch. and SPOC Working Group. 2002. Subduction Processes Off Chile (SPOC) - First Results of the Onshore Seismic Reflection Experiment in Central Chile. 5th ISAG, this volume.

NEOGENE IGNIMBRITES IN THE AREA OF AREQUIPA, SOUTHERN PERU: PALEOMAGNETIC CORRELATIONS AND FLOW DIRECTION.

Orlando MACEDO (1), Perrine PAQUEREAU (2), Pierrick ROPERCH (3), Jean-Claude THOURET (2), and Michel FORNARI (4)

(1) Instituto Geofísico del Perú, Oficina Regional de Arequipa. (omacedo@geo.igp.gob.pe)
(2) Laboratoire Magmas et Volcans, Université Blaise Pascal et CNRS, 63038 Clermont-Ferrand, France (P.Paquereau@opgc.univ-bpclermont.fr) (thouret@opgc.univ-bpclermont.fr)
(3) IRD, UR 104 and Departamento de Geología, Universidad de Chile, Santiago, Chile (properch@cec.uchile.cl)
(4) IRD et UMR Géosciences CNRS, Sophia Antipolis, 06 Nice, France (fornari@unice.fr)

KEYS WORDS: ignimbrite, Arequipa, Peru, Paleomagnetism, Anisotropy of Magnetic Susceptibility

INTRODUCTION

In the area of Arequipa, the ignimbrites termed "sillars" (Jenks and Goldich, 1956) are indurated, nonwelded pyroclastic-flow deposits of dacitic and rhyolitic composition and middle Miocene to late Pliocene in age. In a companion abstract (Thouret et al., this volume), we aim to establish correlations based on petrology, mineralogy and Ar-Ar datings. We have also undertaken a detailed paleomagnetic sampling of 35 sites within most of the ignimbrites in the Arequipa region. Here we report preliminary paleomagnetic results.

PALEOMAGNETIC SAMPLING

Most sites were drilled to the west of the city of Arequipa where most quarries in the "sillar" can be found. The ignimbrite units are several tens of meters thick. Within the quarries in the depression of Arequipa, the main sillar has always a typical white color. This white unit is covered by a nonwelded pink unit. Field evidence suggests a gradual transition between these two units. The unit drilled at site 31 is however beneath the white "sillar" and separated by about 10 meters of volcanoclastic sediments. Site 32 was drilled in the ignimbrite filling valleys carved in the Mesozoic Batholith. Site 39 corresponds to poorly welded ignimbrite interbedded within late Neogene conglomerates overlying the Moquegua Formation. Sites 5,6 and 27 were drilled in non welded tuffs near the locality of Yura.

It is especially difficult to follow the "white sillar" when we cross the Arequipa's city toward the canyon of Chili river eastward. Several outcrops of ignimbrites are found in the Chili canyon (sites 14, 15, 16, 18, 19, 20, 21 and 40) and near the Aguada Blanca dam. At this locality, sites 22 and 23 were drilled in the same unit, while site 24 corresponds to a lowest unit. On the Altiplano north of El Misti, only two other sites were drilled. Unfortunately, no result is yet available for site 25. Site 26 corresponds to a thick ignimbrite sampled near the Rio Sumbay valley. Finally, site 17 corresponds to an ignimbrite about 30 km southeast of Arequipa.

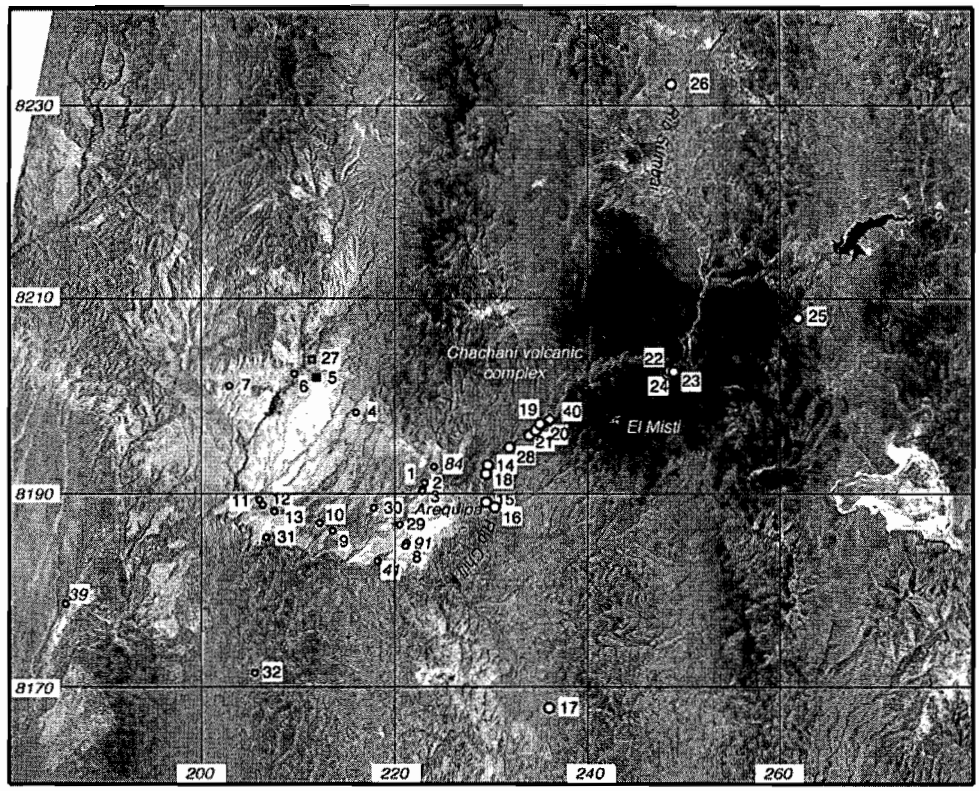

Figure 1 : Landsat image showing paleomagnetic sampling sites. Large circles correspond to sampling in or east of the Chili River. Small circles correspond to the paleomagnetic sampling within a composite thick unit to the west of the city of Arequipa. Different symbols are shown for sites 5, 24, 27 and 40, where we observe different paleomagnetic directions (see text).

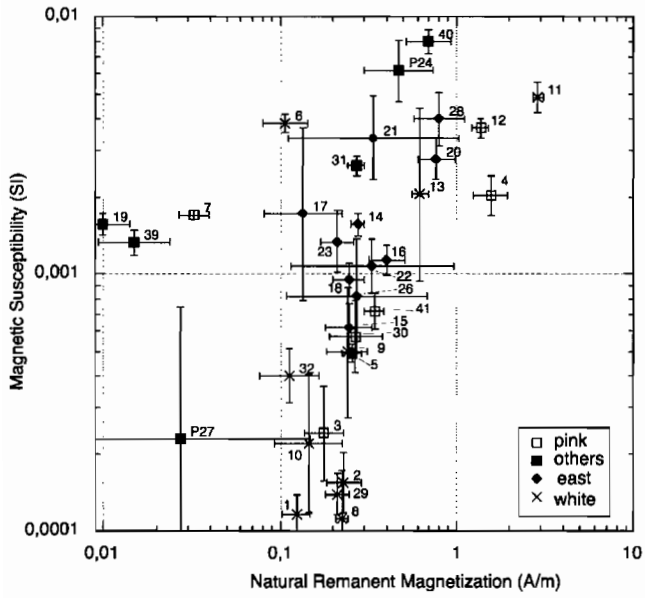

Figure 2: Geometric mean values of NRM versus magnetic susceptibility and associated standard deviations. Open squares correspond to sites in the pink unit above the white "sillar" (crosses).

MAGNETIC PROPERTIES

Figure 2 shows the variations of magnetic susceptibility versus the intensity of the Natural Remanent Magnetization (NRM). The large variation in magnetic susceptibility from 0.0001 to 0.01 SI may be attributed to oxidation conditions during the emplacement of the ignimbrite. Sites with the lowest magnetic susceptibility correspond to the quarries where the bricks of ignimbrites are used for construction in Arequipa. All these sites are located to the west of the city. The highest magnetic susceptibility values are due to a significant content in

magnetite and are usually (but not only) observed toward the base of the ignimbrite units. The very high stability of the NRM allows us to discard the hypothesis that susceptibility changes are due to post-emplacement alteration. Apparent significant alteration was only observed at few sites, especially at site 19. Sites with the lowest NRM values correspond to nonwelded rocks and we interpret the low NRM values as evidence for temperature of emplacement significantly lower than the Curie Point of magnetite (578°C).

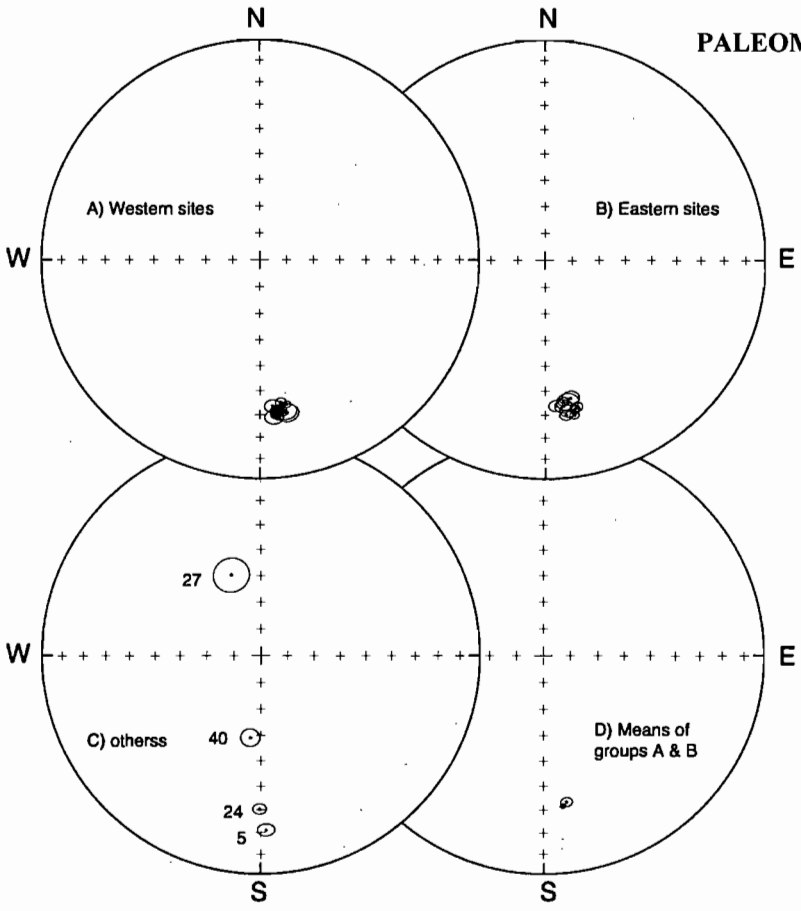

Figure 3: Equal-area projections of site-mean results.

PALEOMAGNETIC CORRELATIONS

At most sites, NRM directions are well grouped and the very high stability of the magnetization allows to use NRM directions for correlation purpose. Previous results obtained by one of us (O.M) based on detailed demagnetization confirms the high stability of the magnetization. Alternating field demagnetization was performed only for a few sites where evidence for secondary magnetization due to lightning was observed. Available results are shown in Figure 3.

Sites located to the west of Arequipa record the same paleomagnetic direction regardless they were drilled in the white or pink unit (Figure 3a). This confirms the stratigraphic succession and gradual transition observed in field. The average direction calculated from paleomagnetic results at 18 sites is (Declination : 172.7°; Inclination: 31.1°; □ 95: 0.9°, k : 1426). The very high Fisher concentration parameter (k) demonstrates that all these sites correspond to a single or successive volcanic event only separated by at most a few tens of years.

Only near Yura, two different directions can be observed, one with a normal polarity (site 27) and one with reverse polarity (site 5).

To the east of Arequipa, a similar paleomagnetic direction was observed at 10 sites (Declination : 171.2°; Inclination: 32.6°; □95: 1.9°, k : 656). Only two different directions of reverse polarity at site 24 and 40 are statistically distinct from this group.

CONCLUSION

Comparison of the average directions calculated from the groups east and west of Arequipa (Figure 3d) suggests that most ignimbrites in the Arequipa region may belong to a single or to a few successive units erupted during a major short-lived volcanic event. Available radiometric ages are in conflict with this hypothesis. Vatin-Perignon et al., (1996) report Fission Track age of 2.42 +/- 0.11 Ma old (Airport quarry) while an Ar-Ar age of 4.87 ± 0.02Ma on sanidine was determined for an ignimbrite near La Joya.

Ar-Ar ages of 13.8 ± 0.1 and 13.12 ± 0.05 Ma, on biotite single grain have been obtained for the ignimbrite sampled at site 40. These ages and the observation of a distinct paleomagnetic signature for this site (40) indicate that this ignimbrite could be of limited geographic extent.

Further high precision radiometric Ar-Ar dating are needed to confirm the hypothesis that most of the paleomagnetic sites were drilled in the same or contemporaneous ignimbritic flows.

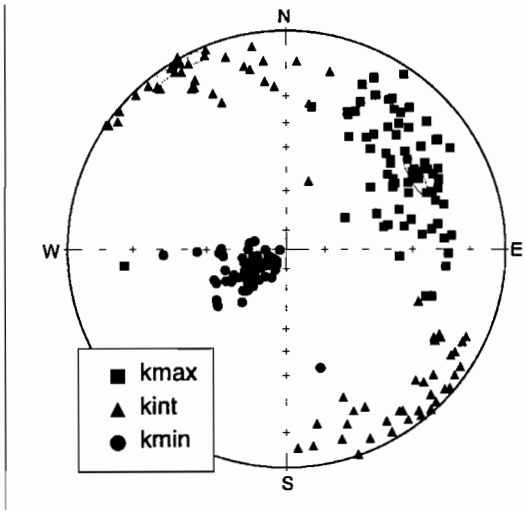

Figure 4 : Example of AMS data obtained at 5 sites (site 9,10,11,12,13) located on the south-western side of the Arequipa depression (see Figure 1).AMS data show imbrication foliations dipping about 20° toward the E-NE (N60) with magnetic lineations slightly more dispersed but oriented along the dip direction of the foliation plane.

Anisotropy of magnetic susceptibility (AMS) was performed for most sites. An example of AMS results is shown in figure 4. Magnetic foliations and lineations indicate a flow direction oriented roughly N60. Unfortunately most sites located in the Chili River have foliation planes less well defined than those located to the west. Two potential sources are proposed by Thouret et al. (this volume): one is thought to be buried beneath the Chachani volcanic complex ; the second source may be located in the Pampa Llantapallana north of El Misti volcano (Fig.1). At this stage, AMS data are too preliminary to constrain clearly a source for the ignimbrites.

REFERENCES

Jenks W.F.and Goldish S.S., 1956, Rhyolitic tuff flows in southern Peru, Journal of Geology, 64, 156-172.

Vatin-Perignon N., Oliver R., 1996, Trace and rare-earth element characteristics of acidic tuffs from Southern Peru and Northern Bolivia and a fission-track age for the Sillar of Arequipa, Journal of South America Earth Science, 9, 91-109.

ANDEAN ADAKITES FROM SLAB MELTING, CRUSTAL THICKENING, AND FOREARC SUBDUCTION EROSION

Suzanne MAHLBURG KAY (1)

(1) Snee Hall, Cornell University, Ithaca, NY, 14853, USA, smk16@cornell.edu

KEYWORDS: Andes, adakites, magmatism, slab melting, subduction erosion, crustal thickening

Neogene Andean magmas with chemical characteristics of adakitic magmas as defined by Defont and Drummond (1990) are common in the Central Andes. Their high-pressure source mineralogy as signaled by trace element characteristics (steep REE patterns, low heavy REE and high Sr contents, etc.) can be produced in at least three ways. In order of descending importance, these are subduction of young oceanic crust, subduction-erosion of forearc crust, and tectonic thickening of the Andean crust. Melting of old subducting oceanic crust in shallow subduction zones (Gutcher et al. 2000) is not required. The origins of adakitic magmas are best deciphered by matching them with specific tectonic conditions and events along the evolving Andean margin (Fig. 1).

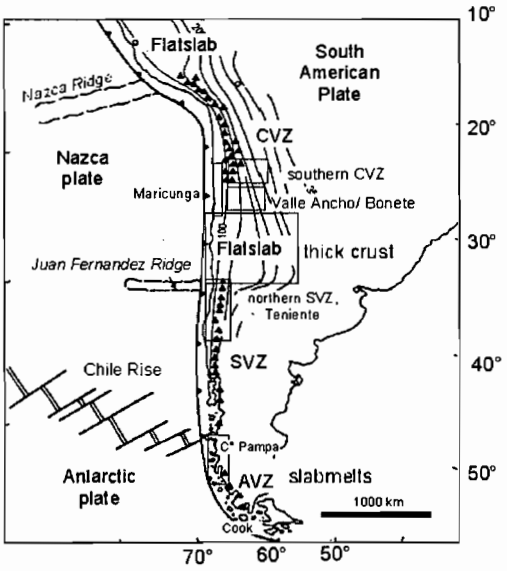

Figure 1. Map of southern and central Andes showing regions referred to in text.

Some of the most convincing Phanerozoic slabmelts on Earth are found among the Neogene to Recent adakitic magmas in the southernmost Andes. The two most convincing cases are lavas erupted at the Recent Mt. Cook center in the southernmost Austral Volcanic Zone (see Stern and Kilian 1996) and at the ~ 12 Ma Cerro Pampa center, which is located east of where the Chilean Rise collided with the Chile trench at ~ 12 Ma (see Kay et al., 1993). The combination of low $^{87}Sr/^{86}Sr$ ratios (~ 0.7028; Fig. 2), extreme Sr concentrations (>1000 ppm; Fig. 3), and steep REE patterns (La/Yb ~ 30; Fig. 4) in these adakites is difficult to explain in other contexts as is the case for the first proposed Neogene slabmelt at Adak Island in the Aleutian arc in Alaska (Kay, 1878). Slab

melting in southern Patagonia is further supported by thermal models for young subducting oceanic plates (Peacock et al, 1994). The Cook and Cerro Pampa adakites contrast with other proposed slabmelts in the AVZ whose higher $^{87}Sr/^{86}Sr$ ratios > 0.705 (Fig. 2) can be explained by crustal contamination of melts from the young subducting Antarctic plate (Kay et al. 1993; Stern and Kilian, 1996).

In contrast to southern Andean adakites, Central Andean magmas with adakitic characteristics have

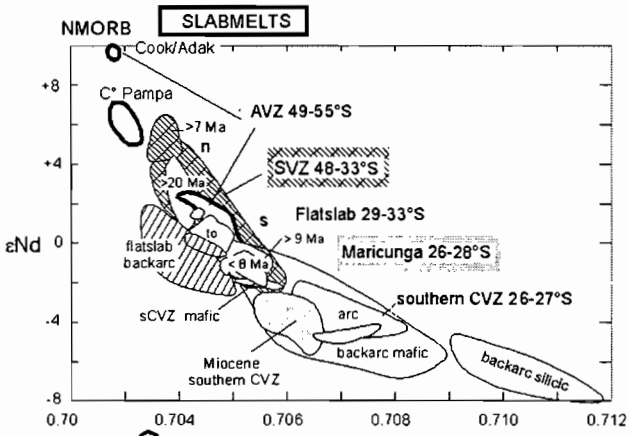

Figure 2. Plot of Nd and Sr isotopic ratios in Miocene to Recent magmas showing characteristics of slabmelt adakites versus those erupted through thickened crust in the central Andes. Data from Stern and Kilean (1994), Kay (1978), Kay et al. (1991, 1993, 1994, 1999, 2002), Hildreth and Moorbath (1988) and sources cited in those papers.

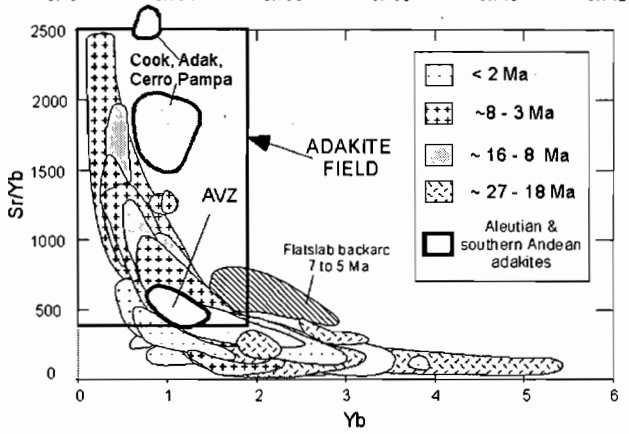

Figure 3. Plot of Sr/Yb ratio versus Yb concentration in ppm for Miocene to Recent magmas showing characteristics of well established slabmelt adakites (Cook, Adak, Cerro Pampa) relative to other central and southern Andean magmas. Graph is one of the discriminants for slabmelt adakites employed by Defant and Drummond (1990). The plot illustrates the increased importance of Andean magmas with adakitic characteristics in the middle to Late Miocene and early Pliocene. This increase correlates with increasing thickness of the Andean crust and frontal arc migration, rather than subduction of hot, young oceanic crust. Data sources as in Figure 2.

erupted over older, colder portions of the subducting Nazca plate. None have the depleted isotopic signatures of the Cook and Cerro Pampa adakites (Fig. 2), and all have lower Sr contents (Fig. 3). A significant number have steeper REE patterns. Their adakitic characteristics are better attributed to partial melting of granulitic to eclogitic facies continental crust. This crust can be added as contaminants in mantle-derived mafic magmas at the base of tectonically thickened crust (e.g., Kay et al., 1991, 1999) or can be incorporated into the mantle wedge as forearc crust removed by the subduction erosion processes (e.g., von Huene and Scholl, 1991; Stern, 1991, Ranero and von Huene, 2000). The chemical characteristics of these two groups are better matches for Archean TTG suite magmas with La/Yb ratios over 100 than are southern Andean slab melts.

Neogene to Recent adakites in the Andean Central Volcanic Zone (CVZ), northern Southern Volcanic Zone (SVZ), and over the Chilean flatslab (Fig. 1) have erupted through crust which has been thickened by structural shortening of ductile crust under compression. Partial melting at the base of this crust in association with injection of mantle-derived basaltic arc magmas in a high-pressure MASH (melting, assimilation, storage and homogenization – Hildreth and Moorbath, 1988) zone leads to magmas with adakitic characteristics. This process is supported by temporal correlations of deformation in foreland fold/thrust belts with eruption of adakitic magmas whose isotopic ratios are best explained by crustal contaminants (e.g., see Kay et al. 1991, 1999, 2002; Figs. 2 to 4). At the extreme, backarc southern Puna Antofalla region adakites with extreme REE

characteristics (La/Yb to 100, Sm/Yb > 8; see Fig. 4) are associated with melting of over thickened lower crust that became negatively buoyant relative to the underlying mantle (Kay et al. 1994). Rapid sinking ("delamination") of this gravitationally unstable granulitic to eclogitic crust along with the underlying mantle lithosphere produced a void in the mantle wedge that was filled by asthenosphere. Mafic magmas with intraplate like chemical signatures that segregated in this asthenosphere caused transient heating and partial melting of the crust, including the delaminating lower crust. These melts left eclogitic residues that are denser than the pre-existing (unmelted) lower crust.

Evidence that forearc crust incorporated into the mantle through the forearc subduction erosion (see von Huene and Scholl 1991; Stern 1991) process also plays a role in producing Andean adakitic signatures comes from correlations of eastward migrations of the arc front with abrupt changes in magmatic geochemistry, including the transient appearance of distinctive adakitic signatures at times of arc migration (Kay and Mpodozis, 2000, 2002; Kay et al. 2002). During arc front migrations, peak periods of subduction erosion bring

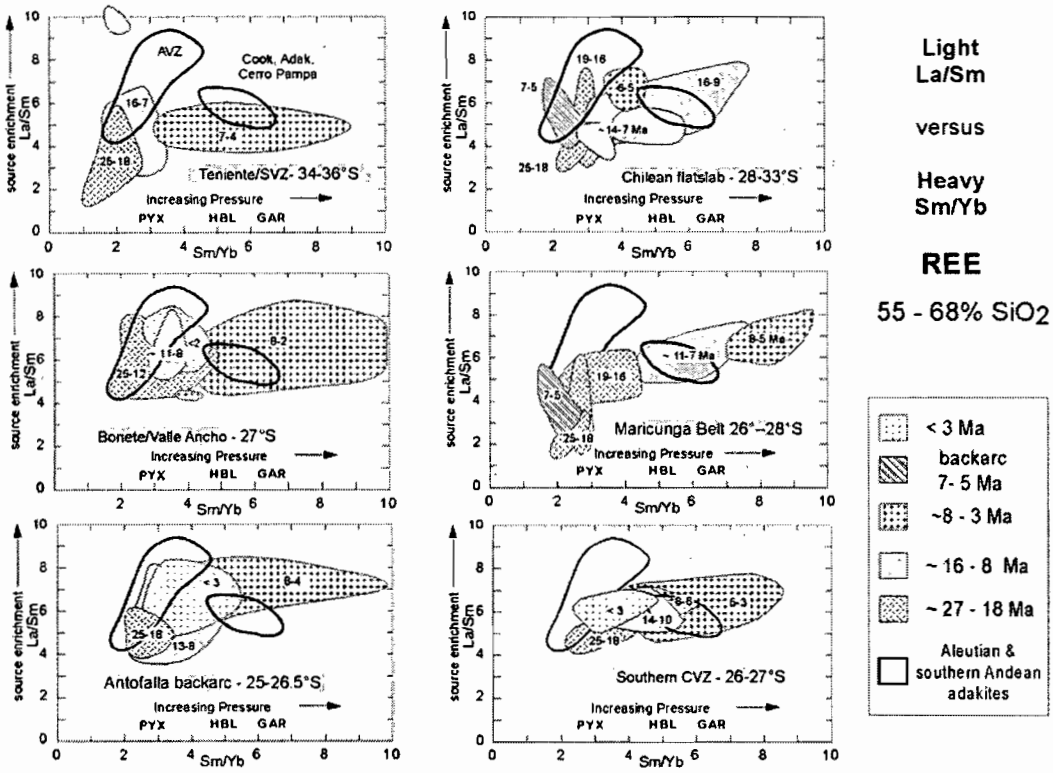

Figure 4. Plot of La/Sm ratio versus Sm/Yb ratios for Miocene to Recent magmas showing characteristics of well established slabmelt adakites (Cook, Adak, Cerro Pampa) along with other proposed AVZ slabmelt adakites relative to central and southern Andean magmas. High Sm/Yb ratios signal a high pressure garnet-bearing residual mineralogy as garnet preferentially fractionates the heavier REEs leading to relatively high Sm/Yb ratios. As in Figure 3, plot illustrates the increased importance of Andean magmas with adakitic characteristics in the middle to Late Miocene and early Pliocene coincident with increasing thickness of the Andean crust and frontal arc migration. As the highest Sm/Yb ratios tend to occur in the most silicic magmas, the garnet signature is a signal of a higher pressure residual crustal mineralogy. Localities shown in Figure 1. Data sources as in Figure 2.

forearc basal crustal material (not only sediment) to high-pressure under the arc, where this transformed granulitic to eclogitic faces crust melts to produce the adakitic signature. The most extreme examples are dacites with ratios of $^{87}Sr/^{86}Sr > 0.705$, La/Yb up to 100, Sm/Yb > 6 (Fig. 4), and La/Ta up to 80 that erupted as volcanism waned in the Maricunga arc near 26° to 28°S and before the frontal arc was reestablished in the CVZ to the east. Other extreme examples are magmas erupted as volcanism ceased in the southernmost CVZ in the Bonete region near 28°S. Distinctive adakitic magmas are also associated with frontal arc migration at 20 to 16

Ma and at 8 to 4 Ma over the Chilean flatslab and in the northern SVZ (Kay et al. 2002). As crustal thickening accompanied arc migration, these adakites also contain partial melts of thickened continental crust.

In conclusion, most Miocene to Recent central and southern Andean adakites are still best explained by equilibration of mantle wedge derived arc magmas with garnet-bearing continental crust rather than by melting of subducted oceanic slabs. Strong support comes from the positive temporal correlation between the abundance of Central Andean adakitic magmas (Figs. 3 and 4) and patterns of crustal thickening and eastward arc front migration. Marked increases in adakitic magmas at about 19 to 16 Ma and again at 8 to 4 Ma can be correlated with peaks in crustal thickening and forearc subduction erosion that are most likely linked with changes in convergence parameters between the Nazca and South American plate.

REFERENCES

Defant, MJ and Drummond MS, (1990), Derivation of some modern island arc magmas by melting of young subducted lithosphere. Nature 347: 662-665.

Gutscher MA, Maury R, and Eissen JP (2000), Can slab melting be caused by flat subduction? Geology 28: 535-538.

Hildreth, W. and Moorbath, S, (1988), Crustal contributions to arc magmatism in the Andes of Central Chile. Contrib. Mineral. Petrol. 98: 455-489

Kay RW, (1978), Aleutian magnesian andesites-melts from subducted Pacific ocean crust. J. Volcanol. Geother. Res. 4: 117-132.

Kay SM and Mpodozis C, (2002) Magmatism as a probe to the Neogene shallowing of the Nazca Plate beneath the modern Chilean flatslab. J. South Am. Earth Sci., In Press

Kay SM, Coira B, and Viramonte J, (1994), Young mafic back-arc volcanic rocks as indicators of continental lithospheric delamination beneath the Argentine Puna Plateau, Central Andes. J. Geophys. Res. 99: 24323-24339.

Kay, SM, Godoy E, and Kurtz A, (2002), Crustal thickening and subduction erosion: their roles in the Neogene Andean Southern Volcanic Zone. Geol. Soc. Amer. Bull. (submitted).

Kay SM, Mpodozis C, and Coira B, (1999), Neogene magmatism, tectonics, and mineral deposits of the Central Andes (22 to 33° S), in Skinner BJ (ed.), Geology and Ore Deposits of the Central Andes, Soc. Economic Geol. Spec. Publ 7:27-59.

Kay SM, Mpodozis C, Ramos VA, and Munizaga F, (1991), Magma source variations for mid-late Tertiary magmatic rocks associated with a shallowing subduction zone and a thickening crust in the central Andes (28 to 33°S). Geol. Soc. Amer. Spec. Paper 265: 113-137.

Kay SM, Ramos VA, and Marquez M, (1993), Evidence in Cerro Pampa volcanic rocks for slab melting prior to ridge-trench collision in southern South America. J. Geol. 101: 703-714.

Ranero CR and von Huene R, 2000, Subduction erosion along the Middle America convergent margin. Nature, 404: 748-752.

Stern CR, (1991a), Role of subduction-erosion in generation of Andean magmas. Geology 19: 78-81.

Stern CR and Kilian R, (1996), Role of the subducted slab, mantle wedge and continental crust in the generation of adakites from the Andean Austral Volcanic Zone. Contrib. Mineral. Petrol. 123: 263-281.

von Huene R and Scholl DW, (1991), Observations at convergent margins concerning sediment subduction, subduction erosion, and the growth of continental crust. Rev. Geophys. 29: 279-316.

LATE QUATERNARY SLIP RATES OF THE MEJILLONES FAULT, NORTHERN CHILE (23°S), USING ^{10}BE DATES

Carlos MARQUARDT (1,4), Régis BRAUCHER (2), Jean-François RITZ (3), Hervé PHILIP (3), Didier BOURLES (2), Alain LAVENU (4), Bertrand DELOUIS (5), Luc ORTLIEB (6).

(1) SERNAGEOMIN, Av. Santa María 0104, Santiago, Chile (cmarquar@sernageomin.cl)
(2) CEREGE, Europole Méditerranéen de l'Arbois, Aix-en Provence, France (braucher@cerege.fr)
(3) LGTS, U. Montpellier II, 34095 Montpellier Cedex 05, France (ritz@dstu.univ-montp2.fr)
(4) IRD-LMTG, U. Paul Sabatier, 38 rue des 36 Ponts, 31400 Toulouse, France (lavenu@cict.fr)
(5) Géosciences Azur, U. Nice, 250 Rue Albert Einstein, 06560 Valbonne, France (delouis@geoazur.unice.fr)
(6) IRD, 32 Avenue Henri Varagnat, 93143, Bondy Cédex, France (Luc.Ortlieb@bondy.ird.fr)

KEY WORDS: Neotectonics, normal faulting, uplift, *in-situ* cosmogenic ^{10}Be dates, northern Chile

INTRODUCTION

The Mejillones Peninsula is located along the arid coast of northern Chile and belongs to the Central Andes fore arc. It is the fore arc emerged part the closest to the subduction trench. Quaternary alluvial fans and uplifted abrasive marine terraces (and associated deposits) are well preserved, and both are affected by several normal faults. Our study aims to date the displaced alluvial fans surfaces, using *in-situ* produced cosmogenic ^{10}Be, to quantify the slip rate along the faults.

THE MEJILLONES FAULT

Located at the northern part of the Mejillones Peninsula, the Mejillones Fault belongs to the Mejillones Faulting System but can also be considered as the most western part of the Atacama Fault System which has a Mesozoic origin (Fig. 1). The Mejillones peninsula is deformed by an E-W extension during the Plio-Quaternary and is affected by numerous normal faults, tension gashes, tilted blocks and vertical motions (*e.g.*: Okada, 1971; Armijo and Thiele, 1991; Hartley and Jolley, 1995; Niemeyer *et al.*, 1996; Delouis *et al.*, 1998). This extensional deformation is expressed in the morphology by a series of horsts and grabens (or half grabens).

The Mejillones Fault limits to the east the uplifted peninsula (Morro Mejillones range) which displays a staircase morphology corresponding to wave-cut platforms abraded in basement rocks. To the east, the Pampa Mejillones defines an isthmus, filled by Neogene marine deposits and covered by Quaternary sequence of beach-ridges. The whole system (Mejillones fault, Morro Mejillones and Pampa Mejillones) can be described as a half graben developed at least from the Neogene time, in the northern half part of the peninsula.

The last movements along the Mejillones Fault affect several generations of alluvial fans at outlets of deep-incised drainage basins developed in the eastern flanks of the Morro Mejillones. This alluvial fans cover Quaternary beach-ridges of Pampa Mejillones formed during the last half million years (Ortlieb, 1995; Ortlieb *et al.*, 1996). These faults are supposed to have a very recent activity, but no historical seismic activity has been

reported along this fault, and moreover, no significant crustal seismicity is associated to the fore arc at this latitude.

Delouis *et al.* (1998) proposed that the state of stress in the outer fore arc is linked to the seismic cycle in the subduction zone. As observed during the 1995, Mw = 8.0 Antofagasta earthquake, subduction earthquakes produced coseismic E-W extension and vertical movement in the coastal area, that would produce the reactivation of some branches of the Atacama Fault System and the formation of superficial cracks.

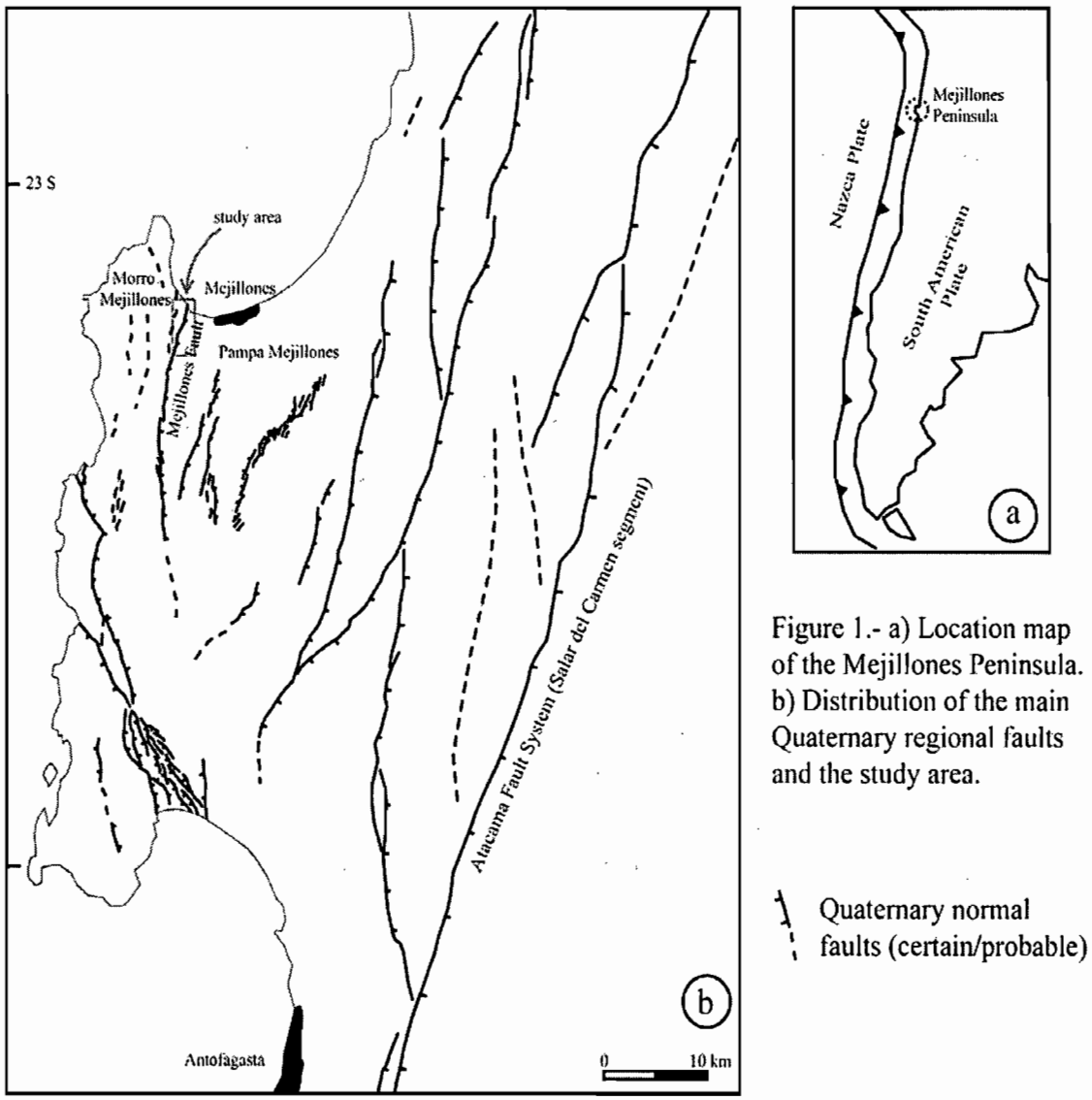

Figure 1.- a) Location map of the Mejillones Peninsula. b) Distribution of the main Quaternary regional faults and the study area.

Quaternary normal faults (certain/probable)

PRELIMINARY MORPHOTECTONICS AND DATINGS RESULTS

We surveyed morphotectonic markers along the northern part of the Mejillones Fault where they were the best preserved from erosion. Three sites were selected in order to measure the cumulated displacements along the fault (Fig. 1). The mean offsets were determined from Digital Elevation Models (DEMs) calculated from differential GPS measurements with 1 cm accuracy. Series of cross-sections in DEMs allowed us to estimate the mean vertical cumulated offsets. We obtained 13 ± 1 m and 5.5 ± 0.5 m for the offsets of two

surfaces, S1 and S2 respectively (age of S1 > S2). We collected samples from granitic boulders well incased in the two alluvial surfaces. S1 and S2 surfaces were sampled, and on both sides of the fault scarp. For each surface, 5 boulders were sampled with two or three samples by boulders: one at the top, one in the core and one at the bottom. These samples were dated using in-situ produced cosmogenic ^{10}Be.

The assumption of negligible erosion of boulders allows us to estimate the minimum exposure ages using ^{10}Be production rates, calculated from the latitude and altitude dependent polynomials of Lal (1991). Preliminary available results from S2 surface give a minimum exposure age of 20000 ± 3000 yrs (Table 1), which yields a slip rate of 0.28 ± 0.05 mm/yr.

Table 1.- ^{10}Be concentrations and calculated minimum exposure ages.

Sample	Surface unit	10Be (atoms/g)	Uncertainty (atoms/g)	Minimum age (yr)	Uncertainty (yr)
C99-13	S2	86 480	10 383	18 882	2 267
C99-14	S2	59 561	9 585	20 435	3 289
C99-15	S2	62 145	12 568	13 552	2 741
C99-16	S2	47 136	9 533	19 145	3 872
C99-17	S2	69 121	12 394	15 079	2 704
C99-19	S2	93 154	13 340	20 346	2 914
C99-20	S2	93 630	14 237	32 423	4 930

DISCUSSION

These results, although preliminary (the rest of ^{10}Be analyses are in progress and will be presented during the ISAG workshop), allow us to draw several preliminary conclusions concerning the recent paleoclimatic and tectonic processes along this part of the Mejillones Peninsula.

According with the preliminary ages resulting of S2 (one of the oldest alluvial surface), we estimated that the alluvial unites developed along the northern part of the Mejillones Fault have been deposited during different paleoclimatic events next to last interglacial time (< 125 ka). This way, the sequence of beach-ridge covered by this alluvial fans, in this part of the Pampa Mejillones, can be assigned as maximum to the last interglacial time.

The long-term regional Pleistocene average uplift estimated from the study of marine terraces of the Pampa de Mejillones is 0.2 mm/yr and the double (0.4 mm/yr) for the Morro Mejillones (Ortlieb, 1995). The difference would represent the amount of uplift that is occurring by normal faulting. These calculations are consistent with our estimation of the vertical slip rate along the Mejillones Fault.

Concerning paleoseismology, the features observed along the fault (two offset alluvial surfaces), show that there were at least two events since the abandonment of the surfaces S1. The difference of riser heights of the inset secondary surfaces observed within the main S2 surface, on both sides of the fault, suggest in fact that the cumulated displacements are the results of much more numerous events. Within the most recent alluvial surfaces, inset in S2, we observed a set of cracks trending NS along the trend of the fault scarp. No surface ruptures were reported in the Antofagasta area during the 1995 Mw = 8.0 earthquake (located at the southern part of the peninsula). Nevertheless, tension gashes were described along some faults of the Atacama fault

system (Delouis *et al.*, 1998). Therefore, we think that the activity of the Mejillones Fault (and all the system fault of this peninsula) could be related to the occurrence of strong subduction earthquakes (Mw $\geq$ 8.0).

CONCLUSIONS

Late Quaternary deformation in the Mejillones Peninsula is characterised by general coastal uplift and extensional deformation. Tectonic blocks with different uplift rates are separated by normal faults. We estimate the preliminary vertical slip rate along the Mejillones Fault (calculated for the last 20 ka) at 0.28 $\pm$ 0.05 mm/yr. This normal faulting is still active and could be closely associated with subduction earthquakes.

ACKNOWLEDGEMENTS

This study was supported by the Chilean Servicio Nacional de Geología y Minería (SERNAGEOMIN) in collaboration with the Intitut de Recherche pour le Développement (IRD). We thank Nicolas Marinovic (SERNAGEOMIN) and Gerard Hérail (IRD) for their support displayed to this study. The dates was supported by the Centre Européen de Recherche et d'Enseignement de Géosciences de l'Environnement (CEREGE) and by the Laboratoire de Géophysique, Tectonique et Sédimentologie of the Montpellier University (UMR5573). We thank Mourice Arnold for his support in the Tandétron of CNRS-Gif (France).

REFERENCES

Armijo R., Thiele R. 1990. Active faulting in northern Chile: ramp stacking and lateral decoupling along a subduction plate boundary? Earth and Planetary Science Letters, Vol. 98, 40-61.

Delouis B., Philip H., Dorbath L., Cisternas A. 1998. Recent crustal deformation in the Antofagasta region (northern Chile) and the subduction process. Geophys. J. Int. 132, 302-338.

Hartley A.J., Jolley J. 1995. Tectonic implications of Late Cenozoic sedimentation from the Coastal Cordillera of northern Chile (22-24°S). Journal of the Geological Society of London, Vol. 152, 51-63.

Lal D. 1991. Cosmic ray labelling of erosion surfaces: In-situ nuclide production rates and erosion models. Earth and Planetary Science Letters, v. 104, 424-439.

Niemeyer H., González G., Martínez De los Rios E. 1996. Evolución tectónica cenozoica del margen continental activo de Antofagasta, norte de Chile. Revista Geológica de Chile, Vol. 23, No 2, 165-186.

Okada A. 1971. On the neotectonics of the Atacama fault zone region. Preliminary notes on late Cenozoic faulting and geomorphic development of the Coast Range of northern Chile. Bull. of the Dep. of Geography Kyoto Univ., 3, 47-65.

Ortlieb L. in coll. with J.L. Goy, C. Zazo, Cl. Hillaire-Marcel and G. Vargas 1995. Late Quaternary Coastal Changes in northern Chile. Guidebook for a fieldtrip, II annual meeting of the IGCP, Project 367, ORSTOM.

Ortlieb L., Díaz A., Guzmán N. 1996. A warm interglacial episode during isotope stage 11 in Northern Chile. Quaternary Science Reviews, 15, 819-831.

TECTONICS FROM THE NORTHERN SEGMENT OF THE LIQUIÑE-OFQUI FAULT SYSTEM (37°-39°S), PATAGONIAN ANDES

Daniel MELNICK (1), Andrés FOLGUERA (2), Matthias ROSENAU (3), Helmut ECHTLER (3), Susanne POTENT (4)

(1) Universidad de Concepción, Departamento de Ciencias de la Tierra. (dmelnick@udec.cl)
(2) Laboratorio de Tectónica Andina, Universidad de Buenos Aires. (folguera@gl.fcen.uba.ar)
(3) GeoForschungsZentrum (GFZ) Potsdam, Germany. (rosen@gfz-potsdam.de , helle@gfz-potsdam.de)
(4) Geologisch-Paläontologisches Institut, Universität Hamburg. (potent@geowiss.uni-hamburg.de)

KEY WORDS: Northern Patagonian Andes, Volcanic Arc Segmentation, Oblique Subduction, Transtension

INTRODUCTION

The Andean cordillera is charaterized by segmentation along strike, due to differences in the subduction geometry and the age and nature of the subducting plate, inherited continental basement features and the differencial partitioning of deformation.

The northern Patagonian Andes (37°30′-46°S) are a relatively low relief mountain chain with a normal crustal thickness (~40km), and a volcanic arc controled by the active Liquiñe-Ofqui fault zone (LOFZ), a more than 1000 km long dextral strike-slip fault system, produced by oblique subduction of the Nazca plate and ridge-push stress from the Chilean rise (Nelson et al. 1994). The LOFZ seems to control the main efusions of Quaternary volcanism indicated by fisural-stratovolcanoes and the alignement of monogenetic cones, after the westward shifting of the arc towards the trench possibly due to steeppening of the subducting Nazca plate during the late Pliocene (Stern, 1989). The nature of deformation along the LOFZ has been described as transpressive in the southern segment (46°-39°S) (Lavenu and Cembrano 1999), and transtensive in the northern (37°30′-39°S) part of the LOFZ (Folguera et. al. 2001, Potent and Reuther, 2001).

SEGMENTATION OF THE NORTHERN PATAGONIAN INTRA-ARC ZONE

Mainly based on kinematic field data, interpretation of Landsat images and digital elevation models, we establish two transitional segments (TS1 and TS2, Figure 2) between the main transpressional southern segment (SS) and the northern segment (NS) characterized by quaternary shortening in the hinterland of the cordillera.

TS1 is characterized by a principal strike-slip deformation along N-S trending faults, its southern boundary is the Gastre fault zone, a main NW-SE trending Paleozoic inherited structure (Rapela and Pankhurst, 1992) where actually the Villarica-Quetrupillán-Lanín volcanic lineament is located (Figure 2). The geometry of TS1 shows important E-W faults cross cutting the main N-S striking LOFZ these orthogonal faults have well preserved triangular facets along their northern side of the valley, inferring Quaternary extension, microtectonic measurements in the Miocene granitoides show sinistral transtensional deformation. TS2 shows mostly

transtentional deformation during Quaternary and recent times dominated by mainly eastward bending horsetail-like structures (Figure 2) as the Lonquimay and el Barco areas (Figure 3).

At the transition between TS2 and the northern segment at 38°S (Figure 2 and 3) the LOFZ cuts the Bío-Bío–Aluminé fault zone (BBAFZ, Figures 2 and 3) and then bends eastwards against the Callaqui-Copahue-Mandolegüe (CCM) transtensional volcanic lineament (Melnick and Folguera, 2001), producing the El Agrio Caldera, a pull-apart basin developping from late Pliocene to early Pleistocene times. Postglacial deformation inside the caldera and the adjacent Copahue Volcano shows a clockwise rotation of the strain patterns into the small compressive Chancho-Co fold and thrust system, limited by a main NW-SE trending sinistral fault (Figure 4), these are the first evidences of recent compression along the intra-arc zone of the Patagonian Andes.

Stratigraphic data from the Curamallín basin show that the CCM lineament acted as a transfer zone during Oligocene continental rifting events (Radic et. al. in prep), which has been reactivated during Pliocene to Quaternary times as an important NE-SW trending 80 km long volcanic fissure (Figure 3).

The northern segment (Figure 2) shows Quaternary and Postglacial shortening in the back-arc zone (Folguera et. al. in prep) and Quaternary compressional deformation along the central valley (Lavenu and Cembrano, 1999). Quaternary deformation in the southern segment, (TS1 and TS2), shows a combination of simple and pure shear along the intra-arc zone, contrasting with the northern segment where pure shear is observed in the hinterland and simple shear along the Central Valley. At 38°S, the low stress/strain partitioning LOFZ splits into two main zones of deformation and the partitioning splits over a wider area.

The limits of both transitional segments are the two longest Quaternary volcanic lineaments of the Southern Andes volcanic zone, to the south the Villarica-Quetrupillán-Lanín 50 km long and the 80 km long Callaqui-Copahue-Mandolegüe to the north (Figure 2).

INFLUENCE OF THE SUBDUTED PLATE GEOMETRY

Bathymetric and topographic data from the Patagonian Andes zone (Figure 1) show the geometry of the subducted Nazca plate at 38°S where the Mocha fracture zone, trending N60°E, is subducted under the uplited Arauco Peninsula and Nahuelbuta Range in the forearc Coastal Cordillera and the also N60°E trending CCM in the principal Cordillera. This fracture zone separates different oceanic crustal structures with Oligocene to the north and Miocene ages (Figure 1). North of the Mocha fracture zone, the depth of the trench increase to more than 4000 m and the mean altitude of the principal cordillera becomes higher than 2000 m.

These features emphasize to correlate the subduction of this oceanic fracture zone and the associated differences in ages, physical parameters and geometry of the subducting slab with the structural segmentation and differential strain partitioning described in the intra-arc zone since Pliocene times.

ACKNOWLEDGEMENTS

This work has benefit from the following projects: GeoForschungsZentrum Potsdam Southern Andes project, SFB 267 "Deformation in the Andes" , PIP 4162 (Conicet) and PICT 059 for the "Study of the segment

of normal subduction -33° to 38°S", "Geological and Volcanological Study of the Copahue Volcano" UNESCO. Re 461 (DFG) for the study of the Arauco-Bío-Bío Trench-Arc-System.

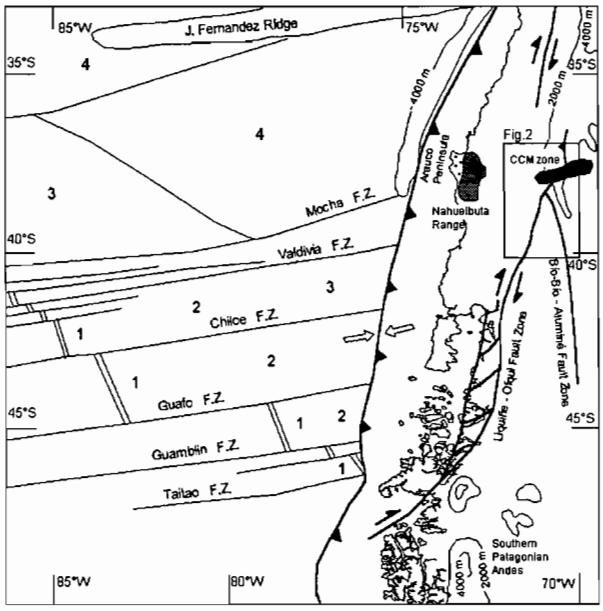

Figure 1. Bathymetric and topographic data from the Nazca plate and Patagonian Andes, Data from Smith and Sandwell, 1997. Age of the ocean floor: 1. Quaternary, 2. Pliocene, 3. Miocene, 4. Oligocene (Dewey and Lamb, 1992).

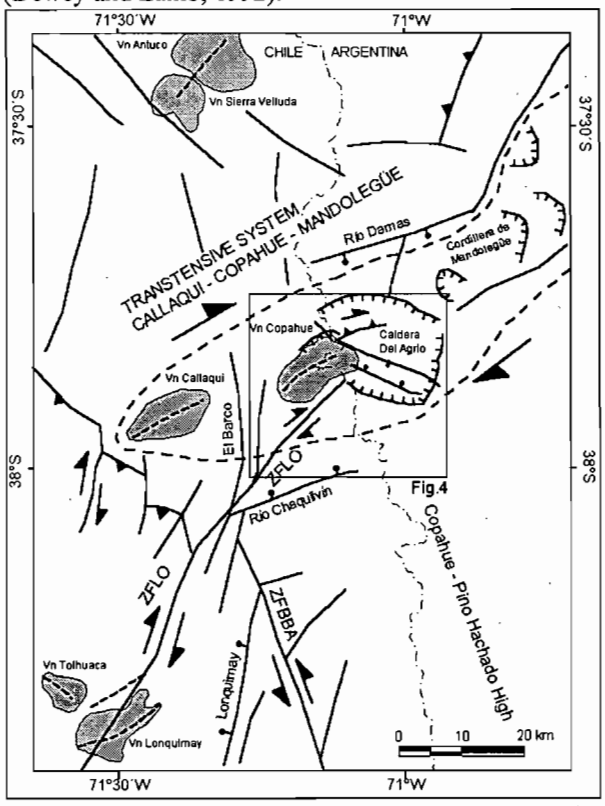

Figure 3. Structural interpretation of the Callaqui–Copahue–Mandolegüe transtensional system. Based on field data, and Landsat interpretation.

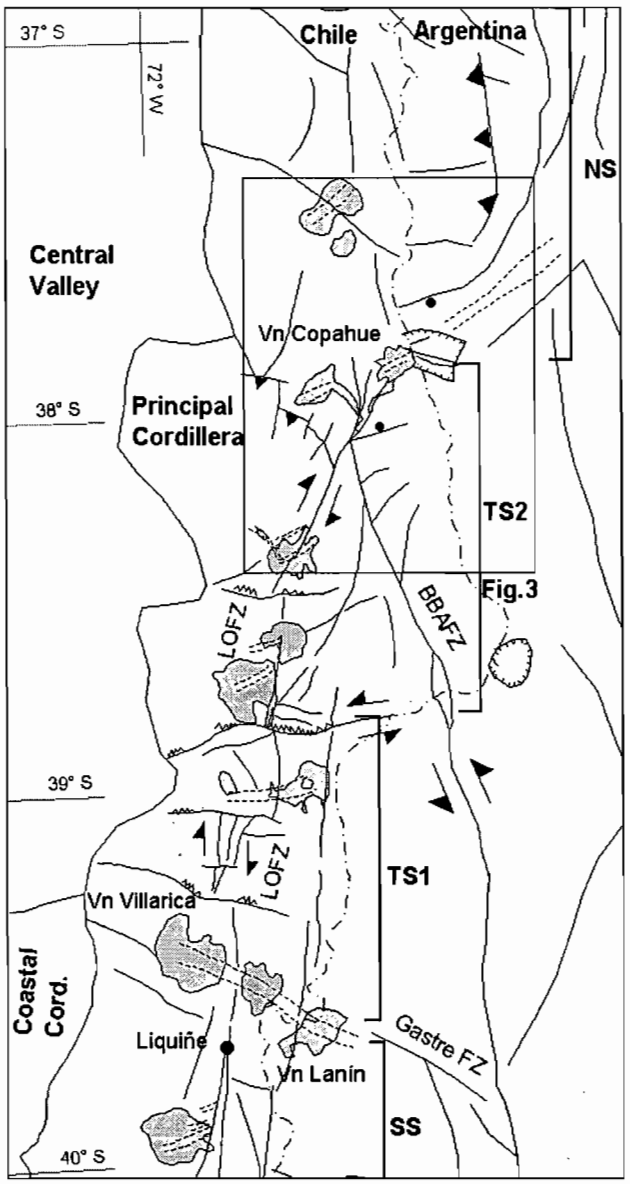

Figure 2. Structural sketch of the Northern Patagonian Andes Segmentation of the intra-arc zone and the Liquiñe-Ofqui Fault zone. Based on field data, LandSat TM and DEM interpretation

→

Figure 4. Structural Map of the Copahue Volcano and El Agrio Caldera.

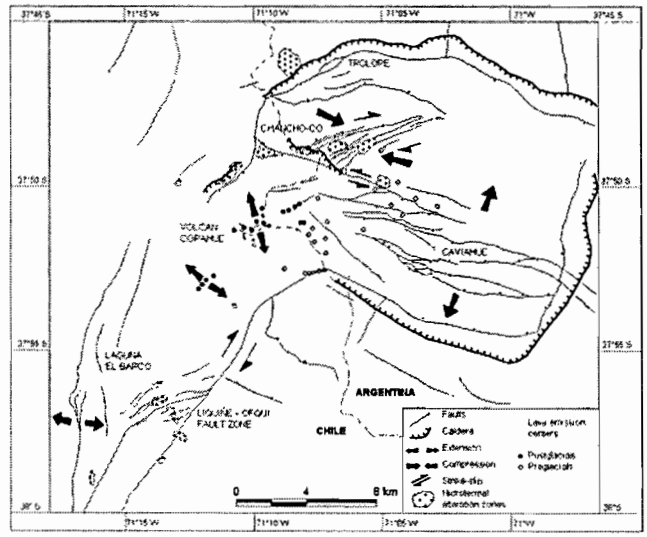

REFERENCES

Dewey, J.F. and Lamb, S.H. 1992. Active Tectonics in the Andes. Tectonophysics, 205 (1992) 79-95.

Folguera, A., Yagupsky, D., Zlotnik, S., Iaffa, D., Melnick, D. 2001. Transtensión como mecanismo de transición entre estados de baja y alta partición de la deformación entre 37° y 40°S en el Plioceno y Cuaternario. 11° Congreso Latinoamericano de Geología, Simposio "Evolución tectónica de los Andes" 3. Electronic files. Montevideo.

Andrés Folguera, Victor A. Ramos, Daniel Melnick, Diego Iaffa, Daniel Yagupsky, Sergio Zlotnik. (in prep). Recurrencia en el desarrollo de cuencas de intraarco. Colapso de estructuras Orogénicas. Cordillera Neuquina (37°30'). Acepted, Revista de la Asociación Geológica Argentina.

Lavenu, A. And Cembrano, J. 1999. Compressional and tranpressional stress pattern for Pliocene and Quaternary brittle deformation in fore arc and intra arc zones (Andes of Central and Southern Chile). Journal of Structural Geology , 21, 1669-1691.

Melnick, d. And folguera, a. 2001. Geologia del complejo volcánico copahue - caldera del agrio, un sistema transtensional activo desde el plioceno en la transición de los andes patagónicos a los andes centrales (38°s - 71°o). Xi congreso geológico latinoamericano, simposio "evolución tectónica de los andes": 6. Electronic files. Montevideo.

Nelson, M.R., Forsythe, R., Arit, I. 1994. Ridge collision tectonics in terrane development. Journal of South American Earth Sciences 7, 271-278.

Potent, S. And Reuther, C.-D. 2001. Neogene Deformationsprozesse im aktiven magmatischen Bogen Südzentralchiles zwischen 37° und 39°S. Mitt. Geol.-Paläont. Inst. Univ. Hamburg 85, 1-22.

Radic, J.P. et. Al. (in prep). Evolución Tectónica de la cuenca Terciaria de Cura-Mallín Región Cordillerana Chileno Argentina (36°30'-39°00'S) acepted XV Argentinian Geological Congress. Calafate.

Rapela, C. W. And Pankhurst, R. J. 1992. The granites of northern Patagonia and the Gastre Fault System in relation to the break-up of Gondwana. Geol. Soc. Spec. Publ. 68, 209-220

Smith, W. H. F., and D. T. Sandwell. 1997. Global seafloor topography from satellite altimetry and ship depth soundings, Science, v. 277, p. 1957-1962, 26 Sept., 1997.

Stern, C. 1989. Pliocene to present migration of the volcanic front, Andean Southern Volcanic Front. Revista Geológica de Chile, 16 (2), 145-162

ENVIRONMENT, PROVENANCE AND PALEOGEOGRAPHIC SETTING OF TWO LATE APTIAN-EARLY ALBIAN OPEN-SEA SEDIMENTARY SEQUENCES IN THE WESTERN PIEDMONT OF THE CENTRAL CORDILLERA, SOUTH PIJAO, QUINDIO DEPARTMENT, COLOMBIA.

Jairo MOJICA (1) and Oscar J. ARÉVALO (1)

(1) Departamento de Geociencias, Universidad Nacional, Apartado 14490, Bogotá - Colombia. (jmojica@ciencias.unal.edu.co ; oscarjarevalo@hotmail.com)

KEYWORDS: Aptian-Albian, open-sea sedimentites, turbidites, Cordillera Central, Quindío, Western Colombia

INTRODUCTION

The geologic evolution of the Colombian Western Andes has been interpreted in several and controversial ways due to complex tectonic relationships and occurrence of incomplete and "mixed" suites of low to medium grade metamorphic rocks ophiolite-like associations, assumed mélanges or mélange zones, as well as volcano-clastic sedimentary units. Those interpretations are based on adopted or adapted models that include accretion of far coming suspected terrains, compressive deformation due to oceanic ridge or arc-continent collision, transpressive deformation and even extensional opening of marginal seas. These discrepancies may be consequence of low state of the art, lack of detailed stratigraphic studies and reliably ages for many of the rock units cropping out west of the water-divide of the Central Cordillera

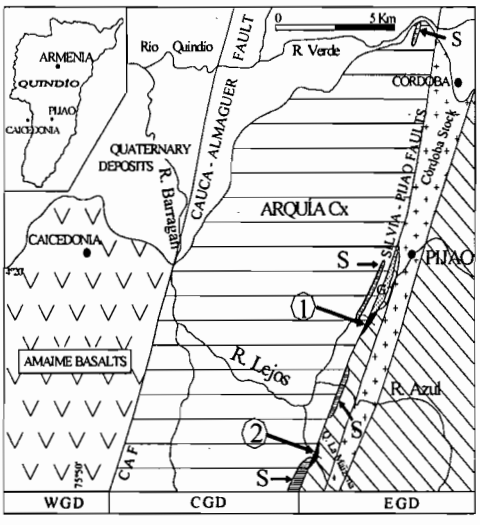

Fig. 1. Tectonic setting and outcrops of the Aptian - Albian sedimentites (1 & 2), serpentinized ultramafic bodies (S) and gabbro (G). Details: see text.

With the intention of helping in the solution of part of the aforementioned problems, this work is dedicated to the description and interpretation of two sedimentary sequences exposed in the half portion of the western piedmont of the Colombian Central Cordillera. The outcrops are located south of the Pijao village, one in the riversides of the Río Lejos –place Puente Tabla- and another in the half portion of the La Maizena creek (Fig. 1). The sedimentites of both sections contain well-preserved fossils including planktonic forams and ammonites of late Aptian – early Albian, identified respectively by Professors N. Tchegliakova and P. Patarroyo (Department of Geosciences, National University, Bogotá).

TECTONIC SETTING

Mojica *et al.* (2001) divide the studied area in three geologic domains (Fig. 1) separated by two master fractures, the Cauca-Almaguer Fault (CAF) and Silvia-Pijao Faults (SPF). The cretaceous sedimentites described in this paper occur in the most western part of the Eastern Geologic Domain (EGD), which is composed also of: a) diabases, pyroclastites and green phyllitic rocks; b) a narrow gabbro body that intrudes the sedimentites; and c) a granodioritic stock with mineral ages K/Ar between 58 and 83 Ma, known as Córdoba Stock or Igneous Córdoba Complex. The Central Geologic Domain (CGD) is separated from the EGD by the SPF, and is composed of medium to low temperature and medium to high-pressure metamorphic rocks (McCourt & Feininger, 1984; McCourt *et al.*, 1984). These rocks have been referred as to Arquía Complex (ACx) and are composed of graphitic, micaceous and amphibolic schists, garnet-bearing amphibolites, as well as amphibolitized eclogites, glaucophanic schists and bodies of serpentinized ultramafics. The ACx is assumed to be Paleozoic by McCourt *et al.* (1984), Cretaceous by González & Núñez (1991) and Maya & González (1995). Westwards of the CAF appears the Western Geologic Domain (WGD), a wide region composed of oceanic basalts (=Amaime Formation or Amaime Complex) with scarce intercalations of weak calcareous sands bearing middle Albian planktonic forams (Mojica *et al.* 2001).

THE APTIAN-ALBIAN SEDIMENTITES

The Puente Tabla and the La Maizena sequences illustrated in Fig. 2, maintain typical Andean strike directions (N10E to N30E) and persistent east dipping; locally the conglomeratic sandstones show normal gradation, thus an indication of normal layering.

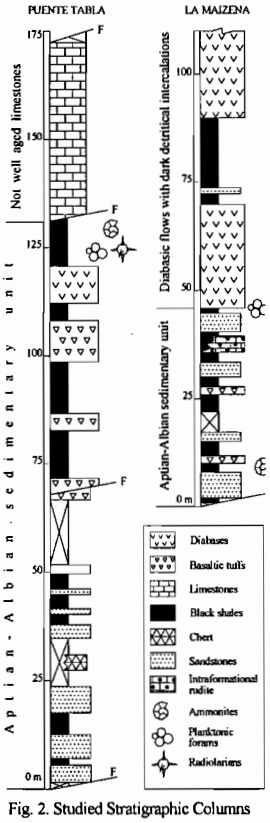

Fig. 2. Studied Stratigraphic Columns

In Puente Tabla the sedimentites conserve a thickness of 175m and are cut by several small faults that hide the stratigraphic relationships. The supposed lower part is composed of very mature, fine-grained quartzose sandstones (quartz >90%) with abundant micaceous matrix, sandy claystones, and scarce cherty beds. The sandstones represent approximately 15% of the Puente Tabla succession. In thin section, besides quartz they show rounded zircon and angular garnet and tourmaline grains, as well as scarce lithics of felsic volcanic rocks and quartz-phyllites. According to their composition the sandstones vary between quartzarenites and lithoarenites - subarcoses.

The middle third is made mainly of bituminous black shales that partially conserve an original plain-parallel lamination. The shales contain frequent intercalations of mafic tuffs and diabasic sills. Their fossil content is composed of scarce ammonites, small inoceramids, other bivalves, planktonic forams and radiolarians. The presence of *Riedelites obliquum* (Riedel) indicates a late Aptian age for this central interval.

The highest part of the Puente Tabla sequence is conformed by some 55m of limestone in faulted contact with the shales of the intermediate segment. Thin sections reveal the presence of micritic, peloidal and lithoclastic limestones as well as calcareous claystones. Until present, the limestones have yielded only isolated samples of ostreids and small inoceramids, but no index fossils. Gabbro dikes locally cut the limestones and generate metric marble-fringes. Basaltic microinjections are also present in some limestones.

At La Maizena the sequence is cut at the base by the SPF and lies in direct contact with the Arquía Complex; the top is marked by the appearance of a thick succession of diabasic flows with intercalations of dark pelites and quartzose sandstones. The preserved section is only 45m thick. It is composed mainly of black, conspicuously sheared dark shales. Very mature quartzose sandstones constitute ca. 35% of the section and appear dispersed through the whole section; due to intense tectonic deformation they adopt the form of squeezed lens-like bodies or boudins. In opposition to the situation observed at Puente Tabla, limestones have not been found at La Maizena; instead of that, there are some graded, friable, conglomeratic-lithic sandstones and intra-formational rudites.

In terms of composition, the conglomeratic sandstones are lithoarenites, the lithoclasts being of felsic vulcanite and plutonites. The rudites are composed of abundant clasts of shales, quartz-siltstones, quarzarenites and subordinated calcareous fragments (micritic and oolithic limestones), bounded by secondary calcite. The shales contain abundant spherical and ellipsoidal concretions (not observed at Puente Tabla) and have yielded well-preserved ammonites, small inoceramids and other bivalves, as well as planktonic forams. The ammonites (*Acanthohoplites aff. odiosus* and *Phyllopachiceras sp.*) and the forams indicate a late Aptian to early Albian age.

ENVIRONMENTAL AND TECTONIC INTERPRETATION

The petrographic results suggest that the mature sandstones and the lithoclastic and peloidal limestones represent turbidites deposited in an open sea of relatively deep waters. The ternary diagrams (Fig. 3) indicate provenance from a craton (very mature sandstones), located far eastward, and from an eroded orogen (lithic sandstones). A Proto-Cordillera Central, i. e. the postulated partially emerged basement high shown in Fig. 4, may have represented the orogen. Mature sandstones similar to those treated here are also known East of Manizales, West of Pácora (Álvarez 1995) and maybe at the type section of the "Fm. Quebradagrande" (Quebrada Campanas SW Medellín; Botero 1963), now called "Quebradagrande Complex" (QCx); more details about the nomenclature of lithodemic units Maya & González (1995).

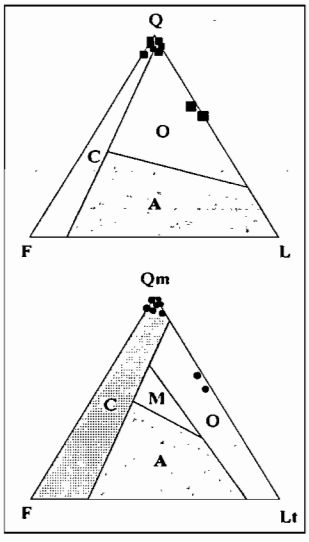

Fig. 3. QFL and QmFLt ternary diagrams

Episodes of submarine volcanism occurred simultaneously with the sedimentation and contributed with different kinds of materials to the basinal area, first with basic pyroclastics, later with diabases and basalts coming from West that ended drowning the previous sedimentation. To this volcanic event may also be related the lavic flows that gave place to the Amaime Complex and the gabbros that intrude the Puente Tabla sedimentites. Geochemical analysis of the diabases and

basalts associated to the QCx suggest distinct origin under extensional tectonics, either in an oceanic rift zone, a back-arc basin or in a marginal sea (Grösser 1989; Nivia *et al.* 1996).

The mature sandstones may have been partially derived from the region located SE of the embayment indicated in the paleogeographic map for Aptian times (shown in the inset of Fig. 4), together with other materials derived from the Proto Cordillera Central (felsic igneous-volcanic and clasts of low-grade metamorphics). The lithoclastic and peloidal limestones may have had a source in small calcareous platforms, located on one or both sides of the eastern basament high.

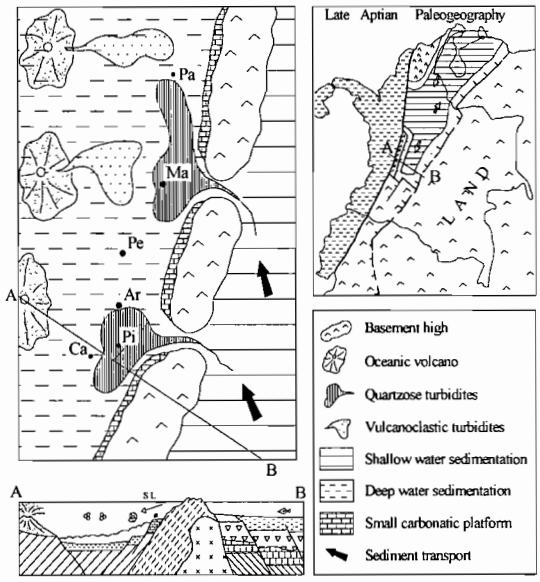

Fig. 4. Proposed geological setting during the depositation of late Aptian - early Albian sedimentites present in the studied area. Pa: Pácora; Ma: Manizales; Pe: Pereira; Ar: Armenia; Pi: Pijao; Ca: Caicedonia.

Anyhow, the proposed tectonic scenario during the accumulation of the Aptian-Albian sedimentites is sketched in Fig. 4. It shows an open-sea basinal area prone to the accumulation of alternating strata in form of: a) turbidites derived from eastern located cratonic and eroded orogen sources, separated from the basinal area by a partially emerged basement high (or "arc"); b) "indigenous" hemipelagic decantation products; c) sub-aquatic and sub-aerial tuffs and diabasic flows originated in oceanic volcanic-chains located "far" west in a Paleo-Pacific ocean.

The basement underlying the Aptian-Albian sedimentites is hitherto unknown; however, it could partly correspond with the Arquía Complex, which may represent a metamorphic oceanic crust accreted to the continental margin of the Northern Andes prior to the accumulation of the aforementioned Aptian-Albian sediments.

REFERENCES

Alvarez J. 1995. Geología del Complejo Ofiolítico de Pácora y secuencias relacionadas de Arcos de Islas (Complejo Quebradagrande), Colombia. INGEOMINAS. Bol. Geológico, 35(1): 3-38. Bogotá.

Botero G. 1963. Contribución al conocimiento de la geología parte central de Antioquia. An. Fac. Min. 57: 1-101.

González H. & Núñez, A. 1991. Mapa geológico generalizado del Departamento del Quindío (Escala 1:100.000), Geología y Recursos Minerales. INGEOMINAS. Mem. Explic. 42 p.

Grösser, J. 1989. Geotectonic Evolution of the Western Cordillera of Colombia new aspects from geochemical data on volcanic rocks. Jour. South. Am. Earth Sc. 2(4): 359-396.

Maya, M. & González, H., 1995: Unidades Litodémicas en la Cordillera Central de Colombia. INGEOMINAS Boletín Geológico, 35 (2-3), p. 43-57.

McCourt, W. J. & Feininger, T. 1984: High-pressure metamorphic rocks in the Central Cordillera of Colombia. Rep. Br. Geol. Surv., No. 84 (1), p. 28-35.

McCourt W., Mosquera D., Nivia A. & Núñez, A. 1984. Mapa Geológico Preliminar. Plancha 243 – Armenia. Escala 1:100.000. INGEOMINAS.

Mojica J., Arévalo O. J., Blanco M., Malagón F., Caicedo H. & Espinosa. A. 2001. Geología del piedemonte occidental de la Cordillera Central entre Salento, y Caicedonia. Quindío-Valle, Colombia. Mem. 8 Congr. Col. Geol.

Nivia, A., Marriner, G. & Kerr, A. 1996. El Complejo Quebradagrande una posible cuenca marginal intracratónica del Cretáceo inferior en la Cordillera Central de Los Andes Colombianos. Mem. 7 Congr. Col. Geol. TII, 108-123.

STRUCTURAL COMPLEXITIES ASSOCIATED WITH LATERAL RAMPS IN THE EASTERN CORDILLERA, CENTRAL ANDES OF ARGENTINA

Ricardo MON (1), César Rubén MONALDI (2) and José SALFITY (3)

(1)Universidad Nacional Tucumán-CONICET, Miguel Lillo 205, 4000 Tucumán, Argentina, (monr@satlink.com)
(2) CONICET, La Rioja 698, 4400 Salta, Argentina, (crmonaldi@arnet.com.ar)
3) Universidad Nacional de Salta-CONICET, Buenos Aires 177, 4400 Salta, Argentina, (salfity@sinectis.com.ar)

KEY WORDS Eastern Cordillera, curved structure, folding interference patterns

INTRODUCTION

The geology of the Eastern Cordillera of north Argentina, a Tertiary fold-and-thrust belt belonging to the Central Andean orogen has been extensively investigated since the beginning of the 20 th century. In spite of that, many geodynamic processes and structural complexities of this mountain range are still poorly understood. That is the case of the curved structures located at its eastern front between 25° and 26° S lat. (Fig. 1), where the emergent thrust sheets are predominantly vergent to the foreland. The most conspicous curved thrusts coincides with the salient recognized as the Creston arc (Fig. 1).

The aim of this paper is to describe why this structure differs from regions along strike to the north and to the south. We document that the structural fabric associated with the Andean orogeny is latter affected by an important N-S compression, which is responsible for regional scale curved structures.

Major oblique strike-slip faults, associated with strongly curved structures were described by Mon (1979) in the external front of the Eastern Cordillera. Among these major strike-slip faults Vergani & Starck (1989) interpreted the so called "Toro lineament and "El Brete lineament" as lateral ramps of thrust-sheet displaced to the east (Vergani y Starck, 1989). The displacement along these oblique lateral ramps generated N-S stress components responsible of hanging wall complex deformation. Accompanying each lateral ramp there are two belts of strong oblique fault and folding: the Cabra Corral area (Fig. 2) and the El Brete area (Fig.3), described below. The strongly curved thrust front located between the two lateral ramps coincides with the Crestón arc (Fig.1). The Neogene evolution of the Cordillera Oriental is controlled by an eastward propagation of the deformation front and the related foreland

The Cabra Corral area

On both margins of the Juramento upper valley and the area of confluence of the Guachipas an Arias rivers there is extensive map-scale evidence of multiple deformation events. Continuous Cretaceous limestone units (Yacoraite Formation) in the middle of the cover sequence form resistant ridges and dip slopes, which allow the fold geometries to be accurately defined (Fig.2). The two orthogonal fold sets are mainly open to gentle, with

steep axial surfaces and plunging axes, showing dome and basin interference pattern (Type I of Ramsay, 1962). Fold dimensions are variable, amplitudes and wave-lengths ranging between 1 km and 6 km. The N-S striking folds originated during Pliocene Andean Orogeny were subsequently or simultaneously folded by E-W oriented folds. The folds of both sets are asymmetrical, the steep limbs of the north striking folds are facing to the west and the steeply dipping limbs of the E-W directed folds are to the north. Establishing the timing of the development of macroscopic folds in bedding in terrains that have undergone a complex deformation history is potentially difficult. Timing the development of macroscopic folds is further complicated. Both folding events could be practically simultaneous. The upper Juramento valley (Fig. 2) is located in a pronounced structural depression between the north plunging Creston anticline and the southward plunging Mojotoro anticline. Both are major strongly curved basement involved folds with the concave side to the west. Westward of the major anticlines the sedimentary cover and the upper basement levels are supposed to be detached of its substratum and folded according the complex pattern described above. After the deep cross–section based on seismic reflection lines published by Vergani & Strack (1989), the detachment surface coincides with the contact cover – basement.

El Brete area

Two curved thrusts, Rearte Fault and El Brete Fault, convex to the south-east, are supposed to be related to the south lateral ramp of the regional salient of the El Crestón arc (Vergani y Starck, 1989). Both thrusts transported southward thick red beds Cretaceous sequences (Pirgua Subgroup) over Tertiary beds and they are marking an abrupt thickness variation in the Cretaceous strata which are much thinner to the south. These thrusts are associated with an oblique fold in the Tertiary beds (Abascal & Mon, 1998).

DISCUSSION AND CONCLUSIONS

The lateral ramps delimiting the thrust sheet coinciding with the Creston arc salient are strike-slip faults emplaced in the abrupt transitions between thick strata forming the salient and the thin strata outside of it. This situation was recognized by Vergani & Starck (1989) in the northern ramp represented by the El Castillejo fault and in the southern ramp, located in El Brete area, by Abascal & Mon (1998). The basin boundaries evolved into a transfer fault zones according the model proposed by Macedo & Marshak (1999). These authors recognized that the shape of the salients and its locations is strong controlled by the predeformational basin-floor shape and they have noted a spatial association of salients with particularly thick sedimentary basins in the foreland.

The displacement of the northern lateral ramp is sinistral an in the southern ramp dextral. The thrust front, convex to the east represents the Crestón arc. This salient is supposed to be controlled by the predeformational sedimentary thickness of the Metán depocenter (Salfity, 1982; Mon 2001). The salient of the El Crestón arc, according the models of Macedo & Marshak (1999), is a basin-controlled curve but also fault-controlled in response to the interaction of the orogen with strike-slip faults cutting across the thrust front. The asymmetry of the El Crestón salient reflects the basin asymmetry of the Metán depocenter whose northern border is much steeper than the southern one (Salfity, 1982).

Because the lateral ramps of El Crestón thrust sheet are cutting obliquely across the thrust front and they are converging towards the foreland, the eastward displacement of the wedge generated N-S stress components responsible of further deformations and structural complexities. The folding interference pattern of Cabra Corral

area and other curved structures described by Mon (2001) within the Crestón thrust sheet are supposed to be the result of these N-S stress components. According Vergani & Starck (1989) the interference folding pattern of Cabra Corral could be related to the movements along second order lateral ramps.

The southern end of the Eastern Cordillera of Argentina shows a particular structure reflecting pronounced along strike variations related to predeformational sedimentary thickness of the Cretaceous basin. The oblique Cretaceous structures controlled the location of the Andean lateral ramps and the movements along them generated N-S stress components responsible of pronounced curved structures.and a complex fold pattern in the upper valley of Juramento River

REFERENCES

Abascal, L. y Mon, R., 1998. Estructura del extremo sur del rift cretácico Salta, noroeste de Argentina. XIII Congreso Geológico Boliviano, 1: 39-44. Potosí.

Macedo, J. Y Marshak, S., 1999. Controls on the geometry of fold-thrust belt salients. Geological Society of America Bulletin, 111 (12): 1808-1822.

Mon, R. 1979: Esquema estructural del Noroeste Argentino. Revista de la Asociación. Geológica Argentina. 35: 53-60.

Mon, R. 2001. Estructuras curvadas y levantamientos verticales en la Cordillera Oriental (provincias (provincias de Salta y Tucumán). Revista Asociación Geológica Argentina, 56: 367-376.

Ramsay, J.G. 1962. Interference patterns produced by superposition of folds of "similar" type. Journal of Geology 60: 466-481.

Salfity, J.A., 1982. Evolución paleogeográfica del Grupo Salta (Cretácico-Eogénico), Argentina. Actas Quinto Congreso Latinoamericano de Geología, Argentina, 1: 11-26. Buenos Aires.

Vergani, G. y Starck, D., 1989. Aspectos estructurales del valle de Lerma, al sur de la ciudad de Salta. Boletín de Informaciones Petroleras, diciembre: 4-9.

STRUCTURAL STYLE AND TIMING OF DEFORMATION IN THE PIEDRAS-GIRARDOT FOLD BELT, COLOMBIA: EARLY TRANSPRESSIONAL DEFORMATION IN THE NORTHERN ANDES

Camilo MONTES

Corporación Geológica ARES, camilom@mac.com

KEYWORDS: Strain, Syntectonic sedimentation, Transpression, Andes, Cordillera Oriental, Three dimensions.

INTRODUCTION

Reconstruction of deformed strata in two and three dimensions is a kinematic exercise commonly constrained by surface geology and/or subsurface seismic reflectors. Additional constraints derived from detailed geologic mapping such as strain markers, kinematic indicators, and timing of deformation, greatly improve the quality of these reconstructions. This short paper summarizes data (Montes, 2001) regarding the strain state and timing of deformation of the Piedras-Girardot foldbelt (Fig. 1). Two manifestations of deformation in the Piedras-Girardot foldbelt are briefly discussed in this paper: first, the stratigraphic signature of deformation is analyzed to establish the timing, and approximate locus of deformation along mapped faults or folds. Second, the structural signature of deformation is analyzed to approximately define the orientation of finite strain axes, and the magnitude of strain recorded by mesoscopic fabric elements. Together, these stratigraphic and structural criteria were used to propose a history of deformation and sedimentation that was geometrically and kinematically tested using two- and three-dimensional models (Montes et al., in press).

The Piedras-Girardot foldbelt

This foldbelt is located in the only segment of the northern Andes where the Cordilleras Central and Oriental overlap, thus opening a unique window into an area key to understanding the interaction between the Caribbean, South American, and Nazca plates (Fig. 1). This anomalous geomorphic province exposes critical relationships between the Cordilleras Oriental and Central covered elsewhere by Neogene deposits. Two very distinctive stratigraphic packages are exposed in the Piedras-Girardot foldbelt: a Late Cretaceous marine carbonate and siliciclastic sequence, and a Tertiary nonmarine, coarse grained, and mostly red siliciclastic sequence. These sequences rest on a volcanoclastic, and plutonic basement of Triassic-Jurassic age.

Syntectonic sedimentation, Late Cretaceous

Stratigraphic pinchouts occur in two sandstone units of Campanian age: the sandy member of the Nivel de Lutitas y Arenas, and the sandy member of the Nivel Intermedio. Pinchouts on two sandstone units of Campanian age were interpreted to record mild uplift during the early Campanian along the northern, northeast-trending segments of two of the major faults of the Piedras-Girardot foldbelt, and along the easternmost (also northeast-trending) structure of

this foldbelt. These coarse-grained marine clastic units represent gentle deformation within the Piedras-Girardot foldbelt during the early and late Campanian (~84 and ~ 74 Ma). Although uplift took place, no major unconformities were developed at this time, as overlying units rest apparently in conformity with syntectonic units below. Since bedding geometry remained mostly parallel, it is unlikely that the faults propagated to the surface at this time.

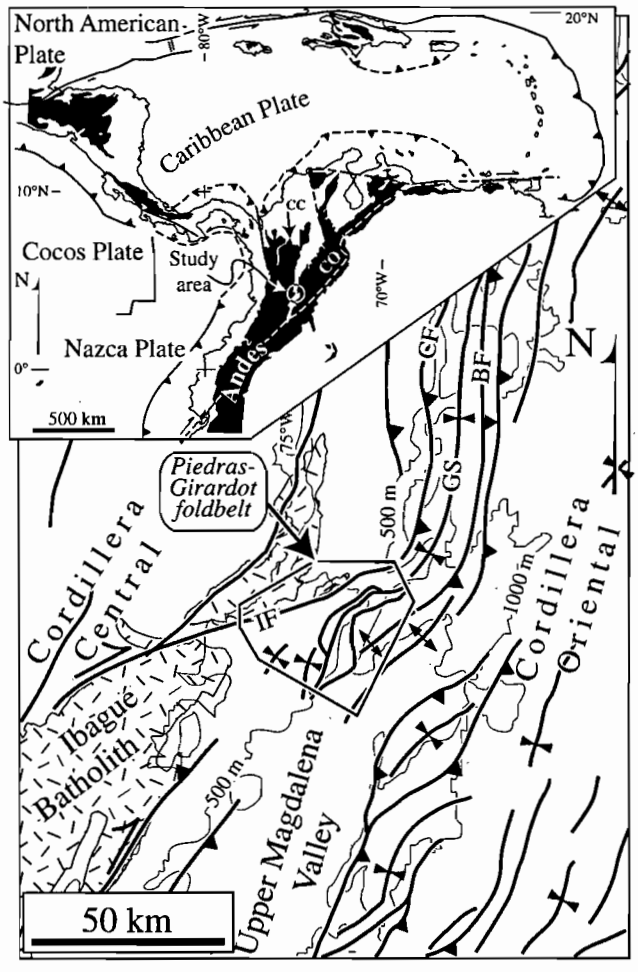

Figure 1: Tectonic map of the Caribbean and part of the northern Andes modified after Schamel, (1991). CC: Cordillera Central; CO: Cordillera Oriental; BF: Bituima fault; CF: Cambao fault; GS: Guaduas syncline; HF: Honda fault; IF: Ibagué fault.

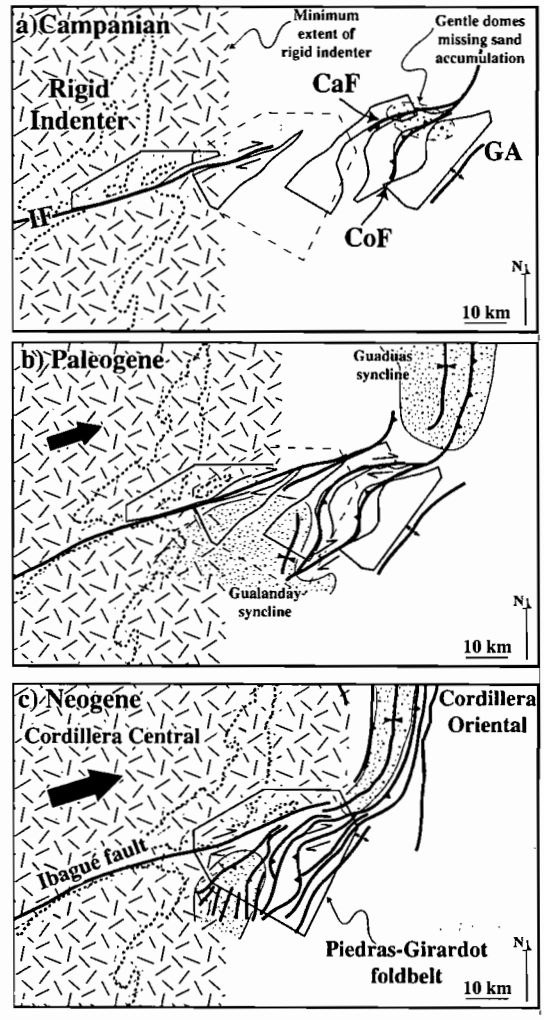

Figure 2: Reconstruction of the ENE translation (~30km) of the rigid indenter of the Cordillera Central along the Ibagué fault (IF). Outline of the study area kept fixed as reference. a) Initial deformation. CaF: Camaito fault, CoF: Cotomal fault; GA: Guaco anticline. b) Continued deformation c) Present configuration.

Syntectonic sedimentation, Paleogene

The Paleocene Guaduas Formation exhibits remarkable thickness changes within the Gualanday syncline that define a fold axial trace morphology that splits in two, with the axial trace delineating a roughly triangular zone that widens downward. The apex of this triangular zone is at the base of the Gualanday Group, marking the end of growth strata. This reveals a time of syntectonic sedimentation, fold growth and propagation (Paleocene Guaduas Formation),

followed by a time of conglomerate accumulation and folding (Gualanday Group). Thickening of the growth strata to the east, the location of the hanging wall cutoff east of the axis of the Gualanday syncline, and preservation of the eastern, but not of the western growth axial traces, indicate that the Cambao thrust sheet was moving westward to southwestward when growth strata accumulated.

Paleogeographic interpretation

Stratigraphic criteria summarized above was interpreted to indicate that the northernmost, northeast-trending segments of the Camaito and Cotomal faults, and the El Guaco anticline started growing during early to late Campanian times (Fig. 2a). These gentle structures were later overlapped by the Maastrichtian conglomerate of the La Tabla Formation, that records unroofing to the west (Cordillera Central). The early Paleogene (Fig. 2b) marks a time of segmentation of accumulation environments due to the west- or southwestward propagation of the Cambao fault (and probably other faults in this foldbelt), and generation of accommodation space in the Guaduas and Gualanday synclines. The Piedras-Girardot foldbelt has been a positive area since then, shedding clastic material into these late Paleogene depocenters, that were being concurrently folded. Only the northern part of the study area contains evidence for post-Miocene (Fig 2c.), and Quaternary deformation, which is at least partially related to the latest movements along the Ibagué fault.

Microscopic and mesoscopic strain

Three fabric elements were investigated: 1) cleavage 2) deformed fossils; and 3) microscopic and mesoscopic veins. Each element provides a partials, and sometimes local story. Together, these elements are used to get a general picture of the contribution of early, nonrigid body deformation in the Piedras-Girardot foldbelt.

Cleavage

Cleavage is a pervasive, uniform, and prominent outcrop-scale element that trends ENE. Microscopically, cleavage surfaces show a sutured morphology where thin films (approximately 0.1 mm) of insoluble material are concentrated. The amount of shortening accommodated by a rock with a 2 cm domain spacing is less than 5 percent. Unfolding the attitude of cleavage surfaces results in an unimodal distribution of poles to cleavage that is still 14 degrees away from vertical. Thus, some gentle folding had already taken place by the time cleavage started to develop (mild folding during late Campanian times). Upper Cretaceous rocks crossed by cleavage, however, constrain cleavage formation to before Paleogene times. After latest Cretaceous times, these early fabrics of deformation were passively rotated by younger structures.

Deformed fossils

Deformed external molds of ammonite shells preserved in black shale of the lower part of the Villeta Group were used as strain markers. The axial ratio ranges between 1.0 and 2.3, with an average of 1.5. After rotation of axial orientations to remove the tilt of bedding, an ENE preferred orientation of the long axes of the ellipses is obtained, which are generally parallel to the trend of cleavage. Axial orientations for the molds indicate E-W and SE-NW shortening directions. Magnitude of axial ratios is related to distance to faults. High ellipticity values are high less than 400 m from a fault, whereas low values to undeformed molds are found more than 1000 m from a fault. These

observations indicate that greater strain occurs closer to faults, and therefore is not a strain pervasive to the entire stratigraphic column.

Shattered pebbles and veins

The conglomeratic unit atop of the Cretaceous sequence of the Piedras-Girardot foldbelt shows a conspicuous deformation fabric of intragranular calcite-filled microscopic veins perpendicular to bedding. The total area change accommodated by intraclastic veins with average intensity is only between 1 and 2 percent. The trends of these microscopic veins is mostly to the northwest, defining a direction of the maximum finite stretch of the finite strain ellipse to the northeast. Such stretch is approximately perpendicular to the direction of minimum finite stretch independently deduced from cleavage and deformed fossils.

CONCLUSIONS

The results above outlined, combined with a palinspastic reconstruction of the Piedras-Girardot foldbelt (Fig. 2) indicate that Late Cretaceous initiation of transpressional deformation in this part of the northern Andes involved small amounts of northwest-southeast contraction along the northeast-trending segments of faults. Although these early faults did not breach the surface, they were probably rooted along a basal detachment along the lower part of the Villeta Group where deformed fossils record high strain values. Continued deformation throughout Late Cretaceous times generated a conspicuous deformation fabric that accommodated small amounts (less than 5%) of internal deformation. Therefore, internal deformation can be ignored when performing two- and three-dimensional modeling of this foldbelt (Montes et al., in press). Large scale Paleogene ENE transpressional deformation, although spectacularly recorded by thick, folded molasse deposits and map-scale faults, is missing a mesoscopic deformation fabric, probably due to strain hardening. Fabric elements associated with Late Cretaceous deformation were passively rotated and translated along thrust sheets developed at this time. Neogene deformation took place only in the western flank of this foldbelt. These results are applicable in a regional scale to the Magdalena Valley, since similar deformation timing has been observed further south (Amézquita & Montes, 1994). This structural style had not been previously identified or quantified in the northern Andes, and is probably related to the onset of oblique interaction between the northern Andes and the deformation front of the Caribbean plate (greater Antilles arc). Continued oblique convergence throughout the Paleogene records the eastwrd relative motion of the Caribbean plate with respect to the northern Andes.

REFERENCES

Amézquita F., and Montes, C., 1994, Sección geológica el Maco-Buenavista: estructura en el sector occidental del valle superior del Magdalena, in Etayo-Serna, ed., Estudios Geológicos del Valle Superior del Magdalena, Ecopetrol, VI-1, VI-36.

Montes, C., 2001, Three dimensional structure and kinematics of the Piedras-Girardot foldbelt in the northern Andes of Colombia, Ph.D. Dissertation, University of Tennessee, Knoxville, 217 p.

Montes, C., Restrepo-Pace, P. A., and Hatcher, R. D., Jr., in press, Three-dimensional structure and kinematics of the Piedras-Girardot foldbelt: surface expression of transpressional deformation in the northern Andes, in Blickwede, J., ed., The circum-Gulf of Mexico and Caribbean region: Plate tectonics, basin formation and hydrocarbon habitats, AAPG Memoir.

Schamel, S., 1991, Middle and upper Magdalena basins, Colombia, in Biddle, K. T., ed., Active margin basins: AAPG Memoir: Tulsa, OK, United States, American Association of Petroleum Geologists, p. 283-301.

EVOLUTION OF THE PICHINCHA VOLCANIC COMPLEX (ECUADOR)

Michel MONZIER (1), Pablo SAMANIEGO (2), Claude ROBIN (1), Bernardo BEATE (2), Joseph COTTEN (3), Minard L. HALL (2), Patricia MOTHES (2), Daniel ANDRADE (2), Erwan BOURDON (4), Jean-Philippe EISSEN (5), Jean-Luc LE PENNEC (5), Andres Gorki RUIZ (2), Theofilos TOULKERIDIS (6)

(1) Institut de Recherche pour le Développement (IRD), UR 031, OPGC / Université Blaise Pascal, 5 rue Kessler, 63038 Clermont-Ferrand, France (M.Monzier@opgc.univ-bpclermont.fr, C.Robin@opgc.univ-bpclermont.fr)
(2) Departamento de Geofisica, Escuela Politecnica Nacional, A. P. 17-01-2759, Quito, Ecuador (geofisico@accessinter.net)
(3) Université de Bretagne Occidentale, UMR 6538- IUEM- Site UFR Sciences, 6 Avenue Le Gorgeu BP 809 29285 Brest Cedex (Jo.Cotten@univ-brest.fr)
(4) Institut de Recherche pour le Développement (IRD), UR 031, 81 Route de Kerfily, 29280 Loc-Maria Plouzane (Erwanbourdon@aol.com)
(5) Institut de Recherche pour le Développement (IRD), UR 031, A. P. 17-12-857, Quito, Ecuador (Jean.Philippe.Eissen@ird.fr, Jean-Luc.Le-Pennec@ird.fr)
(6) Universidad San Francisco de Quito, Campus Cumbayá, A. P. 17-12-841, Quito, Ecuador (theofilost@mail.usfq.edu.ec)

KEY WORLDS: Ecuador, Pichincha, volcanism, chronology, adakite, natural hazards

Since the renewal of eruptive activity at Pichincha in 1999, Quito has been once again threatened by this volcano, whose active vent is only 11 km west of the city. Because the vent is located within a deep caldera largely open to the West, and as ruins of the oldest edifice form a natural barrier between the vent and the city, only ash fall and secondary mud flows represent a serious hazard for Quito. Works by MAE-INEMIN (Barberi et al., 1989; 1992) provided a first interpretation of the Pichincha Volcanic complex (PVC) history. Nevertheless, in order to assess the present-day eruption and its possible evolution, a new appraisal of the evolution of this volcano has been carried out by the Department of Geophysics (EPN) and the French Institute for Development (IRD), including new field observations, new 14C datings and a detailed petro-geochemistry. Preliminary results of this work are presented here.

The PVC consists of five successive volcanoes, whose duration and volume seem to decrease exponentially. The volcanic complex built over the La Esperanza lava pile which would be Pliocene in age (MAE-INEMIN, 1989). A geological sketchmap (Fig. 1) and a SiO_2-Rb diagram (Fig. 2) illustrate such a five-step development.

I- The El Cinto basal edifice. The arcuate ridge that forms a barrier between the Rio Cinto Valley and Quito may represent the remnants of a basal edifice largely dissected by erosion and faulting, as shown by the steep flanks looking toward the Rio Cinto Valley. Barberi et al. (1988) reported two K / Ar ages: 1.17 ± 0.10 for a lava flow from the ridge, and 0.81 ± 0.05 Ma for a sample from the Ungui dome (Fig. 1). El Cinto volcanics are low-Rb acid andesites.

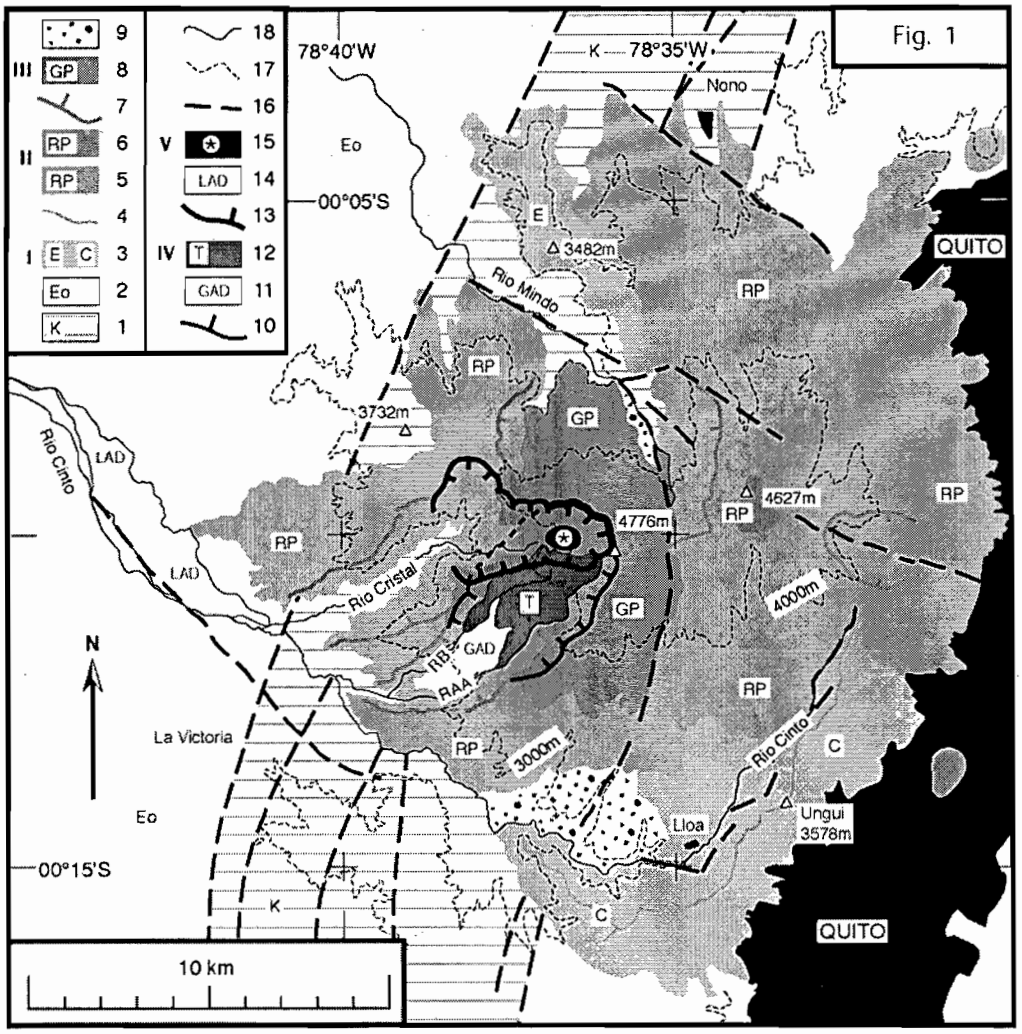

1 = Cretaceous formations ; 2 = Silante Unit (Upper Eocene - Oligocene) ; 3 = La Esperanza lava pile (E) and El Cinto volcano (C) ; 4 = El Cinto crest ; 5 = Rucu Pichincha volcano ; 6 = Rucu Pichincha summital breccias ; 7 = Rucu Pichincha avalanche calderas ; 8 = Guagua Pichincha volcano ; 9 = Guagua Pichincha: Lloa and Rio Mindo "block and ash" fans ; 10 = Guagua Pichincha avalanche caldera ; 11 = Guagua Pichincha avalanche deposit ; 12 = Toaza volcano ; 13 = Toaza avalanche caldera ; 14 = Last avalanche deposit ; 15 = Cristal active volcano ; 16 = fault ; 17 = 3,000 and 4,000 m asl curves ; 18 = main rivers ; Roman numbers refer to the 5th succesive edifices.

II- Rucu Pichincha is a large (23 km-wide), mainly effusive stratovolcano, relatively well preserved from erosion. Two K / Ar ages measured on upper lavas of this edifice (1.32 ± 0.13 and 0.9 ± 0.2 Ma; Barberi et al., 1988), are similar to the age obtained on El Cinto ridge. Ar-Ar datings in progress will attempt to solve this contradiction and define the relationship between El Cinto and Rucu Pichincha edifices. Several flank avalanches affected Rucu Pichincha and the largest, toward the North, probably marked the end of its development. Most products of Rucu Pichincha are medium-Rb acid andesites, but the late subglacial breccias that form the peaks show a clear reversal toward low-Rb compositions.

III- Guagua Pichincha volcano is a 10 km-wide, lava-dominated stratocone, built on the western flank of Rucu Pichincha volcano that collapsed along an arcuate system of normal faults. The beginning of its growth is not yet constrained. We only known that 47,500 y BP ago, (C14 dating), this edifice experienced a major pyroclastic eruption producing dacitic ashflows and probably the formation of a caldera in the summit area. After this event, a complex of domes grew within the caldera and dome activity predominated. Thick block and ash deposits observed near Lloa indicate large dome collapses during two main episodes, the first one dated at 30,320 y BP (C14 on a burried soil), the second one slightly younger (≈ 27,500 y BP ?). Near 23,000 y BP, the

southwestern flank of Guagua Pichincha collapsed. This event, followed by the emission of large volumes of ash and pumice, marked the end of Guagua Pichincha history. Products of Guagua Pichincha volcano are high-Rb acid andesites to dacites.

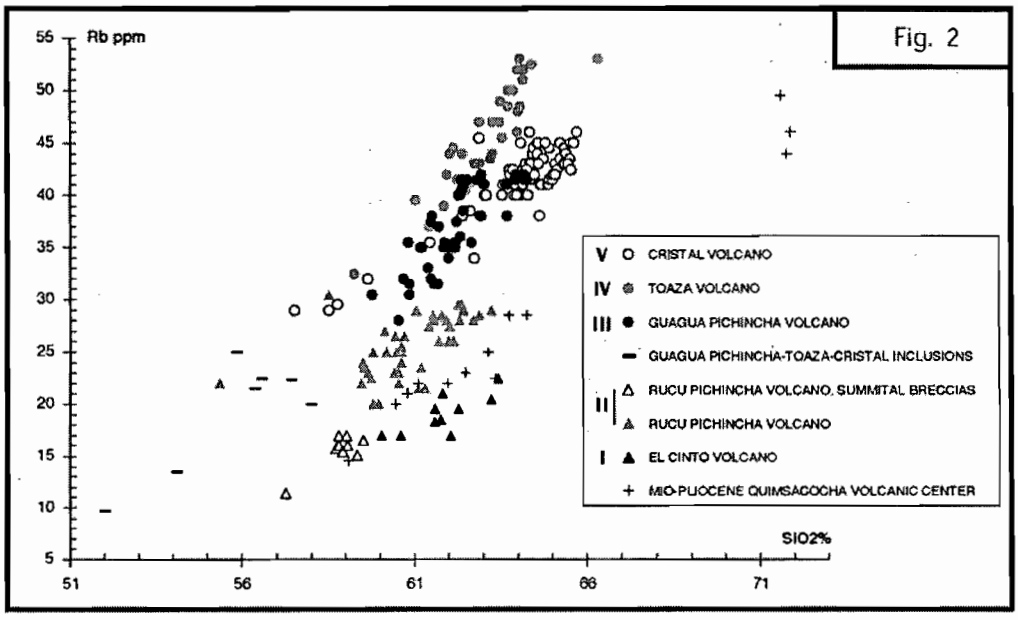

IV- Toaza volcano is a 5 km-wide, dome complex built approximatly from 20,000 to 10, 000 y BP within the avalanche amphitheater of Guagua Pichincha. Block and ash deposits related to this dome complex are recognizable along rivers downstream, but the most striking deposits for this period are those of the late, multistage collapse towards the Rio Cristal valley that affected, 1- part of the western flanks of Rucu and Guagua Pichincha edifices, and 2- the whole summital area of Toaza. The alteration and fracturing of the Cretaceous oceanic basement certainly played a major role in the chronic instability of this western area during the whole evolution of the PVC. This complex avalanche event has been followed by intense pyroclastic activity (numerous ashflows and fallout deposits) well constrained in age from 10,800 to 9,900 y BP (6 new C14 datings). Toaza andesites and dacites have very high Rb contents, a characteristic that distinguishes these deposits from all other PVC products.

V- The presently active Cristal volcano is a small, 1 km-wide, dome complex nested in the Toaza caldera. Deposits from this volcano have been investigated in detail, especially those produced since 2,000 years ago. Five explosive events occurred during this time. The first event, about 2000 y BP, produced a Plinian column accompanied by surges which swept the highest slopes of the mountain. A basal ash layer (surges) topped by a pumice fall deposit are the typical products left by this event. The second and much more powerfull Plinian event, occurred at about 1200 y BP. For about 100 years there followed persistent dome activity which resulted in thick block and ash deposits in the Rio Cristal valley. During historic times, explosive activity resumed in 1566-1582 and 1660 with dense ashfalls over Quito and pyroclastic flows sweeping the Rio Cristal - Rio Cinto valleys (Wolf, 1905; Estupiñan Viteri, 1998). From 1660 to 1980, Cristal volcano was quiet, with fumarolic activity and small outburst of phreatic activity (J. Egred, pers. comm.). Between 1981 and 1998, phreatomagmatism increased, leading to a new magmatic event in september 1999. From this date to March 2001, the activity consisted in the slow growth of small domes alternating with partial dome collapse, releasing minor block and ash pyroclastic flows and derived lahars in the valleys of Rio Cristal and Rio Cinto. Minor ash and pumice emissions also occurred several times, and sometimes slight ashfall affected Quito. Since March

2001, magmatic activity vanished, and seismic activity progressively returned to its pre-eruptive level. Cristal dacites have high Rb contents and, given to their high-silica contents, form a distinct population on the SiO_2-Rb diagram.

As a whole, the volcanic evolution of the PVC is closely accompanied by a remarkable magmatic evolution (Fig. 2). According to Bourdon (1999) and Bourdon et al. (2002), Guagua Pichincha-Cristal products correspond to slab melts, partially modified during their uprise trough a narrow mantle wedge. Interestingly, on the SiO_2-Rb diagram, the Cristal dacites point at rhyolites from the Quimsacocha volcanic center (QVC), a 4,5 km-wide caldera in southern Ecuador that produced true adakites (Beate et al., 2001). Detailed studies (microprobe analyses, laser ablation ICP-MS) are in progress to assess the respective role and variable participation of slab melting, mantle participation, and crustal processes to the magmatic evolution of the PVC.

As the development of PVC is marked by successive decreasing volumes of magmas, the end of the volcanism in this area is probable, maybe related with an ongoing horizontalization of the slab. However, as the adakitic, volatile-rich character of the products becomes more marked with time, highly explosive climax, similar to that of the QVC, is possible. Thus, monitoring should include a close inspection of future magmatic products (and gaz) and the search for a possible shallow magmatic reservoir.

REFERENCES

Barberi, F., Bernardi, A., Figuera, J., Ghigliotti, M. & Rosi, M., 1989. Mapa geologico 1:50,000 del volcan Guagua Pichincha, Instituto Geografico Militar, Quito, Ecuador.

Barberi, F., Coltelli, M., Ferrara, G., Innocenti, F., Navarro, J. M. & Santacroce, R., 1988. Plio-Quaternary volcanism in Ecuador. Geol. Mag. 125 (1): 1-14.

Barberi, F., Ghigliotti, M., Macedonio, G., Orellana, H., Pareschi, M. T. & Rosi, M., 1992. Volcanic hazard assessment of Guagua Pichincha (Ecuador) based on past behaviour and numerical models. J. Volc. Geotherm. Res., 49: 53-68.

Beate, B., Monzier, M., Spikings, R., Cotten, J., Silva, J., Bourdon, E. & Eissen, J.-P., 2001. Mio-Pliocene adakite generation related to flat subduction in southern Ecuador: the Quimsacocha volcanic center. EPSL 192: 561-570.

Bourdon, E., 1999. Conséquences pétrogénétiques de la subduction d'une ride asismique: l'exemple du volcanisme de la marge équatorienne. Thèse de Doctorat, Université de Bretagne Occidentale, Brest, 190 p.

Bourdon, E., Eissen, J.-P., Gutscher, M. A., Monzier, M., Samaniego, P., Robin, C., Bollinguer and Cotten, J., (2002). Adakites and high-Mg andesites at Pichincha volcano (Ecuador): evidence for melting oceanic crust beneath the Northern Volcanic zone of the Andes. Bull. Soc. Géol. Fr, in press

Estupiñan Viteri, T., 1998. Volcan Pichincha. Erupciones, destrucciones e invenciones. Ediciones del Banco Central del Ecuador, Quito, 248 p.

Hughes, R, Bermúdez, R. & Espinel, G., 1998. Mapa geologico de la Cordillera Occidental del Ecuador entre 0° - 1° S. Escala 1 : 200.000. PRODEMINCA - MEM/CODIGEM-BGS. Quito, Ecuador

MAE-INEMIN, 1989. Mitigacion del riesgo volcanico en el area metropolitana de Quito, informe final. Geotermica Italiana, Pisa.

Wolf, T., 1905. Cronica de los fenomenos volcanicos y terremotos en el Ecuador, con algunas noticias sobre otros paises de America central y meridional desde 1533 hasta 1797, Imprenta Universidad Central, Quito, pp. 31-35, 44-51.

EARLY PLIOCENE MAGMATISM AND HIGH EXHUMATION RATES IN THE PATAGONIAN CORDILLERA (46°40'S): K-Ar, AND FISSION TRACK DATA.

Diego MORATA (1), Luis BARBERO (2), Manuel SUAREZ (3) and Rita DE LA CRUZ (3)

(1) Departamento de Geología, Universidad de Chile. Chile, (dmorata@cec.uchile.cl)
(2) Departamento de Geología, Universidad de Cádiz, Spain, (luis.barbero@uca.es)
(3) Servicio Nacional de Geología y Minería, Chile, (msuarez@sernageomin.cl)

KEY WORDS: Window slab, granites, rapid exhumation, Patagonian Cordillera.

INTRODUCTION

The subduction of an active ridge produces specific characteristics in the associated magmatism, tectonism and sedimentation. Apart from the generation from the mantle wedge of typical calc-alkaline acidic magmas associated to subduction, magmatic rock genesis in this context must also be controlled by the presence of the so-called asthenospheric window slab. Another mechanism that produces magmas with particular geochemical features is the partial melting of young altered subducted oceanic crust which, due to its relatively low density, is detached to upper levels. These magmas are represented by adakitic rock types (mostly volcanic and few plutonic rocks) actually restricted to the circum-Pacific margin (Martin, 1999).

In Southern Chile, the subduction of the Chile spreading-ridge is actually active at the latitude of the Taitao Peninsula, in the Chile triple junction (≈ 46°S). The Cabo Raper pluton, a 3-4.2 Ma old biotite- and hornblende bearing granodiorite, is part of this Peninsula, and is interpreted as one of the few adakitic plutons reported in the world (Bourgois et al., 1996, Martin, 1999). In this work we present the geochemistry and thermochronological history of a coeval plutonic body (Río de las Nieves pluton) located at the same latitude 250 km to the east of the present Chile triple junction, near the orogenic front of the Patagonian Cordillera and above the presumed position of the window slab at the time of the granitic generation according to the reconstruction of Gorring et al., (1997). A comparison with other Mio-Pliocene plutons of the North Patagonian Batholith (NPB) is presented.

GEOLOGICAL FRAMEWORK

The Mio-Pliocene tectonic evolution of the Patagonian Andes in southern Chile is mainly controlled by the northeast -trending subduction of the active mid-ocean spreading Chile-Ridge beneath the South American margin (Cande and Leslie, 1986) and the oblique convergence of the Nazca Plate. As a consequence, the long-lived intra-arc dextral strike-slip Liquiñe-Ofqui fault zone was originated (Cembrano et al., 1996), which according to Pankhurst et al., (1999) and Parada et al. (2000) favoured the emplacement and high exhumation rates of the closely related Miocene plutons (e.g., the Paso de las Llaves pluton and the Queulat complex).

The Río de las Nieves pluton (≈46°40'S), a small meta-aluminous biotite quartz-monzonite is located 14 km to the south of the Lago General Carrera. It composition is characterized by SiO_2 contents ≈ 64%, Al_2O_3 = 16%, (FeOt + MgO + MnO) = 6.4, K_2O/Na_2O = 0.88 and moderately high *[mg]* (0.55). On a K-Na-Ca plot, the composition of this pluton fit the typical calc-alkaline trend. Trace elements are characterized by low Ni and Cr contents (5 ppm), Sr = 400 ppm, Sr/Y =15.4, negative Sr anomaly in primitive mantle-normalized multi-element diagram and $(La/Yb)_N$ = 9.6 with Yb_N values (≈13.5) similar to those of the calc-alkaline arc magmas (e.g. Martin, 1999).

GEOCHRONOLOGY

A biotite separate from this pluton was dated by the K/Ar method (Table 1) at the SERNAGEOMIN (Chile) Laboratory (K_2O = 7.699%; Ar rad (nl/g) = 0.960; %Ar atm = 84) obtaining an age of 3.2 ± 0.4 (2σ error), interpreted as a minimum age due to the slightly chloritization observed.

Fission track dating in apatite from the same sample of the Río de las Nieves pluton were carried out in the Universidad de Cádiz, Spain. The apatite fission track age data (4.3 ± 0.7, n = 87, Table 1) overlaps the K-Ar age obtained in biotite and coincide with the K-Ar ages obtained in the Cabo Raper pluton (Table 1), located at the same latitude.

Table 1.- Summary of geochronological data of Late Miocene to Early Pliocene plutonic rocks in the Patagonian Cordillera at *c.* 46°40' Lat. S. ZFT = zircon fission track, AFT = apatite fission track.

Location	Analytical Method				
	K-Ar	$^{40}Ar/^{39}Ar$	Rb/Sr	ZFT	AFT
Rio de las Nieves	3.2 ± 0.4[(1)]				4.3 ± 0.7[(1)]
Cabo Raper	3.3 ± 0.3[(2)]				
	4.1 ± 2.4[(2)]				
Paso de las Llaves	10.0 ± 1.1[(3)]	9.6 ± 0.5[(4)]	10.3 ± 0.4[(5)]	9.7 ± 0.4[(6)]	
		9.6 ± 0.4[(4)]			

Source of data: (1) This work; (2) Mpodozis et al (1985); (3) Suárez and De la Cruz (2001); (4) Petford & Turner (1996); (5) Pankhurst et al. (1999); (6) Thomson et al (2001).

The Late Miocene Paso de las Llaves pluton, close to the Río de las Nieves pluton, was interpreted as a satellite body to the east of the NPB (Pankhurst et al., 1999), shows a fast cooling history as interpreted from K/Ar, Ar/Ar, Rb/Sr and ZFT (Table 1). To the north of the studied area, the Queulat complex (44°30'-44°45'), dated by $^{40}Ar/^{39}Ar$ in 15.6 ± 0.2, also evidence rapid exhumation controlled by the Liquiñe-Ofqui fault as shown by the apatite fission track data (3.3 ± 1.4 Ma) (Parada et al., 2000).

DISCUSSION

The similar K-Ar data shown by the Cabo Raper and the Rio de las Nieves plutons could idicate a common origin. Nevertheless, the geochemistry of the Rio de las Nieves pluton, allows to include it into the recent satellite bodies of the NPB, in contrast to the adakitic nature deduced for the Cabo Raper pluton (Bourgois et al., 1996, Martin, 1999). On the other hand, the location of the Rio de las Nieves pluton, within a fold and thrust zone near the orogenic front of the Patagonian Cordillera and tens of kilometres to the east of the Liquiñe-Ofqui fault zone, exclude the possibility of emplacement and fast exhumation controlled by this fault, as in the case assumed for Miocene plutons, including the Paso de las Llaves pluton (Pankhurst et al., 1999) and the northern Queulat Complex (Parada et al., 2000). However, the tectonic setting of the Paso Las Llaves pluton within the same fold and thrust zone of the Paso Las Nieves pluton, around 100 km eastwards of the Liquiñe Ofqui fault, also precludes a direct influence of this fault in its final emplacement.

The hypotheses presented here for the explanation of the emplacement and fast exhumation rate of the Río de las Nieves pluton is related to the position of the windows slab originated as a consequence of the subduction of the Chile Ridge. According to the tectonic setting and distribution of the oceanic fracture zones and Chile Ridge segments of Gorring et al (1997) and Cande and Leslie (1986), the actual location of the Rio de las Nieves pluton is just in the predicted area in which 3 Ma ago the window slab was located. This window slab could generate the necessary thermal anomaly to produce the Rio de las Nieves pluton as well the tectonic context for a fast exhumation rate. To the south, the San Lorenzo granite (6.6 ± 0.5 Ma, Welkner, 1999; Suárez and de la Cruz, 2001), one of the highest summits of the Patagonian Cordillera (3706 m), is also located in the area in which 6 Ma ago the window slab was present. It is notable that the higher altitude of the Patagonian Cordillera (the San Valentin hill, 4058 m) is also located at the same latitude that the Rio de las Nieves pluton. All these facts could also be consequence of the fast exhumation generated by the subduction of the Chile Ridge and generation of the window-slab.

ACKNOWLEDGEMENTS

This work was funded by the FONDECYT Projects 1000125 and 7000125. Leonardo Zuñiga field work is acknowledged.

REFERENCES

Bourgois. J.; Martin, H.; Lagabrielle, Y.; Le Moigne, J. and Frutos Jara, J. 1996. Subduction-erosion related to the ridge-trench collision: Taitao Peninsula (Chile margin triple junction area). Geology, 24, 723-726.

Cande, S.C. and Leslie, R.B. 1986. Late Cenozoic tectonics of the southern Chile trench. Journal of Geophysical Research, 91, 471-496.

Cembrano, J.; Hervé, F. and Lavenue, A. 1996. The Liquiñe-Ofqui fault zone: a long lived intra-arc fault system in southern Chile. Tectonophysics, 259, 55-66.

Gorring, M.L.; Kay, S.M.; Zeitler, P.K.; Ramos, V.A.; Rubiolo, D.; Fernández, M.I. and Panza, J.L. 1997. A slab window origin for Neogene Patagonian plateau lavas (46.5° to 49.5°S). Tectonics, 16, 1-17.

Martin, H. 1999. Adakitic magmas: modern analogues of Archean granitoids. Lithos, 46, 411-429.

Mpodozis, C.M.; Hervé, M.; Nasi, C.; Soffia, M.J.; Forsythe, R.D. and Nelson, E.P. 1985. El magmatismo plioceno de Península Tres Montes y su relación con la evolución del punto triple de Chile austral. Revista Geológica de Chile, 25/26, 13-28.

Pankhurst, R.J.; Weaver, S.D.; Hervé, F. and Larrondo, P. 1999. Mesozoic-Cenozoic evolution of the North Patagonian Batholith in Aysén, southern Chile. Journal of the Geological Society, London, 156, 673-694.

Parada, M.A.; Lahsen, A. and Palacios, C. 2000. The Miocene plutonic event of the Patagonian Batholith at 44°30'S: thermocronological and geobarometric evidence for melting of a rapidly exhumed lower crust. Transactions of the Royal Society of Edinburgh: Earth Sciences, 91, 169-179.

Petford, N and Turner, P. 1996. Reconnaissance ^{40}Ar-^{39}Ar age and palaeomagnetic study of igneous rocks around Coyhaique, S. Chile (45'30-47°S). Third ISAG, St Malo (France), 17, 625-628.

Suárez, M. and De la Cruz, R. 2001. Jurassic to Miocene K-Ar dates from eastern central Patagonian Cordillera plutons, Chile (45° - 48°S). Geological Magazine, 138, 56-66.

Thomson, S.N.; Hervé, F. and Stöckhert, B. 2001. Mesozoic-Cenozoic denudation history of the Patagonian Andes (southern Chile) and its correlation to different subduction processes. Tectonics, 20, 693-711.

Welkner, D. 1999. Geología del área del Cerro de San Lorenzo: cordillera patagónica oriental, XI región de Aysén Chile (47°25'-47°50'S). Memoria Título Dep. Geología. Univ. Chile, 150 p.

MAGMATIC BASIC EVENTS DURING THE EARLY CRETACEOUS, IN THE COLOMBIAN EASTERN MOUNTAIN RANGE

Manuel MORENO M. (1), Ana CONCHA P. (1), Pedro PATARROYO G. (1), Angela NAVARRETE S.(1)

(1) Department of Geosciences Universidad Nacional de Colombia (mamoreno@ciencias.unal.edu.co), (aconcha@ciencias.unal.edu.co), (pepatar@ciencias.unal.edu.co), (angelachan_nava@yahoo.com)

KEY WORDS: Gabbros, Magmatic Events, Early Cretaceous, Cordillera Oriental, Colombia.

INTRODUCTION

Some basic intrusive bodies represented by dikes and sills of gabbroid composition have been encountered in the western side of the Colombian Eastern Range or "Cordillera Oriental". These intrusive rocks have been studied in detail and are called, in the Boyaca and Cundinamarca regions Gabbros of Puerto Romero – Caceres. Basic intrusive bodies are also present in the eastern flank of the "Cordillera Oriental", en the region of Casanare are called Rodrigoque and La Salina gabbros, an also near of these area are the Pajarito gabbro. In the central area of the "Cordillera Oriental" are recognized La Corona in Muzo and the gabbro located in Pacho at the hill of Tragarepas. Another new discovery of basic intrusive bodies are present toward the southeastern in the Putumayo Basin, in the area close to the Orito Field (Fig. 1).

GABBROS OF PUERTO ROMERO AND CÁCERES

The presence of the gabbro bodies at Puerto Romero y Caceres, in the western side of the "Cordillera Oriental" are lined up in NNE-SSW directions, and suggests the existence of a subsident basin, during Late Cretaceous. The analyzed rocks were studied petrographically by Vasquez (1999), and there is a very important first geochemical classification, which is fundamental because through these results, it is possible to get a better estimate of a geological history of these bodies. Results of the geochemical analysis of the basic intrusive emerged bodies at the Altamira Creek, on the surroundings of Puerto Romero area, and on the Tragarepas - Pacho bodies, confirm that its origin is associated with a stretched domain of a geotectonic interplate environment. Values obtained from the geochemical analysis, were normalized at 100%, water free. Values of the total Fe, were estimated using this formula $Fe_2O_3 = 1,5 + TiO_2$. These bodies have been dated, using radiometric methods and palentologic data of the host rocks, indicating that the basic intrusive rocks are, coetaneous to the Late Albian, but are not younger than the Cenomanian. Analyzed samples have a basic composition with 50 – 57 % of SiO_2, from the diagram of total Alkali ($Na_2O + K_2O$) vs. SiO_2 and first division between alkaline and sub alkaline rocks was obtained. It shows that all the samples are located in the zone of the sub alkaline series. Thus, the sub alkaline rocks were divided into tholeiitic and calcoalkaline. According with this, the diagram AFM was used and shows that even though the samples fall in the tholeiite, all of them are close to the limit. Also, the samples were drawn in the diagram, Alkaline vs. Al_2O_3, where, the rocks have a clear tholeiitic tendency.

Based on these observations, we can deduce that the analyzed samples belong to the subalkaline series with sodium tendency, due to a low concentration of K, and have tholeiite nature. The diagram K_2O vs. SiO_2 shows the variation between Gabbro and Diorite, whit a very low amount of K_2O indicating that these are very primitive and have had a very few cortical contamination (Fig. 2).

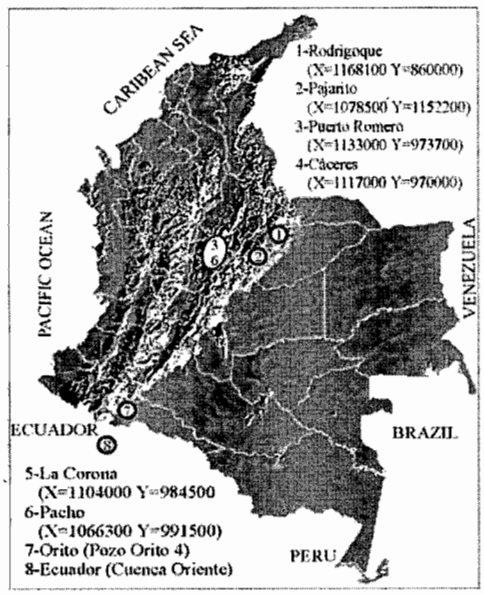

Figure 1- Map of locations of the basic igneous bodies mentioned in this work, reported in Colombia and Ecuador.

To reconfirm this classification the diagram $Na_2O + K_2O$ (total Alkali) vs. SiO_2 of COX (1979), and the TAS of LE BAS method *et al.* (1986), are used on VASQUEZ *et a.l* (2000). When these diagrams are compared, essential differences were not present, therefore, the samples belong to the tholleiitic series, which is poor in K and according whit its composition, that are geochemically classified as gabbros, gabbrodiorite and diorites, VÁSQUEZ *et al.* (2000). In the petrogenetic study, we used the data obtained in the geochemical analysis added to the geotectonic discriminations diagrams, so explaining the geotectonic environment model for these basic rocks of the Caceres and Puerto Romero regions.

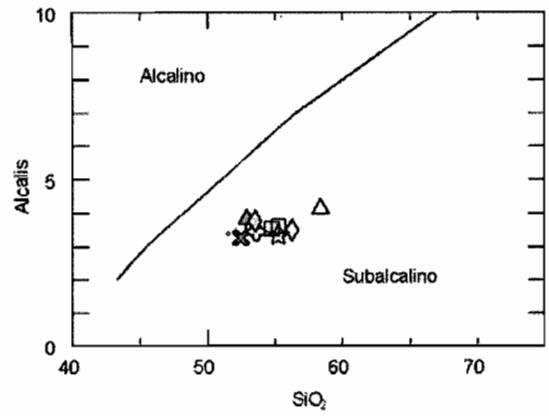

Figure 2- Diagram Alkali vs. SiO_2, (IRVINE & BARRAGÁN 1971)

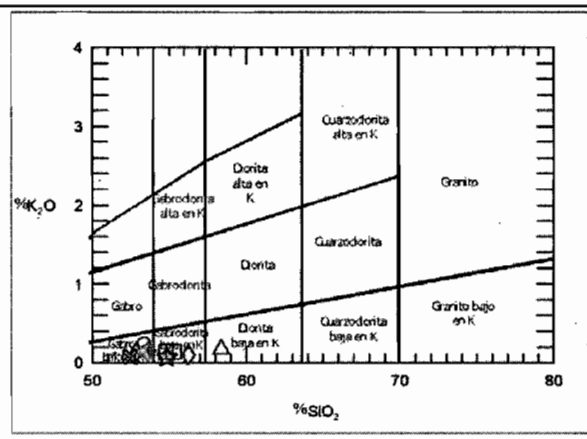

Figure 3- Diagram K_2O vs. SiO_2, (PECCERILLO & TAYLOR 1976).

In the diagram developed by PEARCE *et al.* (1977 *in Vásquez et al. 2000*), the bigger elements: Mg, Fe, and Al, were used in the ternary diagram MgO - FeO_{total} - Al_2O_3, to distinguish 5 different geotectonic environments: dorsal, oceanic ground, oceanic islands, orogenic (Subduction Zone), continental and central islands of expansion. The analyzed samples were generated in an environment of continental intraplates. (Fig. 4). We can establish about the generation of the basic intrusive bodies, that this is caused by formation of an intercontinental rift system, which rise is usually prior to the formation of a soft depression, that will be fulfill with sediments.

Subsequently, the graben was created in which occurred a simultaneous subsidence to the horst rise. During this time, an accumulation of marine sediments happened inside the graben. By this way, the continental crust was reduced very highly, and let the faults from the rift system get enough depth to the emplacement of the basic magma. This intrusion occurred in the most subsidence parts of the basin, due to the high position of the asthenosphere/lithosphere limit, producing partial fusion of the mantle. Along with the work of geochemical characterization and petrogenetic observation and petrographic description of the basic intrusive rocks in the Cáceres and Puerto Romero area were developed. Based on the mineralogical composition seen, these rocks are classified as gabbros and gabbronorite.

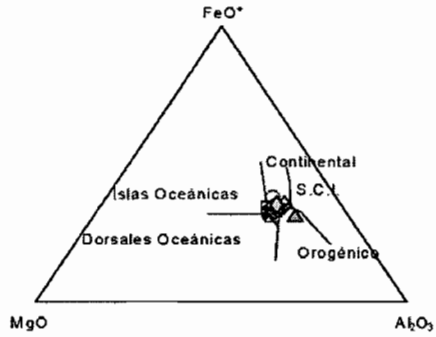

Figure 4- Diagram MgO–FeO–Al_2O_3, (PEARCE et al.1977 in Vásquez et al. 2000), where the analyzed samples were generated in a continental intraplate environment.

GABBRO OF PACHO

This one is located in the Hill of Tragarepas, at north east of Pacho city. Morphologically, this body presents a protuberating conic geometry in the regional topography, and includes sedimentary rocks from the early Cretaceous. Petrographic and geochemical results tell us about a gabbroic body, formed by sericitc plagioclase (andesine–labradorite) and hornblende rich in iron. This last is a result of the clinopyroxene alteration.

Chemical analysis done shows that theses rocks have low concentrations of SiO_2 (45 – 55 %) and K_2O (0,22 – 0,06%). It shows that all the samples are located in a zone of in the sub alkaline series diagram (Fig. 5). Thus, the subalkaline rocks were classificatted like tholleiitic series. These are geochemically classified as gabbros, also like the another intrusive bodies studied in the "Cordillera Oriental", and together with the relations of field and stratigraphic position, let us think about a genetic relation between them (Fig. 6). The existence of the Pacho Gabbro in the central part of the mountain range seems to be genetically related with the appearance of the Iron of the Corradine deposits, in the surroundings of the regions of Pacho.

GABBROS OF PUTUMAYO

The first reports about gabbros in the Putumayo regions, are present in the Orito 4, and close by wells descriptions. The preliminary studies show that basic layered bodies presents thickness between 10 and 40 meters, and were formed as dikes and sills during the Cretaceous and tertiary times in the zone. Its location seems to be by of the Orito Fault. The recognized characteristics in these samples have high resemblance with the rocks mentioned in the Ecuador Oriente-Napo-basin. We could conclude about a continuity and genetic relation of the magma event.

GABBROS OF ECUADOR

Recently, in the Napo-Oriente basin of Ecuador (BARRAGAN & BABY, 1999), intrusive corresponding to gabbroic sills and diabasic dikes with alkaline composition, emplacement in rocks from the Cretaceous were reported. The alkaline composition has a high content of TiO_2, K_2O, P_2O_5. The gabbroic bodies are found aleatory into the Cretaceous rocks, corresponding with the Napo and Hollin formations. The radiometric age obtained from the basic intrusive, represent a range between ~105-110 and ~85 Ma. In contraposition with the Colombian intrusives, the alkaline rocks are genetically associated with magmas, from a continental intraplate environment with hot spots.

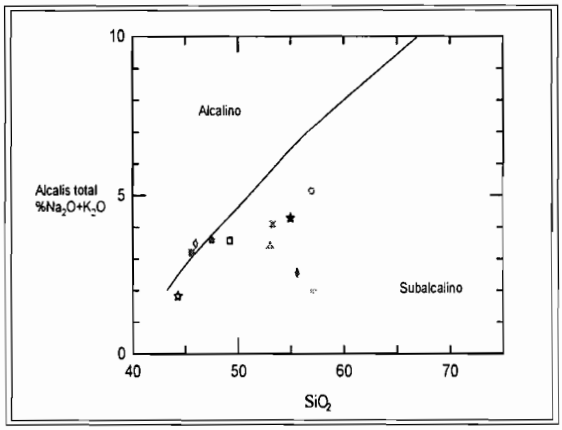

Figure 5- Álcalis Total vs. SiO_2 Diagram (IRVINE & BARAGAR 1971).

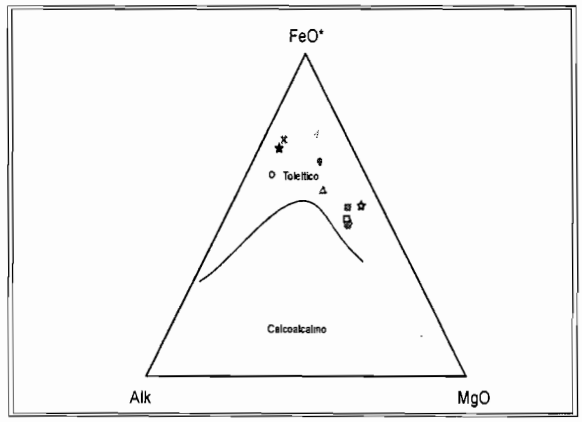

Figure 6- AFM Diagram (IRVINE & BARAGAR 1971).

CONCLUSIONS

The correlative comparisons between the basic intrusive bodies of the Puerto Romero and Caceres, western flank of the "Cordillera oriental" of Colombia, with the intrusive bodies encountered in the Oriente Ecuador basin, permit us to conclude a possible continuity of a similar magma event during the Early Cretaceous. This intrusive, basic body is probably a result of a distensive event, which affected a large portion of the northern part of South America. The new discoveries of these basic rocks into The early Cretaceous sedimentary rocks, only affected in the central part of Colombia, while at the southern part of Colombia, in the Putumayo basin, and in the Oriente Ecuador Basin, the intrusive rocks have affectation also in the Lower and Upper Cretaceous sedimentary rocks, and in the Early Tertiary rocks. The location and description of the present gabbroic bodies in the "Cordillera Oriental", is showed as well as, the igneous bodies found in Ecuador and are related with the tectonic evolution of the Colombian Oriental Mountain Range.

REFERENCES

Barragan R., & Baby P., 1999: A Cretaceous hot spot in the Ecuadorian oriente basin: Geochemical, geochronological and tectonic indicators. Fourth ISAG, International symposium on Andean Geodynamic. Extended Abstracts. Goettingen (Germany).

Vasquez, M., Concha P. A., Moreno J.M., & Patarroyo P., 2000: Caracterización geoquímica y petrográfica de los cuerpos intrusivos básicos aflorantes en la región de Cáceres y Puerto Romero, Departamentos de Cundinamarca y Boyacá, Colombia. Geología Colombiana, 25, pgs. 185 - 198 14 Figs. 3 tablas, 2 laminas.

Vasquez, M. 1999: Evaluación Petrográfica y Caracterización Geoquímica de los cuerpos intrusivos básicos aflorantes en la región de Cáceres y Puerto Romero, departamentos de Cundinamarca y Boyacá (Trabajo de Grado), Universidad Nacional de Colombia, Departamento de Geociencias 74 p., Bogotá.

THE QUEBRADA TURBIA SEQUENCE: A SNAPSHOT OF MAGMATIC DEVELOPMENT WITHIN THE LONG LIVED TATARA-SAN PEDRO VOLCANIC COMPLEX.

George A. MORRIS (1) and Michael A. DUNGAN (1)

(1) Département de Minéralogie, Université de Genève, Rue des Maraîchers 13, CH1211 Genève 4, Switzerland (george.morris@terre.unige.ch)

KEY WORDS: Southern Volcanic Zone, Magmatic Evolution, Magma Mixing.

INTRODUCTION

The Quebrada Turbia Sequence (QTS) forms part of the long lived Tatara - San Pedro volcanic Complex (TSPC, 36°S, Southern Volcanic Zone, Chilean Andes). Geochemical and petrological studies encompassing the entire volcanic complex have eliminated simple fractional crystallisation (FC) as the controlling factor in the evolution of the QTS (Dungan et al., 2001). While assimilation and fractional crystallisation (AFC) processes could theoretically produce the observed array of geochemical data, detailed petrological and mineral chemistry data, presented here, suggest that magma mixing and entrainment of xenocryst phases important factors in the development of this sequence.

GEOLOGY

The QTS is the erosional remnant of a once larger volcano, currently consisting of over 300m of lava flows exposed on the west wall of Quebrada Turbia, on the northwest flank of the Tatara-San Pedro complex (Dungan et al., 2001). The QTS has been dated at ~785 and 771 ka (Singer and Pringle, 1996) and most flows are characterised by transitional virtual geomagnetic pole positions as a result of eruption during the Matuyama-Bruhnes polarity reversal (Brown et al., 1994). Dungan et al. (2001) informally divided the sequence into: a lower group of 5 basaltic andesite to andesite flows (52.7 – 58.8 wt% SiO_2), preserved in a palaedepression; and an upper group of more extensive basaltic andesite flows (54.7 – 56.0 wt% SiO_2). The QTS overlies and is cut by erosion surfaces linked to ice advances at ~785 and 710 ka respectively. All samples contain plagioclase (dominating), clinopyroxene, olivine and spinel phenocrysts.

Orthopyroxene is present in some of the higher silica (>55 wt%) basaltic andesite and andesite flows, occasionally occurring as an overgrowth or replacement of olivine phenocrysts. Small xenoliths (<0.5 cm) of olivine, clinopyroxene and plagioclase are observed throughout the QTS.

WHOLE ROCK AND MINERAL CHEMISTRY

The overall chemical trends within the QTS define coherent arrays on Harker diagrams (decreasing FeO, MgO, and CaO coupled with increasing Na_2O and K_2O with increasing SiO_2). The eruptive sequence shows no progressive chemical ordering for the lower QTS, and little variation for the upper QTS (Fig. 1). In itself, such variations in the eruption order of variably evolved magmas suggests a complex temporal evolution involving multistage differentiation and replenishment.

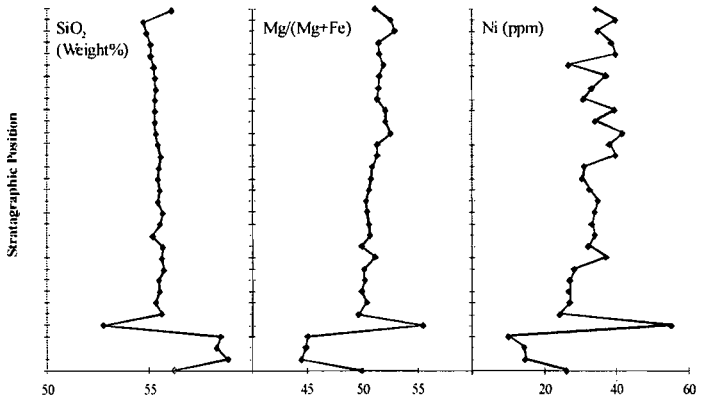

Fig. 1. Selected whole rock chemistry vs. relative stratagraphic position. While, on a Harker style plot, these data display a quasi-coherent array, when examined stratigraphically, compositions of erupted lavas do not show a systematic up-section temporal progression towards more evolved magmas.

In this study we present detailed olivine data for the QTS. Olivine has long been known to have a consistent K_D for the distribution of it's major elements, Fe and Mg, between crystal and host liquid over a large range of compositions, temperatures and water contents ($[Fe/Mg]_{Ol}/[Fe/Mg]_{liq}$ = 0.28 +/-0.05; Sisson and Grove, 1993). Diffusive re-equilibration can however rapidly (on the order of 100's of years) re-equilibrate Fe/Mg ratios to a different host liquid. Olivine compositions therefore present a tool for examining the compositions of magmas within which the phenocrysts have most recently been in equilibrium, and short term open system processes that have occurred prior to eruption

Within the QTS, olivine core compositions typically vary by up to 20% Fo content within an individual sample (Fig. 2), consistent with mixing of multiple magmatic components. In particular, many crystals are Mg-poor with respect to olivine in equilibrium with the host sample, indicating that the magma with which they last equilibrated was more, and often considerably more evolved than the erupted host. The frequency of core compositions in the QTS (Fig. 3) reveals a peak at ~Fo_{67}, in equilibrium with host liquids of Mg# ~35. Such values are not unreasonable, as some basaltic andesites of the TSP have whole rock Mg# as low as 43, (Mg number of whole rock calculated using Fe^{2+} only, based upon calculated Fe^{2+}/Fe^{3+} partitioning assuming log fO_2 = NNO+1, using the Melts program of Ghiorso and Sack, 1995). The range of olivine compositions within each sample (Fig. 2) indicates that several sources of equilibrated olivines contributed to each erupted magma.

A typical mafic andesite from the QTS contains olivines with a range of core compositions (plateaus on Fig. 4). The presence of multiple plateaus within a single sample shows that several discrete batches of olivine-bearing liquid have equilibrated internally before being incorporated into the final magma. Some olivine phenocrysts display a reversely zoned shoulder with higher Fo content than the core. This is normally interpreted as a result of recharge of the olivine-bearing magma by a more primitive magma, increasing the Mg/Fe ratio of both the liquid phase and the crystallising olivine. All olivine phenocrysts have normally zoned rims, apparently due to rapid magma evolution during cooling, but significantly these do not always evolve to the same value at the edge of the crystals within a single sample. In the example illustrated in Fig. 4, high-Fo olivines with reversely zoned shoulders are zoned to Fo_{65} at the rim. Low-Fo olivines do not display a reverse zone but are zoned to rim compositions of $Fo_{55} - Fo_{58}$, although at a shallower gradient.

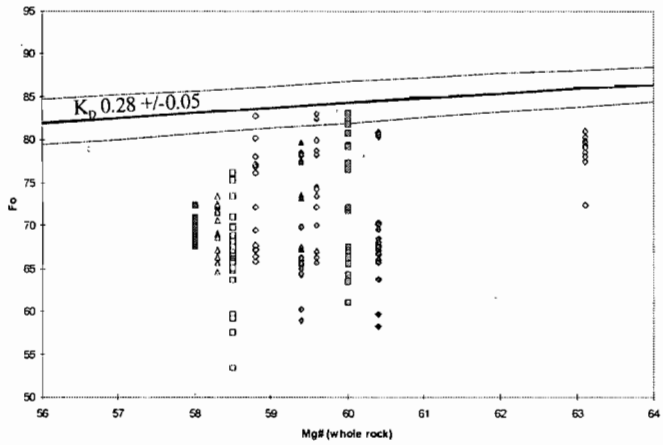

Fig. 2. Fo composition of olivine phenocryst cores vs. Mg number of whole rock host from the QTS. Mg number of whole rock calculated using Fe^{2+} only, based upon calculated Fe^{2+}/Fe^{3+} partitioning assuming log fO_2 = NNO+1.

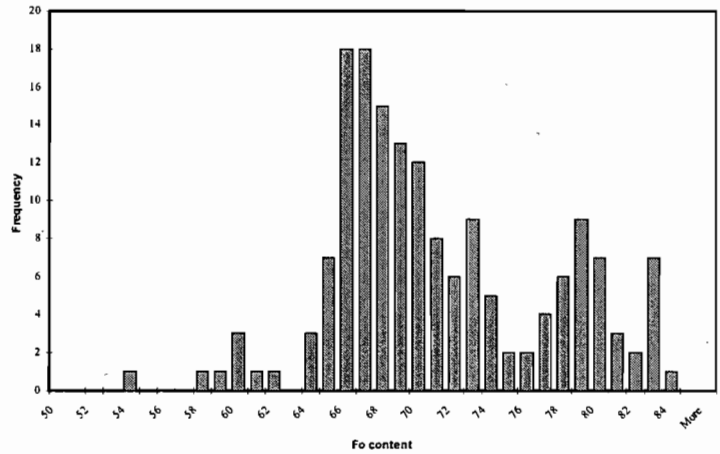

Fig. 3. Histogram showing the core compositions of all analysed olivine phenocrysts from the QTS.

These data suggest a complex evolution of the magma prior to and during eruption with individual olivine-bearing components experiencing radically different evolution paths with mixing between variably evolved magmas occurring at a very late stage. Further, this suggests that multiple discrete batches of crystal-bearing magmas existed beneath the volcano for significant periods of time, evolving along separate paths before being incorporated into the final erupted magma.

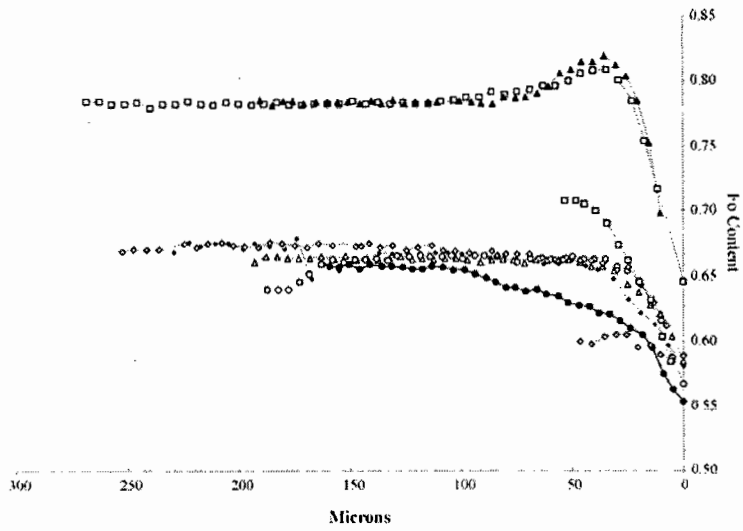

Fig. 4. Core to rim profiles of all olivines analysed within a typical thin section (QTW.11.10: SiO_2 55.54, Mg# 51.3). A bimodal population of olivine core compositions at ~Fo80 and ~Fo65 is interpreted as representing at least two distinct sources for the olivine phenocrysts.

CONCLUSIONS

Lavas from the Quebrada Turbia Sequence (Tatara - San Pedro Complex) are not the products of evolution via FC or AFC from a common parent magma. Instead, multiple magmatic evolution paths were followed, with the final products being a hybrid of primitive and various variably evolved magmas. The compositions of these hybrid magmas was dependant on the proportions and compositions of the blended magmas. Detailed crystal chemistry studies, such as this, can begin to resolve the nature and number of these components.

REFERENCES

Brown L., Pickens J. & Singer B. 1994. Matuyama-Brunhes transition recorded in lava flows of the Chilean Andes: evidence for dipolar fields during reversals. Geology 22, 299-302.

Dungan M.A., Wulff A. & Thompson R. 2001. Eruptive stratigraphy of the Tatara-San Pedro Complex, 36°S, Southern Volcanic Zone, Chilean Andes: Reconstruction Method and Implications for Magma Evolution at Long-lived Arc Volcanic Centres. Journal of Petrology 42, 555-626.

Ghiorso, M. S. & Sack, R. O. 1995. Chemical Mass Transfer in Magmatic Processes. IV. A Revised and Internally Consistent Thermodynamic Model for the Interpolation and Extrapolation of Liquid-Solid Equilibria in Magmatic Systems at Elevated Temperatures and Pressures. Contributions to Mineralogy and Petrology 119, 197-212.

Singer B.S. & Pringle M.S. 1996. Age and duration of the Matuyama-Bruhnes geomagnetic polarity reversal from 40Ar/39Ar incremental-heating analysis of lavas. Earth and Planetary Science Letters 139, 47-61.

Sisson T.W. & Grove T.l. 1993. Temperatures and H_2O contents of low-MgO high Alumina basalts. Contributions to Mineralogy and Petrology 113, 167-184.

TERTIARY TECTONIC EVOLUTION OF THE SOUTHWESTERN EDGE OF THE PUNA PLATEAU: CORDILLERA CLAUDIO GAY (26°-27° S), NORTHERN CHILE

Constantino MPODOZIS (1) and Jorge CLAVERO (2)

(1) Servicio Nacional de Geología y Minería, Santiago, Chile*(cmpodozis@sipetrol.cl)
(2) Servicio Nacional de Geología y Minería, Santiago, Chile (jclavero@sernageomin.cl)
(*) now at SIPETROL, Santiago, Chile

KEY WORDS: Central Andes, Tertiary tectonics, Northern Chile

INTRODUCTION

During the Late Cenozoic the Altiplano-Puna plateau has been the site of repeated cycles of sedimentation, magmatism, and deformation (Allmendinger et al., 1997). This geologic domain has been generally considered to be restricted to the east of the Upper Miocene to Recent volcanic arc of the Central Andes (CVZ). However, recent mapping carried out in Northern Chile (Clavero et al. 1997, 1998) has demonstrated that Neogene sedimentary and volcano-clastic sequences also outcrop along the western border of the CVZ arc that conceals much of the geological features of an otherwise continuous Eocene to Middle Miocene tectonic and magmatic domain. Here we present new field and geochronological data about Cordillera de Claudio Gay (CCG) a 130 km long, 20 km wide range located between the extinct Oligo-Miocene Maricunga volcanic belt and the modern CVZ in the Copiapó region of northern Chile (26°-27° S, Figure 1). Its study may give important clues to reevaluate the Tertiary tectonic evolution of this segment of the Central Andes.

EOCENE TO MIOCENE STRATIGRAPHY AND TECTONICS

The basement of the CCG is formed by metasediments, rhyolitic volcanics and minor granitoid plutons of Late Paleozoic age. Unconformably overlying the basement are Eocene to Upper Miocene volcano-sedimentary sequences cut by basement-involved high angle reverse faults (Clavero et al. 1997, 1998). The oldest Tertiary unit consists of an up to 300 m thick epiclastic and pyroclastic sequence cropping out in the southeastern border of the CCG (Huidobro sequence, Figure 1) which is capped by an up to 400 m

thick pile of altered andesitic lava flows (Vertiente Unit, Figure 1). K-Ar ages, most of which are considered to be resetted, range between 26 and 31 Ma. Equivalent volcanic strata cropping out south of 27°S, both in Chile and Argentina, yield similar, but also some older (ca 38 Ma), K/Ar ages together with disturbed Ar/Ar plateau ages, which span the 36 to 35 Ma time interval (Panteleyev and Cravero, 2000, Mpodozis and Kay in prep).

Volcanism almost totally ceased, at a regional scale, during the Oligocene, when fine-grained continental red beds and evaporites (gypsum) were deposited in the CCG region (Gases Blancos beds, Figure 1). Gentle folding of the Gases Blancos occurred in the Late Oligocene before the reactivation of volcanism at 26 Ma, when activity started again in earnest along the Maricunga arc, 30 km west of the CCG (Mpodozis et al 1995, see Figure 1). A complex array of, mainly dacitic, coarse pyroclastics and associated domes (Claudio Gay Sequence, Figure 1), and basaltic andesitic lavas (Segerstrom basalts) were emplaced between 26 and 22 Ma in the CCG, placed at that time in a "proximal back-arc" position relative to the Maricunga arc. Coeval epiclastic sediments and saline-lake carbonates accumulated in a series of small (extensional?) intramontane basins (Rio Juncalito sequence, Figure 1). Further east, in the far back-arc (Antofalla region, Argentine Puna) alluvial and eolian sediments were deposited in a "broken foreland" environment (i.e., Chacras formation, Kraemer et al 1999). This period ended when east-verging high-angle reverse faults uplifted the Late Paleozoic CCG basement at around 21-20 Ma. Intense volcanism followed. Large dome complexes associated with extensive block-and-ash flow fans erupted along the northern CCG (Sierra de Aliste sequence, 20-19 Ma, Figure 1) to be shortly after covered by a widespread dacitic ignimbrite sheet (Vega Helada Ignimbrite, 18-19 Ma) which probably originated from some 70 km to the north during a collapse event related to the formation of the giant Aguilar Caldera (Naranjo and Cornejo, 1992).

While these events happened in the CCG, a volcanic lull occurred, at the same time, in the Maricunga arc front (Mpodozis et al, 1995) where magmatism made a fresh restart only at 17 to 14 Ma to build large volcanic complexes (Doña Inés, Ojos de Maricunga). In the CCG back arc the mid-Miocene period was a time of uplift, erosion and accumulation of a thick alluvial gravel unit (Rio Lamas sequence) interbedded with distal ignimbrite sheets (15-16 Ma, K/Ar) most likely of western provenance. Progressive unconformities and intraformational folds are common in these Mid-Miocene gravels pointing out to synchronical compressive deformation. Large-scale structures including east-verging folds and, in the northern CCG, west-verging back folds, probably associated with blind basement faults were also formed at that time The geometrical array of the regional structures (that also includes, in the southern CCG, east and west directed high-angle reverse faults) suggests the participation of a strike-slip deformation component.

Finally, the Late Miocene eastward shift of the magmatic foci towards the modern CVZ front (Mpodozis et al, 1985) made the CCG to attain its current "proximal fore-arc" position. Volcanism and sedimentation continued during the Upper Miocene-Pliocene, depositing extensive gravel and ignimbrite sequences of eastern provenance (Figure 1), some of which were deposited along the western CCG flank. Gentle folds affect these sequences, showing evidence of a late stage compressive deformation episode in the Upper Miocene.

DISCUSSION

The CCG exhibits a complete record of Neogene cycles of sedimentation, volcanism and deformation occurred in the proximal back-arc of the Late Oligocene-Mid Miocene volcanic front of the southern Central Andes. One of the most distinctive features of the region is the presence of a previously unreported Eocene-Oligocene volcanic unit (Vertiente sequence) which forms the northern termination of an almost continuous

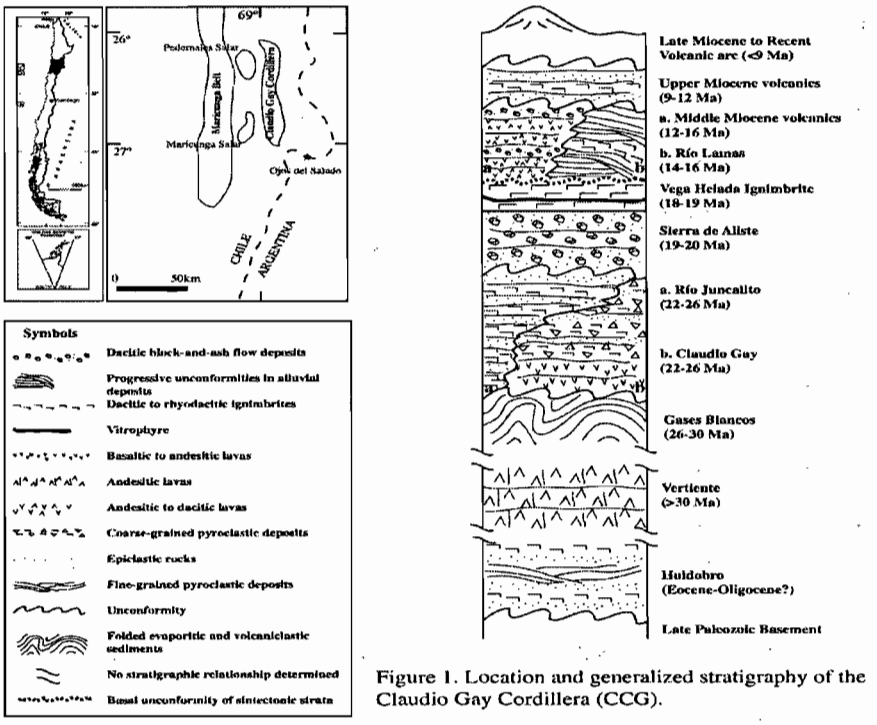

Figure 1. Location and generalized stratigraphy of the Claudio Gay Cordillera (CCG).

volcanic belt continues in Argentina, south of the Ojos del Salado- Pisiss region (27° S) to the Valle del Cura area (31° S), in San Juan (Panteleyev and Cravero, 2000; Limarino et al, 1999; Mpodozis and Kay, in prep).

Any future tectonic reconstruction of the Tertiary volcanic evolution of the Southern Central Andes should consider the causes of the westward shift of magmatism towards the Maricunga Belt occurred after the Oligocene (30-26 Ma), a regionally non magmatic period represented (in the CCG) by the Gases Blancos sequence. The compressional episode preceding the resumption of volcanism at 26 Ma and recorded by the angular unconformity between the Gases Blancos and the overlying Late Oligocene- Early Miocene units (Figure 1) was also, previously unreported. The timing of the younger (Miocene) tectonic events recorded in the Claudio Gay Cordillera is similar to events already reported for other places of the Puna-Altiplano, although, in the Claudio Gay Cordillera, the effects on the Mid-Miocene deformation episode (16-15 Ma) are particularly striking.

REFERENCES

Allmendinger, R. W., Jordan, T. E., Kay, S. M., Isacks, B., 1997. The evolution of the Altiplano-Puna plateau of the Central Andes. Annual Review of Earth and Planetary Sciences, Vol. 25, p. 139-174.

Clavero, J., Mpodozis, C., Gardeweg, M., 1997. Mapa Geológico Preliminar del área del Salar de Wheelwright, Región de Atacama, escala 1:100.000. (unpublished) Servicio Nacional de Geología y Minería, Santiago.

Clavero, J., Gardeweg, M., Mpodozis, C., 1998. Mapa Geológico Preliminar del área del Salar de Piedra Parada, Región de Atacama, escala 1:100.000. (unpublished) Servicio Nacional de Geología y Minería, Santiago.

Limarino, C., Gutiérrez, P. R., Malizia, D., Barreda, V., , Page, S., Ostera, H., Linares, E. 1999, Edad de las secuencias paleógenas y neógenas de las cordilleras de La Brea y Zancarrón, Valle del Cura, San Juan. Revista Asociación Geológica Argentina, Vol. 54(2), p. 177-181.

Mpodozis, C, Cornejo, P., Kay, S. M. Tittler, A., 1995. La Franja de Maricunga: síntesis de la evolución del frente volcánico Oligoceno-Mioceno en la zona sur de los Andes Centrales. Revista Geológica de Chile, Vol. 22, p. 273-313.

Panteleyev, A., and Cravero, O, 2000, Faja del Potro and Cordón de la Brea Ore Deposits, La Rioja and San Juan. Servicio Geológico Minero Argentino (SEGEMAR) Serie Contribuciones Técnicas (Recursos Minerales), Vol. 11, 59 pp., Buenos Aires

Kraemer, B., Aldeman, D,. Alten, M., Schnurr, W., Erpstein, K., Kiefer, E., van den Bogaaard, P, Görler, K.1999. Incorporation of the Paleogene foreland into the Neogene Puna plateau: the Salar de Antofalla area, NW Argentina. Journal of South American Earth Sciences, v. 12(2), p. 157-182.

Naranjo, J. A; Cornejo, P., 1993. Hoja Salar de la Isla. Servicio Nacional de Geología y Minería, Carta Geológica de Chile (1:250.000), Santiago.

TECTONIC RELATION OF METALLOGENIC PROVINCES IN THE CHILEAN LAKE REGION, SOUTHERN ANDES (39-44°S)

Jorge MUÑOZ BRAVO (1), Pedro CRIGNOLA (1), Alexandro ORDOÑEZ (1), Paul DUHART (1)

(1) Servicio Nacional de Geología y Minería, La Paz 406, Puerto Varas, Chile (sernageomin@surnet.cl)

KEY WORDS: Geology, mineralisation, metallogenesis, tectonics

INTRODUCTION

The spatial distribution of the different types of mineral deposits, mineral occurrences, prospects and geochemical anomalies and their relation to geological units along the Chilean Lake Region allow us to propose the existence of Coastal, Central Valley and Main Andean Cordillera Metallogenic Provinces (Crignola, 2000; Ordóñez and Crignola, 2002), which are coincident with the main morphological features of this segment of the Andes (Figure 1). Two metallogenic belts are distinguished in the Main Andean Cordillera Metallogenic Province (Duhart *et al.*, 2000) and two metallogenic epochs are recognised in the Coastal Metallogenic Province. In addition, metallogenic provinces are also coincident in space and time with the tectonic evolution of this segment of the Southern Andes.

GEOLOGIC AND TECTONIC SETTING

Palaeozoic to Triassic metamorphic complexes are the oldest exposed rocks, mainly within the Coastal Cordillera (Figure 1) but also scarcely within the Main Andean Cordillera. Metamorphic rocks include metasedimentary and mafic metavolcanic schists, mylonites and mafic and ultramafic bodies locally emplaced by tectonics. This lithologic association is representative of an accretionary-subduction complex which evolved during Devonian to Triassic times in the southwestern portion of the Gondwana margin (e.g., Hervé, 1988; Duhart *et al.*, 2001). Triassic continental sedimentary, Jurassic volcanics and Late Jurassic-Early Cretaceous marine sedimentary sequences are also locally exposed near the central area of the Main Andean Cordillera. These sequences respectively represent part of northwestern trending Triassic rift basins and an approximately north-south Jurassic-Early Cretaceous arc-backarc system (e.g., Jenchen and Rosenfeld, 1999; Bell *et al.*, 1999). Volcanic rocks representing part of Tertiary and Quaternary magmatic arcs also occur in the Main Andean Cordillera. The Tertiary volcanic complexes and sedimentary basins associated with the Central Valley morphological feature were produced during Late Oligocene-Early Miocene regional crustal extension as a consequence of major tectonic changes in the southeastern part of the Pacific Ocean (Muñoz *et al.*, 2000).

Carboniferous-Permian and Jurassic intrusive rocks were respectively emplaced into the oldest portion of the metamorphic complexes and the Triassic continental sedimentary sequence. Also, along the Main Andean Cordillera, large Late Cretaceous and Miocene intrusive bodies were subsequently emplaced into the Jurassic-Early

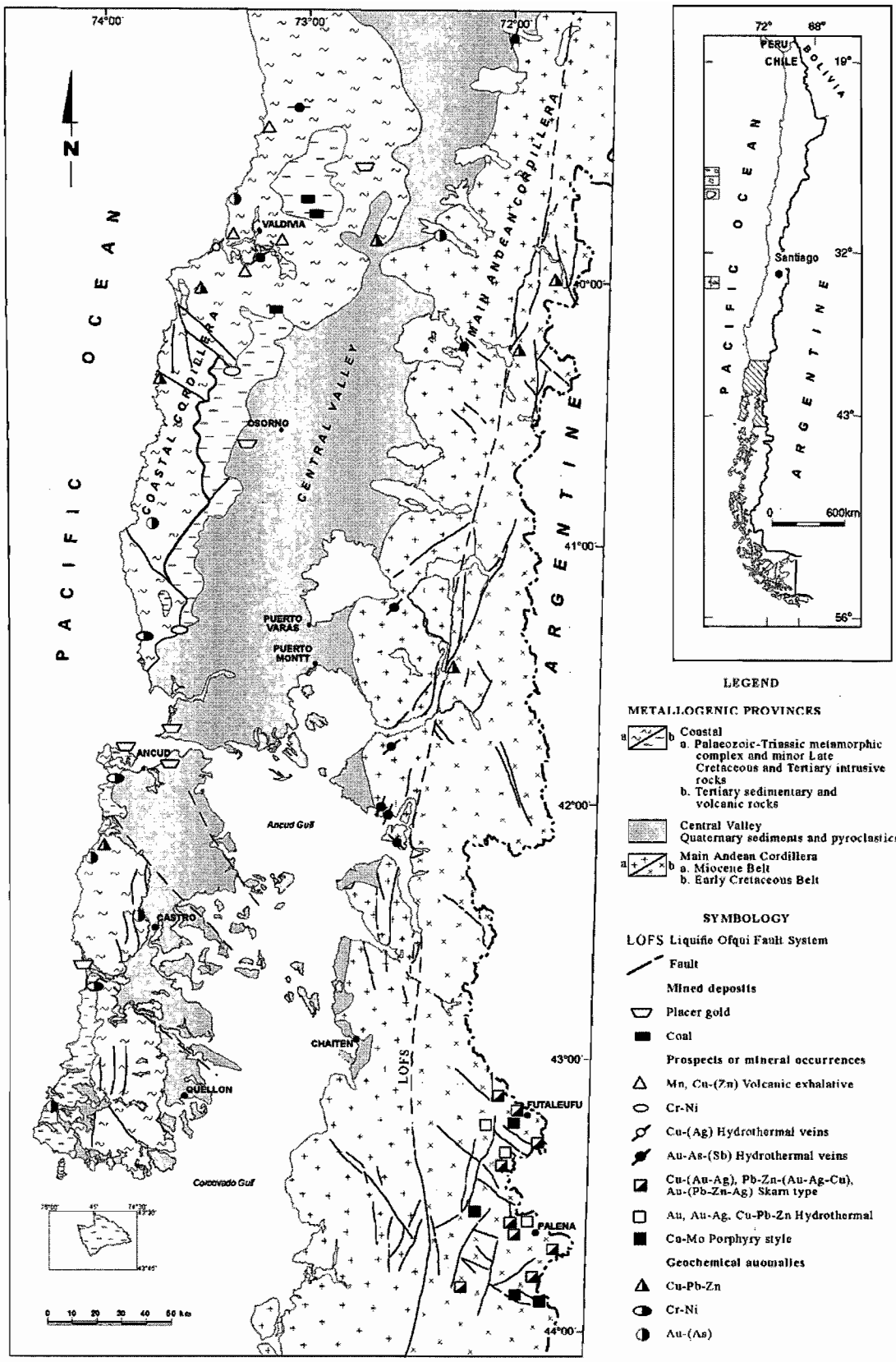

Figure 1. Metallogenic Provinces and mineralisation in the Chilean Lake Region, Southern Andes (39-44°S).

Cretaceous and Tertiary sedimentary and volcanic sequences. Unconsolidated glacial, fluvial, littoral and lacustrine sediments and pyroclastic deposits of Quaternary age are well represented at the Central Valley.

METALLOGENIC PROVINCES

Coastal Province. Includes metallic mineral occurrences and geochemical anomalies representative of two superimposed metallogenic epochs. The oldest Metallogenic Epoch is represented by exhalative Mn and Cu-(Zn) mineral occurrences and geochemical anomalies hosted by Palaeozoic metamorphic rocks and by Cr-Ni geochemical anomalies associated to Palaeozoic mafic volcanics and serpentinized ultramafic bodies. The youngest Metallogenic Epoch includes hydrothermal Cu-(Ag) and Au-As-Sb veins respectively hosted by Late Cretaceous and Early Tertiary felsic intrusive rocks. Also, mined coal beds within Oligocene-Miocene sedimentary sequences and minor placer gold deposits associated to Quaternary sediments are also represented in this Province.

Central Valley Province. Detrital Au forming placer deposits and some industrial rocks and minerals such as gravels, sand, limes and clays are represented along the Central Valley and are mainly associated to the Pleistocene glacial cycles. Gold in placer deposits was mainly transported from the Main Andean Cordillera by ice of different glacial cycles and later concentrated by fluvial and littoral processes. Gold as placer deposits is the only metallic ore mined in the Region.

Main Andean Cordillera Province. Two main metallogenic parallel belts have been recognized along the Main Andean Cordillera, Miocene and Early Cretaceous Belts (Duhart *et al.*, 2000), which extend north and south of the area shown in Figure 1. The Miocene Belt includes Au-As hydrothermal mineralisation represented by northeast and northwest veins and stockwork mainly hosted by Miocene intrusives and Late Oligocene-Early Miocene volcanic and sedimentary rocks. Early Cretaceous Belt includes Au, Au-Ag and Cu-Pb-Zn mineralisation as hydrothermal veins, Cu-Mo porphyry style and Cu-(Au-Ag), Pb-Zn-(Au-Ag-Cu) and Au-(Pb-Zn-Ag) skarn types occurrences, hosted by Jurassic and Early Cretaceous volcanic and sedimentary rocks (Duhart *et al.*, 2000). Polymetallic mineralisation is represented in the eastern portion of the Main Andean Cordillera, it extends into Argentine and is associated to Early Cretaceous magmatism.

TECTONIC RELATION

Palaeozoic Mn and Cu-(Zn) mineral occurrences and geochemical anomalies within the Coastal Province are volcanogenic in origin. Massive sulphide and banded iron formation deposits have been studied to the north (e.g., Pirén, Mahuilque) and associated to oceanic exhalative volcanism (Oyarzún and Clemmey, 1985), the former to proximal and the latter to distal exhalative vents. Similar to Cr deposits to the north (e.g., La Cabaña, Barra *et al.*, 1997), Cr-Ni anomalies within the Coastal Province are related to Palaeozoic oceanic type serpentinized mafic and ultramafic rocks and they are tectonically emplaced mainly along northwestern trending strike slip faults. Northeast hydrothermal Cu-(Ag) and northeast and east-west Au-As-Sb veins in this Province are respectively associated to Late Cretaceous and Early Tertiary magmatism and related to extensional tectonics.

Gold placer mineralisation within the Central Valley was originally deposited within glacial sediments. The morphology of the Central Valley Province probably corresponds to a tectonic basin bounded in its western, and probably eastern boundaries, by Late Oligocene-Early Miocene normal fault systems in part inverted during post Middle Miocene times.

The main branch of the Liquiñe-Ofqui Fault System is the general boundary between the Miocene Belt and the Early Cretaceous Belt, respectively located to the west and east of this major fault system in the Main Andean Cordillera. Miocene Au-As mineralisation is related to magmatism associated to Late Oligocene-Early Miocene crustal extension. Early Cretaceous polymetallic mineralisation is associated to arc type felsic plutons emplaced during extensional tectonics into Jurassic arc type volcanics and Late Jurassic-Early Cretaceous marine sedimentary rocks, which are part of the arc-back arc system.

ACKNOWLEDGEMENTS We thank SERNAGEOMIN for funding and Charles Stern and Waldo Vivallo for review of the manuscript. The Subdirección Nacional de Geología, SERNAGEOMIN, sponsors this publication.

REFERENCES

Barra, F.; Rabbia, O.; Alfaro, G. 1997. Mineralogía y geoquímica de las cromititas de La Cabaña: implicancias en el uso de la cromita como indicador petrogenético para las peridotitas del centro-sur de Chile. Congreso Geológico Chileno, No. 8, Actas, Vol. 2, p. 1205-1209.

Bell, M.; De La Cruz, R.; Suárez, M. 1999. The tectonic evolution of the Mesozoic and Cenozoic Austral basins of southern South America. Fourth International Symposium on Andean Geodynamics, extended abstract, p. 90-93. Göttingen.

Crignola, P. 2000. Depósitos metalíferos, anomalías geoquímicas y recursos energéticos del sector norte de la Región de Los Lagos. Servicio Nacional de Geología y Minería, Mapa de Recursos Minerales de Chile, No. 6, 22 p., 1 mapa escala 1:500.000. Santiago.

Duhart, P.; McDonough, M.; Muñoz, J.; Martin, M.; Villeneuve, M. 2001. El Complejo Metamórfico Bahía Mansa en la cordillera de la Costa del centro-sur de Chile (39°30`-42°00`S): geocronología K-Ar, $^{40}Ar/^{39}Ar$ y U-Pb e implicancias en la evolución del margen sur-occidental de Gondwana. Revista Geológica de Chile, Vol. 28, No. 2, p. 179-208.

Duhart, P.; Crignola, P.; Ordóñez, A.; Muñoz, J. 2000. Franjas metalogénicas en Chiloé continental (41-44°S). In Congreso Geológico Chileno, No. 9, Actas, Vol. 1, p. 201-205. Puerto Varas.

Hervé, F. 1988. Late Palaeozoic subduction and accretion in southern Chile. Episodes, Vol. 1, No. 3, p. 183-188.

Jenchen, U.; Rosenfeld, U. 1999. Contineral Triassic in Argentina: response to tectonic activity. Fourth International Symposium on Andean Geodynamics, extended abstract, p. 372-376. Göttingen.

Muñoz, J.; Troncoso, R.; Duhart, P.; Crignola, P.; Farmer, L.; Stern, C. 2000. The relation of the mid-Tertiary coastal magmatic belt in south central Chile to the Late Oligocene increase in plate convergence rate. Revista Geológica de Chile, Vol. 27, No. 2, p. 177-203.

Ordóñez, A.; Crignola, P. 2002. Depósitos metalíferos, anomalías geoquímicas, rocas y minerales industriales del sector sur de la Región de Los Lagos. Servicio Nacional de Geología y Minería, Carta Geológica de Chile, Serie Recursos Minerales, 1 mapa escala 1:500.000. Santiago. In edition.

Oyarzún, R.; Clemmey, H. 1985. Las mineralizaciones bandeadas de hiero y los sulfuros masivos estratoligados de la Cordillera de Nahuelbuta, Chile. In Geología y Recursos Minerales de Chile (Frutos, Oyarzún, Pincheira, eds.), p. 739-773. Concepción

WBZ AND THERMAL STRUCTURE BENEATH THE ANDES

Miguel MUÑOZ (1)

(1) *Structure and Non-Linear Dynamics of the Earth* - International Centre for Theoretical Physics, Strada Costiera, 11 - 34014 Trieste, Italy. (munozm@ictp.trieste.it)

KEY WORDS: Flat Wadati–Benioff Zones, Andes, Rheological Regimes, Earthquakes.

INTRODUCTION

In the Andes, the cessation of arc and back-arc volcanism has been usually associated to the achievement of flatness of the Wadati-Benioff Zone(s) {WBZ} as representing a continuous shallowing of the subducting Nazca plate. Such a distinct process has been assumed to be related to changing patterns of volcanism, geochemical signatures and tectonophysical processes as uplift, crustal shortening and thickening, although paradoxes and difficult problems are not absent in this context. The flat WBZ in central Chile and Argentina, in Peru and in Ecuador are examined here in the frame of thermal and rheological regimes of the continental lithosphere. It is concluded that seismic activity associated to flat WBZ is really defining seismogenic zones in the continental upper mantle. This kind of seismicity is rare in tectonic environments different to that of western South America. Seismological observations are discussed to confirm the former conclusion. The complete set of publications regarding the WBZ in South America and several works concerning the geology and volcanism of these regions were examined. Reasons of space prevent from giving reference of most of them.

THERMAL RHEOLOGICAL AND SEISMOLOGICAL EVIDENCE FOR THE ABSENCE OF FLAT WBZ

A variable thermal structure with different partition of rheological regimes has been seen to conform significant constraints for the genesis of seismic activity (e.g., Ranalli, 1991). The partition between the brittle and the ductile regimes beneath the Andes has been determined by examining the values that result from a linear frictional fracture criterion (Anderson-Sibson's formulation) and a non-linear flow stress (Dorn's equation for dislocation). The procedure followed to calculate geotherms can be seen in Chapman and Furlong (1992). Thermal conductivity at ambient conditions was taken between 3.0 and 3.3 $Wm^{-1}K^{-1}$. More recent models for the variation of thermal conductivity in the crust and upper mantle (Zoth & Haenel model described in Seipold, 1998; Hofmeister, 1999) are now adopted as compared with the ones used in previous works (e.g., Muñoz, 1994). The general heat flux pattern is taken from Hamza and Muñoz (1996) from features not including geochemical data. When this procedure has been applied in Chile to zones more than about 150-200 km far from the trench, and in regions with Quaternary volcanism, the seismogenic layer lies entirely in the upper crust and its maximum thickness (15-20 km) in the cordilleran area agrees with results of seismological studies (e.g., Campos et al., in press). Rheological parameters were taken from several sources (e.g., Wilks and Carter, 1990;

Ranalli, 1991). Most important is the rheology assumed for the lower crust and for the upper mantle. Rheology of granulites and of diabase were chosen for the lower crust. For the upper mantle, the following dry (D) and wet (W) rheological parametrizations were assumed {E(kJmol $^{-1}$); logA(MPa^{-n}s^{-1}); n}: D: {498; 4.5; 3.6}, {535; 4.5; 3.5}; W: {498; 2.6; 4.5}, {471; 3.3; 4.0}. The strain rate dε/dt is taken to be 10^{-17} s^{-1}. Heat flow measurements in the Precordillera of NW Argentina and in central Chile (28 – 33°S) give extremely low values (21 to 36 mW/m^2), but are few in number (8) and are not representative of several areas. Low heat flow has been ordinary explained as an effect of nearly subhorizontal subduction of the Nazca plate. The allochtonous nature of most of these terranes is instead here considered, and particularly, for the Argentine Precordillera, it is assumed that it is a terrane derived from Laurentia and comprising a basement of Grenville age (e.g., Casquet et al., 2001). The thermal structure of the Grenville province has been extensively studied in the Canadian Shield (e.g., Jaupart and Mareschal, 1999), resulting a heat flux of rather random character of 41 $\pm$ 11 mW/m^2 with an area weighted average of 39 mW/m^2. Geotherms for heat flux at least in that range were computed by assuming a radiogenic heat generation (A) of 0.4-0.6 μW/m^3 for the mid-crust, 0.2-0.4 μW/m^3 for the lower crust and of 0.02 μW/m^3 for the uppermost mantle (e.g., Rudnick et al., 1998). Solutions that do not satisfy conditions for appropriate geothermal gradients in the crust/mantle boundary (cf. Magnitsky, 1971; Rudnick et al., 1998) were discarded. A further constraint is the maximum seismogenic depth observed in the crust. Solutions for Western Argentina (Precordillera) between 31°S and 32°S are highly constrained and result in values of A between 0.7 and 0.8 μW/m^3 for the upper crust when the total crustal thickness is 45 km. The area weighted average for the Canadian Grenville terrane is 0.8 μW/m^3 (Jaupart and Mareschal, 1999). For a crust of 45 km thickness, and for normal (N) and thrust (T) mechanisms of faulting, the following maximum depths of seismogenic zones were obtained for heat flux in the range of 35-40 mW/m^2: I): Crust: N(33 – 40 km), T(28 – 34 km); II): Mantle: N(93 – 104 km), T(76 – 90 km); for strike-slip faulting, intermediate values between N and T are obtained. These values are in full agreement with seismological results of Smalley et al. (1993). In central Chile (28 -32.5°S) there is also indication of a seismogenic lower crust and the brittle mantle extends to about 62 – 98 km depth. In this area and in some areas of NW Argentina, the best constrained models yield values of A between 0.7 and 1.0 μW/m^3. In Peru, three zones were examined, roughly corresponding to the location of earthquakes in vertical sections (A-A', B-B' and C-C') reported in Tavera and Buforn (2001). Values of A obtained for Peru range from 0.7 to 1.2 μW/m^3. Several characteristic values of the crustal thickness were considered for each zone. The morphology of the Peruvian Andes is very complex, and the present rheological results can be briefly summarized as follows: in the northern and central areas, most of the crust is seismogenic and earthquakes in the continental mantle can occur to about 70 – 120 km depth; in the central-southern area (C-C'), where heat flux increases, the crust is seismogenic at least to depths of the mid-crust and seismogenic layers can be found in the upper 20 - 40 km of the continental mantle, whereas other upper mantle zones are in ductile regime. Also to be noted, as for Peru, in other areas, when heat flux is higher than about 45 mW/m^2, the seismogenic zone in the mantle reduces to a minimum or is absent unless a more "extreme" rheology is chosen there. In areas of low heat flow (40-45 mW/m^2) of Ecuador (1°N -2°S), constrained models give values of A between 1.0 and 1.2 μW/m^3. Most of the thin crust (35 km) and the mid-crust when the crust thickens to 40-50 km are seismogenic. As in other cases, depending on the fault mechanism, in Ecuador there is indication of a seismogenic upper mantle down to depths of about 60 – 90 km. These results agree with seismological observations of Guillier et al. (2001). The lithospheric strength, or integrated stress level, for suprahydrostatic pore pressure in some portions of the models and a 'wet' rheology of the upper mantle, in all the areas with earthquakes at depths of

75-100 km, including Ecuador, is generally between 1.0 – 7.0 x 10^{13} Nm^{-1}. These values are of the same order of maximum tectonic forces found in plate tectonics under planetary assumptions.

Taking into account the suggestion of Karato and Wu (1993) that deformation in the cold, shallow upper mantle occurs by diffusion rather than by dislocation creep, this possibility was explored for different creep parameters and grain size. No significant effect on the maximum seismogenic depths in the mantle was obtained for grain size $\geq 10^{-3}$ m. It seems that the transition from dislocation to diffussion creep occurs in the uppermost mantle at very shallow depths and dominates through few tens of kilometers. Also, the effect of relativization of the lithospheric pressure-depth relationship (Petrini and Podladchikov, 2000) was found to be not significant for shortening observed in these areas.

Seismological evidence for the existence of earthquake foci beneath the maximum seismogenic depths in the upper continental mantle can be obtained fron the NEIC database of the U.S. Geological Survey. In the area of western Argentina studied by Smalley et al. (1993), for the period between years 1990 and 2001, the NEIC database reports tens of occurrences at depths between 150 and 250 km. The seismic activity is concentrated at 80-100 km (number of occurrences is one order greater than in deeper levels). Usually it has been concluded that the activity beneath this depth range and that recorded upwards and reaching the crust/mantle boundary is not well located. The situation is similar but less apparent in central Chile. In Peru and Ecuador, the recorded seismic activity below the 80-100 km depth range is much lower. In the area of Ecuador where Gutscher et al. (2000) proposed a flat WBZ, Guillier et al. (2001) showed that the real WBZ can be defined only through intensive local seismological studies. Also, it is worth noting that the high activity observed in NW Argentina at 31-32 °S decreases strongly northwards. Special thermal features of these areas, fluid pulsation phenomena and fault systems and sutures may play an important role. Nucleation of crustal and upper mantle earthquakes occurs close to the level of highest strength where distorsional strain energy is maximum (Bullen and Bolt, 1985).

In Chile (26.5-28.5°S), local seismicity reported by Monfret et al. (2000) describes accurately a WBZ that is not subhorizontal as proposed by previous models. A marginal evidence of the absence of flat WBZ can be taken from Lemoine et al. (2001) that studying a series of earthquakes in central Chile (30-31.5°S) find a reverse pattern of the incremental Coulomb stress for the main earthquake. The slab-push mechanism of this earthquake is then described as a not rare mechanism in nearly flat WBZ in Chile, Peru and Mexico (Lemoine et al., 2001). Norabuena et al. (1994) modeling seismologically a flat subducting slab at 100 km depth beneath central-northern Peru, and using a festooning ray with several reflections inside the slab, by no means could explain the velocities in excess obtained for the flat structure.

CONCLUSIONS

There are not flat WBZ beneath the central and southern Andes. The seismic activity with clusters at depths from about 70 to 100 km is occurring in the continental upper mantle as follows from geotherms and rheological zonation of the lithosphere. Recent seismological studies have been used to confirm this conclusion. Advanced geophysical research is needed to determine the degree of annihilation of the real WBZ in these regions.

REFERENCES

Bullen K.E. and Bolt B.A. 1985. An Introduction to the Theory of Seismology. Cambridge University Press.

Campos J.et al. A seismological study of the 1835 seismic gap in south central Chile.Phys.EarthPlanet.Int.(in press)

Casquet C. et al. 2001. Involvement of the Argentine Precordillera terrane in the Famatinian mobile belt: U-Pb SHRIMP and metamorphic evidence from the Sierra Pie de Palo. Geology, 29, 703-706.

Chapman D.S. and Furlong K.P. 1992. Thermal state of the continental lower crust. Dev.Geot.23, Elsevier,179-199.

Guillier B. et al. 2001. Seismological evidence on the geometry of the orogenic system in central-northern Ecuador (South America). Geophys. Res. Lett., 28, 3749-3752.

Gutscher M.A. et al. 2001. Can slab melting be caused by flat subduction? Geology, 28, 535-538.

Hamza V.M. and Muñoz M. 1996. Heat flow map of South America. Geothermics, 25, 599-646.

Hofmeister A.M. 1999. Mantle values of thermal conductivity and the geotherm from phonon lifetimes. Science, 283, 1699-1706.

Karato S. and Wu P. 1993. Rheology of the upper mantle: A synthesis. Science, 260, 771-777.

Jaupart C. and Mareschal J.C. 1999. The thermal structure and thickness of continental roots. Lithos, 48, 93-114.

Lemoine A., Madariaga R. and Campos J. 2001. Evidence for earthquake interaction in central Chile: the july 1997-september 1998 sequence. Geophys. Res. Lett., 28, 2743-2746.

Magnitsky V.A. 1971. Geothermal gradients and temperatures in the mantle and the problem of fusion. J. Geophys. Res., 76, 1391-1396.

Monfret T. et al. 2000. An accurate Wadati-Benioff zone around Copiapo, northern Chile, using offshore and inland recordings. Abstract Meeting of the European Geophysical Society, Nice, April 2000.

Muñoz M. 1994. Reologia de la litosfera en Norte Chico y Region de los Lagos (Chile). VII Congreso Geologico Chileno, Concepcion, Actas, Vol. 1, 674-678.

Norabuena E.O., Snoke J.A. and James D.E. 1994. Structure of the subducting Nazca plate beneath Peru. J. Geophys. Res., 99, 9215-9226.

Petrini K. and Podladchikov Yu. 2000. Lithospheric pressure-depth relationship in compression regions of thickened crust. J. metamorphic Geol., 18, 67-77.

Ranalli G. 1991. Regional variations in lithosphere rheology from heat flow observations. In: Cermak V. and Rybach L. (Eds.) Terrestrial Heat Flow and the Lithosphere Structure, Springer, Berlin, 1-22.

Rudnick R.L., McDonough W.F. and O'Connell R.J. 1998. Thermal structure, thickness and composition of continental lithosphere. Chemical Geology, 145, 395-411.

Seipold U. 1998. Temperature dependence of thermal transport properties of crystalline rocks – a general law. Tectonophysics, 291, 161-171.

Smalley R. Jr. et al. 1993. Basement seismicity beneath the Andean Precordillera thin-skinned thrust belt and implications for crustal and lithospheric behavior. Tectonics, 12, 63-76.

Tavera H. and Buforn E. 2001. Source mechanism of earthquakes in Peru. Journal of Seismology, 5, 519-539.

Wilks K.R. and Carter N.L. 1990. Rheology of some continental lower crustal rocks. Tectonophysics, 182, 57-77.

SEISMIC STRATIGRAPHY AND TECTONICS OF THE TUCUMÁN BASIN (CRETACEOUS CONTINENTAL RIFT OF SOUTH AMERICA)

María M. PACHECO (1), Nélida Y. MANSILLA (2), Ricardo MON (3)

(1)Goebenstr.15, 30163 Hannover Germany. mp_30163@yahoo.com
(2)Universidad Nacional de Tucumán, Miguel Lillo 205, 4000 Tucumán. Argentina. mansill@unt.edu.ar
(3)Universidad Nacional de Tucumán-CONICET, Miguel Lillo 205, 4000 Tucumán, Argentina. monr@satlink.com

KEY WORDS: Andes Seismostratigraphy Rifting Cretaceous Growth-faulting

INTRODUCTION

The Andean foreland between 26° 30′ and 28°00′ S lat. coincides with a tectonic and topographic depression covered by Quaternary sediments (Fig. 1a). The relief is completely flat and there are no outcrops of rocks older than Quaternary. The mountains bordering the basin are formed by crystalline basement. The crystalline basementis covered by minor Cretaceous and Tertiary units. The southern end of the Eastern Cordillera, formed by low-grade Proterozoic basement cored anticlines, plunges to the south beneath the north border of the depression. In the mountains sourrounding the Tucumán basin there are no signs of Paleozoic depositional successions, and the Cretaceous beds of the Salta Group, which are thousands of meters thick northward of 26° S lat., are poorly represented. In the southwest part of the depression, the Miocene beds lie directly on the crystalline basement. The interpretation of an intersecting network of conventional reflection seismic lines provides evidences about the basement floor geometry of the Tucumán basin. The data represented on the map (Fig. 1a) are two-way travel times (Pacheco et al., 2000). It was possible to recognize a narrow NNE-SSW rift located eastward of the Andean border and aligned with a major regional Cretaceous rift which affected most of the Southamerican continent (Fig. 1b). In the rift two depocenters close to each other were recognized (Fig. 1c y d). In the deepest depocenter of the basin (1c), a sedimetary sequence about 6800 m thick was recognized. The precise composition of the beds forming the sedimentary fill of this basin is unknown because of the absence of drillings deeper than 500 m. The deepest part of the basin is beneath Santa Rosa de Leales (Fig, 1a and 1c). The isochrone lines in Fig. 1c represent the configuration of the top of the syn-rift sequence B (Fig. 2a and 2b), this map view of the basin indicates the two depocenters and the asymmetric shape of the basin, with its west side much steeper than the east one. The seismic cross-sections of Fig. 2a and 2b show different unconformities bounded stratigraphic sequences. The E-W oriented section 2a shows the westward verging deep thrust which passively transports the whole rift to the west. In the west part of the section the crystalline basement is involved in the Andean Tertiary faulting, to the east it is affected only by synsedimentary normal faults. These normal faults, representing the west border of the rift, involve the deepest A sequence and they are unconformably covered and sealed by sequence B. Which is also unconformably covered by the post-rift beds belonging to the C, E and F units. The post-rift beds are involved in the Tertiary compressive deformation. The thick beds represented by sequence F are probably of Miocene age. The older syn-rift beds aresupposed to be Cretaceous.

The easternmost reverse fault registered in this section could represent the inverted border of the rift. In the section 2b the deepest part of the Cretaceous basin is registered. The western border of the main depocenter is a Cretaceous normal fault partially inverted during the Tertiary movements. The sequence B is restricted only to the deepest part of the depocenter. Because of the asymmetric shape of the rift, it is much more extended to the east than to the west (Fig. 2b). In this section the oldest sequence A, present in section 2a, is not represented. The sequence F is younger than to the Cretaceous rift, it is syntectonic deposit in relation to the Tertiary Andean orogeny, in the extreme west of the section it grows from the Cenozoic tectonic front.

CONCLUSIONS

The reflection seismic lines add considerable detailed information about the subsurface features of the Tucumán basin. In the extensional synorogenic rift sequence it was possible to recognize at least four unconformity bounded stratigraphic sequences, sealed by the Miocene which at the west border of the basin are involved in the Cenozoic Andean deformation (Fig. 2a and 2b). Considering both seismic sections, a northward migration of the basin openingcan be detected. In section 2b the sequence B is much thicker and extended than in section 2a. The oldest sequence A of section 2a is not represented in section 2b; this confirms the migration of the sedimentation. The Tucumán basin may represent a buried segment of the major suite of Cretaceous rift basins extending from the coast of Perú to the Atlantic coast (Fig. 1b). To the north it is linked with the Salta rift widely exposed north of 26° S lat. (Salfity, 1982, Welsink et al. 1995) and its southward continuation could coincide with the Cretaceous inverted rift exposed in the north end of the Pampeanas Ranges of Córdoba (Schmidt et al. 1995).

REFERENCES

Pacheco,M.M., Mansilla,N.Y., Mon,R., Sosa,J., Piccioni,L, 2000, The Tucumán Basin as a part of the Cretaceous ontinental Rift of Southamerica : XVII Geowissenschatfliches Lateinamerika-Kollokium (Profil 18-digital publication).

Salfity, J.A., 1982, Evolución paleogeográfica del Grupo Salta (Cretácico-Eogénico), Argentina. Actas del V Congreso Geológico Latinoamericano de Geología: v. 1, p. 11-26, Buenos Aires.

Schmidt,C.J., Astini, R.A., Costa, C.H. Gardini, C.E., Kraemer, P.E., 1995, Cretaceous rifting alluvial fan sedimentation and Neogene inversion, southern Sierras Pampeanas, Argentina, in A.J. Tankard, R. Suárez S. and H.J. Welsink, Petroleum basins of South America: AAPG Memoir 62, p.341-358.

Welsink, C.J., Martínez, E., Aranibar, O and Jarandilla, J. 1995. Structural inversion of Cretaceous rift basin, southern Altiplano, Bolivia, in A.J. Tankard, R. Suárez S. and H. J. Welsink, Petroleum basins of South America: AAPG Memoir 62, p.305-324.

Acknowledgement: We thank to Prof.Dr.Francesc Sàbat for his suggestions and the review of this paper, as well as Mr. Trappe (TEEC Consultant, Germany) and Mr. Luterstein (CNEA, Argentina) for their comments. The seismic lines were provided by Dr. Sosa Gómez.

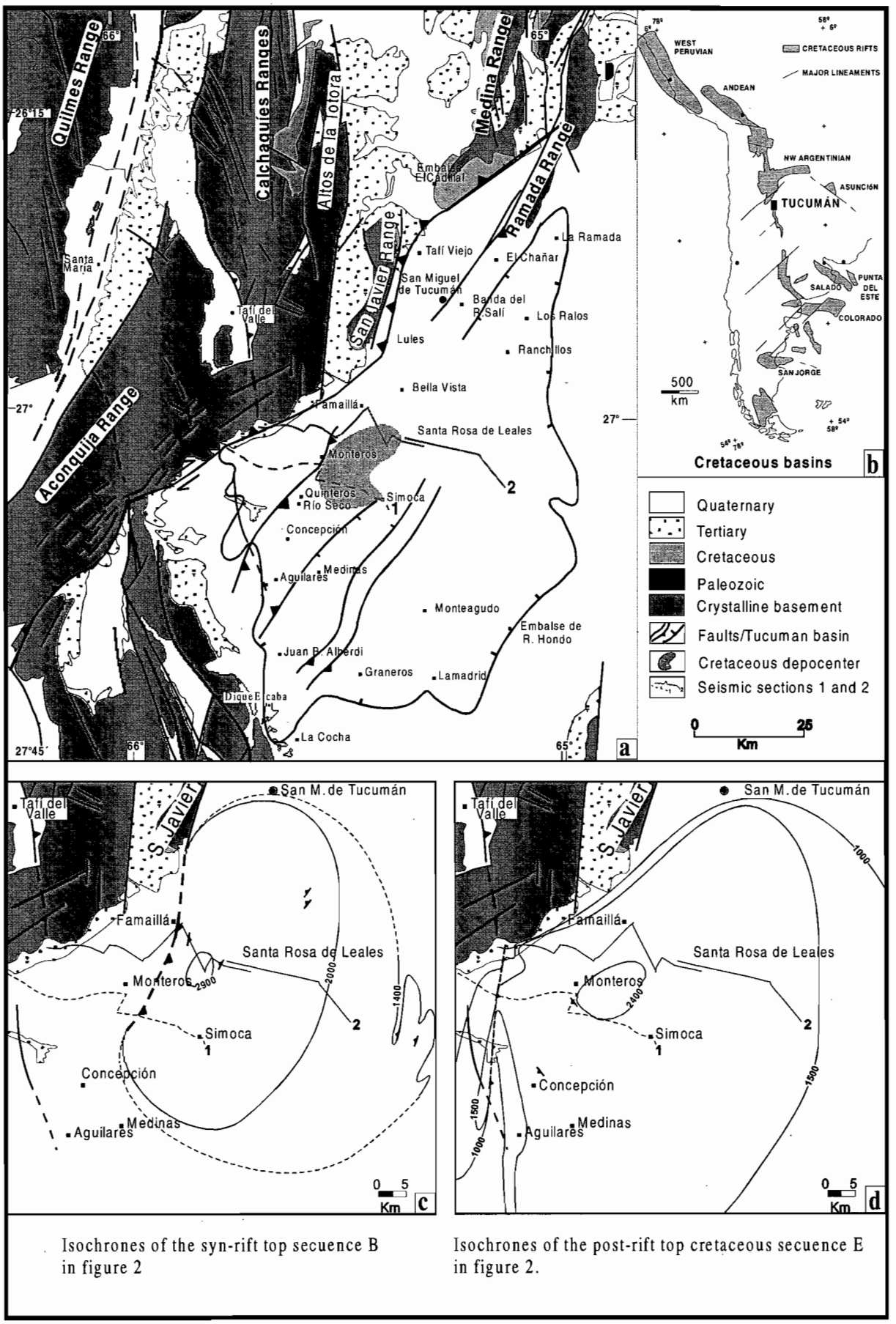

Isochrones of the syn-rift top secuence B in figure 2

Isochrones of the post-rift top cretaceous secuence E in figure 2.

Figure 1

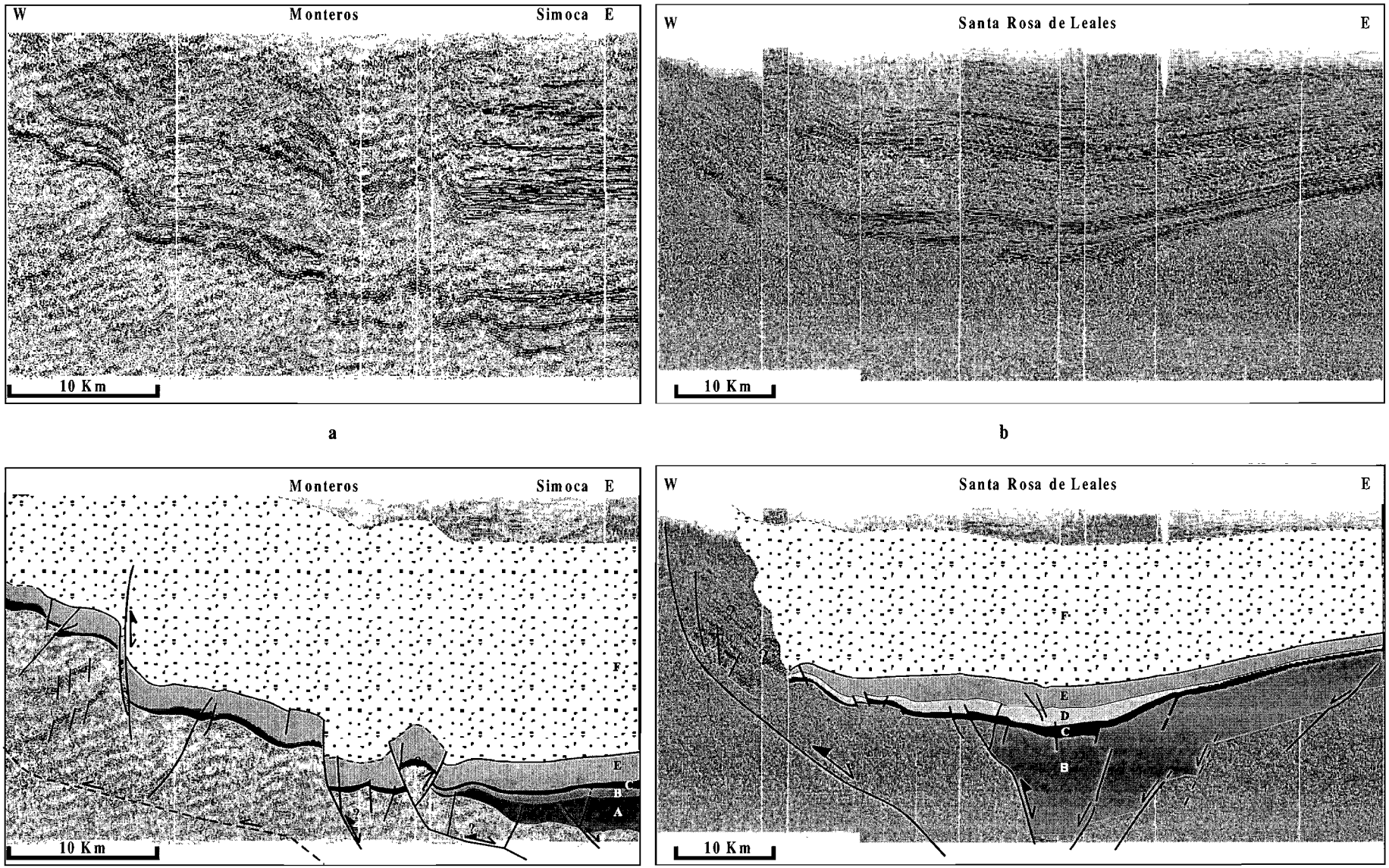

Figure 2: Seismic sections 1 and 2 indicated in figure 1. Lower interpreted: A, B, C, D, E (cretacics) and F (tertiary), seismic secuence.

NEOGENE IGNIMBRITES IN THE AREA OF AREQUIPA, SOUTHERN PERU: CORRELATIONS BASED ON FIELD OBSERVATIONS, GEOCHEMISTRY AND GEOCHRONOLOGY

Perrine PAQUEREAU (1), Jean-Claude THOURET (1), Gerhard WÖRNER (2), and Michel FORNARI (3)

(1) Laboratoire Magmas et Volcans, Université Blaise Pascal et CNRS, 63038 Clermont-Ferrand, France (P.Paquereau@opgc.univ-bpclermont.fr) (thouret@opgc.univ-bpclermont.fr)

(2) GZG, Abt. Geochemie, Goldschmidstrasse 1, Universität Göttingen, 37077 Göttingen, Germany (gwoerne@gwdg.de)

(3) IRD, UMR Géosciences Azur, Sophia Antipolis, Parc Valrose, 06108 Nice cedex 2, France (fornari@unice.fr)

KEY WORDS: ignimbrite, Arequipa, Peru, correlation, mineralogy, chronology.

INTRODUCTION

In the area of Arequipa, the ignimbrites termed "sillars" (Fenner, 1948; Jenks and Goldich, 1956) are indurated, generally nonwelded pyroclastic-flow deposits of dacitic and rhyolitic composition and middle Miocene to late Pliocene in age (this study). They encompass incipiently welded or sintered vitric tuffs, indurated by vapor-phase crystallisation, and previously welded but devitrified tuffs. They mantle an area of roughly 600 km² around the quaternary stratovolcanoes of Chachani and Misti and they fill the depression of Arequipa with a thickness of 100 m to as much as 200 m in the Rio Chili canyon (Fig.1). Similar ignimbrites

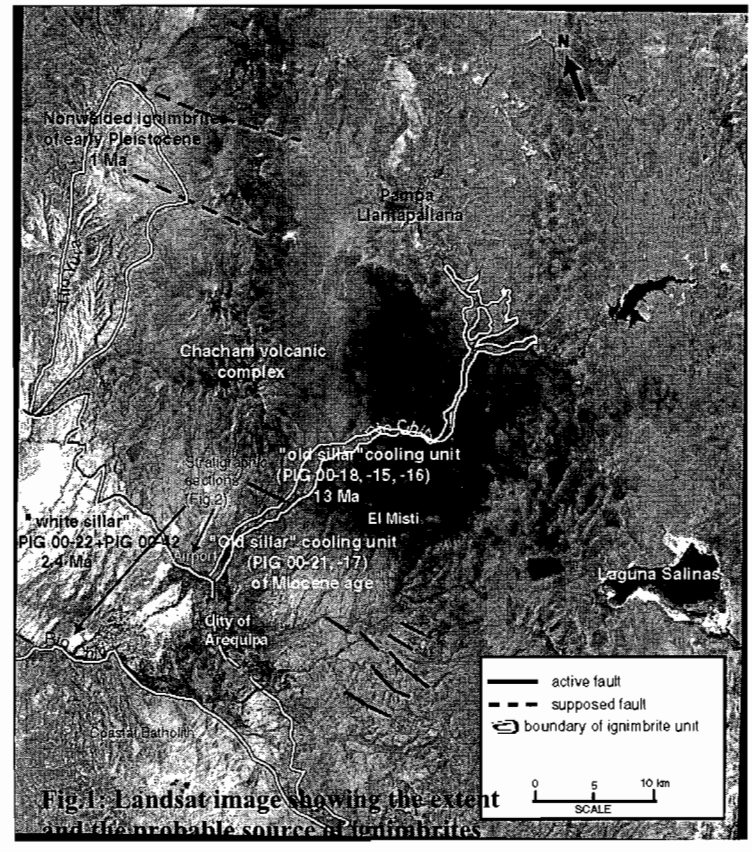

Fig.1: Landsat image showing the extent and the probable source of ignimbrites

have flowed downvalley the Rio Chili and Rio Yura at least 30 km south and southwest of Arequipa beyond the confluence of the three rivers into the Rio Vitor canyon.

Figure 2 shows two stratigraphic sections in the valley of Rio Chili that cuts the flank of the Western Cordillera. They encompass two ignimbrite cooling units above the Jurassic basement: the devitrified, welded 'old sillar' comprises at least two flow units, the lowermost is strongly welded bearing fiammes. The 'old sillar' yielded Ar-Ar

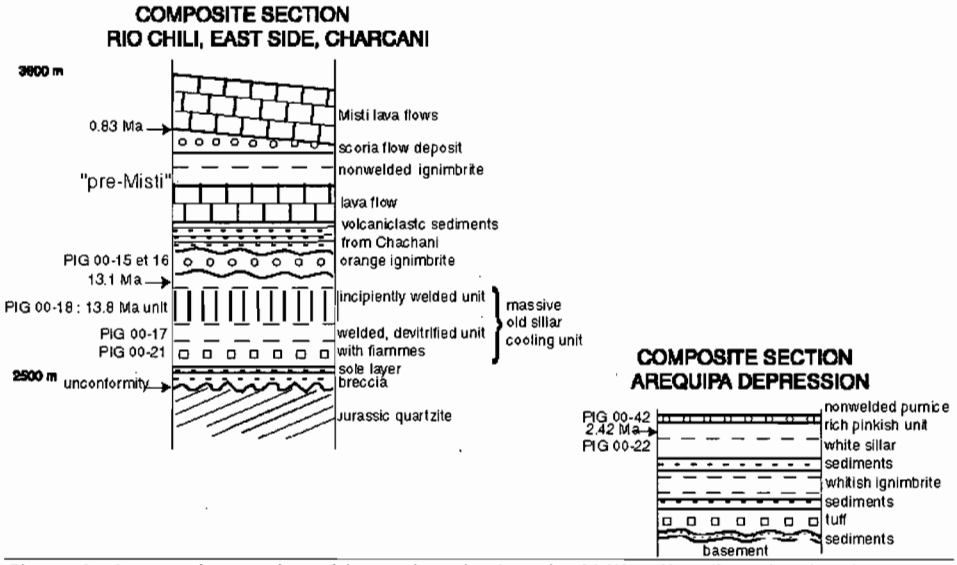

Figure 2: Composite stratigraphic sections in the Rio Chili valley (location in Fig.1)

Ages of 13.8±0.1 and 13.12±0.05 Ma (on biotite single grain). This Miocene ignimbrite is overlain by a 'orange' nonwelded unit of pumice-rich flows. In the Rio Chili valley, the ignimbrites are overlain by volcaniclastic sediments of Plio-Quaternary age and in turn by the lava flows of the base of El Misti stratovolcano (0.833 ± 0.06 Ma whole rock; Thouret et al., 2001).

At least three ignimbrites intercalated with sediments fill the depression of Arequipa. Two 'white sillars', i.e. indurated, nonwelded, crystal-rich vitric tuffs, form the piedmont of Chachani volcanic massif and fill the depression of Arequipa. Towards the WSW of the depression, thick ignimbrites fill paleovalleys and part of the Rio Vitor canyon. The upper whitish ignimbrite (Airport quarry, 2.42 ± 0.11 Ma fission-track Age on glass, *in* Vatin-Perignon et al., 1996) apparently flowed from a NE direction (Fig. 2). One similar whitish ignimbrite (La Joya, Ar-Ar Age of 4.87±0.02 Ma on sanidine) flowed down the Rio Chili valley and ran up the 350-m-high scarp of the coastal batholith south of Arequipa. Finally, on the western side of the Chachani volcanic complex, several nonwelded pumice-flow deposits have filled the Yura valley and flowed downvalley towards the confluence of Rio Vitor. One of these pumice-flow deposits has been dated at 1.02±0.09 Ma (Ar-Ar on biotite).

The goal of our study is to correlate the neogene ignimbrites and to point to their geographic source(s), such as calderas. We have thus used petrological, mineralogical, geochemical analysis, as well as paleomagnetic measurements (Paquereau et al., this volume), for correlating the ignimbrites over widespread areal extents.

GEOCHEMICAL AND MINERALOGICAL CORRELATIONS

1- Petrologic characteristics

The vitric tuffs are pumice and glass rich (50% to 70%), including obsidian. They also contain free crystals (15% to 30%), and accidental fragments, Jurassic sediments and andesite (5% to 10%). Pumice and rocks fragments are surrounded with matrix which contains glass shards and plagioclase microlites. Crystal content ranges between 15% and 40%, and crystals consist of feldspar (plagioclase and sanidine), quartz, biotite, amphibole, and iron-titanium oxyde.

Correlations are based on components proportions (glass and pumice, free crystals, accidental fragments), and percentages of mineral phases. For example, the ignimbrite unit PIG 00-18 is unique in being porphyric and rich in amphiboles, which are absent in the majority of samples. Samples PIG 00-16, -42, -20 rocks are aphyric, with 5% of crystals only. The size of phenocrysts, being highly variable, does not provide a discriminant feature.

2- Mineralogical correlations

Mineral analyses were made using the JEOL JXA 8900R microprobe of the University of Göttingen, on minerals sections and glass shards.

Oxides are present in all samples and the MgO/FeO ratio for titano-magnetites provides discriminative values (Fig. 3). Point analyses on glass shards in matrix or pumice glass, provide good discriminant results.(CaO versus Al_2O_3.diagram : Fig. 4). Figures 3 and 4 show five groups of sillars: group I = most mafic ignimbrite (PIG 00-18) ; group IIa = quite evolved compositions ignimbrites (PIG 00-17) ; group IIb = evolved compositions with large range in degree of differenciation (PIG 00-15, -16, -42, -22) ; group IIc =.PIG 00-20 ; group III (PIG 00-19 and –21).

The feldspars and biotites show a wide range in composition in each ignimbrite unit, therefore adding little discriminative value. Amphiboles which are present in three samples (PIG 00-18, PIG 00-19, and PIG 00-21), are more discriminant. These calcic amphiboles (11% in wt%) show magnesio-hornblende and actinolitic-hornblende composition. The MnO versus Al_2O_3 plot for hornblende is the best discriminant, enabling us to distinguish two compositional groups: PIG 00-18 with high AL_2O_3 (8-9%) and low MnO (0.4-0.6%) and PIG 00-19 and –21, with high Mno (1-1.20%) and low Al_2O_3 (4-5%).

3- Correlations with stratigraphy

These geochemical and mineralogical groups coincide roughly with the pre-established stratigraphy. Group I (PIG 00-18) is dated at 13.8-13.1 Ma using the Ar-Ar method and is termed “old sillar”. Group I underlies rocks PIG 00-15, -16 ("orange cooling unit"), wich belong to the younger ignimbrite type (“white sillar” ignimbrite sequence), is located in compositional group IIb. Ignimbrite unit PIG 00-22, which is locally termed "white sillar", is mineralogically similar to the “orange cooling unit”, and so was linked to it in group IIb. The “pink unit” (PIG 00-42), overlying the “white sillar” and similar in mineralogy, represents the top of the entire ignimbrite sequence. The group IIb present a fractionation trend. The PIG 00-17 ignimbrite unit is stratigraphically beneath PIG 00-18, thus slightly older than 13.8 Ma. The distinct composition of PIG 00-17

points to the group IIa. The group III (PIG 00-19 and -21) comprises two units which belong to the 'old sillar' probably Miocene in age. The whitish, devitrified facies with quartz and sanidine of these two units show similar petrologic and mineralogic characteristics.

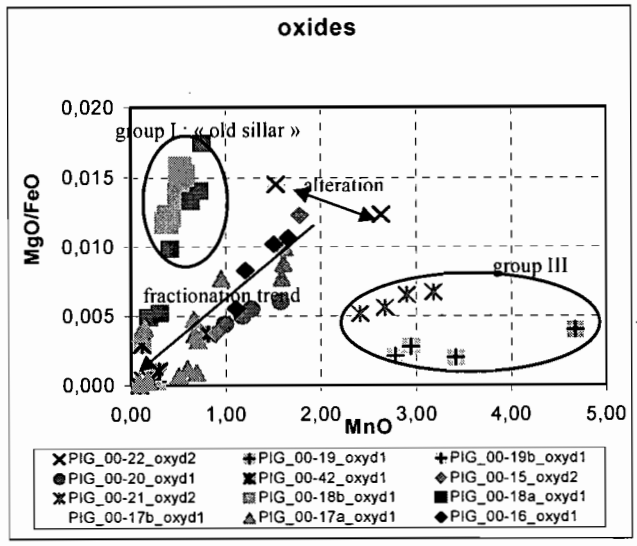

Figure 3: MgO/FeO v. MnO diagram for titano-magnetites

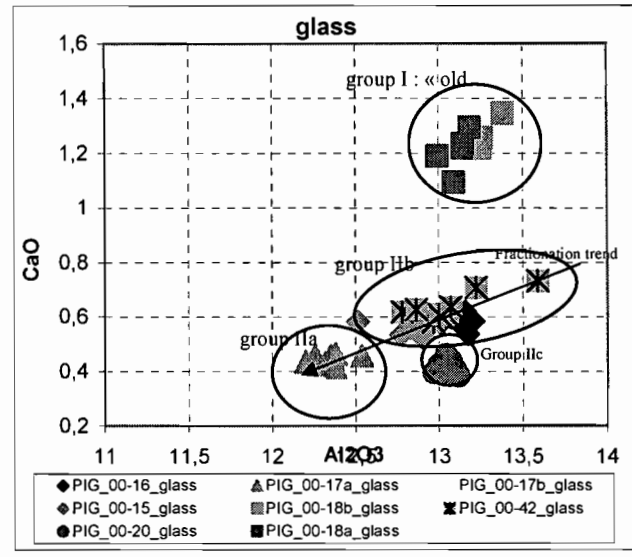

Figure 4: CaO v. Al_2O_3 diagram for glass

CONCLUSION

In order to fingerprint ignimbrites, correlation must depend on a combination of criteria, as suggested by Hildreth and Mahood (1985): careful mapping, field characteristics and geochronology, combined with mineral chemistry or whole-rock chemistry of the juvenile component, glass chemistry of the ignimbrites, and paleomagnetic caracteristics of the ignimbrites (Paquereau et al., this volume). Finally, we aim to localize the geographic source(s), i.e neogene calderas, of the ignimbrites. Our investigation is based on the structural interpretation of one DEM (30m*30m) based on digitized topographic maps and on radar interferometry, as well as Landsat and SPOT satellite images. We also use new ASM data (Paquereau et al., this volume) to attempt to localize the source area. The source of the "white sillar" ignimbrite of Pliocene age is thought to be located NE of the Arequipa depression. At this stage, the study is too preliminary to identify clearly a source for the ignimbrites.

REFERENCES

Fenner C.N., 1948, Incandescent tuff flows in southern Peru, Geological Society of America Bulletin, 59, 879-893.

Hildreth W. and Mahood G., 1985, Correlation of ash-flow tuffs, Geological Society of America Bulletin, 968, 968-974.

Jenks W.F.and Goldish S.S., 1956, Rhyolitic tuff flows in southern Peru, Journal of Geology, 64, 156-172.

Thouret J.C., Finizola A., Fornari M., Legeley-Padovani A., Suni J., Frechen M., 2001, Geology of El Misti volcano near the city of Arequipa, Peru. Geological Society of America Bulletin, 113, 12, 1593-1610.

Vatin-Perignon N., Oliver R., 1996, Trace and rare-earth element characteristics of acidic tuffs from Southern Peru and Northern Bolivia and a fission-track age for the Sillar of Arequipa, Journal of South America Earth Science, 9, 91-109.

MAGNETIC FABRIC AND FIELD EVIDENCE FOR THE CONSTRUCTION OF THE CALEU PLUTON BY MULTIPLE INJECTIONS AND DOMING COAST RANGE OF CENTRAL CHILE

Miguel A. PARADA (1), Pierrick ROPERCH (2,1) and Claudio GUIRESSE(1)

(1) Departamento de Geología, Universidad de Chile. Casilla 13518, Correo 21, Santiago, CHILE (email:maparada@cec.uchile.cl)
(2) Institut de Recherche pour le Development (IRD). Casilla 53390,Correo Central, Santiago, CHILE (properch@cec.uchile.cl)

KEY WORDS: magnetic fabric, pluton, emplacement

INTRODUCTION

Recent field studies on mid- and upper-crustal plutons of different tectonic setting, combined with modelling of emplacement mechanism have shown laccolith-type geometry (fed by vertical dikes), which result from a mechanism of space generation dominated by roof uplift and/or floor depression (e.g. Petford, 1996; Benn et al., 1998). This study presents the results concerning with the construction of a typical Andean shallow-emplaced granitoid pluton, based on the combination of magnetic fabrics and field observations. The dominant processes in the construction of the pluton were 1) multiple upward magma injections by dikes, and 2) thickening of laccolith-shaped pluton by roof doming to accomodate the increasing volume of magma.

THE CALEU PLUTON

The Caleu pluton, located in the Coast Range of central Chile c. 40 km northwest from Santiago, corresponds to the late (94.5 ± 2.2 Ma) event of the Early Cretaceous magmatism. Strata of its volcano-sedimentary envelope were deposited in a Early Cretaceous subsiding basin (Vergara et al., 1995) and currently are tilted about 30-50° to the east. Testimony of the roof have been locally observed near the southern end of the pluton. The anatomy of the pluton consists in three N-S elongated zones (Fig. 1), which define an accross-pluton compositional variation characterized by a westward increase in SiO_2 content. The three zones are: Gabbro-Diorite Zone (GDZ),

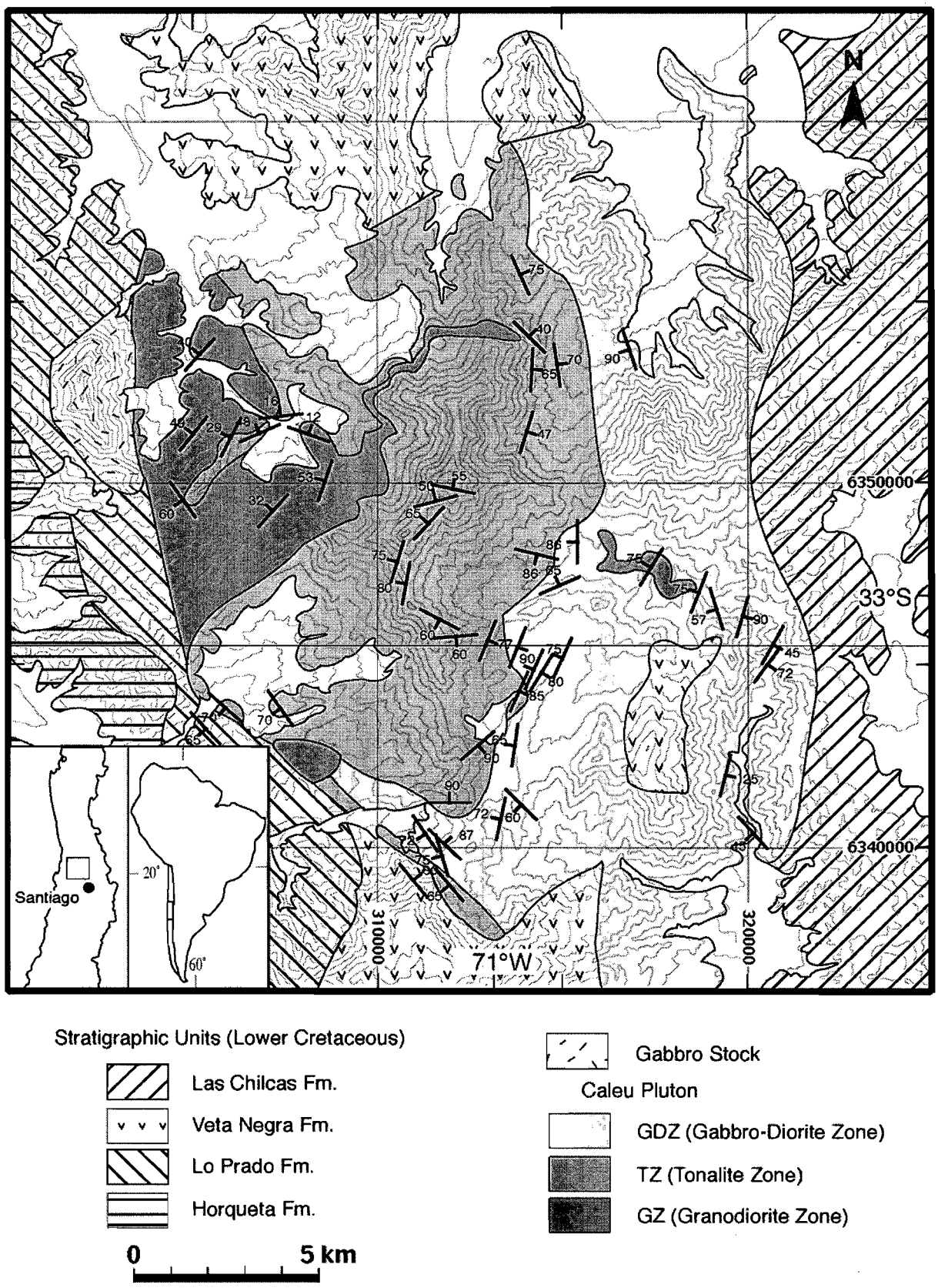

Figure 1: Geological map of the Caleu Pluton. Magnetic foliations define large-scale magmatic structures within the different Pluton units. The numerical values correspond to the dip of the foliation planes.

Tonalite Zone (TZ) and Granodiorite Zone (GZ). The zones were emplaced episodically from mafic to felsic, and their distinct compositional characteristics were not acquired *in situ* but in a subjacent stratified reservoir (Parada et al., 2002). Magnetite is the the ferromagnetic minerals that, by far, make the most significant contributions to the magnetic susceptibility of the three zones, followed by the paramagnetic minerals (mainly biotite and hornblende).

The pluton as a whole is macroscopically isotropic. However, a strong tectonic deformation and recrystallization is locally observed in a rock strip of few meters width along the southwestern margin. This deformation is indicated by a N40°W/65°-80°SW foliation, and a stretching mineral lineation within the foliation plane. Some mafic varieties of the central part of the GDZ exhibit a magmatic mineral lineation, defined by the alignement of euhedral prismatic plagioclase and amphibole crystals.

REMANENT MAGNETIZATIONS AND ANISOTROPY OF MAGNETIC SUSCEPTIBILITY

A total of 547 cores were drilled at 68 sites within the different zones (Fig. 1). The highest values of magnetic susceptibility and remanent magnetization are found in the GDZ (0.04 – 0.1 SI), whereas the lowest values are observed in the GZ (0.01-0.02 SI). Remanent magnetization of samples from the GDZ is more stable than the remanent magnetization of samples from the GZ. This suggests that the increase in magnetite content from the GZ to the GDZ is not associated with an increase in grain size. Normal polarity of the remanent magnetization is observed at all sites. A well-defined characteristic magnetization was determined at 51 sites. Except at four sites near the eastern border of the pluton where deformation can be inferred from the paleomagnetic data, paleomagnetic results show very little dispersion within the three units. The average direction for the pluton (47 sites: declination: 12.4°; inclination: -55.7°; a95: 1.7°) is slightly different from the expected direction at 95Ma determined from the new Apparent Polar Wander Path [Besse and Courtillot; 2002] (declination: 355.7°; inclination: -53.7°). The difference is best explained by a clockwise rotation of the pluton of 16.7°±6.7. This implies that the pluton intruded after tilting of the host volcanic succession.

AMS was measured with the KLY3-S Agico Kappabridge. Five to ten samples were measured at each site. AMS is not very strong and the largest foliation values do not exeed 15%. Shapes of AMS ellipsoids are usually oblate and only a few sites show a prolate ellipsoide. Dip of the foliation planes are steep within the GDZ and TZ zones and shallow dips are observed in the Granite zone of the pluton (Figure 1). On the southwestern border of the Pluton, foliations are sub-parallel to the contact with the Veta Negra country rock. These NW oriented contacts have previously been interpreted as evidence for NW oriented sinistral fault zones. However, only steep vertical magnetic lineations are observed. Moreover remanent magnetizations within the Pluton and within the remagnetized Veta Negra country rock do not show evidence for significant deformation posterior to the intrusion.

SPACE CREATION

Despite the subquadratic shape in plan view of the whole pluton, the zones are elongated exhibiting predominantly concordant magnetic foliation as predicted by emplacement of vertical tabular bodies. It seems likely that each zone was feeded from its respective reservoir by dikes in an episodic way by considering the

westward progression of the zone emplacement with time evidenced by the observed intrusion of TZ into GDZ and GZ into TZ. The space creation for horizontal plutons has been mainly explained by stoping, roof lifting, floor depression, lateral magma propagation and a combination of them (Cruden, 1998). In the case of the Caleu pluton wall-rock xenoliths were not found, thus stoping would have not play a significant role as a mechanism of space creation. We think that roof lifting (doming) and floor depression would have operated. Doming can be evidenced by the dome-like structure generated by the magnetic foliation measured at the center of the pluton (Figure 1). The inflation of the Caleu pluton was produced by succesive pulses that pushed up earlier ones. The lower section of the dome consists of about 800 m of vertical exposure of mafic enclave-bearing tonalite. The upper section is abruptly marked by the ocurrence of enclave-free gabbro-diorites. The density inversion in this rock column is explained by a tonalitic intrusion nested into a previous gabbro-dioritic pulse. The mafic enclaves in the tonalite are crude testimony of mingling between the pulses, particulary if one considers that the larger amount of enclave are observed near the contact with the upper gabbro-diorite. Floor depression seems to be likely by considering the inferred presence of a subjacent reservoir from which the pluton was formed (Parada et al., 2002). In this scenario, downward displacement of the underlying host rocks is promoted by the crustal space vacated by the ascended magma.

ACKNOWLEDGMENTS This research was supported by FONDECYT Grant 1990980.

REFERENCES

Benn, K., Odonne, F. and de Saint Blanquat, M. 1998. Pluton emplacement during transpression in brittle crust: new views from analogue experiments. Geology, 26, 1079-1082.

Besse, J. and Courtillot, V. 2002. Apparent and true polar wander and the geometry of the Geomagnetic Field in the last 200 million years, J. Geophys. Res., *96*, in press.

Cruden, A.R. 1998. On the emplacement of tabular granites. Journal of the Geological Society, London, 155, 853-862.

Parada, M.A., Larrondo, P., Guiresse, C. and Roperch, P. 2002. Magmatic gradients in the Cretaceous Caleu pluton (central Chile): injections of pulses from a stratified reservoir. Gondwana Research, 5, 307-324.

Petford, N. 1996. Dykes or diapirs?. Transaction of the Royal Society of Edinburgh: Earth Sciences, 87, 105-114.

Vergara, M., Levi, B., Nyström, J. O. and Cancino, A. 1995. Jurassic and Early Cretaceous island arc volcanism, extension and subsidence in the Coast Range of central Chile. Geol. Soc. Am. Bull., 107, 1427-1440.

FLAT-SLAB SUBDUCTION ZONE IN CENTRAL CHILE-ARGENTINA: SEISMOTECTONIC AND BODY-WAVE TOMOGRAPHY FROM LOCAL DATA

Mario PARDO (1), Tony MONFRET (2), Emilio VERA (1), Alfredo EISENBERG (1), Stéphane GAFFET (2), Emilio LORCA (1), Adriana PEREZ (1)

(1) Departamento de Geofísica, U. de Chile. Blanco Encalada 2085, Santiago, Chile (mpardo@dgf.uchile.cl)
(2) UMR Géosciences Azur, IRD-CNRS. 250 A. Einstein, 06560 Valbonne, France (monfret@geoazur.unice.fr)

KEY WORDS: flat-slab subduction, central Chile-Argentina, body-waves tomography, seismotectonics

INTRODUCTION

The geodynamic and seismotectonic of central Chile-Argentina are mainly controlled by the subduction of the oceanic Nazca plate beneath the continental South American lithosphere, with a convergence rate of about 8 cm/yr in the N78°E direction (Fig. 1). In this area, the Nazca plate exhibits a flat-slab subduction zone from 28°S to 33°S at depths of ~100 km which extends eastward for hundreds of km before reassuming its downward descent (e.g., Cahill and Isacks, 1991). To the north there is a smooth transition of the slab dip, while to the south there is a sharp change from flat to steep subduction around 32°-33°S, implying bending or tears along the slab (Fig. 1). At the flat-slab zone large thrust and intraplate earthquakes have occurred, crustal shortening of about 150-170 km has been estimated (Allmendinger et al., 1990), and active volcanism is absent since 9-10 Ma (Kay et al., 1988).

In order to analyze the seismotectonic characteristics of this flat-slab region based on local seismicity, focal mechanisms and 3-D body-wave velocity models, we installed a temporary seismological network in central Chile between 30°S and 32°S (Fig. 1). Thirty eight short period stations with three-components and continuously recording, were deployed from Nov. 14, 1999 to Jan. 11, 2000, five of them in a small 100-m triangular array. Thereafter, only 18 stations recorded the seismic activity until March 3, 2000.

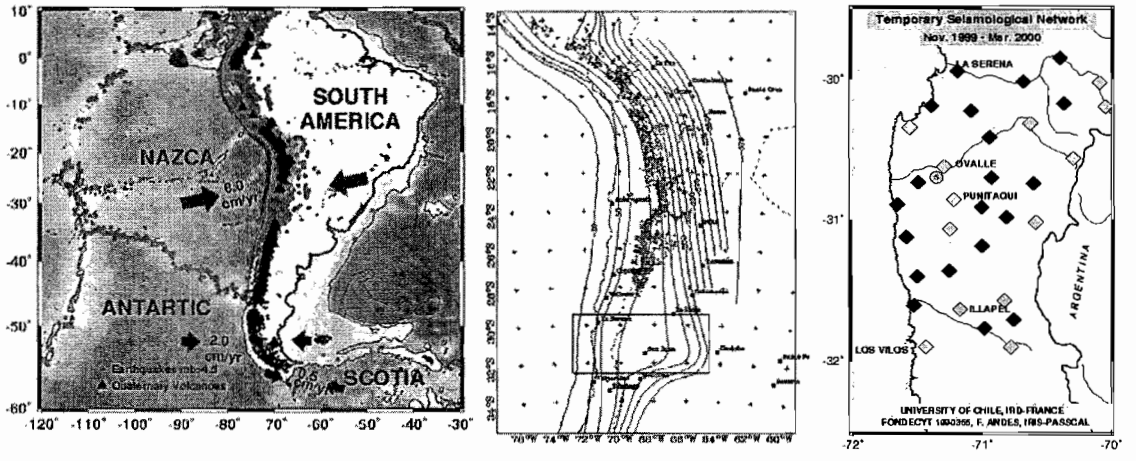

Figure. 1.- [Left] Global South American tectonics. [Center] Nazca plate iso-depth contours after Cahill&Isacks (1991); the rectangle shows the studied zone. [Right] Temporary seismological network deployed between 30°-32°S and used in this study. Stations provided by Iris/Passcal (black) and Lithoscope-France (gray).

DATA AND ANALYSIS

The local network recorded an average of 150 earthquakes per day, from which about half of them were recorded by at least 6 stations allowing a preliminary hypocentral determination. The magnitude of the recorded events ranges from $0.0<m<5.5$, with m determined from the waveform amplitudes and hypocentral distance, calibrated relative to mb from NEIC. The earthquake analysis software SEISAN (Havskov and Ottemöller) was used to create the database of waveforms and phase pickings, and to obtain preliminary hypocenter determinations and focal mechanisms (Fig. 2) based on a 1-D layered velocity model determined according to Kissling et al. (1994). Many of the events correspond to aftershocks of the 1997 Punitaqui earthquake, Mw=7.1, that occurred within the slab at 68 km depth (Fig. 3, Pardo et al., 2002a).

A joint stress tensor and fault plane solutions inversion (Rivera and Cisternas, 1990) was performed using the preliminary focal mechanisms. The results from local data show some differences compared to the obtained with reported mb>5 teleseismic events and focal mechanisms (Pardo et. al., 2002b). At shallow depths, 0-60 km, the teleseismic data show a compressive stress regime, while the local data indicate strike-slip faulting with the compressive principal stress axis ($\sigma 1$) almost parallel to the slab. The stress regime is mainly extensional from teleseismic data at intermediate depths, while the local data show that strike-slip events are predominant, probably due to reactivation of pre-existing faults within the slab and related to the subduction around 32°S of the Juan Fernández Ridge (JFR) (von Huene et al., 1997; Yáñez et al., 2001).

A local seismic tomography inversion was done in the zone using a subset of 1041 events (13295 P-phases and 13476 S-phases time readings) that were recorded by at least 9 stations (rms<0.25). The initial model for this inversion was the previously determined 1-D layered velocity model. We used an update version of Evans et al. (1994) procedure (Simul2000). The zone between 29.5°-32.5°, 69.5°-72.5°W and depths down to 150 km was parameterized in 22x21x18 nodes spaced horizontally in 20 km and vertically in 10 km.

The results are presented in E-W cross-sections showing the obtained 3-D P- and S-wave velocity models, and the final hypocenters relocated using the 3-D model (Fig. 3).

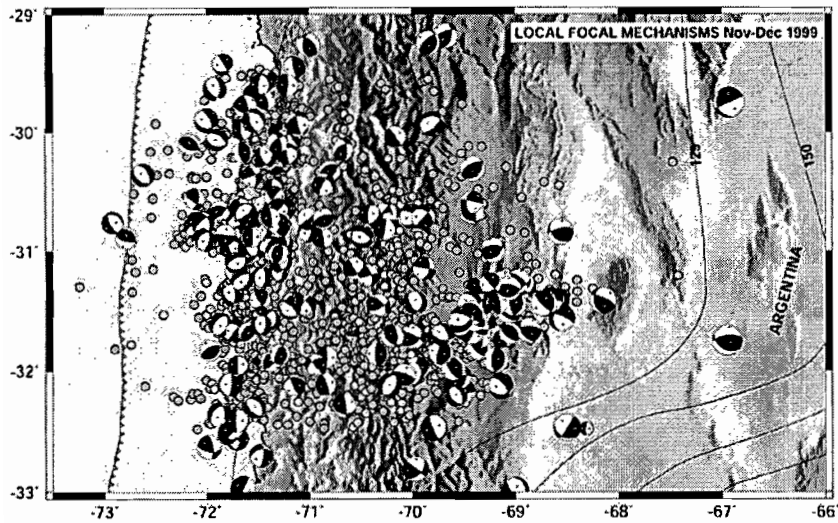

Figure 2.- Seismicity (gray circles) and preliminary focal mechanisms in lower hemispheric projection, of events recorded locally by the temporary network during Nov.-Dec., 1999. Location of the trench and iso-depth contours from Cahill and Isacks (1991) are shown as reference

Assuming that the mantle beneath the Moho interface has P and S waves velocities of about 8 km/s and 4.5 km/s respectively, the local tomography indicates that this interface is located at about 40 km depth below the coastal zone to the Andes foothills, and at about 70 km beneath the Andes cordillera (Fig. 3).

The Benioff zone is well defined by the seismicity and clearly shows the flat-slab subduction of Nazca plate at depths of 100 km. A thick ~30 km seismogenic zone is observed at the top of the downgoing slab, principally in the southern part of the flat-slab zone around the region where the JFR is being subducted. The continental shallow events at the fore-arc are mainly related to mine blasts; nevertheless some of them are crustal tectonic earthquakes. At the back-arc the shallow seismicity (Fig. 3) is associated to the crustal shortening and thin-skinned deformation in the Precordillera in western Argentina (Allmendinger et. al, 1990).

The slab can be correlated with high seismic velocities, particularly at intermediate depths, reaching ~8.5 km/s and ~5 km/s at 100 km depth for P- and S-wave respectively. A low P and S waves velocity anomaly is observed around 71°W, along the whole zone, at 60 km depth (Fig. 3). This depth is considered as the downdip limit of the interface between Nazca and South American plates (Pardo et al., 2002b).

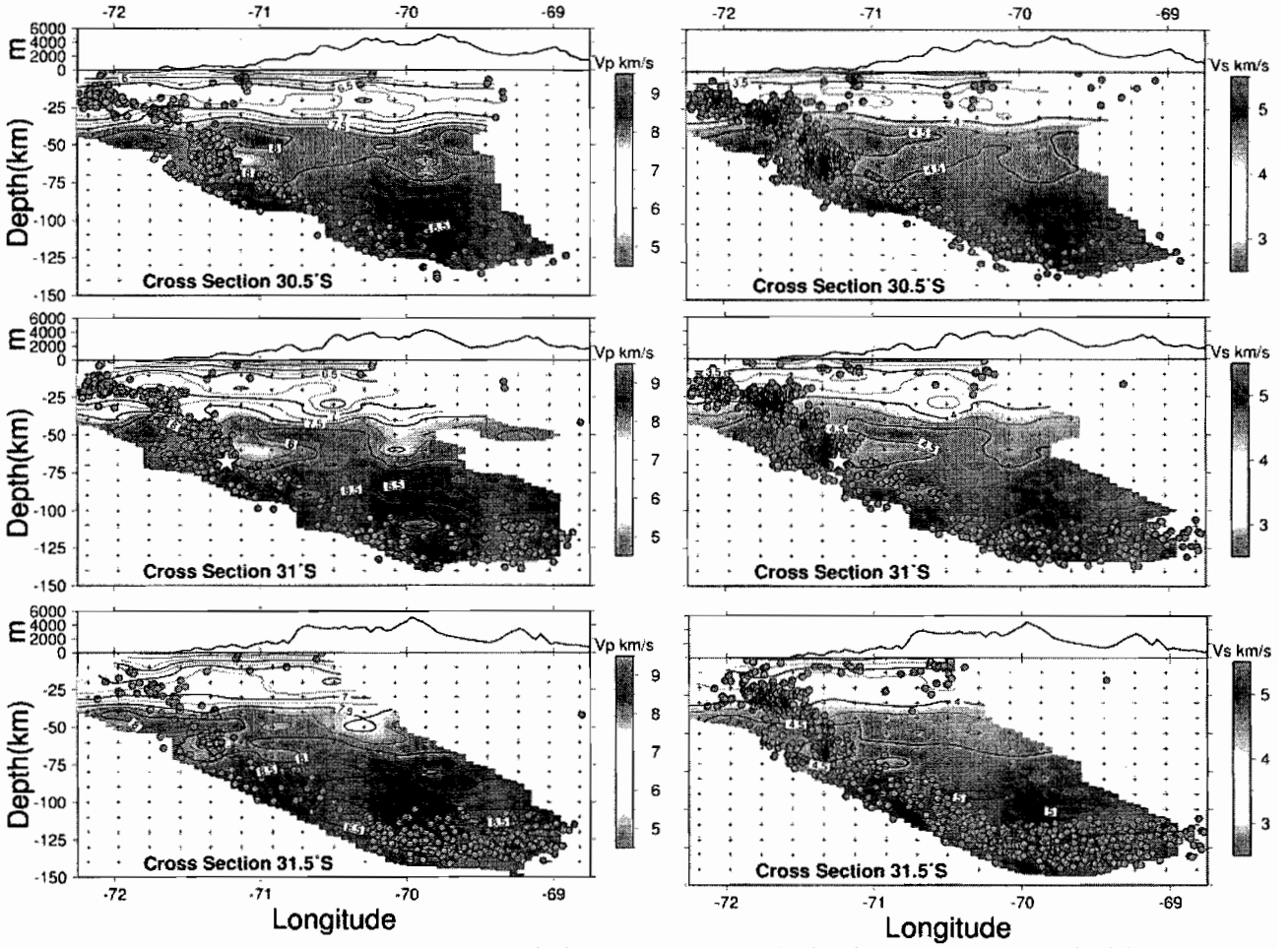

Figure 3.- E-W cross-sections showing body-waves velocity contours each 0.25 km/s only at resolved nodes, seismicity projected from a ±50 km band (circles) and nodes used in the inversion (crosses). The star indicates the location of the 1997 Punitaqui earthquake. At the top of each figure a cross-section of the topography is presented. [Left] P-wave velocity distribution and hypocenters used for the tomography (1041 events). [Right] S-wave velocity distribution and relocated events using the obtained 3-D model (2500 events).

CONCLUSIONS

The flat-slab subduction zone in central Chile-Argentina is analyzed based on local data from a temporary seismological network deployed for more than 3 month in central Chile, between 30°S and 32°S.

The results of the joint inversion of stress tensor and focal mechanisms show predominance of strike-slip faulting at intermediate depths, and strike-slip faulting with compression parallel to the slab at shallow depths.

The 3-D body wave velocity models determined by the local seismic tomography permits to estimate the shape and depth of the Moho discontinuity, and final hypocentral locations of earthquakes within the zone. The Benioff zone, related to the top of the seismicity, clearly shows that the slab is flat at depths of about 100 km. High velocity contrasts of P and S waves, particularly at intermediate depths, are well correlated with the seismicity and the geometry of the slab.

The anomalous thick seismogenic zone within the subducted Nazca plate can be correlated with the JFR subduction, suggesting a thick oceanic crust that might increase the buoyancy of the oceanic lithosphere that contributes to the slab flattening.

ACKNOWLEDGMENTS

We thanks for the instruments used in the temporary network to IRIS/PASSCAL and Lithoscope-France. This work was supported by grants Fondecyt 1990355, F. Andes C-13563, Ecos/Conicyt C00U02 and IRD-France.

REFERENCES

Allmendinger, R.W., Figueroa, D., Snyder, D., Beer, J., Mpodozis, C., Isacks, B., 1990. Foreland shortening and crustal balancing in the Andes at 30°S latitude. *Tectonics*, 9, 789-809.

Cahill, T., Isacks, B., 1992. Seismicity and shape of the subducted Nazca plate. *J. Geophyis. Res.*, 97, 17503-17529.

Evans, J.R., Eberhart-Phillips D., Thurber, C.H., 1994. User's manual for Simulps12 for imaging Vp and Vp/Vs: A derivative of the Thurber Tomographic inversion Simul3 for local earthquakes and explosions. USGS Open-File Report 94-431.

Havskov, J., Ottemöller, L., (Ed.). SEISAN: The earthquake Analysis Software. Institute of Solid Earth Physics, University of Bergen, Norway. (http://www.ifjf.uib.no/seismo/software/seisan.html)

Kay, S.M., Maksaev, V., Moscoso, R., Mpodozis, C., Nasi, C., Gordillo, C.E., 1988. Tertiary magmatism in Chile and Argentina between 28°S and 33°S: Correlation of magmatic chemistry with changing Benioff zone. *J. South American Earth Sciences.*, 1, 21-38.

Kissling, E., Ellsworth, W.L., Eberhart-Phillips, D., Kradolfer, U., 1994. Initial reference models in seismic tomography. *J. Geophys. Res.*, 99, 19635-19646.

Pardo, M., Comte, D., Monfret, T., Boroschek, R., Astroza, M., 2002a. The October 15, 1997 Punitaqui earthquake (Mw=7.1): A destructive event within the subducting Nazca plate in Central Chile. *Tectonophysics*, 345, 199-210.

Pardo, M., Comte, D., Monfret, T., 2002b. Seismotectonic and stress distribution in the central Chile subduction zone. In Press: *J. South American Earth Sciences.*

Rivera, L., Cisternas, A., 1990. Stress tensor and fault plane solutions for a population of earthquakes. *Bull. Seism. Soc. Am.*, 80, 600-614.

von Huene, R., Corvalán, J., Flueh, E.R., Hinz, K., Korstgard, J., Ranero, C.R., Weinrebe, W., and the CONDOR Scientists, 1997. Tectonic control of the subducting Juan Fernandez Ridge on the Andean margin near Valparaiso, Chile. *Tectonics*, 16, 474-488.

Yañez, G., Ranero, C., von Huene, R., Díaz, J., 2001. Magnetic anomaly interpretation across the southern central Andes (32°-34°S): The role of the Juan Fernandez Ridge in the late Tertiary evolution of the margin. *J. Geophys. Res.*, 106, 6325-6435.

EASTERN CORDILLERA FOLD-THRUST BELT, STRUCTURAL FRAMEWORK OF THE CENTRAL ANDES IN NORTHERN ARGENTINA

Gonzalo J. PEÑALOZA (1), Marcos J. JIMÉNEZ (2) and Ricardo MON (1)

(1) CONICET-Universidad Nacional de Tucumán, Miguel Lillo 205, Tucumán, CP 4000, Argentina. (gjp_salta@hotmail.com; monr@satlink.com)
(2) Fundación Miguel Lillo, Miguel Lillo 205, Tucumán, CP 4000, Argentina. (imajime@hotmail.com)

KEY WORDS: high-angle thrust sheets, Andean deformation

INTRODUCTION

The Eastern Cordillera of Argentina between 22° S-24° S represents a narrow basement-involved fold-thrust belt situated between two major geological domains, the Puna Plateau to the west and the Subandean Ranges to the east. The structural analysis led to interprete the area as a *"high-angle shear megazone"* shared in common with the Puna and thrust over the Subandean Ranges along a serie of faults composing the Main Andean Thrust. In this particular area of the Central Andes crustal shortening is related to deep-seated thrust surfaces detaching thick basement sheets. In spite of main thrusts belong to the Pliocene-Pleistocene interval is clear the influence of older structures. After a detailed analysis of minor faults two deformative episodes with contrasting directions where identified within such interval.

The structure of the Eastern Cordillera is characterized by N-S trending basement-involved folds, originally 5 km wavelenght at least, later dislocated by east-verging Pliocene-Pleistocene faults forming an imbricated thrust fan. Probably the original folds are the surface expression of deep propagation faults that do not crop-out. At a regional scale these folds represent second order folds developed on the flanks of two major anticlinorium structures westward and eastward of the Quebrada de Humahuaca respectively (Fig.1).

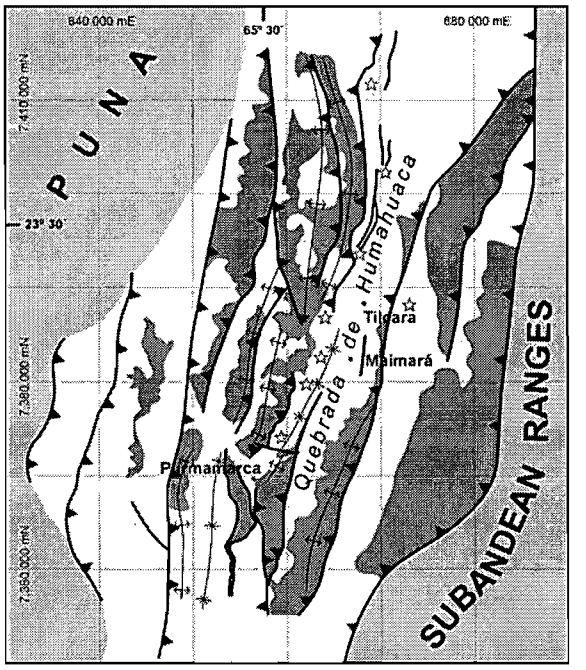

Figure 1. *Map showing main geological features of the area and minor-fault surveyed locations (*). Highlighted outcrops represent basement.*

Both anticlinorium structures would be related to a sole thrust located 20-25 km underneath the Eastern Cordillera from which two thick basement sheets detached and displaced upwards more than 6 km. It's remarkable the fact that at this latitude there are no evident diferences between Puna and Eastern Cordillera but only the geomorphological feature of a water divisory; therefore the Eastern Cordillera shares in common a

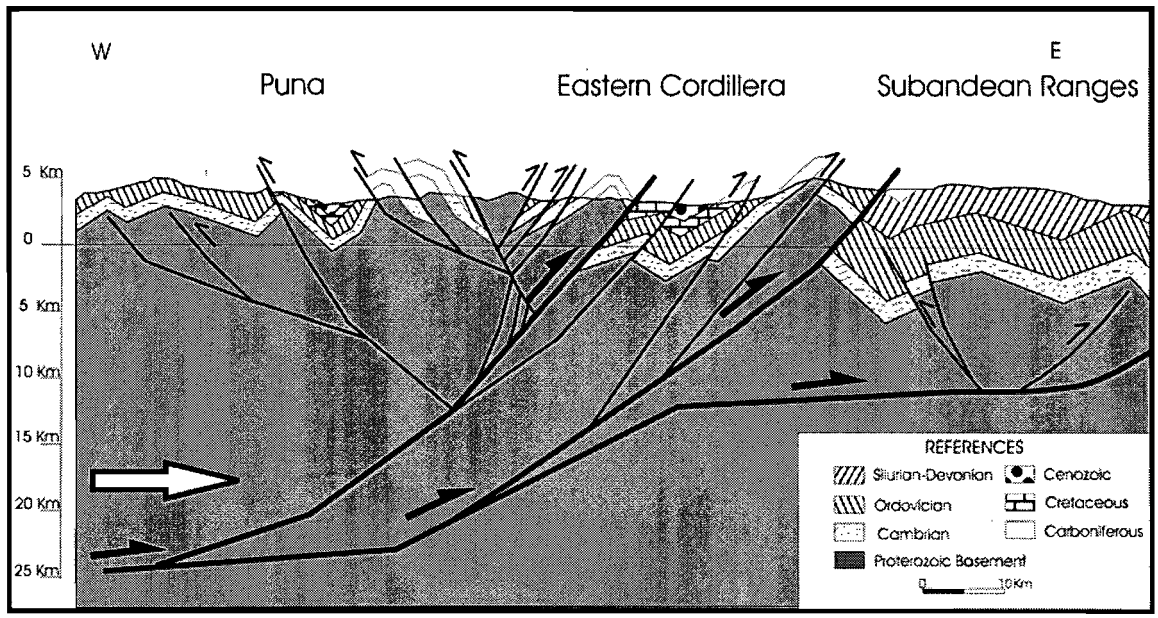

Figure 2. *Simplified geologic cross-section at 23°30'*

unique basement with the Puna (Fig.2).

In terms of the strictly geomety within the imbricated thrust fan is worth to describe it as a *trailing imbricate fan* with increasing minor-fault displacements towards the back and characterized by forelimb-breaking thrusts without evident bed stretching along the fault surfaces. In all cases fault dip-angles are higher than 40°-50°, even close to vertical. Low-angle thrusts as the described by Kley (1996) further north in the Bolivian Eastern Cordillera were not identified.

According to available reconstructions of the deep structure (Mon et al., 1996) and published seismic interpretation further south (Cahill et al., 1992) a ramp between Eastern Cordillera and the Subandean Ranges has been inferred; therefore, in this case, the imbricated thrust sheets of the Eastern Cordillera would be the result of the eastward-migration of the orogen over a detachment surface. As the migration of the hanging wall occurs the ramp between Eastern Cordillera and Subandean Ranges acts as a significant obstacle from which two main thrusts propagated upwards to accommodate major deformation that can not be transferred to the foreland fold-thrust belt (Fig.2). The result of this process is the development of an imbricated east-verging thrust fan recently identified as the *Quebrada de Humahuaca high-angle shear megazone* (Jiménez et al., 2002).

In order to recognize the main cenozoic stress fields, that are still active, minor faults/estriation data from several locations was analyzed. Faults were separated into two different groups, a) Faults in Cretaceous and pre-Pliocene strata; b) Faults in Pliocene-Pleistocene strata; also within both groups reverse faults were distinguished from normal faults. The study shows two contrasting deformation trends affecting both pre-Pliocene and Pliocene-Pleistocene strata. The main crustal shortening ($\sigma 1$) is aligned in a NW-SE trend for the pre-Pliocene rocks and in a NE-SW trend for the Pliocene-Pleistocene rocks; similar results were obtained by

Marret et al. (1994). The interpretation of the extensive deformation turns complicated yet σ3 axes for both groups share orientations with σ 1 axes; it may be suggested that some inversion acted over a part of the fault population in both groups while other faults remained as normal (Fig. 3). These suggestions are not conclusive at all and further observations may improve the interpretation.

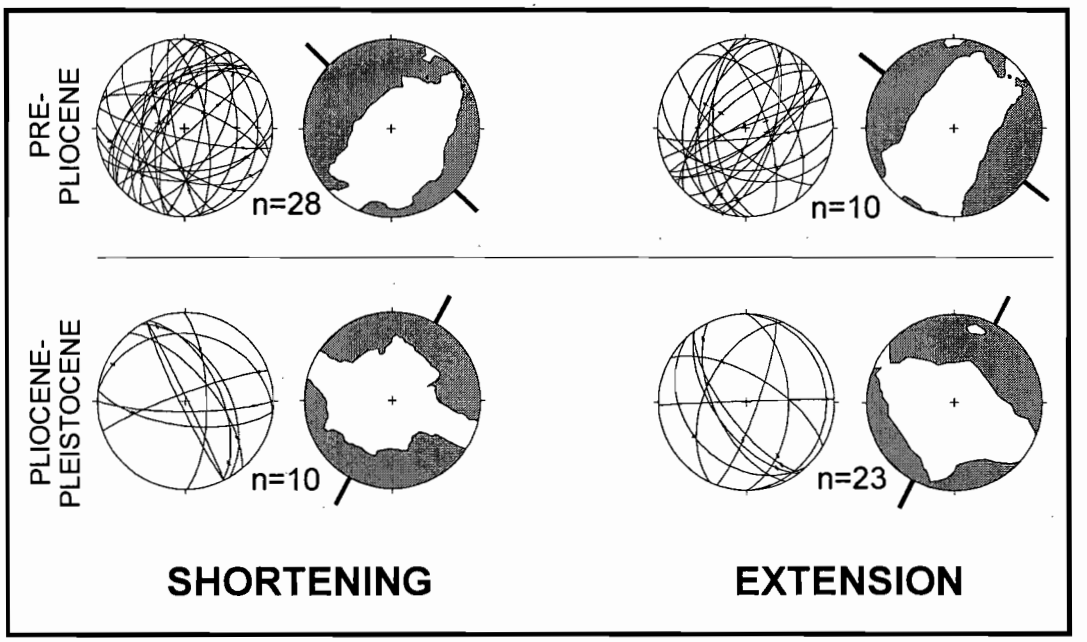

Figure 3. *Statistic analysis of minor fault/estriation data*

CONCLUSIONS

In northern Argentina there is not an evident structural boundary between the Eastern Cordillera and the Puna and both geological provinces share a unique basement. Field observations led to identifie two main east-verging thrust sheets as the principal geometric components of the upper-crust structure. This structural framework would be in close relation to an inferred ramp between Eastern Cordillera and Subandean Ranges, geophysical and deep structure interpretations carried on by diferent authors would support this idea.

Crustal shortening during the andean deformation has been estimated in previous works (Mon et al., 1996; Peñaloza et al., 1999) mainly from balanced cross-sections, averaging 30% and representing a total of 15-20 km for this particular fold-thrust belt. Compresive efforts acted during two diferent episodes with contrasting directions along the Cenozoic, a pre-Pliocene shortening episode with a NW-SE trend and a Pliocene-Pleistocene NE-SW trending episode.

REFERENCES

Cahill, T., B.L. Isacks, D. Whitman, J.L. Chatelain, A. Pérez and J. Mong Chiu, 1992. Seismicity and tectonics in Jujuy province, northwestern Argentina. Tectonics, 11: 944-959.

Kley, J. 1996. Transition from basement-involved to thin skinned thrusting in the Cordillera Oriental of southern Bolivia. Tectonics, 15 (4): 763-775.

Jiménez, M.J., G.J. Peñaloza, R. Mon, R.P. Gambarrutta y J. Eremchuk, 2002. Zona de cizalla de alto ángulo de la Quebrada de Humahuaca (provincia de Jujuy, Argentina). XV Congreso Geológico Argentino, Santa Cruz. In press.

Marret, R.A., R.W. Allmendinger, R.N. Alonso, and R.E. Drake, 1994. Late Cenozoic tectonic evolution of the Puna Plateau and adjacent foreland, northwestern argentine Andes. Journal of South American Earth Sciences, 7: 179-207.

Mon, R., R. Mena y R. Amengual, 1996. Plegamiento cenozoico del basamento proterozoico de la Cordillera Oriental del norte argentino. Revista Asociación Geológica Argentina, 51 (3): 213-223.

Peñaloza, G.J., R.P. Gambarrutta y R. Mon, 1999. Modalidades del acortamiento cenozoico. En Mon R. (autor), Cordillera Oriental. Relatorio de la Geología del Noroeste Argentino, XIV Congreso Geológico Argentino I: 431 – 432. Salta.

THE VOLCANIC ROCKS OF THE CORRALES NEGROS, CORDILLERA PRINCIPAL (33°45'LS) MENDOZA PROVINCE, ARGENTINA

Daniel J. PÉREZ (1)

(1) Laboratorio de Tectónica Andina, Departamento de Ciencias Geológicas, Universidad de Buenos Aires. Ciudad Universitaria 1428, Buenos Aires. (daniel@gl.fcen.uba.ar)

KEYWORD: Plio-Pleistocene volcanism, Andean Cordillera, Corrales Negros, Mendoza, Argentina.

INTRODUCTION

The objective of the present contribution is to analyze the volcanic sequences and their relationship with Mesozoic and Cenozoic sedimentary deposits developed in the Corrales Negros region, to the east of San José volcano. New geochemistry and radiometric date, of this rocks indicated that this volcanic deposits are Pliocene to Pleistocene in age. The study region is located in the Principal Cordillera at 33°45'S-69°45'W, to the east of the San José volcano and north of the Salinillas river, in Mendoza province, Argentina (see Figure 1). These region is in the northern part of the Quaternary Southern Volcanic Zone (SVZ), betwen 33°21'30"S (Tupungato volcano) and 46°S, where the Nazca plate reaches depths 100-150 km, because the subduction angle is 25°-30°.

The first studies in the region correspond to Groeber (1951) and Polanski (1964), and recent studies to Alvarez (1997), Pérez (2001), Ramos et al. (1998), Giambiagi (2000); Tunik (2001).

The stratigraphic sequences of the area are integrated by neopaleozoic Granitic rocks, permotriassic riolites and riodacites rocks of the Choiyoi Group. Continue Jurassic, Cretaccic and Tertiary sedimentary sequences, which are thrusted and folded. Over all of these rocks, were developed the volcanic deposits, composed for andesitic and basaltic plio-pleistoceno sequences.

The volcanic sequences are composed by the Andesita Salinillas and Basalto Corrales Negros. These rocks are pliocene to pleistocene in age. The Andesita Salinillas is composed by dikes, sills and andesitic bodies, with hornblende. These rocks affect the Tertiary sediments of the Tunuyán Conglomerate, the basalts and to the neopaleozoic granitic rocks. A datation on the Salinillas Andesite, by K/Ar method, has give an age of 2,0 ± 0,2 Ma (Pérez, 2002). The Corrales Negros basalt, composed by olivine and pyroxene (augite), developed several lava flow. These rocks unconformably overlying the Tunuyán Conglomerate, the Saldeño Formation and the neopaleozoic granitic rocks. These basaltic rocks have pleistocene in age.

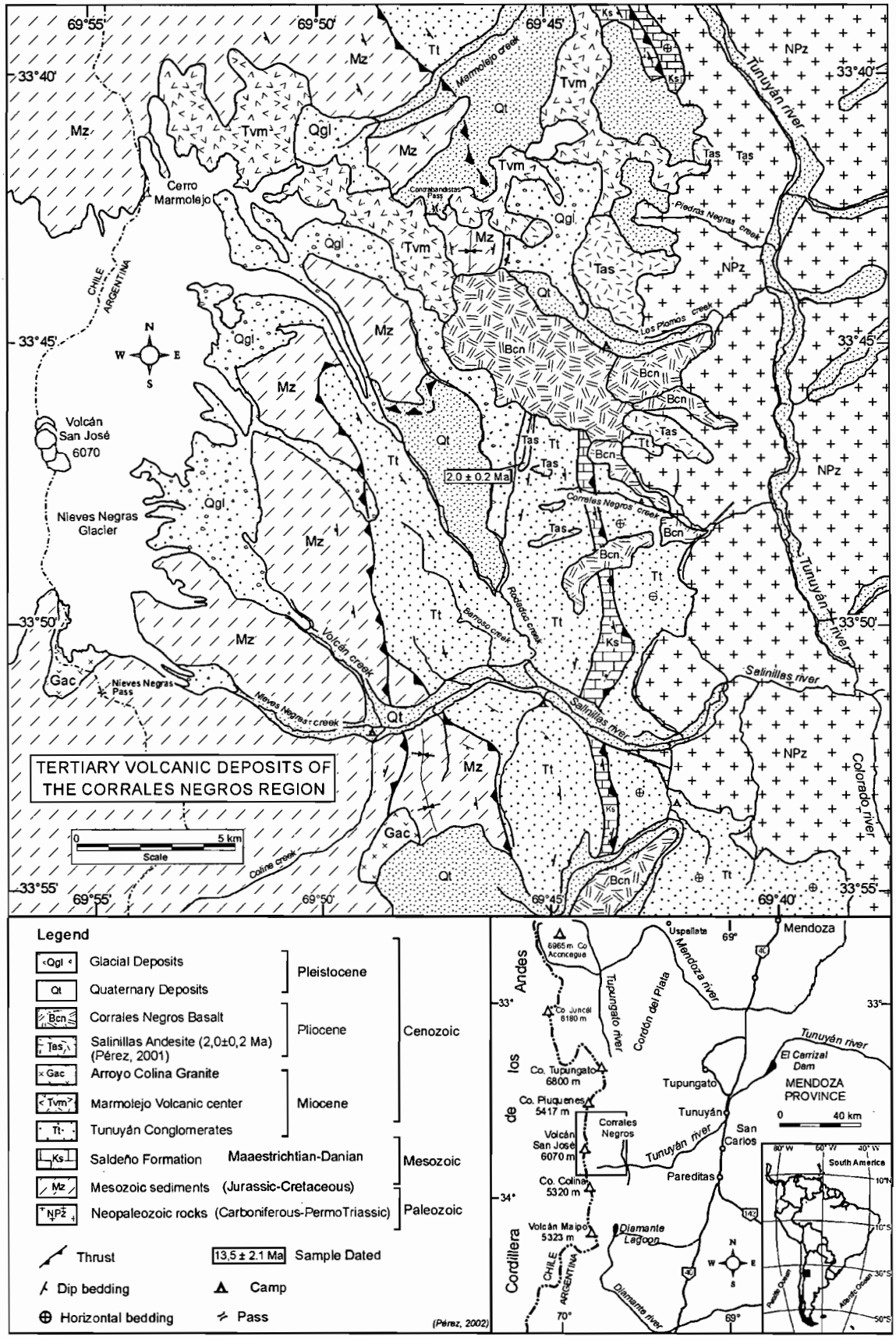

Figure 1: Geologic Map of the studied area.

The geochemistry analysis of the Salinillas and corrales Negros volcanic rocks, show the compositional variation of silica (56-65 %) which locate it between basaltic andesites to dacites rocks. Aluminum values between with 16-17 %, and potassium ones between 1,5-2,6 %, and iron oxides with 3,6-7,3 % (see Figure 2). This geochemistry characteristics are related to subalkaline rocks and calcoalkaline, showing arc magmatism (see Figure 2). In addition this volcanics rock have high Ba/La ratios (31,8-24,7) and La/Ta ratios (29,7-39,8), low La/Yb ratios (7,3-12,2), and medium to low La/Sm ratios (2.7-6.6) (see Figure 2). This geochemistry features allow us to define this rock as a calcoalkaline series developed on magmatic arc (see figure 2a-f).

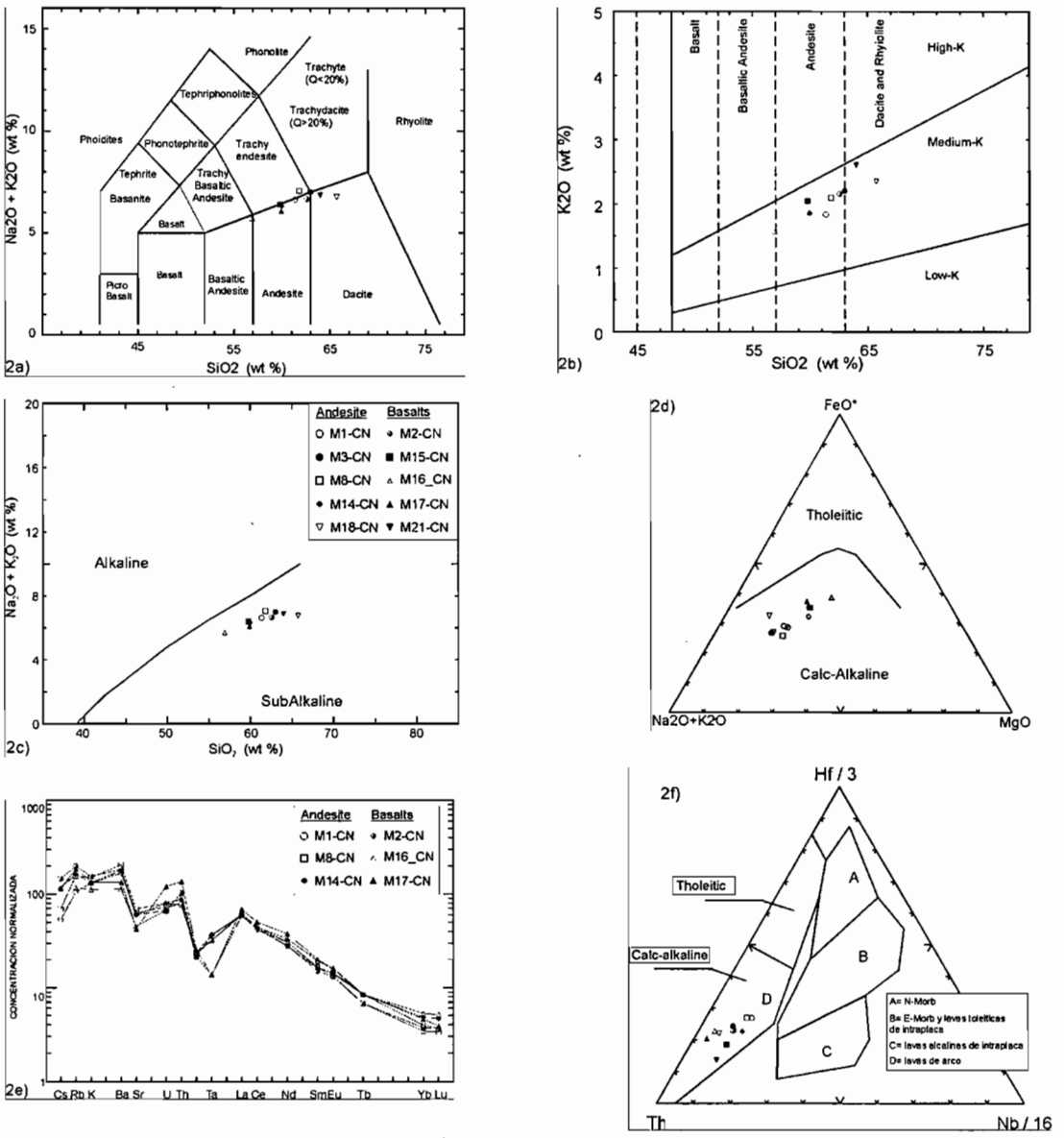

Figure 2a-d: a) TAS diagram, total alkalis versus silica (Le Maitre et al., 1989); b): Plot of K2O versus SiO2; showing low-K, medium-K and high-K arc affinities (Le Maitre et al., 1989); c): volcanic rocks subdivision, in alkaline and subalkaline (Irvine and Baragar, 1971); d): AFM diagram with calcalkaline and tholeiitic fields (Irvine and Baragar, 1971); e) distribution of trace element plots normalized to chondrite by Kay et al. (1987a); f) Wood (1980) diagram showing the magmatic arc association. Legend in figure 2c.

CONCLUSIONS

The volcanic sequences of Andesita Salinillas and Basalto Corrales Negros present similar emplacement characteristics as Mesón de Hierro volcanites of Cordillera de Las Yaretas, located toward southeast of the studied area. All mentioned features suggest that these volcanic rocks, was developed at the same time that the Cerro Papal, Mesón de Hierro and Muralla, between Pliocene and Pleistocene age.

REFERENCES

Giambiagi, L.B., 2000. Estudio de la evolución tectónica de la Cordillera Principal de Mendoza, en el sector comprendido entre los 33°30' y los 33°45' S. Universidad de Buenos Aires, Tesis Doctoral (inédita), 255 pp., Buenos Aires.

Groeber, P., 1951. La Alta Cordillera entre las latitudes 34° y 29°30'. Instituto Investigaciones de las Ciencias Naturales. Museo Argentino de Ciencias Naturales B. Rivadavia, Revista (Ciencias Geológicas) I(5): 1-352, láminas I-XXI, Buenos Aires.

Kay, S.M., Maksaev, V., Mpodozis, C., Moscoso, R., Nasi, C., 1987a. Probing the evolving Andean litosphere: Mid-late Tertiary magmatism in Chile (29°-30.5° S) over the zone of subhorizontal subduction. Journal of Geophysical Research, 92: 6173-6189.

Pérez, D.J., 2001. El volcanismo neógeno de la cordillera de las Yaretas, Cordillera Frontal (34°S) Mendoza. Revista de la Asociación Geológica Argentina, 56 (2):221-23, Buenos Aires.

Polanski, J., 1964. Descripción geológica de la hoja 25a Volcán San José, provincia de Mendoza, Dirección Nacional de Geología y Minería, Boletín 98: 1- 94, Buenos Aires.

Ramos, V.A., Godoy, E., Giambiagi, L., Aguirre-Urreta, M.B., Alvarez, P.P., Pérez, D.J., y Tunik, M., 1998. Tectónica de la Cordillera Principal en la región del Volcán San José (34° LS), Provincia de Mendoza, Argentina. X° Congreso Latinoamericano de Geología (Buenos Aires), Actas II: 104. Tunik, M.A., 2001. Análisis sedimentológico y tectónico de la primera ingresión atlántica en la Alta Cordillera de Mendoza. Universidad de Buenos Aires, Facultad de Ciencias Exactas y Naturales, Tesis Doctoral, (inédita), 257 pp., Buenos Aires.

EROSION TRACING OF THE CHILEAN-BOLIVIAN OROCLINE BY HEAVY MINERAL AND MAJOR AND TRACE ELEMENTS DISCRIMINATION IN SEDIMENTS OF NEOGENE BASINS

Luisa PINTO(1-2), Gérard HERAIL(1), Francois FONTAN(3), Bernard DUPRE(3), Reynaldo CHARRIER(2)

(1) IRD, 39 Allées Jules Guesde, 31000 Toulouse/pinto@cict.fr,gherail@paris.ird.fr

(2) Depto. de Geología, Univ. de Chile, Plaza Ercilla 803, Santiago, Chile/rcharrie@cec.uchile.cl

(3) LMTG-CNRS/UPS-CNRS, 39 Allées Jules Guesde, 31000 Toulouse/ fontan@cict.fr,dupre@lucid.ups-tlse.fr

KEY WORDS: Neogene, basins, oroclino, volcanic arc, crystalline and metamorphic basement.

INTRODUCTION

In northern Chile and northwestern of Bolivia, the main mountain ranges i.e., Precordillera, Western Cordillera and Eastern Cordillera (Fig. 1) are parallel to the Andean basins: Central Depression, the Mauri, Corque and Oriental basins in the Altiplano, and the piggyback basins in the Subandean Zone (Fig. 1). The basins are aligned throughout the mountainous fronts, and the deposits reach up to 10.000 m thickness (Fig. 1). In general, they are characterised by detrital deposits, with coarse sands and gravels in the Central Depression and Altiplano, and sandy to silty sediments in the Subandean Zone. Several stratigraphic units have been defined because of the strong facies variations existent in these basins (Fig. 2). Masek *et al.* (1994) indicates that the northern segment of the orocline in the Subandean Zone would have undergone a greater erosion with respect to the southern segment during Andean uplift. Nevertheless, the recent estimations of shortening indicate that the greater shortening has taken place in the southern segment (*e.g.* Rochat *et al.*, 1999). In addition, it is not known with certainty when the Eastern Cordillera and the Western Cordillera were constituted as mountain ranges. In the frame of this geological setting, it would turn out interesting to determine the nature of the rocks exposed to erosion during the Neogene in order to give light on the evolution of the relief in this region at that time. The analysis of the stratigraphic register in the Neogene basins is essential for solving this tectonic and sedimentary problem. In this work we present the preliminary results on the heavy mineral content, and major and trace element analyses of sedimentary deposits from the Cenozoic basins in this region as a tool for the determination of rocks that were subjected to erosion during the Neogene, discuss and its significance in the Andean paleogeographic evolution in the North segment of the orocline. The heavy minerals were identified by X-Ray (Debye Scherrer method) and determined by SX50-CAMEBAX electron-microprobe (UPS-CNRS, Toulouse); the major elements were analysed by ICP-AES at the Service d'Analyse des Roches et des Minéraux, CRPG, Nancy, and the trace elements by ICP-MS at the Laboratoire de Mécanismes de Transfert in Géologie, UPS-CNRS, Toulouse.

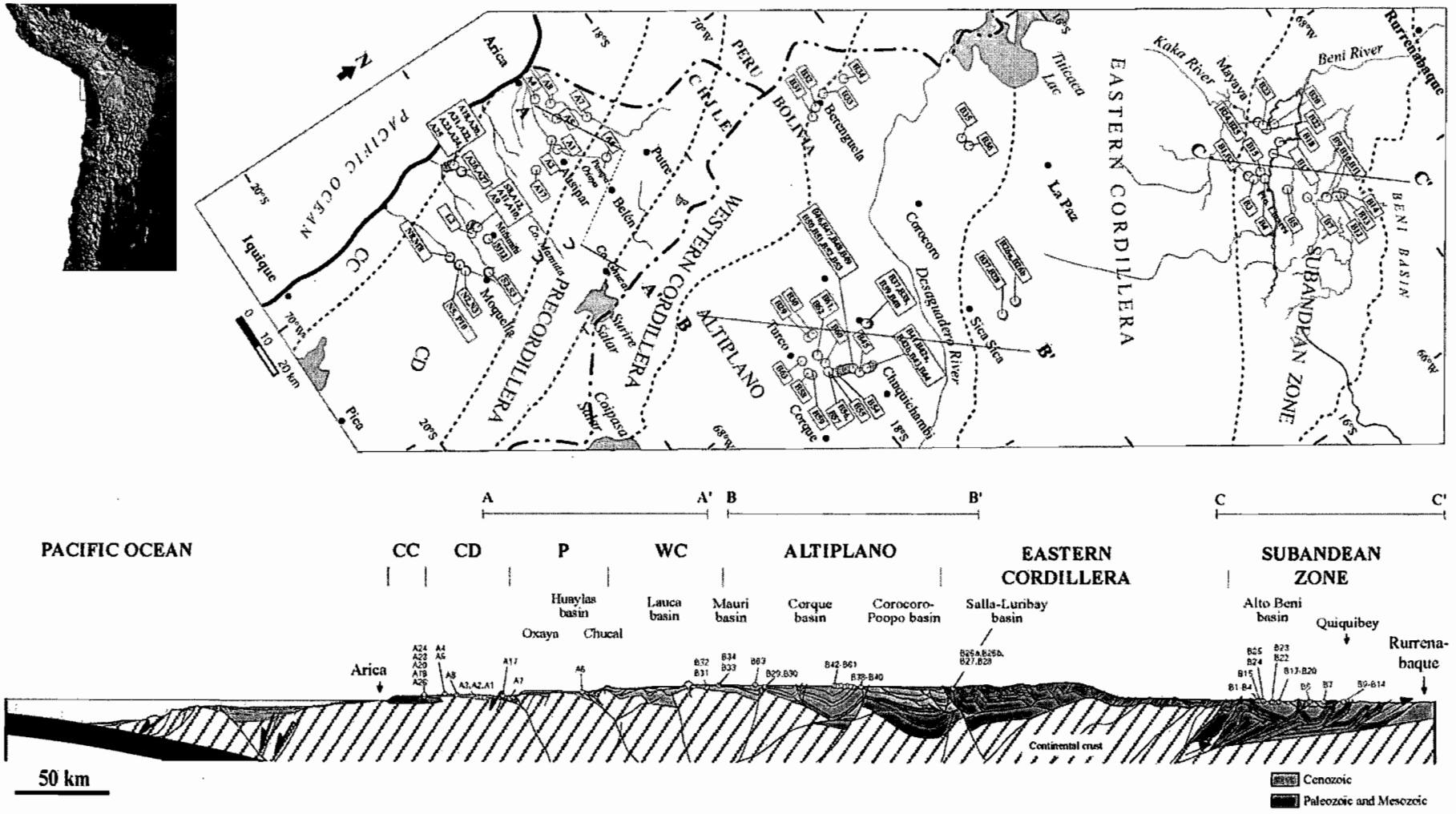

Figure 1. Distribution of Cenozoic basins and location of samples along a SW-NE profile un the Central Andes. CC: Coastal Cordillera, CD: Central Depression; P: Precordillera; WC: Western Cordillera.

RESULTS AND DISCUSSION

The mineral components in the the heavy mineral fraction and the element content in the Neogene sediments (Fig. 3) suggest the continuous erosion of volcanic arcs and the discontinuous erosion of a crystalline and metamorphic basement. (a) The sediments in the Central Depression indicate a intermediate to basic volcanic character of the sediment sources reflected in the low concentrations of SiO_2 and Ta and high concentration in Al_2O_3 with respect to the other basins. This is confirmed by the presence of Diopside and Actinolite in the Oligocene to Early Miocene sediments, and Enstatite, Augite and Forsterite in the Middle Miocene deposits. While the intermediate volcanic components decrease consistently with time in the Central Depression, the basic component increase progressively. While the granitic and metamorphic components are well represented by heavy minerals in the Oligocene to Early Miocene sediments, these are completely absent in the Middle Miocene units. The metamorphic components in the oldest series proceed very possibly from the chilean Belén and the bolivian Cerro Uyarani Metamorphic Complexes. The intermediate volcanic source can correspond either to the Mesozoic Coastal Cordillera or the Precordillera substratum, whereas the basic volcanic source evidently corresponds to the Middle Miocene volcanoes of the Western Cordillera. (b) The presence of granitic material (garnet of the Almandine-Pyrope-Spessartine series) and the greater concentration of SiO_2 in the sediments of the Altiplano basins demonstrate the erosion of mature sedimentary deposits and intrusive bodies – quartzites, granites and/or gneiss – with a continuous supply of volcanic material. The absence of Enstatite and Forsterite and a greater percentage of Magnesiohastingsite, Phlogopite (Fig. 3), Fluorapatite and Titanite, and the greater concentration of SiO_2 indicates that the volcanic supply to the Altiplano basins was more acid than the sedimentary supply to the Central Depression. The volcanic supply to these basins would correspond to the igneous rocks from the Western Cordillera and Eastern Cordillera. (c) An opposite signal is obtained from the analysis of the Subandean Zone sediments, which display a clear predominance of quartz during all its evolution. In this region, the greater concentration of Al_2O_3, Rb and REE, indicates the predominance of the clay fraction in the deposits. In addition, the low Na, Sr and high SiO_2 concentrations (Fig. 3) would be associated to a great alteration or maturity of the sediment (Bathia and Crook, 1986). Nevertheless, the good roundness of tourmalines, zircons, and garnets supports the hypothesis of a long transport or recycling of the material more than an alteration. Thus, these results would indicate that the metamorphic basement and basic volcanic buildings of the Western Cordillera supplied material mainly to the Central Depression. The crystalline basement and acid volcanic deposits of the Western Cordillera and igneous and sedimentary rocks of the Eastern Cordillera supplied material to the Altiplano basins. Whereas the basins of the Subandean Zone only received material from sedimentary rocks eroded along the eastern edge of the Eastern Cordillera being isolated from the volcanic source during all their evolution.

REFERENCES

Bhatia, M., Crook, K., 1986. Trace element characteristics of graywackes and tectonic setting discrimination of sedimentary basins. Contrib. Mineral. Petrol., 92, 181-193.

Masek, J., Isacks, B., Gubbels, T., Fielding, E., 1994. Erosion and tectonics at the margins of continental plateaus. *Journal of Geophysical Research*, 99(B7), 13941-13956.

Rochat, Ph., Hérail, G., Baby, P., Mascle, G., 1999. Bilan crustale et contrôle de la dinamique sédimentaire sur les mécanismes de formation de l'Altiplano. CRAS Paris, 328, 189-195.

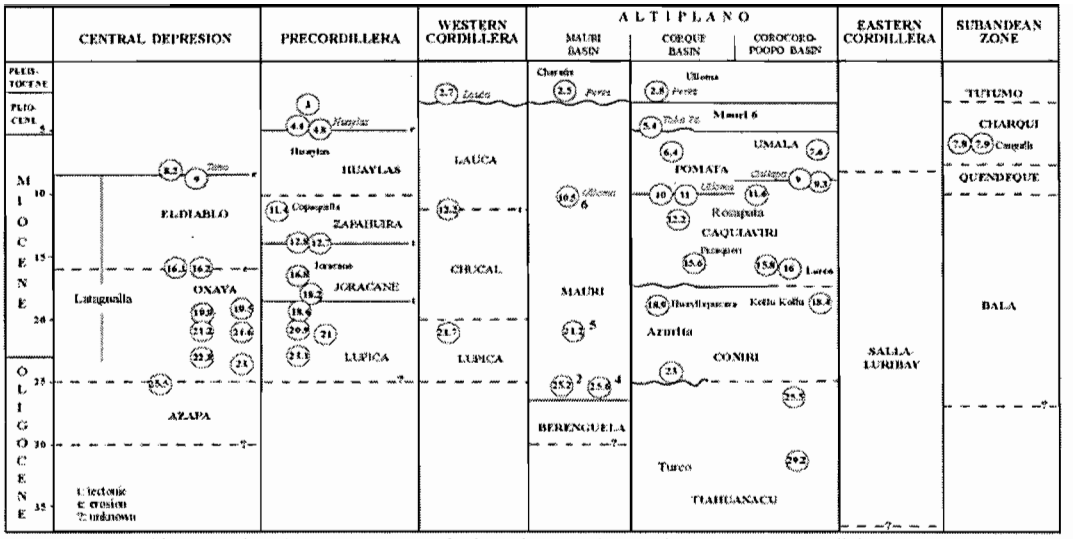

Figure 2. Stratigraphic correlations between the Cenozoic formations, northern Chile and northwest Bolivia. The names in capital letters represent regional formation and the names in italic to local formations or facies. The radiometric ages are in circles and million years. The waved lines represent tectonic pulse and the segmented lines represent not well-known relations between formations.

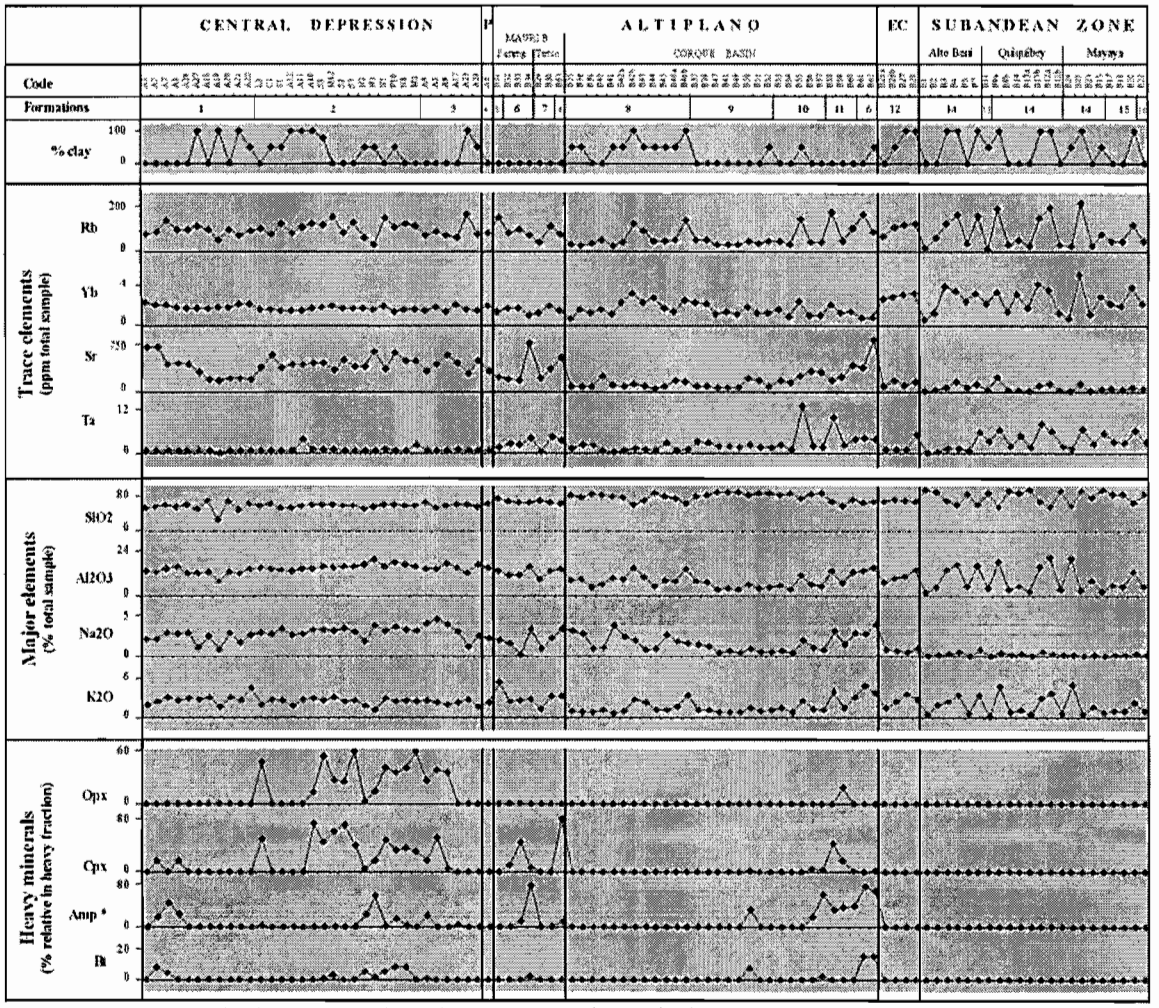

Figure 3. Some trace and major element concentrations and heavy mineral relative concentration in sediments of the Cenozoic basins. P: Precordillera; EC: Eastern Cordillera; Opx: orthopyroxene (Enstatite); Cpx: clinopyroxene (Diopside, Augite); Amp: calcic amphiboles (Magnesiohornblende, Pargasite, Magnesiohastingsite); (*) The A7 sample of the Azapa Fm. contains 24% of Actinolite and 20% of others amphiboles; Bt: biotites. Formations: (1) Azapa-Oxaya Fm., (2) Latagualla Fm., (3) El Diablo Fm., (4) Huaylas Fm., (5) Berenguela Fm., (6) Mauri Fm., (7) Azurita Fm., (8) Tiahuanacu Fm., (9) Coniri Fm., (10) Caquiaviri Fm., (11) Pomata Fm., (12) Salla-Luribay Fm., (13) Bala Fm., (14) Quendeque Fm., (15) Charqui Fm., (16) Tutumo Fm.

ORTHOGONAL DEFORMATION IN THE EASTERN ANDES OF ECUADOR

Warren T PRATT, Pablo DUQUE2 and Miguel PONCE1

(1) Ecuanor SA, Alonso Jerves 134 y Orellana, Casilla 17-07-9312, Quito, Ecuador (wpratt@pi.pro.ec)
(2) Departamento de Geología, Escuela Politécnica Nacional, Casilla 17-01-2759, Quito, Ecuador (pduque@mac.com)

KEY WORDS : Ecuador, Peltetec Event, metamorphism, Pastaza corridor, orthogonal deformation

Patterns of seismicity, volcanism and mineralization leave little doubt that the Pacific Plate is being consumed beneath South America (Gansser 1973). The Andes have grown by compression, uplift, intrusion, crustal thickening and volcanism. Along most of their length subduction has been perpendicular since at least the Jurassic. However, a large part of the northern Andes is regarded as allocthonous, accreted by strike-slip during the Cretaceous and Tertiary (Feininger & Bristow 1980; McCourt *et al.* 1984; Aspden & Litherland 1992) (Fig.1). The Huancabamba Deflection, where the Andes swing from NNW to NNE, probably marks the southern limit of the allocthonous Andes.

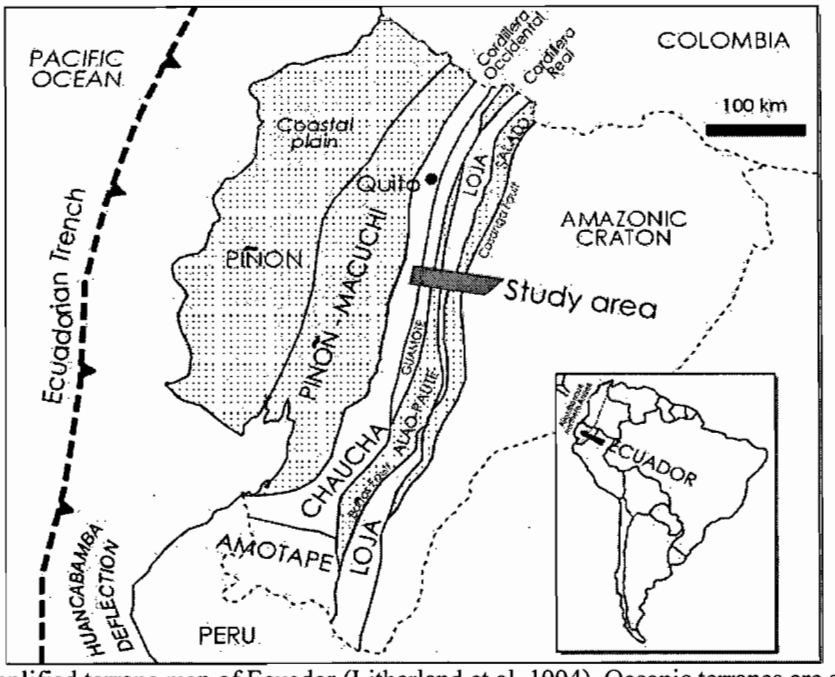

Fig.1. Simplified terrane map of Ecuador (Litherland et al, 1994). Oceanic terranes are stippled

In Ecuador, the Andes separate a broad coastal plain, underlain by Jurassic/Cretaceous oceanic basalts (Piñón Formation), from the Amazon basin and underlying Precambrian Guyana Shield. A topographic trough, the "inter-Andean Graben", divides the Andes into two ranges: the Cordillera Occidental (W) and the Cordillera Real (E). The

Cordillera Occidental comprises Cretaceous pillowed basalt, correlated with the Piñón Formation of the coast (Sauer 1965), and an Eocene island arc (Eguez 1986) (Fig. 1). The Cordillera Real comprises N-striking Palaeozoic and Mesozoic metamorphic rocks. Both cordilleras, and the trough, are partly concealed by subduction-related Tertiary to Recent volcanic rocks. The boundary between oceanic and continental crust is not clear.

We mapped a well-exposed E-W corridor across the Cordillera Real (Figs. 1, 2). The main rocks are graphitic phyllites, mica schists, greenschists, marbles and calc-schists (Table 1). We recognize clear lithostratigraphical divisions in these metamorphosed sedimentary and volcanic rocks (Fig. 2). Four major granitoids, and minor amphibolites, complete the section. Recent lavas from the active volcano Tungurahua occur as erosional outliers along the Río Pastaza.

The strata strike N-S and are commonly sub-vertical. Metamorphic grade ranges from low to high greenschist facies. Schistosity is generally sub-parallel to bedding or compositional layering. The most important structures, both still active, are the Peltetec and Sub-Andean faults (Fig. 2). The Peltetec defines the western edge of the Cordillera Real and includes serpentinite slivers. The Sub-Andean is a reverse fault that separates the true metamorphic Andes, in the W, from the Sub-Andean Zone, a weakly metamorphosed thrust belt, in the E.

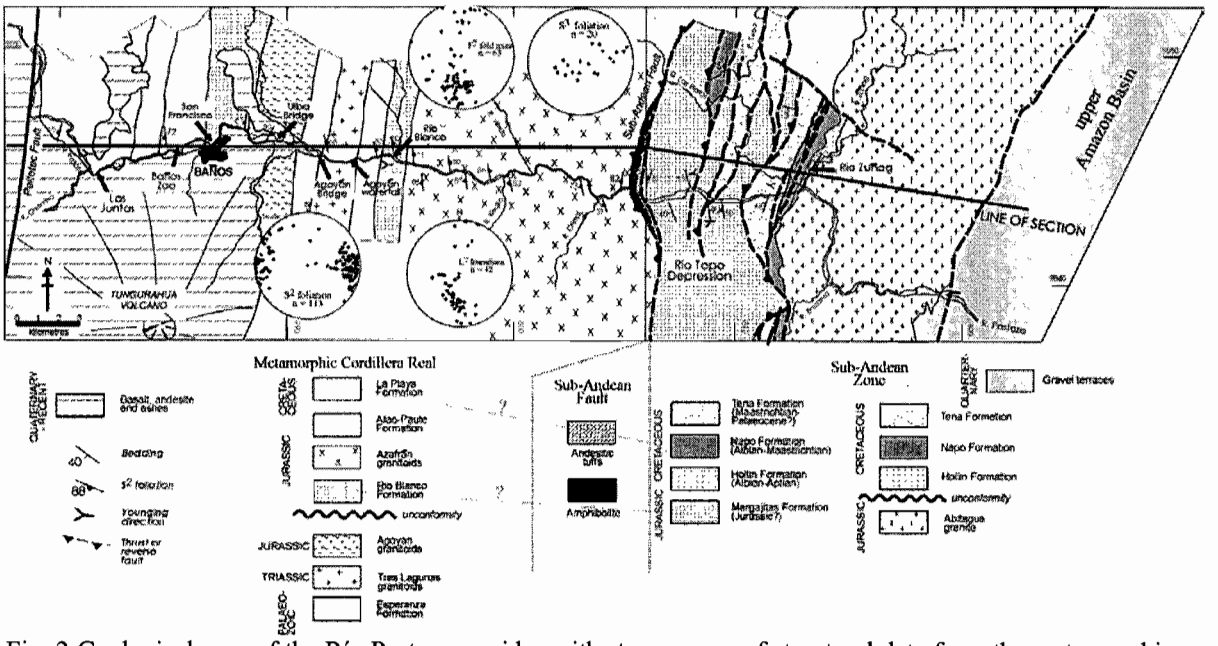

Fig. 2 Geological map of the Río Pastaza corridor with stereograms of structural data from the metamorphic portion of the Cordillera Real. Minor outcrops of amphibolite and Recent lava are omitted.

METAMORPHISM

There are two discrete phases of regional metamorphism in the main metamorphic Cordillera Real. Low greenschist conditions accompanied the formation of the S1 slatey cleavage; graphite was preserved. Subsequently, a high greenschist regional metamorphism occurred in the anticlinal core of the Cordillera Real. This began with porphyroblast formation (albite, garnet) and a foliation (S2) defined by quartz, muscovite, biotite and chlorite. With progressive metamorphism and deformation, pressure shadows of quartz and muscovite developed around the garnets. Subsequently, the S2-related metamorphism had a strong thermal (static) component. It caused widespread

granoblastic recrystallization of quartz and randomly oriented coarse muscovite. Garnet was commonly retrogressed to chlorite at this stage.

Stratigraphic Unit	Age	Petrography and geological setting
Metamorphic Cordillera Real		
Esperanza Formation)	*Triassic-Palaeozoic*	Pelites forming the anticlinal core of the Cordillera. Intruded by granitoids. Includes the highest grade metamorphic rocks
Río Blanco Formation (= Margajitas Fmn?)	*Jurassic?*	Chloritoid schists meta-volcanic, and metamorphosed clastic, rocks. Metamorphic grade reaches high greenschist facies
Alao-Paute Formation	*Jurassic-Cretaceous(?)*	Greenschists, greenstones, metabasalts and metadolerites in the greenschist facies.
La Playa Formation)	*Cretaceous?*	Calcareous phyllite with pyrite and quartz lenses, calc-schists (calcite + talc + chlorite ± fuchsite), scattered marbles
Sub-Andean Zone and Amazon Basin		
Margajitas Formation	*Jurassic ? pre-Albian?*	Pyritous non-calcareous cleaved mudstones, scattered quartzites with distinctive blue quartz grains
Hollín, Napo and Tena formations	*Aptian to Maastrichtian / Palaeocene*	Occur as a complete outcrop in the W flank of the Abitagua granite and as thrusted fragments in the Margajitas Fm
Intrusions		
Tres Lagunas granite	*late Triassic-early Jurassic*	Foliated granite (kfs and blue qz phenocrysts). The western contact is sharply defined against crystalline Esperanza schists
Agoyán granitoids	*late Triassic-early Jurassic*	Metadiorite to metagranodiorite. Good gneissose banding enhanced by boudinaged garnetiferous amphibolites.
Azafrán granitoids	*Jurassic*	Metadiorite to metagranodiorite. Schistosity reflects mica growth and strong grain-size reduction. Micaceous domains
Abitagua granite	*Jurassic*	Jurassic Kfs rich batholith in the eastern foothills of the Cordillera. Shows no evidence of metamorphism.

Table 1. Summary of lithostratigraphic units in the Cordillera Real (Study area)

TECTONIC EVENTS

We see no evidence of the Triassic "Tres Lagunas" dextral strike-slip event of Litherland *et al.*, (1994). The Tres Lagunas granite does not have an old (syn- to late-emplacement) schistosity. Furthermore, the amphibolite dykes and pegmatites were clearly deformed during S1/S2 development. The foliation in the granitoids throughout the Pastaza corridor was formed by relatively brittle processes and was dominated by grain size reduction rather than new mineral growth. There is no structural evidence of pervasive or localized strike-slip deformation. Lineations are instead consistent with oblique dip-slip.

We envisage a structural history with a single progressive deformation. This began with slatey cleavage development (S1) and developed into a low to high greenschist regional metamorphism and deformation (S2). This progressive event was probably the Cretaceous Peltetec deformation. It affected the entire Cordillera. Grades were highest in the core. The Peltetec Event was orthogonal. Its age is poorly known.

The Peltetec Event is younger than the Lower Cretaceous and it occurred at the Napo-Tena formation transition (Maastrichtian), when the Cordillera emerged and carbonate shelf sedimentation in the Amazon basin switched to continental red-bed deposition (Tena Formation) (Baldock 1982). The deformed Napo (Albian/Maastrichtian) limestones, or deeper water equivalents, occur in the Cordillera Real at Baños (La Playa Formation) and Cerro Hermoso (Tschopp 1956). The Margajitas Formation is broadly equivalent to the Río Blanco Formation. Our correlations suggest a mid- to Late Cretaceous age for the Peltetec Event. This is closer to the substantial peak in

(reset) K-Ar dates at about the Cretaceous/Tertiary boundary (Feininger, 1982; Litherland *et al.* 1994). Compressive deformation continued into the Tertiary, probably in pulses, and continues at the present time.

We model the Cordillera Real as an anticlinal core of Palaeozoic basinal or deep shelf sedimentary rocks. They were deposited on the edge of the Precambrian Guyana Shield, on a stable shelf. They probably link with the Palaeozoic rocks of the Peruvian Andes and with the Palaeozoic and Triassic mudstones and limestones of the Amazon basin of Ecuador. The Palaeozoic rocks were intruded by a Triassic S-type granite (Tres Lagunas), reflecting possible rifting (Aspden & Litherland, 1992), and subsequently eroded and overlain unconformably by Jurassic/Cretaceous sediments and submarine basalts/andesites (Alao-Paute). We interpret these rocks as the fill of a marginal basin on thinned continental crust. The Alao-Paute basalts/andesites may correlate with the Misahuallí intermediate volcanic rocks. Major I-type magmatism in the Jurassic (Azafrán and Agoyán granitoids) is probably related to subduction.

The Jurassic/Cretaceous depositional environment was probably controlled by N-S faults, not dissimilar to the current disposition of strata and intrusions in the Sub-Andean Zone. Basin geometry was probably also affected by the intrusion of linear, buoyant batholiths (Abitagua and Azafrán). Local horst and graben tectonics are indicated by the unconformity of the Hollín quartzites (Aptian-Albian) directly upon the Abitagua granite (Jurassic). Immediately to the W, Margajitas Formation is preserved beneath the Hollín unconformity in the Río Topo Depression (Fig. 2). Early on, the unroofing of the Tres Lagunas granite provided blue quartz grains to many Jurassic/Cretaceous sedimentary formations in Ecuador. This blue quartz provides links between the two sides of the Cordillera and is additional evidence for a coherent stratigraphy.

The boundary between oceanic and continental crust must lie W of the Cordillera Real. Collision between the Pallatanga/Piñón crust and continental South America in the late Cretaceous may have driven the orthogonal Peltetec deformation of the Cordillera Real. Alternatively, changes in plate convergence rates and vectors may be responsible. Choking up of the subduction zone by an oceanic plateau or ridge, as appears to happen presently with the Carnegie Ridge off Ecuador, may explain the deformation. The profound shortening of the Cordillera Real implies a strong orthogonal component to this collision.

REFERENCES

Aspden, J A & Litherland, M. 1992. The geology and Mesozoic collisional history of the Cordillera Real, Ecuador. *Tectonophysics*, **205**, 187-204.

Baldock, J W. 1982. *Geology of Ecuador: explanatory bulletin of the National Geological Map of the Republic of Ecuador*. Dirección General de Geología y Minas, Quito.

Egüez, A. 1986. Evolution Cenozioque de la Cordillere Occidentale Septentrionale d` Equateur : Les mineralisation associees. Doctoral thesis. Université Pierre et Marie Curie, Paris.

Feininger, T. 1982 The metamorphic "basement" of Ecuador. *Bulletin of the Geol Society of America*, **93**, 87-92.

Feininger, T. & Bristow, C R. 1980. Cretaceous and Paleogene geologic history of coastal Ecuador. *Geologische Rundschau*, **69**, 849-874.

Gansser, A. 1973. Facts and theories on the Andes. *Journal of the Geological Society of London*, **129**, 93-131

Litherland, Aspden, J A & Jemielita, R A. 1994. The metamorphic belts of Ecuador. *Overseas Geology and Mineral Resources*, **11**, 147 pp. 2 map enclosures at 1:500,000 scale. British Geological Survey, Nottingham

McCourt, W J, Aspden, J A & Brook, M. 1984. New geological and geochronological data from the Colombian Andes: continental growth by multiple accretion. *Journal of the Geological Society of London*, **141**, 831-845.

Sauer W. 1965. Geología del Ecuador. Editorial del Ministerio de Educación, Quito.

Tschopp H J. 1956. Upper Amazon Basin geological province. In: W F JENKS (ed.), Handbook of South American geology. Memoir of the Geological Society of America, 65, 253-267.

RHEOLOGY AND THE EVOLUTION OF THE CENTRAL ANDES

Claudia B. PREZZI (1)

(1) CONICET – Universidad de Buenos Aires. INGEODAV, Dpto. de Cs. Geológicas, FCEyN, Universidad de Buenos Aires, Ciudad Universitaria, Pabellón 2, 1418, Buenos Aires, Argentina. (prezzi@gl.fcen.uba.ar)

KEY WORDS: Central Andes, rheology, flexural compensation, geodynamic evolution.

INTRODUCTION:

Along the Argentine Puna two distinct phases of Cenozoic deformation are observed, a mio-pliocene phase and a plio-quaternary one. Both deformation phases were not synchronous (Toth *et al.* 1996). Cladouhos *et al.* (1994) determined that in the Northern Puna the oldest deformation ceased at about 10 Ma, while Marrett *et al.* (1994) concluded that in the Southern Puna it continued to 4 Ma. Since Late Cenozoic the most intense shortening took place in the Sierras Subandinas and the Santa Bárbara System. While the Sierras Subandinas are a thin skinned fold and thrust belt, the Santa Bárbara System is a thick skinned thrust belt. Watts *et al.* (1995) suggested that the existence of a more rigid lithosphere favoured the formation of thin skinned fold and thrust belts in the central zone (18-19° S), while in the northern and southern ends, where the lithosphere is weaker, the structures involve the basement (thick skinned). Several authors have proposed that the observed diachronism could be due to lateral changes in the lithosphere structure and thickness (e.g.: Allmendinger *et al.* 1997).

The aim of this paper is to propose a very simplified flexural model trying to explain the observed diachronism of Mio-Pliocene deformation along the Argentine Puna. Different authors (among others: Watts *et al.* 1995, Toth *et al.* 1996) have previously proposed lithospheric flexural models for the Central Andes.

METHODOLOGY:

Vening-Meinesz (1939) regarded the lithosphere as an infinite elastic plate of density δ_l that floats horizontally on the astenosphere of density δ_m. The plate bends under the load of a mountainous chain. Such bent of the elastic plate depends on the load geometry, the load density, and the lithosphere effective elastic thickness (Te). Several studies carried out in the Central Andes have considered broken elastic plates instead of infinite ones (e.g. Lyon-Caen *et al.* 1985). During the implementation of this type of models the problem arises about the localization of the elastic plate edge with respect to the topographic load. The deflection (w) of a two dimensional semi-infinite (broken) elastic plate, not subjected to horizontal forces, under a line load Vo (N/m) is given by: $w = [Vo\ \alpha^3/4D]\ e^{-x/\alpha} \cos(x/\alpha)$; with α being the flexural parameter (m), D the flexural rigidity (Nm) and x (m) the horizontal distance with x=0 in the plate edge.

In the model proposed here, the continental lithosphere under the Central Andes is regarded as a two dimensional thin elastic broken plate with its western edge under the actual magmatic arc (68°W). This localization of the plate fracture was chosen trying to avoid lateral variations of the plate flexural rigidity,

considering that under the magmatic arc very low values of electrical resistivity have been registered (2 to 50 Ohmm) (Schwarz and Krüger 1997). These low values suggest the existence of a partial melting zone. If we consider that the thermal state of the lithosphere controls the plate flexural rigidity (Tassara and Yañez 1997), we could expect lateral variations of rigidity under the magmatic arc. It is considered that the plate extends continuously towards the east without lateral variations of the flexural rigidity. However, rigidity would increase towards the east due to the presence of the Brazilian Shield (Watts *et al.* 1995). Nevertheless, taking into account that this model is very simplified and that only the zone between the Argentine Puna and the Sierras Subandinas – Santa Bárbara System will be considered, this oversimplification will be accepted. The possible forces applied to the elastic plate due to the subduction of the Nazca plate under South America plate, and to the thrusting of the Sierras Subandinas over the Brazilian Shield, will not either be considered (Isacks 1988). It is worthy to note that Springer (1999) determined low values of shear strain (lower than 15 MPa) along the contact between the Nazca and South America plates. Once the model constrains have been set, the deflection (w) of the elastic plate 10 Ma ago along two E-W profiles at approximately 22°S (Northern Puna) and 24°S (Southern Puna) will be calculated.

A Poisson's ratio of 0.25, a Young's modulus of 10^{11} N/m^2, a lithospheric density (δ_i) of 2930 kg/m^3 and an upper mantle density (δ_m) of 3320 kg/m^3 were used in the calculations. Different values of elastic thickness (Te) were considered for each modelled profile. Götze *et al.* (1994) determined a Te value of 25 km for the Andean zone extending between 20-22°S and a Te value of 20 km for the zone extending between 22-26°S. Watts *et al.* (1995) observed that Te values increase from nearly 0km in the northern and southern ends, up to approximately 50 km in the central zone. Tassara and Yañez (1997) determined Te values between 15 and 5 km for the Andean segment extending between 12-24°S and Te values between 10 and 0 km for the Andean segment extending between 24-28°S. In this paper, Te values of 25 km and of 15 km were used for the Northern Puna (22°S) and the Southern Puna (24°S), respectively.

In order to calculate the deflection of the elastic plate at 10 Ma, the weight per unit length supported by the plate must be estimated. Cladouhos *et al.* (1994) determined that the deformation that ceased at about 10 Ma, produced 50 km of shortening and an elevation of 2 km for the Northern Puna. Kley *et al.* (1997) reported 75-100 km of shortening across the Altiplano and the western edge of the Eastern Cordillera at 21°15′S; this shortening took place between 25 and 10 Ma. Kley and Monaldi (1998) calculated 80-106 km of shortening across the Altiplano and the Eastern Cordillera at 21°S. Here, a shortening value of 90 km was adopted. Considering a local isostatic compensation for the Puna (Watts *et al.* 1995), the topographic area (At) elevated over an altitude (h) can be estimated from the shortening (S) underwent by the studied zone, the initial crustal thickness (Ho), the initial elevation (ho) and the height of the crustal root (r), (Isacks 1988). In this study, the topographic area (At) elevated over 2 km (h) 10 Ma ago along 22°S was calculated from: S = 90 km, Ho = 35 km (Cladouhos *et al.* 1994), ho = 0 km and r = 15 km. A value of 370.6 km^2 was obtained for At. The weight per unit length (Vo) is given by: $Vo = At\ g\ \delta_t$, with δ_t being the topography's density (2670 kg/m^3).

In the case of the profile modelled along 24°S, the shortening and the elevation occurred previous to 10 Ma are unknown. So, the Vo value calculated for the profile extending along 22°S will be used. This value could be somewhat excessive, as several authors (among others: Isacks 1988, Kley *et al.* 1997) have reported that shortening diminishes from Arica elbow to the south.

OBTAINED RESULTS

The deflections (w) of the elastic plate at 22 and 24°S at 400 km from the edge of the plate were compared. Such distance was chosen considering the shortening occurred later than 10 Ma. The foreland basins would be localized at that distance 10 Ma ago. While, under the model constrains, the plate under the Andean foreland belts at 22°S underwent an elevation of 538m, at 24°S it underwent a subsidence of 96m. These results indicate that the foreland basins supported different strains in both zones of the Andean orogene 10 Ma ago. Therefore, this flexural model could provide an explanation for the above mentioned diachronism.

The compressive deformation that continued to 4 Ma in the Southern Puna produced more shortening and an increment of the topographic load so that, in a particular moment, the foreland basins at 24°S would also undergo elevation. To test this hypothesis the deflection (w) of the plate with the same Te values along the same profiles was calculated, but now considering the load exerted by the actual topography. The digital elevation model produced by the EROS Data Center of the United States Geological Survey was used for the calculation through integration of the corresponding At values. The deflections (w) of the elastic plate at 22 and 24°S at 64°30′W and at 65°15′W respectively were compared. These longitudes correspond to the actual localization of the westernmost zones of the Sierras Subandinas and the Santa Bárbara System. At 22°S-64°30′W the elastic plate underwent an elevation of 1997m. At 24°S-65°15′W the elastic plate underwent an elevation of 467m. These values would indicate that both zones of the plate would suffer deformations giving way to peripheral flexural bulges, subsidence being not registered. On the other hand, the plate shape predicted by the model resembles that of the corresponding Bouguer anomalies (Götze *et al.* 1994) supporting the proposed hypothesis.

Oversimplifications could exist in the proposed model, which would restrict the validity of the obtained results. Nevertheless, it provided a workable hypothesis to explain the observed diachronism in the eastward shift of the deformation along the Argentine Puna. Such diachronism would be controlled by variations in the effective elastic thickness of the lithosphere along the Central Andes.

CONCLUSIONS

It is evident that a great variety of processes has produced the present configuration of the Central Andes and several questions remain unanswered: why did the plateau uplift, crustal thickening and increase in the width of the mountain belt take place during the past 25 Ma?, which is the exact origin of the extraordinary over-thickened crust?, which is the cause of the extreme low values of lithospheric rigidity observed in the high intra mountainous basins?, why is the end of mio-pliocene compressive deformation diachronic along the Argentine Puna?, which are the driving mechanisms leading to the Central Andes vertical axis rotation pattern?, etc. (among others: Baumont *et al.* 1999, Götze and Schmidt 2000, Prezzi and Alonso 2002).

Trying to assay possible answers to these questions, and considering the results obtained in this very simplified model the future course of action is to carry out a 3 D flexural modelling of the crust and mantle rheology for different geological times (constrained by the available geologic and geophysical data) for the zone of the Altiplano-Puna plateau. From such 3D rheology modelling several features of the Central Andes (different styles, timing and rates of deformation, crustal thickening, orogenic shortening, backarc basins evolution, rates of deposition and erosion, gravimetric and geoidal anomalies, pattern of heat-flow density, vertical axis rotation

pattern, volcanic activity, magmatic evolution, ore deposits setting, etc.) could be predicted and compared with the real-world available data, giving a new insight of the orogen geodynamic evolution.

REFERENCES

Allmendinger, R., T. Jordan, S. Kay, and B. Isacks. 1997. The Evolution of the Altiplano-Puna Plateau of the Central Andes. Earth Planet. Sci. Annual Review, *25,* 139-174.

Baumont, D., A. Paul, H. Pedersen, G. Zandt, and S. Beck. 1999. Shear wave velocity in the lithosphere across the Central Andes, paper presented at 4th. ISAG, Goettingen, Germany.

Cladouhos, T. , R. Allmendinger, B. Coira, and E. Farrar. 1994. Late Cenozoic deformation in the Central Andes: fault kinematics from the northern Puna, northwestern Argentina and southwestern Bolivia. Journal of South American Earth Sciences, 7, 209-228.

Götze, H., and S. Schmidt. 2000. Rigidity of the Central Andes and their isostatic state by density modelling, paper presented at IX Congreso Geologico Chileno, Puerto Varas, Chile.

Götze, H., B. Lahmeyer, S. Schmidt, and S. Strunk. 1994. The Lithospheric Structure of the Central Andes (20°-26°S) as inferred from Quantitative Interpretation of Regional Gravity, in Tectonics of the Southern Central *Andes,* edited by Reutter, Scheuber, Wigger, pp. 7-21, Springer Verlag Heidelberg,.

Isacks, B. 1988. Uplift of the Central Andean Plateau and Bending of the Bolivian Orocline. Journal of Geophysical Research, 93, 3211-3231.

Kley , J., and C. Monaldi. 1998. Tectonic shortening and crustal thickness in the Central Andes: How good is the correlation?. Geology, 26(8), 723-726.

Kley, J., J. Müller, S. Tawackoli, V. Jacobshagen, and E. Manutsoglu. 1997. Pre-Andean and Andean-Age deformation in The Eastern Cordillera of Southern Bolivia. Journal of South American Earth Sciences, 10(1), 1-19.

Lyon-Caen, H., P. Molnar and G. Suárez. 1985. Gravity Anomalies and flexure of the Brazilian shield beneath the Bolivian Andes. Earth and Planetary Science Letters, 75, 81-92.

Marrett, R., R. Allmendinguer, R. Alonso, and R. Drake. 1994. Late Cenozoic tectonic evolution of the Puna Plateau and adjacent foreland, northwestern Argentine Andes, Journal of South American Earth Sciences, 7(2), 179-207,.

Prezzi, C. and R. Alonso. 2002. New Paleomagnetic data from the Northern Argentine Puna: Central Andes Rotation Pattern Reanalysed. Journal of Geophysical Research, 107(B2), 10.1029/2001JB000225.

Schwarz, G. and D. Krüger. 1997. Resistivity cross section through the southern Central Andes as inferred from magnetotelluric and geomagnetic deep soundings. Journal of Geophysical Research, 102, 11957-11978.

Springer, M. 1999. Interpretation of heat-flow density in the Central Andes. Tectonophysics, 306, 377-395.

Tassara, A., and G. Yañez. 1997. Segmentación de los Andes (12-50° S): un punto de vista reológico aportado por un análisis flexural, paper presented at VIII Congreso Geológico Chileno, Antofagasta, Chile.

Toth, J., N. Kusznir, and S. Flint. 1996. A flexural isostatic model of lithosphere shortening and foreland basin formation: Application to the Eastern Cordillera and Subandean Belt of NW Argentina. Tectonics, 15(1), 213-223.

Vening Meinesz, F. 1939. Tables fondamentales pour la réduction isostatique régionale. Bulletin Geodinámique, 63.

Watts, A., S. Lamb, J. Fairhead, and J. Dewey. 1995. Lithospheric flexure and bending of the Central Andes. Earth and Planetary Science Letters, 134, 9-21.

THE STRUCTURAL EVOLUTION OF THE CENTRAL ANDEAN FOLD-THRUST BELT, BOLIVIA

Nadine MCQUARRIE (1)

(1) Division of Geological and Planetary Sciences, California Institute of Technology, MC 100-23, Pasadena CA 91125 (nmcq@gps.caltech.edu)

KEY WORDS: tectonics, fold-thrust belt, structure, Andes, Bolivia, megathrust

INTRODUCTION

Many of the key questions in Andean Orogenesis center around the nature, timing and amount of deformation within the Central Andean fold-thrust belt. The Central Andes house one of the world's high elevation plateaus with average elevations of 4 km supported by a ~70 km thick crust (e.g. Beck et al., 1996). Although explanations for this broad area of high elevations have ranged from magmatic additions to thinning of the continental lithosphere, the central Andean plateau is now thought to be primarily the result of tectonic shortening and thickening associated with the Andean fold-thrust belt (Isacks, 1988; Sheffels, 1990; Schmitz, 1994). Even though the high elevation plateau is linked to the shortening accommodated by the fold-thrust belt, the kinematic details of the fold-thrust belt and how it evolved with time still remains a mystery. Balanced cross-sections from the arc to the foreland in conjunction with available timing constraints enable sequential restorations of the fold-thrust belt with time as well as provide realistic estimates of shortening. Cross sections through the Andean fold-thrust belt must account for four regional constraints. These are 1) a 12 km structural step between the Altiplano and the Eastern Cordillera (McQuarrie and DeCelles, 2001), 2) pronounced (~6 km) structural steps between the Interandean zone and the Eastern Cordillera and between the Interandean zone and the Subandean zone (Kley, 1996; 1999), 3) a horizontal, shallow level decollement in lower Paleozoic rocks through the west- and east-verging portions of the Eastern Cordillera (McQuarrie and DeCelles, 2001), and 4) an extensive (~100 km wide) zone of west-verging folds and associated thrust faults. The cross sections and kinematic evolution models presented in this paper propose that the best way to fill these 4 constraints is through the stacking of two basement thrust sheets.

BALANCED CROSS SECTIONS

Balanced cross-sections were constructed along two transects (17°-18° S in the north and (19°-20° S in the south) from the undeformed foreland to the volcanic arc (Figure 1).

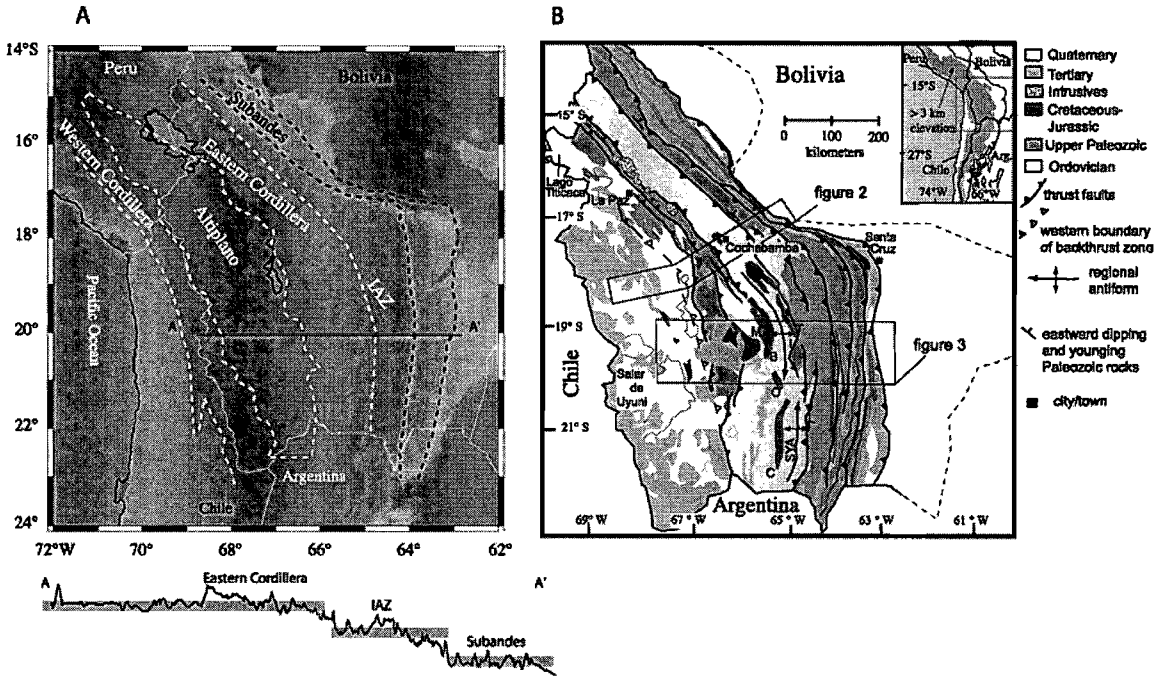

Support for large, basement-involved thrust sheets is found in significant steps in both the topography and the exposed structural elevation of the Andean fold-thrust belt. The structurally highest basement thrust raised folds and faults in predominantly lower Paleozoic rocks of the Eastern Cordillera with respect to Tertiary rocks in the broad, internally drained basin of the Altiplano to the west and east-verging folds and faults in upper Paleozoic rocks of the Interandean zone to the east. The Interandean zone was in turn raised (both structurally and topographically) with respect to the frontal folds and faults of the fold-thrust belt (the Subandean zone) by a second, structurally lower basement thrust sheet. Thus, these two megathrusts divide the Andean fold-thrust belt into four areas of markedly different structural elevations. The Eastern Cordillera can be further subdivided into two zones of west- and east-vergent folds and thrusts.

The balanced cross-sections and the accompanying undeformed sections were simulated using the computer program, 2D-move (Midland Valley) to produce sequentially restored sections that portray how the Andean fold-thrust belt may have evolved through time. The proposed evolution is based almost entirely on the geometric constraints of the structural cross-sections, but is consistent with available basin migration history (Horton et al., 2001, DeCelles and Horton, in review), ages of overlapping syntectonic sedimentary rocks (Sempere et al., 1990; Jordan et al., 1997) and local thermochronology (Benjamin et al., 1987; Farrar et al., 1988; Sempere et al., 1990: Ege, 2001). The kinematic cross-sections were constructed under the assumption that the faults are in-sequence in the direction of transport whenever possible. Dates indicate local timing constraints and arrow shows the location of the Cochabamba area (Figure 2) and the location of the Tarabuco and Incapampa synclines (Figure 3). Scale is in kilometers.

The proposed kinematic model suggests that the eastward propagation of the structurally highest basement thrust fed ~105 km of slip into the Eastern Cordillera along east-vergent and west-vergent faults. This structure also fed ~90 km of eastward slip into the Interandean zone. The initiation and eastward propagation of a lower basement thrust structurally elevated the Interandean zone with respect to the foreland while feeding ~65 km of slip into the

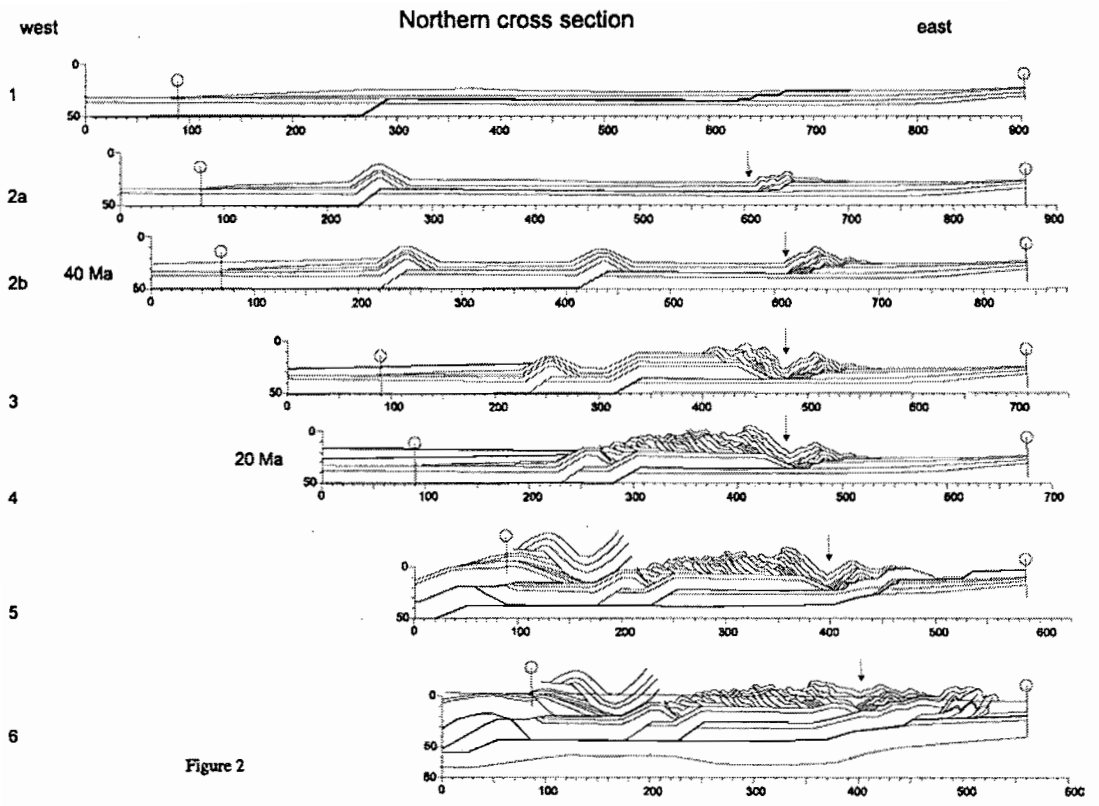

Figure 2

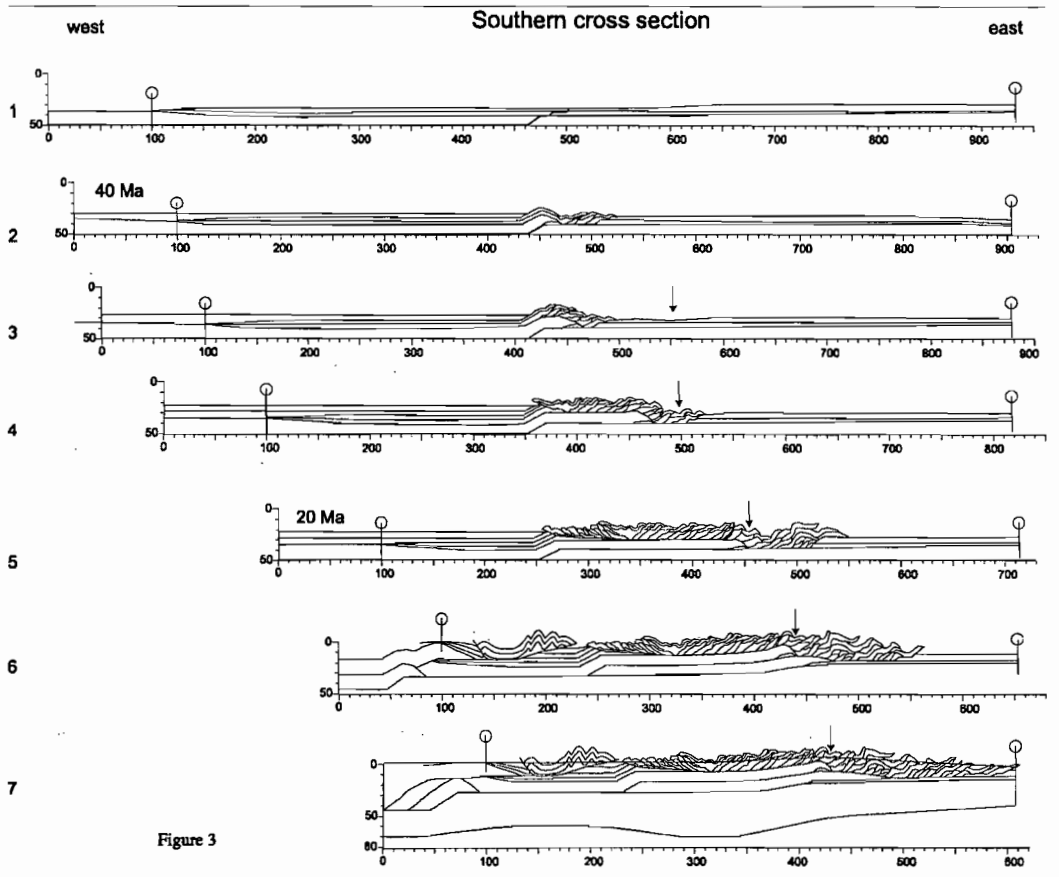

Figure 3

Subandean zone. Out-of-sequence basement thrusting to the west is proposed to have elevated the western edge of the plateau and accommodated ~40 km of shortening within the Altiplano. Total cumulative shortening within the cover rocks of the Andean fold-thrust belt (300-330 km) can be balanced by an equivalent amount of shortening along two basement megathrusts.

REFERENCES

Beck, S. L., Zandt, G., Myers, S. C., Wallace, T. C., Silver, P. G., and Drake, L., 1996, Crustal thickness variations in the Central Andes: Geology, v. 25, p. 407-410.

Benjamin, M. T., Johnson, N. M., and Naeser, C. W., 1987, Recent rapid uplift in the Bolivian Andes: Evidence from fission-track dating: Geology, v. 15, p. 680-683.

DeCelles, P. G. and Horton, B. K., in revision, Implications of early Tertiary foreland basin development for the history of Andean crustal shortening in Bolivia: Geological Society of America.

Ege, H., Jacobshagen, V., Scheuber, E., Sobel, E., Vietor, T., 2001, Thrust related exumation revealed by apatite fission track dating, Central Andes (southern Bolivia): Geophysical Research Abstracts, EGS XXVI General Assembly, Nice, France, v. 3, p. 624.

Farrar, E., Clark, A.H., Kontak, D.J., Archibald, D.A., 1988, Zongo-San Gabon zone: Eocene foreland boundary of Central Andean orogen, northwest Bolivia and southeast Peru: Geology, v. 16, p. 55-58.

Horton, B.K., B.A. Hampton, and G.L. Waanders, 2001, Paleogene synorogenic sedimentation in the Altiplano Plateau and implications for initial mountain building in the Central Andes: Geological Society of America, v. 113, p. 1387-1400

Isacks, B. L., 1988, Uplift of the central Andean plateau and bending of the Bolivian orocline: Journal of Geophysical Research, v. 93, p. 3211-3231.

Jordan, T. E., Reynolds, J. H., and Erikson, J. P., 1997, Variability in age of initial shortening and uplift in the central Andes, 16–33°30' S, *in* Ruddiman, W. F., ed., Tectonic uplift and climate change: New York, Plenum Press, p. 41–61.

Kley, J., 1996, Transition from basement involved to thin-skinned thrusting in the Cordillera Oriental of southern Bolivia: Tectonics, v. 15, p. 763-775.

Kley, J., 1999, Geologic and geometric constraints on a kinematic model of the Bolivian orocline: Journal of South American Earth Science, v. 12, p. 221-235.

McQuarrie, N., DeCelles, P.G., 2001, Geometry and Structural Evolution of the Central Andean Backthrust Belt, Bolivia: Tectonics, v. 17, p. 203-220.

Sempere, T., Hérail, G., Oller, J., and Bonhomme, M. G., 1990, Late Oligocene-early Miocene major tectonic crisis and related basins in Bolivia, Geology, v. 18, p. 946-949.

Sheffels, B. M., 1990, Lower bound on the amount of crustal shortening in the central Bolivian Andes: Geology, v. 23, p. 812-815.

RIDGE COLLISION AND TOPOGRAPHY: FORELAND DEFORMATION IN THE PATAGONIAN ANDES

Victor A. RAMOS

Laboratorio de Tectónica Andina, Universidad de Buenos Aires (andes@gl.fcen.uba.ar)

KEY WORDS: Andes, ridge-collision, Patagonia, deformation, uplift.

INTRODUCTION

The relationship between timing and space of ridge collision and uplift of the Patagonian Andes has been proposed by several authors (Ramos, 1989; Forsythe and Prior, 1992; Ramos and Kay, 1992; Flint et al., 1994; Ramos et al., 1994; Gorring et al., 1997). The Patagonian Andes as a consequence of a series of ridge collisions had several pulses of uplift producing important crustal stacking in the foreland during Late Cretaceous, Eocene, and Late Miocene times. However, recent studies mainly based on the analysis of timing and origin of deformation along the Patagonian fold and thrust belt, proposed that flat-slab subduction result of seismic ridge collision (Suárez et al., 2000). The tectonic setting of both alternatives, in the present region of ridge subduction will be analyzed. The study area in the Patagonian Andes is located in Fig. 1. The collision of the Chile ridge against the trench is taking place at the Taitao Peninsula (46°30'S), just north of Penas Gulf in southern Chile (Forsythe et al., 1986; Lagabrielle et al., 1999; Burgois et al., 1996). The active volcanic front in the Southern Volcanic Zone associated with subduction of the oceanic crust ends in the Hudson volcano (46°00' SL). The arc volcanism resumes in the Austral Volcanic Zone after a gap of about 350 km, with the Lautaro volcano (48°59'SL) with strong adakitic signature, which indicates partial melting of a buoyant young oceanic lithosphere.

RIDGE COLLISION AND TOPOGRAPHY

Bathimetric data from the oceanic crust region adjacent to the Chile ridge, together with the digital topography provided by the U.S.G.S. are illustrated in Fig. 1. The digital elevation indicates an uplift of more than 2,000 m south of the Taitao Fault Zone along the axis of the cordilleran region. This fault zone limits the northern end of a segment subducted more than 3 My ago, as established by Cande and Leslie (1986). North of that zone is the segment where present subduction is under way, colliding the southernmost Chile ridge segment with the Taitao Peninsula (Forsythe and Prior, 1992). As a result, important crustal erosion occurred (Bourgois et al., 1996) and off-scraping is leading to tectonic emplacement of the oceanic crust as an ophiolite (Guivel et al., 1999).

The uplift of Cerro San Valentín to its present elevation at 4,070 m a.s.l. is truncated by the landward projection of the Taitao Fault Zone. On the other hand, south of this mountain is Cerro San Lorenzo (3,706 m) and the mountain chain encompassed by the Hielo Continental Patagónico Norte (*Northern Continental Ice Cap*). Several peaks within this chain are over 3,000 m above sea level (Cerro Fitz Roy, 3,375 m; Cerro Bertrand 3,200 m, among others). The elevation of these granitic mountains is indicating a minimum uplift, as these Miocene intrusives have been unroofed by erosion that eliminated at least a couple of kilometers of the country rocks. Another striking feature is the north-south trend of these uplifts which is parallel to the trench (Fig. 1).

The uplift mechanism could be considered as thermal driven. However, at these latitudes the collision of this southern segment took place at 6 to 10 Ma ago, and the oceanic asthenospheric window is far away beneath the foreland, more than 400 km to the east of these mountains (Murdie et al. 1993; Gorring et al., 1997). Therefore, the heat produced by the ridge subduction or the asthenospheric windows has long been dissipated, and the present topographic anomaly is hard to relate to a thermal anomaly.

Figure 1: Bathymetric data in the oceanic side combined with digital topography of the Andes at these latitudes. Note the major topographic change in the Patagonian Andes, south and north of the projection in the continent of Taitao Fault Zone. The Hudson is the last active volcano in a segment where the subduction of the Chile Ridge has not occurred yet (based on Forsythe and Prior, 1992).

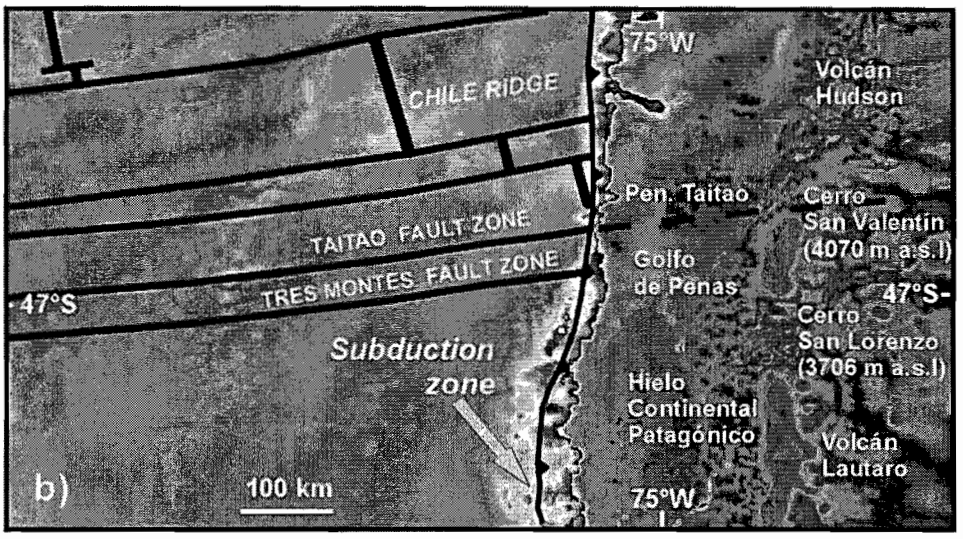

On the other hand, crustal stacking seems to be a more appropriate mechanism as there is a space coincidence between this southern segment and the development of the Patagonian fold and thrust belt. South of the triple junction there is important shortening absorbed by the sedimentary cover, that can be correlated with the basement shortening and uplift of the inner Patagonian Andes. North of the triple junction there is only a mild deformation, with minor shortening controlled by partial tectonic inversion, and large areas of the extensional Mesozoic basin are still preserved beneath the surface at these latitudes (Ramos, 1989).

VOLCANIC GAP

An alternative mechanism has been proposed to explain the volcanic gap by Suárez et al. (2000). These authors suggested that the shallowing of the Wadati-Benioff zone could have produced flat-slab subduction with nil magmatism. However, there is abundant evidence that in areas of present flat-slab subduction the thermal flux is low, and always flat-slab segments are associated with cold continental lithosphere, since the asthenospheric wedge has retreated far away into the foreland. Another feature closely linked to flat-slab subduction is the strong coupling between the continental and oceanic lithospheres that leads to basement foreland deformation. As a result of that, the foreland is broken and Sierras Pampeanas basement uplifts are developed (Jordan et al., 1983).

The thermal state near the triple junction has been studied by Murdie et al. (1993) and Daniel et al. (1996). These authors assumed that temperature field required to explain the observed gravity anomalies, indicates an active asthenospheric wedge and a higher than normal heat flux. The petrologic studies on the retroarc plateau basalts indicate an abnormal heat source in the mantle located at 80-90 km depth with temperatures of the order of 1400 to 1450°C (Cheadle and Petford, 1993), not compatible with the low thermal gradient of a flat-slab subduction. Geochemical and isotopic models of the plateau basalts suggest an abnormal hot mantle (Kay et al., 1993; Kay and Gorring, 1999). The basalt volumes of these plateau basalts require eruptions of 0.2 km^3/year, rates similar to other flood basalt provinces around the world, as the high thermal gradients of Paraná basalts (Petfrord *et al.*, 1996). The foreland basement at these latitudes is exposed in the Deseado Massif, where Mesozoic grabens only have a mild inversion in the subsurface (Ramos, 2002; Homovc and Constantini, 2001). The Wadati-Benioff zone according to the model elaborated by Daniel et al. (1996) south of the triple junction,

has a 30° dipping of the oceanic slab which is not consistent with the flat-slab subduction proposed by Suárez et al. (2000) to explain the volcanic gap. The dehydration of the oceanic slab in the subduction complex prior to the interaction with the asthenospheric wedge was the cause of the volcanic gap as proposed by Mpodozis et al. (1985).

TIMING OF DEFORMATION

Some authors pointed out that deformation is not restricted to the time of ridge collision (Ray, 1996, unpublished Ph. D. thesis; Suárez et al., 2001), doubting about the cause-effects relationship between these two processes, mainly because they found Paleogene and even older deformation in several areas of the Patagonian Cordillera. Although there is no doubt that major orogenic uplift in the Tres Montes-Esmeralda segment has occurred at about 6-8 million years ago, as indicated by new Ar/Ar data on the granitoids of Cerro San Lorenzo (Welkner, 2000), it does not mean that this is the only episode of deformation recorded in the region. The synorogenic deposits of Río Frías and Santa Cruz Formations has begun their deposition as far back as 19 My ago (Feagle et al., 1995). However, effective topographic uplift, as inferred from isotopic studies of paleosoils of the Santa Cruz Formation (Blisniuk and Strecker, 2001), occurred at a younger time. A period of rapid convergence started at about 20 My ago, which accounts for the beginning of deformation, but final uplift seems to be closely linked with the subduction of this Chile Ridge segment. The time and space coincidence between the uplift of Cerro San Lorenzo and the age of collision proposed by Cande and Leslie (1986), fits better with the isotopic data derived from paleosoils (Blisniuk and Strecker, 2001). The time lag between rapid uplift and collision was interpreted as a result of an increase of transpression as young and buoyant oceanic lithosphere was approaching the trench in a low partitioned regime (Folguera and Ramos, 2001).

There are several ridge collisions registered in the Pacific margin of Patagonia (Cande and Leslie, 1986; Ramos and Kay, 1992; and Ramos et al., 1994). The first collision took place at about 80 My ago, as indicated by the emplacement of the Puesto Nuevo Adakite (49°S) and the magmatic arc gap that prevailed during most of the Late Cretaceous at these latitudes (Ramos et al., 1994). There is evidence of widespread deformation in this time interval from 52 to 44°S, described as part of the Patagónides deformation (see review in Ramos, 2002).

Paleogene deformation produced unconformities in the inner region of the Southern Patagonian Andes mainly south of 50°S, and locally in the Cosmelli basin at Meseta Buenos Aires latitudes (Flint et al., 1994). This tectonism is also related to a period of rapid convergence, that leaded to collision of the Farallon-Aluk ridge south of 43°30' (Cande and Leslie, 1986; Ramos and Kay, 1992) and the widespread eruption of OIB retroarc plateau Posadas Basalt between 44° and 52°S.

The third episode is related to the collision of the Chile Ridge that shifted from south to north, from 14 My ago to present time and is well documented by off-scraping of oceanic crust and emplacement of ophiolites, near-trench felsic and MORB-like magmatism, adakite emplacement, rapid mountain uplift, development of a fold and thrust belt, and retro-arc OIB magmatism.

CONCLUDING REMARKS

There is a robust amount of evidence that ridge subduction in the last 80 My interacted with the subduction zone. This interaction is documented by abrupt changes in uplift, deformation, and magmatism. As the collisions of these ridges were associated with periods of rapid convergence in the Late Cretaceous, in the Paleogene and the Neogene, their effects were superimposed to an increase of orogenic activity generated by acceleration of the convergence rates. However, the climax of this deformation and the rapid uplift coincided in time and space with the ridge collision, as documented in the most recent interactions between the seismic ridge and the trench.

REFERENCES

Blisniuk, P.M. and M. R. Strecker, 2001. The interaction between orographic and climatic processes in the southern Patagonian Andes.In Deformation Processes in the Andes, Sonderforschungsbereich 267: 345-356, Berlin.

Bourgois, J., H. Martin, Y. Lagabrielle, J. Le Migne and J. Frutos Jara, 1996. Subduction erosion related to spreading ridge subduction: Taitao Peninsula (Chile Margin triple junction area). Geology 24(8): 723-726.

Cande, S.. and R.B. Leslie, 1986. Late Cenozoic Tectonic of the Southern Chile Trench. J. G. R. 91 B1: 471-496.

Cheadle, M. and N. Petford, 1993. Origin of Patagonian flood basalts. EOS Transactions A. G. U., 74: 663.

Daniel, A.J., N.J. Kusznir and P. Styles, 1996. A temperature and gravity model of spreading Centre subduction, with application to southern Chile. 30th. International Geological Congress, Abstracts 1: 128, Beijing.

Feagle, J., T. Brown, C. Swisher and G. Buckley, 1995. Age of the Pinturas and Santa Cruz Formations. VI°Congreso Argentino de Paleontología y Bioestratigrafía (Trelew), Actas: 129-135, Trelew.

Flint, S.S., D.J. Prior, S.M. Agar and P. Turner, 1994. Stratigraphic and structural evolution of the Tertiary Cosmelli basin and its relationship to the Chile triple junction. Journal of the Geological Society 151: 251-268.

Folguera, A. and V.A. Ramos, 2001. Distribución de la deformación en los Andes Australes (33°-46°S). In Avances en Microtectónica, J.M. Cortés, E. Rossello and L. Dalla Salda (eds.), Asoc. Geol. Arg., Serie D: 5: 13-18.

Forsythe, R. and D. Prior, 1992. Cenozoic continental geology of South America and its relations to the evolution of the Chile triple junction. Proceedings of the Ocean Drilling Program, Initial Reports 141: 23-31.

Forsythe, R., E. Nelson, M. Carr, M. Keading, M. Hervé, C. Mpodozis, J. Soffia and S. Harambour, 1986. Pliocene near trench magmatism in Southern Chile: a possible manifestation of ridge collision. Geology 14: 23-27.

Gorring, M., S. Kay, P. Zeitler, V. Ramos, D. Rubiolo, M. Fernandez and J.L. Panza, 1997. Neogene Patagonian plateau lavas: continental magmas associated with ridge collision at the Chile Triple Junction. Tectonics 16(1): 1-17.

Guivel, C., Y. Lagabrielle, J. Bourgois, R.C. Maury, S. Fourcade, H. Martin and N. Arnaud, 1999. New geochemical constraints for the origin of ridge subduction-related plutonic and volcanic suites from the Chile triple junction (Taitao Peninsula and site 862, Leg ODP 141 on the Taitao ridge), Tectonophysics 311(1-4): 83-113.

Homovc, J.F. and L.A. Constantini, 2001. Hydrocarbon exploration potential within intraplate shear-related depocenters, Deseado and San Julián basins, southern Argentina. A.A.PG., Bulletin 85(10): 1795-1816.

Jordan, T., B. Isacks, V. Ramos and R. Allmendinger, 1983. Mountain building in the Central Andes. Episodes 1983(3): 20-26.

Kay, S.M. and M.L. Gorring, 1999. Evolution of the Patagonian mantle: evidence from isotopic studies of Tertiary to Recent plateau lavas. II South American Symposium on Isotope Geology (Córdoba), Actas: 556-565.

Kay, S.M., V.A. Ramos and M. Márquez, 1993. Evidence in Cerro Pampa volcanic rocks for slab-melting prior to ridge-trench collision in southern South America. Journal of Geology 101: 703-714, Chicago.

Lagabrielle, Y., J. Bourgois, M. Suárez, R. de la Cruz, E. Garel, O. Dauteuil, and M.A. Gutscher, 1999. From compressional to extensional tectonic regime at the front of the Patagonian Andes 46°S-47°S: a response to the subduction of the Chile spreading ridge?. 4th. International Symposium on Andean Geodynamics: 411-416.

Mpodozis, C., M. Hervé, C. Nassi, J. Soffia, R. Forsythe, E. Nelson, 1985. El magmatismo plioceno de Península Tres Montes y su relación con la evolución del Punto Triple de Chile Austral. Rev. Geol. Chile 25-26: 13-28.

Murdie, R.E., D.J. Prior, P. Styles, S.S. Flint and S.M. Agar, 1993. Seismic responses to ridge-transform subduction: Chile tiple junction. Geology 21: 1095-1098.

Petford, N., M. Cheadle and B. Barreiro, 1996. Age and origin of southern flood basalts, Chile Chico region (46°45'S). III° Andean Geodynamics (Saint Maló), Expanded abstracts: 629-632.

Ramos, V., 1989. Foothills structure in Northern Magallanes Basin, Argentina. A.A.P.G., Bulletin 73: 887-903.

Ramos, V.A., 2002. Evolución tectónica. In M.J. Haller (ed.) Geología y recursos naturales de Santa Cruz. XV° Congreso Geológico Argentino (El Calafate), Relatorio I(23): 365-387, Buenos Aires.

Ramos, V.A. and S.M. Kay, 1992. The Southern Patagonian plateau basalts: retroarc testimony of a ridge collision, Argentina. In Andean geodynamics Symposium (Grenoble, France). Tectonophysics 205: 261-282.

Ramos, V.A., S. Mahlburg Kay and L. Sacomani, 1994. La dacita Puesto Nuevo y otras rocas magmáticas: colisión de una dorsal oceánica cretácica. VII°Congreso Geológico Chileno (Concepción), Actas II: 1172-1176.

Suárez , M., R. de la Cruz and C.M. Bell, 2000. Timing and origin of deformation along the Patagonian fold and thrust belt. Geological Magazine 137(4): 345-353, United Kingdom.

SECONDARY GOLD DEPOSITS IN THE LÍPEZ REGION (BOLIVIA)

Wilfredo RAMOS C. (1) and Raúl FERNÁNDEZ (2)

(1) Instituto de Recursos Minerales, FCNyM, Universidad Nacional de La Plata - DAAD
(wramoscollorana@yahoo.com)
(2) Instituto de Recursos Minerales, FCNyM, Universidad Nacional de La Plata-CICBA

KEY WORDS: Bolivia, secondary deposits, gold.

INTRODUCTION

In the Lípez region small secondary gold-deposits are being exploited in minor scale (Fornari et al., 1989, Ramos, 1992, Ramos and Fornari, 1994). This paper summarizes general characteristic of gold grains, such as its distribution, morphoscopy and chemical composition. These results were used to relate it with the geological environment, the primary sources and to deduce exploration criteria in the district.

The zone is located in the Lípez region, southwest of Bolivia, near to Argentina border (Fig 1). The zone belongs to the geological provinces of the Cordillera Occidental, Altiplano and the Cordillera Oriental; the older outcrops consist of Ordovician rocks, which consist of sandstones, siltstones, quarzites and shales (Llandeillian-Caradocian, Kley et al, 1997). They are overlain by limestones, reddish and violaceous argillites of El Molino Formation (Cretaceous), whose outcrops are often limited by regional faults.

The Cenozoic consists of several km of detrital continental deposits associated with volcanic rocks which cover most part of the Altiplano. The magmatism is represented effusive volcanism of andesitic composition (Rondal lavas 22.1 ± 0.6 Ma Fornari et al., 1993), followed by the superposition of mainly dacitic volcanism from about 18 Ma. It includes explosive products (ignimbrites, pyroclastic deposits) and lavas, erupted from extended stratovolcanoes and caldera structures, besides of intrusive subvolcanics stocks (14.6 ± 0.5 Ma, Lema and Ramos, 1997).

The main tectonic features in the Lípez basin result from a compression of Oligocene age, which actuated two main boundary faults: the Uyuni-Khenayani fault to the west by and the San Vicente fault to the east (Baby et al., 1990).

DISTRIBUTION, CHARACTERISTICS AND CHEMICAL COMPOSITION OF GOLD PARTICLES

The distribution of secondary gold-deposits in Lípez region (Fig. 4), show that Vilader, Guadalupe-Morokho and Esmoraca-Viluyo areas have greater concentrations; however they are small size, but some areas are being worked.

Systematic description of the gold particles (about 2100 particles) was based on the observation under binocular microscope of several morphological characters (e.g. length, wide, shape, ...) and chemical compositions were determined by electronic microprobe.

The studied gold particles show different morphologies and chemical analysis which are related with the ore sources (Fig. 3 and Table 1).

The gold particles form two contrasting groups; one consists of particles with angular, irregular morphology; in some cases they are still accompanied by quartz inclusions; the flatness index value is low (1 to 6), but increases in few cases up to 11. The chemical composition varies from 92 to 95 % Au and 8 up to 14 % Ag.

The other group consists of particles with sub-spherical shapes, sub-rounded to rounded morphologies, regular topographies and a low content of silver (<2 % Ag) and traces of Te and Hg. The flatness index is low (from 1 to 5).

The mean size of the particles is about 1 mm; however, they are some exceptions in Vilader and Esmoraca areas with particles up to 6 mm.

Gold particles with the different characteristics mentioned above are mixed in the secondary gold deposits in some areas. In such cases, these characteristics can be used to identify the relative contribution from several primary ore deposit; then the study gold particle is an important tool for mineral exploration.

Similar characteristics are described in the NW Argentine (Rinconada), where the chemical analysis of gold grains vary from 98.84 to 92.59% Au and from 1.16 to 6.71% Ag, but the gold from vein quartz (El Torno), contains 30.26 to 35.86 % Ag (Segal et al., 1997).

PRIMARY MINERALIZATION

The primary mineralization consists of quartz gold veins in Ordovician rocks, polymetallic veins and zones of hydrothermal alteration in volcanics.

The greatest deposits formed by gold-quartz veins are located in the eastern area: e.g. Sucre, Candelaria, Khorykhoya, Chilcobija and Chilco; and can be related the "Au-Sb belt"(Lehrberger, 1988) in the austral part of the Cordillera Oriental; Vilader and Candelaria are in the western area (Fig.1).

For the vein mineralizations included in Ordovician outcrops, controls are structural and lithologic; exploration criteria are the same as those known regionally in the Central Andes, from southern Peru, Bolivia (Yani, Amayapampa, etc.) and northern Argentina (Sierra Rinconada, Segal et al., 1997, Zappettini et al., 1999).

The polymetallic veins and alterations zones of volcanites have gold traces. In some areas with propylitic, argillic and silicic alterations, the anomalies are up to 30 ppm Au, (e. g. 804 to 28400 ppb Au at the Galán Volcanic Complex, Ramos et al., 2001). In the Lípez zone, anomalous gold values are known at the Cerro Bonete (Lípeña, La moza, Barrayhuayco mines), Cerro Morokho and Cerro Lípez (Mesa de Plata and Machu

Socavon) between others. So, the volcanic complex in the southwest of Bolivia, appears as an important area for gold prospecting.

CONCLUSIONS

The secondary gold deposits in the Lípez region are small, but in some cases they are interesting for exploitations in minor scale. The morphoscopic and chemical characteristics of the gold particles which are correlated with the geological environment, are used to characterize the primary sources of the mineralization and provide an efficient tool for mineral exploration.

ACKNOWLEDGEMENTS: We are grateful to Dr. Michel Fornari and Dr. Gerard Herail for their suggestions.

REFERENCES

Fornari M., Herail G., Viscarra G. 1989. Los yacimientos de oro de los Lípez (Bolivia) Tomo I: Estratigrafía y dinámica de emplazamiento de las volcanitas del área de Guadalupe. ORSTOM, Bolivia N° 19. La Paz. 27 p.

Fornari M., Pozzo L., Soler P., Bailly L., Leroy J., Bonhomme M. 1993. Miocene volcanic centers in the southern Altiplano of Bolivia. The Cerro Morokho & Cerro Bonete area (Sur Lípez). Second ISAG, Oxford (UK), p. 363-366

Herail G., Fornari M., Pozzo L. 1993. Émission d'or particulaire au cours des phases de volcanisme explosif du Miocene du Sud de l'Altiplano de Bolivie. C.R. Acad. Sci. Paris, t.316, Série II, p. 1431-1438.

Kley J., Muller J, Tawackoli S., Jacobshagen V., Manutsoglu E. 1997. Preandean and Andean-Age Deformation in the Eastern Cordillera of Southern Bolivia. Journal of South American Earth Sciences. Vol. 10, No 1, p. 1-19.

Lehrberger, G. 1988. Gold-antimonite deposits in marine sediments of the Eastern Cordillera of the Bolivian Andes. Bicentenial Gold 88. Melbourne. 319-321

Lema J.C., Ramos W., 1997. Mapa Geológico de Esmoraca. Publicación SGM Serie I-CGB-50, Cuadrángulo N° 6328. Escala 1:100000. SERGEOMIN, Bolivia.

Ramos C., W., 1992. El placer de Vilader, un yacimiento aluvial de oro de la cuenca alta del Río Lípez. Tesis de Grado, Facultad de Ciencias Geológicas, Universidad Mayor de San Andrés. La Paz. 150 p. Inedito.

Ramos W., Fornari M., 1994. Problemática de la presencia de oro en los Lípez. Boletín de la Sociedad Geológica de Bolivia, No 28. p.248-259.

Ramos C. W., Etcheverry R., Fernández R. 2001. Características de las partículas de oro de los depósitos aluvionales auríferos en el área de Esmoraca suroeste de Bolivia. Congreso Latinoamericano de Geología. Metalogénesis N° 184, p. 7. CD.

Ramos C. W., Fernández R., Lehmann B., 2001. Anomalías de Au-Ag en el Complejo Volcánico Galán (Mioceno), suroeste de Bolivia. Congreso de Geología Económica, Salta – Argentina. Actas 1. p. 123-128.

Segal S., Zappettini, E., Craig J., 1997. Metalogénesis del oro de la Sierra de Rinconada, Provincia de Jujuy. Serie contribuciones técnicas, Recursos Minerales 2. Inst. de Geología y Recursos Minerales. SEGEMAR. P.31.

Zappettini, E. O., Segal S., 1999. Depósitos aluvionales de la Puna, Jujuy. In Recursos Minerales de la República Argentina (Ed. E.O. Zapettini), Inst. de Geología y Recursos Minerales SEGEMAR, Anales 35: 1841-1844, Buenos Aires.

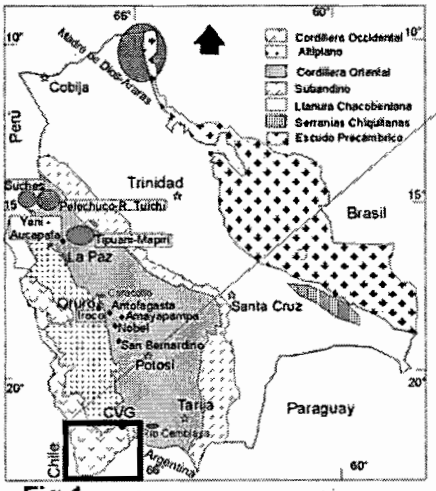

Fig.1 . Geologic provinces, major gold secondary and primary deposits of Bolivia Andes

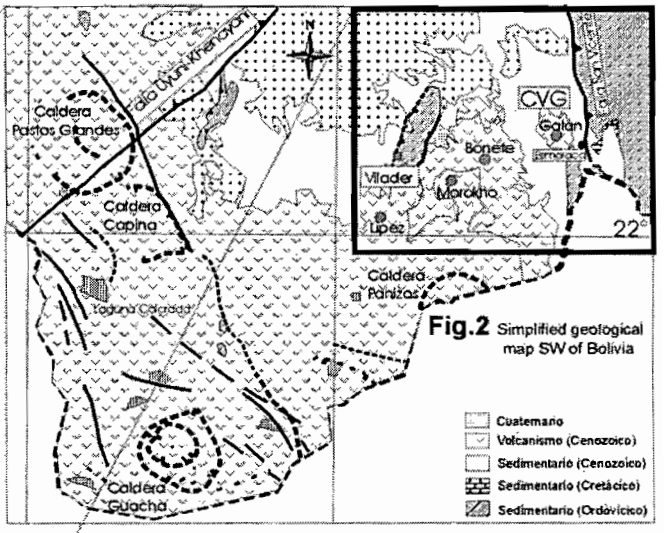

Fig.2 Simplified geological map SW of Bolivia

Fig.3 MORPHOLOGY OF GOLD GRAINS
Lipez region

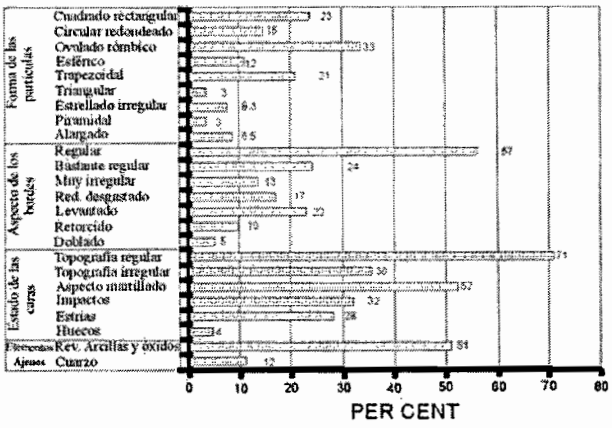

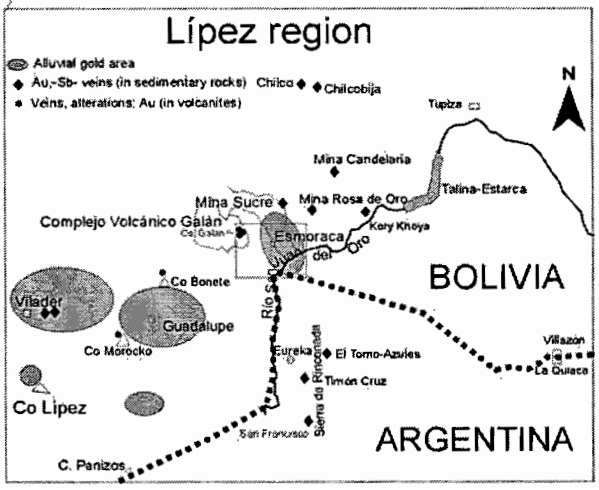

Fig.4. Secondary and primary gold deposits in the Lípez

Secondary deposits				Primary ore deposits		
Size - shape	flatness index	Grade	Chemical composition	Related ore sources	Chemical composition	Grade
Mean 1 mm, some up to 5.6 mm, -angular,	Major until 4, rare up to 11	Major <1 g/t, some up to 3 g/t	92 % Au, 8 % Ag. rare 83% Au, 14 Ag (Vilader)	Quartz veins in ordovician rocks	92 a 95 % Au, until 8 % Ag (Vilader)	Up to 2.5 g/t and 69 g/t (max) (Vilader)
Mean < 1 mm, some up to 3.3 mm, -rounded	Major until 5, rare up to 8	<1 g/t	98 % Au, hasta 2 % Ag.	Ignimbrites. Veins and alterations in volcanic rocks		6 to 24800 ppb de Au; <5 to 328 ppm de Ag (Galán)

Table 1. Related secondary and primary gold deposits in the Lípez region (Bolivia).

NEW PALEOMAGNETIC DATA FROM THE WESTERN PUNA OF ARGENTINA: SOME TECTONIC SPECULATIONS ON ITS EARLY PALEOZOIC EVOLUTION.

A.E. RAPALINI (1,2), M.S.VELASCO (3) and M.KOUKHARSKY (2,4)

(1) INGEODAV, Departamento de Ciencias Geológicas, FCEyN, Universidad de Buenos Aires, Buenos Aires, Argentina. (rapalini@gl.fcen.uba.ar)

(2) Consejo Nacional de Investigaciones Científicas y Técnicas

(3) Center for Earthquake Research and Information, University of Memphis, Memphis, USA.

(4) Departamento de Ciencias Geológicas, FCEyN, Universidad de Buenos Aires, Buenos Aires, Argentina

KEY WORDS: Puna, paleomagnetism, Antofalla terrane, Gonwana

The tectonic evolution of the western South American margin (SW Gondwana) in the latest Proterozoic and Early Paleozoic is dominated by several controversies. In the recent years, however, a broad picture has emerged that incorporates the accretion of terranes as a fundamental mechanism in the configuration of the margin (see Pankhurst and Rapela, 1998, Keppie and Ramos, 1999, etc.). One of the still unsolved questions is the tectonic evolution of the Antofalla terrane in northwestern Argentina and northern Chile. This block has been defined on the basis of a few and small outcrops of Late Proterozoic metamorphic rocks in Chile (Ramos, 1988; Damm et al., 1990), but it is characterized by abundant and widespread Early Paleozoic magmatism and sedimentary successions (Damm et al., 1990, Coira et al., 1999). Whether the Antofalla block is an accreted terrane and its relations with the Arequipa Massif in Perú has not got consensus yet (Bahlburg and Hervé, 1996).

Forsythe et al. (1993) published the first paleomagnetic results form Early Paleozoic rocks of this region. These authors interpreted their results as evidence of a para-autochthonous Arequipa-Antofalla block that successively rotated clockwise and counterclockwise opening and closing a small ocean between it and the western Gondwana margin. Rapalini et al. (1999), however, pointed out that the paleomagnetic data obtained so far belong only to the Antofalla block and suggest a possible latitudinal displacement of this terrane respect to Gondwana in pre-Silurian times.

An important Early Paleozoic magmatism is exposed in the western Puna of Argentina, known as the "Faja Eruptiva de la Puna Occidental" (Western Puna eruptive belt, Palma et al., 1986) which continues in the Cordon de Lila and Sierra de Almeida in Chile. New paleomagnetic data was obtained from some Early Paleozoic units in the western Puna of Argentina (24.3°S, 67.3°W). These units include the Early Ordovician ignimbrites and lavas exposed at Vega Pinato (Koukharsky et al., 1996) and the Chachas and Taca-Taca plutonic complexes (Koukharsky, 1988). Sampling comprised six sites in the effusive rocks of Vega Pinato (three in ignimbrites and three in rhyolitic flows), six sites in the Chachas complex and three sites in the Taca-Taca formation. At each site six to seven independently oriented samples were collected with a portable drilling machine.

All samples were submitted to stepwise AF or thermal cleaning in 10 to 16 steps up to maximum fields of 140 mT or temperatures of 600°C. Magnetic components were determined by principal component analysis

(Kirschvink, 1980). Some sites were ruled out due to unstable magnetic behaviour or low within site directional consistency. These were three sites in the Chachas complex, two in the Taca-Taca granite and one in the volcanics of Vega Pinato. Samples from the remaining sites showed good magnetic behavior with either single or two components. In most cases, unblocking temperatures around 500°C and medium destructive fields lower than 50 mT suggested magnetite as the magnetic carrier.

Mean site characteristic remanence directions were obtained from sites TG 7, TG8, and TG11 from the Chachas complex, site TG13 from the Taca-Taca Fm and sites TG16, TG17, TG18 from ignimbrites and TG19 and TG20 from rhyolites from Vega Pinato. Bedding correction for the volcanics and ignimbrites of Vega Pinato was measured in the field. The Taca-Taca direction was corrected by the attitude of Tertiary clastic sediments that overlie the granitic rocks. No structural correction was applied to the Chachas complex, as no paleohorizontal could be determined. Consistency of directions of these sites with the others after bedding correction suggests that tilting of the Chachas complex is probably negligible. A virtual geomagnetic pole (VGP) was computed for each site. VGPs show a distribution following the proposed APWP of the Antofalla block by Forsythe et al. (1993) and Rapalini et al. (1999). A paleomagnetic pole (CHA) was computed from the average direction from sites TG7, TG11, TG13, TG16, TG17 and TG18 (Vega Pinato ignimbrites and Chachas and Taca-Taca complexes), which is consistent with the OP and OL poles (see fig.1). The age of the ignimbrites at Vega Pinato has been determined as Tremadoc to Arenig (Koukharsky et al., 1996). The age of the Chachas and Taca-Taca plutons is not well determined yet. An Early to Middle Ordovician age is possible according to a dating of the Taca-Taca pluton by Palma et al (1986) and a recent dating by Koukharsky et al. (in press) of the neighbouring Macón intrusive. Mean site remanence directions from TG-19 and TG-20 (rhyolitic flows from Vega Pinato), however, are consistent after bedding correction with the remanence directions from the Tremadoc Las Vicuñas Fm exposed in the Lari creek (Rapalini et al., 1999) .A unique paleomagnetic pole was computed combining the remanece direction of sites from both localities (FV, Fig.1).

The Early Paleozoic paleomagnetic poles for the Western Puna (Antofalla terrane) are presented in Table 1. Figure 1 shows the distribution of these after rotation into a Gondwana reconstruction (Lottes and Rowley, 1990). Their distribution suggests that they are ordered defining the Antofalla apparent polar wander path (APWP) between the Late Cambrian and the Silurian. However, FV position is not consistent, as the rocks from which it was computed are accurately dated as Tremadoc. A possible explanation is that it represents a pretectonic remagnetization in the latest Ordovician, associated to the Ocloyic tectonic phase (Rapalini et al., 1999). Our new results confirm the APWP previously proposed by Forsythe et al. (1993). However, its tectonic interpretation is controversial. According to Forsythe et al. (1993) it suggests just a ccw rotation of a para-authochtonous Arequipa-Antofalla terrane. But Rapalini et al. (1999) pointed out that the CHO pole of ca. 500 Ma shows a large paleolatitude anomaly of at least 1000 km. The Early to Middle Ordovician CHA pole does not show that anomaly in paleolatitude, although its quite large oval of confidence precludes determining anomalies of 10°. Nevertheless, a significant ccw rotation respect to the available Gondwana reference poles for the Early and Middle Ordovican is evident. Lack of well defined reference poles for Gondwana for the Middle and specially the Late Ordovician precludes to unambiguously define if the OP and OL poles show any relative movement between Antofalla and Gondwana. FV pole is consistent with the Silurian and Early Devonian poles of Gondwana. Despite the uncertainties and ambiguities, the simplest interpretation of the paleomagnetic data

obtained so far suggest relative displacement between Antofalla and Gondwana prior to the latest Ordovician, which include large ccw rotation and perhaps significant latitudinal displacements.

Further paleomagnetic data from Early Ordovician or older rocks from the Western Puna as well as reliable Middle to Late Ordovician reference poles for Gondwana will clarify the present uncertainties.

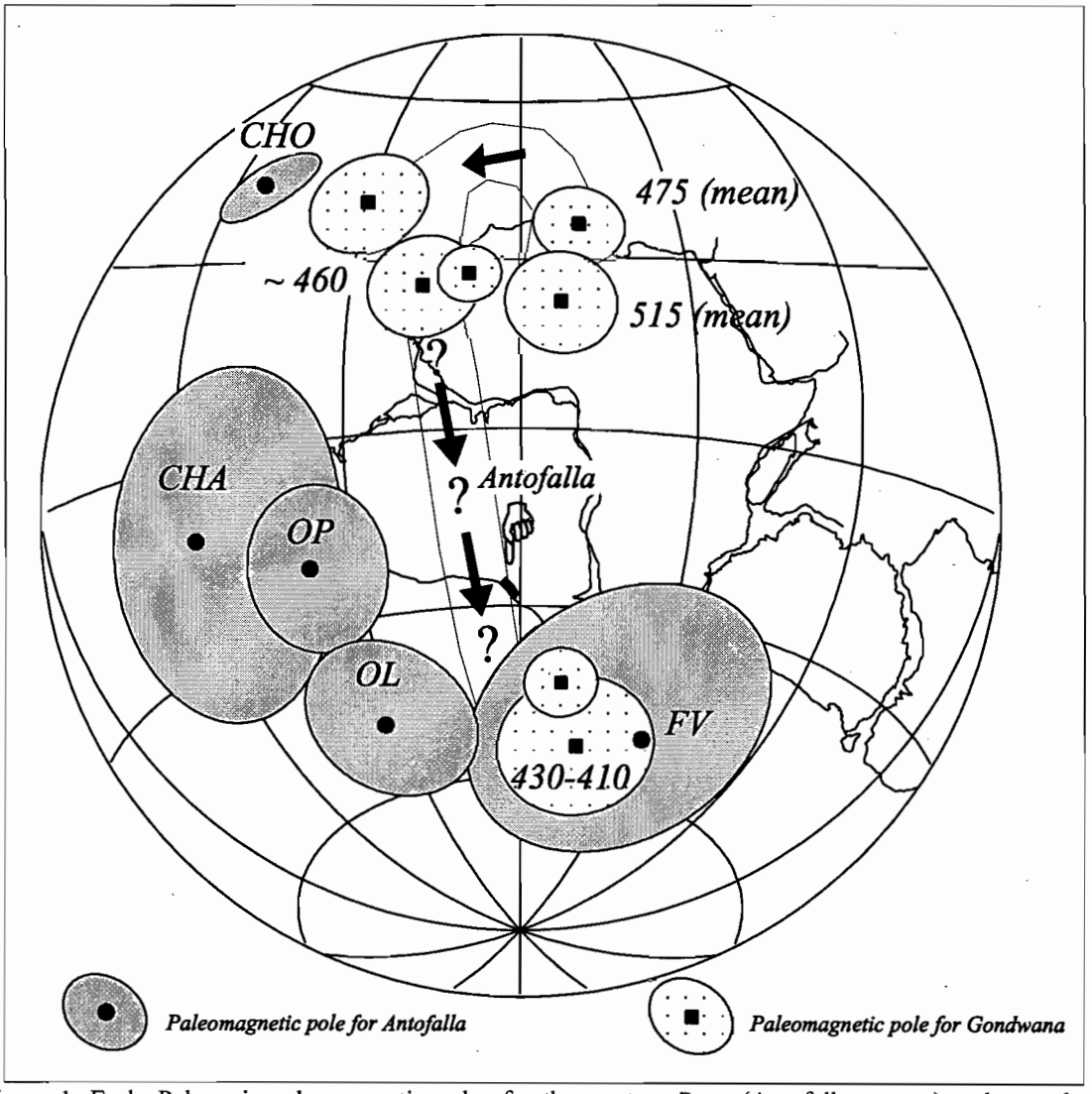

Figure 1: Early Paleozoic paleomagnetic poles for the western Puna (Antofalla terrane) and coeval reference poles for Gondwana with its hypothetical apparent polar wander path. Numbers indicate age of the reference poles in Ma., which are taken from Grunow (1995) and Conti et al. (1995). All poles have been rotated into African coordinates according to Lottes and Rowley (1990).

REFERENCES

Bahlburg, H. and F. Hervé, 1997. Geodynamic evolution and tectonostratigraphic terranes of northwestern Argentina and northern Chile. *Geol. Soc. Amer. Bull., 109,* 869-881

Coira, B., B. Perez, P. Flores, S. Mahlburgh Kay, B. Woll and M. Hanning, 1999. Magmatic sources and tectonic setting of Gondwana margin Ordovician magmas, northern Puna of Argentina and Chile. In *D.Keppie y V.Ramos (eds.), Laurentia - Gondwana connections before Pangea, Geol. Soc. Amer., Special Paper, 336,* 143-170.

Conti, C.M., A.E.Rapalini y J.F.Vilas; 1995. Palaeomagnetism of the Silurian Lipeon Formation, NW Argentina, and the Gondwana apparent polar wander path. *Geophys. J. Internat., 121,* 848-862.

Damm, K., S. Pichowiak, R.Harmon, W. Todt, S. Keley, R. Omarini and H.Niemeyer, 1990. Pre-Mesozoic evolution of the Central Andes: the basement revisited. In *S. Mahlburgh Kay and C.Rapela, Eds., Plutonism from Antarctica to Alaska, Geol. Soc. Amer., Special Paper, 241,* 101-126.

Forsythe, R., J. Davidson, C. Mpodozis and C. Jesinkey, 1993. Lower Paleozoic relative motion of the Arequipa block and Gondwana: paleomagnetic evidence from Sierra de Almeida of northern Chile. *Tectonics, 12*, 219-236.
Grunow, A., 1995. Implications for Gondwana of new Ordovician paleomagnetic data from igneous rocks in southern victoria Land, east Antarctica. *J. Geophys. Res., 100*, 12589-12603.
Keppie, D. and V.Ramos (eds.), 1999. Laurentia - Gondwana connections before Pangea. *Geological Society of America, Special Paper, 336.*
Kirschvink, J.L. 1980. The least-squares and plane and the analysis of paleomagnetic data. *Geophys. J.R. Astron. Soc., 67*: 699-718
Koukharsky, M., 1988. Geología de la Puna en la región que media entre Cerro Socompa y Tul Tul, prov. De Salta. *University of Buenos Aires, Unpublished PhD. Thesis, 83 pp.*
Koukharsky, M., R. Torres Claro, M. Etcheverría, N.E.Vaccari and B.G. Waisfeld, 1996. Episodios volcánicos del Tremadociano y del Arenigiano en Vega Pinato, Puna Salteña, Argentina. *13 Cong. Geol. Arg., 5*, 535-542.
Lottes, A.L and D.B.Rowley; 1990. Reconstruction of the Laurasian and Gondwanan segments of Permian Pangaea. *Geol. Soc. Memoir, 12*, 383-395.
Palma, M.A., P.D. Párica and V.A. Ramos, 1986. El granito Archibarca: su edad y significado tectónico, provincia de Catamarca. *Rev. Asoc. Geol. Arg., 41,* 414-419.
Pankhurst, R.J. and C.A. Rapela (eds.), 1998. The Proto-Andean margin of Gondwana. *Geological Society of London, Special Publications, 142.*
Ramos, V. A.; 1988. Late Proterozoic - Early Paleozoic of South America - a collisional history. *Episodes, 11, 3* : 168-174.
Rapalini, A.E., R.A. Astini and C.M.Conti, 1999. Paleomagnetic constraints on the tectonic evolution of Paleozoic suspect terranes from southern South America. In *D.Keppie y V.Ramos (eds.), Laurentia - Gondwana connections before Pangea, Geological Society of America, Special Paper, 336*, 171-182.

Pole	Geologic Unit	Paleomagnétic Pole (PP) Lat. (°)	Long. (°)	(dp/dm)	Paleomagnetic Results	Age of PP
CHO[1]	Plutón de Choschas + lavas presilúricas	58.1	309.2	(3.8°/7.5°)	AF/T demag., both polarities, n=24 samples	Latest Cambrian
CHA[2]	Chachas andTaca-Taca plutons +Vega Pinato ignimbrites	16.9	260.3	(20.4°/27.8°)	AF/T demag, tilt test, N=6 sites	Early-Middle Ordovician
OP[1]	Tucucaro, Tilipozo and Alto del Inca Plutons	0.0	271.0	(12.4°/13.7°)	AF/T demag., tilt test, n=20 samples	Late Ordovician
OL[1]	PreSilurian lavas	-25.2	260.5	(13.7°/15.0°)	AF/T demag., both polarities, n=20 samples	Silurian ?
FV[3]	Las Vicuñas Fm + Vega Pinato rhyolites	-59.1	289	(19.1°/22.0°)	AF/T demag, tilt test, N=6 sites	Late Ordovician?

Table 1: List of Early Paleozoic paleomagnetic poles for the Western Puna. AF/T demag: alternating field and thermal demagnetization. Negative (positive) latitudinal values correspond to southern (northern) hemisphere. [1] pole obtained by Forsythe et al. (1993); [2] pole obtained in this study; [3] pole obtained combining results from Rapalini et al. (1999) and this study.

ADAKITIC MAGMATISM AT THE LOS PELAMBRES GIANT PORPHYRY COPPER DEPOSIT, CHILE

Martin REICH (1), Miguel Angel PARADA (1), Carlos PALACIOS (1), Andreas DIETRICH (2) and Bernd LEHMANN (2)

(1) Departamento de Geología, Fac. Cs. Fís. y Mat., Universidad de Chile, Santiago-Chile (mreich@cec.uchile.cl).

(2) Institut für Mineralogie und Mineralische Rohstoffe, Technische Universität Clausthal, Germany.

KEY WORDS: Los Pelambres, porphyry copper, adakites.

INTRODUCTION

The Andes of central Chile host several Miocene-Pliocene world-class porphyry copper deposits such as Los Pelambres, Río Blanco-Los Bronces and El Teniente. Their formation has been related to crustal thickening, rapid uplift and exhumation of plutonic systems, together with exsolution of copper-bearing magmatic fluids responsible of brecciation, alteration and mineralization [1]. In this paper we focus on the petrogenesis of the copper porphyries at the Los Pelambres deposit (31°43'S, 70°29'W), located in the high Andes 190 km north of Santiago, near the Chile-Argentina border. The aim of this study is to constrain the nature and source(s) of the magmas associated with the formation of the Los Pelambres porphyry copper deposit, based on whole-rock major and trace elements data. The chemical composition of the Los Pelambres porphyries is then compared with the coeval and barren La Gloria pluton and Aconcagua volcanics, within the same Late-Miocene belt. Whole rock, major and trace elements data from Los Pelambres, La Gloria and Aconcagua magmatic rocks are reported by [2], [3] and [4], respectively.

GEOLOGIC BACKGROUND

The Los Pelambres deposit (32°S) is located in the flat-slab segment (28-33°S) of the Chilean Andes, below which the angle of subduction zone dips gently 10-15° to the east, and which displays a lack of recent volcanic activity. The Los Pelambres porphyry copper mineralization is hosted in an intrusive complex emplaced in andesitic rocks of the Los Pelambres Formation (Late Cretaceous). The intrusive complex has an age of about 10 Ma [5,6] and consists of a main tonalite stock, porphyry dykes of quartz diorite, quartz monzodiorite and

quartz monzonite, and minor post-mineralization andesite and aplite dykes. Magmatic/hydrothermal breccia pipes are also present within the deposit. A detailed petrographic description and characterization of these bodies is given in [6].

GEOCHEMISTRY OF THE LOS PELAMBRES INTRUSIONS

The Los Pelambres fresh (LOI<1.5wt%) mineralized intrusions (tonalite stock, tonalite porphyry and quartz monzodiorite porphyry) form a calc-alkaline suite covering a SiO_2 range from 62 to 72 wt% (Fig.1). They are characterized by high Al_2O_3 (15.2-17.8 wt%) and Na_2O (4.8-6.6 wt%) abundances, with $K_2O/Na_2O<1$ (0.23-0.71). The Na-rich intrusive rocks from Los Pelambres, when plotted on an Ab-An-Or normative diagram show a trondhjemitic character (Fig.2). Trace element abundances of the Los Pelambres intrusions show high Sr (306-750 ppm) and low Y (1.6-6.6 ppm), with high Sr/Y ratios (~100-300) (Fig.3). Cr (1-17 ppm), Ni (2-12 ppm) and Nb (1-10 ppm) contents of the Los Pelambres rocks are low. Chondrite-normalized rare earth element (REE) patterns of Los Pelambres rocks are strongly fractionated, with light rare earth element (LREE) enrichment and heavy REE (HREE) depletion (low Yb (0.143-0.592) and high $[La_N/Yb_N]$ ~25-60) (Fig.3). REE patterns display a steep negative slope with an inflection at Tb, and no positive or negative Eu anomalies are recognized ($[Eu/Eu^*]$~1). When compared to the La Gloria and Aconcagua coeval and barren magmatic rocks, the Los Pelambres porphyries are Al_2O_3 and Na_2O-enriched, together with higher Sr/Y and La/Yb ratios. These particular geochemical features reflect a deeper, high pressure (>15 kbar), and garnet-bearing magmatic source [7,8].

ADAKITIC SIGNATURE: AN ODDITY IN THE LATE MIOCENE MAGMATISM OF CENTRAL CHILE

The intrusive rocks from the Los Pelambres porphyry copper deposit display an adakitic signature, according to the criteria given in [8]. The principal differences between adakitic and "normal" calc-alkaline rocks are recorded by REE, Y and Sr. These relationships can be clearly seen in the $[Sr/Y]$*vs.*Y and $[La_N/Yb_N]$*vs.*Yb_N discrimination diagrams (Fig.3). Along the Chilean Andes (18-54°S), adakitic volcanoes (i.e. slab melts) are documented only in the Austral Volcanic Zone (AVZ, 49-54°S) [9], where young, hot and buoyant oceanic lithosphere (<24 Ma) is subducted under a relatively thin crust (<35 km). The Late Miocene adakitic plutons at Los Pelambres formed closely related in time and space with a changing subduction geometry. In fact, tectonic reconstructions by [10] revealed that the Juan Fernández Ridge (JFR) migrated from north to south along the Chilean margin since Early Miocene to its actual position in central Chile. At the end of the Miocene (~10-7 Ma), the JFR was subducting exactly under the Los Pelambres area, producing relevant modifications of the thermal structure of the subducted lithosphere [11], and thus providing favorable conditions for slab melting. A recent thermal model by [12] has shown that slab melting is viable under flat-slab conditions. Slab melting would occur at an early stage of flat subduction (10-7 Ma), which is consistent with the main shallowing phase of the subduction zone [11] and coeval emplacement of adakitic intrusives at Los Pelambres. In a later stage of flat subduction (6-4 Ma), the model predicts eastwards migration of adakitic magmatism until the slab cools down and the present volcanic gap is formed. Melting of newly underplated

basalts at the base of an overthickened crust has been suggested as an alternative explanation for adakitic signatures in magmatic arcs associated with older subducted crust [13]. However, the southernmost portion of the segment (32-33°S), which includes the Los Pelambres, Aconcagua and La Gloria igneous rocks, never reached more than 35 km of crustal thickness in the Late Miocene, as documented by [4]. Under this setting, the extreme HREE depletion of the Los Pelambres magmas is an exception that can not be explained by partial melting of lower crust, which would require an unlikely crustal overthickening (> 50 km) in the Los Pelambres area in order to stabilize a garnet residue in the source.

Recently, a causal relationship between adakitic magmatism and the size of porphyry copper in northern Chile has been suggested by [14]. They proposed that Late Eocene-Early Oligocene giant porphyry copper deposits like Chuquicamata, with no clear volcanic connections, are intrinsically related to adakitic, highly oxidized, water rich intrusions. They suggested that these magmas were eventually derived from a slab source under flat subduction conditions, evolving in depth as closed systems. We see a similar pattern for the Los Pelambres porphyry copper deposit. The Los Pelambres region during the Miocene-Pliocene is characterized by flat subduction, adakitic magmatism, lack of significant coeval volcanism, and the formation of a giant porphyry copper deposit. Unlike the typical sulfur-poor calc-alkaline barren rocks from La Gloria and Aconcagua, the Los Pelambres slab-derived adakitic porphyries might have contributed with at least part of the sulfur budget of the hydrothermal system. Their inherent oxidation state favors the mineralization, since in the upper part of the system, hydrothermal copper mobility is largely controlled by oxidation state – f H_2S/f SO_2 –, in which much higher Cu solubility in oxidized fluid systems is buffered by magnetite-series porphyries. The Juan Fernandez Ridge-trench collision (and probably its subduction) at time of the ore deposit formation would has played a role maintaining a major thermal gradient in the zone, allowing the partial melting of the oceanic basaltic crust.

REFERENCES

[1] Skewes, M.A., and Stern, C.R., 1994. Tectonic trigger for the formation of late Miocene Cu-rich breccia pipes in the Andes of central Chile. *Geology*, v. 22, 551-554.

[2] Dietrich, A., 1999. Metallogenie, Geochemie und Schmelzeinschluss-Untersuchungen von tin potphyry und copper porphyry Lagerstätten der zentralen Anden (Bolivien, Chile). *UnpublishedPh.D.Thesis*, Technischen Universität Clausthal, 198 p.

[3] Cornejo, P., 1990. Geology, mineral compositions, and magmatic gradients of a zoned pluton: La Gloria pluton, central Chilean Andes. *Unpublished Msc. Thesis*, Stanford University, 160 p.

[4] Kay, S.M., Mpodozis, C., Ramos, V.A., and Munizaga, F., 1991. Magma source variations for mid-late Tertiary magmatic rocks associated with a shallowing subduction zone and a thickening crust in the central Andes (28-33°S). *In* Harmon, R. S., Rapela, C. W. (eds.). Andean magmatism and its tectonic setting. *Geological Society of America Special Paper*, v. 265, 113-137.

[5] Sillitoe, R., 1973. Geology of the Los Pelambres porphyry copper deposit, Chile. *Economic Geology*, v. 68, 1-10.

[6] Atkinson, W.W. Jr., Souviron, A., Vehrs, T.I., and Faunes G.A., 1996. Geology and mineral zoning of the Los Pelambres porphyry copper deposit, Chile: *In* Camus, F., Sillitoe, R.H., and Petersen, R. (eds.). Andean copper deposits: New discoveries, mineralization, styles and metallogeny. *Society of Economic Geology Special Publication*, v. 5, 131-156.

[7] Defant, M.J., and Drummond, M.S., 1990. Derivation of some modern magmas by melting of young subducted lithosphere. *Nature*, v. 347, 662-665.

[8] Martin, H., 1999. Adakitic magmas: modern analogues of Archean granitoids. *Lithos*, v. 46, 411-429.

[9] Stern, C.R., Kilian, R., 1996. Role of the subducted slab, mantle wedge and continental crust in the generation of adakites from the Austral Volcanic Zone. *Contributions to Mineralogy and Petrology*, v. 123, 263-281.

[10] Yáñez, G., Ranero, C., von Huene, R. and Díaz, J., 2001. Magnetic anomaly interpretation across the southern Central Andes (32-34°S): The role of the Juan Fernández Ridge in the late Tertiary evolution of the margin. *Journal of Geophysical Research*, v. 106, 6325-6347.

[11] Kay, S.M., and Abruzzi, J.M., 1996. Magmatic evidence for Neogene lithospheric evolution of the central Andean "flat-slab" between 30°S and 32°S. *Tectonophysics*, v. 259, 15-25.

[12] Gutscher, M.A., Maury, R., Eissen, J.P., and Bourdon, E., 2000. Can slab melting be caused by flat subduction? *Geology*, v. 28, 535-538.

[13] Petford, N., and Atherton, M., 1996. Na-rich partial melts from newly underplated basaltic crust: the Cordillera Blanca batholith, Peru. *Journal of Petrology*, v. 37, n. 6, 1491-1521.

[14] Oyarzún, R., Márquez, A., Lillo, J., López, I. and Rivera, S., 2001. Giant versus small porphyry copper deposits of Cenozoic age in northern Chile: adakitic versus normal calc-alkaline magmatism. *Mineralium Deposita*, v. 36, 794-798.

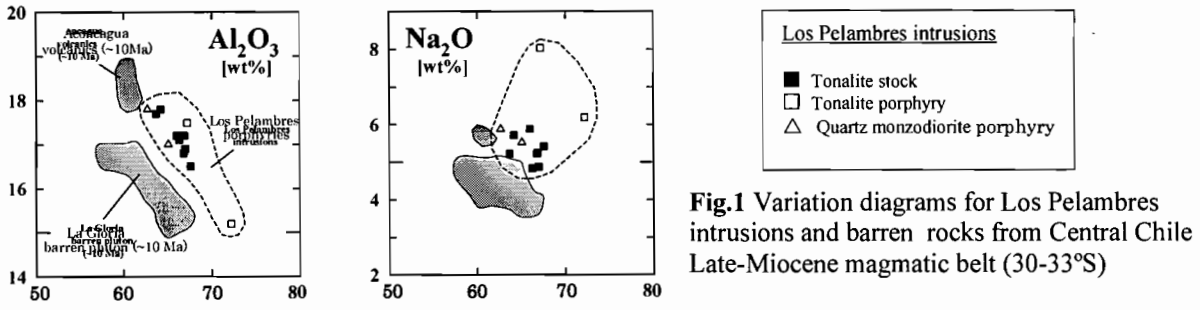

Fig.1 Variation diagrams for Los Pelambres intrusions and barren rocks from Central Chile Late-Miocene magmatic belt (30-33°S)

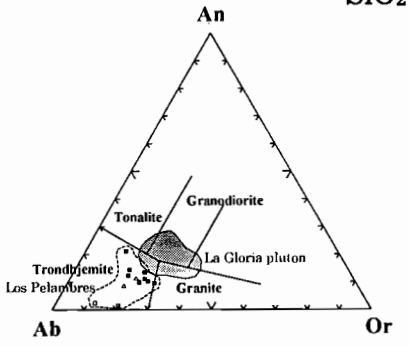

Fig.2 Ab-An-Or normative diagram for Los Pelambres rocks.

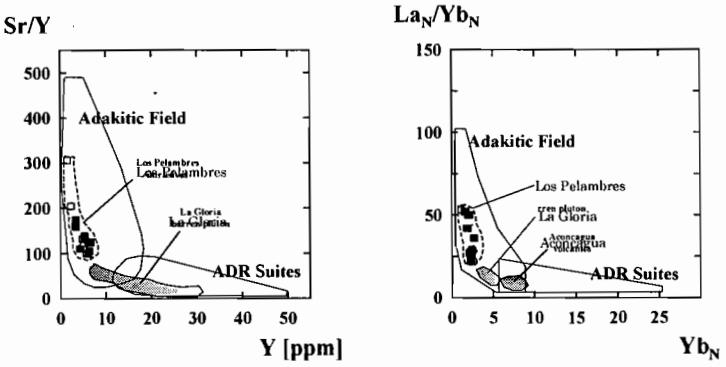

Fig.3 Sr/Y and La_N/Yb_N discrimination diagrams for adakitic rocks from Los Pelambres deposit.

MODELLING THE HYDROLOGICAL CHANGES DURING THE HOLOCENE IN THE ALTIPLANO

Anne RIBSTEIN-COUDRAIN (1), Thomas CONDOM (2), François DELCLAUX (1), Alain DEZETTER (1), Michel LOUBET (3), Laurent LI (4), Alain GIODA (5), Edson RAMIREZ (6)

(1) HydroSciences UMR CNRS–IRD–UMII, Maison des Sciences de l'Eau, 34 095 Montpellier cédex 5, Fax: 33 4 67 14 47 74; Phone: 33 4 67 14 90 85 ; coudrain@msem.univ-montp2.fr

(2) Sisyphe UMR CNRS-UPMC, case 123, 4 place Jussieu, 75 252 Paris cédex 5, France; condom@biogeodis.jussieu.fr

(3) UMR géochimie CNRS Université Paul Sabatier, 38 rue des trente-six ponts, 31 400 Toulouse, France; loubet@lucid.ups-tlse.fr

(4) LMD/CNRS, CC 99, UPMC, 4 place Jussieu, 75 252 Paris cedex 05; li@lmd.jussieu.fr

(5) Great Ice, IRD, 213 rue La Fayette, 75 480 Paris, cedex 10; gioda@msem.univ-montp2.fr

(6) Instituto Hidrología e Hidráulica, UMS, La Paz, Bolivia; ramirez@biogeodis.jussieu.fr

KEY WORDS : endoreic catchment, groundwater, palaeolake, paleohydrology, general circulation model

INTRODUCTION

The Altiplano presents different caracteristics that are interesting to carry on quantitative studies on the relations between climate and hydrology. It is situated at the boundary between different types of climate (10°S-24°S). The hydroclimatic conditions have varied drastically over the past 20 000 years. At present the rainfalls originate mainly from the low latitudes of the Atlantic ocean. The tropical conditions induce a marked season of rains (November to February) and a marked latitudinal gradient of the rain amount (750 mm yr^{-1} in the north, 250 mm yr^{-1} in the south). During the past, the chemical composition of oceanic sediments in front of the Chilean coast (Lamy *et al.*, 2000) show that the latidudinal gradient of rain amount was probably much lower. Such situation could be linked to water vapour flow from high latitudes.

The aim of the presentation is to testify the usefulness of convergent approaches from transient hydrologic modelling and from general atmospheric circulation modelling to reconstruct and/or predict future hydrological changes in response to climate modifications and to the extent of human influence on continental area.

CONSTRAINTS OF HYDROLOGIC MODELLING TO CLIMATIC RECONSTRUCTION

Two hydrologic proxies of the Altiplano were used to carry on hydrologic simulations over the period from 15 000 years B.P. to present. One corresponds to the different water levels of two major lakes in the northern and southern sub-catchments of the Altiplano (10°S-24°S). The other is the evolution of chemical composition of groundwater along the flow paths in a phreatic aquifer in the central part of the Altiplano.

TRANSIENT MODELLING OF LACUSTRINE REGRESSIONS

The Altiplano is an endoreic catchment (196,000 km^2) whose low point is situated in the southern part. Around 15 000 years ago, this low point was occupied by a huge lake of 54 000 km^2. Isotopic data and hydrological constraints indicate that this lake was fed mainly by rainfall on the southern part of the Altiplano and not mainly by inflow from the northern part of the catchment (Coudrain *et al.*, 2001). This study reinforces the argument that the latitudinal gradient of rain amount was probably much lower during this lacustrine phase. Just before or during the early stage of the Holocene, the two major lakes of the Altiplano experienced a water level decrease of around 100 m (Abott *et al.*, 1997). Different simulations with climate changes (precipitation decrease, temperature increase and disappearance of a seasonal rainfall distribution) were carried out. The two subcatchments, the Titicaca one in the northern part, and the Uyuni one in the southern part, present very different shapes. Because of their morphologic difference, the duration of a 100 m decrease of the water level may be interpreted in different ways (Condom *et al.*, submitted). For the northern subcatchment, a 100 m decrease in less than one thousand years should correspond to a change of the climatic parameters among the highest values considered (decrease of rain amount of 15%, increase of temperature of 5°C, and/or disappearance of the seasonal repartition of rain over the year). For the southern sub-catchment, the reservoir effect is negligible. Hence, a 100 m decrease in more than one century must correspond to a progressive change of the climatic conditions.

TRANSIENT MODELLING OF CHEMICAL ELEMENT TRANSFER IN SUB-SURFACE

In an area of 3500 km^2 in the upstream part of the southern sub-catchment of the Uyuni salar transient modelling was carried on over 11 000 years (Coudrain *et al.*, 2001 & 2002). The progressive transfer of different chemical elements (chloride, strontium) between surface, unsaturated zone and the phreatic aquifer was computed. The amounts of the different terms of inflow and outflow have changed during the Holocene according to the climatic evolution. As a consequence, the input, transport and output of chemical elements have also changed during this period. The objective of the study was to reconstruct the time evolution of these terms of the water and chemical balances of the aquifer during the Holocene in accordance to present observed data. The results of the hydrogeological simulations are consistent with the following conclusions: (i) the southern sub-catchment was not fed by significant flow from the northern catchment between approximately 9000 and 4000 years B.P., and (ii) major rain events occurred between 4000 and 2000 years.

CONSTRAINTS OF CLIMATIC MODELLING TO HYDROLOGIC RECONSTRUCTIONS

A study is under development on the links between the general atmospheric circulation and the regional climatic conditions in the central Andes. The first step conducted was on the present variability of the climatic conditions. A simulation on 1000 years with the present orbital conditions was carried on with the coupled

model that takes into account the associated processes between ocean and atmosphere. The results show that the sea surface temperatures change with a periodicity of about one to two centuries. However, considering the extreme situations of these computed results, the rainfall amounts over South America are not changed significantly. Hence, at this stage the working hypothesis is that the coupled processes between oceanic and atmospheric flows are not sufficient to induce significant changes in the rainfall amount in the Andes. Significant changes in precipitation should be bound to orbital variations and/or to changes in the land surface as it has been already computed and published for Western Africa. However, more work is needed to check the validity of such preliminary conclusion.

CONCLUSIONS

Quantitative approach has been largely developed in hydrology/hydrogeology to study the repartition of continental water through different processes (evapotranspiration/runoff/underground flow) and into different reservoirs (lake/river/soil/aquifers/glacier). It is mainly used for the present and the last decades with available instrumental hydrologic data. It can be extended to other periods for which only proxy are available. For distant periods in the past or in the future, modelling continental flow can be very valuable. For example, it can be used for estimating the duration of the impacts of climate change on hydrological terms. In the case of the Altiplano, it has been shown that the present salinity of soil and groundwater is bound to the hydroclimatic conditions that prevailed since 15 000 years. Another example of usefulness of paleo-hydrological modelling is the computation of the duration of the changes of inundated area as a consequence of climatic change. This is important to evaluate the delay between the climate change and the corresponding water level changes of inland area.

It is finally important to note that major changes of inundated area may occur in few decades for modifications of rainfall amount and/or temperature of the order of what is predicted for the future decades of the present century. It is then urgent to strengthen convergent approaches between the ocean/atmospheric studies and the transient hydrological modelling.

REFERENCES

Abbott M. B., Binford M.W., Brenner M. & Kelts K.R. .1997. A 3500 14C yr High-Resolution Record of Water-Level Changes in Lake Titicaca, Bolivia/Peru. *Quaternary Research* **47**, 169-180.

Condom T., Coudrain A., Dezetter A., Brunstein D., Delclaux F., Sicart J.-E. submitted. Transient modelling of lacustrine regressions . Two case studies from the Andean Altiplano.

Coudrain A., Talbi A., Ledoux E., Loubet M., Vacher J., Ramirez E. .2001. Subsurface transfer of chloride after a lake retreat in the central Andes. *Ground Water* **39**, 751-759.

Coudrain, A., M. Loubet, Condom T., Talbi A., Ribstein P., Pouyaud B., Quintanilla J., Dieulin C., Dupre B. .2002. Données isotopiques (87Sr/86Sr) et changements hydrologiques depuis 15 000 ans sur l'Altiplano andin. *Hydrol. Sc. J.* **47**, 293-306.

Lamy F., J. Klump, J. Hebbeln, & G. Wefer .2000. Late Quaternary rapid climate change in northern Chile. *Terra Nova* **12**, 8-13.

PETROGRAPHY, MINERALOGY AND GEOCHEMISTRY OF THOLEIITIC GABBROIC ROCKS OF COASTAL RANGE AT NORTHERN ANTOFAGASTA, CHILE

Alejandra RIOSECO(1), Oscar FIGUEROA(1), Silvino CÓRDOVA(2), Bernard DÉRUELLE(3) and Christian CREIXELL(1).

1. Departamento de Ciencias de la Tierra, Fac. Cs. Químicas, Universidad de Concepción, Chile. E-mail: ofiguero@udec.cl.
2. Departamento de Ciencias Geológicas, Universidad Católica del Norte, Chile.
3. IUFM de l'académie de Versailles & Laboratoire de Magmatologie et Géochimie Inorganique et Expérimentale, Université Pierre et Marie Curie, France.

Keywords: North Chilean Coastal Range, tholeiitic gabbro, pyroxene exsolutions, mineralogical composition.

INTRODUCTION

The first stages of the building of the Jurassic-Lower Cretaceous magmatic arc of northern Chile are evidenced in the north of Antofagasta by a fringe of small stocks and dykes of basic composition (e.g. Hornitos Initial Basic (HIB) of Pichowiack, 1994). South of Antofagasta these gabbroic bodies commonly show igneous layering (e.g. Caleta Coloso Gabro (CCG) Complex; Lucassen & Franz, 1994). The age of these gabbros is 185 M.a. (Lucassen & Thirlwall, 1998) and they have a tholeiitic affinity (Pichowiack et al., 1990; Lucassen & Franz, 1994), which is in contrast with the abundant calcalkaline magmatism that characterizes the arc. The occurrence of this tholeiitic mantle-derived magmatism occurs in an extensional tectonic regime at the continental border (Scheuber et al., 1994).In order to analyze the evolutionary history of the crystallization at the beginning of the Jurassic arc, a petrographic, mineralogical and geochemical study was carried out on the tholeiitic gabbroic rocks of Punta Grande (PG), Hornitos (Ho) and Quebrada Mejillones (QM), located between Antofagasta and Tocopilla (fig. 1).

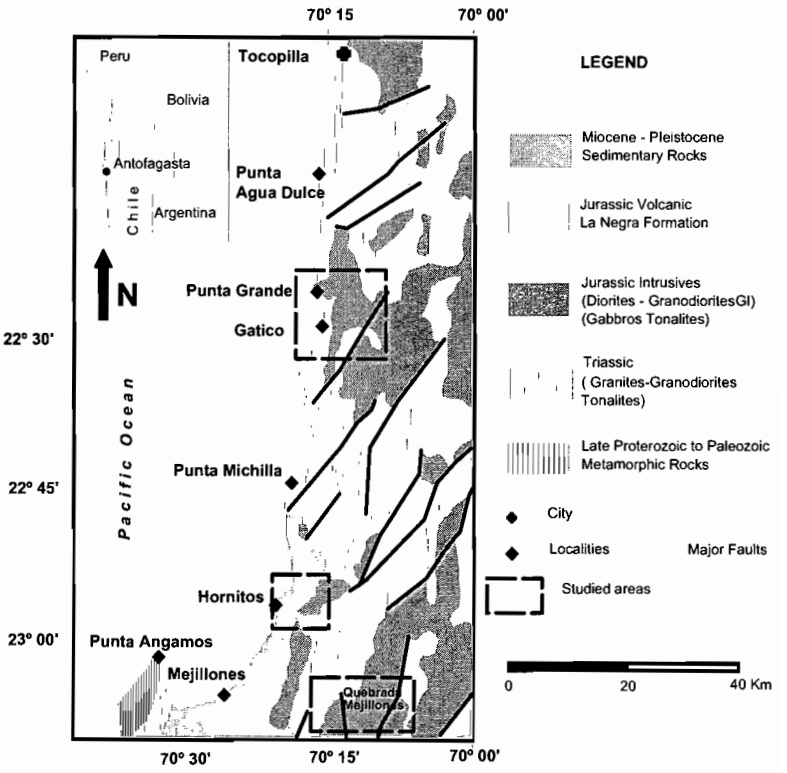

Fig 1. Location of the studied area and geologic map. Modified from Boric et al (1990).

GEOLOGY

The tholeiitic gabbroic rocks are essentially gabbros and gabbronorites that occur as small stocks and NS elongated bodies. They cover areas from 1,2 km^2 at Ho and 1,4 km^2 at PG. At QM they only exist in the gulch because they are almost entirely covered for tertiary sediments. These rocks are intruded by calcalkaline granodioritic, dioritic and monzodioritic bodies, whose Rb-Sr age is 155.4 M.a. (Pichowiak, 1994). Those intrusions occurred by magmatic stoping or by fault. Net or intensely fractured contacts can be found. Abundant aplitic to granodioritic dykes (up to 4 m) also cut the gabbroic rocks. These dykes and their associated little veins, produce gabbros fragmentation and metasomatic patches of more differentiated mineral inside them. This changes gabbro composition, even towards a granitoid rock. Andesitic dykes related to La Negra Formation are also present. They can also be found as andesitic inclusions in aplitic dykes at PG. They have pillow shape which is a characteristic of magma mixing.

PETROGRAPHY

The gabbroic rocks show a hypidiomorphic granular texture with medium to coarse grain size at PG and QM, and porphyritic to intergranular texture with medium to fine grain at Ho (diabase). These rocks are mostly constituted by 2 to 4 mm crystals of plagioclase (pl; 47-61%), clinopyroxene (cpx; 11-20%), orthopyroxene (opx; 7-8%), Fe-Ti oxides (~ 1%) and biotite. Apatite and sphene are accessory minerals. A brownish-greenish amphibole includes resorpbed crystals of cpx and pl. The opx is bastitized in various degrees, especially at Ho. Actinolite-magnetite-calcite microveins and quartz microveins cut the rocks, and variable amount of secondary minerals as quartz (e,g. in intergrowth with vermicular alkali feldspar) and tourmaline are also observed.

All the gabbroic rocks, with the exception of the Ho diabase, are characterized by the presence of opx that show cpx exsolutions, and to a lesser extent, by cpx with opx exsolutions (fig. 2). The cpx exsolutions are irregular blebs or lamellar, and in some twinned individuals may have a herring-bone pattern, which is characteristic of inverted pigeonite (Deer et al., 1992).

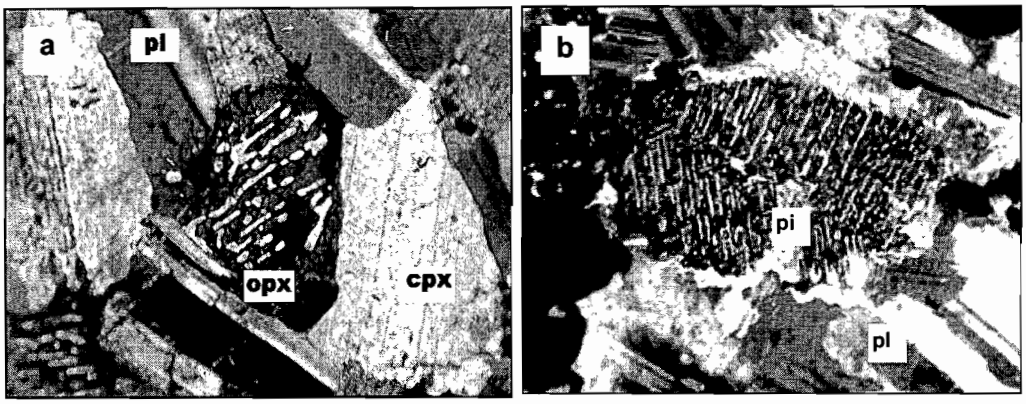

Fig 2 Microphotographies of clinopyroxene exsolutions in: a) orthopyroxene, b) in inverted pigeonite showing "herring bone" texture.

MINERALOGY AND GEOTHERMOMETRY

Pl shows a zonation resulting of a secondary process, with labradorite cores (An51) and andesine rims (An33-34). According to Marimoto's classification (1989; fig. 3), the cpx corresponds to diopside and augite (Wo36En42Fs21 to Wo45En38Fs17) and the opx to enstatite (Wo2En56Fs41 to Wo2En54Fs44). These cpx and opx are respectively richer and poorer in Ca than pyroxenes of the tholeiitic Skaergaard intrusion (Deer et al., 1992). This is probably related to the change in primary pyroxene composition by exsolutions. Therefore, some of Ca-poor pyroxene correspond to pigeonite, as indicated by petrographic observation. In a same rock,

exsolutions have a similar composition to normal crystals (fig. 3). According to the classification of Leake (1997), the brown amphibole corresponds to a magnesium-hornblende. Their mg# (= Mg/(Mg + Fe2+)) varies between 0.72 and 0.81 and their Al_2O_3 content between 3.9 and 5.7%. The Fe-Ti oxides correspond to magnetite and ilmenite. The biotite mg# varies between 0.54 and 0.58 and its contents of Al (IV) vary between 2.47 and 2.36.

Crystallization temperatures were estimated based on the two pyroxenes and the amphibole equilibrium compositions. For the calculation a lithostatic pressure of 3 kbar was assumed (Lucassen et al., 1996) and the program QUILF was used (Andersen et al., 1993). The opx-cpx geothermometer of Lindsley (1983) give temperatures between 850 and 911°C, while the amphibole one of Holland and Blundy (1994) give lower temperatures (around 770°C).

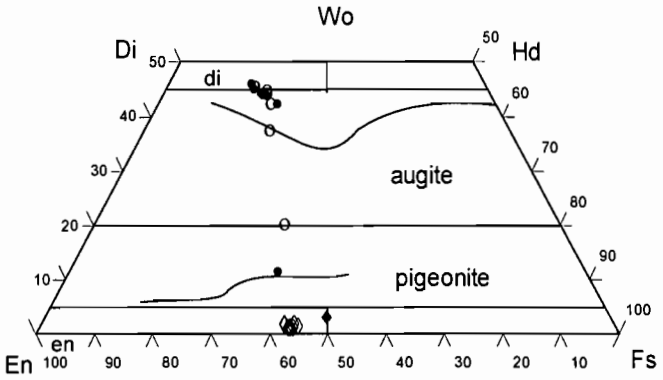

O cpx; ◊ opx; • cpx exsolution in opx; ♦ opx exsolution in cpx.

Fig 3. Pyroxene classification diagram (Marimoto, 1987), showing the Skaergaard pyroxene solidus trend.

GEOCHEMISTRY

Five geochemical analyses were carried out of 3 representative samples of the tholeiitic gabbroic rocks from PG (GT-01, GT-03 and GT-05), and from Ho (Ho-1). One andesitic dyke (GT-02), was also analized. Gabbroic composition varies in relation with the metasomatic event that affects them. SiO_2 contents vary between 51.2 and 61.3% and K_2O contents vary between 0.69 and 2.69% (fig. 4). Normalized rare-earth diagram shows relatively flat patterns ($(La/Yb)_N$ = 2.2-5.1) as in the multi-element (fig. 5), although this one shows a variable Nb depletion. The andesitic dyke have similar patterns to the gabbroic rocks.

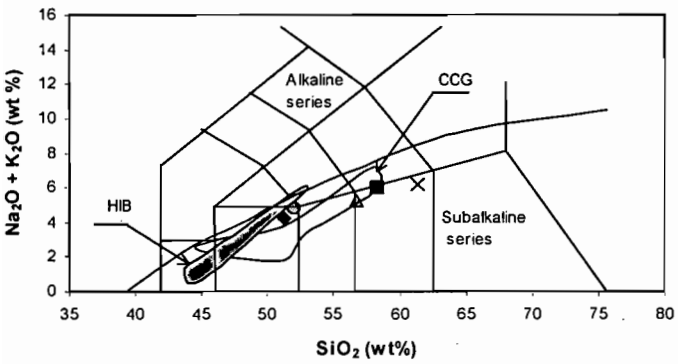

Fig 4. TAS Diagram (Le Maitre et al, 1989). Alkaline and subalkaline fields are after Irvine & Baragar (1971). Representative fields of HIB (Pichowiak, 1994) and the CCG (Lucassen & Franz, 1994) are added.

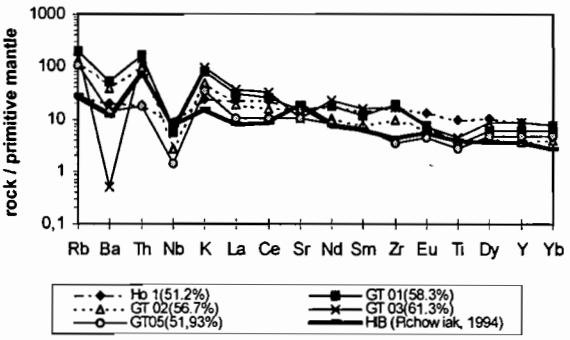

Fig 5 Multi-element Diagram, normalized to primitive

Gabbroic rocks in the north of Antofagasta are characterized by the occurrence of exsolutions in the pyroxenes. This is the first time that such exsolutions are described in Chile. They are similar to those found in stratified gabbros complexes, such as Skaergaard, were formed in continental environments from tholeiitic

magmas (Cox et al., 1979). The tholeiitic affinity of the studied rocks is supported by their relatively flat patterns in the rare earths and multi-elements diagrams (fig. 4).

The occurrence of exsolutions indicates that these intrusives underwent a slow cooling, which provided mineralogical subsolidus reequilibrium such as the pigeonite inversion. Therefore, the intrusion temperature should be higher than the one calculated from the pyroxenes composition, since the composition of both pyroxenes were modified by the exsolutions. The lower estimated temperatures based on the composition of the amphibole that surround resorpbed crystals of pyroxene and pl, indicate the amphibole came from the subsolidus reaction between pyroxenes and pl, in the presence of a fluid. This observation is in agreement with the one made in the study of the amphiboles in basic igneous and metaigneous near Antofagasta (Lucassen & Franz, 1994), where the amphibolitization probably obliterated the original exsolutions. During this stage of slow cooling of the intrusive, biotite was also formed. Due to the long time that these intrusives remained at high temperature, they became permeable to injections of more differentiated material. This would explain why these rocks are richer in silica, potassium and incompatible elements than the HIB and CCG. This more-differentiated material would also have introduced a calcalkaline component in the tholeiitic gabbroic rocks, as evidenced in the multi-element diagram by the negative Nb anomaly (fig. 4).

ACKNOWLEDGEMENTS: We are grateful to Prof. Dr. G. Franz whose remarks helped to clarify this presentation.

REFERENCES

Andersen, D.J.; Lindsley, D.H. & Davidson P.M., 1993. QUILF, a Pascal program to assess equilibria among Fe-Mg-Mn-Ti oxides, pyroxenes, olivine and quartz. Computers and Geosciences, 19 (9): 1333-1350.

Boric, R.; Diaz, F. & Maksaev, V., 1990. Geología y yacimientos metalíferos de la Región de Antofagasta. Sernageomin, boletín 40, 246.

Deer, W., Howie, R. & Zussman, J., 1992. An Introduction to the Rock-forming Minerals-2nd ed. Longman Group UK Limited. 696.

Irivine T.N. & Baragar W.R.A., 1971. A guide to the chemical classification of the common volcanic rorks. Can. J.Earth Sc., 8, 523-548.

Leake, B., 1997. Nomenclature of Amphiboles: Report of the International Mineralogical Association Comission on New Minerals and Mineral Names. Mineralogical Magazine, 61, 295-321.

Le Maitre R.W. and 10 others authors, 1989. A classification of igneous rocks and glossary of terms. Blackwell, Oxford. 193.

Lucassen, F., Fowler, C.M.R. & Franz, G., 1996. Formation of magmatic crust at the Andean continental margin during early Mesozoic: a geological and thermal model of the North Chilean Coast Range. Tectonophysics, 262, 263-279.

Lucassen, F. & Franz, G., 1994. Arc related Jurassic igneous and meta-igneous rocks in the Costal Cordillera of northern Chile / Region Antofagasta. Lithos, 32, 272-298.

Lucassen, F. & Thirlwall, M., 1998. Sm-Nd ages of mafic rocks from Coastal Cordillera at 24° S, Nothern Chile. Geol. Rundsh, 86, 767-774.

McDonough, W.F. & Sun, S.-s., 1995. The composition of the Earth. Chem. Geol., 120: 223-253.

Marimoto, N., 1987. Nomenclature of Pyroxenes. The Canadian Mineralogist, 27, 143-156.

Pichowiak, S., 1994. Early Jurassic to early Cretaceous Magmatism in the Coastal Cordillera and the Central Depression of North Chile. *In* K.-J. Reutter, E. Scheuber & P. J. Wigger eds., Tectonics of the Southern Central Andes. Springer, Berlin, 203-217.

Pichowiak S., Buchelt M., Damm K.W., 1990. Magmatic activity and tectonic setting of the early stages of the Andean cylcle in North Chile. In, Mahlburg Kay S., Rapela C.W. (eds).Plutonism from Antactica to Alaska. Geol Soc Am Spec Pap, 241, 127-144.

Scheuber, E., Bogdanic, T., Jensen, A. & Reutter, K.-J., 1994. Tectonic development of the North Chilean Andes in relation to plate convergence and magmatism since the Jurassic. *In* K.-J. Reutter, E. Scheuber & P. J. Wigger eds., Tectonics of the Southern Central Andes. Springer, Berlin, 121-139

NEOGENE TECTONICS OF THE CENTRAL DEPRESSION AND PRECORDILLERA (NORTH CHILE) FROM THE ANALYSIS OF A DRAINAGE BASIN EVOLUTION

Rodrigo RIQUELME (1,2,3), José DARROZES (2) , Gerard HÉRAIL (3) & Reynaldo CHARRIER (1).

(1) Depto. Geologia Universidad de Chile. Plaza Ercilla 803. Santiago, Chile (rriquelme@lmt.ups-tlse.fr, rcharrie@cec.uchile.cl).
(2) LMTG, UMR 5563, Univ. Paul Sabatier, Toulouse, France. (darrozes@lmt.ups-tlse.fr).
(3) IRD, LMTG, 38 Rue des 36 Ponts, 31400, France. (gherail@paris.ird.fr).
(1,2,3) Convenio Universidad de Chile-IRD.

KEY WORDS: Neogene, landscape surface, Atacama Desert.

INTRODUCTION

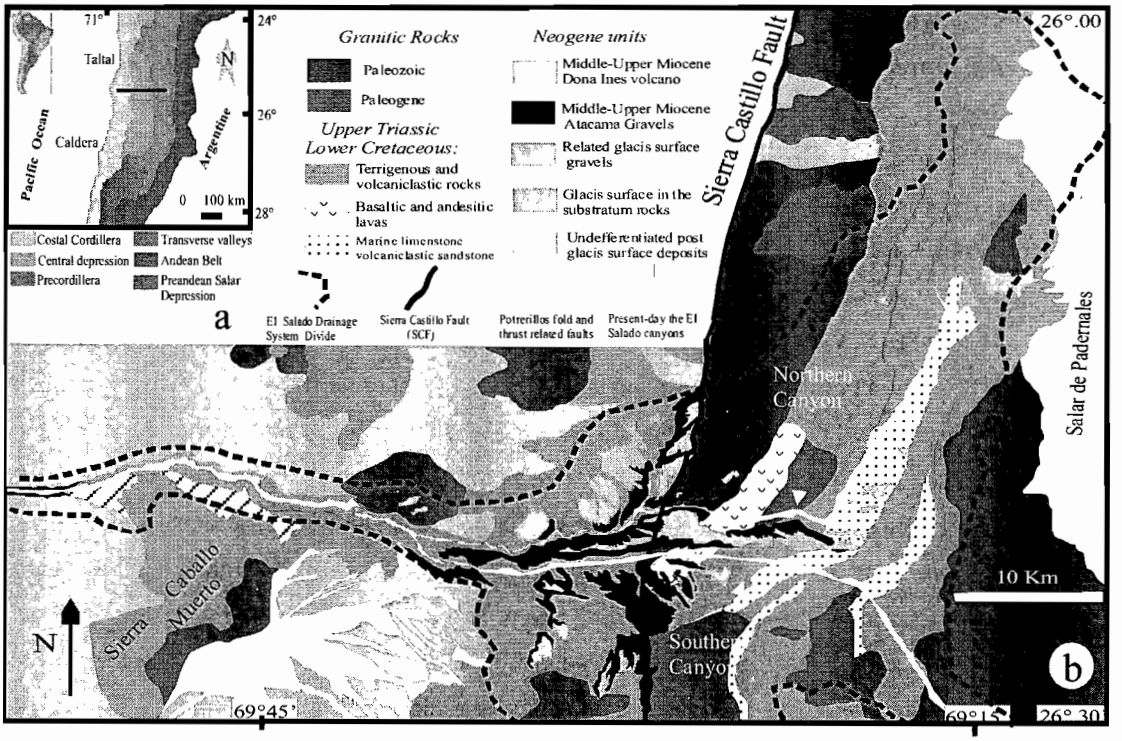

Figure 1: location map of the studied area; a) Principal morphologic units crossed by El Salado valley. b) Main geologic features.

The drainage basin of the El Salado river valley corresponds to the most important drainage system in the southern Atacama Desert between 25° to 27° S.L. (Central Andes). The El Salado river valley cross the Chilean fore-arc perpendicularly to the main morphologic units of the region (fig.1a). Throughout the El Salado river valley in the Central Depression and Precordillera three landscape surfaces corresponding to different stages of the Noegene geomorphologic evolution of this area can be differentiated: (1) the base of a thick series of Middle to Upper Miocene gravel deposits (Atacama Gravels of Sillitoe et al., 1968), (2) the extensive glacis surface that composes the top of the Atacama Gravels (Atacama Pediplain of Sillitoe, 1968), (3) the landscape surface related to the present-day the El Salado river valley development. Here, we present the main features of

these landscape surfaces, we discuss their meaning in the erosional or depositional evolution and their implications for the Neogene tectonic evolution of Central Andes.

GEOLOGIC AND TECTONIC SETTING

The studied area is located in the forearc region. The major structural feature of the area is located in the Precordillera and corresponds to the Sierra Castillo Fault (SCF) that forms part of the Domeyko Fault System (fig.1b). It is a north-south trending subvertical master faults (Tomlinson et al., 1993) active since the Mesozoic (Cornejo et al., 1993). The last important movements recorded in this fault have been dated at the Eocene-Oligocene boundary (Tomlinson et al., 1993). The El Salado Drainage System (SDB) is composed in the Central Depression for a single E-W oriented canyon, without development of tributary basins (fig.1b). Upstream, in the Precordillera, the single canyon is divided in two, very close to each other (3-4 kilometers) sub-parallel tributary canyons. These two canyons are perpendicular to the structural Potrerillos fold and thrust belt. Further East, in the Precordillera-Puna the northern canyon becomes NS oriented, paralleling the structural orientation of the Potrerillos fold and thrust belt, whereas the southern canyon becomes NW-SE oriented, oblique to the Potrerillos fold and thrust belt.

GEOMORPHOLOGIC LANDSCAPE SURFACES IN THE SDB

Atacama Gravel paleosurface: The Atacama Gravels overlies a deep incised paleosurface extensively and continuously exposed in the Precordillera. This allows the reconstruction of the paleo-drainage network in which these gravels were deposited (Paleo-SDB, fig. 3a). The main stream of the Paleo-SDB runs parallel to the southern present-day canyon of the SDB (1-2 km to the North). In the sides of this canyon a longitudinal profile of the Atacama Gravels Base is well expose (fig.4a). The line drawn up between the bottoms of the paleo-valley exposed in the canyon side, which must approximate the line corresponding to the longitudinal profile of the main stream of paleo-SBD. A change in the slope of the main stream is evidenced at the intersection with the SCF. East of the SCF, the slope of the main stream is greater than West of the fault. The main stream drains into the Central Depression toward the SW, following the eastern slope of Sierra Caballo Muerto.

Glacis surface: The upper glacis surface in the Central Depression corresponds to a smoothly-waved surface. The surface is slightly and regularly incised by very linear E-W oriented channels coming from the eastern reliefs (fig.3a). Some of these channels, developed only tens of meters away of the El Salado canyon, run parallel to the canyon several kilometers before falling into it. Immediately East of Sierra Caballo Muerto an old alluvial cone on the glacis surface is cut by the El Salado valley (fig.3b). Both the elongation of the alluvial cone and the preserved markers of stream flow direction indicate that the river has flowed in a N-S direction. This shows that at this time the relief of Caballo Muerto was not still cut by the El Salado. The longitudinal profiles of the glacis surface are approximately parallel to the present-day talweg profile in the western most section of the Central Depression. Towards the east up to the Precordillera it becomes strongly divergent to the present-talweg of the northern canyon. The divergence is not registered for the southern canyon, but as we show below this canyon is less incised than the northern one.

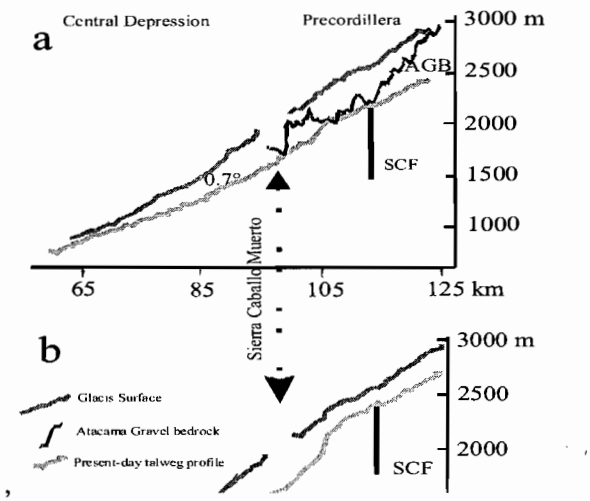

Figure 2: EW profiles of the Atacama Gravel base, glacis surface and present-day valley for the SDB;
a) Northern canyon, b) Southern canyon.

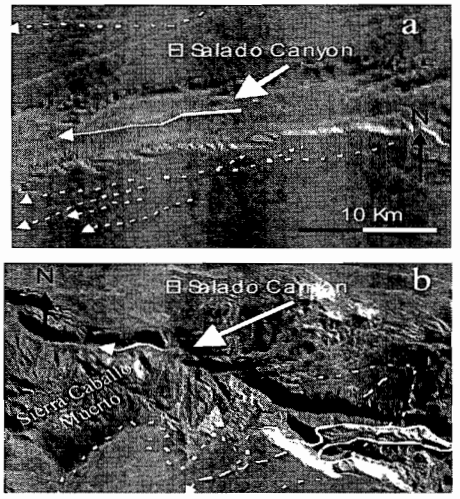

Figure 3: Morphologic features : a) E-W streams of the glacis surface in the Central Depression; b) Oblique Alluvial cone cuts by the EI Saldo canyon.

The present-day morphology of the SDB: Differences can be established for the drainage systems of the northern and southern canyons of the SDB. Tributary basins of the northern canyons show N-S oriented geometries that follow the strike of the lithologic substratum and they are well correlated with the substratum fracturation pattern (figs.2a and 2b). On the contrary, for the southern canyon the elongation of the tributary basins as well as the mainly direction of the drainage network are oblique to nearly perpendicular to the lithologic unit distributions and fracturation pattern. Therefore, lithologic control can be established for the northern part of the drainage system development, whereas this control is less important in the southern part. Longitudinal talweg profile in the Central Depression shows a regular concave curve. In the Precordillera talweg profiles for northern and southern parts differ from each other. The northern talweg profile registers a clear slope break immediately after junction with the southern canyon (500 m altitude difference in 15 km). For the southern canyon the slope break is not registered, however, the talweg profile becomes slightly convex. Talweg altitudes of northern canyon are smaller than those of the southern one, indicating greater incision degree in the first one.

DISCUSSION AND CONCLUSION

The paleo-SDB lies 2 km below the highest regional summits showing that it incises an already high Precordillera. We show that paleo-SDB is developed mainly on the Western part of the SCF. There is no evidence that the SCF accommodate important movements after the Eocene-Oligocene (Tomlinson et al., 1993). This indicates that the SCF has a passive N-S structural control in the SDB development (fig. 4c). This differs than the present-day SDB (fig. 4b) development where E-W canyon rather suggests a drainage development controlled by the E-W regional slope. The Atacama Gravels glacis corresponds in the Precordillera to a continuous process of sedimentation. The infill of the incised landscape is due to the normal activity of the Atacama Fault System (Riquelme et al., 2002) which creates a barrier for sediments coming from the Precordillera.

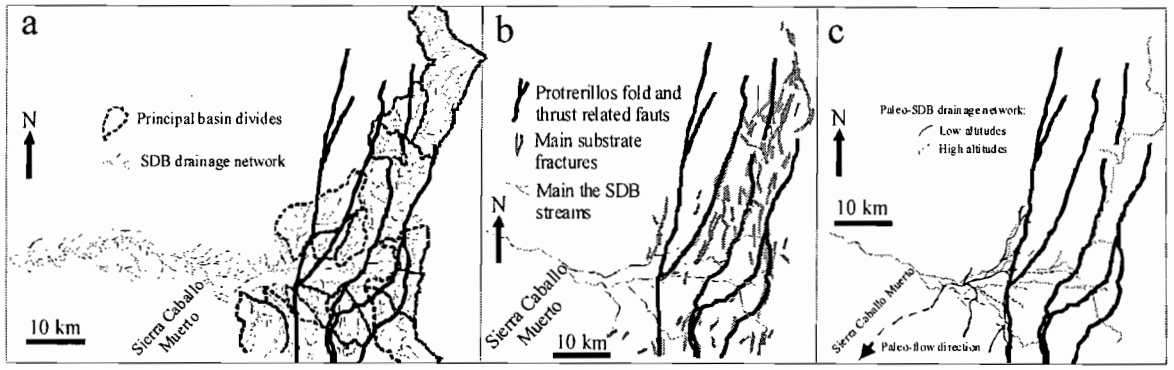

Figure 4: SDB Drainage evolution; a) Present-day SDB drainage network and principal tributary basins; b) SDB Fracturation map; c) Paleo-SDB drainage network showing the influence of the main tectonic structures

At that time, the regional E-W slope was smaller than that of the current. An increase of the E-W regional slope leads to the E-W incision registered in the present-day SDB (Fig. 4b) and it occurred after the glacis formation contrary to the assumptions of other authors (Mortimer, 1973; Naranjo and Paskoff, 1980). A maximum age of 10-11 Ma BP can be established for the reactivation of the E-W incision by considering the ignimbrite that seals the glacis in the Precordillera (Cornejo et al., 1993). The Upper Miocene incision corresponds to the important uplift of the Altiplano and Puna (Gregory-Wodzicki, 2000). The generalized observed tilting (≈3° for Lamb et al.; 1997 in the entire fore-arc and ≈1° for us in the Precordillera) can be explain by an uplift without main fault activities in the Precordillera. The fore-arc tilting explains the anomalous formation of the two parallel canyons of the SDB and the E-W linear streams developed in the glacis surface.

REFERENCES

Cornejo, P., Mpodozis, C., Ramirez, C.F., and Tomlinson, A.J. 1993. Estudio Geológico de la Región de Potrerillos y El Salvador (26°-27° Lat.S). Servicio Nacional de Geología y Minería-CODELCO, Informe Registrado IR-93-01, 12 cuadrángulos escala 1:50.000 y texto 258 pp. Santiago, Chile.

Gregory-Wodzicki K.M., 2000. Uplift of the Central and Northern Andes: A review. Geol. Soc. Am. Bull. 112, 1091-1105.

Lamb, S., Hoke, L., Kennan, L., and Dewey, J., 1997. Cenozoic evolution of the Central Andes in Bolivia and northern Chile. Geol. Soc. Special Publication, 121, 237-264.

Mortimer, C., 1973. The Cenozoic history of the southern Atacama Desert, Chile. J. Soc. Lond., 129, 505-526.

Naranjo, J.A., Paskoff, R., 1980. Evolucion geomorphologica del Desierto de Atacama entre los 26° y 33° latitud sur: Revision cronologica.

Riquelme, R., Martinod, J., Hérail, G., Darrozes, J., Charrier, R., 2002. Geomorphological approach of the Neogene to Recent tectonic activity of the Atacama Fault System (26°-27° South, Northern Chile. Submitted

Sillitoe, R.H., Mortimer, C., Clark, A.H., 1968. A chronology of landform evolution and supergene mineral alteration, southern Atacama Desert, Chile, Inst. Min. Metall., Trans., Sect. B., Vol.77, p.166-169.

Tomlinson, A.J., Cornejo, P., Mpodozis, C., Ramirez, C. 1993. Structural Geology of the Sierra Castillo-Agua Amarga Fault System, Precordillera of Chile, El Salvador-Potrerillos. 2nd International Symposium on Andean Geodynamics, pp. 259-262. Editions de l'ORSTOM, Colloques et Séminaires, Paris.

PETROLEUM GEOLOGY OF THE EASTERN EDGE OF THE ORIENTE BASIN

Marco V. RIVADENEIRA M (1)

(1) mrivadeneira@petroecuador.com.ec

The eastern edge of the Oriente Basin, corresponds to the Capirón-Tiputini System defined by Baby et al (1997), characterized by a right strike-slip faulted System, that in-depth is connected at a detached level, defined previously by Balkwill et al. (1995). The mentioned faults limit the half-grabens of possible Permo-Triassic age.

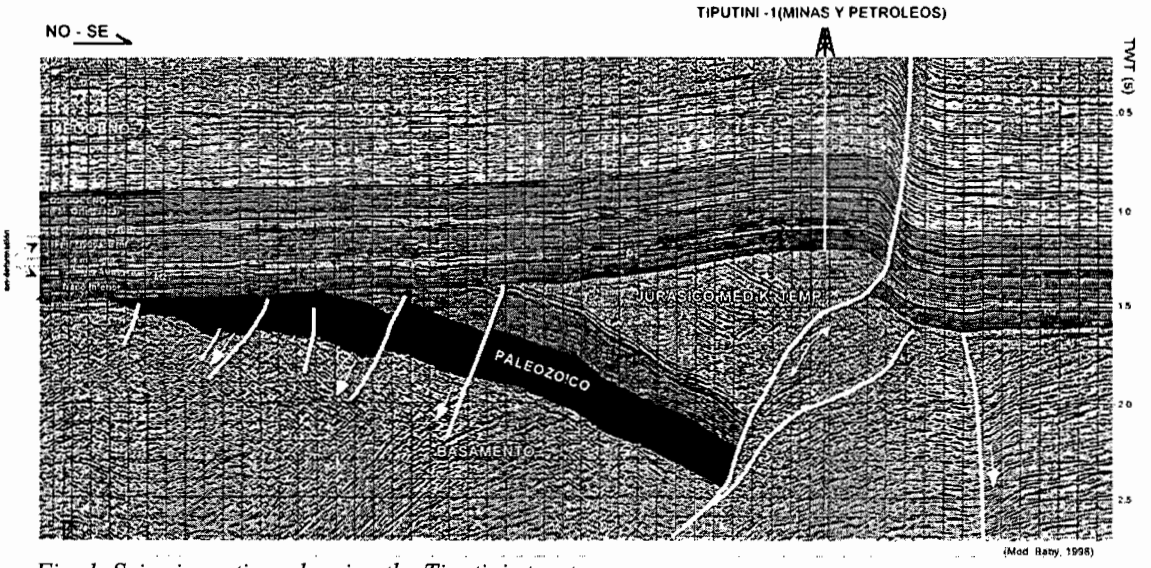

Fig. 1. Seismic section, showing the Tiputini structure

Tiputini it is one of the most impressive structures of the Oriente basin (fig. 1 and 4), in it develops an spectacular half-graben and associated faulted anticline, which contains the oil field of the same name, related with the Yasuní fault, developed as a result of the tectonic inversions. The oil productive anticlines were formed mainly in the first two inversion stages: 1) late turonian-paleocenic and 2) lower eocenic. The Ishpingo, Tambococha and Tiputini structures located in the part most eastern of the eastern border of the basin (fig. 4), are being affected by the last tectonic inversion, which continues at the present time as evidence the current topography.

The stratigraphy is characterized by the progressive decrease of the cretaceous and tertiary formations thickness to the east until disappearing as in the case of the Albian Hollin formation, in the area of the Ishpingo-Tambococha-Tiputini fields (fig.2). The marker fossils, show that the basal sediments correspond to the lower part of the Napo Formation (middle Albian), what demonstrates that the oriental basin edge was presenting rising

relief since the lower cretaceous time, cut by rivers that were carrying their sediments westward, without remain sedimentary records, and it is only from the middle Albian, that the basin border begun to receive sediments.

Under the post –aptian sequence, are found Paleozoic sedimentary patches, preserved of the late Jurassic erosion within the half-grabens, between the Precambrian terrains, related to the Guyana shield. Over the Paleozoic deposits the landfill of the half-grabens is constituted by detritic sediments

of the jurassic age, represented possibly by equivalent continental facies of the marine Santiago formation, known as Sacha formation (Rivadeneira M., 1989), by deposits of the Chapiza formation and by marine upper jurassic sediments, defined as new Tambococha Formation (Díaz M. 2000).

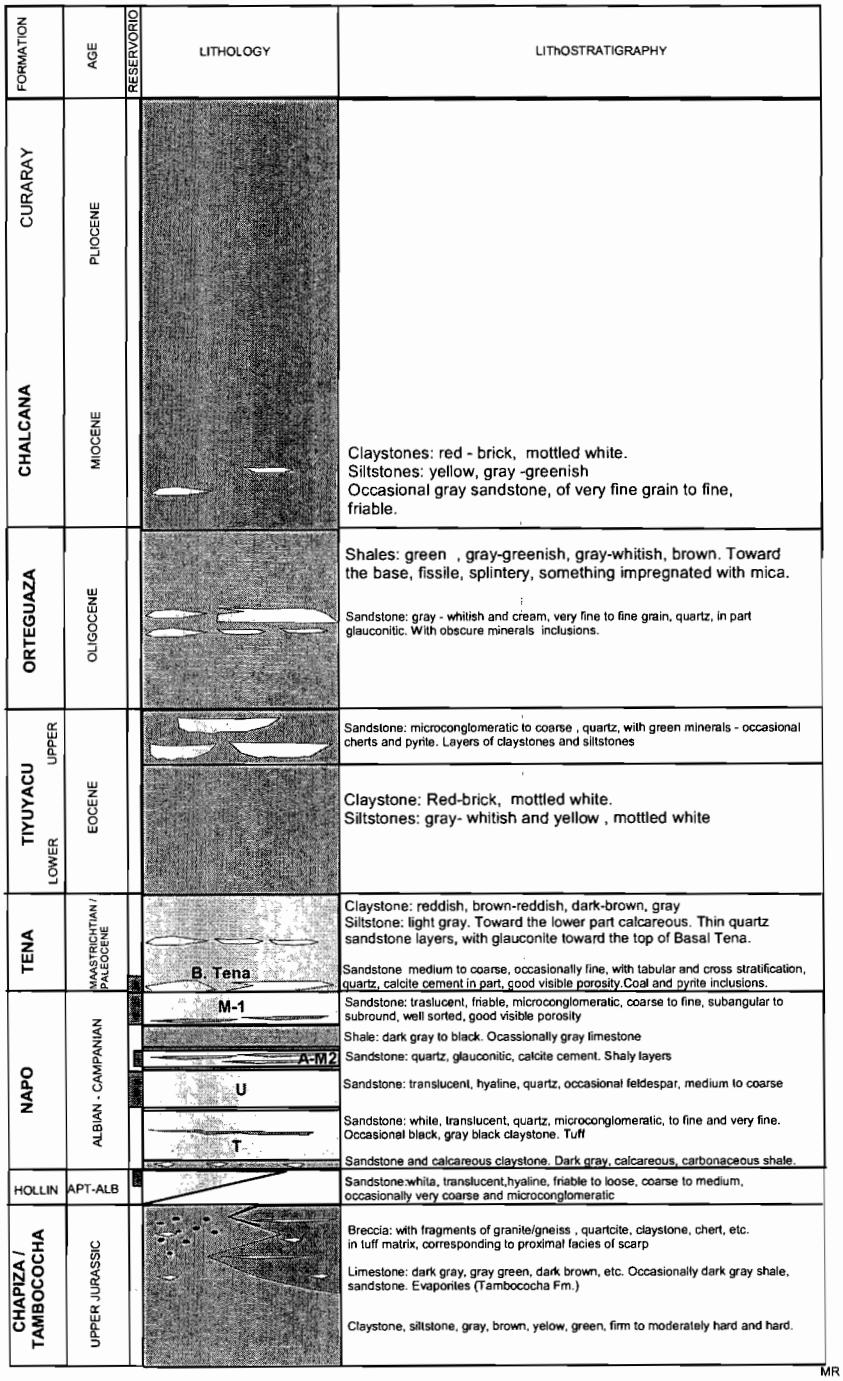

Fig. 2. Stratigraphic column of the eastern border of the Oriente Basin

The Napo deposits in this part of the Oriente Ecuadorian basin are characterized by the great sandy development of the "T" and "U" sequences, whose individualization is difficult by the absence of clayey and calcareous markers (fig. 3). The "A" and lower "M2" turonian limestone are absent, and in their place is developed a sandy/clayey sequence. The radioactive marker "L" of

the coniacian "M1" limestone, together to the top of the M2 limestone, are the best markers of the basin and could be easily recognized even in this part of the basin, specially the M2 top is an excellent seismic marker. The "M2" and "M1" sandstones of the turonian and campanian ages respectively, have a tectonic-stratigraphic control, being restricted their development to the Eastern Corridor of the basin (fig. 3).

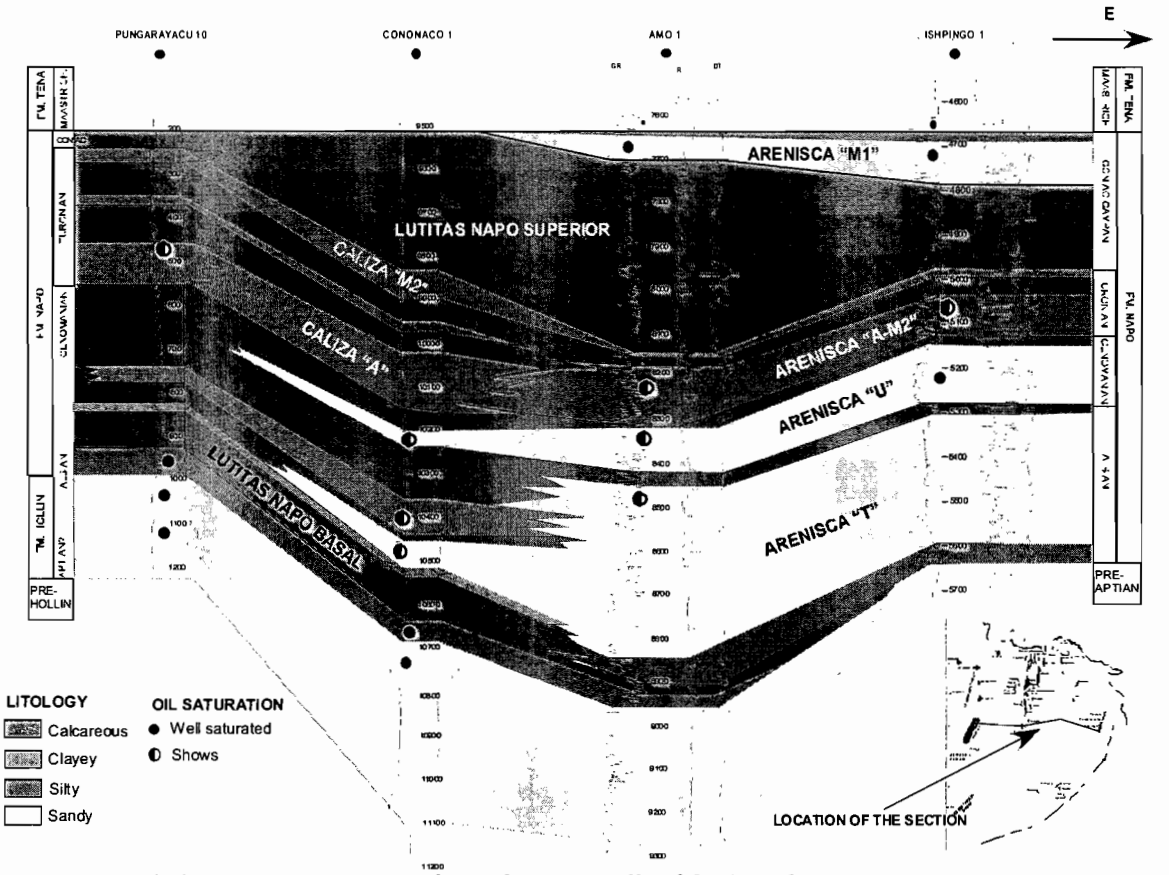

Fig. 3. E-W stratigraphic correlation between wells of the Ecuadorian Oriente Basin

The Tertiary sequence, shows a strong thick nesses decrease, however, are maintained the characteristics of the same, with the following particularities: -Exist difficulty in defining the Tena formation top, since the detritic deposits of the lower Tiyuyacu formation frequently disappear (fig. 2). -The conglomeratic Tiyuyacu bodies are replaced in this part of the basin by sandy facies (fig. 2), product of the greater maturity of the sediments due to the long distance to the Andean source of deposits. -Toward surface, outcrops the Curaray formation, that would be reflecting the raising of this edge, before the absence of deposits more youths, solely restricted to the current river valleys.

It is a heavy oil zone of great economic importance since accumulates about 7.6 billion of barrels, that equal to the 28% of the on-site original oil of all the basin.

Shows a great oil concentration since 34% of the on-site oil discovered in this "petroleum play", is located in the Ishpingo field (fig. 4). This "play" shows a certain areal distribution for quality of the crudes, prevailing toward the NNO the medium quality crudes, while toward the center and east, is extended the

dominance of the heavy crudes. Southward, about the frontier with Peru, are found several fields with heavy and medium gravity oils.

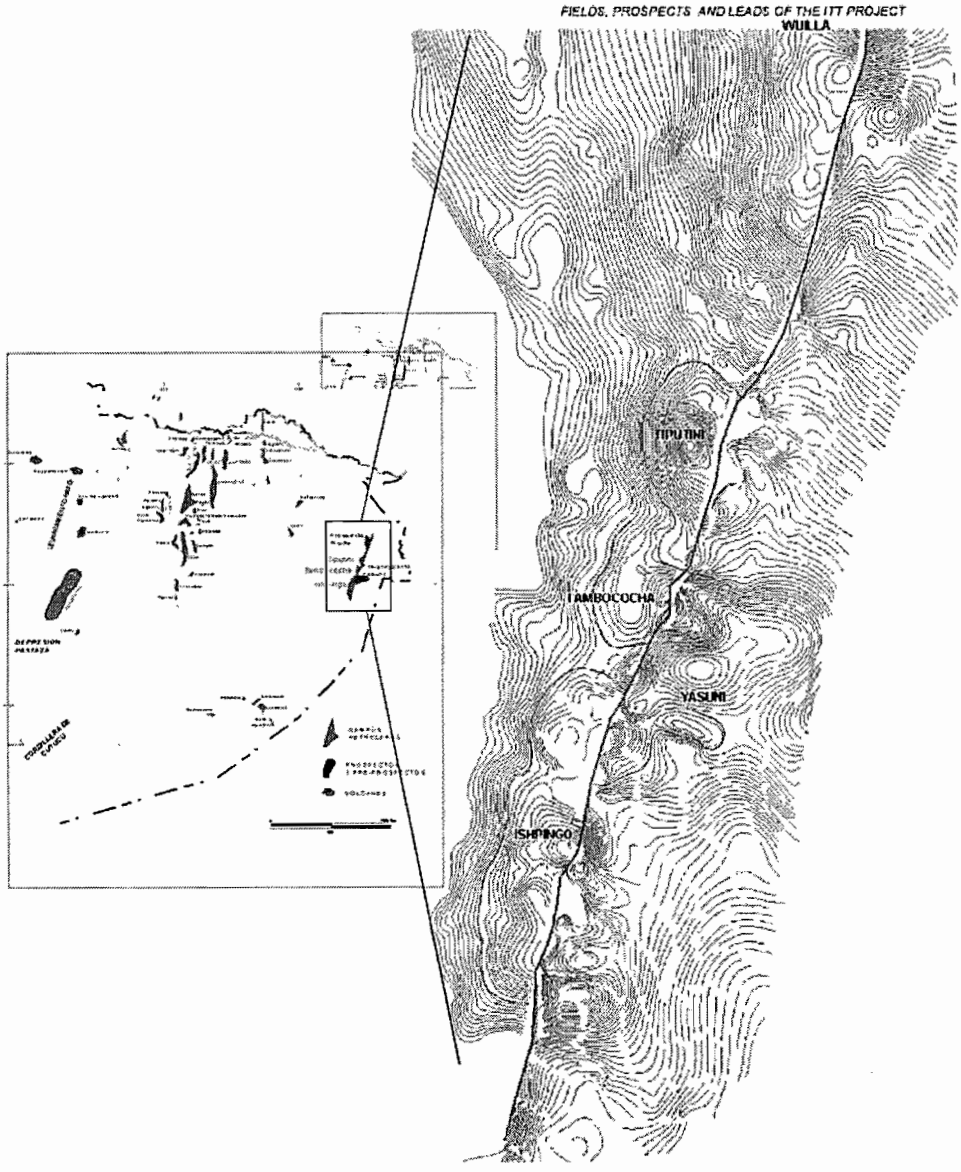

Fig. 4. Structural seismic map showing the biggest structure of the eastern border of the Oriente basin

References

Balkwill H., Rodriguez G., Paredes F. and Almeida J. P., 1995. Northern part of the Oriente Basin Ecuador: Reflection Seismic Expression of Structures. AAPG Memoir 62, pp. 559-571.

Baby P. et. Al., 1997. Estilo Tectónico y Etapas de Deformación de la Parte Norte de la Cuenca Oriente Ecuatoriana. Memorias del VI Simposio Bolivariano, Cartagena, Colombia, v.1, pp 288-302

Diaz B. Marlon A. 2000. Caracterización y Reconstrucción Paleogeográfica de las Cuencas Pre-Aptenses en el Oriente Ecuatoriano

Rivadeneira M., Sánchez H., 1989. Consideraciones Geológicas del Preaptense de la Cuenca Oriente. Memorias del Sexto Congreso Ecuatoriano en Geología, Minas, Petróleo y Geotecnia, pp.214-252.

FORELAND BASIN DYNAMICS IN WESTERN AMAZONIA INFERRED FROM FOREBULGE EVOLUTION: THE CASE STUDY OF THE ARCH OF IQUITOS (PERU)

Martin RODDAZ (1), Patrice BABY (2), Stéphane BRUSSET (3) and Wilber HERMOZA (4)

(1) IRD UR 104 LMTG-UMR 5563, 38 rue des 36 Ponts 31400 Toulouse-France; mroddaz@lmtg.ups-tlse.fr;
(2) IRD UR 104 LMTG-UMR 5563, 38 rue des 36 Ponts 31400 Toulouse-France; baby@cict.fr;
(3) IRD UR 104 LMTG-UMR 5563, 38 rue des 36 Ponts 31400 Toulouse-France; brusset@cict.fr;
(4) IRD UR 104 LMTG-UMR 5563, 38 rue des 36 Ponts 31400 Toulouse-France; hermoza@lmtg.ups-tlse.fr;

KEY WORDS: Foreland basin, Forebulge evolution, Miocene, Marañón, Peru

INTRODUCTION

The modern foreland basin system adjacent to the Andes is considered the type example of retroarc foreland basin (Horton and DeCelles, 1997). In the Central Andes, these authors have defined a four components foreland basin system (i.e. the wedgetop, the foredeep, the forebulge and the backbulge depozones). This system is elongated parallel to the orogenic wedge, which propagated eastward since the late Cretaceous-Paleocene. According to latest studies (Gil, 2001; Hermoza et al., 2002), a continuous orogenic loading was not the rule in the Amazonian foreland basin system.

The Amazonian basin contains actually the world's largest fluvial basin (actual drainage area of 5.8×10^6 km^2, depositional area of approximately $2.5\text{-}3\times10^6$ km^2). The Amazonian basin encompasses several Cenozoic sub-basins delimited by structural/geomorphological arches. From West to East, the Amazon runs across (figure 1): i) the Marañón foreland basin, ii) The Solimoes (intracratonic basin, Caputo, 1991) basin limited to the East by the Purus Arch and to the West by the Iquitos Arch (Caputo, 1991) and divided into two sub-basins separated by the Carauari Arch and iii) the Amazonas basin (Paleozoic intracratonic basin) limited to the East by the Gurupua Arch and to the West by the Purus Arch.

The Marañón basin started to develop in the Late Cretaceous-Paleocene. During this period, it constituted probably the backbulge depozone of a foreland basin system (Gil, 2001). From Eocene to Oligocene, the development of the Andean foreland basin system was controlled by the decrease of tectonic loading (orogenic unloading, Christophoul et al., 2002). From Upper Oligocene to Middle Miocene, the Marañón basin constituted the foredeep depozone of the Andean foreland basin system as a result of orogenic loading context (Gil, 2001). From Middle Miocene to Upper Miocene, Gil (2001) recognizes in the Marañón basin an orogenic unloading

episode with well constrained foresag depozone, which would be filled up by the Pebas Formation. The origin of the Pebas Fm has been widely discussed. According to latest studies (see for example Räsänen et al., 1995), the Pebas Fm consists of tidal deposits, which set up in a shallow marine environment (i.e. the "Pebasian Sea"). The origin of the Pebasian Sea, which extended toward the Purus Arch, is generally correlated and ascribed to the latest Serravallian rise of the global sea level ~ 10 Ma. Contrary to these authors, we impute the presence of the Pebasian Sea to the Middle Miocene-Upper Miocene unloading episode. Based on sedimentation accumulation rate, Hermoza et al., (2002) confirm this Middle Miocene orogenic unloading episode and propose that the foreland basin system has then evolved continuously from Upper Miocene to Pleistocene with a foredeep type sequences that migrates progressively to the East. This latter author has shown that the sedimentation accumulation rate increased strongly during the Upper Miocene-Pleistocene period. From this short literature review of the evolution of the Marañón foreland basin since Paleogene, the Geodynamic evolution of the Peruvian Andes as recorded in the dynamic of the Marañón foreland basin system set out, at least, a 4 steps evolution: i) orogenic loading during the Paleocene; ii) orogenic unloading from Eocene to Oligocene; iii) orogenic loading from Upper Oligocene to Middle Miocene; and iv) orogenic unloading from Middle Miocene to Upper Miocene.

The aim of this paper is to investigate the evolution of the Marañón foreland basin system from Upper Miocene to actual times with emphasis on the evolution of the forebulge depozone.

RESULTS

We have investigated the region of Iquitos (Loreto, Peru; Figure 1). Geomorphologically, this region presents two domains: the non floodable terrains known as the "tierra firme" (about 150 m above sea level) and the Quaternary floodable alluviums plains (100 m above sea level). The "tierra firme" terrains constitute the main part of the Iquitos Arch. The Iquitos Arch is trending NW-SE parallel to the Andean chain and is from 140m abs to 200m abs. It has more than 1000 km long and between 100 and 150 km wide. It is situated at more than 400 km from the orogenic front. From numerical modeling and gravimetrical map (Sanchez et al., 1999), the Iquitos Arch is inferred to correspond to the forebulge of the Marañón foreland basin system.

A 100 km long cross sections has been set out perpendicularly to the axe of the Iquitos Arch (along the Nauta-Iquitos road). Two representative sedimentological logs (IQ35 and IQ40, see Figure 2) have been selected to set up the sedimentology of the Iquitos Arch.

The section IQ 40 is marked by four sequences of tidal-like deposit separated from each other by transgressive surfaces. The four transgressive surfaces dip to the East. These tidal deposits, which present paleocurrent direction to the SW, are succeeded by a fluvial formation with paleocurrent to the NE. From the base to the top, this formation consists of facies Sp, Fsh, Sh, Gh, Sh and Gh. The section IQ 35 displays an erosive contact between the mud/clay sediments of the Pebas Fm and the white sand of the "Iquitos formation".

From this two representative logs, the facies succession displays the competition between uplift and quiescence stages of the forebulge. Uplift stages are marked by prograding stacking pattern from shallow water to embouchure environments while quiescent stages are recorded by the transgressive stacking pattern of tide-influenced units. The sedimentary succession is slumped affected by syn-sedimentary normal faults. Such soft-sediment deformation bear witness to tectonic activity. This movement of the substratum of the forebulge

depozone can be ascribed to reactivation of Proterozoic normal basement-faults well-imaged on seismic section. The Iquitos Arch is still tectonically active since normal faults affect Holocene fluvial deposit (our study and Dumont et al., 1988 in the southern part of the Arch). This indicates that the forebulge is still growing.

CONCLUSIONS

This study has showed that i) the Arch of Iquitos corresponded to the forebulge of the Marañón foreland basin system, ii) the uplift of the forebulge was recorded in the sedimentation by marine facies grading upward to estuary-like facies and to actual fluvial system with shifting in the orientation of the drainage network, and iii) the uplift of the forebulge is still active and associated to neo-tectonic activity ascribed to the reactivation of Proterozoic normal fault. From these results, it appears that the Marañón foreland basin system is controlled by increase in tectonic loading since Upper Miocene. This increase has caused the emergence of the Iquitos forebulge, which have probably induced the retreat of the Pebasian sea and modified the drainage network. The emergence of the forebulge is not as continuous as expected (i.e. transgressive surfaces). The area comprised between the Iquitos Arch and the Carauari Arch is expected to be the backbulge depozone of the Marañón foreland basin system since at least the Upper Miocene.

ACKNOWLEDGEMENTS : Research supported by INSU grant 99PNSE59 and IRD (Tectonique, érosion et sédimentation dans le bassin de l'Amazone : du Mio-Pliocène à l'Actuel).

REFERENCES

Caputo V. 1991 Solimoes megashear: Intraplate tectonics in northwestern Brazil. Geology, 19, 246-249.

Catuneanu O, Beaumont C. and P. Waschbusch. 1997. Interplay of static loads and subduction dynamics in foreland basins: Reciprocal stratigraphies and the "missing" peripheral bulge. Geology, 25, 1087-1090.

Catuneanu O, Sweet A.R. and A.D. Miall. 2000. Reciprocal stratigraphy of the Campanian-Paleocene Western Interior of North America. Sedimentary Geology, 134, 235-255.

Christophoul F., Baby P. and C. Davila. 2002. Stratigraphic responses to a major tectonic event in a foreland basin: the Ecuadorian Oriente Basin from Eocene to Oligocene times. Tectonophysics, 345, 281-298.

DeCelles P.G. and K.A. Giles. 1996. Foreland basin systems. Basin Research, 8, 105-123.

Dumont J.F., Lamotte S and M. Fournier. 1988. Neotectonica del Arco de Iquitos (Jenaro Herrera, Peru). Boletin de la Sociedad Geologica del Peru, 77, 7-17.

Gil W. 2001. Evolution latérale de la déformation d'un front orogénique: Exemple des bassins subandins entre 0° et 16°S. Phd thesis,Université Paul Sabatier, Toulouse, 150pp.

Hermoza W., Baby P., Brusset S., Christophoul F. and W Gil. 2002. Foreland basin system evolution of the Peruvian Andes: new insights from mass balance computation. 5th ISAG, Toulouse.

Horton B.K. and P.G. DeCelles. 1997. The modern foreland basin system adjacent to the central Andes. Geology, 25, 895-898.

Räsänen M. E., Linna A.M, Santos J.C.R. and F.R. Negri. 1995. Late Miocene Tidal Deposits in the Amazonian Foreland Basin. Science, 269, 386-390.

Sanchez A. and 8 contributors. 1999. Geologia de los cuadrangulos 4-p, 5-p, 5-q, 5-r, 6-p, 6-q, 6-r, 7-p, 7-q, 7-r, 8-p, 8-q, 8-r, 9-p, 9-q, 9-r, 10-p, 10-q, 10-r. INGEMMET, Boletin n° 132, Serie A : Carta Geologica Nacional.

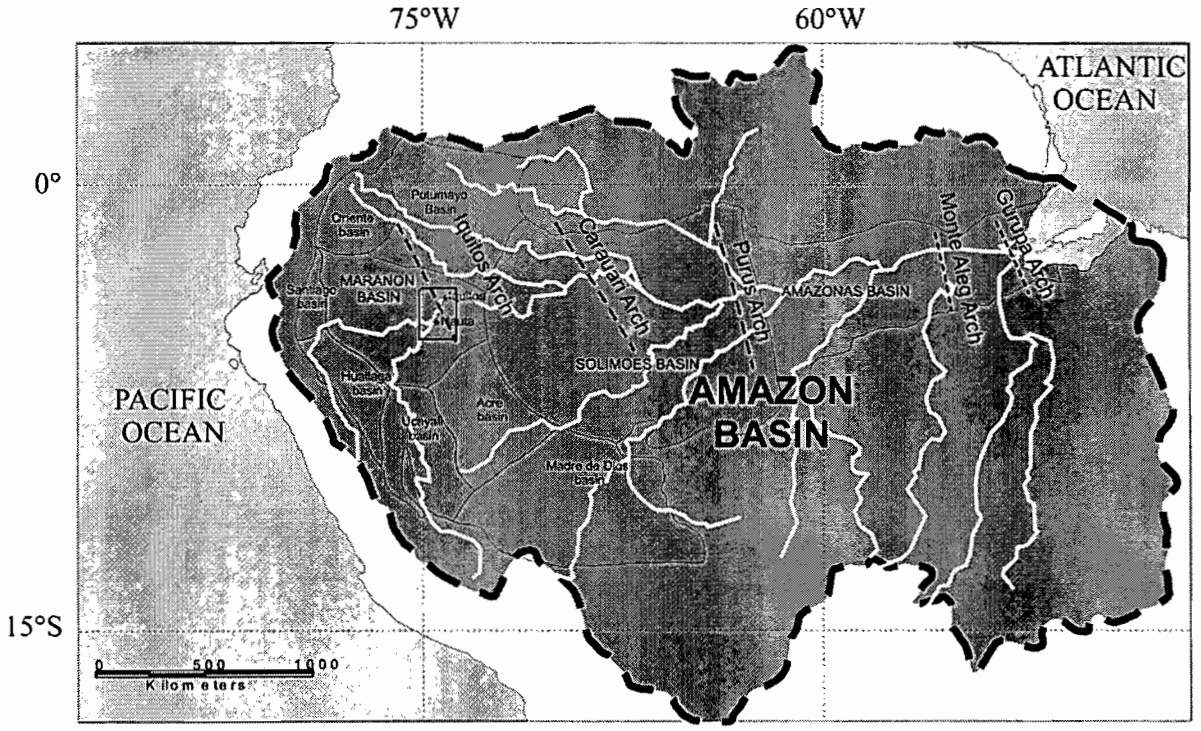

Figure 1: Map of the actual Amazon Basin The dark grey set delimited by sharp dashed lines represents the actual Amazon basin. Rivers are in white, solid lines indicate the limit of the basins. Axes of the Amazon arches are in dashed lines. The rectangle delineates the studied area.

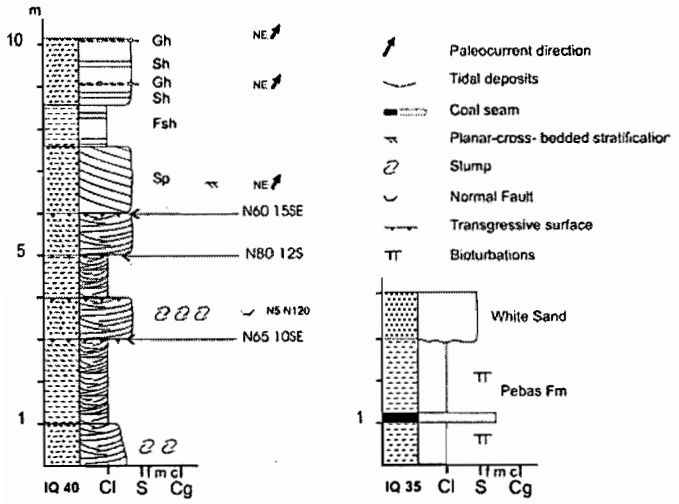

Figure 2: The two representative sedimentary logs. Strike and dip of the transgressive surfaces and faults are given.

GRAVITY and MAGNETIC MODELLING ACROSS THE GUARICO SUB-BASIN, ESPINO GRABEN, VENEZUELA

Inírida RODRÍGUEZ (1) and Josmat RODRÍGUEZ (2)

(1) iniromil@yahoo.com.mx
(2) josmatr@hotmail.com

Key words: gravity, magnetic, modelling, Espino, graben.

INTRODUCTION

This work examines the subsurface structure of the Guarico Sub-basin, across the southwestern extension of the Espino Graben in the central part of Venezuela (Fig. N° 1), through an analysis of gravity and magnetic anomalies.

CENTRAL VENEZUELA TECTONIC SETTING:

The Guarico Sub-basin is an east-northeastern trending and east plunging structural depression located in the central part of Venezuela (Fig. N° 2). It is approximately 200 km long and 120 km wide, and it is bounded on the South by the Guayana Shield, on the North by the Coastal Cordillera –Cordillera de La Costa- with the Villa de Cura complex and nappes up to the Guarico Frontal Thrust; on the west by El Baul Swell (an alkaline granite, 287±10 m.y. (Rb/Sr), 270±10 m.y. (K/Ar), Santamaria and Schubert, 1974; González de Juana et al., 1980)). On the East the Guarico Sub-basin is limited by the Urica Fault, a possible paleofracture of Precambrian age, reactivated during the collision process as a right-strike-slip fault (Daal et al., 1989; Erikson, 1994), and then continues through the Eastern Venezuelan Foreland Basin. The crystalline basement of the Precambrian Guayana Shield, which crops up southward of the Orinoco River, is made up mostly of metasedimentary and igneous rocks, with granite batholiths of homogeneous composition (Case et al., 1984).

One of the earliest apparent traces of some extensional regime in central Venezuela is the existence of a graben-type structure in the Espino area, where a complete record through the pre-rifting into the rifting stages seems to be present. Feo Codecido et al. (1984) have reported there the presence of 1.6km sequence of red-beds and interbedded basaltic flow (113m thick and 162 m.y. in age) at the northeasterly trending Espino Graben. It seems to indicate that a rifting event might have been felt in that area as early as in Mid to Late Jurassic times. Sedimentation took place from the initial rifting phase, over the Atlantic-type ocean margin developed onto the continental northeastern edge of the South American plate. Towards the end of the Cretaceous and into the Paleocene, the Guayana and the El Baul cratonic areas with their Cretaceous sedimentary cover were uplifted, exposing to erosion the Cretaceous Guarico Sub-basin. While erosion was going on in the South, sedimentation was continuous in the North. At this

time Erlich and Barrett (1990) relate the beginning of the first phase of compression-transpression and foreland basin development in Guarico Sub-basin.

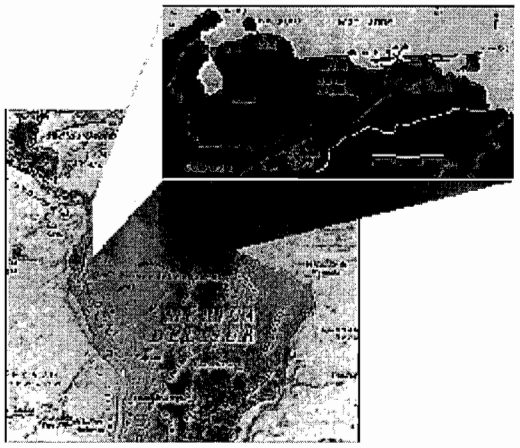

Fig. N° 1 - Location Map of the study area

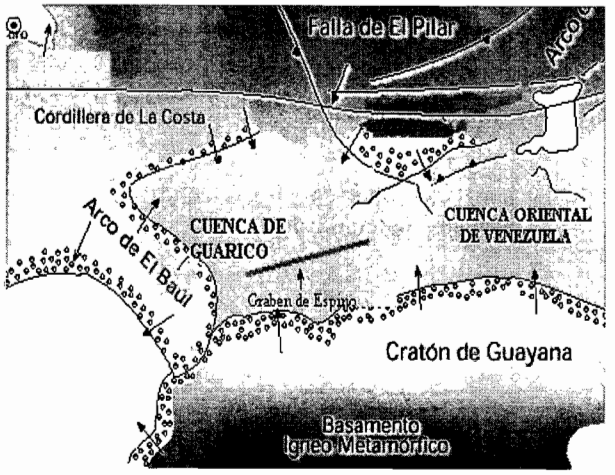

Fig. N° 2 - Geological Setting

GRAVITY and MAGNETIC DATA ANALYSIS

Gravity data from stations between 7°30´N – 8° 30´N of latitude, and 66°45´W-67°45´W of longitude, product of the survey carried out during the course of Field Geophysics 2001, as well as those provided by Cartografia Nacional, Venezuela, were processed to produce the Bouguer Anomaly Map of the area of study (Fig. N° 3). The regional structure is dominated by the East-West to East-Northeast trend of the Guarico Sub-basin and Espino Graben, and is clearly related to the gravity anomaly trend with the same orientation. A positive gravity anomaly belt, which reaches maximum values in excess of 30 mGals occurs over the northern part of the area. Further South the trend is marked by a negative anomaly belt with local minimum more negative than 6 mGals. Along the northern periphery of the basin there is a series of local negative anomalies of the order of 6 mGals.

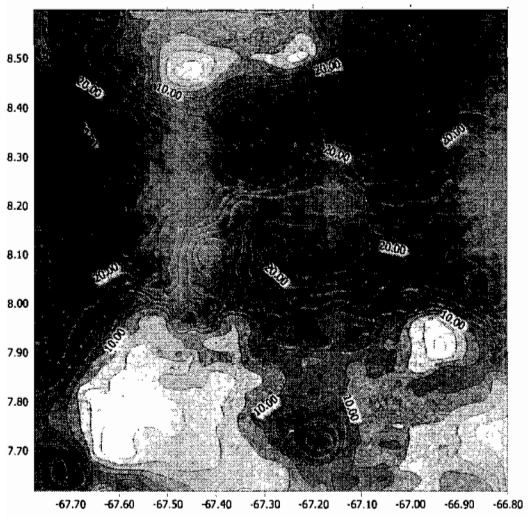

Fig. N° 3.- Bouguer Anomaly Map.

Fig. N° 4.- Total Magnetical Intensity Map.

Magnetic data from the aeromagnetic survey of Venezuela (compiled by Navarro (1989)), were used to produce the Total Magnetical Intensity Map of the area (Fig. N° 4). The magnetic anomalies exhibit a little variable non-symmetrical pattern throughout the region. Nearly East-West trending anomalies dominate the area in clear correlation with the orientation of the basin. Anomalies of the order of 9900 gammas have been identified in the Northern extreme of the area. The most prominent feature in the Magnetic Map is the minimum of 9660 gammas coincident with the Espino Graben.

From the analysis of regional effects in both gravity and magnetic data, a third degree polynomial trend surface was chosen (Figs. N° 4, 5). In those maps the most prominent feature is signed by a negative anomaly (-10 mGals, 9600 gammas) that marks the trace of the Espino Graben.

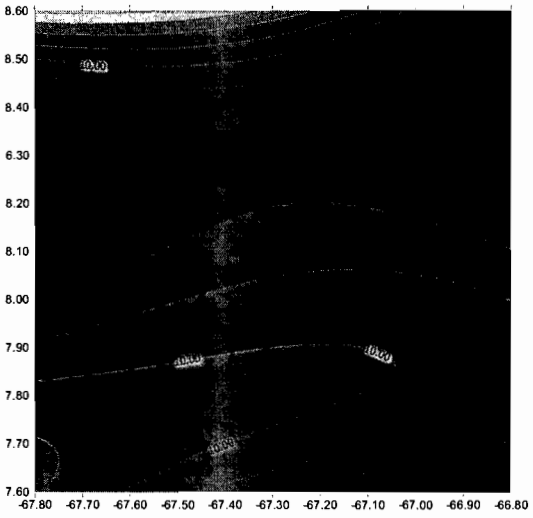

Fig. N° 5.- Regional Bouguer Anomaly Map.

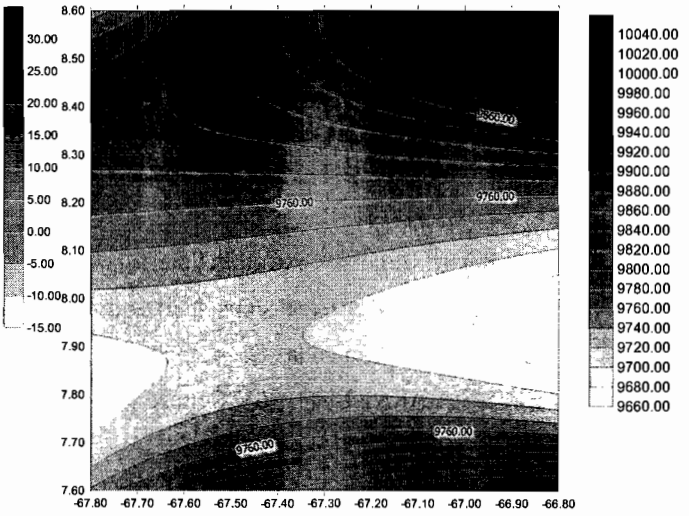

Fig. N° 6.- Regional Total Magnetical Intensity Map.

In order to constrain the models, generalized geological cross-sections based on surface and subsurface data were constructed, and the geological models were converted into a series of polygons with its correspondent densities and magnetic properties to provide the initial input models. Main geological and geophysical constraints imposed to the model come from borehole data (Feo Codecido et al., 1984) seismic and aeromagnetic data (Navarro, 1989). The inclination of the magnetization was assumed parallel to the present field accordingly with the magnetic susceptibility of the rocks in the area, except for the basaltic flows which exhibit significant changes in their magnetic properties.

CONCLUSIONS

A fairly good regional fit is achieved for a model across the Guarico Sub-basin, with a thickness of Tertiary-Cretaceous sediments (ρ = 2.3-2.35 g/cc) of about 1 km, followed by rocks of Paleozoic age (thickness: 5 km, ρ = 2.65 g/cc) overlying a crystalline basement (ρ = 2.75 g/cc). Associated to the Espino Graben there is a sequence of Jurassic rocks (ρ = 2.6 g/cc) with an interbedded basaltic layer (ρ = 2.9 g/cc, thickness 110 km). The modeling also indicates that the whole sedimentary sequence in the basin reaches thicknesses of the order of 6.5km.

REFERENCES

CASE, J.E., T.L HOLCOMBE and R. G. MARTIN (1984) "Map of geologic provinces in the Caribbean region" Scale 1: 5.000.000 In: Bonini, W.E., R.B Hargraves and R. Shagam, Eds. The Caribbean-South American plate boundary and regional tectonics. Geol. Soc. of Amer. Mem. 162: 1-30.

DAAL, A., A. GONZÁLEZ; G HERNÁNDEZ and R. PRIETO (1989) "Exploración de Hidrocarburos en el norte de Monagas ". Internal Report EPHINOM, Comité interfilial CPV-LGV-IM

ERIKSON, J.P. (1994) "A Lower Cretaceous shelf and delta in the Eastern Venezuela Basin". Mem. V Simposio Bolivariano: Exploración Petrolera en las Cuencas Subandinas, Puerto La Cruz, Venezuela. P:174-189

ERLICH, R. N. and S. F BARRETT (1990) "Cenozoic plate tectonic history of the northern Venezuela and Trinidad area". Tectonics 9 (1): 161-184.

FEO CODECIDO, G., F. SMITH, N. ABOUD. and E. Di GIACOMO (1984) "Basement and Paleozoic rocks of the Venezuelan llanos basins". Caribbean- South American plate boundary and regional tectonics. Geol. Soc. of AMER. Mem 162:175-187

GONZÁLEZ DE JUANA, C., J ITURRALDE and X. PICARD (1980) "Geología de Venezuela y sus cuencas petrolíferas". Caracas. Ed. Foninves. Vol I-II. 103p.

NAVARRO, J. (1989) "Mapa de anomalías de intensidad magnética de Venezuela". Corpovén, S.A. Venezuela. Scale: 1:500.000.

SANTAMARIA F and C SCHUBERT (1974) "Geochemistry and geochronology of the southern Caribbean-northern Venezuela plate boundary" Geol. Soc. of Amer. Bull 85(7): 1085-1098.

SEDIMENTOLOGIC EVOLUTION OF THE TINAJANI INTERMONTANE BASIN (LATE OLIGOCENE-MIDDLE MIOCENE, SOUTHEAST PERU)

Rildo RODRIGUEZ (1), Tomasa FLOREZ (2), René MAROCCO (3), Victor CARLOTTO (4) and José CARDENAS (5)

(1) INGEMMET, Av. Canadá 1470, apartado postal 889, Lima 41, Peru (rildo@ingemmet.gob.pe)
(2) Facultad de Ingeniería Geológica, Universidad Nacional San Antonio Abad del Cusco, Cusco, Peru
(3) IRD (ex-ORSTOM) Apartado Postal 18-1209, Lima 18; Peru (marocco@chavin.rcp.net.pe)
(4) Universidad Nacional San Antonio Abad del Cusco UNSAAC. (carlotto@chaski.unsaac.edu.pe)
(5) Universidad Nacional San Antonio Abad del Cusco UNSAAC. (cardenas@inti.unsaac.edu.pe)

KEY WORDS: Sedimentology, intermontane basin, Oligocene-Miocene, SE Peru

RÉSUMÉ

Le bassin intramontagneux de Tinajani (Oligocène supérieur-Miocène moyen; Altiplano du sud du Pérou) montre une évolution tectono-sédimentaire qui peut être divisée en 2 périodes. La première (membre inférieur) correspond au début du remplissage vers 28 Ma, en relation avec des mouvements sénestres-inverses (événement Quechua 0, 28-26 Ma). La seconde (membre supérieur) correspond au reste du remplissage et semble liée a l'événement Quechua 1 (20 Ma) qui produisit un jeu inverse des failles contrôlant le bassin.

INTRODUCTION

The Tinajani intermontane basin (Late Oligocene-Middle Miocene) is located in the Altiplano of southern Peru (Fig. 1). This basin was first studied by Audebaud & Vatin-Pérignon (1974) and considered to be Mio-Pliocene. Sébrier et al. (1988) assigned a Miocene age to the basin, based on some datations which however were not well located in the stratigraphic column.

The substratum of the Tinajani basin consists of Paleozoic rocks (Umachiri series), Triassic-Jurassic sandstones, Cretaceous strata (Ayavacas Formation and Vilquechico Group) and Eocene-Middle Oligocene deposits (Ayaviri Formation and Monterino volcanics). The Monterino volcanics (Florez & Rodriguez, 1999) or Lower Tinajani volcanics (Sébrier et al., 1988) were dated between 26 and 28 Ma (K/Ar; Bonhomme et al., 1985; Fig. 2).

The Tinajani basin has a rhombohedral shape elongated in a NW-SE direction. Its southern edge is controlled by the Pasani and Surimarca fault system, the northeastern edge by the Ayaviri reverse fault, and the northwestern edge by the Huisachita fault.

SEDIMENTOLOGIC EVOLUTION

The Tinajani Formation (Late Oligocene-Middle Miocene) which forms the basin infilling is divided in 4 sequences, named A, B, C and D (Fig. 2).

Sequence A (125-145 m) is conformed by pebbly facies of proximal alluvial fan origin, by sandy facies of a distal braided system, and argillaceous and calcareous facies of lacustrine environment. The sequence evolution is fining-upward and the paleocurrents are from the SW.

Sequence B (650 m) consists of sandy facies of braided rivers, pebbly facies of longitudinal bars and channels of proximal rivers, and lacustrine argillaceous facies, which are interbedded with volcanic tuffs. This unit is a fining-upward sequence that indicates retrogradation of the proximal environment installed in the NE and eastern edges of the basin.

Sequences A and B form a fining-upward megasequence (lower member; Fig. 2) that characterizes the beginning of the sedimentary infilling. This period starts ≈ 28 Ma (Quechua 0 tectonic event) in relation to sinistral inverse motions (caused by a E-W compression, Fig. 3), with the installation of alluvial fan deposits along the southern edge controlled by the Pasani and Surimarca Faults. In the distal part (north) lacustrine deposits developed. Later on, the Pasani and Surimarca Faults stabilized, and the Ayaviri Fault controlled fluvial sedimentation proceeding from the NE (Fig. 3).

Sequence C (150 to 450 m) consists of sandy facies of proximal braided rivers, pebbly facies of proximal rivers and of alluvial fans, which show a coarsening-upward evolution. The alluvial fans are located along the NE and SW edges. Near the base of the unit, volcanic tuffs are dated (K/Ar) between 18 and 14 Ma (Bonhomme et al, 1985, Fig 2), and at 20.5 ± 0.7 Ma (Carlotto, unpublished).

Sequence D (370-160 m) exclusively consists of sandy and conglomeratic (debris flow) alluvial fans coming from the SW. They form coarsening-upward sequences.

Sequences C and D form a coarsening upward megasequence (upper member; Fig. 2) that indicates closure of the basin. This period seems to be in relation with the Quechua 1 tectonic event (20 Ma) that produced reverse motions (compression NE-SW) of the Pasani and Ayaviri faults, creating reliefs that fed alluvial fans and proximal rivers (Fig. 3). Later on, only the Pasani and Surimarca faults were active, feeding fans toward the NE, and also producing NW-SE folds and progressive unconformities.

The Pasani and Ayaviri faults that have controlled the evolution of the Tinajani basin are the structural limits of a threshold which is the continuation of the Cusco-Puno Threshold studied in the Cusco region (Carlotto, 1998). It is on this structural high that the Tinajani basin developed.

Gabbroic and granodioritic plutons are located south of the Pasani and Surimarca faults (Carlier et al., 1996). Erosion of reliefs produced by the surrounding uplift provided detritic material which filled the Tinajani basin, which is compatible with the paleocurrents data.

CONCLUSIONS

Intermontane basins (Late Oligocene-Middle Miocene) aligned on strike-slip faults, are located in the Altiplano and in the Eastern Cordillera-Altiplano limit (Punacancha, Pusi-Capachica, Crucero, Rumichaca, Tinajani basins). These basins present a beginning stage and a closing stage. The filling beginning is related to sinistral transtension or transpression movements along the faults that define the basins, during the Quechua 0 tectonic event (28-26 Ma). The closing of those basins implies reverse and reverse-sinistral motions due to a NE-SW compression, in relation with the Quechua 1 tectonic event (20-17 Ma). These periods of beginning and of closing of the basins seem to coincide with changes in the speed and direction of the Nazca and South American plates, particularly around 26 Ma and 20 Ma.

REFERENCES

AUDEBAUD, E., & VATIN PÉRIGNON, N. (1974).- The volcanism of the northern part of the Peruvian Altiplano and of the Oriental Cordillera on a traverse Quincemil-Sicuani-Arequipa. Proceedings of the Symposium on Andean and Arctic Volcanology. 5-37. Santiago, Chile.

BONHOMME, M.G.; AUDEBAUD, E. & VIVIER, G. (1985).- K-Ar ages of hercynian and neogene rocks along an east-west croos section in southern Perú. Comunicaciones, 35, 27-30.

CARLIER, G., LORAND, J. P., BONHOMME, M. & CARLOTTO, V. (1996).- A reappraisal of the Cenozoic Inner Arc magmatism in the Southern Peru : Consequences for the evolution of the Central Andes for the past 50 Ma. International Symposium on Andean Geodynamics, St Malo, France, Extended abstracts, ORSTOM, série "Colloques et Séminaires", 551-554.

CARLOTTO, V. (1998). Evolution Andine et Raccourcissement au Niveau de Cusco (13-16°S) Perou. Enregistrement sedimentaire, chronologie, controles paleogeographiques, evolution cinematique. Tesis Doctor. Universidad de Grenoble. Francia. 159p.

FLOREZ, T., & RODRIGUEZ, R. (1999). Las Cuencas Neógenas del Sur del Perú. Evolución Sedimentológica, Estratigráfia, Paleogeografía y Tectónica (Ayaviri-Puno). Tesis Ingeniero Geólogo. Universidad Nacional de San Antonio Abad del Cusco. Perú. 68p.

SÉBRIER; M.; LAVENU, A.; FORNARI, M.; SOULAS, P. (1988). Tectonics and uplift in Central Andes (Peru, Bolivia and Northem Chile) from Eocene to present. Géodinamique Paris, vol. 3, 139-161.

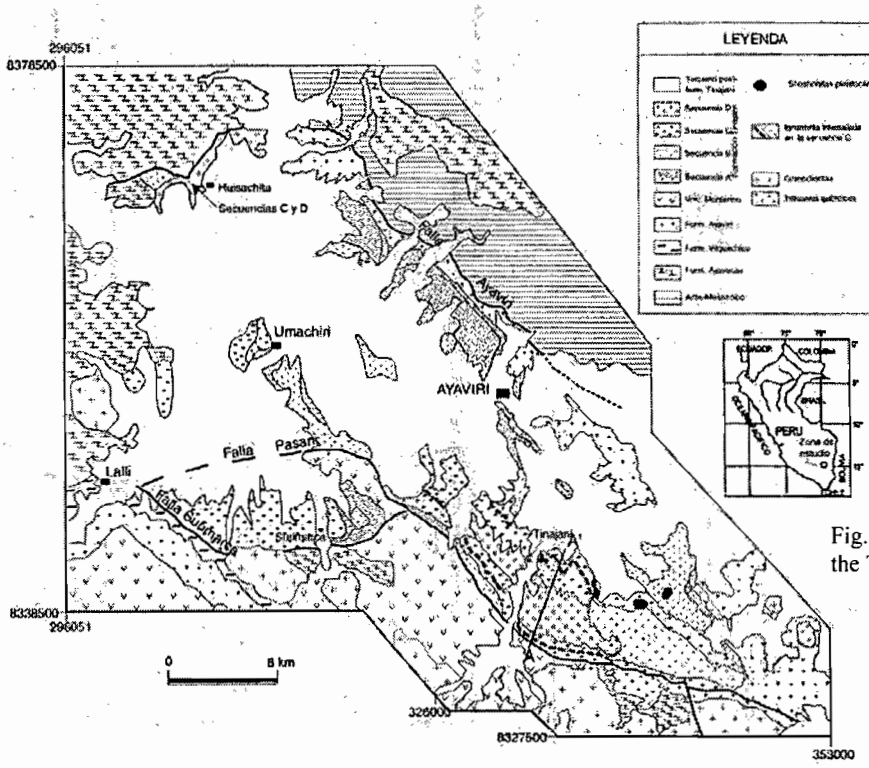

Fig. 1: Geological map of the Tinajani Basin

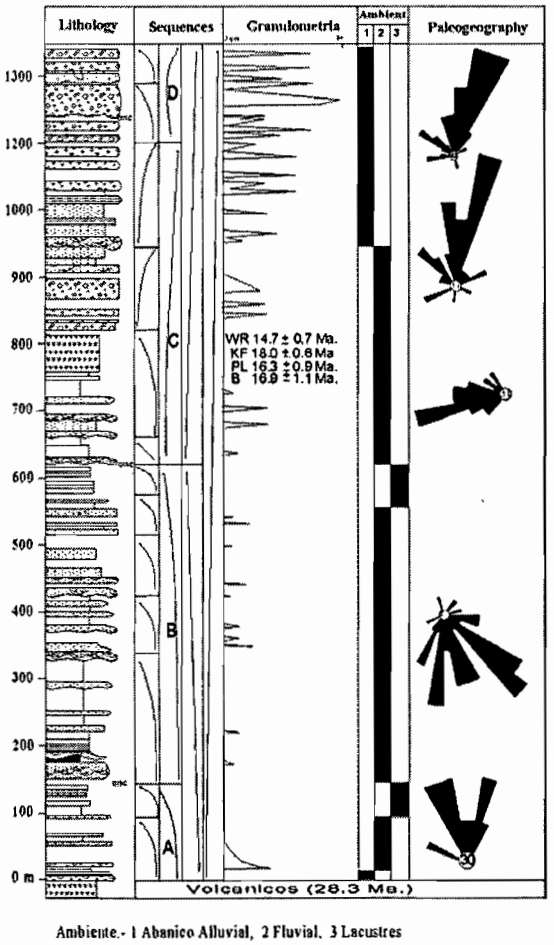

Fig. 2: Lithostratigraphic log of the Tinajani Basin sediments

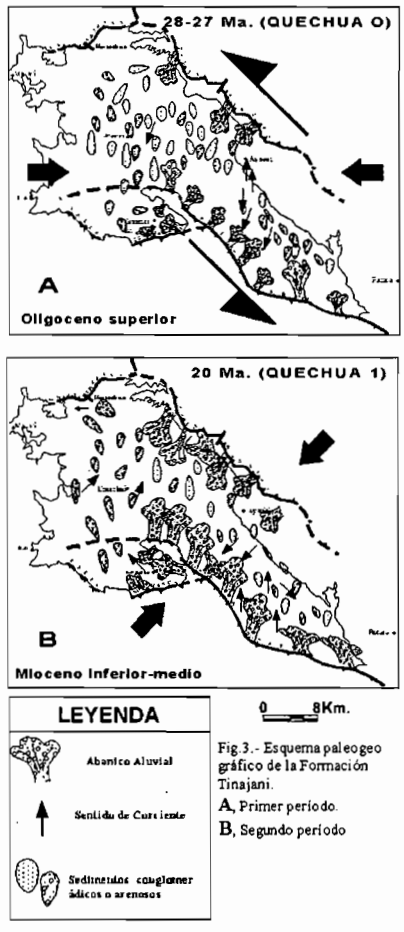

Fig.3.- Esquema paleogeo gráfico de la Formación Tinajani.
A, Primer período.
B, Segundo período

Fig. 3: Paleogeographic map of the Tinajani Formation

TRANSPRESSIONAL MOTIONS ALONG THE CORDILLERA OCCIDENTAL – COASTAL BELT BOUNDARY SINCE THE LATE CRETACEOUS (SOUTHERN PERU, 16° S)

Darwin ROMERO(1), Agapito SANCHEZ(1), Maria CRUZ(1), Pedro TICONA(1), Rildo RODRIGUEZ(1)

(1)Instituto Geológico Minero y Metalúrgico (INGEMMET). Av. Canada 1470, San Borja. Apartado Postal 889. Lima 41, PERU (e-mail: dromero@ingemmet.gob.pe, darofe@hotmail.com)

KEY WORDS: tectonics, transpression, Late Cretaceous, southern Peru, Cordillera Occidental, Coastal Batholith

INTRODUCTION

The study area is located in southern Peru NW of the city of Arequipa (16° S) at the boundary between the Cordillera Occidental and coastal belt. Previous studies sustain that exists in the area a large overthrust, named the Cincha-Lluta overthrust (Vicente et al., 1979). Recent studies realized in the Huambo (32-r) (Romero & Ticona, 2002; Cruz, 2002) and Aplao (33-r) sheets permit to observe NE-vergent thrusts (areas of Andamayo and Ayo). To the SW, however, in the Majes valley (areas of Aplao and Santa Elena), SW-vergent thrusts are observed. In the central areas of Andamayo and Aplao, faults are subvertical and display evidence of senestral motions, affecting rocks of the Coastal. This work presents the results of an integrated regional study that permits to better understand which tectonic, sedimentary and magmatic processes occurred in the area. We interpret the mentioned fault system as a large flower-structure, which resulted from transpressional motions.

STRATIGRAPHY

The study area displays Proterozoic to Quaternary rocks (Fig. 1). The basement consists of gneisses and micaschists, that yielded 1811±39 y 1900 Ma (Cobbing et al., 1977). It is overlain by the Ongoro Fm (Devonian?), composed of schists, slates and sandstones. **The Mesozoic** consists of: the Chocolate Fm (Early Jurassic; conglomerates, volcanic breccias and flows); the Socosani Fm (Toarcian-Bathonian; limestones); the Yura Group (Callovian-Neocomian), with its Puente Fm (sandstone-shale), Cachios Fm (shale), Labra Fm (sandstone-shale), Gramadal Fm (shale-limestone) and Hualhuani Fm (sandstone); the Murco Fm (Barremian-early Albian), composed by mudstones and sandstones; the Arcurquina Fm (middle Albian-Turonian; limestones); the Seraj Fm (Senonian-Maastrichtian?; sandstones, shales, limestones, gypsum, conglomerates). **The Cenozoic** consists of: the Huanca Fm (Middle Eocene – Early Oligocene), which crops out in the NE and

includes the Querque (volcanic-clast conglomerates), Huasamayo (sandstones) and Tarucani (polymictic conglomerates) members; to the SW, the Sotillo Fm (Eocene-Oligocene) is coeval with the latter, and consists of mudstones and sandstones; the Tacaza Group (Miocene) is composed by tuffs, and the Barroso Group (Pliocene-Pleistocene), by volcanic breccias and flows; the Quaternary deposits include the notable Andahua Group (Pleistocene), which consists of andesites and basaltic andesites.

INTRUSIVE ROCKS

The plutons that crop out in the central part of the study area belong to the Coastal Batholith and include granites, granodiorites, tonalites and diorites. Isotopic dates from near the study area (Weibel et al., 1978), range between 97 ± 4.0 and 58.9 ± 2.0 Ma. In the NE area, two plutons (granite-tonalite) are assigned to the Eocene.

STRUCTURAL GEOLOGY

In the study area, folds are mainly observed to the NE, being of kilometric scale with tight to locally recumbent flanks. To the north, the main structure are: the NW-SE, NE-vergent, Jasmin reverse fault, which puts the Arcurquina Fm onto the Huanca Fm; and the NW-SE, NE-vergent, Andamayo reverse fault, which puts Paleozoic-Proterozoic and intrusive rocks against Mesozoic strata; these two faults correspond to the so-called Cincha-Lluta overthrust. In the central part of the area, two faults are noteworthy: the WNW-ESE-trending Santa Rosa fault is a strike-slip fault with a reverse component that uplifted the basement; and the NW-SE-trending Ongoro fault is a senestral strike-slip fault that uplifted Coastal Batholith plutons. To the SW, the NW-SE-striking Cosos and Santa Elena faults are SW-vergent reverse faults that thrust strata of the Yura Group onto Cenozoic rocks.

SEDIMENTARY AND GEODYNAMIC EVOLUTION

In the study area, the Late Cretaceous – Oligocene interval can be divided into two tectonic periods, during which distinct sedimentary environments were originated, in association with peculiar magmatic processes. **First period (Late Cretaceous - Early Eocene)**. After deposition of the lower part of the Arcurquina Fm, probably in an extensional context (Fig. 2), the accumulation of its middle and upper parts possibly corresponded to the onset of a transcurrent tectonic regime, in relation with the onset of the abundant magmatism recorded by the Coastal Batholith, for which a date of 97 ± 4.0 Ma is registered (Weibel et al., 1978). In the area, mainly dextral displacements on local faults increase after the Senonian, creating space for the emplacement of large plutonic masses. The Seraj Fm is deposited to the NE, while to the SW the thick volcanic Toquepala Group accumulates (Fig. 3), indicating a progressive increase in magmatic activity. This suggests that the volcanic-clast conglomerates of the Seraj Fm (Querque Member) probably reflect a Paleocene paroxysm that occurred in a large part of the study area. Dextral displacements may be related to the convergence of the Nazca and South American plates: between anomalies 30-31 and 21 (≈ 68 and 49 Ma), the mean direction of convergence was NNE-SSW (Pardo & Molnar, 1987). On the other hand, in central Peru Bussell (1983) showed that dextral displacements developed within the Coastal Batholith between 69 and 65 Ma. **Second period (Middle Eocene - Oligocene)**. In the Middle Eocene, the study area underwent a change in tectonic context. Displacements on

faults were now senestral with a reverse component, generating the Huanca basin and the deposition of the Querque Member; these motions would have progressively uplifted the Coastal Batholith plutons. In the Late Eocene, reverse displacements were less important, as suggested by the Huasamayo Member deposits. In the Early Oligocene, the Tarucani Member deposits suggest that displacements on faults in the NE area were principally reverse and NE-vergent, which uplifted Paleozoic-Proterozoic and Coastal Batholith rocks. In the SW area, displacements were reverse and SW-vergent, albeit of a lesser amplitude, as suggested by the Sotillo Fm. These motions can be related to the change in convergence direction between the Nazca and South American plates: between anomalies 21 (≈ 49 Ma) and 13 (≈ 35 Ma) the average convergence direction was N 67° E, and would have generated senestral displacements on NW-SE faults, as well as the Huanca basin, which can be interpreted as a pull-apart (Cruz, 2002). From the Miocene to the Recent, the average convergence direction was N 76° E, and the latter system was maintained. This evolution has resulted in the present configuration, formed by a large positive flower-structure generated by faults with mainly senestral displacements and reverse components (Fig. 3).

CONCLUSIONS

The regional Early Cretaceous tectonic context was probably extensional or transtensional. The Late Cretaceous-Paleocene magmatism (Coastal Batholith - Toquepala Group), at least in the study area, occurred probably in a dextral transcurrent regime; dextral displacements would have produced the necessary spaces for the emplacements of these enormous magma masses. The last motions of this fault system were transpressional, senestral with reverse components, and resulted in the observed large positive flower-structure.

REFERENCIAS

Bussell M. 1983. Timing of tectonic and magmatic events in the Central Andes of Perú. Jour. Geol. Soc. London, 140, 2, 279-286.

Cobbing, Ozard, Snelling, (1977): Reconnaissance geochronology of the costal cordillera of the southern Perú. Geol. Soc. of American. Bull. Vol. 88 n 2, 241-246.

Cruz M. 2002. Estratigrafía y evolución Tectono-sedimentaria de los depósitos Sin-orogénicos del Cuadrángulo de Huambo (32-r): Las formaciones Seraj y Huanca. Departamento de Arequipa. Tesis Universidad Nacional San Agustín de Arequipa (en preparación).

Pardo F. & Molnar P. 1987. Relative motion of the Nazca (Farallon) and South American Plates since late Cretaceous time. TECTONICS, Vol. 6, N°. 3, 233-248.

Romero D. & Ticona P. 2002. Actualización Geológica del Cuadrángulo de Huambo (32-r). INGEMMET.

Vicente J.C., Sequeiros F., Valdivia M.A., Zavala J. 1979. El Sobre-escurrimiento de Cincha Lluta: Elemento del accidente mayor andino al NW de Arequipa. Boletin de la Sociedad Geológica del Perú. Tomo 61, 67-99.

Weibel M. & Fejer Z. 1978. El Nevado Coropuna, Dpto de Arequipa. Soc. Geol. del Perú, tomo 57-58, 87-98.

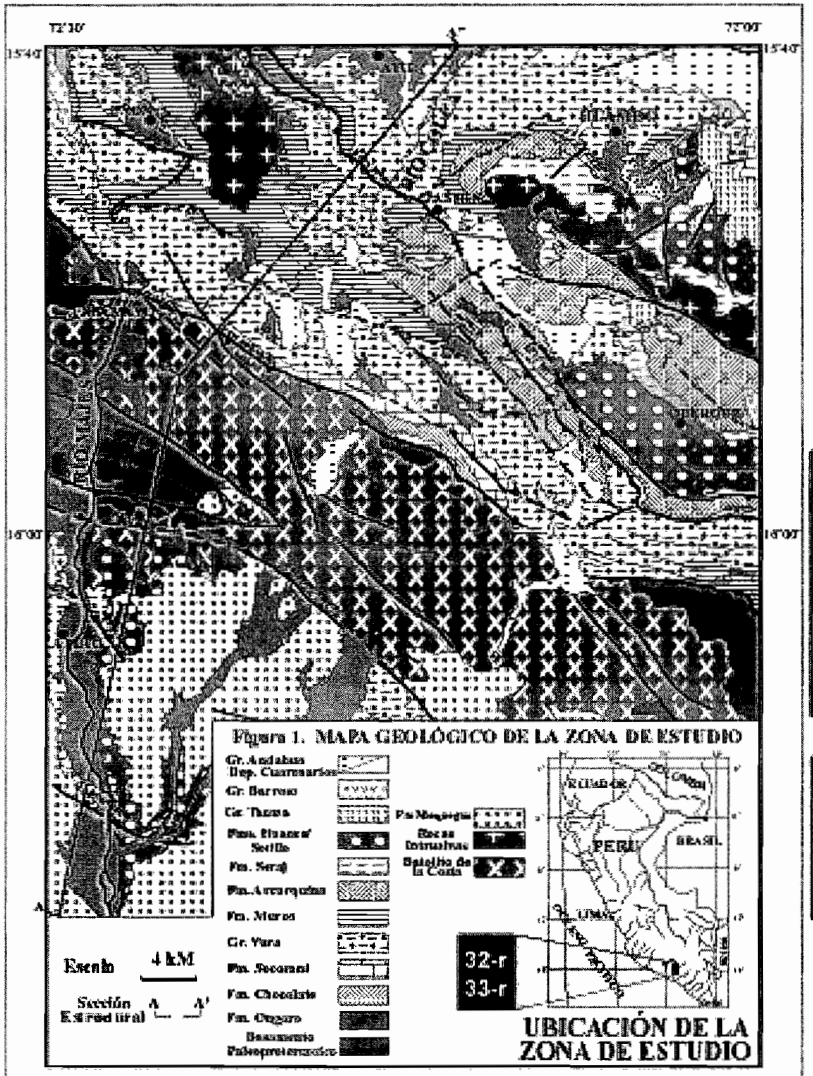

Figura 1. MAPA GEOLÓGICO DE LA ZONA DE ESTUDIO

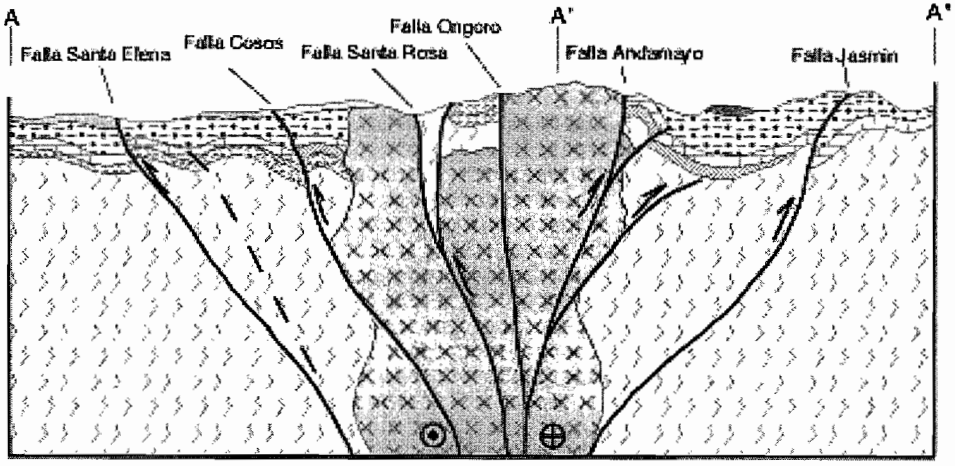

Figura 3. Sección Estructural A-A'-A". En la actualidad

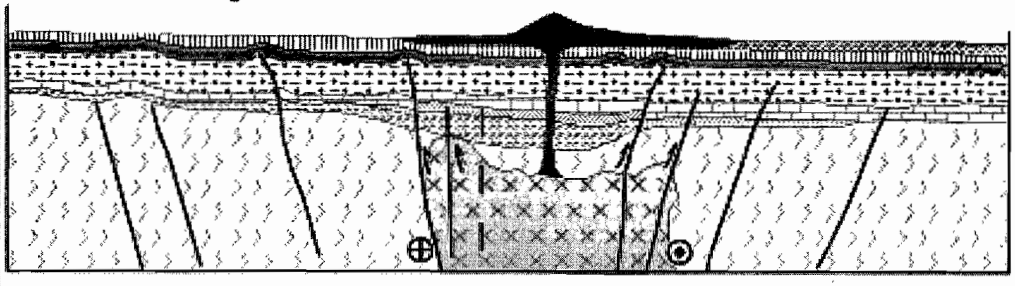

Figura 2. Sección reconstruida para el Cretácico superior - Paleoceno

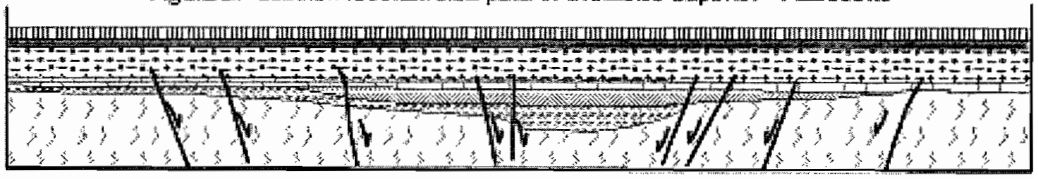

Figura 1. Sección reconstruida para el Albiano medio - superior

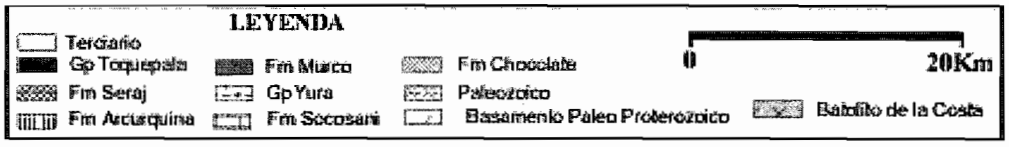

COUNTERCLOCKWISE ROTATION OF THE SOUTH PERUVIAN FOREARC AND IMPLICATIONS FOR THE FORMATION OF THE BOLIVIAN OROCLINE

Pierrick ROPERCH (1), Thierry SEMPÉRÉ (2), Orlando MACEDO (3), César ARRIAGADA (1), and Michel FORNARI (4)

(1) IRD UR 104 and Departamento de Geología, Universidad de Chile, Santiago, Chile (properch@cec.uchile.cl; cearriag@cec.uchile.cl)

(2) IRD UR 104 and Universidad San Marcos, Lima, Peru (sempere@terra.com.pe)

(3) Instituto Geofísico del Perú, Oficina Regional de Arequipa. (omacedo@geo.igp.gob.pe)

(4) IRD, UMR Géosciences Azur, Université Nice-Sophia Antipolis, 06108 Nice, France (fornari@unice.fr)

KEYS WORDS: paleomagnetism, tectonic rotations, orocline, Peru,

INTRODUCTION

Paleomagnetic studies undertaken in the Central Andes demonstrate that tectonic rotations are a key feature of the deformation. Paleomagnetic results obtained in Mesozoic rocks (Roperch and Carlier, 1992; Macedo Sanchez, 1993) and Paleocene rocks (Macedo Sanchez, 1993) demonstrate counterclockwise rotations of Southern Peru larger than 30 degrees supporting the hypothesis of oroclinal bending of the Central Andes. However, the timing of the rotations remains poorly determined. In this study we present new paleomagnetic evidence for a late Paleogene counterclockwise rotation of Southern Peru.

PALEOMAGNETIC SAMPLING

In Southern Peru, the Moquegua Formation, which corresponds to a thick continental sedimentary sequence deposited during the Paleogene, is an especially good paleomagnetic target to further constrain the timing of oroclinal bending. The Lower Moquegua formation corresponds to fine claystones and siltsones deposited unconformably on a well-developed paleosurface postdating the Paleocene Toquepala volcanics. The Upper Moquegua Formation consists of more than 500 m of upward coarsening siltstones and conglomerates with interbedded late Oligocene and Early Miocene tuffs and ignimbrites.

In southern Peru, we sampled 15 sites in claystones and silstones of the Lowwer Moquegua formation and 15 sites in the overlying ignimbrites. In northern Chile to the south of the Arica bend, we sampled the Azapa Formation (equivalent to the Lower Moquegua Fm) and the lower Miocene Oxaya ignimbrites.

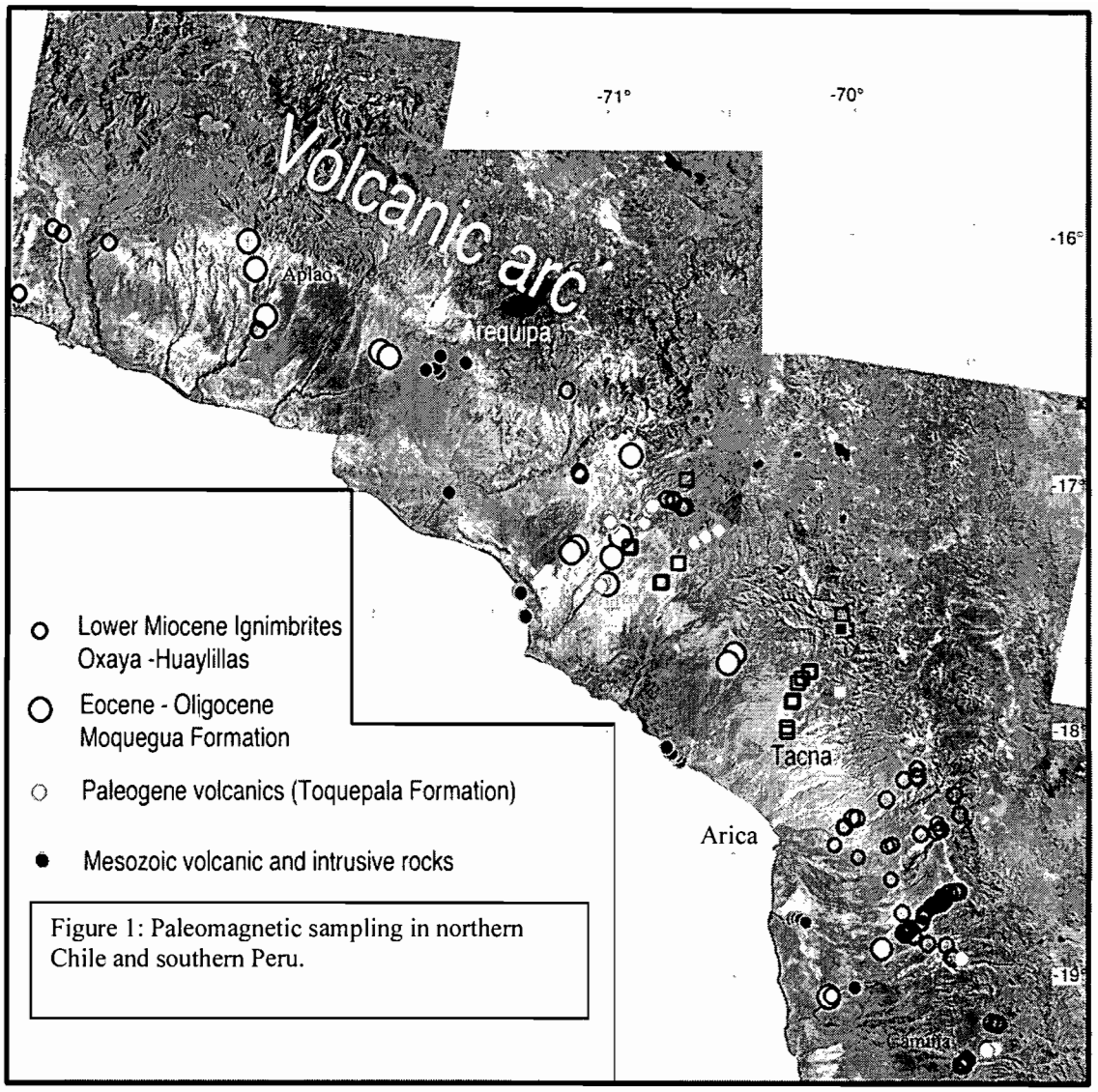

Figure 1: Paleomagnetic sampling in northern Chile and southern Peru.

Ten to twenty cores were drilled at each site. At most sites in the Moquegua Formation, cores were drilled in several claystones and siltstones beds in stratigraphic succession.

PALEOMAGNETIC RESULTS

Moquegua Formation in Southern Peru:

Magnetization is very stable and a characteristic direction was determined in 12 sites out of the 15 sites sampled in the Moquegua formation (figure 2b). Normal and reverse polarity magnetizations are found. At some sites, changes in polarity are observed within the thickest sampled sections.

The average direction calculated for the Aplao and Arequipa area is : (Declination=138.7° Inclination 29.0° $\alpha 95$=17.0° N=4 sites). Near Moquegua, the average paleomagnetic direction is :(Declination=146.0° Inclination 33.3° $\alpha 95$=4.8° N=8 sites).

Paaleogene rocks in northern Chile:

Two sites, drilled in the Azapa Formation underlying the Lower Miocene Oxaya Formation, provide a characteristic magnetization with normal polarity.

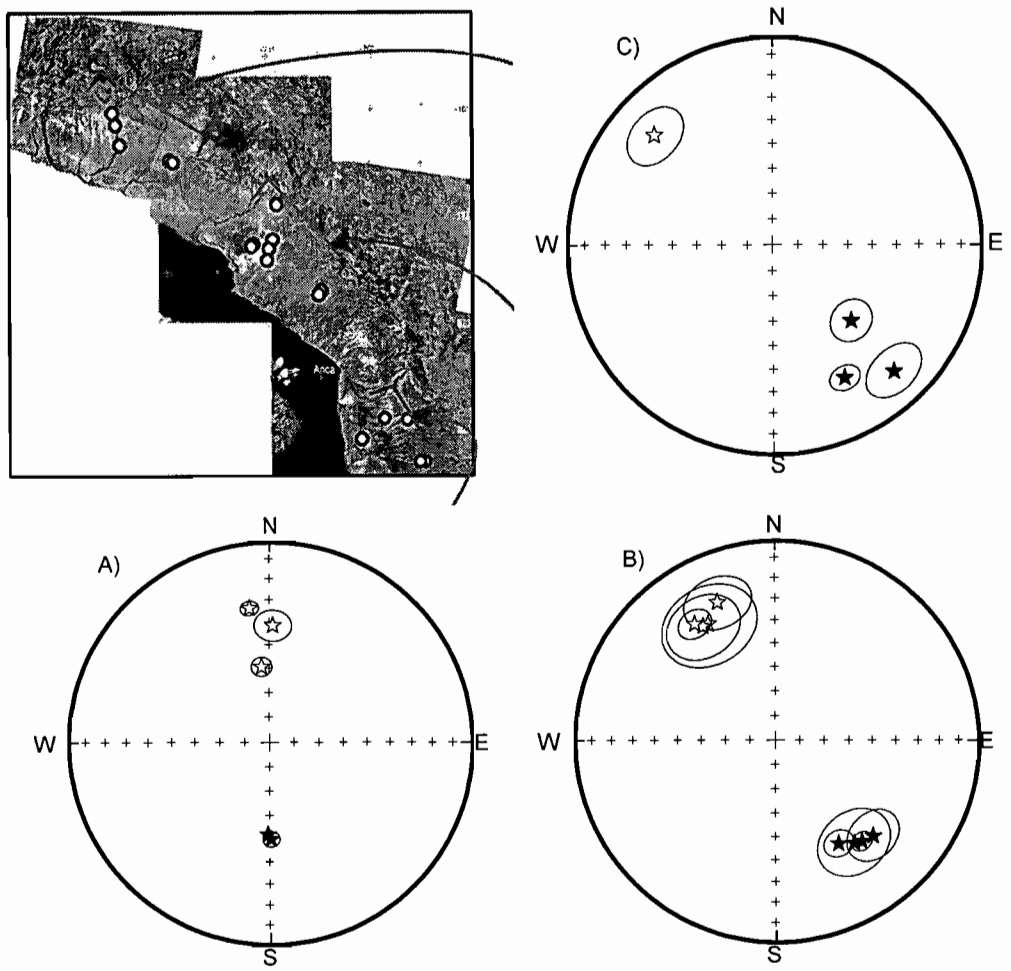

Figure 2: Eocene-Oligocene characteristic magnetizations south (A) and north (B&C) of the Arica bend. Equal area projections of site-mean directions with 95% confidence angle.
Open (filled) stars are characteristic directions of normal (reverse) polarity. Data set (A) corresponds to sites located in Chile, (B) corresponds to the Moquegua region and (C) to the Arequipa and Aplao region.

Near Camiña, a remagnetization of reverse polarity was found in Cretaceous-lower Tertiary sediments underlying the lower Miocene ignimbrites. The remagnetization, not observed in the overlying ignimbrites, is interpreted as a magnetization acquired during the Paleogene. A paleomagnetic result was also obtained in a lower Tertiary intrusive. The average direction calculated from these 5 sites is: (Declination=177.5° Inclination 47.2° α95=17.0° N=4 sites).

Lower Miocene Ignimbrites:

In northern Chile (A) and southern Peru (B) there is no evidence for significant relative rotations. This observation is in good agreement with the apparent continuity in the distribution of flat-lying thick ignimbrites. Near Moquegua (C), several sites were drilled in two large ignimbrites recording intermediate paleomagnetic directions with steep inclinations. These results cannot constrain tectonic rotations. North of Arequipa (D), evidence for significant counterclockwise rotations is also lacking.

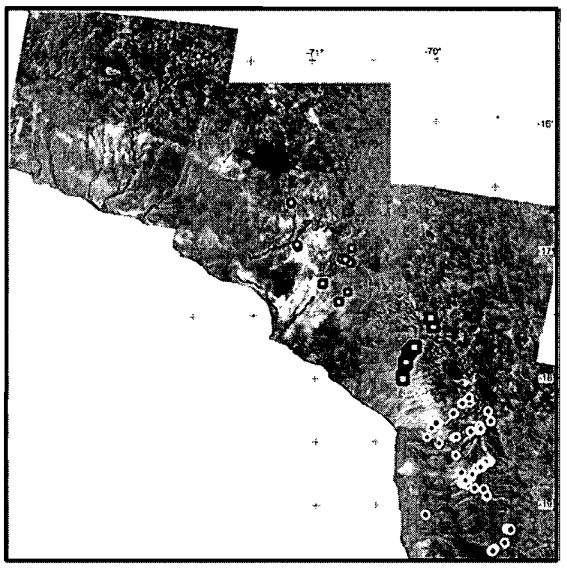

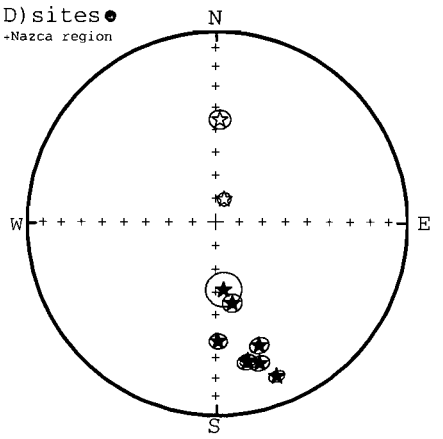

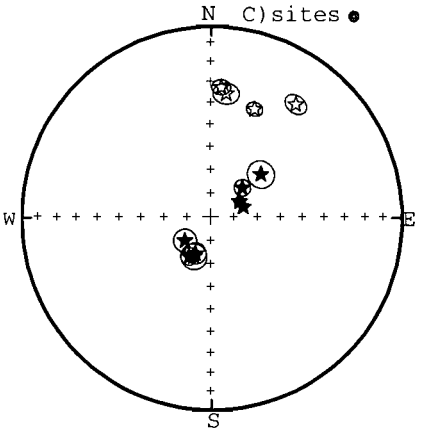

Figure 3: Paleomagnetic sampling in Lower Miocene ignimbrites and equal-are projections of characteristic directions. Angle of confidence at 95% have been omitted for results from northern Chile (A). Results from the Tacna region (squares) are shown in B. Results from the Nazca tuff are shown in D but the sampling sites are located further to the west and not shown on the satellite image.

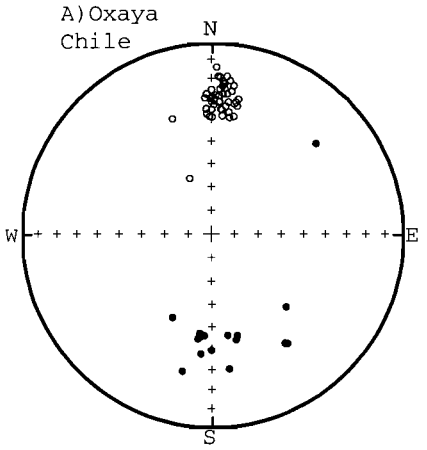

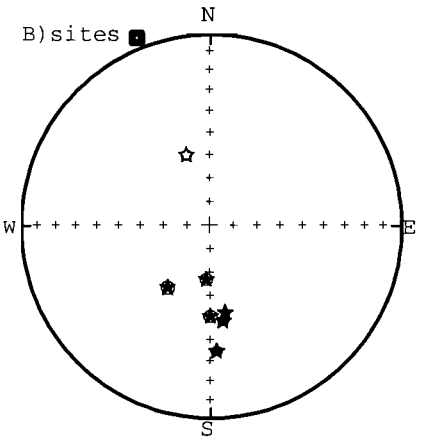

CONCLUSION

The new paleomagnetic results demonstrate that sediments from the lowermost part of the Moquegua Formation record the same large (>30°) counterclockwise tectonic rotation previously observed in Cretaceous and Paleocene rocks in southern Peru. The lack of rotation shown by the paleomagnetic results in lower Miocene ignimbrites support the hypothesis that oroclinal bending in the forearc occurred mostly during Oligocene time. We will discuss the implications of these results for our understanding of the early stages of deformation in the Central Andes.

AUCA MAHUIDA (NEUQUEN BASIN, ARGENTINA): A QUATERNARY SHIELD VOLCANO ON A HYDROCARBON-PRODUCING SUBSTRATE

Eduardo A. ROSSELLO (1), Peter R. COBBOLD (2), Marc DIRAISON (2), Nicolas ARNAUD (3)

(1) CONICET y Departamento de Ciencias Geológicas, Universidad de Buenos Aires, 1428 BUENOS AIRES, Argentina (rossello@gl.fcen.uba.ar)

(2) Géosciences-Rennes (UMR 6118 du CNRS), Université de Rennes I, 35042 RENNES Cedex, France (cobbold@univ-rennes1.fr)

(3) Laboratoire "Magmas et Volcans" (UMR 6524 du CNRS), Université Blaise-Pascal, 6300 CLERMONT-FERRAND, France (arnaud@opgc.univ-bpclermont.fr)

KEY WORDS: Auca Mahuida, volcano, Quaternary, substrate, sediment, hydrocarbons

INTRODUCTION

Auca Mahuida, a Quaternary shield volcano, lies in splendid isolation on the Andean foreland, some 100 km E of the current deformation front (Figs. 1 and 2). At 2253 m, the summit has a well-preserved central crater and an andesitic plug. Flows of basaltic lava, up to 300 m thick, cover the gently sloping flanks. The entire edifice is about 50 km in diameter. More than 100 parasitic vents dot the slopes.

The substrate is mainly sedimentary rock of the Neuquén Basin. This formed as a rift basin near the Pacific margin of South America in the early Mesozoic. Auca Mahuida lies near the NE edge of the basin. The basin centre contains over 5000 m of Triassic to Early Cretaceous marine strata (Urien and Zambrano, 1994; Vergani et al., 1995; Legarreta and Uliana, 1999). From 100 Ma onwards, the Neuquén Basin further developed in a foreland setting. Up to 1300 m of fluvial and alluvial conglomerates of the Neuquén Group filled a Late Cretaceous foreland basin. At about 80 Ma, a temporary incursion of Atlantic waters resulted in shallow-marine carbonates. In the Auca Mahuida area, Tertiary Andean compression caused Early Cretaceous normal faults to reactivate in reverse and strike-slip mode, producing gentle folds in overlying strata (Vergani et al., 1995; Veiga et al., 1999). At the southern edge of the volcano, uplift and erosion have exposed Cretaceous strata, which dip regionally eastward at less than 5°. The basaltic lavas are unconformable upon them.

Currently, the area around the volcano produces oil and gas. The main source rocks are Tithonian black pelites (Vaca Muerta Fm.) and the main reservoir rocks are sandstones (Tordillo Fm.). However, there is also significant production from fractured volcanic sills in or near the source rocks (Orchuela et al., 1989; Zencich and García, 1999). Data for regional sections (Fig. 2) come from more than 330 wells, 18 000 km of 2D seismic profiles and 860 km^2 of 3D surveys (Veiga et al., 1999).

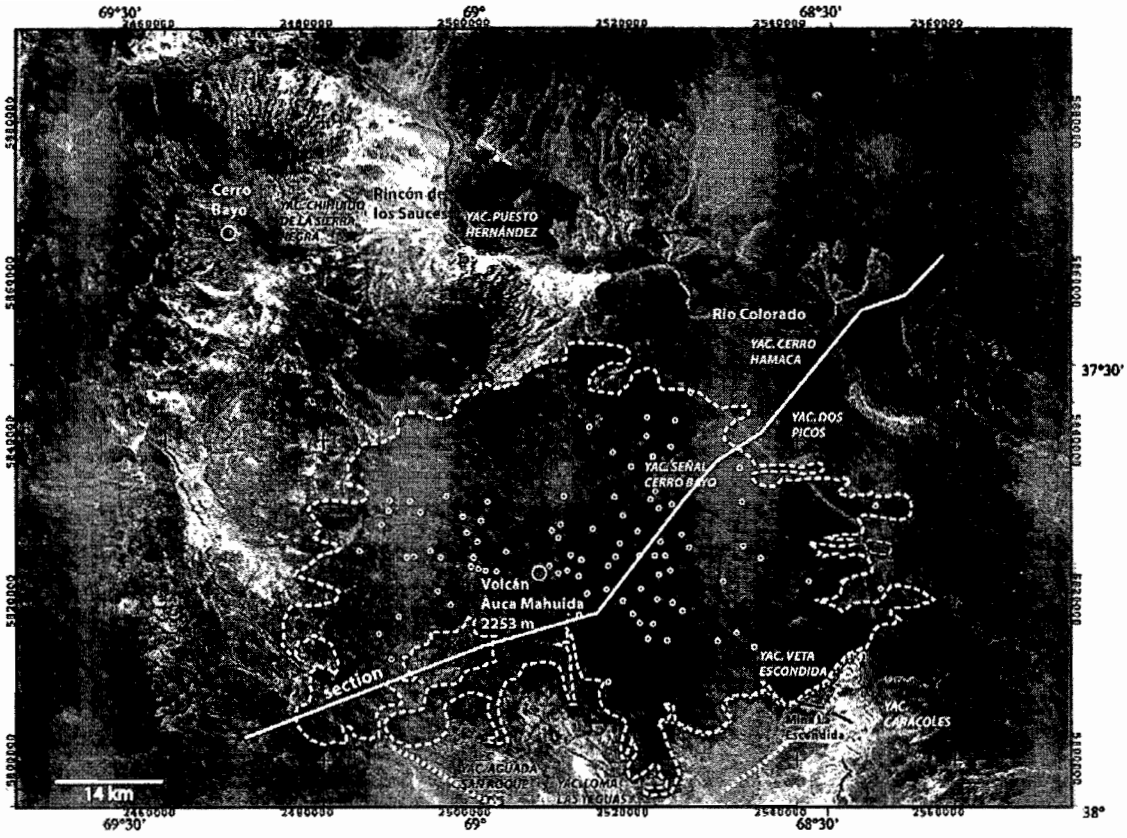

Figure 1. Satellite image of Auca Mahuida volcano. For section, see Fig. 2. Notice summit at 2253 m, edge of basalts (dashed line), traces of breached rim anticlines (dotted lines), vents (open circles), oil fields (YAC.) and outcropping bitumen veins (black lines). Cerro Bayo (to NW) is a more eroded Miocene volcano.

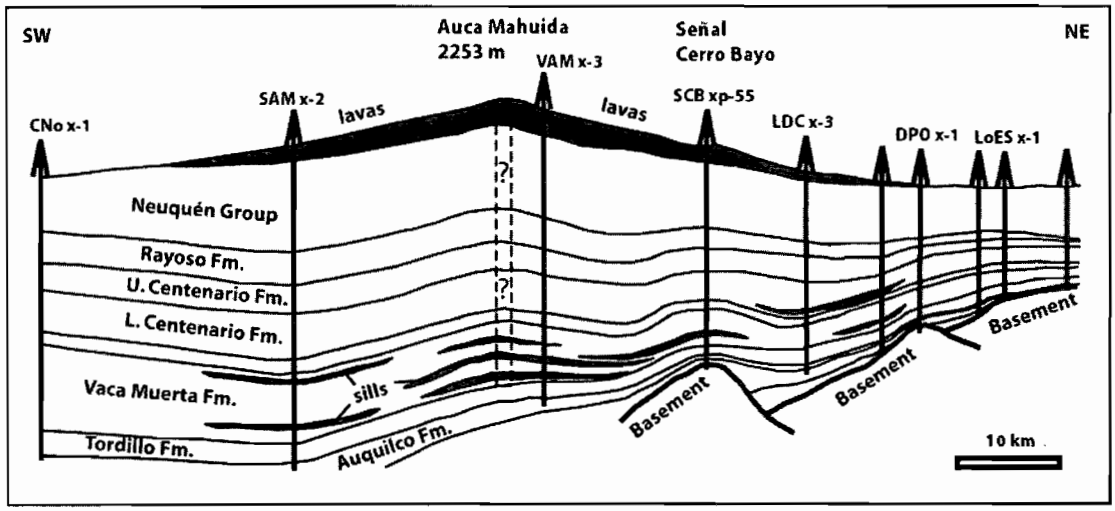

Figure 2. Regional section of Auca Mahuida volcano (modified from Veiga et al., 1999). Vertical scale is about 6 times horizontal scale. Well data have been projected onto section. For location, see Fig. 1.

AGES OF LAVAS

By regional correlation, Holmberg (1964) inferred that all lavas on Auca Mahuida were Quaternary, except for the lowermost basalt, which he assigned to the Pliocene. At 11 surface localities on Auca Mahuida, we took samples for whole-rock Argon-Argon dating at the University of Clermont-Ferrand (Table I). Resulting ages (0.88 to 1.7 Ma) are all Pleistocene, except for one (on the lowermost basalt), which is latest Pliocene.

TABLE 1. Argon-Argon ages (in Ma)

Sample	*Northing*	*Easting*	*Rock type*	*Plateau age*	*Isochron age*	*Preferred age*
ASR1	37° 49' 12"	68° 54' 20"	Basalt	1.4 ± 0.3	1.7 ± 0.1	1.4 ± 0.3
AM1	37° 32' 06"	68° 41' 43"	Basalt	1.18 ± 0.04	1.51 ± 0.06	1.18 ± 0.04
AM3	37° 47' 31"	68° 42' 57"	Basalt	1.61 ± 0.07	2.7 ± 0.1	1.61 ± 0.07
AM4	37° 44' 16"	68° 55' 28"	Andesite	1.8 ± 0.1	1.1 ± 0.2	1.1 ± 0.2
AM5	37° 44' 17"	68° 55' 12"	Andesite	1.19 ± 0.05	-	1.19 ± 0.05
AM6	37° 39' 45"	69° 00' 23"	Basalt	-	-	0.88 ± 0.03
AM7	37° 39' 10"	69° 02' 50"	Basalt	-	-	1.0 or younger
AM8	37° 54' 21"	69° 10' 22"	Basalt	1.97 ± 0.04	1.7 ± 0.2	1.7 ± 0.2
AM9	37° 46' 50"	68° 41' 45"	Basalt	1.78 ± 0.06	0.9 ± 0.07	1.0 or younger
AM10	37° 43' 46"	68° 54' 30"	Andesite	1.16 ± 0.04	-	1.16 ± 0.04
AM11	37° 42' 57"	68° 55' 41"	Andesite	2.03 ± 0.03	1.26 ± 0.07	1.26 ± 0.07

STRUCTURES

Sills. Under Auca Mahuida, numerous wells have intersected sills of basaltic composition, which show up as strong reflectors on seismic data (Orchuela et al., 1989; Zencich and García, 1999). Sills are commonest in or near pelitic source rocks of the Vaca Muerta Fm. (Fig. 2). On the NW flank of Auca Mahuida, a horizontal well follows one sill at depth (Zencich and García, 1999). At Aguada San Roque and Loma Las Yeguas (Fig. 1), sills make good reservoirs (Orchuela et al., 1989). A Pleistocene age for sills is likely, but reliable data are lacking.

Dome. Strata beneath Auca Mahuida volcano form a large dome (Figs. 1 and 2). The amplitude is almost constant down to the Vaca Muerta Fm. and diminishes greatly beneath it. The dome therefore appears to result from emplacement of sills or laccoliths. Near Cerro Bayo (Fig. 1), which is an eroded Miocene volcano, another hydrocarbon-producing dome also contains intrusions at depth (Orchuela et al., 1989).

Rim anticlines. Around the southern rim of Auca Mahuida, erosion has breached two anticlines in strata of the Neuquén Group (Fig. 1). Limb dips are smaller than 5° (Holmberg, 1964). Overlying lavas tilt toward the summit. We infer that these rim anticlines grew in the Pleistocene, impeding southward flow of lava.

Parasitic vents. On Auca Mahuida, parasitic vents form radial alignments (Fig. 1). Most of these trend nearly E-W. Probably they formed parallel to maximum horizontal stress, reflecting the weight of the volcano.

Bitumen dykes. At La Escondida (Fig. 1), dykes of solid hydrocarbon also trend radially (Cobbold et al., 1999). The source rocks are Vaca Muerta pelites. Maturation may have been accelerated by igneous activity.

Thrust faults. At Aguada San Roque, sills ramp up across bedding. Overstepping lenses appear to lie above or along thrust faults, which detach in Vaca Muerta pelites (Orchuela et al., 1989). This association is evidence for interaction between magmatic emplacement and deformation.

CONCLUSIONS

1. Auca Mahuida is a large Quaternary shield volcano, lying well to the east of the Andean deformation front.
2. Andesites surround the well-preserved crater, whereas basaltic lavas cover the gently sloping flanks.
3. According to new Argon-Argon ages, surface lavas are almost all Pleistocene.
4. The substrate consists mainly of Mesozoic sedimentary rocks.
5. The substrate forms a large dome, as a result of multiple igneous intrusions at depth.
6. Basaltic sills have intruded Early Cretaceous pelites, contributing to maturation and providing good reservoirs.
7. Rim anticlines, aligned parasitic vents and bitumen dykes are evidence for radial stresses, due to gravity.
8. At the southern rim of the volcano, sills lie along reverse faults.

ACKNOWLEDGEMENTS

We are grateful to CONICET and to YPF (now part of REPSOL-YPF) for funding our fieldwork and age dating. Ricardo Manoni, Sylvia Zencich and Daniel García, all of YPF, provided invaluable data and assistance.

REFERENCES

Cobbold, P.R., Diraison, M., Rossello, E.A. 1999. Bitumen veins and Eocene transpression, Neuquén Basin, Argentina. Tectonophysics, 314, 423-442.

Holmberg, E. 1964. Descripción geológica de la Hoja 33d, Auca Mahuida (Provincia del Neuquén). Dirección Nacional de Geología y Minería, Buenos Aires, Boletín, 94, 1- 88.

Legarreta, L., Uliana, M.A. 1999. El Jurásico y Cretácico de la Cordillera Principal y la Cuenca Neuquina. 1. Facies Sedimentarias. In: Geología Argentina (edited by Caminos R.), Instituto de Geología y Recursos Minerales, SEGEMAR (Buenos Aires, Argentina), Anales 29, Capítulo 16, 399-416.

Orchuela, I.A., Arteaga, M., Palade, S.E. 1989. Reservorios en rocas ígneas de yacimientos gasíferos en Cuenca Neuquina. Boletín de Informaciones Petroleras, 18, 114-124.

Urien, C.M., Zambrano, J.J. 1994. Petroleum systems in the Neuquén Basin, Argentina. In: The petroleum system - from source to trap (edited by Magoon, L.B., Dow, W.G.), American Association of Petroleum Geologists Memoir, 60, 513-534.

Veiga, R., Lara, M., Bruveris, P. 1999. Distribución de hidrocarburos sobre el margen externo en una cuenca de tras-arco. Ejemplos en la cuenca Neuquina, Argentina. Boletín de Informaciones Petroleras, 60, 142-164.

Vergani, G.D., Tankard, A.J., Belotti, H.J., Welsink, H.J. 1995. Tectonic evolution and paleogeography of the Neuquén basin, Argentina. In: Petroleum basins of South America (edited by Tankard, A.J., Suárez S., R., Welsink, H.J.), American Association of Petroleum Geologists Memoir, 62, 383-402.

Zencich, S., García, D. 1999. Investigación de un cuerpo intrusivo mediante la perforación de un sondeo horizontal. Zona Volcán Auca Mahuida, Cuenca Neuquina, Argentina. Boletín de Informaciones Petroleras, 59, 71-84.

PALEOMAGNETIC EVIDENCE FOR LATE MIOCENE VERTICAL-AXIS ROTATIONS IN THE PERUVIAN CORDILLERA

Sonia ROUSSE (1), Stuart GILDER (1), Daniel FARBER (2), Brendan McNULTY (3), Victor R. TORRES (4), Oscar PALACIOS (4)

(1) Institut de Physique du Globe de Paris, Laboratoire de Paléomagnétisme, 4 Place Jussieu, 75252 Paris cedex 05, FRANCE, rousse@ipgp.jussieu.fr, gilder@ipgp.jussieu.fr

(2) Lawrence Livermore National Laboratory, Livermore, CA 94550, USA, Farber2@llnl.gov

(3) Earth Science Dept., California State University Dominguez Hills, Carson CA 90747, USA, bmcnulty@CSUDH.EDU

(4) Instituto de Geológico Minero y Metalurgico, Lima, 1470 Avenida Canadá, San Borja, Lima 41, PERU, torresbazanvictor@hotmail.com

KEY WORDS : Paleomagnetism, Neogene, Rotation, Tectonics, Peru

INTRODUCTION

The Andes form the longest non-collisional mountain belt on Earth. They are the widest at the Bolivian Orocline, around 19°S, where a change occurs in the strike direction of the major structures that define the chain. Thirty years of Andean paleomagnetic research has demonstrated a fairly coherent pattern of Cretaceous to Pliocene paleomagnetic rotations that generally vary in concert with the changing structural trends. Counterclockwise rotations are found north of the orocline where structures are northwest oriented, while south of the bend, where the regional fabric strikes north-northeast, rotation sense is mainly clockwise. Uncertainty persists surrounding the origin of this pattern and its link with the deformational history of the chain, especially regarding the length scale and timing of the block rotations. Models proposed to explain this pattern range from wholesale oroclinal bending with large-scale (> 1000 km) rotations and/or differential shortening, to smaller block rotation via local partitioning of strike-slip and thrust-related tectonics (see review in Beck, 1998; Randall, 1998). The obliquity of the Nazca plate convergence direction relative to the South-American margin also likely influences the pattern of the paleomagnetic rotations. The Peruvian Cordillera, which is structurally continuous over a long distance and strikes at a relatively high angle with respect to the convergence direction, provides an excellent setting to study the link between mountain building and paleomagnetism, and eventually discriminate between scale dependant tectonic models. For the Peruvian Andes between 9° and 15°S, Rousse et al (2002) demonstrated that Cretaceous to 9 Ma rocks across the Peruvian Cordillera recorded similar and statistically

significant amounts of rotation (on the order of 15°), and that these rotations took place in a rather brief time at ca. 8 Ma.

To verify the coherence of the paleomagnetic rotations and to better understand their timing and extent, we collected more than 800 cores from widely distributed areas in the Cordillera and the Subandean zone. We report results obtained in the Neogene intracordilleran basins of Cajabamba, San Marcos and the Callejon de Huaylas, as well as in Miocene formations of the Tarapoto region.

PALEOMAGNETIC SAMPLING

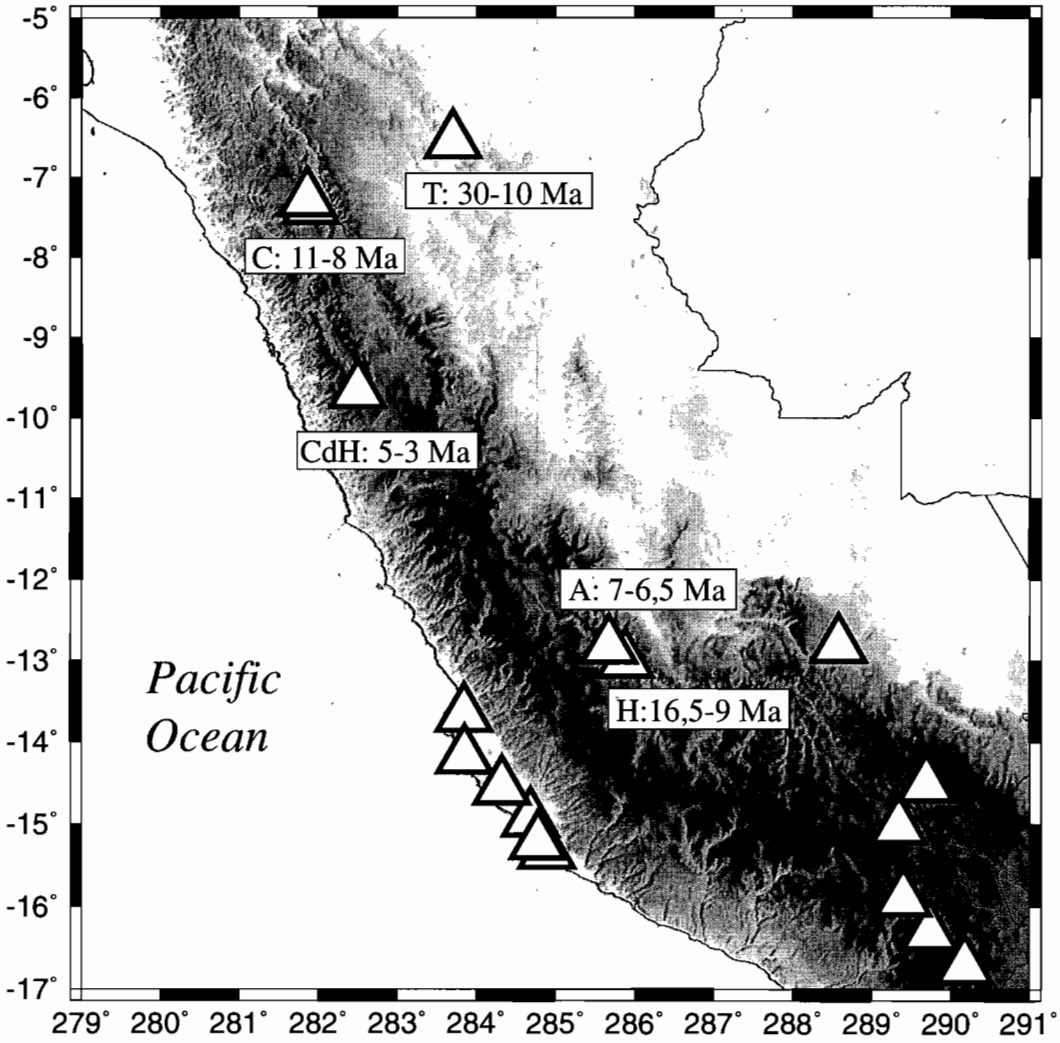

Figure 1: Geographic repartition of the Neogene paleomagnetic sites; A: Ayacucho basin, Ayacucho Formation, C: Cajabamba and San Marcos basins, CdH: Canyon de Huaylas, H: Ayacucho basin, Huanta Formation, T: Tarapoto, Chambira and Ipururo formations. Unlabeled sites were collected in 2001 -results are presently not available.

The subandean zone

In northern Peru, the Subandean zone is a thin-skinned fold and thrust belt which initiated during the Upper Miocene (Audebaud et al., 1973, Nobel and McKee, 1977) and continues today as evinced by high levels of

crustal seismicity (Dorbath et al., 1996). In the Tarapoto region (6.6°S, 283.7°E; Fig. 1) we sampled ten sites of Cenozoic sediments from the Chambira (3 sites) and Ipururo (7 sites) formations. The Chambira Formation is constrained in age by palaeontology as Upper Oligocene to Lower Miocene while a Mio-Pliocene age is inferred for the Ipururo Formation by stratigraphic correlation.

The intracordilleran basins

Several Mio-Pliocene basins crop out in the western Cordillera of North and Central Peru. We collected 245 paleomagnetic samples from three of these basins (Cajabamba, San Marcos and Callejon de Huaylas).

The Cajabamba (8 sites) and San Marcos (8 sites) basins lie within the Cajamarca deflection, a major structural feature of northern Peru, characterized by a progressive reorientation of the strike of the fold axes from the NW-directed Andean trend to a more E-W trend. These basins were filled with 1000 to 1300-m-thick fluvial and fluviolacustrine sediments deposited around 11 to 8 Ma (Fourtanier et al., 1993). An extensive paleomagnetic study of the Cajamarca deflection was carried out by Mitouard et al. (1990, 1992) on Cretaceous to Paleogene rocks, who found evidence for significant counterclockwise rotations, on the order of 22°, except for one isolated region which was not significantly rotated. They concluded that the age of the rotations post-dated the Late Eocene.

The Callejon de Huaylas basin lies west of the Cordillera Blanca batholith, which today forms the highest peaks of the Peruvian Andes. The batholith was emplaced at 8.2±0.2 Ma (concordant U-Pb zircon age; McNulty et al., 1998). The basin's southern part is filled with the 2000 m-thick Lloclla Formation, from which we sampled two sections. Three K-Ar whole rock ages of 5.4±0.1 and 4.65±0.1 Ma were obtained from a tuffaceous horizon at the base of the Lloclla Formation (Bonnot, 1984).

RESULTS AND DISCUSSION

A combined mean direction was calculated for the Chambira and Ipururo formations from the subandean zone. The fold and reversals tests are positive, suggesting a primary origin of the remanence. Relative to the 20 Ma reference pole from Besse and Courtillot (2001), no significant rotation or flattening is recorded. The pole we obtained is also concordant with the Neogene 5 to 24 Ma reference pole from Randall (1998) and lies close to the only Late Miocene pole available for South America (Remedios formation, Brazil, Shultz et al., 1986). The Tarapoto pole can thus be considered as a South American reference pole for the time period ~ 28 to 7 Ma. It probably defines the eastern limit of the Miocene anticlockwise rotations. For the intracordilleran basins, thermal and alternating field demagnetization isolate stable magnetic components which pass fold and reversals tests. Site mean directions show rotations ranging between -21° and +6°. Interestingly, when rotations were found in Cretaceous rocks (Mitouard et al., 1992), the same amount of rotation was registered in nearby Miocene rocks. Moreover, in one case, when Cretaceous rocks recorded no rotation, none was observed either in Miocene rocks. This suggests that, despite several episodes of deformation between the Cretaceous to Present, only the latest one has provoked vertical axis block rotations. These results corroborate with our previous work in the Ayacucho basin (Rousse et al., 2002), and confirm the Neogene origin of the paleomagnetic rotations in the Peruvian Cordillera.

REFERENCES

Audebaud, E. et al., 1973. Les traits Géologiques essentiels des Andes Centrales (Pérou-Bolivie). Revue de Géographie Physique et de Géologie dynamique, 15(1-2): 73-113.

Beck, M.E., 1998. On the mechanism of crustal block rotations in the central Andes. Tectonophysics, 299: 75-92.

Besse, J. and Courtillot, V., 2001. Apparent and True Polar Wander and the Geometry of the Geomagnetic Field in the last 200 Million Years. Journal of Geophysical Research.

Bonnot, D., 1984. Neotectonique et tectonique active de la Cordillère Blanche et du Callejon de Huaylas, Andes Nord-peruviennes. Thèse de doctorat Thesis, Paris XI, Orsay, 115 pp.

Dorbath, C., 1996. Velocity structure of the Andes of central Peru from locally recorded earthquakes. Geophys. Res. Lett., 23(2): 205-208.

Fourtanier, E., Gasse, F., Bellier, O., Bonhomme, M.G. and Robles, I., 1993. Miocene non-marine diatoms from the Western Cordillera basins of northern Peru. Diatom Research, 8(1): 13-30.

McNulty, B.A., Farber, D.L., Wallace, G.S., Lopez, R. and Palacios, O., 1998. Role of plate kinematics and plate-slip-vector partitioning in continental magmatic arcs: Evidence from the Cordillera Blanca, Peru. Geology, 26(9): 827-830.

Mitouard, P., Kissel, C. and Laj, C., 1990. Post-Oligocene rotations in southern Ecuador and northern Peru and the formation of the Huacabamba deflection in the Andean Cordillera. Earth and Planetary Science Letters, 98: 329-339.

Mitouard, P., Laj, C., Mourier, T. and Kissel, C., 1992. Paleomagnetic study of an arcuate fold belt developed on a marginal orogen: The Cajamarca deflection, northern Peru. Earth and Planetary Science Letters, 112: 41-52.

Noble, D.C. and McKee, E.H., 1977. Comment on Spatial distribution of earthquakes and subduction of the Nazca plate beneath South America. Geology, 5: 576-578.

Randall, D.E., 1998. A new Jurassic-Recent apparent polar wanderpath for South America and a review of central Andean tectonic models. Tectonophysics, 299: 49-74.

Rousse, S., Gilder, S., Farber, D., McNulty, B. and Torres, V.R., 2002. Paleomagnetic evidence for rapid vertical-axis rotation in the Peruvian Cordillera ca. 8 Ma. Geology (Boulder), 30(1): 75-78.

Schultz, A., Rathert, M.C., Guerreiro, S.D.C. and Bloch, W., 1986. Paleomagnetism and rock magnetism of Fernando de Noronha, Brazil. Earth and Planetary Science Letters, 79: 208-216.

REGIONAL ASPECTS OF THE SOUTHERN END OF THE CENTRAL VOLCANIC ZONE (BETWEEN 27° - 28° S), ARGENTINA

Daniel RUBIOLO (1), Eduardo ZAPPETTINI (1), Antonio LIZUAIN (1), Catherine HICKSON (2)

(1) Instituto de Geología y Recursos Minerales – IGRM, Servicio Geológico Minero Argentino – SEGEMAR, Avda. J. A. Roca 651, pisos 8 y 10, C1067ABB, Buenos Aires - Argentina (drubio@secind.mecon.gov.ar ; ezappe@secind.mecon.gov.ar ; alizua@secind.mecon.gov.ar)
(2) Geological Survey of Canada, Pacific Division, 101-605 Robson Street, Vancouver, BC, V6B 5J3, Canada (chickson@nrcan.gc.ca)

KEY WORDS: Argentina, Gondwana, Famatina, Mineralization, Precordillera, Volcanism

INTRODUCTION

The Andes mountain range between 27° and 28° S includes the northern end of the flatslab zone and the southern end of the Central Volcanic Zone (CVZ). In a region from the Chaco-Pampean plain in Argentina to the Chilean border four morphostructural units converge: Sierras Pampeanas, Famatina, Precordillera and Cordillera Frontal (Figure 1). This is also a zone of transition between the Altiplano-Puna Plateau to the north and the Sierras Pampeanas to the south, where the subduction angle of the Nazca plate changes from 30° E, (under the Puna), to sub-horizontal south of 27° S (Cahill & Isacks 1992). Cenozoic andesitic volcanism also disappears in this direction.

This part of the Argentinean Andes is increasingly important in terms of economic mineralization associated with Cenozoic volcanism. Exploration targets similar to the Maricunga Belt are localized on the western border of the area (Mpodozis et al. 1995). Farther east, in the Sierras Pampeanas, important Cu-Au porphyries and epithermal deposits are also found (Sasso & Clark 1998, Zappettini et al. 2000).

New regional studies by the Geological Survey of Argentina (SEGEMAR) done in part under the Multinational Andean Project, from Sierras Pampeanas to the Chilean border between 27° and 28° S, are summarised here and provide additional information for the study of Andean geodynamics.

CONCLUSIONS

Famatina : The northern end of Famatina morphostructural unit occupies an area between Bolsón de Fiambalá and the Chaschuil valley. A famatinian granitic stock (Las Angosturas granite) shows a U-Pb intrusion age of 485 ± 7 Ma (Rubiolo et al. 2002). This isotopic date confirms a Tremadoc-Arenig age for the intrusion, which is in accordance with other famatinian granites presented by Pankhurst et al. (2000). Nevertheless, zircon fractions of Las Angosturas granite shows inheritances of 1,2 Ga keeping the discussion open regarding age of the basement and the magmatism's geotectonic position within the Famatina unit (Toselli et al. 1996; Quenardelle & Ramos 1999; Rapela 2000).

Precordillera : A region between the Chaschuil valley on the east and the Bolsón de Laguna Verde and Río La Punilla on the west, displays lithologic and structural features showing strong analogies with the Riojana area of the Precordillera. In this region, outcrops of a pre-Ordovician metamorphic basement of uncertain age are found. Slates, meta-volcanic, and gray and black limestones affected by a regional low-grade metamorphic event suggest a probable Ordovician age based on their strong lithological similarity to the precordilleran Grupo Río Bonete as defined in La Rioja (Aceñolaza 1970). Thus, we propose to extend the Precordillera northward from its conventionally defined limits (Ramos 1999).

Cordillera Frontal : This unit is partly covered by an important Cenozoic volcanic event, morphologically similar to volcanism of the same age and type in the Puna region. This morphostructural unit is characterized by a Neopaleozoic magmatic event, represented by granodioritic porphyries, felsic volcanic rocks and pyroclastic deposits, associate with skarn containing Cu mineralization. Fluvial and aeolian sediments indicate the presence of a Mesozoic extensional rift basin within which alkalic basalts are interbedded. This rifting has taken place in both the Precordillera and Cordillera Frontal morphostructural units.

Cenozoic volcanism was controlled by changing geometries of the subduction zone (Kay et al. 1999). This new regional geological work has added petrologic and geochronologic data, permitting the reconstruction of the volcanic history of the region. The Cenozoic magmatic history began with the development of a Paleogene magmatic arc in Chile (Mpodozis et al. 1997). During the Oligocene-Lower Miocene a volcanic arc formed the Maricunga Belt (Mpodozis et al. 1995). In the Upper Miocene the volcanic arc rapidly broadened to the east (Mpodozis et al. 1996). The volcanism in this period is characteristic of a thickened crust and was accompanied by the emplacement of copper porphyries and epithermal precious metal deposits. Evidence of subglacial volcanism in the Cordillera Frontal during Upper Miocene time implies important tectonic implications surrounding the uplift of Sierras Pampeanas on the east (Rubiolo et al. 2000). During Pliocene time, the volcanic arc contracted and is now active only in the region bordering with Chile. During the Quaternary, explosive volcanic activity has occurred and at the present time volcanism is represented by fumarolic activity on Nevado's Ojos del Salado volcano.

Figure 1: Regional overview of andean geology between 27° y 28° S (Argentina).

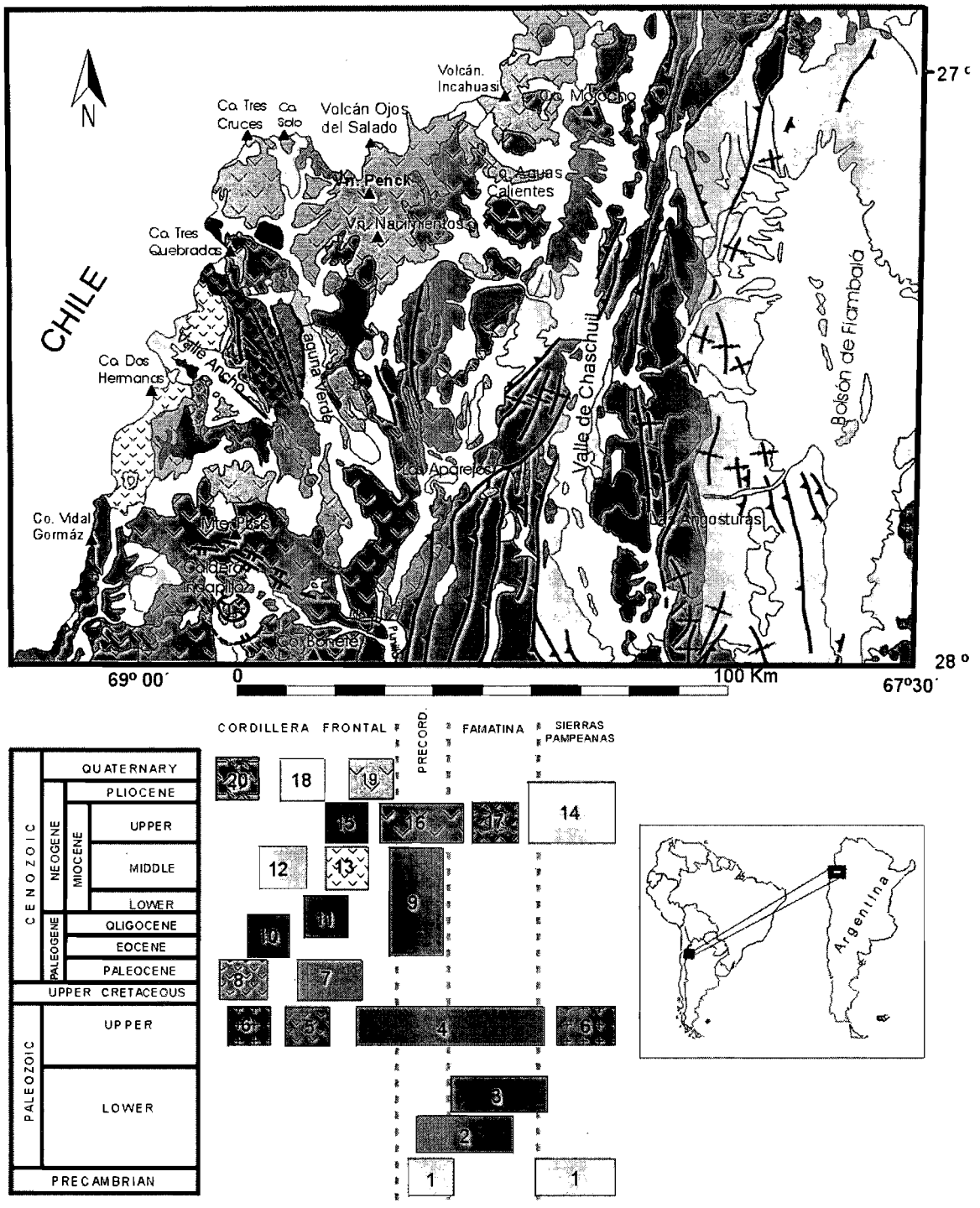

1- Igneous and metamorphic basement; 2- Marine sedimentary rocks with interbedded volcanic sequences; 3 -Famatinian Granites; 4- Marine & continental sequences; 5 - Volcanic & volcano-sedimentary rocks; 6 - Granites; 7- Continental sedimentary rocks; 8 - Volcanic & volcano-sedimentary rocks; 9 - Paleogene-Neogene continental sedimentary rocks; 10 - Volcanic rocks; 11 - Volcanic rocks associated with the epithermal mineralized Maricunga Belt (28-17 Ma); 12 - Felsic volcanic and pyroclastic rocks (17-11 Ma); 13 - Intermediate volcanic rocks (17-11 Ma); 14- Neogene continental sedimentary rocks; 15 - Felsic & intermediate volcanic rocks (11-5 Ma); 16 - Intermediate volcanic rocks (11-5 Ma);17 - Domes & dome complexes associated with hidrothermal alterations (11-5Ma); 18 -Felsic Volcanic & piroclastic rocks (< 5 Ma); 19 - Intermediate volcanic rocks (< 5 Ma); 20 - Domes & dome complexes (< 5Ma).

REFERENCES

Aceñolaza F.G. 1970. Fósiles ordovícicos del área del Río Bonete, departamento de Jagüé, provincia de La Rioja. Acta Geologica Lilloana, 10, 315-328.

Cahill T. & Isacks B. 1992. Seismicity and shape of the subducted Nazca Plate. Journal of Geophysical Research, B, Solid Earth and Planets, 97, 17503-17529.

Kay S.M., Mpodozis C.; Coira B. 1999. Magmatism, tectonism and mineral deposits of the Central Andes (22° - 33° S latitude): In Geology and ore deposits of the Central Andes. (Skinner, B.J.; editor). Soc. Economic Geol. Special Publication, 7, 27-59.

Mpodozis C., Cornejo P., Kay,S. & Tittler A. 1995. La Franja de Maricunga: Síntesis de la evolución del frente volcánico Oligoceno-Mioceno en la zona sur de los Andes Centrales: Revista Geológica de Chile, 22, 273-313.

Mpodozis.C., Kay S. M., Gardeweg M. & Coira B. 1996. Geología de la región Ojos del Salado (Andes centrales, 27° S). Implicancias de la migración hacia el este del frente volcánico Cenozoico superior: In 13° Congreso Geológico Argentino, Actas, 3, 539-548, Buenos Aires.

Mpodozis C., Kay S., Gardeweg M. & Coira B. 1997. Geología de la región de Valle Ancho-Laguna Verde (Catamarca, Argentina). Una ventana al basamento del extremo sur de la zona volcánica de los Andes Centrales: In *8°* Congreso Geológico Chileno, Actas, 3, 1689-1693, Antofagasta.

Pankhurst R.J., Rapela C.W. & Fanning C.M. 2000. Age and origin of coeval TTG, I- and S-type granites in the Famatinian belt of NW Argentina. Transactions of the Royal Society of Edinburgh: Earth Sciences, 91, 151-168.

Quenardelle S. M. & Ramos V.A. 1999. Ordovician western Sierras Pampeanas magmatic belt: Record of Precordillera accretion in Argentina. Geological Society of America, Special Paper, 336, 63-86.

Ramos V. 1999. Las Provincias Geológicas del Territorio Argentino. Geología Argentina, Instituto de Geología y Recursos Minerales, Anales 29, 41-96; Buenos Aires.

Rapela C. W. 2000. El ambiente geotectónico del Ordovícico de la región del Famatina. Revista de la Asociación Geológica Argentina, 55, 134-135.

Rubiolo D., Hickson C., Busteros A., Villeneuve M. & Edwards B. 2000. Petrología del cerro Morocho: Volcán del Mioceno superior en ambiente glacial? (valle de Chaschuil, Catamarca, Argentina). Actas del 9° Congreso Geológico Chileno, 2, 329-333; Puerto Varas.

Rubiolo D., Cisterna C., Villeneuve M. & Hickson C. 2002. Edad U/Pb del granito de Las Angosturas en la sierra de Narváez (Sistema de Famatina, Provincia de Catamarca). Actas del 15° Congreso Geológico Argentino; Buenos Aires (in press).

Sasso, A.M. & Clark, A.H., 1998. The Farallón Negro Group, Northwest Argentina: Magmatic, Hydrothermal and Tectonic Evolution and Implications for Cu-Au Metallogeny in the Andean Back-arc. Society of Economic Geologists Newsletter, 34, 7-18.

Toselli A.J., Durand F., Rossi de Toselli J. & Saavedra J. 1996. Esquema de evolución geotectónica y magmática eopaleozoica del Sistema de Famatina y sectores de Sierras Pampeanas. 13° Congreso Geológico Argentino y 3° Congreso de Exploración de Hidrocarburos, 5, 443-462, Buenos Aires.

Zappettini E., Miranda-Angles, V., Rodríguez C., Palacios O., Cocking R., Godeas M., Uribe-Zeballos H., Vivallo W., Paz M.M., Seggiaro R., Heuschmidt B., Gardeweg M., Boulangger E., Korzeniewski L., Mpodozis C., Carpio M. & Rubiolo D. 2001. Mapa Metalogénico de la Región Fronteriza entre Argentina, Bolivia, Chile y Peru (14° - 28°S). Servicio Nacional de Geología y Minerría, Pulicación Geológica Multinacional, 2, 1 mapa escala 1:1.000.000, Santiago de Chile

COSEISMIC AND ASEISMIC SLIP OBSERVED
from continuous gps measurements
FOR THE 2001 SOUTHERN PERU EARTHQUAKE (Mw = 8.4)

J.C. RUEGG [1], M. OLCAY [2] and D. LAZO [2]

1 CNRS, UMR 7580 & 7578, Institut de Physique du Globe, Paris, France.
ruegg@ipgp.jussieu.fr
2 Universidad Arturo Prat, Iquique, Chile.

KEY WORDS: co-seismic slip, aseismic slip, slow earthquake, gps

INTRODUCTION

On June 23, 2001 at 20:33, UTC, a major earthquake occurred near the coast of southern Peru, about 190 km west of Arequipa (16.15°S, 73.40°W) .A magnitude of 8.4 was computed for this earthquake by the USGS (NEIC). The earthquake occurred along the west coast of Peru (Figure 1) at the boundary between the Nazca and South American plates and resulted from thrust faulting along this boundary as the Nazca plate subducts beneath the South American plate. The two plates are converging towards each other at a rate of 78mm/yr (DeMets et al., 1990). This earthquake took place at a zone of the plate boundary where no major rupture occurred since the 1868 earthquake of magnitude approximately 8.5 – 9 (Dorbath et al., 1990, Comte and Pardo, 1991). The June 23 shock filled partially the South Peru seismic gap (Nishenko, 1985).

DATA

GPS data of the IGS station of AREQ (Arequipa, Peru) are used to determine the quasi-static displacement associated with the Mw = 8.4 Southern Peru earthquake on June 23, 2001. Daily processing of the AREQ data together with those from other IGS stations in South America and one close station in Chile (UAPF, Iquique) gives the position of the AREQ station with respect to other GPS permanent stations in the far field. It results a time history of the source relaxation seen from AREQ station (figure2).

INTERPRETATION

At the time of the main shock (day 174/2001) a co-seismic displacement is evidenced of about 50 cm WSW in the opposite direction to the known interseismic velocity. The observed co-seismic AREQ vector is consistent with the modelled displacement (0.52 m) associated with a reverse fault on the subduction interface (dimension 240x110 km2, 4.50 m slip, rake 76°, Mw = 8.35) fitting approximately the aftershock zone. The computed magnitude and mechanism are consistent with those given by the USGS (NEIC).

The time serie of the observed displacement (Figure 2) shows that the main shock is followed by a significant post seismic signal occuring in the same direction as the co-seismic movement: (1) a first period lasting two week shows a rate of about 4 mm/day (about 8 cm of after-slip); during this period the strong aftershock (Mw=

7.6) of July 7, is seen as a step of about 2-3 cm on the time series, (2) a lower rate period is following (0.3 mm/day) during at least 9 month after the main shock and seems to continue for the beginning of the year 2002. Altogether the post-seismic signal reaches 12-15 cm, that is 30 % of the co-seismic size. This afterslip signal is consitent with a progressive relaxation of accumulated strains (slow earthquake) in the deeper part of the subduction plane.

A slight preseismic displacement (20-30 mm) is detectable during the 6 months before the main shock. It is particularly evidenced as a change in the slope of the time series during the 30 days preceeding the June 23, 2001 event (rate of about 0.7 mm/day). This pre-seismic signal seems also consistent with slow strain events in the deeper part of the rupture zone.

CONCLUSIONS

The daily analysis of GPS data from Arequipa (Peru) and other continuous GPS stations in South America, during the year 2000-2001 reveals four stages of the seismic cycle associated with the subduction of the Nazca plate beneath the South American continent. During the year before the earthquake the end of the interseismic loading is seen as the almost stability of the baseline UAPF-AREQ. A weak pre-seismic signal is emerging from the background noise during the month preceeding the mainshock and is evidenced by a change in the slope of the time series. The mainshock is characterized by an abrupt change of the baseline (day 174) corresponding with the rupture of the locked zone. A significant afterslip movement is seen for the month following the co-seismic rupture. It is continuing at the end of our investigation (March 2002), reaching 30% of the co-seismic displacement.

The June 23, 2001 South Peru earthquake (Mw=8.4) is very similar in size and in seismotectonic context to the 1995 Mw=8.1 Antofagasta earthquake (Ruegg et al., 1996). Each one occurred at the northern and southern extremity of the 1877 Northern Chile seismic gap which has now a strong probability to undergo a similar event.

REFERENCES

Bevis, M., E.C. Kendrick, , R. Smalley, T. Herring, J. Godoy and F. Galban, Crustal motion North and South of the Arica deflection : comparing recent geodetic results from Central Andes, *Geochem., Geophys., Geosyst.*, **1**, 1999.

Comte, D. and M. Pardo, Reappraisal of great historical earthquakes in the Northern Chile and southern Peru seismic gaps, *Natural Hazards,* **4**, 23-44, 1991.

DeMets, C., R.G. Gordon, D.F. Argus and S. Stein, Current plate motions, *Geophys. J. Int.*, **101**, 425-478, 1990.

Dorbath L., A. Cisternas and C. Dorbath, Quantitative assessment of great earthquakes in Peru, *Bull. Seism. Assoc. Amer.*, **80**, 551-576, 1990.

Nishenko, S.P., Seismic potential for large and great intraplate earthquakes along the Chilean and southern Peruvian margins of South America: A quantitative reappraisal, *J. Geophys. Res.*, **90**, 3589-3615, 1985.

Okada Y, Surface deformation to shear and tensile faults in a half space, *Bull. Seism. Assoc. Amer.*, **75**, 1135-1154, 1985.

Ruegg J.C., J. Campos, R. Armijo, S. Barrientos, P. Briole, R. Thiele, M. Arancibia, J. Canuta, T. Duquesnoy, M. Chang, D. Lazo, H. Lyon-Caen, L. Ortlieb, J.C. Rossignol and L. Serrurier, The Mw=8.1 Antofagasta earthquake of July 30, 1995 : First results from teleseismic and geodetic data, *Geophys. Res. Lett.*, **23**, 9, 917-920, 1996.

J.C. Ruegg , M. Olcay and D. Lazo , Co, post and pre(?) -seismic displacements associated with the Mw = 8.4 Southern Peru earthquake of June 23, 2001 from continuous GPS measurements, Seismological Research Letters, vol.72, number 6, pp. 680-685, Nov.-Dec. 2001.

Figure Caption:

Figure 1 – Map of the Southern Peru aera, showing the main shock Mw=8.4 earthquake (red star inside a white circle), the focal mechanism, the main aftershock Mw = 7.6, and the aftershocks (red dots) as determined by the USGS. The observed co-seismic displacement vectors associated with the main shock is shown by an heavy blue arrow and the modelled vector by a thin pink arrow. The total displacement vector (co-seismic + post-seismic) reached after 9 months following the mainshock is shown in green (65 cm). The interseismic velocity vectors for AREQ and other regional GPS sites are shown by thin colored arrows [yellow from Norabuena et al. (1998), green from Bevis et al.(1999), blue from Angerman et al. (1999), and red from Ruegg et al. (preprint, 2001)]. The Nuvel 1A plate convergence vector is show in brown. The modeled rupture zone contour is shown in yellow.

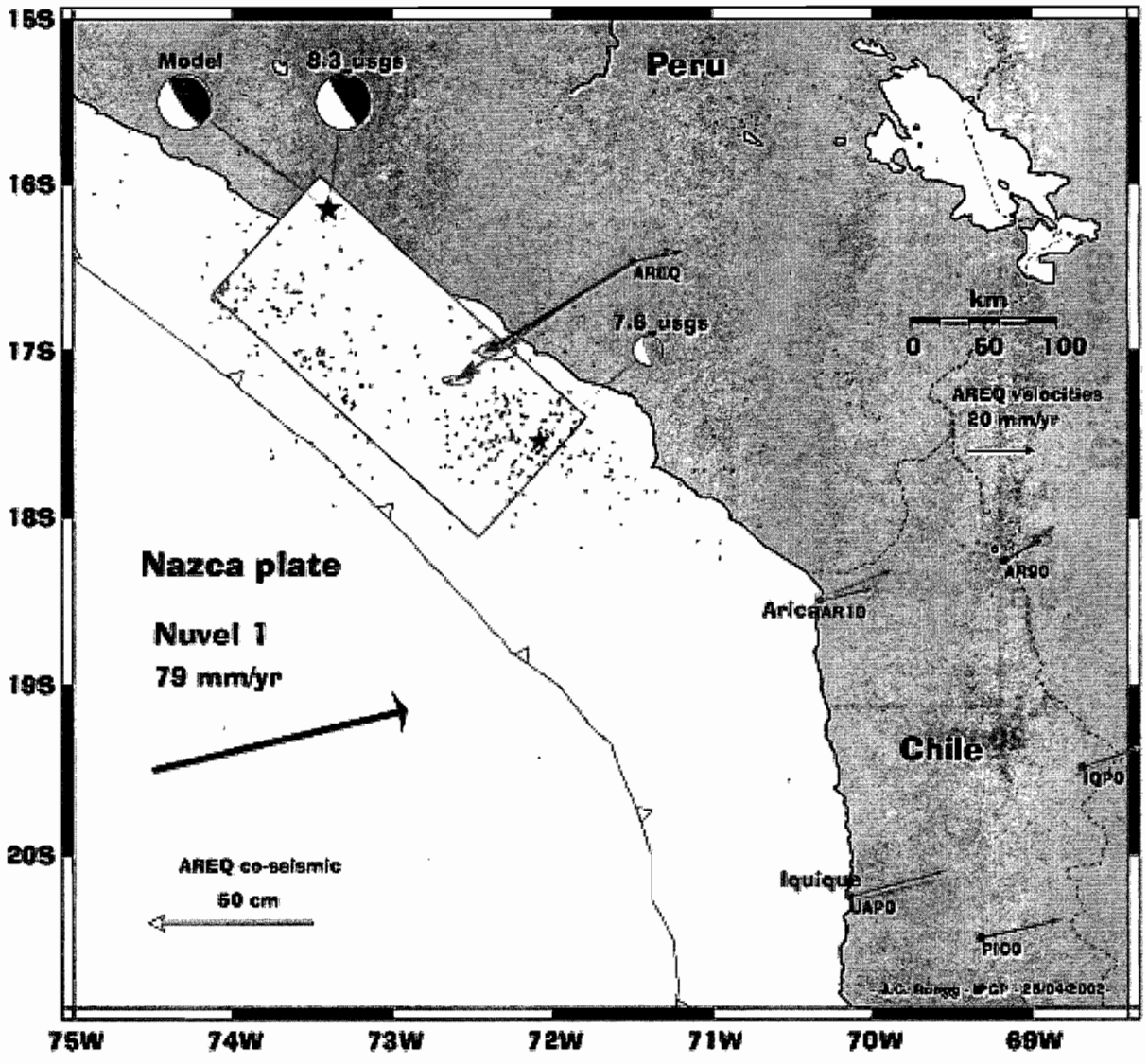

Fig_1

Figure 2 – Variations of the displacement vector of the GPS station AREQ (Arequipa) deduced from the baseline AREQ_UAPF between January 2000 and April 2002. The main shock (Mw=8.4) occured on day 174/2001. During the 6 months preceeding the main shock a signal of about 2-3 cm is seen on the time serie. During the two week following the main shock an after-slip with a mean rate of about 4 mm/days is partly associated with the strongest aftershocks. This afterslip is continuing a a lower rate (0.3 mm/day) during the 9 following months

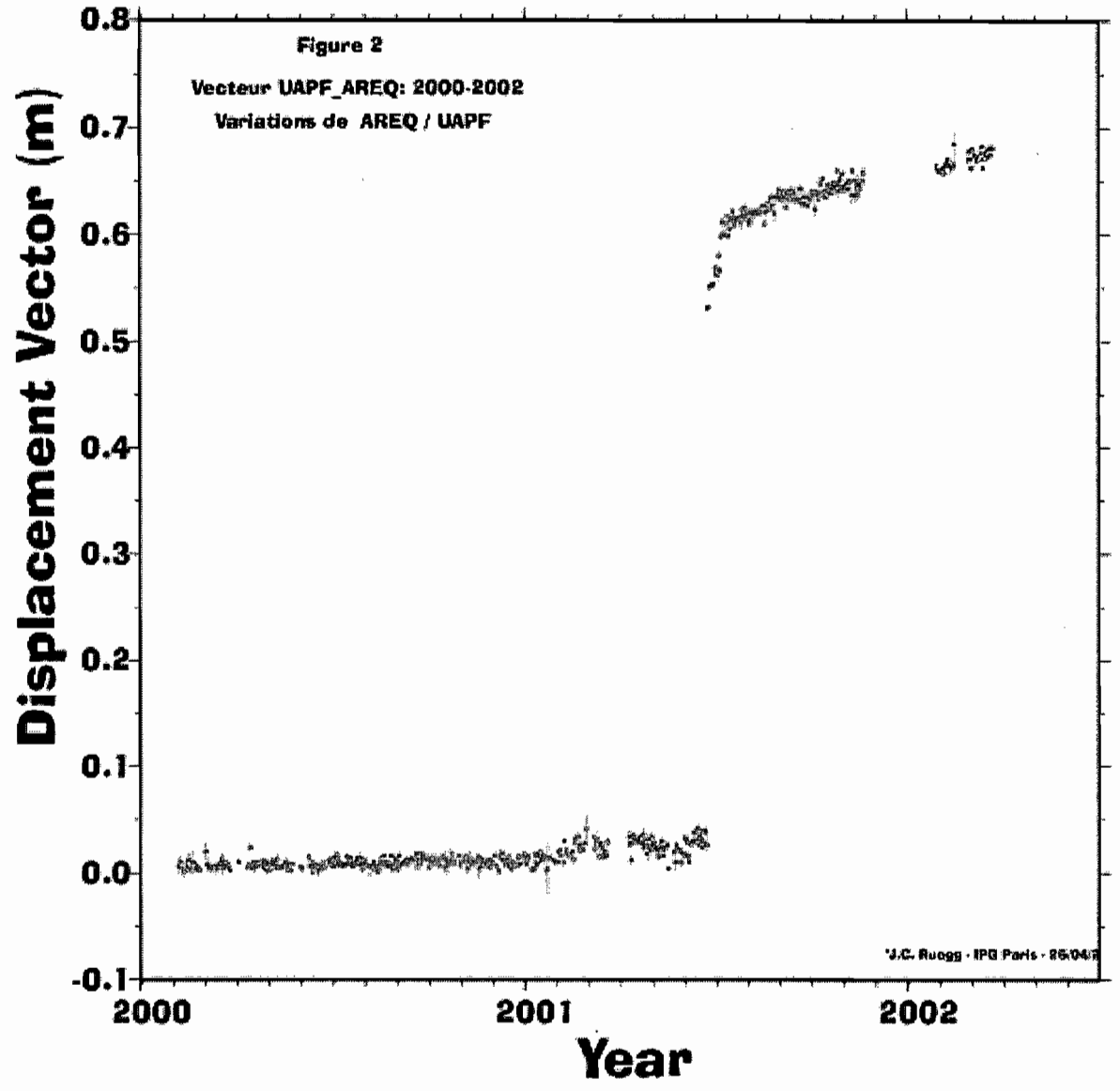

DETRITAL PROVENANCE AND EXHUMATION IN THE ECUADORIAN SUB-ANDEAN ZONE: A KEY REGION LEADING TO THE UNDERSTANDING OF ANDEAN GEODYNAMICS

Geoffrey RUIZ (1), Diane SEWARD (1), Wilfried WINKLER (1) and Richard SPIKINGS (2)

(1) Geological Institute, ETH-Zentrum, CH-8092 Zürich, Switzerland (ruiz@erdw.ethz.ch)
(2) Section des Sciences de la Terre, Université de Genève, Rue des Maraîchers 13, CH-1211 Genève 4, Switzerland (spikings@terre.unige.ch).

KEY WORDS: detrital fission-track ages, heavy minerals, exhumation, Andean Amazon Basin

INTRODUCTION

Tectonic activity at or near plate margins results in orogenic uplift and exhumation of rocks in the Earth's crust by erosion or faulting. Exhumation of a rock is accompanied by cooling and hence the genetic relationship between tectonic and geomorphic processes can be accurately investigated using low-temperature thermochronometers, due to their sensitivity to the movement of rocks through the uppermost, cooler crust. The temperatures of partial to full track annealing in apatite (60-120°C) and zircon (230-310°C) fission-track thermochronometers are particularly useful for this purpose. Since Naeser (1979), several workers have attempted to utilise changes in detrital fission-track grain ages through time to reconstruct the geodynamic development of the source region. This was a major innovative development because, in general, source regions tend to be continually overprinted in active margins and the only thermal record of relic exhumation of the source is in the site of deposition of the eroded material.

The timing and rate of the exhumation within source regions of the Ecuadorian Andean Amazon Basin (AAB; Fig. 1) during Cretaceous and Cenozoic times has been constrained on a regional scale through a thermochronology study of the Ecuadorian Andes (Spikings et al., 2000); whereas, the AAB is assumed to have originated during the Maastrichtian, when the main detrital supply from the Cordillera Real to the west became evident (Fig. 1). Fission-track methodology was thus applied to both (1) rocks constituting the substrate of the AAB in the northern Ecuadorian Sub-Andean Zone region (SAZ; Fig. 1), and (2) Aptian to Recent basin fill series of the AAB, to constrain and refine the geodynamic development of the Andean orogenic system.

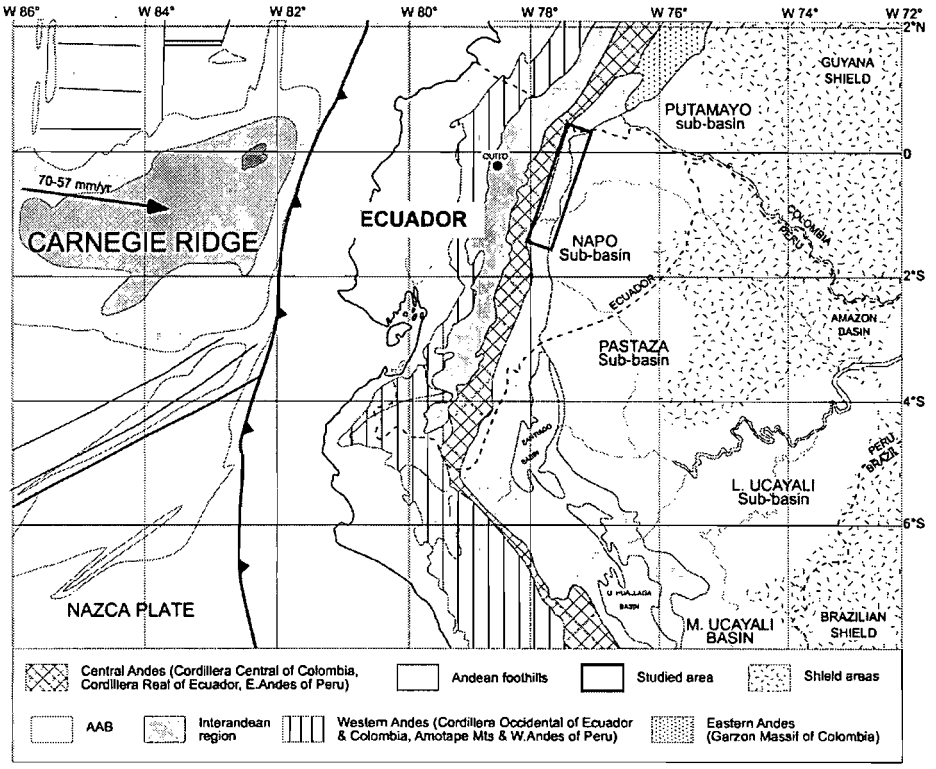

Figure 1: Simplified tectonic map of Ecuador.

RESULTS

-*Basement*: Approximately 40 fission-track ages have been determined from the Jurassic basement of the Andean Amazon Basin in the northern Ecuadorian Sub-Andean Zone (Fig. 1). Temperature-time envelopes reveal that several phases of cooling have occurred since the Middle Eocene (~ 50-35 Ma, 25-20 Ma, 12-0 Ma) and burial did not exceed ~ 4 kilometers (assuming a 30°C/km geothermal gradient).

-*Sediments*: Up to 30 siliciclastic sediments from the entire stratigraphic column across the Ecuadorian Andean Amazon Basin were separated and analysed. Reset apatite and zircon fission-track ages are restricted to a narrow depression within the Cordillera Real, whereas only one apatite fission-track (AFT) age from basin fill series east of the Andes exhibits an AFT age conspicuously younger than its assumed stratigraphic age. Therefore, it is reasonable to assume that the zircon fission-track ages of the sediments from the AAB preserve their detrital character. Seventy detrital zircon fission-track (DZFT) age populations from the Aptian-Albian to Recent basin fill series were extracted from 950 individual grain ages using statistical techniques (Brandon, 1992) and labelled as P_1, P_2... to P_n with increasing ages (Fig. 2). The DZFT age populations show a significant variation from 579 ± 65 Ma to 22.9 ± 1.2 Ma (1σ), and lagtimes vary from 450 to 0 My. The distribution in the cooling ages of detrital grains reflects the varied thermal histories of the source regions.

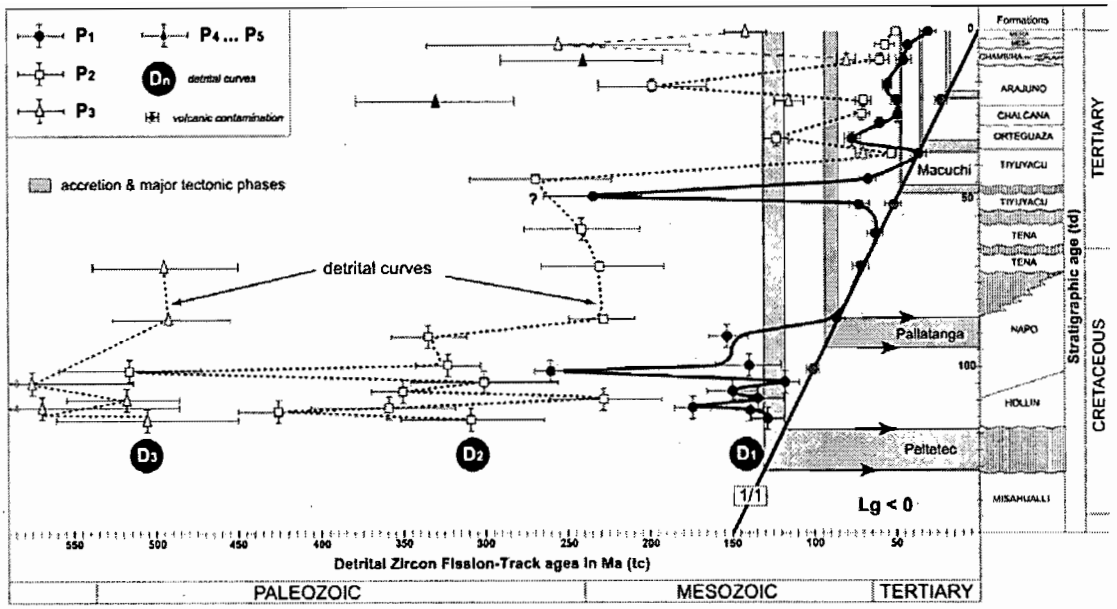

Figure 2: Detrital zircon fission-track age populations (DZFT) from the sedimentary formations of the northern Ecuadorian Subandean Zone. The y-axis represents the stratigraphic age (td) of the host sediment and the x-axis is the ZFT age (tc). Three detrital curves D_1, D_2 & D_3 linking the respective P_1, P_2 & P_3 DZFT age populations are drawn where possible.

Complementary constraints for the identification of source rocks, such as heavy mineral analysis (HM), also provide highly detailed information for diagnosing a large variety of source lithologies. Short-term cycles from ZTR (zircon-tourmaline-rutile) to metamorphic mineral grain dominance are observed stratigraphically upward within both members of the Eocene Tiyuyacu Fm., and the Oligocene Chalcana and Orteguaza Fms. These changes in the heavy mineral contents represent lithological variations within the source rocks from, reworked sediments or shields regions to (1) low to medium-grade, and even (2) high-grade metamorphic rocks. These observed cycles indicate the repeated exhumation and erosion of lower crustal levels that contributed, in variable proportions, to the sedimentary formations of the Ecuadorian AAB. Furthermore, the presence of older detrital zircon fission-track ages from the Tiyuyacu Fm. to the Orteguaza Fm. (Fig. 2) indicates a change of source region (Ruiz et al., 2002), which correlates with a change in the respective heavy mineral association.

CONCLUSIONS

1- The abundance of DZFT populations with Proterozoic and Middle Jurassic to Early Cretaceous ages in the Hollin Fm. (Aptian-Albian) suggests that several distinct source regions, which may have been significantly geographically dispersed, contributed to the early infilling of the AAB. The old populations indicate a probable sourcing in the Guyana-Brazilian Shield regions to the east (Fig. 1). Furthermore, the Early Cretaceous detrital zircon fission-track populations suggest a Late Jurassic-Early Cretaceous phase of exhumation along the Ecuadorian margin (Peltetec event?), which may be responsible for the 60 My hiatus between the Jurassic Misahualli volcanic arc and the overlying Middle Cretaceous AAB sedimentary sequence.

2- Rapid Coniacian/Santonian to Paleocene exhumation (>2 $mm.y^{-1}$) within the source region is coeval with the burial of the basement of the AAB in the northern SAZ. Exhumation during this period is synchronous with the accretion of the oceanic Pallatanga Terrane to the west and therefore may be considered as a minimum constraint for the accretion of the Pallatanga Terrane (e.g. Hughes and Pilatasig, 2002).

3- Distinct provenance changes during the Eocene were coeval with the deposition of proximal sedimentary facies in the AAB (Tiyuyacu Fm.), suggesting that the contemporaneous tectonic development along the Ecuadorian margin was more protracted. Rapid exhumation in the hinterland was restricted to the Middle to Late Eocene (Fig. 2), while lower crustal levels were eroding into the AAB. This phase probably ended with the final docking of the Macuchi oceanic island arc against the Ecuadorian margin where it currently constitutes part of the Cordillera Occidental (Fig. 1; Hughes and Pilatasig, 2002).

4- An almost constant lagtime of 25-35 My can be seen on the D_1 curve during the last 25 Ma (Fig. 2), which indicates that the sediments were being shed from relatively slowly exhuming regions. Therefore, the slow rise of the Eastern Cordillera during the Lower Miocene (Spikings et al., 2000), which was probably related to the break-up of the Farallon plate into the Nazca and Cocos plates at 27-25 Ma, may have sourced the AAB during the Miocene.

5- A clear change of provenance, characterized by the introduction of a pyroxene-olivine dominated heavy mineral assemblage, is observed between the Late Miocene Chambira Fm. and the Pliocene-Pleistocene Mesa and Mera Fms. Therefore, rocks with an oceanic affinity, such as those in the Western Cordillera and Interandean region, have been eroding into the AAB since the Pliocene suggesting a probable coeval exhumation of the region by this time.

REFERENCES:

Brandon, M.T, 1992. Decomposition of fission-track grain age distributions. American Journal of Science, v. 292, p. 535-564.

Hughes R.A., Pilatasig L.F. 2002. Cretaceous and Tertiary terrane accretion in the Cordillera Occidental of the Ecuadorian Andes. Tectonophysics, 345, 29-48.

Naeser, C.W., 1979. Thermal history of sedimentary basins; fission-track dating of subsurface rocks. In: P.A. Scholle and P.R. Schluger (Editors), Aspects of diagenesis. SEPM, Spec. Publ., 26, p.109-112.

Ruiz, G.M., Seward, D., and Winkler W., 2002. Reconstructing polyphased exhumation histories using detrital thermochronology, an example from the zircons of the northern Ecuadorian Sub-Andean Zone, Geotemas.

Spikings R.A., Seward D., Winkler W. and Ruiz G. 2000. Low-temperature thermochronology of the northern Cordillera Real, Ecuador: Tectonic insights from zircon and apatite fission track analysis. Tectonics, 19, 649-668. Supported by Swiss Science Foundation grant no. 20-56794.99.

WIDE-ANGLE SEISMIC CONSTRAINTS ON THE EVOLUTION OF GALAPAGOS HOTSPOT – COCOS-NAZCA SPREADING CENTER INTERACTION

Valentí SALLARES (1), Philippe CHARVIS (2), and Ernst R. FLUEH (3)

(1) IRD-Géosciences Azur, B.P. 48, 06235 - Villefranche-sur-mer, France (valenti.sallares@obs-vlfr.fr)
(2) IRD-Géosciences Azur, B.P. 48, 06235 - Villefranche-sur-mer, France (philippe.charvis@obs-vlfr.fr)
(3) GEOMAR, 1-3 Wischhofstrasse, 28034 - Kiel, Germany (eflueh@geomar.de)

KEY WORDS: Galapagos, hotspot, spreading center, mantle melting, seismic tomography

INTRODUCTION

The presence of a hotspot near to a spreading center generate melting anomalies along the ridge axis [Morgan, 1978]. Typically, the melting anomalies enable higher melt production beneath the ridge, resulting in shallower seafloor and thicker crust than that generated at normal spreading centers. This is evidenced in the long-wavelength bathymetry and gravity anomalies which extends hundreds of kilometers away from hotspots [Ito and Lin, 1995; Escartin et al., 2001]. The main parameters that control the excess of magmatism seem to the size and volume flux of the plume (mainly a function of the temperature anomaly) and the distance between the ridge and the hotspot [e. g., Ito et al., 1999; Ribe, 1996]. Since the seismic velocities are sensitive to the rock composition (and thus to the mantle temperature) and the crustal thickness is proportional to the amount of melting, crustal seismology seems to be an adequate geophysical method to constrain the volume and composition of melt. Hence, the comparison of the observed seismic structure at different periods of time along a hotspot track can give valuable information on the temporal evolution of the hotspot-ridge interaction.

The Galapagos Volcanic Province, located in the northernmost Nazca plate and adjacent Cocos plate, constitutes an excellent example to investigate mantle melting processes due to hotspot-ridge interaction. It is constituted by several blocks of thickened oceanic crust thought to have originated from the interaction between the Galapagos hotspot and the Cocos-Nazca Spreading Center during the last 20 Ma. The most prominent are the Cocos, Malpelo and Carnegie Ridges, which traces the path of the Galapagos hotspot over the Cocos and Nazca plates. In this work we compare the crustal seismic structure of these ridges along five wide-angle profiles acquired during the PAGANINI-1999 and SALIERI-2001 experiments. Two of these profiles are located in the Cocos Ridge, another one in Malpelo, and the last two in Carnegie, at the conjugate positions of Malpelo (at about 20 Ma) and southern Cocos (at about 12 Ma). The 2D velocity field and the Moho geometry along these

profiles have been obtained using a joint refraction/reflection traveltime inversion method, and the uncertainty and robustness of the results have been estimated by performing a Monte Carlo-type analysis.

CONCLUSIONS

The results show that maximum crustal thickness along these profiles is highly variable, ranging from 19-20 km in northern Cocos, Malpelo, and its conjugate Carnegie profile, to 16.5 km in southern Cocos and only 13 km in its conjugate position (Figure 1). Oceanic Layer 2 thickness is quite uniform regardless of total crustal thickness variations, and thus crustal thickening is mainly accomodated in Layer 3. This velocity also shows very similar seismic velocities along all profiles. The notable temporal variations on the crustal thickness at both sides of the ridge axis suggest the existence of important variations on the Galapagos hotspot activity and/or on its relative position with respect to the spreading center. At 20 Ma, the hotspot-ridge system would be dominated by a vigorous on-ridge magmatic activity, while at 12 Ma it would show a significantly lower, off-ridge centered activity.

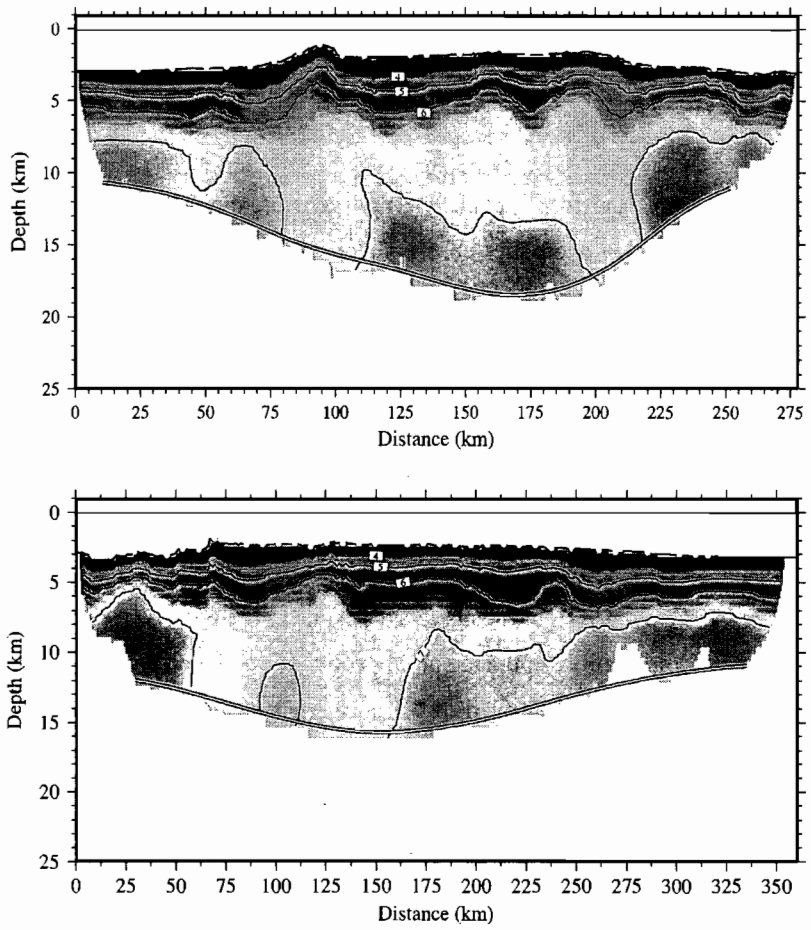

Figure 1.- Crustal seismic structure along southern Cocos profile (up) and its conjugate Carnegie Profile (down). Left side is north and right side is south. Both profiles are located over 12 Ma seafloor. White circles show receiver locations. Note the similar seismic velocities and the different crustal thicknesses.

The mean Layer 3 seismic velocities are generally lower where the crust is the thickest (Figure 1). This leads to an overall anticorrelation between crustal thickness and bulk lower crustal velocities, hence the contrary of that expected if overthickened crust were generated by passive decompression melting of an abnormally hot mantle with an uniform composition [McKenzie and Bickle, 1988; White et al., 1992]. It is thus necessary to consider active upwelling components and/or compositional heterogeneities in the mantle source, and not only high temperatures, to explain the observed seismic structure. This is in agreement with the results of recent studies in the Greenland margin [Korenaga et al., 2000] and in Iceland [McLennan et al., 2001], where active upwelling has been considered to account for the geophysical and geochemical observations. The northernmost segment of Malpelo Ridge shows a rapid crustal thinning and displays high lower crustal velocities, similarly to rifted margins. This could be an evidence of a rifting process which splitted the ancient Malpelo Ridge into Regina and Malpelo Ridges after the initiation of the movement along the Panamá Fracture Zone.

REFERENCES

Escartin, J. et al. 2001. Crustal thickness of V-shaped ridges south of the Azores : Interaction of the Mid-Atlantic Ridge (36°-39° N) and the Azores hotspot. J. Geophys. Res., 106, 21718-21735.

Ito, G., and J. Lin. 1995. Oceanic spreading center – hotspot interactions: Constraints from along-isochron bathymetric and gravity anomalies. Geology, 23, 657-660.

Ito, G., Y. Shen, G. Hirth, and C. J. Wolfe. 1999. Mantle flow, melting, and dehydration of the Iceland mantle plume. Earth Planet. Sci. Lett., 165, 81-96.

Korenaga, J., et al. 2000. Crustal structure of the southeast Greenland margin from joint refraction and reflection seismic tomography. J. Geophys. Res., 105, 21591-21614.

McKenzie, D., and M. J. Bickle. 1988. The volume and composition of melt generated by extension of the lithosphere. J. Petrol., 29, 625-679.

McLennan, J., D. McKenzie, and K. Gronvold. 2001. Plume-driven upwelling under central Iceland. Earth Planet. Sci. Lett., 194, 67-82.

Morgan, W. J. 1978. Rodriguez, Darwin, Amsterdam,... A second type of hotspot island. J. Geophys. Res., 83, 5355-5360.

Ribe, N. 1996. The dynamics of plume-ridge interaction, 2., Off-ridge plumes, J. Geophys. Res., 101, 16159-16204.

Sleep, N. H. 1996. Lateral flow of hot plume material ponded at sub-lithospheric levels, J. Geophys. Res., 101, 28065-28083.

White, R. S., D. McKenzie, and K. O'Nions. 1992. Oceanic crustal thickness from seismic measurements and rare-earth element inversions, J. Geophys. Res., 97, 19683-19715.

CALC-ALKALINE TO ADAKITIC TRANSITION IN THE NORTHERN VOLCANIC ZONE (ECUADOR)

Pablo SAMANIEGO(1,2), Michel MONZIER(2), Claude ROBIN(2), Hervé MARTIN(3), Jean-Philippe EISSEN(1,4), Erwan BOURDON (1,4) and Joseph COTTEN (5)

(1) Departamento de Geofísica, Escuela Politécnica Nacional; Ap. 17-01-2759; Quito, Ecuador (pablosam@hotmail.com).
(2) IRD, UR Processus et Aléas Volcaniques. Laboratoire Magmas et Volcans, Université Blaise Pascal; 5, rue Kessler, 63038 Clermont-Ferrand, France.
(3) Laboratoire Magmas et Volcans; OPGC-Université Blaise Pascal-CNRS; 5, rue Kessler, 63038 Clermont-Ferrand, France.
(4) IRD, Whymper 442 y Coruña, Ap. 17-12-857, Quito, Ecuador.
(5) UMR 6538, Université de Bretagne Occidentale, BP 809, 29285 Brest Cedex, France

KEY WORDS: Andes, Northern Volcanic Zone, Ecuador, adakites, slab melting, mantle metasomatism.

INTRODUCTION

In subduction zone settings, the location of magma genesis is controlled by the thermal state of the mantle-wedge / subducted-slab system (Peacock *et al.*, 1994; Martin, 1999). When old (> 20 Ma) and relatively cold oceanic crust is subducting, the source of calc-alkaline magmas is the mantle wedge metasomatised by hydrous fluids issued from the dehydration of the subducting slab. In contrast, in some rare cases related to the subduction of young and still warm oceanic crust, peculiar magmas called adakites are produced by direct partial melting of the basaltic subducting slab (Defand and Drummond, 1990). Nevertheless, between these two contrasted models several intermediate situations exist, especially in subductions experiencing geodynamical changes.

Such a situation seems to occur in the Quaternary Ecuadorian Volcanic Arc. This arc results from the subduction of the Miocene (12-20 Ma) Nazca oceanic plate beneath the South-American continental plate. But the main part of this arc has developed in front of the Carnegie ridge, an aseismic ridge representing the trace of the Galapagos hotspot on the Nazca Plate (Fig. 1). The ridge is subducting since at least 6-8 Ma and its front is now 300-400 km away from the trench (Gutscher *et al.*, 1999). This subducting ridge also presents a lower subduction angle (~ 25°) compared to the North (> 30°) and with a scarce seismicity (Guillier *et al.*, 2001), possibly resulting of a thermaly warmer environment. Lastly, both high-Y calc-alkaline rocks and low-Y "adakite-like" lavas have been recognised in this arc (Monzier *et al.*, 1997; Bourdon, 1999; Samaniego, 2001; Bourdon *et al.*, 2002a; 2002b). Particularly, several volcanoes of this arc, located at different distances from the trench, are presenting sequentially the two magmatic series. For instance: Pichincha volcano constructed on the Western Cordillera (Bourdon, 1999; Bourdon *et al.*, 2002a; Monzier *et al.*, this volume); Mojanda-Fuya Fuya on the Interandean Valley (Robin *et al.*, 1997; submitted); and Cayambe on the Eastern Cordillera Real (Samaniego, 2001; Samaniego *et al.*, submitted).

The aim of this contribution is to present the temporal magmatic evolution in these three well-studied volcanoes, to constrain the petrogenetic processes active during the transitional period and to relate them to the particular geodynamic setting of Ecuador.

CALC-ALKALINE TO ADAKITIC TRANSITION

The recognition of the presence of two contrasted magmatic series in these three volcanoes is maily based in a strong depletion in Y and HREE and subsequently high La/Yb and Sr/Y ratios for adakite-like rocks, compared to other "classic" calc-alkaline lavas (Fig. 2). Petrogenetic studies of these edifices (Samaniego, 2001; Bourdon *et al.*, 2002a; Samaniego *et al.*, submitted; Robin *et al.*, submitted) are showing that the geochemical characteristics of the adakite-like rocks cannot be related to crustal process like fractional crystallisation or assimilation of the lower crust, suggesting the intervention of a magma related to partial melting of the basaltic subducting slab. On the other hand, Figure 2 shows a "continuum" between the two series, revealing an intermediate situation between the two end-member models mentioned above. Moreover, this evolution seems to occur rapidly; for Cayambe and Mojanda-Fuya Fuya volcanic complexes, the transition between the older edifices (Viejo Cayambe and Mojanda) and the younger ones (Nevado Cayambe and Fuya Fuya) occurred over a short time interval (0.1-0.2 Ma: Samaniego, 2001; Robin *et al.*, 1997; Barberi *et al.*, 1988). In contrast, at Pichincha volcanic complex (PVC) (Monzier *et al.*, this volume), the period between the old (Rucu Pichincha) and young (Guagua Pichincha) edifices seems more important (nearly 1 Ma).

Figure 3 shows some histograms of Y contents of lavas for the old edifices compared to the younger ones. For PVC, the two edifices show the same distribution of Y content (6-23 ppm) but the maximum population show a slight Y decrease from 10-13 ppm for Rucu Pichincha to 8-10 ppm of Y for Guagua Pichincha volcano. In contrast, Mojanda-Fuya Fuya and Cayambe volcanic complexes present a clear bimodality, with higher values of Y content for the older Mojanda (13-20 ppm) and Viejo Cayambe (13-28 ppm) edifices than for the younger Fuya Fuya (7-13 ppm) and Nevado Cayambe (7-20 ppm) volcanoes. Lastly, this figure shows that the "low-Y" adakitic series is present in the three volcanoes independently of their distance from the trench (Western Cordillera, Interandean Valley or Cordillera Real). Conversely, the calc-alkaline series is not well developed on the PVC, but well represented in the basal calc-alkaline series of Mojanda and Viejo Cayambe volcanoes. Thus, the existence of a basal "high-Y" calc-alkaline series could be correlated with trench distance (*i.e.* with mantle wedge thickness).

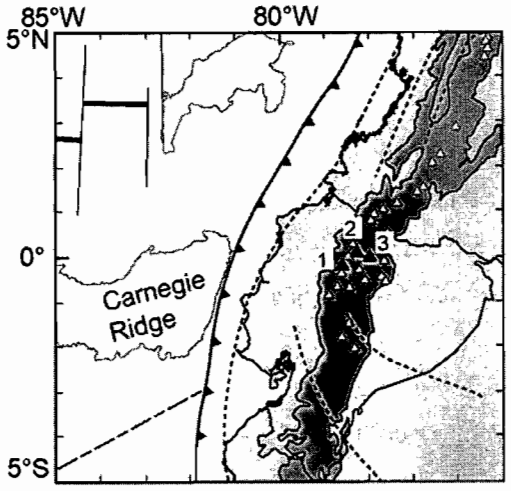

Figure 1. Geodynamical setting of the Ecuadorian Andes (modified from Gutscher et al., 1999). 1: Pichincha; 2: Mojanda-Fuya Fuya; 3: Cayambe

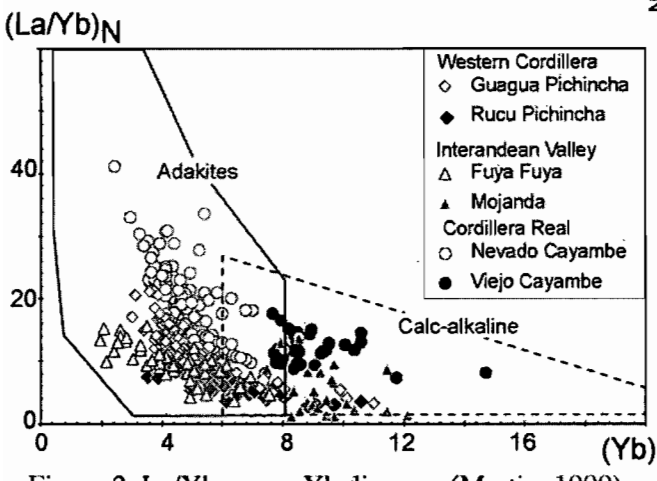

Figure 2. La/Yb versus Yb diagram (Martin, 1999).

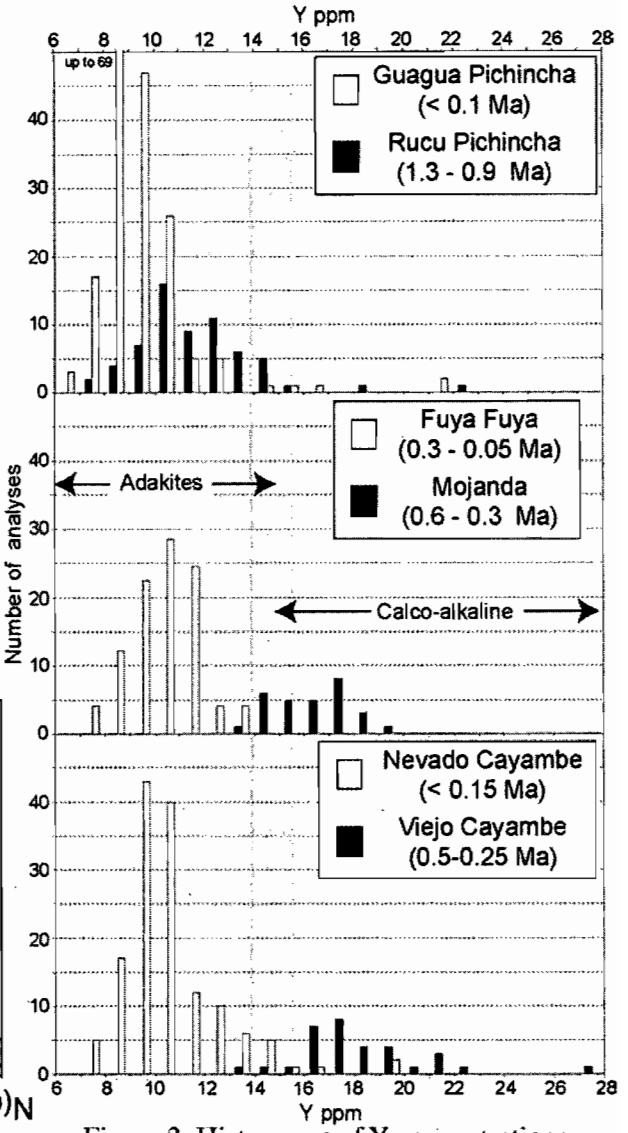

Figure 3. Histograms of Y concentrations.

DISCUSSION: GEODYNAMIC IMPLICATIONS

Geochemical modelling (Samaniego 2001; Samaniego *et al.*, submitted;) led to the conclusion that partial melting of an enriched mantle metasomatised by slab-derived adakitic magmas could generate the calc-alkaline VCAY lavas. A similar model has been proposed to explain intermediate rocks erupted at Antisana volcano (Bourdon, 1999; Bourdon *et al.*, 2002b) situated at 60 km southward of Cayambe. Thus, it is plausible that such a model could explain the genesis all of "high-Y" calc-alkaline series studied here. The same approach reveals that "low-Y" adakite-like rocks display geochemical features intermediate between pure adakitic slab-derived magmas and calc-alkaline mantle-derived magmas. This fact suggests that the interactions between adakitic magmas and the peridotitic mantle wedge are more advanced, allowing to an increase of the adakitic signature in the resulting magmas.

On the other hand, the fact that adakite-like rocks in PVC occur almost 0.8-1 Ma before that in Mojanda-Fuya Fuya or Cayambe volcanic complexes, favoured the hypothesis that the calc-alkaline to adakitic transition is related to a geodynamical change (*i.e.* the arrival under the arc of the subducted Carnegie ridge), allowing slab melting instead of mantle wedge melting. Nevertheless the short time interval for the transition observed in Cayambe and Mojanda-Fuya Fuya (0.1-0.2 Ma) favoured a second scenario in which the increase of the adakitic

features of magmas are related to degree of interaction between slab-derived melts and the mantle wedge. Such a scenario could be related to an increase of adakite / mantle ratio (*cf.* Rapp *et al.* 1999), a process that can be accounted by an increase of slab melting rate associated with the ongoing flattening of the subducting slab (following the model of Gutscher *et al.* 2000); or conversely, to a kind of "saturation" by adakitic magmas of the mantle wedge.

Further studies of Ecuadorian volcanoes in progress will test this model and better constrain the observed calc-alkaline to adakitic transition. Concomitantly, new $^{39}Ar/^{40}Ar$ geochronological data of these magmatic series will help us to better constrain the spatial and temporal evolution of the magmatism in this part of the Andean chain.

In this scenario adakitic magmas have not been completely consumed by metasomatic reactions in the mantle and they could eventually reach the surface as mantle metasomatised adakitic magmas (Bourdon, 1999; Samaniego, 2001; Bourdon *et al.*, 2002a, 2002c).

REFERENCES

Barberi F., Coltelli M., Ferrara G., Innocenti F., Navarro J.M. & Santacroce R. 1988. Plio-Quaternary volcanism in Ecuador: *Geological Magazine*, 125 (1):1-14.

Bourdon E., Eissen J.-P., Gutscher M.-A., Monzier M., Samaniego P., Robin C., Bollinger C. & Cotten J., 2002a. Slab melting and slab melt metasomatism beneath the North Andean Volcanic Zone: adakites and High-Mg andesites from Pichincha volcano. *Bull. Soc. Géol. France*, (in press).

Bourdon E., Eissen J.-P., Monzier M., Robin C., Martin H., Cotten J. & Hall M.L. 2002b. Adakite-like lavas from Antisana volcano (Ecuador): Evidence for slab melt metasomatism beneath the Andean Northern Volcanic Zone: *J. Petrol.* 43:199-217.

Bourdon E., Eissen J.-P., Gutscher M.A., Monzier M., Hall M.L. & Cotten J., 2002c. Magmatic response to early aseismic ridge subduction : the Ecuadorian margin case (South America). *Earth Planet. Sci. Lett., (in press).*

Bourdon E. 1999. Conséquences pétrogénétiques de la subduction d'une ride asismique: l'exemple du volcanisme de la marge équatorienne. Université de Bretagne Occidentale, Brest. *PhD Thesis*, 190 p.

Defant M.J. & Drummond M.S., 1990. Derivation of some modern arc magmas by melting of young subducted lithosphere. *Nature*, 347:662-665.

Guillier B., Chatelain J.-L., Jaillard E., Yepes H., Poupinet G. & Fels J.-F. 2001. Seismological evidence on the geometry of the orogenic system in central-northern Ecuador (South-America): *Geoph. Res. Let.*, 28:3749-3752.

Gutscher M.-A., Malavieille J., Lallemand S. & Collot J.-Y. 1999. Tectonic segmentation of the North Andean margin: impact of the Carnegie Ridge collision: *Earth Planet. Sci. Let.*, 168:255-270.

Gutscher M.A., Maury R.C., Eissen J.P., & Bourdon E., 2000. Can slab melt be caused by flat slab ? *Geology*, 28/6:535-538.

Martin H. 1999. Adakitic magmas: modern analogues of Archean granitoids: *Lithos*, 46:411-429.

Monzier M., Robin C., Hall M.L., Cotten J., Mothes P., Eissen J.-P. & Samaniego P. 1997. Les adakites d'Équateur: modèle préliminaire: *Comptes Rendus Acad. Sci., Paris*, 324:545-552.

Peacock S.M., Rushmer T. & Thompson A.B. 1994. Partial melting of subducting oceanic crust, *Earth Planet. Sci. Lett.*, 121:227-244.

Rapp R.P., Shimizu N., Norman M.D. & Applegate G.S. 1999. Reaction between slab-derived melts and peridotite in the mantle wedge: experimental constraints at 3.8 Gpa. *Chem. Geology*, 160:335-356.

Robin C., Eissen J.-P., Samaniego P., Martin H., Monzier M., Hall M.L., & Cotten J. From calc-alkaline andesites to adakitic dacites at late Pleistocene Mojanda – Fuya Fuya volcanic complex (Ecuador). Submitted to *J. Petrol.*

Robin C., Hall M.L., Jimenez M., Monzier M. and Escobar P. 1997. Mojanda volcanic complex (Ecuador): development of two adjacent contemporaneous volcanoes with contrasting eruptive styles and magmatic suites. *J. South Amer. Earth Sci.*, 10(5-6):345-359.

Samaniego P. 2001. Transition entre magmatismes calco-alcalin et adakitique dans le cas d'une subduction impliquant une ride océanique: le volcan Cayambe (Equateur). Université Blaise Pascal, Clermont-Ferrand, *PhD Thesis*, 305 p.

Samaniego P., Martin H., Robin C. & Monzier M. Transition from classical calc-alkaline to adakitic magmatism at Cayambe volcano, Ecuador: Insights into slab melts/mantle wedge interactions. Submitted to *Geology*.

THE SAN LORENZO FAULT, A NEW ACTIVE FAULT IN RELATION TO THE ESMARALDAS-TUMACO SEISMIC ZONE

Essy SANTANA (1) and Jean François DUMONT (2)

(1) INOCAR, Laboratorio de Geologia Marina, Base Naval Sur, Guayaquil, Ecuador (geologia@inocar.mil.ec)
(2) IRD, A.P. 09 03 30096 Guayaquil, Ecuador (dumontjf@ecnet.ec)

KEY WORDS: South America, earthquakes, neotectonics, subduction, faults

INTRODUCTION

The coast of northwest Ecuador and southwest Colombia has registered some of the most important earthquake of South America (Herd et al., 1981)(1906, Ms 8.7; 1942, Ms 7.9; 1958, Ms 7.8; 1979, Ms 7.9) (Fig. 1). Most of these earthquakes (1906, 1958 and 1979) have been accompanied by tsunamis (Espinoza, 1992). From Rio Verde (Ecuador) to Buenaventura (Colombia) the coast is low, and consists in a wide margin of beach ridges, tidal channels and mangroves. Wet tropical climate as well as the proximity of the Western Cordillera about 50 km away to the southeast provides precipitation through a dense network of rivers. Such conditions, low topography, dense river network and active deformations are basically favorable to observe river patterns anomalies related to active deformation (Schumm et al., 2000).

GEOLOGIC AND GEODYNAMIC BACKGROUND

Northeast of Esmeraldas the morphology of the coast changes drastically (Fig. 1). The coastal cordillera of Manabi sinks in the Pacific Ocean near Esmeraldas, leaving place to a low coast, and finally the tidal channels, swamps and mangroves of the Bay of Ancon de Sardinas. The city of San Lorenzo is located at the border between wetland and terra firme (Fig. 2). The San Lorenzo area is part of the Borbon Basin, a NE-SW trending fore arc basin (Deniaud, 2000). The Borbon basin comprises up to 5000 m of tertiary mudstone resting on a basement of Cretaceous basalts. The Pliocene is represented by deep-water mudstone. The area was folded into NE-SW structures and subsequently emerged during the late Pliocene (Evans and Whittaker, 1982). During the late Pliocene the sedimentation continued in the northern Borbon Basin, is the area of the Gulf of Ancon de Sardinas. The structure of this basin trends E-W to WNW-ESE, nearly orthogonal to the structure of the previous Mio-Pliocene basin (Deniaud, 2000). To the south it is bordered by NW-SE trending faults showing a left hand offset of the NE-SW tertiary structures (CODIGEM and BGS, 1993). The northern limit of the basin follows the Mataje River, which is also the northern limit of the Bay of Ancon de Sardinas.

Along the North Andean margin the Nazca plate is subducting eastwards beneath South America at a rate of about 5-7 cm/a (see a synthesis in (Gutscher et al., 1999), and a nearly W-E trend. The convergence obliquity that increases northward from the Gulf of Guayaquil to south Colombia (Fig. 1) controls the slip rate in the upper plate along the Pallatanga-Bocono wrench fault zone (Ego et al., 1996). The recent deformation in the coastal

areas of Ecuador is represented by near N-S extension (Dumont et al., 1997). The Nazca plate, which is subducted in the Ecuadorian-south Colombian trench, has been formed since the break out of the Farallon plate about 25 Ma (Hey, 1977). The structure is rather complex, including the Carnegie ridge in front of the Manabi region of Ecuador, and the Malpelo Rift in front of north Ecuador-south Colombia. The E-W trending Malpelo Rift is interpreted as a former part of the Galapagos rift, (Gutscher et al., 1999; Lonsdale and Klitgord, 1978) active from ca. 17 to 8 Ma. The Yakina Graben a N-S transform structure of the Malpelo rift fronts obliquely the subduction zone, closer to the south than to the north.

THE SAN LORENZO SCARP LINE AND FAULT

The new fault has been first observed on aerial photos. The morphological evidence is a linear line of bluff observed along about 25 km, from the south of San Lorenzo to the Colombian border, and extending to Colombia according preliminary observations. Southward the line of bluff joins the border of the Rio Los Atajos, but another bluff line appears westward towards Valdez (Fig. 2). The interpretation of the lineament as a fault is supported by the continuous linear trend, and different drainage pattern on each side of the line (Fig. 2).

South of San Lorenzo the main scarp line limits mangrove and tidal channels to the west from 10 to 20 m elevation upland to the east. Near San Lorenzo the fault divides in two segments, the main scarp following the eastern segment. However this segment suddenly stops 10 km the north, and the scarp line shift west to the main fault line (Fig. 2). The wetlands located west of the scarp include drowned beach ridges. Along the Rio Los Atajos these beach ridges were C14 dated of 5000 BP (Tihay, 1989).

Near Tambillo (Fig.2) a very chaotic accumulation of pebbles and trees trunks in a limy matrix crops out at the foot of the scarp below 1 m of recent sediments. The chaotic aspect leaves no doubt to the fact that the material has been takes off down the scarp, because there is no river able to transport the material. The C14 dating of a tree trunk gave 111 year BP. This catastrophic deposition is hypothetically correlated with the 1906 earthquake. This earthquake occurred the 31 of January, that is during the rainy season on the coast. Therefore weather conditions may have favored up root trees on the slope of the scarp. A tsunami with a 5m runup is associated with this earthquake (NOAA-NESDIS wesbsite). However, the possibility to the wave to reach the scarp with a high energy is relatively low, because it is distant of 15 km from the open sea through an area of mangroves, and in indirect line with respect to the main tidal channels.

FAULT DATA

The tectonic observations have been made on the NE trending secondary fault scarp south of San Lorenzo (Fig. 2). The fault cuts weathered material from the paleo San Lorenzo alluvial cone, probably of late Pliocene early quaternary age (Winckell and Zebrowski, 1997).The San Lorenzo river cuts the escarpment, describing a local swing against the scarp line. Observed along 20 m, the fault plane trends to the NE, with W-E trending deviations. The observations were made at the lower part of the morphologic scarp, in an area not related to landslide. The fault planes have a high dip to the northwest except one plane dipping to the south-southeast (fig.

2). The slickensides (see stereogram Fig. 2) show a relative dispersion due to the high dip of the fault planes. High dip fault planes are frequently observed where a normal fault plane reaches the topographic surface. The calculation of the main axis with the Carey method (Carey et al., 1987) gives a NNW extension with a maximum stress vector near vertical.

CONCLUSION

Morphologic and tectonic data are coherent to identify the scarp between wetland and terra firme as a fault, formed after the upper Pleistocene, and existing since 5000 y/BP(Tihay, 1989). This scarp has been reactivated during the 1906 earthquake, or affected by the corresponding tsunamis. The tectonic elements suggest a N-S extension, with a trantensive movement of the faults. This geometry of the deformation seems to favor a tectonic origin of the movement instead of a simple gravitational effect. On a regional scale these NNE trending right hand transtension faults are geometrically coherent with the NW trending left hand faults bordering the late Pliocene to Quaternary Borbon Basin (CODIGEM and BGS, 1993). The lineament line along the Rio Mataje may be part of this system. This main structural pattern may result in a division of the area in coastal blocks bordered by trantension faults, prone to favor gravitational sliding in the slope of the margin. The relatively important effect of the N-S extension accompanied here by a notable subsidence may be related either to the increasing of the obliquity in this area, or to elements related to the structure of the subducting plate, such as the presence of deep fracture like the Malpelo Ridge or the Yaquina Graben.

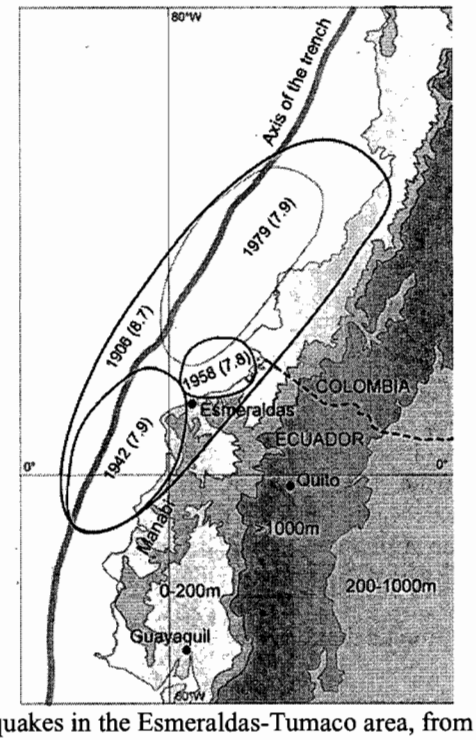

Fig. 1. Position of earthquakes in the Esmeraldas-Tumaco area, from Herd et al. (1981)

Fig 2: synthetic map of the San Lorenzo area. Point A is the location of the C14 sample of 111 year BP.

References

Carey, E., Gailhardis and Mercier, J.L., 1987. A numerical model for determining the state of stress using focal mechanisms of earthquake population:application to Tibetan teleseims and microseismicity of Southern Perou. Earth Planet Sci. Len., 82: 165-177.

CODIGEM and BGS, 1993. Mapa geologico de la Republica del Ecuador. British Geological Survey.

Deniaud, Y., 2000. Enregistrements sédimentaire et structural de l'évolution géodynamique des Andes Equatoriennes au cours du Néogène: Etude des bassins d'avant arc et bilan de masse. Doctor Thesis, Joseph Fourrier, Grenoble, 243 pp.

Dumont, J.F. et al., 1997. Extensional tectonics in the coastab block of Ecuador: preliminary resulta and implications., Workshop on Late Quaternary Coastal Tectonics, London.

Ego, F., Sebrier, M., Lavenu, A., Yepes, H. and Egues, A., 1996. Quaternary state of stress in the Northern Andes and the restraining bend model for the Ecuadorian Andes. Tectonophysics, 259: 101-116.

Espinoza, J., 1992. Terremotos Tsunamigénicos en el Ecuador. Acta Oceanográfica del Pacífico, 7(1): 21-28.

Evans, C.D.R. and Whittaker, J.E., 1982. The geology of the western part of the Borbón Basin, North west Ecuador: Trench forearc Geology. Geol. Soc. London, 10: 191-200.

Gutscher, M.A., Malavielle, J., Lallemand, S. and Collot, J.Y., 1999. Tectonic segmentation of the North Andean margin: impact of the Carnegie Ridge collision. Earth and Planetary Sciences Letters, 168: 255-270.

Herd, D.G. et al., 1981. The Great Tumaco Colombia earthquake of 12 december 1979. Science, 211: 441-445.

Hey, R., 1977. Tectonic evolution of the Cocos-Nazca speading center. Geological Society of America Bulletin, 88: 1404-1420.

Lonsdale, P. and Klitgord, K.D., 1978. Structure and tectonic history of the eastern Panama basin. Geol. Soc. of Am. Bull., 89: 1-9.

Schumm, S.A., Dumont, J.F. and Holbrook, J.M., 2000. Active Tectonics and Alluvial Rivers. Cambridge University Press, 276 pp.

Tihay, J.P., 1989. Aspects geomorphologiques de l'environnement du site archéologique de la Tolita (Equateur), Universite de Pau et des Pays de l'Adour, Pau.

Winckell, A. and Zebrowski, C., 1997. Los paisajes costeros. Los paisajes naturales del Ecuador, Geografía física del Ecuador. CEDIG, pp. 208-319.

MESOZOIC AND CENOZOIC RHEOLOGICAL EVOLUTION OF THE LITHOSPHERE OF THE EASTERN CORDILLERA AND HYPOTHESES ABOUT ITS DEEP STRUCTURE

L. F. SARMIENTO-ROJAS[a*], *F ROURE*[b] *and S. CLOETINGH*[c]

[a]Ecopetrol-ICP Instituto Colombiano del Petróleo, Piedecuesta, Santander, P O Box 4185-Bucaramanga, Colombia.
[b] Institute Francais du Petrole, 1 et 4 Avenue de Bois Préau, 92852, Rueil Malmaison Cedex, France.
[c]Tectonics Group, Faculty of Earth Sciences, Free University, De Boelelaan 1085, 1081 HV Amsterdam, The Netherlands.

Backstripping analysis of stratigraphic columns from the Eastern Cordillera (EC), Llanos and Magdalena Valley (MV) along a regional section, forward modelling of these columns, standard rheological models and flexural models indicate that during the Mesozoic and Palaeogene a weak lithosphere resulted from lithosphere stretching in the area of the EC where Mesozoic extensional basins were developed. However, for the present time, flexural models indicate a weak lithosphere under the EC in open disagreement with standard rheological models that suggest a strong lithosphere in the EC. Two important effects not considered in the standard rheological models may explain the difference: (1) The presence of crustal discontinuities that weaken the lithosphere; and (2) The presence of an anomalous heat input into the lithosphere, as indicated by local Neogene volcanic rocks and several hot springs in the EC. Two major controls on lithosphere dynamics of the extensional basin formation and inversion history of the EC have been (1) lithosphere rheology, and (2) plate-related tectonic stresses. During the Triassic and Jurassic tensional/transtensional stresses, probably initially related to the break-up of Pangea and to backarc extension, produced lithosphere stretching and generated narrow rifts (< 150 km wide), located in the places of the present day MV and the western flank of the EC (Magdalena-Tablazo sub-basin). Repeated stretching events in the same area suggest strain localisation affecting a weak lithosphere. Thermal heating associated with stretching and reactivation of crustal discontinuities probably contributed to such a strain localisation. During the Early Cretaceous tensional/transtensional stresses probably related to backarc extension produced new episodes of lithosphere stretching and generated a wide (> 180 km wide) system of asymmetric half-rift basins, one of which with a depocenter located along the palaeo-eastern flank of the EC, with a major normal fault system in its eastern border (Cocuy sub-basin). A less developed second order half-rift occurred in the place of the south-western flank of the Cordillera (Magdalena-Tablazo sub-basin). While stretching of the Magdalena-Tablazo sub-basin affected lithosphere previously weakened during earlier rifting episodes, development of the new Cocuy cub-basin only can be explained by reactivation of older crustal discontinuities, probably the pre-Mesozoic Guaicáramo palaeo-fault. During the Palaeogene, compressional/transpresional stresses, initially related to collision of the South American plate margin with a relatively buoyant oceanic plateau and later related to acceleration of rates of plate convergence and collision to the Chocó Block during Neogene time, affected the weakened lithosphere of the former extensional basins. This resulted in inversion episodes of the former extensional basins: During the Palaeogene, incipient basin inversion affected the weak lithosphere of the former Magdalena-Tablazo and Cocuy sub-basins, while during the Neogene, the EC resulted from the complete inversion of the Mesozoic extensional basin area. During the whole Meso-Cenozoic time

flexural and rheological models indicate crust-mantle decoupling. Flexural models suggest that in the EC mantle began to contribute to lithosheric strength probably only since Neogene time. In this region lithospheric strength increased during Neogene time.

Based on surface geological data, limited geophysical data (gravity, seismicity), comparison with similar mountain belts and analogue and numerical models from the literature, it is possible to narrow the uncertainity range on the deep structure of the EC. Probably it resembles that of the Pyrenees: Lithospheric shortening has been accommodated in the upper brittle crust by development of a double vergent asymmetric wedge, while the mantle lithosphere accommodated shortening by west-dipping subduction of the cooler and denser LLA mantle lithosphere under the buoyant and hotter Andean lithosphere. The lower ductile crust probably accommodated shortening by thickening. Probably the EC has been strongly affected by transpression with important transcurrent components.

Intermediate seismicity beneath the EC suggest that a subducted slab fragment is present below its NW margin (Taboada *et al.*, 2000). A small, but very active zone of intermediate-deep seismicity, the Bucaramanga earthquake nest (Schneider *et al.*, 1987), may result from deep oblique convergence of Palaeo-Caribbean plate fragment connected to the Panamá Block and the Caribbean Plate from the north. This may explain the NW-SE lineation of the nest (Schneider *et al.*, 1987). Two particularities of the EC, *i.e.* the local presence of Neogene volcanic rocks at Paipa and Iza, and the intermediate seismicity, may be the expression of slab break-off of the eastward-subducting Caribbean-type mantle lithosphere fragment under the EC. Subduction resistance of the relatively buoyant Caribbean type crust may have produced break-off of its denser mantle lithosphere under the Colombian Andes or a fragment of a normal denser lithosphere of the old Farallon Plate. The deep slab suggested by tomographic images (Taboada *et al.*, 2000) may be a subducted slab, which is no longer connected to the surface plates. This hypothesis would explain the east-dipping slab fragment suggested by seismological studies (Schneider *et al.*, 1987; Taboada *et al.*, 2000) and the Paipa-Iza volcanic rocks. These volcanic rocks may be related with upwelling hot asthenosphere where slab break-off occurs. Possibly partial melting of the lower crust beneath the EC may have generated rising magmas, generated a thermal anomaly under the EC and weakened its lithosphere.

Deep seismic studies could offer reliable data in order to support or contradict the suggested hypotheses.

REFERENCES

Schneider, J. F., Pennington, W. D. and Meyer, R. P., 1987. Microseismicity and focal mechanisms of the intermediate-depth Bucaramanga nest, Colombia. J. Geophys. Res. , 92: 13.915-13.926.

Taboada, A., Rivera, L.A., Fuenzalida, A., Cisternas, A., Philip, H., Bijwaard, H., Olaya, J. and Rivera, C., 2000, Geodynamics of the northern Andes: Subductions and intracontinental deformation (Colombia). Tectonics, 19 (5): 787-813.

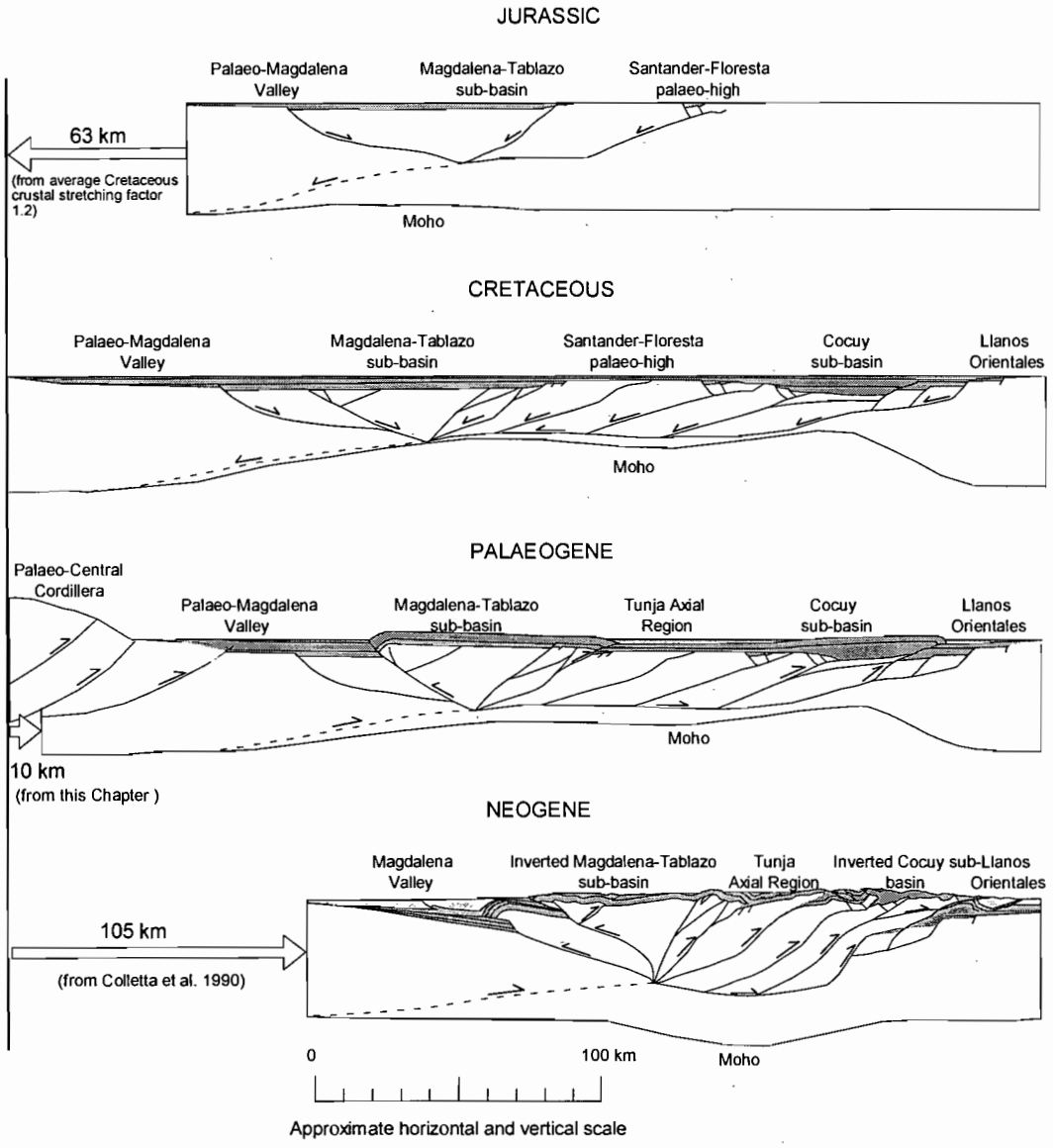

Figure 1: Cartoon showing the suggested tectonic evolution of the Eastern Cordillera since Mesozoic time. Flexural models indicate an incipient inversion of Mesozoic basins and generation of local topography within the study area Cretaceous shortening estimated from Cretaceous extension factors, Palaeogene shortening estimated from kinematic modelling and Neogene shortening from Colletta *et al.* (1990).

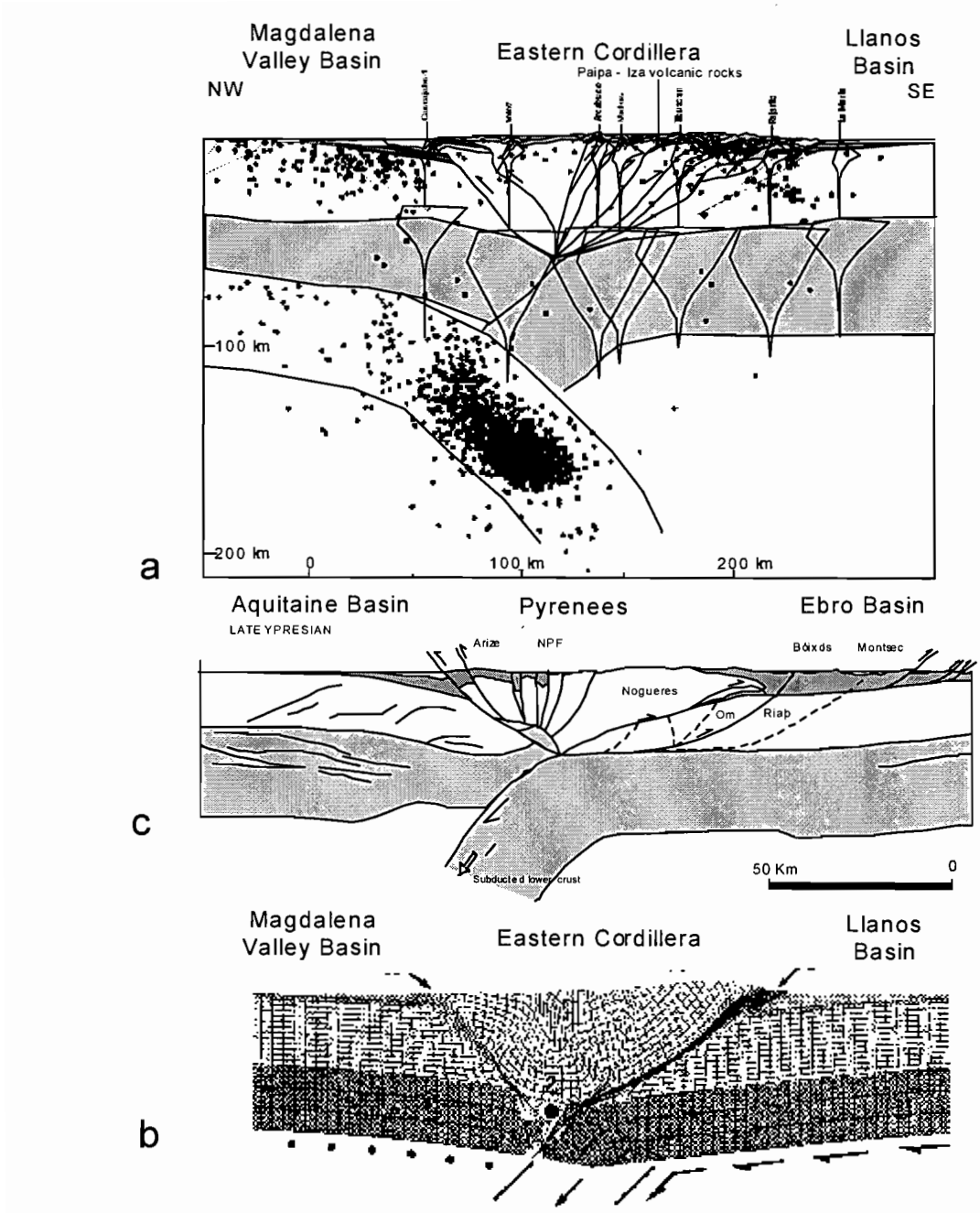

Figure 2: (a) Depth dependent rheological models of the EC at present time (0 Ma) along a regional section of the EC showing the structure (after Colletta *et al.*, 1990) and observed seismicity (after Taboada *et al.*, 2000). The schematic deep structure of the EC is the hypothesis proposed here. (b) Numerical geodynamic model of a collisional orogen (from Beaumont *et al.*, 2000). (c) Crustal cross-section of the Pyrenees (from Beaumont *et al.*, 2000). Compare the hypothetical structure of the EC (a) with the geodynamic numerical model of a collision orogen (b) and with the structure of the Pyrenees.

ARIDISATION AND ENHANCED RATES OF FLUVIAL INCISION IN THE ANDES OF NORTHERN CHILE

Fritz SCHLUNEGGER (1), Florian KOBER (2), Guy SIMPSON (2), Heinz SCHNEIDER (3)

(1) Institute of Geology, Univ. Bern, Baltzerstrasse 1, 3012 Bern, fritz.schlunegger@geo.unibe.ch
(2) Institute of Geology, ETH Zürich, Sonneggstr. 5, 8092 Zürich
(3) Universidad Catolica del Norte, Av. Angamos 0610, Antofagasta, Chile

KEY WORDS: valley formation and climate, Central Andes, landscape evolution

RESUME

Les Andes situées dans la partie septentrionale du Chili ont subi une phase importante d'incision qui est caractérisée par une érosion rétrograde résultant de l'établissement d'un 'knickpoint' classique dans le profile longitudinal des cours d'eau. Cette phase d'incision plus prononcée a débuté il y approximativement 3 Ma, alors que le climat devint hyperaride dans le nord du Chili et que les précipitations allaient être restreintes aux Hautes Andes. Nous interprétons que ce changement climatique, représentant la transition entre un climat semi-aride à hyperaride a initié la phase majeure de formation des vallées.

INTRODUCTION

The Western Escarpment of the Andes of Northern Chile are a tectonically active mountain belt that is characterized by the presence of gently folded surfaces (or pediplains) tens to hundreds of km^2 wide and >1500 m deep valleys that dissect these surfaces (Fig. 1). Although that erosion in these valleys scales rates of relief formation, and despite the fact that these valleys form the most impressive geomorphic features in this part of the Andes, determinations of ages of incision, and more important, interpretations of possible controls on valley formation have been controversial. Depending on interpretations of relationships between ages of surfaces into which incision has occurred and geometries of the drainage network, phases of enhanced rates of incision have been considered to be the result of (i) an eustatic sea level fall, (ii) onset of glaciation in the Pleistocene (which is considered to have increased fluvial runoff) and (iii) differential tectonic movements (see Garcia et al., 1999, and Wörner et al., 2002 for overview of hypotheses).

Here, we present geomorphic and stratigraphic data from the Arica area, Northern Chile, based on which we show that a phase of enhanced fluvial incision rates was initiated in the Late Pliocene at ca. 3 Ma, at a time when climate became hyperarid in the Atacama Desert, and when precipitation became restricted to the High Andes (Hartley & Chong, 2002). We will interpret that this change in palaeoclimate resulted in stabilization of the surfaces in the lower reaches (formation of a salt crust on the Oxaya and Diablo Surfaces), which caused the sediment discharge from the surfaces to the fluvial transport systems to decrease. This change

in the pattern of sediment yield is likely to shift the transport systems to the stage of undercapacity, which, in turn, promotes downcutting and backward erosion.

GEOMORPHIC ELEMENTS

The landscape of the study area consists of two major landform elements that blanket the Western Andean Escarpment in a N-S direction. The Oxaya Surface in the east (Fig. 1) forms the top of the Oxaya and Azapa Formations. These units are made up a > 1000 m-thick succession of tens of m-thick ignimbrite sheets and interbedded fluvial clastics (Carcia et al., 1999; Wörner et al., 2002). Dating of ignimbrites yielded ages of between 25 and 19 Ma for the Azapa and Oxaya Formations (Carcia et al., 1999; Wörner et al., 2002 and references therein). Deformation of the Oxaya Surface caused formation of the Oxaya anticline that displays an amplitude of >500 m, and thrusting along the Ausipar fault (Fig. 1). West of this fault is the Diablo Surface. This geomorphic element is made up of a several tens to hundreds of m-thick succession of fluvio-lacustrine sediments (Carcia et al., 1999; Wörner et al., 2002) that onlap eastward onto the Oxaya Surface west of the Ausipar fault (Fig. 1). The age of the top of the Diablo Formation becomes successively younger towards the south. Indeed, in the Arica area, accumulation of sediment is considered to have terminated in the Upper Miocene (e.g. Wörner et al., 2002). Approximately 100 km farther south (Tana valley), the top of the Diablo Formation is made up of a >70 m-thick succession of calcrete beds, marginal lacustrine limestones and stromatolites. This facies association, dated to have established between ca. 6-3 Ma, appears to be widespread in the Western Escarpment of Northern Chile and is considered as an isochronous marker horizon (Hartley & Chong, 2002, and references therein).

INCISION INTO THE OXAYA AND DIABLO SURFACES

The topographic data of the Arica area reveals that growth of the Oxaya anticline that occurred sometime between the Middle and Late Miocene (Wörner et al., 2002) caused the rivers to cut down to the base level of the Camarones valley (Figs. 1, 2). After the Late Miocene, the rivers feeding the Micoene Camarones river were rerouted in a southward direction into the Azapa drainage system (Figs. 1, 2), and the Camarones valley became abandoned. Because the sediments of the Diablo Formation onlap onto the Oxaya Surface in an eastward direction, and since the elevation of the easterly tip of the Diablo Surface corresponds to the elevation of the Camarones base level, it is likely that the Camarones river represented one of the feeding systems of the fluvio-lacustrine deposits of the Diablo Formation.

The phase of aggradation (which resulted in accumulation of the Diablo Formation) was succeeded by a phase of rapid incision and backward erosion resulting in a significant increase in relief (Figs. 1, 2). At present, the location of enhanced vertical and backward erosion is found immediately west of the knickpoint of the stream profiles (Fig. 2) There the bedrock is exposed on the channel floor, and the hillslopes are oversteepened. In the lower valley reaches, however, accumulation of sediment and long-wavelength meandering has resulted in establishment of wide valleys with planar bases, which increase in width downstream. In the upper reaches above the location of active incision and backward erosion, the

geomorphologies display relatively smooth hillslopes with parabolic cross-sectional geometries indicative of a more mature landscape.

The geomorphic characteristics of this stage of enhanced rates of vertical and backward incision are found all along the Western Escarpment of the Andes of Northern Chile for which we assign an age of Late Pliocene for initiation. Indeed, the youngest sediments that are cut by fluvial incision represent the fluvio-lacustrine sediments found in the Tana valley ca. 100 km south of Arica. As discussed above, these sediments were presumably deposited between ca. 6-3 Ma as a result of a humid phase (Harley & Chong, 2002).

CLIMATE CHANGE AND VALLEY FORMATION

As outlined above, the stratigraphic data from the Western Escarpment of Northern Chile imply an age of ca. 3 Ma for initiation of the phase of enhanced incision. This time, however, is characterized by a shift from more humid climatic conditions to a hyperaric climate especially in the Atacama Desert (Hartley & Chong, 2002). As a result, precipitation became restricted to the High Andes where the major rivers are sourced that deeply cut into the Oxaya and Diablo Surfaces. The hyperarid conditions that established in the lower elevations of the Northern Andes of Chile caused the Pliocene strata to become covered by a thick crust of salt and anhydrite that even blanket hillslopes and summits. We interpret that this stabilization of surfaces decreased the sediment discharge from e.g. the Oxaya and Diablo Surfaces (Fig. 1) to the fluvial transport systems, shifting the rivers into the stage of undercapacity. In case that the fluvial systems are transport-limited, then a decrease in sediment discharge especially at lower elevations causes incision and backward erosion to increase. In support of this hypothesis, a change towards enhanced arid conditions is anticipated to increase the ratio of high-magnitude floods, i.e. the frequencies of large floods, which, in turn, is likely to contribute to the enhancement of incision and backward erosion (see also Tucker & Slingerland, 1997).

REFERENCES

Garcia M., Herail G. & Charrier, R. 1999. Age and structure of the Oxaya Anticline: A major feature of the Miocene compressive structures of northernmost Chile. 4th ISAG, Goettingen. pp. 249-252.

Hartley A.J. & Chong, G. 2002. Late Pliocene age of Atacama Desert: Implication for the desertification of western South America. Geology 30, 43-46.

Molnar P. 2001. Climate change, flooding in arid environments, and erosion rates. Geology 29,1071–1074.

Tucker G.E. & Slingerland R. 1997. Drainage basin response to climate change. Water Resources Research, 33, 2031-2047.

Wörner G., Uhlig D., Kohler I. & Seyfried H. 2002. Evolution of the West Andean Escarpment at 18°S (N. Chile) during the last 25 Ma: uplift, erosion and collaps through time. Tectonophysics 345, 183-198.

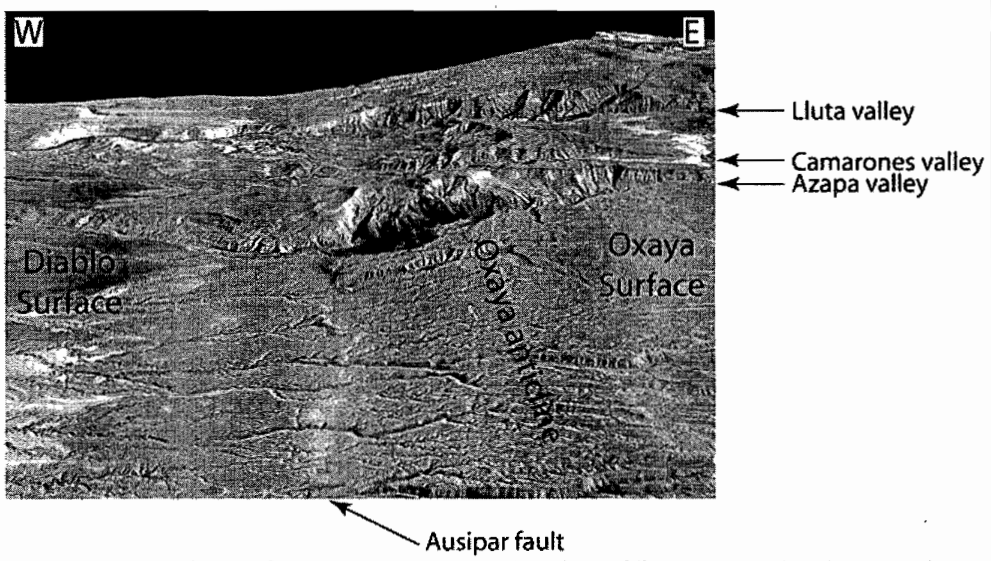

Fig. 1 Geomorphology of the Western Escarpment of Northern Chile. The digital elevation model has a spatial resulution of 50 m.

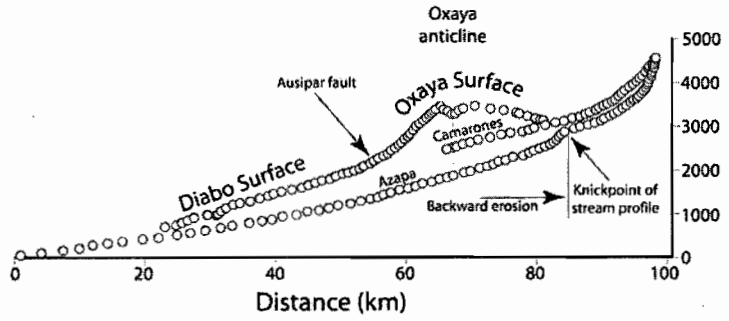

Fig. 2 Stream profiles, elevation of base levels and knickpoint migration of the Azapa river. See Fig. 1 for location

CRUSTAL THICKNESS IN THE EASTERN VENEZUELAN BASIN FROM SEISMIC WIDE ANGLE DATA

Michael SCHMITZ. (1), Ana MARTINS (2,1), Jesús CASTILLO (2)

(1) Fundación Venezolana de Investigaciones Sismológicas, FUNVISIS, Caracas, Venezuela (mschmitz@internet.ve)
(2) Universidad Simón Bolívar, USB, Sartenejas, Caracas, Venezuela (anamartins59@hotmail.com)

KEY WORDS: Venezuela, Eastern Venezuelan Basin, wide angle seismics, crustal structure, Moho

INTRODUCTION

The Eastern Venezuelan Basin with a length of 500 km and a width of 200 km covers the region between the Interior Range to the north and the Guayana Shield to the south all along eastern Venezuela (Fig. 1). Towards the north, the Interior Range fold and thrust belt marks the plate boundary of the South American continent with the Caribbean plate along a mayor strike slip fault system. Towards the south, the basin sediments onlap above the cristalline rocks of the Guayana Shield, which are exposed south of the Orinoco river. As the Eastern Venezuelan Basin is a mayor petroleum bearing province, many studies have been carrying out regarding the stratigraphy and mayor structural trend of the basin (e.g. Hedberg, 1950; Gonzalez de Juana et al., 1980; Parnaud et al., 1995; Passalaqua et al., 1995). Nevertheless, no seismic information is available up to the date on the maximum depth of the basin and the crustal thickness.

Seismic wide angle measurements were designed to investigate the depth of the sedimentary coverage and the crustal structure of the Eastern Venezuelan Basin along a 300 km north - south line and a 80 km line in SW-NE direction (Fig. 1). The total depth of the sediments in the Eastern Venezuelan Basin achieves about 12 km, whereas crustal depth varies between 35 in the north to 38 on the northern edge of the Guayana Shield. In this contribution, we present examples of the seismic data and the derived crustal model.

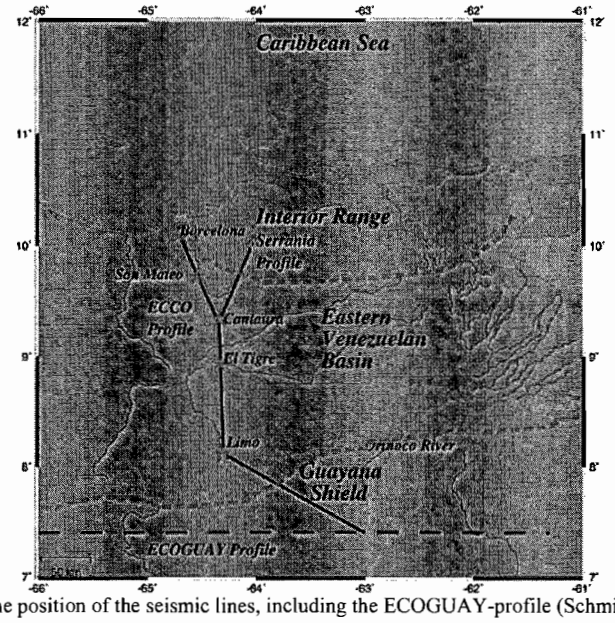

Figure 1. Location map indicating the position of the seismic lines, including the ECOGUAY-profile (Schmitz et al., 2002).

SEISMIC DATA

Seismic field work has been done within the scope of the ECCO project (Estudio Cortical de la Cuenca Oriental) in July 2001 using o total of 193 Texan recorders. Along the main 300 km long north-south line (ECCO-profile) from the Caribbean coast in the north to the Guayana Shield in the south, 5 shots (150 to 550 kg of explosives) were fired. A secondary line in SW-NE direction (Serranía-profile, 80 km length), crossing the intersection between the Eastern Venezuelan Basin and the Interior Range, was fired with a total of 10 smaller shots (75 to 100 kg). Blasts were fired in boreholes between 10 and 30 m in depth using emulsion as explosives (for details see Martins, 2002).

The data quality varies strongly for the different seismic sections due to shotpoint conditions. First arrivals of the sedimentary layers are best on the Serranía profile (Fig. 2) with first arrivals up to 60 km recording distance and up to 4 s (reduced time with 6 km/s). Clear arrivals from the crust-mantle boundary can be derived on the El Tigre - south (Fig. 3) and Limo - north and - south record sections for the southern part of the Eastern Venezuelan Basin and the Guayana Shield. Reflections from the Moho can be observed between 90 and 77 km distance and 4-5 s on the El Tigre-south record section. The derived crustal thickness amouts to 38 km. Deeper arrivals on the other record sections are somewhat doubtful and should be interpreted with caution.

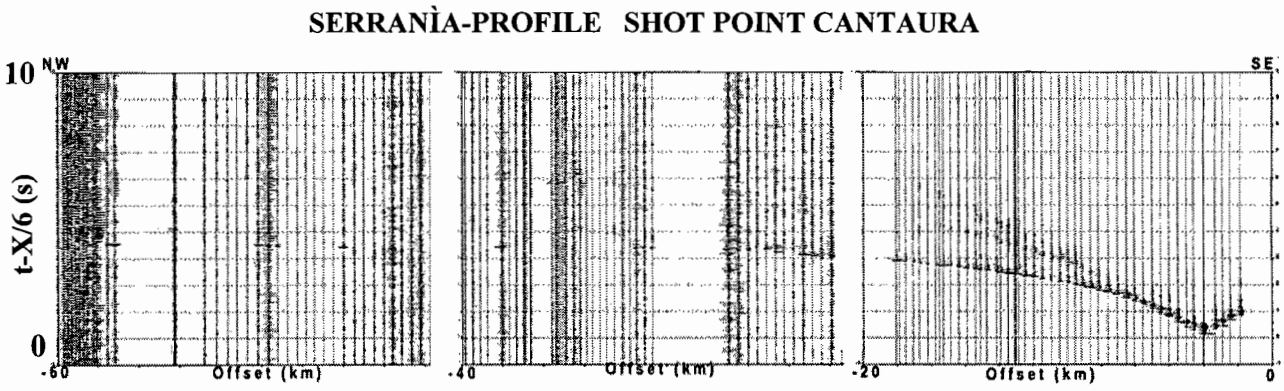

Figure 2. Record section from shot point Cantaura to northeast, recorded along the Serranía-profile with correlated travel time branches (red lines).

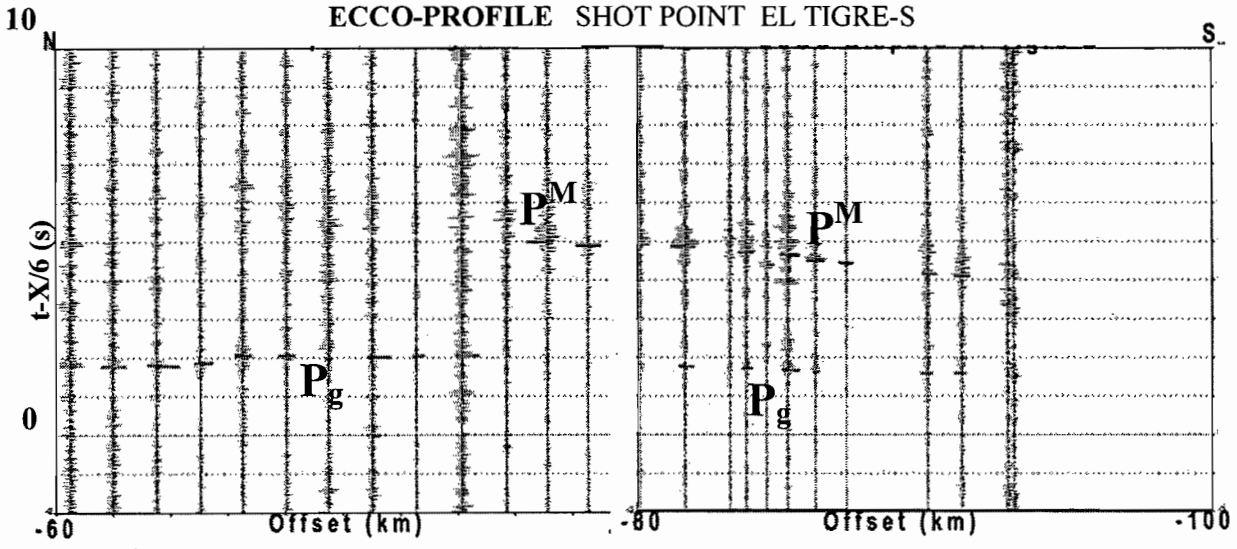

Figure 3. Record section from shot point El Tigre to south, recorded along the ECCO-profile with correlated travel time branches (red lines) from the cristalline basement (P_g) and the Moho reflection (P^M).

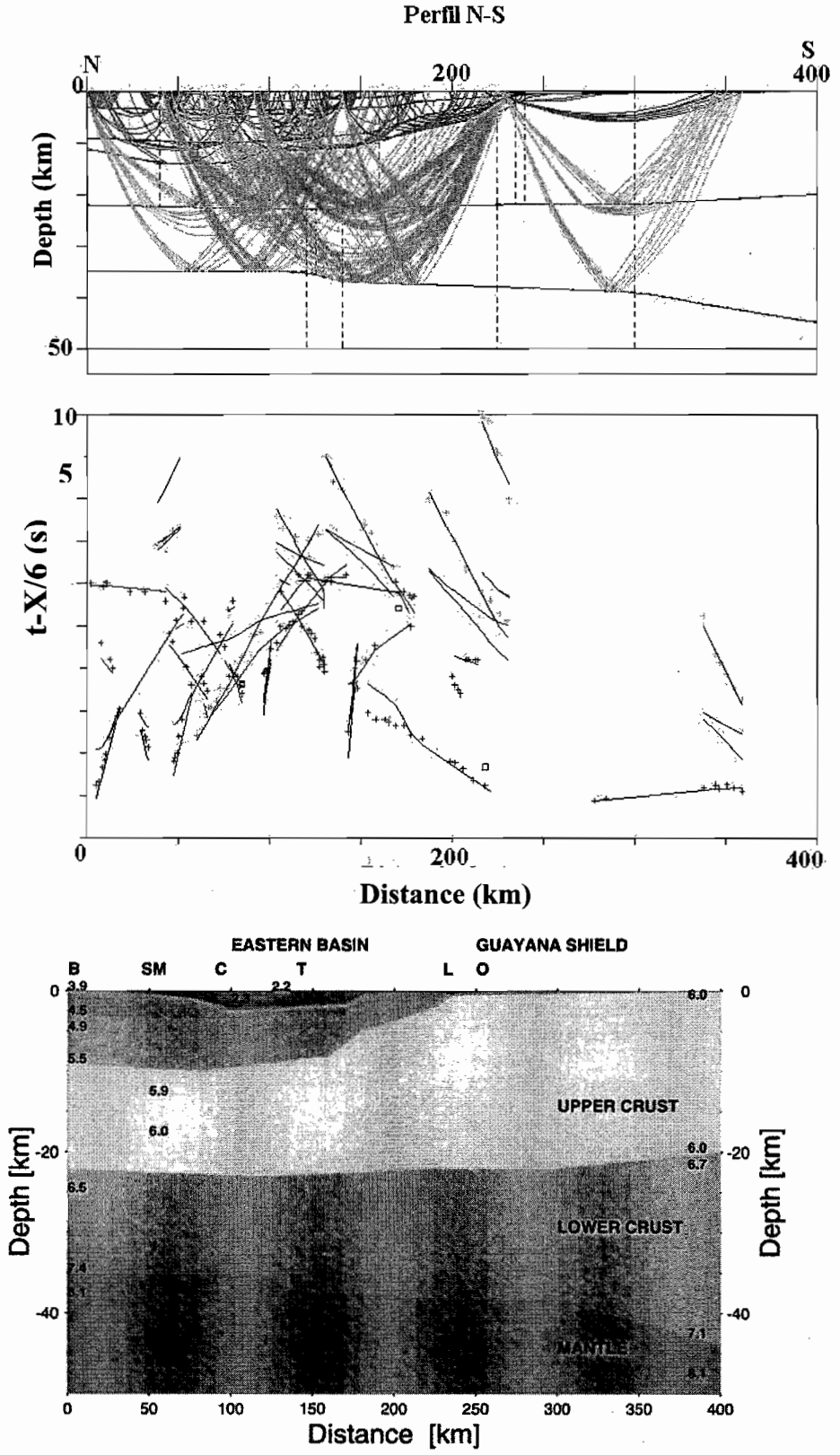

Figure 4. 2-D modeling along the ECCO N - S profile with the calculated raypaths for the upper crustal (red) and lower crustal (light blue) phases (top), the observed (crosses) and calculated (black lines) traveltimes (center), and the derived velocity model (bottom). Shot points: B = Barcelona, SM = San Mateo, C = Cantaura, T = El Tigre, L = Limo; O = position of the Orinoco river.

INTERPRETATION AND CONCLUSIONS

After identifying the main crustal phases, 2-D modeling using the RAYINVR ray tracing program (Zelt, 1992) was applied to the data (Fig. 4). Arrivals from the upper crust can be observed up to 100 km recording distance

with maximum delays of about 3 s on the ECCO-profile and 4 s on the Serranía-profile. Along the ECCO N - S profile the seismic velocities of the sedimentary cover vary between 2.2 km/s down to 2 km depth in the central part of the basin and 3.9 to 5.9 km/s down to about 12 km in the northern part of the basin (Fig. 4).

Arrivals from intermediate levels of the crust cannot be observed in the record sections of the ECCO - profile. Nevertheless, clear refractions from intermediate crustal levels have been observed for the Guayana Shield (ECOGUAY - profile in W-E direction crossing at profile-km 400) with a velocity of 6.7 km/s at 20 km in depth (Schmitz et al., 2002). The total crustal thickness is derived from weak Moho reflections in the northern part of the profile (35 km) and stronger Moho reflections in the south (38 km).

The ECCO-profile crosses the whole Eastern Venezuelan Basin and indicates strong lateral velocity variations for the upper 10-12 km. From geodynamic modeling done some 50 km further east (Jácome, 2001), foreland sediments with a thickness of 7 km were derived, with the passive margin sediments reaching down to 10-15 km in depth. These results coincide well with the velocity model presented here, where strata with a seismic velocity up to 5.5 km/s reach down to a maximum of 9 km, possibly corresponding to the foreland sediments. The strata with a velocity of 5.9 km/s, which reach down to 11-13 km in depth, might correspond to the passive margin sediments. There is only few information on the cristalline crust below. The total crustal thickness increases from 35 km in the north to 38 km close to the Orinoco river in the south (on the northern edge of the Guayana Shield). Further south, a crustal thickness of 42-46 km had been derived for the shield region (Schmitz et al., 2002).

ACKNOWLEDGEMENTS

The seismic field work required the active participation of FUNVISIS, USB, UCV, INTEVEP and IRIS staff and students which were very enthusiastic: A. Martins, Angel Diaz, Alex. Diaz, B. Greschke, G. Malavé J. García, M. Romero, M. Bonilla, M. Schmitz, L.M. Rodríguez, L. Cabrera, L. Castillo, L. Melo, R. Castilla, V. Cano, V. Rocabado, W. Zamora - our sincere thanks to all of them. Many thanks to REPSOL-YPF (Campo Quiamare-La Ceiba), A. Puertas (Hato Ojo de Agua), L. Bolivar (Finca La Candelaria, G. Martínez, (Finca El Sabilar), L.H. Yaselli (Fundo Sabaneta), M. Freites (Cantaura), R. Mazzumaccelli (Hato Nuevo), M. A. García (Hato Loma Blanca) for permits for drilling and blasting. We also thank W. Hidalgo (Rotopercusiones Caroní) and C. Roberts and O. Valera (Suelopetrol) for drilling and L. Pregitzer, M.E. Afanador and F. Chirinos (CAVIM) for blasting. Special thanks to the IRIS/PASSCAL Instrument Centre, which gave the 193 TEXANs for recording and technical support in preparation and field work. The data collected during the experiment will be available via the IRIS Data Management Centre. The IRIS Consortium is supported by NSF grant EAR-9023505. Project financed by CONICIT No. S1-2000000685 with aditional funds for drilling and blasting from PDVSA-FUNVISIS No. 450050709.

REFERENCES

González de Juana, C., Arozena, C.J. and Picard, X.C., 1980. Geología de Venezuela y de sus cuencas petrolíferas. FONINVES, Caracas, pp. 1031.

Hedberg, J.D., 1950. Geology of the eastern Venezuela basin (Anzoategui-Monagas-Sucre-eastern Garico portion). GSA Bull., 61, 1173-1216.

Jácome, M.I., 2001. The formation of the Monagas foreland basin: eastern Venezuela. PhD tesis, Univ. of Liverpool, 204 pp.

Martins, A., 2002. Estructura cortical en la Cuenca Oriental con énfasis en la determinación del espesor de la capa de sedimentos. Tesis, Universidad Simón Bolívar, Sartenejas, 142 pp.

Parnaud, F., Gou, Y., Pascual, J.-C., Truskowski, I., Gallango, O., Passalaqua, H. and Roure, F., 1995. Petroleum Geology of the central part of the Eastern Venezuelan Basin. In : Petroleum basins of South America, Tankard, Suárez and Welsink (eds.), AAPG Memoir 62, 741-756.

Passalaqua, H., Fernandez, F., Gou, Y. and Roure, F., 1995. Crustal architecture and strain partitioning in the Eastern Venezuelan Ranges. In : Petroleum basins of South America, Tankard, Suárez and Welsink (eds.), AAPG Memoir 62, 667-679.

Schmitz, M., Chalbaud, D., Castillo, J. and Izarra, C., 2002. The Crustal Structure of the Guayana Shield, Venezuela, from seismic refraction and gravity data. Tectonophysics, 345 (1-4), 103-118.

Zelt, C., 1992. Seismic traveltime inversion for 2-D crustal velocity structure. Geophys. J. Int., 108, 16-34.

LOW PALEOZOIC EXTENSIONAL TECTONIC EVIDENCE IN THE QUEBRADA DE HUMAHUACA. CORDILLERA ORIENTAL ARGENTINA.

Raúl E. SEGGIARO(1), Eduardo F. GALLARDO (2)

(1)Universidad Nacional de Salta – Buenos Aires 177 -(4400) – Salta – Argentina (raul@ciunsa.edu.ar)
(2)Universidad Nacional de Salta – Buenos Aires 177-(4400) – Salta – Argentina (egallardo@ciunsa.edu.ar)

KEY WORDS: Cordillera Oriental – Argentina- Extensional tectonic – Paleozoic structures

INTRODUCTION

The Cordillera Oriental mountain belt presents a steep relief cut by erosion, with an excellent outcrop exposition. The stratigraphy is integrated by the Puncoviscana Formation leptometamorphic basement, Meson Group cambrian sandstones, quarzites and pelites, Salta Group cretacic and paleogene continental deposits, Maimara formation neogene fluvial deposits and quaterary alluvial fans.

There are several tectonic events superposed that make it difficult to interpret the oldest structures. The structural features registered up to the present consist of short radius curvature folds with axial planes clivaje related in the basement, folds and thrusts attributed to the upper ordovician Ocloyic diastrophic phase (Mon et al., 1993), extensional cretacic faults some of them reactivated (Rodriguez et al, 1997) and andean thrusts with detachment levels that involve large basement thickness.

In this paper, the first evidence of extensional fault temporality limited between cambrian and low tremadoc deposits is presented.

PALEOZOIC EXTENSIONAL STRUCTURES

Coquena creek

The ordovician beds that outcrop in Coquena creek, located to the west of Purmamarca village (figure1), show a faunistic association from low Tremadoc to Llanvir ages (Harrington y Leanza, 1957).

The low Tremadoc sediments overlap in unconformity the Puncoviscana Formation and brecciated relictic outcrops belonging to the Meson Group. In the contact with the ordovician deposits the quarzite cambrian blocks and olistolites are evolved within pelitic ordovician matrix . Cambrian deposits show discontinuous outcrops of beds broken by a 10 to 20m thick fault zone.

The ordovician beds cover the fault zone irregularities and unlike the underlying rocks, do not present evidence of having been affected by the fault.

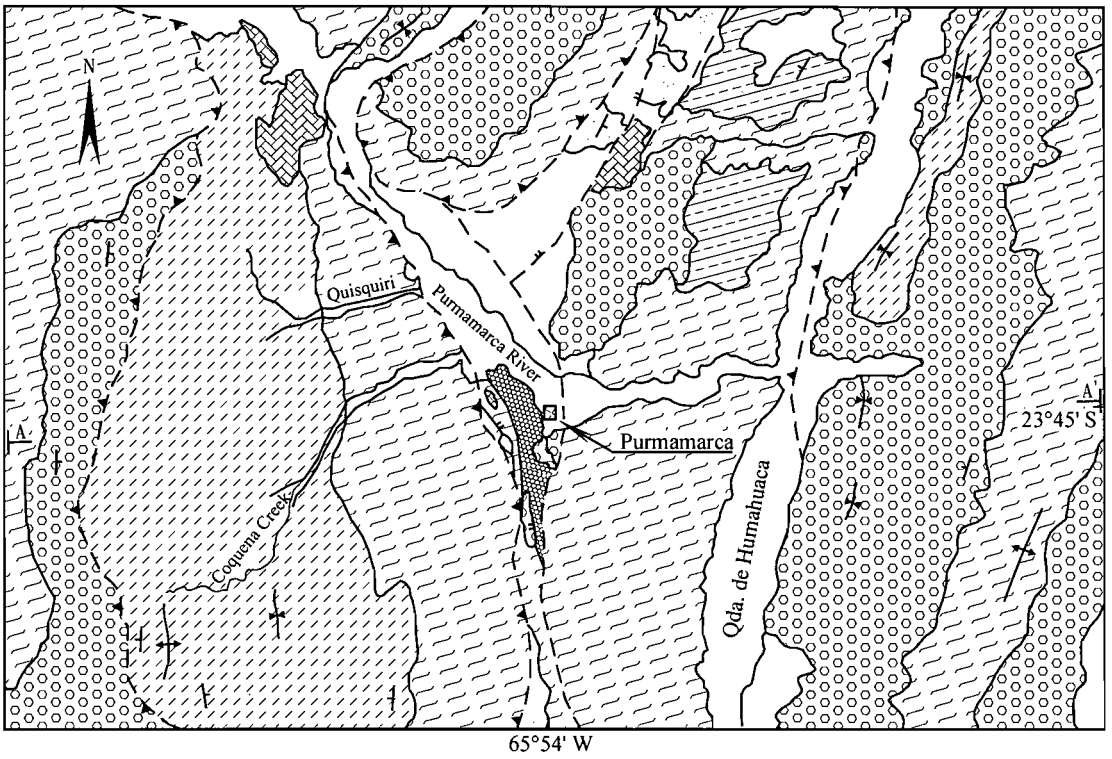

Figure N°1 - Geological map. References in figure N°2

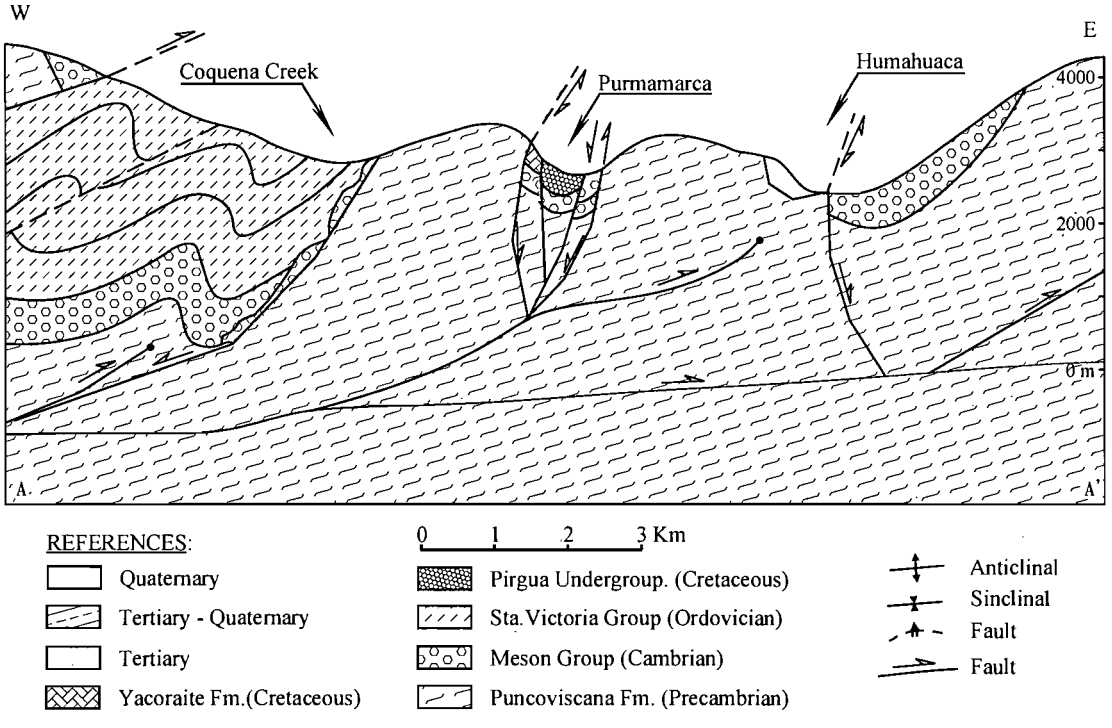

Figure N°2 - Cross section A - A'.

The relationship observed between the units involved, indicates that low tremadoc sediments fill the floor wall of a west dipping normal fault that affected only Cambrian and basement rocks (figure2).

The low tremadoc ordovician deposits occurred sintectonically or immediately after a first order extensional tectonic event. As the generation time of the normal fault is between upper cambric and low tremadoc ages, it is the first structural evidence that indicates the extensional tectonic nature of the Iruya diastrophic phase.

Quebrada de Humahuaca - Rio Grande river

Along the Quebrada de Humahuaca between Tumbaya and Maimará villages, a fault puts in contact the Meson Group with the Puncoviscana Formation (figure 3).

The geometric relations and the unit disposition involved show an extensional east dipping fault (figure4). This fault was folded in some stretch and rotated to subvertical 80° dip in others by the Andean movements.

The original orientation of the fault plane previous to the Andean tectonics was obtained by restoring to the horizontal the tertiary beds lying on Puncoviscana Formation in the footwall and the Cambrian beds of the hanging wall fault block. As a result an original deep fault plane ranging between 45° to 60° E was obtained. The Yacoraite Formation cretacic carbonatic deposits overlap unconformably both the basement rocks of the occidental fault block and Cambrian rocks of the oriental block.

A similar relationship occur in the Alfarcito valley (figure 3) where Yacoraite Formation covers a fault within basement and ordovician deposits (figure 4).

The base relations of the Yacoraite Formation show a precretacic floor structured by normal faults with more than 500 m vertical displacement (figure 4).

The normal faults covered by the Yacoraite Formation and the absence of the cretacic sin rift Pirgua Subgroup are evidences that these faults occurred in a precretacic tectonic extensional event. We consider that both precretacic normal faults could belong together with the already discussed Coquena normal fault to the Iruya diastrophic phase. The Iruyics structures may influence the development of the diastrophic fases detected within the ordovician basin and the structuration of the Cordillera Oriental during the Andean tectonics.

ACKNOWLEDGEMENTS : This is a contribution to the CIUNSa Project N°927 and the SEGEMAR Project: Tectonic Inversion in Western Cordillera and Puna.

REFERENCES

Harrington,H.J. y Leanza, A.F., 1957. Ordovician trilobites of Argentina. University of Kansas, Special Publication, 259. Kansas.

Heredia,N, Rodriguez Fernández, R. Seggiaro,R. y Gonzalez M. 1997. Estructuras de Inversión Tectónica en la Cordillera Oriental de los Andes, entre 23° y24° S, Provincia de Jujuy, NO de Argentina. Acta Geológica Hispánica. V.32 N°1-2 P.93 – 102. Barcelona.

Mon, R., Rahmer, S. y Mena,R. 1993. Estructuras superpuestas en la Cordillera Oriental, provincia de Jujuy. 12° Congreso Geológico Argentino y 2° Congreso de Exploración de Hidrocarburos. Actas III: 48 –54, Mendoza.

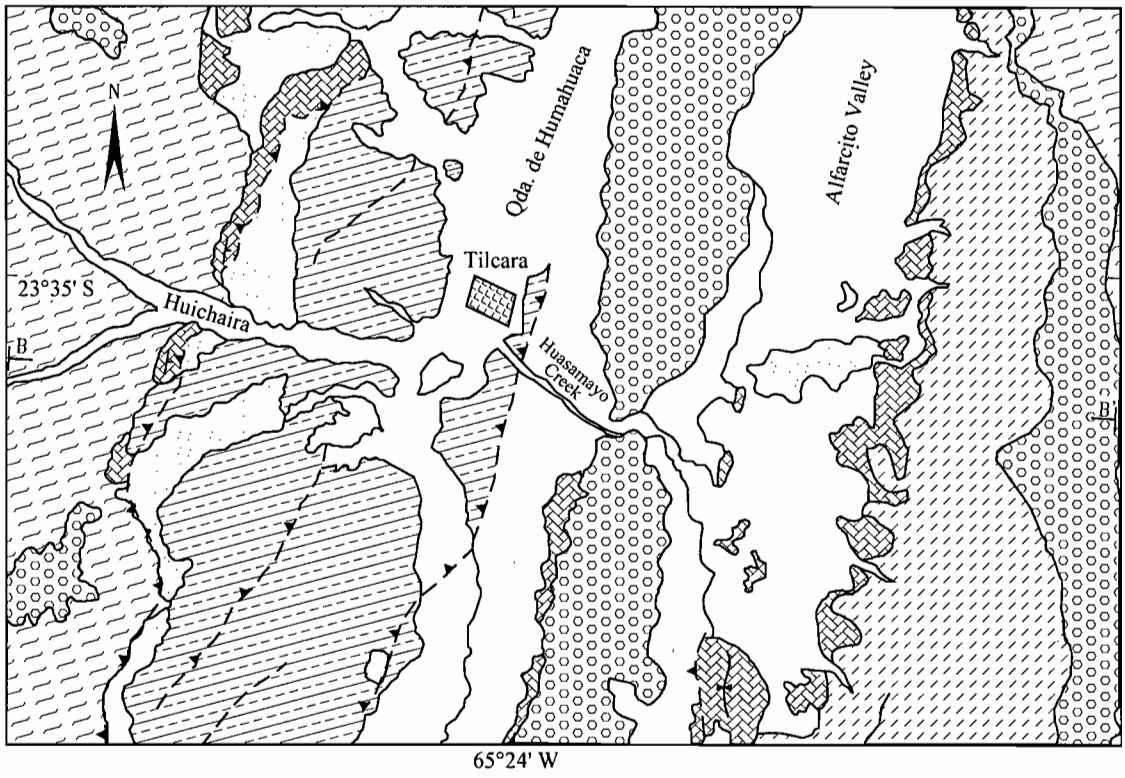

Figure N°3 - Geological map. References in figure N°4

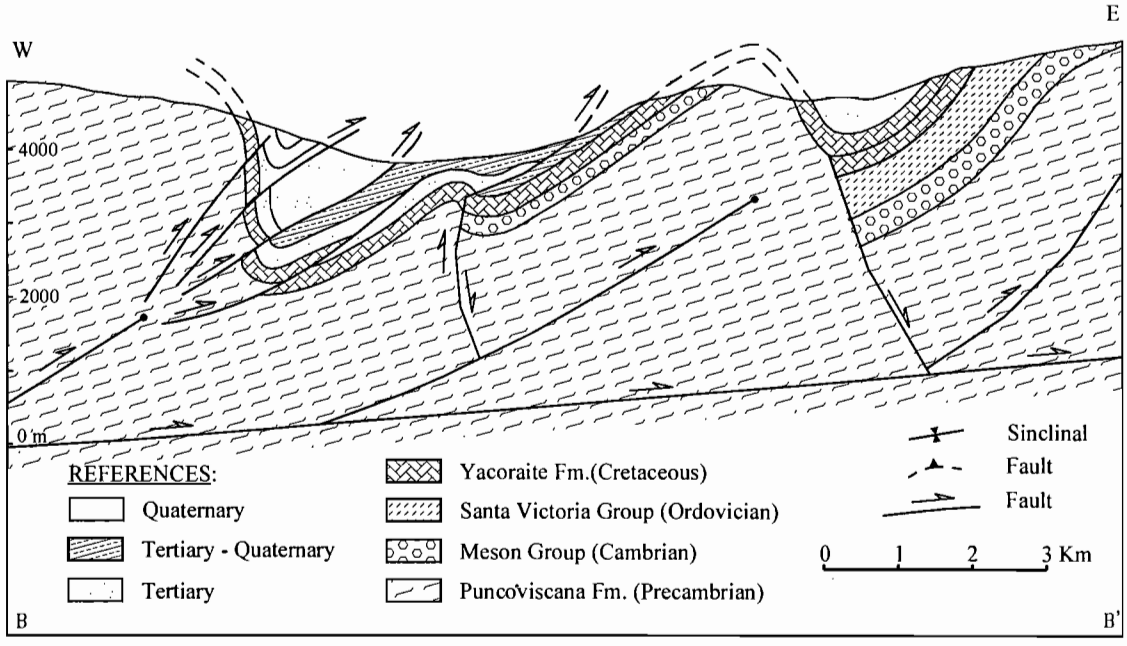

Figure N°4 - Cross section B - B'.

NEVADO DE LONGAVÍ: ANOMALOUS INCOMPATIBLE ELEMENT-POOR COMPOSITIONS IN THE SVZ OF THE ANDES (36.25°S).

Daniel SELLÉS (1), Carolina RODRÍGUEZ (1) and Michael DUNGAN (1).

(1) Section des Sciences de la Terre, Université de Genève, 13 Rue des Maraîchers, 1211 Genève 4, Switzerland. (Daniel.Selles@terre.unige.ch)

KEY WORDS: SVZ, amphibole, low-K dacites, Longaví-Osorno Segment.

INTRODUCTION

Nevado de Longaví (NL) is a dominantly andesitic late Quaternary stratovolcano located at 36°12'S-71°10'W in the Southern Volcanic Zone of the Chilean Andes (Fig. 1). It is the northernmost center of the Longaví-Osorno Segment (segmentation scheme of Dungan et al., 2001), whose front is located some 15-18 Km trench-wards with respect to the southern terminus of the segment just to the north (Tatara-San Pedro complex; 36°S). A general feature of the SVZ is that volcanoes within segments are commonly similar in comparison to abrupt changes in magma chemistry and mineralogy across segment boundaries. In contrast, the compositional and mineralogical characteristics of Longaví magmas violate all expectations based on the petrologic character of adjacent volcanic centers, and these magmas are unique in the SVZ. They were unusually wet, anomalously low in most incompatible elements (K, Rb, Nb, Y), and have many features in common with inferred slab-melts even though this origin appears to be untenable on the basis of it geodynamic framework.

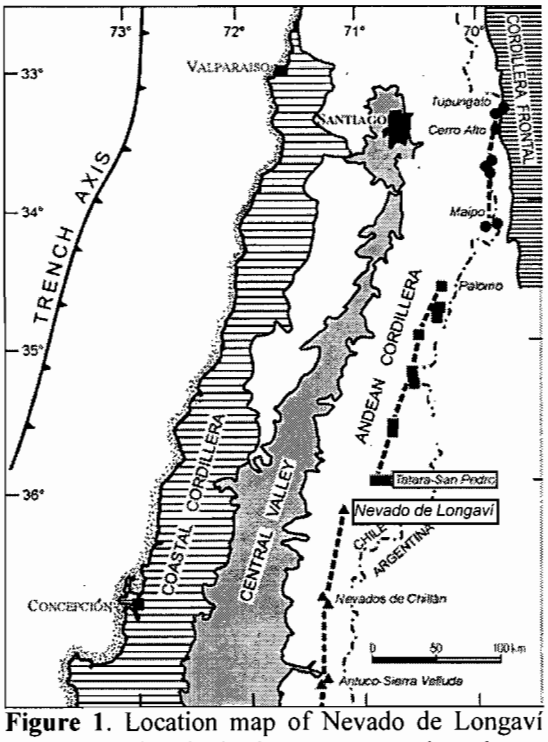

Figure 1. Location map of Nevado de Longaví volcano and neighboring centers. Also shown segmentation scheme of the SVZ used in text (from Dungan *et al.*, 2001)

VOLCANIC GEOLOGY

Nevado de Longaví (NL) overlies folded and weakly metamorphosed continental volcaniclastic and sedimentary strata (Eocene-Early Miocene Cura-Mallín Formation; Muñoz & Niemeyer, 1984), which in turn are intruded by Miocene plutons. The aerially extensive, impressively voluminous, and dominantly mafic Pleistocene Villalobos volcanic complex extends to the south of NL and occupies the gap between this and Nevados de Chillán.

Main cone: The late Quaternary main edifice comprises primarily thick andesitic lavas that radiate from a source coincident with Holocene summit domes. Reconnaissance sampling of the E-SE flanks (around 30

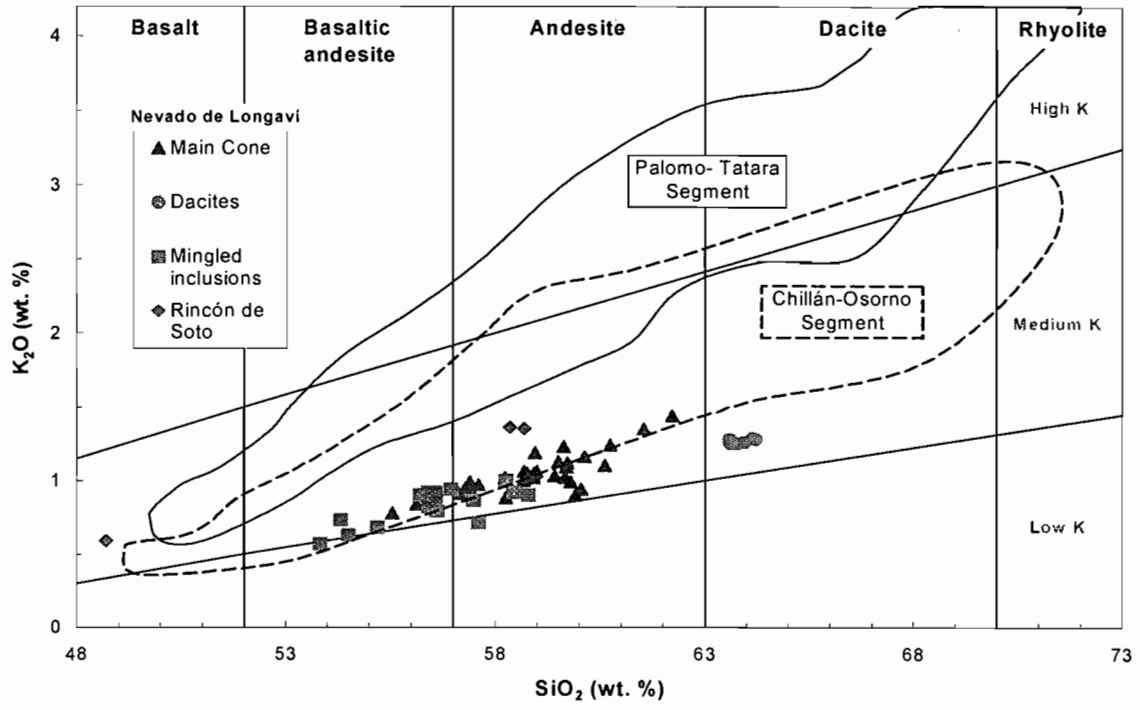

Figure 2: K2O vs. SiO2 diagram, showing samples from Nevado de Longaví volcano as compared to contents in Palomo-Tatara segment and center between Chillán and Osorno.

samples) has yielded only andesitic lavas (55-62% SiO_2), but many contain mafic mingled inclusions and a variety of plutonic-textured xenoliths (both as yet poorly sampled). The phenocryst assemblage is generally plag + cpx ± opx, but both olivine and hornblende are occasionally present, probably as xenocrysts recording magma mixing. We infer that a large depression on the E flank of Longaví is a pre-Holocene sector-collapse, now partly filled with Holocene pyroclastic and volcaniclastic deposits.

Holocene pyroclastic deposits: In contrast with the apparently dominantly effusive activity preserved in the main edifice, demonstrably Holocene units are pyroclastic deposits and associated summit domes. Proximal Holocene eruptive products are preserved mainly within a sector-collapse basin on the east flank as a coarse block and ash flow deposit, perhaps with some distal fall-out equivalents (J.A. Naranjo, pers. comm.). The two youngest deposits recognized are: (1) a widespread andesitic (62% SiO_2) white pumice deposit which is up to 25 m thick proximally (single pumices >30 cm) that extends as a thin fall deposits at least 20 Km to the east, and (2) a block and ash deposit of variable thickness (from 65 to 15 m) marked by distinctive prismatically jointed blocks (up to 5 m length) of a hornblende porphyritic silicic andesite (63-64% SiO_2) that contains abundant mingled mafic magmatic inclusions (53-58% SiO_2; exceptionally rich in hornblende). Unsampled summit domes are presumed to be near-vent equivalents of these pyroclastic units. An unusual aspect of the pumiceous andesite deposit is the widespread occurrence of nearly monolithologic rounded and polished granitoid lithic fragments (10-50 cm) many kilometers from the vent, which are compositionally distinct from local granite outcrops.

Rincón de Soto satellite center: The previously unrecognized monogenetic Rincón de Soto center (vent located 10 Km to the south of the summit of NL) forms a single Holocene cone and andesitic flow (59% SiO_2) which is spectacularly charged with both mingled basaltic magmatic inclusions (49% SiO_2; hbl + plag + mgt) and a variety of plutonic-textured xenoliths that locally approach 20 vol. % of the flow. This mingled flow

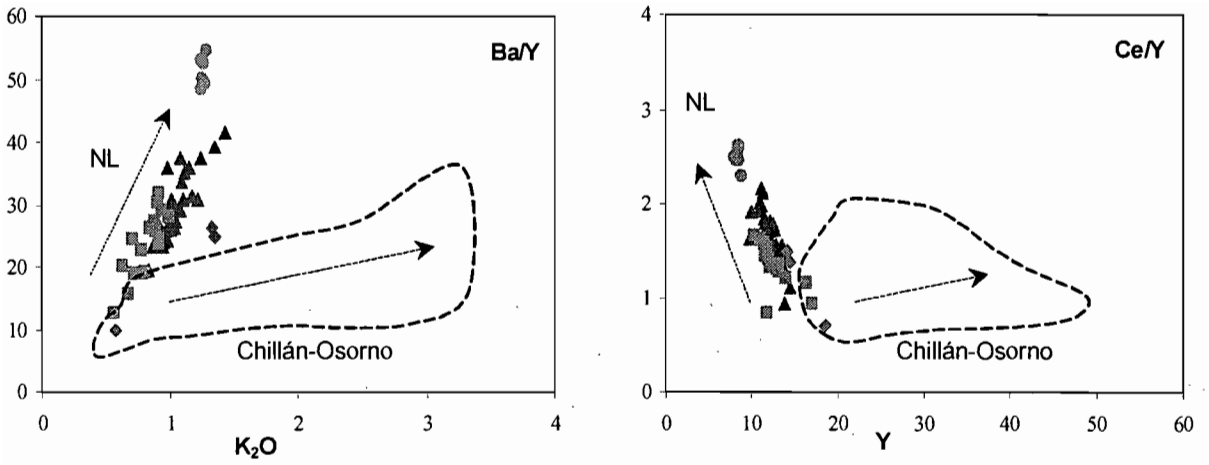

Figure 3: Selected diagrams comparing Nevado de Longaví evolutionary trends to the behavior of the rest of the segment (Chillán-Osorno). Arrows indicate direction of increasing silica contents. Other symbols as in Fig. 2

exhibits many characteristics in common with Holocene and pre-Holocene products of NL, and is considered to be a manifestation of a physically separate but fundamentally similar magmatic system.

CHEMISTRY AND PETROLOGY

The magmatic products at NL are strikingly anomalous in terms of combined mineralogy and chemistry compared to all other volcanoes of the SVZ. Differentiation trends at other centers in the same arc segment (Nevados de Chillán southward to Osorno; 36.8-41.1°S) are characterized by more pronounced increases in K with increasing silica (Fig. 2) and are notably devoid of hydrous minerals, even in rare rhyolites that appear to be products of extreme fractional crystallization. The NL silicic andesites and dacites that contain hornblende (62-64% SiO_2) and associated hornblende-rich quenched inclusions (49-59% SiO_2) are characterized by unusually low incompatible elements contents combined with high Mg#'s (around 50 for the dacites, while the most mafic inclusions have values around 60), K/Rb, Ce/Y, Sr/Y, and Ba/Y. The high Ba/Y and Sr/Y ratios of NL magmas are due in part to decreasing Y with increasing SiO_2 (marked suppression of Y and HREE enrichments with increasing differentiation), which is contrary to the trends at all other volcanoes within the segment as far south as Osorno (Fig. 3). The only evolved magmas in the SVZ with similar phenocryst assemblages and increasing Sr/Y with increasing differentiation are from the andesite-dacite cones near 33.5°S (e.g. Tupungato and Cerro Alto). At these centers, however, the high ratios are accompanied by much higher K_2O and other incompatible trace element contents than any Longaví lava. Crustal assimilation is thought to be a dominant factor on controlling the chemistry of evolved magmas in the northern segment of the SVZ (Hildreth & Moorbath, 1988), but such a process seems difficult to invoke for Longaví whose basement does not substantially differ in composition or in thickness from the crust underlying neighboring centers.

By far the closest Andean compositional analogies to the Longaví dacites are lavas from Mt. Burney in the southern AVZ (54.4°S) which are proposed to be partial melts of hot young subducted oceanic crust (e.g. Stern & Kilian, 1996). Such a magma generation mechanism finds little support in the geodynamic setting of NL, in that mid Tertiary oceanic crust is currently being subducted beneath this center (36-37°S). On the other hand, mafic end-members from NL seem to respond to the latitudinal systematic variations predicted by Hildreth &

Moorbath (1988). Although no detailed modeling has been carried out so far, simple variation diagrams point towards a mixing trend between a "normal" (but highly hydrated) basaltic end-member and an "anomalous" more silicic component.

CONCLUSIONS

There is little doubt that both magma generation and evolution conditions at Longaví differ dramatically from those volcanoes located immediately to the north and south. The low-K hornblende-bearing Longaví magmas were exceptionally water-rich and anomalously low in many incompatible elements. Although the abundance of granitic xenoliths suggests important physical magma-crust interaction, chemical interactions seem to be minor in the light of the unusually low concentrations of incompatible elements. We provisionally infer enhanced amphibole stability conditions, related to the highly hydrous character of the magmas, which could play a major role in trapping incompatible elements during magma evolution. We suspect that proximity to the subducted Mocha Fracture Zone may play a role in their water-rich character.

ACKNOWLEDGEMENTS

This work is supported by Swiss Fonds National Grants 20-63950.00 and the collaboration of SERNAGEOMIN-Chile. Special thanks to Dr. Moyra Gardeweg.

REFERENCES

Dungan. M, Wulff, A., Thompson, R. 2001. Eruptive stratigraphy of the Tatara-San Pedro complex, 36°S, Southern Volcanic Zone, Chilean Andes: Reconstruction method and implications for magma evolution at long-lived arc volcanic centers. Journal of Petrology, v. 42, N. 3, pp. 555-626.

Hildreth, W. & Moobath, S. 1988. Crustal contributions to arc magmatism in the Andes of Central Chile. Contributions to Mineralogy and Petrology, 98:455-489.

Muñoz, J. & Niemeyer, C. 1984. Hoja Laguna del Maule, Regiones del Maule y del Bío Bío. Servicio Nacional de Geología y Minería, Carta Geológica de Chile No.64.

Stern C.R. & Kilian R. 1996. Role of the subducted slab, mantle wedge and continental crust in the generation of adakites from the Andean Austral Volcanic zone. Contrib. Mineral. Petrol., 123, 263-281.

LITHOSPHERIC-SCALE TRANSCURRENT FAULT SYSTEMS IN ANDEAN SOUTHERN PERU

Thierry SEMPERE (1), Javier JACAY (2), Michel FORNARI (3), Pierrick ROPERCH (4), Harmuth ACOSTA (5), Conrado BEDOYA (6), Luis CERPA (5), Alexander FLORES (6), Laurent HUSSON (1), Ivanoff IBARRA (5), Omar LATORRE (5), Mirian MAMANI (5), Paola MEZA (5), Francis ODONNE (7), Yovani ORÓS (5), Adán PINO (6) and Rildo RODRÍGUEZ (8)

(1) I.R.D.-Perú, La Mariscala 115, Lima 27; apartado postal 18-1209, Lima 18, Peru (sempere@terra.com.pe)
(2) Escuela de Ingeniería Geológica, Universidad Nacional Mayor de San Marcos, apartado 3973, Lima 100, Peru
(3) I.R.D. and Laboratoire de Géochronologie, UMR Géosciences Azur, Université de Nice, France
(4) I.R.D.-Chile, casilla 53390, Correo Central, Santiago, Chile
(5) Facultad de Ingeniería Geológica, Universidad Nacional San Antonio Abad del Cusco, Cusco, Peru
(6) Escuela de Ingeniería Geológica – Geotecnia, Universidad Nacional Jorge Basadre Grohmann, Tacna, Peru
(7) Laboratoire de Dynamique des Bassins Sédimentaires, Université Paul Sabatier, Toulouse, France
(8) INGEMMET, Av. Canadá 1470, apartado postal 889, Lima 41, Peru

KEY WORDS: Peru, Bolivian Orocline, transcurrent tectonics, magmatism, syntectonic basins

INTRODUCTION

Although Andean southern Peru forms the northwestern termination of the Bolivian Orocline, knowledge of its geology has little progressed in the last 20 years, partly due to the civil war that spread in the region during the 1980s and early 1990s. As a consequence, outdated information and concepts are generally still used in current assessments and syntheses, and updated data are needed. This short descriptive contribution presents the principal tectonic elements we currently recognise in southern Peru, and their relationships with syntectonic sedimentary basins. We observe that the most prominent deformational systems in this part of the Bolivian Orocline are dominantly transcurrent, and that many magmatic manifestations are associated with them.

LARGE-SCALE TECTONIC STRUCTURE OF ANDEAN SOUTHERN PERU

One of the main structural and paleotectonic element in southern Peru appears to be the Cusco-Lagunillas-Laraqueri-Abaroa structural corridor (CECLLA in Spanish), which strikes ~N150E and shows a remarkable 20°-obliquity to the regional Andean trend (Fig. 1). This large dextral wrench system is ~40-to-~80 km-wide and displays a variety of tectonic, magmatic and sedimentary features:

- Along the CECLLA, pre-Oligocene rocks are locally intensely deformed (folded, sheared, and/or pervasively fractured), whereas northeast of it they are not, and reverse and strike-slip faults are observed. Paleozoic rocks crop out only northeast of the CECLLA, which moreover coincides with the northeastern limit of the Dogger-age deep-water facies of the Jurassic Arequipa basin. Immediately southwest of the CECLLA, the rarely exposed pre-Cenozoic rocks are much deformed Jurassic strata and unconformable, less deformed, mid-Cretaceous deposits. Immediately northeast of the CECLLA, the little deformed Jurassic strata are preserved below the Early Cretaceous erosional unconformity, and constrastingly display terrestrial and subordinate shallow-marine facies (Sempere et al., 2000). In the latest Jurassic - Early Cretaceous interval, deformational and thermal phenomena affected at least parts of the CECLLA, which locally resulted in an angular unconformity, and uplifts (Newell, 1949; Clark et al., 1990; Sempere et al., 2002). South of 15°S, thick Late Cretaceous - Paleogene strata, representing the foreland fill of the paleo-Andes, are known only from northeast of the CECLLA (excepted one occurrence within it). Eocene plutons (southwest of Cusco, north of Tacna) are known only from west of (or within) the CECLLA (Andahuaylas-Yauri batholith southwest of Cusco; Ataspaca-Ticaco batholith northeast of Tacna-Mal Paso). Due to these characteristics, the Intra-Andean Boundary Fault (FLIA in Spanish) conjectured by Sempere (1995) should be identified with the CECLLA.

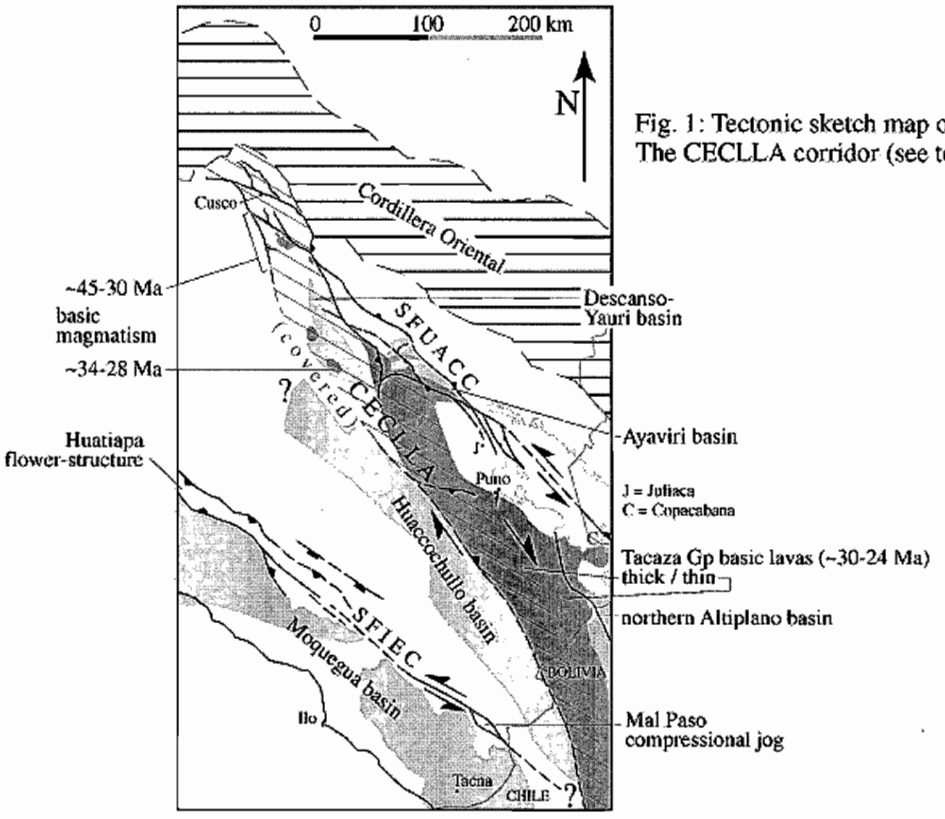

Fig. 1: Tectonic sketch map of Andean southern Peru. The CECLLA corridor (see text) is obliquely hatched.

- The CECLLA was the locus of emplacement of the Tacaza Group igneous rocks, which include mostly alkaline basic volcanics (dated 30-24 Ma; Fornari et al., 2002) and basic to felsic intrusions that also display alkaline affinities (Mamani and Ibarra, 2000). Their geometric and geochemical characteristics show that this magmatic corridor was not directly linked to subduction but rather functioned as a lithospheric-scale wrench system that permitted mantle melts to access the surface. Folding of the Tacaza basic flows in the CECLLA is post-dated by Late Miocene or younger strata.

- The Tacaza Group *sensu lato* also includes volcano-sedimentary units that were deposited in twin Oligo-Miocene basins west (Huaccochullo basin, Peru) and east (northern Altiplano basin, Bolivia) of the CECLLA during its tectonic-magmatic activity; the infills of these two basins display noteworthy stratigraphic similarities and symmetries. The basal Tacaza volcano-sedimentary strata commonly post-date previous strata with an angular unconformity even outside the CECLLA. Some smaller basins, such as the Early-Middle Miocene Descanso-Yauri basin and the Late Miocene Paruro basin, developped within the CECLLA.

- Normal or transtensional faulting is currently particularly active within the CECLLA (areas of Pomacanchis, Langui-Layo, Lagunillas, etc.), creating hemigrabens in which lakes are formed. Senestral N120E faulting (including one focal mechanism solution for a crustal seism in the Lagunillas area) is common, and compatible with the dextral, ~N150E-oriented, CECLLA system. Late Neogene basic volcanism and hydrothermalism are also documented in the corridor area.

The ~N130E-trending Urcos-Ayaviri-Copacabana-Coniri fault system (SFUACC in Spanish) is a senestral transcurrent system that bounds the Cordillera Oriental domain and has an important SW-verging reverse component (Fig. 1). Although it was previously considered as a thrust in nearby Bolivia (Sempere et al., 1990), many SFUACC faults appear (sub) vertical. The close association of Neogene magmatism with the SFUACC (Redwood and Macintyre, 1989), including mantle-derived rocks occurring right on the main faults in Peru (Carlotto, 1998) and Bolivia (Hérail et al., 1993), definitely demonstrates that it is a crustal to lithospheric wrench system. The CECLLA and SFUACC become coalescent south of Cusco and in their NNW prolongation the Cordillera Oriental presents a major oroclinal deflection (Fig. 1). The development and syndepositional deformation of the rhombic Oligo-Miocene Ayaviri basin was controlled by major SFUACC faults.

The structure of southernmost Peru is dominated by the senestral, N125E-trending, Incapuquio-El Castillo fault system (SFIEC in Spanish; Jacay et al., this symposium), which is still seismically active and includes large and small flower-structures that have exhumed Precambrian basement (Fig. 1). Faults in this system have dips ranging from 90° (dominant) down to 35°, and a reverse component generally uplifting the NE compartments. The SFIEC serves as a first-approximation boundary for the plateau that extends to the northeast and supports the Plio-Quaternary volcanoes. At least east of 70°10'W, specific SFIEC faults display gouge facies that grade into subvertical mylonite bands (reaching ultramylonite and possibly even pseudotachylite facies in the east), which are ~100 m to ~3 km - wide. These fault rocks are particularly found in restraining bends and compressional jogs of the eastern SFIEC, i.e. in the internal region of the symmetry axis of the Bolivian Orocline. Conglomerate distribution and thickness show that the SFIEC formed the active northeastern boundary of the Oligocene Moquegua basin. It is likely that the abundant arc magmatism represented by the nearby, deformed, Late Cretaceous-Early Paleogene Toquepala Group was emplaced in relation with transpression along the SFIEC (following Saint-Blanquat et al.'s [1998] model); significantly enough, many coeval plutons occur in the Huatiapa flower-structure. Although it is largely buried in northern Chile below the thick Neogene volcanic rocks of the Cordillera Occidental, the SFIEC may interrupt against the CECLLA or coalesce with it.

CONCLUSIONS

Because magmas tend to ascend subvertically from depths ranging from the mid-crust to the lithospheric mantle, the close association of igneous rocks, partly derived from the mantle, with the CECLLA, SFUACC, and SFIEC, demonstrates that these fault systems are of lithospheric scale and subvertical.

We believe that recognition of lithospheric-scale wrench zones in southern Peru challenges the paradigmatic assumption that the Bolivian Orocline Andes were built by pure crustal shortening. Tectonic and magmatic phenomena akin to lateral expulsion of large lithospheric blocks now appear to have played significant roles. It is probably no coincidence, for instance, that >30° counterclockwise tectonic rotations of the Moquegua basin (Roperch et al., 2002) and intense mantle-derived magmatism along the CECLLA (Fornari et al., 2002) both developed during the Oligocene.

REFERENCES

Carlotto, V., 1998. Evolution andine et raccourcissement au niveau de Cusco (13°-16°S, Pérou). Ph.D. dissertation, Université de Grenoble, France, 159 p.

Clark, A.H., Kontak, D.J., Farrar, E., 1990. The San Judas Tadeo W (–Mo, Au) deposit: Permian lithophile mineralization in southeastern Peru. Economic Geology, v. 85, p. 1651–1668.

Fornari, M., Mamani, M., Ibarra, I., Carlier, G., 2002. Datación del período volcánico "Tacaza" en el Altiplano de Perú y Bolivia. XI Congreso Peruano de Geología, Lima, in press.

Hérail, G., Soler, P., Lizeca, J.L., Bonhomme, M.G., 1993. Evolution géodynamique de la transition entre l'Altiplano et la Cordillère Orientale au nord d'Oruro (Bolivie): implications sur le déroulement de l'orogénèse. Comptes Rendus de l'Académie des Sciences de Paris, série II, v. 317, p. 515-522.

Jacay, J., Sempere, T., Husson, L., Pino, A., 2002. Structural characteristics of the Incapuquio fault system, southern Peru. V International Symposium on Andean Geodynamics, Toulouse, this volume.

Mamani, M., Ibarra, I., 2000. Magmatismo y tectónica meso-cenozoica del Altiplano y del borde noreste de la Cordillera Occidental de la región de Puno. Tesis de grado, Universidad Nacional San Antonio Abad del Cusco, 82 p.

Newell, N.D., 1949. Geology of the Lake Titicaca region, Peru and Bolivia. Geological Society of America Memoir 36, 111 p.

Redwood, D.S., Macintyre, R.M., 1989. K-Ar dating of Miocene magmatism and related epithermal mineralization of the northeastern Altiplano of Bolivia. Economic Geology, v. 84, p. 618-630.

Roperch, P., Sempere, T., Arriagada, C., Fornari, M., Macedo-Sánchez, O., Tapia, C., 2002. New paleomagnetic constraints on the formation of the Bolivian Orocline. EGS 02-A-05121, in press.

Saint-Blanquat, M. de, Tikoff, B., Teyssier, C., & Vigneresse, J.-L., 1998. Transpressional kinematics and magmatic arcs. In: R.E. Holdsworth, R.A. Strachan & J.F. Dewey (eds), *Continental transpressional and transtensional tectonics*, Geological Society, London, Special Publications, v. 135, p. 327-340.

Sempere, T., 1995. Phanerozoic evolution of Bolivia and adjacent regions. *In*: A.J. Tankard, R. Suárez & H.J. Welsink (eds.), *Petroleum basins of South America*, AAPG Memoir 62, p. 207-230.

Sempere, T., Hérail, G., Oller, J., Bonhomme, M.G., 1990. Late Oligocene-early Miocene major tectonic crisis and related basins in Bolivia. Geology, v. 18, p. 946-949.

Sempere, T., Acosta, H., Carlotto, V., 2000. Estratigrafía del Mesozoico y Paleogeno en la region del Lago Titicaca: hacia una solución? X Congreso Peruano de Geología, Lima, p. 52 (abs.) and CD-ROM file GR50A (41 p.).

Sempere, T., Carlier, G., Soler, P., Fornari, M., Carlotto, V., Jacay, J., Arispe, O., Néraudeau, D., Cárdenas, J., Rosas, S., Jiménez, N., 2002. Late Permian - Middle Jurassic lithospheric thinning in Peru and Bolivia, and its bearing on Andean-age tectonics. Tectonophysics, v. 345, p. 153-181.

TRACE ELEMENTS GEOCHEMISTRY IN THE BOLIVIAN PROVINCE OF AMAZON BASIN

*Patrick SEYLER, Jean-Loup GUYOT, Laurence MAURICE-BOURGOIN**

LMTG-IRD, Université Paul Sabatier, 38, rue des trente-six ponts, F-31400 TOULOUSE.
* IRD-UnB Brasilia, Brazil.

KEY WORDS: Rivers, Geochemistry, Trace Elements, Bolivia, Amazon basin

INTRODUCTION

The geochemical studies on river water provide an insight into the weathering processes that control the distribution of elements and their fluxes. The upper drainage basins of the Amazon provide most of the dissolved and sediment yields leading to the Amazonian basin (Gibbs 1972; Stallard & Edmond, 1983, Guyot *et al,* 1995). The geochemistry of the Bolivian rivers have been extensively studied during the PHICAB (Hydrology and Climatology of Bolivia) program (Guyot *et al*, 1995, and ref. therein). But, geochemical studies concerned essentially the major element distribution. A limited number of papers inverstigate riverine transport of trace elements in the upper Amazon basin (Seyler et al, 1998; Elbaz-Poulichet et al, 1999) Our aim in the present work is to gain additional insight into origin and geochemical behavior of trace elements in a tectonically active area within the humid tropics. Because it represents an important part of the largest world river basin and also because it is a relatively pristine region where the contribution of the atmospheric marine source is limited (Stallard and Edmond, 1981), the Mamore and Beni basins are ideally suited to assess the different factors which act to the trace element transport by rivers.

STUDIED AREA AND SAMPLING

The Bolivian Amazon region lies in the upper middle part of the Madeira river basin. The basin extends from the Eastern Cordillera of the Andes to the Amazon Floodplain and the Brazilian Shield. The Madeira basin is large (900 000 km^2 upstream the Brazilian boundary) and provides most of the yield of the Amazon River for both dissolved loads and sediments (Roche and Fernandez1988; Guyot et al, 1995). Most of the samples analysed in the present study, have been collected in areas marked by pronounced topographic heights (Fig.1), decreasing from 3000 m to 100 m above sea level.

The Andean tributaries of the Beni River are draining intrusive granitic rocks covered by thick sedimentary deposits from the Ordovicien dominated by gray-green to dark shales and sandstones with ages ranging from the lower Paleozoic to Tertiary.

Carbonate rocks and evaporite formations form abundant outcrops in the Mamore subbasin, especially in the Grande river catchment whereas intrusive granites, associated with sulfide mineralization exist in the Beni subbasin.

Surface water samples were collected during three field campaigns, during the rainy season (march 1994), at the end of rainy season (may 1996), and at the end of dry season (November 1994). Trace elements analysis were performed on acidified samples using inductively coupled plasma mass spectrometry technique, according to the method described elsewhere (Seyler & Elbaz-Poulichet, 1996). Organic Carbon (DOC and POC) was determined by a high-temperature catalytic oxidation method (HTCO), using a TOC-5000 Instrument (Shimadzu). More detailled information is given by Cauwet (1994).

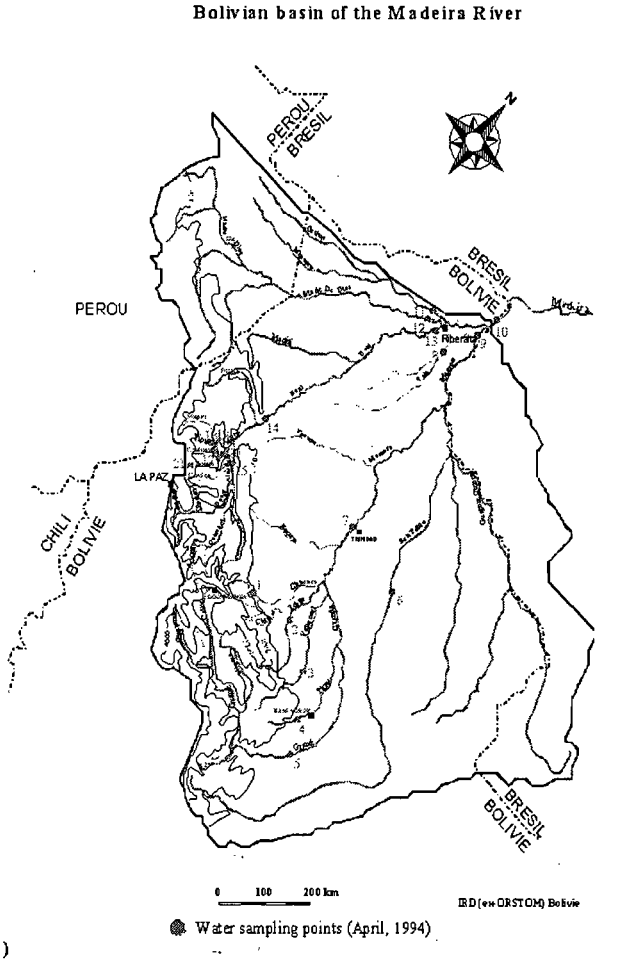

Fig. 1; Map of the Beni and Mamore subbasins showing sampling stations

RESULTS AND DISCUSSION

Dissolved material

Major constituent data allows us to distinguish two groups of river waters on the basis of pH and alkalinity (Fig 2). The first type has a low pH (<7.5) and low alkalinity (<1meq.l^{-1}) and is represented by 6 rivers from the Beni basin and 3 rivers from the Mamore Basin. Sulfate, which probably results from pyrite weathering, is the major anion in the rivers having pH ≤6.6. The other rivers are dominated by carbonate. The second water type with pH values >7.5 and with variable and often high alkalinity includes 8 rivers from the Mamore basin and 5 rivers from the Beni basin. In these rivers, pH increases regularly with alkalinity. SO_4^{2-} is the dominant anion in some of these waters and tends to increase with chloride and alkalinity. The weathering of sulphur contained in shales is probably a major source for sulfate, however some contribution from gypsum cannot be excluded. The ratio R= Si/Na+K-Cl (for most of the analysed

waters is generally low (< 2) indicating either a low contribution from weathering of silicate phases or formation of cation rich clays (Stallard, 1985) (Fig. 3)

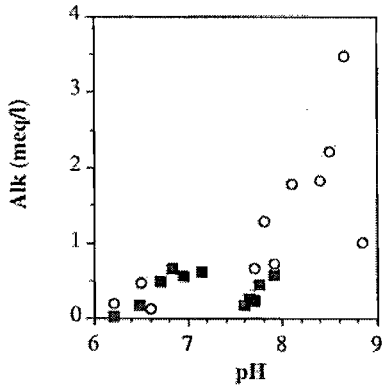

Fig. 2. Plot of Alkalinity vs. pH. Full squares: Beni subbasin; open circles: Mamore subbasin.

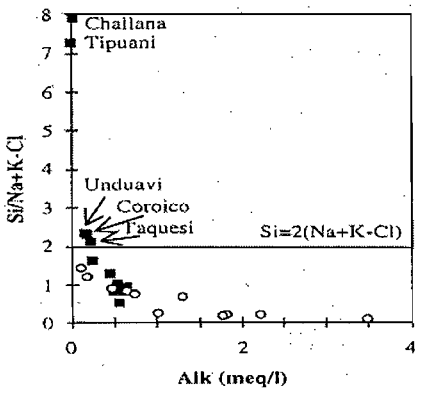

Fig 3 Si/Na+K-Cl vs. Alkalinity. Symbols as in Fig. 2

The plot of R versus Alkalinity displays an asymptotic trend and suggests a predominant role of carbonate as source for major dissolved cations.

The geochemistry of trace elements in. the Andean tributaries of the Mamore River are characterized by high concentrations of Mn (55 to 4290 nM), Sr (894 to 1943 nM), Mo (2.5 to 20.3 nM), Ba (99 to 399 nM) and U (0.3 to 3.9 nM) while high concentrations of As (1.9 to 310.6 nM), Zn (3.8 to 218.5 nM), Cd (0.03 to 1.66 nM) and Cs (0.06 to 2.57 nM) characterize Andean tributaries of the Beni River with maximum values measured in the Taquesi R. The geochemistry of trace elements can be divided into two groups according to their relationships with major elements and pH: (1) those with are correlated with major ions (Mo, Rb, Ba, U and to a lesser extent Zn and Cd) are controlled by their abundance in the most weatherable lithologies (carbonate rocks, evaporates and sulfides contained in shales), while silicate rocks have only a limited influence; (2) those witch are not correlated with major ions (Mn, Ni, Cu) are controlled by adsorption processes and/or complexation. Regarding to the anthropogenic influence, the high Zn, As, and Cd concentrations measured in the Taquesi river can be explained by important mining activities. High values of V measured at the end of the dry season in plain rivers ('black waters') can be correlated with the decreasing of the phytoplankton biomass.

Suspended Particulate Material (SPM)

Detailed evaluation of the mineralogy and major element chemistry of SPM have been already undertaken (Guyot, 1993). SPM is made up of clays (57 to 76%) and quartz (15 to 33%) with subordinate amounts of plagioclase and K-feldspar. Illite (53%), kaolinite (20%), chlorite (18%) and smectite (9%) are the main clay minerals in the Madeira basin. There is a high degree of correlation among the trace metals in SPM (Fig. 4). No obvious difference has been detected between the Beni and Mamore sub-basins. The fractionation of trace elements in the solid load results mainly from a binary mixing between quartz and

muscovite+illite. These minerals which are amongst the most resistant to chemical weathering have been introduced in river waters by physical erosion

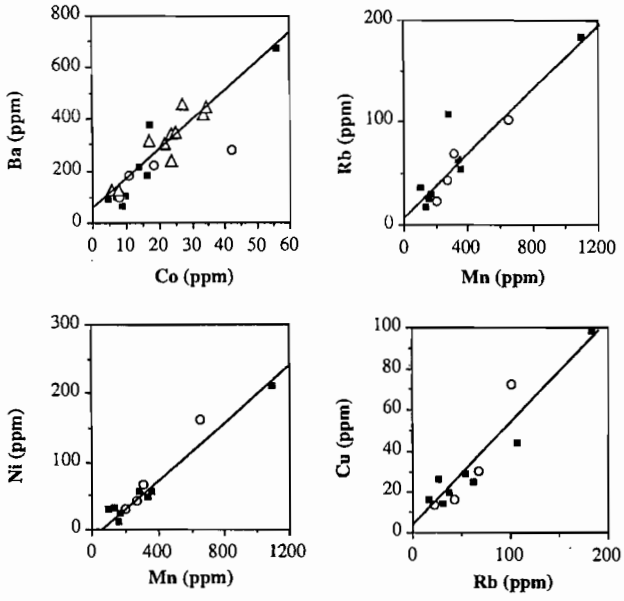

Fig. 4. Ba vs Co, Rb vs Mn, Ni vs Mn and Cu vs Rb in SPM; Full squares: Beni subbasin; open circles Mamore subbasin, triangles: Congo basin

ACKNOWLEDMENTS

This work was funded by IRD "Hydrology and Geochemistry of Amazon river basin" Project and INSU-IRD PNSE program.

REFERENCES

Cauwet, G.(1994) HTCO method for dissolved organic carbon in seawater: influence of catalyst on balanck estimation. *Mar. Chem.* 47, 55-64

Elbaz-Poulichet, F., Seyler, P., Maurice-Bourgoin, L., Guyot, J.L., & Dupuy, C. (1999) Traceelement geochemistry in the upper Amazon drainage basin (Bolivia). *Chemical Geology*, 157, 319-334.

Gibbs R.J. 1972. Water Chemistry of the Amazon River. *Geochim. Cosmochim. Acta* **36**, 1061-1066.

Guyot J.L. (1993) Hydrogéochimie des fleuves de l'Amazonie bolivienne. *Coll. Etudes & Thèses*, ORSTOM, Paris, 261p.

Guyot J.L., Quintanilla, J. Cortes, J. & Filizola, N. (1995) Les flux de matières dissoutes et particulaires des Andes de Bolivie vers le Rio Madeira en Amazonie brésilienne, 39-49. In: *Aguas, Glaciares y Cambios Climaticos en los Andes Tropicales*, La Paz, June 1995.

Seyler P., Guyot J.L., Maurice-Bourgoin L., Sondag F., Elbaz-Poulichet F., Etcheber H., Quintanilla J. 1998. Origin of trace elements in the Bolivian Amazonian drainage basin. In *Hydrology in the Humid Tropic Environment,* IAHS Pub. 253, 47-60.

Stallard, R.F.& Edmond, J.M. 1983. Geochemistry of the Amazon. 2. The influence of geology and weathering environment on the dissolved load. *Journal of Geophysical Research* **88** (14): 9671-9688.

MAGNETIC FABRIC IN THE ANTENA GRANODIORITE, CHUQUICAMATA AREA, NORTHERN CHILE

Silvia SINGER (1), Rubén SOMOZA (2), Andrew TOMLINSON (3),Mónica LOPEZ DE LUCHI (4), and Irene BARTOLOMEU RAPOSO (5)

(1) Departamento de Ciencias Geológicas, FCEyN, Universidad de Buenos Aires; Argentina
(2) CONICET - Depto. Cs. Geológicas, FCEyN, Universidad de Buenos Aires, Argentina
(3) SERNAGEOMIN, Santiago, Chile
(4) CONICET - INGEIS, Buenos Aires, Argentina
(5) Laboratório de Anisotropias Magnéticas, Instituto de Geociências, Universidade de São Paulo, Brasil

KEYWORDS: Anisotropy of magnetic susceptibility, Fortuna Complex, Chuquicamata, northern Chile.

INTRODUCTION

The Fortuna Complex is composed of shallow plutons that crop out immediately west of Chuquicamata, northern Chile, forming a NNE-elongate body of about 5 x 20 km. The complex consists of an earlier (ca 39 Ma), large intrusion called the Antena granodiorite (Fig. 1); a younger (ca 37.5 Ma), more central intrusion called the Fiesta granodiotite (Fig. 1); and later granitoid porphyries genetically linked to the Fiesta unit (Dilles et al., 1997). Information about the internal structure of these plutons is sparse, a fact that encouraged us to perform anisotropy of the magnetic susceptibility (AMS) measurements. Here we present the main characteristics observed from the magnetic fabric in the larger body of the Fortuna Complex, the Antena granodiorite.

PALEOMAGNETIC AND ROCK MAGNETIC DATA

Most sampled sites did not give suitable paleomagnetic results. However, 14 sites yielded a well-defined remanence interpreted as thermoremanent magnetization. Sites carrying reversed polarity remanence are interspersed with others that show normal polarity remanence. The shallow nature of the intrusion suggests that cooling and locking of remanence at each site did not span a long time-interval. This, coupled with the presence of antipodal magnetizations and the length to width ratio of the body, suggests that the Antena unit was constructed by several episodes of magma injection and cooling through the blocking temperatures.

Acquisition of isothermal remanence (IRM) and hysteresis loops were performed on samples of selected sites in order to obtain information about the magnetic mineralogy. The results indicate that the magnetic signal is mostly dominated by multidomain (MD) magnetite, with bulk susceptibilities ranging from 13 to 71 10^{-3} SI, mean value = 34.1, σ = 11.5.

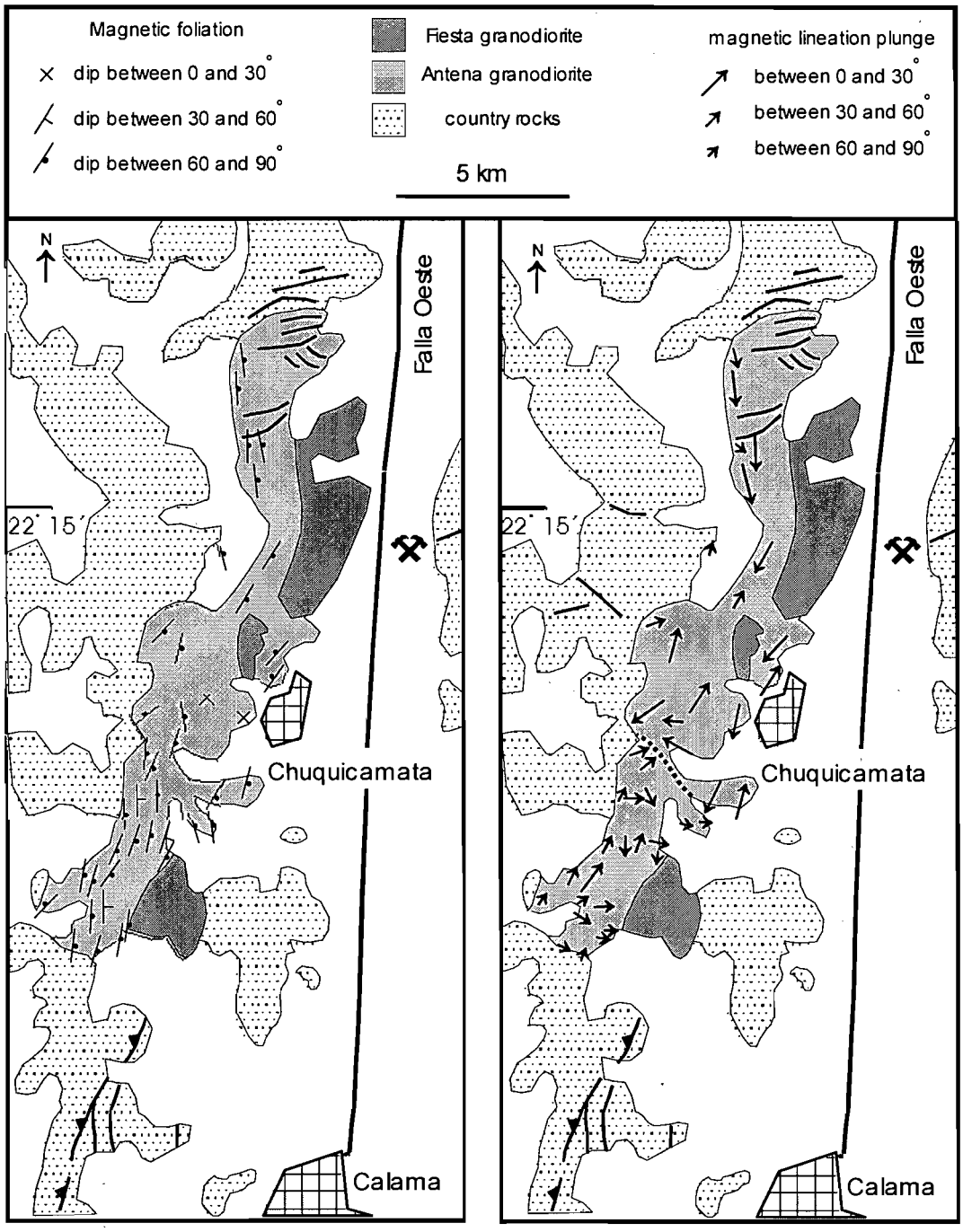

Figure 1. Sketch map of the Antena and Fiesta granodiorites. The younger porphyries are not shown for simplicity. Antena granodiorite: the map on the left shows the pattern of magnetic foliation while that on the right the pattern of magnetic lineation. Magnetic foliations match very well the shape of the body. Note that foliation in the southernmost sites is oriented at high angles to the contact with the wallrock. Magnetic lineations in the southern part of the body tend to be steep, whereas shallower lineations predominate at the latitude of Chuquicamata and farther north. Dotted line depicts an arbitrary boundary between these two lineation families.

ANISOTROPY OF THE MAGNETIC SUSCEPTIBILITY

AMS constitutes an important tool to explore the internal structure of plutonic units (e.g. Bouchez and Gleizes, 1995; Trindade et al., 1999; McNulty et al., 2000). AMS results from the Antena granodiorite depict a consistent pattern of foliation and lineation (Fig. 1). At the site, ellipsoid shape is predominantly triaxial (79% of the cases), with oblate ellipsoids being subordinate (21% of the cases). Foliation predominates over lineation (mean F = 9.9 %, σ = 6; mean L = 3.8 %, σ = 2.7). Degree of anisotropy ranges from 36 to 2.7%, with a mean of

14.1 % (σ = 8.4). The greater values of degree of anisotropy are observed in sites from the area SW of Chuquicamata, whereas the lower values correspond to sites located in the northern part of the unit. This spatial distribution of degree of anisotropy is controlled by foliation, since the contribution of lineation is roughly uniform throughout the pluton. Anisotropy of anhysteretic remanence (AARR) measurements performed on two sites yield ellipsoids with similar shape and similar axis orientation as the corresponding AMS ellipsoids; the degree anisotropy being about 50% greater in AARM, however.

The magnetic foliation tends to be steep (in most sites dipping between 60 and 90° toward the E) and remarkably resembles the shape of the intrusion (Fig. 1). Two families of magnetic lineation can be distinguished. Lineations in the southern part of the body plunge moderately to steeply without a preferred azimuth; whereas shallow, margin-parallel lineations predominate in the central and northern parts of the pluton (Fig. 1).

The high values of magnetic susceptibility suggest that the AMS signal is imposed by magnetite. The fact that magnetite is of MD size suggests the observed fabric is of normal type. The AMS signal may reflect either a single process of magnetic fabric acquisition or be the final product of superimposed processes. In the first case we can take into account two possibilities. If the magnetic fabric and petrofabric are coeval, the presence of MD magnetite encourages the interpretation that the ellipsoid axes of the magnetic fabric will correspond one to one to the petrofabric axes. Alternatively, the magnetic fabric may reflect a later process affecting titanomagnetites; for instance a stress-related alignment of intragranular domain walls of magnetite (e.g. Borradaile and Kehlenbeck, 1996). Below is a discussion and tentative interpretation of the origin of the magnetic fabric in the Antena granodiorite. Petrographic studies (work in progress) may help to refine this interpretation.

Some observations to take into account when interpreting the AMS results of the Antena granodiorite are: 1) the degree of anisotropy is rather constant across the strike of the pluton, lacking a contrast between the center and border of the body; 2) the AMS ellipsoid shows a similar orientation in both microgranitoid enclaves and surrounding matrix; 3) foliation cuts at high angle to xenoliths; 4) the trend shown by foliation in sites carrying normal remanence is similar to those carrying reversed remanence; and 5) foliation at the southern end of the body is oriented at high angles the pluton-wallrock contact, showing parallelism with foliation detected in the Los Picos monzodiorite (host rock) (unpublished data). Point (1) argues against an important contribution from magmatic flow in the magnetic fabric. Points (2) and (3) suggest that matrix and enclaves had similar viscosities when the magnetic fabric formed. Point (4) suggests that either the magnetic fabric postdates diachronous pulses of magma injection or that a similar ambient stress field (e.g. regional stress) was present during injection of different pulses. Point (5) suggests that, at least locally, foliation behaves independently of the pluton boundary. These points suggest that the magnetic fabric may postdate magma chamber construction, and could have been developed late in (or after) the crystallization history (e.g. Paterson et al., 1998). In this case the magnetic foliation pattern in the pluton may reflect regional strain. This idea is in agreement with the fact that the Antena granodiorite was emplaced during regional deformation (Incaic orogenic phase; Tomlinson and Blanco, 1997), shows an overall orientation that matches regional Eocene structures (e.g. reverse faults in Figure 1), and the presence of mylonites (Maksaev et al., 1988) in the area where higher anisotropies are observed.

The significance of the magnetic lineation pattern is more enigmatic. The steep lineations are consistent with horizontal shortening and vertical stretching that are seen in the regional deformational pattern, but the shallow lineations in the central and northern parts of the pluton are not. The presence of roof pendants and the

shallower stratigraphic level of emplacement suggest that the northern part of the pluton is nearer the roof of the body. In this context, the steep lineations in the southern part of the body may be interpreted as reflecting, in part, vertical magma ascent in the deeper parts of the pluton, while the shallow lineations represent lateral flow near the roof of the pluton.

We tentatively conclude that the magnetic fabrics may be polygenetic. The shallow lineations and locally shallow foliations in the central and northern parts of the pluton probably reflect lateral flow near the roof of the pluton. The steep lineations and foliations in the southern, deeper part of the pluton are interpreted to result from both magmatic flow during vertical ascent and a regional horizontal shortening strain which erased wall-to-core and enclave-to-matrix fabric contrasts, and produced foliations discordant to the southern wall of the body. The north-south (shallow-deep) differences in the degree of anisotropy may reflect superposition of a more or less uniform regional horizontal shortening strain over a pluton having, from magmatic flow, domains with different initial magnetic fabric orientations and/or degrees of anisotropy. In this interpretation, the greater values of the degree of anisotropy in the south represent enhancement of the anisotropy by superposition of similarly oriented ellipsoids. The lower values in the north reflect superposition of regional strain on an initially weak and/or shallowly dipping magnetic foliation. Strain was sufficient to invert the foliation axes, but not the lineation.

Acknowledgements: Part of AMS measurements was performed in the Universidad de Chile at Santiago under cordial invitation of Pierrick Roperch. Fieldwork was supported by the Servicio Nacional de Geología y Minería (Chile).

REFERENCES

Borradaile, G., and M. Kehlenbeck, 1996. Possible cryptic tectono-magmatic fabrics in "post-tectonic" granitoid plutons of the Canadian Shield, Earth and Planetary Science Letters, v. 137, p. 119-127.

Bouchez, J., and G. Gleizes, 1995. Two-stage deformation of the Mont-Louis - Andorra granite pluton (Variscan Pyrenees) inferred from magnetic susceptibility anisotropy; Journal of the Geological Society of London, v. 152, p. 669-679.

Dilles, J.; A. Tomlinson; M. Martin; and N. Blanco; 1997. El Abra and Fortuna complexes: a porphyry cooper batholit sinistrally displaced by the Falla Oeste; VIII Congreso Geológico de Chile, vol. III, p. 1883-1887.

Maksaev, V., M. Zentilli, and P. Reynolds, 1988. Geocronología ^{40}Ar-^{39}Ar de depósitos de tipo pórfiro cuprífero del norte de Chile, V Congreso Geológico Chileno, v.1, p. B109-B133.

McNulty, B., O. Tobisch, A. Cruden, and S. Gilder, 2000. Multistage emplacement of the Mont Givens pluton, central Sierra Neveda batholith, California; Geological Society of America Bulletin, v. 112, p. 119-135.

Paterson, S., T K Flower Jr., K. Schmidt, A. Yoshinobu, E. S Yuan, R. Miller, 1998. Interpreting magmatic fabric patterns in plutons, Lithos, v. 44, p. 53-82.

Trindade, R., M.I. Bartolomeu Raposo, M. Ernesto, and R. Siqueira, 1999. Magnetic susceptibility and partial anhysteretic remanence anisotropies in the magnetite-bearing granite pluton of Turão, NE Brazil, Tectonophysics, v. 314, p. 443-468.

Tomlinson, A.; and N. Blanco, 1997. Structural evolution and displacement history of the west fault system, Precordillera, Chile: Part 1, synmineral history, VIII Congreso Geológico Chileno, v.3, p. 1873-1877.

ESTIMATING THE AGE OF THE FLAT SLAB BENEATH THE CENTRAL ANDES

Rubén SOMOZA

CONICET - Universidad de Buenos Aires <somoza@gl.fcen.uba.ar>

KEYWORDS: Central Andes, flat subduction, Neogene, magmatic arc

The age of subduction is estimated for some portions of the slab beneath the Central Andes. Hypothetical, trench to foreland trajectories on the Earth surface of particles of the Nazca plate were calculated at selected latitudes. This was achieved by combining Nazca-South America relative motions and convergence between the trench and the craton due to horizontal shortening in the eastern deforming belt of the Central Andes. Transferring these superficial trajectories on the Wadati-Benioff zone shows the current position (latitude, longitude, and depth) of particles of oceanic lithosphere which entered in subduction at 10, 7.5, 5, and 2.5 Ma (Fig. 1 and 2). Application of this exercise assumes that: 1) the slab is physically continuos; 2) the area of the oceanic lithosphere is conserved after subduction; 3) the relative position of the trench respect to the foreland has not been significantly modified by tectonic erosion during the last 10 m.y.; and 4) the azimuth of the slab motion with respect to a fixed South America is the same as that of the Nazca plate. The position of particles entering the subduction zone at 10 Ma are not well constrained because they lye in a zone where the depth of the slab is not well defined.

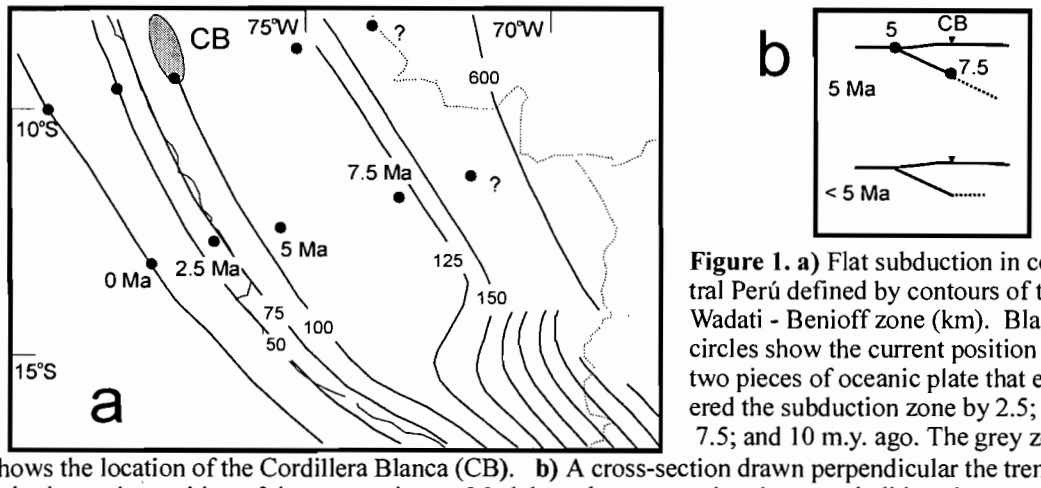

Figure 1. a) Flat subduction in central Perú defined by contours of the Wadati - Benioff zone (km). Black circles show the current position of two pieces of oceanic plate that entered the subduction zone by 2.5; 5; 7.5; and 10 m.y. ago. The grey zone shows the location of the Cordillera Blanca (CB). **b)** A cross-section drawn perpendicular the trench axis shows the position of the magmatic arc. Model results suggest that the oceanic lithosphere entering the subduction zone 7.5 m.y. ago was likely beneath the CB (depth of ~ 100 km) about 5 m.y. ago. Further sinking of that piece of slab during the last 5 m.y. would have been lower than 25 km (Fig. 1a).

The current vertical level of particles entering the central Andean subduction zone 7.5 m.y. ago is about 100 km shallower in the zones of flat subduction (Fig. 1 and 2). The preferred age for the slab inflexion defining flat subduction beneath Perú is around 5 Ma, and possibly a similar age could be adopted for the flat slab in Chile.

The most important intrusive phase in the Cordillera Blanca batholith (CB in Fig. 1a) occurred between 5 and 6 Ma (Petford et al., 1996). The last record of magmatic activity in this zone are volcanic rocks dated between 2.7 and 3 Ma (Petford and Atherton, 1992). Petford et al. (1996) suggested that the source of CB magmas was newly underplated mantle-derived material. The reconstructions suggest that particles entering the subduction zone 7.5 m.y. ago were located beneath the current position of CB by 5 m.y. ago (Fig. 1b). The occurrence of CB suggests the presence of a well-developed asthenospheric wedge by those times, allowing the speculation that the slab was at a depth ~100 km beneath the 5 Ma magmatic arc in this area (Fig. 1b). The current depth of that portion of slab is shallower than 125 km (Fig. 1a), suggesting very low additional sinking (< 25 km) during the last 5 m.y., which may be interpreted as the development of the slab inflexion in Perú central. This suggests that the most recent (younger than 5 Ma) magmatic activity in the area would have been associated with a progressively thinner asthenospheric wedge.

Figure 2 shows the calculated position of particles that entered in subduction in the southern central Andes. Because of poorly constrained crustal shortening data for the southern Puna, the southern points in Figure 2 represent particles entering the subduction zone at different latitudes (30 and 32°S, see caption). Differential sinking of about 100 km is observed for the particles that entered in subduction 7.5 m.y. ago. On the other hand, the "slab isochron" defined by the 7.5 Ma particles is discordant with the depth contours of the Benioff zone, suggesting that the strike of these later south of 22°S does not represent the strike of the late Miocene continental margin.

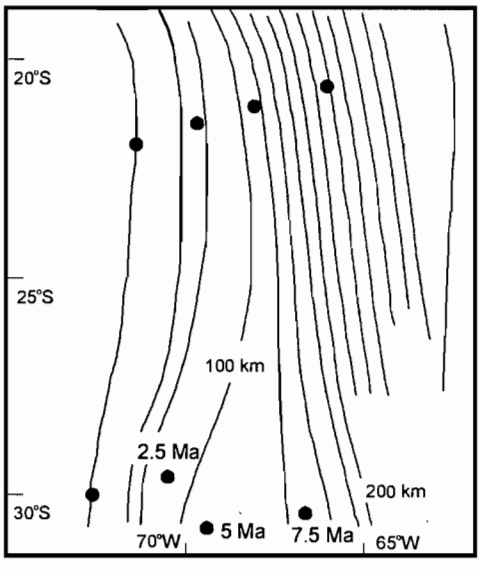

Figure 2. Contours of the Wadati-Benioff zone beneath the southern Central Andes. The southern 2.5 Ma point corresponds to a particle entering the subduction zone at 30°S, whereas the corresponding 5 and 7.5 Ma points were subducted at 32° S. Oceanic lithosphere entering the subduction zone 7.5 m.y. ago is currently about 100 shallower in the region of flat subduction in central Chile. The pattern suggests that "subduction isochrons" created by the points are discordant respect to the contours of the W-B zone.

REFERENCES

Petford, N., and M. Atherton, 1992, Granitoid emplacement and deformation along a major crustal lineament: the Cordillera Blanca, Perú: Tectonophysics, v. 205, p. 171-185.

Petford, N., M. Atherton, and A. Halliday, 1996, Rapid magma production rates, underplating and remelting in the Andes: isotopic evidence from northern-central Perú (9-11°S): Journal of South American Earth Sciences, v. 9, p. 69-78.

TERRANE ACCRETION AND OROGENIC GROWTH IN ECUADOR

R.A. SPIKINGS[1], W. WINKLER[2], D. SEWARD[2], G. RUIZ[2] and R. HANDLER[3]

1. Section des Sciences de la Terre, Université de Genève, Rue des Maraîchers 13, CH-1211 Genève 4, Switzerland. spikings@terre.unige.ch

2. Geologisches Institut, ETH-Zentrum, Zürich CH-8092, Switzerland. winkler@erdw.ethz.ch, seward@erdw.ethz.ch, ruiz@erdw.ethz.ch

3. Institute for Geology and Paleontology, University of Salzburg, Hellbrunner Str. 34, 5020 Salzburg, Austria

KEYWORDS: Northern Andes, Thermochronology, Terranes, Caribbean Plate, Carnegie Ridge,

INTRODUCTION

Oceanic hotspot activity, generating large oceanic igneous plateau provinces, plate rearrangements and the generation of new spreading centers since at least 90 Ma has resulted in large structural, thickness and density heterogeneities in the approaching and subducting oceanic slab offshore NW South America (SOAM; Figure 1). At the present day, various oceanic allochthonous terranes comprise western Ecuador and the relatively thick and buoyant Carnegie Ridge is subducting beneath the upper plate with a flat configuration (Gutscher et al., 2000). We present the results of $^{40}Ar/^{39}Ar$ (white mica and biotite) and fission track (FT; zircon and apatite) data from traverses (labelled a – f in Figure 1) across the Eastern Cordillera and the Amotape Complex, which collectively define the palaeo-continental margin, that is presently sutured against oceanic basement in the vicinity of the Inter-Andean Valley (Figure 1). A quantitative framework for the thermal and exhumation history of the palaeo-continental margin since ~70 Ma has been established, which reveals systematic and distinctive along-strike trends, which can be correlated with contemporaraneous heterogeneities in the approaching and subducting oceanic crust. These results will be compared with preliminary thermochronological data from the Western Cordillera (Pallatanga and Macuchi terranes), which is built upon a part of allochthonous Ecuador, above oceanic crust.

RESULTS, THERMAL MODELLING AND INTERPRETATION

The distribution of $^{40}Ar/^{39}Ar$ ages and FT ages from the palaeo-continental margin can be split into three groups; 1, Traverse A, where the ZFT and AFT ages are ≤15 Ma, with long AFT lengths (>14 μm) occuring at ~9 Ma; 2, Traverses B and C where a larger range in FT ages is observed with AFT ages ranging

between 44 – 9 Ma and ZFT ages ranging between 67 – 28 Ma, with long AFT lengths occurring at ~41 Ma. Plateau $^{40}Ar/^{39}Ar$ ages range between 66 – 56 Ma; 3, Traverses D, E and F, where AFT ages are distinctly older and range between 64 – 11, ZFT ages range between 68 – 33 Ma and the longest AFT lengths occur at ~59 Ma.

Forward modelling of the AFT data from individual samples has been combined with overlapping ZFT and $^{40}Ar/^{39}Ar$ ages (obtained from the same respective sample) to generate potential thermal history paths for several samples from temperatures ≤380°C (Figure 2). Various regions of all of the traverses experienced rapid cooling rates (~ 30 - 20°C/My) during 70 – 55 Ma and 43 – 30 Ma. However, the region to the north of S1°30' (Traverses A, B and C) experienced rapid cooling (up to 50°C/My) at 15 and 9 Ma, whereas the region to the south (traverses D, E and F) remained thermally stable.

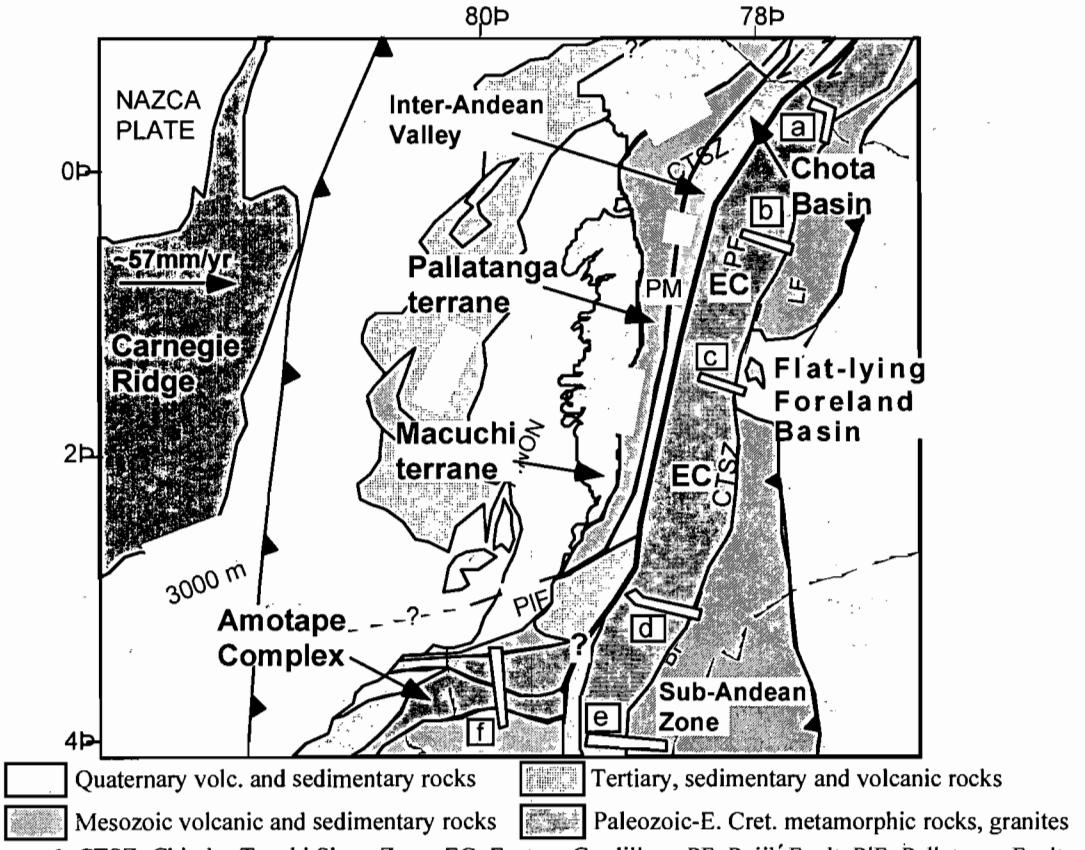

Figure 1. CTSZ: Chimbo-Toachi Shear Zone, EC: Eastern Cordillera, PF: Pujilí Fault, PIF: Pallatanga Fault, PM: Pujilí Melange. Thick black line is the ocean continent suture.

Field mapping (Hughes and Pilatasig, 2002) and geochemical and geochronological similarities between the basement peridotites and basalts of the allochthonous oceanic Pallatanga and Macuchi terranes and the Caribbean Plateau, combined with kinematic reconstructions of the Caribbean Plateau (citations listed in Spikings et al., 2001), provide convincing evidence that the oceanic allochthonous terranes originally formed as island arcs at the leading and trailing edges of the buoyant Caribbean Plateau. The Plateau and southern branches of the island arc systems collided with the NW SOAM continental margin, resulting in the accretion of the Pallatanga and Macuchi terranes during the late Cretaceous and Eocene, subsequently causing the entire contemporaneous continental margin to uplift and exhume.

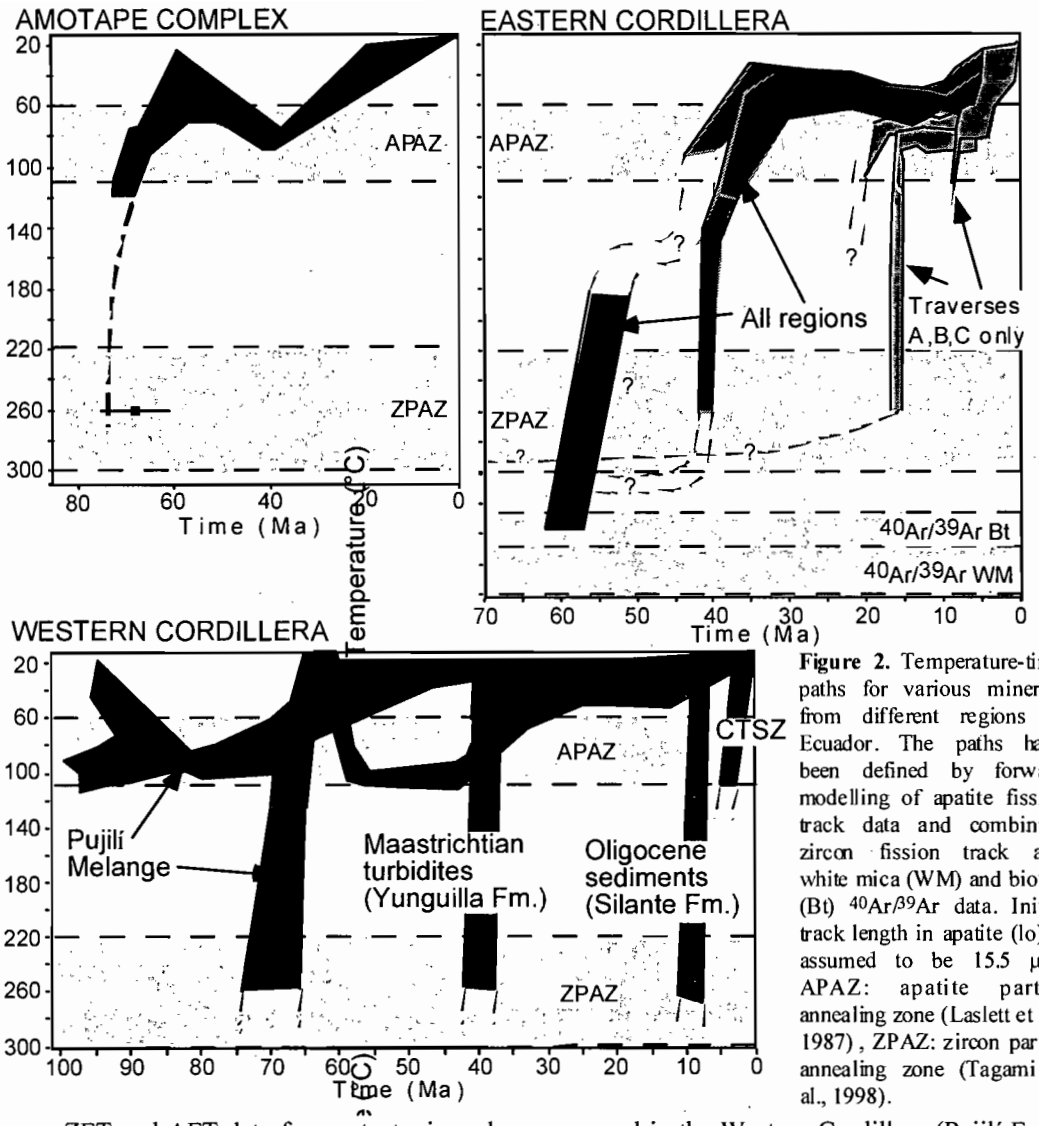

Figure 2. Temperature-time paths for various minerals from different regions of Ecuador. The paths have been defined by forward modelling of apatite fission track data and combining zircon fission track and white mica (WM) and biotite (Bt) $^{40}Ar/^{39}Ar$ data. Initial track length in apatite (lo) is assumed to be 15.5 μm. APAZ: apatite partial annealing zone (Laslett et al., 1987), ZPAZ: zircon partial annealing zone (Tagami et al., 1998).

ZFT and AFT data from a tectonic melange exposed in the Western Cordillera (Pujilí Fm.; Figure 1), which formed in the suture zone between oceanic crust of the Pallatanga Terrane and the continental margin (Hughes and Pilatasig, 2001), experienced increased cooling rates during 80–60 Ma (Figure 2). The cooling was probably a result of both regional exhumation that accompanied the collision and thermal relaxation following frictional heating within the melange. Therefore, assuming that the melange formed during the early stages of the collision, the suture can be dated at ~80 Ma and the progressive formation of the melange via reactivation of the suture probably continued until 60 Ma, as recorded in the Amotape Complex and the Eastern Cordillera. Rapid cooling of Maastrichtian sandstones (Figure 2) in the far northern Cordillera Occidental at ~40 Ma was probably a result of increased rates of exhumation, driven by the accretion of the Macuchi Terrane.

The timing of collision of the Carnegie Ridge with the North Andean margin (Figure 1) has been a matter of conjecture for over 20 yr and previous estimates for the timing of the onsett of collision range between 25 – 1 Ma (e.g. Lonsdale and Klitgord, 1978). However, we propose that the distinct and dramatic increase in cooling rates observed in parts of traverses A,B and C (Figure 2), which lie directly above or close to the flat subducted slab segment that is supported by the buoyant Carnegie Ridge (Figure 1), was caused by the collision of the Carnegie Ridge with the trench at ~15 Ma. This estimate corroborates with limits imposed by the relative convergence rates of the SOAM plate and the Nazca Plate (Spikings et al., 2001). The collision produced

increased compressive stress, uplift, exhumation and cooling in northern Ecuador. Coupling of the Carnegie Ridge and upper plate may have caused isostatic disequillibrium and a further period of increased stress, resulting in increased exhumation rates at 9Ma, which is also recorded in parts of the Western Cordillera (Fig. 2).

Late Miocene and younger FT ages (< 6 Ma) from the cordilleras are restricted to highly strained rocks, which form part of the CTSZ in the Western Cordillera (Figure 1). Furthermore, rapid late Miocene exhumation rates of ~0.7km/My during 5 - 0 Ma are recorded in the northernmost Eastern Cordillera (Spikings et al., 2000). Finally, ZFT chronostratigraphy of the intermontane Chota Basin, located in the far northern Inter-andean Valley, suggests the oldest sedimentary rocks are 5.4±0.4 Ma, which are the oldest inter-montane sediments in the Inter-Andean Valley. Collectively, this evidence suggests that late Miocene and younger fission track ages from the CTSZ may record cooling that followed a period of shearing and exhumation at ~6 - 5 Ma. Dextral strike-slip displacement of the allochthonous oceanic terranes towards the north-northeast since ~6 Ma produced a complex transcurrent system that included the CTFZ, and uplifted fault blocks comprising the northern Eastern Cordillera. The same system generated the pull-apart Chota Basin and younger basins to the south which collectively form parts of the Inter-Andean Valley.

REFERENCES

Gutscher M-A., Malavieille J., Lallemand S., Collot J-Y. 1999. Tectonic segmentation of the North Andean margin :impact of the Carnegie Ridge collision. Earth and Planetary Science Letters, 168, 255–270.

Hughes R.A., Pilatasig L.F. 2002. Cretaceous and Tertiary terrane accretion in the Cordillera Occidental of the Ecuadorian Andes. Tectonophysics, 345, 29-48.

Laslett G.M., Green P.F., Duddy I.R., Gleadow A.J.W. 1987. Thermal annealing of fission tracks in apatite 2: A quantitative analysis. Chemical Geology, 65, 1–15.

Lonsdale P., Klitgord P.D. 1978. Structure and tectonic history of the eastern Panama Basin. Geological Society of America Bulletin. 89, 98 –999.

Spikings R.A., Seward D., Winkler W., Ruiz G. 2000. Low-temperature thermochronology of the northern Cordillera Real, Ecuador: Tectonic insights from zircon and apatite fission track analysis. Tectonics, 19,649-668.

Spikings R.A., Winkler W., Seward D., Handler R. 2001. Along strike variations in the thermal and tectonic response of the continental Ecuadorian Andes to the collision with Heterogeneous oceanic crust. Earth and Planetary Science Letters, 186, 57–73.

Tagami T, Galbraith R.F., Yamada R., Laslett G.M. 1998. Revised annealing kinetics of fission tracks in zircon and geological implications, in: P Van den Haute, F. de Corte (Eds.), Advances in Fission-Track Geochronology, Solid Earth Sciences Library 10, Kluwer Academic, Norwell, 1998, pp. 99–112.

SUBDUCTION PROCESSES OF CHILE (SPOC) - FIRST RESULTS OF THE ONSHORE SEISMIC REFLECTION EXPERIMENT IN CHILE (38° S)

Manfred STILLER (1), Charlotte KRAWCZYK (2), SPOC Working Group (3)

(1) GFZ Potsdam, Telegrafenberg, D-14473 Potsdam, Germany, manfred@gfz-potsdam.de

(2) GFZ Potsdam, Telegrafenberg, D-14473 Potsdam, Germany, lotte@gfz-potsdam.de

(3) See text for details

KEY WORDS : Near-vertical reflection seismics, Nazca-Plate, seismogenic coupling

INTRODUCTION

Between 36° and 39° S, the multi-disciplinary offshore project SPOC (Subduction Processes Off Chile; Reichert & SPOC Scientific Shipboard Party, 2002; Ladage et al., 2002) was extended landwards in November 2001 by different active and passive seismic experiments, with the zone of seismogenic coupling, generally located between 20-40 km depth, as the prime target (see Krawczyk et al., this volume; SPOC Working Group (Land), 2002). Here, we mainly report the first results from the near-vertical incidence reflection (NVR) seismic experiment component on land which was designed to image that part of the subduction zone between the S-America and Nazca-Plate located in the offshore-onshore transition zone.

CONCLUSIONS

The NVR land profile is located at a latitude of about 38° 15`S. Covering the westernmost part of a longer E-W refraction line (one amongst three), the receiver spread of the reflection line was 54 km long, with three spread set-ups of 18 km length each, being twice entirely shifted from the coast in the W to the western margin of the Longitudinal valley in the E. With each set-up 180 geophone-groups (string of six 4.5 Hz p-detectors per group) were deployed at 100 m spacing. The recording equipment consisted of 30 Teledyne PDAS100 seismological recorders (6 channels each). All instruments were provided by the GIPP Potsdam and the FU Berlin.

A total of two explosive shots in the Pacific Ocean (50 kg and 25 kg charge fired at ocean bottom), 10 borehole shots (75 kg charge fired at 20 m depth) at 6 different locations within the onshore reflection line, and two shots east of the active spread (75 kg and 150 kg charge, the latter with 2 holes at 20 m) were recorded (see Figure, light-blue asterisks). This NVR-land experiment thereby resulted in a 72 km long CDP line (see Figure, white

line), with a 2-fold coverage in the innermost 45 km and single-fold coverage at the margins, extending the seismic imaging to the Pacific ocean and to the Longitudinal valley.
In addition, all airgun shots of the offshore E-W profile SO168-038, surveyed by the R/V SONNE, were recorded with the first 18 km of the onshore reflection spread (laying in prolongation of the marine line).

The (onshore) *SPOC Working Group*:
M. Araneda [1], K. Bataille [2], J. Bribach [3], A. Cser [4], C.M. Krawczyk [3], S. Lüth [5], S. Martin [6], J. Mechie [3], L. Rabenstein [5], W. Schnurr [5], M. Stiller [3], P. Wigger [5]

[1] SEGMI (Santiago, Chile)
[2] Universidad de Concepcion (Concepcion, Chile)
[3] GeoForschungsZentrum Potsdam (Germany)
[4] Universidad de Concepcion (Los Angeles, Chile)
[5] Free University Berlin (Germany)
[6] Potsdam University (Germany)

Location map of the SPOC onshore NVR reflection experiment component in South Chile (blue asterisks: explosive shots, white line: CDP profile).

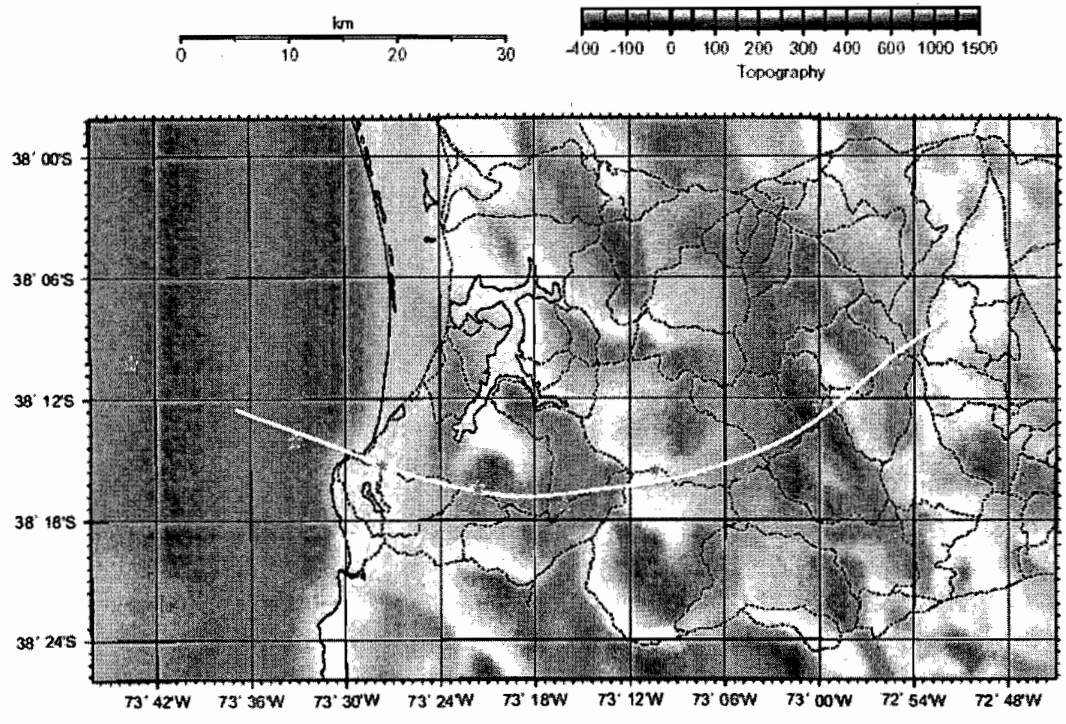

The preliminary data processing of the onshore NVR component, consisting of the 14 single shots, gives even with the only 1-2fold CDP coverage a clear image of different reflection bands in the upper and middle crust. Along the entire profile, a 1 s TWT thick strong reflection band is observed between 3 and 4 s TWT, which

shows almost no dip. On the western half of the profile, prominent reflections dip eastward from ca. 6 s TWT down to ca. 8 s TWT. Finally, in the central part of the seismic reflection profile, some relatively weaker reflections are found between 10 to 14 s TWT. All these eastward dipping reflection bands between 6 and 14 s TWT could be interpreted as indications for the downgoing plate which moreover is confirmed by the result of the CDP image after depth-migration. From this, the top of the oceanic plate can be estimated dipping with an angle of roughly 20° to the E from a depth of about 25 km to about 45 km along the NVR line.

The data of the offshore airgun shots recorded with the onshore NVR spread, covering a broad offset range from 18 km to 180 km, show decreasing signal quality for distances greater than 100 km. But with respect to the high redunancy (all 3600 airgun shots, 50 m spaced, were recorded with all 180 receiver groups, 100 m spaced) they allow for a proper enhancement of the signal/noise ratio by a moving common-offset stacking technique. Evaluation of densely sampled wide-angle sections prepared in this manner shall be used to extend the velocity-depth model, derived from the corresponding land refraction line (see Lüth et al., this volume), to the W far into the Pacific Ocean.

REFERENCES

Ladage S., Reichert C., Schreckenberger B., Block M., Bönnemann C., Canuta J., Damaske D., Diàz J., Gaedicke C., Krawczyk C., Kus J., Sepulveda J. & Urbina O. 2002. SPOC-Experiment: Seismic Imaging and Bathymetry of the Central Chile Margin - First Results. Geophysical Research Abstracts, 4.

Reichert C. & SPOC Scientific Shipboard Party, 2002. Subduction Processes off Chile: Initial Geophysical Results of SONNE Cruise SO-161(2+3). Geophysical Research Abstracts, 4.

SPOC Working Group (Land) 2002. SPOC - Subduction Processes off Chile - First Results from Seismic Onshore Observations. Abstract Volume, 211-212. 62. Jahrestagung der Deutschen Geophysikalischen Gesellschaft (DGG), Hannover, Germany, March 2002.

NAZCA - SOUTH AMERICA INTERACTION: REVIEW OF A 2D FLEXURAL ANALYSIS ALONG THE CENTRAL ANDEAN FOREARC.

Andrés TASSARA O. (1)

(1)Institut für Geologische Wissenschaften, Frei Universität Berlin, Malteserstrasse 74-100, D-12249 Berlin, Germany (andres@geophysik.fu-berlin.de). Formerly: SERNAGEOMIN, Santiago de Chile.

KEY WORDS: Central Andes, Forearc, Elastic Thickness, Compressive Stress, Rheology.

INTRODUCTION

The Andean Cordillera is the classical example of mountain chains constructed by the convergence between oceanic and continental plates. Along the Central Andes segment (15° - 33.5°S), the orogen reaches its maximum height (> 6000 m) and width (600 km), presenting between 15° and 28°S the second biggest continental plateau of the Earth, the Altiplano-Puna. These high topographies are primarily compensated by a 60-70 km thick crustal root (i.e. Beck et al., 1996). The huge crustal volume of the Central Andes is thought to have been principally acquired through neogene-to-recent tectonic shortening of the backarc and foreland regions (Allmendinger et al., 1997; Kley et al., 1999). The subduction angle of the Nazca oceanic plate below the Altiplano-Puna plateau increases east and downward until 550-600 km depth, but south of these latitudes the deep angle (> 100 km depth) diminish gradually to flat subduction conditions (Cahill and Isacks, 1992), generating a volcanic arc gap between 28° and 33.5°S. These changes correlate with a slab age reduction, from 50 Ma under the Plateau to 40 Ma at the southern limit of the segment. At both limits, buoyant aseismic ridges are subducted; Nazca at 15°S and Juan Fernandez at 33.5°S. Interpretations of GPS observations along the margin (Klotz et al., 2001; Bevis et al., 2001) indicate that the thrust interface between Nazca and South America plates is 100% locked and <10% of the convergence is absorbed within the continent as lithospheric deformation. This result suggests that would be there a strong thermomechanical interaction between both plates in the forearc region. However, it is still poorly understood, which tectonic and mechanic influence has the forearc in the construction of the orogen and how is transferred the shortening component of convergence from the interplate contact *through* the forearc to the deformation front. In this context, I review the results of a flexural analysis applied to the Andean margin (Tassara y Yanez, 1996). In contrast to others flexural approaches (i.e. Steward and Watts, 1997), this analysis gives estimates on the flexural rigidity variations in the forearc and

on along-strike gradients of horizontal compressive stress. These results are linked with tectonic variables and they contribute to best understand which roll play the forearc in the orogenic process of the Andes.

METHODS AND RESULTS

A 2D flexural analysis (see Turcotte and Schubert, 1982) was applied to 15 topographic and gravimetric profiles between 15° and 50°S (Tassara, 1997; Tassara and Yanez, 1996). Here are considered 10 of those profiles between 15° and 33.5°S. Each section is orthogonal to the principal trend of the Andes and runs from the Peru-Chile trench to the stable South American craton. The 2D flexural analysis developed assumes that the lithosphere is an elastic plate of variable thickness *Te* (effective elastic thickness), downward deflected under the vertical weight of topographic loads and horizontal tectonic stress *P*. Into the model, P=HCF*[5*10^{12} N/m], with HCF (Horizontal Compression Factor) between 0 and 1. The inclusion of this factor in the analysis, generally not considered in traditional flexural approaches, respond to the high relative influence of compressive forces on flexure expected under conditions of very low rigidity below the mountain axis (Tassara and Yanez, 1996) and strong horizontal coupling between Nazca and South America plates. The Bouguer anomaly across each modelled section, was extracted from a grid produced by the Chilean Geological Survey (SERNAGEOMIN), and used as an actual signal of the Moho morphology and lithospheric deflection. A forward modelling of this signal for each section gives a *Te* profile and a value for HCF. The final model shows a good fit between actual and calculated Bouguer anomalies across each section, with residuals lower than ±25 mGal at 200 km long wavelength (Tassara, 1997). Nevertheless the forearc region shows relatively higher residuals than the orogen axis, suggesting that the quality of the estimates is here lower than there, it can be delineated the following first order characteristics of the flexural results:

1) For each section, *Te* increase drastically from <5 km on the western margin of the orogen to values of 50-70 km at the trench axis.
2) Maximum *Te* at the trench decreases along-strike, from ~70 km north of 28°S to ~50 km at 33.5°S.
3) To compare this variation, I have calculated for each section the average *Te* incremental gradient from the trench to the orogen (ΔTe). Between 15° and 28°S ΔTe falls in the range 0.3 to 0.45, while between 28° and 33.5°S this value decreases gradually southward to 0.19.
4) These results suggests a southward decrease in the forearc rigidity.
5) HCF is 0.5 between 15° and 18°S, zero between 18° and 29°S, and increase gradually southward until 0.8 at 33.5°S.

DISCUTION AND IMPLICATIONS

The high rigidity of the forearc region is a direct consequence of the strong thermomechanical control exerted by the cold and rigid subducted plate on the rheological properties of the overriding continental edge, following thermal models proposed for the Andean margin (i.e. Olesckevich et al., 1999) that explains in this way the very low heat flow values reported for the forearc (Springer and Foster, 1998). The slab thermal control

on the forearc is powered in the Andean context by the high mechanical coupling between both plates. In this thermomechanical frame, the rigid and coupled slab-forearc system can be seen as a solid indenter, pushing eastward and transferring, with minimal internal deformation, the non-seismic component of the convergence to the rheologially weakened regions of the orogen. Paleomagnetic evidences (Roperch et al., 2000; Lamb, 2001) indicates almost no tectonic rotations in the forearc since at least 10 Ma, supporting such a rigid mechanical behaviour. This active, indenter-like behaviour is consistent with the occurrence of high angle, high vertical throw compressive structures, described as the transition between the forearc and the Altiplano at 18°-20°S (i.e. Garcia et al., 1999).

The relevant influence of the oceanic plate thermal conditions on the rigidity of the forearc region, can be good appreciated in the clear along-strike correlation between the Nazca plate age at the trench and the *Te* values. The reduction of the age from 50 Ma at 28°S to 40 Ma at 33.5°S implies a ~30% increment of the heat flow derived from the oceanic slab (i.e. Turcotte and Schubert, 1982). Assuming that *Te* is inversely proportional to the heat flow, this variation can satisfactory explain the southward decrease in ΔTe, without unconstrained changes in others rheological parameters (crust and mantle compositions or strain rate, see Burov and Diament, 1995).

In addition, the along-strike reduction of the Nazca plate age generates an increment of the slab buoyancy. This phenomena is linked with the southward increase of the mechanical coupling between both plates (Gutscher et al., 2000). This relationship is reinforced at the northern and southern limits of the Central Andes by the subduction of the buoyant Nazca and Juan Fernandez aseismic ridges. The total effect of the along-strike buoyancy and mechanical coupling variations on the horizontal stress transmitted from the plate interface through the continental margin, is clearly delineated by the northward and principally southward positive gradients in HCF values. The quantification presented here of such kind of gradients could help to constrain dynamical models of continental deformation.

REFERENCES

Allmendinger, R; Jordan, T; Kay, S; Isacks, B. 1997. The evolution of the Altiplano-Puna plateau of the Central Andes. Annual Reviews on Earth and Planetary Sciences, 25, 139 – 174.

Beck, S; Zandt, G; Myers, S; Wallace, T; Silver, P; Drake, L. 1996. Crustal thickness variations in the central Andes. Geology, 24, 404 – 410.

Bevis, M., E. Kendrick, R. Smalley Jr, B. A. Brooks, R. W. Allmendinger, B. L. Isacks. 2001. On the strength of interplate coupling and the rate of back arc convergence in the central Andes: An analysis of the interseismic velocity field. Geochem. Geophys. Geosyst., 2, 10.129/2001GC000198.

Burov, E. and M. Diament. 1995. The effective elastic thickness (T_e) of continental lithosphere: What does it really mean?. Journal of Geophysical Research, 100, 3905 - 3927.

Cahill, T. and B. Isacks. 1992. Seismicity and shape of the subducted Nazca plate. Journal of Geophysical Research, 97, 17503 - 17529.

García, M.; Hérail, G.; Charrier, R. 1999. Age and structure of the Oxaya Anticline, a major feature of the Miocene
compressive structures of northernmost Chile. In International Symposium on Andean Geodynamics, No. 4, Göttingen, Extended Abstracts Volume, 249-252.

Gutscher, M-A; Spakman, W; Bijwaard, H; Engdahl, R. 2000. Geodynamics of flat subduction: Seismicity and tomographic constraints from the Andean margin. Tectonics, 19, 814 - 833.

Kley, J; Monaldi, C; Salfity, J. 1999. Along-strike segmentation of the Andean foreland; causes and consequences. Tectonophysics, 301, 75 - 94.

Klotz, J., G. Khazaradze, D. Angermann, C. Reigber, R. Perdomo, O. Cifuentes. 2001. Earthquake cycle dominates contemporary crustal deformation in Central and Southern Andes. Earth Planet. Sci. Lett., 193, 437–446.

Lamb, S. 2001. Vertical axis rotations in the Bolivian orocline, South America: 2. Kinematic and dynamical implications. J. Geophys. Res., 106, 26.633 – 26.654.

Oleskevich, D. A., R. D. Hyndman, K. Wang. 1999. The updip and downdip limits to great subduction earthquakes: Thermal and structural models of Cascadia, south Alaska, SW Japan, and Chile. J. Geophys. Res., 104, 14,965–
14,992.

Roperch, P; M. Fornari, G. Herail, G. Parraguez. 2000. Tectonic rotations within the bolivian Altiplano: Implications for the geodynamic evolution of the central Andes during the late Tertiary. J. Geophys. Res., 105. 795 – 820.

Springer, M. and A. Foster. 1998. Heat-flow density across the central Andean subduction zone. Tectonophysics, 291, 123 – 139.

Tassara, A. 1997. Segmentación andina desde el análisis flexural de la anomalía de Bouguer. Memoria de título y tesis de magister (Inédito), Universidad de Chile, Departamento de Geología, 140 p.

Tassara, A. and G. Yanez, 1996. Thermomechanic segmentation of the Andes (15° - 50°S): a flexural analysis approach. In International Symposium on Andean Geodynamics, No. 3, St. Malo, Extended Abstracts Volume, 115 – 118.

Turcotte, D. And G. Shubert. 1982. Geodynamics; applications of continuum physics to geological problems", John Wiley & Sons Eds.

MAGNETIC AND GRAVITY ANOMALIES IN THE CENTRAL PART OF THE TIERRA DEL FUEGO ISLAND. ARGENTINE: EVIDENCES OF TRANSTENSIVE TECTONICS

TASSONE, A[(1)]; LIPPAI, H[(1)]; COMBA, A.[(1)], LODOLO, E[(2)]; MENICHETTI, M[(3)]; HORMAECHEA, J.L[(4)]; VILAS, J.F[(1)]

[1]Instituto de Geofisica "Daniel A. Valencio", Dpto. Cs. Geologicas. FCEyN. U.B.A, Ciudad Universitaria C1428EHA, Argentina. E:mail: atassone@gl.fcen.uba.ar, lippai@gl.fcen.uba.ar, vilas@gl.fcen.uba.ar

[2]Istituto Nazionale di Oceanografia e di Geofisica Sperimentale (OGS), Borgo Grotta Gigante 42/C, 34016 Trieste, Italia. E-mail: elodolo@ogs.trieste.it

[3]Istituto di Geodinamica e Sedimentologia, Università di Urbino, Campus Universitario, 61029 Urbino, Italia, E-mail; menichetti@uniurb.it

[4]Estación Astronómica Río Grande. UNLP-CONICET. Tierra del Fuego. E-mail: jlhor@earg.gov.ar

KEY WORDS: Gravity, Magnetic, Paleomagnetic; Tierra del Fuego, Magallanes-Fagnano Fault System

INTRODUCTION

The Tierra del Fuego region, is one of the least known places on Earth because its remoteness and the difficult access to most of its length. The intersection of the South America-Scotia plate boundary in the Tierra del Fuego region is represented by a mainly strike-slip lineament, known as the Magallanes-Fagnano Fault System (MFS), running from the western part of the North Scotia Ridge to the Chile Trench south of 50°S (*Fuenzalida*, 1972; *Dalziel*, 1989). The MFS, substantially splits the Tierra del Fuego Island in two continental blocks. The MFS is a mainly transcurrent lineament which runs from the Pacific entrance of the Magellan's Strait to the Atlantic coast of the Island (Fig. 1), where significant deformation related to left-lateral strike-slip faults has been surveyed both onshore and offshore (Winslow, 1982; Cunningham, 1993; Klepeis and Austin 1997; Olivero et al., 1999; Menichetti et al., 2000; Diraison et al., 2000; Lodolo et al., 2002).

Three geophysical and geological field surveys have been carried out in the in the central part of the Tierra del Fuego island. The difficulties of access in most of the study areas have prevented the realization of a regular grid with closely-spaced geophysical and geological data points, and for this reason some parts remain still unsurveyed (Fig.2a: see shaded areas). Gravity and magnetic data points have been acquired on 420 GPS-fixed data points based on the geodetic local net from the *Estación Astronómica de Rio Grande,* with a LaCoste-Romberg gravimeter and EG&G Geometrics proton magnetometer. The topographic correction necessary for producing the Bouguer anomaly map has been in fact computed using the obtained Digital Elevation Model. Within this area, a paleomagnetic and magnetic anisotropy survey was performed on the outcrops of the Cerro Hewhoepen intrusive.

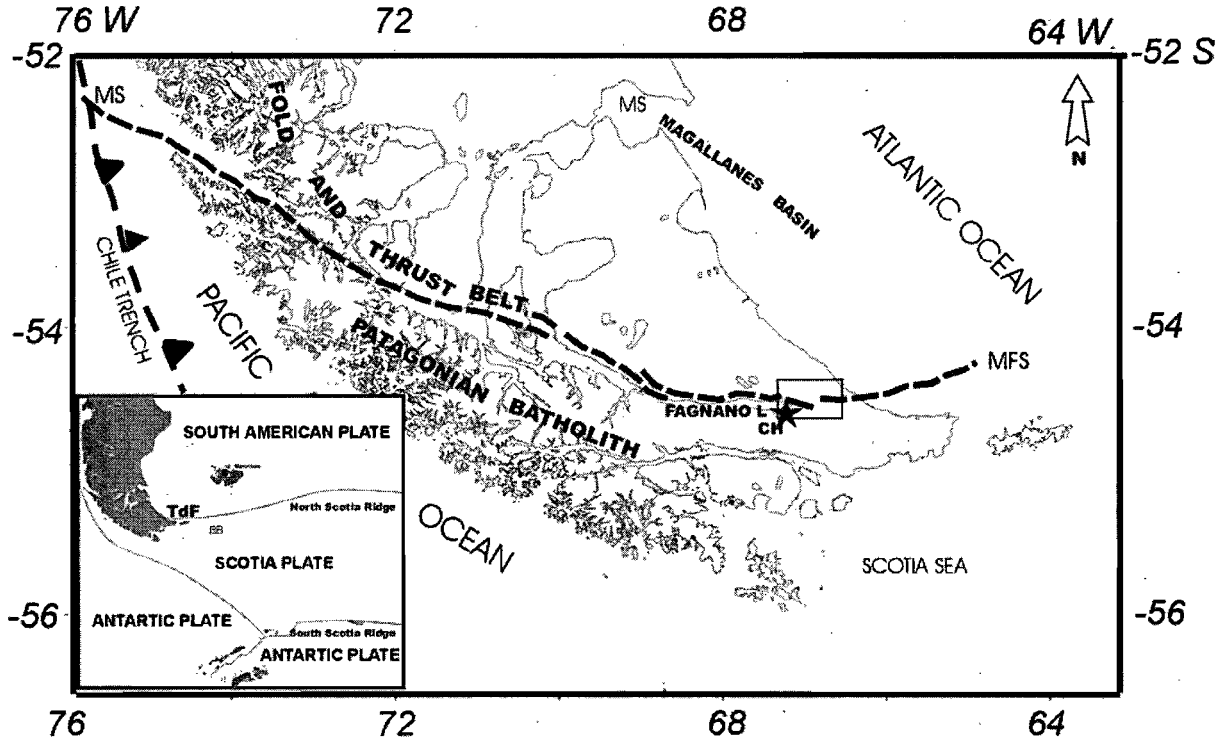

Fig. 1 –Simplified geological map of the Tierra del Fuego Island, with the main tectonic provinces and locations cited in the text. MS: Magallanes Strait; MFS = Magallanes-Fagnano Fault System. Box refers to the corresponding figures 2a and 2b. The inset shows the regional tectonic map with the plate boundaries.

Several maps were constructed with the data acquired (Bouguer anomaly map, map of anomaly of the total magnetic field) and sections combining the information gained from gravity and magnetic data.

Fig. 2 a)

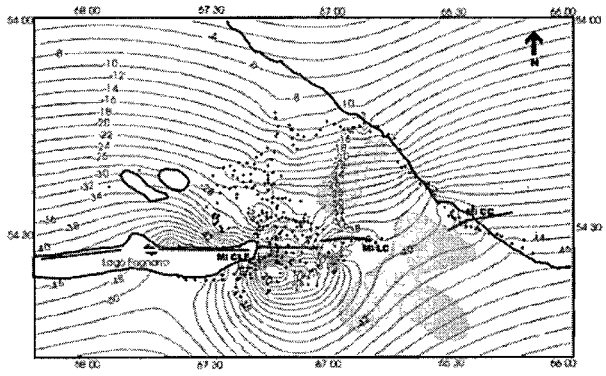

Fig. 2 b)

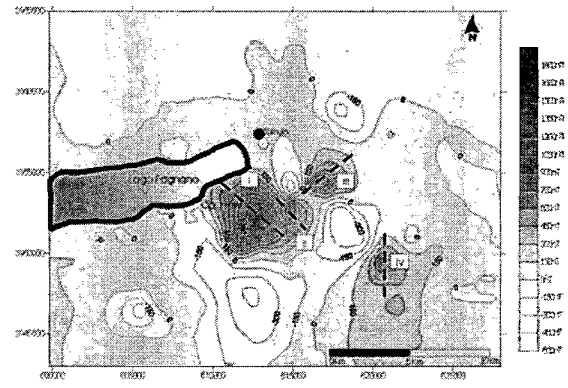

Fig. 2: a) Complete Bouguer gravity map of the central part of Tierra del Fuego Island. Contour lines each 2 miliGal. The measurement stations are indicated by dots. FMF: Magallanes-Fagnano Fault; Mi CLF: Bouguer minimum anomaly in Lago Fagnano located in correspondence of a sag pond at the estuary of the Rio Turbio; Mi LC: Bouguer minimum anomaly in the sector de la Ea. La Correntina located at the eastern termination of the valley occupied by the Rio Turbio; Mi CC: Bouguer minimum anomaly in the Cabo Colorado; CH: Bouguer maximum anomaly in the Cerro Hewhoepen.

b) Magnetic map of one sector of the surveyed area. Four (I, II, III, IV) significant positive magnetic anomalies are located in ESE of Lago Fagnano. Contour lines each 150 nT. Thick segment refers to the total field magnetic preferential orientation for each recognised intrusive body.

The Bouguer anomaly map (Fig. 2a) shows a regional decreasing through South indicating a major

thickness of continental crust. The regional anomaly trend onshore is characterized by anomalies ranging from about -2 miliGals to -60 miliGals. A delimited maximum in the anomaly (-18 miliGal, CH) is related to the higher density of the Cerro Hewhoepen monzodioritic intrusion, a crystalline body that occupies an area approximately 3 x 3 km wide, and coinciding with an isolated relief about 750 m high. The sector to E of the Lago Fagnano to Atlantic coast present two anomaly minimums owing to the existence of two pull apart basins. One of the anomaly minimums is the Cabo Colorado (-42 miliGal, Mi CC) where important evidences of shear tectonism, overprinted on folding and thrusting, have been surveyed. The second is located at the eastern termination of the valley occupied by the Rio Turbio (-42 miliGal, Mi LC), the eastern tributary of Lago Fagnano. Another minimum, less pronounced than the two above mentioned, is located in correspondence of a sag pond at the estuary of the Rio Turbio (-40 miliGal, Mi CLF). The free-air anomaly data obtained from satellite in the Atlantic offshore (Sandwell, 1995), show a regional anomaly trending E-W which may be correlated with the free-air anomaly data collected in the central area of Tierra del Fuego Island (Tassone et al., 1999). The magnetic map shows part of the surveyed area (54° 27'-54° 37' S and 66° 59' y 67° 27'W) in which the Cerro Hewhoepen is included. The values of the anomaly vary between 600 nT and 1800 nT. The map displays four anomaly maxims in correspondence with the intrusive bodies. These bodies are located in the area which would have rotated due to MFS movements. The maximum I corresponds to the intrusive which outcrops in Cerro Hewhoepen. There, the magnetic data are mainly oriented WNW-ESE displaying the strongest value gradients in the ENE-WSW direction. The maximum II is oriented as the maximum I. The maximum III is located close to the MFS trace with maximum values oriented NE-SW, whereas the maximum IV (located farther to the south of MFF) shows a minor rotation with anomaly values oriented near the N-S direction.

DISCUSSION AND CONCLUSIONS

In the surveyed area, the MFF segments have a clear morphological expression, and are associated with localized gravity minima in correspondence of their unconnected ends. The gravimetric minimums (Mi LC: La Correntina basin and Mi CC: Cabo Colorado basin) associated with the MFF, along with the field structural data suggest a transtensive scenario, and are interpreted as pull-apart basins associated with the MFF. Basins like these have been recognized through bathymetric and reflexion seismic surveys along the MFF both to the west of the studied area in the Magallanes Strait and to the east in the Atlantic offshore; the sedimentary architecture of these basins reflects a close relation between transform-normal extension and strike-slip motion (Lodolo et al., 2002). To the ESE of Lago Fagnano, near the Cerro Hewhoepen intrusive, the magnetic data suggest the existence of several intrusive bodies in the subsurface. As reflected by geophysical modelling, the Hewhoepen body has a piston shape, which along with its location and alkaline nature, might suggest that its emplacement was localized at a releasing bend of the MFF (Cerredo et al., 2000). The magnetic anomaly for each of the bodies indicates a rotation in relation to the NS direction. These values agree with the calculated rotation of the magnetic pole of the intrusive I of Cerro Hewhoepen. (counterclockwise rotation of 33.4° ±7.5°, inclination anomaly of 39.7° ± 6.0°). Furthermore, the MSA values of the intrusive I suggest an EW lineament, which coincides with the transtension direction of the MFF (Baraldo et al., 2002).

The gravity and magnetic data provided critical information in those areas where rock outcrops are lacking. These data combined with the paleomagnetic, MSA, bathymetric, seismic reflexion data and field structural information support the transtensive tectonic regimen for the Magallanes Fagnano Fault System.

REFERENCES

Baraldo; A.; Rapalini; A.; Tassone, A.; Lippai, H.; Menichetti, M.; Lodolo, E. 2002. Estudio paleomagnético del intrusivo del Cerro Hewhoepen, Tierra del Fuego, y sus implicancias tectónicas. XV Congreso Geológico Argentino. Calafate. Argentina. Actas.

Cerredo, M. E., Tassone, A., Coren, F., Lodolo, E. Lippai, H. 2000. Postorogenic, alkaline magmatism in the Fuegian Andes: The Hewhoepen intrusive (Tierra del Fuego Island). IX Congreso Geológico Chileno. Puerto Varas. Chile. Actas. Vol. 2. Simposio Nacional Nro. 2: 192-196

Cunningham, W.D. 1993. Strike-slip faults in the southernmost Andes and the development of the Patagonian orocline, *Tectonics*: 169-186.

Dalzield, L. W. D. 1989. Tectonics of the Scotia Arc., Antartica. Field trip Guidebook, Vol. T180: 206 pp.

Diraison, M., Cobbold, P.R., Gapais, D., Rossello, E.A. and Le Corre, C., 2000. Cenozoic crustal thickening, wrenching and rifting in the foothills of the southernmost Andes. *Tectonophysics*, 316: 91-119.

Fuenzalida, R.H., 1972, Geological correlation between the Patagonian Andes and the Antarctic Peninsula and some tectonic implications: Master Thesis, 75 pp., Stanford Univ, CA.

Kirschvink, J.L. 1980. The least-squares and plane and the analysis of paleomagnetic data. Geophys. J.R. Astron. Soc., 67: 699-718

Klepeis, K.A. and J.A. Austin, 1997. Contrasting styles of superposed deformation in the southernmost Andes, *Tectonics*, 16: 755-776.

Lodolo, E., M. Menichetti; A. Tassone, R. Geletti, P. Sterzai, H. Lippai; and J. Hormaechea. 2002. Researchers Target a continental transform Fault in Tierra del Fuego. EOS Transactions AGU, 83 (1): 1-6.

Menichetti, M.; Coren, F.; Lodolo, E.; Tassone, A. 2000. Wrenh tectonics in the Tierra del Fuego Island (Argentina). Analysis from field and remote sensing data. The first Stephan Mueller Conference of the European Geophysical Society (EGS): >From continental breakup to collision. Grand Nirvana Hotel, Dead Sea, Israel, junio 11-16. Actas.

Olivero, E.B., Martinioni, D.R., Malumian, N. and Palamarczuck, S., 1999. Bosquejo geológico de la Isla Grande de Tierra del Fuego, Argentina. *Actas XIV Cong. Geol. Arg.*: 291-294.

Sandwell, D.T., 1995. Ocean basin tectonics revealed with declassified Geosat altimeter data. EOS Transactions AGU, 76 (46), Fall Meeting: 149.

Tassone A.A., Lodolo E. and TESAC Group (Lippai H. , Zanolla C., Hormaechea J.L., Coren F., Vidmar R., Rinaldi C.). 1999. Indicadores geofísicos sobre la localización del límite entre las placas Sud América-Scotia en Tierra del Fuego (Argentina). XIV Congreso Geológico Argentino. Salta. Argentina. Actas I: 326-329.

Winslow, M.A.. 1982. The structural evolution of the Magallanes Basin and neotectonics in the southernmost Andes. In: *Antarctic Geoscience* (C. Craddock, ed.). Madison, University of Winsconsin Press: 143-154.

NEW PALAEOMAGNETIC RESULTS FROM THE COASTAL CORDILLERA/PRECORDILLERA BOUNDARY NORTHERN CHILE: IMPLICATIONS FOR PLATE MARGIN DEFORMATION.

Graeme TAYLOR. (1), Mark GIPSON (1), John GROCOTT (2)

(1) Department of Geological Sciences, University of Plymouth, Plymouth, UK, PL4 8AA, GTaylor@Plymouth.ac.uk
(2) School of Earth Sciences and Geography, Kingston University, Penrhyn Road, Kingston-upon-Thames, Surrey, UK, KT1 2EE, j.grocott@kingston.ac.uk

KEY WORDS: Palaeomagnetism, Northern Chile, Crustal Rotation, Timing

INTRODUCTION

Crustal rotation is an important part of Andean deformation in the Central Andes. Numerous palaeomagnetic results from the Coastal Cordillera of northern Chile (see Randall, 1998 and Beck, 1998 for reviews) indicate substantial rotations have affected the Jurassic-Cretaceous rocks of the then magmatic/volcanic arc and which now forms part of the present-day forearc. The area is transected by a number of major margin parallel, sinistrally transtensive to transpressive, fault systems (the Atacama Fault Zone - AFZ, the Coastal Cordillera-Precordillera Boundary Fault system - CC-PC, and the Sierra Castilla / Agua Amarga / La Ternara fault zones which all form part of the larger Domeyko Fault System - DFS). Any or all of these fault systems may have contributed to the recorded rotations. Furthermore it has long been suggested that larger scale processes, associated with the development of the Andes as a whole, have contributed to the observed crustal rotations. It has however proved difficult to elucidate the timing of the actual rotations and to relate these to their causative deformational event or events. During the past five years we have conducted integrated palaeomagnetic, geochronological and structural studies of various geologic units along a 200 km length of the boundary between the Coastal Cordillera and the Precordillera zone (CC-PC) in order to better constrain the timing of rotation in relation to deformation (Grocott & Taylor, 2002). The boundary between these two areas/morphotectonic units is recognised as a sinistrally transpressive fault system exemplified in the Copiapó region by a narrow fold and thrust system whose outcrop pattern and kinematics imply that they are part of a more steeply inclined sinistral transpressive fault zone (the CC-PC FZ, Arévalo et al., in prep.). We present new palaeomagnetic data from units of Cretaceous to Paleogene age from Inc de Oro in the north (26.8°S) to Vallenar in the south (28.8°S) along this boundary and evaluate them in relation to this deformation.

GEOLOGICAL SETTING AND PALAEOMAGNETIC DATA

The area has been the locus for a number of previous palaeomagnetic studies (Forsythe et al., 1987, Riley et al., 1993, Dupont-Nivet et al., 1996, Randall et al., 1996, Randall et al., 2001) and these data plus those of Table 1 are represented on Figure 1. In addition Fernández et al. (2000) have studied two profiles from Inca de Oro to east of the Domeyko Fault System. The new data of Table 1 include results from Tertiary plutonic

complexes (Inca de Oro, Cabeza de Vaca and of the Vallenar area - results 1, 3, 7). To the north and south of Vallenar itself field studies indicate that the emplacement of these complexes was syn-tectonic to the transpressive deformation and displacement on the boundary system. This is evidenced by granitic components of the complex having high-temperature fabrics parallel to the deformational fabric and ductile shear zones, which show a range of pre, syn and post tectonic relationships to the granite margins themselves. Here this deformation has been dated, based on Ar-Ar geochronology of hornblende and biotite separates from the granites, to be between 66 and 62 Ma. This age for deformation is consistent with our own and others (Matthews et al. 2001) results from the syntectonic Inca de Oro granite situated in the north of the belt and is consistent with K-Ar ages for plutons and minor intrusions (e.g. Cabeza de Vaca) in the central part of the belt (Arévalo 1994, 1995). Palaeomagnetic results from sediments and volcanics of the Punte del Cobre Fm, the Chañarcillo Gp. and Cerillos Fm. (results 2, 4, 6, 8), both east and west of the boundary itself, all fail fold tests indicating that they were remagnetised and rotated post deformation. In total the palaeomagnetic data from the entire area show no significant differences in rotation across the major fault systems but appear to diminish rapidly east of the DFZ.

The vast majority of samples were collectedwoth portable drills and orientated using both sun and magnetic compasses. Most sites/samples, with the exception of dykes from the Cachiyuyo complex, yielded a characteristic remanence component during standard stepwise AF and thermal demagnetisation. Mean site directions were computed giving unit weighting to samples and unit means from mean site directions. The data as a whole straddle the CC-PC boundary zone and indicate a statistically significant clockwise rotation in all units varying between 28-56°, mean 40". These results are not significantly different from those of the Coastal Cordillera (e.g. Randall et al. 1996 and unpublished data from the Vallenar region, Figure 1) nor from the area immediately east of the DFS (Randall et al. 2001). While we would argue that at least 15° of rotation is related to observed faulting (Grocott & Taylor 2002), the data implies a large-scale process is responsible for the bulk of rotation seen throughout the area. At a more local scale, and particularly highlighted by the study of Fernández et al. (2001), is that between site variation is a function of local small scale block rotations which may be more closely related to the fault systems.

Table 1 Palaeomagnetic Data from the Coastal Cordillera-Precordillera Boundary region, 26-29°S

	Unit	Lat	Long	Age	N	Dec	Inc	A95	R
1	Inca de Oro Granite	26.8	290.1	65	11/12	39.3	-43.4	7.0	44.7 ± 9.8
	Cachiyuyo Dyke complex	27.1	289.9	<62	9/9	Unstable			
2	Cerillos Fm., Remag, Qbda. Condores/Paipote	27.3	289.8	< 62	8/9	34.1	-41.7	5	39.6 ± 7.3
3	Cabeza de Vaca Pluton	27.5	289.9	62	9/10	25.8	-42.7	9.3	31.3 ± 11.3
4	Cerillos Fm., Remag, Elisa de Bordo, Copiapo	27.6	289.8	< 62	8/12	50.5	-42.7	8.3	56.0 ± 10.4
5	S. La Dichusa volcs., Hornitos Fm., los Loros.	27.7	289.8	77-62	7/7	29.3	-42.1	8.0	34.8 ± 10.0
6	Cerillos Fm. Remag, Q Totoralillo/Copiapo	27.7	289.9	< 62	5/5	42.2	-44.3	10.2	47.7 ± 12.5
7	Tertiary pluton complex	28.4	289.5	66-62	11/15	27.9	-54.3	8.3	28.6 ± 10.1
8	Quebrada del Cama sequence, Punte del Cobre Fm., S of Vallenar	28.8	289.3	< 65	9/9	31.5	-50.7	4.3	37.1 ± 7.4

4 modified from Riley et al .1993, 5 from Taylor et al. 1996.

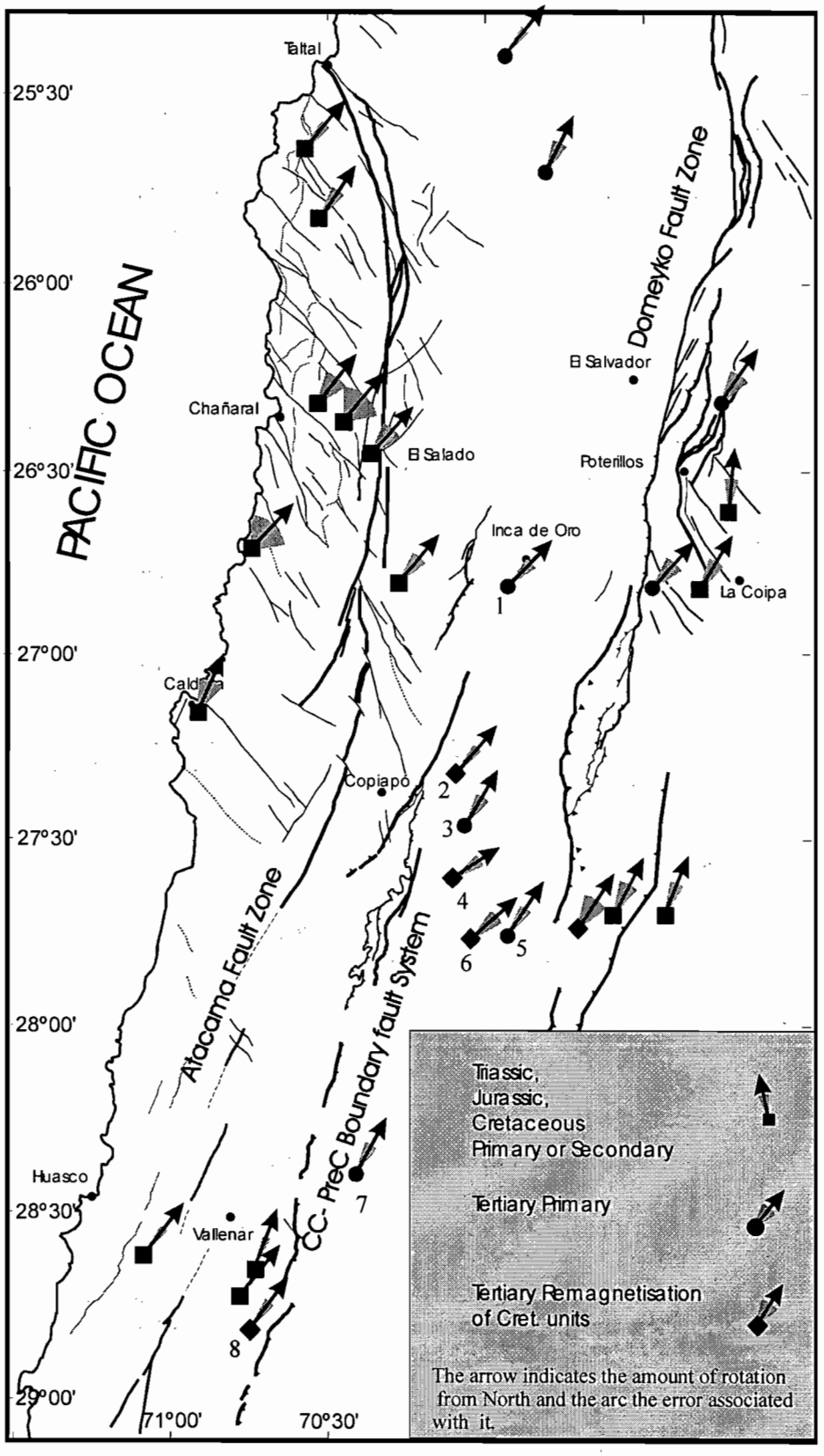

Figure 1 Map of the region showing the palaeomagnetic rotations in Table 1 plus those from Randall et al.1996, Randall et al., 2001, Riley et al. 1993, Forsythe et al. 1987 and unpublished data of the authors.

CONCLUSIONS

The Coastal Cordillera and Precordillera boundary zone of northern Chile between 26 and 29°S is affected by substantial clockwise rotations averaging some 40°. The consistency of these rotations with those to the west from older Jurassic-Cretaceous rocks would suggest a substantial part, if not all, of their rotation is also of Tertiary age. The timing of this rotation would appear to be post 62 Ma as shown by results from both plutonics and remagnetized and rotated Cretaceous units along the boundary zone. The data as a whole suggest a large-scale process has operated and is responsible for the bulk of observed rotations.

REFERENCES

Arévalo, C., 1994. Mapa geológico del cuadrángulo Los Loros (1:100,000), Servicio Nacional de Geologia y Minería, Documentos de Trabajo, No. 6.

Arévalo, C., 1995. Mapa geológico del cuadrángulo Copiapó (1:100,000), Servicio Nacional de Geologia y Minería, Documentos de Trabajo, No. 6.

Arévalo, C., Grocott J., & Taylor. G.K. (in prep). Emplacement of arc plutonic complexes, deformation and the setting of the Candelaria mineral deposit at the Coastal Cordillera-Precordillera boundary in the Andes of northern Chile (27°30'S).

Dupont-Nivet, G., Roperch, P. Gautier, P, Chauvin, A., Gerard, M & Carlier, G., 1996. Clockwise rotations in northern Chile: Oroclinal bending and in situ tectonic rotations?. 3rd ISAG, ORSTOM Colleques & Seminaires, 355-358.

Fernández , R., Roperch, P., Mpodozis, C & Tomlinson A., (2000). Paleomagnetesimo y rotatciones tectonicas en la Cordillera de Domeyko, entre los 26° y 27° S, Region de Atacama, Chile. IX Congreso Geologico Chileno, Actas 2, pp 562-566.

Forsythe, R. D., Kent, D. V., Mpodozis, C. & Davidson, J., 1987. Paleomagnetism of Permian and Triassic rocks, central Chilean Andes. In: G.D. Mackenzie (Editor), Gondwana 6: Structure, Tectonics and Geophysics. A.G.U. Monograph series, 40, pp. 241-252.

Grocott, J. & Taylor, G.K. 2002. Deformation partitioning, magmatic arc fault systems and emplacement of granitic complexes in the Coastal Cordillera, north Chilean Andes (25-27°S). J. Geol. Soc. Lond, in press.

Matthews, Stephen J., Pérez de Arce, C., Cornejo, P., & Cuitiño, L. Dating quartz: Ar/Ar analyses of coexisting muscovite and fluid inclusion - rich quartz from a Paleocene metamorphic aureole. PS. III South American symposium on Isotope Geology, Pucon, Chile, 2001

Randall, D.E., G.K. Taylor, & J. Grocott, Major crustal rotations in the Andean Margin: Paleomagnetic results from the Coastal Cordillera of northern Chile. J. Geophys. Res., 101, 15,783-15,798, 1996.

Randall, D.E., Tomlinson A. & Taylor, G.K. (2001). Palaeomagnetically defined rotations from the Precordillera of northern Chile: evidence of localised in situ fault-controlled rotations. Tectonics, 20, 235-254.

Riley, P. D., Beck, M. E., & Burmester, R. F., Mpodozis, C. and Garcia, F., 1993. Palaeomagnetic evidence of vertical axis block rotations from the Mesozoic of Northern Chile. J. Geophys. Res., 98: 8321-8333.

Taylor, G.K., Randall, D.E. & Grocott, J. (1996). Palaeomagnetism, strike-slip fault systems and crustal rotation in the region 25-27°S of northern Chile. 3rd ISAG, ORSTOM Colleques & Seminaires, 509-512.

ACKNOWDLEGEMENTS

We are grateful to NERC for research grant GR3/99111 that has supported our research studies in northern Chile. We have been greatly helped by the collaboration and co-operation of many geologists in the Sernageomin in Santiago, Chile, in particular Carlos Arévalo, Andy Tomlinson and Pirzio Godoy. We also express our appreciation for the support and kindness shown to us in the field by all our Sernageomin drivers.

AN EXTENSIVE NEW FISSION-TRACK THERMOCHRONOLOGICAL DATABASE FROM THE COASTAL PATAGONIAN ANDES (47°S TO 53°S): A RECORD OF CENOZOIC DENUDATION AND MAGMATISM

Stuart N. THOMSON (1) and Francisco HERVÉ (2)

(1) Institut für Geologie, Mineralogie und Geophysik, Ruhr-Universität Bochum, D-44780 Bochum, Germany (email: stuart.thomson@ruhr-uni-bochum.de)

(2) Departamento de Geologia, Universidad de Chile, Casilla 13518 Correo 21, Santiago, Chile (email: fherve@cec.uchile.cl)

KEY WORDS: Patagonian Andes, Batholith, Geochronology, Fission-track Dating, Thermal History, Erosion

INTRODUCTION

Over the past few years a number of boat excursions to the remote and poorly studied parts of the coastal Patagonian Andes of Chile between latitudes 47°S and 53°S have permitted the collection of at least 100 samples for the purpose of fission-track (FT) low temperature thermochronological analysis. The sampling strategy was largely restricted to collection of regionally distributed shoreline exposures of granitoid rocks from the south Patagonian batholith. The collection of sample profiles with large elevation contrast (to allow good estimation of the timing of changes in cooling and denudation rates) has so far been prevented by a lack of time and the very steep slopes covered in impenetrable temperate rainforest. The present database comprises 84 zircon FT ages, 70 apatite FT ages and 57 apatite FT length distributions are presented. These data complement an international research program in this part of the Andean Cordillera which includes the application of conventional geochronological dating, geochemistry, petrology, palaeomagnetism, and field observation. FT thermochronology provides unique information on the low-temperature thermal history of rocks in the upper ca. 10km of the Earth's crust and hence on geological processes such as erosional denudation and heating related to localised upper crustal magmatism. In the coastal Patagonian Andes such data can be used, for example, to assess the geomorphic response of the overriding continental plate to the subduction of the active Chile rise oceanic spreading centre and variations in the rates of relative plate convergence, and also to better estimate the extent of Cenozoic magmatism. The FT database from the coastal Patagonian Andes is represented in map form in Figure 1. Interpretation of the apatite and zircon FT data is dealt with separately in the next sections.

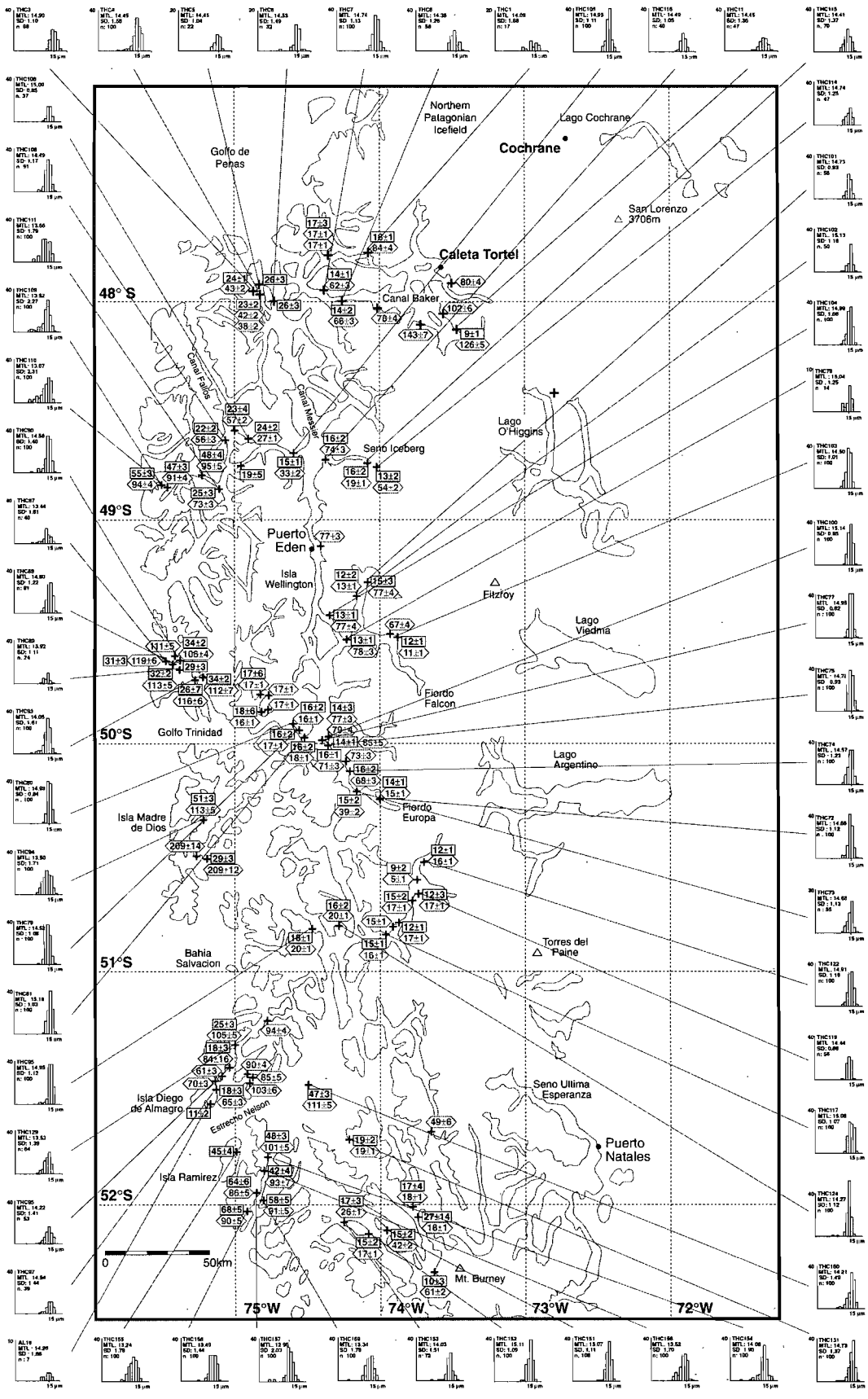

Figure 1: Apatite and zircon fission-track data largely from batholithic rocks of the coastal Patagonian Andes of Chile between 47°S and 53°S.

APATITE FT RESULTS

Over geological time fission tracks in apatite are only stable below 110±10°C, only becoming fully stable at temperatures below about 60°C (a range of temperatures known as the apatite partial annealing zone or APAZ). Track stability over time can be evaluated by measuring track lengths. Above 60°C tracks begin to shorten or anneal at a rate which over geological time leads to measurable shortening. Above 110±10°C the rate of annealing is so fast with respect to geological time that all tracks effectively disappear immediately after they form. Consequently, if a sample cools quickly tracks have no time to shorten within the APAZ and mean track length will be long (>14μm). For slowly cooled samples or samples with complex histories involving longer periods of time at temperatures between 60°C and 110±10°C then tracks have time to shorten significantly, leading to a higher proportion of shorter tracks (<14μm) in an analysed sample. In the coastal Patagonian Andes (Figure 1) most samples have a high mean track length (>14μm) indicative of rapid cooling at the time given by the apatite FT age. However, in the westernmost parts of the studied region, closest to the trench, noticeably shorter mean track lengths are observed. This pattern is mirrored in the apatite FT ages. In the far west ages are older (up to 68 Ma) while further east more rapidly cooled samples have younger ages decreasing from about 30 to 25 Ma down to between about 18 and 10 Ma in those samples nearest the present Andean topographic divide. Thomson et al. [2001] interpreted the 30-25 Ma ages to represent the onset of a phase of accelerated cooling caused either by uplift and erosion linked to a coeval increase in plate convergence rates, or increased erosion caused by climate change linked to opening of the Drake passage at this time. Since this study, older apatite FT ages with shorter mean track lengths have been obtained further west. These data imply that these samples were closer to the surface (at temperatures well below 110±10°C , but within the APAZ to allow preservation of the shorter tracks) before undergoing accelerated cooling at around 30 to 25 Ma. This is supported by the good fit between the real data and the ages and lengths predicted by such a time-temperature history according to experimentally determined apatite FT annealing kinetics. The westernmost part of the study area has thus undergone the least amount of total erosion in the region since the Cretaceous. Younger apatite ages (<ca. 18 Ma) even further east reflect rapid cooling following heating related to Miocene magmatism (see zircon FT results below). However, the regional distribution of such ages, particularly those between 15 and 10 Ma well away from the potential influence of Miocene magmatism, are best interpreted as representing a further period of regional rapid cooling at this time linked to increased uplift and erosion. Interestingly this is coeval with subduction/collision of the Chile rise spreading centre at these latitudes and suggests a causal link. Since about 10 Ma no significant cooling is recorded in the region by the apatite FT data.

ZIRCON FT RESULTS

Fission-tracks in zircon remain stable to much higher temperatures than those in apatite. For rocks undergoing steady cooling, the FT age records the time when the sample cooled to temperatures below about 280±30°C, while the temperatures of partial annealing in zircon is between about 240±20°C and 310±20°C. Track length measurement is very difficult in zircon, meaning that interpretation of the time-temperature histories from zircon FT data is more speculative. However, where the stratigraphic or crystallisation age of the dated sample is known, then later partial or total resetting of the FT age can still provide vital information on the temperature history of such rocks not detectable by other methods. The zircon FT ages from the coastal

Patagonian Andes show a huge variation from 5 Ma to 209 Ma (Figure 1). Particularly prevalent are several local clusters of Miocene ages between 16 and 20Ma. These ages mark areas of localised Miocene plutonism. In some cases this has been confirmed by independent Miocene crystallisation ages from the same samples [Fanning et al., 2001]. In many cases however, the young Miocene FT ages are found in granitoids of early Cretaceous age and instead imply heating or contact metamorphism of these rocks to above >310±20°C. Thus, although actual Miocene magmatism itself may have been very restricted, its thermal influence is much more regional in extent. This may have important implications concerning the distribution of hydrothermal mineralisation in the region. In several other samples later heating of Cretaceous plutons in confirmed by differential partial resetting of zircon FT ages in individual samples. One independently dated Paleocene pluton [C.M. Fanning, pers. comm.] has also locally reset or partially reset some nearby zircon FT ages in older early Cretaceous rocks. Many other of the older Cretaceous zircon FT ages from the Patagonian batholith can be interpreted to represent the slow cooling of these rocks following their earlier emplacement. Two late Triassic ages of ca. 209 Ma (Figure 1) from older basement metamorphic rocks near Isla Madre de Dios date cooling below 280±30°C following metamorphism [Thomson and Hervé, 2002, submitted]. New Late Cretaceous zircon FT ages from HP-LT metamorphosed Jurassic sedimentary rocks on Isla Diego de Almagro may reflect cooling and final tectonic unroofing of these HP-LT rocks related to the nearby Seno Arcabuz shear zone, where dated syn-kinematic white micas imply a Late Cretaceous phase of deformation.

ACKNOWLEDGEMENTS

Boat Excursions in Chile were supported by Catedra Presidencial en Ciencias and Fondecyt Grant 1980741 to FH. SNT was supported by DFG Stipendium Th 573/2-1 and by DFG Grants Sto196/11-1 and Sto196/11-2 to Bernhard Stöckhert at the Ruhr-Universität Bochum, Germany.

REFERENCES

Fanning, C.M., Hervé, F., Pankhurst, R.J., Thomson, S.N. and Faúndez, V. (2001). Late Cenozoic magmatism in the South Patagonian Batholith : SHRIMP U - Pb zircon age evidence. III South American Symposium on Isotope Geology (Pucón, Chile). Revista Comunicaciones (Universidad de Chile), v. 21, p. 11.

Thomson, S. N., Hervé, F. & Stöckhert, B. (2001). The Mesozoic-Cenozoic denudation history of the southern Chilean Andes and its correlation to different subduction processes. Tectonics, v. 20, p. 693-711.

Thomson, S. N. & Hervé, F. (2002). Integrating detrital zircon fission-track and U-Pb SHRIMP ages to estimate the age of deposition, metamorphism and later reheating of metamorphic complexes at the ancestral Gondwana margin of southern Chile (42°S-52°S). Revista geológica de Chile. Submitted.

VALLEY EVOLUTION, UPLIFT, VOLCANISM, AND RELATED HAZARDS IN THE CENTRAL ANDES OF SOUTHERN PERU

Jean-Claude THOURET(1), Gerhard WÖRNER(2), A. FINIZOLA(1), and A. LEGELEY-PADOVANI(3)

(1) Laboratoire Magmas et Volcans, Université Blaise Pascal et CNRS, 63038 Clermont-Ferrand cedex, France (thouret@opgc.univ-bpclermont.fr)
(2) Geoschemisches Institut, Goldschmidtstrasse 1, Universitât Göttingen, 37077, Göttingen, Germany (gwoerne@dwdg.de)
(3) IRD, Centre Ile de France, 34 rue Henri-Varagnat, 93193 Bondy cedex, France (A.Legeley-Padovani@bondy.ird.fr)

KEY WORDS: Andes, Peru, valley history, volcanoes, ignimbrites, uplift, canyons, downcutting, hazards.

INTRODUCTION

Interpretation of satellite images, field work, and geochronology identify three principal types of volcanoes in the areas of Rio Cotahuasi-Rio Ocoña, and Arequipa in southern Peru (Figs. 1-3): (1) relatively youthful stratovolcanoes of Pleistocene to Recent age e.g. El Misti (≤0.8 Ma) and older, larger complexes such as Nevado Coropuna, (2) deeply eroded stratovolcanoes of Plio-Quaternary age (4-1.5 Ma) such as Nevado Solimana and Chachani, and; (3) subdued 'shield' volcanoes of Late Miocene age. While the former are rather varied in petrography and hence chemical composiotion of erupted magmas, the latter tend to be comprised more of monotonous mafic andesites. Ignimbrites form of several hundreds of km^2 in area and several tens of km^3 in volume are also observed and have been dated at middle Miocene (13-14 Ma), Pliocene (5-2 Ma), and Pleistocene age (~1 Ma) (Thouret et al., 2001).

In the area of Arequipa, 13-14 M ignimbrites outcrop above the Jurassic basement in the Rio Chili valley that cuts the flank of the Western Cordillera (Fig. 2). The upper flanks of Rio Chili valley are built in part by lava flows and volcaniclastic sediments of Plio-Quaternary age, whose sources are the Chachani massif and El Misti. Downcutting by 250 m has been achieved within the past 3 My (Fig. 2).

In contrast, the headvalleys of the deepest canyons on Earth of Rios Ocoña, Cotahuasi and Colca NW of Arequipa, have been cut 2 km down in Miocene volcanic rocks and 1 km further down in Cretaceous intrusive and Jurassic sedimentary rocks. The headvalleys were repeatedly filled by pyroclastics and lava flows of Neogene age (< I Ma, Fig. 3) and have subsequenty been recut below their original thalweg. These canyons are thus much deeper and older (middle Miocene) than Rio Chili.

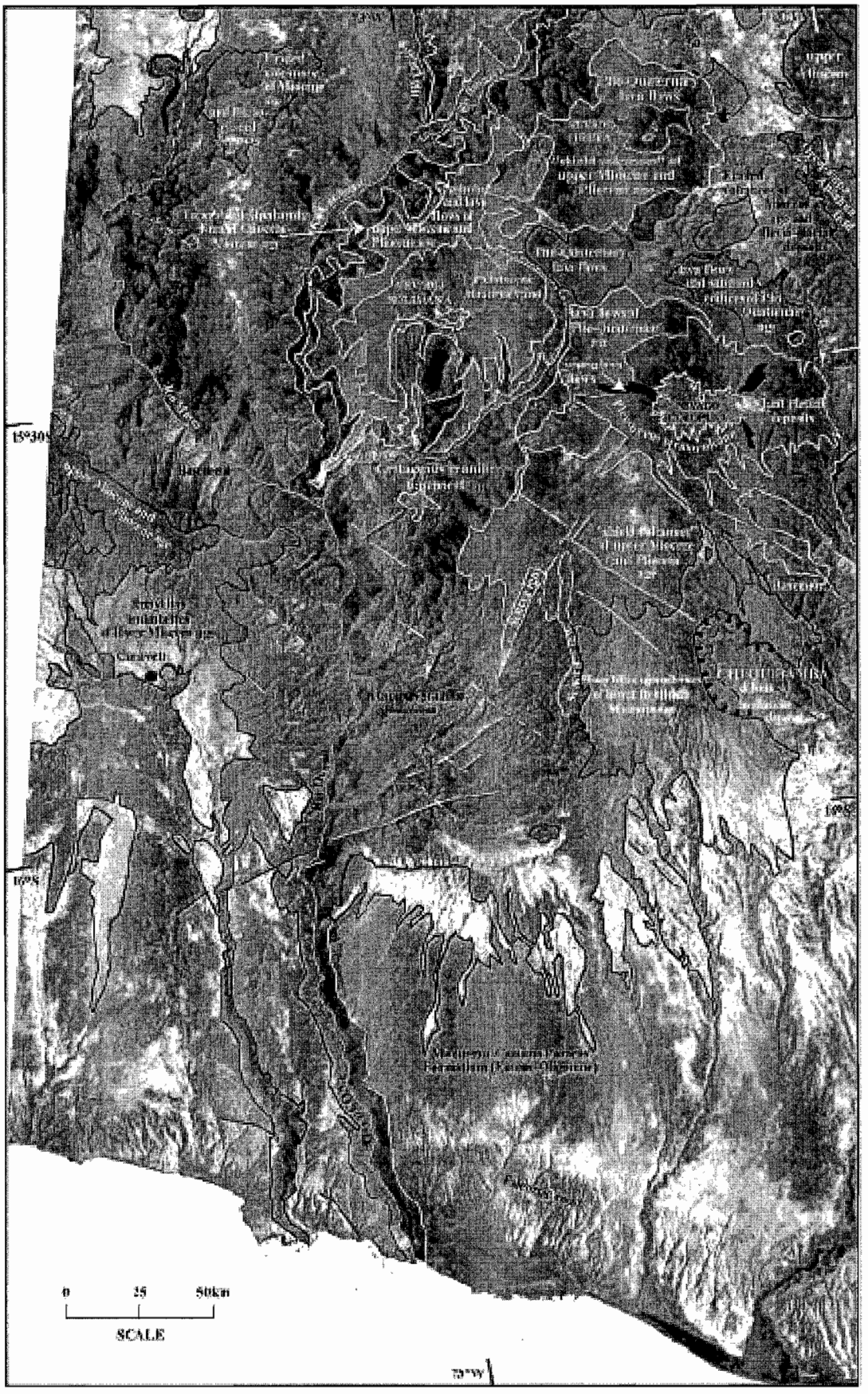

Fig. 1 showing the area of the canyons of Rio Ocoña and Rio Cotahuasi in the Western Cordillera, ignimbrites, and three types of volcanoes. Main geologic units and faults are also shown.

Marine sediments and conglomerates of Eogene age are uplifted to as much as 2000 m asl. in the area of Caraveli and on the east side of the Rio Ocoña (Fig. 3). The main palaeosurface, which has been mantled by the Huaylillas ignimbrites of lower Miocene age, is tilted and ist eastern parts uplifted from about 2500 m to 4000 m asl. in the area of Chuquibamba (Fig. 3). More than half of the uplift (about 2000 m) of the Western Cordillera postdates the emplacement of the Huaylillas ignimbrites (Kennan, 1999). This uplift, combined with the increase of water discharge from glacial sources since Upper Pliocene times triggered the downcutting by at least 1500 m of the Ocoña, Cotahuasi and Colca Canyons since the middle Miocene to Pliocene. Further downcutting of the canyon occured after the emplacement and infilling of the Pliocene lava flows and ignimbrites

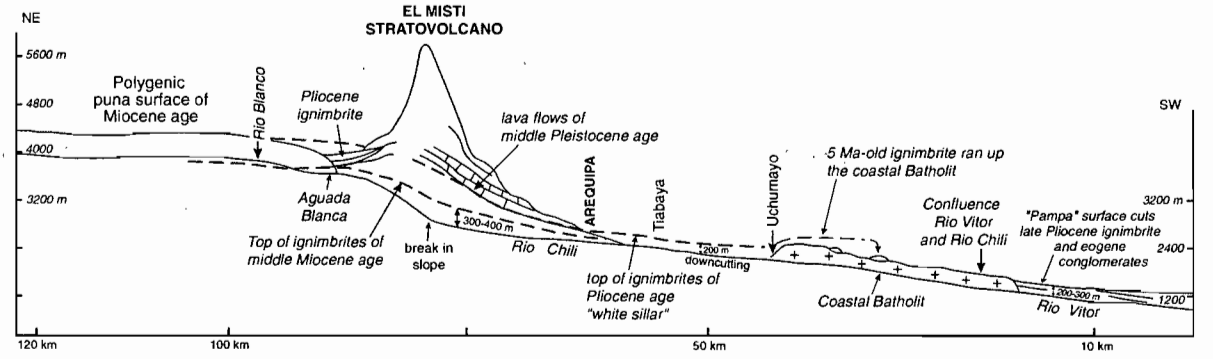

Fig. 2 showing the Rio Chili valley through the Western Cordillera and the depression of Arequipa, El Misti stratovolcano and three groups of ignimbrites (middle Miocene, Pliocene, and early Pleistocene). The amount of uplift and downcutting is estimated using the Miocene surface remnants and the base of ignimbrites and lava flows.

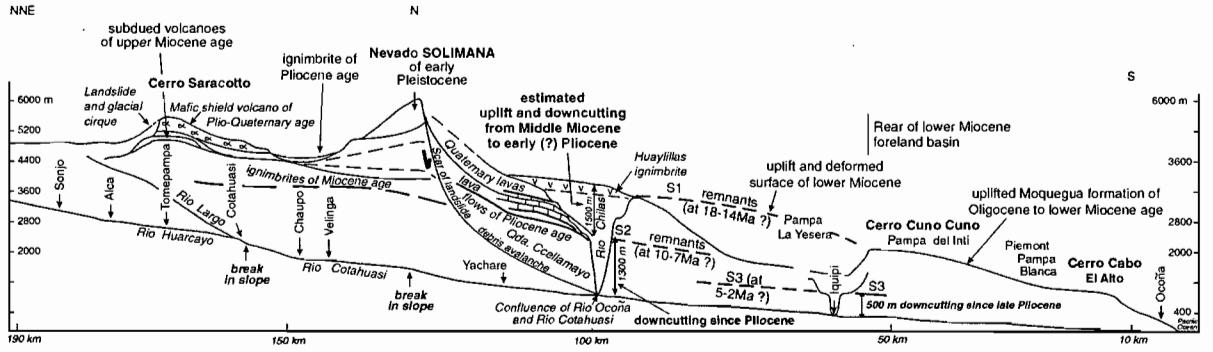

Fig. 3 showing the canyons of the Rio Ocona and Cotahuasi through the western Cordillera, three groups of volcanoes (upper Miocene, Plio-Quaternary, and Pleistocene in age), and three groups of ignimbrites (Alpabamba, Huaylillas, and Sencca) . The amount of uplift and downcutting is estimated using the S1, S2, and S3 surface remnants.

CONCLUSIONS

Digital elevation model (DEM) based on six digitized topographic maps (1:250.000) will be used to illustrate the relationships between the generations of ignimbrites and volcanoes, the uplift of the surface remnants and the downcutting of the canyons. The rapid rate of uplift of the western Cordillera and the distinct rate of the downcutting in the deep Rio Ocoña canyon versus that of Rio Chili are inferred from calculations using the DEM and Ar-Ar geochronology on volcanic rocks.

Downcutting of the deepest canyons on Earth has triggered huge landslides. Collapses involved the Miocene ignimbrites that form the highest canyons walls, e.g., above the town of Cotahuasi, and the edge of the

Huaylillas plateau near Chuquibamba (Fig. 3). Downcutting also triggered flank failures on the Plio-Quaternary volcanoes, such as the southwest flank of Nevado Solimana. Subsequent debris avalanches have dammed the upper course of Rios Cotahuasi and Rio Huarcaya in Pleistocene time. Downcutting continues and valley flanc and volcano instabilites pose a major hazard in these ultr-deep canyons. Further hazards are also related to potential dam breakouts that may trigger devastating debris flows toward the populated lower valleys.

REFERENCES

Kennan L., 1999. Large-scale geomorphology in the Andes: interelationships of tectonics, magmatism, and climate. *In*: M.A. Summerfield, ed., Geomorphology and Global Tectonics, p. 167-199, J. Wiley, New York.

Thouret J.-C., Finizola A., Fornari M., Suni J., Legeley-Padovani A., and Frechen M., 2001. Geology of El Misti volcano nearby the city of Arequipa, Peru. *Geological Society of America Bulletin*, vol. 113, n°12, 1593-1610.

PALEOGEOGRAPHYC EVOLUTION OF THE SOUTHWEST GONDWANA BOUNDARY DURING THE LATE PALEOZOIC. NEWS STUDIES IN THE PRE-ANDEAN VOLCANISM OF THE SAN RAFAEL BLOCK, MENDOZA PROVINCE, ARGENTINA

Renata N TOMEZZOLI(1,2), Laura E. KLEIMAN(3), Julio A. SALVARREDI(4), Carla TERRIZZAN(1*) and ERNESTO O. CRISTALLINI(1,2*).*

[1]Consejo Nacional de Investigaciones Científicas y Técnicas (CONICET).
[2]Universidad de Buenos Aires. Departamento de Ciencias Geológicas, Facultad de Ciencias Exactas y Naturales, Ciudad Universitaria, 1428, Pabellón 11. Buenos Aires, Argentina. E-mail: *renata@gl.fcen.uba.ar; *cterrizzano@hotmail.com; *ernesto@gl.fcen.uba.ar
[3]CNEA. Unidad de Actividad de Geología. Av. del Libertador 8250, 1429. Buenos Aires. E-mail: kleiman@cae.cnea.gov.ar
[4]CNEA. Regional Cuyo, Godoy Cruz, 5500, Mendoza. E-mail: cneacuyo@ciudad.com.ar

KEYWORDS: Gondwana ; Volcanism ; Choiyoi ; Petrogenic model ; Paleomagnetism ; Pangea

Work is in progress on the Permian - Triassic section of South - Central Argentina along a zone believed to be the Devonian collision of Patagonia with South America known as "SamFrau geosyncline" of Du Toit (1927) in Argentina (Figure 1). In order to improve knowledge of this part of Gondwana and to explore regional relationships between sedimentation, volcanism and age of deformation, new studies are involve rocks from the San Rafael block, in Mendoza Province, Argentina, deformed during the late Paleozoic. This collision model is still uncertain and there are many controversies related to the age of the deformation of this belt.

Gondwanic magmatism in the Bloque de San Rafael, is represented by the Choiyoi magmatic province which can be divided in a lower sequence that represents the products of a subduction-related magmatic arc, and an upper sequence which corresponds to a period of pos-orogenic extensional collapse (Kleiman, 1999). The lower Choiyoi volcanics in San Rafael are made up of the Cochicó Group which overlie unconformably the Carboniferous sediments of El Imperial Formation (Figure 2). The Yacimiento Los Reyunos Formation, at the base of the sequence, is composed of four interbedded facies: conglomerates (Psefítico Member), andesitic breccias (Andesítico Member), ignimbrites (Toba Vieja Gorda Member, TVG), and epiclastic redeposited eolian sandstones (Areniscas Atigradas Member). These rocks were deposited in two N-S troughs. At the eastern trough the ignimbritic facies is predominant, up to seven eruptive units have been identified that were interpreted as cooling units (Meza 1988; Meza and Mazzoni, 1996). They can reach thicknesses of up to 200 m. Outcrops at the western trough are not well exposed and the cooling units are not so easily identified. Whole rock K/Ar ages on ignimbrites range from 282 to 266 Ma. A recent $^{40}Ar/^{39}Ar$ age on sanidine from an ignimbrite from the central portion of the sequence yielded 266.31 ± 0.82 Ma (Melchor 2000).

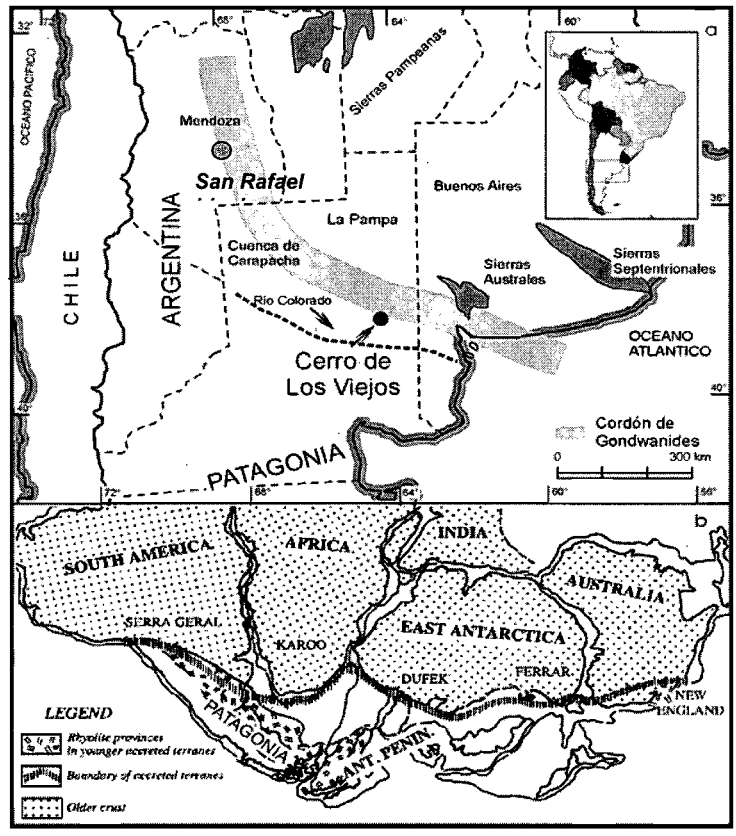

Figure 1: Location of the study area of the San Rafael block, Mendoza province, Argentina, exposed in the orogenic belt known as "Gondwanides" (Keidel 1916). This deformed belt has the same distribution of the gondwanic magmatism of Carboniferous-Permian age. Part b, modified from Kay *et al*, 1989)

Systematic sampling was done in the Cochicó Group, in different localities including several sites for each cooling unit (Figure 2). At least six drill cores or four hand samples were collected per site. They were oriented in the field using magnetic and/or sun compasses. Usually three cylindrical specimens (2.2 cm long. x 2.5 cm diameter) were cut from each core. The specimens are submitting to standart studies.

The outcrops of these ignimbrites present a massive appearance with the basal portion of the unit forming less eroded rounded scarps and the upper portion, slightly more welded, with columnar joints. Colors are predominantly gray, brown red or red. As these rocks are poorly welded the typical zonation of ignimbrites are not observed. These rocks are crystal-rich (up to 50%), with quartz, plagioclase (oligoclase and andesine), sandine, and biotite as the main minerals. Accesory phases are Ti-magnetite, apatite and zircon. Their modal composition is mainly dacitic. The alteration assemblage comprises calcite, siderite, chlorite, sericite, montmorillonite, caolinite, epidote, barite, rutile, anatase, hematite. Pumice fragments range between 2 and 15% and seldom comprises 20% of the rock. Lithic fragments are accidental (metamorphites and sedimentites from the bedrock), accesories (ignimbrites and andesites) and cognates (glassy fragments). They can account for 10% of the rock. The matrix is devitrified with micro-and crypto-crystalline textures being the more abundant features though some axiolitic ans spherulitic textures are also observed. The interbedded eolian sandstones are reworked from the ignimbrites, they can reach thicknesses of up to100 m.

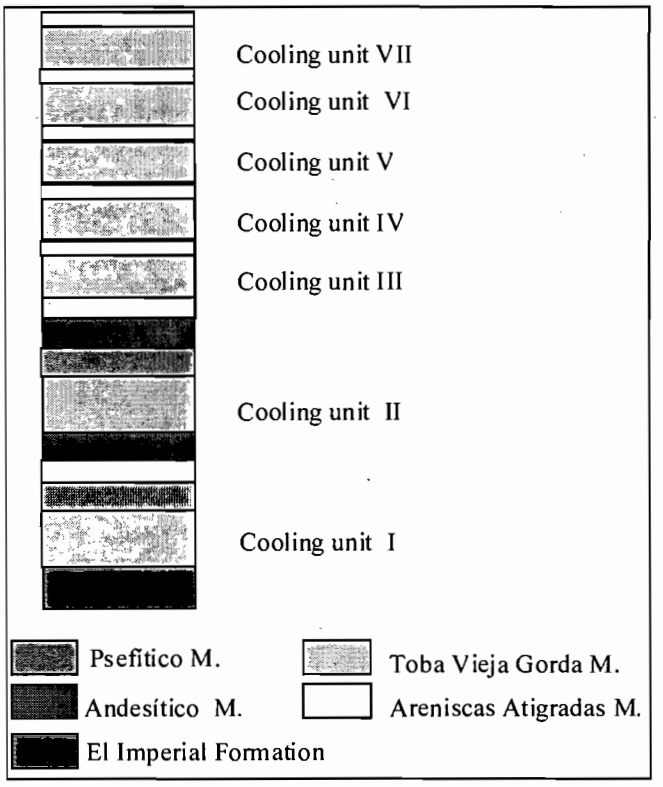

Figure 2: Stratigraphic section of the Yacimiento Los Reyunos Formation showing the position of the different interbedded facies, and the seven cooling units of the Toba Vieja Gorda ignimbrites.

The San Rafael block is located north of the Colorado River in south-central Argentina (Figure 1a). According to Ramos (1984), an ocean was consumed by subduction towards Patagonia along the northern boundary of Patagonia at the southern margin of Gondwana (Figure 1b), before the continental blocks collided in the mid-to late Paleozoic. Associated with this collision, and perhaps continuing for a period thereafter, deformation in the Sierras Australes (east of San Rafael block, Figure 1) may have started in mid-Paleozoic to Permian (Tomezzoli and Vilas, 1999; Tomezzoli, 2001). The main objective of this integrated study of paleomagnetism, anisotropy of magnetic susceptibility (AMS; MacDonald and Ellwood, 1987), petrographic and structural features is to investigate the kinematic history of this area, and to distinguish multiple tectonic events that account for the fabrics of the outcropping rocks (Tomezzoli *et al.*, 2002). The current studies involve rocks from Mendoza (El Imperial Formation) and La Pampa (Carapacha basin) to carried out regional comparisons along this deformed belt to establishing the age of the deformation by region to evaluate time - transgressive deformation. Further objectives are location of the top of the Kiaman and improving the apparent polar wander path of the late Paleozoic - early Mesozoic of South America. The stability of the area imply that the obtained paleomagnetic poles will be representative of South America and can be useful to evaluate a better understanding of the assembly, deformation, and fragmentation of Gondwana / Pangea. The exploration of the AMS will be use as a tool to determine the procedure sources of the ignimbrites from the TVG member and to correlating the cooling units from the eastern and western troughs.

REFERENCES

Du Toit, A., 1927. A geological comparison of South America with South Africa, Carnegie Intitute of Washington Publications. 381, 1-157. Washington.

Kay, S.M., Ramos, V.A., Mpodozis, C. and Sruoga, P., 1989. Late Paleozoic to Jurassic silicic magmatism at the Gondwana margin: Analogy to the Middle Proterozoic in North America?. Geology. 17: 324-328.

Keidel, J. 1916. La geología de las sierras de la Provincia de Buenos Aires y sus relaciones con las montañas del Cabo y los Andes. Ministerio de Agricultura Nacional. Anales Dirección Nacional de Geología y Mineria. T IX (3), Buenos Aires.

Kleiman, L.E., 1999. Mineralogía y petrología del volcanismo permo-triásico y triásico del bloque de San Rafael en el área de Sierra Pintada, provincia de Mendoza, y su relación con las mineralizaciones de uranio. Tesis doctoral, Facultad de Ciencias Exactas y Naturales, Universidad de Buenos Aires: 286 p. Unpublished.

MacDonald, W.D., and B.B. Ellwood, 1987. Anisotropy of magnetic susceptibility: sedimentological, igneous and structural-tectonics application. Review of Geophysics, 25: 905-909

Melchor, R.N., 2000. Stratigraphic and biostratigraphic consequences of a new ^{40} Ar/ ^{39} Ar date for the base of the Cochicó Group (Permian) Eastern Permian Basin, San Rafael, Mendoza, Argentina. Ameghiniana 37: 271-282.

Meza, J.C., 1988. Informe mensual del mes de julio. CNEA, informe interno, Buenos Aires, 2p. Unpublished.

Meza J.C. y M. M. Mazzoni, 1996. Depósitos de flujos de detritos volcaniclásticos en la Formación Yacimiento Los Reyunos (Pérmico). Sierra Pintada de San Rafael, Mendoza. XIII Congreso Geológico Argentino y III Congreso de Exploración de Hidrocarburos, Actas II: 73.

Ramos, V.A., 1984. Patagonia: un continente paleozoico a la deriva?, IX Cong. Geol. Argentino, Actas II: 311-325, S. C. Bariloche, Buenos Aires.

Tomezzoli, R.N., Vilas, J. F., 1999. Paleomagnetic constraints on age of deformation of the Sierras Australes thrust and fold belt, Argentina. Geophysical Journal International, 138: 857-870.

Tomezzoli, R.N., 2001. Further Palaeomagnetic results from the Sierras Australes fold and thrust belt, Argentina. Geophysical Journal International, 147: 356-366.

Tomezzoli, R.N, MacDonald, W.D. and H. Tickyj, 2002. Composite magnetic fabrics and S-C petrofabric in granitic gneiss of Cerro de los Viejos, La Pampa province, Argentina. Journal of Structural Geology. In press.

DETERMINATION OF THE PRESENT STRESS TENSOR FOR THE NORTH SEGMENT OF THE ANDES FROM FOCAL MAJOR EARTHQUAKES MECHANISMS

Toro-Ramírez A. M. y Osorio N. J. A.

INGEOMINAS, Instituto de Investigación e Información Geocientífica Minero-Ambiental y Nuclear. Diag. 53 # 34-53. Bogotá (Colombia). Fax 0.57-1-2223764. atoro@ingeomin.gov.co

The northwestern extreme of South America (between latitudes 4°S and 13°N and longitudes 67° and 82° to the west Greenwich) is of special interest due to its location in the interaction zone of large three tectonic plates (Fig 1), the Nazca plate is converging eastward at 6 cm/yr relative to northwestern of South America (NWSA); the Caribbean plate is moving at 1-2 cm/yr to the E-SE relative to NWSA (Freymueller et al., 1993; Kellogg and Vega, 1995),Taboada, et al., 2000.

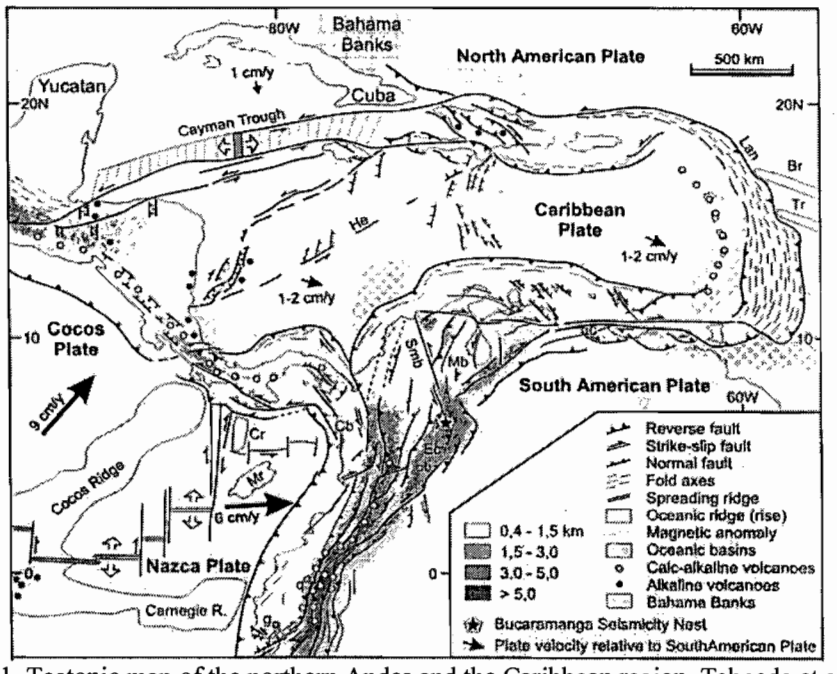

Figure 1. Tectonic map of the northern Andes and the Caribbean region, Taboada et al, 2000

Because of such situation some authors have centered their studies in this region, highlight accomplished them by Ego et al., 1996 and Carvajal et al, 2001 who calculated the stress state for the Andes of the North from of focal earthquake mechanisms, concluding that the difference of stress in this region is due to forces balance between the Nazca, Caribbean and South American plates; however in none of these projects has been spoken of the classification of the tectonic regime for the region.

This study presents the stress state of the Andes of the North and the distribution of the shape of tensor (R) that permits to give a classification of the tectonic regime, for which were applied several focal earthquakes mechanism analysis methods: the inversion method of Reches (Reches et al., 1992) based on the equation of Bott, the graphic method of the straight dihedral and the spatial distribution of the axis P and T. For the inversion were used the focal mechanisms of 219 earthquakes registered by the seismic network (NEIC - HARVARD) for a period of 41 years since 1960s and magnitude mb= 5.0, located within the study zone; the epicentral concentration of these seismic events and their relationship to a specific structural province permitted the definition of 15 areas, 12 of them associated with shallow seismicity and the 3 others with deep seismic activity (Fig. 2).

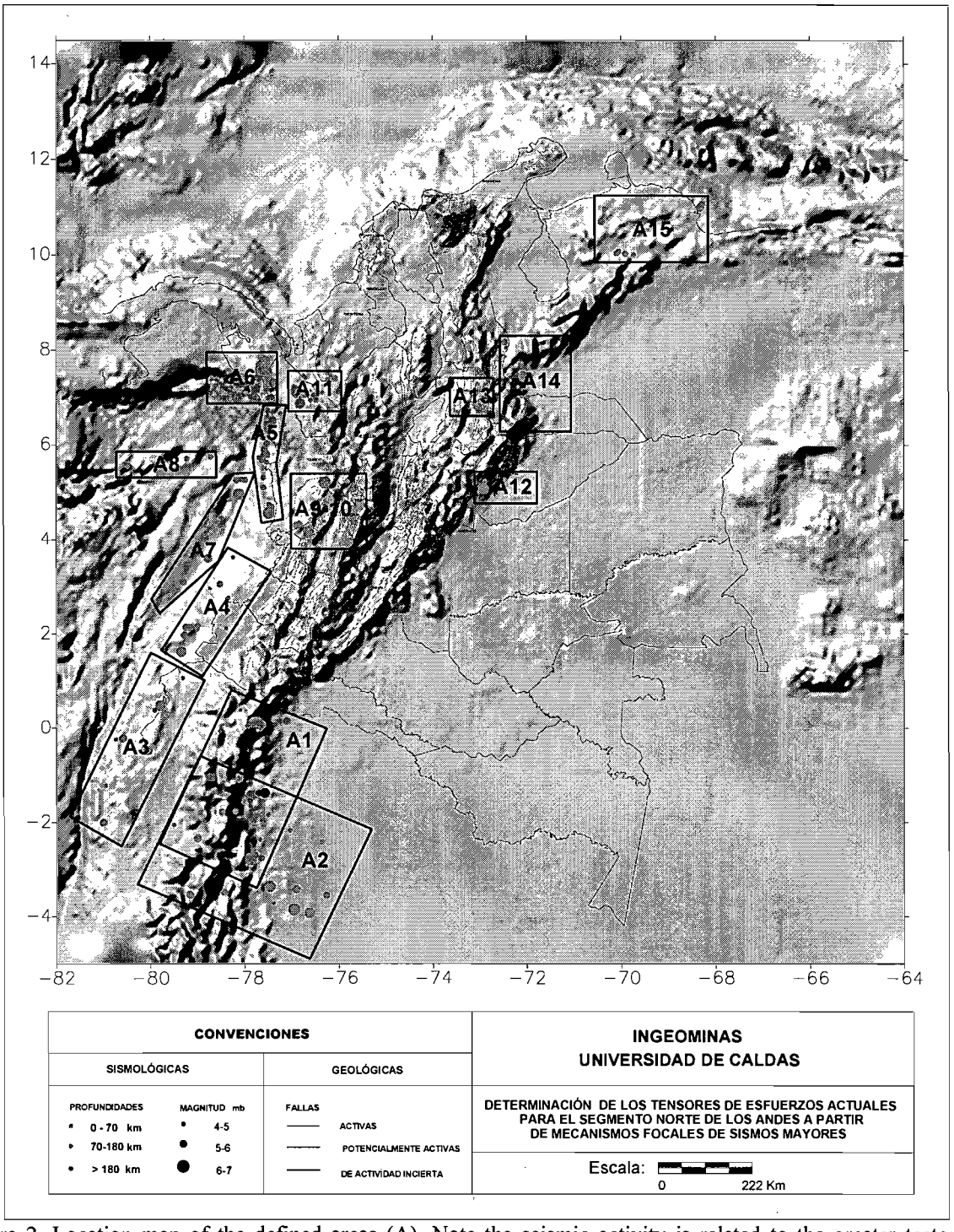

Figura 2. Location map of the defined areas (A). Note the seismic activity is related to the greater tectonic features and main active fault systems.

The results from the inversion for the northwest of South America (Fig. 3), show an stress state compressive in the convergence strike of the Nazca plate with respect to the South American plate in sense W-E, in this region is appreciated a rotation of the stress counterclockwise from one trend W-E to the south of 5°N to other trend WSW -ENE to the north of this latitude, its result of the decomposition of the vector of convergence of the Nazca plate in two vectores, the first normal to the margin of the coast (deformation vector) and the second parallel to the margin (displacement vector), which are transferred to the zone of couple and to the continent, favoring the reactivation of preexistents the major fault systems NS (Romeral Fault System and Guaicáramo Fault) those which control the cordilleran foothills, and the transpressive faulting systems NNE, (Garrapatas, Algeciras, Ibagué, Palestina and Santa Marta – Bucaramanga Faults), imprinting them a displacement strike that it is in favor of the tensor, consequent with documented at continental scale by Dewey, 1992.

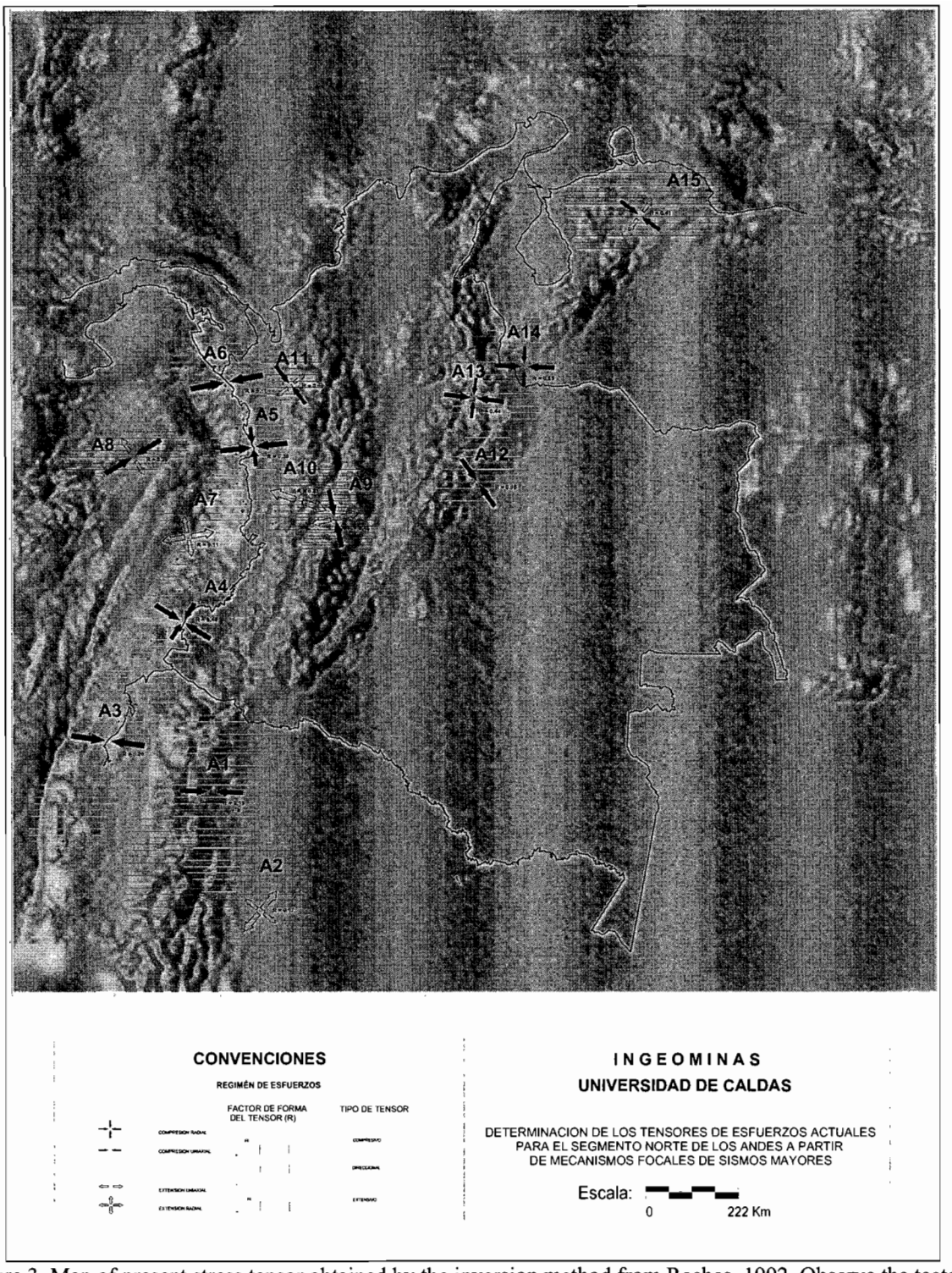

Figura 3. Map of present stress tensor obtained by the inversion method from Reches, 1992. Observe the tectonic regime of each area is given by the shape of factor (R) .

The distensive stress regime obtained from the inversion of focal mechanisms of deep earthquakes in the areas A2 and A10 evidence clearly the subduction process of the plate Nazca under the South American plate. The areas A3, A4, A5, A6 and A12 associated with shallow sismicity are related to a compressive regime product of the interaction of the Nazca plate and South American plate. In Ecuador (A1) the presence of the Carnegie rigde (overthickened oceanic slab product of the activity of the hot spot of Galapagos) makes difficult the subduction process by which the stress transference is manifested in high seismic activity rate in the zone of couple (earthquake of Tumaco) and intense deformation to the interior of the continental plate.

In the areas A9 and A11 corresponding with the regions of the Eje cafetero and Murindó respectively, the directional stress regime is product of the push of the Chocó Block (CB) in trend southeast with respect to the

NWSA (Fig. 1) occurred near the Mioceno middle (12 m.a) (Duque-Caro, 1990), though is not discarded for the area A9 the influence of a displacement vector due to the partition of the stress by the oblique interaction between the Nazca and South American plates.

The inversion of deep focal mechanisms (<150 km) in the region of the Nest of Bucaramanga (A13) shows an stress regime compressive is not coherent whith the models in which the nest is proposed as a manifestation of the subduction of the plate Nazca under South American plate (e.g. Taboada et al .,2000), by such reason is necessary carry out structural and seismologics studies in the Colombian Caribbean that provide base information in order to the formulation of a tectonic model for this region.

Finally, in the northeast region of Venezuela (A15) the interaction of the Caribbean plate and the Maracaibo block is absorbed by the major fault systems strike-silp (Boconó and Santa Marta – Bucaramanga faults) that limit the Andes of Merida, coherent with the obtained directional regime.

REFERENCES

Bohorquez, O., et al., Tensor de esfuerzos preliminar y estudios de réplicas. En edición revista Horizontes Naturales de la Universidad de Caldas.

Bott, M.H.P., (1959). The mechanism of oblique-slip faulting. Geol. Mag., Vol 96, p.109-117.

Carvajal, C., et al., (2001). Estado actual de la deformación en el territorio colombiano. En edición revista Horizontes Naturales de la Universidad de Caldas.

Dewey, et al., (1992). Active tectonics of the Andes. Tectonophysics, 205, p. 79-95.

Dimate, C., (1995). The 19 january 1995 Tauramena (Colombia) earthquake: geometry and stress regime. (Inf. Int. Ingeominas).

Duque-Caro., (1990b). The Chocó Block in the northwestern corner of South America: structural, tectonostratigraphic, and paleogeographic implications. J South Am. Earth Sci. 3, p. 71-84.

Ego, F., et al., (1996). Quaternary state of stress in the northern Andes and the restraining bend model for the Ecuadorian Andes, Tectonophysics 259, p. 101-116.

Phillip, H., (1987). Plio-Quaternary evolution of the strees field in Mediterranean zones of subduction and Collision, Geophysicae 5B, (3), p 301-320.

Reches, Z., Baer, G. y Hatzor, Y., (1992). Constraints on the strength of the Upper Crust from stress inversion of fault slip data. J. Geophys.Res., Vol 97, p.12481-12493.

Taboada, A., et al., (2000). Geodynamics of the Northern Andes, Tectonics, Vol. 19, N. 5, p. 787-813.

PROVENANCE OF THE UPPER CRETACEOUS TO MIDDLE EOCENE CLASTIC SEDIMENTS OF THE WESTERN CORDILLERA OF ECUADOR

Jorge TORO ÁLAVA (1, 3) and Etienne JAILLARD (2, 3)

(1) Petroproducción, Av. 6 de Diciembre y G. Cañero, Quito, Ecuador, PO Box 17-01-1006 jedutoro@hotmail.com
(2) IRD, UR 106, 38 rue des 36 Ponts, 31 000 Toulouse, France.
(3) IRD-LGCA, Maison des Géosciences, BP 53, 38 041 Grenoble Cedex, France ejaillar@ujf-grenoble.fr

KEY WORDS: Western Cordillera of Ecuador, mineralogy modes, modal analysis, clastic sediments, source areas, maturity.

INTRODUCTION

The petrographic study of the upper Cretaceous to middle Eocene clastic sediments of the Western Cordillera of Ecuador (WCE), aims to determine their sources and their relationship with the tectonic evolution of the Andes. Sandstone petrography reflects both the source areas and the tectonic setting of the depositional areas. Quantitative sandstone detrital modes, determined by point counting on thin sections, can be used to index provenance studies (Schwab 1986). Sandstone framework mineralogy modes are expressed by Q-F-L, Qm-P-K, and Qp-Lv-Ls diagrams. In these diagrams and in the classical classification diagrams of sandstones, Q = Qt = total quartz grains (monocrystalline Qm, and policrystalline Qp); F = total feldspar grains, K = K feldspar, P = plagioclase; and Lt = total lithic fragments (stable, and total unstable lithic fragments L), Lv = volcanic rock fragments, and Ls = sedimentary rock fragments (Tucker 1991). In addition, we used the FLvLs and QMxOM diagrams, where: Mx = total matrix content, and OM = estimated organic matter content in thin section.

GEOLOGICAL SETTING

The basement of the WCE (Fig. 1) is made of several oceanic terranes accreted successively to the Andean margin between the Late Cretaceous (~80-85 Ma) and the Eocene (~40 Ma, Feininger & Bristow 1980, Hughes et al. 1999, Reynaud et al. 1999). In the study areas (Fig. 1), the Late Cretaceous - Palaeogene, mainly turbiditic deposits comprise (Fig. 2): the black cherts, greywackes and limestones of the upper Campanian - Maastrichtian Yunguilla Fm. These are unconformably overlain by the Saquisilí Fm (1000 m) of lower to middle Palaeocene age (Hughes et al. 1999), composed of siltstones and fine- to medium-grained quartz-sandstones, rich in muscovite and heavy minerals. Although dominated by conglomerates, the overlying Gallo Rumi Fm (1000 m) exhibits the same composition as the Saquisilí Fm. It is ascribed to the upper Palaeocene, and grades upwards

into siltstones and very fine-grained sandstones. An angular unconformity separates the Gallo Rumi Fm from the middle Eocene Apagua Fm (2000 m). The latter comprises mainly medium-grained quartz-sandstones. The Apagua Fm is overlain by the continental Rumi Cruz Fm (1500 m) assigned to the upper Eocene (Hughes et al. 1999). The Rumi Cruz conglomerates are rich in clasts of black cherts and quartz.

RESULTS

Standard diagrams for arenites and greywackes classification (Dott 1964, Folk et al. 1970, Pettijohn et al. 1987), evidence that (1) the Yunguilla Fm sediments are mainly fine-grained feldspathic greywackes; (2) the Saquisilí Fm sediments are mainly lithic greywackes, litharenites and sublitharenites; and (3) the turbidites of the Apagua Fm are mainly sublitharenites, litharenites, and lithic greywackes.

According to the Q-F-L diagram (Dickinson 1985, Fig. 3), the Yunguilla Fm derived mainly from the erosion of a transitional magmatic arc terrane, and in a minor part from the erosion of basement rocks. Between the Maastrichtian and the Palaeocene, the source area changed dramatically. The Palaeocene Saquisilí Fm recycled an orogen rich in both quartz grains and lithic fragments. Finally, the petrography of the middle Eocene Apagua Fm suggests that it recycled an uplifted orogen marked by abundant metamorphic clasts. This evolution of the source areas correlates with variations of the grain size (Fig. 9), and of the matrix and organic matter contents (Fig. 4). Both the average grain size and median of the maximum grain size increase from the Yunguilla Fm (183.8 μ and 683.8 μ, respectively) to the Apagua Fm (374.4 μ and 1514.2 μ, respectively) (412.4 μ and 1788.8 μ, respectively in the Saquisilí Fm). The Q-Mx-OM diagram shows a clear trend from matrix and OM rich samples in the Yunguilla Fm, to medium to poor contents in matrix and OM in the Saquisilí and Apagua Fms.

According to the Qm-P-K diagram (Dickinson & Suczek 1979), which characterizes the tectonic setting of the source areas, the latest Cretaceous Yunguilla Fm is dominated by volcanic grains and clasts, indicating a magmatic arc source (Fig. 5). The Paleocene Saquisilí Fm shows a clear increase of the plutonic/volcanic ratio, evolving from a magmatic arc source to a circumpacific VP suite of modes. Finally, the composition of the Apagua Fm and the increasing maturity and stability of its clastic components indicates an evolution to continental block, dominantly crystalline source areas. The Qp-Lv-Ls diagram (Dickinson & Suczek 1979) suggests a complex evolution of source areas (Fig. 6). The Yunguilla Fm is marked by fine clastic sediments of basin to shelf environment, rich in volcanic lithics and in fine-grained siliceous sediments, some of diagenetic origin. In the overlying Saquisili Fm, the sandstones rich in cherts of chemical to biochemical origin indicate the influence of collisional orogenic setting. The sandstones of the Apagua Fm are rich in cherts, Lv and Ls, suggesting a composite tectonic setting, dominated by both collisional orogenic and subduction complex sources.

The F-Lv-Ls diagram (Fig. 7) shows another well defined trend. The fine-grained sediments of the Yunguilla Fm are very rich in feldspars, whereas the sandstones of the Saquisilí Fm are rich in feldespars and in volcanic rock fragments. The Apagua Fm is characterized by roughly equal proportions of the three modal components: F, Lv and Ls. Therefore, from the Palaeocene to the Eocene, the source areas changed from a transitional plutonic arc terrane to an arc orogen. We interpret this trend as the result of the progressive uplift of the source areas.

CONCLUSIONS

The upper Campanian-lower Maastrichtian Yunguilla Fm is made of fine-grained feldspathic greywackes, deriving from a transitional magmatic/volcanic arc terrane, and possibly deposited in a marine forearc basin.

The lower to middle Palaeocene Saquisilí Fm is made of sandstones, classified as lithic greywackes, litharenites, sublitharenites, rich in feldspars and in volcanic rock fragments. It was deposited in a collisional setting, and recycled probably a metamorphic and partly plutonic uplifted basement.

The middle Eocene sandstones of the Apagua Fm are sublitharenites, litharenites and lithic greywackes, marked by a high maturity and stability of the clastic components. It may have deposited in a composite tectonic environment, recycling uplifted plutonic and metamorphic areas (continental block sources/crystalline source).

The increasing occurrence of plutonic or metamorphic fragments in the Saquisilí and Apagua Fms indicates that the crystalline basement was uplifted and increasingly eroded during the lower Paleocene-middle Eocene interval. The trend from volcanic (Yunguilla Fm) to plutonic/metamorphic (Saquisilí and Apagua Fms) source areas correlates with a coarsening upwards trend, and with a decrease of the matrix and organic matter contents.

REFERENCES

Dickinson W.R. 1985. Interpreting provenance relations from detrital modes of sandstones, *in*: Provenance of arenites, Zuff G.G. Eds., 333-362, D. Reidel Publ. Co.

Dickinson W. R., Suczek C. A. 1979. Plate tectonic and sandstone composition, AAPG Bull., 63, 2164-2182.

Dott R.H. 1964. Wacke, graywacke and matrix-what approach to inmature sandstone clasification?, J. Sedim. Petr., 34, 625-632.

Feininger T., Bristow C.R. 1980. Cretaceous and Paleogene history of coastal Ecuador, Geol. Rundschau, 69, 849-874.

Folk R.L., Andrews P.B., Lewis D.W. 1970. Detrital sedimentary rock classification and nomenclature for use in New Zealand, NZ J. Geol. Geophys., 13, 937-968.

Hughes R.A., Bermúdez R., Espinel G. 1999. Mapa Geológico de la Cordillera Occidental del Ecuador entre 0°-1°S., 1:200 000, Codigem - Ministerio de Energía, y Minas - BGS Publs., Quito, Nottingham.

Jaillard E., Benites S., Mascle G. H. 1997. Les déformations paléogènes de la zone d'avant-arc sud-équatoriennes en relation avec l'évolution géodynamique. Bull. Soc. Géol. France, 168, 403-412.

Pettijohn F. J., Potter P. E., Siever R. 1987. Sand and sandstone. Springer Verlag, New York, 553 pp.

Reynaud C., Jaillard É., Lapierre H., Mamberti M., Mascle G.H. 1999. Oceanic plateau and island arcs of Southwestern Ecuador: their place in the geodynamic evolution of Northwestern South America,Tectonophysics, 307, 235-254,

Tucker M.E. 1991. Sedimentary Petrology: an introduction to the origin of the sedimentary rocks, Blackwell Publ., 2nd ed., Oxford, 259 p.

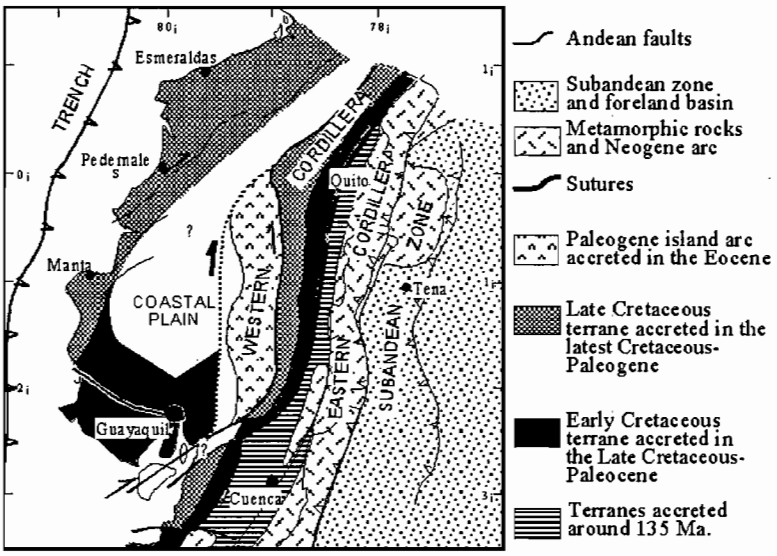

Fig. 1 : Oceanic terranes accreted in Ecuador

Unit	Age
Saraguro	Oligo-Miocene
Rumi Cruz	Upper Eocene
Apagua	Middle Eocene
Gallo Rumi	Upper Paleocene ?
Saquisilí	Low.-Mid. Paleocene
Yunguilla	Up. Camp.-Low. Maastr.

Fig. 2 : Stratigraphic succession of the study area

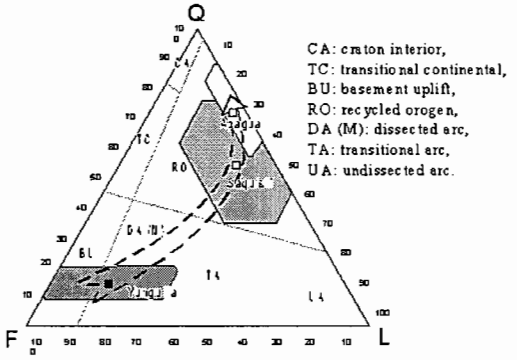

Fig. 3. Q-F-L diagram (discrimination of source areas)

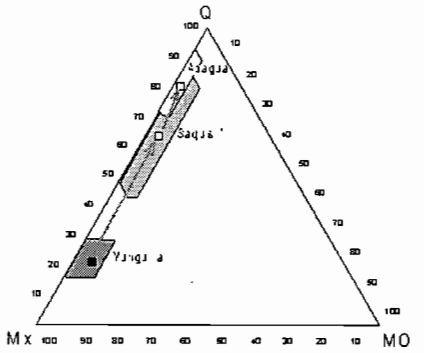

Fig. 4. Matrix (Mx) and organic (MO) contents.

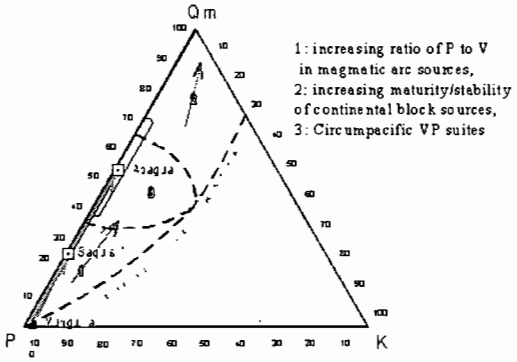

Fig. 5. Q-P-K diagram.

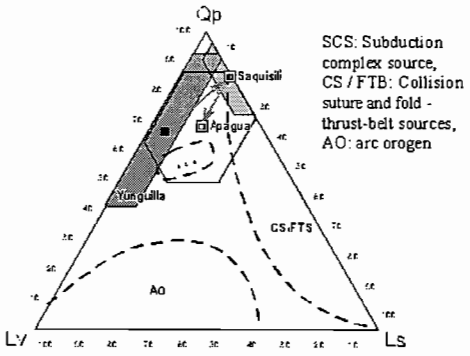

Fig. 6. Qp-Lv-Ls diagram.

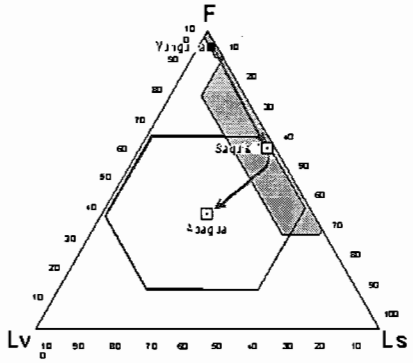

Fig. 7. F-Lv-Ls diagram.

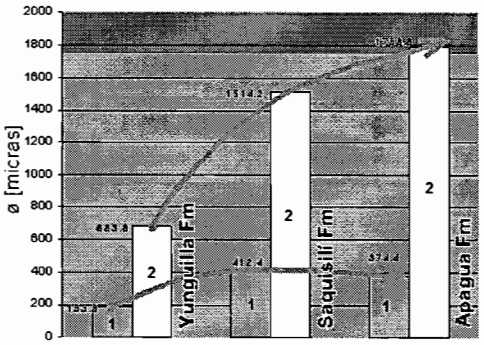

Fig. 8. Grain size variation (1: phi moyen, 2: phi max)

K-Ar GEOCHRONOLOGY OF THE SAN LUIS GOLD BELT, CENTRAL ARGENTINA: A REVIEW

Nilda E. Urbina (1)

(1) Universidad Nacional de San Luis. Ejército de los Andes 950. 5700 San Luis, Argentina. urbina@unsl.edu.ar

KEY WORDS: Geochronology, Tertiary, Gold, Deposits, Ore, Metallogeny

INTRODUCTION

The San Luis Tertiary metallogenic belt is located between latitudes 32° 45' - 33° 14' S and longitudes 65° 24' – 66° 05' W in the Sierras Pampeanas of San Luis, central Argentina (Fig. 1a). This belt comprises several deposits and hydrothermal alteration zones hosted by volcanic rocks, stocks which intruded them, and Precambrian to Paleozoic igneous-metamorphic basement rocks. K-Ar ages have demonstrated that the volcanic event and the associated mineralization process took place during the late Miocene to late Pliocene period. This short paper presents a geochronological data compilation of 11 radiometric ages that, as a whole, could contribute to understand the evolution of the San Luis metallogenic belt.

GEOLOGICAL SETTING

The volcanic rocks and associated mineralizations in the Sierras Pampeanas of San Luis occur within a west-northwest-trending magmatic belt which is roughly perpendicular to the main reverse faults that constitute the western boundary of the San Luis range (Fig.1a). The mineralizations and the volcanic rocks with which they are related were generated on the inner side of an arc environment as a consequence of the subduction zone shallowing between latitudes 28° and 33° S (Kay et al., 1999). Mesosilicic magmas belonging to normal to high-K calc-alkaline and shoshonitic types (Brogioni, 1987; Urbina et al., 1997) show at both regional and local scales a K enrichment with decreasing ages (Urbina et al., 1997). The resulting volcanic rocks cropping out from La Carolina in the west to El Morro in the east (Fig.1b) can be grouped into andesites, dacites, latites, and trachytes that were emplaced as domes, flows, cones, sills, dykes and pyroclastic deposits. Low sulphidation epithermal and porphyry-type deposits have been recognized in relation with the Tertiary volcanic event. Sulphide-rich base metals, gold and silver epithermal deposits and the Diente Verde gold-rich porphyry copper are associated with eroded volcanic centers and a high-level stock in the western part of the belt while carbonate epithermal deposits are predominant in the eastern side of the belt. Elsewhere in the San Luis belt, the emplacements of volcanics and associated mineralizations appear to be controled by intersections of NNE-SSW, E-W and NW-SE structural trends.

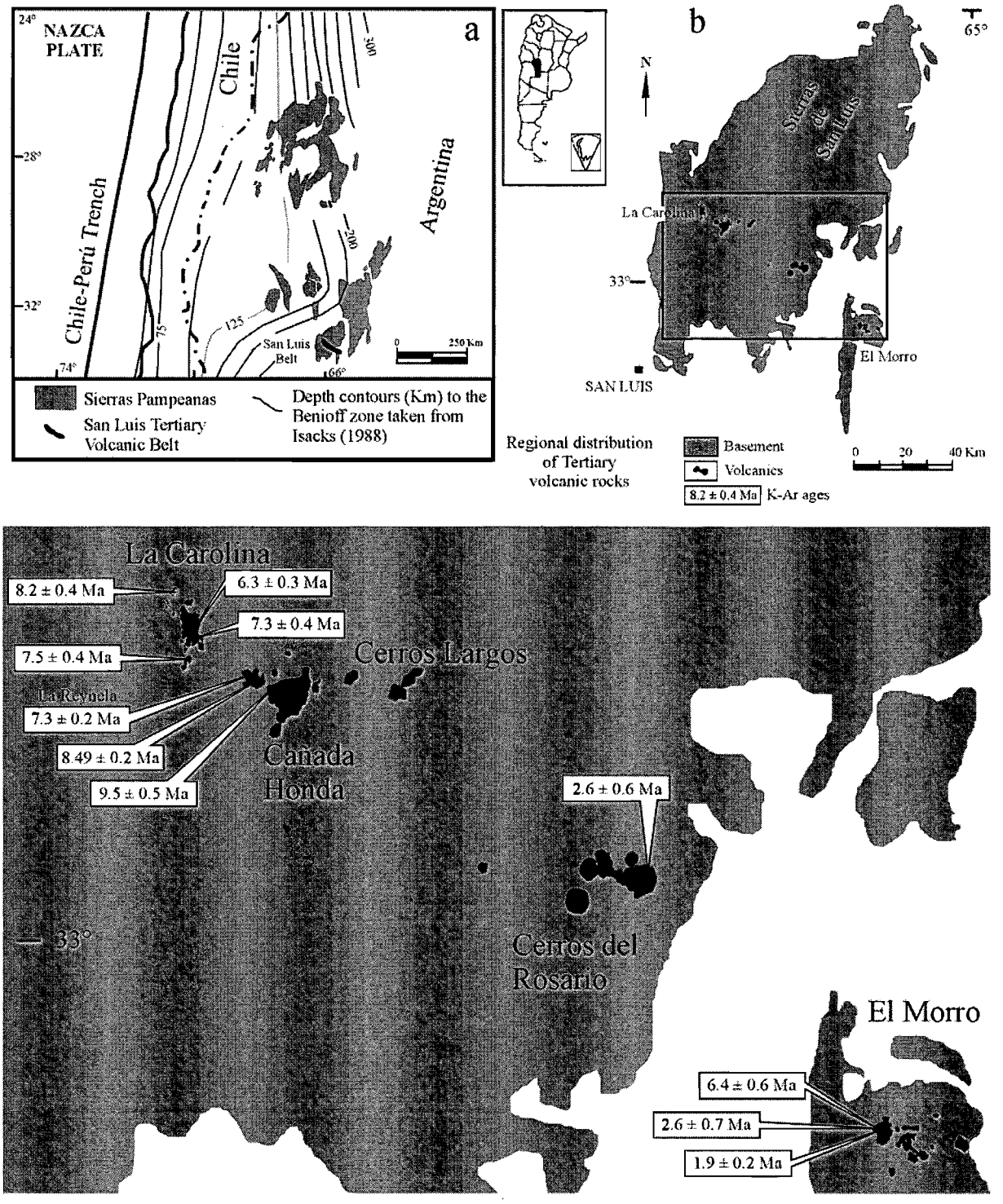

Figure 1. a) Location of the San Luis Tertiary metallogenic belt in the Central Andean flat slab region. b) Simplified map of the Sierra de San Luis showing the regional distribution and ages of Tertiary volcanic rocks.

GEOCHRONOLOGY

The four most important volcanic centers in the San Luis belt (Tres Cerritos-La Carolina, Cañada Honda-Cerros Largos, Cerros del Rosario, Sierra del Morro) and the hydrothermal alteration of La Reynela low sulphidation carbonate-base metals epithermal vein were previously dated by the K-Ar method indicating a late

Miocene to late Pliocene age for the belt (Ramos et al., 1991; Urbina et al., 1995; Sruoga et al., 1996; Urbina and Oggier, 2001). The eleven existing ages are presented in Table 1 with locations shown in Figure 1 b.

At Tres Cerritos, one sample from andesitic dome was dated at 8.2 ± 0.4 Ma. At La Carolina district, two very similar ages, 7.5 ± 0.4 and 7.3 ± 0.4 Ma, were obtained respectively for both fresh and altered lacites from Tomolasta and Pan de Azucar domes, whereas a distinctly younger age of 6.3 ± 0.3 Ma was yielded by sanidine from a trachytic dyke. Farther east, at Cañada Honda district, the andesitic walls of Diente Verde volcanic cone were dated at 9.5 ± 0.5 Ma. For the same district, an age of 8.49 ± 0.2 Ma was obtained for an andesite from Cerro del Valle dome. An even younger age of 7.3 ± 0.2 Ma was provided by illite accompanying La Reynela epithermal vein which cuts Cerro del Valle andesite. A single age of 2.6 ± 0.6 Ma was obtained by Ramos et al. (1991) from a biotitic dacite at Cerros del Rosario district. And finally, at Sierra del Morro district in the eastern end of the belt, the same authors reported ages of 6.4 ± 0.6 Ma for a pre-caldera andesite, 2.6 ± 0.7 Ma for an andesite from the top of the intra-caldera pyroclastic sequence and 1.9 ± 0.2 Ma for latest trachyandesitic dykes.

Table 1. K-Ar data for samples from the San Luis Gold-bearing Volcanic Belt, Central Argentina

Sample n° and locality	Sample description	Material dated	K-Ar age	Reference
C 41, Tres Cerritos, Tres Cerritos-La Carolina district	Andesite from the dome	Whole-rock	8.2 ± 0.4 Ma	Sruoga et al. (1996)
C 3, Cerro Tomolasta, La Carolina district	Lacite from the dome	Sanidine	7.5 ± 0.4 Ma	Urbina et al. (1995)
C 4, Cerro Pan de Azucar, La Carolina district	Lacite from the dome	Whole-rock	7.3 ± 0.4 Ma	Urbina et al. (1995)
C 46, trachytic dyke, La Carolina district	Trachyte from dyke	Sanidine	6.3 ± 0.3 Ma	Sruoga et al. (1996)
DV5, Cerro Diente Verde, Cañada Honda district	Andesite from the wall of the volcanic cone	Whole-rock	9.5 ± 0.5 Ma	Urbina et al. (1995)
CVM7, Cerro del Valle, Cañada Honda district	Andesite from the dome	Whole-rock	8.49 ± 0.2 Ma	Urbina and Oggier (2001)
LR 1-4 III, La Reynela deposit, Cañada Honda district	Hydrothermal alteration	Illite	7.3 ± 0.2 Ma	Urbina and Oggier (2001)
7124 H706/88, Cerros del Rosario district	Dacite	Whole-rock	2.6 ± 0.6 Ma	Ramos et al. (1991)
7121 H704/88, Sierra del Morro district	Pre-caldera andesite	Whole-rock	6.4 ± 0.6 Ma	Ramos et al. (1991)
7122 P574/88, Sierra del Morro district	Intracaldera andesite	Whole-rock	2.6 ± 0.7 Ma	Ramos et al. (1991)
7123 P596/88, Sierra del Morro district	Trachyandesitic dyke	Whole-rock	1.9 ± 0.2 Ma	Ramos et al. (1991)

DISCUSSION AND CONCLUSIONS

Volcanic activity in the San Luis belt began at 9.5 Ma and ended at 1.9 Ma. Volcanism took place immediately prior to, and during the final stages of the slab flattening between 28° and 33° S Lat. Volcanic rocks and associated mineralizations were generated 700 km east from the Chilean trench during a period of 7.6 Ma and over a west-east distance of about 80 km. For that reason the San Luis belt represents the easternmost and youngest Tertiary volcanic and metallogenic event in Argentina.

The results above demonstrate that, as a whole, the rock ages become progressively younger from west to east in the belt. Nevertheless, the ages obtained for Cañada Honda district show that this is the oldest volcanic field in the belt. La Reynela deposit with 7.3 ± 0.2 Ma postdates the main volcanic episode at Cañada Honda district which took place between 9.5 and 8.49 Ma, and predates the El Morro eruptions to the east. The lifespan of the hydrothermal system at Cañada Honda district may therefore be established in a period of time of approximately 1.2 Ma. At the same time, La Reynela deposit seems to have been formed at least partly overlapping the volcanic activity at La Carolina district, where the ages of both fresh and altered rocks range from 7.5 ± 0.4 to 7.3 ± 0.4 Ma suggesting that the hydrothermal alteration is closely linked to the volcanic emplacement in that area. On the other hand, the latest emplacement of a trachytic dyke in La Carolina district at 6.3 ± 0.3 Ma is simultaneous with Sierra del Morro pre-caldera andesite and clearly predates the major volcanic activity in the eastern side of the belt, which is interpreted as the final stage of waning volcanism between 6.4 ± 0.6 Ma and 1.9 ± 0.2 Ma. Therefore, the volcanic activity at La Carolina district ceased when the eruptions began at Sierra del Morro district.

As noted above, the evidence suggest the probable existence of at least two different magmatic pulses and associated mineralization periods accompanying the eastward migration of the volcanic front: 9.5 to 6.3 Ma in the west and 6.4 to 1.9 Ma in the east. In addition, contrasting deposit types are present along the belt: sulphide-rich base metals, gold and silver low sulphidation epithermal deposits and the Diente Verde gold-rich porphyry copper appear in the western side of the belt (La Carolina and Cañada Honda district) whilst those in the eastern part of the belt are carbonate dominated epithermal deposits (Cerros del Rosario district). This change of mineralizations along the belt, with concentration of metal deposits in the western side, might probably reflect an eastward-decreasing depth of erosion and mineralization ages.

REFERENCES

Brogioni N. 1987. Petrología del vulcanismo Mio-Plioceno de la Provincia de San Luis. Revista Museo de La Plata, Sección Geología, X, 83, 71-100.

Isacks B. L. 1988. Uplift of the central Andean plateau and bending of the Bolivian Orocline. Journal of Geophysical Research, 93, 3211-3231.

Kay S. M., Mpodozis C. and Coira B. 1999. Neogene Magmatism, Tectonism, and Mineral Deposits of the Central Andes (22° to 33° S Latitude). In: Skinner B. J. (Ed.) Geology and Ore Deposits of the Central Andes, Special Publication 7, Society of Economic Geologists, 27-59.

Ramos V., Munizaga F. and Kay S. M. 1991. El magmatismo Cenozoico a los 33 ° S de Latitud: Geocronología y Relaciones Tectónicas. 6 ° Congreso Geológico Chileno, 892-896.

Sruoga P., Urbina N. and Malvicini L. 1996. El Volcanismo Terciario y los depósitos hidrotermales (Au, Cu) asociados en La Carolina y Diente Verde, San Luis, Argentina. XIII Congreso Geológico Argentino, 3, 89-100.

Urbina N. and Oggier F. P. 2001. New K-Ar ages of volcanic rocks and associated mineralization in Cañada Honda district, San Luis, Argentina. III South American Symposium On Isotope Geology Volume (CD-ROM), Sociedad Geológica de Chile, Santiago, Chile: 539-542.

Urbina N., Sruoga P. and Malvicini L. 1995. El volcanismo Mioceno y la mineralización aurífera asociada en La Carolina y Diente Verde, provincia de San Luis, Argentina. IX Congreso Latinoamericano de Geología, Caracas, Venezuela (CD-ROM) TE M5-252, 1-13.

Urbina N., Sruoga P. and Malvicini L. 1997. Late Tertiary Gold-Bearing Volcanic Belt in the Sierras Pampeanas of San Luis, Argentina. International Geology Review, 39, 4, 287-306.

PARTICULATE ORGANIC MATTER ANALYSES AND OIL POTENTIAL OF THE NAPO GROUP, SUBANDEAN ZONE, ECUADOR

Cristian VALLEJO (1), Peter A. HOCHULI (1, 2) Wilfried WINKLER (3)

(1) Department of Earth-Sciences, ETH Zürich, CH-8092 Zürich, Switzerland (cristian.vallejo@erdw.ethz.ch)
(2) Stratigraphic Consulting, Rue des Alpes 3, CH-1580 Avenches, Switzerland (peter.hochuli@erdw.ethz.ch)
(3) Department of Earth-Sciences, ETH Zürich, CH-8092 Zürich, Switzerland (wilfried.winkler@erdw.ethz.ch)

KEY WORDS: Napo Group, organic matter, source potential, Oriente Basin

INTRODUCTION

The Subandean Zone of Ecuador (SAZ) is the westernmost and proximal part of the Oriente Basin. In this area the Paleozoic basement and the Mesozoic to Tertiary volcanic and sedimentary formations are exposed in large-scale antiforms and thrust slices. This architecture is due to the eastward thrusting of the Cordillera Real over the Guyana Shield and Oriente Basin fill series.

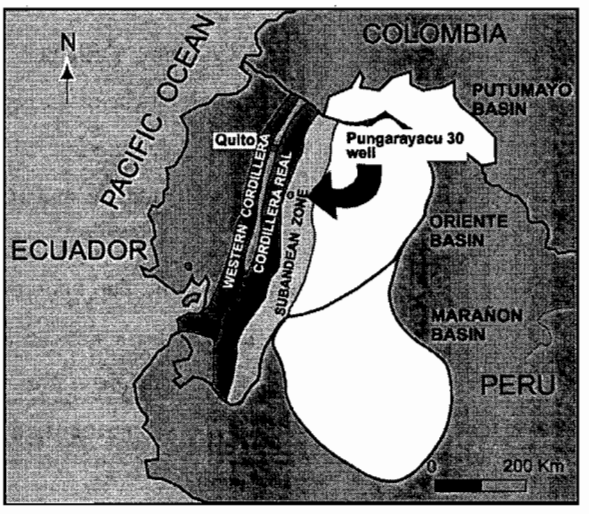

Figure 1. Location Map

The Napo Group is a sedimentary series including organic rich shales, sandstones and limestones of Late Albian to Campanian age. It is subdivided in four formations: Napo Basal, Lower Napo, Middle Napo and Upper Napo (Jaillard, 1997), which were deposited in the epicontinental Oriente Basin (Fig. 1). This basin has yielded the

majority of hydrocarbons that have been extracted from the Putumayo-Oriente-Marañon oil province (Rivadeneira & Baby, 1999). Sandstones of the Napo Group are the main oil reservoir rocks in the Oriente Basin, whereas organic rich intervals are assumed to be the oil source rock.

In this study we use sedimentological, and particulate organic matter (POM) data, in order to reconstruct the depositional environment, and to evaluate the oil source potential of the Napo Group. For this we have selected the Pungarayacu 30 well (Fig. 1), which contains the most complete record of the Napo Group in the SAZ, including the oil reservoir rocks and the presumed oil source intervals.

DISCUSION

Based on POM and sedimentological evidence (Fig. 2), several stratigraphic sequences have been recognized within the Napo Group in the Pungarayacu 30 well. These sequences are comprised in two larger scale sedimentary stages: the first one including the Napo Basal and Lower Napo Formations is characterized by important input of terrestrial derived phytoclast and palynomorphs (up to 90%), deposited during well-developed lowstand system tracts (LST). Whereas in the second stage (Middle and Upper Napo Fm.) the POM assemblages are characterized by high abundance of well preserved (fluorescent) amorphous organic matter (AOM), a general decrease in the terrestrial derived material, and high TOC values, ranging between 9,8–12%. Anoxic-dysoxic conditions, that enhanced the preservation of the organic matter, produced high quality source rocks. During this latter stage, restricted marine environments prevailed and LSTs are not preserved or are of minor importance.

According to paleogeographic reconstructions (Pindell & Tabbutt, 1995), the northwestern South American basins were connected during the Late Cretaceous. During most of this period, the Ecuadorian segment was probably separated from the Pacific Ocean by a proto-Cordillera Real, which isolated the basin from open marine conditions, enhancing organic matter preservation by restricted water circulation. Such barriers have been also recognized for contemporaneous formations in Colombia (Villeta Fm.) and in Venezuela (La Luna Fm.), where they are also assumed to play a role in the development of anoxic bottom waters. The described POM and paleontological data (e.g. oysters) and the high accumulation rate of organic matter, suggest a prevailing shallow water column (ca. 20-40 m deep), where oxidative and respiratory losses were minimal, allowing the preservation of the organic matter in sediments.

In the studied well, oil prone intervals are found in the Middle Turonian interval, corresponding to the Lower A Limestone and Lower M2 Limestone Members (Fig. 2). They are characterized by high abundance of well preserved AOM (up to 70%) associated with high TOC values (10–12%). Time equivalent sediments in Colombia and Venezuela have been related to maximum flooding events, that allowed the preservation of organic matter in anoxic bottom water conditions (Erlich *et al.*, 1999; Ramon *et al.*, 2001). Therefore, this interval is regionally identified and corresponds to a widespread event. However, according to our data it does not coincide with the early Turonian global flooding event (OAE2). In the Oriente Basin this event seems to fall

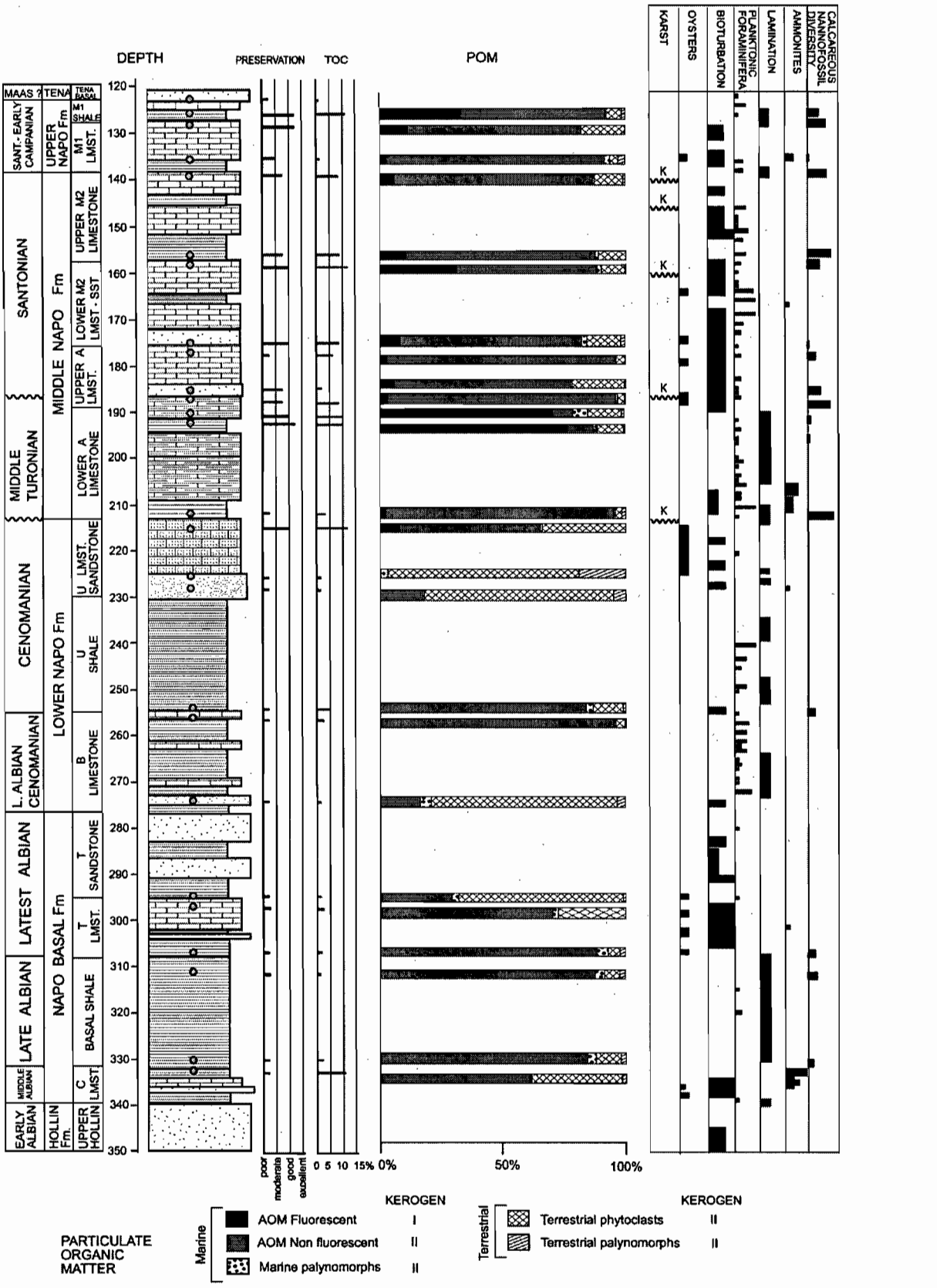

Figure 2. Lithostratigraphy, sedimentary structures (modified from Jaillard, 1997), TOC, preservation and POM of the Pungarayacu 30 well.

within the Early Turonian hiatus.

The colour of palynomorphs is used as a direct indicator of thermal maturation. In the Pungarayacu 30 well the colour of the palynomorphs varies between pale yellow to yellow, corresponding to a value of 2 in the Thermal Alteration Scale (TAS of Batten, 1982). This correlates well with average T max values of 428°C, as determined by pyrolysis. Vitrinite reflectance of values 0.4–0.5% from the same area are also in line with these features. These data indicate thermally immature conditions for oil generation, with an equivalent temperature being below 60 °C.

The origin of the oil accumulation in the Pungarayacu area remains to be explained. Thermally immature conditions of the sediments indicate that they were not able to generate major quantities of liquid hydrocarbons. It is possible that the oil was generated and migrated from an equivalent source of a neighboring area, or that it was sourced from pre-Cretaceous rocks of which the oil potential remains to be proved.

REFERENCES

Batten, D. J. 1982. Palynofacies, palaeoenvironments and petroleum. *Journal of Micropaleontology* **1**, 107-114

Erlich R. N., Macsotay, O., Nederbragt, A. J., Lorente, A. 1999. Palaeoecology, palaeogeography and depositional environments of Upper Cretaceous rocks of western Venezuela. *Palaeogeography, Palaeoclimatology, Palaeoecology* **153**, 203–238.

Jaillard, E. 1997. Síntesis Estratigráfica y Sedimentológica del Cretácico y Paleógeno de la Cuenca Oriental del Ecuador. Informe final del convenio Orstom-Petroproducción. 164 pp.

Pindell, J. & Tabbutt K. 1995. Mesozoic-Cenozoic Andean paleogeography and regional controls on hydrocarbon systems, In *Petroleum basins of South America* (eds Tankard, A. J., Suarez, R. & Welsink, H.J.), *American Association of Petroleum Geologists, Memoir* **62**, 101-128.

Ramon, J. C., Dzou L. I., Hughes, W. B., Holba, A. B. 2001. Evolution of the Cretaceous organic facies in Colombia: implications for oil composition. *Journal of South American Earth Sciences* **14**, 31-50.

Rivadeneira, M. & Baby P. 1999. La Cuenca Oriente: Estilo Tectonico, Etapas de Deformacion y Caracteristicas Geologicas de los principales campos de Petroproducción. Petroproecuador - IRD, Quito.

This work was supported by a Swiss Government Fellowship Grant provided to CV.

NEOPROTEROZOIC DIAMICTITES FROM FOUR DIFFERENT CRATONS: PROVENANCE AND PALEOTECTONIC SETTING – FIRST RESULTS

Anelda VAN STADEN[1] and Udo ZIMMERMANN[1]

[1]Department of Geology, RAU, Auckland Park 2092, South Africa (E-mail: uz@na.rau.ac.za)

KEY WORDS: Neoproterozoic, diamictites, snowball earth, Sierras Pampeanas, Sierra Tandil, provenance

INTRODUCTION

Tillites (glacial deposits) or diamictites are seldomly studied with provenance as a focus. In this case study probable glacial deposits of Neoproterozoic ages are investigated related to the so-called "Snowball Earth hypothesis" (Hoffman, et al., 1998; Fig. 2). Conglomeratic rocks and diamictites from four regions related to different cratonic areas: northwestern Argentina, southern Bolivia and southwest Brazil (Sierra Pampeanas block and Amazonian craton), Sierra Tandil in the Buenos Aires Province (Rio de la Plata craton), northern Namibia (West-Congo craton) and northwest South Africa (Kalahari craton) (Fig. 1, 2) were selected. The provenance study of the Gondwana-wide exposed diamictites of Neoproterozoic age could provide a new tool to compare the probable source rocks of the glacial deposits on different Gondwana-cratons. Geochemical and isotopic approaches to constraining provenance of these sedimentary rocks compliment the information inferred from petrography. The final goal of this project involves the modelling of the evolution of upper crustal processes in these four regions and the paleogeographic distribution of tectonic plates during the Neoproterozoic in Central Gondwana (Fig. 2). We will combine "classical" methods (quantification of framework minerals and heavy minerals) with advanced methods of whole rock analysis (geochemistry and isotope geochemistry) and single grain characterisation. This should provide a possibility of modelling source and depositional areas and also processes of transportation and sedimentation.

CONCLUSIONS

With this we represent the first results of our fieldwork in the Sierra Tandil (Rio de la Plata craton) and the Sierras Pampeans (northwest Argentina). In both regions conglomeratic and diamictites are related with carbonates (e.g. Aceñolaza et al, 1990; Poire, 1993; Spalletti and Del Valle, 1984).

In the northwestern part of Argentina small conglomeratic outcrops are distributed in the Puncoviscana Formation, interpreted as the basement in that region (e.g. Aceñolaza et al., 1990). They are associated with fine-

grained turbidites and shales as well as carbonates. The Puncoviscana Formation is generally considered to represent a passive margin deposit of latest Precambrian-Early Cambrian age on the western margin of the Pampia Craton representing the western Gondwana margin during the Neoproterozoic (e.g. Jezek, 1985). In contradiction Keppie and Bahlburg (1999) interpret the formation as foreland basin deposits and Omarini et al. (1999) propose a back-arc position. However, quantitative petrological and geochemical data for the sedimentary rocks of the Puncoviscana Formation are insufficient for a provenance and a tectonic setting of these successions. The conglomeratic layers are thin (< 5 m) and widely distributed in the Puncoviscana Formation (Poman, Sierra Ovejerria, Cachi and Rosario de Lerma in northwest Argentina; Fig. 1). Quantifications of these layers and single-grain analyses with SEM to determine a possible glacial transport as well as stable isotope measurements of the carbonatic layers are in progress. The source areas of the Puncoviscana Formation is difficult to determine since older basement material was not found thus far. The regional exposed medium- to high-grade metamorphic rocks are interpreted as equivalents of the same formation (e.g. Aceñolaza et al., 1990). However, only few Nd-model ages were presented (Lucassen et al., 1999) and provenance analyses of the metasedimentary units are absent.

In the Sierra Tandil (Fig. 2) the diamictites (< 1,1 m) overly crystalline basement and are followed by orthoquartzites. The diamictites are composed mainly of sandstones, sandy shales with scattered dropstones of variable sizes. The clasts are of granitoid origin or represented by ortoquartzites. The provenance of the diamictites, based on petrological evidence, is represented by the underlying crystalline basement (Spalletti and Del Valle, 1984). More detailed characterisation of the diamictites and a comparison with the basement rocks of the same region will be accomplished by single-grain analyses and geochemical data. The relationship between the Sierra Pampeanas block and the Rio de la Plata craton during the Neoproterozoic is unknown.

The project is a contribution to the IGCP 436: Structure and Evolution of the Gondwana Margin.

REFERENCES

Aceñolaza, F.G. , Miller, H. and Toselli, A.J. 1990. El Ciclo Pampeanas en el Noroeste Argentino. Universidad Tucumán Correlación Geológica, 4, 227pp.

Hoffman, P.F., Kaufman, A.J., Halverson, G.P. and Schrag, D.P. 1998. A Neoproterozoic Snowball Earth. Nature, 281, 1342-1346.

Jezek, P.; Willner, A. P.; Aceñolaza, F. G.; and Miller H. 1985. The Puncoviscana trough- a large basin of Late Precambrian to Early Cambrian age on the Pacific edge of the Brazilian shield. Geol. Rundschau, 74/3, 573-584.

Keppie, J.D. and Bahlburg, H. 1999. Puncoviscana Formation of northwestern and central Argentina: Passive margin or foreland basin deposits?. In: *Laurentia-Gondwana connections before Pangaea* (Eds. V.A. Ramos and J.D. Keppie), Geological Society of America Special Paper, 336, 139-144.

Lucassen, F., Becchio, R., Wilke, H.G., Franz, G., Thirlwall, M.F., Viramonte, J. and Wemmer, K. 2000. Proterozoic-Paleozoic development of the basement of the Central Andes (18-26°S) – A mobile belt of the South American Craton. Journal of South American Earth Sciences, 13:697-715.

Omarini, R.H., R. J. Sureda, h.-j., Götze, a. Seilacher and f. Pflüger, 1999. Puncoviscana folded belt in northwesatern argentina. Testimony of late proterozoic rodinia fragmentation and pre-gondwana collisional episodes. *International journal of earth science.* 88, 76-97.

Poiré, D. G. 1993. Estratigrafía del Precámbrico sedimentario de Olavarría, Sierras Bayas, Provincia de Buenos Aires, Argentina. XII Congreso Geológico Argentino y II Congreso de Exploración de Hidrocarburos, actas, 2, 1-11.

Spalletti, L. and Del Valle, A. 1984. Las diamictitas del Sector Oriental de Tandilia: Caracteres sedimentológicos y orígen. Rev. Asoc. Geol. Arg., 39:188-206.

Unrug, R. (1996) The assembly of Gondwanaland. *Episodes,* 19, 11-20.

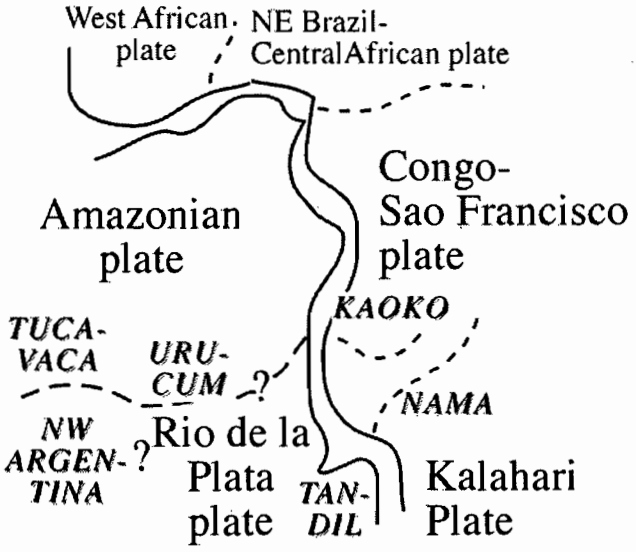

Fig. 1: Outcrop locations of probable Neoproterozoic glacial deposits in southern Southamerica.

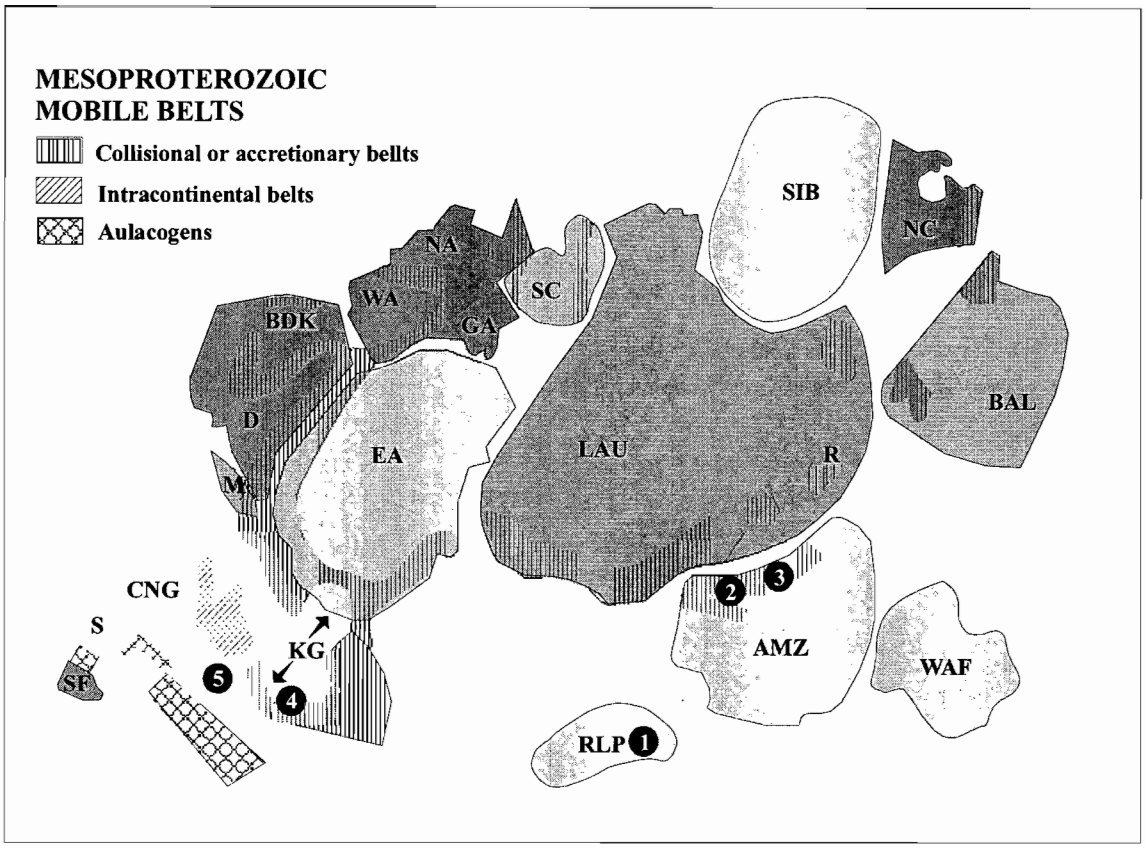

Archean and Paleoproterozoic cratons:

AMZ Amazonian
BDK Bundelkhand
CNG Congo
D Dharwar
EA East Antarctica
GA Gawler
ESN East Sahara-Nile
KG Kalahari-Grunehogna
LAU Laurentia
MD Madagascar-Dharwar
NA North Australian
NC North China
R Rockall
RLP Rio de la Plata
S Salvador
SC South China
SF Sao Francisco
SIB Siberia
WA Western Australian
WAF West African

Relative location of sampling:

1 Sierra de Tandil (Buenos Aires Province)
2 Tucavaca (S-Bolivia)
3 Urucum (SW-Brazil)
4 Gariep (NW-South Africa)
5 Kaoko (N-Namibia)
6 Sierras Pampeanas
(basement Gondwana age unknown and hence not indicated on map)

Fig. 2: The Rodinia supercontinent assembled at c. 1000 Ma (modified after Unrug, 1996).

STATE OF STRAIN AND STRESS IN NORWESTERN OF SOUTHAMERICA

Carlos A. VARGAS-JIMÉNEZ(1), Juan Pablo DURÁN-TOVAR(2)

[1]Departamento de Geociencias, Universidad Nacional de Colombia, Santafé de Bogotá - COLOMBIA. Email:cavj@hotmail.com
[2] Magister student of gephysic, Departamento de Geociencias, Universidad Nacional de Colombia, Santafé de Bogotá - COLOMBIA. Email: jpduran@hotmail.com

KEY WORDS: satellital geodesy, Colombia, Bucaramanga, seismicity

Application of satellital geodesy in campaigns CASA of 1991, 1994 and 1996 (See fig. 1), stress inversion analysis of 96 focal mechanisms for period 1976 – 2000 (See fig 2) obtained of Harvard University (Mw > 5) allowed to establish a compressive tendency in the west - east sense of the Panama-Costa Rica Block (BPC), that hit the North Andes Block (BNA). Nevertheless, some seismic evidences would allow to confirm the existence of the proposed Chocó Block (BC), with western limit already Darién Range, and eastern limit in the zone of Murindó, demonstrated by the stress inversion of these two zones, with sub-parallel tendency north - south. The southern limit, already 4° N, also shows stress with north - south tendency. Some located superficial earthquakes in the Pacific Coast, apparently western limit of Chocó Block, shows stress with NW tendency. Additionally, the vectors of displacement and the main stress axis in the Colombian southwest, near to the zone of Tumaco, shows clear tendencies west-east. Finally, the deep seismicity in the zone of Bucaramanga displays stress with tendency NNW - SSE, coherent with the Caribbean Plate subduction under Sudamerica.

The results of shear wave analysis of accelerograms recorder in the National Network of Accelerometers of Colombia from January of 1994 to December of 1997 allowed to estimate the direction of shear wave polarization in 6 regions (See fig 3) that should be parallel or sub parallel to the maximum horizontal compressive stress (Kaneshima, 1990). The leading shear waves in the region seismicity in the zone of Bucaramanga from deep earthquakes (depth > 40 km) are polarized in E-SE direction. In the region 2, throughout the System of Faults of Borde Llanero, leading shear waves from shallow earthquakes (depth < 40 km) are polarized NE-SE direction. In the region 3 to the latitude 1°N in the Colombian Pacific Coast, leading shear waves from shallow earthquakes are polarized NE direction. In the region 4 and 5 in the cordillera Western, leading shear waves from deep earthquakes (depth > 40 km) are polarized NE direction NNE-SE. In the region 6 in the Pacific Coast, leading shear waves from shallow earthquakes are polarized SE, direction. The discrepancies in orientation between the leading shear wave and the maximum horizontal compression can be result of local crustal heterogeneities.

REFERENCES

Kellog, J.N. & Vega, V. (1995). Tectonic development of Panama, Costa Rica, and the Colombian Andes: Constrainst from Global Positioning System geodetic studies and gravity. Geol. Soc. America Bull., Special Paper **295**: 75-90.

Kaneshima, Satoshi. (1990). Origin of Crustal Anisotropy: Shear Wave Splitting Studies in Japan. Journal of Geophysical Research, Vol 95, No B7, pages 11,121-11,133.

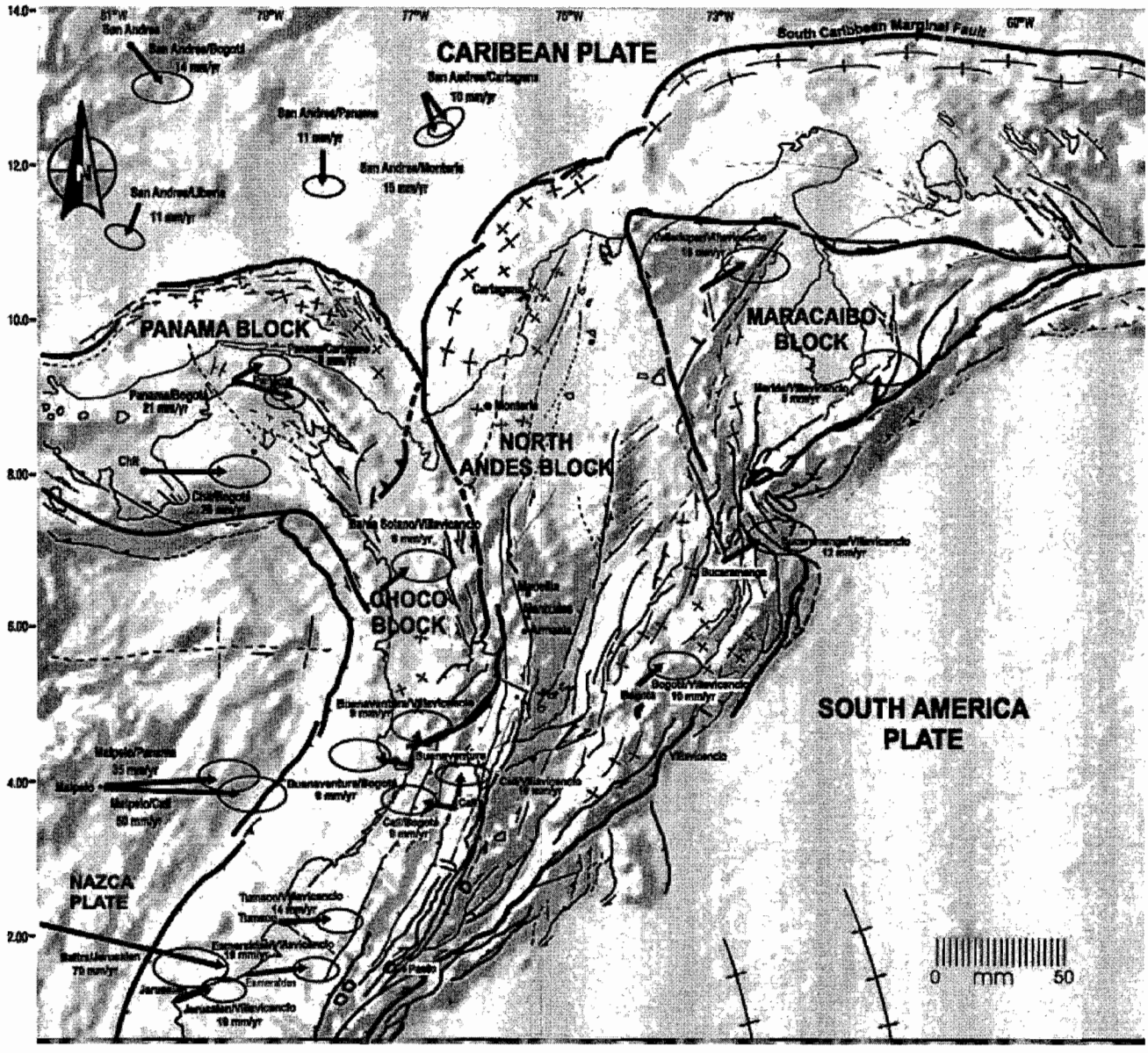

Figure 1. Deformation vectors from CASA project. The error ellipses are in the same scale of Vector. Modify from de Kellog & Vega (1995), Mora (1995) y Trenkamp et al. (2001).

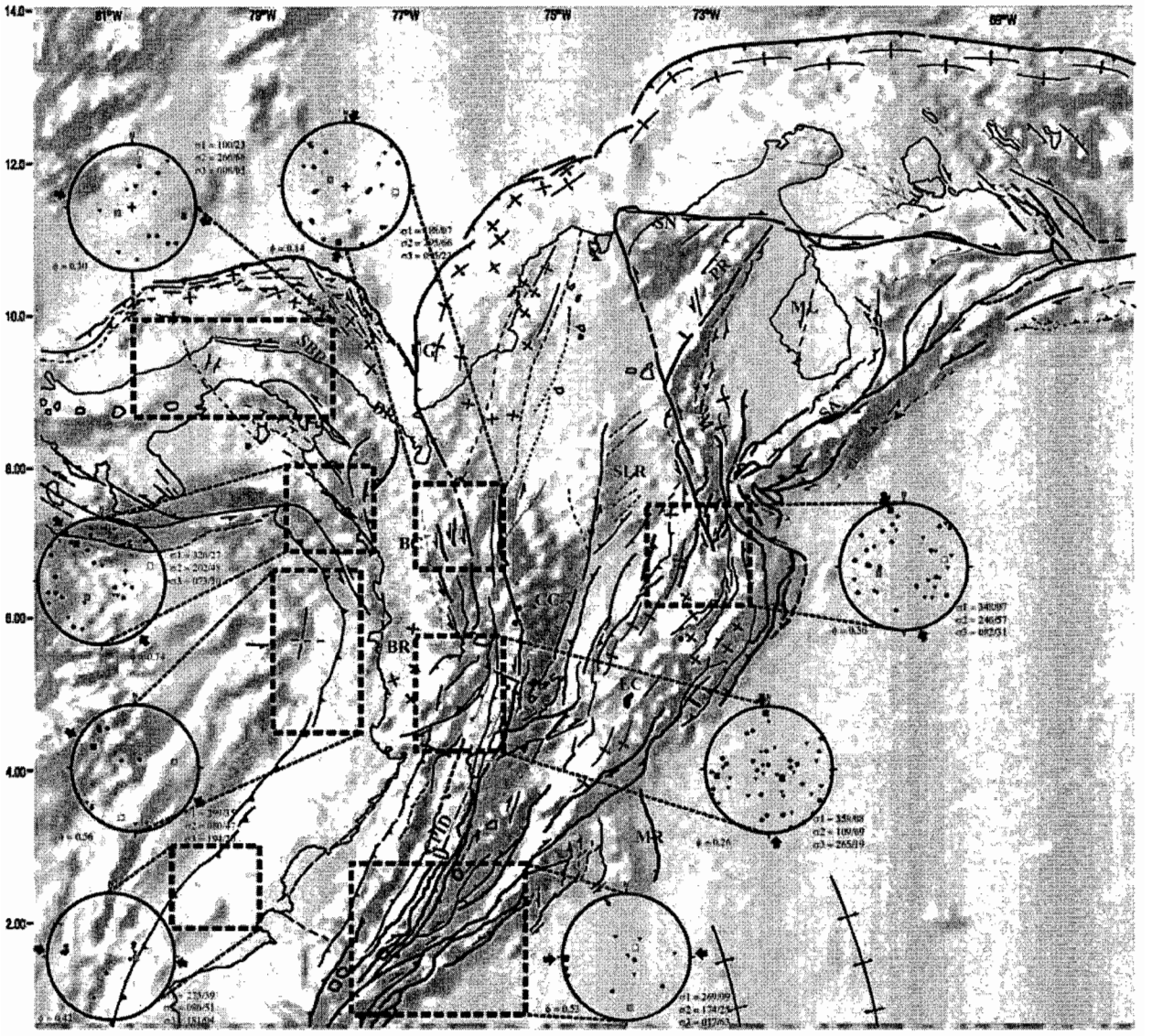

Figure 2. Determination of principal stress axis by means of the Method of Reches (Reches, 1983; Reches, 1987) from 94 solutions of focal mechanisms (CMT) reported by the University of Harvard for period 1976 to 2000 and with Mw > = 5.0.

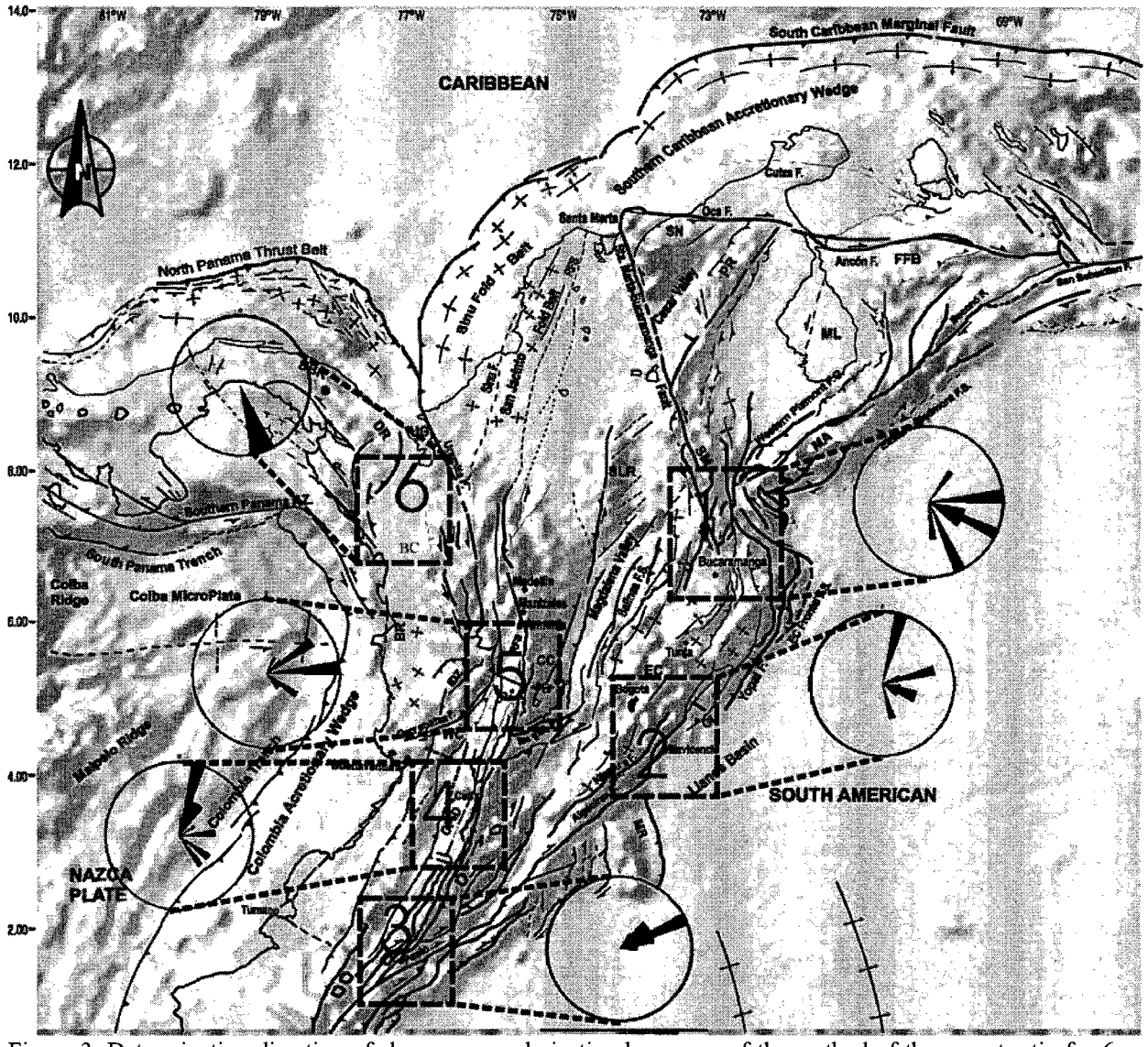

Figure 3. Determination direction of shear wave polarization by means of the method of the aspect ratio for 6 regions. The data used are three component accelerograms recorder in the National Network of Accelerometers of Colombia from january of 1994 to december of 1997.

RADIOCHRONOLOGY IN A MARINE SEQUENCE OF NORTHERN CHILE, FOR HIGH RESOLUTION PALEOSISMOLOGICAL AND PALEOCLIMATIC RECONSTRUCTIONS

Gabriel VARGAS(1,2,3), Luc ORTLIEB(2), Jorge VALDES(4)

1: Departamento de Geología, Universidad de Chile, Plaza Ercilla 803, Santiago, Chile. gvargas@cec.uchile.cl
2: IRD, 32 Avenue Henri Varagnat, 93143, Bondy Cédex. Luc.Ortlieb@bondy.ird.fr
3: D.G.O., Université Bordeaux I, Avenue des Facultés, 33405 Talence Cédex.
4: Facultad de Recursos del Mar, Universidad de Antofagasta, Casilla 170, Antofagasta. jvaldes@uantof.cl

KEY WORDS: Radiochronology, ^{210}Pb, ^{14}C, laminated sediments, paleoclimate, paleoceanography

THE BAHIA MEJILLONES SEDIMENTARY SYSTEM

A particular depositional environment. Mejillones bay (23°S) is a particular sedimentary system along the coast off central-northern Chile. Its geographical situation, protected from the prevalent southwestern winds, together with the presence in the vicinity of an important upwelling cell (Rodríguez et al., 1991; Marín et al., 1993), that drives primary productivity processes specially intensified during the spring, favour vertical deposition of biogenic debris, organic matter and some eolian lithogenic particles. The result is the prevalence, generally at depths greater than 70 m, of hemipelagic sedimentation within the bay. The exceptionally good preservation of the sediments, which is related to the prevalence of waters with depleted concentrations of O_2 (generally <0.1 ml/l below 50 m depth) (Escribano, 1998), gives to this sedimentary record the potential for paleoclimatic and paleosismological studies at a high resolution time scale.

Constraints for radiocarbon geochronology. The determination of a precise chronology from radiocarbon data for recent coastal marine sedimentary sequences, presents some problems. In addition to the methodological constraints due to variations in the production rate of ^{14}C in the atmosphere trough time, the "Suess Effect", the "Bomb Effect" and the difference between the ^{14}C stock in the atmospheric and oceanic reservoirs (Global Oceanic Reservoir Effect, *"R"*) (Stuiver et al., 1998), local variations of the *R* factor trough time (ΔR) must be considered. In eastern boundary coastal areas, these variations result from variations of the input, during strong upwelling events, of CO_2 with depleted activity of ^{14}C, from deeper waters to the surface of the sea (*e.g.* Brown et al., 1993). This type of processes hampers the determination of a precise chronology from high resolution sedimentary records. In this communication, we show some results and geochronological interpretations from ^{210}Pb and ^{14}C data, and we discuss the significance of anomalous structural and textural features within the sedimentary sequence of Mejillones bay.

^{210}Pb AND RADIOCARBON GEOCHRONOLOGY FROM CORE F981A

The core F981A was retrieved from the zone of maximal biogenic accumulation. After corresponding assumptions, the application of the CF-CS (Constant Flux-Constant Sedimentation) model from ^{210}Pb results, the net mass accumulation rate calculated for the upper 10 cm of the core F981A is W=

3.24 ±0.18 g/cm^2/100 years (➔ Mean sedimentation rate ~R= 13.1 ±0.7 cm/100 years). The application of the CRS (Constant Rate of Supply) model gives a mean mass accumulation rate of W= 3.78 ±0.03 g/cm^2/100 years (➔ Mean sedimentation rate ~R= 15.57 ±0.03 cm/100 years), for the same segment.

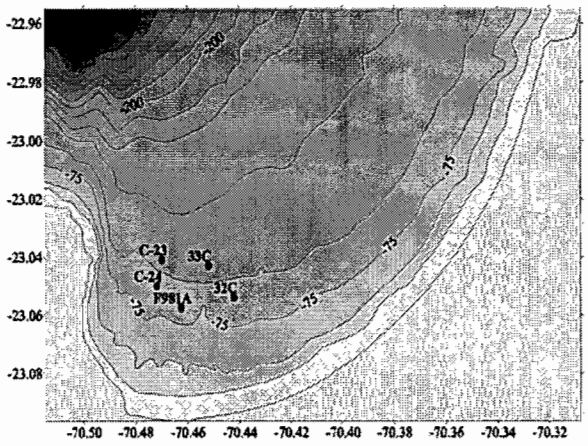

Fig. 1. Situation of cores retrieved from the Mejillones bay, northern Chile. Bathymetric curves every 25 m.

$\delta^{13}C$ and C/N measurements on the organic fraction of the sediments samples from core F981A, clearly reflect the phytoplanktonic origin of the organic matter deposited in the bay. All the radiocarbon measurements were made on this fraction of the sediment. ^{14}C results from core F981A suggest that the sudden increase of the conventional radiocarbon age is linked to sudden increases of ΔR in the Mejillones system, most probably resulting from the intensification of the upwelling cell (Fig. 2). The anomalously low value of the conventional radiocarbon age of the most superficial sample, suggests an input of ^{14}C due to the Bomb Effect.

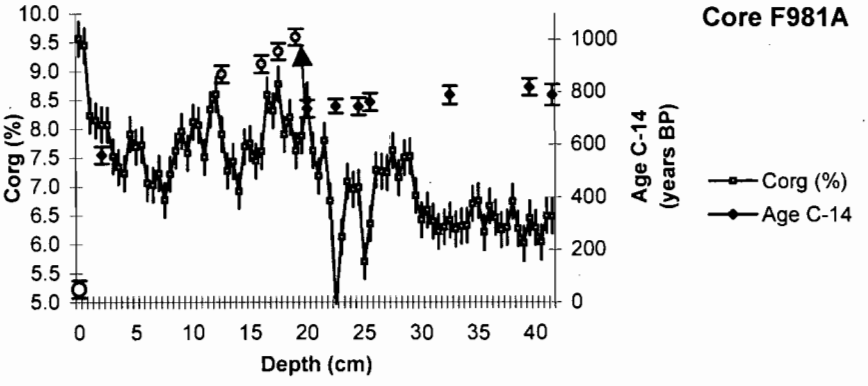

Fig. 2. Conventional radiocarbon ages and organic carbon content from the core F981A. The anomalous increase of the radiocarbon ages at about 18 cm depth (black arrow, grey circles), is correlated with an increase of the organic carbon content, that results from a primary productivity intensification, due to intensified upwelling processes. The white circle shows the superficial sample affected by the Bomb Effect.

These considerations lead to exclude from the geochronological model the ages affected by an increased ΔR and the age affected by the Bomb Effect. Using a linear regression for the remaining data, it is possible to calculate a net mass accumulation rate of W= 3.4 ±0.5 g/cm^2/100 years (➔ Mean sedimentation rate ~R= 16.7 ±2.2 cm/100 years) for the whole core F981A. The accuracy and precision of the ^{210}Pb and ^{14}C chronologies, are confirmed by the close values of W. This high value of W in the zone of the maximal biogenic accumulation within the bay, makes possible high resolution paleoclimatic and paleosismological reconstructions. Based on the extrapolated chronology from ^{210}Pb data, and by using the Marine Calibration

Curve for radiocarbon data (Stuiver et al., 1998), we calculate a mean ΔR= 262±13 years for the period between 1730 AD and 1880 AD.

ON THE OCCURRENCE OF DISCONTINUITIES IN THE SEDIMENTARY SEQUENCE

The occurrence of anomalous features in the sedimentary sequence at Mejillones was reported in previous works and assumed to be linked to a seismic event (Valdés, 1998; Ortlieb et al., 2000). Ortlieb et al. (2000) reported a slump between 46 cm and 57.5 cm depth in the core 23 (Fig. 3), which was correlated with an angular unconformity also observed in several other cores. It was interpreted that such a strong seismic event occurred about 1200 yrs B.P. (uncalibrated). In cores 24 and 32C, the angular discontinuity was observed at about 70 cm and 75 cm depth, respectively (Fig. 3).

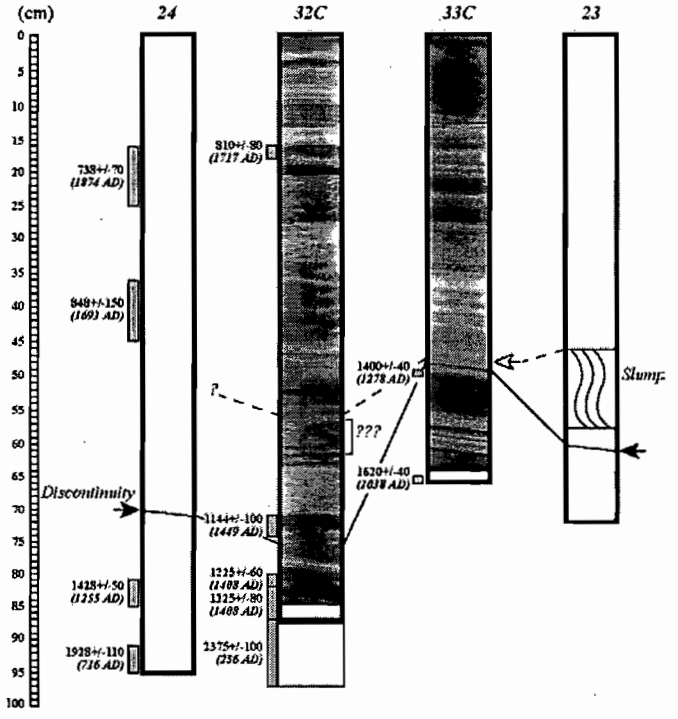

Fig. 3. Anomalous structures and radiocarbon data from cores of Mejillones Bay. A discontinuity level (black arrow and continuous line) observed in all the cores is interpreted as the result of a strong seismic event. A second anomalous feature, which was observed in core 33C (white arrow), is interpreted as a second event, that caused a hiatus estimated to encompass about 30 cm of the sedimentary sequence. This second event is tentatively correlated with the slump observed in the core 23.

In the core 33C, this discontinuity is located at a 47.5 cm depth. It is associated with a slight change in the geometric disposition of the layers, and with a lenticular anomalous deposit enriched in lithogenic debris (visible in thin sections). Another anomalous lenticular deposit was observed several centimeters above the angular discontinuity, suggesting the occurrence of a second event. Taking into account the stratigraphic position of the discontinuity in the core 33C, with respect to the cores 24 and 32C, and the presence of this second anomalous feature in the sequence, we interpret that the occurrence of this second event was responsible for the disparition (erosion) of about 20-30 cm of sequence. As the angular discontinuity was observed at a 60 cm depth in the core 23, we interpret that the slump is more probably associated with this second seismic event than with the first one. Both lenticular deposits should result from reworking of material from shallower areas of the basin. Therefore, after these detailed observations of the

structure, the texture and the mineralogical composition of the sediments, we interpret that structures like angular discontinuities, lenticular deposits enriched in lithogenic debris and slumps, can effectively be associated to the occurrence of strong seismic events or tsunamis in the region.

The radiocarbon data avalaible for cores 24, 32C and 33C, after calibration using Calib.4.3 (Stuiver & Reimer, 1993) and taking into account a ΔR= 262 ±13 years, suggest that the first strong seismic event occurred after 1400 AD, possibly between 1400 AD and 1450 AD, and that the second event occurred at about 1700 AD, or before. For the two last major historical earthquakes in this region, in august 1868 and may 1877, Kausel (1986) inferred magnituds of M_w= 7 and M_w= 5, respectively. The observation from thin sections of sequence in cores F981A and 33C, did not reveal anomalous structural or textural features in the upper sequence, especially in the upper half of the core 33C. This suggests that the two seismic (and/or tsunami) events interpreted from the structural and textural anomalous features in the sedimentary series, were probably more intense, at least in the region of the Mejillones bay, than M_w= 7.

REFERENCES

Escribano R., 1998. Population dynmics of *Calanus chilensis* in the eastern boundary Humboldt current. *Fisheries Oceanography* 7: 245-251.

Kausel E., 1986. Los terremotos de Agosto de 1868 y Mayo de 1877 que afectaron el sur de Perú y el norte de Chile. *Bol. Acad. Ciencias*, 3 (1): 8-13.

Marín V., Rodríguez L., Vallejos L., Fuenteseca J., Oyarce E., 1993. Efectos de la surgencia costera sobre ela productividad primaria primaveral de Bahía Mejillones del Sur (Antofagasta, Chile). *Rev. Chilena de Historia Natural*, 66: 479-491.

Ortlieb L., Goy J.L., Zazo C., Hillaire-Marcel Cl., Vargas G., 1995. Late Quaternary coastal changes in northern Chile. Guidebook for a fieldtrip (Antofagasta-Iquique, 23-25 november). IGCP Project 367, 1995 Meeting, ORSTOM, Univ. de Antofagasta, 175 p.

Ortlieb L., Escribano R., Follegati R., Zuñiga O., Kong I., Rodríguez L., Valdés J., Guzmán N., & Iratchet P., 2000.Recording ocean-climate changes during the last 2,000 years in a hypoxic marine environment off northern Chile (23°S). *Rev. Chilena de Historia Natural*, 73: 221-242.

Rodríguez L., Marín V., Farías M., Oyarce E., 1991. Identification of an upwelling zone by remote sensing and *in situ* measurement, Mejillones del Sur Bay (Antofagasta-Chile). *Sci. Mar.*, 55 (3): 467-473.

Ruegg J.C., Campos J., Armijo R., Barrientos S., Briole P., Thiele R., Arancibia M., Cañuta J., Duquesnoy T., Chang M., Lazo D., Lyon-Caen H., Ortlieb L., Rossignol J.C., Serrurier L., 1996. The M_W= 8.1 Antofagasta (North Chile) Earthquake of July 30, 1995: First results from teleseismic and geodetic data. *Geophys. Res.Letters*, 23 (9): 917-920.

Stuiver M., Reimer P., Bard E., Beck W., Burr G.S., Hughen K., Kromer B., McCormac G., Van Der Plicht J. & Spurk M., 1998. Intcal98 radiocarbon age calibration, 24,000-0 cal BP. *Radiocarbon*, 40 (3): 1041-1083.

Valdés J., 1998. Evolución oceanográfica reciente de la Bahía Mejillones del Sur (23°S). Evidencia geoquímica en sedimentos marinos. Ph.D Thesis, Centro EULA-Chile, Universidad de Concepción, 114 p.

MINERAL COMPOSITION VARIATIONS AS EFFECT OF CONTACT-METAMORPHISM IN THE METAPELITES OF THE EASTERN SERIES, NAHUELBUTA-MOUNTAINS, SOUTH CENTRAL CHILE

Paulina VASQUEZ ILLANES (1), Gerhard FRANZ (2), Friedrich LUCASSEN (3) & Oscar FIGUEROA (1

(1) Departamento de Ciencias de la Tierra, Fac. Cs. Químicas, Universidad de Concepción, Chile (pauvasqu@udec.cl)

(2) Technische Universität Berlin, Fachgebiet Petrologie Sekr. EB 15, D-10623 Berlin, Germany

(3) GeoForschungszentrum Potsdam, Telegrafenberg, D-14473 Potsdam Germany

KEY WORDS: Central Chile, contact aureole, Buchan type metamorphism, conditions of metamorphism, mineral composition variations.

INTRODUCTION

The accretionary complexes from the Coastal Cordillera of south central Chile are subdivided in a Western Series (medium to high P/T) and an Eastern Series (low P/T), which mimic a paired metamorphic belt (González Bonorino and Aguirre, 1970). The Eastern Series has been affected by a Buchan type of regional contact metamorphism (Vásquez, 2001) contemporaneous to the intrusion of the Southern Coastal Batholith (Hervé, 1988). Towards the intrusive biotite, andalusite and sillimanite zones can be observed in the metapelites (Hervé, 1977; Vásquez, 2001). In the Eastern Series of Laraquete-Colcura area, local occurrences of pretectonic staurolite, garnet and biotite evidence a Barrovian metamorphism. The thermal effect of metamorphism in the mineral chemistry can be seen in the most common mineral in the metapelites (biotite, white mica, plagioclase and garnet). For this reason, rock forming minerals located a different distances to the border of the intrusive have been analysed. From the furthest to the nearest to the intrusive, they are:

- I : biotite-garnet phyllite at Colcura area (00-47).
- II : mineral inclusions in andalusite phyllite near Curanilahue (00-71).
- III : matrix of phyllite near Curanilahue (00-71).
- IV : migmatite at Caramávida (00-37) located in the contact with the intrusive.
- V : xenolite of garnet-cordierite schist from Parque Nahuelbuta (00-11).
- VI : xenolite of a nodular sillimanite schist near Piedra del Águila.

Paragenesis II and III correspond to the same rocks but they represent distinct equilibrium events: the paragenesis of the andalusite inclusions (II) represents a previous equilibrium than that of the matrix.

Biotite: The Al_2O_3, TiO_2, annite component (Ann) and MnO biotite contents vary with metamorphic grade. Biotite in paragenesis I is altered to chlorite, therefore its compositional variation was studied from paragenesis

II to VI. Al_2O_3 and MnO contents diminich and Ann component and TiO_2contents increase from paragenesis II to V. In paragenesis VI their respective contents are higher or lower than in paragenesis V (fig. 1, table 1).

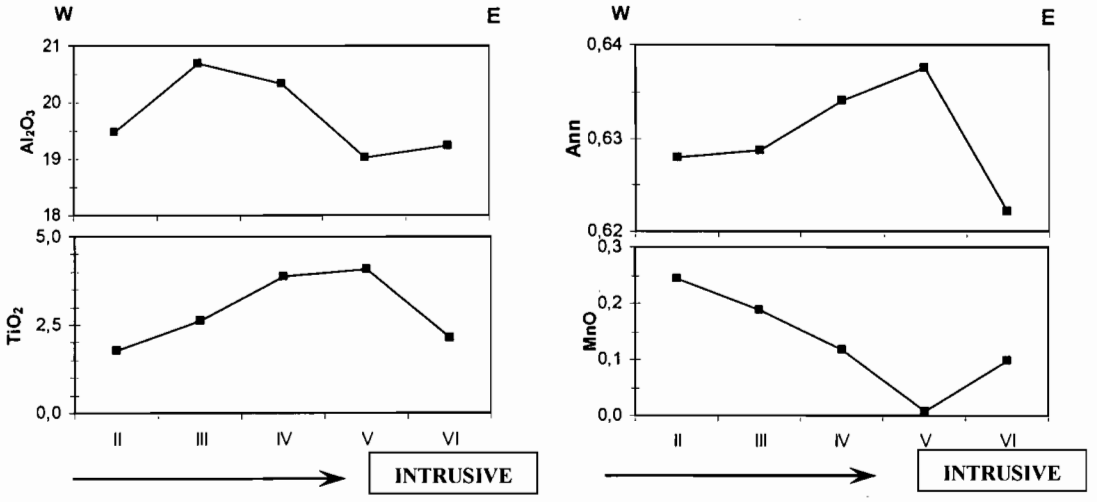

Figure 1: Scheme representing variations in the biotite composition of the Nahuelbuta Mountains. Paragenesis II and III are the furthest and V and VI the closest to the intrusive (see explication in text).

Plagioclase: Plagioclase has been studied in paragenesis I, II, IV and V. It shows almost no zonation. With increasing proximity to the intrusive, the anortitic component increases from An_1 to An_{31} (fig. 2).

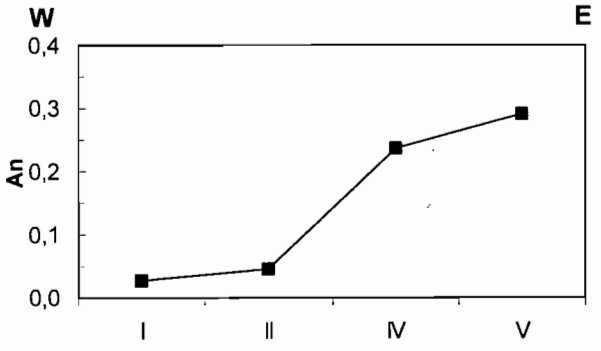

Figure 2: Variation in anortite content (Ca/(Ca+Na+K)) in plagioclase as function of proximity to the intrusive (details in text).

White mica: White mica has been studied in paragenesis I, II, III, y VI. Approaching the intrusive from paragenesis I through III, paragonite contents (Na/(Na+K)), TiO_2 and the ratio Fe/(Mg+Fe) increase (fig. 3). These contents are lower in paragenesis VI. MgO and FeO contents diminish from I through VI while Al_2O_3 has remained relatively constant.

Garnet: Two garnets are distinguished: garnet of paragenesis I is a product of Barrovian metamorphism while the one in paragenesis V represents a Buchan metamorphism. Barrovian metamorphism garnets show moderate to weak zonation, with crystal core richer in spessartine and poorer in almandine than in crystal rims. This reflects growth due to fractionate metamorphic crystallization (Hollister, 1966; Spear, 1988). Considering that the rocks have low MnO contents (0,08%; Vásquez, 2001), such zoning implies that at the beginning of metamorphism garnet incorporate in structure more MnO and become lower to the rim, according to MnO diminishing in the host rock. Comparing to the Barrovian garnet, those of paragenesis V (Buchan metamorphism) have higher almandine and pyrope contents and lower spessartine and grossular contents (table 1).

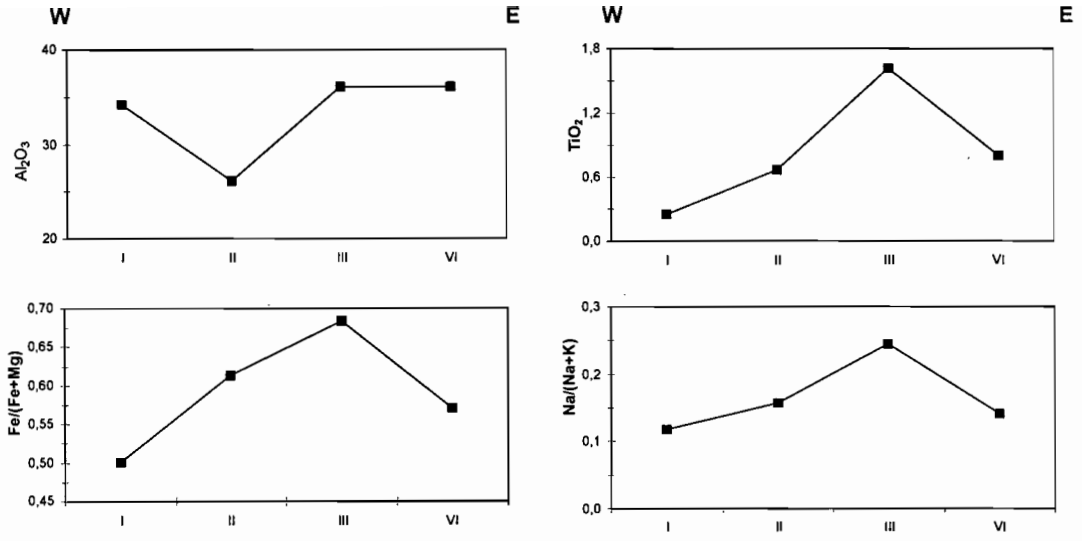

Figure 3: Scheme representing variations in the composition of white mica originated by contact metamorphism as function of proximity to the intrusive (see text for details).

CONCLUSIONS

Table 1 shows a summary of the variation of composition of the minerals of Buchan metamorphism in Nahuelbuta Ranges as function of proximity to the intrusive body. With increasing metamorphic grade plagioclase is more anortitic, garnet is poorer in Mn and richer in Fe, biotite is slightly more magnesic and mica in general is richer in Ti. White mica and biotite of paragenesis VI behave different than the general tendency (fig 1 y fig. 2), especially in relation with diminishing content of TiO_2. Many studies have described that with increasing metamorphic grade Ti content increases as well in white mica (e.g. Kwak, 1968; Guidotti, 1978, 1984; Guidotti *et al.*, 1977) as in biotite (Guidotti, 1984). For this reason it is concluded that the compositions of white mica and biotite of paragenesis VI are products of retrograde metamorphism which, however, could not be confirmed by petrographic observations.

Minerals	**I**	**II**	**III**	**IV**	**V**	**VI**
	Colcura	**Incl. in andalusite Curanilahue**	**Matrix Curanilahue**	**Caramávida**	**Parque Nahuelbuta**	**Piedra del Águila**
Garnet (*)	Alm 69-73	-----	-----	-----	Alm 83-86	-----
	Sp 18-13	-----	-----	-----	Sp 2-3	-----
	Py 8-9	-----	-----	-----	Py 9-11	-----
	Gr 4-6	-----	-----	-----	Gr 3-3	-----
Biotite	w.a.	Phlg 36	Phlg 37	Phlg 36	Phlg 35	Phlg 38
Plagioclase	An 4	An 0-5	-----	An 26	An 29	-----
White mica	Ms 75-Ms 88	Ms 86	Ms 75	-----	-----	Ms 86
	Pg 11-22	Pg 14	Pg 24	-----	-----	Pg 14

Table 1: Summary of variation in mineral composition originated by contact metamorphism as a function of proximity to the intrusive (see text for details).

(*) Minerals with zonation. Abbreviations: Alm = almandine; An = anortite; Gr = grossular; Incl = inclusions; Ms = muscovite; Pg = paragonite; Phlg = phlogopite; Py = pyrope; Sp = spessartine; w.a. = with alteration.

ACKNOWLEDGMENTS

This study is a contribution within the SFB 267 "Deformationsprozesse in den Anden" of the Deutsche Forschungsgemeinschaft and Proyecto DIUC N° 200.025.018-1: "Petrología y Geotermobarometría de la Serie Oriental del Basamento Metamórfico del Centro-Sur de Chile" . Univ. Concepción.

REFERENCES

Gonzalez-Bonorino, O. & Aguirre, L. 1970. Metamorphic facies series of the crystalline basement of Chile. Geologische Rundschau, 59, 979-993.

Guidotti, C.V. 1978. Compositional variation of muscovite in medium- to high-grade metapelites of Northwestern Maine. American Mineralogist, 63, 878-884.

Guidotti, C.V. 1984. Micas in metamorphic rocks. In Bailey, S.W. (ed.): Micas. Mineralogical Society of America, 13, 357-467.

Guidotti, C., Cheney, J.T. & Guggenheim, S. 1977. Distribution of titanium between coexisting muscovite and biotite in pelitic schist form northwestern Maine. American Mineralogist, 62, 438-448.

Hervé, F. 1977. Petrology of crystalline basement of the Nahuelbuta mountains, south central Chile. In Ishikawa, T. y Aguirre, L. (eds.): Comparative Studies on the Geology on the Circumpacific Orogenic Belts in Japan-Chile. Japan Society for the Promotion of Science, 1-51.

Hervé, F. 1988. Late Palaeozoic subduction and accretion in Southern Chile. Episodes, 11, 183-188.

Hollister, L.S. 1966. Garnet zoning: an interpretation based on the Rayleigh fractionation model. Science, 154, 1147-1150.

Kwak, T.A.P. 1980. Ti in biotite and muscovite as an indication of metamorphic grade in almandine facies rocks from Sudbury, Ontario. Geochimica et Cosmochimica Acta, 32, 1222-1229.

Spear, F.S. 1988. Metamorphic fractional crystallization and internal metasomatism by diffusional homogenization of zoned garnet. Contributions of Mineralogy and Petrology, 99, 507-517.

Vásquez Illanes, P.S. 2001. Petrología y geotermobarometría del basamento metamórfico de la Cordillera de la Costa entre los 36°30'S y 38°00'S. Memoria para obtener el título de geólogo. Universidad de Concepción (Inédito), 173 pp.

CURRENT MOVEMENT EXPRESSION ALONG THE NORTHERN ANDES BOUNDARY IN SW COLOMBIA

Francisco VELANDIA, Roberto TERRAZA, Henry VILLEGAS

Ingeominas, Diag. 53 N° 34-53, Bogotá, Colombia; fcovelan@ingeomin.gov.co

INTRODUCTION

The study area comprises a fringe of 350 km long in the SW of Colombia, between 2° and 5° north latitude (Fig. 1). Metamorphic, plutonic, volcanic and sedimentary rocks with ages from Precambrian to Neogene, as well as Quaternary deposits, have been mapped in the area.

A structural interpretation was carried out from five Landsat TM5 scenes mosaic with the following path (P), row (R) and date: P9R58, P9R59 and P9R60 of August 7, 1989 and P8R58 and P8R59 of January 2, 1988. The images were processed in order to obtain a 4R-5G-2B false color composite, with histogram equalization and edge enhancement filters.

The regional models consider the Northern Andes as a tectonic block moving NE in relation to the South American Plate (Pennington, 1981; Kellogg et al., 1985; Freymueller et al., 1993; Mann, 1995; Kellogg & Vega, 1995), along a series of faults denominated East Andean Frontal Fault System. For the Quaternary, this limit has been interpreted with a transpressive righ lateral movement (Freymueller et al., 1993), with an active tectonic setting and related to the subduction of the Nazca Plate under the South American Plate (Fig. 2).

Velandia (1997) used radar images to characterize this structure like wrench fault and to point out the continuity to the NE reaching the Guaicaramo Fault System. The present work seeks to show the continuity of the Algeciras Fault System toward the SW of Colombia up to the border line with Ecuador, and to indicate the wrenching associated features, including the main pull-apart basins.

THE ALGECIRAS FAULT SYSTEM

Most of the interpreted lineaments from the satellite images are related to the mapped regional faults, but these lineaments had not been considered for an integrated analysis. The name of Algeciras Fault System (AFS) is proposed for the set of faults with SW-NE rectilinear and regional patterns, which are identified from Ecuador up to the Guaicaramo Fault System (east side of the Eastern Cordillera of Colombia). This set can be genetically related to progressive phases of the Andean Orogeny. The name of the system responds to the place where, right lateral displacement and geomorphic indicators of neotectonic activity were initially defined by Vergara (1993, in Paris and Romero, 1994). Major historical earthquakes (1834, 1827, 1967, 1917), can be related to the traces of the AFS (Fig. 3), as well as seismic events registered by the National Seismic Network of Colombia (Fig. 4).

Features analysis (Fig. 5) allows to classify the AFS as a wrench complex structure type, or strike slip faults, typically subvertical at depth, involving igneous and metamorphic basement rocks as well as supracrustal sediments and sedimentary rocks (Biddle & Christie-Blick, 1985), besides this, it presents important vertical movement. Weathering and topography make it difficult to observe a clear expression of these faults; however, in some areas it is possible to recognize patterns and arrangements in surface, which can be compared with those shown by diverse authors (Naylor et al., 1986; Mandl, 1988; Dooley & McClay, 1997) as corresponding to strike slip faults under simple shear conditions.

The identification of Riedel, synthetic and antithetic type faults (Fig. 5), allows to determine the dextral sense of movement of the ASF. Principal displacement zones (PDZ) are observed in Zuluaga, Yunguillo and south of Monopamba, as well as lazy S-shaped releasing bend basins, in Balsillas, El Paraiso, Algeciras (Fig. 5-A), near Pitalito (Fig. 5-B) and in San Juan de Villalobos (Fig. 5-C); also, extensive and rhomboidal shaped basins, developed by releasing sidestep of right lateral displacement, as those of Pitalito (Fig. 5-B) and Sibundoy (Fig. 5-D) are observed. Other basins like La Cocha and Estero (Fig. 5-D) are also assumed as areas of local tension by right stepovers of the ASF.

Folds like Garzón Syncline, Zuluaga Anticline and others of shorter extension near by Altamira-Pitalito, San Juan de Villalobos and Yunguillo, are located oblique to the main trace of the ASF. They correspond to the arrangements of structures associated with right slip faults (Biddle & Christie-Blick, 1985).

Also, by comparison with the evolution of experimental wrench fault zones (Naylor et al., 1986), it is possible to identify lenses in the study area, which consist of segments with neotectonic activity, reported by Vergara (1996), Chorowicz et al. (1996) and Velandia et al. (1999) in Algeciras area; Diederix & Gómez (1991) and Van Der Wiel (1991) in Zuluaga-Garzón surroundings. Neotectonic indicators are also identified near Altamira (Fig. 5-B), San Juan of Villalobos-Yunguillo (Fig. 5-C), Sibundoy and Monopamba.

The splay and bend distribution of segments located toward the SW and NE extremes of the structure are interpreted as horse tail patterns of the ASF.

CONCLUSIONS

The Algeciras Fault System (AFS) is defined as a wrench fault structure, with important vertical component, in which, besides the sedimentary cover, basement rocks are involved. Despite the fault system outcrops in mountainous land, it is possible to determine indicative features of its neotectonic activity and associated Riedel type faults, which in some areas are conforming lenses, where the most active segments are located. The identification and arrangement of synthetic and antithetic faults, pull-apart basins and associated folds, allow to confirm the right lateral displacement of the wrench fault.

The NE trend of the AFS constitutes the expression of the simple shear caused by the W-E subduction of the Nazca Plate under the South American Plate. The system is part of the megastructure or Northern Andes regional boundary, which begins at the Gulf of Guayaquil in Ecuador and continues through the Guaicaramo Fault System in the east side of the Eastern Cordillera of Colombia up to reach the Boconó Fault Zone in Venezuela northeastward.

The AFS does not correspond exactly to the morphological boundary of the Eastern Cordillera of Colombia, well-known as the East Andean Frontal Fault System.

REFERENCES

BIDDLE, K. & CHRISTIE-BLICK, N. (editors), 1985. Strike-slip deformation, basin formation, and sedimentation. Society of Economic Palontologists and Mineralogistics. Special Publication, 37. Oklahoma.

CHOROWICZ, J., CHOTIN, P. & GUILLANDE, R., 1996. The Garzon fault: active southwestern boundary of the Caribbean plate in Colombia. Geol Rundsch, 85: 172-179.

DIEDERIX, H. y GÓMEZ, H., 1991. Mapa geológico del sur del departamento del Huila. Escala 1:100.000. IGAC. Publicación especial Revista CIAF, 13 (2). Bogotá.

DOOLEY, T., & McCLAY, K., 1997. Analog modeling of pull-apart basins. AAPG Bulletin, 81 (11): 1804-1826.

FREYMUELLER, J., KELLOGG, J. & VEGA, V., 1993. Plate motions in the North Andean region. Journal of Geophysical Research, 98: 21853- 21863.

INGEOMINAS, 1999. Mapa de grandes sismos de Colombia 1566-1999. Escala 1:200.000. Santa Fe de Bogotá.

KELLOGG, J., OGUJIOFOR, I. & KANSAKAR, D., 1985. Cenozoic tectonics of the Panama and North Andes blocks. Memorias VI Congreso Latinoamericano de Geología, I: 40-59. Bogotá.

KELLOGG, J. & VEGA, V., 1995. Tectonic development of Panama, Costa Rica and the Colombian Andes: Constraints from Global Positioning System geodetic studies and gravity. Geological Society of America. Special Paper, 295: 75-90.

MANDL, G., 1988. Mechanics of tectonic faulting, models and basic concepts. Series Editor: H.J. Zward. Elsevier.

MANN, P. (editor), 1995. Geologic and tectonic development of the Caribbean Plate Boundary in Southern Central America. Geological Society of America. Special Paper 295, preface.

NAYLOR, M., MANDL, G. & SIJPESTEIJN, C., 1986. Fault geometries in basement-induced wrench faulting under different initial stress states. Journal of Structural Geology, 8: 737-752.

PARÍS, G. y ROMERO J., 1994. Fallas activas en Colombia. Boletín Geológico INGEOMINAS. 34 (2/3): 3-25.

PENNINGTON, W., 1981. Subduction of the eastern panama basin and seismotectonics of northwestern South America. Journal of Geophysical Research, 86: 10753- 10770.

VAN DER WIEL, A.M., 1991. Uplift & volcanism of the SE Colombian Andes in relation to Neogene sedimentation in the Upper Magdalena Valley. Thesis of PhD U. Agriculture University of Wageningen. Amsterdam. The Netherlands.

VELANDIA, F., 1997. SAR imagery analysis of geological lineaments in an area of SW Colombia, the Northern Andes. Thesis of MSc. Shimane University. Matsue. Japan.

VELANDIA, F., MORALES, C., CAICEDO, J. y NÚÑEZ, A., 1999. Geología de la Plancha 345 - Campoalegre. Escala 1:100.000. INGEOMINAS. Bogotá.

VERGARA, H., 1996. Rasgos y actividad neotectónica de la Falla de Algeciras. Memorias VII Congreso Colombiano de Geología. I: 491-500. Santa Fe de Bogotá.

NUMERICAL MODELLING OF PLATEAU KINEMATICS IN THE CENTRAL ANDES

Tim VIETOR (1) & Onno ONCKEN (1)

(1) Geoforschungszentrum, Potsdam, Telegrafenberg, 14473 Potsdam, Germany,
tvietor@gfz-potsdam.de, oncken@gfz-potsdam.de

ABSTRACT (TO BE TRANSLATED INTO FRENCH)

The numerical simulation of plateau formation in the Central Andes suggests that the material flux directions with respect to the plateau control the asymmetry of its flanks. On the E side the plateau grows by accretion of foreland material while the W side is essentially a product of backthrusting of the plateau onto the forearc region. The different kinematics result in different geometries: large taper in the W, small taper in the E.

INTRODUCTION

Asymmetric kinematics and topography of orogens are well known from collisional setting. These orogens inherit their fundamental asymmetry from the preceding subduction zone. After initial collision subduction of the leading edge of the lower plate proceeds and the corresponding crust moves towards the subduction zone. In contrast, the upper plate crust initially remains fixed with respect to the subduction zone. It is this asymmetry of the mass flux directions for the two sides of the collisional mountain belts that controls their different kinematic and topographic evolution (Wang and Davis, 1996; Willett et al., 1993). On the lower plate side where the material moves towards the orogen the resulting pro-wedge is characterised by a small taper, a low surface slope and high shortening rates. In contrast, in the upper plate retro-wedge the material is pushed away from the subduction zone and exhibits a large taper, a high surface slope and much lower shortening rates.

The plateau orogen of the Central Andes shows a similar asymmetry of its flanks. However, the polarity is reversed: on the western - lower plate - side the taper of the marginal wedge is large and deformation rates are slow; on the eastern - upper plate - flank the taper is small and deformation rates are high.

In contrast to the collisional orogens the two flanks of the Central Andes are separated by a wide plateau region. The plateau is the result of vertical decoupling at crustal scale weak zones (Pope and Willett, 1998; Wdowinski and Bock, 1994a; Wdowinski and Bock, 1994b). These weak detachments at or near the base of the crust prevent the formation and conservation of orogenic-scale topographic gradients. In a set of numerical experiments we test the influence of detachment expansion and contraction on the kinematics of plateau orogens in general and compare the kinematic evolution of the resulting end-member plateau types to the geology of the Central Andes. We show how the boundary conditions of the plateau orogen control the contrasting evolution of the two flanks including their kinematics and topography.

NUMERICAL METHOD

For our numerical experiments we make use of the distinct element technique that easily handles the large strains involved in orogeny but restricts the rheology to non-cohesive Navier-Coulomb behaviour of perfectly plastic behaviour. The starting configuration is a rectangular box, 800 x 300 km in size, containing some 5500 disk-shaped elements and represents a vertical crustal profile. The lower boundary of the box is cut in two, in order to allow convergence of the model boundaries (fig. 1). The deformation of the model material is driven by kinematic boundary conditions applied as fixed velocities of the right side wall and lower boundary. The properties of the disks are homogeneous and the lower boundary contains a decoupled- (zero shear stress-) section in its center. During convergence of the model halves the size of the decoupling zone may be changed arbitrarily in order to test detachment widening or narrowing.

RESULTS

Figure 1A shows the reference **experiment A** simulating the collision of two pieces of laterally and vertically homogenous continental crust after 175 km of convergence. This experiment lacks a central detachment and generates a doubly vergent orogen which owes its asymmetry to the unequal boundary conditions of the two model halves as described above. Continuous frontal accretion broadens the pro-wedge thrust belt on the right side forming average surface slopes of 8% and a taper angle of 29°. The retro-wedge on the left side grows by underthrusting and uplift at its back which allows larger surface slopes (26%) and larger tapers (~48°). Deformation rates are up to 3 times higher on the pro-side on the right than on the retro-side on the left.

Experiment B introduces a fixed width detachment into the lower boundary of the crust that extends over a distance of 75 km from the subduction point to the sides. In the detached section no shear stresses are interchanged between the model material and the lower boundary segments. In this experiment the right side foreland (lower plate) moves towards the detachment while the left side foreland (upper plate) remains fixed.

After 250 km of convergence (fig 1.B) the configuration of the model sides has developed an asymmetry in both geometry and deformation rate. Deformation is focused to the right side of the orogen where the marginal wedge grows by accretion of thrust slices at high shortening rates. In contrast, the left flank of the plateau is pushed outward onto the unmoving foreland at very slow rates. The taper angles / surface slopes are 50° / 10% and 35° / 6.6% for the right and left sides respectively.

In **experiment C** an initial, 100 km wide decoupling zone at the base of the crust starts to spread towards the right side foreland after 125 km of convergence. The speed of the lateral expansion is equal to half the convergence velocity. The early model evolution is identical to experiment P2. Subsequently, shortening localizes exclusively to right flank of the orogen as soon as the subcrustal detachment starts to expand towards the right side. Plateau deformation and uplift dies down after ca. 150 km of convergence and the orogen grows solely towards the foreland.

SUMMARY AND DISCUSSION

The experiments on simplified plateau orogens performed in this study suggest that

(1) The material flux directions with respect to the plateau detachment control the asymmetry of the plateau flanks. A plateau margin where material moves into the detached zone (the right side of the plateau experiments) develops a pro-flank with a small taper and a high rate of shortening due to the accretion of foreland material. Plateau flanks where the material is pushed out of the plateau zone produce large tapers and slow deformation rates; accretion of foreland material is negligible.

(2) The kinematic patterns observed in the geological record reflect the evolution of the detachment width. A widening subcrustal detachment below the plateau enables the lateral growth of the orogen without simultaneous vertical uplift.

In the Central Andes the topography and the kinematic of the plateau flanks at 21°S are asymmetric. At the western margin deformation rates are low (5E-17/s) and the taper is ~50° (Muñoz and Charrier, 1996; Victor, 2000). Accretion of foreland material is restricted to its eastern margin. Here deformation rates are 30 times higher (1.5E-15/s) than at the Western flank and the taper is as low as ~8° (Kley et al., 1997). This suggests that the material flux is directed towards the plateau detachment in the East leading to the formation of a pro-flank. At the western plateau rim the material flux is directed away from the detachment and produces a retro-flank.

The stability of the retro-flank on the W side of the orogen can tentatively be attributed to the mechanical contrast between the forearc and the plateau region. While the plateau is soft and partly molten at depth, the forearc is cooled from below by the subducting Nazca plate and consequently strong. We speculate that the thermal situation at the boundary of the plateau prevents the propagation of the deformation into the forearc and is responsible for the formation of a retro-wedge.

In the last 8 to 10 Ma the unilateral accretion has not induced any shortening of the plateau or the western flank. Concluding from the numerical 2D-experiments this requires widening of the regional weak detachment below the plateau at a rate that is ~ half the convergence velocity. Quicker or slower widening of the detachment would lead to plateau extension or shortening respectively.

REFERENCES

Kley, J., Müller, J., Tawackoli, S., Jacobshagen, V. and Manutsoglu, E., 1997. Pre-Andean and Andean-age deformation in the Eastern Cordillera of southern Bolivia. Journal of South American Earth Sciences, 10(1): 1-19.

Muñoz, N. and Charrier, R., 1996. Uplift of the western border of the Altiplano on a west-vergent thrust system, northern Chile. Journal of South American Earth Sciences, 9(3-4): 171-181.

Pope, D.C. and Willett, S.D., 1998. Thermal-mechanical model for crustal thickening in the Central Andes driven by ablative subduction. Geology (Boulder), 26(6): 511-514.

Victor, P., 2000. Die Entwicklung der Altiplano Westflanke und ihre Bedeutung für die Plateaubildung und Krustenverdickung in N-Chile (20-21°S). Dissertation. GeoForschungszentrum Potsdam.

Wang, W.H. and Davis, D.M., 1996. Sandbox model simulation of forearc evolution and noncritical wedges. Journal of Geophysical Research, B, Solid Earth and Planets, 101(5): 11,329-11,339.

Wdowinski, S. and Bock, Y., 1994a. The evolution of deformation and topography of high elevated plateaus 1. Model, numerical analysis, and general results. Journal of Geophysical Research, 99(B4): 7103-7119.

Wdowinski, S. and Bock, Y., 1994b. The evolution of deformation and topography of high elevated plateaus 2. Application to the Central Andes. Journal of Geophysical Research, 99(B4): 7121-7130.

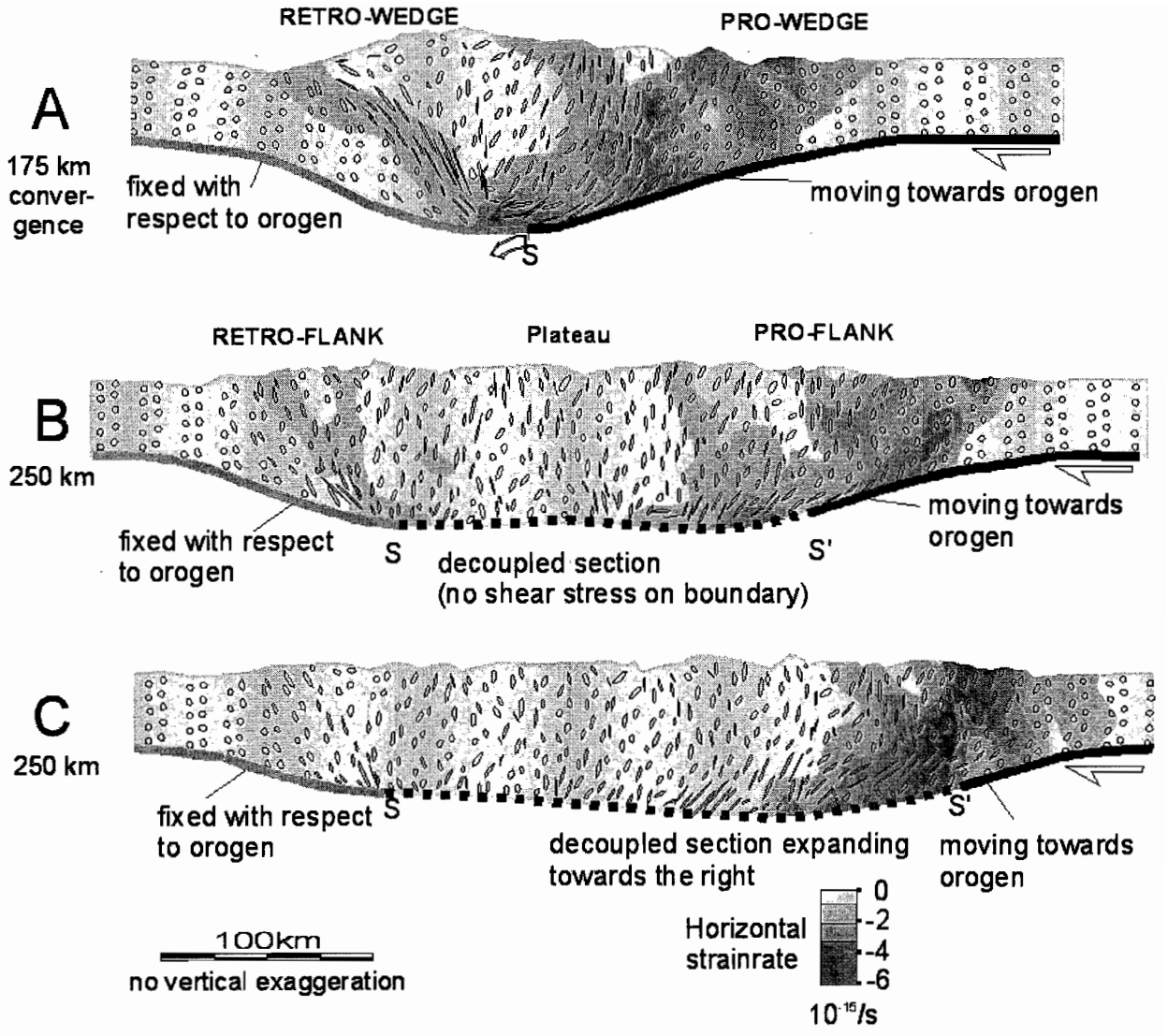

Willett, S., Beaumont, C. and Fullsack, P., 1993. Mechanical model for the tectonics of doubly vergent compressional orogens. Geology (Boulder), 21(4): 371-374.

Fig. 1. Finite strains (ellipses) and horizontal strain rates (shading) of numerical models: A) Collisional orogen, S indicates position of velocity discontinuity. B) Asymmetric plateau orogen with a constant-width decoupling zone at the base of the crust. C) Asymmetric orogen with expanding decoupling zone at the base of the crust. In the plateau experiments S and S` represent the shear stress discontinuities at the tips of the decoupled section of the lower boundary below the plateau.

PLIO-QUATERNARY SEDIMENTARY AND TECTONIC EVOLUTION OF THE CENTRAL INTER-ANDEAN VALLEY IN ECUADOR

Diego VILLAGÓMEZ [1], Arturo EGÜEZ [2], Wilfried WINKLER [3], Richard SPIKINGS [4]

[1] Departamento de Geología, EPN. Ap. 17-1-2759. Quito, Ecuador (fravil@uio.satnet.net)

[2] Instituto Geofísico, EPN Ap. 17-1-2759. Quito, Ecuador (geofisico@accessinter.net)

[3] Geological Institute, ETH-Zürich, Sonneggstrasse 5, 8092 Zürich, Switzerland (winkler@erdw.ethz.ch)

[4] Section Sciences de la Terre, Université de Genève, 1211 Genève, Switzerland (spikings@terre.unige.ch)

KEYWORDS: Pliocene-Quaternary, Inter-Andean Valley, basins, tectonics, Quito active fault system.

INTRODUCTION

The Inter-Andean Valley (IAV) is an elongated geomorphic depression (about 2000 m), which is situated between the Cordillera Occidental and Real in northern Ecuador. It is approximately a 25km wide and 300km long NNE oriented tectonic structure and extends from latitude 2°S to the Colombian border in the north (~ 1°N). The IAV exhibits intensive Quaternary volcanic activity and active faults are widespread, dense population centers exist in the valley. Therefore, it is important to understand the geodynamics of this region, in order to assess the seismic and volcanic hazard in the area.

The present study focuses on the Central IAV between latitude 0°02'30"N and 0°12'30"S with an emphasis on the Quito uplift structures. We carried out a detailed facies and structural mapping of the Quito-San Antonio-Guayllabamba area in order to derive a new geodynamic model for the region. Several radiometric datings are available in literature (Olade 1980, Barberi et al. 1988, Geotermia Italiana 1989, Lavenu et al 1992, 1996). However, these represent mostly data from volcanic edifices, which were correlated into the basin fill series. Further radiometric dating ($^{40}Ar/^{39}Ar$) of six samples of the basin fill is in progress.

MORPHOSTRUCTURAL FEATURES ON THE CENTRAL IAV

The Central IAV is bounded by the Calacalí-Pallatanga Fault in the W, and the Peltetec Fault in the E. The most prominent geologic feature in the Central IAV is the so-called 'Quito active fault system', which forms a key part in the tectonic evolution of the region. The morphological expression of this system is defined by a set of three ridges that, although they have a common N to NNE orientation, they are not connected with each other. From north to south, the ridges are called: Calderón-Catequilla ridge (**CCR**), Batán-La Bota ridge

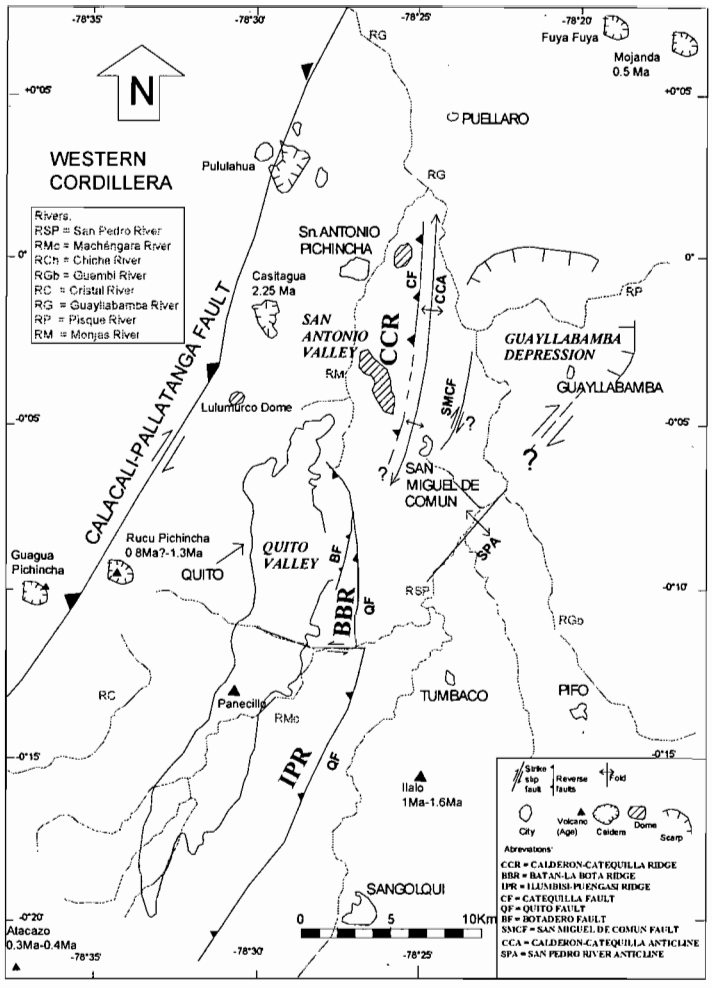

Fig 1: Actual tectonic scheme of the Central IAV.

(**BBR**) and Ilumbisí-Puengasí ridge (**IPR**) (Fig. 1). These ridges divide the younger Central IAV in three sub-basins (Quito, San Antonio and Guayllabamba) and are important controls in the sedimentation pattern (see below). Previous work (Ego et al. 1996, Alvarado 1996) considered the ridges as fold structures associated with a blind reverse fault dipping to the west. Detailed studies in the two northern ridges show a more complicated tectonic evolution in time. The morphological, tectonic, and stratigraphic evidences suggest that the northern **CCR** correspond to a double plunging fold, associated with an active thrust fault (Catequilla Fault), which began to work earlier than the other structures. In contrast, the **BBR** and **IPR** are active 'flexure-and-thrust' structures, which represent a different and younger fault segment. This southern segment, called the Quito Fault, was active during recent times and is composed of a set of smaller active faults (e.g. the recently mapped Botadero fault, Fig. 1). All these faults form the 'Quito active fault system'.

SEDIMENTARY AND TECTONIC EVOLUTION OF THE CENTRAL IAV.

The opening of the IAV presumably started first in the north (Chota Basin) during the late Miocene (Winkler et al., Spikings et al., this volume). Preliminary stratigraphic data suggest that the Central IAV opened during the late Pliocene. The aperture was mainly driven by major strike slip movements along the Calacali-Pallatanga Fault at the western margin of the basin. The basement of the Central IAV consists of rocks of the Pallatanga Unit (late Cretaceous) to the west, and andesitic lavas and breccias of the lower **Pisque Fm.** to the east. The oldest basin fill deposits, which unconformably cover the basement rocks, show an important supply of rock material derived from the Cordillera Occidental. The basin fill series can be divided in two main sequences (Fig. 2) separated by a major unconformity. The lower sequence, the **Pisque** and **San Miguel Fms.** were deposited in a dominantly E-W extensional regime from late Pliocene to early Pleistocene. The upper sequence (**Guayllabamba, Chiche, Machángara, Mojanda, Cangahua Fms.**) was deposited mainly during the middle Pleistocene-Holocene and was related to important volcanic activity in the area and an inversion in the stress regime to E-W compression.

The lower part of the **PISQUE Fm.** (Fig 2) is mainly composed of andesitic lavas and breccias, which are unconformably topped by tuffs and lahars. The upper part of the formation consists of eastward prograding

alluvial fan system sediments and braided river deposits, which indicate enhanced subsidence of the Central IAV and uplift in the Cordillera Occidental. After this, a large lake developed in the NE part of the Central IAV, which received high amounts of detrital volcaniclastic material from the W (fluvial and deltaic facies). These volcaniclastic sediments correspond to the **SAN MIGUEL Fm.** Abundant tuff layers in the lacustrine deposits document the syn-eruptive character of the San Miguel Fm. The progradation of the deltas towards the center of the basin suggests that it must have subsided rapidly with respect to the western margin. Many syn-sedimentary and post-sedimentary deformation features imply that the Pisque Fm. and San Miguel Fm. were deposited in an E-W oriented extensional regime, which corroborates with the observations of Tibaldi and Ferrari (1992) and Samaniego et al (1994).

Subsequently, an important change to intense tectonic activity and volcanism along the remaining lacustrine basin margin produced the unconformably deposition of the **GUAYLLABAMBA Fm**. of middle Pleistocene age. In the lake deposits several intrusions occurred (Catequilla and Pacpo domes). The formation consists of primary volcanic deposits in the south and west, and lahar deposits towards the lake in the northeast. When the lahars entered the lake, they deformed the unconsolidated sediments of the San Miguel Fm. by developing giant slumps. In the west, the top of the Guayllabamba Fm. consists of alluvial fan system sediments that record the uplift of the CCR. The inversion of the stress regime to E-W compression occurred sometime during the Guayllabamba Fm. deposition. A relatively quiescent period followed with the deposition of the **CHICHE Fm.**, which is characterized by lacustrine and fluvial deposits interbedded with lahars (Fig. 2). Facies analysis reveals that many different source regions contributed to the Chiche Fm. Compressive deformation was then revived in the area at the end of the deposition of the Chiche Fm. (~0.5 Ma, Lavenu 1996), in particular with the start of the activity of the reverse Quito fault. This fault has risen the Quito sub-basin with respect to the rest of the Valley, and formed the BBR and IPR structures. Quito is a type of piggyback basin and a main trap of the products derived from the Pichincha and Atacazo volcanic complexes. The correlative deposits correspond to the **MACHÁNGARA Fm.,** which consist at the base of primary volcanic deposits and lahars. At the top it consists of fluvial sediments. The succession of these two well defined facies, the primary volcanic and the epiclastic ones, mark the westward retreat of the Pichincha volcanic complex (Alvarado, 1996). The Máchangara Fm. shows progressive unconformity geometries along the BBR and IPR structures, due to the activity of the Quito fault. Coeval with the Machángara Fm., in the north the **MOJANDA Fm.** with volcanics and volcanoclastic products of the Mojanda volcanic complex was deposited.

During the late Pleistocene the deposition of the tuffs of the **CANGAHUA Fm**. took place, which are widely distributed in the entire Inter-Andean Valley. Towards the end of the Pleistocene, the conspicuous Guayllabamba depression began to form due to the interaction of the Quito Fault System and a NE trending inherited fault (Samaniego et al, 1994). (See Fig. 1). This depression is a pull-apart basin that contains large blocks that have collapsed towards the center of the basin. Finally, during the Holocene the San Antonio sub-basin was filled with pyroclastic products of the Pululahua volcano, and the Quito sub-basin filled with local lacustrine deposits (so-called La Carolina deposits).

CONCLUSIONS

The opening of the Central IAV occurred on an E-W extensional stress regime sometime in the late Pliocene or early Pleistocene. During this time a major basin developed which was a dumpsite for lacustrine, fluvial,

alluvial, lahar and other volcanic deposits. Later, during the middle Pleistocene, the tectonic regime was inverted to E-W oriented compression, which was probably driven by major dextral displacement along the western border faults (e.g. Calacalí-Pallatanga Fault) of the IAV. This compression produced a set of ridges, and the major basin was split into three sub-basins, which then developed individually. The formation of the ridges was not simultaneous, and they played an important role in the sedimentation of the sub-basins. The ridges are the morphological expression of thrust propagation towards the east. Uplift of the ridges is still active today as documented by seismicity (Calahorrano, 2001) and the abundance of landslides and creeps along their oversteepened slopes.

REFERENCES

Alvarado. 1996, Tesis de grado, EPN, Quito. 380 pp.
Barberi et al. 1988, Geological Magazine 125, 1-14.
Calahorrano. 2001, Tesis de grado, EPN, Quito. 190 pp.
Ego & Sebrier. 1996, Annales Tectonicae. 10, 31-59.
Geotermia italiana. 1989, Informe final. Pisa, Italia.
Lavenu et al. 1992, Journal of South American Earth Science. 5, 309-320.
Lavenu et al. 1996, Bulletin Institut francais d'études andines. 25, 1-15.
OLADE. 1980, Organización Latinoamericana de Energía. Quito.
Samaniego et al. 1994, Resúmenes Terceras Jornadas Ciencias de la Tierra, EPN-Quito, 49-50.
Tibaldi & Ferrari. 1992, Journal Geodynamics. 15, 59-83.

This work is supported by the Swiss National Science Foundation (WW and RS, grant # 100000000000).

ANOMALOUS LOWER MIOCENE FOREARC MAGMATISM AFTER AN EXTENSIONAL REGIME IN CENTRAL ANDES (33°S), CHILE

Renate WALL (1); Luis LARA (1)

(1) SERNAGEOMIN. Av. Santa María 0104. Santiago. Chile. rwall@sernageomin.cl; lelara@sernageomin.cl

KEY WORDS: Alkaline volcanism, forearc, convergence rate, Lower Miocene, Central Chile

INTRODUCTION

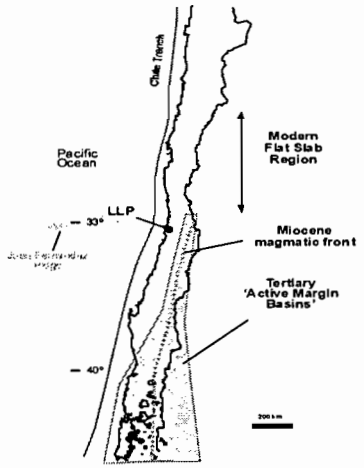

Fig. 1. Sketch for location of LLP. Tertiary 'Active Margin Basins' are from Jordan *et al.* (2001).

In the coastal area of Central Chile (33°S) a small and unique group of volcanic rocks (Lavas Las Pataguas; LLP) of Lower Miocene age (*ca.* 18 Ma) crops out, whose geochemical features contrast with those typical of a volcanic arc. Its position, 80 km west of the Oligo-Miocene arc front, geochemistry and age suggest a relationship with the transient conditions prevailing at the end of an extensional regime and before the Miocene crustal thickening (Fig. 1). The general features of LLP were discussed by Wall & Lara (2001). In this work, we want to discuss a genetic model for the lavas and set them into the geodynamic evolution of the South American margin.

LAVAS LAS PATAGUAS: BASALTIC TRACHYANDESITES IN THE FOREARC REGION

LLP consists of 3 small outcrops (1.15 km^2) of multiple lava flows with elongated and aligned tumuli over flat floors, without evidence of vents or feeding dykes. The volcanic facies suggest fissural volcanism related to a NNW fault, reactivated later as a normal fault. K-Ar whole rock ages gave 17.8±0.7 and 18.8±0.8 Ma while plagioclase gave values between 12.0±1.5 and 14.8±1.8 Ma; the latter with lower reproducibility than the former. The most convincing age (*ca.* 18 Ma) coincides with other regional events like the end of the volcanism of the Coastal

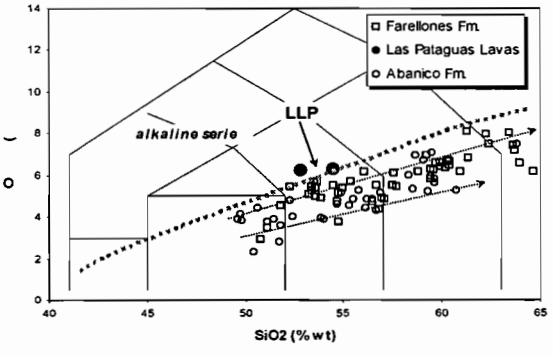

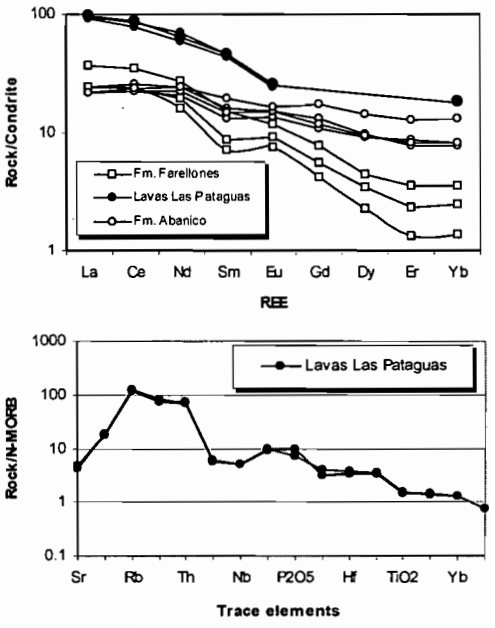

Fig. 2. Alkalis/SiO_2; REE patterns and trace elements diagram for LLP, Abanico and Farellones formations. Data from Wall & Lara (2001), Sellés (1999) and Kay & Kurtz (1995).

Magmatic Belt (38°-42°S; Muñoz *et al.*, 2000), the end of extensional regime coeval with the volcanism of Abanico (Coya-Machalí) Formation (Charrier *et al.*, 1994; Wall *et al.*, 1999), the singular presence of adakitic magmas in the Andean Range at the same latitude (Sellés & Godoy, 2000) and the clear crustal contribution increasing since 18 Ma (Godoy & Lara, 1994; Kay & Kurtz, 1995). The LLP plots in the alkaline series of differentiation, far from the Abanico Formation lavas (tholeiitic trend) and the Farellones Formation (calkalkaline trend) (Sellés, 1999) (Fig.2). The high values of TiO_2 and P_2O_5 are typical of alkaline lavas. The REE pattern is significantly enriched in LREE (La/Sm=3.4), related to a lower melting degree of the source. The HFSE shows values 120 times higher than the N-MORB with high values of Rb and Th and a deep negative anomaly of Ta-Nb. The rates of La/Nb (2.5) and Ba/Nb (39-44) suggest a lithospheric source after Thompson y Morrison (1988), Thompson *et al.* (1989) and Fitton *et al.* (1991). A small batch of melt would have evolved later in the crust with olivine, clinopiroxene and magnetite crystallization.

DISCUSSION

The thermal conditions to induce melting in the fore-arc region are unusual and could be reached only with high buoyancy young slabs (<5 Ma) (Iwamori, 1998). Similar conditions are neccesary for melting the slab below the arc region (Peacock, 1996). The extrusion of the LLP at the same time of the adakitic magmas in the volcanic arc requieres a common explanation.

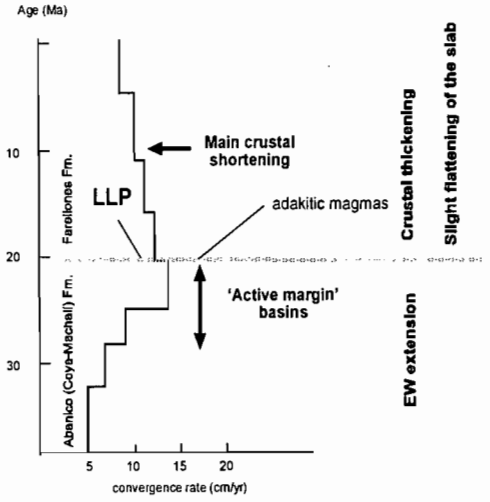

Fig. 3. Summary of volcanic events and geodynamic conditions. Convergence rate from Somoza (1998).

The subduction parameter that changed at *ca.* 20 Ma is the convergence rate (with a high velocity that began to decrease). A slight flattening of the slab also began and was associated later with the crustal thickening that reached a maximun at 10-8 Ma in the region (Godoy & Lara, 1994; Kay & Kurtz, 1995). Nevertheless, current models link the convergence rate and the tectonic regime in the upper plate in an ambiguos way. For instance, according to Uyeda & Kanamori (1979) and Ruff & Kanamori (1980), high convergence rate causes strong coupling and tectonic compression on the upper plate which does not agree with the available data from Central-Southern Chile. Muñoz *et al.* (2000) and Jordan *et al.* (2001) suggest, instead, that the strong increase of convergence velocity in the South American margin at 28-26 Ma caused high asthenospheric circulation, high slab dehydratation and thermal weakening of the continental lithosphere and an extensional regime in the upper plate. These conditions were prevailing until 20 Ma when a decrease in the convergence rate (Somoza, 1998) would have allowed the recovery of the long-term compressive regime. We speculate that, at 20-18 Ma, the inherited thermal conditions and the decrease of convergence rate caused strong coupling in the subduction zone heating the fore-arc region and promoting a sligth flattening of the slab that allowed anomalous volcanism west to the arc front and the adakitic volcanism production in the arc during a short time (Fig. 3). This complete cycle, until the creation of a volcanic gap, is recognized in the actual flat slab region (Kay & Abbruzzi, 1996) with similar tectonic history.

In the other hand, at 33°S a transversal long lived NW-SE fault system, which constitutes a first order Andean feature, could have determined the location of LLP in the forearc.

ACKNOWLEDGEMENTS

We are grateful to SERNAGEOMIN for the support for this research that is part of Hoja Santiago Project. C. Pérez de Arce made the K-Ar dating and S.M. Kay obtained some of the geochemical data.

REFERENCES

Charrier, R.; Wyss, A.; Flynn, J.; Swisher III, C.C.; Spichiger, S.; Zapatta, F. 1994. Nuevos antecedentes estratigráficos y estructurales para las formaciones Coya-Machalí y Abanico, entre los 33°50' y 35°S, Cordillera Principal Chilena. In Congreso Geológico Chileno, No. 7, Actas, Vol. 2, p. 1316-1319. Concepción.

Godoy, E.; Lara, L. 1994. El Teniente 2ª Fase. Informe Final. Corporación Nacional del Cobre-Servicio Nacional de Geología y Minería, 40 p. Santiago.

Fitton, G.; James, D.; Leeman, W. 1991. Basic magmatism associated with Late Cenozoic Extension in the Western United States: compositional variations in space and time. Journal of Geophysical Research, Vol. 96, No. B8, p. 13.693-13.711.

Kay, S.; Kurtz, A. 1995. Magmatic and tectonic characterization of the El Teniente region. Final Report, Corporación Nacional del Cobre, 180 p.

Kay, S.; Abbruzzi, J. 1996. Magmatic evidence for Neogene lithospheric evolution of the central Andean 'flat slab' between 30°S and 32°S. Tectonophysics No. 259, p.15-28.

Iwamori, H. 1998. Transportation of H_2O and melting in subduction zones. Earth and Planetary Science Letters, Vol. 160, p. 65-80.

Jordan, T.E.; Burns, W.M.; Veiga, R.; Pángaro, F.; Copeland, P.; Kelley, S.; Mpodozis, C. 2001. Extension and basin formation in the southern Andes cused by increased convergence rate: A mid-Cenozoic trigger for the Andes. Tectonics, Vol. 20, No.3, p. 308-324.

Muñoz, J.; Troncoso, R.; Duhart, P.; Crignola, P.; Farmer, L.; Stern, C.R. 2000. The relation of the mid-Tertiary coastal magmatic belt in south-central Chile to the late Oligocene increase in plate convergence rate. Revista Geológica de Chile, Vol. 27, No. 2, p. 177-203.

Peacock, S.M. 1996. Thermal and petrologic structure of subduction zones. In Bebout, G.E et al., eds., Subduction: Top to bottom. American Geophysical Union Geophysical Monograph 96, p. 119-133.

Ruff, L.; Kanamori, H. 1980. Seismicity and the subduction process. Physics of the Earth and Planetary Interiors No. 23, p.240-252.

Sellés, D. 1999. La Formación Abanico en el Cuadrángulo Santiago (33°15'-33°30'S; 70°30'-70°45'O), Chile Central. Estratigrafía y Geoquímica. Memoria de Título (Inédito). Universidad de Chile, Departamento de Geología, 154 p. Santiago, Chile.

Sellés, D.; Godoy, E. 2000. Residual garnet signature in early miocene subvolcanic stocks from the andean foothills of central Chile. In Congreso Geológico Chileno, No. 9. Actas, Vol. 1, p. 697-699. Puerto Varas.

Somoza, R. 1998. Updated Nazca (Farallon)- South America relative motions during the last 40 My: implications for mountain building in the central Andean region. Journal South America Earth Science, Vol. 11, No. 3, p. 211-215.

Thompson, R.N.; Morrison, M.A. 1988. Asthenospheric and lower lithospheric mantle contributions to continental extensional magmatism: an example from the British Tertiary Province. Chemical Geology, Vol. 68, p. 1-15.

Thompson, R.N.; Leat, P.; Dickin, A.; Morrison, M.A.; Hendry, G.; Gibson, S. 1989. Strongly potassic mafic magmas from lithospheric mantle sources during continental extension and heating: evidence from Miocene minettes of northwest Colorado, U.S.A. Earth and Planetary Science Letters, No.98, p. 139-153.

Uyeda, S.; Kanamori, H. 1979. Back-arc opening and the mode of subduction. Journal of Geopphysical Research No. 84, p.1049-1061.

Wall, R.; Sellés, D.; Gana, P. 1999. Area Tiltil-Santiago, Región Metropolitana. Servicio Nacional de Geología y Minería, Mapas Geológicos, No. 11, 1 mapa escala 1:100.000, 1 anexo. Santiago, Chile.

Wall, R.; Lara, L. 2001. Lavas Las Pataguas: volcanismo alcalino en el antearco andino del Mioceno Inferior, Chile Central. Revista Geológica de Chile, V. 28. No. 2, p. 243-258.

THE CARRIZAL BAJO BRECCIAS: INDICATIONS OF CONTEMPORANEITY BETWEEN TWO END MEMBER MAGMAS IN A LATE TRIASSIC EXTENSIONAL SETTING, NORTHERN CHILE (27°45'-28°20'S)

Daniela WELKNER R. (1) and Carlos AREVALO V. (2)

(1) SERNAGEOMIN. Avenida Santa María 0104, Providencia, Santiago, Chile (dwelkner@sernageomin.cl)
(2) SERNAGEOMIN. Avenida Santa María 0104, Providencia, Santiago, Chile (carevalo@sernageomin.cl)

KEY WORDS: Late Triassic composite intrusions, mafic enclaves, mixing, felsic-mafic complexes

INTRODUCTION

Igneous textures where rounded to angular mafic rock fragments are immerse in a felsic igneous matrix are common in areas where contemporaneous plutonic bodies of extreme compositions occur together. Generally such arrays are interpreted as fabrics where granitic materials contains enclaves of pre-existing mafic rocks, a suitable explanation but incorrect in most cases. Detailed examination reveals that in much the mafic material is coeval with or even younger than the granitic component. This is the case of the Late Triassic Carrizal Bajo Intrusive Complex (CBIC), that crops out in the Coastal Cordillera of northern Chile (27°45'-28°20'S). It is a bimodal intrusive made up of a stack of four flat lying plutonic layers which was emplaced during a Late Triassic extensional period in the Andes (Mpodozis and Kay, 1992). These plutonic subunits are petrographically and alternately formed by two end members: (1) granites to granodiorites; (2) diorites to quartz diorites. Directly to the north of the area, the felsic and mafic units have been collectively called Sierra Galena Granite and Los Cachos Pluton respectively (Blanco *et al.*, in press). In the following we call these units Sierra Galena granites and Los Cachos diorites. The interface between the layers is sharp and, in most cases, made up of irregular bodies to concordant horizons of intrusion breccias (*sensu* Harker, 1908 *in* Pitcher and Berger, 1972) here called the Carrizal Bajo breccias.

This paper deals with the petrography, geochronology and spatial distribution of the breccias of Carrizal Bajo and its relation with the Sierra Galena granites and Los Cachos diorites. Its main objective is to contribute to a better understanding of the genesis of the breccias and constrain, as far as possible, the intrusion order of the involved mafic and felsic materials.

GEOLOGICAL SETTING

The CBIC is emplaced in a Devonian to Carboniferous metasedimentary complex (Epimetamorphic Complex of Chañaral; Godoy and Lara, 1998). On its eastern margin, the CBIC is intruded by the Early Jurassic Algodones Pluton (197-192 Ma, Table 1). All these units are covered by Quaternary eolic and alluvial deposits (Figure 1).

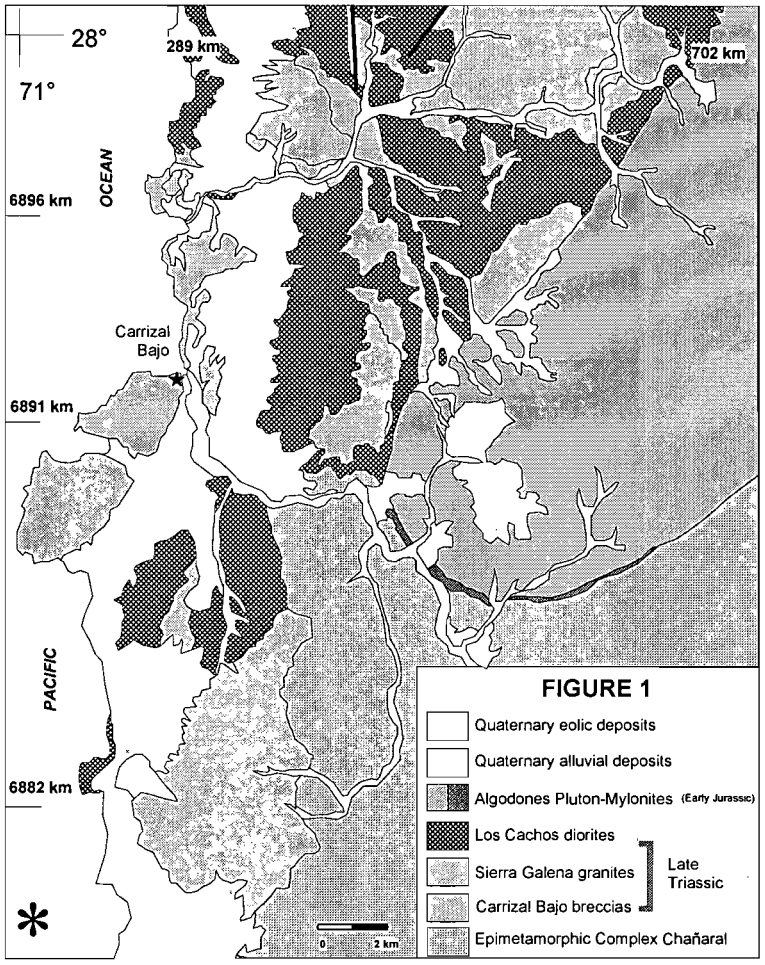

The Sierra Galena granites are biotite-rich monzogranites with minor biotite-hornblende granodiorites. K-Ar biotite ages range from 224 to 221 Ma (Table 1). Los Cachos diorites are hornblende-biotite diorites and quartz diorites, hornblende-olivine apatite-bearing norites and pyroxene-hornblende gabbros with a K-Ar biotite age of 243±8 Ma (Table 1). The Carrizal Bajo breccias are exposed in areas where layers of Sierra Galena granites and Los Cachos diorites are in contact. They also form the interface between felsic and mafic dykes within complexes of sheeted sub-vertical dykes, near Carrizal Bajo, that probably correspond to feeders of the Carrizal Bajo Intrusive Complex (Arévalo *et al.*, 2002).

The breccias crop out as a network of small dykes and irregular veinlets of felsitic material hosted in the gabbros and quartz diorites which, in some cases, becomes a mappeable unit. They are interpreted as intrusion breccias whose fragments, either granitic or dioritic, show a broad variety in size and shape (Figure 2). The felsic fragments range from biotite-hornblende syenogranites to tonalites and have a K-Ar biotite age of 224±5 Ma, while the mafic fragments range from olivine gabbros to biotite quartz monzodiorites and have a K-Ar biotite age of 208±5 Ma (Table 1).

Sample	Lithology	Material	%K	rad Ar (nl/g)	%Atm Ar	Age(Ma) ± Error(2s)
Los Cachos diorites						
VW-1	olivine-hornblende norite	biotite with actinolite	3.25	32.88	12	243±8
Sierra Galena granites						
VW-5	biotite-hornblende monzogranite	biotite	6.18	57.38	6	224± 5
VW-15	biotite-hornblende granodiorite	biotite	7.00	63.94	10	221±5
Carrizal Bajo breccias						
VW-11	biotite-hornblende tonalite	biotite	6.75	62.49	8	224±5
VW-67	quartz monzodiorite	biotite	7.01	59.93	7	208±5
Algodones Pluton						
VW-10	biotite-hornblende monzogranite	biotite	6.52	51.38	6	192±5
VW-28	quartz monzodiorite	biotite	7.29	59.17	9	197±5

TABLE 1. K-Ar AGES OF THE CARRIZAL BAJO INTRUSIVE COMPLEX.

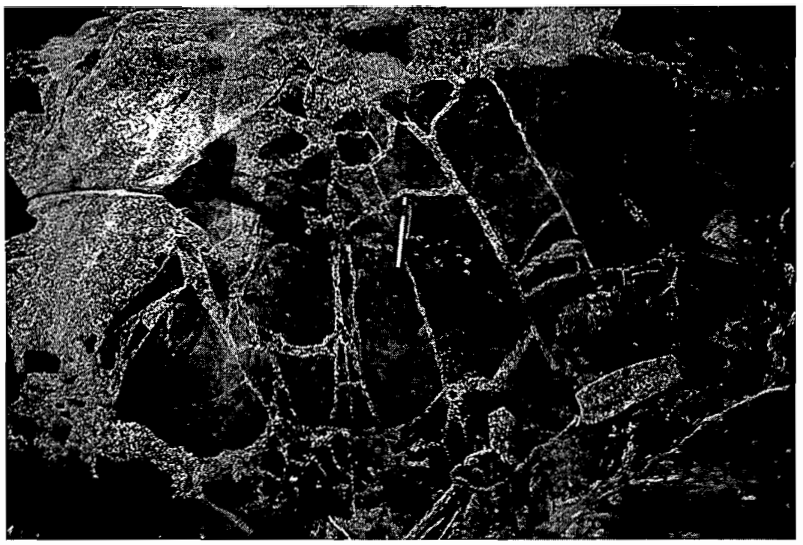

Figure 2. The Carrizal Bajo breccias showing a fragmented gabbroic pillow with angular blocks (Los Cachos diorites) enclosed in and veined by granites (Sierra Galena granites).

THE ORDER OF INTRUSION IN THE CARRIZAL BAJO BRECCIAS

According to Blake (1981), composite fabrics like the Carrizal Bajo breccias can be classified in two types regarding the age of the end members involved. In the first one, felsic material already crystallized is intruded, subsequently melted and mobilized by younger mafic magma. In the other type, the felsic material is partially or entirely liquid when it is intruded by contemporaneous mafic magma. In the latter case, the temperature gradient of the magmas results in a rapid cooling of the mafic material leading to the formation of angular gabbroic fragments (Figure 2).

In the Carrizal Bajo breccias the existence of pillow-like mafic bodies with crenulate-contacts within the felsic material, points to the simultaneous existence of the bimodal components in a liquid state. The presence of internal fragmentation and jig-saw textures within the mafic lobe could therefore indicate a rapid quenching of the pillow. Moreover, the existence of apatite needles together with fine grain textures in the gabbroic fragments also suggest a rapid cooling (Vernon *et al.*, 1988) after the pillow was formed. In the whole, these observations suggest that both felsic and mafic fractions are contemporaneous and consequently they should be close in age.

K-Ar radiometric data presented in this work show good correlation between the Sierra Galena granites and their felsic equivalent in the breccias. However, these ages are not consistent at all with those obtained from Los Cachos diorites and from the mafic fraction in the breccias. We favor instead an interpretation based on field evidence which indicates that when the mafic melt became in contact with the felsic component, the latter was at the liquid state and thus they crystallized together.

The disagreement between the radiometric ages from felsic and mafic fractions is matter of current research. The use of $^{40}Ar/^{39}Ar$ high precision geochronology will help to confirm or not the field based hypothesis.

DISCUSSION AND CONCLUSIONS

Field evidence points to the simultaneous existence of a mainly granitic and dioritic magma which were at the liquid state when they became in contact to form the Carrizal Bajo breccias. However, the available radiometric K-Ar data is not sufficiently precise to prove the simultaneity of both end member magmas.

Considering that in both Late Triassic Los Cachos diorites and Sierra Galena granites homogeneous lithologies predominates (diorites-quartz diorites and granites-granodiorites respectively), and taking into account that some lithological variations are observed in the fragments that form the Carrizal Bajo breccias, it is possible to infer that mixing processes occurred during (or after) the genesis of the breccias.

In the literature of breccias like those described here, the mafic material involved has commonly been interpreted as xenoliths in a granitic intrusive, implying that it is older than its granitic host. From our results we can state that this is not the correct interpretation, and probably felsic and mafic materials are coeval although the possibility that the mafic component could be younger should not be discarded.

REFERENCES

Arévalo, C., Grocott, J., Valenzuela, J. and Welkner, D. 2002. Tabular plutons from the Coastal Cordillera of the Copiapó-Vallenar area and an approach to their emplacement mechanism. Proceedings of 5th ISAG.

Blake, D. 1981. Intrusive felsic-mafic net-veined complexes in north Queensland. BMR Journal of Australian Geology and Geophysics, 6, 95-99.

Blanco, N., Godoy, E. and Marquardt, C. In press. Mapa Geológico del área Castilla-Totoral Bajo (1:100.000): Región de Atacama. Servicio Nacional de Geología y Minería.

Godoy, E. and Lara, L. 1998. Hojas Chañaral y Diego de Almagro, Región de Atacama. Servicio Nacional de Geología y Minería, Mapas Geológicos No 5-6, 1 mapa escala 1:100.000, Santiago.

Mpodozis, C. and Kay, S. 1992. Late Paleozoic to Triassic evolution of the Gondwana margin: Evidence from Chilean Frontal Cordilleran batholiths(28°-31°S). Geological Society of America Bulletin, 105, 1462-1477.

Pitcher, W. And Berger, A. 1972. The Appinite Suite: Basic Rocks Genetically Associated with Granite, *In* The Geology of Donegal: A Study of Granite Emplacement and Unroofing. *John Wiley and Sons*, 143-168.

Vernon, R., Etheridge, M. And Wall, V. 1988. Shape and microstructure of microgranitoid enclaves: indicators of magma mingling and flow. Lithos, 22, 1-11.

SEQUENCE STRATIGRAPHY OF THE CRETACEOUS ECUADORIAN ORIENTE BASIN: TECTONIC AND SEDIMENTARY EVIDENCES OF AN EARLY FORELAND DEFORMATION

Howard WHITE [1], Roberto BARRAGAN [2], Frederic CHRISTOPHOUL [3], Patrice BABY [4] and Marco RIVADENEIRA [5]

1) Kerr McGee Oil and Gas Corporation, 16666 NorthChase, Houston, Texas 77060
2) Amerada Hess Production Gabon, P.O.Box 20316, Libreville, Gabon-Africa, rbarragan@hess.com
3) Laboratoire des Mécanismes de Transfert en Géologie, 38 rue des 36 ponts, 31400 TOULOUSE
4) IRD (UR104), 38 rue des 36 ponts, 31400, Toulouse, baby@cict.fr
5) Petroproducción, Apartado Postal 17.12.857, Quito, Ecuador

Key Words: Oriente Basin, LST, TST, HST, MFS, sedimentary cycle, tectonic inversion

INTRODUCTION

The Cretaceous section of the Ecuadorian Oriente Basin (Hollin, Napo, and Basal Tena formations), located on the eastern flank of the Andean Cordillera (Fig. 1), exhibits features well suited to a sequence stratigraphic framework. They are characterized by a cyclic sequence of limestones, shales and sandstones whose deposition and distribution were controlled by relative sea level changes (White et al., 1995). The cyclic Cretaceous Hollin-Napo-Basal Tena succession has been subdivided into five, third order stratigraphic sequences associated to the global eustatic chart of Haq et al. (1987). Figure 2 illustrates the inferred depositional sequences within the Hollin-Napo-Basal Tena sandstone intervals positioned opposite to the significant sea level drops.

Within a sequence stratigraphic framework, relative sea level controls basinal accommodation space and excerpts regional controls over sediment distribution. The base of each sandstone interval represents a sign of basinward shifting of facies and is thus classified as a sequence boundary.

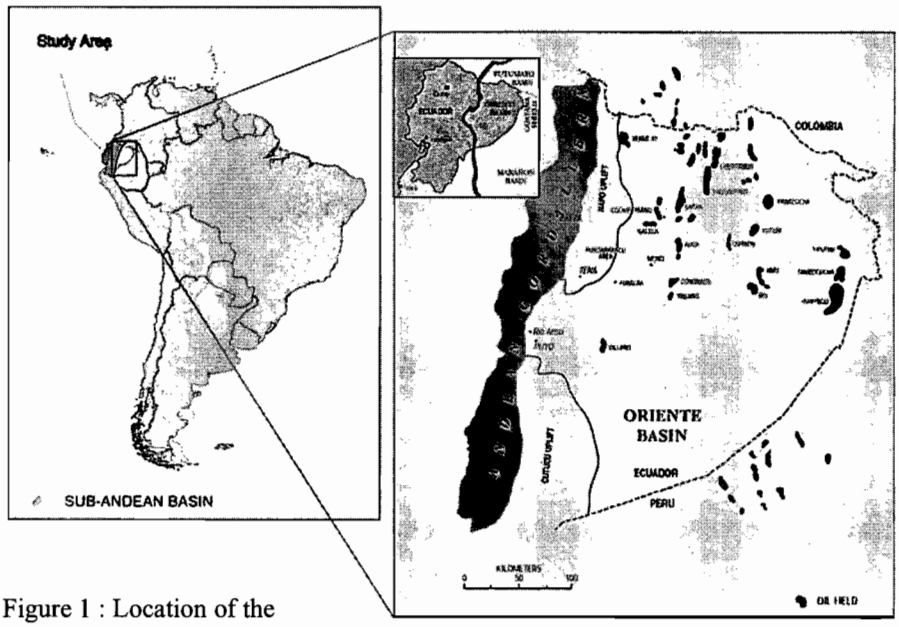

Figure 1 : Location of the study area

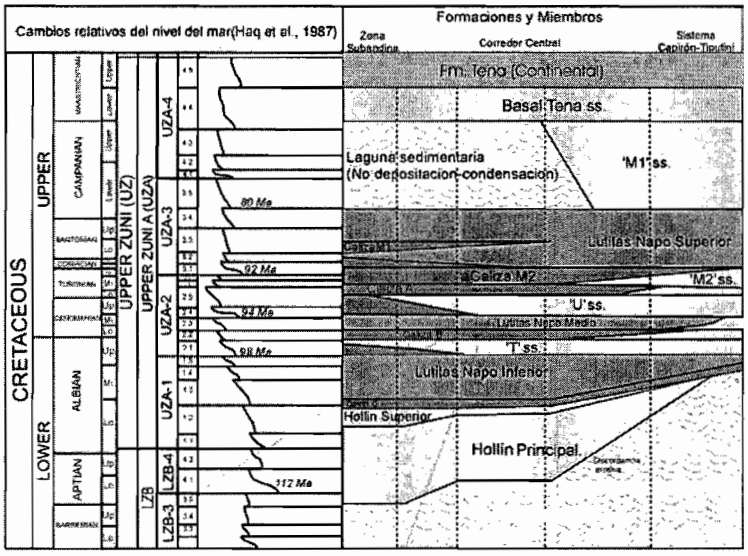

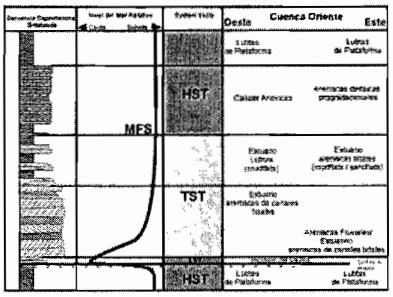

Figure 2 : Cretaceous sedimentary cycles of the Oriente basin and the relationship to the eustatic curve from Haq et al. (1987). Biostratigraphic ages from Jaillard (1997) ; Faucher et al., 1971)

Figure 3 : Ideal sedimentary sequence in the Cretaceous section, Orietne Basin (modfied from Gardner, 1995)

The ideal sedimentary cycle is the record of a completed base-level transit cycle (Gardner, 1995) (Fig 3). It starts with the channeled sands transported from an east-southeast source. These channel sands were deposited within the incised valley, typically within tidal-influenced fluvial environments. Once the estuary is filled, successive deposits spill over the valley margins and reflect the overall transgression of marine facies back toward the east (TST-transgressive system tract). Interbeded tidal- influenced sandstones, thicker shales and thin limestones give way to thick limestone accumulations and marine shales (HST- high stand system tract). This ideal cycle is recognized in the Hollin-Napo-Basal Tena units (Fig. 4). Thus:

Sedimentary cycle I (upper Aptian - Upper Albian): It corresponds in classic stratigraphic terms to the Main Hollin and Upper Hollín formations, Lower Napo Shale, and Basal T Sandstone units. The Main Hollín alluvial braidplain prograded westward across the Oriente during sea level lowstand conditions. The transgressive tidal shoreline and shallower marine shelf deposition occurred during Upper Hollín (TST), from west to east eventually through the entire Oriente Basin shelf. The maximum flooding surface (MFS), recording the transition to highstand condition, occurred during deposition of the Lower Napo Shale. The capping Basal Napo T marine shelf dominated sandstones parasequence prograded westward over the entire Oriente Basin and represents the highstand system tract (HST) of the first sedimentary cycle.

Sedimentary cycle II (upper Albian -middle Cenomanian): It corresponds to the Main 'T' sandstone, Upper 'T'

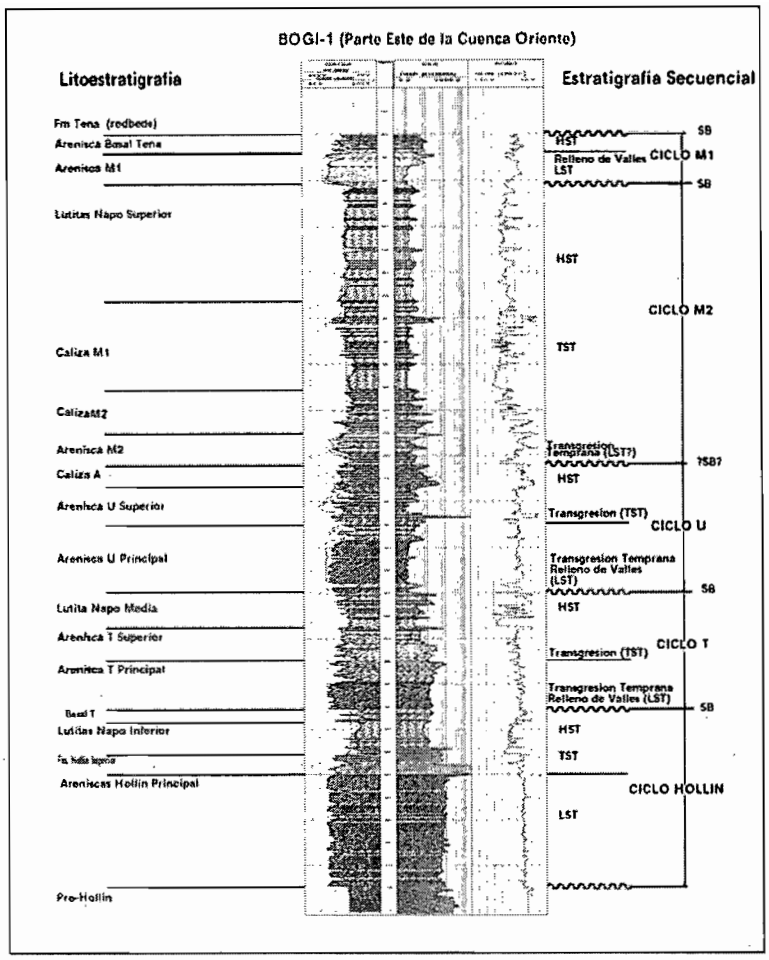

Figure 4 : Sedimentary cycles defined within the Cretaceous section of the Oriente Basin

Sandstone, 'B' limestone and the capping Middle Napo Shale units of the Napo Formation. Sea level drop during the Upper Albian (≈ 98 my) creating a major sequence boundary and an erosive drainage network subsequently filled by the main T incised valley sandstones during early transgressive sea level rise. Overlying are the transgressive to highstand deposits of the Upper T, the Napo B limestone and Middle Napo Shale.

Sedimentary cycle III (lower/middle Cenomanian – lower Turonian?): It consists of the Main 'U' sandstone, Upper 'U' sandstone and 'A' limestone units of the Napo formation. Subsequent sea level drops during the midle Cenomanian (≈94 my) created another erosional sequence boundary at the top of Middle Napo Shale. The Main U Sandstone represents the subsequent incised valley fill deposited during early transgression. Limestone packages of the A limestone represents highstand carbonate deposition on the open marine shelf.

Sedimentary cycle IV (Turonian – Campaniano Inferior): The M2 cycle includes the 'M2' Sandstone, the 'M2' Shale and M2 Limestone plus the capping M1 Limestone and Upper Napo Shale. In the western-central basin, the M2 sedimentary cycle is completely marine shelf without any coarse terrigenous input. Equivalent shorelines to alluvial clastics for the M2 interval are confined to the eastern Oriente Basin and Marañon Basin (Barragán, 1999) and are interpreted as lowstand to early transgressive system. The M2 and M1 Limestones and the Upper Napo Shale reflect the major transgressive and highstand deposits.

Sedimentary cycle V (Campanian-lower Maastrichtian?): It is formed by the fluvial 'M1' Sandstone evident only in the eastern part of the basin and the Basal Tena sandstones that progradated over the entire basin. The 'M1' Sandstone (in the east/southeastern basin) represents early transgressive incised valley fill. Part of the M1 cycle has been preserved as an entirely sedimentary section (eastern part of the basin) while to the west active

tectonism continued to create surfaces of stratigraphic discontinuity. The Basal Tena sandstone is interpreted to represent the final episode of Napo sedimentary infill and document tide-dominated deltaic facies within a rapidly prograding highstand depositional system (HST). After the Basal Tena progradation, Oriente Basin marine conditions were replaced by a non-marine (continental) foreland basin setting.

Although the sequence IV and V shows a complete base-level sedimentary transit cycle (Gardner, 1995), they exhibits distinctive tectonic synsedimentary features (Fig. 4), and active volcanism that records the first phase of basin inversion of pre-Cretaceous structures (Baby et al., 1999). The difference from the previous sedimentary cycles is the fact that Upper Napo Cretaceous sediments are condensed or almost absent in the sub-Andean zone as a consequence of a ravinement and starving event associated with late Cretaceous tectonism.

CONCLUSIONS

Within the Albian-Maastrichtian section, five third-order sequence stratigraphic intervals have been identified in the Ecuadorian Oriente Basin. They represent the Hollín-Napo-basal Tena depositional system that document westerly shoreline shifts across the Oriente Basin and vertical changes in facies which interrupt otherwise consistent marine shelf sedimentation. Seismic sections, regional well log correlations and facies distribution reveal key synsedimentary features and active volcanism attesting a tectonic control during Upper Napo deposition (M2 limestone to Basal Tena Fm). We conclude that from the Aptian to Turonian, the Oriente Basin existed as the expression of a pre-tectonic cratonic passive margin under eustatic influence (White et al., 1999), and from the Turonian to Maastrichtian, the basin underwent a syntectonic period and/or the beginning of the Andean foreland system recording the first phase of basin inversion of pre-Cretaceous structures (Baby et al., 1999) where eustatic influence is still present.

REFERENCE

Baby, P., Rivadeneira, M., Christophoul, F., and Barragán, R., 1999. Style and timing of deformation in the Oriente Basin of Ecuador. Extended Abstract *ISAG99*, Gottingen. 68-72.

Barragán, R., 1999. Relations entre Volcanisme, Tectonique d'inversion et Sedimentation dans le Bassin Cretace Equatorien, *Ph.D Thesis,* Laboratoire de Dynamique de Bassins, Universite Paul Sabatier, Toulouse III, Toulouse, France. 223p.

Gardner, M., 1995. Tectonic and eustatic controls on the stratal architecture of mid-Cretaceous stratigraphic sequences, central western interior foreland basin of North America. *SEPM Special Publication*, **52**, 243-281.

Haq, B.U., Hardenbol, J., and Vail, P.R., 1987. Chronology of sea levels since the Triassic. *Science*, **235**, 1156-1167.

Jaillard, E., 1997. Síntesis Estratigráfica y Sedimentológica del Cretáceo y Paleógeno de la Cuenca Oriental del Ecuador: *Petroproduccion – Orstom*, 163 p.

White, H. J., Skopec, R., Ramirez, F., Rodas, J., and Bonilla, G., 1995. Reservoir characteristics of the Hollin and Napo formations, western Oriente basin, Ecuador, *in* Tankard, A. J., Suárez S. R., and Welsink, H. J., eds., Petroleum basins of South America: *American Association of Petroleum Geologist* Memoir **62**, 573–596.

White, H., Barragan, R., Jordan, D., Robbs, E., and Ramirez, F., 1999. Predictability of reservoir facies within a sequence stratigraphic framework, Oriente Basin, Ecuador. *AAPG Annual Convention*, San Antonio Texas, A149

THE CHOTA BASIN AND ITS SIGNIFICANCE FOR THE FORMATION OF THE INTER-ANDEAN VALLEY IN ECUADOR

Wilfried WINKLER (1), Richard SPIKINGS (2), Diego VILLAGOMEZ (3), Arturo EGUEZ (3), Peter ABEGGLEN (1) and Stefan TOBLER (1)

(1) Geological Institute, ETH-Zentrum, 8092 Zürich, Switzerland (wilfried.winkler@erdw.ethz.ch)
(2) Département de Minéralogie, Université de Genève, 1211 Genève, Switzerland (spikings@terre.unige.ch)
(3) Escuela Politécnica Nacíonal EPN-Quito, Ecuador, (superdiegol@hotmail.com) (aeguez007@hotmail.com)

KEY WORDS: Inter-Andean depression, Ecuador, stratigraphy, tectonics, Pliocene-Pleistocene

INTRODUCTION

The Chota Basin lies in the northern Inter-Andean Valley (IAV) (ca 15 km north of Ibarra; Fig. 1) and represents one of a series of sedimentary basins, which were active from the late Neogene to Quaternary (e.g., Winter and Lavenu 1989, Lavenu et al. 1995, 1996, Barragan et al. 1996, Ego and Sébrier 1996, Eguez and Beate 1994). These studies utilized chronostratigraphic, sedimentologic and tectonic data to attempt to reconstruct the tectonic history of the Inter-andean Valley. Recent work (Abegglen 2001, Tobler 2001, Villagomez this volume) has provided new data on the Chota, Guayllabamba and Quito Basins. In particular, a chronostratigraphic framework of the Chota Basin fill, determined from apatite (AFT) and zircon (ZFT) fission track analyses, has improved our understanding of the timing of the IAV formation.

DEFINITION OF THE PLIO-PLEISTOCENE INTER-ANDEAN VALLEY IN ECUADOR

The IAV is limited to the northern half of the Ecuadorian Andes. Morphologically, it is characterized by a row of depressions below 3000m between the Cordillera Real (CR) and the Cordillera Occidental (CO) (Fig. 1). The continuation of the IAV into Colombia (Cauca Valley) is not discussed here. The regional depression is bounded by reactivated crustal scale faults, which formed during the successive accretion of oceanic terranes during the Cretaceous and Tertiary (CPF, PelF, Fig.1). The IAV contains several sub-basins with sedimentary sequences that range between latest Miocene and Pleistocene. At the latitude of ≈ 2°10' the depression swings westwards towards the Gulf of Guayaquil, dissecting the topography of the CO (Fig. 1). This area is characterized by the opening of the Pallatanga pull-apart basin, which has been forming since ca 2.5 Ma (Winter and Lavenu 1989). General right-lateral transpressive movement in the forearc and arc is compensated by extension in the Jambeli Basin. Since ≈ 5 Ma, volcanic activity has been restricted to north of the town of Pallatanga and is concentrated along the bordering faults of the IAV structure (e.g. Barberi et al, 1988). Inverted thermal histories of deformed rocks along the ChTSZ and the CCF (Ferrari & Tibaldi, 1992) (Fig. 1) document increased cooling rates in the bordering cordilleras since ≈ 6-5 Ma (Spikings et al. this volume), which we attribute to displacement and exhumation of the fault zones.

BASINS

The IAV hosts a series of distinct sedimentary basin fill sequences which overlie either exposures of basement rocks of the cordilleras (Pallatanga and Guamote units) or dominantly volcanic successions

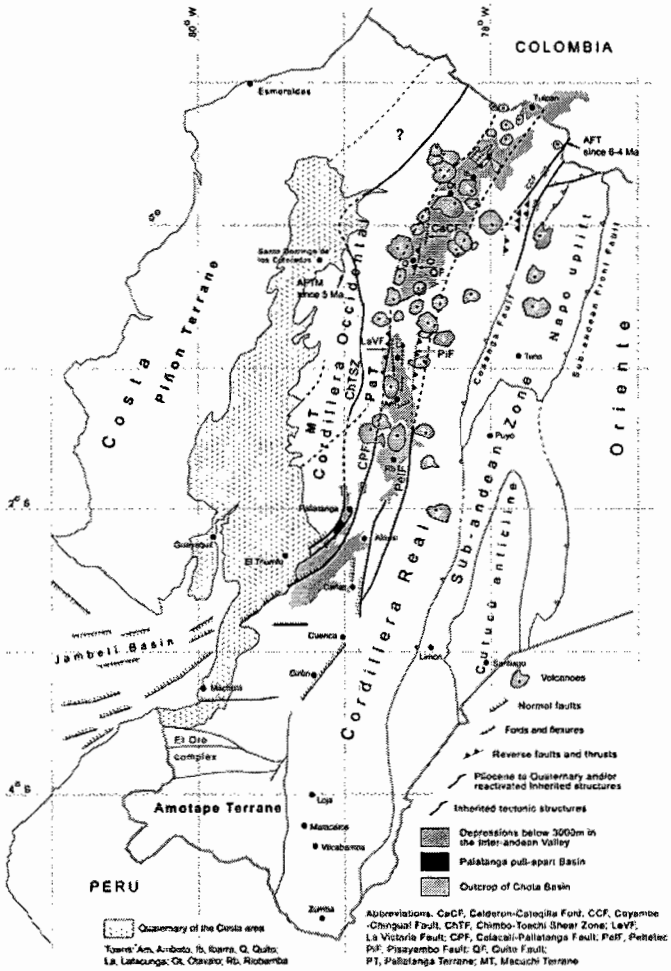

Fig. 1: Simplified geological sketch of the Inter-Andean Valley structure in the Ecuadorian Andes

of Oligocene to late Miocene age, which are also exposed outside the present IAV in the Sierra of southern Ecuador (Fig. 2).

Chota Basin: The basin sequence has a thickness of ≈ 1200-1400m and its exposure is divided into two parts by an extensive lahar sheet, across which (W to E) lithologic correlations are difficult. In contrast to earlier propositions, we find that the Peñas Coloradas Fm., which yields a ZFT age of 5.4±0.4 Ma and is cut by a dyke that yields an AFT age of 3.7±1.7 Ma, is the same age or partly pre-dating the Chota Fm. Alluvial fan deposits of the Peñas Coloradas Fm.were supplied from the east (Barragan et al. 1996) and the heavy mineral assamblage is diagnostic of a source terrane composed of medium to high-grade regional metamorphic rocks (garnet, epidote, clinozoisite, zoisite, kyanite) and low-grade granitic rocks (zircon, tourmaline, rutile) such those as present in the CR today (Abegglen 2001, Tobler 2001). In the east, the formation is overlain by upper sequences of the meandering fluvial to lacustrine (bottom to top) Chota Fm. The dominance of magnesio-hastingite hornblende, basaltic brown hornblende and clinopyroxene of diopsidic composition documents a source region composed of andesitic and basaltic (likely in part coeval) volcanics. The presence of medium to high-grade metamorphic minerals in the lowermost part of the Chota Fm. corroborates the here proposed stratigraphic succession. A total of 5 ZFT and AFT ages (ash beds) in the western sector of the

Chota Fm. range between 4.8±0.4 and 2.9±1.5 Ma. The AFT age of 1.1±0.6 Ma obtained from an ash bed just beneath the lahar in the east is difficult to interpret although we tentatively ascribe it to the Chota Fm. (Abegglen 2001). The alluvial fan facies of the Santa Rosa Fm., including the massive Gavilanes breccia, prograded from the west on the Chota Fm. (Barragan et al. 1996, Tobler, 2001). In addition to andesitic volcanic debris, the reworking of augite, hypersthene and diopside indicates that basic rocks of the Pallatanga unit contributed to the sedimentary flux. The basin series was deposited in a normal fault bounded pull-apart basin, which was subsequently inverted by ≈ E-W shortening, driving intensive folding and thrusting of both the sediments and the dykes/sills (Barragan et al. 1996, Tobler, 2001, Abegglen 2001). Undeformed tuffaceous volcanoclastic rocks unconformably overlie the Santa Rosa Fm. and yield a ZFT age of 0.5±0.2 Ma (ZFT), which constrains the minimum age of the folding event.

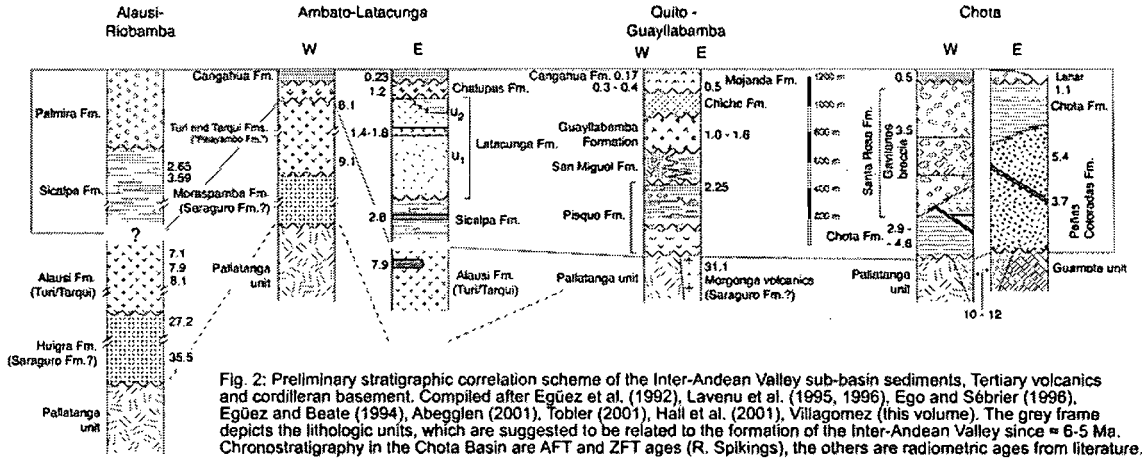

Fig. 2: Preliminary stratigraphic correlation scheme of the Inter-Andean Valley sub-basin sediments, Tertiary volcanics and cordilleran basement. Compiled after Egüez et al. (1992), Lavenu et al. (1995, 1996), Ego and Sébrier (1996), Egüez and Beate (1994), Abegglen (2001), Tobler (2001), Hall et al. (2001), Villagomez (this volume). The grey frame depicts the lithologic units, which are suggested to be related to the formation of the Inter-Andean Valley since ≈ 6-5 Ma. Chronostratigraphy in the Chota Basin are AFT and ZFT ages (R. Spikings), the others are radiometric ages from literature.

Quito and Guayllabamba Basin: The sedimentary rocks of the Quito and Guayllabamba basins consists of a complex series of volcanic and volcaniclastic deposits (Alvarado, 1996; Ego and Sébrier, 1996; Lavenu et al., 1996; Villagomez, this volume; Fig. 2). Lacustrine, deltaic, fluvial and alluvial fan facies prevail in the upper Pisque Fm., the San Miguel and Chiche Fms. In situ radiometric ages of strata are rare although correlations between volcanic edifices into the basins provide approximate chronostratigraphic constraints (e.g. Olade 1980, Barberi et al. 1988, Robin et al. 1977) (Fig.2). Further radiometric analyses are in progress although previous work suggests the sedimentary rocks are younger than 6-5 Ma . The Quito and Guayllabamba basin series are deformed by the large scale ≈ N-S trending Calderon-Catequilla/Quito Folds and the Quito/Botatero thrust Faults (Ego and Sébrier 1996, Villagomez, this volume). Tentative estimates suggest that the main compressive tectonic activity started at ≈ 1.0 Ma (Ego and Sébrier 1996, Villagomez, this volume).

Ambato-Latacunga Basin: In this area the basin fill series wedge out towards the CO in the west. Volcaniclastic rocks of the fluvial/lacustrine Sicalpa Fm. overlie volcanic rocks of the Turi and Tarqui Fm. The lower Latacunga Fm. is mainly of volcanic origin, whereas the upper Latacunga Fm. consists of lacustrine and fluvial deposits (Lavenu et al. 1995). Unconsolidated pyroclastics unconformably overlie these early basin series. The Ambato-Latacunga Basin is bounded by thrusts in the east (east-dipping Pisayambo Fault) and in the west (west-dipping La Victoria Fault). Both faults represent segments of the Calacali-Pallatanga and Peltetec Fault systems respectively. Stratigraphic evidence suggests that a significant phase of

compressive deformation occurred between ≈ 1.85 and 1.2. Ma, i.e during deposition of the U2 unit (Lavenu et al. 1995, 1996).

Alausi-Riobamba Basin: The Pleistocene, alluvial fan and fluvial, conglomeratic Palmira Fm. overlies the Pliocene Sicalpa Fm. with an angular unconformity (Egüez et al. 1992, Lavenu et al 1996) (Fig. 2). The presence of these coarse sediments, which were derived from the east, is an important indication of a significant tectonic and/or climatic change during the late Pliocene (Lavenu et al 1996).

CONCLUSIONS

In the IAV since latest Miocene (≈ 6-5 Ma) several sedimentary sub-basins formed, which are younger than the Intermontane Basins in the Sierra of southern Ecuador. There is general agreement that during the early stages of sub-basin formation, local pull-apart extension occurred, possibly starting in the north (Chota Basin) and prograding southward. Inversion to ≈ E-W compressive deformation presumably started in late Pliocene in the south and in the Pleistocene in the north. The larger IAV Basin can be interpreted as a spindle shaped pull-apart basin which formed since ≈ 6 Ma, presumably in response to enhanced coupling of the eastward subducting Carnegie Ridge with the NNE trending Ecuadorian arc and forearc (Spikings et al. 2001). Volcanic activity appears to be closely linked with deep crustal wrench faults due to the general right-lateral transpressive tectonic regime.

REFERENCES

Abegglen, P. 2001, unpubl. Diploma Thesis ETH-Zürich.
Alvarado, A. 1996, Tesis de grado EPN-Quito.
Barberi, F., Coltelli, M. Ferrara, G., Innocenti, F., Navarro, J.M., Santacroce, R. 1988, Geol. Mag. 125, 1-14.
Barragan, R., Baudino, R., Marocco, R. 1996, J. South Am. Earth Sc. 9, 309-319.
Ego, F., Sébrier, M. 1996, Annales Tectonicae 10, 31-59.
Egüez, A., Dugas, F., Bomhomme, M. 1992, Bol.Geol. Ecuat. 3 47-55.
Egüez, A. & Beate, B. 1994, Excursion Guide to Chota Basin, EPN-Quito.
Ferrari, L. Tibaldi, A. 1992, J. Geodynamics 15, 39-58.
Hall, M. et al. 2001, Cuartas jornadas ciencias Tierra, Quito.
Lavenu, A., Winter, Th., Dávila, F. 1995, Geophys. J. Int. 121, 279-300.
Lavenu, A., Baudino, R., Ego Frédéric, 1996, Bull. Inst. fr. études andines 25, 1-15.
OLADE, 1980, Organizacíon Latinoamericana de Energía, Quito.
Robin, C., Hall, M., Jimenez, M., Monzier, M., Escobar, P. 1997, J. South Am. Earth Sc. 10, 345-359.
Spikings, R., Winkler, W., Seward, D., Handler, R. 2001, Earth and Planetary Sc. Lett. 186, 57-73.
Tobler, St. 2001. unpubl. Diploma Thesis ETH-Zürich.
Winter Th., Lavenu A. 1989, Annales Tectonicae 3, 123-139.

This work was supported by the Swiss Academy of Science (PA and ST) and by the Swiss National Science Foundation (WW and RS, grant # 20-56794.99).

PRELIMINARY FISSIONTRACK DATA ON THE EFFECTS OF THE SUBDUCTING NAZCA RIDGE ON THE GEOMORPHOLOGY IN SOUTH-CENTRAL PERU

M. WIPF , D. SEWARD, F. SCHLUNEGGER

Geological Institute, ETH-Zentrum, Sonneggstr. 5, 8092 Zürich, Switzerland, martin.wipf@erdw.ethz.ch

KEYWORDS : Nazca Ridge, Subduction, Exhumation, Coastal Batholith, Peru

INTRODUCTION :

The subduction of oceanic lithosphere with strong relief such as a ridge may produce superimposed tectonic effects on continental margins (von Heune et al., 1991). Because these ridges are generally believed to have been sourced at hotspots on or near a midocean ridge, they tend to be aseismic and more buoyant than the surrounding ocean floor. This buoyancy leads to low-angle subduction (Pilger, 1981). Where the ridge bearing flat slab enters the subduction zone it has an initial and profound effect on the geomorphology of the associated trench. Furthermore the subduction of a buoyant aseismic ridge is likely to result in enhanced rates of exhumation of the upper crustal sections of the overlying slab compared to neighbouring areas, and in a rerouting of rivers as the buoyant ridge possibly causes an anomaly in the crustal uplift pattern. It is these effects that we intend to quantify. The Peruvian coast provides an ideal location for such a study as it combines "normal" subduction of the Pacific Plate with an intervening ridge subduction. The Coastal Batholith in Peru (12-18°S) offers the unique possibility to study the effects on one lithological unit in one climate zone (desert) therefore decreasing the parameters that might influence the results.

Preliminary fission track data from the Lima and the San Juan region suggest a slight variation in ages. Tracklength modeling however show a almost identical uplift history for the two areas. Initial data do not support an effect on the geomorphology caused by the subducting Nazca Ridge. Fast uplift in Late Eocene is followed by reburial and renewed uplift during Miocene time. That fact that the age of the sample from Lima is very similar to the one in San Juan despite the big difference in stratgraphic age suggests that fissiontrack ages were reset along the whole southern Peruvian coast prior to the Eocene. The data further suggests that significant erosion of Eocene and Miocene sediments have taken place in the coastal areas.

CONCLUSIONS :

The Pacific oceanic crust, specifically the Nazca Plate, is being actively subducted eastwards underneath the Andes at a rate of approximately 8 cm per year. Extending along the west coast of South America is a major oceanic trench, the Peru-Chile trench, which is the geomorphological expression of this subducting plate. However, at the coastal margin of central south Peru, between 14 and 15°S, it is almost obliterated where the Nazca Ridge subducts eastwards under the South American continent (Fig. 1). The effects seen on the change in the geomorphology of the trench can be seen on the continent as the bouyant ridge extends underneath. The drainage patterns of the rivers are for example rerouted over the ridge. Further, a very obvious feature is the coastline, which is extended westwards at the point where the northern margin of the ridge meets the trench and the coastal continental geology is different from this point southwards. Here Late Eocene to Recent sediments lie unconformably on the Precambrian Arequipa Massif. The present day subduction angle is segregated into zones of variable dip with a direct correlation to the position of the ridges at the coastal margins. The changes in slab dip are gradual – there do not appear to be sharp tears in the subducting slab. The region in Peru between 12 and 18°S extends from a flat slab to a steeper slab geometry, and includes the region of the advancing Nazca Ridge. Thus, south-central Peru (12-18°S) provides an ideal position for such a study as it combines "normal" subduction of the Pacific Plate with an intervening ridge subduction. The immediately obvious effects of this approaching ridge seen along the trench should also be measurable inland where the bouyant ridge extends eastwards under the Andes. Specifically, we expect youngest low-T exhumation ages to be on the area overriding the ridge and immediately north.

However, because the Nazca plate is subducting at 080°, and the Nazca Ridge is trending 045° the collision point is migrating southwards at about 10cm a^{-1}. Spence et al. (1999) suggest that the subducting Nazca Ridge would provide a continually refreshed topography into the shallow subduction zone. Depending on the response time of the surface evolution the youngest ages will be either over the ridge or in the region north trailing the southern movement. Specifically, because of the SE-ward shift of the zone where the ridge collides with the continent, through time, we expect successively younger exhumation ages in the same direction on the overriding plate. The area south of the ridge, which has not been affected by the buoyancy is expected to yield oldest low-T exhumation ages. In support of this hypothesis geomorphological data reveal a very clear distinction in the drainage patterns. North of the Nazca Ridge, the drainage is directed dominantly normal to the coast in rivers that are broad and that contain abundant aggradational conglomerates. On the ridge, the river system is complex and appears to have been redirected southwards.

In order to test our hypothesis outlined above and by interpreting the ongoing surface processes we are undertaking a program of low temperature thermochronology combined with analysis of digital elevation models. Samples were collected from Lima to Chala in cross sections normal (NE-SW) to the coastline (Fig.1), in order to cover the regions north, on and south of the Nazca Ridge. The altitudes of the samples vary from 0 to 2500 meters above sea level. They are from the Coastal Batholith Cretaceous intrusives and the Precambrian gneisses of the Arequipa massif.

Preliminary fission track data suggest slight variations in ages which however do not seem to be caused due to the passage of the underlying ridge as it traversed from north to south. Fissiontrack data from the Lima region show a bimodal tracklength distribution whereas the data from the San Juan region just on the southern

edge of the Nazca Ridge is unimodal. However modeling of the data nonetheless shows a very similar history. For the sample from Lima a rapid uplift in Eocene is followed by burial and renewed uplift in Miocene times is asumed. This fits well with the known Eocene ages of the sediments covering the Batholith northeast of Lima. In the more southern area of San Juan modeling of tracklength data also suggests uplift in the Eocene reburial and uplift during the Miocene. Miocene Sediments of the Pisco Formation east of San Juan support this model. The data further leads to the assumption that considerable amounts of sediments had to be eroded during the last 10 to 15 Ma. Further data will be presented

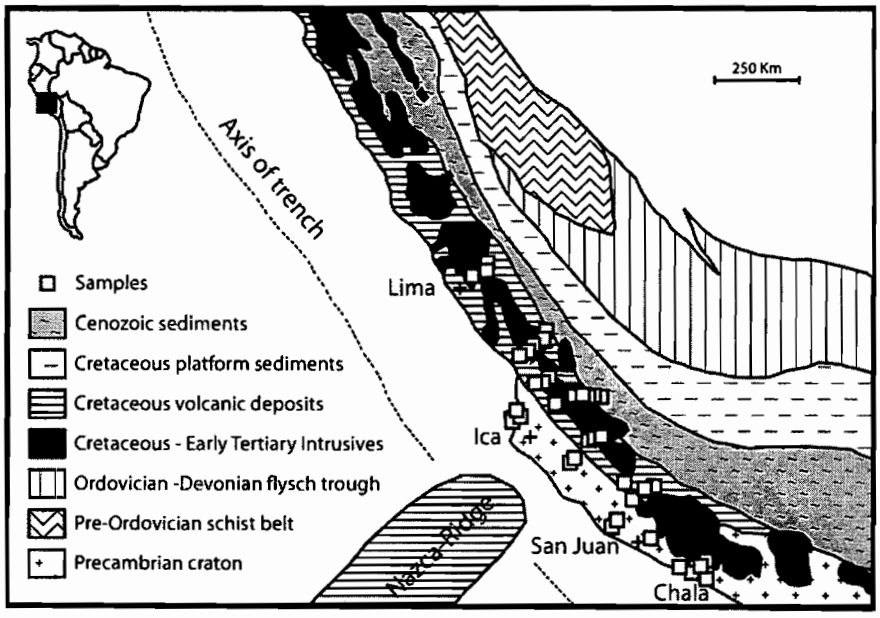

Figure1:
Geology of the Southern Peruvian Andes (Pitcher 1978, modified), including sample locations of the present study.

REFERENCES :

Pilger, R.H., (1981): Plate reconstructions, aseismic ridges, and low-angle subduction beneath the Andes. GSA Bulletin, Part I, v. 92, 448-452.

Pitcher W.S., (1978): The anatomy of a batholith. Journal of the Geo. Soc. of London, 135 part 2: 157-182.

Spence, W., Mendoza, C., Engdahl, E.R., Choy, G.L. and Norabuena, E., (1999): Seismic subduction of the Nazca Ridge as shown by the 1996-97 Peru earthquakes. Pure and Applied geophysics, 154: 753-776.

von Heune, R., and Scholl, D. W., (1991): Observations at convergent margins concerning sediment subduction, subduction erosion, and the growth of continental crust. Rev. Geophys, 29: 279-316.

VISCOUS MODELING OF THE DYNAMIC TRENCH TOPOGRAPHY ALONG THE CENTRAL AND SOUTH AMERICAN ACTIVE MARGIN: IMPLICATIONS ON INTERPLATE RHEOLOGY AND DEGREE OF COUPLING

Gonzalo YAÑEZ C.(1) and Jose CEMBRANO P.(2)

(1) CODELCO-CHILE, Teatinos 258 7° Piso, Santiago-Chile , email: gyane003@stgo.codelco.cl
(2) U. CATOLICA DEL NORTE, Av. Angamos 0610, Antofagasta-Chile , email: jcembrano@ucn.cl

KEYWORDS: Central Andes, Chile, dynamic trench topography, rheology.

INTRODUCTION

Negative Free Air gravity anomaly along convergent margins (i.e. Smith and Sandwell (1994)) demonstrates that this first order topographic feature is not compensated isostatically. Wdowinski (1992) clearly shows that the plate margin topography is the result of a dynamic equilibrium between two competing effects: (1) the tectonic force pulling the overriding plate downwards, and (2) body or buoyant force acting in the opposite sense. By using the viscous long term approach proposed by Wdowinski (1992), three first order parameters appear to control the shape of the dynamic trench topography: (a) the average viscosity of the overriding plate; (b) the degree of coupling between the oceanic and the continental plate; and ; (c) the convergence plate velocity. The last parameter is fairly well constrained from kinematic plate models such as Nuvel-1 (DeMets et al., 1994), whereas the first two parameters are poorly known, and are fundamental for large scale deformation models. The active margin of Central and South America is a natural laboratory to better constrain these two parameters, given the simplicity of the convergence geometry and the existence of different tectonic environments (Figure 1). By looking at Figure 1 we can identify important differences in the shape of the trench topography (for example north and south of the Taitao triple junction). Such an along strike tectonic segmentation allows the isolation of both parameters (plate coupling and overriding plate rheology). Of particular interest is the behavior of outstanding oceanic features such as the subduction of active (Chile Rise, Cocos Ridge) and passive (Juan Fernández, Nazca, and Carnegie) ridges that are likely to commonly believed to affect plate coupling. In fact, shallow seismicity (hypocenters in the range of 0-30km with magnitudes above 5 from CNSS Catalog) show incipient clustering within the vicinity of these features (Figure 1). The approach followed in this investigation is to model the dynamic trench topography along the active margin of Central and South America. Given the fact that the trench topography is already established, the modeling effort is oriented to find the parameters that equilibrate the tectonic and buoyant forces. From preliminary estimates of Wdowinski (1992) the trench topography equilibrium is reached after 2-5 Ma after the onset of subduction regime starting from flat relief topography. Therefore, it is fair to assume that the Central and South American trench topography is essentially in quasi static equilibrium, although the oblique and laterally evolving subduction of active or passive ridges may locally perturb this assumption. We first describe the model characteristics, running then the model along the profiles defined in Figure 1, considering the appropriate plate convergence rate and extracting the parameters that best fit the tectonic and buoyant force equilibrium. We then discuss the tectonic implications of the model results in the framework of the Central and South American plate segmentation.

VISCOUS MODEL Following the Wdowinski (1992) formulation, the long-term deformation along the Central and South American subduction zone can be seen as a 2-D deformable overriding plate in contact with a rigid

subducting slab at the Wadatti-Benioff zone, and the much weaker asthenospheric layer underneath. In this simple model the overriding plate is represented by a viscous rheology (constant), interacting through boundary conditions with the subducting slab and the asthenosphere. The subducting slab effect is represented by a convergence velocity transferred to the overriding viscous plate through a narrow region that accommodates most of the associated deformation (i.e. Shreve and Closs, 1986). In the model, this narrow region parallel to the Wadatti- Benioff zone is called the "slip layer", characterized by a much weaker viscosity. The ratio of the slip viscosity and slip thicknes times the convergence velocity represents the degree of coupling of the subducting slab and overriding plate. At the base of the continental lithosphere the shear traction associated with the flow in the asthenosphere is neglected because its likely effect on the continental plate deformation affects primarily the back-arc region with a longer wavelength (i.e. Yañez 1994). The surface boundary condition has no effect unless it is located below the sea level, in this case it has a positive pressure effect scaled by the crust and water density contrast. The remaining boundary condition corresponds to the vertical side located far away in the foreland region of the overriding plate such that the velocity field is naturally imposed to zero.

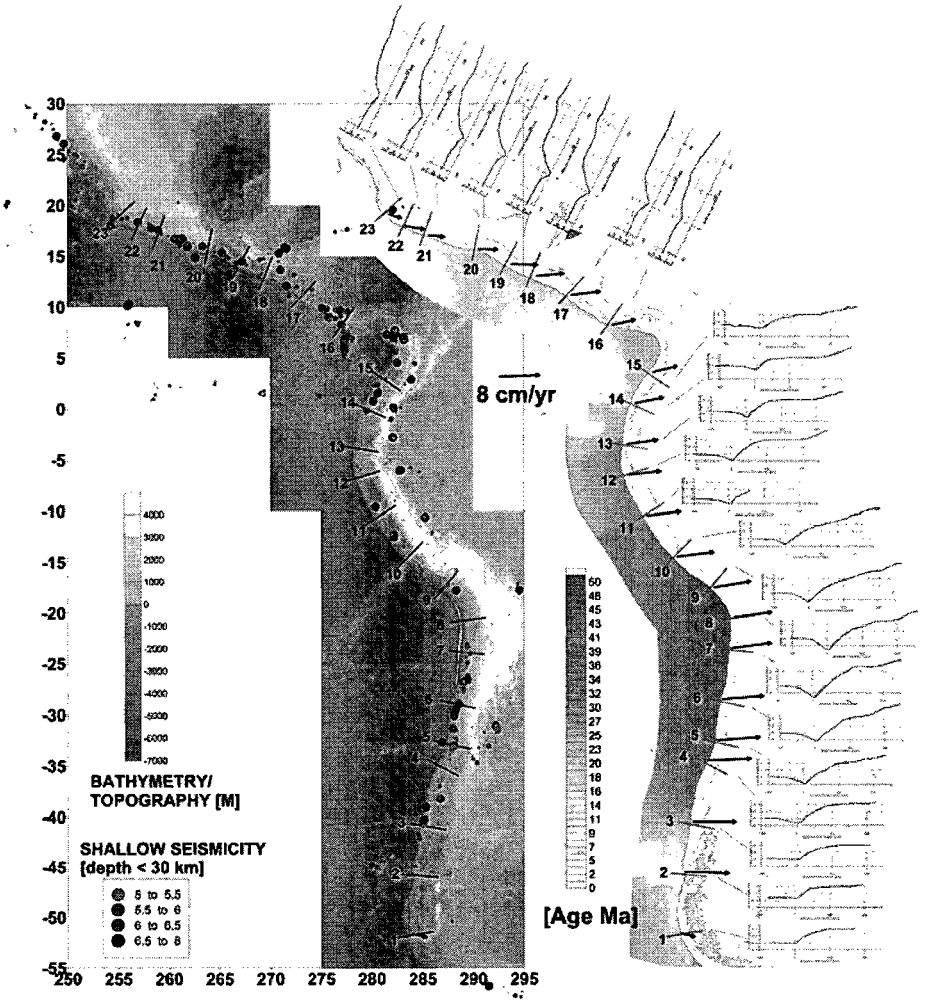

Figure 1: Tectonic framework. Left panel: topography-bathymetry (Smith and Sandwell, 1994), and shallow seismicity (0-30 km, 1970-2000 period, from the CNSS data-base). The analyzed profiles are shown in the panel (numbered from 1 to 23). Convergence rate is shown on the right side as solid black arrows (from DeMets et al., 1994). In the oceanic side of this panel we include the age of the oceanic plate in gray shades. In the right most side, we show the 23 topography-bathymetry analyzed profiles.

The governing equation that represents the physics of the problem involves the force balance equation, the continuity of incompressible materials, and a linear constitutive law for the viscous flow (see Wdowinski, 1992 for further details). The problem is solved using the standard finite element technique with the penalty formulation that replaces the pressure term for an incompressible fluid (i.e. Zienkiewicz and Taylor 1991). The

finite element discretization uses 5,000 triangular elements, and the boundary conditions are established according to the description of the previous paragraph. The competing effects of the buoyant and tectonic forces in the near trench topography deformation can be clearly observed in Figure 2. In this case we imposed a given trench topography, modeling separately the tectonic and the buoyant forces. The associated velocity field, that ultimately controls the trench topography deformation, is spread in the opposite direction: tectonic forces transfer the convergence velocity field downwards and parallel to the Wadatti-Benioff plane, whereas the buoyant forces try to re-establish the original plate configuration with no trench topography. In the following section, we will apply this model to determine the overriding plate and slip layer viscosity that better fit the observed topography with the corresponding convergence velocity boundary condition along the sections defined in Figure 1.

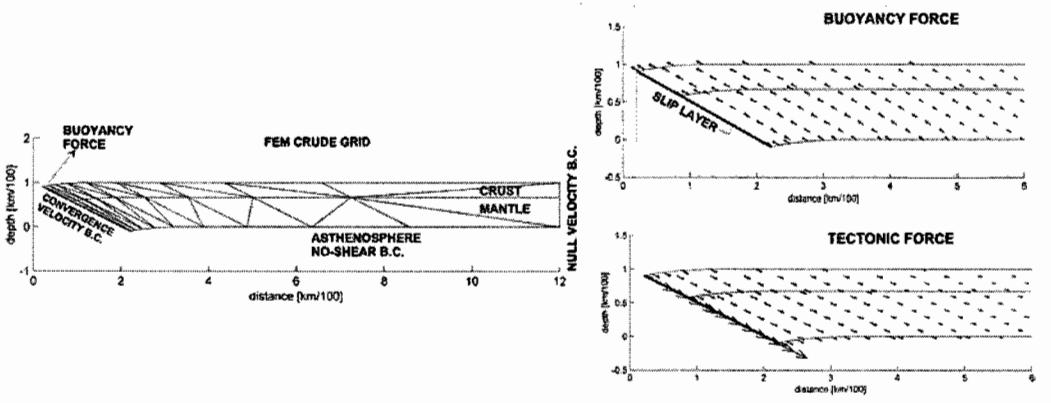

Figure 2: Viscous model deformation. Left panel tectonic forces, right panel buoyant forces

RESULTS In Figure 3, we summarize the model results in terms of the overriding plate and slip layer viscosity that allows the equilibrium between tectonic and buoyant forces across the 20 transects defined in Figure 1. The equilibrium is achieved with simple trial and error forward modeling up to a limit in which the maximum velocity field is less than 5% of the convergence velocity. In this Figure, the convergence velocity and the age of the subducting plate also are shown for further correlation.

DISCUSSION AND CONCLUSIONS The dynamic trench topography along the Central and Southern Andes active plate boundary zone has been modeled considering a viscous approach in which buoyancy and tectonic forces equilibrate with each other. The model results shown in Figure 3 indicate that the viscosity of the slip layer varies along the strike of the trench axis in the range of 1-5 10^{18} [Pas], however is almost insensitive to variations in the continental plate viscosity. Associated shear stresses in the range of 5 to 15 [Mpa] may be established considering a slip layer thickness of 8 km and the convergence velocity of 4-8 [cm/yr]. This stress range represents a direct measure of the relative plate coupling at the Wadatti-Benioff region, which is also in good agreement with the stress drop estimates from seismic activity at convergent margins (10-30 [Mpa]). According to the modelling effort, the degree of coupling shows a direct correlation with the age of the subducting slab in the Nazca Plate. Somewhat surprisingly, the lowest coupling is associated with the collision zones of active ridges at the Taitao T.J. and the Cocos Ridge. The high heat flow released from the seafloor spreading reduces the viscosity of the overriding plate such that the dynamic topography is achieved with just a minor stress transference from the subductiong slab. On the other hand, the oldest oceanic crust near the Arica elbow (45 Ma) shows the maximum coupling. This "highly coupled" region is located in front of a coastal

margin under an extensional regime, suggesting a likely relationship with the tectonic erosion of the margin. Passive ridges, contrary to our common belief do not show the largest degree of coupling; in fact there is a tendency towards smaller values than the surrounding areas (the most remarkable case is that of profile 16 at the Carnegie Ridge subduction). The first order age dependence of the coupling degree, suggests that the relative reduction in the coupling of passive ridge subduction implies a thermal (age) resetting in those zones. Local, and episodic, changes in the sea level (up to tens of meters with wavelengths of ~100 km) may be correlated with the oblique convergence of passive ridges given the perturbation in the degree of coupling. The large coupling observed in the Cocos-Central America plate interaction is not consistent with the age dependence previously outlined (subducting slab younger than 20 [Ma]). This large coupling is also consistent with the observed seismicity (Figure 1). The observed high obliquity in the region (Figure 3) is probably playing an important role to be considered in futures experiments.

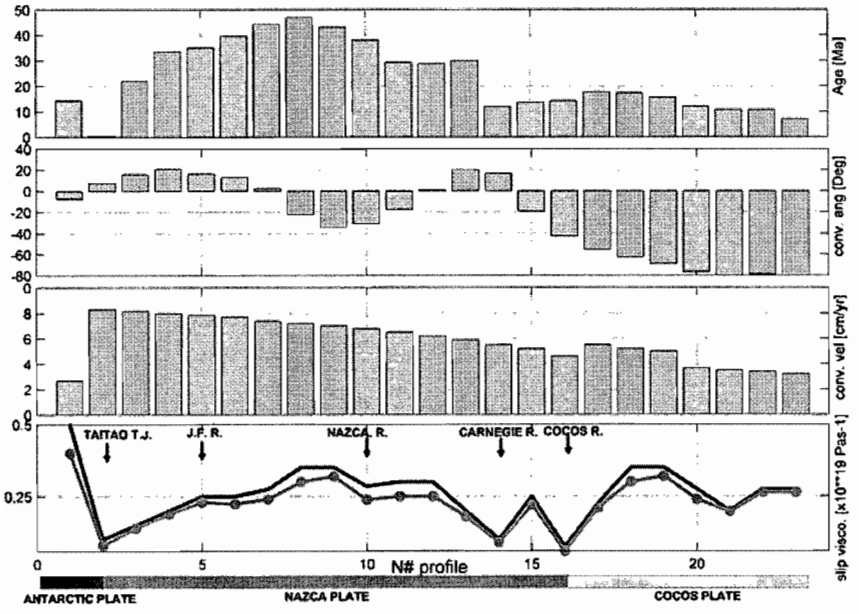

Figure 3: Model results. In the lower panel we present the viscosity of the slip layer for an overriding viscosity of $2 \cdot 10^{21}$ [Pas] (black solid line), and $5 \cdot 10^{21}$ [Pas] (gray solid line).

AKNOWLEDGMENTS This research has been supported by Fondecyt Project 1000136.

REFERENCE

.DeMets C. et al., Effects of recent revisions to the geomagnetic reversal time scale on estimates of current plate motions, Geophys. Res. Lett. Vol 21 N#20 p. 2191-2194, 1994

Shreve R.L. and M. Closs, Dynamics of sediment subduction melange formation, and prism accretion, J.Geophys. Res., 10,229-10,245, V. 91, 1986

Smith W.H.F. and D.T. Sandwell, Bathymetric prediction from dense satellite altimetry and sparse shipboard bathymetry, J. Geophys. Res, 99, 21803-21824, 1994

Wdowinski S. Dinamically Supported Trench Topography, J. Geophys. Res., 17,651-17, 656 ,V. 97, 1992

Yañez G.A., Some aspects of the long term lithospheric evolution: Remanent magnetization of the ocean basins and deformation at convergent margins, Ph. D. Thesis, Columbia University, New York, USA, 1994.

.Zienkiewicz O.C. and R.L. Taylor, The Finite Element Method, vol. 2, Solid and Fluid Mechanics Dynamics and Non-linearity, 4th ed. McGraw-Hill, New York, 1991

PRESTACK DEPTH IMAGING OF DEEP SEISMIC REFLECTION DATASETS : ANCORP & PRECORP

Mi-Kyung YOON (1), Stefan BUSKE(2), Stefan LÜTH(3)

(1) yoon@geophysik.fu-berlin.de

(2) buske@geophysik.fu-berlin.de

(3) stefan@geophysik.fu-berlin.de

KEY WORDS: Deep Seismic Image, Subduction Zone, Prestack Depth Migration, Bright Spot

INTRODUCTION

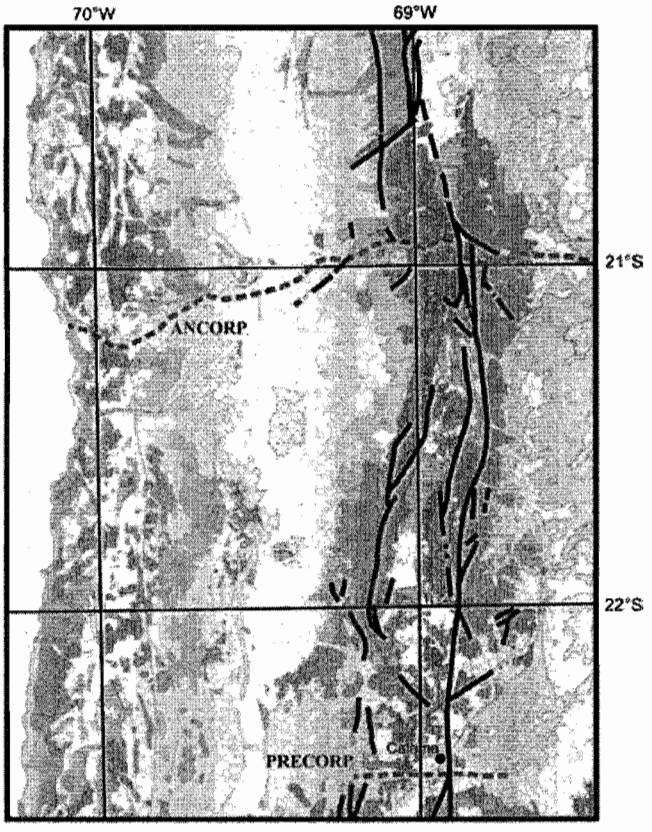

Fig. 1: Location of ANCORP and PRECORP (dashed lines)

In the frame of the Collaborative Research Center 267[1] two deep seismic reflection profiles have been acquired across the Central Andes: PRECORP and ANCORP (fig. 1). The 50km long PRECORP profile has been carried out as a technical feasibility study in 1995. One year later the ANCORP project was realized, a combined refraction and reflection experiment along a 385 km E-W profile with maximal N-S extension of 50 km. The data processing of the PRECORP dataset provided no seismic images, whereas a high quality 2D image of the subduction zone was obtained by a cmp-processing sequence followed by a poststack migration of the ANCORP data (ANCORP Research Group, 1999). This paper presents the results of a reprocessing of both datasets using the Kirchhoff prestack depth migration method. This processing provided a 3D migrated depth section of ANCORP (Yoon, 2001) which gives a detailed image of the subducting oceanic plate, the Nazca reflector and a Bright Spot (Quebrada Blanca Bright Spot). It also resulted in a 2D depth section of the PRECORP line, where parts of the Nazca reflector can be identified and a second bright spot (Calama Bright

[1] Sonderforschungsbereich 267 "Deformation Processes in the Andes", www.fu-berlin.de/sfb267

Spot) is spotted.

DATA PROCESSING

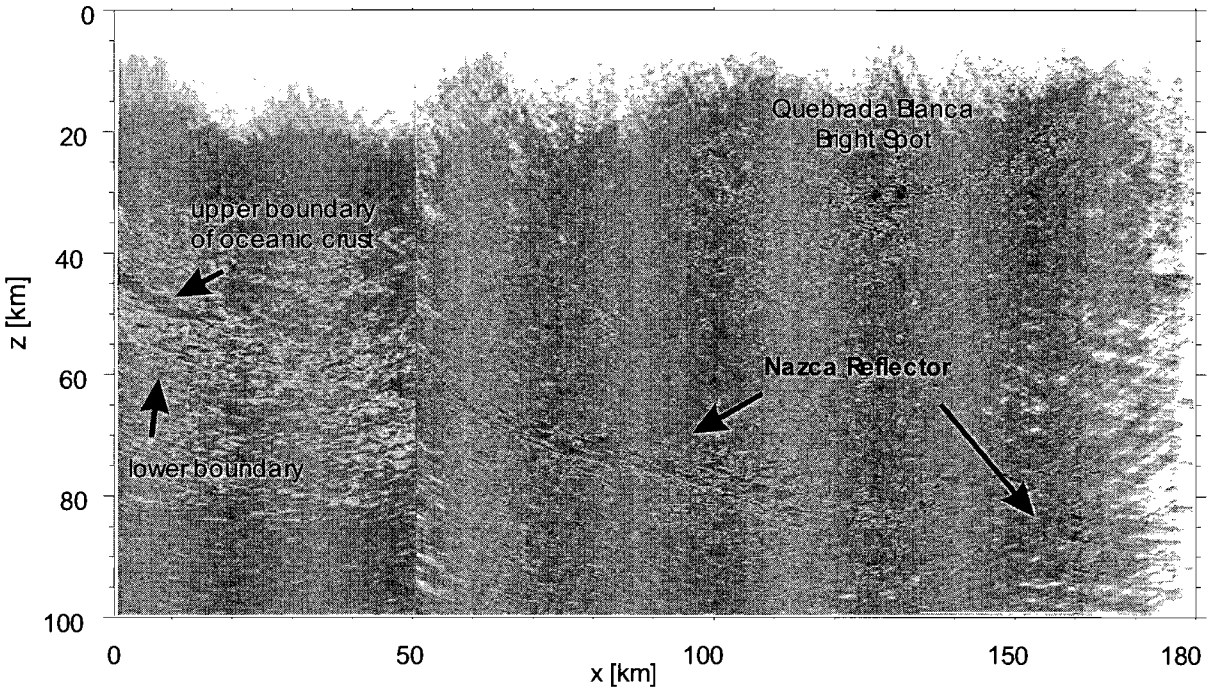

Fig. 2: Prestack depth migrated section of ANCORP.

The prestack depth migration of PRECORP was performed in 2D, whereas - according to the crooked line geometry - it was implemented in 3D for ANCORP. The 2D velocity model, which was used for both data sets, was derived from seismic refraction (Lüth, 2000). Under the assumption of negligible lateral velocity variations perpendicular to the profile the 2D model was extrapolated to 3D. Strong elevation variations of the surface along the profile suggested a migration from topography, thus static corrections were not performed and travel times were calculated from the surface. The travel time calculation was realized by a numerical implementation of a finite difference solver approach of the eikonal equation proposed by Podvin and Lecomte (1991). For each common shot gather a prestack depth migrated section was computed. Optimized selective stacking of these single sections yielded the final 2D or 3D depth slices, respectively. In order to increase the signal-to-noise ratio of the ANCORP image the slides which were located near the profile line were stacked. Hence a final 2D section was obtained (fig. 2).

On account of the low signal-to-noise ratio and a high amplitude dynamic range the prestack depth migration of the PRECORP dataset was splitted into two depth areas, the upper part from the surface down to 50km, and the lower part between 50km and 100km depth. Geometrical Spreading correction was applied for the lower part only in order to enhance deep reflection amplitudes. Stacking of both section produced the final depth section (fig. 3).

RESULTS

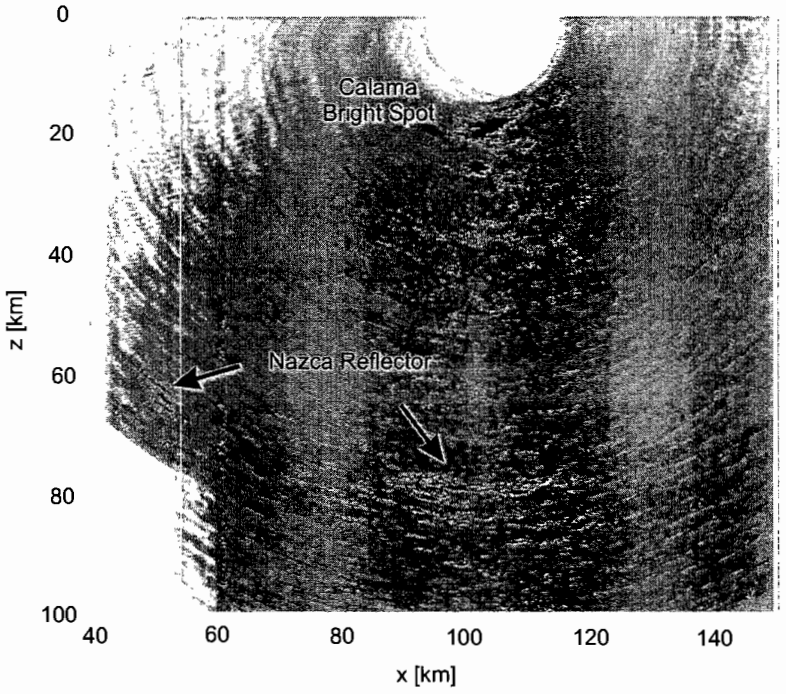

Fig. 3: Prestack depth migrated section of PRECORP.

The 2D depth section of ANCORP yields sharp images of the upper and the lower boundary of the oceanic crust in the depth range between 40-55km (fig. 2). We were also able to work out deep reflections, with a continuous observation of the Nazca reflector to a maximum depth of about 95km. A spatial analysis of the Quebrada Blanca Bright Spot in the 3D section shows both a dipping component to the west and also to the north. While standard data processing provided no image of the PRECORP data, the prestack depth migration combined with separate treatment of lower and deeper reflections succeeded in an seismic depth image showing segments of the Nazca reflector in depth down to 80km (fig. 3). The migration of the upper part provided an image of a feature with highly reflected amplitudes (Calama Bright Spot), which is dipping to the west.

CONCLUSIONS

In this paper we showed two examples of successful application of the Kirchhoff prestack depth migration to deep seismic reflection data: The resulting ANCORP section shows sharp images of the upper and the lower boundary of the oceanic crust at depth between 40-50km. A 3D analysis of the Quebrada Blanca Bright Spot showed in addition to the west dipping component – which was known from previous processing results - a dip component to the north. Furthermore we were able to present a seismic depth section of the PRECORP data set at all, which shows segments of the Nazca reflector and a the Calama Bright Spot.

REFERENCES

ANCORP Research Group 1999. Seismic Reflection Image of the Andean Subduction Zone Reveals Offset of Intermediate-Depth Seismicity into Oceanic Mantle. Nature 349, 341-344.

Lüth, S. 2000. Ergebnisse weitwinkelseimischer Untersuchungen und die Struktur der Kruste auf einer Traverse über die zentralen Anden bei 21°S. Dissertation, Berliner Geowissenschaftliche Abhandlungen, Reihe B: Geophysik, Band 37, Selbstverlag Fachbereich Geowissenschaften, FU Berlin.

Podvin, L., Lecomte, L. 1991. Finite difference computation of travel-times in very contrasted velocity models: amassively parallel approach and its associated tools. Geophysical Journal International 105, pp. 271-284.

Yoon, M. and Buske, S. 2001. Application of Prestack Depth Migration to a deep seismic data set. EGS XXVE General Assembly, Nice, France.

THE PROVENANCE OF THE ORDOVICIAN DEPOSITS OF THE FAMATINA RANGE (NORTHWESTERN ARGENTINA): FIRST RESULTS

Udo ZIMMERMANN[1], Susana ESTEBAN[2] and Heinrich BAHLBURG[3]

[1]*Department of Geology, RAU, Auckland Park 2092, South Africa (uz@na.rau.ac.za)*

[2]Instituto Superior de Correlación Geológica, Universidad Nacional de Tucumán, Miguel Lillo 205, 4000 Tucumán, Argentina (insugeo@unt.edu.ar)

[3]Geologisches-Paläontologisches Institut, Universität Münster, Correnssstr. 24, 48149 Muenster, Germany (bahlbur@uni-muenster.de)

KEY WORDS: Ordovician, provenance analysis, Famatina Range

INTRODUCTION

This contribution presents the first results of a provenance analysis of Pre-Ordovician to Lower Ordovician formations of the Famatina Range (northwestern Argentina) (Fig. 1). The study forms part of a project to model source areas and the depositional history of the Cambrian to Ordovician deposits in the NW part of Argentina (Fig. 1), using petrological (include CL, SEM, microprobe analysis), geochemical and isotope geochemical methods. A comparison with data from the Puna basin, situated to the north of the Famatina region (Fig. 1) are made. The Cambro-Ordovician evolution of the Famatina Range is discussed in detail. Some authors interpreted the region as an exotic block, defined a Puna-Famatinian Terrane (Conti et al., 1996) or modelled an island-arc scenario (Aceñolaza et al., 1996). Furthermore a large retro-arc basin that includes the Puna and Famatina deposits is proposed (Zimmermann, 2000). The stratigraphy begins with the La Aguadita/Negro Peinado Formation which comprises the oldest sedimentary rocks of the Famatina basin. They consist of fine-grained siliciclastic turbidity currents and turbidites, ichnofossils point to an age of late Precambrian to early Cambrian (Rossi et al., 1997). Based on petrography and geochemistry the deposits are interpreted as sedimented on a passive continental margin deposits (Rossi et al., 1997). The Cambro-Ordovician stratigraphic record begins with the deposition of the Volcancito Formation (Harrington and Leanza, 1957) in the uppermost Cambrian (Esteban, 1999), the top and the base of which is not exposed (Toselli, 1977). Pankhurst et al. (1998) confirmed a Tremadocian (SHRIMP data 490 +/- 5 Ma) magmatic activity related to a subduction zone setting at a continental margin. The volcanic influence is represented in highly volcanoclastic and volcanic Arenig formations Suri, Las Planchadas (Mángano and Buatois, 1996) and Portezuelo de las Minitas (Aceñolaza and Gutiérrez-Marco, 2000). The youngest sedimentary rocks were deposited during Upper Arenig to Llanvirn (Molles Formation, Harrington and Leanza, 1957).

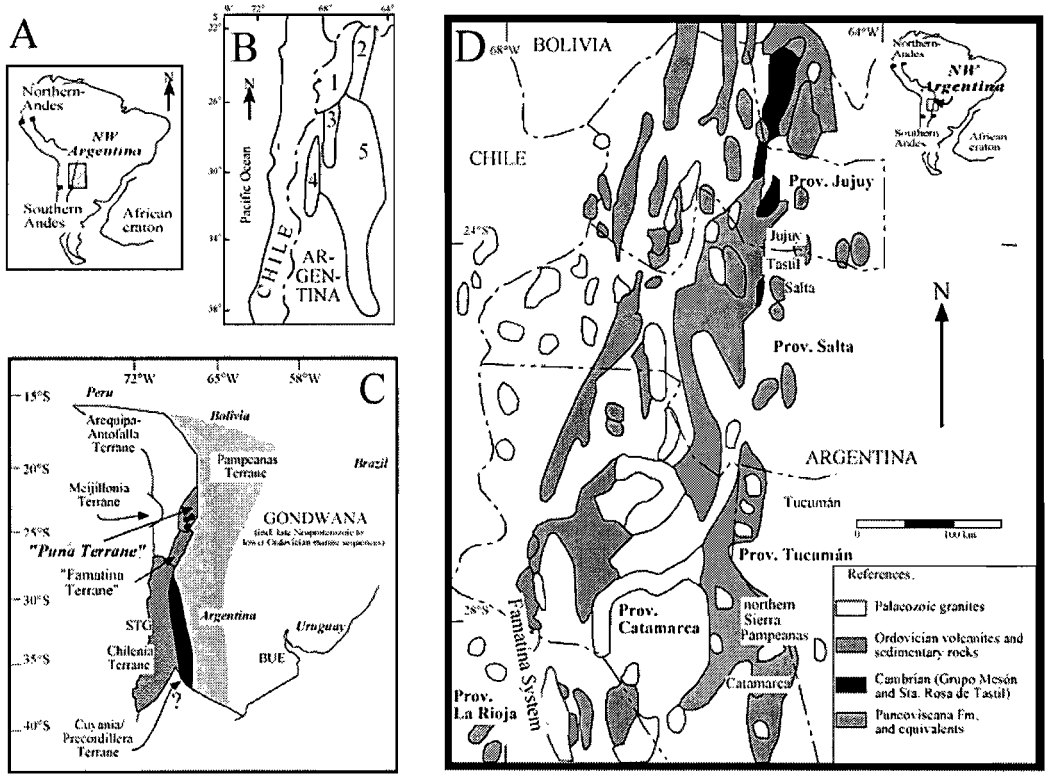

Fig. 1:
A: outcrop ubication
B: Lower Paleozoic geotectonic units and their hypothetical boundaries in NW Argentina. 1= Puna; 2= Cordillera Oriental; 3= Famatina; 4= Precordillera; 5= Sierras Pampeanas (after Rapela et al, 1992).
C: Proposed geotectonic units including the assumed terrane blocks Puna and Puna-Famatina Terrane (Palma et al., 1990; Conti et al., 1996). The black spots indicate the alleged ophiolitic rocks in the southern Puna (e.g. Ramos et al., 1986) which are hypothetically interpreted as the suture zone between the Pampeanas Terrane and westerly terranes/s. However, the mafic magmatites show a calc-alcaline signature and not a MOR (e.g. Zimmermann et al., 1999). Famatina terrane represents the southern part of a probable Puna-Famatina Terrane. (modified after Bahlburg and Hervé, 1997; STG= Santiago de Chile, BUE=Buenos Aires)
D: Schematic geological map of the Paleozoic of the Puna and Famatina region (after Grissom et al., 1998).

CONCLUSIONS

Petrographical, palaeontological and sedimentological data define the rocks of the Volcancito Formation as platform deposits in a low energy environment, partly affected by wave energy or storm events. The provenance of the source/s of the Volcancito Formation, using trace elements and especially REE, has a UCC composition and shows an active continental margin signature. Neither fragments indicating a mafic or volcanic source, nor typical geochemical trends for subduction related volcanism could be found. The samples of central and northern Puna of Tremadocian age are more concentrated in REE and show partly an influence of volcanic material (Zimmermann, 2000; Zimmermann and Esteban, subm.). The volcaniclastic and volcanic formations Suri and Las Planchadas are different and their composition could be classified as rhyodacitic to dacitic (Suri Formation) and dacitic to andesitic (Las Planchadas Formation) respectively. The trace element data show the influence of a continental volcanic arc in

a very strong negative Ta-Nb anomalies. La-Th-Sc and Th-Sc-Zr relations point to a volcanic arc provenance for both formations. According to the petrography the rocks of the Suri Formation show an influence of non-volcanic debris that causes higher Th/Sc values (0,7-0,9), Ta, Nb and lower Ti/Zr values. Coincident to the evolution of the northerly Puna basin, the influence of the volcanic debris starts in the Upper Tremadoc. Middle Ordovician formations of the Famatina Range that shows the extinction of the volcanic arc, like the Llanvirn Falda Ciénaga Formation (Zimmermann, 2000) in the southern Puna for example are not exposed. We propose a similar evolution of the Famatina Range basin like the Puna basin: during the Tremadoc the basin margin changed from a rifted margin composition to an active continental margin with the initiation of a volcanic arc. So far unclear is, if this basin represented the western Gondwana margin or a retro-arc basin, like the Puna deposits. Only further provenance work on single grains and isotopic work could define the source and depositional areas more detailed and could help to review the different palaeotectonic models for the western boundary of Gondwana during the Cambro-Ordovician times.

The project is a contribution to the IGCP 436: Structure and Evolution of the Gondwana Margin.

REFERENCES

Aceñolaza, F.G. and Gutiérrez-Marco, J.C. 2000. Graptolitos de la Formación Portezuelo de las Minitas (Ordovícico Inferior) del Sistema de Famatina, La Rioja, Argentina. Boletin de la Academía Nacional de Ciencias, Cord. Rep. Argentina, 64, 18-26.

Aceñolaza, F.G., Miller, H. and Toselli, A. 1996. Geología del Sistema de Famatina. Münchener Geologische Hefte **19** (Reihe A). 1-410. München.

Bahlburg, H. and Hervé, F. 1997. Geodynamic evolution and tectonostratigraphic terranes of northern Argentina and northern Chile. Geological Society of America Bulletin, 109, 869-884.

Conti, C.M., Rapalini, A.E., Coira, B. and Koukharsky, M. 1996. Paleomagnetic evidence of an early Paleozoic rotated terrane in Northwest Argentina. a clue for Gondwana-Laurentia interaction?. Geology, 24, 953-956.

Esteban, S. 1999. Estratigrafía, Geología Sedimentaria y Paleontología del Ordovícico Basal del Sistema del Famatina. Tesis Doctoral (Inédita). Fac. Cs. Nat. E IML – Univ. Nac. de Tucumán, 1-189.

Grissom, G.C., DeBari, S.M. and Snee, L.W. 1998. Geology of the Sierra de Fiambalá, northwest Argentina: Implications for Early Palaeozoic Andean tectonics; in: Pankhurst, R.J. and Rapela, C.W.: The Proto-andean Margin of Gondwana; Geological Society, London, Special Publication, 142, 297-323.

Harrington, H. and Leanza, A., 1957. Ordovician trilobites of Argentina. Department of Geology University of Kansas, Special Publication, 1, 1-276.

Mángano, M. and Buatois, L. 1996. Shallow marine event sedimentation in a volcanic arc-related setting: the ordovician Suri Formation, Famatina Range, NW Argentina. Sedimentary Geology, 105: 63-90.

Palma, M. A., Brisson, I. and Vujovich, G. 1990. Geológia del bloque de la Quebrada Honda, Puna Cartamarqueña. Revista de la Asociación Geológica Argentina, 45, 145-158.

Pankhurst, R., Rapela, C., Saavedra, J., Baldo, E., Dahlquist, J., Pascua, I. and Fanning, C. 1998. The Famatinian magmatic arc in the central Sierras Pampeanas: an Early to Mid Ordovician continental arc on the Gondwana margin. In: *The Proto-Andean Margin of Gondwana* (Eds. R. Pankhurst and C. Rapela), Geological Society London Special Publication, 142, 181-217.

Ramos, V. A., Jordan, T. E., Allmendinger, R.W., Mpodozis, C., Kay, S.M., Cortés, J.M. and Palma, M. 1986. Paleozoic terranes of the central Argentine-chilean Andes; Tectonics, 5, 855-880

Rapela, C.W., Coira, B., Toselli, A. and Saavedra, J. 1992. El magmatismo del Paleózoico en el Sudoeste de Gondwana. In: *Paleozóico Inferior de Ibero-América* (Eds. J.G. Gutiérrez Marco, J. Saavedra and I. Rábano), 21-68.

Rossi, J.N., Durand, F.R., Toselli, A.J. and Sardi, F.G. 1997. Aspectos estratigráficos y geoquímicos comparativos del basamento metamórfico de bajo grado del Sistema de Famatina, argentina. Revista de la Asociación Geológica Argentina, 52, 469-480.

Toselli, G. 1977. El Paleozoico Inferior y Medio de la region de Volcancito, Sierra de Famatina, Provincia de La Rioja, Rep. Argentina. Acta Geol. Lill., 14, 85-104.

Zimmermann, U. 2000. The evolution of the Ordovician Southern Puna-Basin in NW Argentina - a compilation. IX Congreso Geológico Chileno, 1, 720-725.

Zimmermann, U. and Esteban, S.B. (subm.). Provenance and facies of the Volcancito Formation, Famatina Range (Northwestern Argentina). XV Congreso Geológico Argentino.

Zimmermann, U., Mahlburg Kay, S. and Bahlburg, H. 1999. Petrography and geochemistry of southern Puna (NW Argentina) Pre-Late Ordovician gabbroic to ultramafic units, intermediate plutonites and their host units: a guide to evolution of the western margin of Gondwana. XIV Congreso Geologico Argentino, actas, 2, 143-146.

AUTHOR INDEX

GROUPS

Achevé d'imprimer sur les presses de :

LAVAUZELLE graphic N° d'Imprim. 2066112-02 – Dépôt légal : Sept. 2002